Proton-Activated Catalysts for Efficient and Practical Enantioselective Syntheses

Author: Farid Willem van der Mei

Proton-Activated Catalysts for Efficient and Practical Enantioselective Syntheses

Farid Willem van der Mei

A dissertation

submitted to the Faculty of

the department of Chemistry

in partial fulfillment

of the requirements for the degree of

Doctor of Philosophy

Boston College
Morrissey College of Arts and Sciences
Graduate School

September 2018

Proton-Activated Catalysts for Efficient and Practical Enantioselective Syntheses

Farid Willem van der Mei
Advisor: Professor Amir H. Hoveyda

Abstract

A previously developed catalytic system which can catalyze a variety of efficient and enantioselective allyl additions has been expanded to include regio-, diastereo-, *Z*-, and enantioselective crotyl addition reactions. As discussed in Chapter 1, we were able to carry out efficient crotyl additions to *N*-phosphinoyl imines by discovering a sufficiently Lewis acidic co-catalyst, zinc(II) methoxide. This finding enabled us to vastly improve reaction efficiency, in addition to enabling a 1,3-borotropic shift during the course of the reaction, turning a previously α selective transformation into a γ-selective one. These findings allowed us to develop a catalytic, enantioselective crotyl addition to *N*-phosphinoyl imines utilizing the commercially available *Z*-crotyl–B(pin).

When the reaction conditions elucidated for crotyl additions to imines were utilized on a more electrophilic substrate, such as trifluoromethyl ketones, an entirely different finding was observed (Chapter 2). We found that if direct addition is more facile than 1,3-borotropic shift the transformation will again be α-selective, furnishing a linear product, rather than the typically observed, branched crotyl addition product. This finding allowed us to establish the first broadly applicable, efficient, regio-, *Z*-, and enantioselective crotyl addition to trifluoromethyl ketones. We then highlighted the utility of these products by using this method in tandem with *Z*-selective olefin metathesis, affording complex, enantioenriched, trifluoromethyl-containing homoallylic alcohols. During the course of these studies, and through density functional theory computations, we learned that *Z*- and *E*-crotyl–B(pin) react through distinct transition

states to form the same *Z*-olefin-containing product with varying levels of enantioselectivity.

These findings led us to the results reported in Chapter 3, the first examples of enantioselective aminophenol-promoted allyl additions to aldehydes. We were able to utilize *Z*-CF_3-allyl–B(pin) and *Z*-Cl-allyl–B(pin) (both accessed through catalytic olefin metathesis) in *Z*- and enantioselective additions to aldehydes, affording products which cannot be accessed readily through previously reported methods. We quickly realized the potential of *Z*-chloro-substituted homoallylic alcohols for the synthesis of *Z*-homoallylic alcohols, to demonstrate this potential, we carried out the total synthesis of mycothiazole, which we accomplished in seven steps from commercially available materials and 17% overall yield, a marked improvement over the previous synthetic strategy.

Acknowledgements

When I first started graduate school, I was under the impression that graduate school would often feel like an endless voyage. However, as many people had warned me over these past five years, the experience ended in a flash. While these past five years have often been filled with stress and anxiety, I believe that the underlying reason that accounts for this rapid passage of time is the people I met during this journey. The innumerable amount of gratifying conversations and interactions with these people made this experience irreplaceable to me, and for this I would like to thank all of the people I have connected with over these years.

First and foremost, I would like to thank Professor Amir H. Hoveyda for accepting to me into his group and allowing me to work on the exciting research presented in this thesis. I have learned a lot from Professor Hoveyda over the years and I could not imagine any other lab where I would have had a better education. He has taught me several key lessons that apply not only to lab, but also to life as a whole. For example, we are always instructed to pay great attention to detail and to always think for ourselves, rather than looking to other people for answers. I will greatly miss his stories and hope to be able to hear the new stories as they develop.

I would also like to take this time to thank Professors Marc L. Snapper and James P. Morken for serving as members of my doctoral defense committee as well as reading my dissertation. I was also fortunate enough to also be able to take the synthesis classes that they taught during my first year of graduate school. I would also like to acknowledge Professor Jeffery A. Byers for serving as the head of my orals committee as well as for

being an extremely rigorous and challenging teacher, which I greatly appreciated and enjoyed. I perceive Mechanistic Organic Chemistry to be the most important class which we take at BC and appreciate the strong foundation which I received from his course.

I was fortunate enough to be able to partake in and finish two interesting projects started by Dr. Hiroshi Miyamoto and Dr. Changming Qin. I owe a lot to their hard work and dedication for which I would like to thank them.

During my stay in the Hoveyda lab I have made a tremendous amount of new friends. As I mentioned before, I believe that this experience was greatly enriched by these relationships and for that I would like to thank (in no particular order): Hwanjong Jang, Hao Wu, Keven McGrath, Ying Shi, Ming Joo Koh, Jaehee Lee, KyungA Lee, Thach T. Nguyen, Juan del Pozo del Valle, Stella A. Gonsales, Felix W. W. Hartrampf, Paulo Paioti, Filippo Romiti, and Yucheng Mu. In particular, I would like to thank KyungA Lee and Thach T. Nguyen, two of my closest friends during this time. These two were always available to chat and helped establish a great group atmosphere for which I am deeply thankful.

I would also like to thank Ryan J. Morrison and Diana C. Fager for continuing on with the aminophenol project. I look forward to see the excellent work to come from them, I believe they will leave no stone unturned. In the same vein, I am eager to see what the future generation of Hoveyda lab graduate students (Chaofan, Yuebiao, Shaochen, Ryan, Diana, Mu, Xinghan and Tobias) accomplishes.

Lastly I would like to thank my mom and Emma Edelstein, two people without whom I would have not been able to complete this journey. Their constant encouragement and support meant the world to me.

Table of Contents

Chapter One

Lewis Acid Catalyzed Borotropic Shifts in the Design of Diastereo- and Enantioselective γ-Additions of Allylboron Moieties to Aldimines

1.1. Introduction

Enantioenriched homoallylic amines are synthetically valuable compounds, therefore the development of practical and synthetically useful methods to generate such moieties are of great importance to the field of organic synthesis. Amines are ubiquitous in nature and often have a critical role in the biological activities of their parent compounds.[1] Catalytic enantioselective addition of allyl groups is an expedient and attractive approach to access the aforementioned amines with high enantiomeric purity, while also installing an alkene unit for further elaboration.[2] Alkenes can participate in a number of synthetically useful subsequent reactions such as ozonolysis, olefin metathesis, dihydroxylation, epoxidation, hydroboration, allowing access to a wide variety of more complex products.[2]

(1) Kobayashi, S.; Mori, Y.; Fossey, J. S.; Salter, M. M. *Chem*. *Rev*. **2011**, *111*, 2626–2704.
(2) For a recent review on enantioselective addition of allyl groups to carbonyl compounds and imines, see: (a) Yus, M.; González-Gómez, J. C.; Foubelo, F. *Chem*. *Rev*. **2011**, *111*, 7774–7854. For a recent review on diastereoselective methods for these transformations see: (b) Yus, N.; González-Gómez, J. C.; Foubelo, F. *Chem*. *Rev*. **2013**, *113*, 5595–5698.

Scheme 1.1. Homoallylic Amines as Precursors to Valuable Products

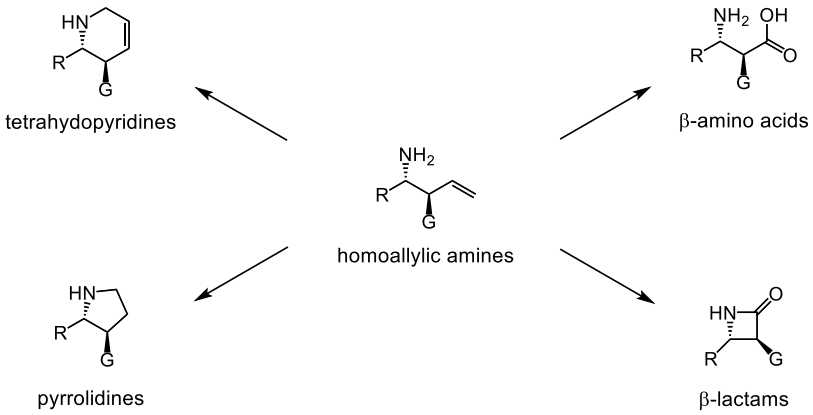

Hence, homoallylic amines can serve as precursors to a variety of valuable enantiomerically enriched nitrogen-containing molecules, such as β-amino acids, lactams, pyrrolidines, and tetrahydropyridines (Scheme 1.1).[3,4]

1.2. Background

1.2.1 State-of-the-Art in Catalytic Enantioselective Crotyl Additions to Imines

Despite the synthetic utility of enantioenriched homoallylic amines, the field of catalytic enantioselective crotyl additions to aldimines is relatively under-developed. Since 1999 there have been ten reports on methods for catalytic enantioselective crotyl additions to imines, the majority which have only carried out the transformation on a singular substrate, the benzaldehyde-derived aldimine. The first disclosed catalytic enantioselective

(3) Ramachandran, P. V.; Burghardt, T. E. *Chem. Eur. J.* **2005**, *11*, 4387–4395.
(4) a) Liu, M.; Sibi, M. P. *Tetrahedron* **2002**, *58*, 7991–8035; b) Fuller, A. A.; Chen, B.; Minter, A. R.; Mapp, A. K. *J. Am. Chem. Soc.* **2005**, *127*, 5376–5383.

crotylation of α-imino esters with *E*-crotyl-tri-*n*-butyl stannane was reported by Fang *et al.* in 1999 (Scheme 1.2).[5]

Scheme 1.2. Jørgensen's Crotyl Additions to *N*-Tosyl α-Imine Esters

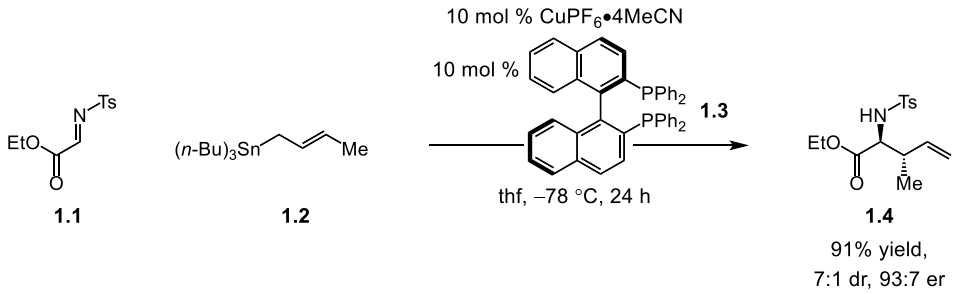

The transformation was catalyzed by a Cu-phosphine system and was found to be moderately diastereoselective (6:1 to 10:1 dr) and enantioselective (50:50 to 93:7 er) depending on the phosphine that was employed. However, diminished reaction temperatures (–78 °C) in addition to lengthy reaction times (12–24 hours) were required. Additionally, only one substrate was examined and the notoriously hard-to-remove *N*-tosyl protecting group was used. In 2001 the Kobayashi group disclosed a similar transformation utilizing a chiral Lewis acidic zirconium-BINOL complex to catalyze allyl stannane additions to *ortho*-hydroxy-phenyl protected aldimines (Scheme 1.3).[6]

(5) Fang, X.; Johannsen, M.; Yao, S.; Gathergood, N.; Hazell, R. G.; Jørgensen, K. A. *J. Org. Chem.* **1999**, *64*, 4844–4849.
(6) Gastner, T.; Ishitani, H.; Akiyama, R.; Kobayashi, S. *Angew. Chem., Int. Ed.* **2001**, *40*, 1896–1898.

Scheme 1.3. Kobayashi's Chiral Zirconium Catalysts for Enantioselective Crotyl Additions

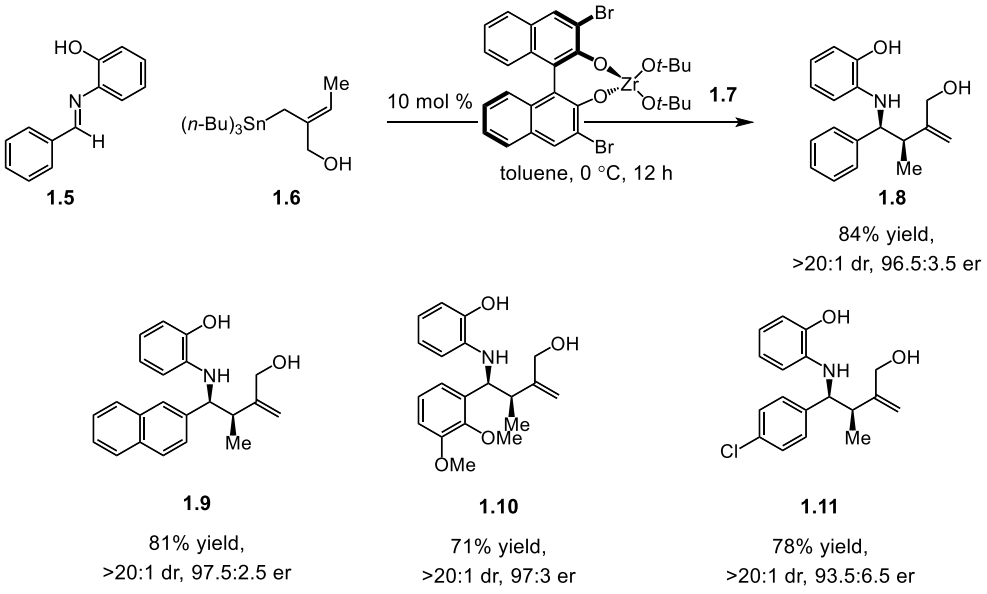

The Kobayashi group found that reactions utilizing *Z*-crotyl-tris-*n*-butyl stannane afforded products with high diastereoselectivity (>95:5 dr) for the *syn* diastereomer and high enantioselectivity (>93:7 er), yet they did not report any results regarding the *E* isomer of the reagent. The reactions could be carried out at 0 °C in twelve hours with 10 mol % of the zirconium-based catalyst. Only six aryl cases were examined and the phenolic protecting group employed, needed for high enantioselectivity, requires two steps, including oxidative conditions (CAN), for removal. In 2007 the Jacobsen group published a protocol in which a chiral urea catalyst could promote the enantioselective allylation of acylhydrazones with an *in situ* generated crotyl indium reagent (Scheme 1.4).[7]

(7) Tan, K. L.; Jacobsen, E. N. *Angew. Chem., Int. Ed.* **2007**, *46*, 1315–1317.

Scheme 1.4. Jacobsen's Chiral Urea Catalysts for Enantioselective Crotyl Additions

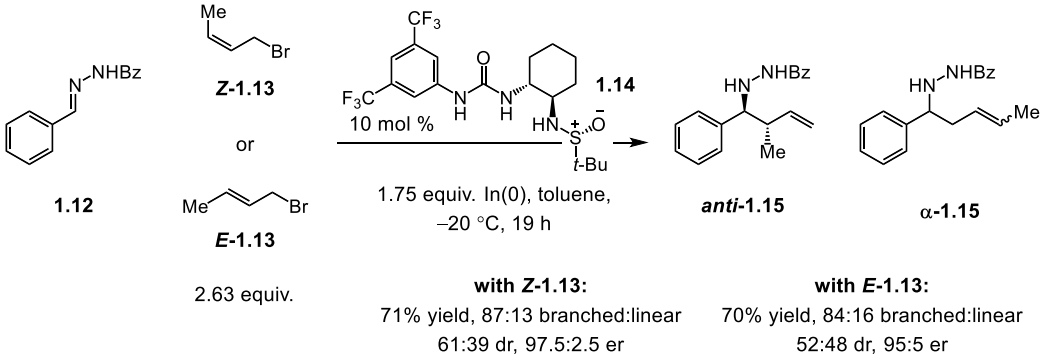

Jacobsen and Tan state that when crotyl bromide (*E* or *Z*) is utilized in their protocol the products are generated with high enantioselectivity (>95:5 er). On the other hand, the diastereoselectivity and regioselectivity of the transformation are moderate. The super-stoichiometric use (1.75 equiv.) of costly indium, in addition to diminished reaction temperatures (–20 °C) and costly cleavage of the hydrazine protecting group (super stoichiometric SmI_2) are considerable disadvantages of this method. Additionally, only the benzaldehyde- derived imine was explored. The same year, the Schaus group also disclosed a catalytic enantioselective allylboration of acyl-protected imines catalyzed by BINOL derivatives (Scheme 1.5).[8]

Scheme 1.5. Schaus' BINOL Catalyzed Crotyl Addition to Acyl Imines

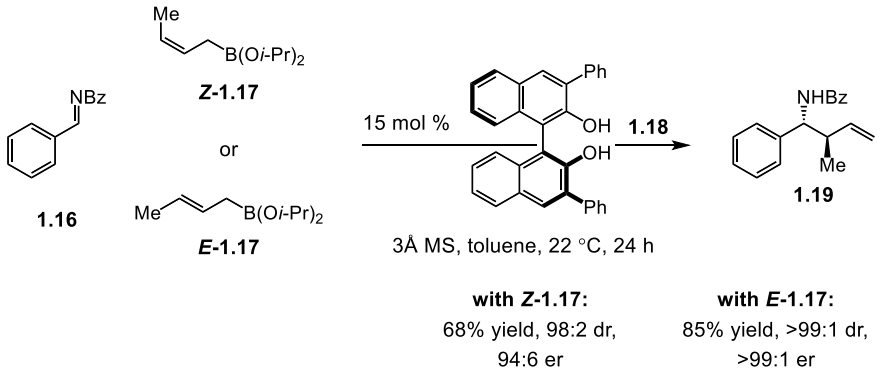

(8) Lou, S.; Moquist, P. N.; Schaus, S. E. *J. Am. Chem. Soc.* **2007**, *129*, 15398–15404.

Therein, Schaus *et al*. reported that *E*- and *Z*-crotyl–B(O*i*-Pr)$_2$ reacted to form the *anti* diastereomer of the crotyl product with exceptional diastereo- and enantioselectivity (>98:2 dr and >94:6 er). Again, only the benzaldehyde-derived aldimine was explored. Additionally, the protocol requires high catalyst loadings (15 mol %), extended reaction times (>24 h), and the use of an air and moisture sensitive crotylboron reagent (which must be stored as a dilute solution). The following year the Kobayashi group disclosed another method for the enantioselective allylation of hydrazone protected α-imino esters (Scheme 1.6).[9]

Scheme 1.6. Kobayashi's Zn-Catalyzed Enantioselective Crotyl Addition to Hydrazone Esters

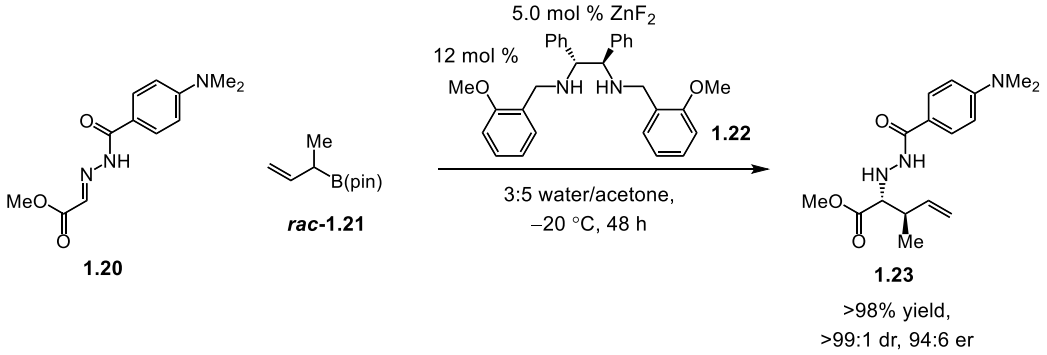

The method, catalyzed by zinc difluoride and a chiral diamine ligand was found to furnish crotylation products with excellent regio- and diastereoselectivity (>99:1, for both) in addition to high enantioselectivity (94:6 er). The method was not limited to methyl substituted allyl boron reagents; ethyl, butyl, *tert*-amyl, and O-benzyl substituents were also tolerated. To access this product however, the Kobayashi group had to use the (not commercially available) branched α-methyl allylboron reagent, as they found that in their method addition to the imine occurred from the α-carbon of the allylboron reagent. When

(9) Fujita, M.; Nagano, T.; Schneider, U.; Hamada, T.; Ogawa, C.; Kobayashi, S. *J. Am. Chem. Soc.* **2008**, *130*, 2914–2915.

γ-substituted crotyl boron reagents were employed, the reaction was found to proceed sluggishly (<25% yield in 110 h) and with low enantioselectivity (<57:43 er). Yet again the transformation was only shown for one substrate and required long reaction times (48 h) and low reaction temperatures (–20 °C). In 2009, the Yamamoto group published a method for a silver-phosphine catalyzed allylation of phenyl-protected aldimines with *Z*-crotyl-Si(OMe)$_3$ (Scheme 1.7).[10]

Scheme 1.7. Yamamoto's Ag-Phosphine-Catalyzed Enantioselective Crotyl Additions

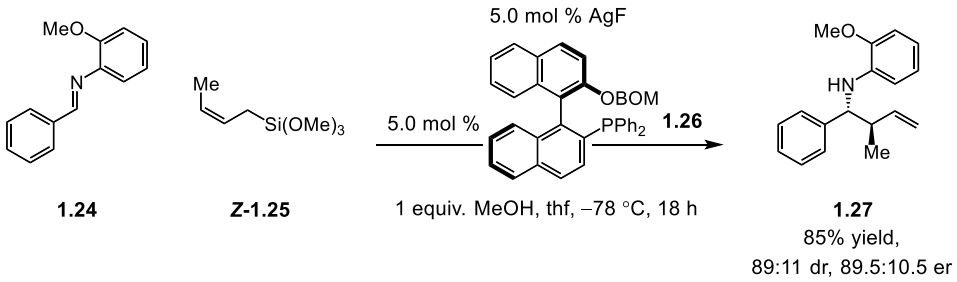

1.24 ***Z*-1.25** **1.27**
85% yield,
89:11 dr, 89.5:10.5 er

The optimal phosphine ligand was found to furnish the product in 89:11 dr (for the *anti* isomer) and 89.5:10.5 er. This method was also shown only for the benzaldehyde-derived aldimine. Additionally, the protocol utilizes low reaction temperatures (–78 °C), long reaction times (18 h) and a non-commercially available crotyl silane. Lastly, whether or not the *E* isomer of **1.25** would furnish the opposite diastereomer was not disclosed. The Zhou group published a Pd-phosphoramidite catalyzed enantioselective crotylation of *N*-tosyl-protected phenyl aldimines utilizing crotyl alcohol as the allyl source (Scheme 1.8).[11]

(10) Naodovic, M.; Wadamoto, M.; Yamamoto, H. *Eur. J. Org. Chem.* **2009**, 5129–5131.
(11) Qiao, X.-C.; Zhu, S.-F.; Chen, W.-Q.; Zhou, Q.-L. *Tetrahedron: Asymmetry* **2010**, *21*, 1216–1220.

Scheme 1.8. Zhou's Pd-Phosphoramide-Catalyzed Enantioselective Crotyl Additions

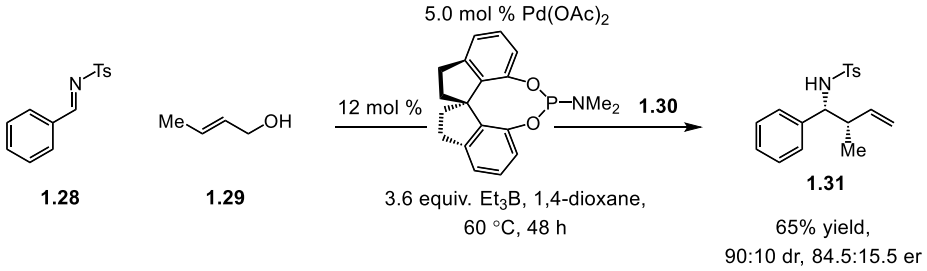

For the case explored, the Zhou group discovered that while diastereoselectivities were high (90:10 dr) the enantioselectivity of the transformation was moderate (84.5:15.5 er). They also found that the method was not limited to methyl-substituted allylic alcohols, phenyl-substituted allylic alcohols where also competent in the reaction and reacted with exceptional diastereoselectivity (>99:1 dr). The Kobayashi group disclosed another method for the crotylation of acylhydrazones utilizing the branched α-methyl allylboron reagent (Scheme 1.9).[12]

Scheme 1.9. Kobayashi's In(I)-Catalyzed Crotyl Additions to *N*-Acyl Hydrazones

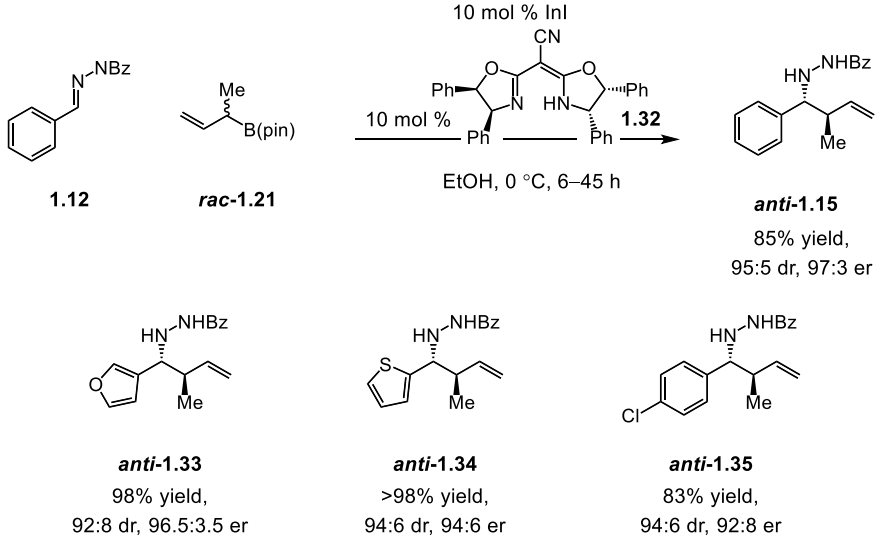

(12) Chakrabarti, A.; Konishi, H.; Yamaguchi, M.; Schneider, U.; Kobayashi, S. *Angew. Chem., Int. Ed.* **2010**, *49*, 1838–1841.

The highly selective transformation was catalyzed by indium iodide and a chiral semicorrin ligand. Eight examples (aryl and heteroaryl) were disclosed and the transformation was found to be very regio-, diastereo- and enantioselective (>98:2, >88:12, and >92:8, respectively). However, no alkyl, alkenyl, or alkynyl examples were shown, nor were any sterically hindered *ortho*-substituted or highly electron deficient examples demonstrated. Despite this, the method was still the most general reported protocol at the time. In 2011, Terada *et al*. demonstrated that the crotylation of *N*-acyl protected phenyl aldimines could be catalyzed by (up to 100 mol % of) a phosphoric acid catalyst (Scheme 1.10).[13]

Scheme 1.10. Terada's Chiral Phosphoric Acid-Facilitated Crotyl Additions

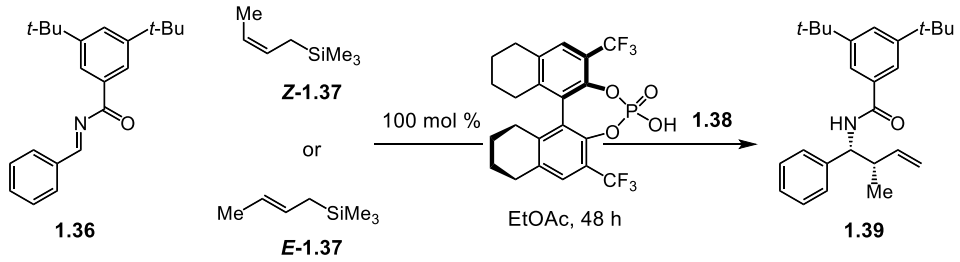

Terada and co-workers found that both *E*- and *Z*-crotyl-$SiMe_3$ furnish the *syn* diastereomer of the product with high diastereoselectivities and high enantioselectivities depending on the olefin isomer of the allylsilane reagent employed (93:7 dr and 99:1 with *E*-crotylsilane, 84:16 dr and 97:3 er with *Z*-crotylsilane). Although the reaction conditions are mild, the reaction is extremely sluggish (48 hours) and necessitates the stoichiometric use of a phosphoric acid derivative (either with 100 mol % catalyst or 20 mol % catalyst

(13) Momiyama, N.; Nishimoto, H.; Terada, M. *Org. Lett.* **2011**, *13*, 2126–2129.

and 80 mol % of an additional, achiral phosphoric acid derivative. In 2012 the Lam group reported what is to date the only catalytic enantioselective method which can access both diastereomers of the crotylation product with high diastereo- and enantioselectivity (Scheme 1.11).[14]

Scheme 1.11. Lam's Rh-Catalyzed Crotyl Additions to Cyclic *N*-Sulfonylimines

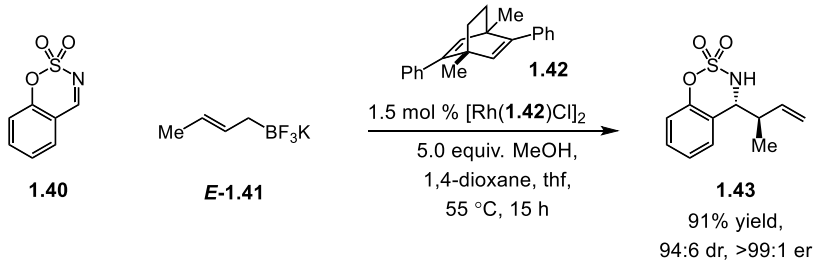

1.40 ***E*-1.41** **1.43**
91% yield,
94:6 dr, >99:1 er

with *Z*-1.41:
89% yield,
16:84 dr, >99:1 er

They found that by utilizing 1.5 mol % of a chiral diene-containing rhodium dimer the product could be synthesized with high diastereo- and enantioselectivities. When the *Z* isomer of the potassium trifluoroborate salt ***Z*-1.41** was used, the *syn* diastereomer of the product could be accessed with slightly diminished diastereoselectivity. The protocol was also amenable to *n*-alkyl substituted allyl boron reagents. However, they found that other less reactive protecting groups could not be employed in this method, which limits the applicability of the protocol. As illustrated above, there is still a need for practical and efficient catalytic methods for crotyl additions to imines which do not necessitate low temperature reaction conditions, high catalyst loadings, and/or long reaction times.[15]

(14) Luo, Y.; Hepburn, H. B.; Chotsaeng, N.; Lam, H. W. *Angew. Chem., Int. Ed.* **2012**, *51*, 8309–8313.

(15) For diastereoselective allyl additions with enantiomerically pure reagents or substrates, see: a) Hanessian, S.; Yang, R.-Y.; *Tetrahedron Lett.* **1996**, *37*, 5273–5276; b) Gao, Y.; Sato, F. *J. Org. Chem.* **1995**, *60*, 8136–8137; c) Berger, R.; Rabbat, P. M. A.; Leighton, J. L. *J. Am. Chem. Soc.* **2003**, *125*, 9596–9597; d) Kobayashi, S.; Ogawa, C.; Konishi, H.; Sugiura, M. *J. Am. Chem. Soc.* **2003**, *125*, 6610–6611; e) Reddy, L.

1.2.2 Aminophenol Compounds as Efficient Ligands for Allyl Additions to N-Phosphinoyl Imines

In 2013, the Hoveyda group disclosed a new protocol for efficient and highly enantioselective allyl additions to *N*-phosphinoyl imines and isatin derivatives.[16] It was shown that an aminophenol ligand (Scheme 1.12, **1.46**), in the presence of methanol and a catalytic amount of base, could catalyze efficient allyl additions to imines and carbonyls utilizing allylboronic acid pinacol ester (allyl–B(pin), **1.45**) as an allyl source. The aminophenol was easily prepared (4 steps from commercially available materials) and highly modular. The high efficiency and enantioselectivity of this transformation is proposed to originate from the embedded proton in the active complex. As illustrated by transition state **1.51** (Scheme 1.12), the protonated ammonium group serves two key roles in the transformation. First, it renders the boron in the complex more Lewis acidic, which facilitates substrate binding and the subsequent C–C bond formation. Additionally, the proton serves as a second point of binding for the substrate, improving enantiotopic differentiation, rendering the transformation highly enantioselective.[17] Scheme 1.12 depicts that the method is not only amenable to aryl *N*-phosphinoyl imines, but that heteroaryl (**1.48**), alkyl (**1.49**) and alkenyl and alkynyl *N*-phosphinoyl imines also react

R.; Hu, B.; Prashad, M.; Prasad, K. *Org. Lett.* **2008**, *10*, 3109–3112; f) Takahashi, M.; McLaughlin, M.; Micalizio, G. C. *Angew. Chem. Int. Ed.* **2009**, *48*, 3648–3652; g) Feske, M. I.; Santanilla, A. B.; Leighton, J. L. *Org. Lett.* **2010**, *12*, 688–691; h) Liu, M.; Shen, A.; Sun, X.-W.; Deng, F.; Xu, M.-H.; Lin, G.-Q. *Chem. Commun.* **2010**, *46*, 8460–8462; i) Arena, G.; Zill, N.; Salvadori, J.; Girard, N.; Mann, A.; Taddei, M. *Org. Lett.* **2011**, *13*, 2294–2297; j) Guo, T.; Song, R.; Yuan, B.-H.; Chen, X.-Y.; Sun, X.-W.; Lin, G.-Q. *Chem. Commun.* **2013**, *49*, 5402–5404; k) Soares de Rogo Barros, O.; Sirvent, J. A.; Foubelo, F.; Yus, M. *Chem. Commun.* **2014**, *50*, 6898–6901.

(16) Silverio, D. L.; Torker, S.; Pilyugina, T.; Vieira, E. M.; Snapper, M. L.; Haeffner, F.; Hoveyda, A. H. *Nature* **494**, 216–221.

(17) For a full account of the intricacies of this transformation, see ref. (16).

efficiently and with high enantioselectivity. In the same report, the method was also expanded to another class of substrates, isatins. Isatins were chosen due to that fact that the carbonyl of the amide moiety could also interact with the proton on the aminophenol-boron complex, once again engendering a second point of binding. Scheme 1.12 shows that indeed, **1.50** was also synthesized in high enantioselectivity. We have since found that this catalyst system is amenable to the allylation and allenylation of a variety of other electrophiles, such as methyl ketones, trifluoromethyl ketones, and Boc-protected imines).[18]

Scheme 1.12. Initial Disclosure of Aminophenol Catalyzed Allyl Additions

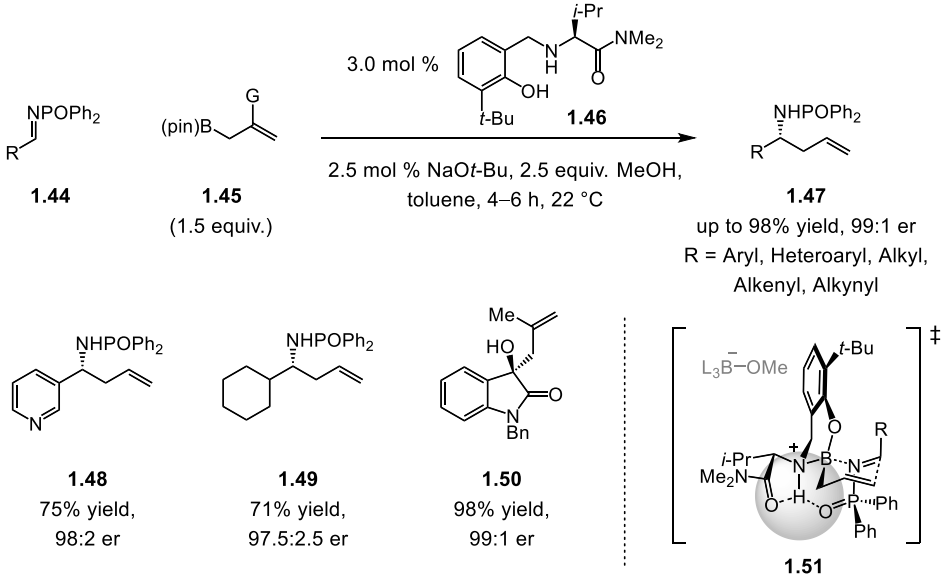

One of the most exciting features of this protocol, however, is its regioselectivity. When the reaction was carried out with deuterated allyl–B(pin) (***d*₂-1.45**, Scheme 1.13) we discovered that the reaction proceeded with exceptional α selectivity. Which is to say that

(18) (a) Wu, H.; Haeffner, F.; Hoveyda, A. H. *J. Am. Chem. Soc.* **2014**, *136*, 3780–3783. (b) Lee, K.; Silverio, D. L.; Torker, S.; Haeffner, F.; Robbins, D. W.; van der Mei, F. W., Hoveyda, A. H. *Nature Chem*. **2016**, *8*, 768–777. (c) Robbins, D. W.; Lee, K.; Silverio, D. L.; Volkov, A.; Torker, S.; Hoveyda, A. H. *Angew. Chem. Int. Ed.* **2016**, *55*, 9610–9614.

the carbon, which was initially attached to the boron atom of the allyl–B(pin) reagent, is the carbon involved in the C–C bond formation. This was a fascinating result, because in general allylation reactions proceed with C–C bond formation occurring from the γ-carbon of the allyl reagent. This discovery is what prompted us to propose the following α-selective catalytic cycle (Scheme 1.14).

Scheme 1.13. Regioselectivity of Aminophenol Promoted Allyl Additions to Imines

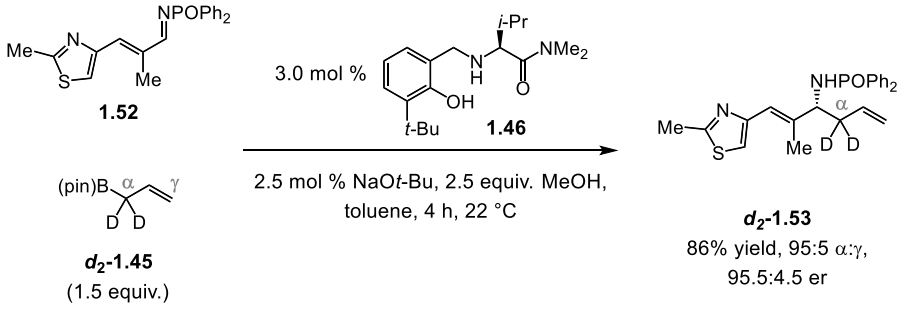

We proposed that, in the presence of aminophenol ligand, sodium *tert*-butoxide, and methanol, allyl–B(pin) can react to form a trace amount of complex **1.54** (Scheme 1.14). This chiral aminophenol-boron-methoxide complex could then undergo an allyl exchange with allyl–B(pin), as depicted in the transition state ***d*$_2$-1.55**. This allyl exchange would occur from the γ-carbon of the allyl–B(pin) reagent, generating the chiral aminophenol-boron-allyl complex ***d*$_2$-1.56**. The newly formed chiral allylboron is highly electrophilic and reactive due to the protonated amine moiety, facilitating substrate coordination and subsequent C–C bond formation, shown by transition state ***d*$_2$-1.58**. This process also occurs by a γ-addition, however due to the initial allyl exchange, this produces the net α-addition product ***d*$_2$-1.60**, after product release. Thus, the net α selectivity of the overall transformation is due two consecutive γ-addition events: 1) the initial allyl transfer (**1.54** → ***d*$_2$-1.56**) and 2) the allyl addition to the electrophile (***d*$_2$-1.56** → ***d*$_2$-1.59**).

Scheme 1.14. Proposed α-Selective Catalytic Cycle

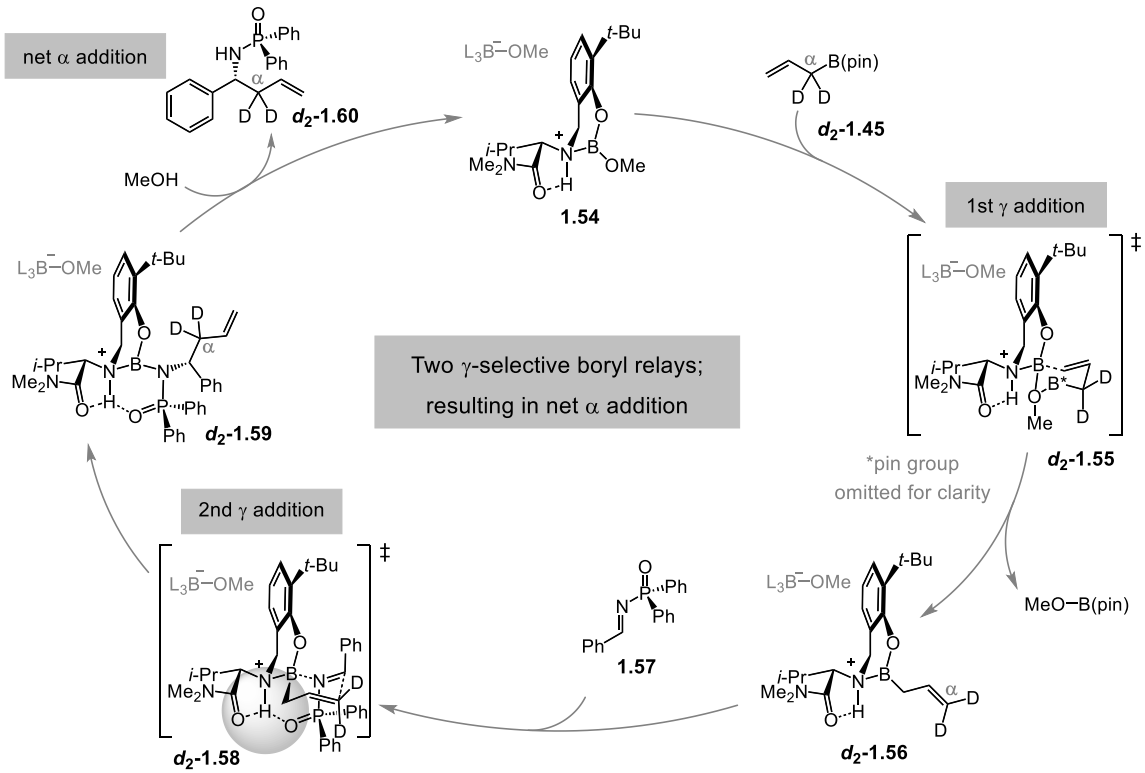

As alluded to in Scheme 1.15, this discovery led us to ask the following questions: What would the reaction outcome be if a γ-substituted allyl boron reagent, such as ***E*-1.61**, was used? Would the reaction be α-selective? Could we modify the reaction conditions, to achieve a net γ-addition, in order to access the branched product **1.63**? Would the transformation be efficient, regio-, diastereo-, and enantioselective?

Scheme 1.15. Accessing a Net γ-Addition Product

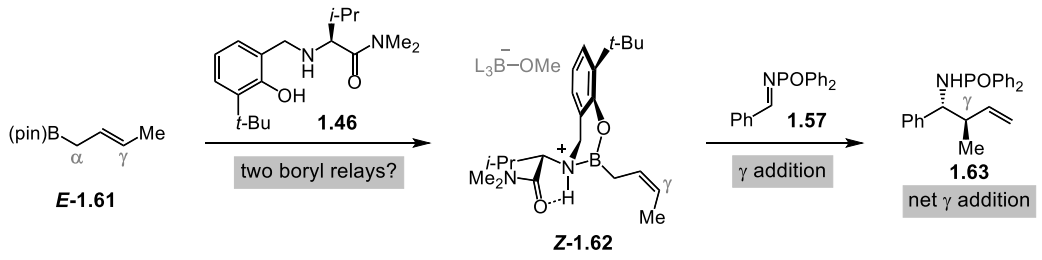

At this stage, our objective was to alter the α-selective catalytic cycle into a γ-selective transformation. Scheme 1.16 demonstrates how we envisioned this process to

occur. The catalytic cycle would again initiate from the chiral aminophenol-boron-methoxide complex **1.54**. Upon coordination of a substituted allyl–B(pin) (***Z*-1.61**, for example) and subsequent allyl exchange via transition state **1.64**, diastereomeric complex **1.65**, would be accessed. We envisioned that complex **1.65** could then undergo an intramolecular 1,3-borotropic shift by the means of transition state **1.66**, driven by the release of steric strain, to attain the linear olefin isomer of the aminophenol-boron-crotyl intermediate ***Z*-1.62**. Upon substrate coordination (**1.44**) with complex ***Z*-1.62**, C–C bond formation could occur through transition state **1.67**. After protonolysis of the N–B bond, the γ-addition product **1.68** would be produced. Whereas the previous α-selective cycle underwent two consecutive γ-addition events to access the α-addition product, the γ-selective pathway would undergo three γ-addition events to access the γ-addition product by the inclusion of a 1,3-borotropic shift (**1.65** → ***Z*-1.62**).

Scheme 1.16. Plausible γ-Selective Catalytic Cycle

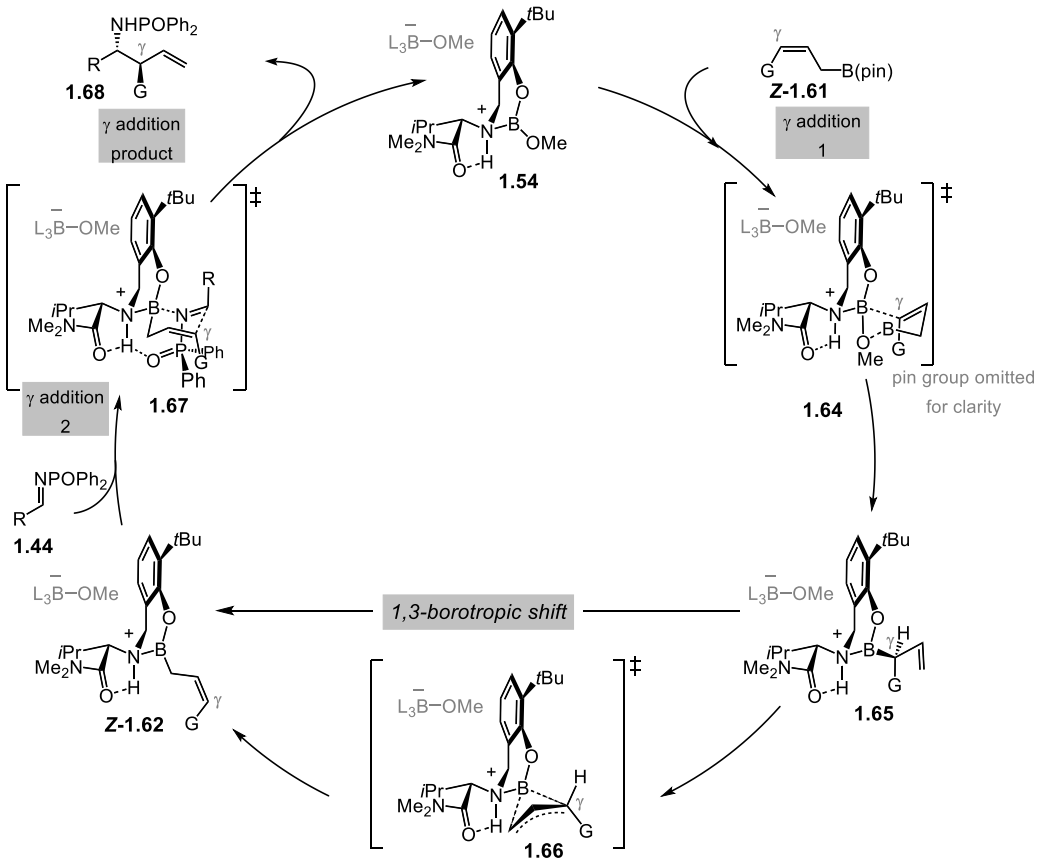

With this goal in mind, we set out to modify the reaction conditions in order to catalyze a 1,3-borotropic shift during the course of the reaction.

1.3. Borotropic Shift as a Means to Access the γ-Addition Product

Since early reports originating in the 1970's, 1,3-borotropic rearrangements, intermittently referred to as permanent allylic rearrangements, have been comprehensively examined and studied by several research groups.[19] Since the seminal reports on 1,3-

(19) For discussion on the mechanism of 1,3-borotropic rearrangement, see: a) Hancock, K. G.; Kramer, J. D. *J. Am. Chem. Soc.* **1973,** *95*, 6463–6465; b) Hancock, K. G.; Kramer, J. D. *J. Organomet. Chem.* **1974**, *64*, C29–C31; c) Henriksen, U.; Snyder, J. P.; Halgren, T. A. *J. Org. Chem.* **1981**, *46*, 3767–3768; d) Bühl,

borotropic shift, a vast number of experimental outcomes have been attributed to the occurrence of 1,3-borotropic rearrangements.[20] Due to the ability of 1,3-borotropic rearrangements to isomerize enantiomerically enriched stereocenters and even olefin geometry, Lachance and Hall have referred to borotropic rearrangements as the, "bane of stereoselective synthesis."[21] Although there have been numerous reports on 1,3-borotropic rearrangements, there have been no methods which have invoked them to access the desired regioisomer in a catalytic approach.

Scheme 1.17. Mechanism of 1,3-Borotropic Shift

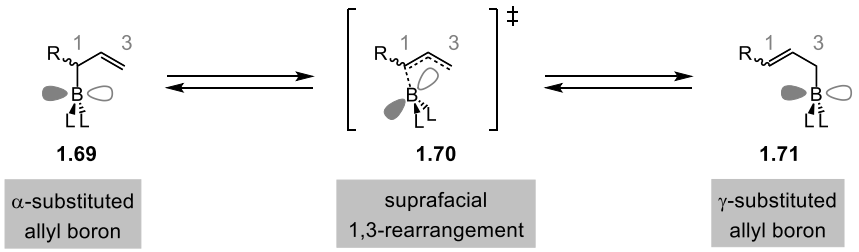

M.; Schleyer. P. v. R.; Ibrahim, M. A.; Clark, T. *J. Am. Chem. Soc.* **1991**, *113*, 2466–2471; e) Bubnov, Y. N.; Gurskii, M. E.; Gridnev, I. D.; Ignatenko, Y. A.; Ustynyuk, Y. A.; Mstislavsky, V. I. *J. Organomet. Chem.* **1992**, *424*, 127–132; f) Gridnev, I. D.; Gursky, M. E.; Bubnov, Y. N.; *Organometallics* **1996**, *15*, 3696–3702; g) Bubnov, Y. N.; *Pure Appl. Chem.* **1987**, *59,* 895–906; h) Choi, J. Y.; Kim, C. K.; Kim, C. K.; Lee, I. *J. Phys. Chem. A* **2002**, *106*, 5709–5715; i) Ess, D. H.; Kister, J.; Chen, M.; Roush, W. R. *Org. Lett.* **2009**, *11*, 5538–5541; j) Gurskii, M. E.; Belyakov, P. A.; Lyssenko, K. A.; Semenova, A. L.; Bubnov, Y. N. *Russian Chem. Bull. Int. Ed.* **2014**, *63*, 480–486.

(20) For examples of 1,3-borotropic rearrangement in synthetic methods, see: a) Zweifel G.; Horng A.; *Synthesis* **1973**, 672 – 674; b) Kramer, G. W.; Brown, H. C. *J. Organomet. Chem.* **1977**, *132*, 9–27; c) Zweifel, G.; Backlund, S. J.; Leung, T. *J. Am. Chem. Soc.* **1978**, *100*, 5561–5562; d) Brown, H. C.; Liotta, R.; Kramer, G. W. *J. Am. Chem. Soc.* **1979**, *101*, 2966–2970; e) Hoffmann, R. W.; Zeib, H.-J. *J. Org. Chem.* **1981**, *46*, 1309–1314; f) Wang, K. K.; Nikam, S. S.; Ho, C. D. *J. Org. Chem.* **1983**, *48*, 5376–5377; g) Brown, H. C.; Jadhav, P. K.; Bhat, K. S. *J. Am. Chem. Soc.* **1985**, *107*, 2564–2565; h) Brown, H. C.; Rangaishenvi, M. V.; Jayaraman, S. *Organometallics* **1992**, *11*, 1948–1954; i) Lombardo, M.; Morganti, S.; Tozzi, M.; Trombini, C. *Eur. J. Org. Chem.* **2002**, 2823–2830; j) Burgos, C. H.; Canales, E.; Matos, K.; Soderquist, J. A. *J. Am. Chem. Soc.* **2005**, *127*, 8044–8049; k) Gonzalez, A. Z.; Soderquist, J. A. *Org. Lett.* **2007**, *9*, 1081–1084; l) Canales, E.; González, A. Z.; Soderquist, J. A. *Angew. Chem. Int. Ed.* **2007**, *46*, 397–399; m) Fang, G. Y.; Aggarwal, V. K. *Angew. Chem. Int. Ed.* **2007**, *46*, 359–362; n) González, A. Z.; Román, J. G.; Alicea, E.; Canales, E.; Soderquist, J. A. *J. Am. Chem. Soc.* **2009**, *131*, 1269–1273; o) Chen, J. L.-Y.; Scott, H. K.; Hesse, M. J.; Willis, C. L.; Aggarwal, V. K. *J. Am. Chem. Soc.* **2013**, *135*, 5316–5319; p) Chen, M.; Roush, W. R. *J. Am. Chem. Soc.* **2013**, *135*, 9512–9517.

(21) Lachance, H.; Hall, D. G.; Allylboration of Carbonyl Compounds, in *Organic Reactions*, Denmark, S. E., Ed; Wiley: New York, **2009**; Vol. *73*, p 17.

The mechanistic nuances of 1,3-borotropic shift are fascinating as the rate of the rearrangement depends immensely on the ligands on the boron atom (L, Scheme 1.17). To understand the effect that the ligands have on 1,3-borotropic rearrangements one must first understand the mechanism by which this rearrangement proceeds. As illustrated in Scheme 1.17, the initial interaction of the rearrangement is the coordination of the π-bond of the olefin with the partially vacant *p*-orbital on the boron atom. This coordination, depicted in transition state **1.70** (Scheme 1.17), allows for the isomerization of the boron from C_1 to C_3, a thermodynamic process driven by the release of steric strain. This allows the boron to isomerize from the sterically crowded internal position (**1.69**) to the comparatively less crowded terminal position (**1.71**). This rearrangement has been proposed to be an intramolecular process in the seminal report by Hancock and co-workers.[19a]

Scheme 1.18. 1,3-Borotropic Shift Cross-Over Experiment

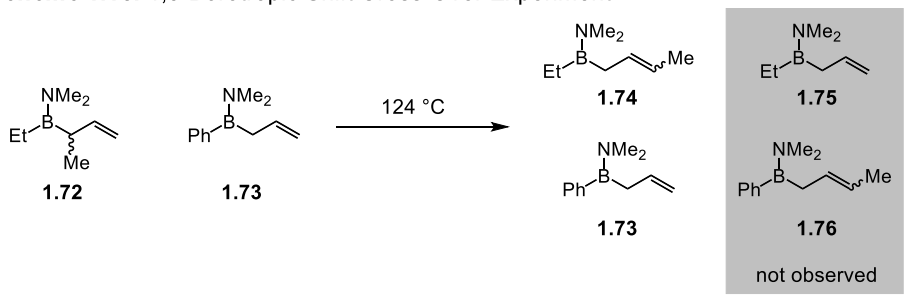

Hancock and co-workers carried out two key mechanistic probes in order to determine that 1,3-borotropic rearrangement is an intramolecular process. The first experiment that was carried out was a kinetic analysis of the thermal isomerization of but-1-en-3-yl-(dimethylamino)ethylborane (**1.72**, Scheme 1.18). In this analysis, Hancock and co-workers were able to conclude that the isomerization proceed with first-order kinetics, suggesting that the isomerization proceeds intramolecularly. In a second experiment (Scheme 1.18), Hancock and co-workers carried out a cross-over experiment between **1.72**

and **1.73**. If 1,3-borotropic shift occurs by an intermolecular mechanism, then the crossover products **1.75** and **1.76** should be observed. If products **1.75** and **1.76** are not detected after the isomerization, that would suggest that 1,3-borotropic shift is an intramolecular process. As Hancock and co-workers could not detect any of the cross-over products (**1.75** and **1.76**), it led them to conclude that borotropic shift occurs via an intramolecular mechanism. As the mechanism of 1,3-borotropic shift depends on the ability of the olefin to coordinate *p*-orbital of the boron atom, the importance of the ligand on boron becomes apparent (L, Scheme 1.17)

Scheme 1.19. Experimental and Calculated Barriers for 1,3-Borotropic Shifts

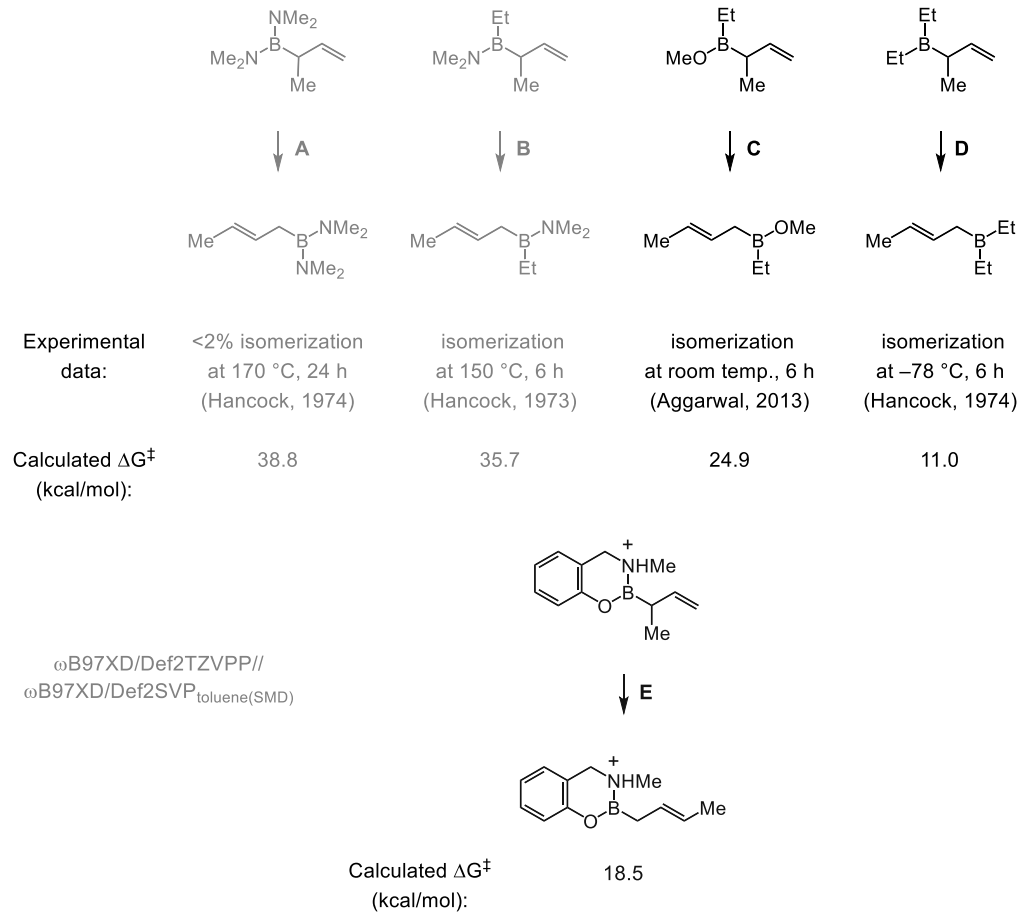

As shown in Scheme 1.19, we set out to compare several experimentally observed instances of 1,3-borotropic shift and the respective calculated barrier to the isomerization. As can be seen, compounds with highly electron donating ligands, such as the dimethylamino ligand (**A** and **B**, Scheme 1.19) undergo 1,3-borotropic shift extremely sluggishly (confirmed by the high calculated barrier to isomerization of 38.8 and 35.7 kcal/mol, respectively). Once one considers the mechanism by which 1,3-borotropic shift occurs this observation should seem evident. Since 1,3-borotropic shift initially proceeds by coordination of the alkene to the partially empty *p*-orbital on the boron, it follows that electron-donating ligands would hinder this coordination and subsequently hamper 1,3-borotropic shift. By utilizing allylboron compounds with less donating ligands, such as alkyl ligands (**C** and **D**, Scheme 1.19) 1,3-borotropic shifts become quite facile at room temperature, again supported by the lower calculated barriers to isomerization. To probe the feasibility of going through a 1,3-borotropic shift with a chiral aminophenol-boron-allyl complex, the barrier of the isomerization for a truncated system (**E**, Scheme 1.19) was calculated and shown to be 18.5 kcal/mol, a lower barrier than the barrier for an isomerization that has been shown to occur below room temperature (24.9 kcal/mol, **C**, Scheme 1.19). The data shown in Scheme 1.19 suggests that the rate of 1,3-borotropic shift depends greatly on the Lewis acidity of the boron atom. This led us to question if the addition of a Lewis acidic co-catalyst could facilitate the rate of 1,3-borotropic shift and subsequently invert the regioselectivity of aminophenol-promoted allyl additions from an α-selective process to a γ-selective process.

Scheme 1.20. Potential Modes of Activation by a Lewis Acid

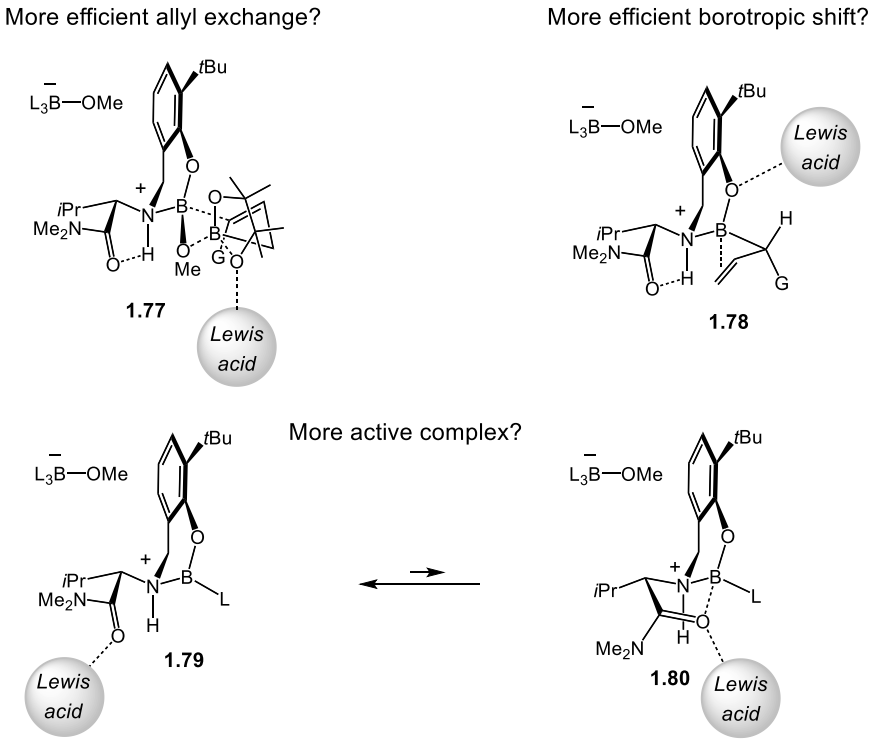

As depicted in Scheme 1.20, we envisioned various modes wherein a Lewis acidic co-catalyst could facilitate the desired transformation. For example, as has been proposed by various researchers, a Lewis acid could facilitate allyl transfer by coordination of the Lewis acid to the pinacolato oxygen of the B(pin) unit, as shown in transition state **1.77**.[22] This would render the boron more Lewis acidic, facilitating coordination with the chiral aminophenol-boron-methoxide complex and accelerating the initial allyl exchange. As has been alluded to earlier, we also wondered if the Lewis acid could chelate to the phenoxide oxygen of the chiral aminophenol-boron-allyl complex, rendering the boron more Lewis

(22) For reports where Lewis acid association with a B(pin) moiety has been proposed, see: a) Yamamoto, H.; Futatsugi K. *Angew. Chem. Int. Ed.* **2005**, *44*, 1924–1942; b) Rauniyar V.; Zhai, H.; Hall, D. G. *J. Am. Chem. Soc.* **2008**, *130*, 8481–8490; c) Barnett, D. S.; Moquist, P. N.; Schaus S. E. *Angew. Chem. Int. Ed.* **2009**, *48*, 8679–8682; d) Wang, H.; Jain, P.; Antilla, J. C.; Houk, K. N. *J. Org. Chem.* **2013**, *78*, 1208–1215.

acidic and promoting the 1,3-borotropic shift from the internal allyl boron to the terminal allyl boron. Lastly, during our computational studies of these aminophenol systems we located a potential resting state, complex **1.80**, where the amide carbonyl group coordinates to the boron atom. In this complex (**1.80**) the boron is coordinatively saturated, preventing the coordination of another allyl–B(pin) or the substrate and preventing the desired reaction. We hoped that the inclusion of a Lewis acidic co-catalyst could favor the coordinatively unsaturated boron complex, shown by complex **1.79**, allowing for the transformation to proceed efficiently. With these concepts in mind, we aimed to achieve a γ-selective crotyl addition to imines utilizing the aminophenol ligands developed in our laboratories.

1.4. Development of Aminophenol-Promoted Crotyl Additions to Phosphinoyl Imines

1.4.1 Initial Result for Crotyl Additions to Phosphinoyl Imines

Preliminary investigations into the development of crotyl additions to *N*-phosphinoyl imines commenced by subjecting benzaldehyde derived phosphinoyl imine **1.57** and *E*-crotyl–Boronic acid pinacol ester ***E*-1.61** (*E*-crotyl–B(pin)) to the optimal reaction conditions disclosed in our 2013 report.[16] The result of these studies, summarized in Scheme 1.21, show that there are several challenges that need to be overcome. It was found that under the aforementioned reaction conditions, the reaction sluggishly proceeded to 35% conversion, generating the product in 25:75 γ:α regioselectivity and moderate (88:12) diastereoselectivity.

Scheme 1.21. Initial Result for Crotyl Addition to Phosphinoyl Imines

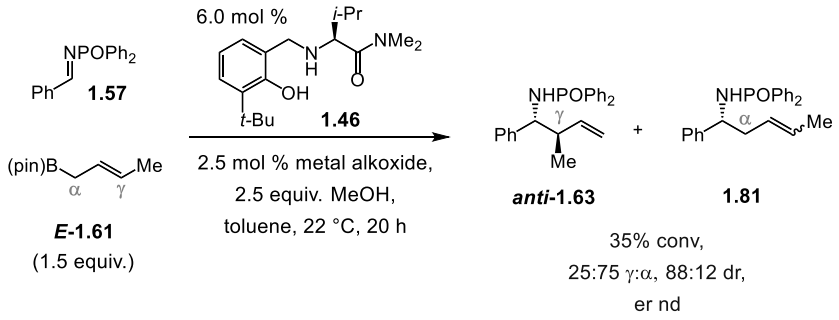

While the initial results were disappointing, the fact that 25% of the product was the branched isomer arising from γ-addition (***anti*-1.63**) was an exciting finding. What this result suggests is that indeed there is the possibility of catalyzing a 1,3-borotropic shift (as depicted in Scheme 1.16) in the transformation in order to access the γ-addition product. Nevertheless, in order to achieve a synthetically useful, efficient, and selective transformation, several issues needed to be addressed. While the low regioselectivity was clearly in need of improvement, the reaction efficiency was also very low. As was discussed earlier (Scheme 1.20), we hypothesized that perhaps by utilizing a more Lewis acidic metal alkoxide we could improve not only the reaction efficiency, but also accelerate the 1,3-borotropic shift and improve the regioselectivity for the γ-addition product.

1.4.2 Reaction Optimization through Lewis Acid Screening

Several metal salts and bases were examined, with the objective of finding a Lewis acidic co-catalyst. The results, summarized in Table 1.1, showed that organic bases such as 1,8-diazabicyclo[5.4.0]undec-7-ene (DBU, Table 1.1, entry 9) were ineffective in catalyzing an efficient transformation. Other metal alkoxides, including ytterbium(III) *iso*-propoxide, neodymium(III) *iso*-propoxide, strontium(II) *iso*-propoxide and magnesium(II)

tert-butoxide (entries 5–8), where found to have a modest influence on the efficiency and selectivity of the transformation.

Table 1.1. Lewis Acid Screening

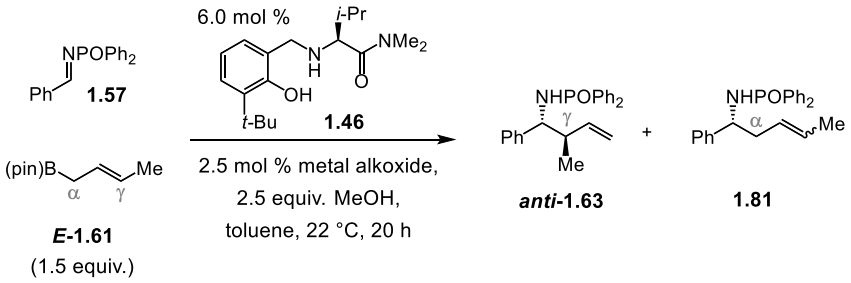

Entry	Base [mol %]	Conv. [%]; Yield [%]	γ:α	dr	er
1	NaO*t*-Bu [5.0]	35, ND	25:75	88:12	ND
2	$Zn(Ot\text{-}Bu)_2$ [2.5]	>98, 92	75:25	89:11	95:5
3	$ZnCl_2/Et_2O$ [2.5]	0, NA	NA	0, NA	0, NA
4	$ZnBr_2/Et_2O$ [2.5]	0, NA	NA	0, NA	0, NA
5	$Y(Oi\text{-}Pr)_3$ [2.5]	33, 3	60:40	88, 12	96:4
6	$Nd(Oi\text{-}Pr)_3$ [2.5]	54, 20	46:54	97, 3	97:3
7	$Sr(Oi\text{-}Pr)_2$ [2.5]	72, 5	54:46	87, 13	96:4
8	$Mg(Ot\text{-}Bu)_2$ [2.5]	31, 9	37:63	89, 11	97:3
9	DBU [2.5]	<10, ND	60:40	ND	ND
10	$Zn(Ot\text{-}Bu)_2$ [2.5] + NaO*t*-Bu [12.5]	>98, 81	54:46	92:8	96:4

However, the desired product, ***anti*-1.63**, was obtained in high enantioselectivity, regardless of the identity of the additive. Zinc(II) halides ($ZnCl_2$, and $ZnBr_2$, Table 1.1, entries 3 and 4) where found to be completely ineffective in catalyzing any crotyl addition. However, when zinc(II) *tert*-butoxide was added to the reaction, the transformation was found to proceed to complete conversion, while the regioselectivity was reversed, favoring the desired γ-addition product (75:25 γ:α). With this finding in hand, we turned to examine other zinc(II) salts in order to further optimize the reaction.

1.4.3 Zinc(II) Alkoxides as Competent Lewis Acidic Co-Catalysts

A variety of commercially available zinc(II) salts were obtained and examined under the reaction conditions, as summarized in Table 1.2. We found that zinc(II) salts that are too Lewis acidic, such as zinc(II) acetate, triflate or fluoride, were ineffective co-catalysts in this system (Table 1.2, entries 1–3) and furnished none of the desired product. Zinc(II) bis[bis(trimethylsilyl)amide] was found to be effective in improving the reaction efficiency, however the regioselectivity of the transformation was found to be lower than when zinc(II) *tert*-butoxide was used (entry 5, 69:31 γ:α vs. 75:25 with Zn(O*t*-Bu)$_2$).

Table 1.2. Zinc(II) salt screening

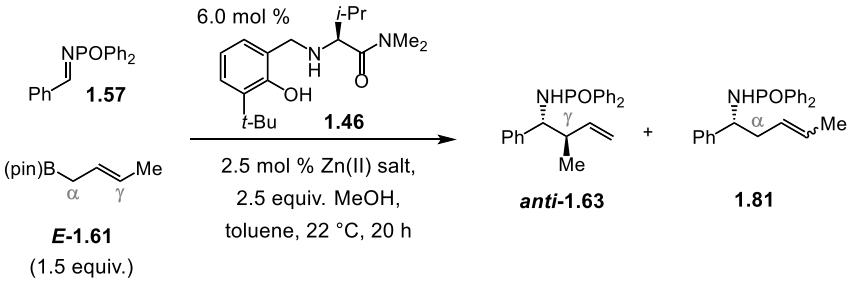

Entry	Zn salt	Conv. [%]; Yield [%];	γ:α	dr	er
1	none	<2; ND	NA	NA	NA
2	$Zn(OAc)_2$	<2; ND	NA	NA	NA
3	$Zn(OTf)_2/Et_2O$	<2; ND	NA	NA	NA
4	ZnF_2	<2; ND	NA	NA	NA
5	$Zn(hmds)_2$	>98; 88	69:31	95:5	94:6
6	Zn(O*t*-Bu)$_2$	>98; 83	75:25	89:11	95:5
7	$Zn(OMe)_2$	>98; 84	90:10	94:6	96:4

We rationalized that a larger Lewis acidic zinc salt would not be able to chelate as efficiently with the phenoxide arm of the crotyl-aminophenol-boron complex (as illustrated in Scheme 1.20, complex **1.78**). This could in turn hinder 1,3-borotropic shift, diminishing the γ selectivity of the transformation. Following this logic, we turned toward a smaller

zinc salt, zinc(II) methoxide. We found that indeed, with a smaller Zn salt, the reaction became more γ-selective allowing for the product to be obtained in 90:10 γ:α and high diastereo- and enantioselectivity (entry 7). After finding the optimal Lewis acidic co-catalyst we turned to determining the optimal aminophenol ligand.

1.4.4 Aminophenol Ligand Screening and Reaction Optimization

In the hopes of further improving the regioselectivity of the transformation, we turned to screening a variety of aminophenol ligands. With the aminophenol ligand that was previously found to be optimal for the allylation of *N*-phosphinoyl imines (**1.46**), we found that the desired product could be obtained in 84% yield with 90:10 γ:α, 94:6 diastereoselectivity, and 96:4 enantioselectivity. With the sterically larger, *tert*-leucine derived aminophenol ligands (**1.82** and **1.86**) the regioselectivity was slightly improved (96:4 and 97:3 γ:α, respectively), however, due to *tert*-leucine being an expensive, non-proteinogenic amino acid, we opted to use the valine-derived aminophenol ligands.

Scheme 1.22. Aminophenol Screening Data

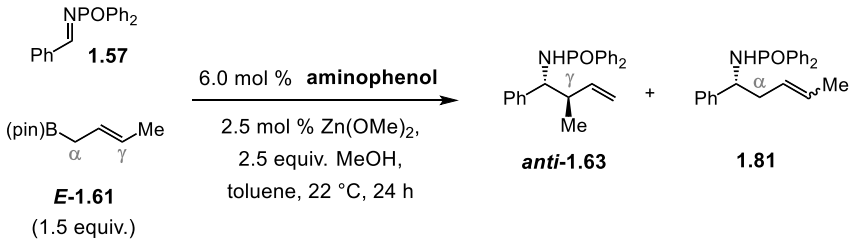

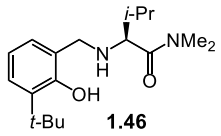

>98% conv, 84% yield,
90:10 γ:α, 94:6 dr,
96:4 er

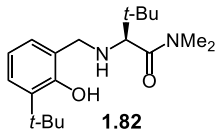

>98% conv, 84% yield,
96:4 γ:α, 94:6 dr,
96.5:3.5 er

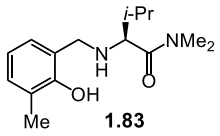

77% conv, 48% yield,
95:5 γ:α, 83:17 dr,
86:14 er

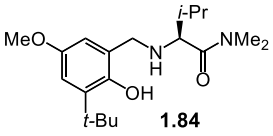

>98% conv, 84% yield,
84:16 γ:α, 90:10 dr,
94:6 er

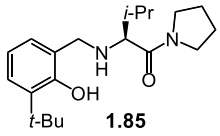

>98% conv, 90% yield,
92:8 γ:α, 97:3 dr,
97:3 er

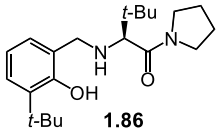

>98% conv, 88% yield,
97:3 γ:α, 95:5 dr,
99:1 er

Reducing the size of the substituent on the aryl ring from a *tert*-butyl unit to a methyl group (**1.83**) led to lower reaction efficiency and have a detrimental effect on the diastereo- and enantioselectivity of the transformation. Electronic modification of the aryl ring (**1.84**) was also found to have an adverse effect on the selectivity of the reaction. Notably there was a drastic reduction in the γ selectivity, which can be explained by the requirements for 1,3-borotropic shift. By utilizing a more electron-rich ligand, the Lewis acidity of the boron is reduced, hindering 1,3-borotropic shift from occurring efficiently. Lastly, modification of the amide group from a dimethyl-substituted amide to a pyrrolidine-substituted amide (**1.85**, Scheme 1.23) was found to induce a slight improvement in

selectivities (92:8 γ:α, 97:3 dr, and 97:3 er). We decided that aminophenol **1.85** was optimal and after a brief aminophenol and zinc methoxide loading optimization, we found that the product could be obtained with 95:5 regioselectivity, 96:4 diastereoselectivity, and 96:4 enantioselectivity (Scheme 1.24).

Scheme 1.24. Increased Reactivity and Regioselectivity with *Z*-Crotyl–B(pin)

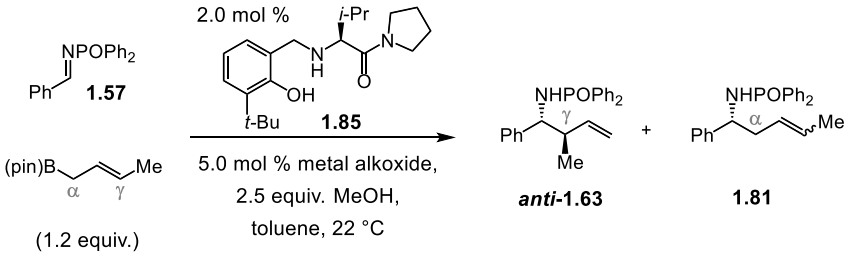

with ***E*-1.61**:
24 h
>98% conv, 83% yield,
95:5 γ:α, 96:4 dr,
96:4 er

with ***Z*-1.61**:
3 h
>98% conv, 87% yield,
>98:2 γ:α, 96:4 dr,
96:4 er

Notably, when we used *Z*-crotyl–B(pin) (***Z*-1.61**) in the reaction, it was found that the transformation occurred much more efficiently (3 h, vs. 24 h with ***E*-1.61**). Even more fascinating was the fact that regardless of the stereoisomer of the crotylboron reagent used, we only obtained the *anti* diastereomer of the product, an outcome which will be discussed in detail below.

Scheme 1.25. Rationale for Diminished Efficiency with *E*-crotyl–B(pin)

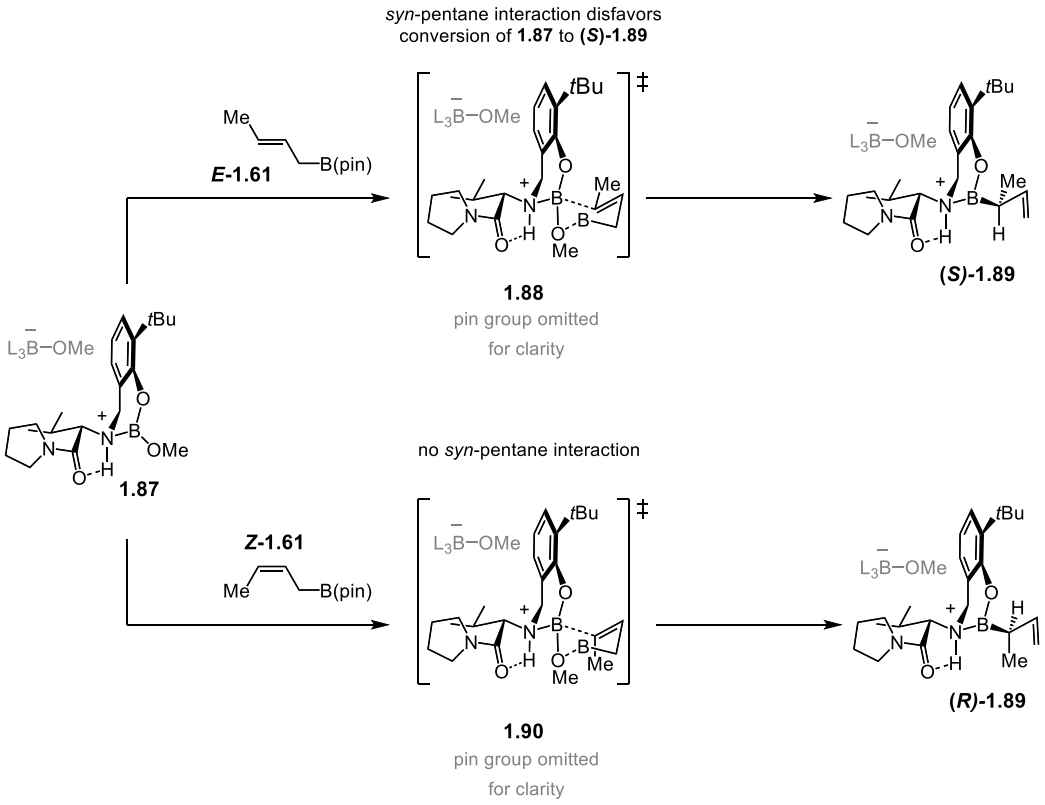

To explain the increased efficiency of the *Z*-crotyl–B(pin) reagent, one must consider the transition states for the allyl transfer. As illustrated in Scheme 1.25, in the transition state for the allyl transfer when ***E*-1.61** is used (transition state **1.88**, Scheme 1.25), the methyl group of the crotyl boron reagent results in a *syn*-pentane interaction with the aminophenol ligand. This steric interaction greatly increases the barrier for this allyl transfer, causing the decrease in reaction efficiency. However, when ***Z*-1.61** is used there is no such steric interaction in the transition state (transition state **1.90**).

1.4.5 Scope of the Method

With the optimal conditions in hand (*Z*-crotyl–B(pin), 2.0 mol % **1.85**, 5.0 mol % $Zn(OMe)_2$, 2.5 equivalents of methanol) we set out to show the broad applicability of the protocol. We found that *ortho*-substituted substrates (Scheme 1.26, **1.91**–**1.94**) were tolerated, with only a slight decrease in diastereoselectivity. *Meta*-substituted aryl substrates also reacted with no substantial effect on the regio-, diastereo- and enantioselectivity of the transformation (**1.95** and **1.96**). Electron rich substrates, such as *para*-methoxyphenyl substituted *N*-phosphinoyl imine (**1.97**), reacted with high regio-, diastereo- and enantioselectivity (98:2, 94:6, and 93:7, respectively). However, the very Lewis basic *para*-dimethylaniline-derived phosphinoyl imine (**1.98**) reacted sluggishly and with low enantioselectivity (80:20 er). We propose that this may be due to the ability of the Lewis basic amine group to sequester the zinc(II) salt, perhaps allowing non-selective pathways to more effectively compete with the enantioselective pathway.

Scheme 1.26. Aryl Phosphinoyl Imines in the Catalytic, Enantioselective Approach

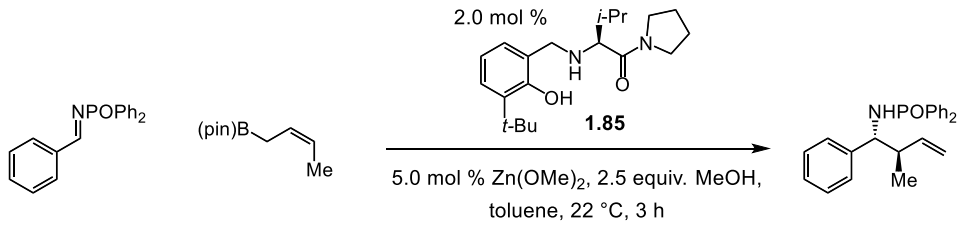

1.57 | ***Z*-1.61** (1.2 equiv.) | **1.63** 87% yield, >98:2 γ:α, 96:4 dr, 96:4 er

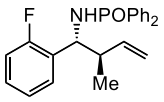

1.91
80% yield, 96:4 γ:α,
93.5:6.5 dr, 98:2 er

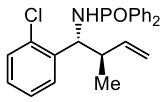

1.92
84% yield, 98:2 γ:α,
90:10 dr, 99:1 er

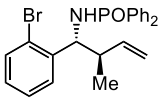

1.93
92% yield, 95:5 γ:α,
92:8 dr, 98:2 er

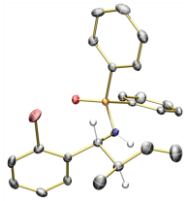

X-ray of **1.93**

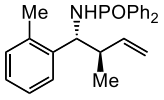

1.94[a]
89% yield, >98:2 γ:α,
92:8 dr, 94:6 er

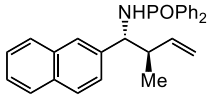

1.95
92% yield, 97:3 γ:α,
93:7 dr, 95:5 er

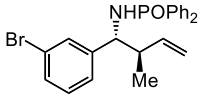

1.96
88% yield, >98:2 γ:α,
92:8 dr, 96:4 er

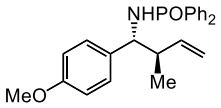

1.97
94% yield, 98:2 γ:α,
94:6 dr, 93:7 er

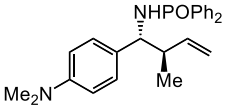

1.98[b]
75% yield, >98:2 γ:α,
91.5:8.5 dr, 80:20 er

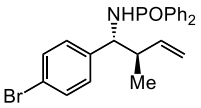

1.99
92% yield, >98:2 γ:α,
94:6 dr, 97.5:2.5 er

gram scale

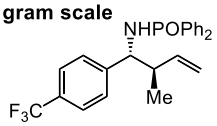

1.100
96% yield, >98:2 γ:α,
92.5:7.5 dr, 99:1 er

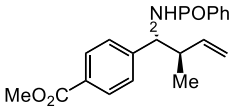

1.101
86% yield, >98:2 γ:α,
91:9 dr, 97:3 er

[a] 5.0 mol % **1.85.** [b] Reaction time: 24 h.

Electronically deactivated imines, such as *para*-bromophenyl (**1.99**), *para*-trifluoromethylphenyl (**1.100**), or *para*-methyl ester-phenyl substituted imines reacted well, generating products in high yield and high regio-, diastereo-, and enantioselectivity. The reaction with *para*-trifluoromethyl substituted *N*-phosphinoyl imine **1.100** was also

carried out on gram scale, with no erosion in the selectivities, demonstrating the scalability of the method.

Scheme 1.27. Scope of the Protocol for Heteroaromatic Substrates

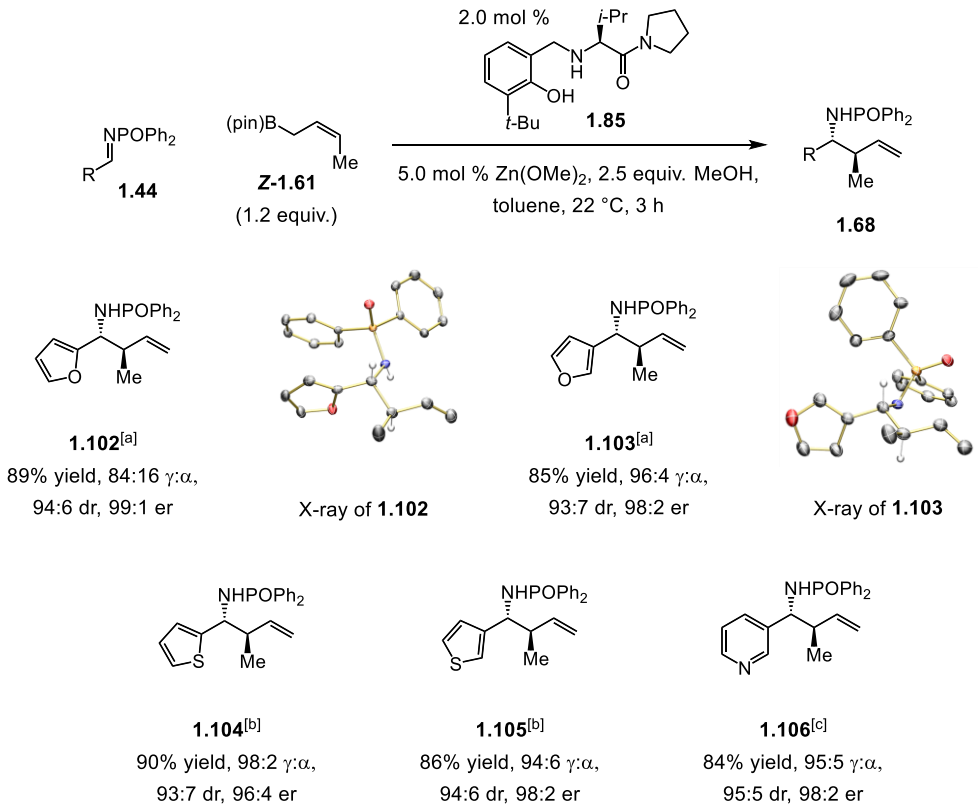

[a] Reaction time: 5 h. [b] Reaction time: 4 h.
[c] With 10 mol % **1.85** and 10 mol % $Zn(OMe)_2$ after 8 h.

As shown in Scheme 1.27, hetero-aromatic substrates such as 2-furyl (**1.102**), 3-furyl (**1.103**), 2-thienyl **(1.104**), and 3-thienyl **(1.105**) substituted imines reacted efficiently and with high selectivities, though slightly longer reaction times were required to achieve full conversion of the starting materials (4 h for furyl imines and 5 h for thienyl imines). 3-Pyridyl substituted imine **1.106** was synthesized in 95:5 regioselectivity, 95:5 diastereoselectivity and 98:2 enantioselectivity, however higher catalyst loadings and reaction times were required (10 mol % **1.85**, 10 mol % $Zn(OMe)_2$, 8 h), likely due to the ability of the pyridine to chelate with and subsequently sequester the zinc additive. While

we found that the method was broadly applicable to a wide variety of aryl and hetero-aryl substrates, we quickly found that the same was not true for alkenyl and alkyl substrates, as depicted in Scheme 1.28.

Scheme 1.28. Crotyl Additions to Non-Aromatic Electrophiles

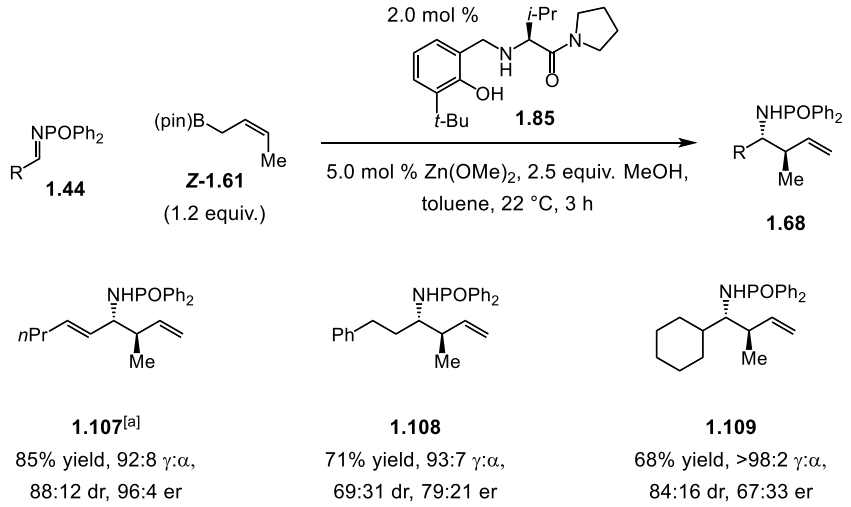

[a] With 12.5 mol % **1.85** and 7.5 mol % $Zn(OMe)_2$.

Trans-hexenal derived phosphinoyl amine (**1.107**) was synthesized in 85% yield, good regioselectivity (92:8 γ:α), moderate diastereoselectivity (88:12 dr) and high enantioselectivity (96:4 er). However, to achieve these levels of selectivity high catalyst and zinc methoxide loadings were required (12.5 mol % and 7.5 mol %, respectively. However, when alkyl imines were employed in the reaction, such as the parent imines of **1.108** and **1.109**, the products were isolated with extremely poor diastereo- and enantioselectivity. We believe that these low selectivities stem from the ability of these substrates to undergo tautomerization to their enamine form. This tautomerization is capable of scrambling the imine from an *E*-imine to a Z/*E* mixture of imine, which affects which enantiotopic face of the imine the crotyl group adds to, eroding the diastereo- and

enantioselectivity of the reaction.[23] To date, there are still no catalytic, enantioselective protocols which can access these crotyl addition products with high diastereo- and enantioselectivities. Scheme 1.29 highlights that the method is not only useful for a variety of *N*-phosphinoyl imines, it is also amenable to a variety of substituted allyl boron reagents.

Scheme 1.29. Additions Utilizing Various Substituted Allyl Boron Reagents

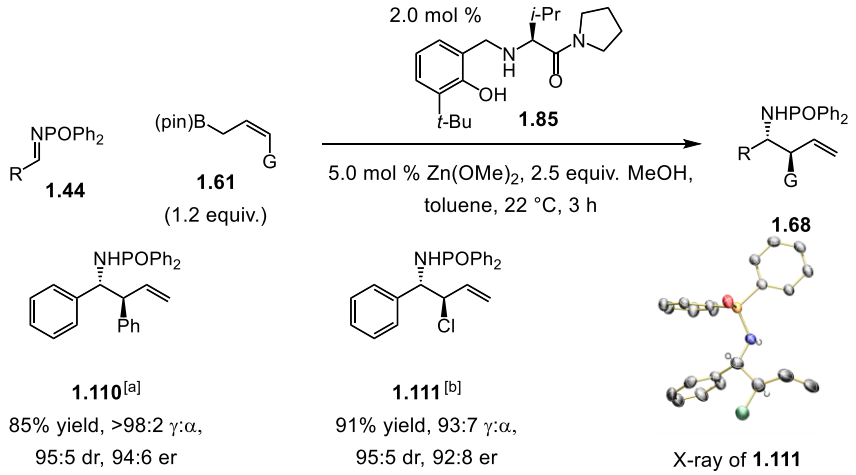

(>98% *E* for phenyl-substituted allylboronate and >98% *Z* for the Cl-substituted allylboronate)
[a] At 50 °C, after 6 h. [b] With 10 mol % **1.85** and 10 mol % $Zn(OMe)_2$ after 24 h.

The *E*-phenyl-substituted allyl boron reagent, easily synthesized through a palladium-catalyzed boryl addition allyl chlorides[24], required elevated temperatures (50 °C) to react with the phosphinoyl imine, however the product was isolated with high diastereoselectivity and enantioselectivity (**1.110**, 95:5 dr, 94:6 er). *Z*-Chloro-substituted allyl–B(pin), readily accessible in one step utilizing *Z*-selective cross-metathesis[25], could also be added to a phosphinoyl imine, producing α-chloro amine **1.111** in 91% yield with high diastereo- and good enantioselectivity (95:5 and 92:8, respectively).

---

(23) Whereas we have observed some formation of the *Z*-imine during substrate synthesis, we have not been able to detect isomerization of the imine *in situ* by ^{1}H NMR spectroscopy. This could be due to the fact that the *Z*-imine is formed in low concentrations and immediately consumed.
(24) Zhang, P.; Roundtree, I. A.; Morken, J. P. *Org. Lett*. **2012**, *14*, 1416–1419.
(25 Koh, M. J.; Nguyen, T. T.; Zhang, H.; Schrock, R. R.; Hoveyda, A. H. *Nature* **2016**, *531*, 459–465.

1.5. Mechanistic Implications in the Aminophenol-Promoted Crotyl Additions to Phosphinoyl Imines

During the optimization of the reaction conditions we observed the peculiar result that both *E*- and *Z*-crotyl–B(pin) produced the same *anti*-diastereomer of the product, as depicted in Scheme 1.30. This was highly unexpected since, generally, when crotyl reagents are used and C–C bond formation occurs *via* a closed, six-membered ring transition state, each olefin isomer should produce a different diastereomer of the product.

Scheme 1.30. *E*- and *Z*-Crotyl–B(pin) Reagents Produce the Same Diastereomer

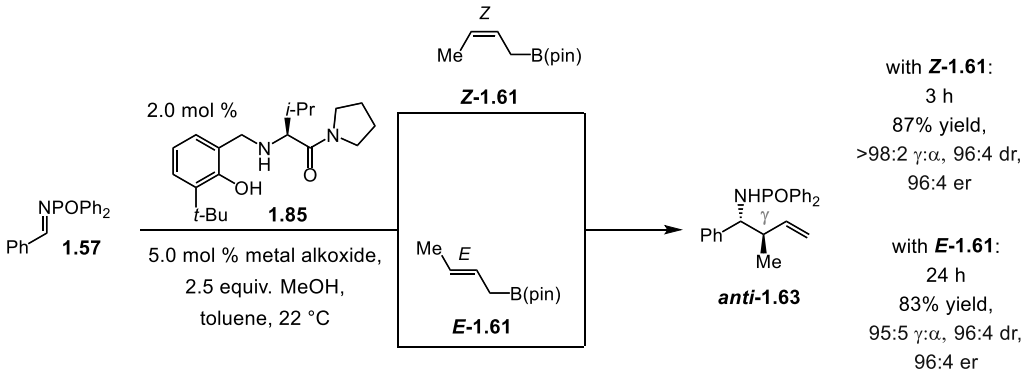

This experimental outcome could arise from several distinct possibilities. One possibility could be that, under the reaction conditions, the crotylboron starting materials could be isomerizing to the same olefin isomer. However, ^{1}H NMR analysis of the reaction mixture over the course of the reaction showed no discernible isomerization of the starting materials. A second possibility could be that the initial allyl transfer from the starting materials onto the chiral aminophenol-boron-methoxide complex (Scheme 1.16, **1.54** → **1.65**) is not stereospecific, i.e. *E*- and *Z*-crotyl–B(pin) undergo the allyl transfer in such a way that the same diastereomeric intermediate (**1.65**) is produced. However, in our initial report on aminophenol-promoted allylation reactions we found that when a chiral

allylboron reagent is used, the stereochemistry is retained during the course of the reaction, suggesting that the allyl transfer is indeed stereospecific.[16]

Scheme 1.31. Stereospecific Allyl Transfer for *E*- and *Z*-crotyl–B(pin) Reagents

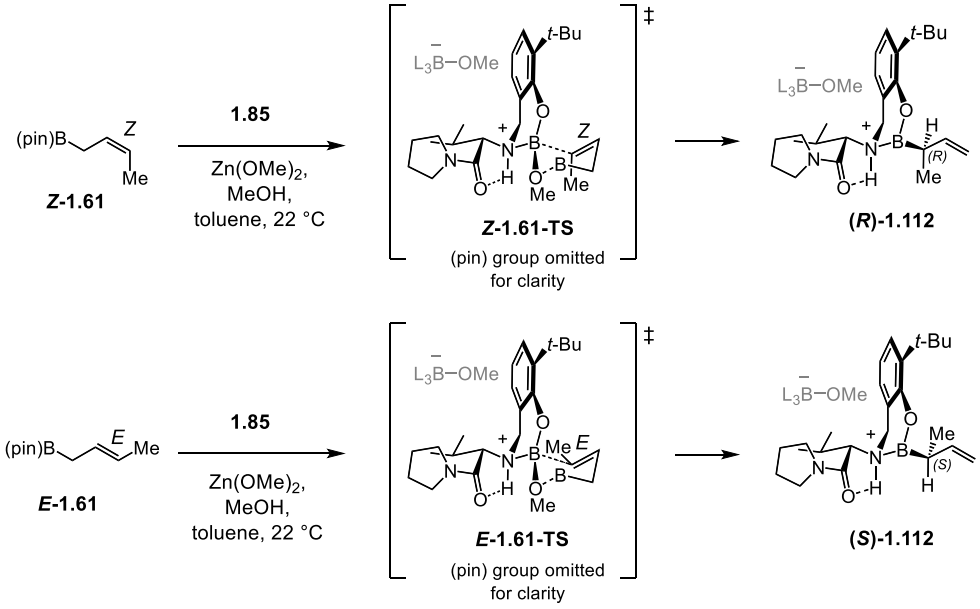

As shown in Scheme 1.31, there are two diastereomeric intermediates (**(*R*)-1.112** and **(*S*)-1.112**) that are formed when *Z*- and *E*-crotyl–B(pin) are used in the reaction. When ***Z*-1.61** is subjected to the reaction conditions (catalytic aminophenol **1.85**, $Zn(OMe)_2$ and methanol), it associates with the aminophenol-boron-methoxide complex as shown in transition state ***Z*-1.61-TS**, this closed, six-membered ring transition state allows for a stereospecific allyl transfer, generating the diastereomeric aminophenol-boron-allyl complex **(*R*)-1.112**. An analogous process is proposed when ***E*-1.61** is used, generating the other diastereomeric complex, **(*S*)-1.112**. Now the question becomes, how do these two diastereomeric intermediates react to yield the same product? The three possible mechanistic scenarios are demonstrated in Scheme 1.32.

Scheme 1.32. Potenial Mechanistic Scenarios

A Could the Reaction be Under Curtin-Hammett Control?

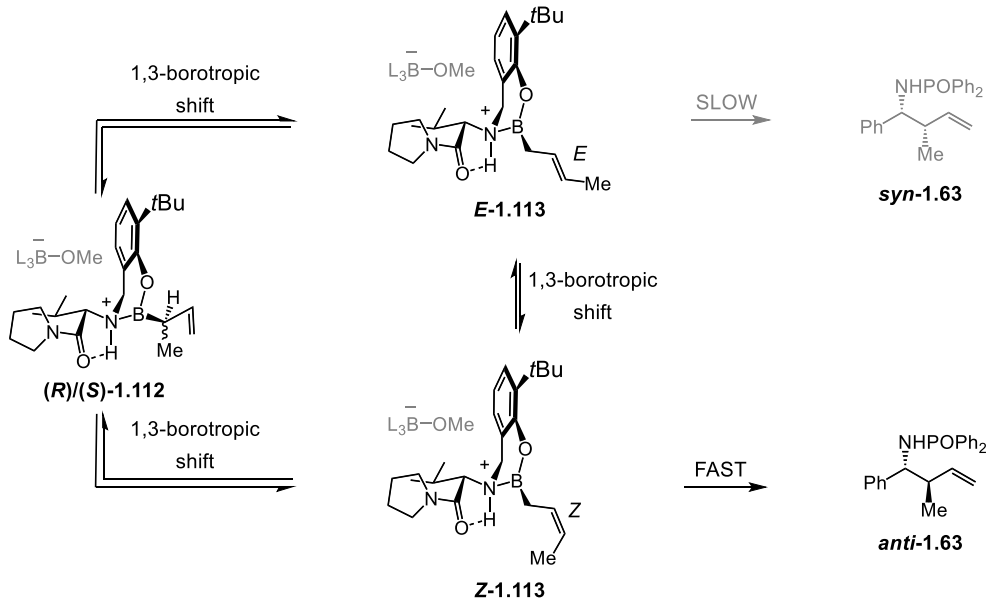

B Could the Chiral *E*- and *Z*- Crotyl Boron React by Different Transition States?

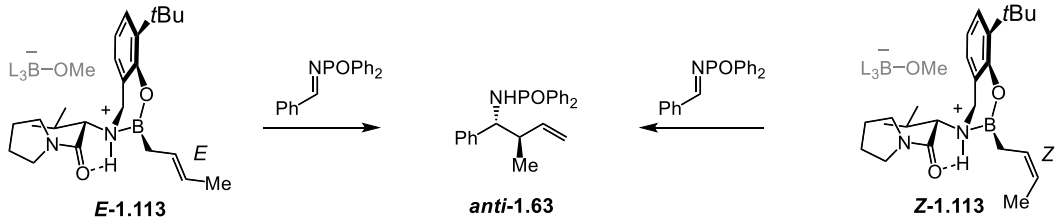

C Could the 1,3-Borotropic Shift be a Stereoconvergent Process?

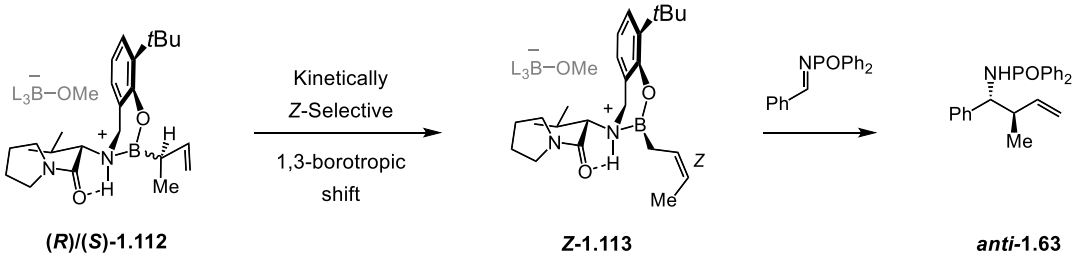

One plausible explanation is that the transformation is under Curtin-Hammett control, wherein the 1,3-borotropic shift is so facile that these intermediates could interconvert rapidly, shown in **A**, Scheme 1.32. In this case ***E*-1.113** and ***Z*-1.113**, generated from a 1,3-borotropic shift of intermediate **1.112**, can rapidly interconvert through

successive 1,3-borotropic shifts. This allows the product distribution to be determined by the energy difference between the transition states leading to ***syn*-1.63** and ***anti*-1.63**. In this situation one would observe a single product regardless of which starting material was used. A second plausible scenario would be that ***E*-1.113** and ***Z*-1.113** simply react through different transition states which generate the same diastereomer of product, as shown in **B**, Scheme 1.32. For example, if ***Z*-1.113** reacted through a chair transition state while ***E*-1.113** reacted through a boat transition state, then the same product would be generated.[26] The last possible scenario is shown in **C**, Scheme 1.32. In this plausible scenario **(*R*)-1.112** and **(*S*)-1.112** undergo 1,3-borotropic way in a kinetically *Z*-selective fashion, causing these two diastereomeric intermediates to converge to the same, linear chiral aminophenol-boron-crotyl complex, ***Z*-1.113**. To rule out scenarios **A** and **B**, we devised the mechanistic probe shown in Scheme 1.33. The hypothesis was that if we used α-substituted allylboron reagent, *rac*-**1.114**, that after the initial allyl transfer we would generate a mixture of ***Z*-1.113** and ***E*-1.113**. If scenarios **A** or **B** are operative we would still expect the product to be synthesized with high diastereoselectivity. If the product was of low diastereoselectivity, then we could conclude that ***E*-1.113** and ***Z*-1.113** cannot rapidly interconvert through successive 1,3-borotropic shifts (scenario **A**) and that ***E*-1.113** and ***Z*-1.113** do not react through distinct transition states to access the same diastereomer (scenario **B**).

(26) Preliminary DFT calculations suggest that, for this system, the chair transition state is always lower in energy than the boat transition state, regardless of *E*/*Z* geometry of the intermediate, making this scenario unlikely. These calculations also suggest that the *E*-intermediate would preferentially react to form the *syn* diastereomer of the product.

Scheme 1.33. Probing the Reaction Pathway with α-Methyl-Allyl–B(pin)

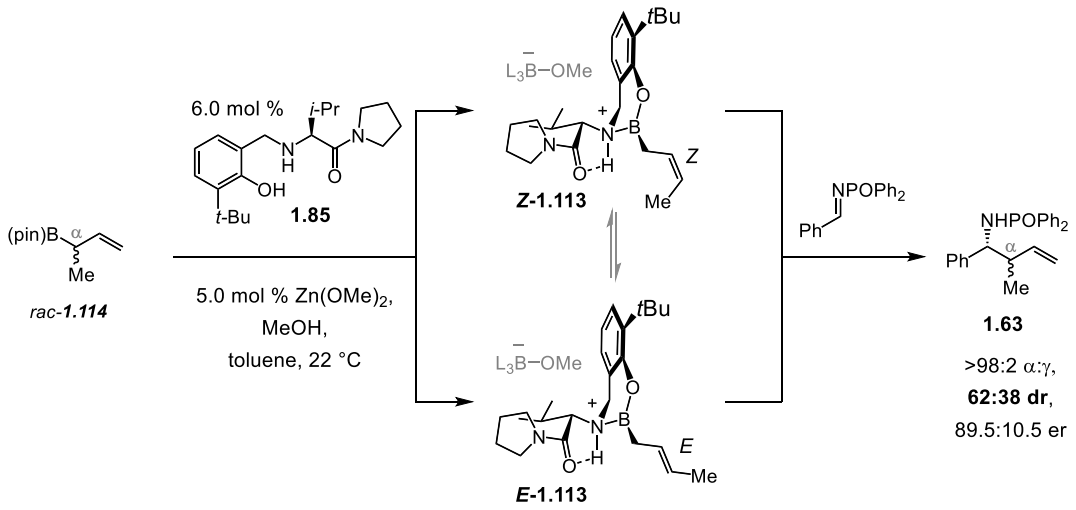

When we subjected *rac*-**1.114** to the reaction conditions we found that the product was isolated with complete regioselectivity for the branched isomer. However, the diastereoselectivity of the transformation was found to be extremely low (62:38). This allowed us to rule out scenarios **A** and **B** from being operative. These findings suggest that *Z*- and *E*-crotyl–B(pin) produce the same product as a result of the 1,3-borotropic shift isomerizing **(*R*)-1.112** and **(*S*)-1.112** to a common intermediate, ***Z*-1.113**, which reacts with the phosphinoyl imine to produce ***anti*-1.63**. The rationale for how this isomerization is kinetically *Z*-selective can be found in Scheme 1.34.

Scheme 1.34. Rationale for the Kinetic *Z* Selectivity in the 1,3-Borotropic Shift

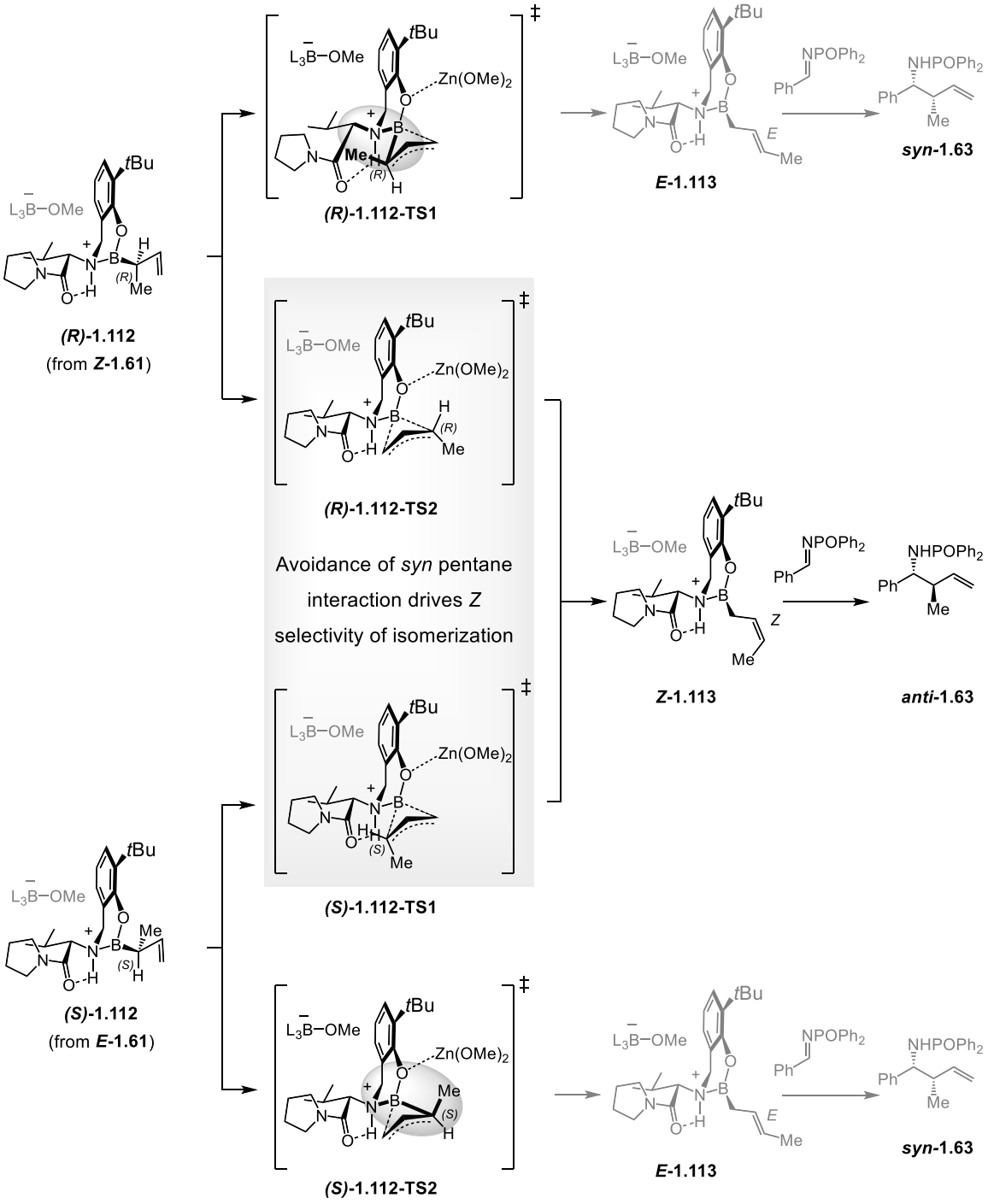

To summarize the rationale in Scheme 1.34, we propose that **(*R*)-1.112** and **(*S*)-1.112** undergo 1,3-borotropic shift in a manner where the methyl substituent is pointed away from the complex backbone, as shown in **(*R*)-1.112-TS2** and **(*S*)-1.112-TS1**. The

driving force for this mode of isomerization becomes evident when one considers the alternative transition states for the isomerization. As shown in transition states **(*R*)-1.112-TS1** and **(*S*)-1.112-TS2** (Scheme 1.34), isomerization occurring with the methyl group pointed towards the backbone of the complex, generates a *syn*-pentane interaction. To avoid this steric penalty, the isomerization occurs with the methyl group pointed away from the backbone of the complex, generating ***Z*-1.113** regardless of which diastereomeric intermediated was formed during the course of the reaction ((***R*)-1.112** and **(*S*)-1.112**).

1.6. Conclusions

Through mechanistic understanding of the aminophenol-promoted allylation reaction, in addition to the factors involved in 1,3-borotropic shifts, we were able to develop a highly efficient, regio-, diastereo-, and enantioselective crotyl addition to *N*-phosphinoyl imines. By finding an appropriate Lewis acidic co-catalyst we were able to greatly enhance the reaction efficiency as well as completely reverse an α-selective transformation to a γ-selective reaction by enabling a kinetically *Z*-selective 1,3-borotropic shift within the catalytic cycle. Additionally, this protocol is represents the only catalytic, enantioselective method which constructively utilizes a 1,3-borotropic shift as a means to access the desired regioisomer of the product to date. Future work has included adapting the newly discovered catalytic system to other substrate and reagent classes, such as alkoxy-substituted allyl–B(pin) reagents. These studies have also served as a platform for future studies on additions of substituted allylboron species with aminophenol ligands.

1.7. *Experimental Section*

1.7.1. *General*

Infrared (IR) spectra were recorded on a Bruker FT-IR Alpha (ATR mode) spectrophotometer, ν_{max} in cm^{-1}. Bands are characterized as broad (br), strong (s), medium (m), and weak (w). ^{1}H NMR spectra were recorded on a Varian Unity INOVA 400 (400 MHz) or 600 (600 MHz) spectrometer. Chemical shifts are reported in ppm from tetramethylsilane with the solvent resonance as the internal standard ($CDCl_3$: δ 7.26 ppm). Data are reported as follows: chemical shift, integration, multiplicity (s = singlet, d = doublet, t = triplet, q = quartet, br s = broad singlet, m = multiplet, app. = apparent), and coupling constant (Hz). ^{13}C NMR spectra were recorded on a Varian Unity INOVA 400 (100 MHz) or 600 (150 MHz) spectrometer with complete proton decoupling. Chemical shifts are reported in ppm from tetramethylsilane with the solvent resonance as the internal standard ($CDCl_3$: δ 77.16 ppm). High-resolution mass spectrometry was performed on a JEOL AccuTOF DART (positive mode) at the Mass Spectrometry Facility, Boston College. Enantiomeric ratios were determined by high-performance liquid chromatography (HPLC) with a Shimadzu chromatograph (Chiral Technologies Chiralpak AZ-H (4.6 x 250 mm), Chiralcel OZ-H (4.6 x 250 mm), Chiralpak AD-H (4.6

x 250 mm)) in comparison with authentic racemic materials. Optical rotations were measured on a Rudolph Research Analytical Autopol IV Polarimeter. Unless otherwise noted, all reactions were carried out with distilled and degassed solvents under an atmosphere of dry N_2 in oven- (135 °C) or flame-dried glassware with standard dry box or vacuum-line techniques. Solvents were purified under a positive pressure of dry argon by a modified Innovative Technologies purification system: toluene, benzene and hexanes were purified through a copper oxide and alumina column; CH_2Cl_2 and Et_2O were purged with Ar and purified by passage through two alumina columns. Tetrahydrofuran (Aldrich Chemical Co.) was purified by distillation from sodium benzophenone ketyl immediately prior to use unless otherwise specified. All work-up and purification procedures were carried out with reagent grade solvents (purchased from Fisher) in air.

Reagents:

***d*$_2$-Allylboronic acid pinacol ester** was prepared according to a previously reported procedure.[1]

Aminophenol catalysts were prepared according to previously reported procedures.[2]

(1) Sieber, J. D.; Morken, J. P. *J. Am. Chem. Soc.* **2008**, *130*, 4978–4983.

(*Z*)-2-(3-Chloroallyl)-4,4,5,5-tetramethyl-1,3,2-dioxaborolane was prepared according to a newly reported procedure.[3]

2-Cinnamyl-4,4,5,5-tetramethyl-1,3,2-dioxaborolane was prepared according to a previously reported procedure.[4]

(*E*)-Crotylboronic acid pinacol ester was purchased from Aldrich Chemical Co. and used as received.

(*Z*)-Crotylboronic acid pinacol ester was purchased from Aldrich Chemical Co. and used as received.

Magnesium(II) *tert*-butoxide was purchased from Alfa Aesar and used as received.

Methanol (extra dry over molecular sieves) was purchased from Acros organics and distilled over magnesium turnings.

α-Methyl allylboronic acid pinacol ester was prepared according to a previously reported procedure.[5]

---

(2) Silverio, D. L.; Torker, S.; Pilyugina, T.; Vieira, E. M.; Snapper, M. L.; Haeffner, F.; Hoveyda, A. H. *Nature* **2013**, *494*, 216-221.

(3) Koh, M.J.; Nguyen, T. T.; Zhang, H.; Schrock, R. R.; Hoveyda, A. H. *Nature* **2016**, *531*, 459–465.

(4) Zhang, P.; Roundtree, I. A.; Morken, J. P. *Org. Lett.* **2012**, *14*, 1416–1419.

Neodymium(III) *iso*-propoxide was purchased from Strem and used as received.

***N*-Phosphinoyl imines** were prepared according to previously reported procedures.[1,6]

Sodium(I) *tert*-butoxide was purchased from Strem and used as received.

Sodium periodate was purchased from Aldrich Chemical Co. and used as received.

Sodium sulfate was purchased from Fisher and used as received.

Strontium(II) *iso*-propoxide was purchased from Strem and used as received.

Yttrium(III) *iso*-propoxide was purchased from Strem and used as received.

Zinc(II) acetate was purchased from Aldrich Chemical Co. and used as received.

Zinc(II) bis[bis(trimethylsilyl)amide] was purchased from Aldrich Chemical Co. and used as received.

Zinc(II) bromide in diethyl ether was freshly prepared from Zinc(II) bromide from Strem and diethyl ether from the solvent purification system.

Zinc(II) *tert*-butoxide (powder) was purchased from Alfa Aesar and used as received.

---

(5) Fandrick, K. R.; Fandrick, D. R.; Gao, J. J.; Reeves, J. T.; Tan, Z.; Li, W.; Song, J. J.; Lu, B.; Yee, N. K.; Senanayake, C. H.; *Org. Lett.* **2010**, *12*, 3748–3751.

(6) Vieira, E. M.; Snapper, M. L.; Hoveyda, A. H. *J. Am. Chem. Soc.* **2011**, *133*, 3332–3335.

Zinc(II) chloride in diethyl ether was purchased from Aldrich Chemical Co. and used as received.

Zinc(II) fluoride was purchased from Aldrich Chemical Co. and used as received.

Zinc(II) methoxide (97%, powder) was purchased from Aldrich Chemical Co. and used as received.

Zinc(II) triflate was purchased from Aldrich chemical company and used as received.

1.7.2. *Catalytic Enantioselective Crotyl Additions to Phosphinoyl Imines*

Representative Procedure for Additions to *N*-phosphinoyl imines

In a N_2-filled glovebox, $Zn(OMe)_2$ (1.9 mg, 0.015 mmol, 5 mol%) was added to an oven-dried 8 mL vial equipped with a stir bar followed by a solution of aminophenol **1.46** in toluene (2.0 mg, 0.006 mmol in 1.0 mL toluene). The mixture was allowed to stir at 22 °C for 15 min, after which phosphinoylimine **1.57** (91.6, 0.30 mmol), (*Z*)-crotylboronate ***Z*-1.61** (74 μL, 0.36 mmol, 1.2 equiv), MeOH (30 μL, 0.75 mmol, 2.5 equiv) and toluene (2 mL) were added sequentially. The vial was sealed with a cap and electrical tape and taken out of the glovebox. The mixture was allowed to stir for 3 h at

22 °C. The cap was removed and 3 mL of a saturated solution of aqueous $NaIO_4$ was added and the biphasic mixture was allowed to stir at 22 °C for 20 min. The layers were separated and the aqueous layer was washed with ethyl acetate (4 x 4 mL). The organic layers were combined and dried over Na_2SO_4 and the volatiles were removed *in vacuo.* The unpurified residue, obtained as off-white solid, was purified by silica gel chromatography (gradient eluting with 10:0 to 3:1 to 1:3 hexanes:EtOAc) to yield 93.8 mg (0.26 mmol, 87% yield) of **1.63** as a mixture of diastereomers as white crystalline solid in 96:4 e.r.

1.7.3. *Analytical Data for New Compounds*

***N*-((1*R*,2*R*)-2-Methyl-1-phenylbut-3-en-1-yl)-*P*,*P*-diphenylphosphinic amide (1.63):** White solid; m. p. = 151–153 °C; **IR (neat):** 3179 (w, br), 1436 (m), 1181 (m), 1124 (m), 1110 (m), 1059 (m), 901 (m), 750 (m), 722 (m), 692 (s), 576 (m), 537 (s) cm^{-1}; **^{1}H NMR (400 MHz, $CDCl_3$):** δ 7.85–7.78 (2H, m), 7.67–7.61 (2H, m), 7.50–7.45 (1H, m), 7.44–7.38 (2H, m), 7.38–7.32 (1H, m), 7.24–7.14 (5H, m), 7.12–7.07 (2H, m), 5.81 (1H, ddd, *J* = 17.2, 10.4, 7.6 Hz), 5.17–5.08 (2H, m), 4.08 (1H, ddd, *J* = 10.8, 8.8, 6.8 Hz), 3.38 (1H, dd, *J* = 8.8, 6.4 Hz), 2.56 (1H, ddq, *J* = 7.6, 6.8, 6.4 Hz), 0.99 (3H, d, *J* = 6.4

Hz); **^{13}C NMR (100 MHz, $CDCl_3$):** δ 142.7 (d, *J* = 3.7 Hz), 140.2, 133.4 (d, *J* = 127 Hz), 132.7 (d, *J* = 9.7 Hz), 132.1 (d, *J* = 130 Hz), 131.87 (d, *J* = 9.7 Hz), 131.85 (d, *J* = 2.2 Hz), 131.6 (d, *J* = 3.0 Hz), 128.6 (d, *J* = 11.9 Hz), 128.2, 128.1 (d, *J* = 12.7 Hz), 127.3, 127.0, 116.8, 59.5, 45.7 (d, *J* = 5.2 Hz), 17.2; **HRMS (DART):** Calcd for $C_{23}H_{25}NOP$ $[M+H]^+$: 362.1674; Found: 362.1682; **Specific Rotation:** $[\alpha]_D^{23}$ +59.9 (*c* 0.50, $CHCl_3$) for a >98:2 γ/α, 98:2 d.r. and 98:2 e.r. sample. Enantiomeric purity was determined by HPLC analysis in comparison to authentic racemic material (Chiralpak AZ-H, 96:4 hexanes:*i*PrOH, 0.65 mL/min, 220 nm) t_R : 129 min (major) and 106 min (minor).

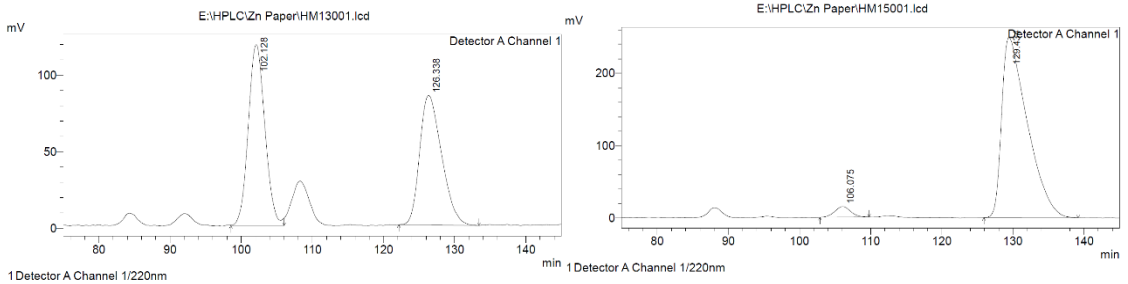

PeakTable

Detector A Channel 1 220nm

Peak#	Ret. Time	Area	Height	Area %	Height %
1	102.128	19258483	118203	51.405	58.275
2	126.338	18205728	84633	48.595	41.725
Total		37464212	202836	100.000	100.000

PeakTable

Detector A Channel 1 220nm

Peak#	Ret. Time	Area	Height	Area %	Height %
1	106.075	2224251	14648	3.444	5.547
2	129.434	62367380	249425	96.556	94.453
Total		64591631	264072	100.000	100.000

Peak #	Ret. Time (min)	Area %	Peak #	Ret. Time (min)	Area %
1	102.128	51.405	1	106.075	3.444
2	126.338	48.595	2	129.434	96.556

***N*-((1*R*,2*R*)-1-(2-Fluorophenyl)-2-methylbut-3-en-1-yl)-*P*,*P*-diphenylphosphinic amide (1.91):** White solid; m.p. = 125–128 °C; **IR (neat):** 3160 (w, br), 1452 (m), 1437 (m), 1182 (s), 1124 (m), 1109 (m), 1067 (m), 908 (m), 749 (m), 724 (m), 692 (s), 529 (s)

cm^{-1}; **^{1}H NMR (400 MHz, $CDCl_3$):** δ 7.84–7.78 (2H, m), 7.70–7.64 (2H, m), 7.52–7.46 (1H, m), 7.44–7.35 (3H, m), 7.28–7.22 (2H, m), 7.20–7.10 (2H, m), 7.02 (1H, td, *J* = 7.6, 1.2 Hz), 6.91 (1H, ddd, *J* = 10.8, 8.0, 1.2 Hz), 5.84 (1H, ddd, *J* = 17.2, 10.4, 7.6 Hz), 5.19–5.15 (1H, m), 5.12 (1H, dt, *J* = 17.2, 1.6 Hz), 4.26 (1H, td, *J* = 10.0, 7.2 Hz), 3.47 (1H, dd, *J* = 9.2, 7.2 Hz), 2.69–2.59 (1H, m), 0.99 (3H, d, *J* = 6.8 Hz); **^{13}C NMR (100 MHz, $CDCl_3$):** δ 160.4 (d, *J* = 244 Hz), 140.3, 133.2 (d, *J* = 90.3 Hz), 132.5 (d, *J* = 9.9 Hz), 131.9 (d, *J* = 93.4 Hz), 131.9 (d, *J* = 9.1 Hz), 131.9 (d, *J* = 3.1 Hz), 131.6 (d, *J* = 3.0 Hz), 129.9 (dd, *J* = 12.9, 3.0 Hz), 129.4 (d, *J* = 4.6 Hz), 128.7 (d, *J* = 8.3 Hz), 128.5 (d, *J* = 12.2 Hz), 128.2 (d, *J* = 12.9 Hz), 123.9 (d, *J* = 3.0 Hz), 116.7, 115.5 (d, *J* = 22 Hz), 55.0, 44.5 (dd, *J* = 5.3, 1.5 Hz), 17.3; **HRMS (DART)** Calcd for $C_{23}H_{23}FNOP$ $[M+H]^+$: 380.15795, Found: 380.15776; **Specific Rotation:** $[\alpha]_D^{21}$ +49.9 (*c* 1.00, $CHCl_3$) for a 95:5 γ/α, 95:5 d.r. and 98.5:1.5 e.r. sample. The enantiomeric purity was determined by HPLC analysis in comparison to authentic racemic material (Chiralcel OZ-H, 96:4 hexanes:*i*PrOH, 0.6 mL/min, 220 nm) t_R: 104 min (major) and 157 min (minor).

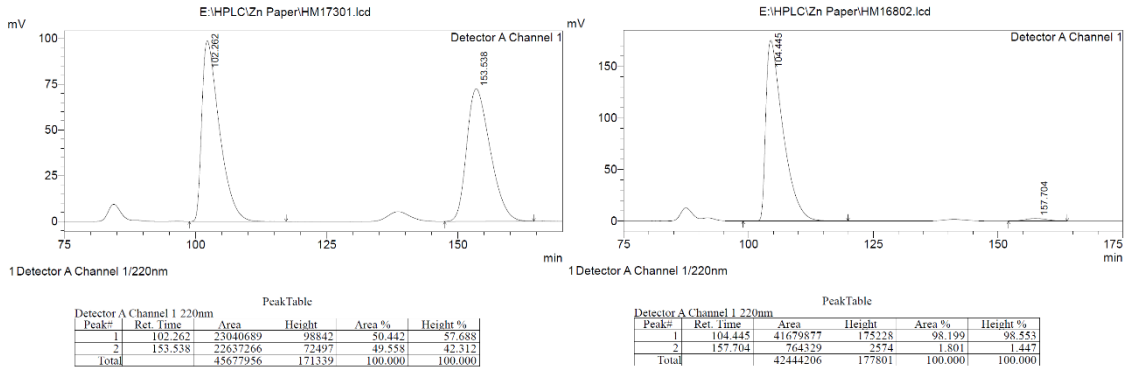

PeakTable

Detector A Channel 1 220nm

Peak#	Ret. Time	Area	Height	Area %	Height %
1	102.262	23040689	98842	50.442	57.688
2	153.538	22637266	72497	49.558	42.312
Total		45677956	171339	100.000	100.000

PeakTable

Detector A Channel 1 220nm

Peak#	Ret. Time	Area	Height	Area %	Height %
1	104.445	41679877	175228	98.199	98.553
2	157.704	764329	2574	1.801	1.447
Total		42444206	177801	100.000	100.000

Peak #	Ret. Time (min)	Area %	Peak #	Ret. Time (min)	Area %
1	102.262	50.442	1	104.445	98.553
2	153.538	49.558	2	157.704	1.447

***N*-((1*R*,2*R*)-1-(2-chlorophenyl)-2-methylbut-3-en-1-yl)-*P*,*P*-diphenylphosphinic amide (1.92):** White solid; m.p. = 164–165 °C; **IR (neat):** 3176 (w, br), 1437 (m), 1184 (s), 1108 (m), 909 (m), 751 (m), 724 (m), 693 (s), 543 (s) 531 (m), 513 (m) cm^{-1}; **^{1}H NMR (400 MHz, $CDCl_3$):** δ 7.86–7.78 (2H, m), 7.69–7.62 (2H, m), 7.51–7.46 (1H, m), 7.45–7.16 (8H, m), 7.16–7.11 (1H, m), 5.81 (1H, ddd, *J* = 17.2, 10.8, 7.2 Hz), 5.20 (1H, dt, *J* = 10.8, 1.2 Hz), 5.13 (1H, dt, *J* = 17.2, 1.6 Hz), 4.56–4.40 (1H, m), 3.54–3.38 (1H, m), 2.72–2.60 (1H, m), 1.10 (3H, d, *J* = 6.4 Hz); **^{13}C NMR (100 MHz, $CDCl_3$):** δ 140.5, 139.0, 133.0 (d, *J* = 97.9 Hz), 132.7, 132.5 (d, *J* = 9.8 Hz), 132.0 (d, *J* = 9.1 Hz, peaks overlapped at 131.93), 131.9 (d, *J* = 2.3 Hz, peaks overlapped at 131.9), 131.7 (d, *J* = 2.3 Hz), 131.6 (d, *J* = 100 Hz), 129.6, 128.6 (d, *J* = 12.2 Hz, peaks overlapped at 128.50), 128.5 (peaks overlapped at 128.50), 128.18 (d, *J* = 12.1 Hz), 128.15, 126.6, 117.4, 56.1, 43.3 (d, *J* = 5.4 Hz), 17.0; **HRMS (DART):** Calcd for $C_{23}H_{24}ClNOP$ $[M+H]^+$: 396.12840,

Found: 396.12892; **Specific Rotation:** $[\alpha]_D^{21}$ +29.9 (*c* 1.00, $CHCl_3$) for a 98:2 γ/α, 90:10 d.r. and 99:1 e.r. sample. The enantiomeric purity was determined by HPLC analysis in comparison to authentic racemic material (Chiralpak AZ-H, 96:4 hexanes:*i*PrOH, 1.0 mL/min, 220 nm) t_R: 97 min (major) and 58 min (minor).

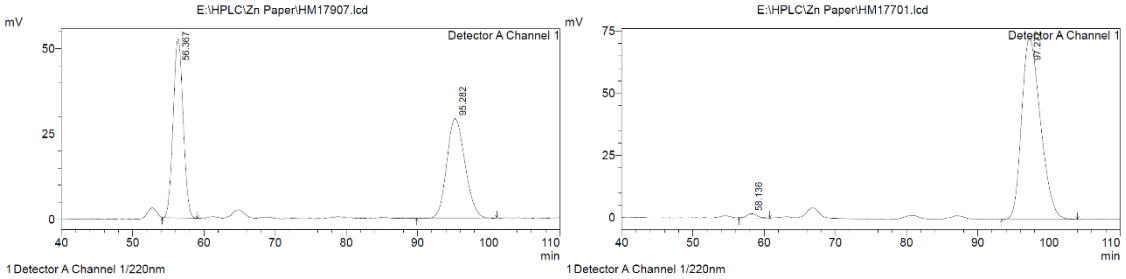

PeakTable

Detector A Channel 1 220nm

Peak#	Ret. Time	Area	Height	Area %	Height %
1	56.367	5119779	52469	49.847	64.294
2	95.282	5151307	29139	50.153	35.706
Total		10271086	81608	100.000	100.000

PeakTable

Detector A Channel 1 220nm

Peak#	Ret. Time	Area	Height	Area %	Height %
1	58.136	166767	1606	1.229	2.162
2	97.272	13406269	72640	98.771	97.838
Total		13573035	74245	100.000	100.000

Peak #	Ret. Time (min)	Area %	Peak #	Ret. Time (min)	Area %
1	56.367	49.847	1	58.136	1.229
2	95.282	50.153	2	97.272	98.771

***N*-((1*R*,2*R*)-1-(2-Bromophenyl)-2-methylbut-3-en-1-yl)-*P*,*P*-diphenylphosphinic amide (1.93):** White solid; m.p. = 166 °C, decomposition; **IR (neat):** 3210 (w, br), 1437 (m), 1186 (s), 1124 (m), 1109 (m), 999 (m), 911 (w), 750 (m), 726 (m), 695 (s), 544 (m) cm^{-1}; **^{1}H NMR (400 MHz, $CDCl_3$):** δ 7.86–7.81 (2H, m), 7.69–7.64 (2H, m), 7.50–7.46 (1H, m), 7.44–7.37 (4H, m), 7.29–7.24 (4H, m), 7.08–7.04 (1H, m), 5.80 (1H, m), 5.22–5.11 (2H, m), 4.48 (1H, app s), 3.48 (1H, app s), 2.65 (1H, app s), 1.15 (3H, app s); **^{13}C NMR (100 MHz, $CDCl_3$):** δ 143.2, 138.5, 132.9 (d, *J* = 128 Hz), 132.9, 132.7 (d, *J* = 9.0 Hz), 132.5 (d, *J* = 9.8 Hz), 132.0 (d, *J* = 9.9 Hz), 131.9 (d, *J* = 130 Hz), 131.9 (d, *J* =

2.3 Hz), 131.7 (d, J = 3.0 Hz), 128.6 (d, J = 12.1 Hz), 128.5, 128.2 (d, J = 12.9 Hz), 127.2, 123.2, 117.6, 58.0, 43.1 (d, J = 5 Hz), 17.0; **HRMS (DART):** Calcd for $C_{23}H_{24}BrNOP$ $[M+H]^+$: 440.07789, Found: 440.07861; **Specific Rotation:** $[\alpha]_D^{24}$ +10.4 (*c* 1.6, $CHCl_3$) for a 96:4 γ/α, 91:9 d.r. and 98:2 e.r. sample; The enantiomeric purity was determined by HPLC analysis in comparison to authentic racemic material (Chiralpak AZ-H, 96:4 hexanes:*i*PrOH, 0.8 mL/min, 220 nm) t_R: 119 min (major) and 68 min (minor).

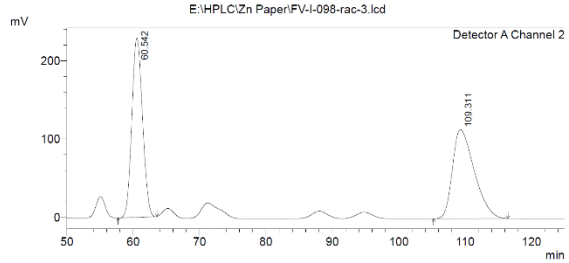

PeakTable

Detector A Channel 2 220nm

Peak#	Ret. Time	Area	Height	Area %
1	60.542	25567310	228792	49.618
2	109.311	25960818	113443	50.382
Total		51528128	342236	100.000

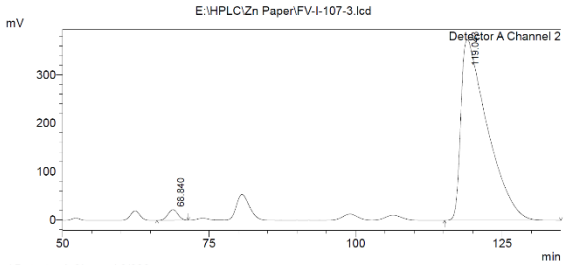

PeakTable

Detector A Channel 2 220nm

Peak#	Ret. Time	Area	Height	Area %
1	68.840	2618215	21937	2.188
2	119.043	117066425	373912	97.812
Total		119684640	395849	100.000

Peak #	Ret. Time (min)	Area %	Peak #	Ret. Time (min)	Area %
1	60.542	49.618	1	68.840	2.188
2	109.311	50.382	2	119.043	97.812

***N*-((1*R*,2*R*)-2-Methyl-1-(o-tolyl)but-3-en-1-yl)-*P*,*P*-diphenylphosphinic amide (1.94):**

White solid; m.p. = 123–125 °C; **IR (neat):** 3189 (w, br), 1437 (m), 1184 (s), 1122 (m), 1109 (m), 1062 (w), 997 (m), 907 (m), 850 (m), 724 (m), 695 (m), 532 (m) cm^{-1}; **^{1}H NMR (400 MHz, $CDCl_3$):** δ 7.86–7.80 (2H, m), 7.61–7.56 (2H, m), 7.49–7.45 (1H, m), 7.43–7.38 (2H, m), 7.36–7.30 (2H, m), 7.25–7.16 (3H, m), 7.09–6.96 (1H, td, J = 7.2,

1.6 Hz), 6.95–6.93 (1H, m), 5.86 (1H, ddd, *J* = 17.2, 10.0, 7.2 Hz), 5.20–5.10 (2H, m), 4.30 (1H, ddd, *J* = 19.6, 9.2, 6.4 Hz), 3.397 (1H, dd, *J* = 8.8, 6.4 Hz), 2.49 (1H, ddq, *J* = 13.6, 6.8 Hz), 1.86 (3H, s), 1.05 (3H, d, *J* = 6.8 Hz); **^{13}C NMR (100 MHz, $CDCl_3$):** δ 141.6 (d, *J* = 3.8 Hz), 139.9, 135.1, 133.5 (d, *J* = 127.5 Hz), 132.7 (d, *J* = 9.8 Hz), 131.9 (d, *J* = 3.0 Hz), 131.9 (d, *J* = 9.9 Hz), 131.9 (d, *J* = 130.0 Hz), 131.5 (d, *J* = 2.3 Hz), 130.2, 128.6 (d, *J* = 12.9 Hz), 128.1 (d, *J* = 12.1 Hz), 126.9, 126.6, 126.0, 117.1, 54.7, 44.8 (d, *J* = 5.3 Hz), 19.2, 17.1; **HRMS (DART):** Calcd for $C_{24}H_{27}NOP$ $[M+H]^+$: 376.18303, Found: 376.18341; **Specific Rotation:** $[\alpha]_D^{24}$ +16.93 (*c* 1.18, $CHCl_3$) for a >98:2 γ/α, 93:7 d.r. and 94:6 e.r. sample; The enantiomeric purity was determined by HPLC analysis in comparison to authentic racemic material (Chiralpak AZ-H, 96:4 hexanes:*i*PrOH, 0.8 mL/min, 220 nm) t_R: 73 min (major) and 59 min (minor).

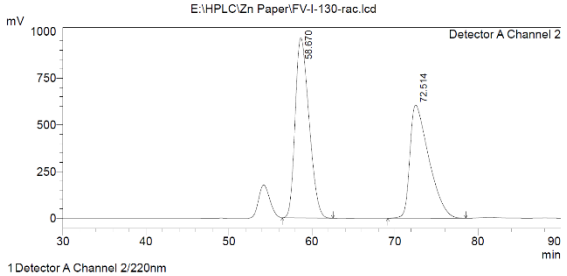

PeakTable
Detector A Channel 2 220nm

Peak#	Ret. Time	Area	Height	Area %
1	58.670	111599818	965185	53.670
2	72.514	96338613	606549	46.330
Total		207938431	1571734	100.000

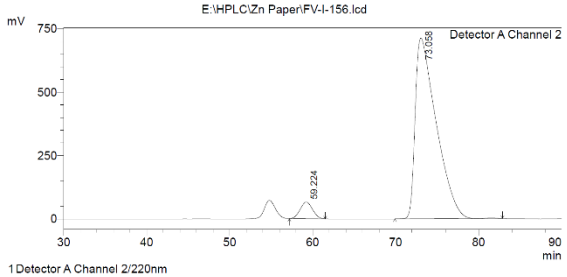

PeakTable
Detector A Channel 2 220nm

Peak#	Ret. Time	Area	Height	Area %
1	59.224	6774514	65667	5.116
2	73.058	125652286	713347	94.884
Total		132426800	779014	100.000

Peak #	Ret. Time (min)	Area %	Peak #	Ret. Time (min)	Area %
1	58.670	53.670	1	59.224	5.116
2	72.514	46.330	2	73.058	94.884

***N*-((1*R*,2*R*)-2-Methyl-1-(naphthalen-2-yl)but-3-en-1-yl)-*P*,*P*-diphenylphosphinic amide (1.95):** Off-white solid; m.p. = 164–166 °C; **IR (neat):** 3184 (w, br), 1508 (m), 1187 (s), 1123 (m), 1109 (m), 998 (w), 911 (m), 746 (m), 724 (m), 696 (m), 537 (m) cm^{-1}; **^{1}H NMR (400 MHz, $CDCl_3$):** δ 7.85–7.69 (5H, m), 7.62 (2H, dd, *J* = 12, 7.2 Hz), 7.50–7.39 (6H, m), 7.31 (1H, d, *J* = 7.2 Hz), 7.22 (1H, d, *J* = 8 Hz), 7.10 (2H, td, *J* = 7.6, 3.2 Hz), 5.86 (1H, ddd, *J* = 17.6, 10.4, 7.6 Hz), 5.21–5.14 (2H, m), 4.25 (1H, dt, *J* = 9.6, 8.0 Hz), 3.49 (1H, app t, *J* = 7.2Hz), 2.72–2.63 (1H, m), 1.02 (3H, d, *J* = 6.4 Hz); **^{13}C NMR (100 MHz, $CDCl_3$):** δ 140.3, 139.9 (d, *J* = 2.5 Hz), 133.4 (d, *J* = 126.4 Hz), 133.1, 132.7, 132.6 (d, *J* = 9.3 Hz), 132.0 (d, *J* = 130.7 Hz), 131.9 (d, *J* = 2.6 Hz), 131.9 (d, *J* = 9.3 Hz), 131.5 (d, *J* = 3.4 Hz), 128.6 (d, *J* = 11.8 Hz), 128.0 (d, *J* = 11.8 Hz), 128.0, 128.0, 127.6, 126.5, 126.0, 125.8, 125.2, 116.9, 59.7, 45.6 (d, *J* = 5.9 Hz), 17.3; **HRMS (DART):** Calcd for $C_{27}H_{27}NOP$ $[M+H]^+$: 412.18303, Found: 412.18303; **Specific Rotation:** $[\alpha]_D^{24}$ +64.56 (*c* 1.47, $CHCl_3$) for a 97:3 γ/α, 93:7 d.r. and 95:5 e.r. sample; The enantiomeric purity was determined by HPLC analysis in comparison to authentic racemic material (Chiralpak AZ-H, 94:6 hexanes:*i*PrOH, 0.4 mL/min, 220 nm) t_R: 346 min (major) and 194 min (minor).

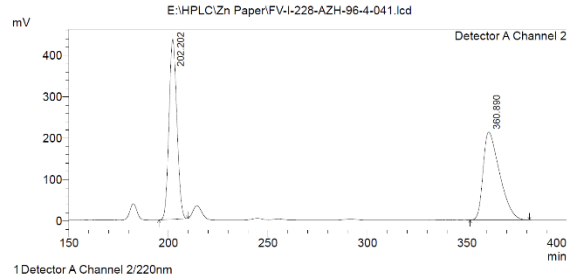

PeakTable

Detector A Channel 2 220nm

Peak#	Ret. Time	Area	Height	Area %
1	202.202	119670606	434734	49.545
2	360.890	121870850	212145	50.455
Total		241541456	646878	100.000

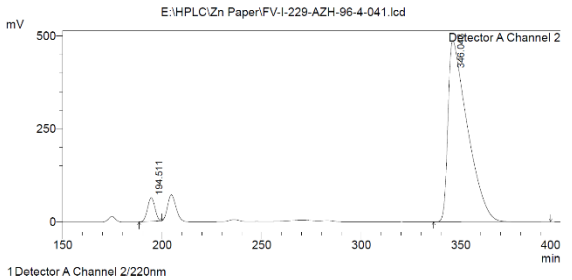

PeakTable

Detector A Channel 2 220nm

Peak#	Ret. Time	Area	Height	Area %
1	194.511	16320450	63546	4.711
2	346.043	330086570	486586	95.289
Total		346407020	550132	100.000

Peak #	Ret. Time (min)	Area %	Peak #	Ret. Time (min)	Area %
1	202.202	49.545	1	194.511	4.711
2	360.890	50.455	2	346.043	95.289

***N*-((1*R*,2*R*)-1-(3-Bromophenyl)-2-methylbut-3-en-1-yl)-*P*,*P*-diphenylphosphinic amide (1.96):** White solid; m.p. = 130–132 °C; **IR (neat):** 3160 (w, br), 1436 (m), 1178 (m), 1123 (m), 1107 (m), 1069 (m), 902 (m), 724 (m), 692 (s), 550 (s), 526 (s) cm^{-1}; **^{1}H NMR (400 MHz, $CDCl_3$):** δ 7.83–7.77 (2H, m), 7.66–7.59 (2H, m), 7.52–7.47 (1H, m), 7.45–7.34 (3H, m), 7.29–7.22 (3H, m), 7.21–7.19 (1H, m), 7.08–7.02 (2H, m), 5.78 (1H, ddd, *J* = 17.2, 10.4, 7.6 Hz), 5.20–5.10 (2H, m), 4.05 (1H, dt, *J* = 10.0, 7.2 Hz), 3.38 (1H, dd, *J* = 7.2, 5.2 Hz), 2.56–2.46 (1H, m), 0.97 (3H, d, *J* = 6.8 Hz); **^{13}C NMR (100 MHz, $CDCl_3$):** δ 145.0 (d, *J* = 2.2 Hz), 139.9, 133.0 (d, *J* = 120 Hz), 132.5 (d, *J* = 9.0 Hz), 132.0 (d, *J* = 2.2 Hz), 131.8 (d, *J* = 124 Hz), 131.7 (d, *J* = 9.1 Hz, peaks overlapped at 131.7), 131.7 (d, *J* = 2.3 Hz, peaks overlapped at 131.7), 130.4, 130.1, 129.7, 128.5 (d, *J* = 12.2 Hz), 128.1 (d, *J* = 12.1 Hz), 126.2, 122.3, 117.3, 58.9 (d, *J* = 1.5 Hz), 45.6 (d, *J* = 5.3 Hz), 17.3; **HRMS (DART):** Calcd for $C_{23}H_{24}BrNOP$ $[M+H]^+$: 440.07789, Found:

440.07783; **Specific Rotation:** $[\alpha]_D^{21}$ +59.9 (*c* 1.00, $CHCl_3$) for a >98:2 γ/α, 91:9 d.r and 96:4 e.r sample; The enantiomeric purity was determined by HPLC analysis in comparison to authentic racemic material (Chiralcel OZ-H, 96:4 hexanes:*i*PrOH, 0.6 mL/min, 220 nm) t_R: 85 min (major) and 78 min (minor).

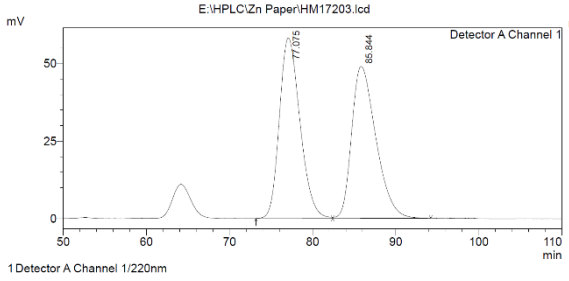

PeakTable
Detector A Channel 1 220nm

Peak#	Ret. Time	Area	Height	Area %	Height %
1	77.075	10042359	58225	50.305	54.295
2	85.844	9920651	49014	49.695	45.705
Total		19963009	107239	100.000	100.000

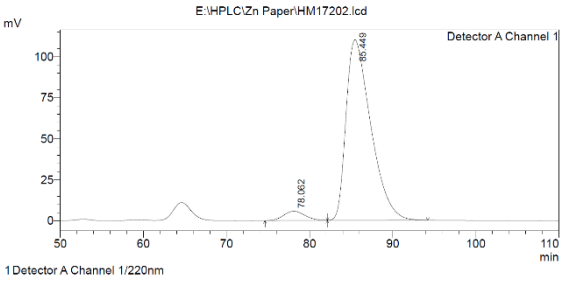

PeakTable
Detector A Channel 1 220nm

Peak#	Ret. Time	Area	Height	Area %	Height %
1	78.062	1008946	5704	4.232	4.931
2	85.449	22829527	109982	95.768	95.069
Total		23838473	115686	100.000	100.000

Peak #	Ret. Time (min)	Area %	Peak #	Ret. Time (min)	Area %
1	77.075	50.305	1	78.062	4.232
2	85.844	49.695	2	85.449	95.768

***N*-((1*R*,2*R*)-1-(4-Methoxyphenyl)-2-methylbut-3-en-1-yl)-*P*,*P*-diphenylphosphinic amide (1.97):** White solid; m.p. = 136–138 °C; **IR (neat):** 3209 (w, br), 1612 (w), 1513 (m), 1436 (m), 1251 (m), 1178 (s), 1122 (m), 1107 (m), 1068 (m), 1027 (m), 906 (m), 749 (m), 721 (m), 692 (s), 533 (s) cm^{-1}; **^{1}H NMR (400 MHz, $CDCl_3$):** δ 7.83–7.77 (2H, m), 7.68–7.62 (2H, m), 7.50–7.45 (1H, m), 7.43–7.34 (3H, m), 7.27–7.22 (2H, m), 7.03–6.99 (2H, m), 6.76–6.72 (2H, m), 5.80 (1H, ddd, *J* = 17.2, 10.8, 7.6 Hz), 5.16–5.08 (2H, m), 4.03 (1H, dt, *J* = 10.4, 8.4 Hz), 3.78 (3H, s), 3.35 (1H, dd, *J* = 8.4, 6.0 Hz), 2.57–2.47 (1H, m), 0.96 (3H, d, *J* = 7.2 Hz); **^{13}C NMR (100 MHz, $CDCl_3$):** δ 158.5,

140.5, 134.7 (d, J = 3.0 Hz), 133.4 (d, J = 113 Hz), 132.6 (d, J = 9.8 Hz), 132.2 (d, J = 117 Hz), 131.8 (d, J = 9.9 Hz), 131.8 (peaks overlapped at 131.8), 131.5 (d, J = 2.3 Hz), 128.5 (d, J = 12.9 Hz), 128.3, 128.1 (d, J = 12.1 Hz), 116.6, 113.5, 59.0 (d, J = 1.5 Hz), 55.3, 45.8 (d, J = 6.0 Hz), 17.1; **HRMS (DART)**: Calcd for $C_{24}H_{27}NO_2P$ $[M+H]^+$: 392.17794, Found: 392.17705; **Specific Rotation:** $[\alpha]_D^{21}$ +69.9 (*c* 1.00, $CHCl_3$) for a >98:2 γ/α, 94:6 d.r. and 93:7 e.r. sample; The enantiomeric purity was determined by HPLC analysis in comparison to authentic racemic material (Chiralcel OZ-H, 96:4 hexanes:*i*PrOH, 1.0 mL/min, 220 nm) t_R: 117 min (major) and 88 min (minor).

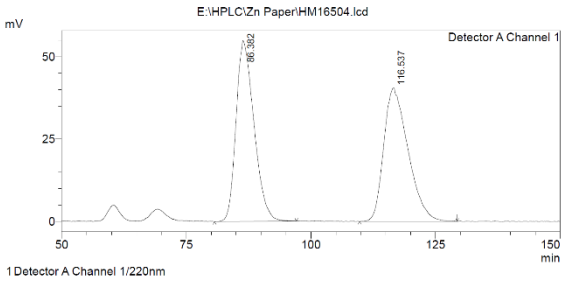

PeakTable
Detector A Channel 1 220nm

Peak#	Ret. Time	Area	Height	Area %	Height %
1	86.382	13719670	54895	49.986	57.490
2	116.537	13727489	40591	50.014	42.510
Total		27447159	95486	100.000	100.000

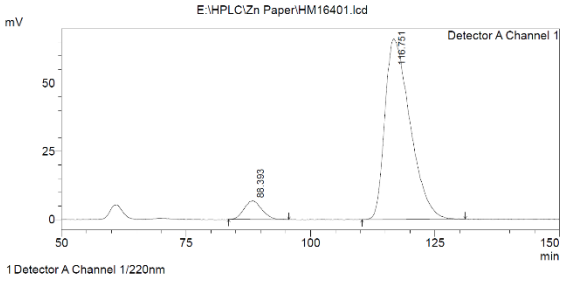

PeakTable
Detector A Channel 1 220nm

Peak#	Ret. Time	Area	Height	Area %	Height %
1	88.393	1678280	6805	6.721	9.326
2	116.751	23292336	66165	93.279	90.674
Total		24970616	72971	100.000	100.000

Peak #	Ret. Time (min)	Area %	Peak #	Ret. Time (min)	Area %
1	86.382	49.986	1	88.393	6.721
2	116.537	50.014	2	116.751	93.279

***N*-((1*R*,2*R*)-1-(4-(Dimethylamino)phenyl)-2-methylbut-3-en-1-yl)-*P*,*P*-diphenylphosphinic amide (1.98):** White solid; m.p. = 128–129 °C; **IR (neat):** 3232 (w, br), 3075 (w), 2957 (w), 2798 (w), 1616 (w), 1523 (m), 1435 (m), 1346 (w), 1184 (s), 1122 (m), 1105 (m), 1058 (m), 905 (m), 808 (m), 721 (s), 691 (s), 530 (s) cm^{-1}; **^{1}H NMR**

(400 MHz, $CDCl_3$): δ 7.84–7.77 (2H, m), 7.70–7.64 (2H, m), 7.49–7.44 (1H, m), 7.43–7.33 (3H, m), 7.28–7.22 (2H, m), 6.95 (2H, d, *J* = 8.4 Hz), 6.60 (2H, d, *J* = 8.4 Hz), 5.81 (1H, ddd, *J* = 17.2, 10.4, 7.6 Hz), 5.14–5.06 (2H, m), 4.02-3.94 (1H, m), 3.32 (1H, dd, *J* = 8.8, 6.4 Hz), 2.92 (6H, s), 2.59–2.49 (1H, m), 0.98 (3H, d, *J* = 7.2 Hz); **^{13}C NMR (100 MHz, $CDCl_3$):** δ 149.6, 140.8, 133.6 (d, *J* = 126 Hz, peaks overlapped at 132.9), 132.6 (d, *J* = 9.9 Hz), 132.3 (d, *J* = 131 Hz, peaks overlapped at 132.9), 131.8 (d, *J* = 9.1 Hz), 131.6 (d, *J* = 2.3 Hz), 131.4 (d, *J* = 2.3 Hz), 130.4 (d, *J* = 3.8 Hz), 128.4 (d, *J* = 12.1 Hz), 128.0 (d, *J* = 12.9 Hz), 127.9, 116.2, 112.3, 59.1, 45.7 (d, *J* = 5.3 Hz), 40.7, 17.0; **HRMS (DART):** Calcd for $C_{25}H_{30}N_2OP$ $[M+H]^+$: 405.20957, Found: 405.20853; **Specific Rotation:** $[\alpha]_D^{22}$ +79.8 (*c* 1.00, $CHCl_3$) for a >98:2 γ/α, 93:7 d.r. and 80:20 e.r. sample; The enantiomeric purity was determined by HPLC analysis in comparison to authentic racemic material (Chiralpak AZ-H, 96:4 hexanes:*i*PrOH, 1.0 mL/min, 220 nm) t_R: 197 min (major) and 120 min (minor).

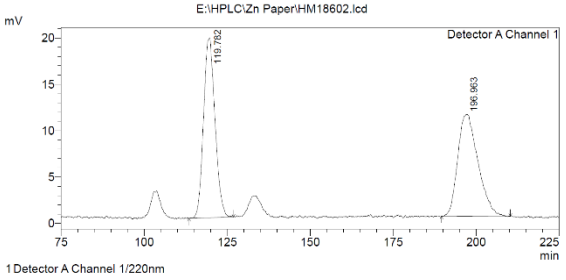

PeakTable
Detector A Channel 1 220nm

Peak#	Ret. Time	Area	Height	Area %	Height %
1	119.782	4656398	19432	50.014	63.877
2	196.963	4653865	10989	49.986	36.123
Total		9310263	30421	100.000	100.000

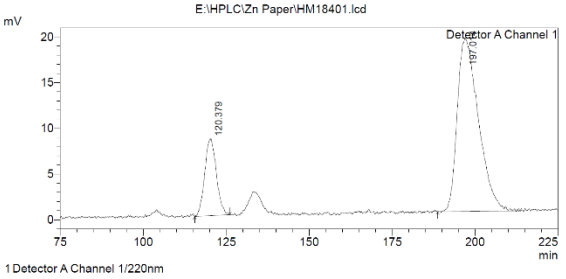

PeakTable
Detector A Channel 1 220nm

Peak#	Ret. Time	Area	Height	Area %	Height %
1	120.379	2045518	8435	19.544	30.780
2	197.014	8420625	18969	80.456	69.220
Total		10466143	27404	100.000	100.000

Peak #	Ret. Time (min)	Area %	Peak #	Ret. Time (min)	Area %
1	119.782	50.014	1	120.379	19.544
2	196.963	49.986	2	197.014	80.456

***N*-((1*R*,2*R*)-1-(4-Bromophenyl)-2-methylbut-3-en-1-yl)-*P*,*P*-diphenylphosphinic amide (1.99) :** White solid; m.p. = 145–147 °C; **IR (neat):** 3215 (w, br), 1435 (m), 1180 (m), 1123 (m), 1109 (m), 999 (m), 917 (m), 748 (m), 723 (m), 692 (s), 535 (s) cm^{-1}; **^{1}H NMR (400 MHz, $CDCl_3$):** δ 7.83–7.77 (2H, m), 7.66–7.60 (2H, m), 7.52–7.47 (1H, m), 7.45–7.36 (3H, m), 7.34–7.30 (2H, m), 7.28–7.22 (2H, m), 7.00–6.96 (2H, m), 5.77 (1H, ddd, *J* = 17.6, 10.8, 8.0 Hz), 5.20–5.10 (2H, m), 4.04 (1H, dt, *J* = 9.6, 8.0 Hz), 3.37 (1H, dd, *J* = 8.0, 5.6 Hz), 2.55–2.46 (1H, m), 0.97 (3H, d, *J* = 6.8 Hz); **^{13}C NMR (100 MHz, $CDCl_3$)**: δ 141.7 (d, *J* = 3.1 Hz), 139.8, 133.1 (d, *J* = 95.6 Hz), 132.5 (d, *J* = 9.1 Hz), 131.9 (d, *J* = 3.1 Hz), 131.8 (d, *J* = 99.4 Hz), 131.8 (d, *J* = 9.9 Hz), 131.6 (d, *J* = 3.0 Hz), 131.2, 129.1, 128.6 (d, *J* = 12.9 Hz), 128.2 (d, *J* = 12.9 Hz), 120.9, 117.2, 58.9 (d, *J* = 1.6 Hz), 45.5 (d, *J* = 6.0 Hz), 17.1; **HRMS (DART):** Calcd for $C_{23}H_{24}BrNOP$ $[M+H]^+$: 440.07789, Found: 440.07672; **Specific Rotation:** $[\alpha]_D^{21}$ +79.8 (*c* 1.00, $CHCl_3$) for a >98:2 γ/α, 93:7 d.r. and 97:3 e.r. sample; The enantiomeric purity was determined by HPLC analysis in comparison to authentic racemic material (Chiralcel OZ-H, 96:4 hexanes:*i*PrOH, 0.6 mL/min, 220 nm) t_R: 74 min (major) and 52 min (minor).

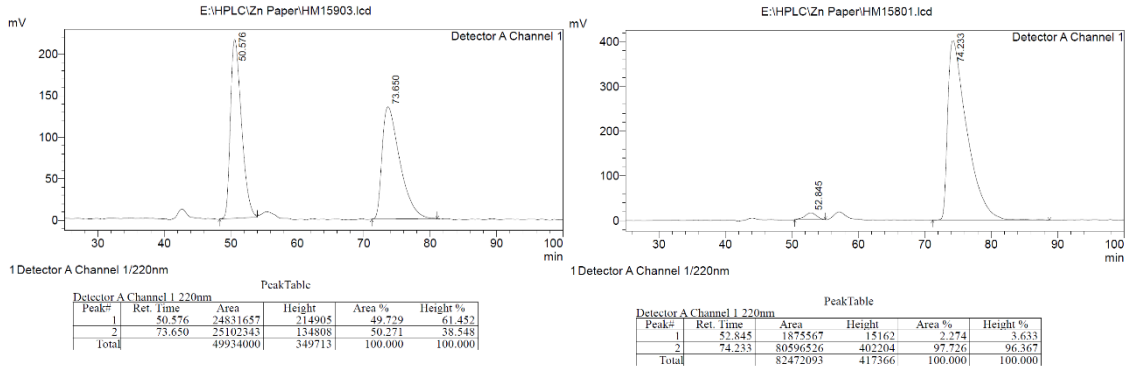

Peak #	Ret. Time (min)	Area %	Peak #	Ret. Time (min)	Area %
1	50.576	49.729	1	52.845	2.274
2	73.650	50.271	2	74.233	97.726

***N*-((1*R*,2*R*)-2-Methyl-1-(4-(trifluoromethyl)phenyl)but-3-en-1-yl)-*P*,*P*-diphenylphosphinic amide (1.100):** White solid; m.p. = 159–162 °C; **IR (neat):** 3168 (w, br), 1438 (m), 1326 (s), 1182 (m), 1122 (S), 1067 (m), 999 (m), 725 (w), 695 (m), 534 (m) cm^{-1}; **^{1}H NMR (400 MHz, $CDCl_3$):** δ 7.84–7.78 (2H, m), 7.64–7.58 (2H, m), 7.52–7.47 (1H, m), 7.45–7.40 (4H, m), 7.38–7.33 (1H, m) 7.26–7.19 (4H, m), 5.77 (1H, ddd, *J* = 17.2, 10.4, 7.6 Hz), 5.21–5.13 (2H, m), 4.34 (1H, dt, *J* = 10, 7.6 Hz), 3.46 (1H, dd, *J* = 7.6, 5.6 Hz), 2.59–2.50 (1H, m), 0.98 (3H, d, *J* = 6.8 Hz); **^{13}C NMR (100 MHz, $CDCl_3$):** δ 146.7, 139.7, 132.9 (d, *J* = 126.8 Hz), 132.5 (d, *J* = 9.8 Hz), 132.1 (d, *J* = 3.0 Hz), 131.9 (d, *J* = 131.9 Hz), 131.8 (d, *J* = 9.1 Hz), 131.7 (d, *J* = 3.0 Hz), 129.3 (q, *J* = 32.6 Hz), 128.7 (d, *J* = 12.1 Hz), 128.9 (d, *J* = 12.9 Hz), 127.8, 125.1 (q, *J* = 3.8 Hz), 124.3 (q, *J* = 270.2 Hz) 117.5, 59.1, 45.6 (d, *J* = 6.8 Hz), 17.2; **HRMS (DART):** Calcd

for $C_{24}H_{24}F_3NOP$ $[M+H]^+$: 430.15476, Found: 430.15583; **Specific Rotation:** $[\alpha]_D^{24}$ +49.77 (*c* 1.41, $CHCl_3$) for a 95:5 γ/α, 92:8 d.r. and >99:1 e.r. sample; The enantiomeric purity was determined by HPLC analysis in comparison to authentic racemic material (Chiralcel OZ-H, 96:4 hexanes:*i*PrOH, 0.4 mL/min, 220 nm) t_R: 58 min (major) and 37 min (minor).

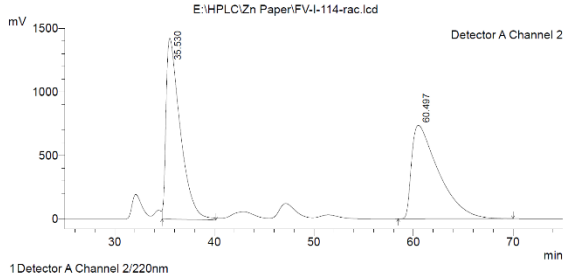

Peak Table

Detector A Channel 2 220nm

Peak#	Ret. Time	Area	Height	Area %
1	35.530	140989685	1424468	50.418
2	60.497	138652905	735470	49.582
Total		279642590	2159938	100.000

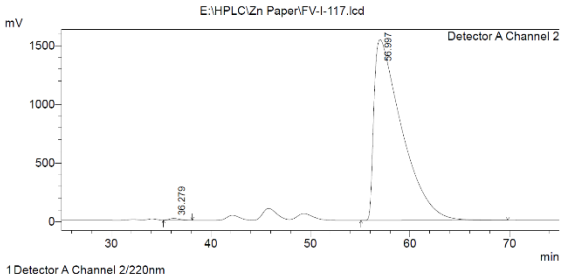

Peak Table

Detector A Channel 2 220nm

Peak#	Ret. Time	Area	Height	Area %
1	36.279	1156284	15979	0.385
2	56.997	298934571	1542206	99.615
Total		300090855	1558184	100.000

Peak #	Ret. Time (min)	Area %	Peak #	Ret. Time (min)	Area %
1	35.530	50.418	1	36.279	0.385
2	60.497	49.582	2	56.997	99.615

Methyl 4-((1*R*,2*R*)-1-((diphenylphosphoryl)amino)-2-methylbut-3-en-1-yl)benzoate (1.101): m.p. = 139–140 °C**; IR (neat):** 3201 (w, br), 3058 (w), 2979 (w), 2871 (w), 1717 (s), 1435 (m), 1279 (s), 1179 (s), 1107 (s), 909 (m), 725 (m), 696 (s), 540 (s), 529 (s) cm^{-1}; **^{1}H NMR (400 MHz, $CDCl_3$):** δ 7.91–7.88 (2H, m), 7.84–7.78 (2H, m), 7.65–7.59 (2H, m), 7.52–7.47 (1H, m), 7.45–7.39 (2H, m), 7.38–7.33 (1H, m), 7.24–7.16 (4H, m), 5.77 (1H, ddd, *J* = 18.0, 10.8, 8.0 Hz), 5.20–5.16 (1H, m), 5.12 (1H, dt, *J* = 18.0, 1.2 Hz), 4.13 (1H, ddd, *J* = 10.4, 8.4, 6.8 Hz), 3.91 (3H, s), 3.41 (1H, dd, *J* = 8.4, 5.2 Hz),

2.60–2.50 (1H, m), 0.99 (3H, d, J = 6.8 Hz); **^{13}C NMR (100 MHz, $CDCl_3$):** δ 167.0, 148.1 (d, J = 3.0 Hz), 139.6, 132.9 (d, J = 127 Hz), 132.5 (d, J = 9.8 Hz), 132.0 (d, J = 3.0 Hz), 131.8 (d, J = 9.9 Hz), 131.8 (d, J = 131 Hz), 131.7 (d, J = 2.3 Hz), 129.5, 128.9, 128.6 (d, J = 12.9 Hz), 128.2 (d, J = 12.9 Hz), 127.3, 117.2, 59.2, 52.2, 45.5 (d, J = 6.0 Hz), 17.1; **HRMS (DART):** Calcd for $C_{25}H_{27}NO_3P$ $[M+H]^+$: 420.17285, Found: 420.17224; **Specific Rotation:** $[\alpha]_D^{21}$ +79.8 (*c* 1.00, $CHCl_3$) for a >98:2 γ/α, 91:9 d.r. and 97:3 e.r. sample; The enantiomeric purity was determined by HPLC analysis in comparison to authentic racemic material (Chiralpak AD-H, 94:6 hexanes:*i*PrOH, 1.0 mL/min, 220 nm) t_R: 136 min (major) and 65 min (minor).

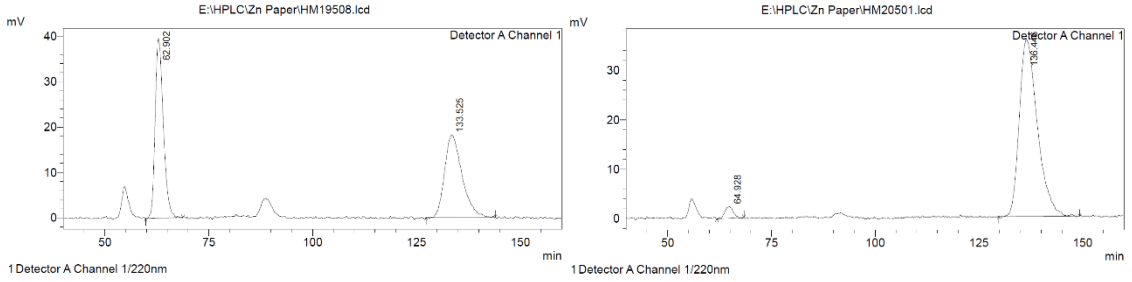

PeakTable

Detector A Channel 1 220nm

Peak#	Ret. Time	Area	Height	Area %	Height %
1	62.902	5412906	39609	50.624	68.581
2	133.525	5279500	18146	49.376	31.419
Total		10692406	57755	100.000	100.000

PeakTable

Detector A Channel 1 220nm

Peak#	Ret. Time	Area	Height	Area %	Height %
1	64.928	322317	2356	2.888	6.163
2	136.446	10838652	35883	97.112	93.837
Total		11160969	38239	100.000	100.000

Peak #	Ret. Time (min)	Area %	Peak #	Ret. Time (min)	Area %
1	62.902	50.624	1	64.928	2.888
2	133.525	49.376	2	136.446	97.112

***N*-((1*R*,2*R*)-1-(Furan-2-yl)-2-methylbut-3-en-1-yl)-*P*,*P*-diphenylphosphinic amide (1.102) :** Off-white solid; m.p. = 102–105 °C; **IR (neat):** 3176 (w, br), 3077 (w), 2963 (w), 2925 (w), 1437 (s), 1189 (s), 1149 (s), 1109 (s), 914 (m), 724 (s), 696 (s), 530 (s)

cm^{-1}; **^{1}H NMR (400 MHz, $CDCl_3$):** δ 7.84–7.73 (4H, m), 7.50–7.47 (1H, m), 7.45–7.32 (3H, m), 7.35 (2H, td, *J* = 8.0, 3.2 Hz), 7.28 (1H, d, *J* = 2.0 Hz), 6.19 (1H, dd, *J* = 3.2, 2.0 Hz), 6.04 (1H, d, *J* = 3.2 Hz), 5.78 (1H, ddd, *J* = 17.2, 10.8, 7.6 Hz), 5.13–5.09 (2H, m), 4.17 (1H, td, *J* = 9.6, 6.4 Hz), 3.31 (1H, app t, *J* = 8.4 Hz), 2.77–2.74 (1H, m), 1.02 (3H, d, *J* = 6.8 Hz); **^{13}C NMR (100 MHz, $CDCl_3$):** δ 154.5 (d, *J* = 4.2), 141.5, 140.1, 133.1 (d, *J* = 126.5 Hz), 132.5 (d, *J* = 9.3 Hz), 132.2 (d, *J* = 129.9 Hz), 131.9 (d, *J* = 2.6 Hz), 131.9 (d, *J* = 10.2 Hz), 131.7 (d, *J* = 3.4 Hz), 128.6 (d, *J* = 12.7 Hz), 128.3 (d, *J* = 12.7 Hz), 116.7, 110.2, 107.6, 53.4, 42.2 (d, *J* = 5.0 Hz), 16.4; **HRMS (DART)**: Calcd for $C_{21}H_{23}NO_2P$ $[M+H]^+$: 352.14664, Found: 352.14635; **Specific Rotation:** $[\alpha]_D^{21}$ +70.80 (*c* 1.27, $CHCl_3$) for a 84:16 γ/α, 94:6 d.r. and 99:1 e.r. sample; The enantiomeric purity was determined by HPLC analysis in comparison to authentic racemic material (Chiralpak AZ-H, 96:4 hexanes:*i*-PrOH, 0.6 mL/min, 220 nm) t_R: 106 min (major) and 98 min (minor).

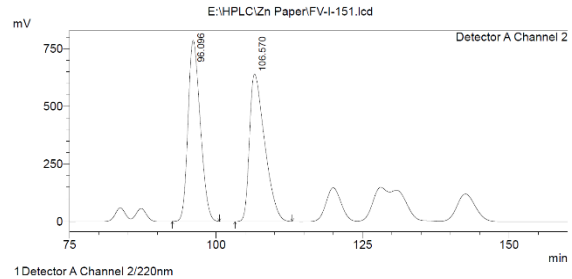

PeakTable

Detector A Channel 2 220nm

Peak#	Ret. Time	Area	Height	Area %
1	96.096	113995706	785505	49.715
2	106.570	115303166	639969	50.285
Total		229298872	1425474	100.000

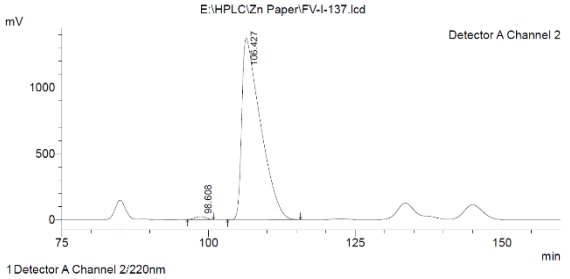

PeakTable

Detector A Channel 2 220nm

Peak#	Ret. Time	Area	Height	Area %
1	98.608	2792418	21701	0.911
2	106.427	303841759	1372878	99.089
Total		306634177	1394579	100.000

Peak #	Ret. Time (min)	Area %	Peak #	Ret. Time (min)	Area %
1	96.096	49.715	1	98.608	0.911
2	106.570	50.285	2	106.427	99.089

***N*-((1*R*,2*R*)-1-(Furan-3-yl)-2-methylbut-3-en-1-yl)-*P*,*P*-diphenylphosphinic amide (1.103) :** Off-white solid; m.p. = 113–116 °C; **IR (neat):** 3167 (w, br), 3074 (w), 1500 (w), 1483 (m), 1184 (s), 1123 (m), 1108 (m), 913 (w), 874 (w), 724 (m), 695 (m), 599 (w), 564 (m), 530 (m) cm^{-1}; **^{1}H NMR (400 MHz, $CDCl_3$):** δ 7.86–7.78 (4H, m), 7.51–7.34 (6H, m), 7.31 (1H, app t, *J* = 2.0 Hz), 7.21–7.20 (1H, m), 6.30–6.29 (1H, m), 5.79 (1H, ddd, *J* = 17.6, 10.0, 7.2 Hz), 5.15–5.09 (2H, m), 4.10 (1H, td, *J* = 9.6, 6.0 Hz), 3.17 (1H, dd, *J* = 8.8, 6.8 Hz), 2.61–2.57 (1H, m), 1.05 (3H, d, *J* = 6.4 Hz); **^{13}C NMR (100 MHz, $CDCl_3$):** δ 143.1, 140.2, 140.0, 133.2 (d, *J* = 129.0 Hz, overlaps with the peak at 132.5), 132.6 (d, *J* = 9.1 Hz), 132.5 (d, *J* = 131.3 Hz, overlaps with the peak at 131.8), 132.0 (d, *J* = 9.1 Hz), 131.9 (d, *J* = 3.1 Hz, overlaps with the peak at 131.8), 131.8 (d, *J* = 3.1 Hz), 128.6 (d, *J* = 12.2 Hz), 128.4 (d, *J* = 12.9 Hz), 127.0 (d, *J* = 4.5 Hz), 116.8, 109.3, 51.8, 44.0 (d, *J* = 5.3 Hz), 16.3; **HRMS (DART):** Calcd for $C_{21}H_{23}NO_2P$ $[M+H]^+$: 352.14664, Found: 352.14572; **Specific Rotation:** $[\alpha]_D^{24}$ +37.99 (*c* 1.49, $CHCl_3$) for a 96:4 γ/α, 96:4 d.r. and 98:2 e.r. sample; The enantiomeric purity was determined by HPLC analysis in comparison to authentic racemic material (Chiralpak AD-H, 97:3 hexanes:*i*PrOH, 0.6 mL/min, 220 nm) t_R: 128 min (major) and 78 min (minor).

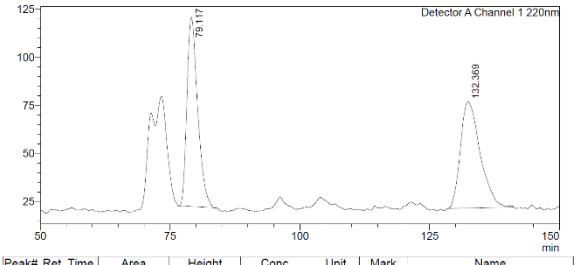

Peak#	Ret. Time	Area	Height	Conc.	Unit	Mark	Name
1	79.117	14164962	98354	49.326		M	
2	132.369	14552188	55362	50.674		M	
Total		28717150	153716				

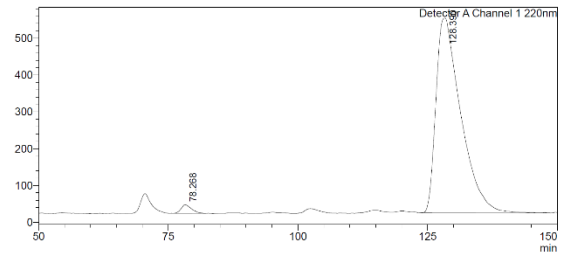

Peak#	Ret. Time	Area	Height	Conc.	Unit	Mark	Name
1	78.268	3232032	23234	1.805		M	
2	128.390	175871523	528534	98.195		M	
Total		179103555	551767				

Peak #	Ret. Time (min)	Area %	Peak #	Ret. Time (min)	Area %
1	79.117	49.326	1	78.268	1.805
2	132.369	50.674	2	128.390	98.195

***N*-((1*R*,2*R*)-2-Methyl-1-(thiophen-2-yl)but-3-en-1-yl)-*P*,*P*-diphenylphosphinic amide (1.104):** Off-white solid; m.p. = 126–128 °C; **IR (neat):** 3148 (w, br), 1436 (m), 1186 (s), 1124 (m), 1107 (m), 748 (m), 726 (m), 694 (s), 543 (w), 530 (m) cm^{-1}; **^{1}H NMR (400 MHz, $CDCl_3$):** δ 7.89–7.74 (4H, m), 7.51–7.39 (4H, m), 7.32–7.28 (2H, m), 7.15 (1H, dd, *J* = 5.2, 1.2 Hz), 6.83 (1H, dd, *J* = 4.8, 3.6 Hz), 6.74 (1H, d, *J* = 3.6 Hz), 5.84 (1H, ddd, *J* = 17.6, 10.4, 7.2 Hz), 5.17–5.12 (2H, m), 4.41 (1H, td, *J* = 10.0, 6.4 Hz), 3.34 (1H, app t, *J* = 6.8 Hz), 2.72–2.64 (1H, m), 1.09 (3H, d, *J* = 6.8 Hz); **^{13}C NMR (100 MHz, $CDCl_3$):** δ 147.4 (d, *J* = 4.2 Hz), 139.6, 133.2 (d, *J* = 127.3 Hz), 132.6 (d, *J* = 9.3 Hz), 132.0 (d, *J* = 4.2 Hz, overlaps with peak at 132.0), 132.0 (d, *J* = 9.2 Hz) 131.9 (d, *J* = 130.7 Hz), 131.7 (d, *J* = 3.3 Hz), 128.6 (d, *J* = 12.6 Hz), 128.3 (d, *J* = 12.6 Hz), 126.6, 125.0, 124.0, 117.2, 55.6, 45.8 (d, *J* = 4.2 Hz), 16.7; **HRMS (DART):** Calcd for $C_{21}H_{23}NOPS$ $[M+H]^+$: 368.12380, Found: 368.12446; **Specific Rotation:** $[\alpha]_D^{24}$ +34.00

(*c* 1.76, $CHCl_3$) for a 98:2 γ/α, 93:7 d.r. and 96:4 e.r. sample; The enantiomeric purity was determined by HPLC analysis in comparison to authentic racemic material (Chiralpak AD-H, 96:4 hexanes:*i*PrOH, 0.6 mL/min, 220 nm) t_R: 68 min (major) and 55 min (minor).

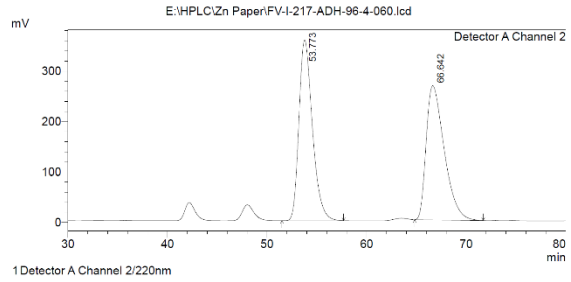

PeakTable

Detector A Channel 2 220nm

Peak#	Ret. Time	Area	Height	Area %
1	53.773	33706775	358311	50.156
2	66.642	33496886	266038	49.844
Total		67203660	624349	100.000

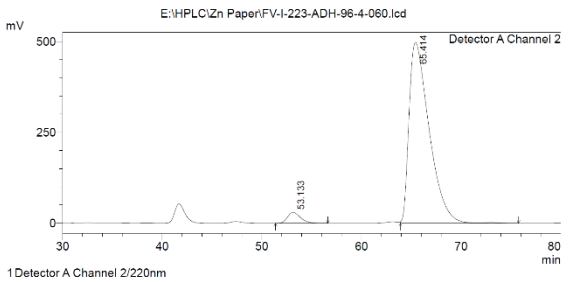

PeakTable

Detector A Channel 2 220nm

Peak#	Ret. Time	Area	Height	Area %
1	53.133	2789808	30171	3.824
2	65.414	70164783	498370	96.176
Total		72954591	528540	100.000

Peak #	Ret. Time (min)	Area %	Peak #	Ret. Time (min)	Area %
1	53.773	50.156	1	53.133	3.824
2	66.642	49.844	2	65.414	96.176

***N*-((1*R*,2*R*)-2-Methyl-1-(thiophen-3-yl)but-3-en-1-yl)-*P*,*P*-diphenylphosphinic amide (1.105):** Off-white solid; m.p. = 130–132 ℃; **IR (neat):** 3158 (m, br), 1436 (m), 1183 (s), 1124 (m), 1108 (m), 1083 (w), 1067 (w), 912 (w), 746 (m), 724 (m), 694 (m), 658 (w), 561 (m), 530 (m) cm^{-1}; **^{1}H NMR (400 MHz, $CDCl_3$):** δ 7.83–7.78 (2H, m), 7.73–7.68 (2H, m), 7.50–7.46 (1H, m), 7.43–7.38 (3H, m), 7.32–7.27 (2H, m), 7.20–7.18 (1H, m), 6.94–6.92 (2H, m), 5.79 (1H, ddd, *J* = 18.0, 10.8, 7.6 Hz), 5.15–5.09 (2H, m), 4.22 (1H, ddd, *J* = 9.6, 6.8 Hz), 3.29 (1H, app t, *J* = 7.2 Hz), 2.61 (1H, ddq, *J* = 13.2, 6.4 Hz), 1.02 (3H, d, *J* = 6.8 Hz); **^{13}C NMR (100 MHz, $CDCl_3$):** δ 143.8 (d, *J* = 4.2 Hz), 140.2, 133.3

(d, J = 127 Hz), 132.6 (d, J = 9.2 Hz), 132.2 (d, J = 130 Hz), 131.87 (d, J = 2.6 Hz), 131.85 (d, J = 9.3 Hz), 131.65 (d, J = 2.6 Hz), 128.55 (d, J = 12.6 Hz), 128.24 (d, J = 12.7 Hz), 126.3, 125.7, 122.0, 116.8, 55.6, 44.9 (d, J = 5.9 Hz), 16.8; **HRMS (DART):** Calcd for $C_{21}H_{23}NOPS$ $[M+H]^+$: 368.1238, Found: 368.1243; **Specific Rotation:** $[\alpha]_D^{23}$ = +62.44 (c = 1.76, $CHCl_3$) for a 94:6 γ:α, 94:6 d.r. and 98:2 e.r. sample; The enantiomeric purity was determined by HPLC analysis in comparison to authentic racemic material (Chiralpak AZ-H, 97:3 hexanes:*i*PrOH, 0.6 mL/min, 220 nm) t_R : 83 min (major) and 56 min (minor).

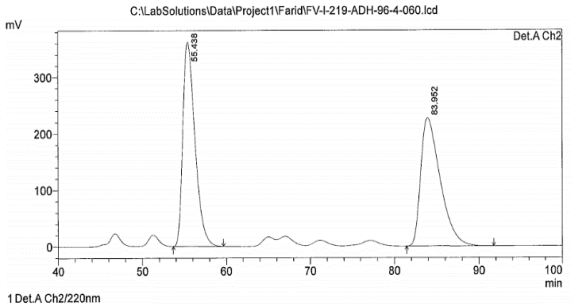

PeakTable

Detector A Ch2 220nm

Peak#	Ret. Time	Area	Height	Area %
1	55.438	36218964	361995	49.818
2	83.952	36484065	226987	50.182
Total		72703028	588982	100.000

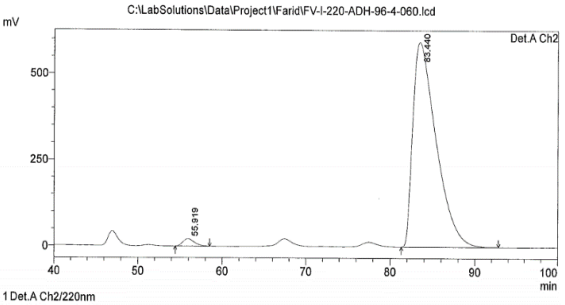

PeakTable

Detector A Ch2 220nm

Peak#	Ret. Time	Area	Height	Area %
1	55.919	2000472	21144	1.741
2	83.440	112907839	593470	98.259
Total		114908311	614615	100.000

Peak #	Ret. Time (min)	Area %	Peak #	Ret. Time (min)	Area %
1	55.438	49.818	1	55.919	1.741
2	83.952	50.182	2	83.440	98.259

***N*-((1*R*,2*R*)-2-Methyl-1-(pyridin-3-yl)but-3-en-1-yl)-*P*,*P*-diphenylphosphinic amide (1.106):** White solid; m.p. = 137–141 °C; **IR (neat):** 3177 (w, br), 2962 (w), 2926 (w), 2871 (w), 1438 (m), 1184 (s), 1122 (s), 1109 (s), 909 (m), 751 (m), 724 (s), 697 (s), 540

(s) cm^{-1}; **^{1}H NMR (600 MHz, $CDCl_3$):** δ 8.40 (1H, d, *J* = 4.8 Hz), 8.32 (1H, s), 7.80 (2H, dd, *J* = 11.4, 7.8 Hz), 7.63 (2H, dd, *J* =11.4, 7.8 Hz), 7.49 (1H, t, *J* = 7.8 Hz), 7.45–7.40 (3H, m), 7.34 (1H, t, *J* = 7.8 Hz), 7.24 (2H, td, *J* = 7.8, 3.0 Hz), 7.12 (1H, dd, *J* = 7.2, 4.2 Hz), 5.78 (1H, ddd, *J* = 17.4, 9.6, 7.2 Hz), 5.20–5.12 (2H, m), 4.11 (1H, dt, *J* = 10.2, 7.8 Hz), 3.45 (1H, t, *J* = 6.6 Hz), 2.57–2.53 (1H, m), 0.98 (3H, d, *J* = 6.6 Hz); **^{13}C NMR (100 MHz, $CDCl_3$):** δ 149.1, 148.5, 139.5, 137.9 (d, *J* = 2.3 Hz), 135.0, 132.8 (d, *J* = 128.3 Hz, overlaps with peak at 132.1), 132.5 (d, *J* = 9.1 Hz), 132.1 (d, *J* = 3.0 Hz), 131.8 (d, *J* = 130 Hz), 131.8 (d, *J* = 9.1 Hz), 131.8 (d, *J* = 3.1 Hz), 128.7 (d, *J* = 12.9 Hz), 128.3 (d, *J* = 12.1 Hz), 123.0, 117.6, 57.3 (d, *J* =1.5 Hz), 45.6 (d, *J* = 6.1 Hz), 17.1; **HRMS (DART):** Calcd for $C_{22}H_{24}N_2OP$ $[M+H]^+$: 363.1626, Found: 363.1625; **Specific Rotation:** $[\alpha]_D^{24}$ +50.74 (*c* 1.50, $CHCl_3$) for a 95:5 γ/α, 95:5 d.r. and 98:2 e.r. sample; The enantiomeric purity was determined by HPLC analysis in comparison to authentic racemic material (Chiralpak AZ-H, 94:6 hexanes:*i*PrOH, 0.6 mL/min, 220 nm) t_R: 407 min (major) and 367 min (minor).

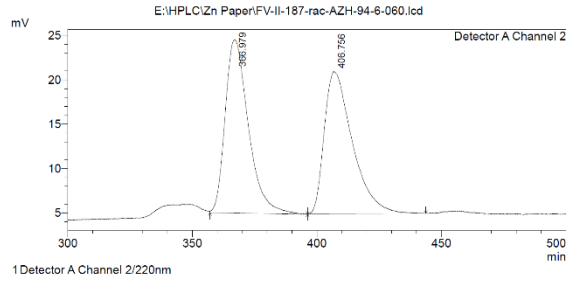

PeakTable

Detector A Channel 2 220nm

Peak#	Ret. Time	Area	Height	Area %
1	366.979	12673357	19551	50.277
2	406.756	12533913	16058	49.723
Total		25207270	35608	100.000

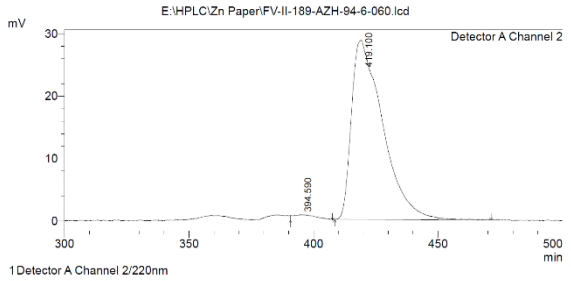

PeakTable

Detector A Channel 2 220nm

Peak#	Ret. Time	Area	Height	Area %
1	394.590	588336	882	2.289
2	419.100	25118836	28731	97.711
Total		25707172	29613	100.000

Peak #	Ret. Time (min)	Area %	Peak #	Ret. Time (min)	Area %
1	366.695	49.591	1	386.086	1.675
2	406.742	50.409	2	419.026	96.571

***N*-((3*R*,4*S*,*E*)-3-Methylnona-1,5-dien-4-yl)-*P*,*P*-diphenylphosphinic amide (1.107):** White solid; m.p. = 87–90 °C; **IR (neat):** 3176 (w, br), 2958 (w), 2925 (w), 1436 (m), 1186 (s), 1123 (m), 1108 (m), 1057 (w), 969 (w), 724 (m), 694 (m), 540 (m) cm^{-1}; **^{1}H NMR (400 MHz, $CDCl_3$):** δ 7.93–7.81 (4H, m), 7.50–7.38 (6H, m), 5.77 (1H, ddd, *J* = 16.8, 10.8, 7.6 Hz), 5.45–5.38 (1H, m), 5.32–5.26 (1H, m), 5.10–5.04 (2H, m), 3.57–3.50 (1H, m), 2.97 (1H, app t, *J* = 8.4 Hz), 2.42–2.34 (1H, m), 1.89 (2H, dd, *J* = 14.0, 6.8 Hz), 1.32–1.27 (2H, m), 1.02 (3H, d, *J* = 6.8 Hz), 0.84 (3H, t, *J* = 7.6 Hz); **^{13}C NMR (100 MHz, $CDCl_3$):** δ 140.6, 133.7 (d, *J* = 127.3 Hz), 133.3 (d, *J* = 128.2 Hz, overlaps with peak at 132.6), 132.8, 132.7 (d, *J* = 9.3 Hz), 132.0 (d, *J* = 9.3 Hz), 131.7 (d, *J* = 2.5 Hz), 131.7 (d, *J* = 2.5 Hz), 130.3 (d, *J* = 4.2 Hz), 128.5 (d, *J* = 12.1 Hz), 128.4 (d, *J* = 12.6 Hz), 116.1, 57.8, 44.0 (d, *J* = 5.9 Hz), 34.4, 22.4, 15.8, 13.8; **HRMS (DART):** Calcd for $C_{22}H_{29}NOP$ $[M+H]^+$: 354.19868, Found: 354.19808; **Specific Rotation:** $[\alpha]_D^{24}$ –3.23 (*c*

0.43, $CHCl_3$) for a 92:8 γ/α, 88:12 d.r. and 96:4 e.r. sample; The enantiomeric purity was determined by HPLC analysis in comparison to authentic racemic material (Chiralpak AD-H, 96:4 hexanes:*i*PrOH, 0.6 mL/min, 220 nm) t_R: 34 min (major) and 25 min (minor).

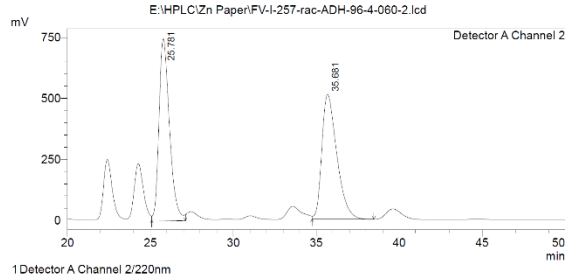

Peak Table

Detector A Channel 2 220nm

Peak#	Ret. Time	Area	Height	Area %
1	25.781	32768667	745909	50.506
2	35.681	32111920	512366	49.494
Total		64880586	1258275	100.000

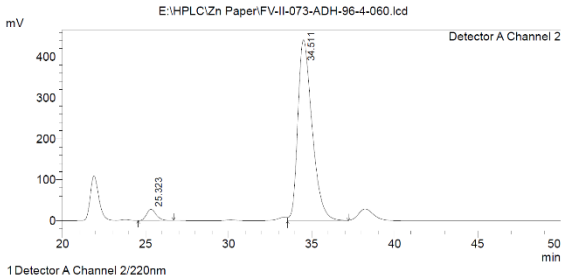

Peak Table

Detector A Channel 2 220nm

Peak#	Ret. Time	Area	Height	Area %
1	25.323	1081537	27314	3.911
2	34.511	26571292	441937	96.089
Total		27652829	469251	100.000

Peak #	Ret. Time (min)	Area %	Peak #	Ret. Time (min)	Area %
1	26.215	50.506	1	25.323	3.911
2	36.638	49.494	2	34.511	96.089

***N*-((3*S*,4*R*)-4-Methyl-1-phenylhex-5-en-3-yl)-*P*,*P*-diphenylphosphinic amide (1.108):** Off-white solid; m.p. = 91–94 °C; **IR (neat):** 3184 (w, br), 2924 (w), 1437 (m), 1185 (s), 1121 (s), 1109 (s), 909 (m), 722 (s), 696 (s), 593 (w), 533 (s) cm^{-1}; **^{1}H NMR (400 MHz, $CDCl_3$):** δ 7.96–7.86 (4H, m), 7.53–7.42 (6H, m), 7.23 (2H, d, *J* =7.6 Hz), 7.17–7.12 (3H, m), 5.77 (1H, ddd, *J* = 17.6, 10.4, 6.8 Hz), 5.11–5.03 (2H, m), 3.12-3.03 (1H, m), 2.81–2.71 (1H, m), 2.66–2.59 (1H, m), 2.66–2.59 (1H, m), 1.91–1.76 (1H, m), 1.06 (3H, d, *J* = 7.2 Hz); **^{13}C NMR (150 MHz, $CDCl_3$):** δ 142.0, 139.7, 133.2 (d, *J* = 129 Hz), 133.1 (d, *J* = 128 Hz), 132.4 (d, *J* = 8.9 Hz), 132.3 (d, *J* = 8.9 Hz), 131.9 (d, *J* = 2.6 Hz), 131.8 (d, *J* = 2.6 Hz), 131.8, 128.6 (d, *J* = 11.4 Hz), 128.4, 128.5 (d, *J* = 10.1 Hz), 125.9,

116.2, 55.6, 41.5 (d, J = 3.8 Hz), 36.2 (d, J = 3.9), 32.5, 15.4; **HRMS (DART):** Calcd for $C_{25}H_{29}NOP$ $[M+H]^+$: 390.19868, Found: 390.19967; **Specific Rotation:** $[\alpha]_D^{24}$ +10.454 (*c* 0.73, $CHCl_3$) for a >98:2 γ/α, 61:39 d.r. and 79:21 e.r. sample; The enantiomeric purity was determined by HPLC analysis in comparison to authentic racemic material (Chiralpak AD-H, 96:4 hexanes:*i*PrOH, 0.6 mL/min, 220 nm) t_R: 39 min (major) and 69 min (minor).

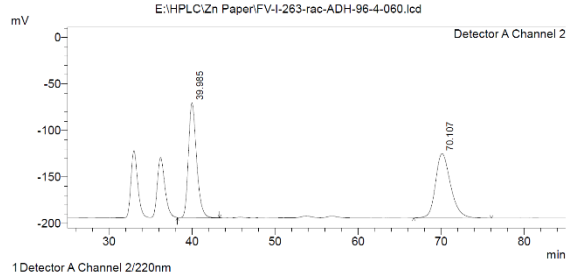

PeakTable
Detector A Channel 2 220nm

Peak#	Ret. Time	Area	Height	Area %
1	39.985	8416593	123361	48.959
2	70.107	8774398	69339	51.041
Total		17190991	192700	100.000

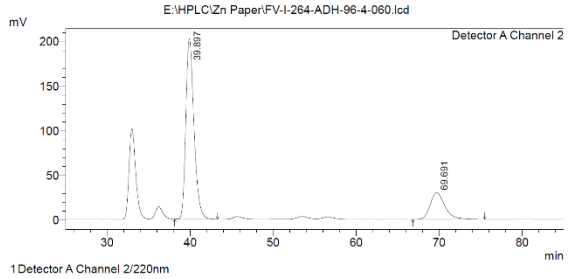

PeakTable
Detector A Channel 2 220nm

Peak#	Ret. Time	Area	Height	Area %
1	39.897	13800591	202321	78.925
2	69.691	3685073	29879	21.075
Total		17485664	232201	100.000

Peak #	Ret. Time (min)	Area %	Peak #	Ret. Time (min)	Area %
1	39.985	48.959	1	39.897	78.925
2	70.107	51.041	2	69.691	21.075

***N*-((1*S*,2*R*)-1-Cyclohexyl-2-methylbut-3-en-1-yl)-*P*,*P*-diphenylphosphinic amide (1.109):** White solid; m.p. = 174–176 °C; **IR (neat):** 3212 (w, br), 2922 (m), 2852 (w), 1436 (m), 1189 (s), 1121 (m), 1109 (m), 1037 (w), 910 (w), 718 (m), 694 (m), 538 (s) cm^{-1}; **^{1}H NMR (400 MHz, $CDCl_3$):** δ 7.93–7.83 (4H, m), 7.51–7.39 (6H, m), 5.83 (1H, ddd, J = 17.2, 10.0, 6.8 Hz), 5.09–5.02 (2H, m), 2.81–2.73 (1H, m), 2.68–2.63 (1H, m), 2.52–2.43 (1H, m), 1.85–1.56 (6H, m), 1.47–1.36 (1H, m), 1.23–1.10 (4H, m), 1.01 (3H,

d, J = 6.8 Hz); **^{13}C NMR (100 MHz, CDCl3):** δ 140.8, 133.5 (d, J = 129 Hz), 133.4 (d, J = 129 Hz), 132.5 (d, J = 9.3 Hz), 132.4 (d, J = 9.2 Hz), 131.8 (d, J = 2.5 Hz), 131.7 (d, J = 2.5 Hz), 128.4 (d, J = 12.9 Hz), 128.3 (d, J = 11.8 Hz), 115.7, 60.9 (d, J = 2.5 Hz), 42.3 (d, J = 3.4 Hz), 40.5 (d, J = 5.0 Hz), 30.9, 29.4, 26.7, 26.6, 26.5, 17.6; **HRMS (DART):** Calcd for $C_{23}H_{31}NOP$ $[M+H]^+$: 368.21433, Found: 368.21578; **Specific Rotation:** $[\alpha]_D^{24}$ +3.220 (*c* 0.825, $CHCl_3$) for a >98:2 γ/α, 84:16 d.r. and 67:33 e.r. sample; The enantiomeric purity was determined by HPLC analysis in comparison to authentic racemic material (Chiralpak AD-H, 96:4 hexanes:*i*PrOH, 0.6 mL/min, 220 nm) t_R: 40 min (major) and 29 min (minor).

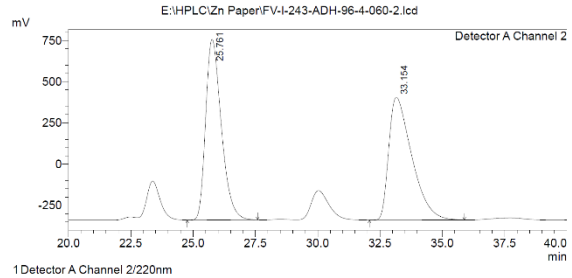

PeakTable
Detector A Channel 2 220nm

Peak#	Ret. Time	Area	Height	Area %
1	25.761	47877882	1095459	50.045
2	33.154	47792538	744707	49.955
Total		95670421	1840166	100.000

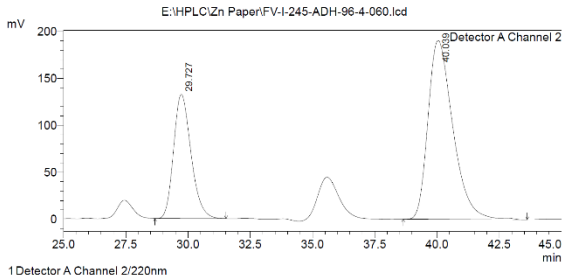

PeakTable
Detector A Channel 2 220nm

Peak#	Ret. Time	Area	Height	Area %
1	29.727	6441705	132144	32.726
2	40.039	13242038	190379	67.274
Total		19683743	322523	100.000

Peak #	Ret. Time (min)	Area %	Peak #	Ret. Time (min)	Area %
1	25.761	50.045	1	29.727	32.726
2	33.154	49.955	2	40.039	67.274

***N*-((1*R*,2*S*)-1,2-Diphenylbut-3-en-1-yl)-*P*,*P*-diphenylphosphinic amide (1.110):** White solid; m.p. = 208–209 °C; **IR (neat):** 3211 (w, br), 3058 (w), 3027 (w), 1435 (w), 1181 (m), 1107 (m), 750 (m), 722 (m), 693 (s), 532 (s) cm^{-1}; **^{1}H NMR (400 MHz, $CDCl_3$):** δ

7.67–7.56 (4H, m), 7.50–7.44 (1H, m), 7.40–7.34 (3H, m), 7.28–7.20 (5H, m), 7.19–7.13 (3H, m), 7.02–6.98 (2H, m), 6.88–6.84 (2H, m), 6.03 (1H, ddd, *J* = 19.6, 10.0, 9.2 Hz), 5.16–5.10 (2H, m), 4.46 (1H, td, *J* = 10.0, 6.4 Hz), 3.82 (1H, dd, *J* = 9.2, 6.4 Hz), 3.45 (1H, dd, *J* = 10.0, 6.4 Hz); **^{13}C NMR (100 MHz, $CDCl_3$):** δ 140.8 (d, *J* = 3.8 Hz), 140.4, 136.6, 133.1 (d, *J* = 127 Hz), 132.5 (d, *J* = 9.9 Hz), 132.2 (d, *J* = 131 Hz), 131.8 (d, *J* = 3.0 Hz, peaks overlapped at 131.8), 131.8 (d, *J* = 9.1 Hz, peaks overlapped at 131.8), 131.7 (d, *J* = 3.0 Hz), 128.8, 128.5, 128.5 (d, *J* = 12.1 Hz), 128.2 (d, *J* = 12.9 Hz), 127.9, 127.7, 127.2, 127.0, 118.6, 59.7, 58.1 (d, *J* = 4.5 Hz); **HRMS (DART):** Calcd for $C_{28}H_{27}NOP$ $[M+H]^+$: 424.18378, Found: 424.18303; **Specific Rotation:** $[\alpha]_D^{21}$ +10.0 (*c* 1.00, $CHCl_3$) for a >98:2 γ/α, 95:5 d.r. and 94:6 e.r. sample; The enantiomeric purity was determined by HPLC analysis in comparison to authentic racemic material (Chiralpak AZ-H, 96:4 hexanes:*i*PrOH, 1.0 mL/min, 220 nm) t_R: 95 min (major) and 62 min (minor).

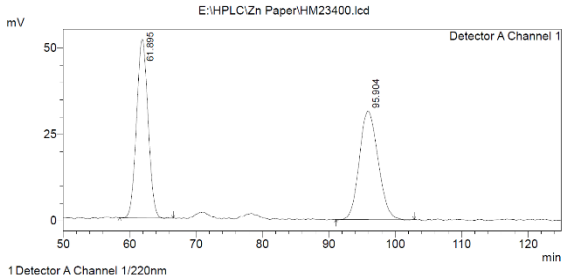

PeakTable

Detector A Channel 1 220nm

Peak#	Ret. Time	Area	Height	Area %	Height %
1	61.895	6215684	51692	50.268	62.150
2	95.904	6149433	31481	49.732	37.850
Total		12365117	83173	100.000	100.000

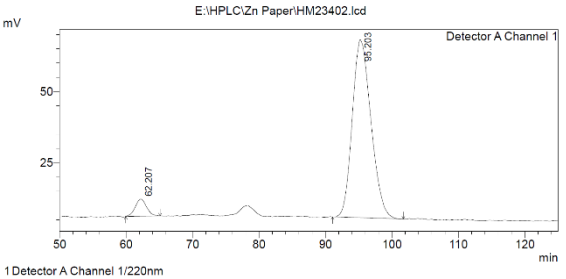

PeakTable

Detector A Channel 1 220nm

Peak#	Ret. Time	Area	Height	Area %	Height %
1	62.207	703226	6001	5.440	8.764
2	95.203	12224075	62467	94.560	91.236
Total		12927300	68468	100.000	100.000

Peak #	Ret. Time (min)	Area %	Peak #	Ret. Time (min)	Area %
1	61.895	50.268	1	62.207	5.440
2	95.904	49.732	2	95.203	94.560

***N*-((1*S*,2*R*)-2-Chloro-1-phenylbut-3-en-1-yl)-*P*,*P*-diphenylphosphinic amide (1.111):**

White solid; m.p. = 135–137 °C; **IR (neat):** 3161 (w, br), 3058 (w), 1456 (w), 1437 (m), 1181 (s), 1124 (m), 1108 (m), 928 (w), 748 (w), 725 (m), 695 (s), 535 (m) cm^{-1}; **^{1}H NMR (400 MHz, $CDCl_3$):** δ 7.90 – 7.81 (m, 2H), 7.76 – 7.68 (m, 2H), 7.55 – 7.48 (m, 1H), 7.48 – 7.39 (m, 3H), 7.34 – 7.27 (m, 5H), 7.20 (dd, *J* = 6.7, 3.0 Hz, 2H), 5.54 (ddd, *J* = 16.8, 10.1, 8.2 Hz, 1H), 5.33 (dd, *J* = 16.9, 1.3 Hz, 1H), 5.15 (dd, *J* = 10.2, 1.1 Hz, 1H), 4.98 (dd, *J* = 8.3, 4.0 Hz, 1H), 4.50 (td, *J* = 10.8, 4.1 Hz, 1H), 4.00 (dd, *J* = 11.1, 7.0 Hz, 1H).; **^{13}C NMR (100 MHz, $CDCl_3$):** δ 138.1 (d, *J* = 5.3 Hz), 135.1, 132.8 (d, *J* = 127 Hz), 132.7 (d, *J* = 9.9 Hz), 132.2 (d, *J* = 2.2 Hz), 132.0 (d, *J* = 2.3 Hz), 131.8 (d, *J* = 9.8 Hz) 131.7 (d, *J* = 131 Hz), 128.7 (d, *J* = 12.9 Hz), 128.5 (d, *J* = 12.2 Hz), 128.2, 128.1, 128.0, 119.2, 69.3 (d, *J* = 3.8 Hz), 59.0; **HRMS (DART):** Calcd for $C_{22}H_{21}ClNOP$ $[M+H]^+$: 382.11275, Found: 382.11295; **Specific Rotation:** $[\alpha]_D^{20}$ +29.2 (*c* 1.25, $CHCl_3$) for a 91:9 γ/α, 95:5 d.r. and 92:8 e.r. sample; The enantiomeric purity was determined by HPLC analysis in comparison to authentic racemic material (Chiralpak AD-H, 96:4 hexanes:*i*PrOH, 0.7 mL/min, 220 nm) t_R: 136 min (major) and 85 min (minor).

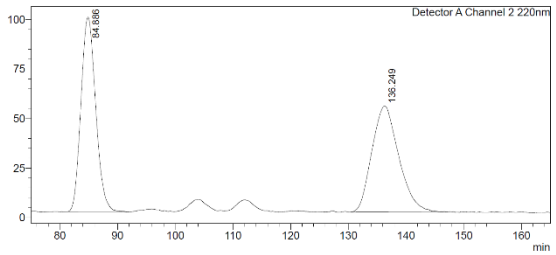

<Peak Table>
Detector A Channel 2 220nm

Peak#	Ret. Time	Area	Height	Conc.	Unit	Mark	Name
1	84.886	17438667	98193	50.203		M	
2	136.249	17297622	53528	49.797		M	
Total		34736289	151721				

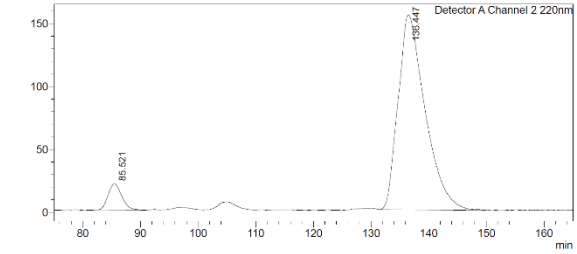

<Peak Table>
Detector A Channel 2 220nm

Peak#	Ret. Time	Area	Height	Conc.	Unit	Mark	Name
1	85.521	3403793	20975	6.326		M	
2	136.447	50398995	154776	93.674		M	
Total		53802788	175751				

Peak #	Ret. Time (min)	Area %	Peak #	Ret. Time (min)	Area %
1	84.866	50.203	1	85.521	6.326
2	136.249	49.797	2	136.447	93.674

1.7.4. *DFT Calculations*

DFT calculations were performed with the Gaussian 09 suite of programs[7] employing the dispersion corrected ωB97XD functional.[8] The Def2SVP[9] basis set and the SMD[10] solvation model (toluene) was used for geometry optimization and frequency calculation.

(7) Frisch, M. J.; Trucks, G. W.; Schlegel, H. B.; Scuseria, G. E.; Robb, M. A.; Cheeseman, J. R.; Scalmani, G.; Barone, V.; Mennucci, B.; Petersson, G. A.; Nakatsuji, H.; Caricato, M.; Li, X.; Hratchian, H. P.; Izmaylov, A. F.; Bloino, J.; Zheng, G.; Sonnenberg, J. L.; Hada, M.; Ehara, M.; Toyota, K.; Fukuda, R.; Hasegawa, J.; Ishida, M.; Nakajima, T.; Honda, Y.; Kitao, O.; Nakai, H.; Vreven, T.; Montgomery, Jr., J. A.; Peralta, J. E.; Ogliaro, F.; Bearpark, M.; Heyd, J. J.; Brothers, E.; Kudin, K. N.; Staroverov, V. N.; Kobayashi, R.; Normand, J.; Raghavachari, K.; Rendell, A.; Burant, J. C.; Iyengar, S. S.; Tomasi, J.; Cossi, M.; Rega, N.; Millam, J. M.; Klene, M.; Knox, J. E.; Cross, J. B.; Bakken, V.; Adamo, C.; Jaramillo, J.; Gomperts, R.; Stratmann, R. E.; Yazyev, O.; Austin, A. J.; Cammi, R.; Pomelli, C.; Ochterski, J. W.; Martin, R. L.; Morokuma, K.; Zakrzewski, V. G.; Voth, G. A.; Salvador, P.; Dannenberg, J. J.; Dapprich, S.; Daniels, A. D.; Farkas, Ö.; Foresman, J. B.; Ortiz, J. V.; Cioslowski, J.; Fox, D. J. Gaussian 09, Revision D.01, Gaussian, Inc., Wallingford CT, 2009.

(8) Chai, J.-D.; Head-Gordon, M. *Phys. Chem. Chem. Phys.*, **2008**, *10*, 6615.

(9) Weigend, F.; Ahlrichs, R.; *Phys. Chem. Chem. Phys*. **2005**, *7*, 3297−3305.

(10) Marenich, A. V.; Cramer, C. J.; Truhlar, D. G. *J. Phys. Chem. B*, **2009**, *113*, 6378−6396.

The nature of all stationary points was checked through vibrational analysis. Single point electronic energy (ΔE_{sp}) calculations applying the ωB97XD functional and the Def2TZVPP[8] basis set in solution with the SMD solvation model were performed on the geometries obtained with the Def2SVP basis set. The single point electronic energies (ΔE_{sp}) at the Def2TZVPP level were corrected by addition of thermal corrections to the Gibbs free energy (ΔG_{corr}) obtained at the corresponding Def2SVP level. Tables of electronic and free energies and single point energies are given below.

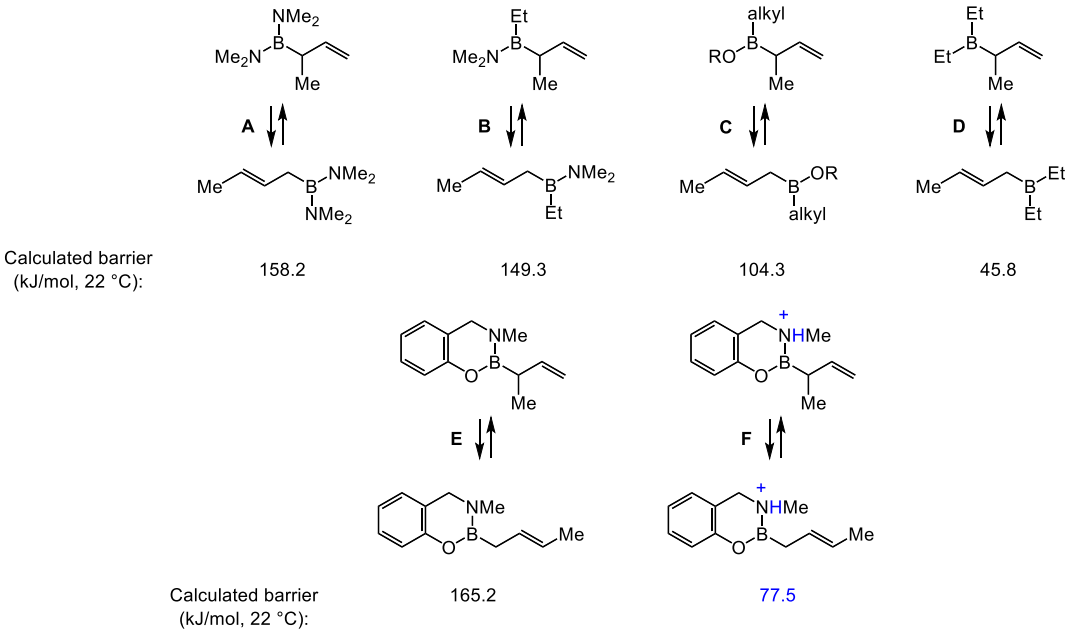

***Scheme S1.1*:** Energy barriers for borotropic rearrangement

Table S1.1: Borotropic rearrangement energies and Gibbs free energies calculated with ωB97XD/Def2SVP, calculations were carried out in toluene with the SMD solvation model.

Structure	**E [Hartree]**	**ΔE [kcal/mol]**	**G [Hartree]**	**ΔG [kcal/mol]**	**ΔG_{corr} [kcal/mol]**	**Freq [cm^{-1}]**
A-gs	-450.23365580	0.00	-450.002578	0.00	0.00	46.97
A-ts	-450.17572772	36.35	-449.945105	36.06	-0.29	-378.74
B-gs	-394.92607219	0.00	-394.712044	0.00	0.00	34.03
B-ts	-394.87260447	33.55	-394.657733	34.08	0.53	-286.43
C-gs	-375.50579463	0.00	-375.330809	0.00	0.00	42.65
C-ts	-375.47124946	21.68	-375.294301	22.91	1.23	-216.63
D-gs	-339.59587263	0.00	-339.398483	0.00	0.00	35.60
D-ts	-339.58455040	7.10	-339.384068	9.05	1.94	-191.59
E-gs	-621.18511508	0.00	-620.9629	0.00	0.00	31.50
E-ts	-621.12547954	37.42	-620.903271	37.42	0.00	-379.55
F-gs	-621.58799325	0.00	-621.349225	0.00	0.00	47.47
F-ts	-621.56245890	16.02	-621.323154	16.36	0.34	-297.62

***Table S1.2*:** Borotropic rearrangement single point energies calculated with ωB97XD/Def2TZVPP//Def2SVP, calculations were carried out in toluene with the SMD model.

Structure	E_{sp} [Hartree]	ΔE_{sp} [kcal/mol]	ΔG_{sp} [kcal/mol]	ΔG_{sp} [kJ/mol]
A-gs	-450.72099443	0.00	0.00	0.0
A-ts	-450.66028826	38.09	37.81	158.2
B-gs	-395.35272601	0.00	0.00	0.0
B-ts	-395.29668547	35.17	35.70	149.3
C-gs	-375.91776528	0.00	0.00	0.0
C-ts	-375.88002028	23.69	24.92	104.3
D-gs	-339.96164138	0.00	0.00	0.0
D-ts	-339.94728282	9.01	10.95	45.8
E-gs	-621.85190065	0.00	0.00	0.0
E-ts	-621.78898039	39.48	39.48	165.2
F-gs	-622.25598199	0.00	0.00	0.0
F-ts	-622.22698208	18.20	18.53	77.5

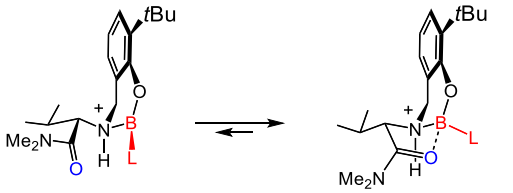

***R*-allyl** **ΔG = 0 kcal/mol**

***R*-allyl'** **ΔG = -75.6 kJ/mol**

***Scheme S1.2*:** Preference for carbonyl bound species.

***Table S1.3*:** Ground state energies and Gibbs free energies for ***R*-allyl** and ***R*-allyl'** calculated with ωB97XD/Def2SVP, calculations were carried out in toluene with the SMD solvation model.

Structure	**E [Hartree]**	**ΔE [kcal/mol]**	**G [Hartree]**	**ΔG [kcal/mol]**	**ΔG_{corr} [kcal/mol]**	**Freq [cm^{-1}]**
***R*-allyl**	-1260.23766903	0.00	-1259.669967	0.00	0.00	24.02
***R*-allyl'**	-1260.27575595	-23.90	-1259.701591	-19.84	4.06	43.16

***Table S1.4*:** Ground state single point energies for ***R*-allyl** and ***R*-allyl'** calculated with ωB97XD/Def2TZVPP//Def2SVP, calculations were carried out in toluene with the SMD model.

Structure	**E_{sp} [Hartree]**	**ΔE_{sp} [kcal/mol]**	**ΔG_{sp} [kcal/mol]**	**ΔG_{sp} [kJ/mol]**
***R*-allyl**	-1261.58635767	0.00	0.00	0.0
***R*-allyl'**	-1261.62161470	-22.12	-18.07	-75.6

1.7.5. *Crystallographic Data*

X-ray structure data for compound 1.63:

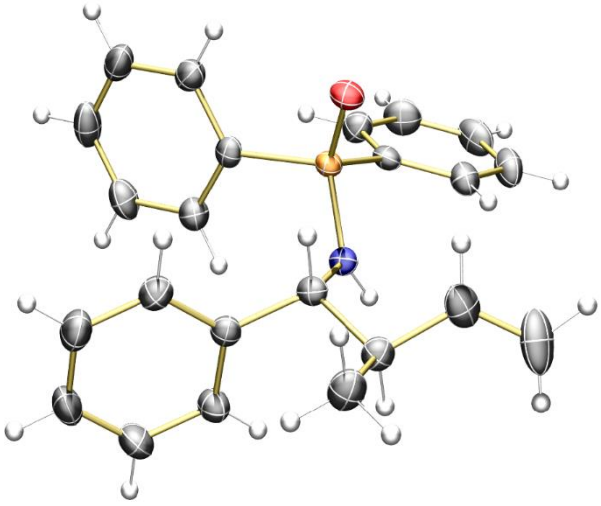

Table S1.5: Crystal data and structure refinement for **1.63**.

Identification code	C23H24NOP	
Empirical formula	C23 H24 N O P	
Formula weight	361.40	
Temperature	100(2) K	
Wavelength	1.54178 Å	
Crystal system	Orthorhombic	
Space group	P2(1) 2(1) 2(1)	
Unit cell dimensions	a = 10.2191(4) Å	α= 90°.
	b = 10.3468(4) Å	β= 90°.
	c = 38.1838(15) Å	γ = 90°.
Volume	4037.4(3) $Å^3$	
Z	8	
Density (calculated)	1.189 Mg/m^3	
Absorption coefficient	1.276 mm^{-1}	
F(000)	1536	
Crystal size	0.28 x 0.25 x 0.06 mm^3	
Theta range for data collection	4.43 to 69.20°.	
Index ranges	-11<=h<=11, -12<=k<=9, -44<=l<=44	
Reflections collected	29528	

Independent reflections	6927 [R(int) = 0.0263]
Completeness to theta = 66.50°	97.5 %
Absorption correction	Semi-empirical from equivalents
Max. and min. transmission	0.9274 and 0.7164
Refinement method	Full-matrix least-squares on F^2
Data / restraints / parameters	6927 / 0 / 469
Goodness-of-fit on F^2	1.060
Final R indices [I>2sigma(I)]	R1 = 0.0271, wR2 = 0.0713
R indices (all data)	R1 = 0.0275, wR2 = 0.0719
Absolute structure parameter	0.004(11)
Extinction coefficient	na
Largest diff. peak and hole	0.334 and -0.238 e.$Å^{-3}$

Table S1.6: Atomic coordinates ($x10^4$) and equivalent isotropic displacement parameters ($Å^2x10^3$)
for **1.63**. U(eq) is defined as one third of the trace of the orthogonalized U^{ij} tensor.

	x	y	z	U(eq)
P(1)	5297(1)	7119(1)	5233(1)	19(1)
O(1)	6709(1)	7329(1)	5165(1)	28(1)
N(1)	4424(1)	6989(1)	4878(1)	21(1)
C(1)	4531(1)	8423(2)	5472(1)	22(1)
C(2)	4325(2)	9599(2)	5302(1)	29(1)
C(3)	3852(2)	10649(2)	5489(1)	36(1)
C(4)	3582(2)	10528(2)	5840(1)	39(1)
C(5)	3774(2)	9367(2)	6011(1)	39(1)
C(6)	4245(2)	8312(2)	5826(1)	30(1)
C(7)	5084(2)	5715(1)	5509(1)	23(1)
C(8)	6147(2)	5262(2)	5699(1)	31(1)
C(9)	5992(2)	4255(2)	5935(1)	40(1)
C(10)	4776(2)	3712(2)	5986(1)	42(1)
C(11)	3711(2)	4139(2)	5792(1)	37(1)
C(12)	3865(2)	5139(2)	5552(1)	28(1)
C(13)	4871(2)	6155(1)	4590(1)	22(1)
C(14)	4577(2)	6816(2)	4238(1)	26(1)

C(15)	5213(2)	8122(2)	4228(1)	36(1)
C(16)	4708(2)	9175(2)	4093(1)	53(1)
C(17)	5054(2)	5971(2)	3934(1)	36(1)
C(18)	4326(2)	4793(2)	4616(1)	24(1)
C(19)	5161(2)	3748(2)	4656(1)	30(1)
C(20)	4690(2)	2494(2)	4674(1)	38(1)
C(21)	3360(2)	2272(2)	4651(1)	39(1)
C(22)	2512(2)	3303(2)	4614(1)	37(1)
C(23)	2982(2)	4559(2)	4597(1)	30(1)
P(2)	9972(1)	7651(1)	7342(1)	17(1)
O(2)	10160(1)	9048(1)	7416(1)	24(1)
N(2)	9863(1)	6790(1)	7701(1)	19(1)
C(24)	11317(1)	6910(1)	7109(1)	19(1)
C(25)	12500(2)	6718(2)	7283(1)	26(1)
C(26)	13568(2)	6228(2)	7106(1)	30(1)
C(27)	13470(2)	5918(2)	6754(1)	27(1)
C(28)	12307(2)	6111(2)	6578(1)	29(1)
C(29)	11234(2)	6607(2)	6755(1)	24(1)
C(30)	8562(1)	7410(2)	7063(1)	21(1)
C(31)	8041(2)	8445(2)	6879(1)	27(1)
C(32)	7043(2)	8240(2)	6637(1)	33(1)
C(33)	6589(2)	7005(2)	6579(1)	34(1)
C(34)	7080(2)	5972(2)	6769(1)	32(1)
C(35)	8064(2)	6174(2)	7012(1)	25(1)
C(36)	9074(1)	7270(1)	7994(1)	21(1)
C(37)	9775(2)	6987(1)	8343(1)	24(1)
C(38)	11152(2)	7497(2)	8334(1)	31(1)
C(39)	12178(2)	6925(2)	8466(1)	40(1)
C(40)	9027(2)	7599(2)	8647(1)	34(1)
C(41)	7676(2)	6766(2)	7984(1)	22(1)
C(42)	6642(2)	7619(2)	7937(1)	32(1)
C(43)	5361(2)	7176(2)	7926(1)	42(1)
C(44)	5093(2)	5877(2)	7960(1)	36(1)
C(45)	6117(2)	5018(2)	8004(1)	31(1)
C(46)	7396(2)	5457(2)	8016(1)	26(1)

***Table S1.7*:** Bond lengths [Å] and angles [°] for **1.63**.

P(1)-O(1)	1.4820(11)
P(1)-N(1)	1.6298(12)
P(1)-C(1)	1.8068(15)
P(1)-C(7)	1.8083(15)
N(1)-C(13)	1.4705(18)
N(1)-H(1N)	0.8800
C(1)-C(6)	1.387(2)
C(1)-C(2)	1.394(2)
C(2)-C(3)	1.386(2)
C(2)-H(2A)	0.9500
C(3)-C(4)	1.376(3)
C(3)-H(3A)	0.9500
C(4)-C(5)	1.382(3)
C(4)-H(4A)	0.9500
C(5)-C(6)	1.387(2)
C(5)-H(5A)	0.9500
C(6)-H(6A)	0.9500
C(7)-C(8)	1.388(2)
C(7)-C(12)	1.389(2)
C(8)-C(9)	1.387(3)
C(8)-H(8A)	0.9500
C(9)-C(10)	1.378(3)
C(9)-H(9A)	0.9500
C(10)-C(11)	1.389(3)
C(10)-H(10A)	0.9500
C(11)-C(12)	1.391(3)
C(11)-H(11A)	0.9500
C(12)-H(12A)	0.9500
C(13)-C(18)	1.518(2)
C(13)-C(14)	1.539(2)
C(13)-H(13A)	1.0000
C(14)-C(15)	1.500(2)

C(14)-C(17)	1.533(2)
C(14)-H(14A)	1.0000
C(15)-C(16)	1.310(3)
C(15)-H(15A)	0.9500
C(16)-H(16A)	0.9500
C(16)-H(16B)	0.9500
C(17)-H(17A)	0.9800
C(17)-H(17B)	0.9800
C(17)-H(17C)	0.9800
C(18)-C(19)	1.387(2)
C(18)-C(23)	1.396(2)
C(19)-C(20)	1.386(3)
C(19)-H(19A)	0.9500
C(20)-C(21)	1.381(3)
C(20)-H(20A)	0.9500
C(21)-C(22)	1.381(3)
C(21)-H(21A)	0.9500
C(22)-C(23)	1.388(3)
C(22)-H(22A)	0.9500
C(23)-H(23A)	0.9500
P(2)-O(2)	1.4851(10)
P(2)-N(2)	1.6388(11)
P(2)-C(24)	1.8078(15)
P(2)-C(30)	1.8094(15)
N(2)-C(36)	1.4662(18)
N(2)-H(2N)	0.8800
C(24)-C(29)	1.388(2)
C(24)-C(25)	1.394(2)
C(25)-C(26)	1.381(2)
C(25)-H(25A)	0.9500
C(26)-C(27)	1.386(2)
C(26)-H(26A)	0.9500
C(27)-C(28)	1.379(2)
C(27)-H(27A)	0.9500
C(28)-C(29)	1.387(2)

C(28)-H(28A)	0.9500
C(29)-H(29A)	0.9500
C(30)-C(31)	1.388(2)
C(30)-C(35)	1.391(2)
C(31)-C(32)	1.393(2)
C(31)-H(31A)	0.9500
C(32)-C(33)	1.377(3)
C(32)-H(32A)	0.9500
C(33)-C(34)	1.386(3)
C(33)-H(33A)	0.9500
C(34)-C(35)	1.382(2)
C(34)-H(34A)	0.9500
C(35)-H(35A)	0.9500
C(36)-C(41)	1.521(2)
C(36)-C(37)	1.541(2)
C(36)-H(36A)	1.0000
C(37)-C(38)	1.504(2)
C(37)-C(40)	1.526(2)
C(37)-H(37A)	1.0000
C(38)-C(39)	1.305(3)
C(38)-H(38A)	0.9500
C(39)-H(39A)	0.9500
C(39)-H(39B)	0.9500
C(40)-H(40A)	0.9800
C(40)-H(40B)	0.9800
C(40)-H(40C)	0.9800
C(41)-C(42)	1.390(2)
C(41)-C(46)	1.390(2)
C(42)-C(43)	1.387(3)
C(42)-H(42A)	0.9500
C(43)-C(44)	1.378(3)
C(43)-H(43A)	0.9500
C(44)-C(45)	1.383(3)
C(44)-H(44A)	0.9500
C(45)-C(46)	1.384(2)

C(45)-H(45A)	0.9500
C(46)-H(46A)	0.9500

O(1)-P(1)-N(1)	113.46(6)
O(1)-P(1)-C(1)	113.67(7)
N(1)-P(1)-C(1)	104.17(7)
O(1)-P(1)-C(7)	109.73(7)
N(1)-P(1)-C(7)	110.65(7)
C(1)-P(1)-C(7)	104.72(7)
C(13)-N(1)-P(1)	120.06(10)
C(13)-N(1)-H(1N)	120.0
P(1)-N(1)-H(1N)	120.0
C(6)-C(1)-C(2)	119.56(15)
C(6)-C(1)-P(1)	121.38(12)
C(2)-C(1)-P(1)	118.85(12)
C(3)-C(2)-C(1)	119.88(16)
C(3)-C(2)-H(2A)	120.1
C(1)-C(2)-H(2A)	120.1
C(4)-C(3)-C(2)	119.97(17)
C(4)-C(3)-H(3A)	120.0
C(2)-C(3)-H(3A)	120.0
C(3)-C(4)-C(5)	120.79(16)
C(3)-C(4)-H(4A)	119.6
C(5)-C(4)-H(4A)	119.6
C(4)-C(5)-C(6)	119.47(16)
C(4)-C(5)-H(5A)	120.3
C(6)-C(5)-H(5A)	120.3
C(5)-C(6)-C(1)	120.33(16)
C(5)-C(6)-H(6A)	119.8
C(1)-C(6)-H(6A)	119.8
C(8)-C(7)-C(12)	119.74(15)
C(8)-C(7)-P(1)	118.74(13)
C(12)-C(7)-P(1)	121.38(12)
C(9)-C(8)-C(7)	120.23(17)
C(9)-C(8)-H(8A)	119.9

C(7)-C(8)-H(8A)	119.9
C(10)-C(9)-C(8)	120.04(18)
C(10)-C(9)-H(9A)	120.0
C(8)-C(9)-H(9A)	120.0
C(9)-C(10)-C(11)	120.16(16)
C(9)-C(10)-H(10A)	119.9
C(11)-C(10)-H(10A)	119.9
C(10)-C(11)-C(12)	119.92(17)
C(10)-C(11)-H(11A)	120.0
C(12)-C(11)-H(11A)	120.0
C(7)-C(12)-C(11)	119.85(16)
C(7)-C(12)-H(12A)	120.1
C(11)-C(12)-H(12A)	120.1
N(1)-C(13)-C(18)	112.50(12)
N(1)-C(13)-C(14)	109.32(12)
C(18)-C(13)-C(14)	113.43(12)
N(1)-C(13)-H(13A)	107.1
C(18)-C(13)-H(13A)	107.1
C(14)-C(13)-H(13A)	107.1
C(15)-C(14)-C(17)	110.87(14)
C(15)-C(14)-C(13)	109.83(13)
C(17)-C(14)-C(13)	110.21(13)
C(15)-C(14)-H(14A)	108.6
C(17)-C(14)-H(14A)	108.6
C(13)-C(14)-H(14A)	108.6
C(16)-C(15)-C(14)	126.1(2)
C(16)-C(15)-H(15A)	117.0
C(14)-C(15)-H(15A)	117.0
C(15)-C(16)-H(16A)	120.0
C(15)-C(16)-H(16B)	120.0
H(16A)-C(16)-H(16B)	120.0
C(14)-C(17)-H(17A)	109.5
C(14)-C(17)-H(17B)	109.5
H(17A)-C(17)-H(17B)	109.5
C(14)-C(17)-H(17C)	109.5

H(17A)-C(17)-H(17C)	109.5
H(17B)-C(17)-H(17C)	109.5
C(19)-C(18)-C(23)	118.43(16)
C(19)-C(18)-C(13)	120.33(14)
C(23)-C(18)-C(13)	121.24(14)
C(20)-C(19)-C(18)	121.43(17)
C(20)-C(19)-H(19A)	119.3
C(18)-C(19)-H(19A)	119.3
C(21)-C(20)-C(19)	119.66(17)
C(21)-C(20)-H(20A)	120.2
C(19)-C(20)-H(20A)	120.2
C(20)-C(21)-C(22)	119.71(17)
C(20)-C(21)-H(21A)	120.1
C(22)-C(21)-H(21A)	120.1
C(21)-C(22)-C(23)	120.73(17)
C(21)-C(22)-H(22A)	119.6
C(23)-C(22)-H(22A)	119.6
C(22)-C(23)-C(18)	120.05(16)
C(22)-C(23)-H(23A)	120.0
C(18)-C(23)-H(23A)	120.0
O(2)-P(2)-N(2)	112.32(6)
O(2)-P(2)-C(24)	114.09(7)
N(2)-P(2)-C(24)	103.50(6)
O(2)-P(2)-C(30)	110.39(7)
N(2)-P(2)-C(30)	111.27(7)
C(24)-P(2)-C(30)	104.89(7)
C(36)-N(2)-P(2)	119.44(9)
C(36)-N(2)-H(2N)	120.3
P(2)-N(2)-H(2N)	120.3
C(29)-C(24)-C(25)	119.01(14)
C(29)-C(24)-P(2)	121.92(11)
C(25)-C(24)-P(2)	118.92(11)
C(26)-C(25)-C(24)	120.23(14)
C(26)-C(25)-H(25A)	119.9
C(24)-C(25)-H(25A)	119.9

C(25)-C(26)-C(27)	120.25(15)
C(25)-C(26)-H(26A)	119.9
C(27)-C(26)-H(26A)	119.9
C(28)-C(27)-C(26)	119.98(15)
C(28)-C(27)-H(27A)	120.0
C(26)-C(27)-H(27A)	120.0
C(27)-C(28)-C(29)	119.91(15)
C(27)-C(28)-H(28A)	120.0
C(29)-C(28)-H(28A)	120.0
C(28)-C(29)-C(24)	120.61(14)
C(28)-C(29)-H(29A)	119.7
C(24)-C(29)-H(29A)	119.7
C(31)-C(30)-C(35)	119.82(14)
C(31)-C(30)-P(2)	119.83(12)
C(35)-C(30)-P(2)	120.14(12)
C(30)-C(31)-C(32)	119.97(16)
C(30)-C(31)-H(31A)	120.0
C(32)-C(31)-H(31A)	120.0
C(33)-C(32)-C(31)	119.65(15)
C(33)-C(32)-H(32A)	120.2
C(31)-C(32)-H(32A)	120.2
C(32)-C(33)-C(34)	120.64(16)
C(32)-C(33)-H(33A)	119.7
C(34)-C(33)-H(33A)	119.7
C(35)-C(34)-C(33)	119.84(17)
C(35)-C(34)-H(34A)	120.1
C(33)-C(34)-H(34A)	120.1
C(34)-C(35)-C(30)	120.01(15)
C(34)-C(35)-H(35A)	120.0
C(30)-C(35)-H(35A)	120.0
N(2)-C(36)-C(41)	112.43(12)
N(2)-C(36)-C(37)	109.91(12)
C(41)-C(36)-C(37)	113.09(12)
N(2)-C(36)-H(36A)	107.0
C(41)-C(36)-H(36A)	107.0

C(37)-C(36)-H(36A)	107.0
C(38)-C(37)-C(40)	109.99(13)
C(38)-C(37)-C(36)	110.31(12)
C(40)-C(37)-C(36)	110.25(13)
C(38)-C(37)-H(37A)	108.7
C(40)-C(37)-H(37A)	108.7
C(36)-C(37)-H(37A)	108.7
C(39)-C(38)-C(37)	125.67(17)
C(39)-C(38)-H(38A)	117.2
C(37)-C(38)-H(38A)	117.2
C(38)-C(39)-H(39A)	120.0
C(38)-C(39)-H(39B)	120.0
H(39A)-C(39)-H(39B)	120.0
C(37)-C(40)-H(40A)	109.5
C(37)-C(40)-H(40B)	109.5
H(40A)-C(40)-H(40B)	109.5
C(37)-C(40)-H(40C)	109.5
H(40A)-C(40)-H(40C)	109.5
H(40B)-C(40)-H(40C)	109.5
C(42)-C(41)-C(46)	118.26(16)
C(42)-C(41)-C(36)	120.03(14)
C(46)-C(41)-C(36)	121.70(14)
C(43)-C(42)-C(41)	120.77(16)
C(43)-C(42)-H(42A)	119.6
C(41)-C(42)-H(42A)	119.6
C(44)-C(43)-C(42)	120.52(17)
C(44)-C(43)-H(43A)	119.7
C(42)-C(43)-H(43A)	119.7
C(43)-C(44)-C(45)	119.16(17)
C(43)-C(44)-H(44A)	120.4
C(45)-C(44)-H(44A)	120.4
C(44)-C(45)-C(46)	120.52(16)
C(44)-C(45)-H(45A)	119.7
C(46)-C(45)-H(45A)	119.7
C(45)-C(46)-C(41)	120.76(15)

C(45)-C(46)-H(46A)	119.6
C(41)-C(46)-H(46A)	119.6

Symmetry transformations used to generate equivalent atoms:

***Table S1.8*:** Anisotropic displacement parameters ($Å^2 x\ 10^3$) for **1.63**. The anisotropic displacement factor exponent takes the form: $-2\pi^2[h^2a^{*2}U^{11} + ... + 2hka^*b^*U^{12}]$.

	U^{11}	U^{22}	U^{33}	U^{23}	U^{13}	U^{12}
P(1)	17(1)	21(1)	20(1)	-2(1)	0(1)	0(1)
O(1)	19(1)	32(1)	31(1)	-4(1)	1(1)	-2(1)
N(1)	18(1)	23(1)	22(1)	-3(1)	1(1)	3(1)
C(1)	18(1)	24(1)	25(1)	-5(1)	-2(1)	-3(1)
C(2)	28(1)	25(1)	32(1)	-1(1)	5(1)	-1(1)
C(3)	36(1)	22(1)	50(1)	-2(1)	6(1)	3(1)
C(4)	38(1)	31(1)	48(1)	-18(1)	6(1)	2(1)
C(5)	46(1)	44(1)	27(1)	-12(1)	3(1)	2(1)
C(6)	35(1)	30(1)	26(1)	-3(1)	-3(1)	3(1)
C(7)	28(1)	21(1)	20(1)	-3(1)	2(1)	3(1)
C(8)	37(1)	27(1)	30(1)	-4(1)	-7(1)	4(1)
C(9)	58(1)	27(1)	35(1)	0(1)	-15(1)	7(1)
C(10)	75(1)	25(1)	25(1)	2(1)	0(1)	-1(1)
C(11)	47(1)	30(1)	34(1)	-1(1)	10(1)	-8(1)
C(12)	30(1)	28(1)	27(1)	0(1)	3(1)	0(1)
C(13)	22(1)	24(1)	21(1)	-4(1)	1(1)	2(1)
C(14)	29(1)	28(1)	22(1)	-1(1)	1(1)	1(1)
C(15)	50(1)	35(1)	25(1)	-1(1)	8(1)	-8(1)
C(16)	66(1)	32(1)	61(1)	7(1)	37(1)	2(1)
C(17)	47(1)	37(1)	23(1)	-3(1)	0(1)	5(1)
C(18)	27(1)	25(1)	19(1)	-2(1)	0(1)	0(1)
C(19)	30(1)	31(1)	29(1)	0(1)	-1(1)	4(1)
C(20)	46(1)	28(1)	39(1)	2(1)	-4(1)	7(1)
C(21)	52(1)	24(1)	41(1)	0(1)	-5(1)	-7(1)
C(22)	35(1)	34(1)	43(1)	-3(1)	-4(1)	-8(1)
C(23)	29(1)	27(1)	36(1)	-4(1)	0(1)	1(1)

P(2)	20(1)	14(1)	18(1)	1(1)	2(1)	0(1)
O(2)	29(1)	16(1)	26(1)	1(1)	4(1)	-2(1)
N(2)	24(1)	13(1)	20(1)	0(1)	3(1)	2(1)
C(24)	20(1)	16(1)	21(1)	2(1)	2(1)	-1(1)
C(25)	26(1)	27(1)	24(1)	-3(1)	-4(1)	-1(1)
C(26)	22(1)	32(1)	35(1)	-3(1)	-3(1)	3(1)
C(27)	23(1)	25(1)	34(1)	-2(1)	7(1)	1(1)
C(28)	30(1)	34(1)	22(1)	-2(1)	3(1)	0(1)
C(29)	22(1)	30(1)	21(1)	2(1)	0(1)	2(1)
C(30)	19(1)	24(1)	20(1)	0(1)	4(1)	1(1)
C(31)	25(1)	24(1)	31(1)	6(1)	2(1)	1(1)
C(32)	25(1)	38(1)	36(1)	13(1)	-3(1)	5(1)
C(33)	23(1)	46(1)	33(1)	5(1)	-7(1)	-3(1)
C(34)	28(1)	30(1)	38(1)	-1(1)	-5(1)	-4(1)
C(35)	23(1)	24(1)	28(1)	2(1)	0(1)	2(1)
C(36)	27(1)	16(1)	20(1)	0(1)	3(1)	0(1)
C(37)	32(1)	20(1)	20(1)	-1(1)	1(1)	-3(1)
C(38)	37(1)	32(1)	24(1)	-4(1)	-1(1)	-10(1)
C(39)	34(1)	42(1)	45(1)	-14(1)	-2(1)	-4(1)
C(40)	44(1)	36(1)	21(1)	-3(1)	3(1)	-1(1)
C(41)	25(1)	24(1)	17(1)	-1(1)	2(1)	1(1)
C(42)	35(1)	25(1)	37(1)	0(1)	-1(1)	4(1)
C(43)	29(1)	44(1)	51(1)	2(1)	-6(1)	10(1)
C(44)	26(1)	46(1)	34(1)	0(1)	0(1)	-4(1)
C(45)	32(1)	31(1)	29(1)	-1(1)	6(1)	-7(1)
C(46)	26(1)	24(1)	29(1)	0(1)	5(1)	2(1)

***Table S1.9*:** Hydrogen coordinates ($x10^4$) and isotropic displacement parameters ($Å^2x10^3$)
for **1.63**.

	x	y	z	U(eq)
H(1N)	3685	7419	4858	25

H(2A)	4509	9680	5059	35
H(3A)	3715	11453	5374	43
H(4A)	3259	11252	5967	47
H(5A)	3584	9291	6254	47
H(6A)	4373	7510	5942	36
H(8A)	6985	5643	5667	37
H(9A)	6726	3939	6062	48
H(10A)	4665	3044	6154	50
H(11A)	2877	3748	5823	44
H(12A)	3140	5428	5417	34
H(13A)	5845	6085	4610	27
H(14A)	3609	6931	4216	31
H(15A)	6061	8192	4328	44
H(16A)	3863	9152	3990	64
H(16B)	5187	9961	4099	64
H(17A)	4625	5125	3945	53
H(17B)	6004	5858	3951	53
H(17C)	4838	6389	3711	53
H(19A)	6077	3894	4673	36
H(20A)	5278	1790	4701	45
H(21A)	3029	1415	4661	47
H(22A)	1597	3150	4599	45
H(23A)	2390	5261	4573	37
H(2N)	10275	6045	7718	23
H(25A)	12571	6925	7525	31
H(26A)	14373	6104	7226	36
H(27A)	14205	5572	6633	33
H(28A)	12241	5904	6337	34
H(29A)	10435	6741	6634	29
H(31A)	8364	9294	6918	32
H(32A)	6678	8947	6512	39
H(33A)	5932	6860	6408	41
H(34A)	6742	5127	6733	38
H(35A)	8399	5468	7143	30
H(36A)	9027	8231	7970	25

H(37A)	9805	6030	8379	29
H(38A)	11288	8306	8222	37
H(39A)	12087	6115	8581	48
H(39B)	13015	7319	8448	48
H(40A)	9481	7412	8867	50
H(40B)	8140	7240	8656	50
H(40C)	8979	8536	8613	50
H(42A)	6813	8517	7911	39
H(43A)	4664	7772	7895	50
H(44A)	4215	5575	7954	43
H(45A)	5942	4120	8027	37
H(46A)	8090	4856	8046	31

***Table S1.10*:** Torsion angles [°] for **1.63**.

O(1)-P(1)-N(1)-C(13)	46.39(13)
C(1)-P(1)-N(1)-C(13)	170.51(11)
C(7)-P(1)-N(1)-C(13)	-77.45(13)
O(1)-P(1)-C(1)-C(6)	-103.27(14)
N(1)-P(1)-C(1)-C(6)	132.74(13)
C(7)-P(1)-C(1)-C(6)	16.48(15)
O(1)-P(1)-C(1)-C(2)	71.37(14)
N(1)-P(1)-C(1)-C(2)	-52.62(14)
C(7)-P(1)-C(1)-C(2)	-168.88(12)
C(6)-C(1)-C(2)-C(3)	0.7(2)
P(1)-C(1)-C(2)-C(3)	-174.00(13)
C(1)-C(2)-C(3)-C(4)	-0.3(3)
C(2)-C(3)-C(4)-C(5)	-0.1(3)
C(3)-C(4)-C(5)-C(6)	0.0(3)
C(4)-C(5)-C(6)-C(1)	0.4(3)
C(2)-C(1)-C(6)-C(5)	-0.8(2)
P(1)-C(1)-C(6)-C(5)	173.78(14)
O(1)-P(1)-C(7)-C(8)	18.30(14)
N(1)-P(1)-C(7)-C(8)	144.25(12)
C(1)-P(1)-C(7)-C(8)	-104.06(13)

O(1)-P(1)-C(7)-C(12)	-165.98(12)
N(1)-P(1)-C(7)-C(12)	-40.03(15)
C(1)-P(1)-C(7)-C(12)	71.66(14)
C(12)-C(7)-C(8)-C(9)	-1.2(2)
P(1)-C(7)-C(8)-C(9)	174.61(13)
C(7)-C(8)-C(9)-C(10)	-0.9(3)
C(8)-C(9)-C(10)-C(11)	2.4(3)
C(9)-C(10)-C(11)-C(12)	-1.6(3)
C(8)-C(7)-C(12)-C(11)	1.9(2)
P(1)-C(7)-C(12)-C(11)	-173.79(13)
C(10)-C(11)-C(12)-C(7)	-0.5(3)
P(1)-N(1)-C(13)-C(18)	92.31(14)
P(1)-N(1)-C(13)-C(14)	-140.73(11)
N(1)-C(13)-C(14)-C(15)	56.74(17)
C(18)-C(13)-C(14)-C(15)	-176.84(14)
N(1)-C(13)-C(14)-C(17)	179.17(14)
C(18)-C(13)-C(14)-C(17)	-54.40(18)
C(17)-C(14)-C(15)-C(16)	97.1(2)
C(13)-C(14)-C(15)-C(16)	-140.88(18)
N(1)-C(13)-C(18)-C(19)	-117.82(15)
C(14)-C(13)-C(18)-C(19)	117.44(16)
N(1)-C(13)-C(18)-C(23)	62.56(19)
C(14)-C(13)-C(18)-C(23)	-62.17(19)
C(23)-C(18)-C(19)-C(20)	0.9(2)
C(13)-C(18)-C(19)-C(20)	-178.75(15)
C(18)-C(19)-C(20)-C(21)	-0.1(3)
C(19)-C(20)-C(21)-C(22)	-0.5(3)
C(20)-C(21)-C(22)-C(23)	0.4(3)
C(21)-C(22)-C(23)-C(18)	0.4(3)
C(19)-C(18)-C(23)-C(22)	-1.0(3)
C(13)-C(18)-C(23)-C(22)	178.63(15)
O(2)-P(2)-N(2)-C(36)	42.88(13)
C(24)-P(2)-N(2)-C(36)	166.40(11)
C(30)-P(2)-N(2)-C(36)	-81.45(12)
O(2)-P(2)-C(24)-C(29)	-104.67(13)

N(2)-P(2)-C(24)-C(29)	132.98(13)
C(30)-P(2)-C(24)-C(29)	16.25(15)
O(2)-P(2)-C(24)-C(25)	70.97(13)
N(2)-P(2)-C(24)-C(25)	-51.38(13)
C(30)-P(2)-C(24)-C(25)	-168.12(12)
C(29)-C(24)-C(25)-C(26)	-0.2(2)
P(2)-C(24)-C(25)-C(26)	-176.01(13)
C(24)-C(25)-C(26)-C(27)	-0.4(3)
C(25)-C(26)-C(27)-C(28)	0.7(3)
C(26)-C(27)-C(28)-C(29)	-0.4(3)
C(27)-C(28)-C(29)-C(24)	-0.2(3)
C(25)-C(24)-C(29)-C(28)	0.5(2)
P(2)-C(24)-C(29)-C(28)	176.13(13)
O(2)-P(2)-C(30)-C(31)	16.64(14)
N(2)-P(2)-C(30)-C(31)	142.05(12)
C(24)-P(2)-C(30)-C(31)	-106.68(13)
O(2)-P(2)-C(30)-C(35)	-168.51(12)
N(2)-P(2)-C(30)-C(35)	-43.10(14)
C(24)-P(2)-C(30)-C(35)	68.17(13)
C(35)-C(30)-C(31)-C(32)	-1.5(2)
P(2)-C(30)-C(31)-C(32)	173.34(13)
C(30)-C(31)-C(32)-C(33)	-0.7(3)
C(31)-C(32)-C(33)-C(34)	2.4(3)
C(32)-C(33)-C(34)-C(35)	-1.9(3)
C(33)-C(34)-C(35)-C(30)	-0.3(3)
C(31)-C(30)-C(35)-C(34)	2.0(2)
P(2)-C(30)-C(35)-C(34)	-172.83(13)
P(2)-N(2)-C(36)-C(41)	93.01(13)
P(2)-N(2)-C(36)-C(37)	-140.06(11)
N(2)-C(36)-C(37)-C(38)	52.84(16)
C(41)-C(36)-C(37)-C(38)	179.40(13)
N(2)-C(36)-C(37)-C(40)	174.51(13)
C(41)-C(36)-C(37)-C(40)	-58.92(16)
C(40)-C(37)-C(38)-C(39)	97.2(2)
C(36)-C(37)-C(38)-C(39)	-140.93(17)

N(2)-C(36)-C(41)-C(42)	-115.32(15)
C(37)-C(36)-C(41)-C(42)	119.47(15)
N(2)-C(36)-C(41)-C(46)	63.46(18)
C(37)-C(36)-C(41)-C(46)	-61.75(18)
C(46)-C(41)-C(42)-C(43)	1.0(2)
C(36)-C(41)-C(42)-C(43)	179.82(15)
C(41)-C(42)-C(43)-C(44)	-0.5(3)
C(42)-C(43)-C(44)-C(45)	-0.2(3)
C(43)-C(44)-C(45)-C(46)	0.4(3)
C(44)-C(45)-C(46)-C(41)	0.1(2)
C(42)-C(41)-C(46)-C(45)	-0.8(2)
C(36)-C(41)-C(46)-C(45)	-179.60(14)

Symmetry transformations used to generate equivalent atoms:

***Table S1.11*:** Hydrogen bonds for **1.63** [Å and °].

D-H...A	d(D-H)	d(H...A)	d(D...A)	<(DHA)
N(1)-H(1N)...O(1)#1	0.88	2.04	2.8679(16)	156.8
N(2)-H(2N)...O(2)#2	0.88	2.17	2.8716(15)	135.8

Symmetry transformations used to generate equivalent atoms:

#1 x-1/2,-y+3/2,-z+1 #2 -x+2,y-1/2,-z+3/2

X-ray structure data for compound 1.93:

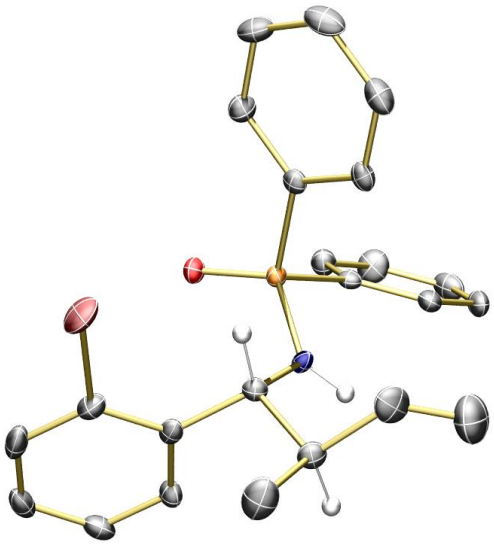

***Table S1.12*:** Crystal data and structure refinement for **1.93**.

Identification code	C23H23BrNOP	
Empirical formula	C23 H23 Br N O P	
Formula weight	440.30	
Temperature	100(2) K	
Wavelength	0.71073 Å	
Crystal system	Orthorhombic	
Space group	$P2_12_12$	
Unit cell dimensions	a = 19.890(3) Å	α= 90°.
	b = 22.115(3) Å	β= 90°.
	c = 14.743(2) Å	γ = 90°.
Volume	6484.9(16) $Å^3$	
Z	12	
Density (calculated)	1.353 Mg/m^3	
Absorption coefficient	1.988 mm^{-1}	
F(000)	2712	
Crystal size	0.550 x 0.320 x 0.210 mm^3	
Theta range for data collection	1.377 to 28.321°.	
Index ranges	-26<=h<=26, -29<=k<=29, -19<=l<=19	
Reflections collected	99712	

Independent reflections	16063 [R(int) = 0.0659]
Completeness to theta = 25.242°	100.0 %
Absorption correction	Semi-empirical from equivalents
Max. and min. transmission	0.7457 and 0.5949
Refinement method	Full-matrix least-squares on F^2
Data / restraints / parameters	16063 / 0 / 733
Goodness-of-fit on F^2	1.037
Final R indices [I>2sigma(I)]	R1 = 0.0365, wR2 = 0.0734
R indices (all data)	R1 = 0.0526, wR2 = 0.0780
Absolute structure parameter	0.003(3)
Extinction coefficient	na
Largest diff. peak and hole	1.075 and -0.815 e.$Å^{-3}$

Table S1.13: Atomic coordinates ($x10^4$) and equivalent isotropic displacement parameters ($Å^2x10^3$) for **1.93**. U(eq) is defined as one third of the trace of the orthogonalized U^{ij} tensor.

	x	y	z	U(eq)
Br(1)	1219(1)	5362(1)	2388(1)	44(1)
P(1)	3333(1)	6446(1)	2094(1)	14(1)
O(1)	2951(1)	6562(1)	1243(2)	20(1)
N(1)	2905(1)	6554(1)	3029(2)	15(1)
C(1)	1586(2)	5494(2)	3569(3)	25(1)
C(2)	1429(2)	5070(2)	4227(3)	33(1)
C(3)	1657(2)	5151(2)	5098(3)	32(1)
C(4)	2048(2)	5645(2)	5306(3)	28(1)
C(5)	2208(2)	6061(2)	4642(2)	22(1)
C(6)	1981(2)	5995(2)	3746(2)	18(1)
C(7)	2177(2)	6471(2)	3048(2)	18(1)
C(8)	1818(2)	7082(2)	3230(2)	20(1)
C(9)	2068(2)	7558(2)	2592(3)	27(1)
C(10)	2447(2)	8017(2)	2827(3)	39(1)
C(11)	1064(2)	7007(2)	3143(3)	31(1)
C(12)	3648(2)	5687(2)	2090(2)	19(1)
C(13)	3684(2)	5332(2)	2862(3)	26(1)

C(14)	3959(2)	4755(2)	2816(3)	34(1)
C(15)	4183(2)	4528(2)	2003(3)	38(1)
C(16)	4143(2)	4876(2)	1227(3)	36(1)
C(17)	3881(2)	5450(2)	1271(3)	29(1)
C(18)	4054(2)	6931(2)	2202(2)	16(1)
C(19)	4009(2)	7518(2)	1852(2)	19(1)
C(20)	4557(2)	7902(2)	1888(2)	24(1)
C(21)	5146(2)	7708(2)	2275(2)	24(1)
C(22)	5202(2)	7129(2)	2619(2)	22(1)
C(23)	4656(2)	6744(2)	2581(2)	18(1)
Br(2)	2093(1)	8992(1)	5242(1)	30(1)
P(2)	3695(1)	7438(1)	5374(1)	12(1)
O(2)	3239(1)	7281(1)	4611(2)	16(1)
N(2)	3382(1)	7578(1)	6378(2)	13(1)
C(24)	1805(2)	8202(2)	5586(2)	19(1)
C(25)	1200(2)	8005(2)	5234(2)	24(1)
C(26)	972(2)	7430(2)	5454(2)	25(1)
C(27)	1350(2)	7074(2)	6031(2)	23(1)
C(28)	1947(2)	7284(2)	6382(2)	17(1)
C(29)	2196(2)	7853(2)	6164(2)	16(1)
C(30)	2880(2)	8049(1)	6518(2)	14(1)
C(31)	2865(2)	8224(1)	7537(2)	18(1)
C(32)	3527(2)	8490(2)	7812(3)	27(1)
C(33)	3963(2)	8244(2)	8355(3)	43(1)
C(34)	2301(2)	8670(2)	7740(3)	32(1)
C(35)	4264(2)	6824(2)	5614(2)	14(1)
C(36)	4288(2)	6352(2)	4994(2)	20(1)
C(37)	4704(2)	5855(2)	5149(3)	28(1)
C(38)	5092(2)	5833(2)	5929(3)	26(1)
C(39)	5072(2)	6302(2)	6548(2)	21(1)
C(40)	4657(2)	6796(2)	6396(2)	17(1)
C(41)	4169(2)	8106(2)	5084(2)	14(1)
C(42)	4194(2)	8287(2)	4175(2)	20(1)
C(43)	4570(2)	8785(2)	3930(3)	26(1)
C(44)	4930(2)	9104(2)	4571(3)	27(1)

C(45)	4902(2)	8934(2)	5479(3)	24(1)
C(46)	4524(2)	8434(2)	5729(2)	18(1)
Br(3)	1058(1)	5660(1)	7658(1)	45(1)
P(3)	3280(1)	6276(1)	8521(1)	15(1)
O(3)	3162(1)	6759(1)	7837(2)	19(1)
N(3)	2754(1)	6253(1)	9367(2)	17(1)
C(47)	1350(2)	5286(2)	8762(3)	32(1)
C(48)	1126(3)	4702(2)	8911(3)	53(1)
C(49)	1320(3)	4408(2)	9683(3)	57(2)
C(50)	1721(2)	4693(2)	10308(3)	40(1)
C(51)	1941(2)	5276(2)	10151(3)	29(1)
C(52)	1758(2)	5595(2)	9367(2)	23(1)
C(53)	2022(2)	6229(2)	9224(2)	19(1)
C(54)	1677(2)	6694(2)	9857(2)	24(1)
C(55)	1855(2)	7320(2)	9557(3)	31(1)
C(56)	2264(3)	7696(2)	9959(3)	47(1)
C(57)	912(2)	6614(2)	9903(3)	39(1)
C(58)	3255(2)	5553(2)	7972(2)	17(1)
C(59)	3172(2)	5017(2)	8464(2)	21(1)
C(60)	3179(2)	4465(2)	8027(3)	25(1)
C(61)	3270(2)	4442(2)	7094(3)	26(1)
C(62)	3359(2)	4967(2)	6600(2)	24(1)
C(63)	3352(2)	5522(2)	7040(2)	20(1)
C(64)	4094(2)	6321(2)	9055(2)	17(1)
C(65)	4608(2)	5927(2)	8812(2)	23(1)
C(66)	5248(2)	5993(2)	9168(3)	30(1)
C(67)	5381(2)	6453(2)	9780(3)	29(1)
C(68)	4870(2)	6844(2)	10038(2)	26(1)
C(69)	4236(2)	6778(2)	9675(2)	22(1)

***Table S1.14*:** Bond lengths [Å] and angles [°] for **1.93**.

Br(1)-C(1)	1.910(4)
P(1)-O(1)	1.489(2)
P(1)-N(1)	1.637(3)

P(1)-C(12)	1.792(4)
P(1)-C(18)	1.798(4)
N(1)-C(7)	1.461(4)
C(1)-C(6)	1.382(5)
C(1)-C(2)	1.384(6)
C(2)-C(3)	1.374(6)
C(3)-C(4)	1.376(6)
C(4)-C(5)	1.381(5)
C(5)-C(6)	1.403(5)
C(6)-C(7)	1.523(5)
C(7)-C(8)	1.552(5)
C(8)-C(9)	1.496(5)
C(8)-C(11)	1.513(5)
C(9)-C(10)	1.312(6)
C(12)-C(13)	1.385(5)
C(12)-C(17)	1.396(5)
C(13)-C(14)	1.389(6)
C(14)-C(15)	1.374(6)
C(15)-C(16)	1.380(6)
C(16)-C(17)	1.375(5)
C(18)-C(23)	1.384(5)
C(18)-C(19)	1.399(5)
C(19)-C(20)	1.383(5)
C(20)-C(21)	1.372(5)
C(21)-C(22)	1.380(5)
C(22)-C(23)	1.382(5)
Br(2)-C(24)	1.907(4)
P(2)-O(2)	1.487(2)
P(2)-N(2)	1.636(3)
P(2)-C(35)	1.803(4)
P(2)-C(41)	1.804(4)
N(2)-C(30)	1.457(4)
C(24)-C(25)	1.382(5)
C(24)-C(29)	1.388(5)
C(25)-C(26)	1.389(5)

C(26)-C(27)	1.381(5)
C(27)-C(28)	1.376(5)
C(28)-C(29)	1.391(5)
C(29)-C(30)	1.520(5)
C(30)-C(31)	1.552(4)
C(31)-C(32)	1.498(5)
C(31)-C(34)	1.524(5)
C(32)-C(33)	1.299(6)
C(35)-C(36)	1.387(5)
C(35)-C(40)	1.395(5)
C(36)-C(37)	1.395(5)
C(37)-C(38)	1.385(5)
C(38)-C(39)	1.380(5)
C(39)-C(40)	1.387(5)
C(41)-C(46)	1.389(5)
C(41)-C(42)	1.400(5)
C(42)-C(43)	1.380(5)
C(43)-C(44)	1.379(6)
C(44)-C(45)	1.391(5)
C(45)-C(46)	1.388(5)
Br(3)-C(47)	1.915(4)
P(3)-O(3)	1.487(2)
P(3)-N(3)	1.628(3)
P(3)-C(58)	1.792(3)
P(3)-C(64)	1.802(4)
N(3)-C(53)	1.473(5)
C(47)-C(52)	1.385(5)
C(47)-C(48)	1.385(6)
C(48)-C(49)	1.367(7)
C(49)-C(50)	1.373(7)
C(50)-C(51)	1.381(6)
C(51)-C(52)	1.402(5)
C(52)-C(53)	1.512(5)
C(53)-C(54)	1.549(5)
C(54)-C(55)	1.495(6)

C(54)-C(57)	1.533(6)
C(55)-C(56)	1.305(6)
C(58)-C(63)	1.389(5)
C(58)-C(59)	1.400(5)
C(59)-C(60)	1.381(5)
C(60)-C(61)	1.388(5)
C(61)-C(62)	1.382(5)
C(62)-C(63)	1.388(5)
C(64)-C(69)	1.391(5)
C(64)-C(65)	1.392(5)
C(65)-C(66)	1.384(5)
C(66)-C(67)	1.386(6)
C(67)-C(68)	1.386(6)
C(68)-C(69)	1.378(5)

O(1)-P(1)-N(1)	114.85(14)
O(1)-P(1)-C(12)	109.69(15)
N(1)-P(1)-C(12)	108.65(15)
O(1)-P(1)-C(18)	112.32(15)
N(1)-P(1)-C(18)	104.66(15)
C(12)-P(1)-C(18)	106.22(16)
C(7)-N(1)-P(1)	120.9(2)
C(6)-C(1)-C(2)	122.6(4)
C(6)-C(1)-Br(1)	120.7(3)
C(2)-C(1)-Br(1)	116.7(3)
C(3)-C(2)-C(1)	119.5(4)
C(2)-C(3)-C(4)	119.9(4)
C(3)-C(4)-C(5)	120.0(4)
C(4)-C(5)-C(6)	121.6(4)
C(1)-C(6)-C(5)	116.3(3)
C(1)-C(6)-C(7)	124.9(3)
C(5)-C(6)-C(7)	118.8(3)
N(1)-C(7)-C(6)	110.7(3)
N(1)-C(7)-C(8)	110.5(3)
C(6)-C(7)-C(8)	111.6(3)

C(9)-C(8)-C(11)	110.7(3)
C(9)-C(8)-C(7)	110.5(3)
C(11)-C(8)-C(7)	110.2(3)
C(10)-C(9)-C(8)	124.7(4)
C(13)-C(12)-C(17)	118.7(3)
C(13)-C(12)-P(1)	123.2(3)
C(17)-C(12)-P(1)	118.1(3)
C(12)-C(13)-C(14)	120.1(4)
C(15)-C(14)-C(13)	120.4(4)
C(14)-C(15)-C(16)	120.1(4)
C(17)-C(16)-C(15)	119.8(4)
C(16)-C(17)-C(12)	120.9(4)
C(23)-C(18)-C(19)	118.7(3)
C(23)-C(18)-P(1)	123.2(3)
C(19)-C(18)-P(1)	118.0(3)
C(20)-C(19)-C(18)	120.4(3)
C(21)-C(20)-C(19)	119.7(4)
C(20)-C(21)-C(22)	120.8(3)
C(21)-C(22)-C(23)	119.6(3)
C(22)-C(23)-C(18)	120.8(3)
O(2)-P(2)-N(2)	119.76(15)
O(2)-P(2)-C(35)	110.87(15)
N(2)-P(2)-C(35)	101.78(15)
O(2)-P(2)-C(41)	109.29(14)
N(2)-P(2)-C(41)	104.97(15)
C(35)-P(2)-C(41)	109.64(16)
C(30)-N(2)-P(2)	121.6(2)
C(25)-C(24)-C(29)	122.9(3)
C(25)-C(24)-Br(2)	116.8(3)
C(29)-C(24)-Br(2)	120.3(3)
C(24)-C(25)-C(26)	119.1(3)
C(27)-C(26)-C(25)	119.2(3)
C(28)-C(27)-C(26)	120.6(4)
C(27)-C(28)-C(29)	121.8(3)
C(24)-C(29)-C(28)	116.5(3)

C(24)-C(29)-C(30)	123.6(3)
C(28)-C(29)-C(30)	119.9(3)
N(2)-C(30)-C(29)	111.1(3)
N(2)-C(30)-C(31)	109.2(3)
C(29)-C(30)-C(31)	112.8(3)
C(32)-C(31)-C(34)	109.9(3)
C(32)-C(31)-C(30)	110.1(3)
C(34)-C(31)-C(30)	111.5(3)
C(33)-C(32)-C(31)	126.1(4)
C(36)-C(35)-C(40)	119.4(3)
C(36)-C(35)-P(2)	117.3(3)
C(40)-C(35)-P(2)	123.2(3)
C(35)-C(36)-C(37)	120.3(3)
C(38)-C(37)-C(36)	119.6(3)
C(39)-C(38)-C(37)	120.4(3)
C(38)-C(39)-C(40)	120.1(3)
C(39)-C(40)-C(35)	120.1(3)
C(46)-C(41)-C(42)	119.2(3)
C(46)-C(41)-P(2)	122.1(3)
C(42)-C(41)-P(2)	118.7(3)
C(43)-C(42)-C(41)	119.9(4)
C(44)-C(43)-C(42)	120.7(3)
C(43)-C(44)-C(45)	120.0(4)
C(46)-C(45)-C(44)	119.5(3)
C(45)-C(46)-C(41)	120.7(3)
O(3)-P(3)-N(3)	116.09(14)
O(3)-P(3)-C(58)	109.29(15)
N(3)-P(3)-C(58)	107.48(16)
O(3)-P(3)-C(64)	113.44(15)
N(3)-P(3)-C(64)	104.07(15)
C(58)-P(3)-C(64)	105.81(17)
C(53)-N(3)-P(3)	121.8(2)
C(52)-C(47)-C(48)	123.1(4)
C(52)-C(47)-Br(3)	120.8(3)
C(48)-C(47)-Br(3)	116.1(3)

C(49)-C(48)-C(47)	119.1(4)
C(48)-C(49)-C(50)	120.2(4)
C(49)-C(50)-C(51)	120.1(4)
C(50)-C(51)-C(52)	121.7(4)
C(47)-C(52)-C(51)	115.8(4)
C(47)-C(52)-C(53)	124.8(3)
C(51)-C(52)-C(53)	119.4(3)
N(3)-C(53)-C(52)	110.9(3)
N(3)-C(53)-C(54)	109.1(3)
C(52)-C(53)-C(54)	112.2(3)
C(55)-C(54)-C(57)	110.8(3)
C(55)-C(54)-C(53)	109.4(3)
C(57)-C(54)-C(53)	112.9(3)
C(56)-C(55)-C(54)	127.1(4)
C(63)-C(58)-C(59)	119.1(3)
C(63)-C(58)-P(3)	119.2(3)
C(59)-C(58)-P(3)	121.6(3)
C(60)-C(59)-C(58)	120.4(3)
C(59)-C(60)-C(61)	119.7(4)
C(62)-C(61)-C(60)	120.6(3)
C(61)-C(62)-C(63)	119.6(3)
C(62)-C(63)-C(58)	120.5(3)
C(69)-C(64)-C(65)	118.3(3)
C(69)-C(64)-P(3)	120.7(3)
C(65)-C(64)-P(3)	120.8(3)
C(66)-C(65)-C(64)	120.8(3)
C(65)-C(66)-C(67)	120.0(4)
C(66)-C(67)-C(68)	119.8(4)
C(69)-C(68)-C(67)	119.9(4)
C(68)-C(69)-C(64)	121.2(3)

Symmetry transformations used to generate equivalent atoms:

***Table S1.15*:** Anisotropic displacement parameters ($Å^2x10^3$) for **1.93**. The anisotropic displacement factor exponent takes the form: $-2\pi^2[h^2a^{*2}U^{11} + ... + 2hka^*b^*U^{12}]$.

	U^{11}	U^{22}	U^{33}	U^{23}	U^{13}	U^{12}
Br(1)	51(1)	44(1)	38(1)	-17(1)	0(1)	-23(1)
P(1)	15(1)	16(1)	12(1)	-2(1)	1(1)	0(1)
O(1)	20(1)	26(1)	14(1)	-3(1)	-1(1)	2(1)
N(1)	15(2)	21(2)	10(1)	-3(1)	-1(1)	0(1)
C(1)	21(2)	23(2)	30(2)	-8(2)	4(2)	-2(2)
C(2)	29(2)	19(2)	51(3)	-5(2)	14(2)	-3(2)
C(3)	29(2)	24(2)	45(3)	13(2)	14(2)	5(2)
C(4)	21(2)	34(2)	28(2)	6(2)	4(2)	9(2)
C(5)	15(2)	26(2)	24(2)	2(2)	3(2)	1(2)
C(6)	14(2)	19(2)	23(2)	-4(2)	4(1)	2(2)
C(7)	14(2)	21(2)	17(2)	-3(1)	-1(1)	-1(2)
C(8)	18(2)	23(2)	18(2)	-2(1)	0(2)	3(2)
C(9)	29(2)	28(2)	25(2)	5(2)	3(2)	10(2)
C(10)	37(3)	29(2)	50(3)	11(2)	9(2)	9(2)
C(11)	26(2)	35(2)	33(2)	0(2)	7(2)	8(2)
C(12)	11(2)	18(2)	27(2)	-4(2)	-1(2)	-4(1)
C(13)	25(2)	23(2)	31(2)	2(2)	-1(2)	-3(2)
C(14)	35(3)	24(2)	45(3)	11(2)	-3(2)	-3(2)
C(15)	34(3)	21(2)	59(3)	-1(2)	2(2)	3(2)
C(16)	42(3)	25(2)	39(2)	-7(2)	5(2)	7(2)
C(17)	35(2)	26(2)	26(2)	-5(2)	5(2)	5(2)
C(18)	18(2)	20(2)	12(2)	-4(1)	4(1)	-2(1)
C(19)	20(2)	22(2)	17(2)	-2(1)	3(2)	-1(2)
C(20)	31(2)	22(2)	20(2)	-2(2)	6(2)	-6(2)
C(21)	23(2)	28(2)	20(2)	-5(2)	3(2)	-9(2)
C(22)	18(2)	29(2)	18(2)	-2(2)	1(2)	-1(2)
C(23)	21(2)	19(2)	16(2)	-1(1)	3(2)	-2(1)
Br(2)	41(1)	23(1)	26(1)	12(1)	-3(1)	4(1)
P(2)	12(1)	14(1)	11(1)	-1(1)	0(1)	0(1)
O(2)	16(1)	19(1)	14(1)	-1(1)	-2(1)	-1(1)
N(2)	14(2)	16(2)	9(1)	0(1)	2(1)	5(1)
C(24)	23(2)	17(2)	16(2)	2(1)	2(2)	2(2)
C(25)	23(2)	36(2)	14(2)	0(2)	-3(2)	10(2)

C(26)	13(2)	41(2)	21(2)	-7(2)	1(2)	0(2)
C(27)	18(2)	25(2)	26(2)	-2(2)	7(2)	-4(2)
C(28)	14(2)	18(2)	20(2)	1(1)	-1(1)	3(1)
C(29)	15(2)	19(2)	13(2)	-1(1)	2(1)	6(1)
C(30)	15(2)	13(2)	15(2)	-1(1)	2(1)	0(1)
C(31)	20(2)	16(2)	16(2)	-3(1)	3(2)	1(1)
C(32)	33(2)	27(2)	21(2)	-12(2)	2(2)	-1(2)
C(33)	40(3)	47(3)	42(3)	-7(2)	-11(2)	-2(2)
C(34)	38(2)	31(2)	26(2)	-7(2)	0(2)	12(2)
C(35)	14(2)	12(2)	17(2)	2(1)	4(1)	-2(1)
C(36)	19(2)	23(2)	19(2)	-2(1)	1(2)	1(2)
C(37)	35(2)	17(2)	32(2)	-3(2)	1(2)	6(2)
C(38)	19(2)	21(2)	39(2)	8(2)	5(2)	6(2)
C(39)	14(2)	27(2)	22(2)	7(2)	-2(2)	2(2)
C(40)	14(2)	19(2)	18(2)	1(1)	2(2)	-2(1)
C(41)	12(2)	13(2)	18(2)	-1(1)	2(1)	3(1)
C(42)	22(2)	19(2)	20(2)	1(1)	0(2)	0(2)
C(43)	32(2)	21(2)	24(2)	6(2)	9(2)	1(2)
C(44)	24(2)	13(2)	45(2)	2(2)	11(2)	0(2)
C(45)	18(2)	18(2)	35(2)	-4(2)	-3(2)	1(2)
C(46)	13(2)	18(2)	22(2)	-2(1)	-1(2)	3(1)
Br(3)	67(1)	42(1)	27(1)	8(1)	-24(1)	-17(1)
P(3)	20(1)	15(1)	10(1)	0(1)	0(1)	3(1)
O(3)	27(2)	18(1)	14(1)	2(1)	2(1)	5(1)
N(3)	18(2)	23(2)	11(1)	1(1)	-3(1)	4(1)
C(47)	45(3)	30(2)	22(2)	8(2)	-10(2)	-7(2)
C(48)	85(4)	39(3)	34(2)	6(2)	-12(3)	-31(3)
C(49)	96(4)	31(3)	44(3)	11(2)	-9(3)	-22(3)
C(50)	62(3)	31(2)	27(2)	12(2)	0(2)	-8(2)
C(51)	35(2)	32(2)	19(2)	8(2)	1(2)	-1(2)
C(52)	25(2)	25(2)	18(2)	4(2)	1(2)	2(2)
C(53)	21(2)	23(2)	14(2)	5(1)	-1(2)	2(2)
C(54)	22(2)	33(2)	18(2)	2(2)	-1(2)	8(2)
C(55)	35(2)	29(2)	29(2)	2(2)	6(2)	8(2)
C(56)	63(4)	40(3)	39(3)	7(2)	9(2)	10(2)

C(57)	31(2)	46(3)	40(3)	2(2)	-5(2)	10(2)
C(58)	17(2)	16(2)	18(2)	-2(1)	-2(2)	1(1)
C(59)	25(2)	21(2)	18(2)	0(2)	-2(2)	2(2)
C(60)	29(2)	18(2)	29(2)	2(2)	-3(2)	-2(2)
C(61)	27(2)	21(2)	29(2)	-8(2)	-3(2)	1(2)
C(62)	25(2)	29(2)	17(2)	-8(2)	-2(2)	-1(2)
C(63)	19(2)	21(2)	18(2)	-1(1)	-3(2)	2(2)
C(64)	22(2)	18(2)	12(2)	4(1)	1(1)	-2(2)
C(65)	26(2)	24(2)	17(2)	-5(2)	-2(2)	2(2)
C(66)	25(2)	40(2)	27(2)	-4(2)	0(2)	9(2)
C(67)	21(2)	40(2)	27(2)	3(2)	-5(2)	-4(2)
C(68)	24(2)	35(2)	19(2)	-7(2)	1(2)	-7(2)
C(69)	25(2)	21(2)	20(2)	-3(2)	5(2)	-1(2)

***Table S1.16*:** Hydrogen coordinates ($x10^4$) and isotropic displacement parameters ($Å^2x10^3$)
for **1.93**.

	x	y	z	U(eq)
H(1N)	3117	6663	3527	18
H(2)	1166	4726	4076	40
H(3)	1545	4866	5556	39
H(4)	2208	5701	5908	33
H(5)	2478	6400	4795	26
H(7)	2033	6323	2438	21
H(8)	1922	7213	3864	24
H(9)	1943	7525	1972	33
H(10A)	2582	8065	3441	47
H(10B)	2587	8302	2383	47
H(11A)	841	7388	3301	47
H(11B)	912	6687	3554	47
H(11C)	952	6897	2517	47
H(13)	3522	5482	3424	32

H(14)	3992	4516	3349	41
H(15)	4365	4132	1974	45
H(16)	4297	4719	664	43
H(17)	3857	5689	736	35
H(19)	3600	7653	1589	23
H(20)	4526	8299	1645	29
H(21)	5520	7974	2307	29
H(22)	5613	6997	2880	26
H(23)	4694	6346	2818	22
H(2N)	3520	7364	6846	15
H(25)	943	8259	4847	29
H(26)	561	7283	5211	30
H(27)	1197	6680	6187	28
H(28)	2195	7033	6785	21
H(30)	3023	8414	6165	17
H(31)	2787	7850	7901	21
H(32)	3638	8875	7567	32
H(33A)	3874	7860	8616	52
H(33B)	4371	8449	8490	52
H(34A)	2294	8760	8391	47
H(34B)	1869	8493	7561	47
H(34C)	2376	9045	7400	47
H(36)	4020	6368	4461	24
H(37)	4722	5534	4723	33
H(38)	5374	5494	6039	32
H(39)	5343	6286	7078	25
H(40)	4640	7115	6827	20
H(42)	3954	8067	3727	24
H(43)	4582	8910	3314	31
H(44)	5196	9441	4393	33
H(45)	5141	9159	5924	28
H(46)	4508	8314	6347	21
H(3N)	2912	6255	9924	21
H(48)	842	4508	8482	63
H(49)	1176	4004	9788	69

H(50)	1848	4490	10849	48
H(51)	2224	5466	10585	34
H(53)	1928	6349	8582	23
H(54)	1861	6636	10482	29
H(55)	1648	7459	9015	37
H(56A)	2485	7580	10503	57
H(56B)	2341	8085	9707	57
H(57A)	720	6922	10305	59
H(57B)	807	6211	10138	59
H(57C)	721	6659	9294	59
H(59)	3111	5033	9103	25
H(60)	3121	4102	8363	31
H(61)	3271	4063	6793	31
H(62)	3425	4948	5962	28
H(63)	3413	5883	6701	23
H(65)	4519	5608	8396	27
H(66)	5596	5723	8993	36
H(67)	5820	6501	10021	35
H(68)	4958	7156	10465	31
H(69)	3890	7049	9852	26

***Table S1.17*:** Torsion angles [°] for **1.93**.

O(1)-P(1)-N(1)-C(7)	28.6(3)
C(12)-P(1)-N(1)-C(7)	-94.6(3)
C(18)-P(1)-N(1)-C(7)	152.2(3)
C(6)-C(1)-C(2)-C(3)	1.7(6)
Br(1)-C(1)-C(2)-C(3)	-177.6(3)
C(1)-C(2)-C(3)-C(4)	-1.1(6)
C(2)-C(3)-C(4)-C(5)	0.3(6)
C(3)-C(4)-C(5)-C(6)	0.0(6)
C(2)-C(1)-C(6)-C(5)	-1.3(6)
Br(1)-C(1)-C(6)-C(5)	178.0(3)
C(2)-C(1)-C(6)-C(7)	179.2(3)
Br(1)-C(1)-C(6)-C(7)	-1.6(5)

C(4)-C(5)-C(6)-C(1)	0.4(5)
C(4)-C(5)-C(6)-C(7)	180.0(3)
P(1)-N(1)-C(7)-C(6)	121.5(3)
P(1)-N(1)-C(7)-C(8)	-114.3(3)
C(1)-C(6)-C(7)-N(1)	-126.7(4)
C(5)-C(6)-C(7)-N(1)	53.8(4)
C(1)-C(6)-C(7)-C(8)	109.8(4)
C(5)-C(6)-C(7)-C(8)	-69.8(4)
N(1)-C(7)-C(8)-C(9)	50.9(4)
C(6)-C(7)-C(8)-C(9)	174.6(3)
N(1)-C(7)-C(8)-C(11)	173.6(3)
C(6)-C(7)-C(8)-C(11)	-62.7(4)
C(11)-C(8)-C(9)-C(10)	128.2(4)
C(7)-C(8)-C(9)-C(10)	-109.4(4)
O(1)-P(1)-C(12)-C(13)	-143.4(3)
N(1)-P(1)-C(12)-C(13)	-17.1(3)
C(18)-P(1)-C(12)-C(13)	95.0(3)
O(1)-P(1)-C(12)-C(17)	38.1(3)
N(1)-P(1)-C(12)-C(17)	164.4(3)
C(18)-P(1)-C(12)-C(17)	-83.5(3)
C(17)-C(12)-C(13)-C(14)	1.0(5)
P(1)-C(12)-C(13)-C(14)	-177.5(3)
C(12)-C(13)-C(14)-C(15)	-1.4(6)
C(13)-C(14)-C(15)-C(16)	0.8(7)
C(14)-C(15)-C(16)-C(17)	0.2(7)
C(15)-C(16)-C(17)-C(12)	-0.5(7)
C(13)-C(12)-C(17)-C(16)	-0.1(6)
P(1)-C(12)-C(17)-C(16)	178.4(3)
O(1)-P(1)-C(18)-C(23)	-143.8(3)
N(1)-P(1)-C(18)-C(23)	91.0(3)
C(12)-P(1)-C(18)-C(23)	-23.9(3)
O(1)-P(1)-C(18)-C(19)	33.6(3)
N(1)-P(1)-C(18)-C(19)	-91.6(3)
C(12)-P(1)-C(18)-C(19)	153.5(3)
C(23)-C(18)-C(19)-C(20)	-0.1(5)

P(1)-C(18)-C(19)-C(20)	-177.6(3)
C(18)-C(19)-C(20)-C(21)	-0.5(5)
C(19)-C(20)-C(21)-C(22)	0.9(5)
C(20)-C(21)-C(22)-C(23)	-0.7(5)
C(21)-C(22)-C(23)-C(18)	0.0(5)
C(19)-C(18)-C(23)-C(22)	0.4(5)
P(1)-C(18)-C(23)-C(22)	177.8(3)
O(2)-P(2)-N(2)-C(30)	-56.8(3)
C(35)-P(2)-N(2)-C(30)	-179.4(3)
C(41)-P(2)-N(2)-C(30)	66.4(3)
C(29)-C(24)-C(25)-C(26)	-0.8(5)
Br(2)-C(24)-C(25)-C(26)	179.1(3)
C(24)-C(25)-C(26)-C(27)	1.1(5)
C(25)-C(26)-C(27)-C(28)	-0.3(5)
C(26)-C(27)-C(28)-C(29)	-0.9(5)
C(25)-C(24)-C(29)-C(28)	-0.3(5)
Br(2)-C(24)-C(29)-C(28)	179.8(2)
C(25)-C(24)-C(29)-C(30)	176.7(3)
Br(2)-C(24)-C(29)-C(30)	-3.2(4)
C(27)-C(28)-C(29)-C(24)	1.2(5)
C(27)-C(28)-C(29)-C(30)	-175.9(3)
P(2)-N(2)-C(30)-C(29)	74.5(3)
P(2)-N(2)-C(30)-C(31)	-160.6(2)
C(24)-C(29)-C(30)-N(2)	-129.7(3)
C(28)-C(29)-C(30)-N(2)	47.2(4)
C(24)-C(29)-C(30)-C(31)	107.4(4)
C(28)-C(29)-C(30)-C(31)	-75.7(4)
N(2)-C(30)-C(31)-C(32)	63.5(4)
C(29)-C(30)-C(31)-C(32)	-172.6(3)
N(2)-C(30)-C(31)-C(34)	-174.3(3)
C(29)-C(30)-C(31)-C(34)	-50.3(4)
C(34)-C(31)-C(32)-C(33)	125.5(4)
C(30)-C(31)-C(32)-C(33)	-111.3(4)
O(2)-P(2)-C(35)-C(36)	10.7(3)
N(2)-P(2)-C(35)-C(36)	139.2(3)

C(41)-P(2)-C(35)-C(36)	-110.1(3)
O(2)-P(2)-C(35)-C(40)	-167.3(3)
N(2)-P(2)-C(35)-C(40)	-38.8(3)
C(41)-P(2)-C(35)-C(40)	72.0(3)
C(40)-C(35)-C(36)-C(37)	-0.3(5)
P(2)-C(35)-C(36)-C(37)	-178.3(3)
C(35)-C(36)-C(37)-C(38)	0.2(6)
C(36)-C(37)-C(38)-C(39)	-0.4(6)
C(37)-C(38)-C(39)-C(40)	0.6(6)
C(38)-C(39)-C(40)-C(35)	-0.7(5)
C(36)-C(35)-C(40)-C(39)	0.5(5)
P(2)-C(35)-C(40)-C(39)	178.4(3)
O(2)-P(2)-C(41)-C(46)	165.7(3)
N(2)-P(2)-C(41)-C(46)	36.1(3)
C(35)-P(2)-C(41)-C(46)	-72.6(3)
O(2)-P(2)-C(41)-C(42)	-16.4(3)
N(2)-P(2)-C(41)-C(42)	-146.0(3)
C(35)-P(2)-C(41)-C(42)	105.3(3)
C(46)-C(41)-C(42)-C(43)	0.0(5)
P(2)-C(41)-C(42)-C(43)	-178.0(3)
C(41)-C(42)-C(43)-C(44)	0.9(6)
C(42)-C(43)-C(44)-C(45)	-1.6(6)
C(43)-C(44)-C(45)-C(46)	1.5(6)
C(44)-C(45)-C(46)-C(41)	-0.6(5)
C(42)-C(41)-C(46)-C(45)	-0.1(5)
P(2)-C(41)-C(46)-C(45)	177.8(3)
O(3)-P(3)-N(3)-C(53)	53.1(3)
C(58)-P(3)-N(3)-C(53)	-69.6(3)
C(64)-P(3)-N(3)-C(53)	178.5(3)
C(52)-C(47)-C(48)-C(49)	-0.8(8)
Br(3)-C(47)-C(48)-C(49)	179.6(4)
C(47)-C(48)-C(49)-C(50)	1.1(9)
C(48)-C(49)-C(50)-C(51)	-1.1(8)
C(49)-C(50)-C(51)-C(52)	0.9(7)
C(48)-C(47)-C(52)-C(51)	0.6(7)

Br(3)-C(47)-C(52)-C(51)	-179.9(3)
C(48)-C(47)-C(52)-C(53)	179.0(4)
Br(3)-C(47)-C(52)-C(53)	-1.4(6)
C(50)-C(51)-C(52)-C(47)	-0.6(6)
C(50)-C(51)-C(52)-C(53)	-179.1(4)
P(3)-N(3)-C(53)-C(52)	102.4(3)
P(3)-N(3)-C(53)-C(54)	-133.5(3)
C(47)-C(52)-C(53)-N(3)	-129.2(4)
C(51)-C(52)-C(53)-N(3)	49.2(4)
C(47)-C(52)-C(53)-C(54)	108.4(4)
C(51)-C(52)-C(53)-C(54)	-73.2(4)
N(3)-C(53)-C(54)-C(55)	68.0(4)
C(52)-C(53)-C(54)-C(55)	-168.7(3)
N(3)-C(53)-C(54)-C(57)	-168.2(3)
C(52)-C(53)-C(54)-C(57)	-44.8(4)
C(57)-C(54)-C(55)-C(56)	127.9(5)
C(53)-C(54)-C(55)-C(56)	-107.0(5)
O(3)-P(3)-C(58)-C(63)	20.3(4)
N(3)-P(3)-C(58)-C(63)	147.0(3)
C(64)-P(3)-C(58)-C(63)	-102.2(3)
O(3)-P(3)-C(58)-C(59)	-162.8(3)
N(3)-P(3)-C(58)-C(59)	-36.1(3)
C(64)-P(3)-C(58)-C(59)	74.7(3)
C(63)-C(58)-C(59)-C(60)	-0.7(5)
P(3)-C(58)-C(59)-C(60)	-177.6(3)
C(58)-C(59)-C(60)-C(61)	0.2(6)
C(59)-C(60)-C(61)-C(62)	0.5(6)
C(60)-C(61)-C(62)-C(63)	-0.5(6)
C(61)-C(62)-C(63)-C(58)	-0.1(6)
C(59)-C(58)-C(63)-C(62)	0.7(6)
P(3)-C(58)-C(63)-C(62)	177.7(3)
O(3)-P(3)-C(64)-C(69)	71.8(3)
N(3)-P(3)-C(64)-C(69)	-55.3(3)
C(58)-P(3)-C(64)-C(69)	-168.5(3)
O(3)-P(3)-C(64)-C(65)	-103.8(3)

N(3)-P(3)-C(64)-C(65)	129.1(3)
C(58)-P(3)-C(64)-C(65)	16.0(3)
C(69)-C(64)-C(65)-C(66)	-1.0(5)
P(3)-C(64)-C(65)-C(66)	174.7(3)
C(64)-C(65)-C(66)-C(67)	0.5(6)
C(65)-C(66)-C(67)-C(68)	0.5(6)
C(66)-C(67)-C(68)-C(69)	-1.0(6)
C(67)-C(68)-C(69)-C(64)	0.5(6)
C(65)-C(64)-C(69)-C(68)	0.4(5)
P(3)-C(64)-C(69)-C(68)	-175.2(3)

Symmetry transformations used to generate equivalent atoms:

***Table S1.18*:** Hydrogen bonds for **1.93** [Å and °].

D-H...A	d(D-H)	d(H...A)	d(D...A)	<(DHA)
N(1)-H(1N)...O(2)	0.88	2.12	2.909(3)	149.4
N(2)-H(2N)...O(3)	0.88	2.11	2.846(4)	141.3
N(3)-H(3N)...O(1)#1	0.88	2.06	2.876(4)	153.7

Symmetry transformations used to generate equivalent atoms:

#1 x,y,z+1

X-ray structure data for compound 1.102:

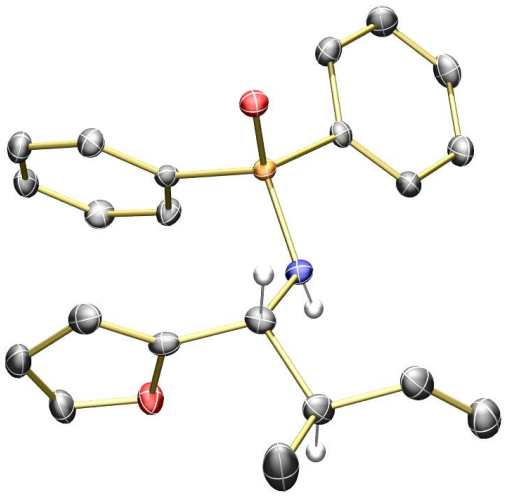

***Table S1.19*:** Crystal data and structure refinement for **1.102**.

Identification code	C21H22NO2P	
Empirical formula	C21 H22 N O2 P	
Formula weight	351.36	
Temperature	100(2) K	
Wavelength	1.54178 Å	
Crystal system	Orthorhombic	
Space group	$P2_12_12_1$	
Unit cell dimensions	a = 5.37280(10) Å	α= 90°.
	b = 17.0264(4) Å	β= 90°.
	c = 20.2126(5) Å	γ = 90°.
Volume	1849.04(7) $Å^3$	
Z	4	
Density (calculated)	1.262 Mg/m^3	
Absorption coefficient	1.420 mm^{-1}	
F(000)	744	
Crystal size	0.430 x 0.120 x 0.070 mm^3	
Theta range for data collection	3.394 to 66.736°.	
Index ranges	-6<=h<=6, -20<=k<=20, -24<=l<=22	
Reflections collected	17934	
Independent reflections	3276 [R(int) = 0.0321]	
Completeness to theta = 66.500°	100.0 %	

Absorption correction	Semi-empirical from equivalents
Max. and min. transmission	0.7528 and 0.6182
Refinement method	Full-matrix least-squares on F^2
Data / restraints / parameters	3276 / 1 / 231
Goodness-of-fit on F^2	1.051
Final R indices [I>2sigma(I)]	R1 = 0.0257, wR2 = 0.0674
R indices (all data)	R1 = 0.0264, wR2 = 0.0679
Absolute structure parameter	0.022(6)
Extinction coefficient	na
Largest diff. peak and hole	0.309 and -0.223 e.$Å^{-3}$

***Table S1.20*:** Atomic coordinates ($x10^4$) and equivalent isotropic displacement parameters ($Å^2x10^3$) for **1.102**. U(eq) is defined as one third of the trace of the orthogonalized U^{ij} tensor.

	x	y	z	U(eq)
P(1)	5612(1)	3474(1)	6875(1)	13(1)
O(1)	3102(2)	3566(1)	7176(1)	18(1)
O(2)	9340(3)	1780(1)	7562(1)	20(1)
N(1)	7807(3)	3428(1)	7443(1)	15(1)
C(1)	6544(4)	4284(1)	6352(1)	15(1)
C(2)	4936(4)	4474(1)	5834(1)	21(1)
C(3)	5462(5)	5100(1)	5422(1)	26(1)
C(4)	7596(4)	5542(1)	5522(1)	25(1)
C(5)	9185(4)	5358(1)	6033(1)	24(1)
C(6)	8677(4)	4728(1)	6452(1)	20(1)
C(7)	5647(4)	2630(1)	6326(1)	15(1)
C(8)	7569(4)	2525(1)	5872(1)	19(1)
C(9)	7555(4)	1887(1)	5446(1)	22(1)
C(10)	5627(4)	1345(1)	5474(1)	21(1)
C(11)	3723(4)	1441(1)	5929(1)	22(1)
C(12)	3720(4)	2085(1)	6354(1)	19(1)
C(13)	7417(4)	2939(1)	8037(1)	17(1)
C(14)	7286(4)	2084(1)	7872(1)	17(1)
C(15)	8789(4)	1012(1)	7419(1)	24(1)

C(16)	6508(4)	830(1)	7632(1)	26(1)
C(17)	5528(4)	1529(1)	7930(1)	23(1)
C(18)	9478(5)	3131(1)	8542(1)	21(1)
C(19)	9107(6)	2649(1)	9177(1)	40(1)
C(20)	9525(5)	3992(1)	8715(1)	24(1)
C(21)	11489(5)	4452(2)	8662(1)	31(1)

***Table S1.21*:** Bond lengths [Å] and angles [°] for **1.102**.

P(1)-O(1)	1.4876(14)
P(1)-N(1)	1.6478(16)
P(1)-C(1)	1.808(2)
P(1)-C(7)	1.8155(19)
O(2)-C(14)	1.371(2)
O(2)-C(15)	1.371(2)
N(1)-C(13)	1.476(2)
N(1)-H(1N)	0.83(2)
C(1)-C(6)	1.387(3)
C(1)-C(2)	1.396(3)
C(2)-C(3)	1.382(3)
C(2)-H(2)	0.9500
C(3)-C(4)	1.387(3)
C(3)-H(3)	0.9500
C(4)-C(5)	1.376(3)
C(4)-H(4)	0.9500
C(5)-C(6)	1.393(3)
C(5)-H(5)	0.9500
C(6)-H(6)	0.9500
C(7)-C(12)	1.391(3)
C(7)-C(8)	1.393(3)
C(8)-C(9)	1.387(3)
C(8)-H(8)	0.9500
C(9)-C(10)	1.388(3)
C(9)-H(9)	0.9500
C(10)-C(11)	1.385(3)

C(10)-H(10)	0.9500
C(11)-C(12)	1.394(3)
C(11)-H(11)	0.9500
C(12)-H(12)	0.9500
C(13)-C(14)	1.495(3)
C(13)-C(18)	1.542(3)
C(13)-H(13)	1.0000
C(14)-C(17)	1.342(3)
C(15)-C(16)	1.335(3)
C(15)-H(15)	0.9500
C(16)-C(17)	1.434(3)
C(16)-H(16)	0.9500
C(17)-H(17)	0.9500
C(18)-C(20)	1.506(3)
C(18)-C(19)	1.536(3)
C(18)-H(18)	1.0000
C(19)-H(19A)	0.9800
C(19)-H(19B)	0.9800
C(19)-H(19C)	0.9800
C(20)-C(21)	1.319(3)
C(20)-H(20)	0.9500
C(21)-H(21A)	0.9500
C(21)-H(21B)	0.9500

O(1)-P(1)-N(1)	111.63(8)
O(1)-P(1)-C(1)	114.20(9)
N(1)-P(1)-C(1)	104.15(9)
O(1)-P(1)-C(7)	110.05(9)
N(1)-P(1)-C(7)	112.38(9)
C(1)-P(1)-C(7)	104.13(9)
C(14)-O(2)-C(15)	106.46(16)
C(13)-N(1)-P(1)	119.45(13)
C(13)-N(1)-H(1N)	112.8(17)
P(1)-N(1)-H(1N)	119.2(17)
C(6)-C(1)-C(2)	119.58(18)

C(6)-C(1)-P(1)	124.05(16)
C(2)-C(1)-P(1)	116.34(15)
C(3)-C(2)-C(1)	120.29(19)
C(3)-C(2)-H(2)	119.9
C(1)-C(2)-H(2)	119.9
C(2)-C(3)-C(4)	120.0(2)
C(2)-C(3)-H(3)	120.0
C(4)-C(3)-H(3)	120.0
C(5)-C(4)-C(3)	119.9(2)
C(5)-C(4)-H(4)	120.0
C(3)-C(4)-H(4)	120.0
C(4)-C(5)-C(6)	120.7(2)
C(4)-C(5)-H(5)	119.7
C(6)-C(5)-H(5)	119.7
C(1)-C(6)-C(5)	119.6(2)
C(1)-C(6)-H(6)	120.2
C(5)-C(6)-H(6)	120.2
C(12)-C(7)-C(8)	119.60(18)
C(12)-C(7)-P(1)	119.65(15)
C(8)-C(7)-P(1)	120.75(15)
C(9)-C(8)-C(7)	120.32(19)
C(9)-C(8)-H(8)	119.8
C(7)-C(8)-H(8)	119.8
C(8)-C(9)-C(10)	120.00(19)
C(8)-C(9)-H(9)	120.0
C(10)-C(9)-H(9)	120.0
C(11)-C(10)-C(9)	119.98(18)
C(11)-C(10)-H(10)	120.0
C(9)-C(10)-H(10)	120.0
C(10)-C(11)-C(12)	120.21(19)
C(10)-C(11)-H(11)	119.9
C(12)-C(11)-H(11)	119.9
C(7)-C(12)-C(11)	119.89(19)
C(7)-C(12)-H(12)	120.1
C(11)-C(12)-H(12)	120.1

N(1)-C(13)-C(14)	112.01(16)
N(1)-C(13)-C(18)	108.52(16)
C(14)-C(13)-C(18)	112.80(17)
N(1)-C(13)-H(13)	107.8
C(14)-C(13)-H(13)	107.8
C(18)-C(13)-H(13)	107.8
C(17)-C(14)-O(2)	109.87(18)
C(17)-C(14)-C(13)	134.4(2)
O(2)-C(14)-C(13)	115.60(17)
C(16)-C(15)-O(2)	110.6(2)
C(16)-C(15)-H(15)	124.7
O(2)-C(15)-H(15)	124.7
C(15)-C(16)-C(17)	106.2(2)
C(15)-C(16)-H(16)	126.9
C(17)-C(16)-H(16)	126.9
C(14)-C(17)-C(16)	106.86(19)
C(14)-C(17)-H(17)	126.6
C(16)-C(17)-H(17)	126.6
C(20)-C(18)-C(19)	109.23(17)
C(20)-C(18)-C(13)	111.81(18)
C(19)-C(18)-C(13)	110.3(2)
C(20)-C(18)-H(18)	108.5
C(19)-C(18)-H(18)	108.5
C(13)-C(18)-H(18)	108.5
C(18)-C(19)-H(19A)	109.5
C(18)-C(19)-H(19B)	109.5
H(19A)-C(19)-H(19B)	109.5
C(18)-C(19)-H(19C)	109.5
H(19A)-C(19)-H(19C)	109.5
H(19B)-C(19)-H(19C)	109.5
C(21)-C(20)-C(18)	125.0(2)
C(21)-C(20)-H(20)	117.5
C(18)-C(20)-H(20)	117.5
C(20)-C(21)-H(21A)	120.0
C(20)-C(21)-H(21B)	120.0

H(21A)-C(21)-H(21B) 120.0

Symmetry transformations used to generate equivalent atoms:

***Table S1.22*:** Anisotropic displacement parameters ($Å^2x10^3$) for **1.102**. The anisotropic displacement factor exponent takes the form: $-2\pi^2[h^2a^{*2}U^{11} + ... + 2hka^*b^*U^{12}]$.

	U^{11}	U^{22}	U^{33}	U^{23}	U^{13}	U^{12}
P(1)	11(1)	14(1)	13(1)	0(1)	0(1)	1(1)
O(1)	14(1)	20(1)	19(1)	0(1)	1(1)	2(1)
O(2)	19(1)	17(1)	24(1)	-2(1)	3(1)	0(1)
N(1)	11(1)	20(1)	14(1)	1(1)	2(1)	0(1)
C(1)	17(1)	13(1)	15(1)	-1(1)	2(1)	1(1)
C(2)	21(1)	22(1)	19(1)	-1(1)	-2(1)	-2(1)
C(3)	33(1)	27(1)	18(1)	3(1)	-7(1)	1(1)
C(4)	33(1)	19(1)	22(1)	6(1)	3(1)	-1(1)
C(5)	22(1)	20(1)	30(1)	3(1)	1(1)	-3(1)
C(6)	20(1)	16(1)	23(1)	1(1)	-4(1)	1(1)
C(7)	15(1)	16(1)	14(1)	0(1)	-3(1)	2(1)
C(8)	15(1)	20(1)	22(1)	-2(1)	1(1)	-2(1)
C(9)	19(1)	27(1)	19(1)	-3(1)	3(1)	3(1)
C(10)	25(1)	17(1)	21(1)	-3(1)	-3(1)	2(1)
C(11)	21(1)	19(1)	25(1)	-2(1)	-1(1)	-4(1)
C(12)	17(1)	21(1)	18(1)	0(1)	2(1)	-1(1)
C(13)	16(1)	21(1)	14(1)	2(1)	3(1)	2(1)
C(14)	14(1)	24(1)	13(1)	4(1)	-1(1)	1(1)
C(15)	31(1)	16(1)	25(1)	-1(1)	-2(1)	1(1)
C(16)	31(1)	19(1)	28(1)	6(1)	-9(1)	-7(1)
C(17)	19(1)	26(1)	24(1)	8(1)	-1(1)	-3(1)
C(18)	27(1)	23(1)	15(1)	-2(1)	-3(1)	4(1)
C(19)	70(2)	28(1)	23(1)	3(1)	-14(1)	-7(1)
C(20)	31(1)	25(1)	16(1)	-2(1)	-2(1)	5(1)
C(21)	40(1)	27(1)	26(1)	-2(1)	-3(1)	-1(1)

***Table S1.23*:** Hydrogen coordinates ($x10^4$) and isotropic displacement parameters ($Å^2x10^3$)
for **1.102**.

	x	y	z	U(eq)
H(1N)	9280(40)	3447(14)	7327(12)	23(6)
H(2)	3473	4172	5764	25
H(3)	4363	5227	5069	31
H(4)	7961	5973	5239	29
H(5)	10644	5663	6101	28
H(6)	9783	4603	6803	24
H(8)	8897	2893	5854	23
H(9)	8863	1820	5135	26
H(10)	5614	908	5181	25
H(11)	2414	1066	5951	26
H(12)	2403	2153	6663	22
H(13)	5787	3094	8237	20
H(15)	9878	659	7198	29
H(16)	5698	336	7594	31
H(17)	3938	1587	8129	28
H(18)	11121	2987	8345	26
H(19A)	10410	2783	9497	60
H(19B)	9201	2088	9072	60
H(19C)	7472	2768	9367	60
H(20)	8026	4220	8873	29
H(21A)	13022	4246	8505	37
H(21B)	11371	4991	8781	37

***Table S1.24*:** Torsion angles [°] for **1.102**.

O(1)-P(1)-N(1)-C(13)	43.85(17)
C(1)-P(1)-N(1)-C(13)	167.55(14)
C(7)-P(1)-N(1)-C(13)	-80.35(17)
O(1)-P(1)-C(1)-C(6)	122.16(17)
N(1)-P(1)-C(1)-C(6)	0.14(19)

C(7)-P(1)-C(1)-C(6)	-117.79(17)
O(1)-P(1)-C(1)-C(2)	-55.73(17)
N(1)-P(1)-C(1)-C(2)	-177.75(15)
C(7)-P(1)-C(1)-C(2)	64.32(17)
C(6)-C(1)-C(2)-C(3)	0.1(3)
P(1)-C(1)-C(2)-C(3)	178.05(16)
C(1)-C(2)-C(3)-C(4)	0.0(3)
C(2)-C(3)-C(4)-C(5)	-0.1(3)
C(3)-C(4)-C(5)-C(6)	0.1(3)
C(2)-C(1)-C(6)-C(5)	0.0(3)
P(1)-C(1)-C(6)-C(5)	-177.84(16)
C(4)-C(5)-C(6)-C(1)	-0.1(3)
O(1)-P(1)-C(7)-C(12)	-14.32(18)
N(1)-P(1)-C(7)-C(12)	110.76(17)
C(1)-P(1)-C(7)-C(12)	-137.13(16)
O(1)-P(1)-C(7)-C(8)	164.98(15)
N(1)-P(1)-C(7)-C(8)	-69.94(17)
C(1)-P(1)-C(7)-C(8)	42.17(18)
C(12)-C(7)-C(8)-C(9)	0.6(3)
P(1)-C(7)-C(8)-C(9)	-178.73(16)
C(7)-C(8)-C(9)-C(10)	-0.5(3)
C(8)-C(9)-C(10)-C(11)	-0.2(3)
C(9)-C(10)-C(11)-C(12)	0.7(3)
C(8)-C(7)-C(12)-C(11)	0.0(3)
P(1)-C(7)-C(12)-C(11)	179.27(16)
C(10)-C(11)-C(12)-C(7)	-0.6(3)
P(1)-N(1)-C(13)-C(14)	66.1(2)
P(1)-N(1)-C(13)-C(18)	-168.69(13)
C(15)-O(2)-C(14)-C(17)	0.8(2)
C(15)-O(2)-C(14)-C(13)	-176.24(17)
N(1)-C(13)-C(14)-C(17)	-117.5(3)
C(18)-C(13)-C(14)-C(17)	119.7(3)
N(1)-C(13)-C(14)-O(2)	58.6(2)
C(18)-C(13)-C(14)-O(2)	-64.1(2)
C(14)-O(2)-C(15)-C(16)	-0.7(2)

O(2)-C(15)-C(16)-C(17)	0.3(2)
O(2)-C(14)-C(17)-C(16)	-0.7(2)
C(13)-C(14)-C(17)-C(16)	175.6(2)
C(15)-C(16)-C(17)-C(14)	0.2(3)
N(1)-C(13)-C(18)-C(20)	56.9(2)
C(14)-C(13)-C(18)-C(20)	-178.38(18)
N(1)-C(13)-C(18)-C(19)	178.64(18)
C(14)-C(13)-C(18)-C(19)	-56.6(2)
C(19)-C(18)-C(20)-C(21)	112.8(3)
C(13)-C(18)-C(20)-C(21)	-124.8(2)

Symmetry transformations used to generate equivalent atoms:

***Table S1.25*:** Hydrogen bonds for **1.102** [Å and °].

D-H...A	d(D-H)	d(H...A)	d(D...A)	<(DHA)
N(1)-H(1N)...O(1)#1	0.83(2)	2.08(2)	2.905(2)	171(2)

Symmetry transformations used to generate equivalent atoms:

#1 x+1,y,z

X-ray structure data for compound 1.103:

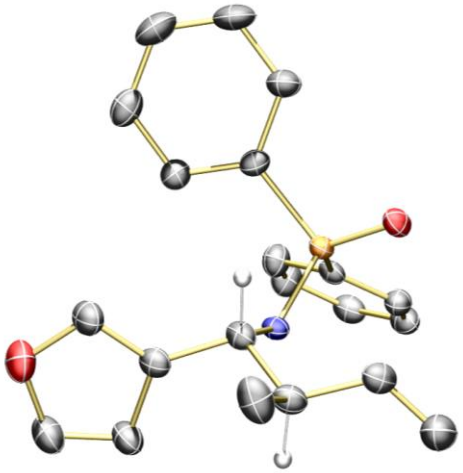

***Table S1.26*:** Crystal data and structure refinement for **1.103**.

Identification code	C21H22NO2P	
Empirical formula	C21 H22 N O2 P	
Formula weight	351.36	
Temperature	100(2) K	
Wavelength	1.54178 Å	
Crystal system	Monoclinic	
Space group	$P2_1$	
Unit cell dimensions	a = 9.8837(3) Å	α= 90°.
	b = 19.6195(5) Å	β= 104.2220(11)°.
	c = 20.0873(6) Å	γ = 90°.
Volume	3775.81(19) $Å^3$	
Z	8	
Density (calculated)	1.236 Mg/m^3	
Absorption coefficient	1.391 mm^{-1}	
F(000)	1488	
Crystal size	0.320 x 0.140 x 0.060 mm^3	
Theta range for data collection	2.269 to 66.630°.	
Index ranges	-9<=h<=11, -23<=k<=23, -23<=l<=23	
Reflections collected	49488	
Independent reflections	13247 [R(int) = 0.0241]	
Completeness to theta = 66.500°	99.6 %	

Absorption correction	Semi-empirical from equivalents
Max. and min. transmission	0.7528 and 0.6145
Refinement method	Full-matrix least-squares on F^2
Data / restraints / parameters	13247 / 5 / 921
Goodness-of-fit on F^2	1.021
Final R indices [I>2sigma(I)]	R1 = 0.0293, wR2 = 0.0793
R indices (all data)	R1 = 0.0297, wR2 = 0.0797
Absolute structure parameter	0.026(2)
Extinction coefficient	na
Largest diff. peak and hole	0.546 and -0.223 e.$Å^{-3}$

***Table S1.27*:** Atomic coordinates ($x10^4$) and equivalent isotropic displacement parameters ($Å^2x10^3$) for **1.103**. U(eq) is defined as one third of the trace of the orthogonalized U^{ij} tensor.

	x	y	z	U(eq)
P(1)	4444(1)	5092(1)	9890(1)	18(1)
O(1)	2932(2)	5001(1)	9836(1)	26(1)
O(2)	4917(2)	6849(1)	8153(1)	34(1)
N(1)	4913(2)	4815(1)	9205(1)	18(1)
C(1)	5553(2)	4618(1)	10584(1)	20(1)
C(2)	5980(3)	3957(1)	10483(1)	27(1)
C(3)	6717(3)	3578(2)	11037(2)	35(1)
C(4)	7040(3)	3856(2)	11695(2)	36(1)
C(5)	6629(3)	4510(2)	11796(1)	34(1)
C(6)	5882(3)	4888(1)	11247(1)	27(1)
C(7)	4930(3)	5979(1)	10050(1)	22(1)
C(8)	3951(3)	6452(1)	10161(1)	30(1)
C(9)	4325(3)	7136(2)	10257(2)	38(1)
C(10)	5635(3)	7349(2)	10231(2)	39(1)
C(11)	6609(3)	6880(2)	10113(2)	32(1)
C(12)	6257(3)	6197(1)	10026(1)	26(1)
C(13)	4172(2)	5054(1)	8514(1)	18(1)
C(14)	4719(2)	5734(1)	8345(1)	20(1)
C(15)	6078(3)	5867(1)	8242(1)	25(1)

C(16)	6134(3)	6537(1)	8124(1)	30(1)
C(17)	4074(3)	6341(1)	8289(1)	27(1)
C(18)	4301(3)	4501(1)	7986(1)	22(1)
C(19)	3585(3)	4722(2)	7250(1)	30(1)
C(20)	3683(3)	3838(1)	8145(1)	29(1)
C(21)	4253(4)	3240(2)	8148(2)	41(1)
P(2)	-726(1)	4734(1)	9512(1)	20(1)
O(3)	-2184(2)	4813(1)	9568(1)	26(1)
O(4)	1896(2)	2891(1)	11525(1)	36(1)
N(2)	408(2)	4850(1)	10249(1)	22(1)
C(22)	-531(3)	3905(1)	9156(1)	26(1)
C(23)	-1698(3)	3490(2)	8941(2)	36(1)
C(24)	-1573(3)	2854(2)	8672(2)	47(1)
C(25)	-283(4)	2626(2)	8611(2)	46(1)
C(26)	880(3)	3037(2)	8820(2)	37(1)
C(27)	763(3)	3673(2)	9093(2)	31(1)
C(28)	-212(2)	5361(1)	8966(1)	23(1)
C(29)	-145(3)	5208(2)	8297(1)	32(1)
C(30)	105(3)	5722(2)	7870(2)	43(1)
C(31)	301(3)	6381(2)	8106(2)	48(1)
C(32)	250(3)	6540(2)	8772(2)	46(1)
C(33)	-13(3)	6029(2)	9203(2)	33(1)
C(34)	209(3)	4528(1)	10879(1)	24(1)
C(35)	1097(3)	3897(1)	11063(1)	24(1)
C(36)	850(3)	3363(1)	11438(2)	32(1)
C(37)	2836(3)	3150(1)	11191(1)	30(1)
C(38)	2408(3)	3751(1)	10907(1)	30(1)
C(39)	506(3)	5059(1)	11474(1)	30(1)
C(40)	-539(3)	5643(2)	11308(2)	32(1)
C(41)	1997(3)	5292(2)	11634(2)	37(1)
C(42)	2440(3)	5898(2)	11504(2)	45(1)
P(3)	8970(1)	5188(1)	4096(1)	19(1)
O(5)	8259(2)	5049(1)	4657(1)	26(1)
O(6)	10453(2)	6569(1)	6327(1)	32(1)
N(3)	10468(2)	5594(1)	4259(1)	21(1)

C(43)	7828(2)	5698(1)	3439(1)	22(1)
C(44)	8288(3)	5992(1)	2905(1)	28(1)
C(45)	7371(3)	6376(1)	2407(2)	33(1)
C(46)	6010(3)	6461(1)	2446(2)	35(1)
C(47)	5545(3)	6170(2)	2977(2)	37(1)
C(48)	6455(3)	5791(1)	3473(2)	31(1)
C(49)	9376(2)	4399(1)	3722(1)	21(1)
C(50)	10479(3)	4333(1)	3403(1)	25(1)
C(51)	10792(3)	3701(1)	3173(1)	28(1)
C(52)	9999(3)	3133(1)	3245(1)	29(1)
C(53)	8878(3)	3203(1)	3546(2)	30(1)
C(54)	8576(3)	3830(1)	3785(1)	26(1)
C(55)	10617(2)	6298(1)	4520(1)	22(1)
C(56)	10757(3)	6318(1)	5284(1)	23(1)
C(57)	9978(3)	6664(1)	5636(1)	29(1)
C(58)	11578(3)	6143(2)	6410(2)	33(1)
C(59)	11797(3)	5970(2)	5800(1)	30(1)
C(60)	11897(3)	6636(1)	4336(1)	26(1)
C(61)	12035(3)	7377(2)	4568(2)	43(1)
C(62)	11911(4)	6539(2)	3590(2)	47(1)
C(63)	11950(4)	6987(3)	3124(2)	64(1)
P(4)	4284(1)	4462(1)	4815(1)	19(1)
O(7)	3239(2)	5017(1)	4604(1)	25(1)
O(8)	8657(2)	3914(1)	7197(1)	39(1)
N(4)	5891(2)	4664(1)	5211(1)	20(1)
C(64)	4524(2)	3977(1)	4084(1)	21(1)
C(65)	4320(3)	4300(1)	3450(1)	26(1)
C(66)	4504(3)	3943(2)	2884(1)	32(1)
C(67)	4886(3)	3265(2)	2943(1)	32(1)
C(68)	5072(3)	2934(2)	3570(2)	35(1)
C(69)	4887(3)	3293(1)	4140(2)	30(1)
C(70)	3690(3)	3871(1)	5375(1)	23(1)
C(71)	2263(3)	3818(2)	5319(2)	32(1)
C(72)	1764(3)	3347(2)	5712(2)	42(1)
C(73)	2670(4)	2925(2)	6164(2)	42(1)

C(74)	4098(3)	2974(2)	6226(2)	34(1)
C(75)	4604(3)	3447(1)	5833(1)	25(1)
C(76)	6288(3)	4991(1)	5893(1)	23(1)
C(77)	7451(3)	4586(1)	6351(1)	25(1)
C(78)	7419(3)	4245(2)	6931(1)	32(1)
C(79)	9486(3)	4062(2)	6758(2)	37(1)
C(80)	8805(3)	4465(2)	6241(2)	32(1)
C(81)	6704(3)	5749(1)	5850(1)	27(1)
C(82)	6941(3)	6084(2)	6558(2)	40(1)
C(83)	5613(3)	6144(1)	5347(1)	28(1)
C(84)	5834(3)	6555(2)	4876(2)	40(1)

***Table S1.28*:** Bond lengths [Å] and angles [°] for **1.103**.

P(1)-O(1)	1.4825(17)
P(1)-N(1)	1.6492(19)
P(1)-C(1)	1.806(2)
P(1)-C(7)	1.812(3)
O(2)-C(16)	1.364(4)
O(2)-C(17)	1.368(3)
N(1)-C(13)	1.478(3)
N(1)-H(1N)	0.85(2)
C(1)-C(2)	1.393(4)
C(1)-C(6)	1.394(4)
C(2)-C(3)	1.386(4)
C(2)-H(2)	0.9500
C(3)-C(4)	1.392(4)
C(3)-H(3)	0.9500
C(4)-C(5)	1.377(5)
C(4)-H(4)	0.9500
C(5)-C(6)	1.383(4)
C(5)-H(5)	0.9500
C(6)-H(6)	0.9500
C(7)-C(12)	1.393(4)
C(7)-C(8)	1.397(4)

C(8)-C(9)	1.393(4)
C(8)-H(8)	0.9500
C(9)-C(10)	1.373(5)
C(9)-H(9)	0.9500
C(10)-C(11)	1.395(4)
C(10)-H(10)	0.9500
C(11)-C(12)	1.385(4)
C(11)-H(11)	0.9500
C(12)-H(12)	0.9500
C(13)-C(14)	1.508(3)
C(13)-C(18)	1.543(3)
C(13)-H(13)	1.0000
C(14)-C(17)	1.343(4)
C(14)-C(15)	1.433(3)
C(15)-C(16)	1.340(4)
C(15)-H(15)	0.9500
C(16)-H(16)	0.9500
C(17)-H(17)	0.9500
C(18)-C(20)	1.503(4)
C(18)-C(19)	1.537(3)
C(18)-H(18)	1.0000
C(19)-H(19A)	0.9800
C(19)-H(19B)	0.9800
C(19)-H(19C)	0.9800
C(20)-C(21)	1.302(4)
C(20)-H(20)	0.9500
C(21)-H(21A)	0.9500
C(21)-H(21B)	0.9500
P(2)-O(3)	1.4812(17)
P(2)-N(2)	1.639(2)
P(2)-C(28)	1.801(3)
P(2)-C(22)	1.806(3)
O(4)-C(36)	1.367(3)
O(4)-C(37)	1.370(3)
N(2)-C(34)	1.468(3)

N(2)-H(2N)	0.85(2)
C(22)-C(23)	1.391(4)
C(22)-C(27)	1.393(4)
C(23)-C(24)	1.377(5)
C(23)-H(23)	0.9500
C(24)-C(25)	1.386(5)
C(24)-H(24)	0.9500
C(25)-C(26)	1.383(5)
C(25)-H(25)	0.9500
C(26)-C(27)	1.378(4)
C(26)-H(26)	0.9500
C(27)-H(27)	0.9500
C(28)-C(33)	1.391(4)
C(28)-C(29)	1.395(4)
C(29)-C(30)	1.384(4)
C(29)-H(29)	0.9500
C(30)-C(31)	1.375(6)
C(30)-H(30)	0.9500
C(31)-C(32)	1.387(6)
C(31)-H(31)	0.9500
C(32)-C(33)	1.392(4)
C(32)-H(32)	0.9500
C(33)-H(33)	0.9500
C(34)-C(35)	1.509(3)
C(34)-C(39)	1.559(4)
C(34)-H(34)	1.0000
C(35)-C(36)	1.347(4)
C(35)-C(38)	1.435(4)
C(36)-H(36)	0.9500
C(37)-C(38)	1.333(4)
C(37)-H(37)	0.9500
C(38)-H(38)	0.9500
C(39)-C(41)	1.500(4)
C(39)-C(40)	1.522(4)
C(39)-H(39)	1.0000

C(40)-H(40A)	0.9800
C(40)-H(40B)	0.9800
C(40)-H(40C)	0.9800
C(41)-C(42)	1.316(5)
C(41)-H(41)	0.9500
C(42)-H(42A)	0.9500
C(42)-H(42B)	0.9500
P(3)-O(5)	1.4917(17)
P(3)-N(3)	1.642(2)
P(3)-C(49)	1.808(2)
P(3)-C(43)	1.814(2)
O(6)-C(57)	1.365(3)
O(6)-C(58)	1.368(4)
N(3)-C(55)	1.472(3)
N(3)-H(3N)	0.83(2)
C(43)-C(48)	1.387(4)
C(43)-C(44)	1.388(4)
C(44)-C(45)	1.394(4)
C(44)-H(44)	0.9500
C(45)-C(46)	1.376(4)
C(45)-H(45)	0.9500
C(46)-C(47)	1.386(5)
C(46)-H(46)	0.9500
C(47)-C(48)	1.383(4)
C(47)-H(47)	0.9500
C(48)-H(48)	0.9500
C(49)-C(54)	1.391(4)
C(49)-C(50)	1.399(3)
C(50)-C(51)	1.384(4)
C(50)-H(50)	0.9500
C(51)-C(52)	1.390(4)
C(51)-H(51)	0.9500
C(52)-C(53)	1.393(4)
C(52)-H(52)	0.9500
C(53)-C(54)	1.380(4)

C(53)-H(53)	0.9500
C(54)-H(54)	0.9500
C(55)-C(56)	1.508(4)
C(55)-C(60)	1.552(3)
C(55)-H(55)	1.0000
C(56)-C(57)	1.349(4)
C(56)-C(59)	1.439(4)
C(57)-H(57)	0.9500
C(58)-C(59)	1.340(4)
C(58)-H(58)	0.9500
C(59)-H(59)	0.9500
C(60)-C(62)	1.514(4)
C(60)-C(61)	1.522(4)
C(60)-H(60)	1.0000
C(61)-H(61A)	0.9800
C(61)-H(61B)	0.9800
C(61)-H(61C)	0.9800
C(62)-C(63)	1.292(5)
C(62)-H(62)	0.9500
C(63)-H(63A)	0.9500
C(63)-H(63B)	0.9500
P(4)-O(7)	1.4899(18)
P(4)-N(4)	1.641(2)
P(4)-C(70)	1.810(2)
P(4)-C(64)	1.813(2)
O(8)-C(78)	1.372(4)
O(8)-C(79)	1.374(4)
N(4)-C(76)	1.477(3)
N(4)-H(4N)	0.84(2)
C(64)-C(69)	1.387(4)
C(64)-C(65)	1.393(4)
C(65)-C(66)	1.386(4)
C(65)-H(65)	0.9500
C(66)-C(67)	1.380(4)
C(66)-H(66)	0.9500

C(67)-C(68)	1.388(4)
C(67)-H(67)	0.9500
C(68)-C(69)	1.393(4)
C(68)-H(68)	0.9500
C(69)-H(69)	0.9500
C(70)-C(71)	1.391(4)
C(70)-C(75)	1.396(4)
C(71)-C(72)	1.383(4)
C(71)-H(71)	0.9500
C(72)-C(73)	1.383(5)
C(72)-H(72)	0.9500
C(73)-C(74)	1.388(5)
C(73)-H(73)	0.9500
C(74)-C(75)	1.389(4)
C(74)-H(74)	0.9500
C(75)-H(75)	0.9500
C(76)-C(77)	1.510(4)
C(76)-C(81)	1.550(4)
C(76)-H(76)	1.0000
C(77)-C(78)	1.350(4)
C(77)-C(80)	1.429(4)
C(78)-H(78)	0.9500
C(79)-C(80)	1.346(4)
C(79)-H(79)	0.9500
C(80)-H(80)	0.9500
C(81)-C(83)	1.499(4)
C(81)-C(82)	1.533(4)
C(81)-H(81)	1.0000
C(82)-H(82A)	0.9800
C(82)-H(82B)	0.9800
C(82)-H(82C)	0.9800
C(83)-C(84)	1.302(4)
C(83)-H(83)	0.9500
C(84)-H(84A)	0.9500
C(84)-H(84B)	0.9500

O(1)-P(1)-N(1)	112.63(10)
O(1)-P(1)-C(1)	113.82(10)
N(1)-P(1)-C(1)	103.46(11)
O(1)-P(1)-C(7)	110.30(11)
N(1)-P(1)-C(7)	110.40(11)
C(1)-P(1)-C(7)	105.84(11)
C(16)-O(2)-C(17)	105.6(2)
C(13)-N(1)-P(1)	120.23(15)
C(13)-N(1)-H(1N)	113.8(18)
P(1)-N(1)-H(1N)	111.9(18)
C(2)-C(1)-C(6)	119.0(2)
C(2)-C(1)-P(1)	120.98(19)
C(6)-C(1)-P(1)	119.72(19)
C(3)-C(2)-C(1)	120.1(3)
C(3)-C(2)-H(2)	120.0
C(1)-C(2)-H(2)	120.0
C(2)-C(3)-C(4)	120.2(3)
C(2)-C(3)-H(3)	119.9
C(4)-C(3)-H(3)	119.9
C(5)-C(4)-C(3)	119.9(3)
C(5)-C(4)-H(4)	120.1
C(3)-C(4)-H(4)	120.1
C(4)-C(5)-C(6)	120.1(3)
C(4)-C(5)-H(5)	120.0
C(6)-C(5)-H(5)	120.0
C(5)-C(6)-C(1)	120.7(3)
C(5)-C(6)-H(6)	119.6
C(1)-C(6)-H(6)	119.6
C(12)-C(7)-C(8)	119.8(2)
C(12)-C(7)-P(1)	119.98(19)
C(8)-C(7)-P(1)	120.2(2)
C(9)-C(8)-C(7)	119.4(3)
C(9)-C(8)-H(8)	120.3
C(7)-C(8)-H(8)	120.3

C(10)-C(9)-C(8)	120.6(3)
C(10)-C(9)-H(9)	119.7
C(8)-C(9)-H(9)	119.7
C(9)-C(10)-C(11)	120.1(3)
C(9)-C(10)-H(10)	120.0
C(11)-C(10)-H(10)	120.0
C(12)-C(11)-C(10)	119.9(3)
C(12)-C(11)-H(11)	120.1
C(10)-C(11)-H(11)	120.1
C(11)-C(12)-C(7)	120.2(2)
C(11)-C(12)-H(12)	119.9
C(7)-C(12)-H(12)	119.9
N(1)-C(13)-C(14)	111.69(19)
N(1)-C(13)-C(18)	108.43(19)
C(14)-C(13)-C(18)	111.94(19)
N(1)-C(13)-H(13)	108.2
C(14)-C(13)-H(13)	108.2
C(18)-C(13)-H(13)	108.2
C(17)-C(14)-C(15)	105.6(2)
C(17)-C(14)-C(13)	127.9(2)
C(15)-C(14)-C(13)	126.4(2)
C(16)-C(15)-C(14)	106.6(2)
C(16)-C(15)-H(15)	126.7
C(14)-C(15)-H(15)	126.7
C(15)-C(16)-O(2)	110.9(2)
C(15)-C(16)-H(16)	124.6
O(2)-C(16)-H(16)	124.6
C(14)-C(17)-O(2)	111.3(2)
C(14)-C(17)-H(17)	124.3
O(2)-C(17)-H(17)	124.3
C(20)-C(18)-C(19)	109.5(2)
C(20)-C(18)-C(13)	110.8(2)
C(19)-C(18)-C(13)	111.4(2)
C(20)-C(18)-H(18)	108.3
C(19)-C(18)-H(18)	108.3

C(13)-C(18)-H(18)	108.3
C(18)-C(19)-H(19A)	109.5
C(18)-C(19)-H(19B)	109.5
H(19A)-C(19)-H(19B)	109.5
C(18)-C(19)-H(19C)	109.5
H(19A)-C(19)-H(19C)	109.5
H(19B)-C(19)-H(19C)	109.5
C(21)-C(20)-C(18)	125.7(3)
C(21)-C(20)-H(20)	117.2
C(18)-C(20)-H(20)	117.2
C(20)-C(21)-H(21A)	120.0
C(20)-C(21)-H(21B)	120.0
H(21A)-C(21)-H(21B)	120.0
O(3)-P(2)-N(2)	112.26(11)
O(3)-P(2)-C(28)	113.57(11)
N(2)-P(2)-C(28)	102.89(11)
O(3)-P(2)-C(22)	108.96(11)
N(2)-P(2)-C(22)	111.53(12)
C(28)-P(2)-C(22)	107.47(12)
C(36)-O(4)-C(37)	105.6(2)
C(34)-N(2)-P(2)	120.78(17)
C(34)-N(2)-H(2N)	119(2)
P(2)-N(2)-H(2N)	113.3(19)
C(23)-C(22)-C(27)	119.3(3)
C(23)-C(22)-P(2)	119.3(2)
C(27)-C(22)-P(2)	121.4(2)
C(24)-C(23)-C(22)	120.4(3)
C(24)-C(23)-H(23)	119.8
C(22)-C(23)-H(23)	119.8
C(23)-C(24)-C(25)	120.0(3)
C(23)-C(24)-H(24)	120.0
C(25)-C(24)-H(24)	120.0
C(26)-C(25)-C(24)	119.9(3)
C(26)-C(25)-H(25)	120.0
C(24)-C(25)-H(25)	120.0

C(27)-C(26)-C(25)	120.3(3)
C(27)-C(26)-H(26)	119.9
C(25)-C(26)-H(26)	119.9
C(26)-C(27)-C(22)	120.1(3)
C(26)-C(27)-H(27)	119.9
C(22)-C(27)-H(27)	119.9
C(33)-C(28)-C(29)	119.7(3)
C(33)-C(28)-P(2)	118.2(2)
C(29)-C(28)-P(2)	121.8(2)
C(30)-C(29)-C(28)	119.9(3)
C(30)-C(29)-H(29)	120.0
C(28)-C(29)-H(29)	120.0
C(31)-C(30)-C(29)	120.2(3)
C(31)-C(30)-H(30)	119.9
C(29)-C(30)-H(30)	119.9
C(30)-C(31)-C(32)	120.6(3)
C(30)-C(31)-H(31)	119.7
C(32)-C(31)-H(31)	119.7
C(31)-C(32)-C(33)	119.7(3)
C(31)-C(32)-H(32)	120.2
C(33)-C(32)-H(32)	120.2
C(28)-C(33)-C(32)	119.9(3)
C(28)-C(33)-H(33)	120.0
C(32)-C(33)-H(33)	120.0
N(2)-C(34)-C(35)	111.8(2)
N(2)-C(34)-C(39)	109.5(2)
C(35)-C(34)-C(39)	111.8(2)
N(2)-C(34)-H(34)	107.9
C(35)-C(34)-H(34)	107.9
C(39)-C(34)-H(34)	107.9
C(36)-C(35)-C(38)	105.3(2)
C(36)-C(35)-C(34)	126.9(2)
C(38)-C(35)-C(34)	127.8(2)
C(35)-C(36)-O(4)	111.3(2)
C(35)-C(36)-H(36)	124.3

O(4)-C(36)-H(36)	124.3
C(38)-C(37)-O(4)	110.9(2)
C(38)-C(37)-H(37)	124.6
O(4)-C(37)-H(37)	124.6
C(37)-C(38)-C(35)	107.0(2)
C(37)-C(38)-H(38)	126.5
C(35)-C(38)-H(38)	126.5
C(41)-C(39)-C(40)	113.3(2)
C(41)-C(39)-C(34)	110.9(2)
C(40)-C(39)-C(34)	110.2(2)
C(41)-C(39)-H(39)	107.4
C(40)-C(39)-H(39)	107.4
C(34)-C(39)-H(39)	107.4
C(39)-C(40)-H(40A)	109.5
C(39)-C(40)-H(40B)	109.5
H(40A)-C(40)-H(40B)	109.5
C(39)-C(40)-H(40C)	109.5
H(40A)-C(40)-H(40C)	109.5
H(40B)-C(40)-H(40C)	109.5
C(42)-C(41)-C(39)	126.2(3)
C(42)-C(41)-H(41)	116.9
C(39)-C(41)-H(41)	116.9
C(41)-C(42)-H(42A)	120.0
C(41)-C(42)-H(42B)	120.0
H(42A)-C(42)-H(42B)	120.0
O(5)-P(3)-N(3)	120.52(11)
O(5)-P(3)-C(49)	110.57(11)
N(3)-P(3)-C(49)	102.48(11)
O(5)-P(3)-C(43)	109.05(11)
N(3)-P(3)-C(43)	104.24(11)
C(49)-P(3)-C(43)	109.41(11)
C(57)-O(6)-C(58)	105.8(2)
C(55)-N(3)-P(3)	122.16(16)
C(55)-N(3)-H(3N)	112(2)
P(3)-N(3)-H(3N)	118(2)

C(48)-C(43)-C(44)	119.6(2)
C(48)-C(43)-P(3)	118.6(2)
C(44)-C(43)-P(3)	121.89(19)
C(43)-C(44)-C(45)	119.9(2)
C(43)-C(44)-H(44)	120.0
C(45)-C(44)-H(44)	120.0
C(46)-C(45)-C(44)	119.9(3)
C(46)-C(45)-H(45)	120.1
C(44)-C(45)-H(45)	120.1
C(45)-C(46)-C(47)	120.5(3)
C(45)-C(46)-H(46)	119.8
C(47)-C(46)-H(46)	119.8
C(48)-C(47)-C(46)	119.7(3)
C(48)-C(47)-H(47)	120.1
C(46)-C(47)-H(47)	120.1
C(47)-C(48)-C(43)	120.4(3)
C(47)-C(48)-H(48)	119.8
C(43)-C(48)-H(48)	119.8
C(54)-C(49)-C(50)	119.4(2)
C(54)-C(49)-P(3)	117.37(19)
C(50)-C(49)-P(3)	123.16(19)
C(51)-C(50)-C(49)	119.9(2)
C(51)-C(50)-H(50)	120.0
C(49)-C(50)-H(50)	120.0
C(50)-C(51)-C(52)	120.3(2)
C(50)-C(51)-H(51)	119.8
C(52)-C(51)-H(51)	119.8
C(51)-C(52)-C(53)	119.7(2)
C(51)-C(52)-H(52)	120.1
C(53)-C(52)-H(52)	120.1
C(54)-C(53)-C(52)	120.0(2)
C(54)-C(53)-H(53)	120.0
C(52)-C(53)-H(53)	120.0
C(53)-C(54)-C(49)	120.5(2)
C(53)-C(54)-H(54)	119.7

C(49)-C(54)-H(54)	119.7
N(3)-C(55)-C(56)	111.3(2)
N(3)-C(55)-C(60)	109.4(2)
C(56)-C(55)-C(60)	110.8(2)
N(3)-C(55)-H(55)	108.4
C(56)-C(55)-H(55)	108.4
C(60)-C(55)-H(55)	108.4
C(57)-C(56)-C(59)	105.1(2)
C(57)-C(56)-C(55)	128.6(2)
C(59)-C(56)-C(55)	126.2(2)
C(56)-C(57)-O(6)	111.4(2)
C(56)-C(57)-H(57)	124.3
O(6)-C(57)-H(57)	124.3
C(59)-C(58)-O(6)	110.7(3)
C(59)-C(58)-H(58)	124.6
O(6)-C(58)-H(58)	124.6
C(58)-C(59)-C(56)	106.8(3)
C(58)-C(59)-H(59)	126.6
C(56)-C(59)-H(59)	126.6
C(62)-C(60)-C(61)	113.7(3)
C(62)-C(60)-C(55)	112.8(2)
C(61)-C(60)-C(55)	110.6(2)
C(62)-C(60)-H(60)	106.4
C(61)-C(60)-H(60)	106.4
C(55)-C(60)-H(60)	106.4
C(60)-C(61)-H(61A)	109.5
C(60)-C(61)-H(61B)	109.5
H(61A)-C(61)-H(61B)	109.5
C(60)-C(61)-H(61C)	109.5
H(61A)-C(61)-H(61C)	109.5
H(61B)-C(61)-H(61C)	109.5
C(63)-C(62)-C(60)	129.8(4)
C(63)-C(62)-H(62)	115.1
C(60)-C(62)-H(62)	115.1
C(62)-C(63)-H(63A)	120.0

C(62)-C(63)-H(63B)	120.0
H(63A)-C(63)-H(63B)	120.0
O(7)-P(4)-N(4)	118.81(10)
O(7)-P(4)-C(70)	109.67(11)
N(4)-P(4)-C(70)	106.13(11)
O(7)-P(4)-C(64)	111.87(11)
N(4)-P(4)-C(64)	102.46(10)
C(70)-P(4)-C(64)	107.11(11)
C(78)-O(8)-C(79)	105.4(2)
C(76)-N(4)-P(4)	123.99(16)
C(76)-N(4)-H(4N)	118(2)
P(4)-N(4)-H(4N)	114(2)
C(69)-C(64)-C(65)	119.4(2)
C(69)-C(64)-P(4)	121.7(2)
C(65)-C(64)-P(4)	118.89(19)
C(66)-C(65)-C(64)	120.1(2)
C(66)-C(65)-H(65)	120.0
C(64)-C(65)-H(65)	120.0
C(67)-C(66)-C(65)	120.3(3)
C(67)-C(66)-H(66)	119.8
C(65)-C(66)-H(66)	119.8
C(66)-C(67)-C(68)	120.1(3)
C(66)-C(67)-H(67)	119.9
C(68)-C(67)-H(67)	119.9
C(67)-C(68)-C(69)	119.6(3)
C(67)-C(68)-H(68)	120.2
C(69)-C(68)-H(68)	120.2
C(64)-C(69)-C(68)	120.4(3)
C(64)-C(69)-H(69)	119.8
C(68)-C(69)-H(69)	119.8
C(71)-C(70)-C(75)	119.2(2)
C(71)-C(70)-P(4)	118.4(2)
C(75)-C(70)-P(4)	122.33(19)
C(72)-C(71)-C(70)	120.1(3)
C(72)-C(71)-H(71)	120.0

C(70)-C(71)-H(71)	120.0
C(71)-C(72)-C(73)	120.7(3)
C(71)-C(72)-H(72)	119.7
C(73)-C(72)-H(72)	119.7
C(72)-C(73)-C(74)	119.8(3)
C(72)-C(73)-H(73)	120.1
C(74)-C(73)-H(73)	120.1
C(73)-C(74)-C(75)	119.7(3)
C(73)-C(74)-H(74)	120.2
C(75)-C(74)-H(74)	120.2
C(74)-C(75)-C(70)	120.5(3)
C(74)-C(75)-H(75)	119.7
C(70)-C(75)-H(75)	119.7
N(4)-C(76)-C(77)	109.0(2)
N(4)-C(76)-C(81)	112.2(2)
C(77)-C(76)-C(81)	111.5(2)
N(4)-C(76)-H(76)	108.0
C(77)-C(76)-H(76)	108.0
C(81)-C(76)-H(76)	108.0
C(78)-C(77)-C(80)	105.8(2)
C(78)-C(77)-C(76)	127.6(2)
C(80)-C(77)-C(76)	126.5(2)
C(77)-C(78)-O(8)	111.2(3)
C(77)-C(78)-H(78)	124.4
O(8)-C(78)-H(78)	124.4
C(80)-C(79)-O(8)	110.8(3)
C(80)-C(79)-H(79)	124.6
O(8)-C(79)-H(79)	124.6
C(79)-C(80)-C(77)	106.7(3)
C(79)-C(80)-H(80)	126.7
C(77)-C(80)-H(80)	126.7
C(83)-C(81)-C(82)	108.9(2)
C(83)-C(81)-C(76)	112.1(2)
C(82)-C(81)-C(76)	109.9(2)
C(83)-C(81)-H(81)	108.6

C(82)-C(81)-H(81)	108.6
C(76)-C(81)-H(81)	108.6
C(81)-C(82)-H(82A)	109.5
C(81)-C(82)-H(82B)	109.5
H(82A)-C(82)-H(82B)	109.5
C(81)-C(82)-H(82C)	109.5
H(82A)-C(82)-H(82C)	109.5
H(82B)-C(82)-H(82C)	109.5
C(84)-C(83)-C(81)	126.0(3)
C(84)-C(83)-H(83)	117.0
C(81)-C(83)-H(83)	117.0
C(83)-C(84)-H(84A)	120.0
C(83)-C(84)-H(84B)	120.0
H(84A)-C(84)-H(84B)	120.0

Symmetry transformations used to generate equivalent atoms:

***Table S1.29*:** Anisotropic displacement parameters ($Å^2x10^3$) for **1.103**. The anisotropic displacement factor exponent takes the form: $-2\pi^2[h^2a^{*2}U^{11} + ... + 2hka^*b^*U^{12}]$.

	U^{11}	U^{22}	U^{33}	U^{23}	U^{13}	U^{12}
P(1)	14(1)	21(1)	19(1)	0(1)	4(1)	-1(1)
O(1)	16(1)	33(1)	28(1)	1(1)	7(1)	-1(1)
O(2)	38(1)	21(1)	41(1)	2(1)	10(1)	-3(1)
N(1)	12(1)	22(1)	20(1)	1(1)	3(1)	0(1)
C(1)	14(1)	26(1)	21(1)	2(1)	6(1)	-4(1)
C(2)	28(1)	28(1)	26(1)	5(1)	8(1)	-1(1)
C(3)	34(2)	33(2)	39(2)	12(1)	11(1)	6(1)
C(4)	27(1)	51(2)	27(1)	17(1)	3(1)	-2(1)
C(5)	32(1)	45(2)	22(1)	4(1)	3(1)	-12(1)
C(6)	26(1)	32(1)	25(1)	0(1)	6(1)	-6(1)
C(7)	22(1)	21(1)	21(1)	-2(1)	3(1)	1(1)
C(8)	28(1)	30(1)	32(1)	0(1)	10(1)	6(1)
C(9)	41(2)	27(1)	46(2)	-7(1)	13(1)	9(1)
C(10)	46(2)	21(1)	47(2)	-6(1)	8(1)	0(1)

C(11)	30(1)	28(1)	38(2)	-4(1)	5(1)	-4(1)
C(12)	23(1)	24(1)	29(1)	-3(1)	5(1)	-1(1)
C(13)	15(1)	20(1)	20(1)	1(1)	3(1)	0(1)
C(14)	18(1)	23(1)	17(1)	0(1)	1(1)	-2(1)
C(15)	22(1)	28(1)	27(1)	2(1)	7(1)	-1(1)
C(16)	31(1)	31(1)	31(1)	-1(1)	10(1)	-8(1)
C(17)	25(1)	24(1)	30(1)	1(1)	6(1)	-2(1)
C(18)	22(1)	23(1)	23(1)	-2(1)	7(1)	-1(1)
C(19)	35(1)	30(1)	22(1)	-4(1)	4(1)	-2(1)
C(20)	36(1)	26(1)	27(1)	-6(1)	9(1)	-6(1)
C(21)	53(2)	26(1)	46(2)	-2(1)	17(2)	-2(1)
P(2)	14(1)	23(1)	22(1)	3(1)	5(1)	1(1)
O(3)	16(1)	31(1)	30(1)	1(1)	5(1)	1(1)
O(4)	41(1)	26(1)	45(1)	8(1)	16(1)	5(1)
N(2)	14(1)	29(1)	24(1)	4(1)	6(1)	0(1)
C(22)	24(1)	25(1)	30(1)	2(1)	9(1)	2(1)
C(23)	25(1)	31(2)	53(2)	-5(1)	13(1)	-3(1)
C(24)	34(2)	35(2)	75(2)	-13(2)	16(2)	-9(1)
C(25)	48(2)	27(2)	66(2)	-10(2)	20(2)	0(1)
C(26)	31(2)	32(2)	50(2)	-2(1)	15(1)	6(1)
C(27)	23(1)	29(1)	40(2)	0(1)	7(1)	1(1)
C(28)	12(1)	32(1)	24(1)	8(1)	2(1)	1(1)
C(29)	19(1)	50(2)	27(1)	5(1)	4(1)	0(1)
C(30)	27(1)	69(2)	31(2)	20(2)	6(1)	1(1)
C(31)	27(2)	64(2)	52(2)	39(2)	7(1)	6(1)
C(32)	33(2)	32(2)	68(2)	18(2)	4(2)	1(1)
C(33)	26(1)	31(1)	40(2)	6(1)	5(1)	2(1)
C(34)	22(1)	27(1)	25(1)	4(1)	8(1)	1(1)
C(35)	25(1)	25(1)	21(1)	0(1)	5(1)	1(1)
C(36)	34(2)	27(1)	39(2)	2(1)	16(1)	1(1)
C(37)	29(1)	31(1)	31(1)	0(1)	9(1)	4(1)
C(38)	27(1)	30(1)	33(1)	8(1)	9(1)	2(1)
C(39)	35(1)	30(1)	24(1)	4(1)	9(1)	2(1)
C(40)	34(2)	30(1)	37(2)	-1(1)	14(1)	1(1)
C(41)	34(2)	39(2)	33(2)	-8(1)	-5(1)	9(1)

C(42)	31(2)	48(2)	54(2)	-18(2)	7(1)	-3(1)
P(3)	17(1)	20(1)	20(1)	-1(1)	5(1)	-2(1)
O(5)	24(1)	32(1)	25(1)	-3(1)	9(1)	-6(1)
O(6)	40(1)	27(1)	31(1)	-4(1)	13(1)	0(1)
N(3)	18(1)	20(1)	23(1)	0(1)	3(1)	1(1)
C(43)	21(1)	19(1)	24(1)	-5(1)	2(1)	0(1)
C(44)	23(1)	32(1)	29(1)	3(1)	5(1)	5(1)
C(45)	36(2)	29(1)	33(2)	4(1)	6(1)	3(1)
C(46)	28(1)	22(1)	46(2)	1(1)	-7(1)	3(1)
C(47)	19(1)	33(2)	57(2)	1(1)	5(1)	2(1)
C(48)	25(1)	28(1)	40(2)	-2(1)	9(1)	-3(1)
C(49)	22(1)	21(1)	18(1)	1(1)	2(1)	1(1)
C(50)	26(1)	26(1)	23(1)	-1(1)	7(1)	-4(1)
C(51)	26(1)	33(1)	27(1)	-6(1)	8(1)	0(1)
C(52)	32(1)	23(1)	31(1)	-2(1)	3(1)	2(1)
C(53)	29(1)	22(1)	37(2)	3(1)	7(1)	-4(1)
C(54)	22(1)	26(1)	30(1)	3(1)	7(1)	-1(1)
C(55)	18(1)	21(1)	25(1)	1(1)	1(1)	0(1)
C(56)	21(1)	19(1)	29(1)	-2(1)	7(1)	-4(1)
C(57)	28(1)	25(1)	32(1)	-2(1)	5(1)	0(1)
C(58)	38(2)	32(2)	30(1)	4(1)	9(1)	2(1)
C(59)	32(1)	32(1)	26(1)	4(1)	7(1)	6(1)
C(60)	22(1)	26(1)	29(1)	4(1)	4(1)	-3(1)
C(61)	38(2)	29(2)	65(2)	-4(1)	20(2)	-9(1)
C(62)	44(2)	55(2)	40(2)	6(2)	8(1)	-26(2)
C(63)	58(2)	86(3)	49(2)	12(2)	17(2)	-2(2)
P(4)	16(1)	19(1)	21(1)	-1(1)	5(1)	0(1)
O(7)	21(1)	22(1)	33(1)	-1(1)	5(1)	1(1)
O(8)	42(1)	42(1)	29(1)	4(1)	3(1)	6(1)
N(4)	16(1)	25(1)	20(1)	-2(1)	7(1)	-2(1)
C(64)	15(1)	26(1)	21(1)	-4(1)	2(1)	-2(1)
C(65)	24(1)	27(1)	27(1)	1(1)	9(1)	0(1)
C(66)	27(1)	45(2)	24(1)	2(1)	7(1)	-1(1)
C(67)	28(1)	41(2)	27(1)	-11(1)	7(1)	-4(1)
C(68)	42(2)	28(1)	35(2)	-6(1)	12(1)	3(1)

C(69)	36(2)	28(1)	28(1)	0(1)	9(1)	3(1)
C(70)	26(1)	21(1)	24(1)	-4(1)	10(1)	-4(1)
C(71)	26(1)	37(2)	36(2)	-1(1)	11(1)	-6(1)
C(72)	33(2)	51(2)	49(2)	-2(2)	21(1)	-15(1)
C(73)	54(2)	35(2)	43(2)	-1(1)	24(2)	-15(1)
C(74)	48(2)	26(1)	30(1)	-1(1)	12(1)	-2(1)
C(75)	29(1)	24(1)	25(1)	-3(1)	9(1)	0(1)
C(76)	21(1)	29(1)	20(1)	-4(1)	6(1)	-1(1)
C(77)	23(1)	29(1)	23(1)	-6(1)	5(1)	-2(1)
C(78)	29(1)	42(2)	25(1)	1(1)	5(1)	0(1)
C(79)	29(1)	45(2)	34(2)	-2(1)	3(1)	6(1)
C(80)	25(1)	42(2)	30(1)	0(1)	6(1)	4(1)
C(81)	23(1)	29(1)	29(1)	-7(1)	7(1)	-4(1)
C(82)	42(2)	36(2)	35(2)	-11(1)	-2(1)	6(1)
C(83)	26(1)	24(1)	34(1)	-6(1)	9(1)	-1(1)
C(84)	34(2)	38(2)	47(2)	4(1)	9(1)	-2(1)

***Table S1.30*:** Hydrogen coordinates ($x10^4$) and isotropic displacement parameters ($Å^2x10^3$) for **1.103**.

	x	y	z	U(eq)
H(1N)	5800(20)	4801(14)	9269(14)	14(6)
H(2)	5766	3767	10035	32
H(3)	7003	3127	10966	42
H(4)	7543	3594	12073	43
H(5)	6859	4702	12244	40
H(6)	5589	5337	11322	33
H(8)	3039	6308	10172	35
H(9)	3668	7458	10340	45
H(10)	5877	7817	10295	46
H(11)	7512	7028	10091	39
H(12)	6923	5876	9949	31
H(13)	3162	5108	8504	22
H(15)	6799	5543	8255	30

H(16)	6917	6765	8032	36
H(17)	3152	6410	8338	32
H(18)	5314	4426	8015	27
H(19A)	3683	4361	6928	44
H(19B)	4023	5141	7138	44
H(19C)	2592	4806	7214	44
H(20)	2800	3858	8253	35
H(21A)	5135	3196	8043	49
H(21B)	3786	2847	8255	49
H(2N)	1240(20)	4917(15)	10210(15)	20(7)
H(23)	-2585	3646	8980	43
H(24)	-2373	2572	8528	57
H(25)	-197	2187	8425	55
H(26)	1763	2881	8775	45
H(27)	1566	3952	9238	37
H(29)	-272	4752	8134	39
H(30)	142	5618	7413	51
H(31)	474	6731	7810	57
H(32)	392	6996	8933	55
H(33)	-55	6135	9659	39
H(34)	-791	4388	10793	29
H(36)	51	3320	11618	39
H(37)	3679	2931	11166	36
H(38)	2881	4029	10649	35
H(39)	358	4825	11892	35
H(40A)	-351	5970	11689	49
H(40B)	-1487	5463	11242	49
H(40C)	-450	5872	10887	49
H(41)	2686	4971	11849	45
H(42A)	1790	6237	11290	54
H(42B)	3410	5998	11626	54
H(3N)	11190(30)	5367(15)	4400(16)	25(8)
H(44)	9227	5931	2879	34
H(45)	7685	6579	2043	40
H(46)	5386	6722	2105	42

H(47)	4604	6230	3001	45
H(48)	6138	5594	3839	37
H(50)	11011	4722	3344	30
H(51)	11553	3655	2965	34
H(52)	10221	2700	3090	35
H(53)	8320	2818	3586	36
H(54)	7816	3874	3993	31
H(55)	9762	6559	4288	27
H(57)	9198	6939	5428	34
H(58)	12128	5992	6841	40
H(59)	12503	5673	5722	36
H(60)	12740	6395	4613	32
H(61A)	12843	7583	4444	64
H(61B)	12165	7398	5067	64
H(61C)	11188	7626	4343	64
H(62)	11888	6078	3442	56
H(63A)	11975	7459	3233	76
H(63B)	11954	6846	2672	76
H(4N)	6430(30)	4717(16)	4949(14)	25(7)
H(65)	4055	4767	3406	31
H(66)	4367	4166	2453	38
H(67)	5021	3024	2555	38
H(68)	5324	2466	3610	41
H(69)	5011	3067	4569	37
H(71)	1630	4106	5011	39
H(72)	788	3313	5671	51
H(73)	2317	2602	6431	50
H(74)	4725	2686	6537	41
H(75)	5580	3482	5876	30
H(76)	5462	4975	6097	28
H(78)	6640	4236	7129	38
H(79)	10414	3902	6812	44
H(80)	9157	4635	5873	39
H(81)	7596	5768	5699	32
H(82A)	7255	6554	6532	59

H(82B)	7654	5829	6890	59
H(82C)	6067	6082	6705	59
H(83)	4674	6089	5375	33
H(84A)	6756	6625	4828	48
H(84B)	5073	6784	4580	48

***Table S1.31*:** Torsion angles [°] for **1.103**.

O(1)-P(1)-N(1)-C(13)	52.9(2)
C(1)-P(1)-N(1)-C(13)	176.23(17)
C(7)-P(1)-N(1)-C(13)	-70.91(19)
O(1)-P(1)-C(1)-C(2)	90.4(2)
N(1)-P(1)-C(1)-C(2)	-32.2(2)
C(7)-P(1)-C(1)-C(2)	-148.3(2)
O(1)-P(1)-C(1)-C(6)	-83.4(2)
N(1)-P(1)-C(1)-C(6)	154.03(19)
C(7)-P(1)-C(1)-C(6)	37.9(2)
C(6)-C(1)-C(2)-C(3)	0.1(4)
P(1)-C(1)-C(2)-C(3)	-173.7(2)
C(1)-C(2)-C(3)-C(4)	-0.3(4)
C(2)-C(3)-C(4)-C(5)	-0.2(4)
C(3)-C(4)-C(5)-C(6)	0.8(4)
C(4)-C(5)-C(6)-C(1)	-1.0(4)
C(2)-C(1)-C(6)-C(5)	0.5(4)
P(1)-C(1)-C(6)-C(5)	174.4(2)
O(1)-P(1)-C(7)-C(12)	-171.20(19)
N(1)-P(1)-C(7)-C(12)	-46.1(2)
C(1)-P(1)-C(7)-C(12)	65.3(2)
O(1)-P(1)-C(7)-C(8)	5.2(2)
N(1)-P(1)-C(7)-C(8)	130.4(2)
C(1)-P(1)-C(7)-C(8)	-118.3(2)
C(12)-C(7)-C(8)-C(9)	-1.0(4)
P(1)-C(7)-C(8)-C(9)	-177.5(2)
C(7)-C(8)-C(9)-C(10)	1.1(5)
C(8)-C(9)-C(10)-C(11)	-0.3(5)

C(9)-C(10)-C(11)-C(12)	-0.5(5)
C(10)-C(11)-C(12)-C(7)	0.5(4)
C(8)-C(7)-C(12)-C(11)	0.2(4)
P(1)-C(7)-C(12)-C(11)	176.7(2)
P(1)-N(1)-C(13)-C(14)	82.8(2)
P(1)-N(1)-C(13)-C(18)	-153.43(16)
N(1)-C(13)-C(14)-C(17)	-109.8(3)
C(18)-C(13)-C(14)-C(17)	128.4(3)
N(1)-C(13)-C(14)-C(15)	67.1(3)
C(18)-C(13)-C(14)-C(15)	-54.7(3)
C(17)-C(14)-C(15)-C(16)	-0.8(3)
C(13)-C(14)-C(15)-C(16)	-178.3(2)
C(14)-C(15)-C(16)-O(2)	0.9(3)
C(17)-O(2)-C(16)-C(15)	-0.7(3)
C(15)-C(14)-C(17)-O(2)	0.5(3)
C(13)-C(14)-C(17)-O(2)	177.8(2)
C(16)-O(2)-C(17)-C(14)	0.1(3)
N(1)-C(13)-C(18)-C(20)	59.2(3)
C(14)-C(13)-C(18)-C(20)	-177.1(2)
N(1)-C(13)-C(18)-C(19)	-178.53(19)
C(14)-C(13)-C(18)-C(19)	-54.9(3)
C(19)-C(18)-C(20)-C(21)	102.1(3)
C(13)-C(18)-C(20)-C(21)	-134.5(3)
O(3)-P(2)-N(2)-C(34)	45.9(2)
C(28)-P(2)-N(2)-C(34)	168.40(19)
C(22)-P(2)-N(2)-C(34)	-76.7(2)
O(3)-P(2)-C(22)-C(23)	4.7(3)
N(2)-P(2)-C(22)-C(23)	129.2(2)
C(28)-P(2)-C(22)-C(23)	-118.8(2)
O(3)-P(2)-C(22)-C(27)	-175.2(2)
N(2)-P(2)-C(22)-C(27)	-50.7(3)
C(28)-P(2)-C(22)-C(27)	61.4(2)
C(27)-C(22)-C(23)-C(24)	0.3(5)
P(2)-C(22)-C(23)-C(24)	-179.6(3)
C(22)-C(23)-C(24)-C(25)	-0.3(6)

C(23)-C(24)-C(25)-C(26)	-0.1(6)
C(24)-C(25)-C(26)-C(27)	0.4(6)
C(25)-C(26)-C(27)-C(22)	-0.4(5)
C(23)-C(22)-C(27)-C(26)	0.1(4)
P(2)-C(22)-C(27)-C(26)	179.9(2)
O(3)-P(2)-C(28)-C(33)	71.6(2)
N(2)-P(2)-C(28)-C(33)	-50.0(2)
C(22)-P(2)-C(28)-C(33)	-167.8(2)
O(3)-P(2)-C(28)-C(29)	-102.1(2)
N(2)-P(2)-C(28)-C(29)	136.4(2)
C(22)-P(2)-C(28)-C(29)	18.5(2)
C(33)-C(28)-C(29)-C(30)	-0.6(4)
P(2)-C(28)-C(29)-C(30)	173.0(2)
C(28)-C(29)-C(30)-C(31)	0.6(4)
C(29)-C(30)-C(31)-C(32)	-0.1(5)
C(30)-C(31)-C(32)-C(33)	-0.4(5)
C(29)-C(28)-C(33)-C(32)	0.1(4)
P(2)-C(28)-C(33)-C(32)	-173.7(2)
C(31)-C(32)-C(33)-C(28)	0.4(4)
P(2)-N(2)-C(34)-C(35)	100.5(2)
P(2)-N(2)-C(34)-C(39)	-135.04(19)
N(2)-C(34)-C(35)-C(36)	-155.1(3)
C(39)-C(34)-C(35)-C(36)	81.8(3)
N(2)-C(34)-C(35)-C(38)	28.0(4)
C(39)-C(34)-C(35)-C(38)	-95.1(3)
C(38)-C(35)-C(36)-O(4)	-0.4(3)
C(34)-C(35)-C(36)-O(4)	-177.8(2)
C(37)-O(4)-C(36)-C(35)	0.4(3)
C(36)-O(4)-C(37)-C(38)	-0.2(3)
O(4)-C(37)-C(38)-C(35)	-0.1(3)
C(36)-C(35)-C(38)-C(37)	0.3(3)
C(34)-C(35)-C(38)-C(37)	177.7(3)
N(2)-C(34)-C(39)-C(41)	-63.1(3)
C(35)-C(34)-C(39)-C(41)	61.3(3)
N(2)-C(34)-C(39)-C(40)	63.2(3)

C(35)-C(34)-C(39)-C(40)	-172.5(2)
C(40)-C(39)-C(41)-C(42)	-15.1(4)
C(34)-C(39)-C(41)-C(42)	109.4(3)
O(5)-P(3)-N(3)-C(55)	-61.9(2)
C(49)-P(3)-N(3)-C(55)	174.85(19)
C(43)-P(3)-N(3)-C(55)	60.8(2)
O(5)-P(3)-C(43)-C(48)	-10.3(2)
N(3)-P(3)-C(43)-C(48)	-140.2(2)
C(49)-P(3)-C(43)-C(48)	110.8(2)
O(5)-P(3)-C(43)-C(44)	170.2(2)
N(3)-P(3)-C(43)-C(44)	40.2(2)
C(49)-P(3)-C(43)-C(44)	-68.8(2)
C(48)-C(43)-C(44)-C(45)	-0.1(4)
P(3)-C(43)-C(44)-C(45)	179.5(2)
C(43)-C(44)-C(45)-C(46)	-0.2(4)
C(44)-C(45)-C(46)-C(47)	0.3(4)
C(45)-C(46)-C(47)-C(48)	0.0(5)
C(46)-C(47)-C(48)-C(43)	-0.4(4)
C(44)-C(43)-C(48)-C(47)	0.4(4)
P(3)-C(43)-C(48)-C(47)	-179.2(2)
O(5)-P(3)-C(49)-C(54)	24.0(2)
N(3)-P(3)-C(49)-C(54)	153.65(19)
C(43)-P(3)-C(49)-C(54)	-96.2(2)
O(5)-P(3)-C(49)-C(50)	-153.5(2)
N(3)-P(3)-C(49)-C(50)	-23.8(2)
C(43)-P(3)-C(49)-C(50)	86.4(2)
C(54)-C(49)-C(50)-C(51)	-2.2(4)
P(3)-C(49)-C(50)-C(51)	175.2(2)
C(49)-C(50)-C(51)-C(52)	1.3(4)
C(50)-C(51)-C(52)-C(53)	0.5(4)
C(51)-C(52)-C(53)-C(54)	-1.5(4)
C(52)-C(53)-C(54)-C(49)	0.6(4)
C(50)-C(49)-C(54)-C(53)	1.2(4)
P(3)-C(49)-C(54)-C(53)	-176.3(2)
P(3)-N(3)-C(55)-C(56)	80.8(2)

P(3)-N(3)-C(55)-C(60)	-156.38(17)
N(3)-C(55)-C(56)-C(57)	-124.5(3)
C(60)-C(55)-C(56)-C(57)	113.5(3)
N(3)-C(55)-C(56)-C(59)	56.7(3)
C(60)-C(55)-C(56)-C(59)	-65.3(3)
C(59)-C(56)-C(57)-O(6)	0.8(3)
C(55)-C(56)-C(57)-O(6)	-178.2(2)
C(58)-O(6)-C(57)-C(56)	-0.1(3)
C(57)-O(6)-C(58)-C(59)	-0.7(3)
O(6)-C(58)-C(59)-C(56)	1.2(3)
C(57)-C(56)-C(59)-C(58)	-1.2(3)
C(55)-C(56)-C(59)-C(58)	177.8(2)
N(3)-C(55)-C(60)-C(62)	48.5(3)
C(56)-C(55)-C(60)-C(62)	171.6(2)
N(3)-C(55)-C(60)-C(61)	177.2(2)
C(56)-C(55)-C(60)-C(61)	-59.7(3)
C(61)-C(60)-C(62)-C(63)	-4.0(5)
C(55)-C(60)-C(62)-C(63)	123.1(4)
O(7)-P(4)-N(4)-C(76)	64.2(2)
C(70)-P(4)-N(4)-C(76)	-59.7(2)
C(64)-P(4)-N(4)-C(76)	-171.9(2)
O(7)-P(4)-C(64)-C(69)	-149.9(2)
N(4)-P(4)-C(64)-C(69)	81.8(2)
C(70)-P(4)-C(64)-C(69)	-29.7(2)
O(7)-P(4)-C(64)-C(65)	29.4(2)
N(4)-P(4)-C(64)-C(65)	-99.0(2)
C(70)-P(4)-C(64)-C(65)	149.60(19)
C(69)-C(64)-C(65)-C(66)	-1.1(4)
P(4)-C(64)-C(65)-C(66)	179.6(2)
C(64)-C(65)-C(66)-C(67)	0.2(4)
C(65)-C(66)-C(67)-C(68)	0.7(4)
C(66)-C(67)-C(68)-C(69)	-0.7(4)
C(65)-C(64)-C(69)-C(68)	1.1(4)
P(4)-C(64)-C(69)-C(68)	-179.6(2)
C(67)-C(68)-C(69)-C(64)	-0.2(4)

O(7)-P(4)-C(70)-C(71)	25.7(2)
N(4)-P(4)-C(70)-C(71)	155.2(2)
C(64)-P(4)-C(70)-C(71)	-95.9(2)
O(7)-P(4)-C(70)-C(75)	-157.6(2)
N(4)-P(4)-C(70)-C(75)	-28.1(2)
C(64)-P(4)-C(70)-C(75)	80.8(2)
C(75)-C(70)-C(71)-C(72)	-0.3(4)
P(4)-C(70)-C(71)-C(72)	176.6(2)
C(70)-C(71)-C(72)-C(73)	0.1(5)
C(71)-C(72)-C(73)-C(74)	0.2(5)
C(72)-C(73)-C(74)-C(75)	-0.1(5)
C(73)-C(74)-C(75)-C(70)	-0.1(4)
C(71)-C(70)-C(75)-C(74)	0.3(4)
P(4)-C(70)-C(75)-C(74)	-176.4(2)
P(4)-N(4)-C(76)-C(77)	128.4(2)
P(4)-N(4)-C(76)-C(81)	-107.6(2)
N(4)-C(76)-C(77)-C(78)	-116.1(3)
C(81)-C(76)-C(77)-C(78)	119.5(3)
N(4)-C(76)-C(77)-C(80)	61.2(3)
C(81)-C(76)-C(77)-C(80)	-63.1(3)
C(80)-C(77)-C(78)-O(8)	-0.1(3)
C(76)-C(77)-C(78)-O(8)	177.7(2)
C(79)-O(8)-C(78)-C(77)	0.2(3)
C(78)-O(8)-C(79)-C(80)	-0.1(3)
O(8)-C(79)-C(80)-C(77)	0.1(4)
C(78)-C(77)-C(80)-C(79)	0.0(3)
C(76)-C(77)-C(80)-C(79)	-177.8(3)
N(4)-C(76)-C(81)-C(83)	52.2(3)
C(77)-C(76)-C(81)-C(83)	174.8(2)
N(4)-C(76)-C(81)-C(82)	173.5(2)
C(77)-C(76)-C(81)-C(82)	-63.9(3)
C(82)-C(81)-C(83)-C(84)	105.5(3)
C(76)-C(81)-C(83)-C(84)	-132.6(3)

Symmetry transformations used to generate equivalent atoms:

***Table S1.32*:** Hydrogen bonds for **1.103** [Å and °].

D-H...A	d(D-H)	d(H...A)	d(D...A)	<(DHA)
N(1)-H(1N)...O(3)#1	0.85(2)	1.94(2)	2.782(3)	171(3)
N(2)-H(2N)...O(1)	0.85(2)	2.00(2)	2.831(3)	164(3)
N(3)-H(3N)...O(7)#1	0.83(2)	2.08(2)	2.886(3)	163(3)
N(4)-H(4N)...O(5)	0.84(2)	2.13(2)	2.926(3)	157(3)

Symmetry transformations used to generate equivalent atoms:

#1 x+1,y,z

X-ray structure data for compound 1.111:

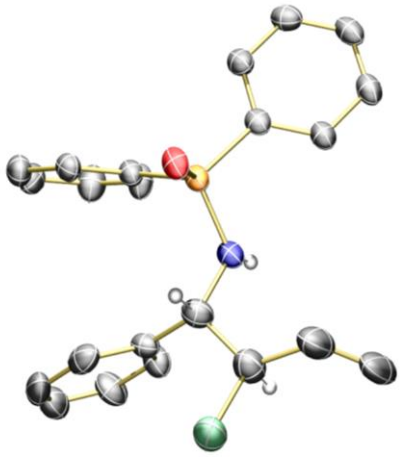

***Table S1.33*:** Crystal data and structure refinement for **1.111**.

Identification code	C22H21ClNOP	
Empirical formula	C22 H21 Cl N O P	
Formula weight	381.82	
Temperature	100(2) K	
Wavelength	0.71073 Å	
Crystal system	Orthorhombic	
Space group	Pbca	
Unit cell dimensions	a = 19.681(5) Å	α= 90°.
	b = 10.131(3) Å	β= 90°.
	c = 20.010(5) Å	γ = 90°.
Volume	3989.9(17) $Å^3$	
Z	8	
Density (calculated)	1.271 Mg/m^3	
Absorption coefficient	0.282 mm^{-1}	
F(000)	1600	
Crystal size	0.510 x 0.220 x 0.160 mm^3	
Theta range for data collection	2.035 to 28.369°.	
Index ranges	-26<=h<=26, -13<=k<=13, -26<=l<=26	
Reflections collected	89034	
Independent reflections	4986 [R(int) = 0.1161]	
Completeness to theta = 25.242°	100.0 %	

Absorption correction	Semi-empirical from equivalents
Max. and min. transmission	0.7457 and 0.3751
Refinement method	Full-matrix least-squares on F^2
Data / restraints / parameters	4986 / 215 / 257
Goodness-of-fit on F^2	1.040
Final R indices [I>2sigma(I)]	R1 = 0.0769, wR2 = 0.2069
R indices (all data)	R1 = 0.1109, wR2 = 0.2331
Extinction coefficient	na
Largest diff. peak and hole	1.003 and -1.011 e.$Å^{-3}$

***Table S1.34*:** Atomic coordinates ($x10^4$) and equivalent isotropic displacement parameters ($Å^2x10^3$) for **1.111**. U(eq) is defined as one third of the trace of the orthogonalized U^{ij} tensor.

	x	y	z	U(eq)
Cl(1)	6173(1)	4601(1)	8639(1)	57(1)
P(1)	7473(1)	4898(1)	6366(1)	26(1)
O(1)	7460(1)	6307(2)	6575(1)	33(1)
N(1)	7269(2)	3917(3)	6990(2)	30(1)
C(1)	6897(2)	4635(3)	5679(2)	29(1)
C(2)	6448(2)	5634(4)	5490(2)	32(1)
C(3)	5953(2)	5394(4)	5011(2)	39(1)
C(4)	5906(2)	4166(4)	4710(2)	42(1)
C(5)	6355(2)	3165(4)	4892(2)	46(1)
C(6)	6845(2)	3397(4)	5378(2)	39(1)
C(7)	8295(2)	4315(3)	6110(2)	28(1)
C(8)	8504(2)	4440(3)	5445(2)	34(1)
C(9)	9160(2)	4082(4)	5261(2)	38(1)
C(10)	9607(2)	3603(4)	5734(2)	37(1)
C(11)	9410(2)	3473(4)	6394(2)	35(1)
C(12)	8754(2)	3825(3)	6585(2)	30(1)
C(13)	6680(2)	4306(4)	7398(2)	38(1)
C(14)	6000(2)	3837(3)	7132(2)	32(1)
C(15)	5460(2)	4720(4)	7081(2)	43(1)
C(16)	4831(2)	4283(5)	6847(2)	50(1)

C(17)	4742(2)	2994(5)	6662(2)	54(1)
C(18)	5267(2)	2132(5)	6702(2)	49(1)
C(19)	5895(2)	2540(4)	6935(2)	41(1)
C(20)	6811(2)	3848(5)	8107(2)	48(1)
C(21)	7475(9)	4365(18)	8333(7)	48(3)
C(22)	7873(7)	3599(17)	8751(9)	64(4)
C(21X)	7519(10)	4100(20)	8466(9)	66(5)
C(22X)	7838(8)	3010(20)	8803(9)	70(4)

***Table S1.35*:** Bond lengths [Å] and angles [°] for **1.111**.

Cl(1)-C(20)	1.815(5)
P(1)-O(1)	1.489(2)
P(1)-N(1)	1.645(3)
P(1)-C(7)	1.797(4)
P(1)-C(1)	1.800(4)
N(1)-C(13)	1.473(5)
N(1)-H(1N)	0.875(19)
C(1)-C(6)	1.396(5)
C(1)-C(2)	1.396(5)
C(2)-C(3)	1.388(5)
C(2)-H(2)	0.9500
C(3)-C(4)	1.386(6)
C(3)-H(3)	0.9500
C(4)-C(5)	1.394(6)
C(4)-H(4)	0.9500
C(5)-C(6)	1.390(5)
C(5)-H(5)	0.9500
C(6)-H(6)	0.9500
C(7)-C(8)	1.399(5)
C(7)-C(12)	1.403(5)
C(8)-C(9)	1.390(5)
C(8)-H(8)	0.9500
C(9)-C(10)	1.381(6)
C(9)-H(9)	0.9500

C(10)-C(11)	1.382(6)
C(10)-H(10)	0.9500
C(11)-C(12)	1.393(5)
C(11)-H(11)	0.9500
C(12)-H(12)	0.9500
C(13)-C(20)	1.514(6)
C(13)-C(14)	1.515(5)
C(13)-H(13)	1.0000
C(14)-C(19)	1.388(5)
C(14)-C(15)	1.394(5)
C(15)-C(16)	1.396(7)
C(15)-H(15)	0.9500
C(16)-C(17)	1.369(7)
C(16)-H(16)	0.9500
C(17)-C(18)	1.356(7)
C(17)-H(17)	0.9500
C(18)-C(19)	1.384(6)
C(18)-H(18)	0.9500
C(19)-H(19)	0.9500
C(20)-C(21)	1.479(18)
C(20)-H(20)	1.0000
C(21)-C(22)	1.383(14)
C(21)-H(21)	0.9500
C(22)-H(22A)	0.9500
C(22)-H(22B)	0.9500

O(1)-P(1)-N(1)	111.20(15)
O(1)-P(1)-C(7)	114.27(15)
N(1)-P(1)-C(7)	103.74(16)
O(1)-P(1)-C(1)	110.20(15)
N(1)-P(1)-C(1)	109.70(16)
C(7)-P(1)-C(1)	107.47(16)
C(13)-N(1)-P(1)	116.8(2)
C(13)-N(1)-H(1N)	118(3)
P(1)-N(1)-H(1N)	117(3)

C(6)-C(1)-C(2)	119.2(3)
C(6)-C(1)-P(1)	120.6(3)
C(2)-C(1)-P(1)	119.9(3)
C(3)-C(2)-C(1)	120.4(3)
C(3)-C(2)-H(2)	119.8
C(1)-C(2)-H(2)	119.8
C(4)-C(3)-C(2)	120.3(4)
C(4)-C(3)-H(3)	119.9
C(2)-C(3)-H(3)	119.9
C(3)-C(4)-C(5)	119.8(4)
C(3)-C(4)-H(4)	120.1
C(5)-C(4)-H(4)	120.1
C(6)-C(5)-C(4)	120.0(4)
C(6)-C(5)-H(5)	120.0
C(4)-C(5)-H(5)	120.0
C(5)-C(6)-C(1)	120.4(4)
C(5)-C(6)-H(6)	119.8
C(1)-C(6)-H(6)	119.8
C(8)-C(7)-C(12)	119.2(3)
C(8)-C(7)-P(1)	120.5(3)
C(12)-C(7)-P(1)	120.2(3)
C(9)-C(8)-C(7)	120.1(4)
C(9)-C(8)-H(8)	119.9
C(7)-C(8)-H(8)	119.9
C(10)-C(9)-C(8)	120.1(4)
C(10)-C(9)-H(9)	120.0
C(8)-C(9)-H(9)	120.0
C(9)-C(10)-C(11)	120.7(4)
C(9)-C(10)-H(10)	119.7
C(11)-C(10)-H(10)	119.7
C(10)-C(11)-C(12)	119.9(4)
C(10)-C(11)-H(11)	120.1
C(12)-C(11)-H(11)	120.1
C(11)-C(12)-C(7)	120.1(3)
C(11)-C(12)-H(12)	120.0

C(7)-C(12)-H(12)	120.0
N(1)-C(13)-C(20)	107.7(3)
N(1)-C(13)-C(14)	114.6(3)
C(20)-C(13)-C(14)	112.6(3)
N(1)-C(13)-H(13)	107.2
C(20)-C(13)-H(13)	107.2
C(14)-C(13)-H(13)	107.2
C(19)-C(14)-C(15)	118.2(4)
C(19)-C(14)-C(13)	121.9(3)
C(15)-C(14)-C(13)	119.9(4)
C(14)-C(15)-C(16)	119.9(4)
C(14)-C(15)-H(15)	120.0
C(16)-C(15)-H(15)	120.0
C(17)-C(16)-C(15)	120.5(4)
C(17)-C(16)-H(16)	119.8
C(15)-C(16)-H(16)	119.8
C(18)-C(17)-C(16)	120.1(4)
C(18)-C(17)-H(17)	120.0
C(16)-C(17)-H(17)	120.0
C(17)-C(18)-C(19)	120.5(4)
C(17)-C(18)-H(18)	119.7
C(19)-C(18)-H(18)	119.7
C(18)-C(19)-C(14)	120.9(4)
C(18)-C(19)-H(19)	119.6
C(14)-C(19)-H(19)	119.6
C(21)-C(20)-C(13)	109.2(8)
C(21)-C(20)-Cl(1)	106.4(7)
C(13)-C(20)-Cl(1)	107.7(3)
C(21)-C(20)-H(20)	111.1
C(13)-C(20)-H(20)	111.1
Cl(1)-C(20)-H(20)	111.1
C(22)-C(21)-C(20)	119.2(16)
C(22)-C(21)-H(21)	120.4
C(20)-C(21)-H(21)	120.4
C(21)-C(22)-H(22A)	120.0

C(21)-C(22)-H(22B)	120.0
H(22A)-C(22)-H(22B)	120.0

Symmetry transformations used to generate equivalent atoms:

***Table S1.36*:** Anisotropic displacement parameters ($Å^2x10^3$) for **1.111**. The anisotropic displacement factor exponent takes the form: $-2\pi^2[h^2a^{*2}U^{11} + ... + 2hka^*b^*U^{12}]$.

	U^{11}	U^{22}	U^{33}	U^{23}	U^{13}	U^{12}
Cl(1)	50(1)	79(1)	43(1)	5(1)	10(1)	18(1)
P(1)	25(1)	17(1)	37(1)	-2(1)	0(1)	-1(1)
O(1)	31(1)	18(1)	50(2)	-4(1)	-2(1)	0(1)
N(1)	28(1)	21(1)	39(2)	-3(1)	3(1)	-2(1)
C(1)	27(2)	22(2)	39(2)	2(1)	-1(1)	-2(1)
C(2)	30(2)	27(2)	39(2)	1(1)	2(1)	3(1)
C(3)	35(2)	36(2)	45(2)	4(2)	-4(2)	4(2)
C(4)	39(2)	41(2)	45(2)	5(2)	-9(2)	-6(2)
C(5)	51(2)	32(2)	57(2)	-4(2)	-16(2)	-4(2)
C(6)	42(2)	26(2)	50(2)	-4(2)	-14(2)	2(2)
C(7)	28(2)	17(1)	40(2)	-2(1)	1(1)	-3(1)
C(8)	32(2)	26(2)	42(2)	3(1)	4(1)	0(1)
C(9)	39(2)	30(2)	45(2)	1(2)	11(2)	-3(2)
C(10)	28(2)	26(2)	57(2)	-3(2)	7(2)	-1(1)
C(11)	28(2)	28(2)	51(2)	-2(2)	-3(2)	1(1)
C(12)	27(2)	25(2)	39(2)	-3(1)	0(1)	-1(1)
C(13)	38(2)	37(2)	39(2)	-6(2)	7(2)	-3(2)
C(14)	32(2)	27(2)	37(2)	0(1)	8(1)	-1(1)
C(15)	56(2)	34(2)	38(2)	6(2)	10(2)	11(2)
C(16)	44(2)	63(3)	44(2)	13(2)	3(2)	23(2)
C(17)	38(2)	74(3)	49(2)	2(2)	0(2)	1(2)
C(18)	34(2)	50(2)	63(3)	-9(2)	0(2)	-9(2)
C(19)	35(2)	31(2)	56(2)	-4(2)	-2(2)	1(2)
C(20)	43(2)	56(3)	46(2)	-4(2)	3(2)	3(2)
C(21)	45(4)	76(7)	23(5)	-16(5)	-9(4)	13(4)
C(22)	29(5)	98(10)	65(8)	29(8)	-25(5)	-18(6)

C(21X)	42(5)	102(11)	55(9)	10(6)	5(5)	-14(5)
C(22X)	34(5)	124(11)	52(7)	7(8)	0(4)	-22(7)

***Table S1.37*:** Hydrogen coordinates ($x10^4$) and isotropic displacement parameters ($Å^2x10^3$)
for **1.111**.

	x	y	z	U(eq)
H(1N)	7350(20)	3070(20)	6930(20)	35
H(2)	6482	6482	5689	38
H(3)	5644	6075	4890	46
H(4)	5569	4007	4380	50
H(5)	6326	2324	4684	56
H(6)	7147	2709	5505	47
H(8)	8198	4770	5118	40
H(9)	9301	4168	4809	46
H(10)	10055	3360	5606	44
H(11)	9721	3143	6716	42
H(12)	8617	3732	7038	36
H(13)	6667	5293	7406	45
H(15)	5519	5617	7206	51
H(16)	4462	4884	6816	61
H(17)	4312	2703	6504	64
H(18)	5204	1239	6570	59
H(19)	6258	1925	6960	49
H(20)	6795	2864	8139	58
H(21)	7626	5212	8194	57
H(22A)	7719	2753	8888	77
H(22B)	8300	3920	8900	77
H(21X)	7727	4942	8458	80
H(22C)	7625	2164	8807	84
H(22D)	8261	3127	9022	84

***Table S1.38*:** Torsion angles [°] for **1.111**.

O(1)-P(1)-N(1)-C(13)	44.9(3)
C(7)-P(1)-N(1)-C(13)	168.1(3)
C(1)-P(1)-N(1)-C(13)	-77.3(3)
O(1)-P(1)-C(1)-C(6)	177.1(3)
N(1)-P(1)-C(1)-C(6)	-60.1(3)
C(7)-P(1)-C(1)-C(6)	52.0(3)
O(1)-P(1)-C(1)-C(2)	-9.6(3)
N(1)-P(1)-C(1)-C(2)	113.2(3)
C(7)-P(1)-C(1)-C(2)	-134.7(3)
C(6)-C(1)-C(2)-C(3)	0.5(6)
P(1)-C(1)-C(2)-C(3)	-172.9(3)
C(1)-C(2)-C(3)-C(4)	-1.0(6)
C(2)-C(3)-C(4)-C(5)	0.5(6)
C(3)-C(4)-C(5)-C(6)	0.4(7)
C(4)-C(5)-C(6)-C(1)	-0.9(7)
C(2)-C(1)-C(6)-C(5)	0.4(6)
P(1)-C(1)-C(6)-C(5)	173.8(3)
O(1)-P(1)-C(7)-C(8)	-88.3(3)
N(1)-P(1)-C(7)-C(8)	150.4(3)
C(1)-P(1)-C(7)-C(8)	34.3(3)
O(1)-P(1)-C(7)-C(12)	86.6(3)
N(1)-P(1)-C(7)-C(12)	-34.6(3)
C(1)-P(1)-C(7)-C(12)	-150.8(3)
C(12)-C(7)-C(8)-C(9)	-0.1(5)
P(1)-C(7)-C(8)-C(9)	175.0(3)
C(7)-C(8)-C(9)-C(10)	0.0(6)
C(8)-C(9)-C(10)-C(11)	0.0(6)
C(9)-C(10)-C(11)-C(12)	0.1(6)
C(10)-C(11)-C(12)-C(7)	-0.2(5)
C(8)-C(7)-C(12)-C(11)	0.2(5)
P(1)-C(7)-C(12)-C(11)	-174.8(3)
P(1)-N(1)-C(13)-C(20)	-147.5(3)
P(1)-N(1)-C(13)-C(14)	86.4(4)
N(1)-C(13)-C(14)-C(19)	48.3(5)

C(20)-C(13)-C(14)-C(19)	-75.2(5)
N(1)-C(13)-C(14)-C(15)	-131.8(4)
C(20)-C(13)-C(14)-C(15)	104.8(4)
C(19)-C(14)-C(15)-C(16)	1.0(6)
C(13)-C(14)-C(15)-C(16)	-178.9(4)
C(14)-C(15)-C(16)-C(17)	-0.5(6)
C(15)-C(16)-C(17)-C(18)	-0.3(7)
C(16)-C(17)-C(18)-C(19)	0.4(7)
C(17)-C(18)-C(19)-C(14)	0.1(7)
C(15)-C(14)-C(19)-C(18)	-0.9(6)
C(13)-C(14)-C(19)-C(18)	179.1(4)
N(1)-C(13)-C(20)-C(21)	53.8(8)
C(14)-C(13)-C(20)-C(21)	-178.9(7)
N(1)-C(13)-C(20)-Cl(1)	169.0(3)
C(14)-C(13)-C(20)-Cl(1)	-63.8(4)
C(13)-C(20)-C(21)-C(22)	-144.7(12)
Cl(1)-C(20)-C(21)-C(22)	99.3(13)

Symmetry transformations used to generate equivalent atoms:

***Table 1.39*:** Hydrogen bonds for **1.111** [Å and °].

D-H...A	d(D-H)	d(H...A)	d(D...A)	<(DHA)
N(1)-H(1N)...O(1)#1	0.875(19)	1.97(2)	2.822(4)	166(4)

Symmetry transformations used to generate equivalent atoms:

#1 -x+3/2,y-1/2,z

1.7.6. *NMR Spectra (^{1}H, ^{13}C)*

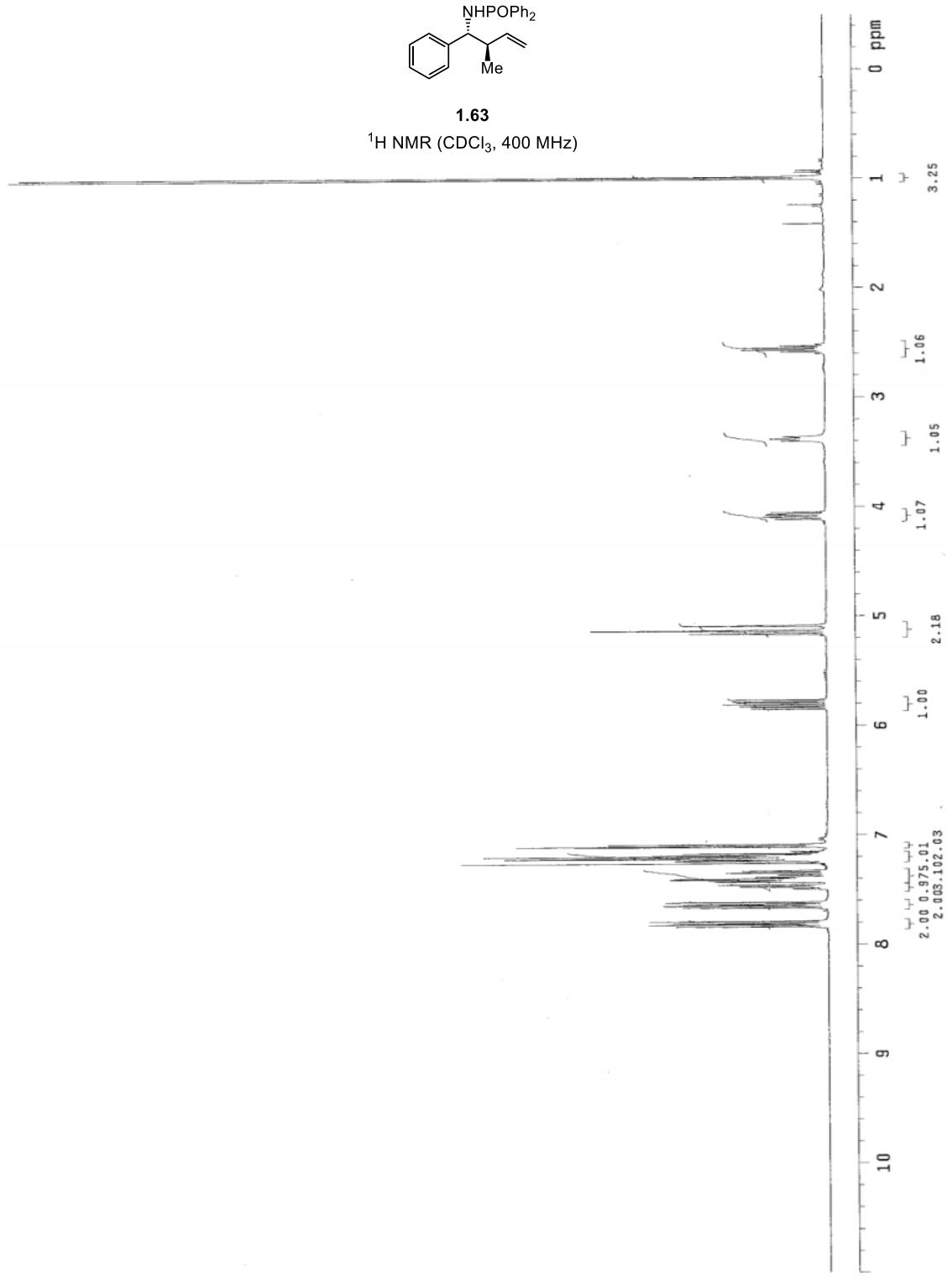

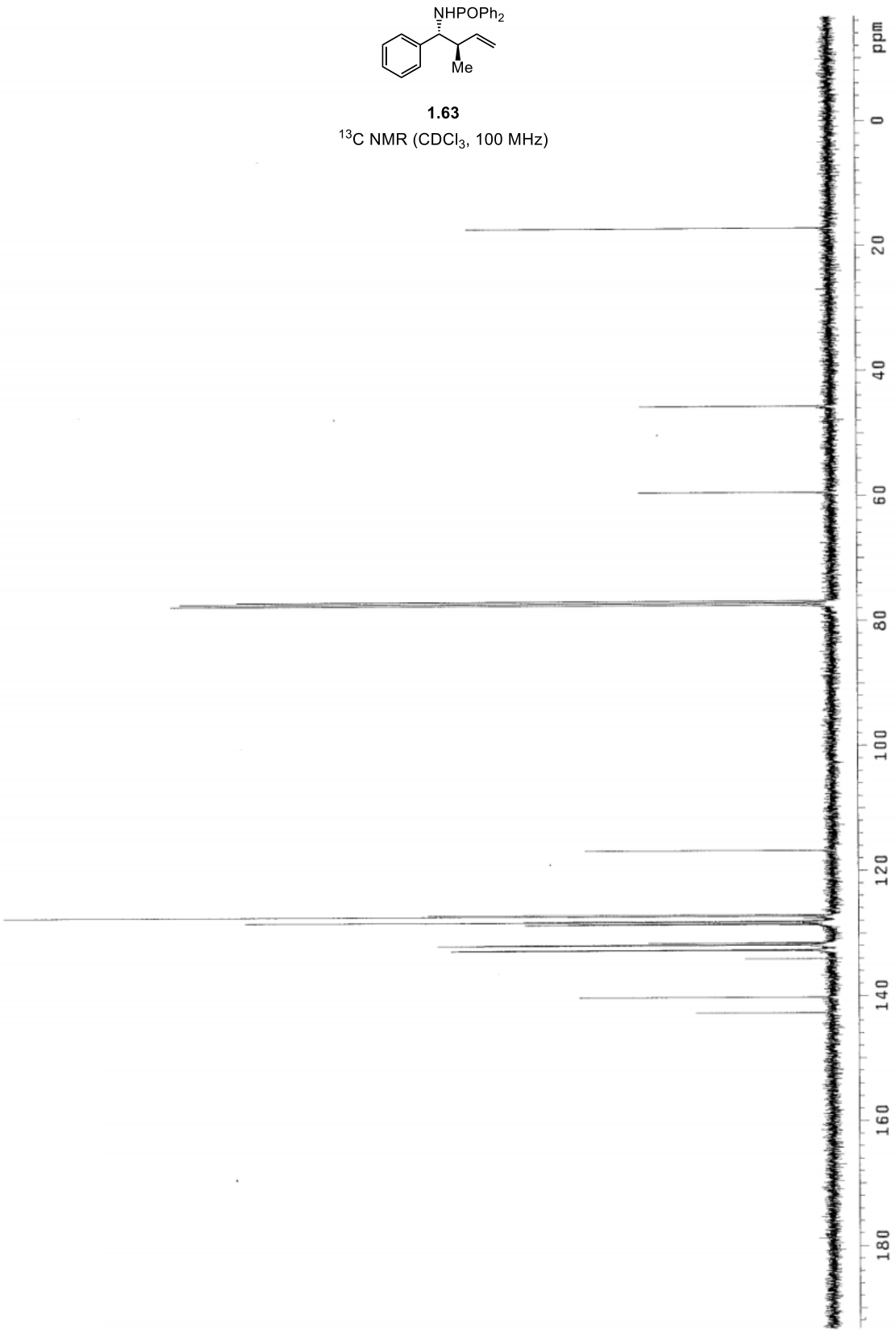

1.63

^{13}C NMR ($CDCl_3$, 100 MHz)

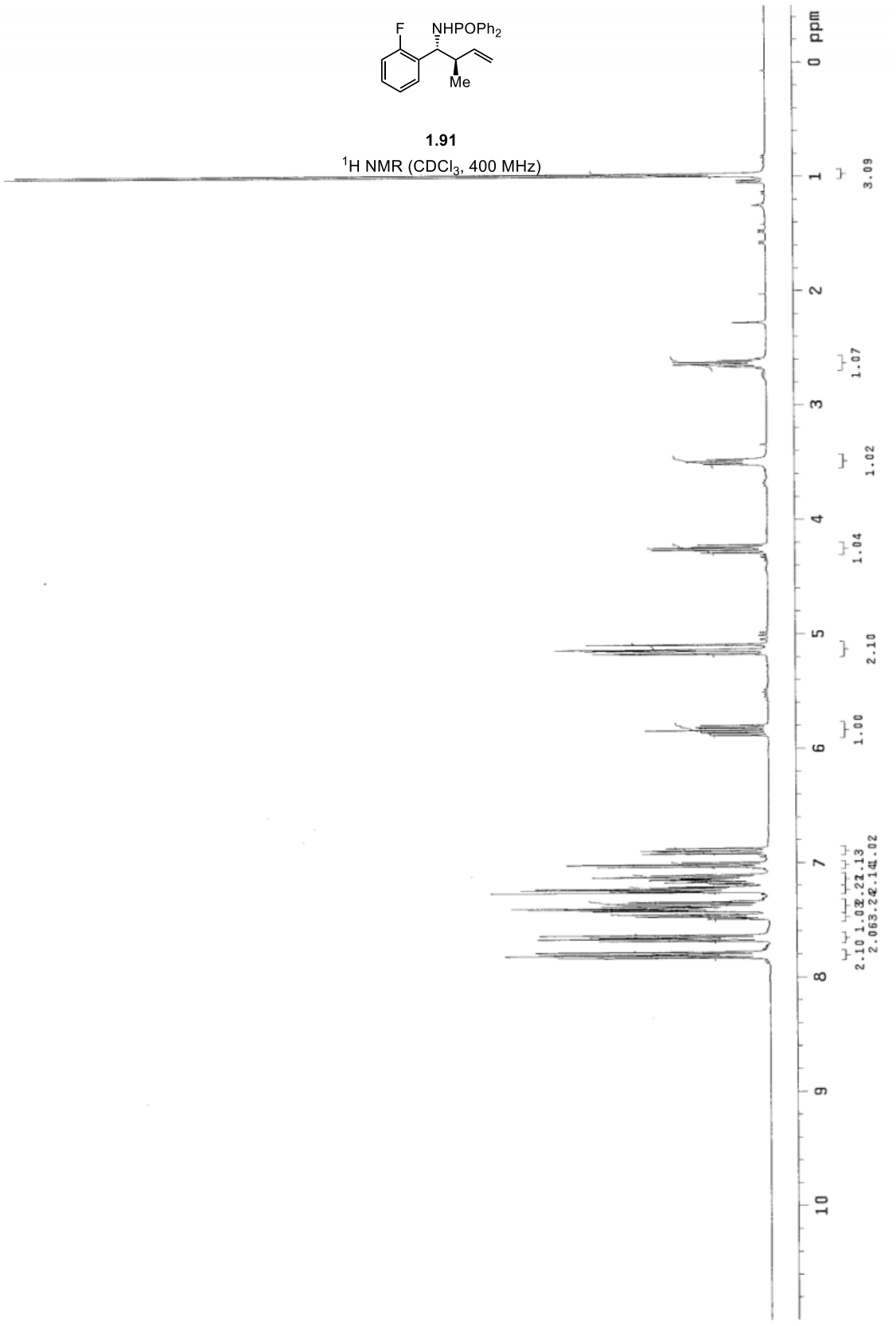
F
NHPOPh2
Me
1.91
1H NMR (CDCl3, 400 MHz)
0 ppm
1
2
3
4
5
6
7
8
9
10
3.09
1.07
1.02
1.04
2.10
1.00

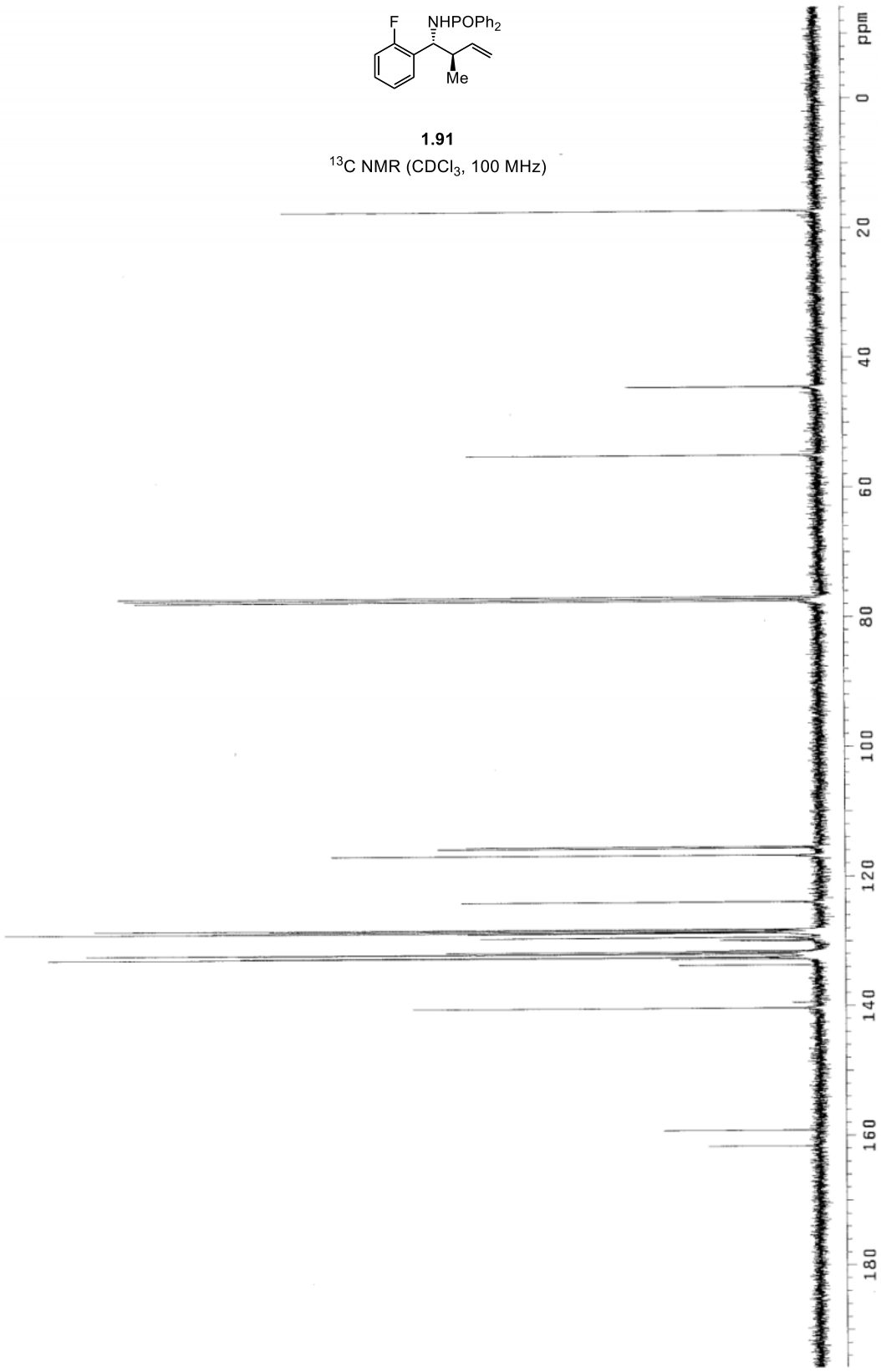

1.91

^{13}C NMR ($CDCl_3$, 100 MHz)

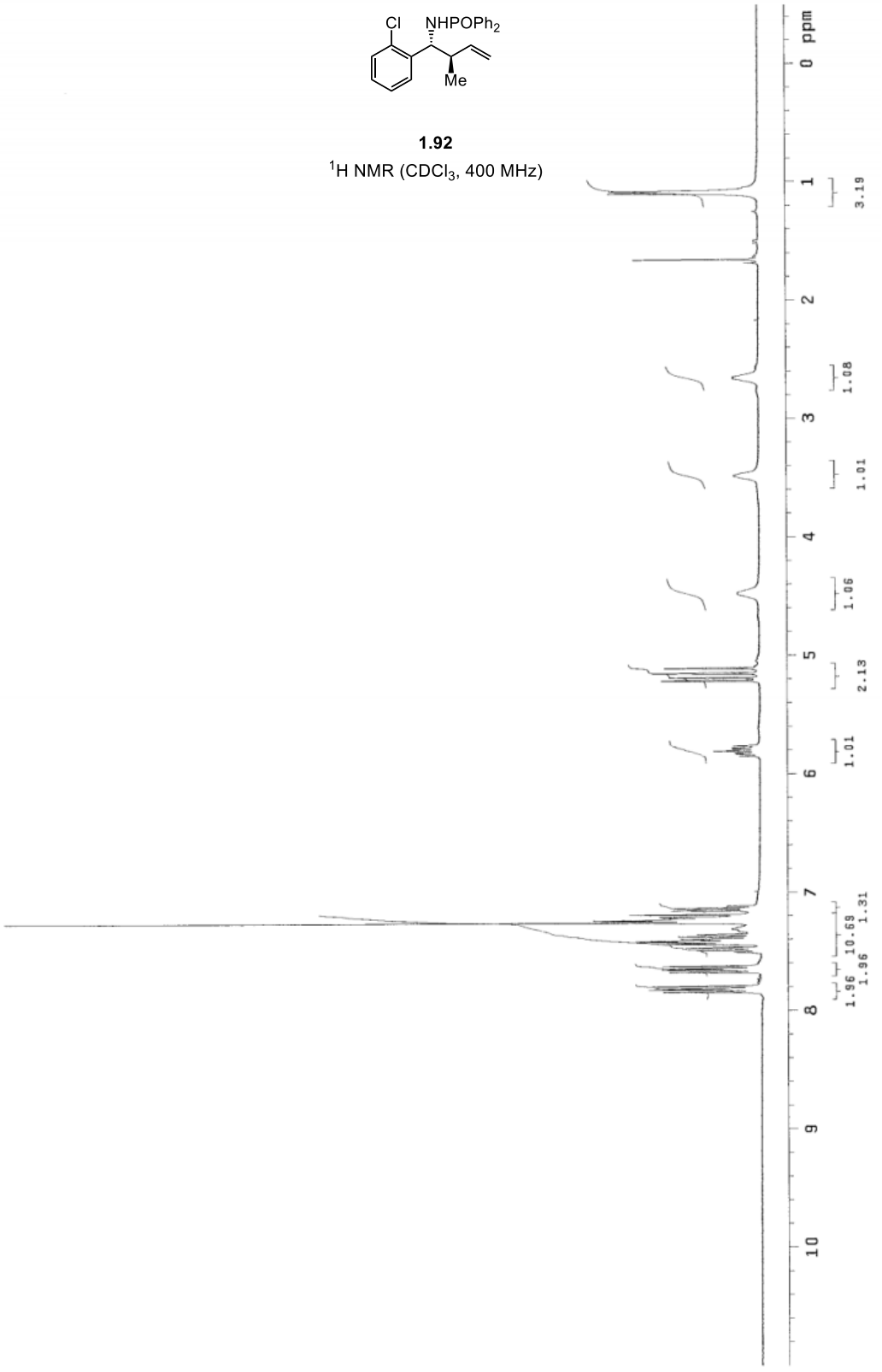
Cl
NHPOPh2
Me
1.92
1H NMR (CDCl3, 400 MHz)
0 ppm
1
2
3
4
5
6
7
8
9
10
3.19
1.08
1.01
1.06
2.13
1.01
1.96
10.69
1.96
1.31

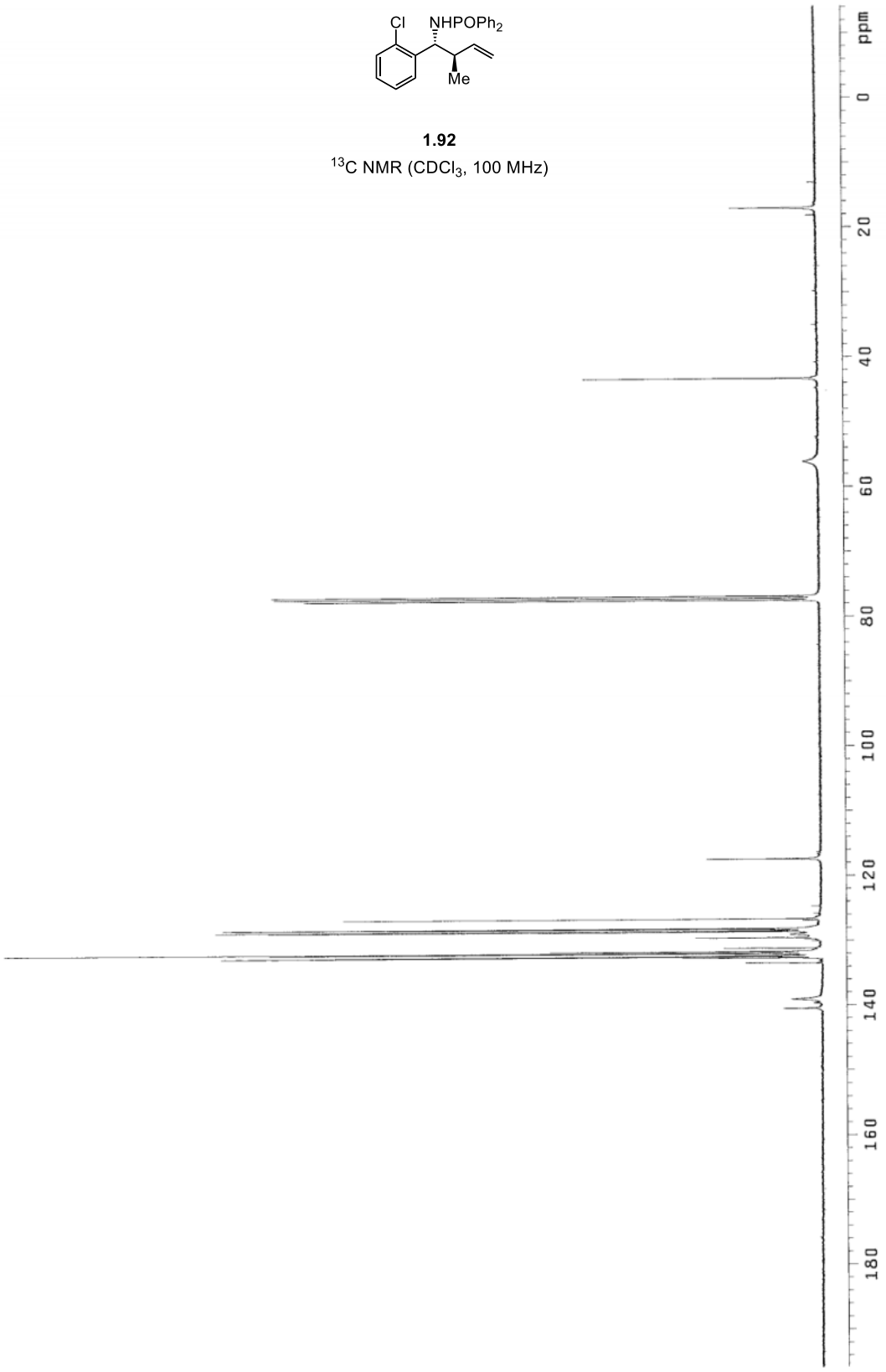

1.92

^{13}C NMR ($CDCl_3$, 100 MHz)

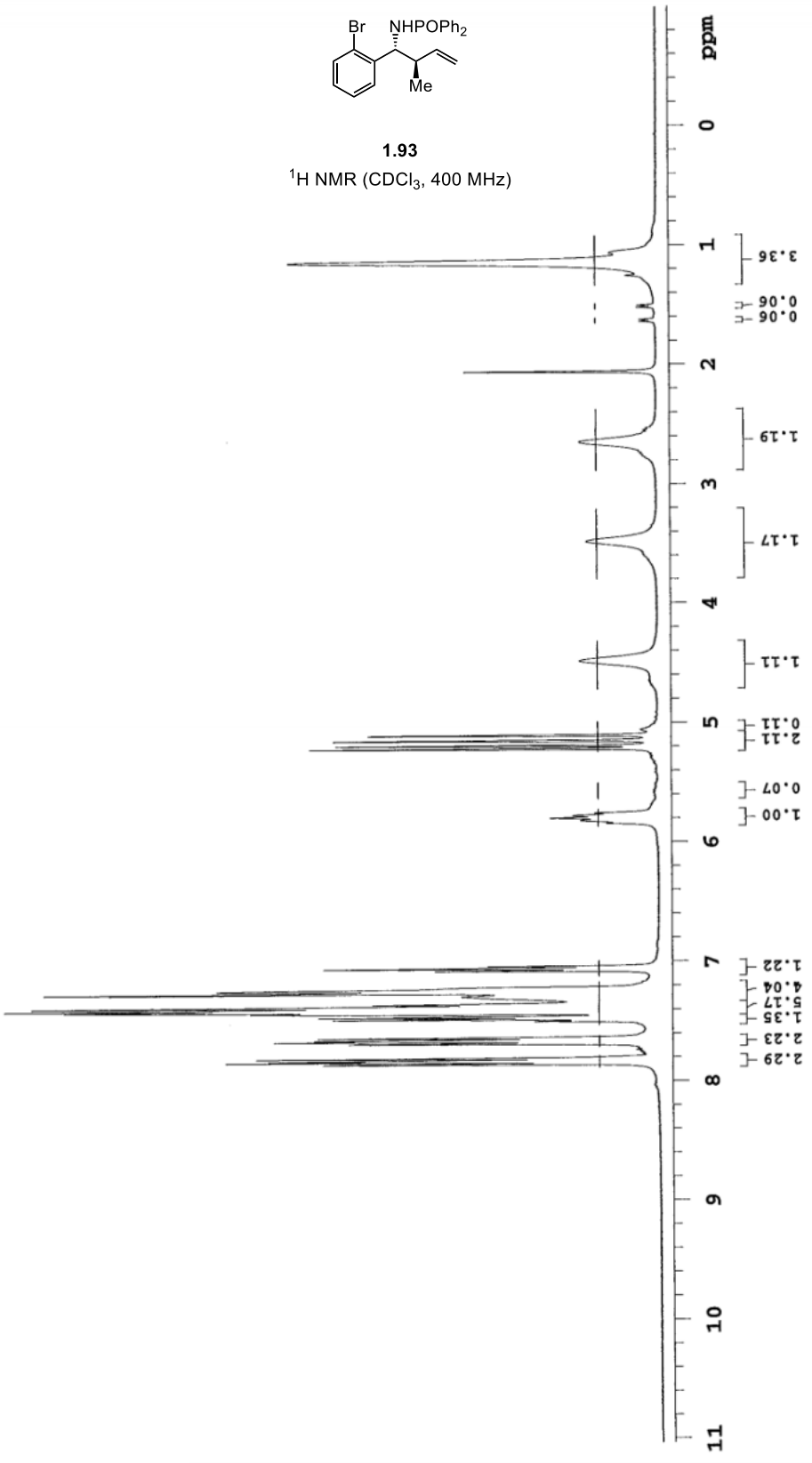
Br
NHPOPh2
Me
1.93
1H NMR (CDCl3, 400 MHz)
ppm
3.36
0.06
0.06
1.19
1.17
1.11
2.11
0.11
0.07
1.00
1.22
4.04
5.17
1.35
2.23
2.29

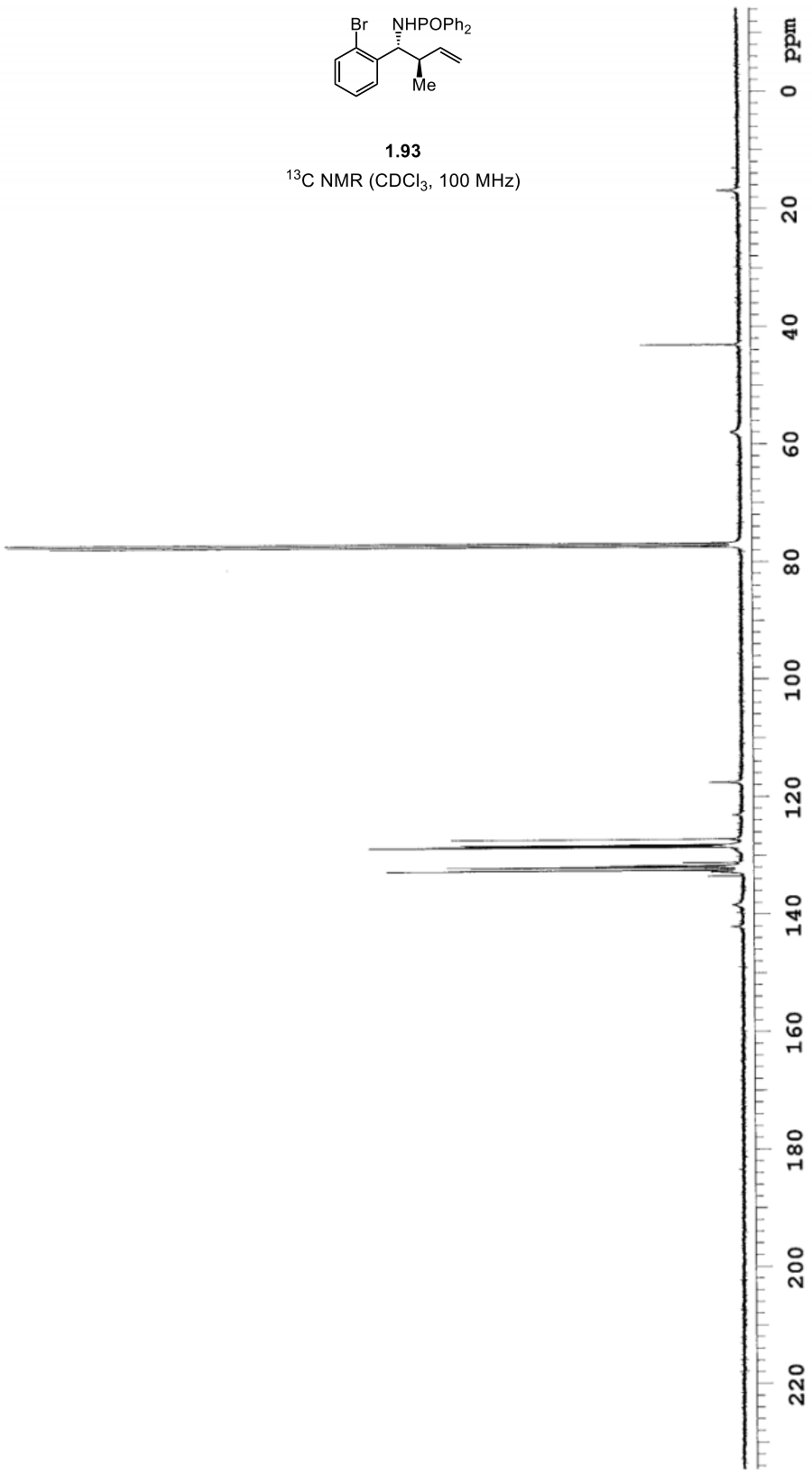

1.93

^{13}C NMR ($CDCl_3$, 100 MHz)

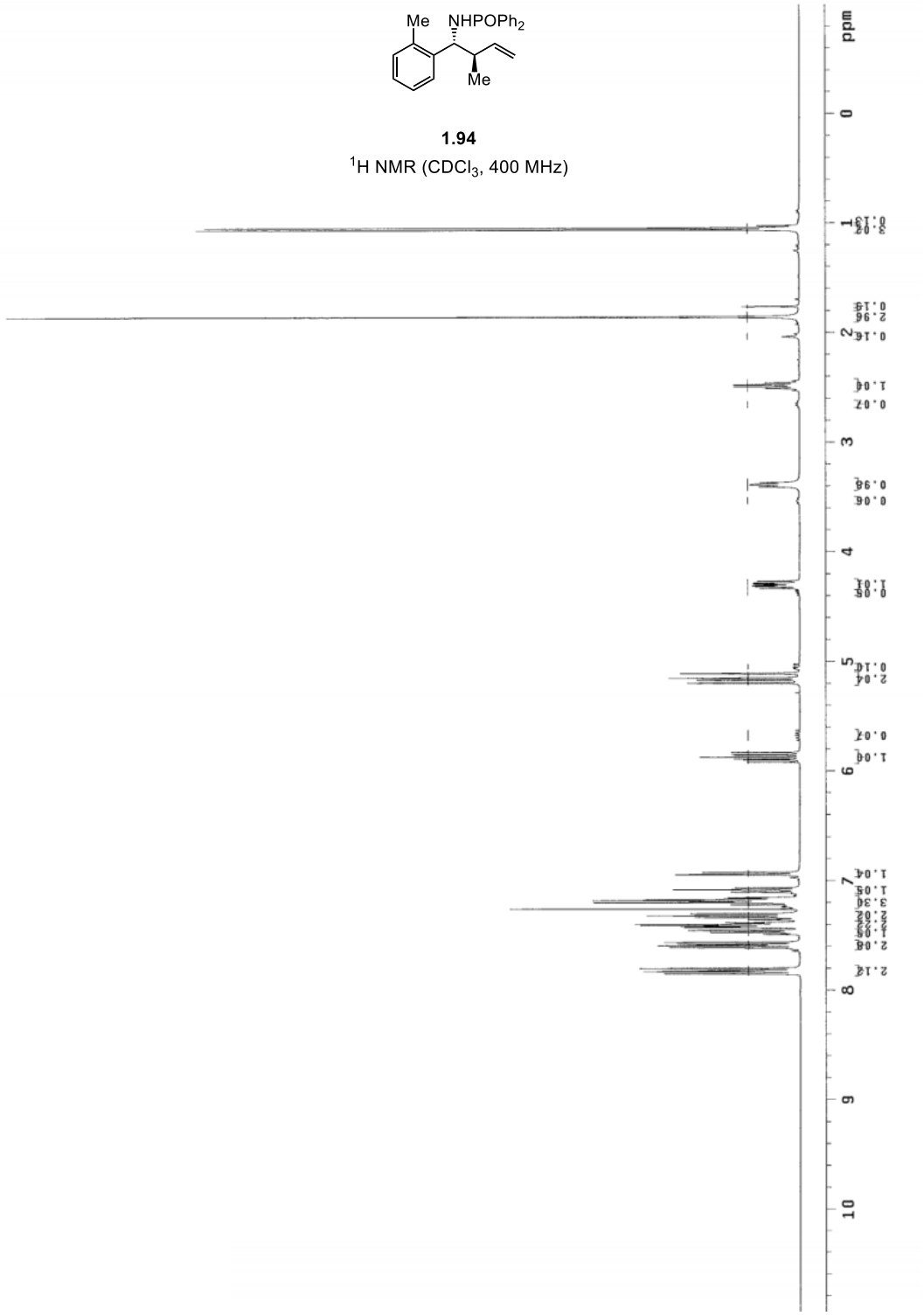

1.94

^{1}H NMR ($CDCl_3$, 400 MHz)

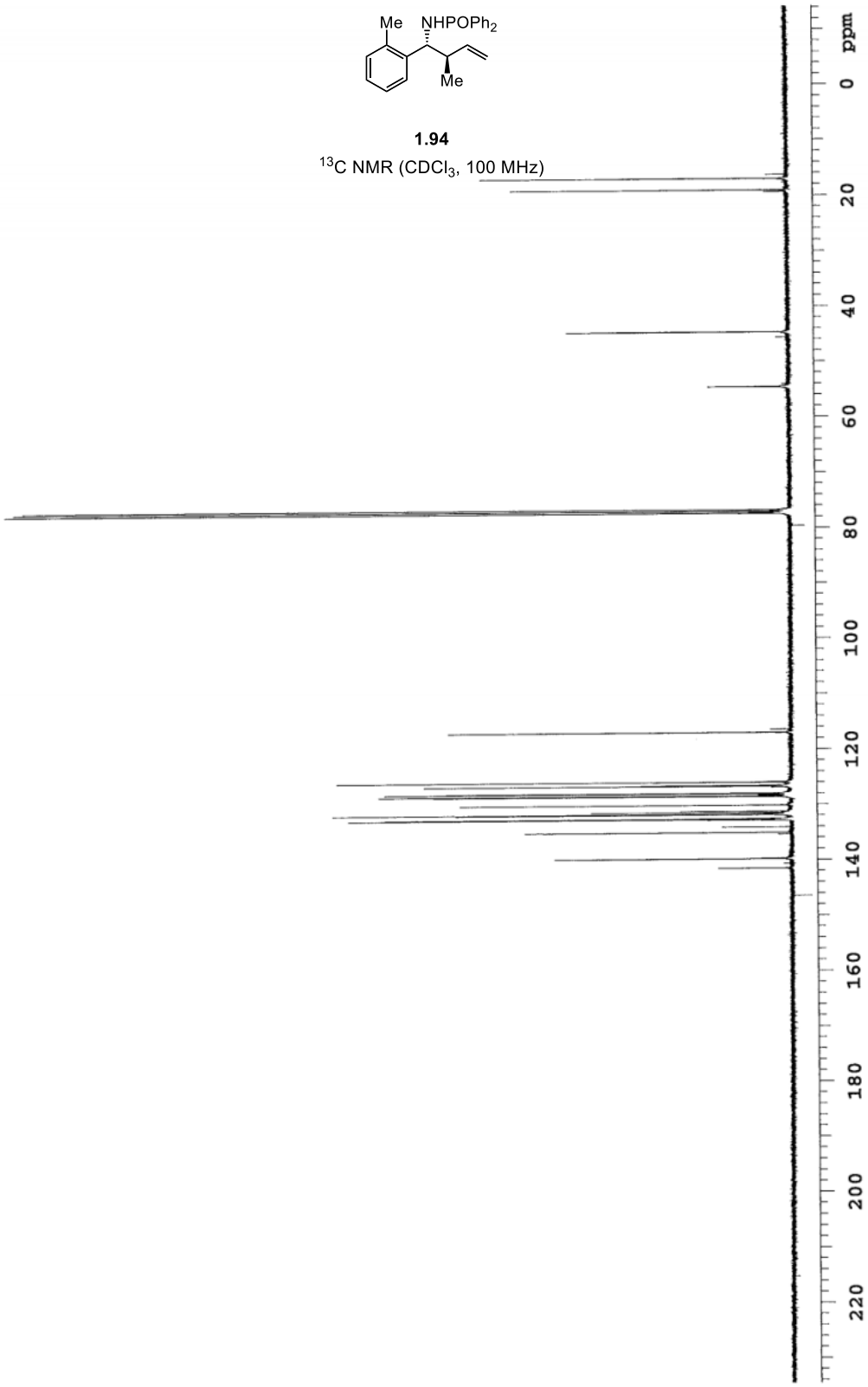
Me
NHPOPh2
Me
1.94
13C NMR (CDCl3, 100 MHz)
ppm
0
20
40
60
80
100
120
140
160
180
200
220

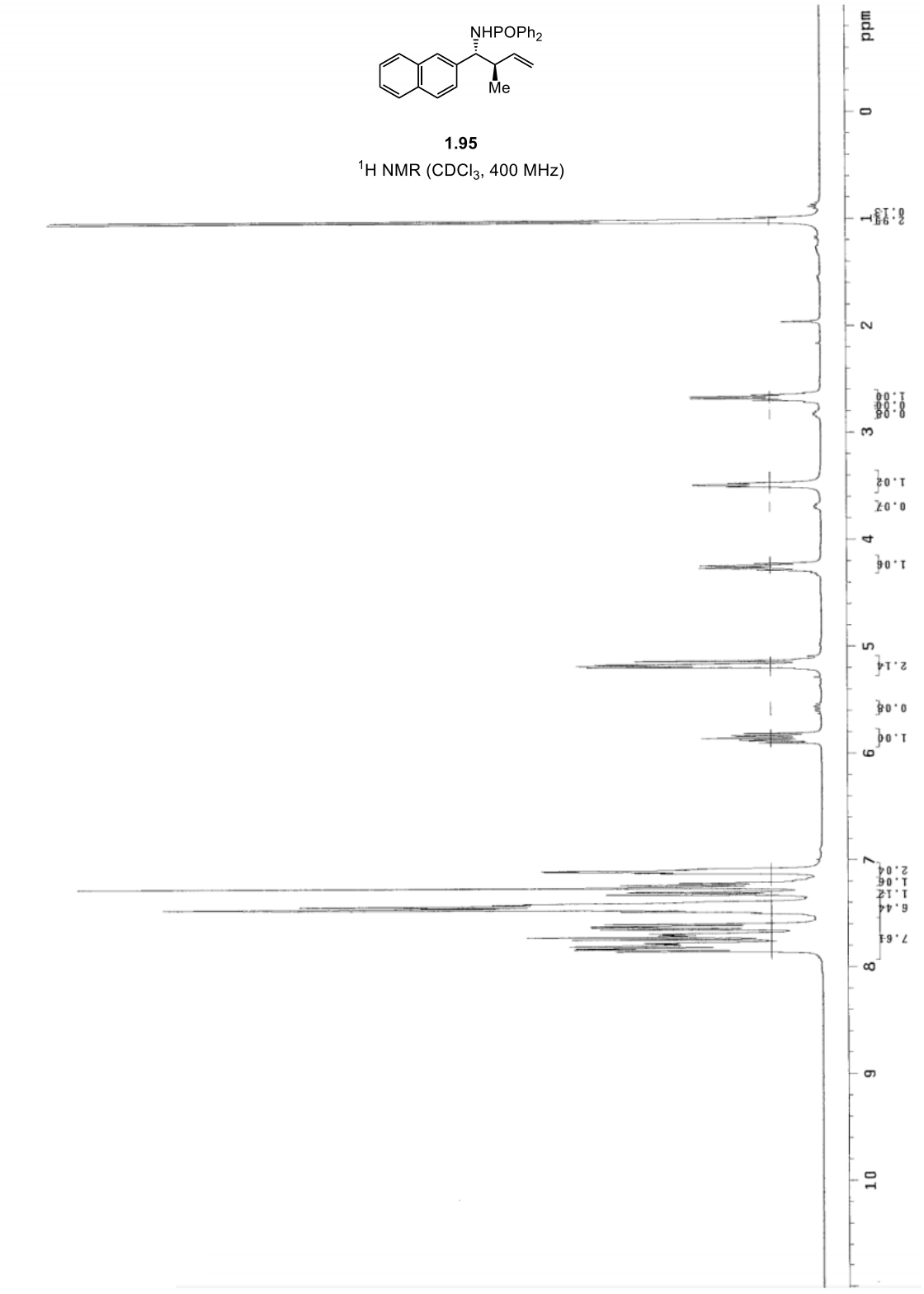

1.95

^{1}H NMR ($CDCl_3$, 400 MHz)

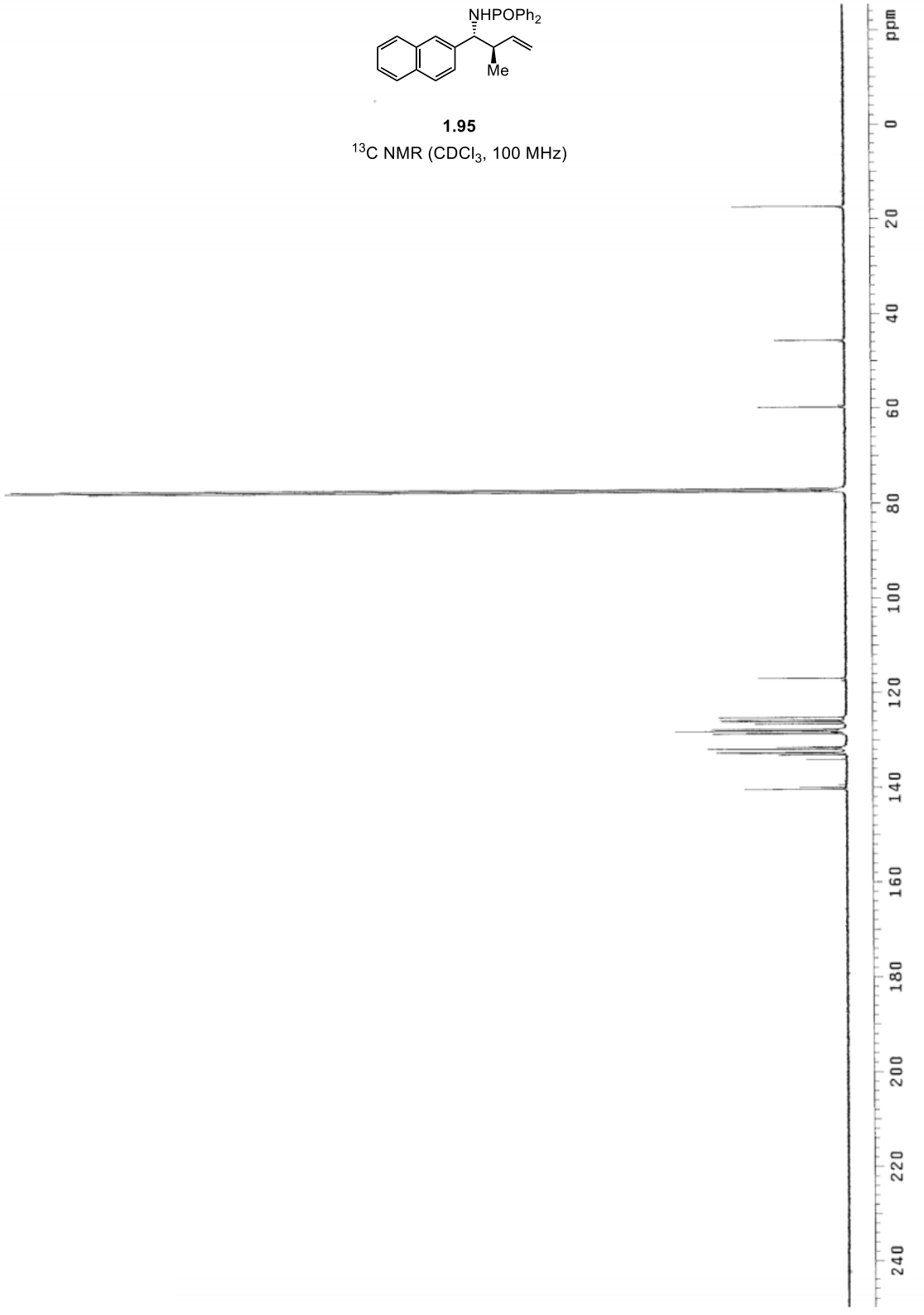

1.95

^{13}C NMR ($CDCl_3$, 100 MHz)

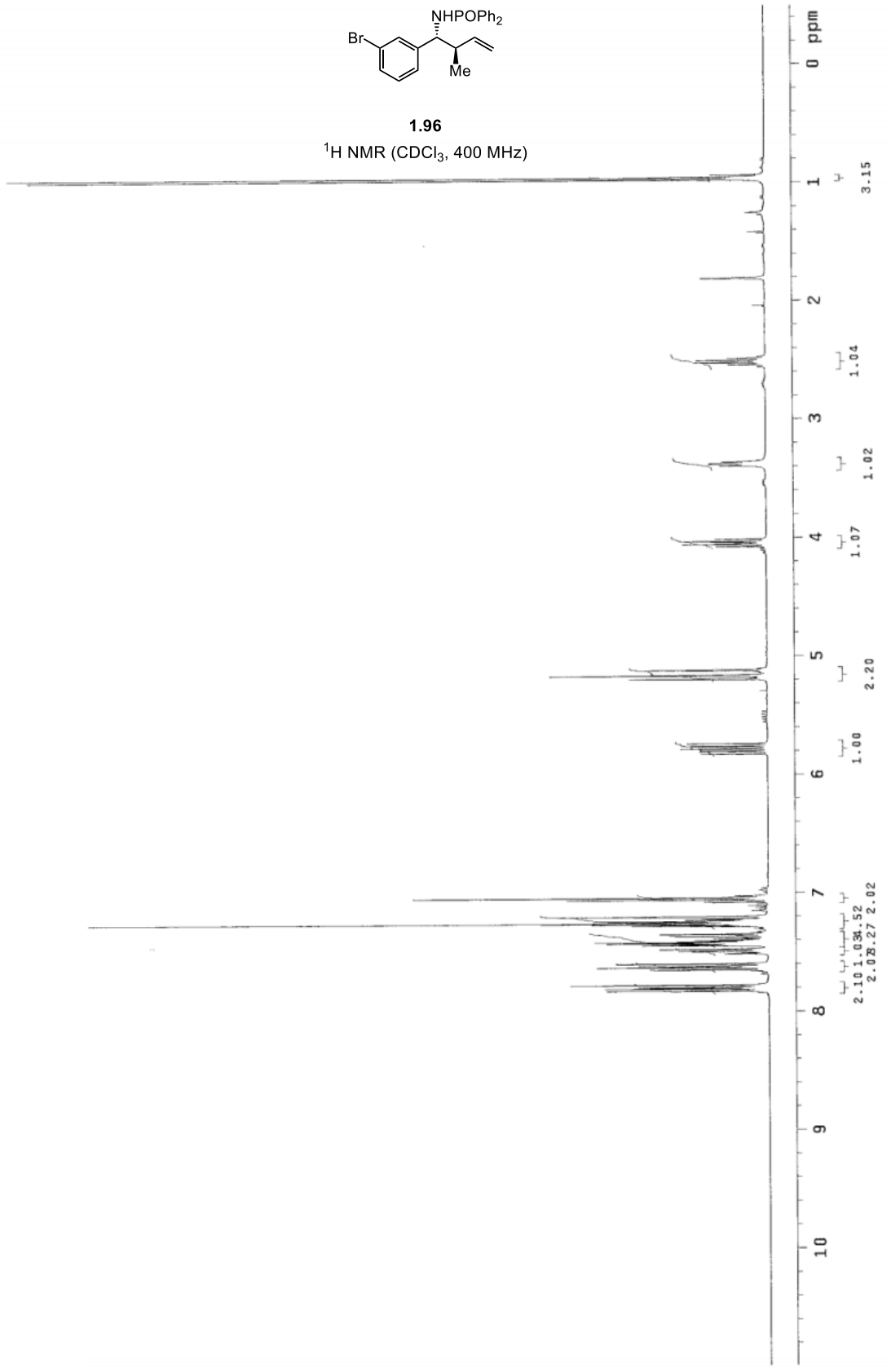
NHPOPh2
Br
Me
1.96
1H NMR (CDCl3, 400 MHz)
0 ppm
1
2
3
4
5
6
7
8
9
10
3.15
1.04
1.02
1.07
2.20
1.00
2.10 1.03 4.52
2.02 2.27 2.02

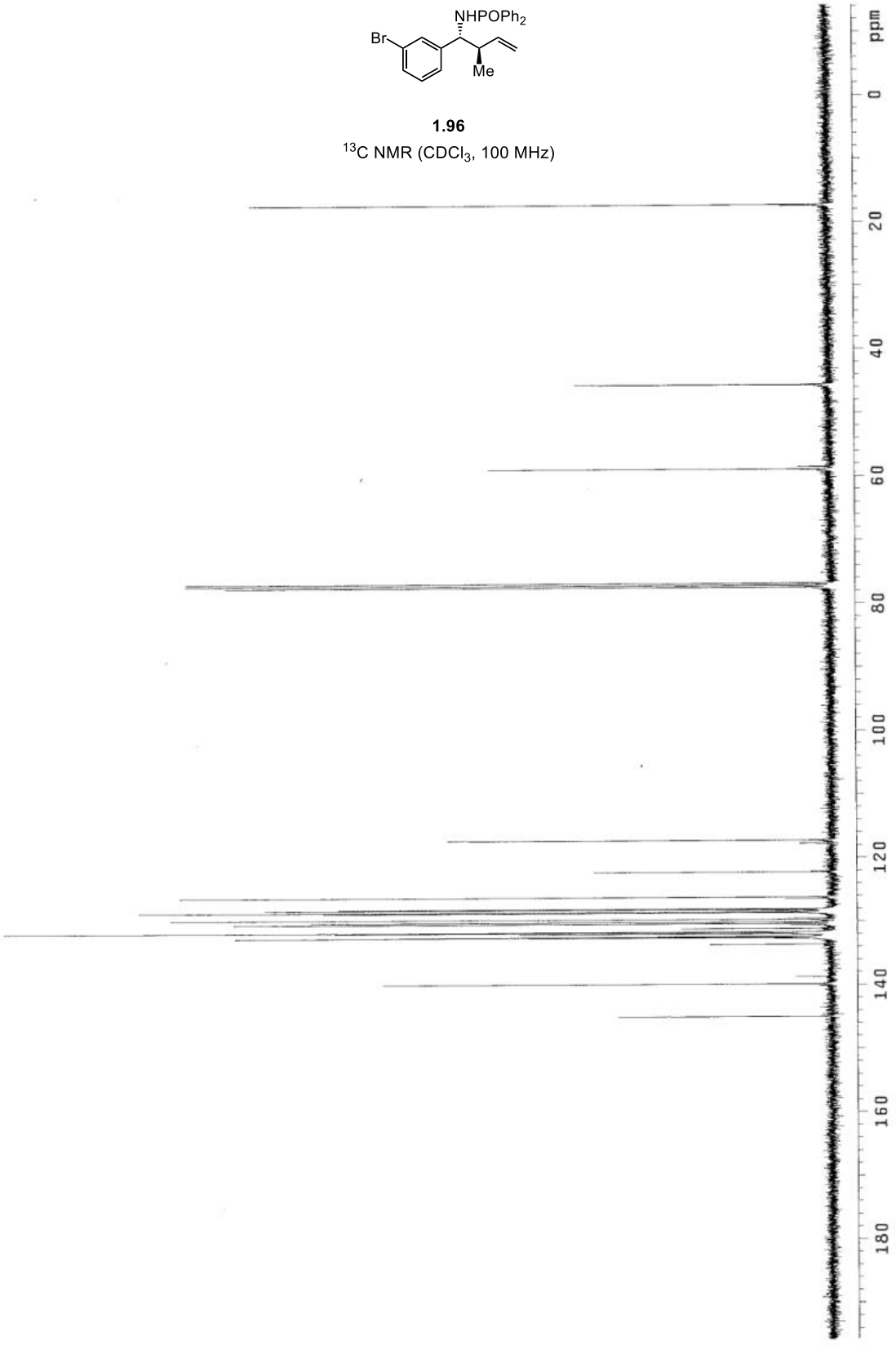

1.96

^{13}C NMR ($CDCl_3$, 100 MHz)

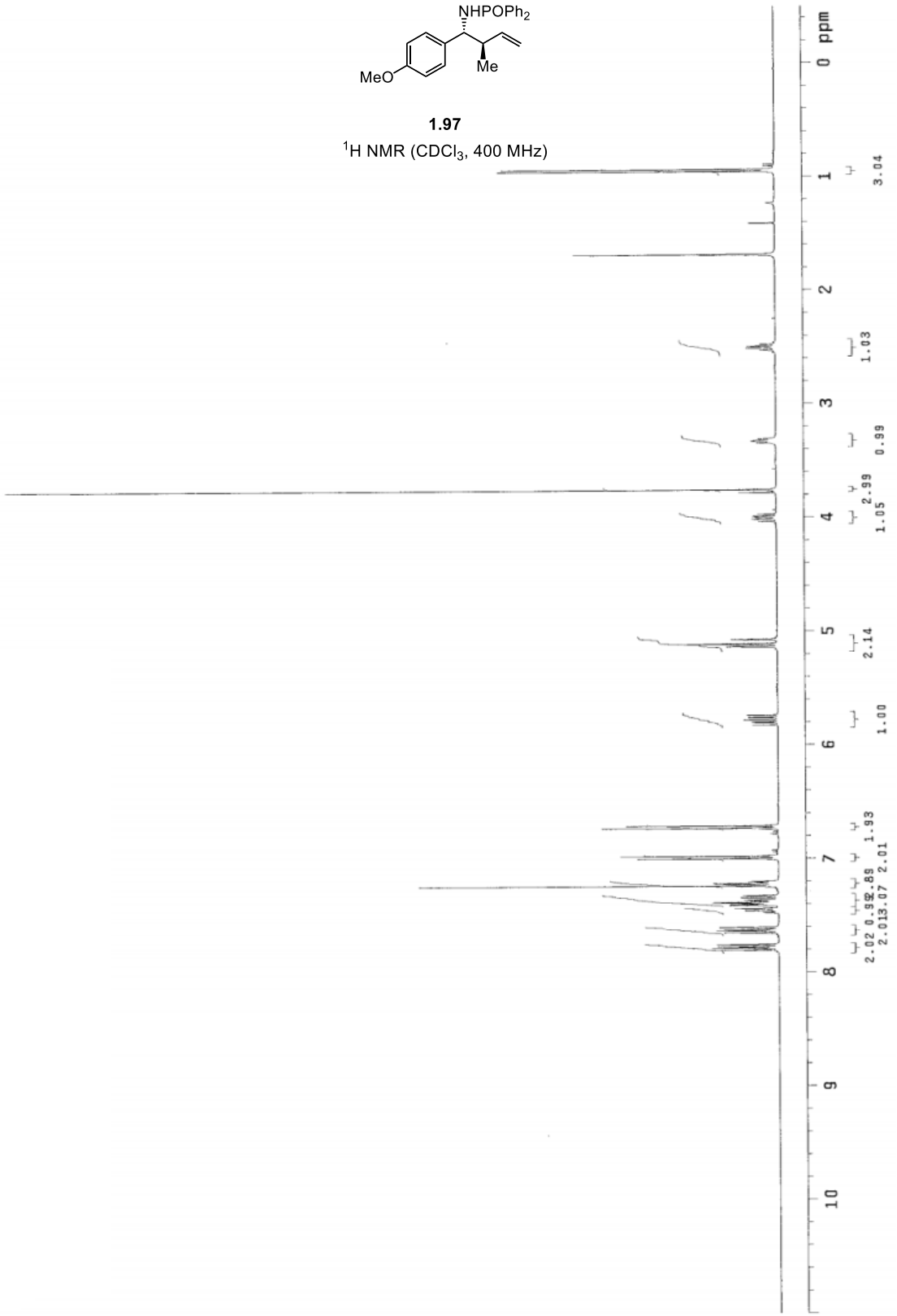
NHPOPh2
Me
MeO
1.97
1H NMR (CDCl3, 400 MHz)
0 ppm
1
2
3
4
5
6
7
8
9
10
3.04
1.03
0.99
2.99
1.05
2.14
1.00
1.93
2.01
2.07
2.02

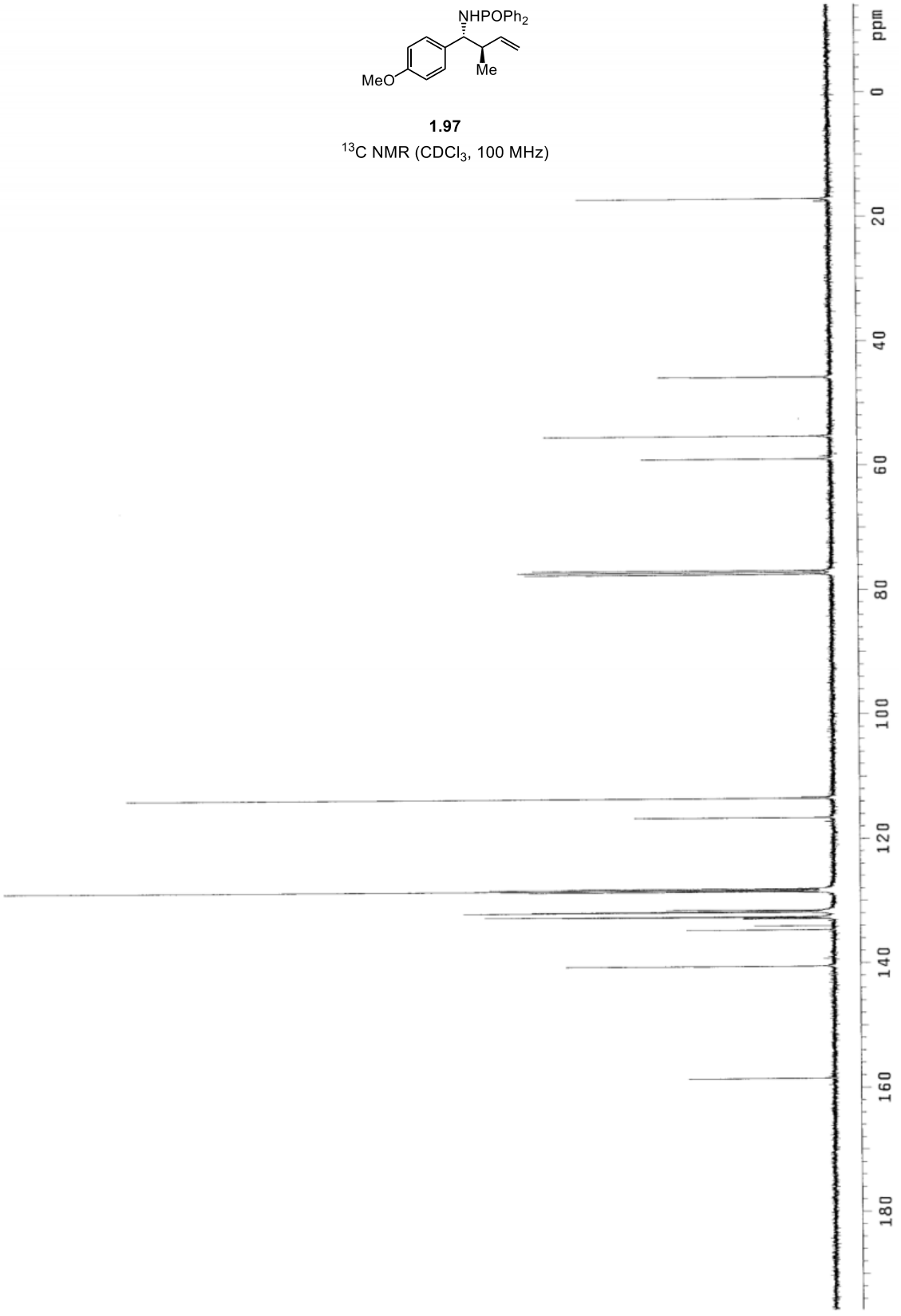

1.97

^{13}C NMR ($CDCl_3$, 100 MHz)

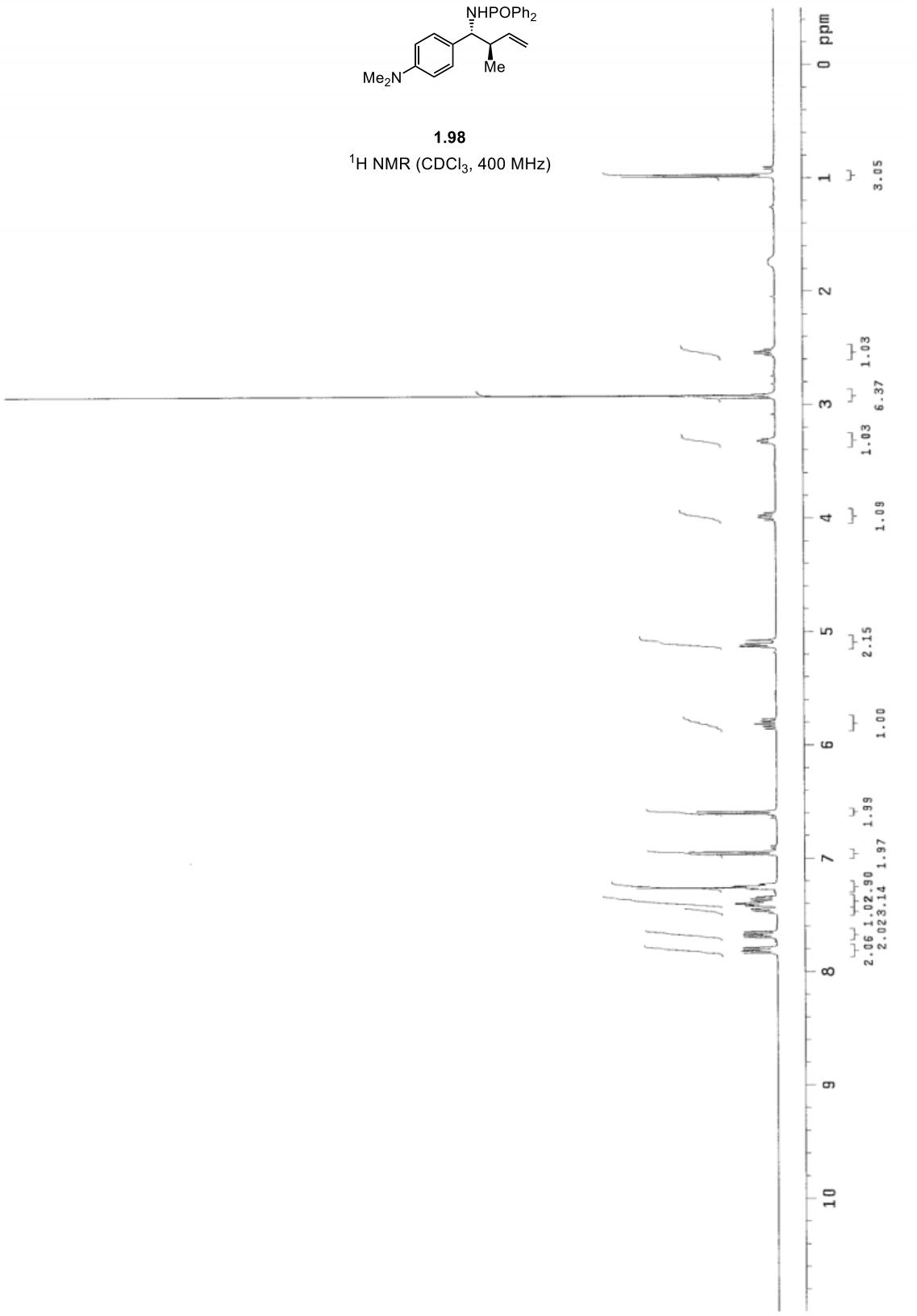
NHPOPh2
Me2N
Me
1.98
1H NMR (CDCl3, 400 MHz)
0 ppm
1
2
3
4
5
6
7
8
9
10
3.05
1.03
6.37
1.03
1.09
2.15
1.00
1.99
2.06 1.02.90 1.97
2.023.14

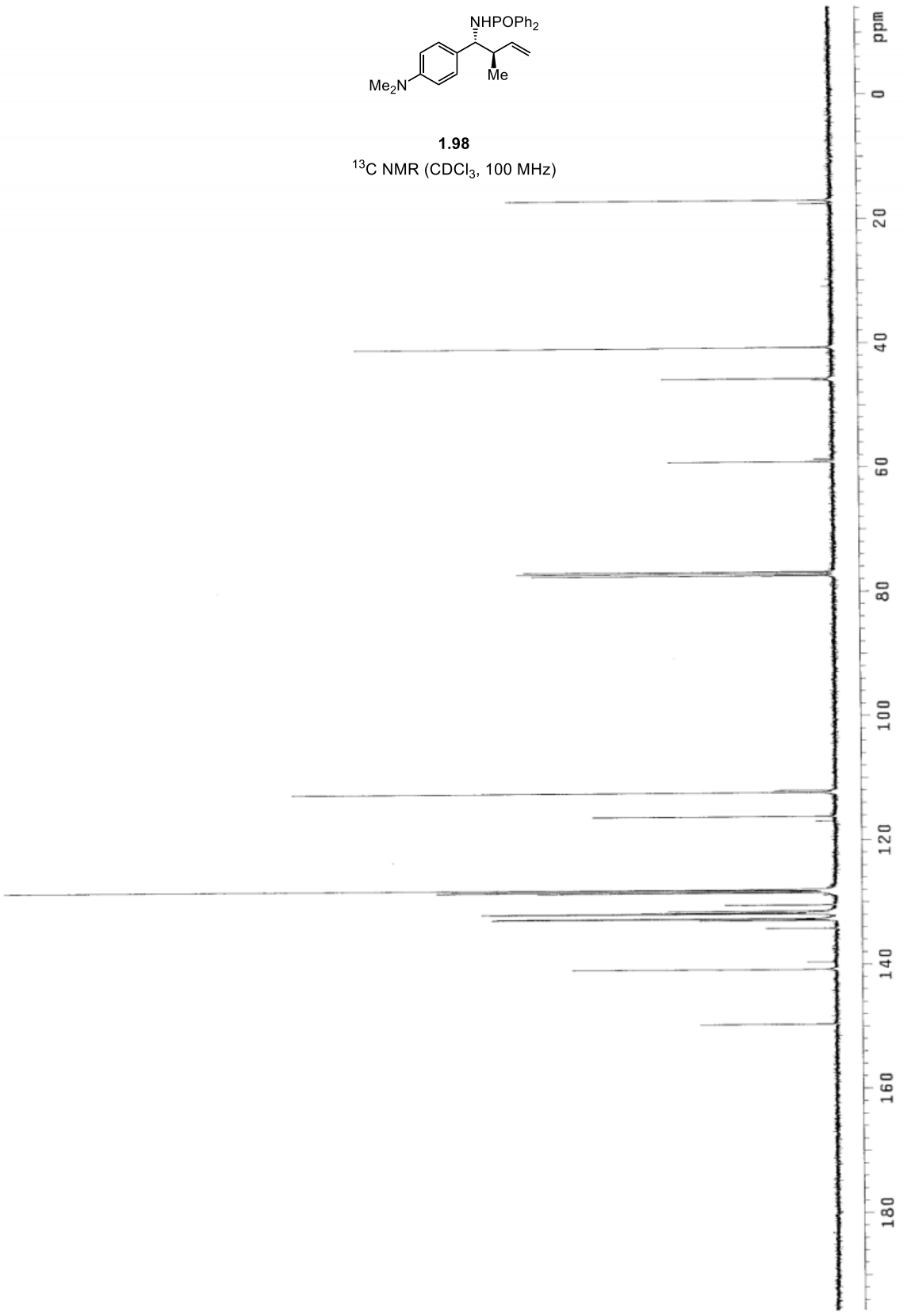

1.98

^{13}C NMR ($CDCl_3$, 100 MHz)

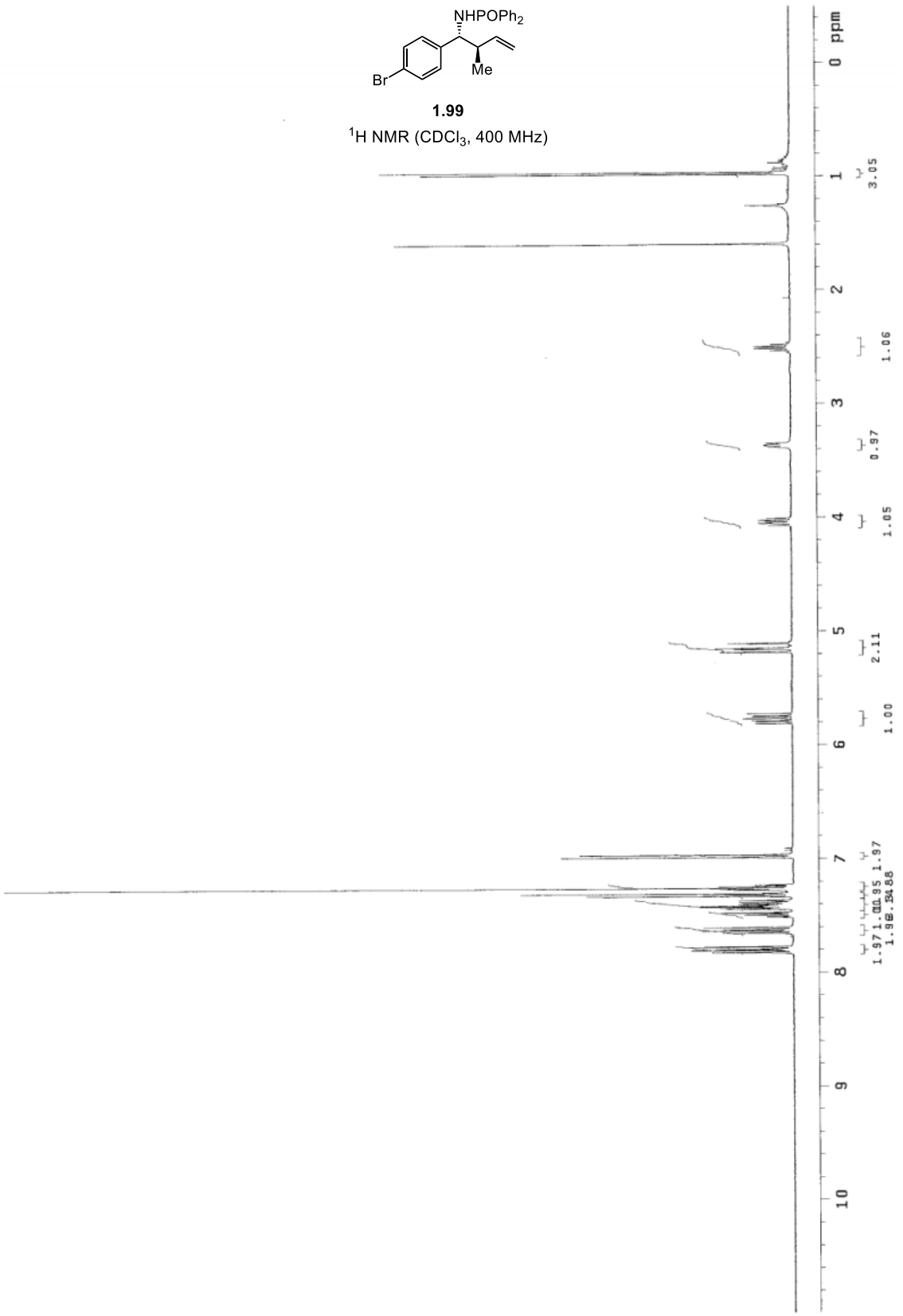
NHPOPh2
Me
Br
1.99
1H NMR (CDCl3, 400 MHz)
0 ppm
1
2
3
4
5
6
7
8
9
10
3.05
1.06
0.97
1.05
2.11
1.00
1.97

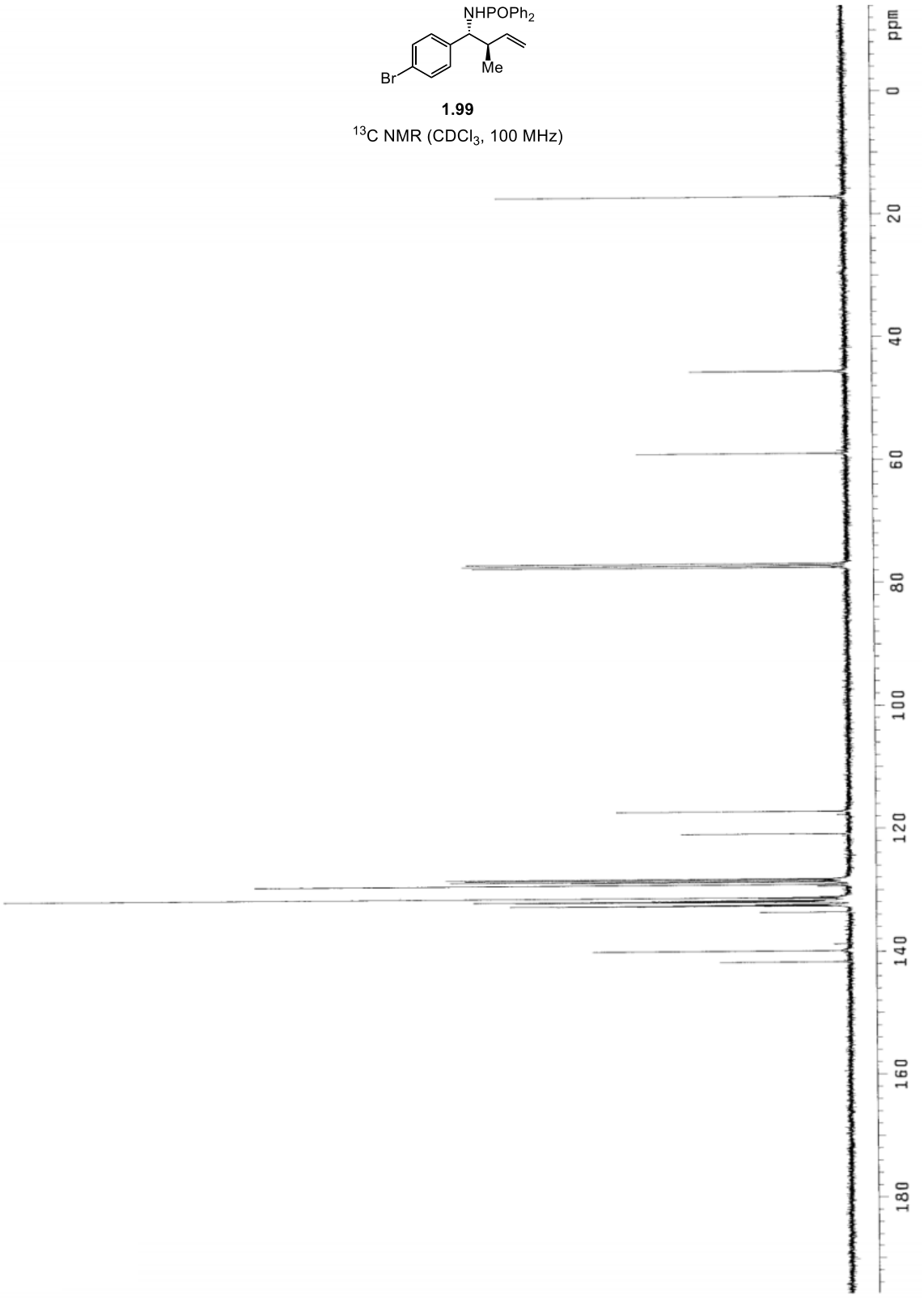

1.99

^{13}C NMR ($CDCl_3$, 100 MHz)

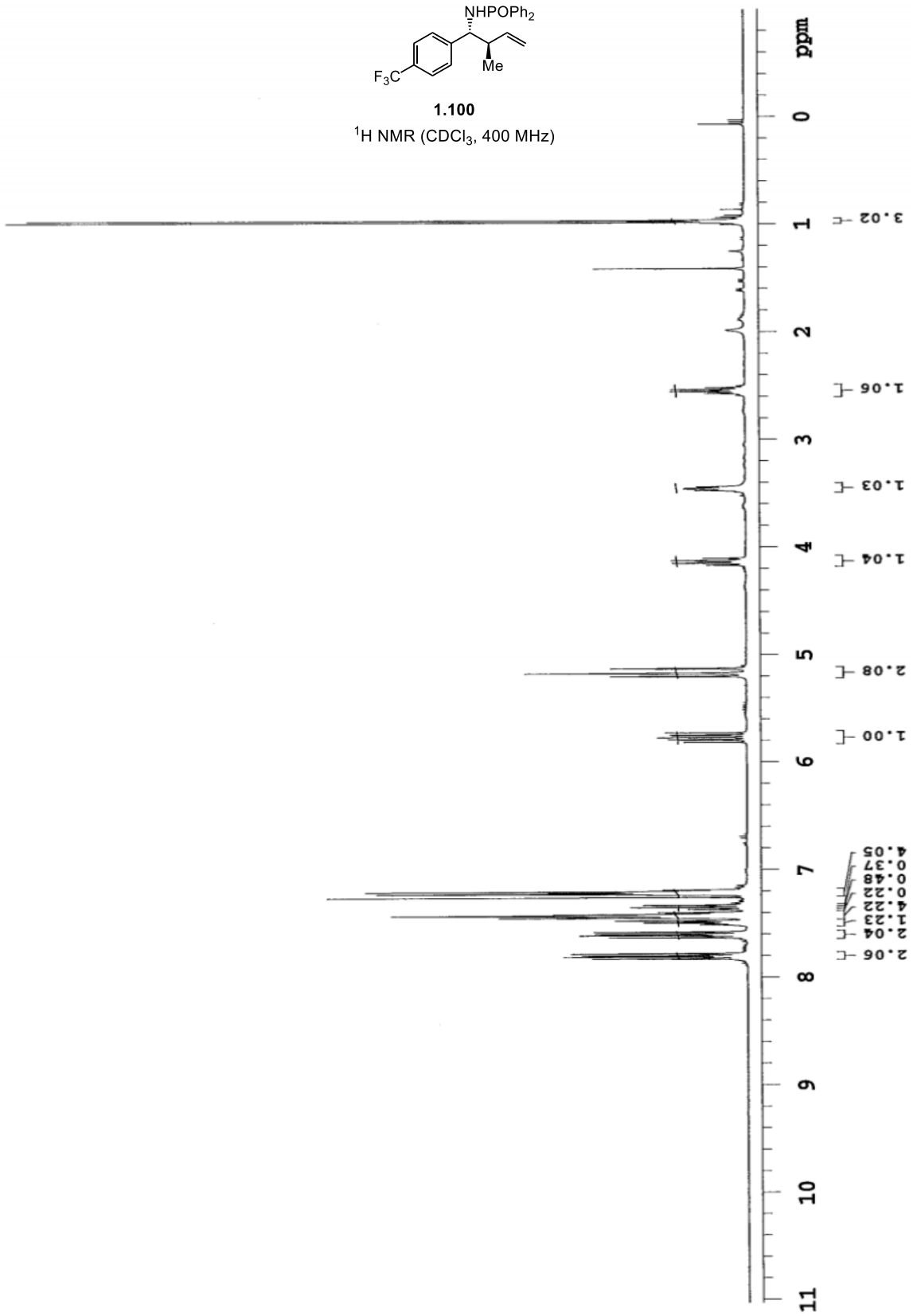
NHPOPh2
F3C
Me
1.100
1H NMR (CDCl3, 400 MHz)
ppm
0
1
2
3
4
5
6
7
8
9
10
11
3.02
1.06
1.03
1.04
2.08
1.00
4.05
0.37
0.48
0.22
4.22
1.23
2.04
2.06

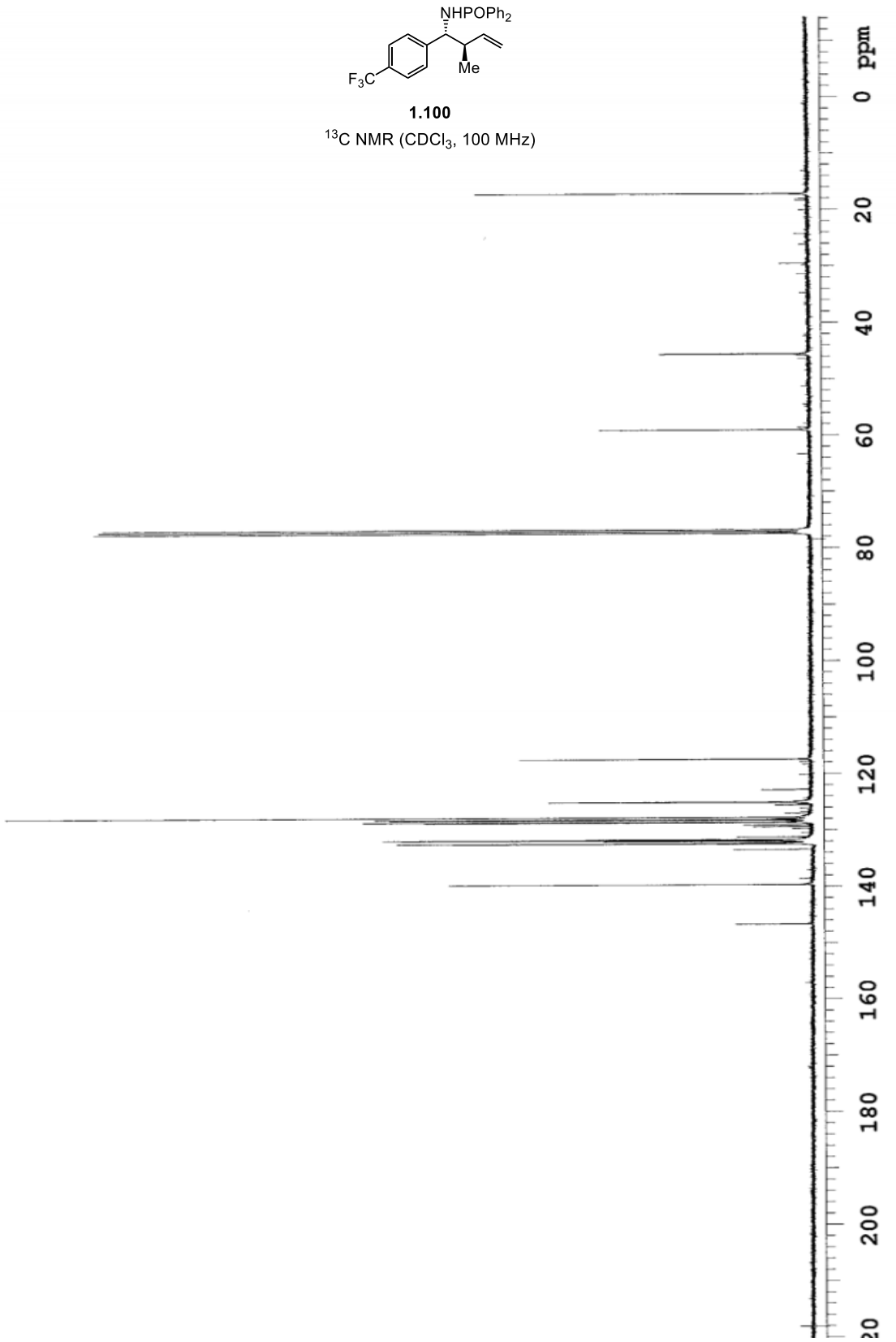

1.100

^{13}C NMR ($CDCl_3$, 100 MHz)

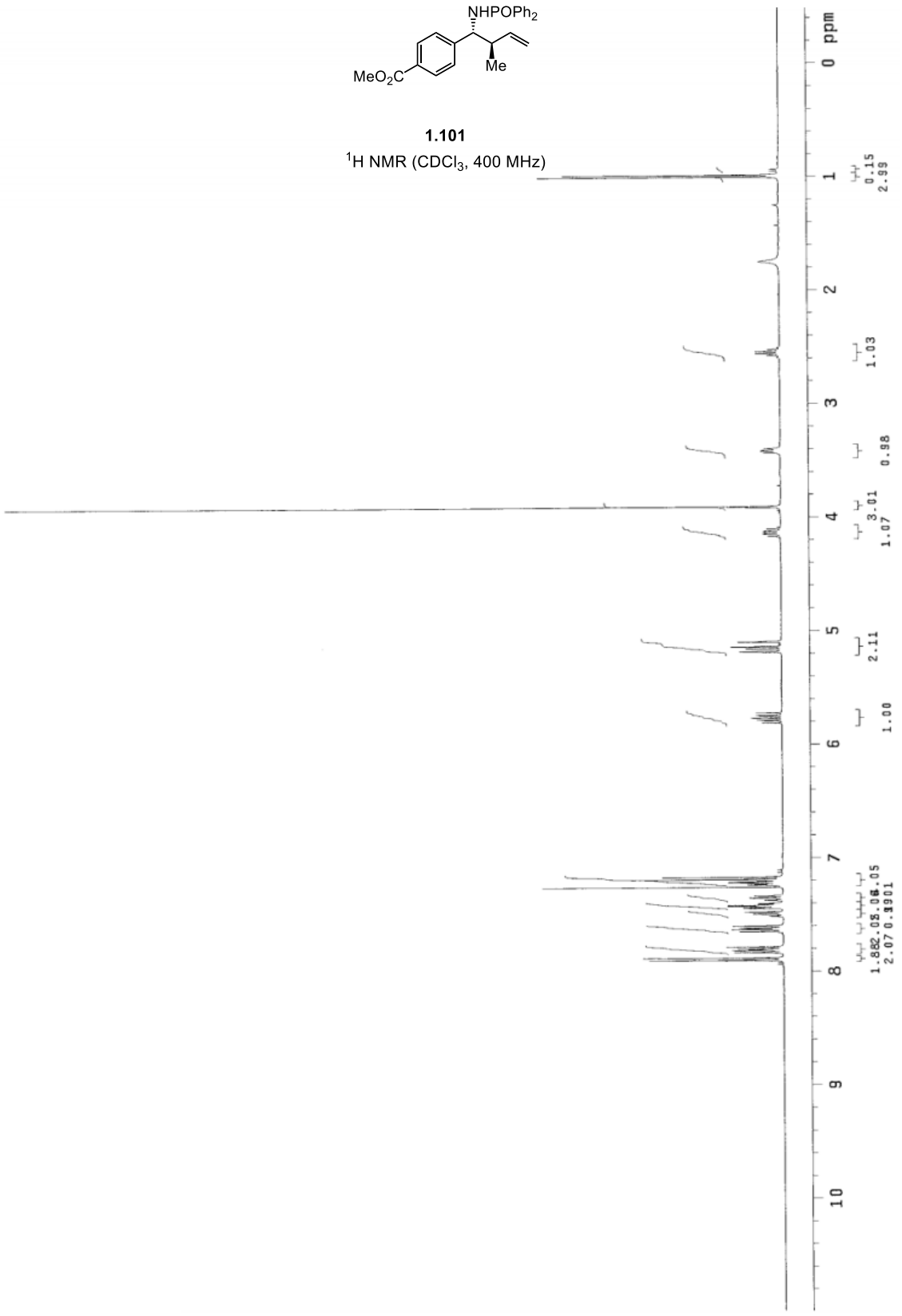

1.101

^{1}H NMR ($CDCl_3$, 400 MHz)

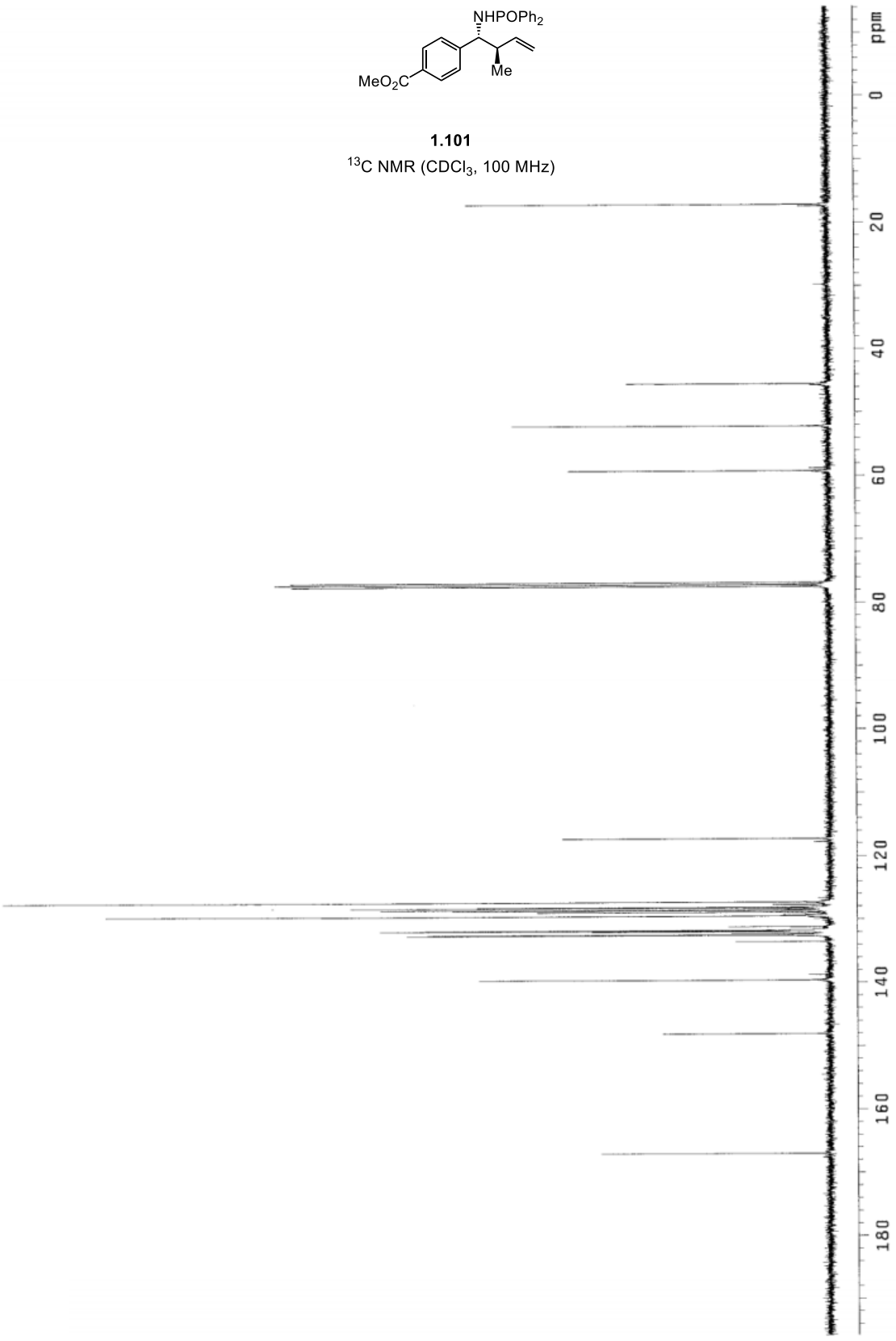

1.101

^{13}C NMR ($CDCl_3$, 100 MHz)

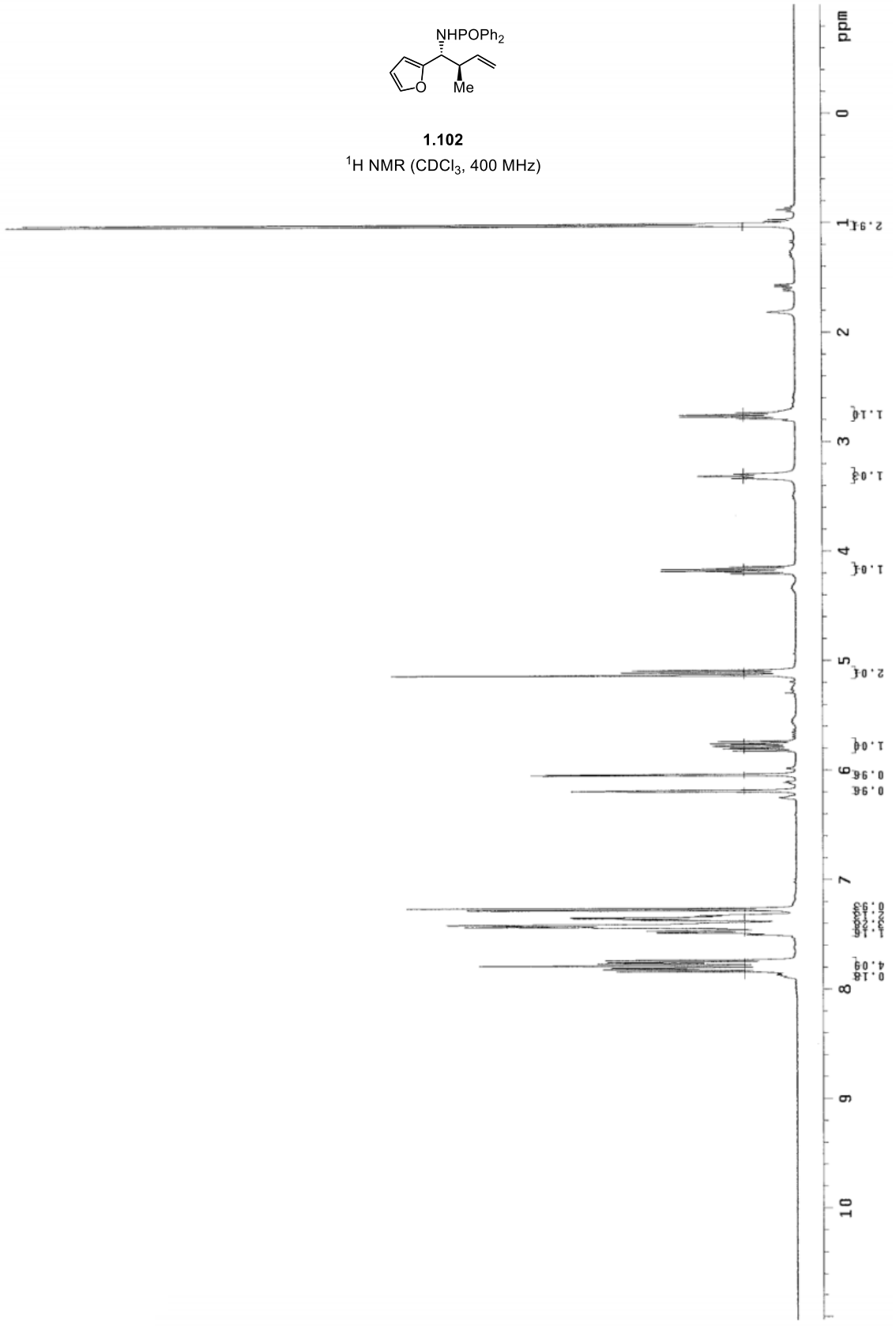

1.102

^{1}H NMR ($CDCl_3$, 400 MHz)

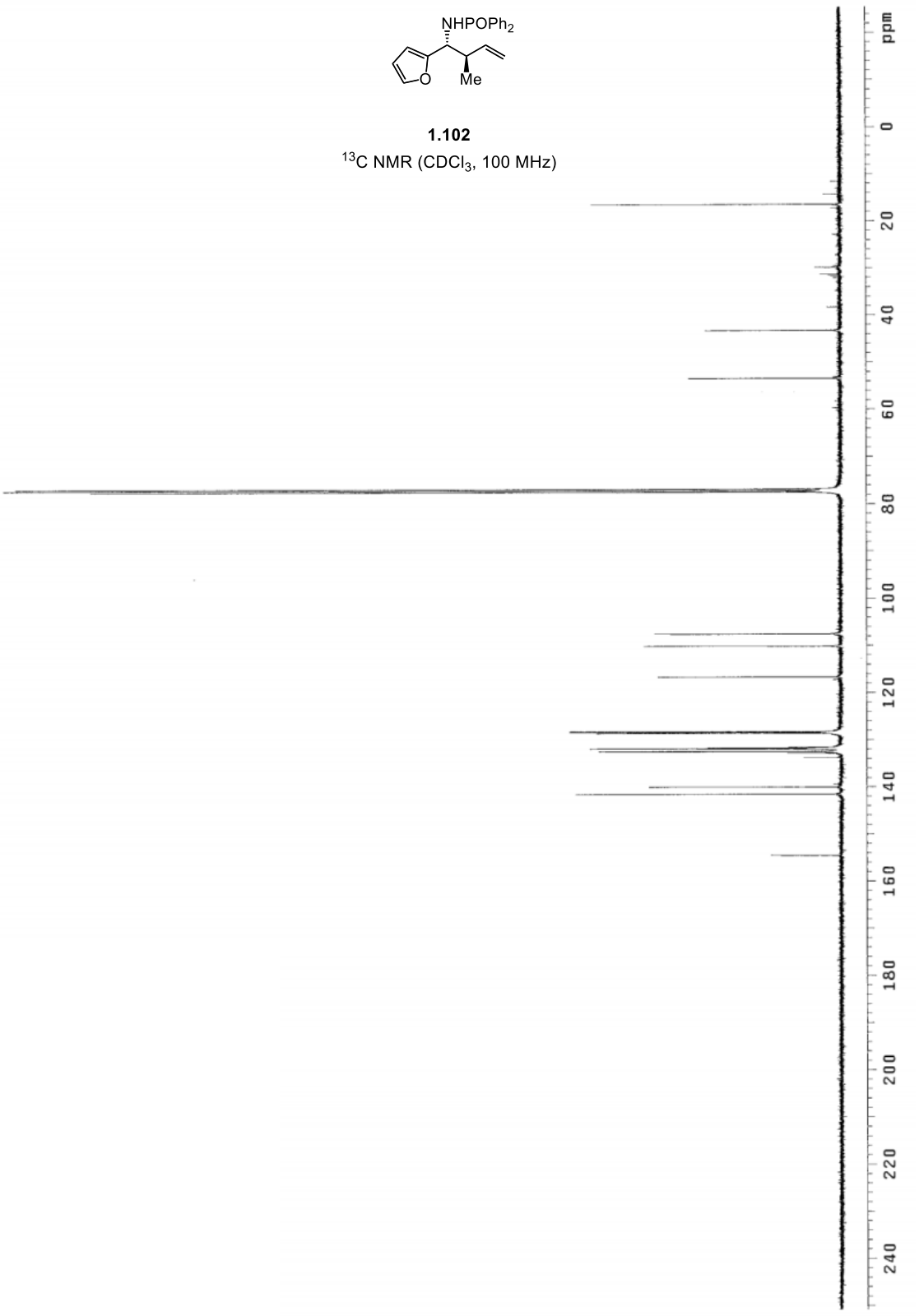

1.102

^{13}C NMR ($CDCl_3$, 100 MHz)

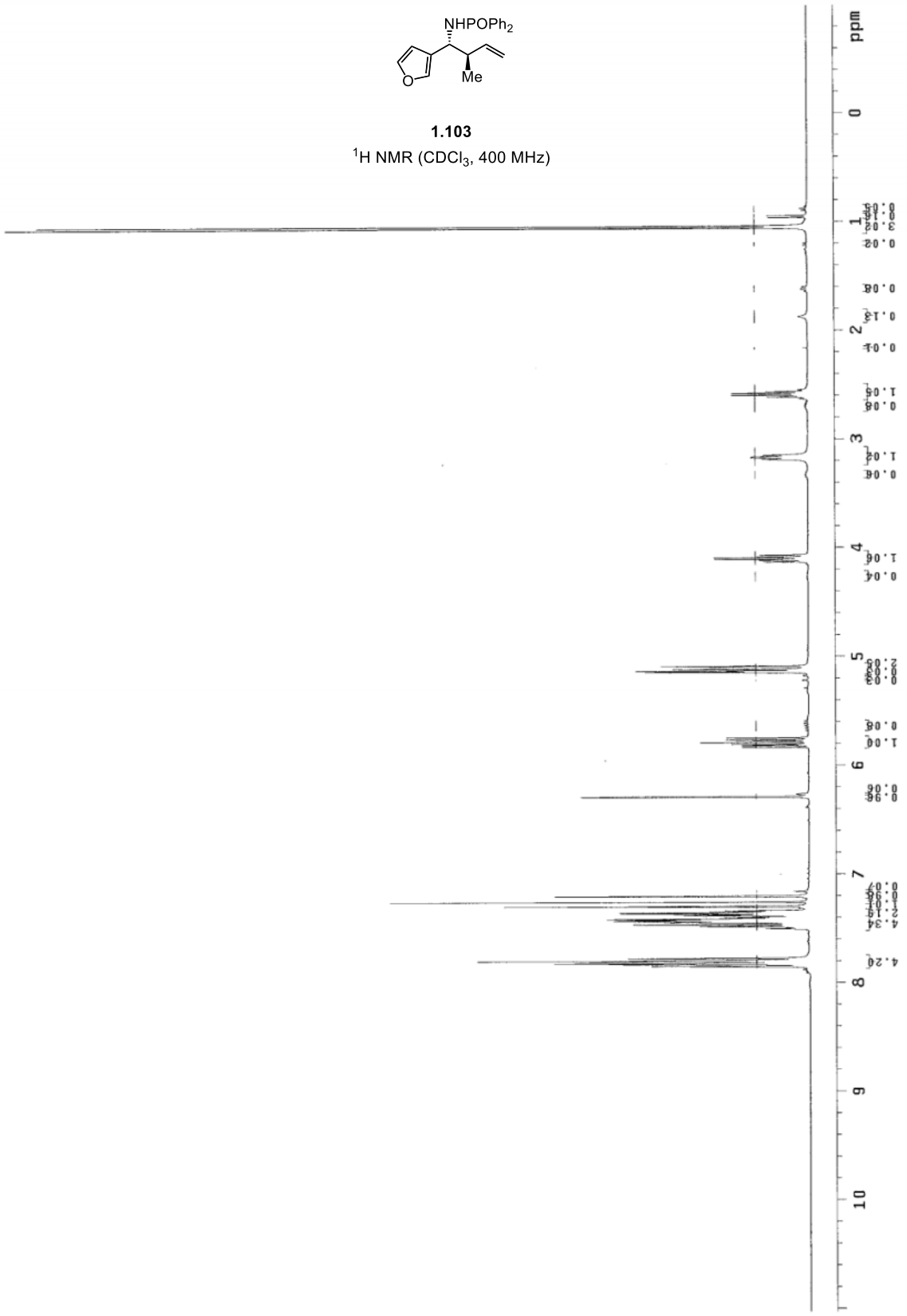

1.103

^{1}H NMR ($CDCl_3$, 400 MHz)

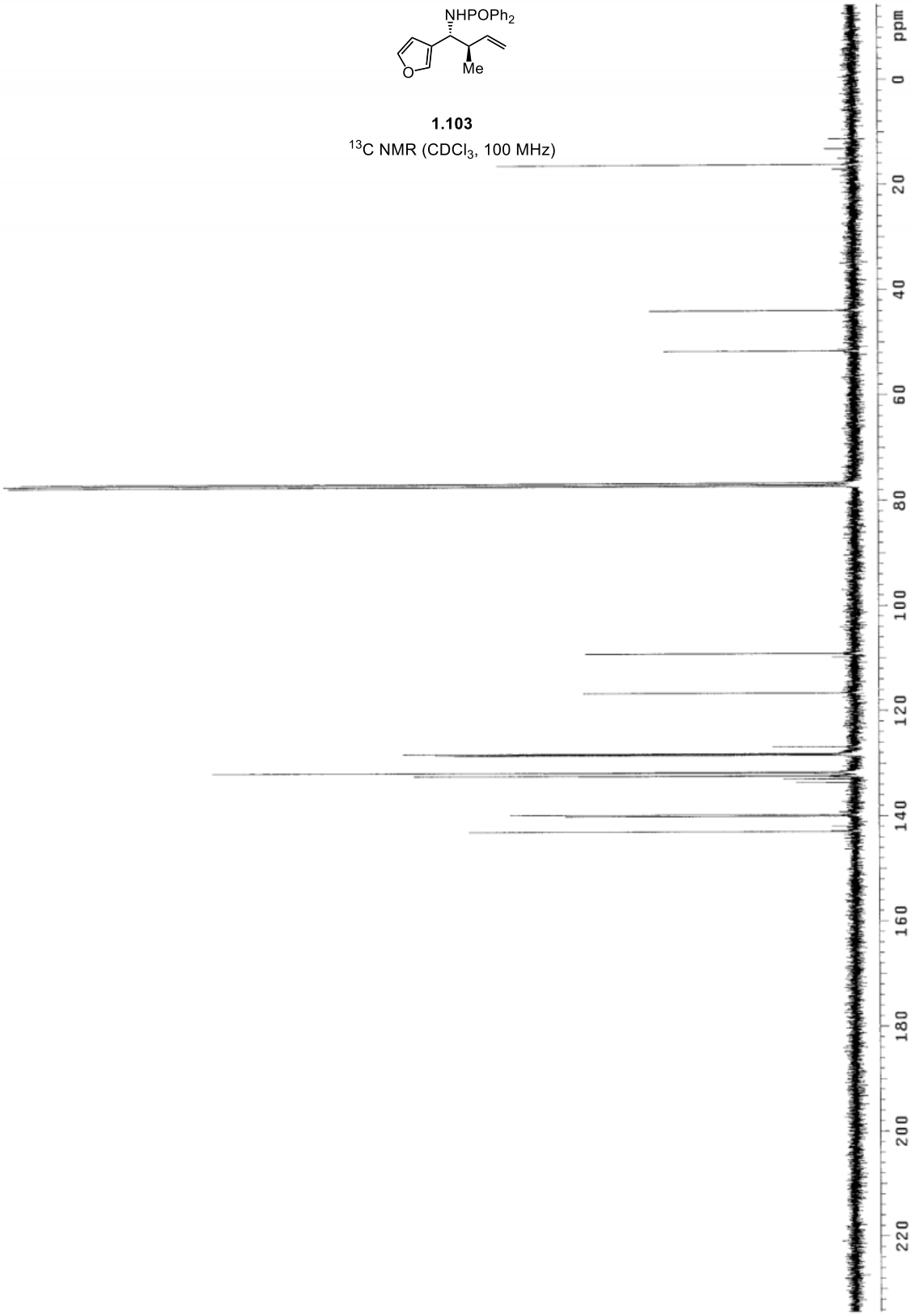

1.103

^{13}C NMR ($CDCl_3$, 100 MHz)

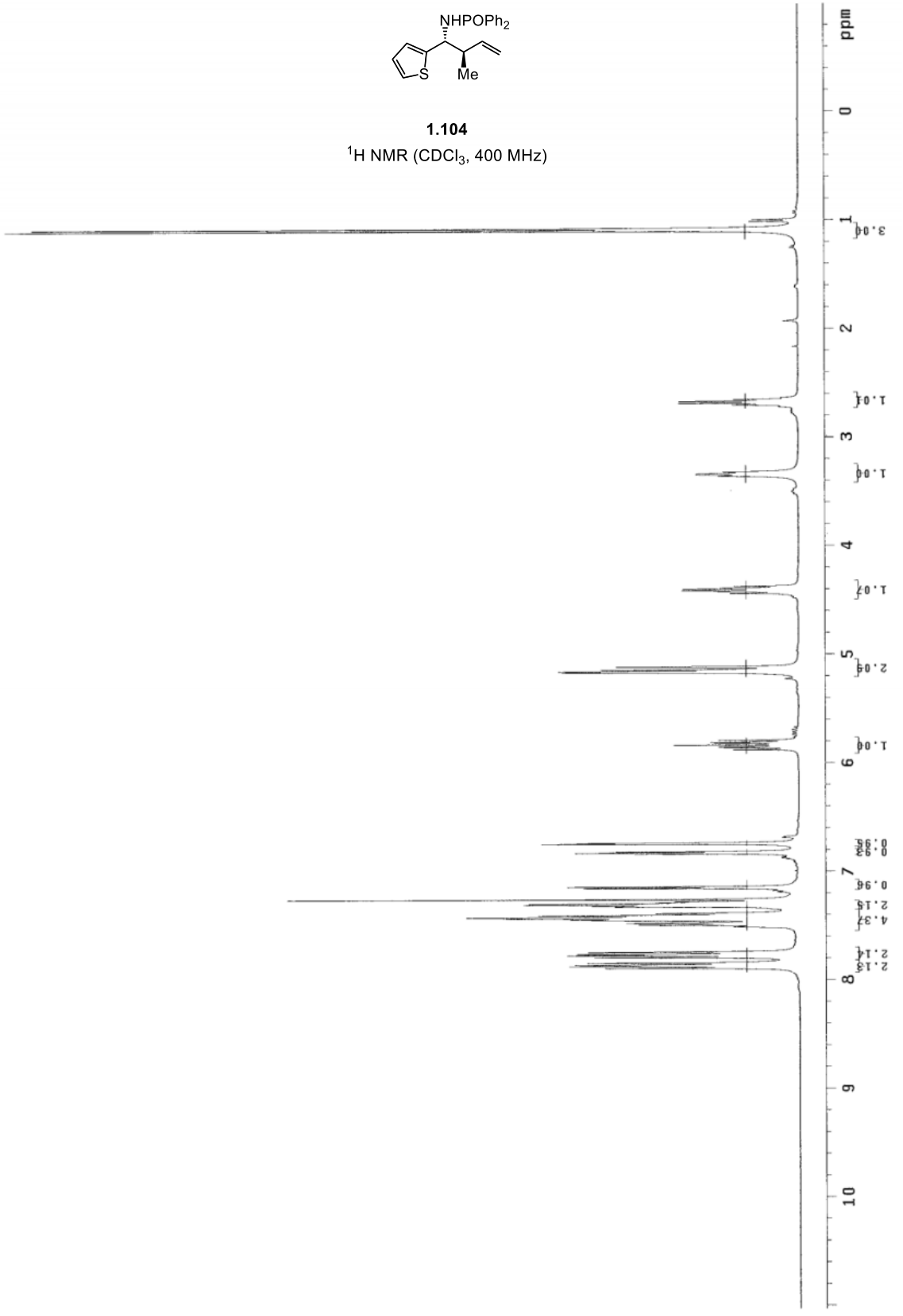

1.104

^{1}H NMR ($CDCl_3$, 400 MHz)

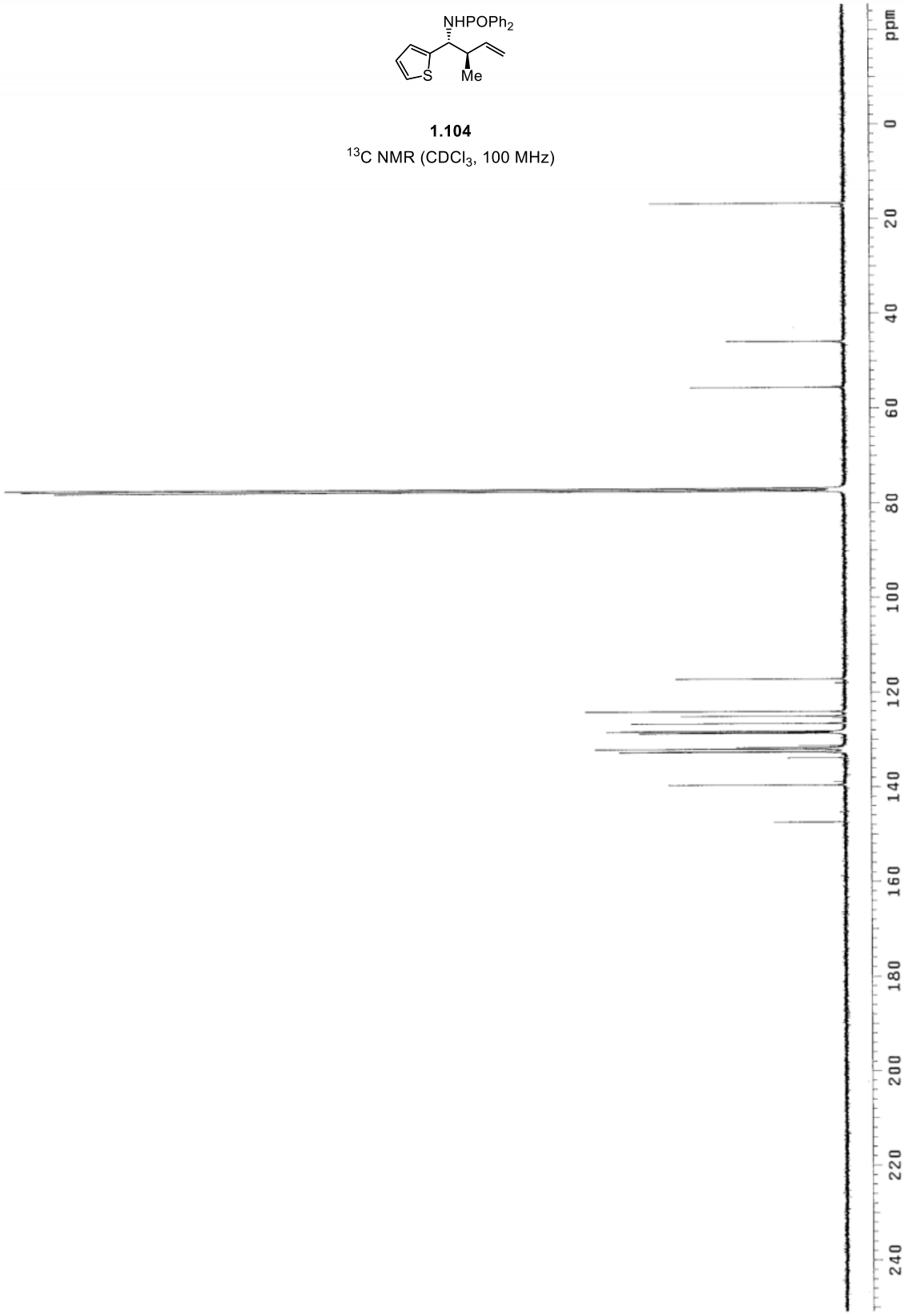

1.104

^{13}C NMR ($CDCl_3$, 100 MHz)

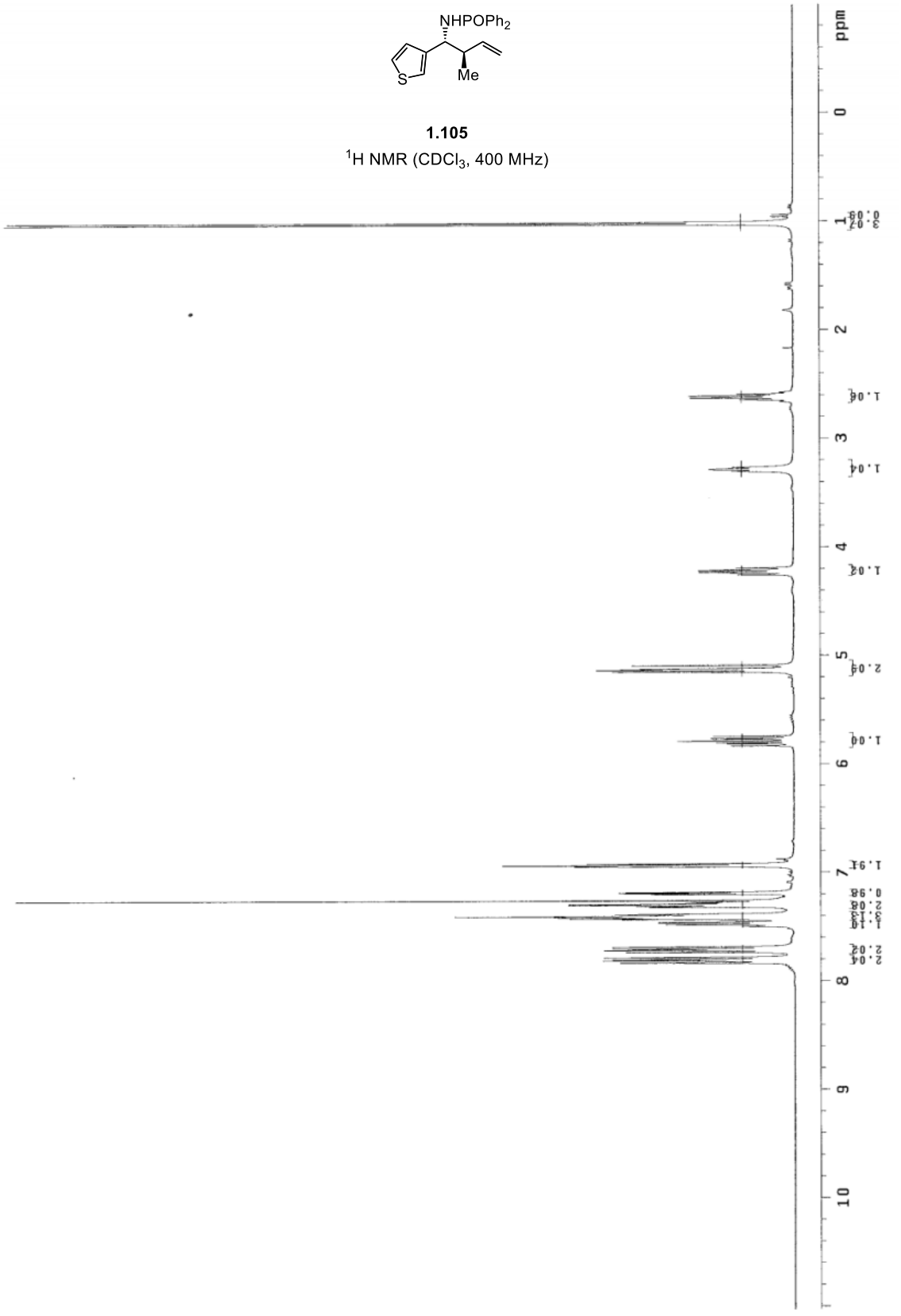

1.105

^{1}H NMR ($CDCl_3$, 400 MHz)

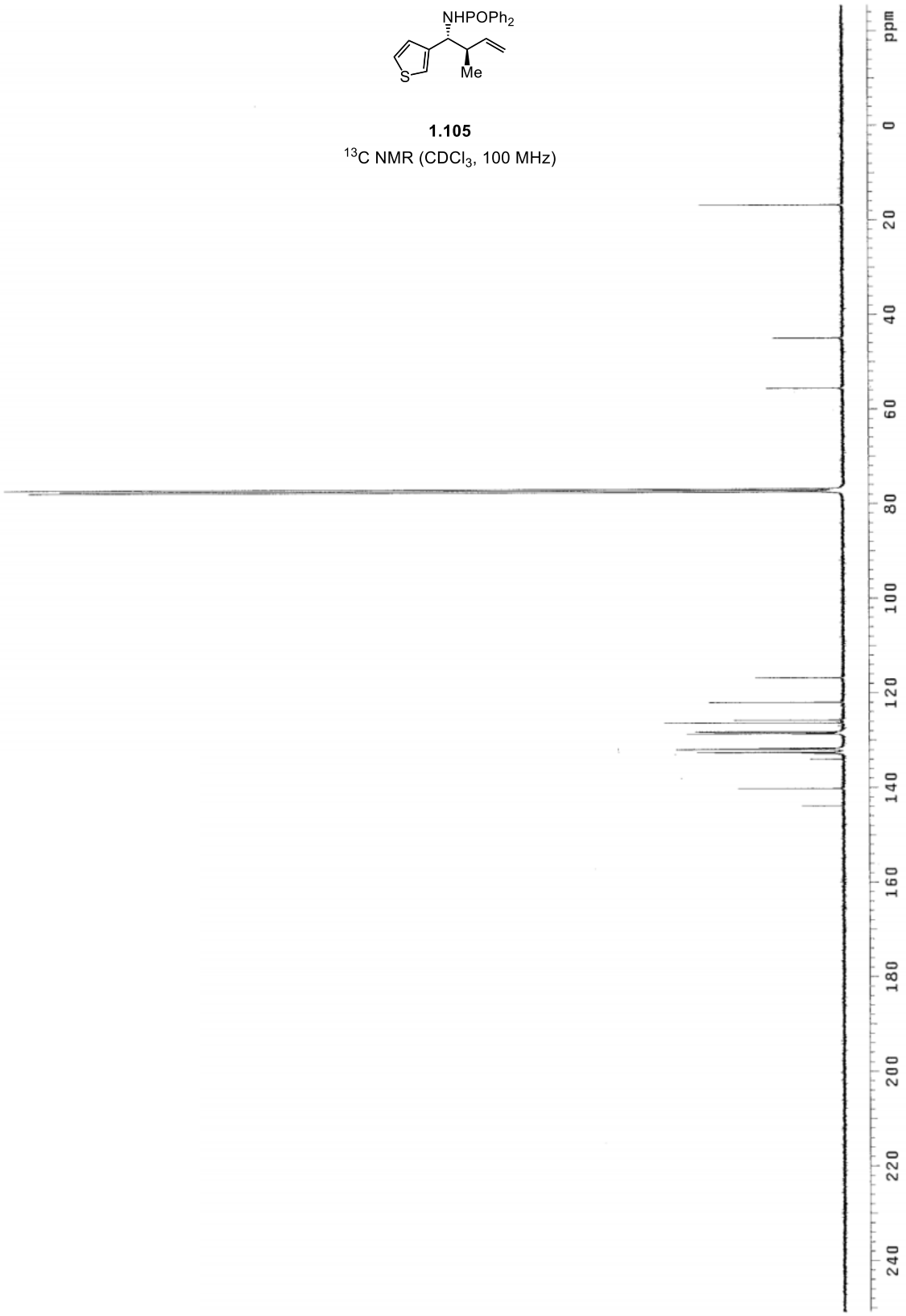

1.105

^{13}C NMR ($CDCl_3$, 100 MHz)

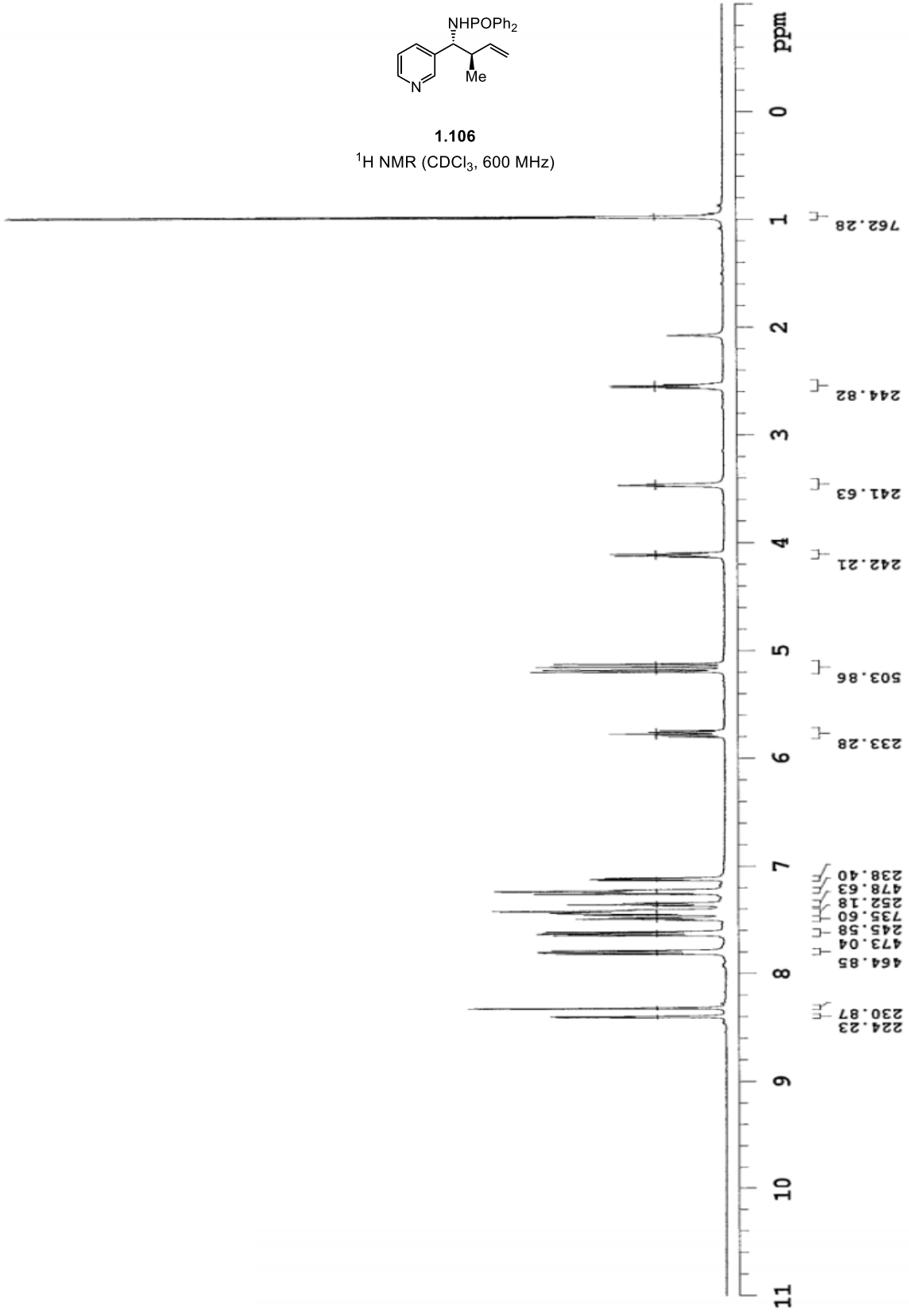
NHPOPh2
Me
N
1.106
1H NMR (CDCl3, 600 MHz)
ppm
0
1
2
3
4
5
6
7
8
9
10
11
762.28
244.82
241.63
242.21
503.86
233.28
238.40
478.63
252.18
735.60
245.58
473.04
464.85
230.87
224.23

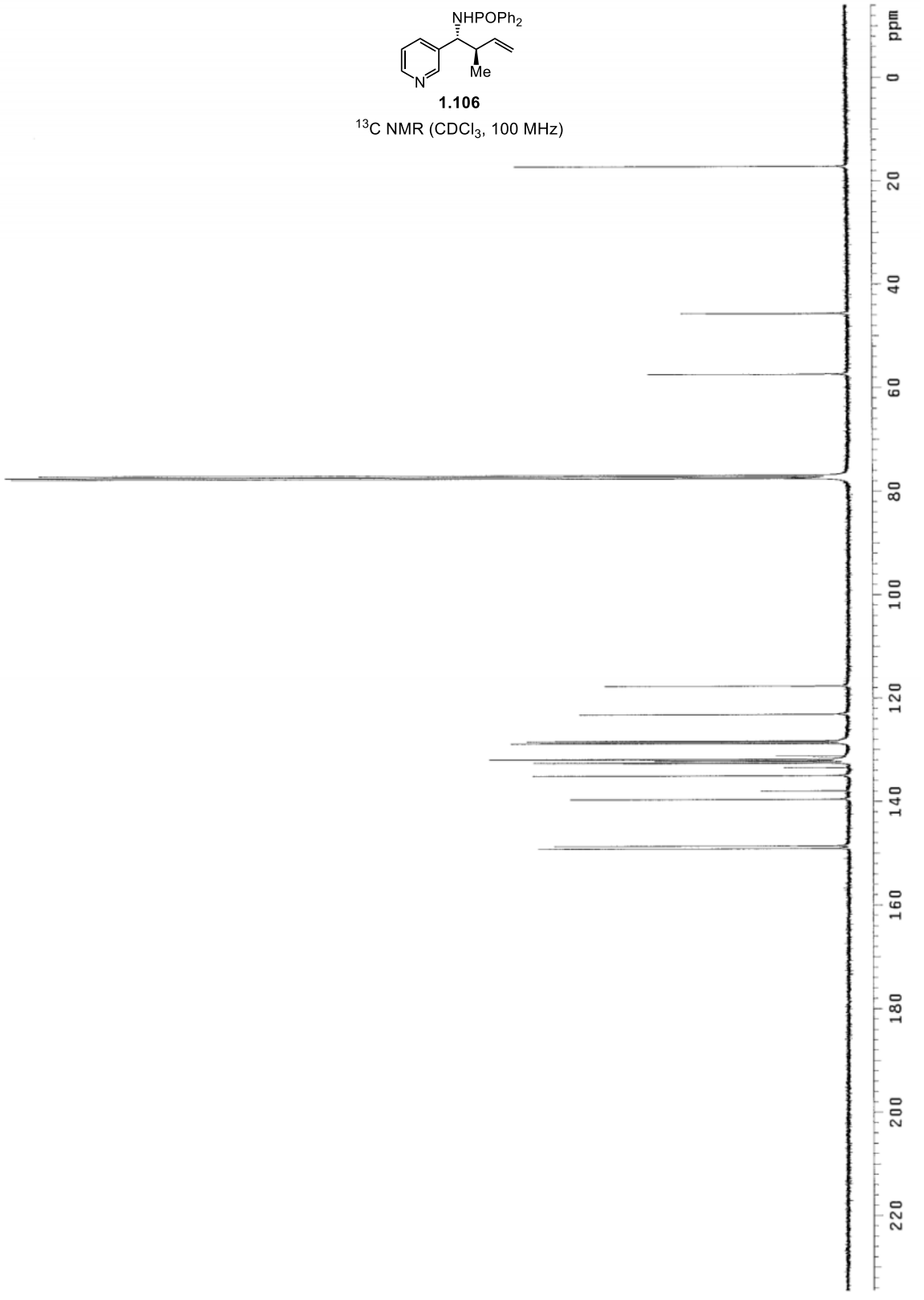

1.106

^{13}C NMR ($CDCl_3$, 100 MHz)

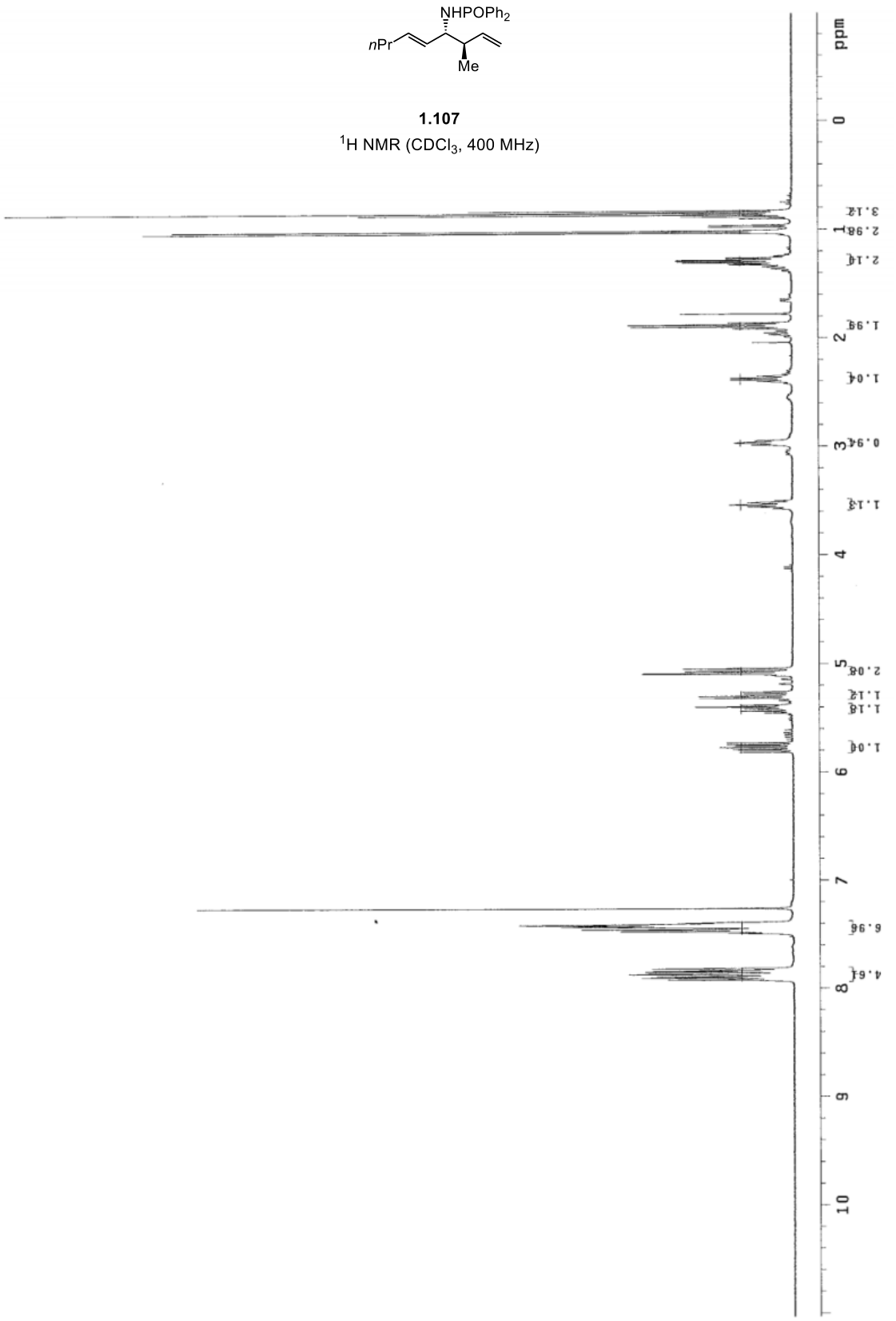

1.107

^{1}H NMR ($CDCl_3$, 400 MHz)

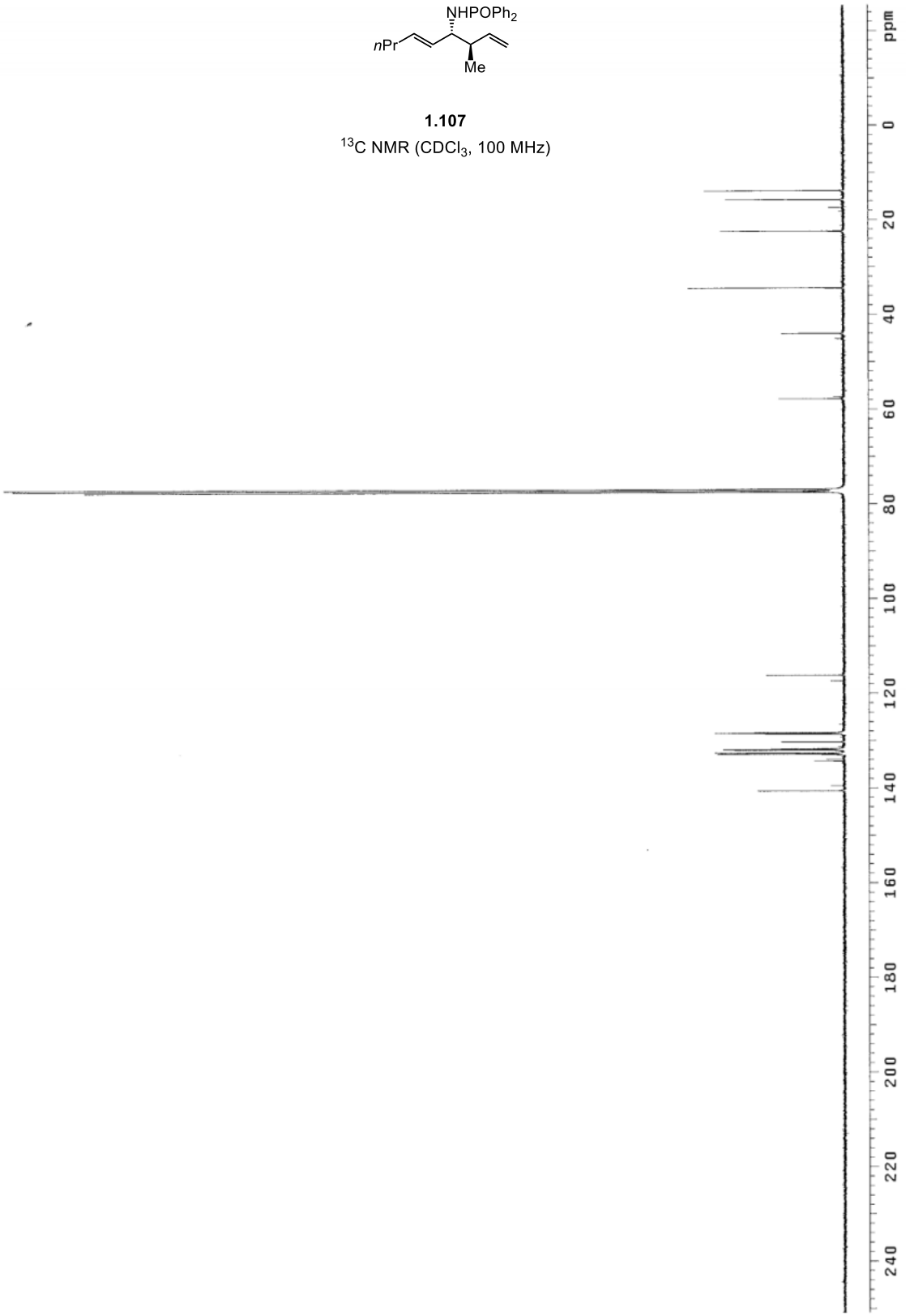

1.107

^{13}C NMR ($CDCl_3$, 100 MHz)

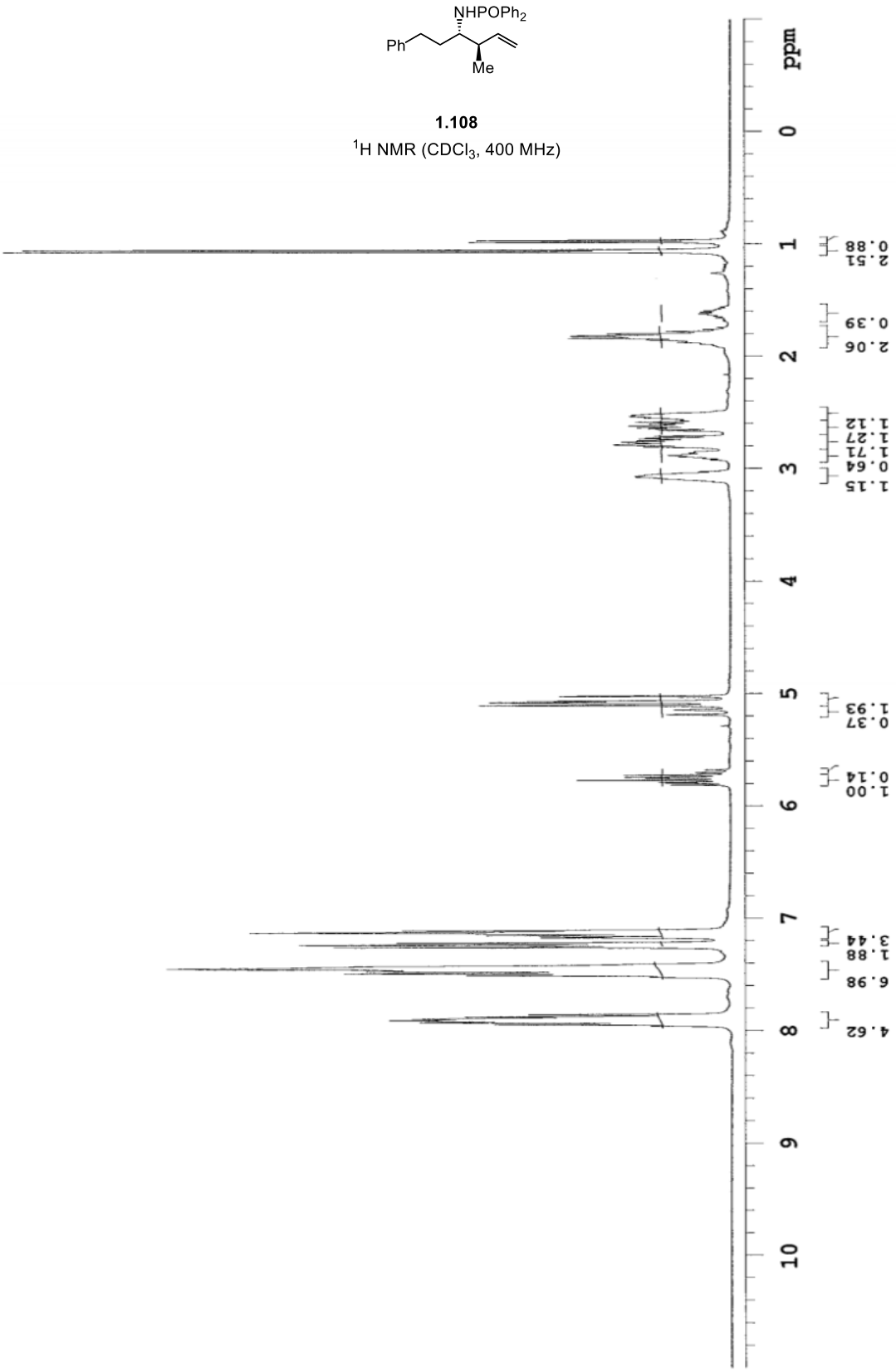

1.108

^{1}H NMR ($CDCl_3$, 400 MHz)

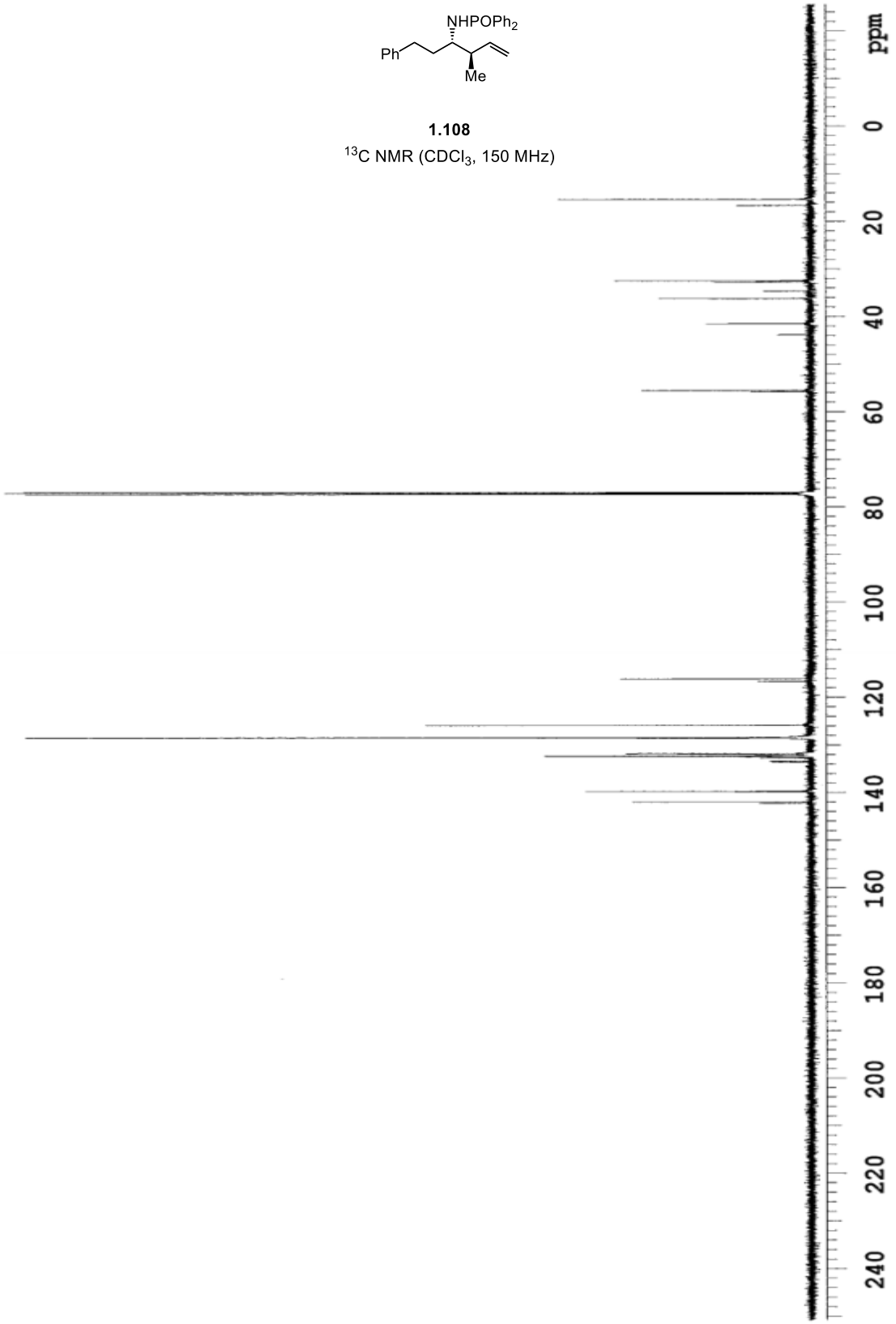

1.108

^{13}C NMR ($CDCl_3$, 150 MHz)

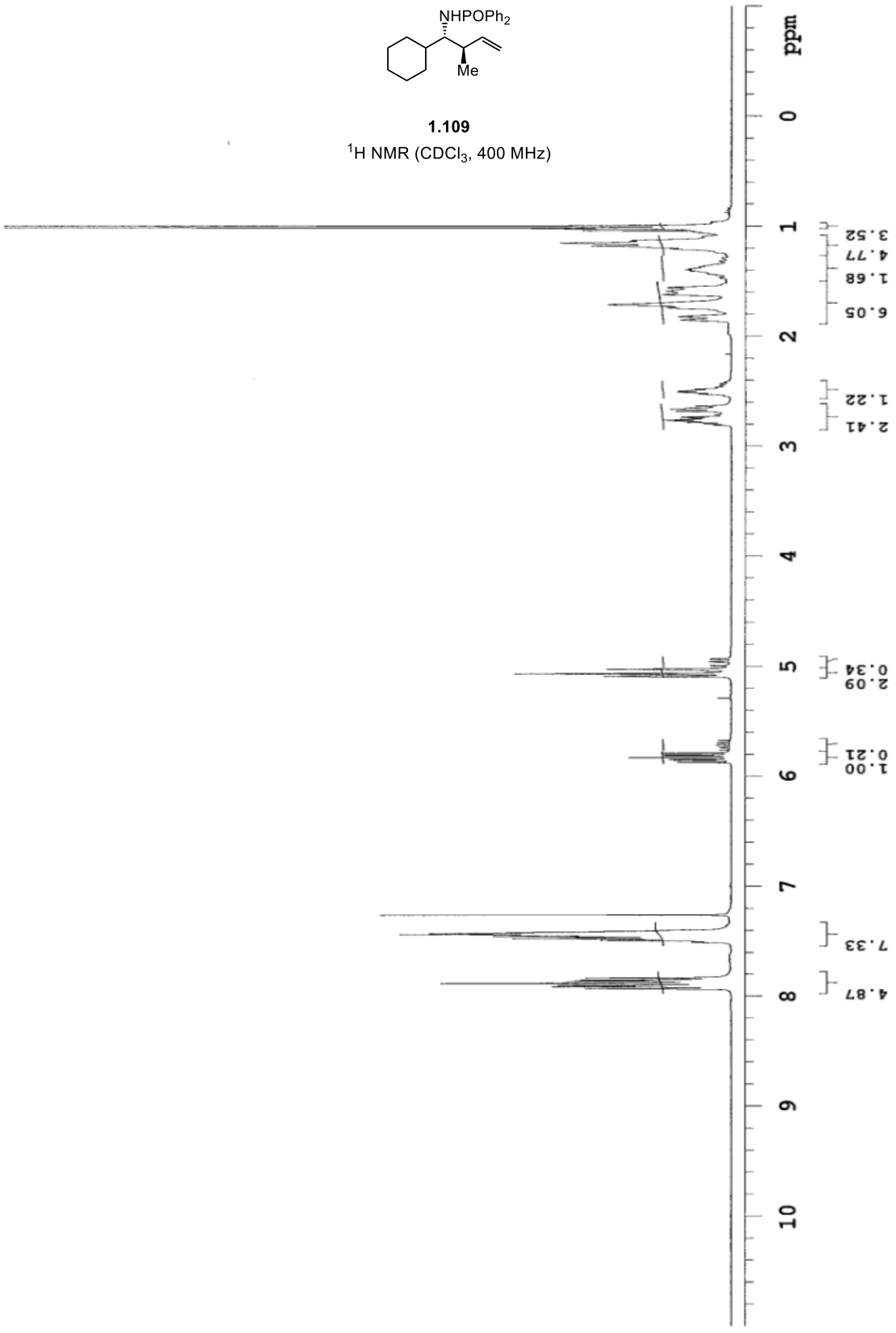

1.109

^{1}H NMR ($CDCl_3$, 400 MHz)

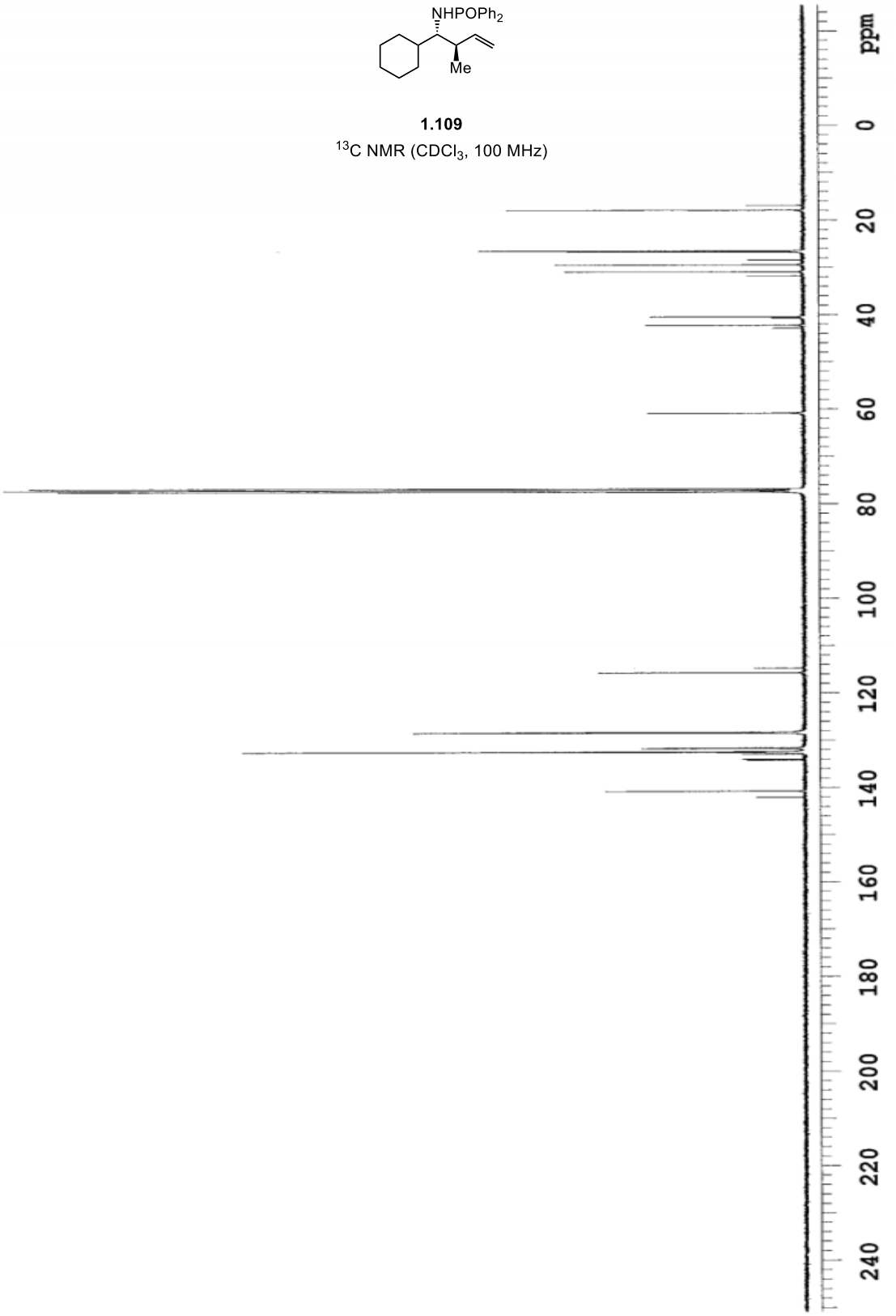

1.109

^{13}C NMR ($CDCl_3$, 100 MHz)

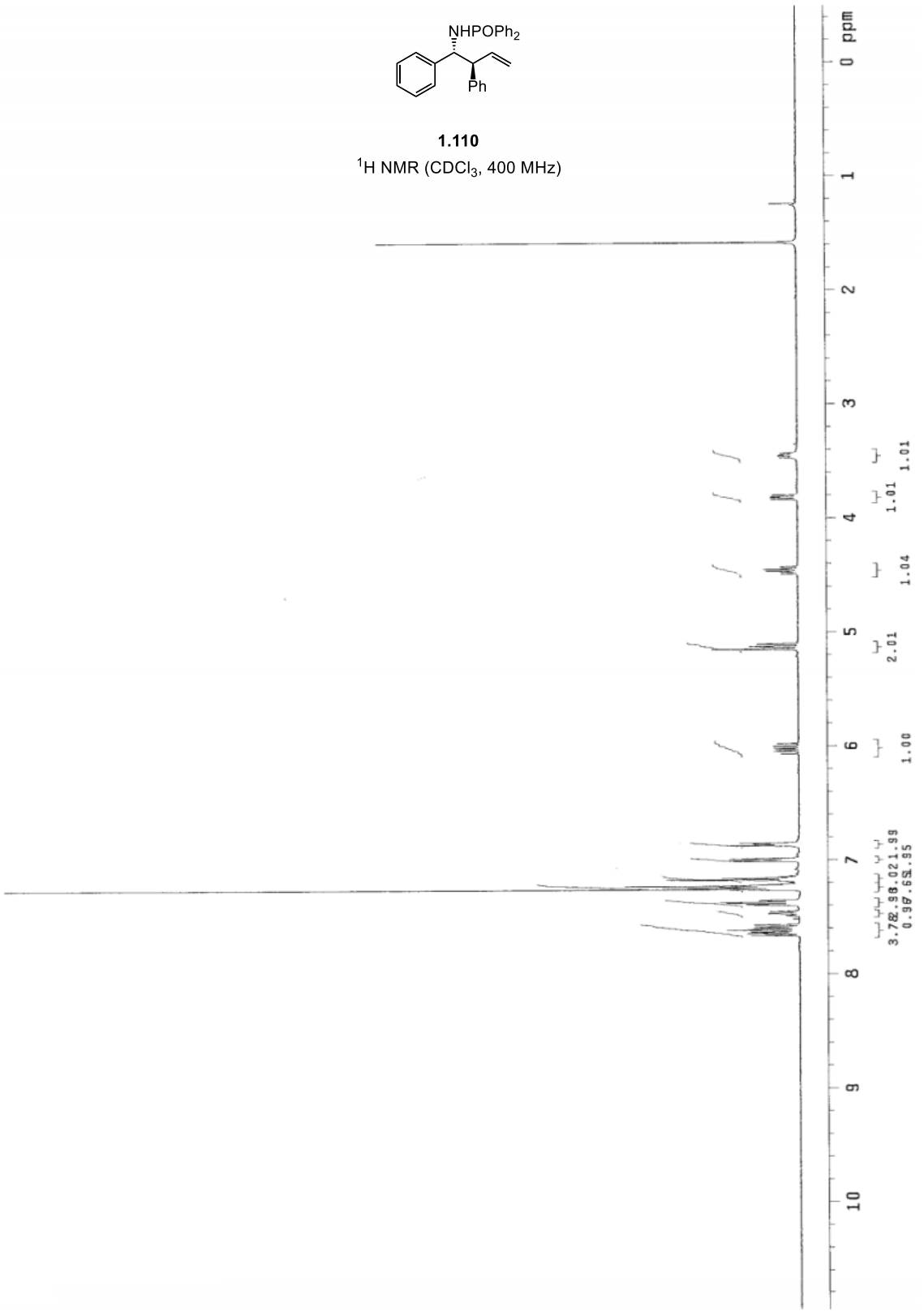

1.110

^{1}H NMR ($CDCl_3$, 400 MHz)

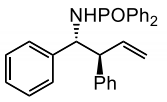

1.110

^{13}C NMR ($CDCl_3$, 100 MHz)

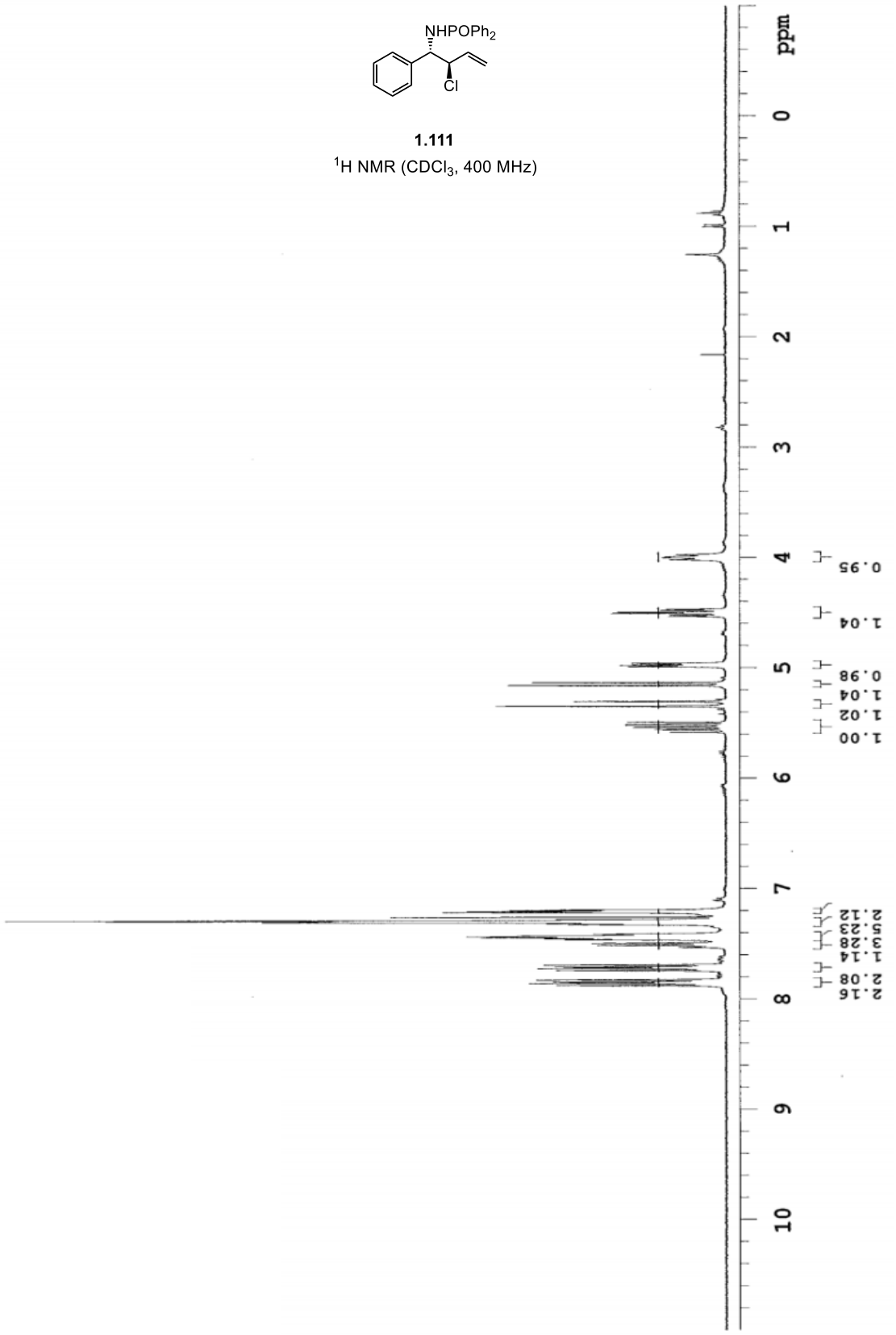

1.111

^{1}H NMR ($CDCl_3$, 400 MHz)

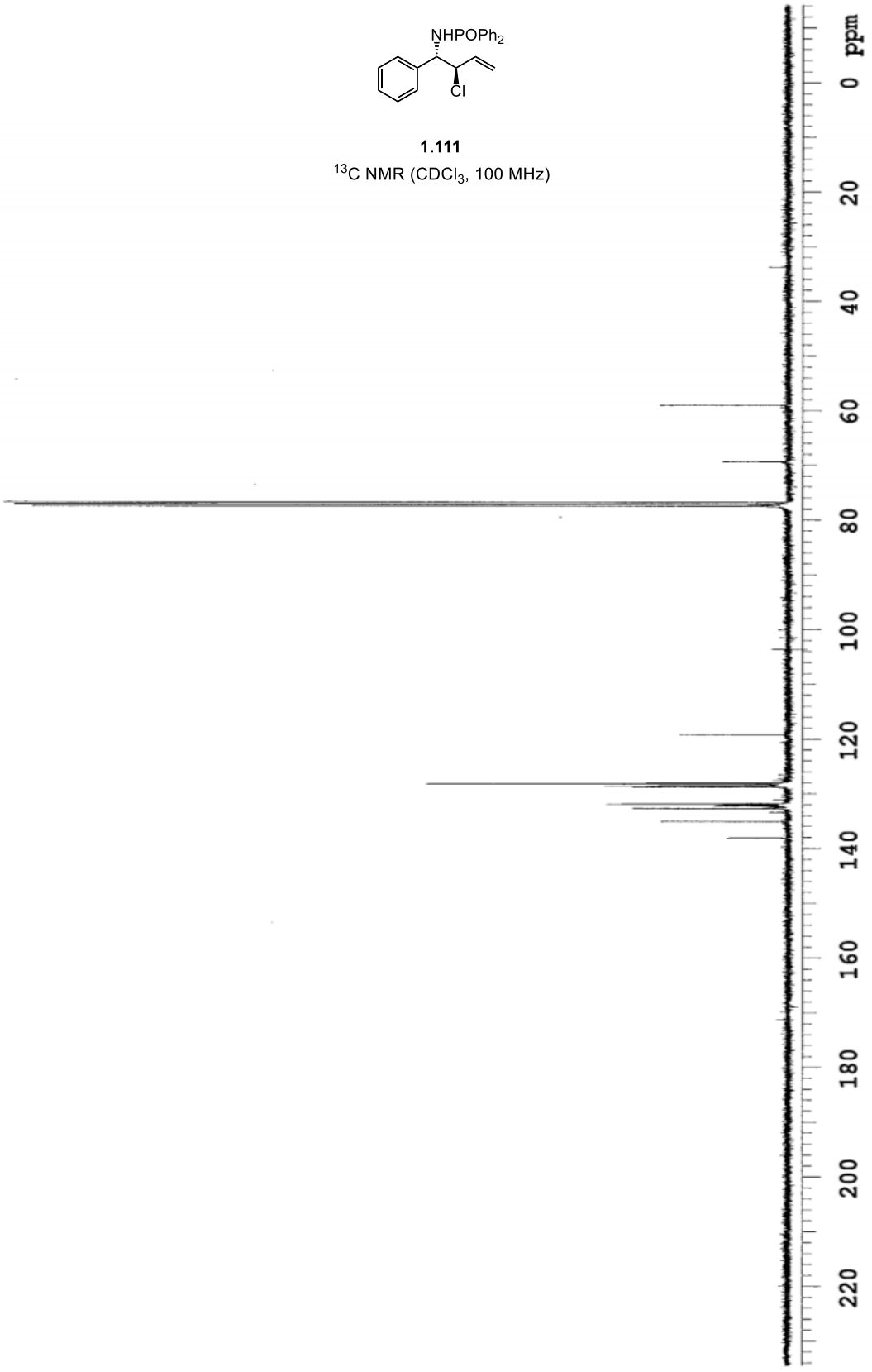

1.111

^{13}C NMR ($CDCl_3$, 100 MHz)

1.7.7. *DFT Calculation Structures*

A-gs

Cartesian coordinates (Angstroms):

C	-2.228	1.325	1.531
C	-2.162	0.299	0.679
C	-1.339	0.256	-0.586
B	0.210	-0.021	-0.204
C	-1.920	-0.692	-1.640
H	-1.376	1.274	-1.005
H	-1.323	-0.667	-2.566
H	-2.955	-0.420	-1.906
H	-1.937	-1.738	-1.298
H	-2.828	1.272	2.444
H	-1.681	2.257	1.349
H	-2.739	-0.606	0.920
N	1.127	1.084	-0.176
N	0.673	-1.339	0.120
C	0.966	2.306	-0.930
H	0.667	3.162	-0.294
H	0.219	2.198	-1.726
H	1.916	2.585	-1.422
C	-0.166	-2.408	0.608
H	-0.237	-3.246	-0.113
H	-1.180	-2.059	0.829
H	0.239	-2.826	1.549
C	2.248	1.154	0.735
C	2.042	-1.766	-0.061
H	2.613	-1.032	-0.643
H	2.071	-2.720	-0.620
H	2.573	-1.939	0.896
H	2.212	0.339	1.469

H 2.217 2.102 1.302

H 3.229 1.117 0.223

SCF Done: E(RwB97XD) = -450.233655796 A.U. after 1 cycles

	1	2	3
	A	A	A
Frequencies --	46.9658	57.9819	78.3375
Red. masses --	2.9116	2.8756	2.8471

Zero-point correction= 0.271392 (Hartree/Particle)

Thermal correction to Energy= 0.285804

Thermal correction to Enthalpy= 0.286748

Thermal correction to Gibbs Free Energy= 0.231078

Sum of electronic and zero-point Energies= -449.962264

Sum of electronic and thermal Energies= -449.947852

Sum of electronic and thermal Enthalpies= -449.946908

Sum of electronic and thermal Free Energies= -450.002578

Item	Value	Threshold	Converged?
Maximum Force	0.000000	0.000015	YES
RMS Force	0.000000	0.000010	YES

A-ts

Cartesian coordinates (Angstroms):

C -0.179 -0.449 2.056

C -1.300 -0.636 1.241

C -1.265 -1.317 0.010

B 0.050 -0.042 0.197

H -0.620 -2.196 -0.061

C -2.401 -1.258 -0.977

H -0.234 0.322 2.827

H 0.545 -1.249 2.211

H -2.103 0.101 1.356

N -0.197 1.312 -0.350

N 1.319 -0.741 -0.132

C	-1.442	2.021	-0.210
H	-1.599	2.456	0.804
H	-2.304	1.380	-0.435
H	-1.486	2.863	-0.923
C	2.561	-0.506	0.561
H	3.141	-1.442	0.679
H	2.386	-0.094	1.564
H	3.229	0.209	0.032
C	0.933	2.212	-0.354
C	1.521	-1.097	-1.514
H	0.579	-1.425	-1.979
H	2.243	-1.930	-1.606
H	1.914	-0.261	-2.132
H	1.851	1.693	-0.656
H	1.125	2.682	0.636
H	0.774	3.034	-1.075
H	-2.051	-0.940	-1.972
H	-3.192	-0.560	-0.664
H	-2.869	-2.248	-1.097

SCF Done: E(RwB97XD) = -450.175727716 A.U. after 1 cycles

	1	2	3
	A	A	A
Frequencies --	-378.7444	51.7757	105.8818
Red. masses --	7.5962	2.6135	2.1976

Zero-point correction= 0.269313 (Hartree/Particle)

Thermal correction to Energy= 0.283028

Thermal correction to Enthalpy= 0.283972

Thermal correction to Gibbs Free Energy= 0.230623

Sum of electronic and zero-point Energies= -449.906414

Sum of electronic and thermal Energies= -449.892699

Sum of electronic and thermal Enthalpies= -449.891755

Sum of electronic and thermal Free Energies= -449.945105

Item	Value	Threshold	Converged?

Maximum Force	0.000001	0.000015	YES
RMS Force	0.000000	0.000010	YES

B-gs

Cartesian coordinates (Angstroms):

C	2.971	0.045	1.211
C	2.240	-0.016	0.095
C	0.992	-0.831	-0.095
B	-0.329	0.080	-0.237
C	1.099	-1.714	-1.354
H	0.906	-1.494	0.782
H	0.217	-2.365	-1.462
H	1.992	-2.361	-1.323
H	1.168	-1.104	-2.270
H	3.866	0.671	1.275
H	2.701	-0.528	2.105
H	2.565	0.580	-0.769
C	-0.205	1.525	-0.906
N	-1.578	-0.406	0.207
C	-0.027	2.626	0.149
C	-2.816	0.341	0.115
H	0.089	3.622	-0.308
H	0.864	2.442	0.770
H	-0.891	2.675	0.832
H	-3.561	-0.197	-0.499
H	-2.662	1.329	-0.333
H	-3.262	0.489	1.115
C	-1.800	-1.711	0.797
H	-0.867	-2.276	0.899
H	-2.491	-2.311	0.179
H	-2.252	-1.620	1.801
H	-1.077	1.763	-1.539
H	0.661	1.546	-1.590

SCF Done: E(RwB97XD) = -394.926072189 A.U. after 1 cycles

	1	2	3
	A	A	A
Frequencies --	34.0285	69.9691	88.3132
Red. masses --	2.9243	2.6674	2.3223

Zero-point correction= 0.253678 (Hartree/Particle)

Thermal correction to Energy= 0.267136

Thermal correction to Enthalpy= 0.268080

Thermal correction to Gibbs Free Energy= 0.214029

Sum of electronic and zero-point Energies= -394.672394

Sum of electronic and thermal Energies= -394.658936

Sum of electronic and thermal Enthalpies= -394.657992

Sum of electronic and thermal Free Energies= -394.712044

Item	Value	Threshold	Converged?
Maximum Force	0.000001	0.000015	YES
RMS Force	0.000000	0.000010	YES

B-ts

Cartesian coordinates (Angstroms):

C	0.112	0.303	1.717
C	1.198	-0.405	1.132
C	0.984	-1.441	0.236
B	-0.042	0.197	-0.028
C	2.024	-1.920	-0.731
H	0.157	-2.125	0.433
H	1.577	-2.107	-1.720
H	2.480	-2.866	-0.395
H	2.830	-1.182	-0.859
H	0.350	1.234	2.236
H	-0.731	-0.258	2.135
H	2.140	0.146	1.023
C	0.654	1.325	-0.957

N	-1.433	-0.212	-0.438
C	1.184	2.580	-0.263
C	-2.375	0.842	-0.129
H	1.626	3.295	-0.976
H	1.968	2.350	0.479
H	0.381	3.111	0.275
H	-3.306	0.724	-0.712
H	-1.953	1.827	-0.380
H	-2.662	0.875	0.947
C	-2.014	-1.512	-0.242
H	-1.442	-2.297	-0.759
H	-3.030	-1.533	-0.673
H	-2.123	-1.817	0.826
H	-0.088	1.623	-1.717
H	1.472	0.864	-1.540

SCF Done: E(RwB97XD) = -394.872604468 A.U. after 1 cycles

	1	2	3
	A	A	A
Frequencies --	-286.4345	29.8426	89.2835
Red. masses --	6.8092	2.5242	2.5153

Zero-point correction= 0.252340 (Hartree/Particle)
Thermal correction to Energy= 0.264577
Thermal correction to Enthalpy= 0.265521
Thermal correction to Gibbs Free Energy= 0.214872
Sum of electronic and zero-point Energies= -394.620264
Sum of electronic and thermal Energies= -394.608028
Sum of electronic and thermal Enthalpies= -394.607084
Sum of electronic and thermal Free Energies= -394.657733

Item	Value	Threshold	Converged?
Maximum Force	0.000000	0.000015	YES
RMS Force	0.000000	0.000010	YES

C-gs

Cartesian coordinates (Angstroms):

C	-2.686	0.289	1.039
C	-1.670	-0.526	0.748
C	-0.878	-0.550	-0.535
B	0.570	0.006	-0.149
C	-0.854	-1.955	-1.148
H	-1.356	0.150	-1.241
H	-0.273	-1.974	-2.083
H	-1.873	-2.308	-1.378
H	-0.392	-2.682	-0.463
H	-3.194	0.244	2.006
H	-3.057	1.026	0.317
H	-1.351	-1.254	1.507
C	0.946	1.546	-0.099
O	1.476	-0.941	0.216
C	-0.077	2.540	-0.645
C	2.781	-0.649	0.650
H	0.269	3.580	-0.541
H	-1.038	2.458	-0.115
H	-0.277	2.368	-1.715
H	3.281	-1.597	0.897
H	2.782	-0.014	1.552
H	3.368	-0.143	-0.133
H	1.917	1.685	-0.610
H	1.166	1.783	0.961

SCF Done: E(RwB97XD) = -375.505794631 A.U. after 1 cycles

	1	2	3
	A	A	A
Frequencies --	42.6485	87.6899	91.5238
Red. masses --	3.1474	1.2193	2.4883

Zero-point correction= 0.212693 (Hartree/Particle)

Thermal correction to Energy= 0.224664

Thermal correction to Enthalpy= 0.225608

Thermal correction to Gibbs Free Energy= 0.174986

Sum of electronic and zero-point Energies= -375.293101

Sum of electronic and thermal Energies= -375.281131

Sum of electronic and thermal Enthalpies= -375.280187

Sum of electronic and thermal Free Energies= -375.330809

Item	Value	Threshold	Converged?
Maximum Force	0.000000	0.000015	YES
RMS Force	0.000000	0.000010	YES

C-ts

Cartesian coordinates (Angstroms):

C	-0.031	0.198	1.859
C	-1.022	-0.539	1.181
C	-1.533	-0.098	-0.053
B	0.267	-0.064	0.085
C	-2.240	-1.035	-0.993
H	-1.785	0.961	-0.154
H	-2.064	-0.738	-2.038
H	-3.330	-1.033	-0.829
H	-1.875	-2.066	-0.878
H	0.550	-0.323	2.624
H	-0.120	1.280	1.984
H	-1.007	-1.624	1.336
C	0.847	1.311	-0.552
O	0.890	-1.277	-0.318
C	0.119	2.640	-0.394
C	2.278	-1.356	-0.367
H	0.704	3.469	-0.822
H	-0.068	2.897	0.662
H	-0.856	2.644	-0.908
H	2.567	-2.393	-0.601
H	2.752	-1.087	0.598
H	2.718	-0.706	-1.148

H 0.967 1.101 -1.631

H 1.875 1.427 -0.164

SCF Done: E(RwB97XD) = -375.471249456 A.U. after 1 cycles

	1	2	3
	A	A	A
Frequencies --	-216.6291	84.1488	119.9267
Red. masses --	5.1941	2.8037	1.8614

Zero-point correction= 0.212420 (Hartree/Particle)

Thermal correction to Energy= 0.223291

Thermal correction to Enthalpy= 0.224236

Thermal correction to Gibbs Free Energy= 0.176948

Sum of electronic and zero-point Energies= -375.258829

Sum of electronic and thermal Energies= -375.247958

Sum of electronic and thermal Enthalpies= -375.247014

Sum of electronic and thermal Free Energies= -375.294301

Item	Value	Threshold	Converged?
Maximum Force	0.000000	0.000015	YES
RMS Force	0.000000	0.000010	YES

D-gs

Cartesian coordinates (Angstroms):

C -2.832 0.667 -1.097

C -2.085 0.282 -0.059

C -1.040 -0.795 -0.083

B 0.443 -0.229 0.077

C -1.240 -1.802 1.070

H -1.121 -1.347 -1.036

H -0.475 -2.594 1.051

H -2.225 -2.290 1.002

H -1.181 -1.307 2.053

H -3.563 1.476 -1.007

H -2.742 0.186 -2.077

H	-2.220	0.799	0.901
C	0.758	0.965	1.065
C	1.568	-0.869	-0.828
C	0.842	2.271	0.252
H	1.079	3.133	0.896
H	-0.109	2.491	-0.257
H	1.623	2.220	-0.524
C	3.032	-0.624	-0.472
H	3.265	0.451	-0.420
H	3.717	-1.069	-1.211
H	3.285	-1.058	0.508
H	1.721	0.805	1.581
H	-0.009	1.079	1.849
H	1.348	-0.455	-1.835
H	1.369	-1.949	-0.949

SCF Done: E(RwB97XD) = -339.595872630 A.U. after 1 cycles

	1	2	3
	A	A	A
Frequencies --	35.6003	73.1625	106.9048
Red. masses --	3.1552	2.9951	1.8957

Zero-point correction= 0.235275 (Hartree/Particle)

Thermal correction to Energy= 0.247509

Thermal correction to Enthalpy= 0.248454

Thermal correction to Gibbs Free Energy= 0.197390

Sum of electronic and zero-point Energies= -339.360597

Sum of electronic and thermal Energies= -339.348363

Sum of electronic and thermal Enthalpies= -339.347419

Sum of electronic and thermal Free Energies= -339.398483

Item	Value	Threshold	Converged?
Maximum Force	0.000001	0.000015	YES
RMS Force	0.000000	0.000010	YES

D-ts

Cartesian coordinates (Angstroms):

C	-0.016	-0.261	1.813
C	1.157	0.075	1.166
C	1.612	-0.670	0.025
B	-0.007	-0.162	-0.161
C	2.748	-0.140	-0.815
H	1.590	-1.761	0.120
H	2.690	-0.533	-1.841
H	3.730	-0.429	-0.406
H	2.726	0.959	-0.882
H	-0.510	0.481	2.443
H	-0.322	-1.299	1.953
H	1.479	1.122	1.233
C	-0.349	1.264	-0.838
C	-0.959	-1.415	-0.540
C	-1.202	2.216	0.004
H	-1.472	3.133	-0.545
H	-0.671	2.535	0.916
H	-2.141	1.740	0.331
C	-2.455	-1.185	-0.334
H	-2.695	-1.028	0.731
H	-3.057	-2.039	-0.686
H	-2.807	-0.295	-0.880
H	-0.877	1.063	-1.788
H	0.575	1.792	-1.135
H	-0.652	-2.342	-0.029
H	-0.773	-1.604	-1.615

SCF Done: E(RwB97XD) = -339.584550403 A.U. after 1 cycles

	1	2	3
	A	A	A
Frequencies --	-191.5908	86.5846	129.9525
Red. masses --	5.2509	2.4844	2.1757

Zero-point correction= 0.235777 (Hartree/Particle)

Thermal correction to Energy=		0.246766	
Thermal correction to Enthalpy=		0.247710	
Thermal correction to Gibbs Free Energy=		0.200483	
Sum of electronic and zero-point Energies=		-339.348773	
Sum of electronic and thermal Energies=		-339.337784	
Sum of electronic and thermal Enthalpies=		-339.336840	
Sum of electronic and thermal Free Energies=		-339.384068	
Item	Value	Threshold	Converged?
Maximum Force	0.000001	0.000015	YES
RMS Force	0.000000	0.000010	YES

E-gs

Cartesian coordinates (Angstroms):

C	-4.101	0.012	-0.154
C	-3.728	-1.319	0.040
C	-2.383	-1.657	0.145
C	-1.404	-0.664	0.054
C	-1.761	0.674	-0.138
C	-3.118	0.994	-0.241
H	-3.404	2.039	-0.391
H	-5.155	0.283	-0.237
H	-4.489	-2.099	0.110
H	-2.064	-2.690	0.299
O	-0.106	-1.038	0.163
C	-0.705	1.742	-0.244
N	0.635	1.258	0.047
H	-0.954	2.566	0.451
H	-0.728	2.189	-1.258
C	1.608	2.325	0.068
H	2.596	1.962	0.369
H	1.307	3.110	0.783
H	1.708	2.800	-0.925
B	0.932	-0.110	0.196

C	2.374	-0.765	0.425
C	3.345	-0.429	-0.677
H	2.182	-1.849	0.369
C	2.944	-0.468	1.822
C	3.618	-1.202	-1.731
H	3.861	0.537	-0.602
H	3.143	-2.180	-1.863
H	4.326	-0.884	-2.501
H	3.151	0.603	1.973
H	3.888	-1.011	1.990
H	2.239	-0.776	2.609

SCF Done: E(RwB97XD) = -621.185115083 A.U. after 1 cycles

	1	2	3
	A	A	A
Frequencies --	31.5031	50.2773	62.8322
Red. masses --	3.8743	3.3175	3.3343

Zero-point correction= 0.264057 (Hartree/Particle)
Thermal correction to Energy= 0.278368
Thermal correction to Enthalpy= 0.279313
Thermal correction to Gibbs Free Energy= 0.222215
Sum of electronic and zero-point Energies= -620.921058
Sum of electronic and thermal Energies= -620.906747
Sum of electronic and thermal Enthalpies= -620.905802
Sum of electronic and thermal Free Energies= -620.962900

Item	Value	Threshold	Converged?
Maximum Force	0.000003	0.000015	YES
RMS Force	0.000001	0.000010	YES

E-ts

Cartesian coordinates (Angstroms):

C	3.856	0.041	-0.201
C	3.474	-1.292	-0.040

C	2.133	-1.621	0.140
C	1.163	-0.614	0.170
C	1.534	0.730	0.008
C	2.882	1.038	-0.180
H	3.170	2.085	-0.315
H	4.906	0.300	-0.348
H	4.226	-2.084	-0.059
H	1.814	-2.658	0.266
O	-0.120	-0.957	0.369
C	0.458	1.782	0.046
N	-0.814	1.267	-0.440
H	0.765	2.629	-0.589
H	0.367	2.194	1.080
C	-1.751	2.334	-0.667
H	-2.678	1.977	-1.135
H	-1.317	3.077	-1.357
H	-2.036	2.885	0.258
B	-1.176	0.006	0.264
C	-2.744	-0.711	-0.433
C	-2.574	-0.839	0.947
C	-2.722	-1.884	-1.369
H	-3.206	0.202	-0.815
C	-2.153	0.251	1.747
H	-2.285	-1.834	1.304
H	-2.617	1.234	1.626
H	-1.771	0.023	2.744
H	-2.177	-1.626	-2.290
H	-3.739	-2.189	-1.662
H	-2.220	-2.751	-0.915

SCF Done: E(RwB97XD) = -621.125479541 A.U. after 1 cycles

	1	2	3
	A	A	A
Frequencies --	-379.5548	29.9674	81.6777
Red. masses --	7.6539	4.2411	3.0642

Zero-point correction=	0.261977 (Hartree/Particle)
Thermal correction to Energy=	0.275406
Thermal correction to Enthalpy=	0.276350
Thermal correction to Gibbs Free Energy=	0.222209
Sum of electronic and zero-point Energies=	-620.863503
Sum of electronic and thermal Energies=	-620.850074
Sum of electronic and thermal Enthalpies=	-620.849130
Sum of electronic and thermal Free Energies=	-620.903271

Item	Value	Threshold	Converged?
Maximum Force	0.000000	0.000015	YES
RMS Force	0.000000	0.000010	YES

F-gs

Cartesian coordinates (Angstroms):

C	4.017	0.107	0.269
C	3.697	-1.229	0.028
C	2.384	-1.601	-0.254
C	1.409	-0.615	-0.295
C	1.706	0.728	-0.062
C	3.024	1.084	0.226
H	3.272	2.131	0.413
H	5.048	0.390	0.491
H	4.476	-1.993	0.060
H	2.110	-2.640	-0.446
O	0.110	-0.977	-0.576
C	0.591	1.721	-0.180
N	-0.681	1.139	0.363
H	0.393	1.982	-1.233
H	0.806	2.648	0.366
C	-1.779	2.143	0.352
H	-2.681	1.702	0.789
H	-1.967	2.455	-0.681
H	-1.466	3.011	0.945

B	-0.981	-0.246	-0.307
C	-2.422	-0.808	-0.551
C	-3.189	-0.780	0.761
H	-2.253	-1.865	-0.818
C	-3.184	-0.158	-1.717
C	-2.747	-1.302	1.908
H	-4.173	-0.294	0.743
H	-1.787	-1.828	1.976
H	-3.347	-1.260	2.820
H	-3.445	0.892	-1.521
H	-4.127	-0.697	-1.896
H	-2.604	-0.197	-2.651
H	-0.507	0.903	1.353

SCF Done: E(RwB97XD) = -621.587993249 A.U. after 1 cycles

	1	2	3
	A	A	A
Frequencies --	47.4740	58.7016	93.1257
Red. masses --	3.7321	3.3314	2.6791

Zero-point correction= 0.279141 (Hartree/Particle)

Thermal correction to Energy= 0.293077

Thermal correction to Enthalpy= 0.294021

Thermal correction to Gibbs Free Energy= 0.238768

Sum of electronic and zero-point Energies= -621.308852

Sum of electronic and thermal Energies= -621.294917

Sum of electronic and thermal Enthalpies= -621.293973

Sum of electronic and thermal Free Energies= -621.349225

Item	Value	Threshold	Converged?
Maximum Force	0.000000	0.000015	YES
RMS Force	0.000000	0.000010	YES

F-ts

Cartesian coordinates (Angstroms):

C	3.839	0.224	0.188
C	3.546	-1.109	-0.105
C	2.246	-1.500	-0.425
C	1.246	-0.533	-0.455
C	1.528	0.809	-0.180
C	2.829	1.185	0.151
H	3.055	2.232	0.367
H	4.860	0.516	0.441
H	4.340	-1.858	-0.081
H	2.002	-2.538	-0.655
O	-0.042	-0.851	-0.765
C	0.377	1.755	-0.324
N	-0.831	1.235	0.409
H	0.079	1.852	-1.380
H	0.605	2.756	0.064
C	-1.998	2.119	0.181
H	-2.839	1.801	0.806
H	-2.283	2.071	-0.876
H	-1.729	3.151	0.442
B	-1.039	-0.325	0.094
C	-2.556	-1.025	-0.376
C	-2.378	-1.031	1.032
H	-2.123	-1.871	-0.925
C	-3.766	-0.412	-1.028
C	-1.126	-1.354	1.573
H	-3.004	-0.333	1.607
H	-0.566	-2.223	1.216
H	-0.907	-1.030	2.592
H	-4.235	0.362	-0.405
H	-4.523	-1.188	-1.217
H	-3.509	0.029	-2.002
H	-0.593	1.293	1.403

SCF Done: E(RwB97XD) = -621.562458903 A.U. after 1 cycles

1 2 3

	A	A	A
Frequencies --	-297.6201	45.6883	82.2454
Red. masses --	6.2477	3.8843	3.7046

Zero-point correction= 0.278007 (Hartree/Particle)
Thermal correction to Energy= 0.291029
Thermal correction to Enthalpy= 0.291973
Thermal correction to Gibbs Free Energy= 0.239304
Sum of electronic and zero-point Energies= -621.284451
Sum of electronic and thermal Energies= -621.271430
Sum of electronic and thermal Enthalpies= -621.270486
Sum of electronic and thermal Free Energies= -621.323154

Item	Value	Threshold	Converged?
Maximum Force	0.000000	0.000015	YES
RMS Force	0.000000	0.000010	YES

***R*-allyl**

Cartesian coordinates (Angstroms):

H	-4.332	-2.711	0.333
H	-4.870	-2.310	-2.029
H	-1.106	0.155	5.242
C	-3.953	-1.683	0.447
H	-4.784	-1.058	0.806
H	-2.652	-3.081	-1.592
C	-4.559	-1.260	-1.927
H	-3.173	-1.696	1.220
H	-5.447	-0.688	-1.618
H	1.088	-0.065	4.228
C	-0.982	-0.394	4.305
C	-3.420	-1.166	-0.903
C	-2.272	-2.065	-1.400
C	0.224	-0.537	3.747
H	-4.251	-0.910	-2.925
H	-1.883	-0.838	3.870

H	-1.465	-2.152	-0.661
H	-1.852	-1.684	-2.344
C	-2.936	0.285	-0.734
C	0.504	-1.284	2.445
H	-4.386	1.167	-2.064
O	-1.225	-0.359	0.827
C	-0.172	-2.651	2.328
H	1.593	-1.391	2.359
C	-3.554	1.360	-1.388
C	-1.873	0.629	0.114
B	-0.029	-0.235	1.424
C	-3.150	2.682	-1.206
C	-1.444	1.945	0.310
H	0.723	0.727	-0.956
H	-3.668	3.483	-1.735
N	0.720	1.099	1.121
H	-0.648	2.127	2.310
C	-2.092	2.981	-0.357
C	-0.307	2.180	1.263
H	1.452	1.216	1.834
C	1.470	0.978	-0.193
O	3.150	-0.123	1.078
C	2.441	-0.185	0.078
H	0.770	2.734	-2.205
H	-1.769	4.014	-0.210
N	2.440	-1.222	-0.767
H	0.591	3.721	-0.738
H	0.158	3.160	1.118
C	3.329	-2.367	-0.539
C	1.587	-1.409	-1.949
C	1.322	3.232	-1.393
H	2.873	1.248	-2.519
C	2.252	2.253	-0.659
C	3.318	1.795	-1.673
H	1.924	4.034	-1.846

H	4.093	1.166	-1.213
H	2.259	3.386	1.237
C	2.961	2.951	0.509
H	3.822	2.679	-2.090
H	3.633	2.262	1.039
H	3.565	3.785	0.122
C	2.173	-2.653	-2.615
H	1.615	-0.531	-2.608
H	0.542	-1.573	-1.639
C	2.746	-3.449	-1.442
H	2.980	-2.361	-3.305
H	1.420	-3.203	-3.193
H	3.498	-4.188	-1.747
H	1.940	-3.986	-0.917
H	3.341	-2.629	0.528
H	4.360	-2.099	-0.825
H	0.135	-3.306	3.156
H	0.108	-3.142	1.385
H	-1.269	-2.576	2.347

SCF Done: E(RwB97XD) = -1260.23766903 A.U. after 1 cycles

	1	2	3
	A	A	A
Frequencies --	24.0164	33.4287	40.5899
Red. masses --	4.0183	3.7103	3.3828

Zero-point correction= 0.627601 (Hartree/Particle)
Thermal correction to Energy= 0.658498
Thermal correction to Enthalpy= 0.659442
Thermal correction to Gibbs Free Energy= 0.567702
Sum of electronic and zero-point Energies= -1259.610068
Sum of electronic and thermal Energies= -1259.579171
Sum of electronic and thermal Enthalpies= -1259.578227
Sum of electronic and thermal Free Energies= -1259.669967

Item	Value	Threshold	Converged?
Maximum Force	0.000000	0.000015	YES

RMS Force 0.000000 0.000010 YES

***R*-allyl'**

Cartesian coordinates (Angstroms):

H	4.858	-1.738	0.955
H	5.599	0.548	1.291
H	0.066	-5.628	-0.963
C	4.127	-1.426	0.193
H	4.615	-1.503	-0.791
H	3.669	-0.265	2.624
C	4.922	0.906	0.501
H	3.287	-2.133	0.215
H	5.479	0.873	-0.447
H	-1.582	-3.929	-0.549
C	0.246	-4.865	-0.200
C	3.670	0.020	0.465
C	2.989	0.110	1.843
C	-0.654	-3.911	0.044
H	4.687	1.958	0.728
H	1.188	-4.932	0.350
H	2.066	-0.482	1.888
H	2.750	1.156	2.090
C	2.693	0.462	-0.637
C	-0.537	-2.784	1.036
H	3.809	2.201	-1.254
O	1.153	-1.352	-0.206
C	0.484	-3.027	2.150
H	-1.531	-2.652	1.503
C	2.923	1.593	-1.434
C	1.524	-0.268	-0.929
B	-0.191	-1.425	0.263
C	2.064	1.984	-2.463
C	0.680	0.085	-1.994

H	-2.106	0.781	-1.443
H	2.293	2.877	-3.048
N	-1.226	-1.084	-0.992
H	-0.068	-1.849	-2.548
C	0.940	1.221	-2.758
C	-0.454	-0.862	-2.252
H	-1.826	-1.897	-1.134
C	-2.058	0.084	-0.596
O	-0.471	-0.165	1.103
C	-1.211	0.684	0.505
H	-4.332	1.692	-0.749
H	0.278	1.491	-3.585
N	-1.181	1.944	0.825
H	-4.399	0.457	-2.028
H	-1.135	-0.502	-3.035
C	-0.229	2.480	1.813
C	-1.928	3.017	0.145
C	-4.501	0.624	-0.944
H	-3.582	0.988	1.648
C	-3.542	-0.276	-0.152
C	-3.744	-0.060	1.354
H	-5.542	0.402	-0.670
H	-3.075	-0.694	1.955
H	-3.776	-1.964	-1.555
C	-3.885	-1.736	-0.481
H	-4.777	-0.316	1.628
H	-3.295	-2.456	0.106
H	-4.940	-1.919	-0.233
C	-1.405	4.297	0.803
H	-3.007	2.878	0.284
H	-1.701	2.982	-0.932
C	-0.023	3.908	1.328
H	-2.062	4.584	1.638
H	-1.382	5.134	0.093
H	0.336	4.569	2.127

H	0.720	3.918	0.515
H	0.676	1.862	1.822
H	-0.691	2.440	2.812
H	0.278	-3.967	2.685
H	0.461	-2.210	2.887
H	1.509	-3.081	1.755

SCF Done: E(RwB97XD) = -1260.27575595 A.U. after 1 cycles

	1	2	3
	A	A	A
Frequencies --	43.1630	44.0769	52.2230
Red. masses --	4.1977	3.8883	3.6714

Zero-point correction= 0.630348 (Hartree/Particle)
Thermal correction to Energy= 0.659550
Thermal correction to Enthalpy= 0.660494
Thermal correction to Gibbs Free Energy= 0.574165
Sum of electronic and zero-point Energies= -1259.645408
Sum of electronic and thermal Energies= -1259.616206
Sum of electronic and thermal Enthalpies= -1259.615262
Sum of electronic and thermal Free Energies= -1259.701591

Item	Value	Threshold	Converged?
Maximum Force	0.000001	0.000015	YES
RMS Force	0.000000	0.000010	YES

Chapter Two

Practical, Broadly Applicable, α- , Z-, Diastereoselective, and Enantioselective Addition of Allylboron Compounds to Mono-, Di-, Tri-, and Polyfluoroalkyl Ketones

2.1. Introduction

Fluorine containing compounds have been steadily gaining importance over the years in multiple fields, such as: therapeutics,[1] agrochemicals,[2] and materials.[3] Therefore, it follows that methods that can generate trifluoromethyl-containing compounds enantioselectively through practical, efficient and broadly applicable catalytic protocols are of the utmost importance to the greater synthetic community. Despite the aforementioned utility and desirability of these products, methods that can generate trifluoromethyl-substituted tertiary alcohols through allyl addition are few and far between.[4] We sought to improve upon the current methods by developing a catalytic

(1) Gillis, E. P.; Eastman, K. J.; Hill, M. D.; Donnelly, D. J.; Meanwell, N. A. *J. Med. Chem.* **2015**, *58*, 8315−8359.
(2) Fujiwara, T.; O'Hagan, D. *J. Fluorine Chem.* **2014**, *167*, 16−29.
(3) Berger, R.; Resnati, G.; Metrangolo, P.; Weber, E.; Hulliger, J. *Chem. Soc. Rev. 2011*, **40**, 3496−3508.
(4) For examples of carbon-based nucleophiles (non-allyl) in catalytic enantioselective additions to trifluoromethyl ketones, see (a) Zhang, G.-W.; Meng, W.; Ma, H.; Nie, J.; Zhang, W.-Q.; Ma, J.-A. *Angew. Chem., Int. Ed.* **2011**, *50*, 3538–3542; (b) Motoki, R.; Kanai, M.; Shibasaki, M. *Org. Lett.* **2007**, *9*, 2997–3000; (c) Cook, A. M.; Wolf, C. *Angew. Chem., Int. Ed.* **2016**, *55*, 2929–2933; (d) Noda, H.; Amemiya, F.; Weidner, K.; Kumagai, N.; Shibasaki, M. *Chem. Sci.* **2017**, *8*, 3260–3269; (e) Zheng, Y.; Tan, Y.; Harms, K.; Marsch, M.; Riedel, R.; Zhang, L.; Meggers, E. *J. Am. Chem. Soc.* **2017**, *139*, 4322–4325; (f) Ma, J.; Kass, S. R. *Org. Lett.* **2018**, *20*, 2689–2692; (g) Borrego, L. G.; Recio, R.; Alcarranza, M.; Khiar, N.; Fernández. *Adv. Synth. Catal.* **2018**, *360*, 1273–1279; (h) Gan, X.-C.; Zhang, Q.; Jia, X.-S., Yin, L. *Org. Lett.* **2018**, *20*, 1070–1073; (i) Jafari, E.; Kundu, D. S.; Chauhan, P.; Gajulapalli, V. P R.; von Essen, C.; Rissanen, K.; Enders, D. *Synthesis* **2018**, *50*, 323–329; (j) Jiang, L.; Hu, B.; Xie, X.; Zhang, Z. *Tetrahedron* **2017**, *73*, 6901–6905.

enantioselective crotyl addition utilizing our aminophenol ligand to access these products efficiently and with high levels of regio-, diastereo-, *Z*, and enantioselectivity. While our motivations for this study are rooted in the value of the products, we were also intrigued in further investigating the generality of 1,3-borotropic shift, as discussed in Chapter 1.

2.2. Background

2.2.1 State-of-the-Art in Catalytic Enantioselective Allyl Additions to Trifluoromethyl Ketones

The field of catalytic enantioselective allyl additions to trifluoromethyl ketones has barely been broached, leaving much room for improvement over the existing methods. The first report of an enantioselective allyl addition to a trifluoromethyl ketone was carried out by Loh *et al.* in 1990, the results are shown in Scheme 2.1.[5]

Scheme 2.1. Loh's Stoichiometric Indium Mediated Allyl Addition

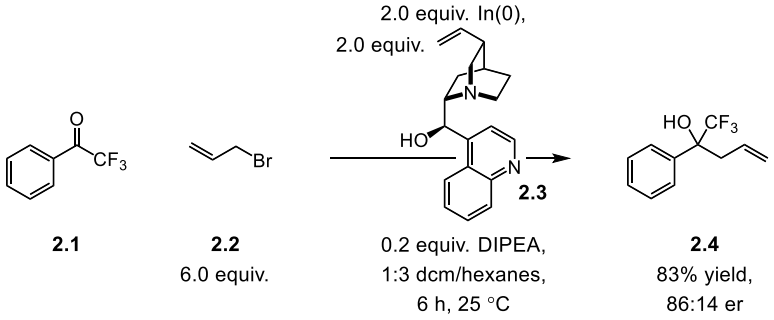

The Loh group was able to perform allyl additions to trifluoromethyl ketones by utilizing stoichiometric indium powder and a cinchona alkaloid (**2.3**) in the presence of six equivalents of allyl bromide. The in situ generated allyl-indium-cinchona species can

(5) Loh, T.-P.; Zhou, J.-R., Li, X.-R. *Tetrahedron Lett.* **1990**, *40*, 9333–9336.

further react with trifluoroacetophenone (**2.1**) to furnish the corresponding trifluoromethyl-substituted homoallylic alcohol (**2.4**) in 83% yield and 86:14 er. While they were able to access the desired product with moderate levels of enantioselectivity, the need for superstoichiometric reagents (including indium and even the cinchona alkaloid ligand) in addition to the limited scope of the transformation (only one case was examined), leaves much room for improvement.

Scheme 2.2. Feng's Indium/*N*-Oxide Catalyzed Allylation of Trifluoroacetophenone

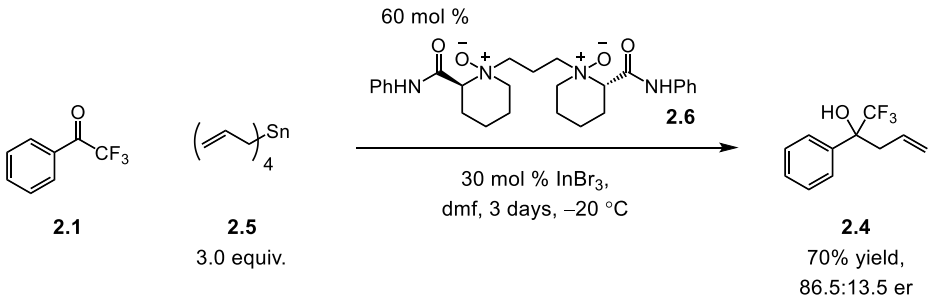

The following report on enantioselective allyl additions to trifluoromethyl ketones was disclosed by Feng et al. in 2007 (Scheme 2.2).[6] Feng and co-workers reported a protocol which utilizes tetraallyltin as an allyl source, which, in the presence of 30 mol % indium(III) bromide and C_2-symmetric *N*-oxide ligand, in situ generates a chiral allylating reagent capable of reacting with trifluoromethyl ketones. Under these reaction conditions it was reported that the desired product could be obtained in similar enantioselectivity (86.5:13.5 er versus 86:14 er), as was obtained by the Loh group (over a decade earlier), and slightly lower yield (70% yield versus 83% yield). Unfortunately, the reaction also required low temperature reaction conditions and took 3 days to reach completion. Lastly, the protocol was not investigated with other trifluoromethyl ketones, limiting the reported

(6) Zhang, X.; Chen, D.; Liu, X.; Feng, X. *J. Org. Chem.* **2007**, *72*, 5227–5233.

scope of the protocol. The following year, the Singaram group published what was, before our groups' entry into the field, the most competitive protocol to achieve allylation of trifluoromethyl ketones efficiently and with high enantioselectivity (Scheme 2.3).[7]

Scheme 2.3. Singaram's Indium/Aminoalcohol Catalyzed Allylation

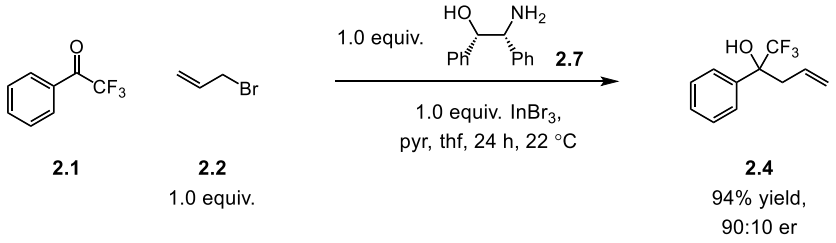

2.1 **2.2** 1.0 equiv. **2.4** 94% yield, 90:10 er

The reported protocol was similar to the method reported by the Loh group (Scheme 2.3), with the exception that indium(III) bromide was used instead of indium powder and aminoalcohol **2.7** was the ligand, rather than cinchona alkaloid **2.3**. With the aforementioned modifications, the Singaram group found that they could synthesize the desired compound (**2.4**) in high yields and 90:10 enantioselectivity. However, again the method was not catalytic nor was it shown to be general and broadly applicable. As can be seen by the previous state-in-the-art in enantioselective allyl additions to trifluoromethyl ketones, there had been no reported broadly applicable, catalytic, and enantioselective method for the synthesis of these valuable building blocks.

2.2.2 Objectives of the Study on Crotyl Additions to Trifluoromethyl Ketones

In 2016, our laboratory developed a protocol to access these trifluoromethyl-containing homoallylic alcohols in a catalytic enantioselective fashion.[8] While previous

(7) Haddad, T. D.; Hirayama, L. C.; Taynton, P.; Singaram, B. *Tetrahedron Lett.* **2008**, *49*, 508–511.
(8) Lee, K.; Silverio, D. L.; Torker, S.; Robbins, D. W.; Haeffner, F.; van der Mei, F. W.; Hoveyda, A. H. *Nature Chem.* **2016**, *8*, 768–777.

efforts at generating the aforementioned compounds enantioselectively were met with moderate levels of enantioselectivity, we found that, by utilizing the aminophenol ligand for this transformation, we could generate these compounds enantioselectively, despite the small size difference between the two substituents of the electrophile (phenyl versus trifluoromethyl), as shown in Scheme 2.4 A. We proposed that the origin of high enantioselectivity in these transformations was not due to steric reasons; rather, due to the embedded ammonium group in the catalytically active complex, the substrate can participate in a second point of binding with the catalyst by means of an electrostatic interaction between the trifluoromethyl group of the substrate and the ammonium moiety of the catalyst.[9] This second point of contact allows for high enantiotopic differentiation of the faces of the electrophile, allowing the allyl addition to occur in a highly enantioselective manner. We found that under the reported reaction conditions (2.5 mol % aminophenol **2.10**, 10 mol % NaO*t*-Bu, 1.3 equiv. methanol, toluene, 4 hours, –4 °C), the protocol was broadly applicable in regard to electrophile (**2.8**) *and* nucleophile (**2.9**). Nineteen examples were demonstrated and the reaction was found to be highly efficient and enantioselective.

(9) For an in-depth analysis and enlightening discussion of this phenomenon, see ref. 8.

Scheme 2.4. Catalytic Enantioselective Additions to Trifluoromethyl Ketones

A Aminophenol Catalyzed Allyl Additions

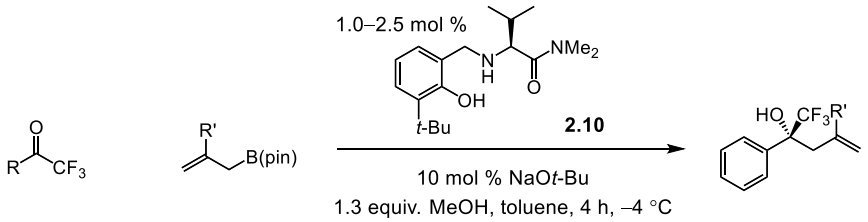

2.8
R = Aryl, Heteroaryl, Alkyl, Alkenyl

2.9
1.1 equiv.
R' = H, Me, Cl

2.11
19 examples
up to 98% yield,
up to >99:1 er

B Aminophenol Catalyzed Allenyl Additions

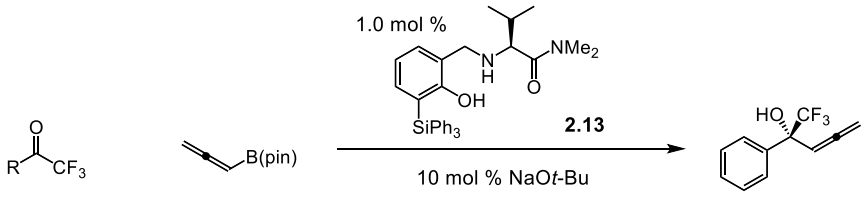

2.8
R = Aryl, Heteroaryl, Alkyl, Alkenyl

2.12
1.1 equiv.

2.14
14 examples
up to 97% yield,
up to >99:1 er

In the same report, we also demonstrated that, with a slight change in the ligand used for the transformation (Scheme 2.4 B, **2.13**), the method could also be expanded to allenyl addition to trifluoromethyl ketones. At that point in time (and as of the writing of this thesis), there had been no reports of a catalytic enantioselective allenyl addition to trifluoromethyl ketones.[10] Again, the protocol proved to be robust and broadly applicable, tolerating a wide variety of trifluoromethyl ketones and furnishing products in exceptionally high yields and enantioselectivities.

(10) There have been two methods to generate these compounds, however in both cases no enantioselectivity was reported for the transformation despite the fact that chiral auxiliaries were employed. For these reports, see: (a) Haddad, T. D.; Hirayama, L. C.; Buckley, J. J.; Singaram, B. *J. Org. Chem.* **2012**, *77*, 889–898; (b) Fandrick, D. R.; Reeves, J. T.; Bakonyi, J. M.; Nyalapatla, P. R.; Tan, Z.; Niemeier, O.; Akalay, D.; Fandrick, K. R.; Wohlleben, W.; Ollenberger, S.; Song, J. J.; Sun, X.; Qu, B.; Haddad, N.; Sanyal, S.; Shen, S.; Ma, S.; Byrne, D.; Chitroda, A.; Fuchs, V.; Narayanan, B. A.; Grinberg, N.; Lee, H.; Yee, N.; Brenner, M.; Senanayake, C. H. *J. Org. Chem.* **2013**, *78*, 3592–3615.

Scheme 2.5. Possible Products in Crotyl Addition to Trifluoromethyl Ketones

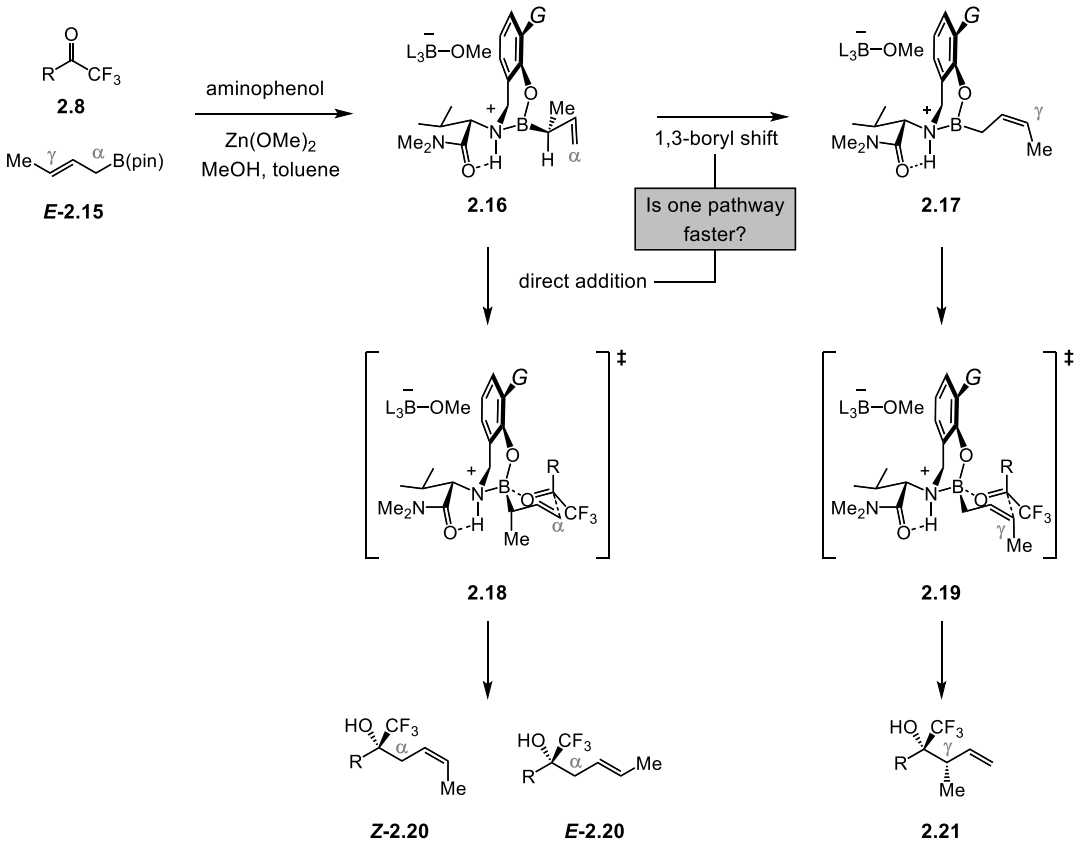

After these developments in our lab, we set out to explore the possibility of using γ-substituted allylboron reagents in this transformation, in order to further understand 1,3-borotropic shift. Particularly, we were wondering if 1,3-borotropic shift would always be more facile than the corresponding direct addition to the electrophile. The questions we aimed to address in this study are discussed in Scheme 2.5. When *E*-crotyl–B(pin) (***E*-2.15**) is subjected to aminophenol, zinc(II) methoxide and methanol, intermediate **2.16** is formed. At this point, one of two outcomes could occur. Either 1,3-borotropic shift could be

extremely facile and intermediate **2.17** would be formed, and after reacting with the electrophile through transition state **2.19** would furnish the γ-addition product **2.21**, similar to the reaction outcome observed in Chapter 1. Alternatively, the electrophile could be reactive enough to undergo direct addition with **2.16** to form α-addition product **2.20** *via* the intermediacy of transition state **2.18**. Thus, the first question became: are trifluoromethyl ketones reactive enough to undergo direct addition or would 1,3-borotropic shift still prevail over direct addition? If the reaction was α-selective (i.e., direct addition occurred), would the reaction be *E*- or *Z*-selective? Would the product be enantioselective? Similar questions arose in regard to the γ-addition product. Would the diastereoselectivity of the transformation be high? Would the transformation be enantioselective? Another interesting possibility is the fact that the rates of direct addition versus 1,3-borotropic shift could be competitive, leading to products with poor regioselectivity. Instead, perhaps more ambiguous scenarios are possible when less electrophilic substrates are used, such as difluoromethyl- and monofluoromethyl ketones. Would these electron-rich substrates react with different levels of regioselectivity? Would they be similarly non-enantioselective, as was the case in the corresponding allyl additions? In order to study all of these possible scenarios, we set out to investigate this transformation in the hopes of gaining more knowledge on the use of substituted allyl boron reagents with the aminophenol ligand.

2.3. Development of Aminophenol-Promoted Crotyl Additions to Trifluoromethyl Ketones

2.3.1 Initial Result for Crotyl Additions to Trifluoromethyl Ketones

When we first subjected trifluoroacetophenone (**2.1**) to similar reaction conditions reported for the crotylation of *N*-phosphinoyl imines (1.2 equivalents of **Z-2.15**, 2.5 mol% aminophenol **2.10**, 5.0 mol % zinc(II) methoxide, and 1.3 equivalents of methanol) we found that the reaction was quite efficient and enantioselective (Scheme 2.6). However, we were surprised at the observed regioselectivity of the transformation, as the reaction was found to proceed with exclusive α selectivity.

Scheme 2.6. Initial Result for Crotyl Addition to Trifluoromethyl Ketones

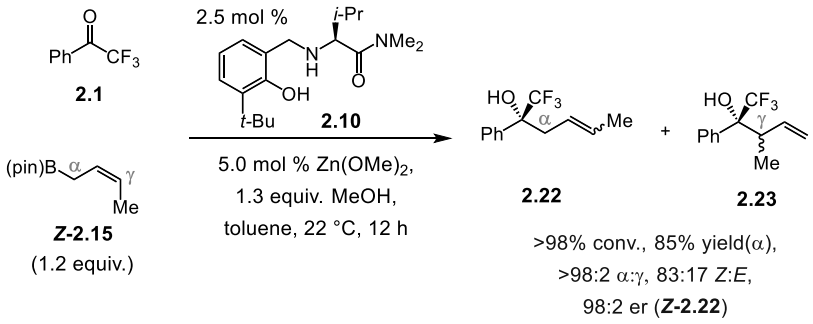

This finding came as a surprise to us, as the recently developed crotyl additions to *N*-phosphinoyl imines were highly γ-selective (see Chapter 1). This suggested to us that the occurrence of 1,3-borotropic shift during a reaction is highly dependent on the electrophilicity of the substrate. Additionally, the reaction was found to be highly enantioselective (98:2 er), which is marginally higher than the enantioselectivity of the corresponding allyl addition to **2.1** (96:4 er, at 4 °C). Though the efficiency, regio- and enantioselectivity were all found to be high, the *Z* selectivity of the transformation was found to be low, with aminophenol **2.10** producing products with 83:17 *Z*:*E* selectivity.

Transformations for this substrate class, particularly the α-selective products of these reactions, were few and far between, thus we set out to improve the selectivities of the transformation through the screening of aminophenol ligands.

2.3.2 Reaction Optimization through Aminophenol Screening

In order to efficiently screen a variety of aminophenol ligands, we decided to carry out the following set of experiments at 60 °C as shown in Scheme 2.7. When we carried out the reaction shown in Scheme 2.6 at elevated temperatures, we found that the enantioselectivity of the transformation was still high, however the regio- and *Z* selectivity was somewhat diminished (96:4 α:γ and 79:21 *Z*:*E* versus >98:2 α:γ and 83:17 *Z*:*E* at 22 °C).

Scheme 2.7. Representative Aminophenol Screening Data

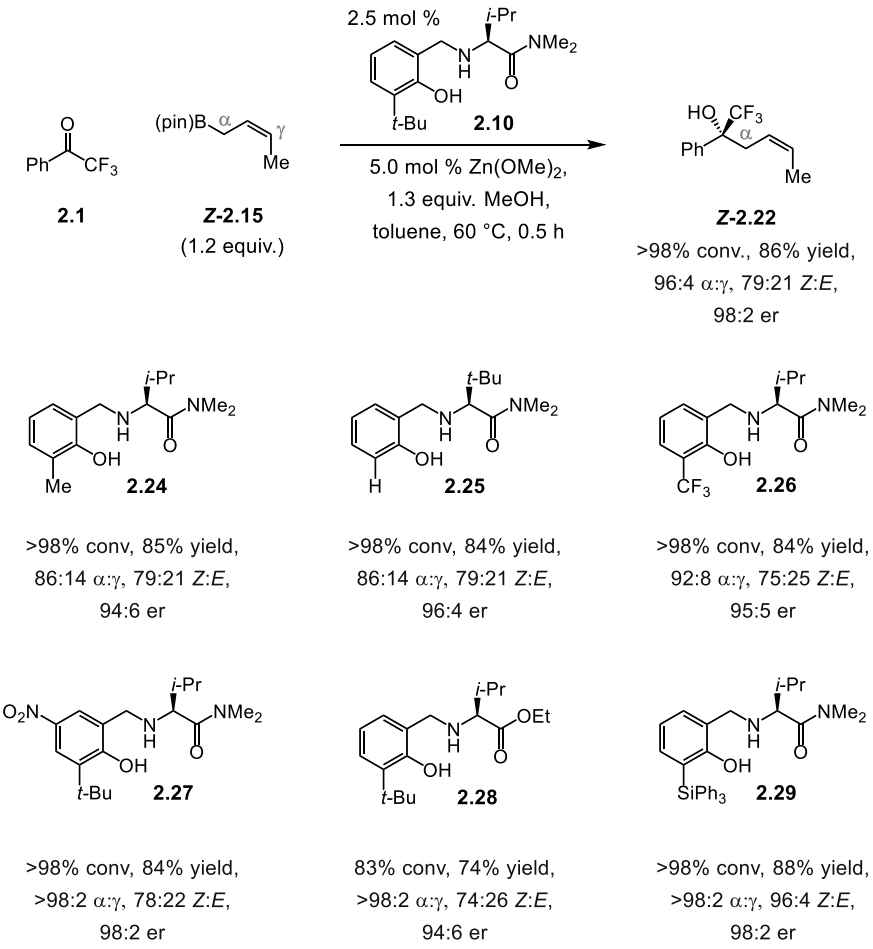

When aminophenol ligands with smaller aryl substituents (such as R = Me (**2.24**), H (**2.25**)) were screened under these reaction conditions regio- and enantioselectivities were lower (86:14 α:γ and 94:6 er for aminophenol **2.24** and 86:14 α:γ and 96:4 er for aminophenol **2.25**), and *Z*:*E* selectivities remained unchanged. Aminophenol ligands with electron withdrawing substituents, which had previously found to be ineffective in catalyzing enantioselective allyl additions to phosphinoyl imines, were found to work under these conditions.[11] While the CF_3-substituted (**2.26**) and nitro-substituted (**2.27**)

(11) Note: We believe that this is related to the use of $Zn(OMe)_2$ rather than the more basic NaO*t*-Bu employed in the allyl additions to *N*-phosphinoyl imines. NMR studies have indicated that acidic phenols

aminophenol ligands were found to catalyze efficient crotyl additions to trifluoromethyl ketones, the selectivities with which the products were formed were not improved. When an ester-containing aminophenol was utilized for the reaction rather than the traditional amide-containing aminophenols, the reaction was found to be less efficient with low *Z* selectivity (74:26 *Z*:*E*).[12] Lastly, when we moved to the triphenylsilyl-substituted aminophenol (**2.29**), developed for allylation of methyl ketones[13], we found that the products were obtained with exceptional regio- and enantioselectivity and high *Z* selectivity (96:4 *Z*:*E*). The exact mechanism by which the triphenylsilyl-substituted aminophenol can access products with such high *Z* selectivity will be discussed in detail below. A variety of other modifications to the aminophenol ligands, whether steric or electronic, were found to produce no further improvements in the selectivity of the transformation.

2.3.3 Optimized Reaction Conditions for Crotyl Additions to Trifluoromethyl Ketones

With the optimal aminophenol ligand (**2.29**) in hand we set out to optimize the other reaction parameters, the final result of these experiments can be found in Scheme 2.8.

---

remain deprotonated in reactions when NaO*t*-Bu is used, however under conditions which utilized $Zn(OMe)_2$, the phenolic proton remains intact. This is a mechanistically interesting finding which could shed light on the initiation of the catalytically competent species.

(12) The exact rationale for why the ester-containing aminophenol reacts inefficiently is currently still unknown. However, we propose that it is likely due to the diminished Lewis basicity of the carbonyl oxygen, which likely plays an integral role in stabilizing the charged ammonium group of the catalytically active species.

(13) Robbins, D. W.; Lee, K.; Silverio, D. L.; Volkov, A.; Torker, S.; Hoveyda, A. H. *Angew. Chem., Int. Ed.* **2016**, *55*, 9610–9614.

Scheme 2.8. Optimized Reaction Conditions for Crotyl Additions

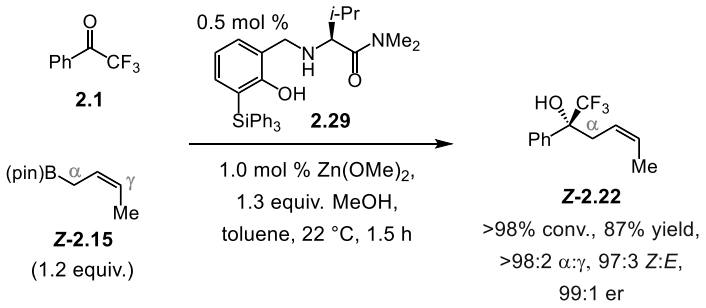

Naturally, we investigated the reaction outcome at room temperature and found that the *Z* and enantioselectivity of the transformation both slightly improved (97:3 *Z*:*E* and 99:1 er versus 96:4 *Z*:*E* and 98:2 er at 60 °C). We also found that the transformation was incredibly efficient with the triphenylsilyl aminophenol ligand, enabling us to perform the transformation at low loadings (0.5 mol % aminophenol **2.29** and 1.0 mol % zinc(II) methoxide) and short reaction times (1.5 hours).

2.4. Scope of the Method

2.4.1 Reactions with Z-Crotyl–B(pin)

In hopes of demonstrating the broad applicability and practicality of the protocol, we carried out an extensive investigation with regard to substrate scope. The reaction was found to tolerate a variety of trifluoromethyl ketones (aryl, heteroaryl, alkynyl, alkenyl and alkyl) in addition to being amenable to different substituted allyl boron reagents as well as mono- and difluoromethyl ketones. The scope of the transformation with respect to aryl-substituted trifluoromethyl ketones is shown in Scheme 2.9.

Scheme 2.9. Reactions with Aryl-Substituted Trifluoromethylketones

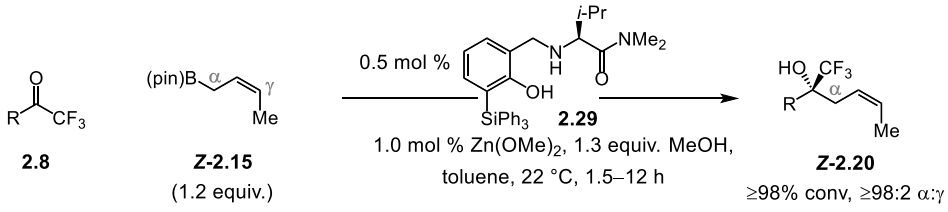

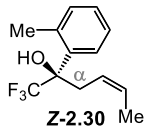
Z-2.30
2 h, 91% yield,
96:4 *Z*:*E*, 98:2 er

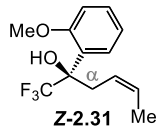
Z-2.31
3 h, 92% yield,
98:2 *Z*:*E*, >99:1 er

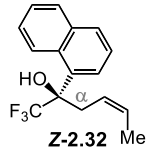
Z-2.32
1.5 h, 95% yield,
>98:2 *Z*:*E*, 97:3 er

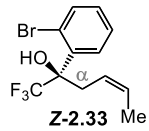
Z-2.33
3 h, 91% yield,
90:10 *Z*:*E*, 98:2 er

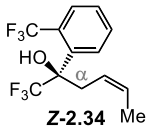
Z-2.34
2 h, 93% yield,
88:12 *Z*:*E*, 98:2 er

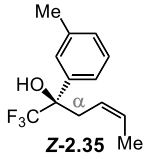
Z-2.35
2 h, 92% yield,
97:3 *Z*:*E*, 99:1 er

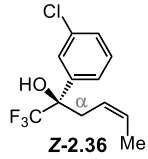
Z-2.36
3 h, 87% yield,
96:4 *Z*:*E*, 98:2 er

gram scale

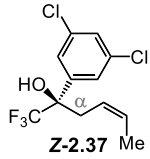
Z-2.37
12 h, 93% yield,
97:3 *Z*:*E*, 96:4 er

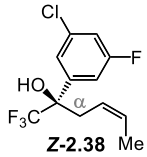
Z-2.38
3 h, 96% yield,
97:3 *Z*:*E*, 97:3 er

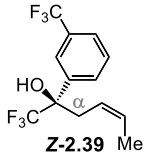
Z-2.39
4 h, 93% yield,
95:5 *Z*:*E*, 98:2 er

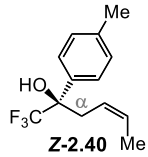
Z-2.40
1.5 h, 92% yield,
96:4 *Z*:*E*, >99:1 er

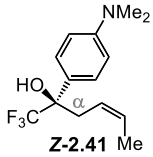
Z-2.41
4 h, 98% yield,
97:3 *Z*:*E*, >99:1 er

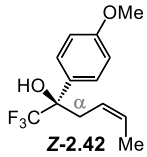
Z-2.42
3.5 h,97% yield,
97:3 *Z*:*E*, >99:1 er

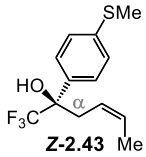
Z-2.43
4 h, 98% yield,
96:4 *Z*:*E*, >99:1 er

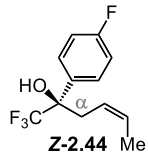
Z-2.44
1.5 h, 94% yield,
96:4 *Z*:*E*, >99:1 er

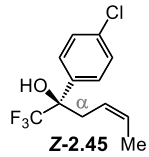
Z-2.45
1.5 h, 92% yield,
96:4 *Z*:*E*, 99:1 er

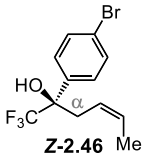
Z-2.46
2 h, 93% yield,
96:4 *Z*:*E*, >99:1 er

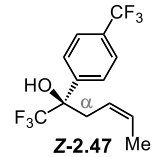
Z-2.47
1.5 h,92% yield,
94:6 *Z*:*E*, 99:1 er

The inclusion of an *ortho*-substituent on the aryl ring was found to not impact selectivity greatly in many cases. For example, when *ortho*-tolyl-substituted

trifluoromethyl ketone (***Z*-2.30**) was subjected to the reaction conditions, the product was generated with 96% *Z* selectivity and 98:2 enantioselectivity. A similar result was obtained when the reaction was carried out on *ortho*-methoxy substituted ***Z*-2.31**, with the product being generated in 98:2 *Z*:*E* selectivity and >99:1 enantioselectivity. 1-Napthyl-substituted trifluoromethyl ketones also reacted with high efficiency and selectivities (>98:2 *Z*:*E* and 97:3 er, ***Z*-2.32**). However, when larger ortho-substituted substrates were utilized, there was a diminution in the *Z* selectivity of the transformation. For instance, *ortho*-bromo- (***Z*-2.33**) and *ortho*-trifluoromethyl-substituted (***Z*-2.34**) trifluoromethyl ketones reacted with moderate *Z* selectivity (90:10 and 88:12 *Z*:*E*, respectively) while enantioselectivities remained high (98:2 er in both cases). A handful of *meta*- and 3,5-disubstituted trifluoromethyl ketones were also evaluated in the transformation. *Meta*-tolyl- (***Z*-2.35**) and *meta*-chloro-substituted (***Z*-2.36**) electrophiles were well tolerated under the reaction conditions, furnishing products with high *Z* selectivity (97:3 and 96:4 *Z*:*E* selectivity, respectively) and enantioselectivity (99:1 and 98:2 er, respectively). We found that the substrates could contain two *meta*-substituents with no observable attenuation in selectivity, as evidenced by the high *Z* and enantioselectivities obtained for 3,5-dichloro- (***Z*-2.37**) and 3,5-chlorofluoro-substituted (***Z*-2.38**) ketones. The protocol was also carried out on gram scale for the 3,5-dichloro-substituted trifluoromethyl ketone without any deterioration of the reaction efficiency. The reaction was also carried out on a host of *para*-substituted trifluoromethyl ketones, where we found out that regardless of the electronic nature of the substituent, electronically activated substrates (i.e., *p*-NMe_2, *p*-OMe, *p*-SMe, and *p*-F) and deactivated substrates (i.e., *p*-Cl, *p*-Br, and *p*-CF_3) reacted efficiently and with high selectivities (≥94:6 *Z*:*E* and ≥99:1 er). Satisfied with the performance of this protocol

on aryl-substituted trifluoromethyl ketones, we then turned to investigate the reaction with heteroaryl-substituted trifluoromethyl ketones (Scheme 2.10).

Scheme 2.10. Reactions with Heteroaryl-Substituted Trifluoromethylketones

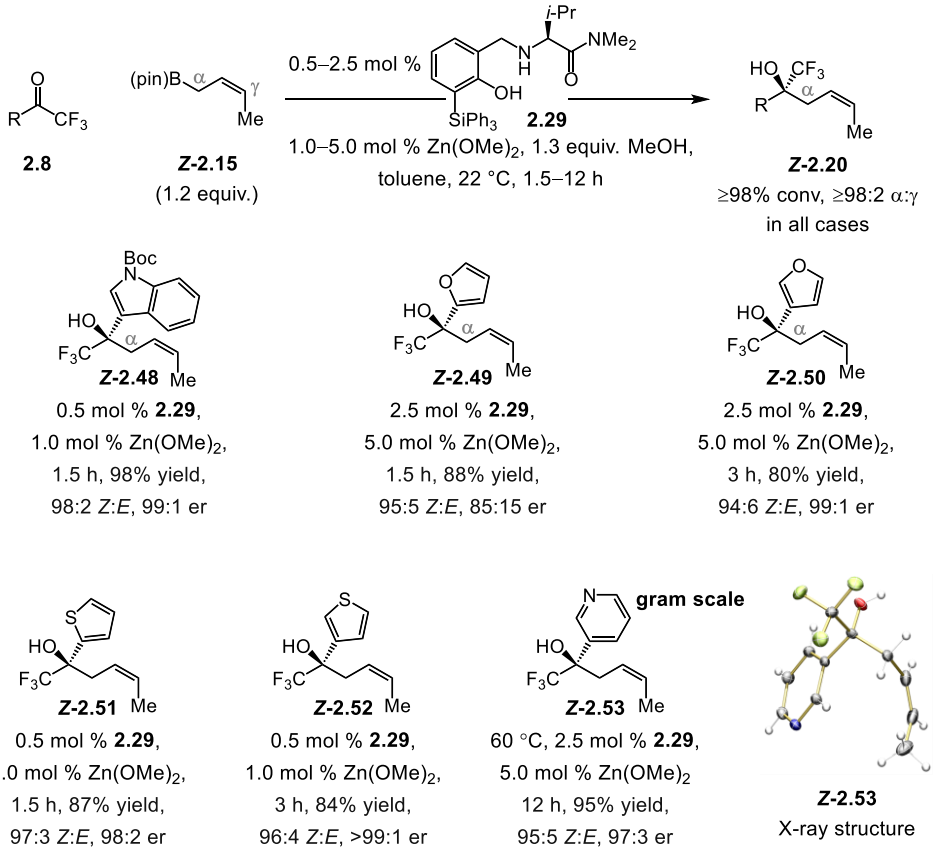

Though the reaction conditions were quite general for the aryl substrates examined in Scheme 2.9, we found that with heteroaryl substrates, occasionally higher catalyst loadings and/or elevated temperatures were required. However, the observed selectivities of the transformation were quite high, for example, 3-Boc-indole-containing tertiary alcohol ***Z*-2.48** was obtained with 98:2 *Z:E* and 99:1 enantioselectivity. When 2-furyl-substituted ketone ***Z*-2.49** was subjected to the reaction conditions, elevated catalyst loadings were required (2.5 mol % aminophenol **2.29** and 5.0 mol % $Zn(OMe)_2$) for an efficient transformation. Additionally, while the *Z* selectivity of the transformation was

high for this case (95:5 *Z*:*E*), the enantioselectivity was much lower than what we had observed for previous cases (85:15 er).[14] However, when the substrate was switched to the analogous 3-furyl-containing ketone, the enantiopurity of the product was again high (99:1 er, ***Z*-2.50**). Interestingly, when corresponding thienyl substrates were subjected to the reaction conditions, enantioselectivities were high, regardless of the location of the heteroatom (98:2 er and >99:1 er for ***Z*-2.51** and ***Z*-2.52**, respectively). We believe that the origin of this discrepancy is due to the fact that sulfur does not readily participate in a competitive electrostatic interaction as well as oxygen can, due to it having worse orbital overlap with hydrogen when compared to oxygen. Lastly, when the hydrate of 3-pyridyl-substituted trifluoromethyl ketone was subjected to the reaction conditions, we found that the reaction required elevated temperatures (60 °C) and catalyst loadings to proceed to completion in 12 hours.[15] However, despite the need for elevated temperatures, the product (***Z*-2.53**) was obtained in high *Z* and enantioselectivity (95:5 *Z*:*E* and 97:3 er). Alkyl, alkenyl and alkynyl substrates were also investigated and found to tolerate the reaction conditions, as shown in Scheme 2.11.

(14) This phenomenon was also observed during the development of the aminophenol promoted allyl additions to trifluoromethyl ketones. For an interesting discussion and analysis of this outcome please see ref. 8.

(15) The ketone form of this substrate was not isolable, hydrate formation occurred immediately upon silica gel column chromatography. Coincidentally, we also believe that high temperatures and catalyst loadings are required for this transformation, due to hydrolysis of the hydrate being slow.

Scheme 2.11. Scope for Alkyl-, Alkenyl-, and Alkynyl-Substituted Trifluoromethylketones

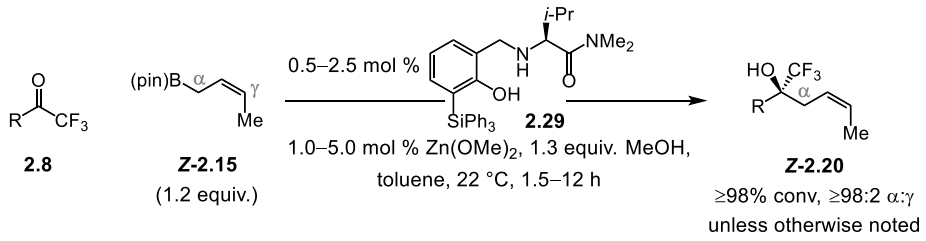

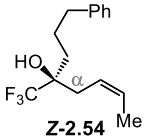

***Z*-2.54**
0.5 mol % **2.29**,
1.0 mol % $Zn(OMe)_2$,
3 h, 93% yield,
92:8 *Z*:*E*, 96:4 er

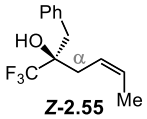

***Z*-2.55**
2.5 mol % **2.29**,
5.0 mol % $Zn(OMe)_2$,
4 h, 80% yield, 97:3 α:γ,
79:21 *Z*:*E*, 96:4 er

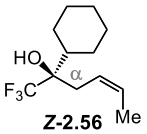

***Z*-2.56**
0.5 mol % **2.29**,
1.0 mol % $Zn(OMe)_2$,
3 h, 88% yield,
>98:2 *Z*:*E*, 90:10 er

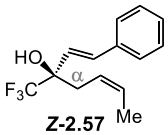

***Z*-2.57**
0.5 mol % **2.29**,
1.0 mol % $Zn(OMe)_2$,
1.5 h, 97% yield,
98:2 *Z*:*E*, 99:1 er

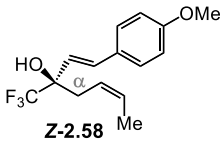

***Z*-2.58**
2.5 mol % **2.29**,
5.0 mol % $Zn(OMe)_2$,
5 h, 95% yield,
>98:2 *Z*:*E*, 99:1 er

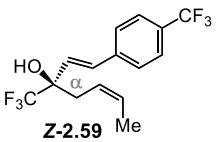

***Z*-2.59**
2.5 mol % **2.29**,
5.0 mol % $Zn(OMe)_2$,
2 h, 93% yield,
96:4 *Z*:*E*, 99:1 er

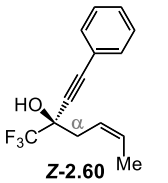

***Z*-2.60**
0.5 mol % **2.29**,
1.0 mol % $Zn(OMe)_2$,
1.5 h, 95% yield,
98:2 *Z*:*E*, 81:19 er

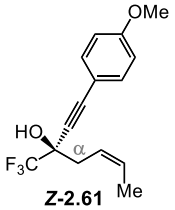

***Z*-2.61**
2.5 mol % **2.29**,
5.0 mol % $Zn(OMe)_2$,
4 h, 80% yield,
>98:2 *Z*:*E*, 82:18 er

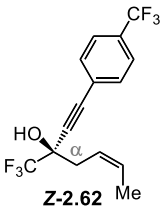

***Z*-2.62**
2.5 mol % **2.29**,
5.0 mol % $Zn(OMe)_2$,
3 h, 88% yield,
97:3 *Z*:*E*, 85:15 er

Alkyl substrates such as phenpropyl- and cyclohexyl- substituted trifluoromethyl ketones were found to react efficiently and with varying selectivities. For example, ***Z*-2.54** was isolated in high yield and enantioselectivity (96:4), but with slightly diminished *Z* selectivity. On the other hand, the cyclohexyl-substituted product ***Z*-2.56** was obtained with high *Z* selectivity (>98:2 *Z*:*E*) but slightly lower enantioselectivity (90:10 er). An

interesting case was the benzyl-substituted trifluoromethyl ketone derived from ***Z*-2.55**, which was isolated with low *Z*:*E* selectivity (79:21 *Z*:*E*). This problem, while not well understood as-of-yet, has been solved, as will be shown in the upcoming section. A variety of alkenyl-substituted electrophiles (***Z*-2.57**, ***Z*-2.58**, and ***Z*-2.59**) were well tolerated in the reaction, regardless of the electronic nature of the electrophile. All products were isolated in high yield (≥93%), *Z* selectivity (≥96:4 *Z*:*E*) and enantioselectivity (99:1 er). However, when we turned to examining the analogous alkynyl-substituted trifluoromethyl ketones, we observed diminished enantioselectivities in all cases (81:19–85:15 er for ***Z*-2.60**–***Z*-2.62**) while *Z* selectivity remained high (≥97:3 *Z*:*E*). We believe that the origin for this interaction could be due to a competing cation-π interaction between the alkyne and the proton of the ammonium group, as shown in Figure 2.1.[16,17] This interaction would work against the electrostatic attraction between the ammonium-trifluoromethyl group, lowering the enantioselectivity of the transformation.

Figure 2.1. Competitive Transition State for Alkynyl Substrates

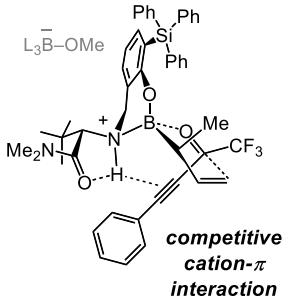

(16) For an interesting study where alkyne moieties affect enantioselectivity, see: Ramachandran, P. V.; Gong, B.; Teodorovic', A. V.; Brown, H. C. *Tetrahedron: Asymmetry* **1994**, *5*, 1061–1074.
(17) While not well studied in the context of ammonium-alkyne interactions, cation-π interactions have been well studied in the case of ammonium-aryl interactions. For examples, see: (a) Dougherty, D. A. *Science* **1996**, *271*, 163–168; (b) Ma, J. C.; Dougherty, D. A. *Chem. Rev.* **1997**, *97*, 1303–1324; (c) Mahadevi, A. S.; Sastry, G. N.; *Chem. Rev.* **2013**, *113,* 2100–2138; (d) Holland, M. C.; Metternich, J. B.; Mück-Lichtenfeld, C.; Gilmour, R. *Chem. Commun.* **2015**, *51*, 5322–5325; (e) Kamps, J. J. A. G.; Khan, A.; Choi, H.; Lesniak, R. K.; Brem, J.; Rydzik, A. M.; McDonough, M. A.; Schofield, C. J.; Claridge, T. D. W.; Mecinović, J. *Chem. – Eur. J.* **2016**, *22*, 1270–1276.

There is *some* support for this hypothesis if one considers the enantioselectivity that was obtained with the para-trifluoromethyl-substituted substrate ***Z*-2.62**. The *para*-trifluoromethyl group should render the alkyne more electron deficient, disfavoring any potential competitive cation-π interaction. However, the fact that the enantioselectivity only improved to 85:15 er (versus 81:19 with ***Z*-2.62**) suggests that perhaps there are other factors in effect in addition to the cation-π interaction. At this stage, we were also interested in investigating the generality of the method with respect to the trifluoromethyl group. Would mono- and difluoromethyl ketones reacted enantioselectively? Could this method be expanded to other perfluoroalkyl ketones? When a variety of difluoromethyl ketones were subjected to the reaction conditions, the products (***Z*-2.65**, ***Z*-2.66**, and ***Z*-2.67**, Scheme 2.12) were obtained in high enantioselectivity (98:2 er) but slightly diminished *Z* selectivity (87:13–92:8 *Z*:*E*). Interestingly, when the analogous monofluoromethyl ketones were examined in the transformation, the *Z* selectivity dropped even further (57:43–78:22 *Z*:*E*), while enantioselectivity remained high (95:5–97:3 er). The high enantioselectivity for these transformations are notable, as allyl additions to mono- and difluoromethyl ketones were minimally enantioselective.[8] These data demonstrate the importance of the number of fluorine atoms on the *Z* selectivity of the transformation, as the *Z*:*E* ratio of the product diminished with each removed fluorine atom (97:3 *Z*:*E* for trifluoromethyl-substituted ***Z*-2.22**, 91:9 for difluoromethyl-substituted ***Z*-2.65**, and 78:22 for monofluoromethyl-substituted ***Z*-2.68**). Lastly, the crystal structure obtained from **2.71**, which was derived from ***Z*-2.68**, showed that the sense of stereochemical induction remained unchanged.

Scheme 2.12. Reactions with Other Fluoroalkyl-Substituted Ketones

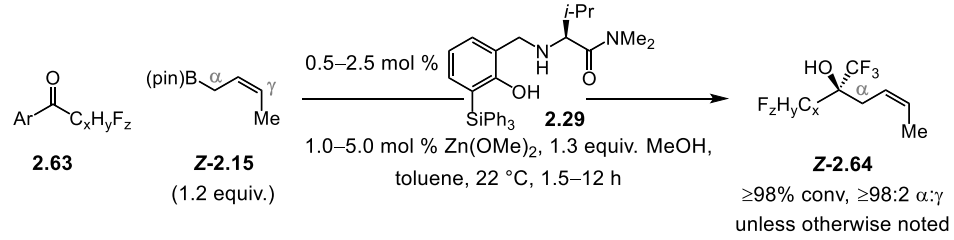

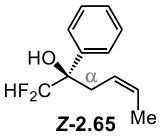

***Z*-2.65**
2.5 mol % **2.29**,
5.0 mol % $Zn(OMe)_2$,
3 h, 86% yield,
91:9 *Z*:*E*, 98.5:1.5 er

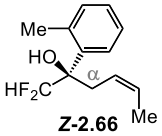

***Z*-2.66**
2.5 mol % **2.29**,
5.0 mol % $Zn(OMe)_2$,
4 h, 95% yield,
87:13 *Z*:*E*, 98:2 er

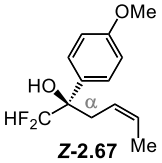

***Z*-2.67**
2.5 mol % **2.29**,
5.0 mol % $Zn(OMe)_2$,
4 h, 94% yield,
92:8 *Z*:*E*, 98.5:1.5 er

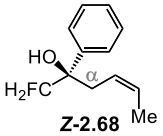

***Z*-2.68**
2.5 mol % **2.29**,
5.0 mol % $Zn(OMe)_2$,
3 h, 86% yield,
78:22 *Z*:*E*, 95:5 er

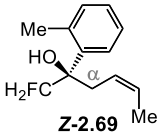

***Z*-2.69**
2.5 mol % **2.29**,
5.0 mol % $Zn(OMe)_2$,
4 h, 93% yield, 88:12 α:γ,
57:43 *Z*:*E*, 96:4 er

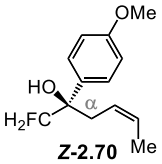

***Z*-2.70**
2.5 mol % **2.29**,
5.0 mol % $Zn(OMe)_2$,
4 h, 94% yield, 92:8 α:γ,
78:22 *Z*:*E*, 97:3 er

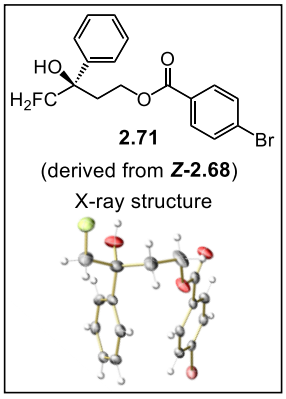

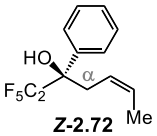

***Z*-2.72**
2.5 mol % **2.29**,
5.0 mol % $Zn(OMe)_2$,
1.5 h, 85% yield,
>98:2 *Z*:*E*, >99:1 er

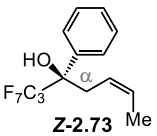

***Z*-2.73**
0.5 mol % **2.29**,
1.0 mol % $Zn(OMe)_2$,
1.5 h, 91% yield,
>98:2 *Z*:*E*, >99:1 er

We found that perfluoroalkyl ketones, such as pentafluoroethyl-substituted and heptafluoropropyl-substituted ketones also reacted with exceptional efficiency, α-, *Z*-, and enantioselectivity. The products, ***Z*-2.72** and ***Z*-2.73**, were obtained in high yield and essentially a single stereoisomer (≥98:2 *Z*:*E* and ≥99:1 er).

2.4.2 Reactions with other γ-Substituted-Allyl–B(pin) Reagents

We then turned to investigating the reactivity with other γ-substituted allyl boron reagents, such as the *n*-heptyl-substituted allyl boron, readily synthesized through a *Z*-selective, Ni-catalyzed 1,4 hydroboration of the corresponding diene.[18] We found that reactions with this reagent proceeded with high enantioselectivities (98:2–>99:1 er, ***Z*-2.76**–**78**, Scheme 2.13), however they also proved to be slightly less *Z*-selective (90:10–94:6 *Z*:*E*) and efficient, with reactions taking between 8 and 24 hours.

Scheme 2.13. Reactions with Other γ-Substituted Allylboron Reagents

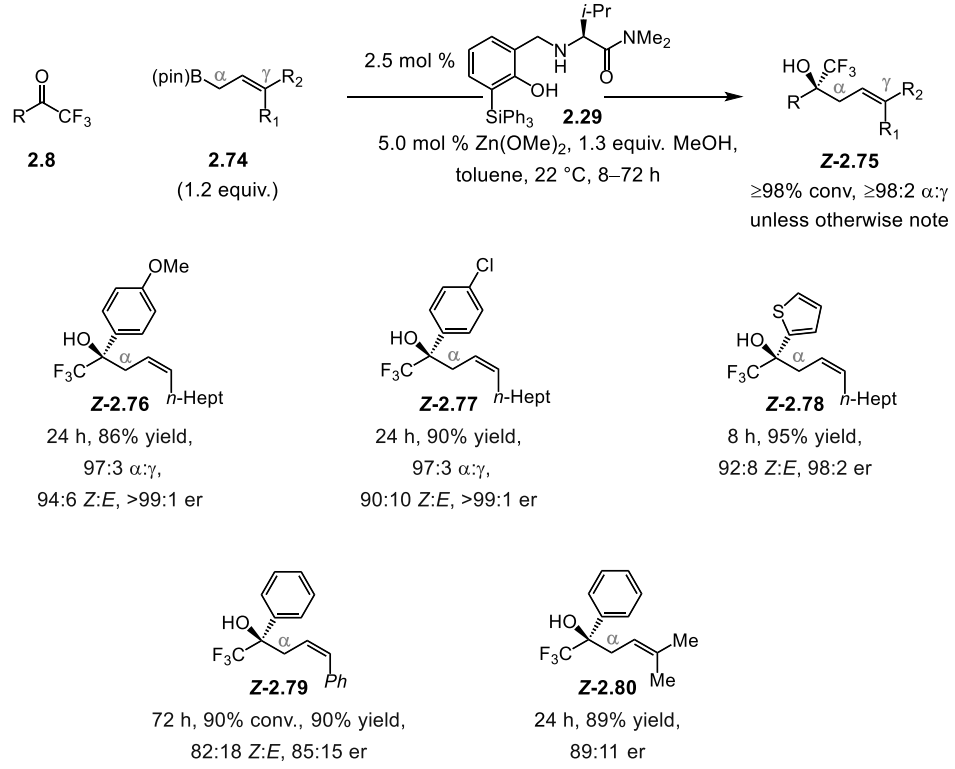

When the *E*-phenyl-substituted allyl boron was utilized in the reaction, the transformation was found to proceed sluggishly, taking 72 hours to reach 90% conversion (***Z*-2.79**) and generating products with moderate *Z* and enantioselectivity (82:18 *Z*:*E* and

(18) Ely, R. J.; Morken, J. P. *J. Am. Chem. Soc.* **2010**, *132*, 2534–2535.

85:15 er). The rate of the reaction could be increased by carrying the reaction out at elevated temperatures. At 60 °C, the reaction went to completion in 6 hours, however the product was obtained with lower selectivities (92:8 α:γ, 76:24 *Z*:*E*, and 80:20 er). *γ*,*γ'*-Dimethyl-substituted allyl–B(pin) also reacted sluggishly and with diminished enantioselectivity (***Z*-2.80**, 24 hours and 89:11 er).

2.4.3 Reactions with E-Crotyl–B(pin)

From the findings of the previous chapter, we were also interested in investigating the reaction outcome with *E*-crotyl–B(pin). Would the two reagents again furnish the same product, as they had with *N*-phosphinoyl imines? At the onset of this study, we initially observed that the major product was again the same stereoisomer, regardless of the identity of the starting crotyl–B(pin) reagent (***Z*-2.22**). However, further investigations with the *E*-crotyl–B(pin) reagent led us to discover some unexpected reactivity trends, as shown in Scheme 2.14.

Scheme 2.14. Variations in Enantioselectivity with *E*-Crotyl–B(pin)

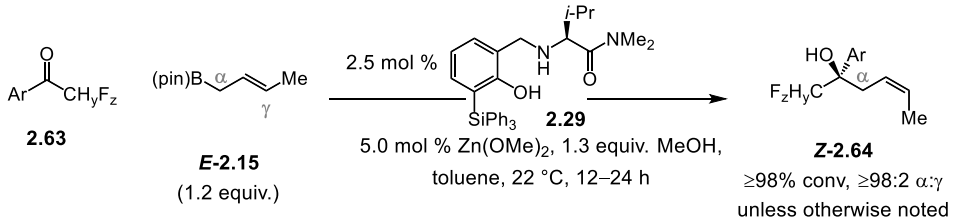

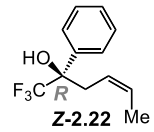

Z-2.22
24 h, 86% yield,
>98:2 *Z*:*E*, 91:9 er

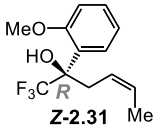

Z-2.31
24 h, 89% yield,
98:2 *Z*:*E*, 85:15 er

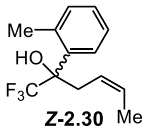

Z-2.30
24 h, 91% yield,
83:17 *Z*:*E*, 44:56 er

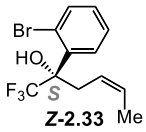

Z-2.33
12 h, 96% yield,
96:4 *Z*:*E*, 24:76 er

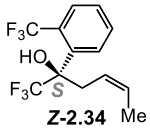

Z-2.34
24 h, 93% yield,
>98:2 *Z*:*E*, 6:94 er

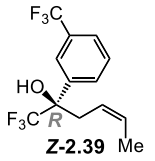

Z-2.39
24 h, 92% yield,
>98:2 *Z*:*E*, 85:15 er

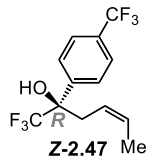

Z-2.47
24 h,90% yield,
>98:2 *Z*:*E*, 96:4 er

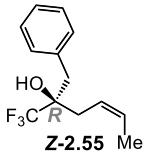

Z-2.55
24 h, 82% yield,
>98:2 *Z*:*E*, 97:3 er

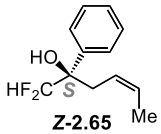

Z-2.65
24 h, 93% yield,
>98:2 *Z*:*E*, 22:78 er

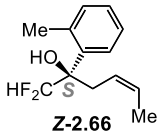

Z-2.66
24 h, 89% yield,
98:2 *Z*:*E*, 9:91 er

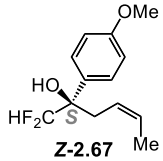

Z-2.67
24 h, 95% yield,
>98:2 *Z*:*E*, 19:81 er

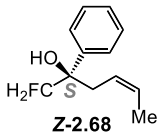

Z-2.68
24 h, 92% yield,
>98:2 *Z*:*E*, 9:91 er

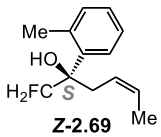

Z-2.69
24 h, 95% yield,
98:2 *Z*:*E*, 4:96 er

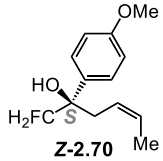

Z-2.70
24 h, 98% yield,
>98:2 *Z*:*E*, 9:91 er

As was just mentioned, when ***E*-2.15** was added to trifluoromethyl ketone **2.1**, in the presence of 2.5 mol % aminophenol **2.29**, 5.0 mol % $Zn(OMe)_2$ and 1.3 equiv. of methanol the *Z* isomer of the α-addition product (***Z*-2.22**) was accessed in >98:2 *Z*:*E* ratio and 91:9 er. The reaction with an *ortho*-methoxy-substituted electrophile (***Z*-2.31**) was highly *Z*-selective (98:2 *Z*:*E*), however slightly less enantioselective (85:15 er). When the

larger *ortho*-methyl-substituted trifluoromethyl ketone was subjected to the reaction conditions, product was obtained in a near racemic form, with a slight preference for the opposite enantiomer of the product (44:46 er, ***Z*-2.30**). *Ortho*-bromo-substituted ***Z*-2.33** was isolated with 96% *Z* selectivity, but 24:76 enantioselectivity in favor of the (*S*)-enantiomer of the product. Following in the same trend, *ortho*-trifluoromethyl-substituted ***Z*-2.34** was generated in >98% *Z* selectivity and high enantioselectivity for the (*S*)-enantiomer of the product (6:94 er). While this reversal of enantioselectivity was consistent for *ortho*-substituted substrates, the same was not observed for the *meta*-substituted analogues. For example, *meta*-CF_3-substituted (***Z*-2.39**) and *para*-CF_3-substituted (***Z*-2.47**) electrophiles were isolated as the (*R*)-enantiomer of the product (85:15 and 96:4 er, respectively), regardless of the crotyl–B(pin) reagent used. A similar phenomenon was observed when the electrophile was modified from a trifluoromethyl ketone to a di- and a monofluoromethyl ketone. Additions to difluoro- (***Z*-2.65**, Scheme 2.12) and monofluoro acetophenone (***Z*-2.68**, Scheme 2.12) were highly enantioselective for the (*R*)-enantiomer of product (98.5:1.5 and 95:5 er, respectively) when *Z*-crotyl–B(pin) was used. However, when these reactions were carried out with *E*-crotyl–B(pin) there was a reversal of enantioselectivity with the products being isolated as the (*S*)-enantiomer (22:78 er for ***Z*-2.65** and 9:91 er for ***Z*-2.68**, Scheme 2.14). An interesting trend was observed when a similar analysis was carried out on *ortho*-methyl substituted mono-, di-, and trifluoroacetophenone (***Z*-2.69**, ***Z*-2.66**, ***Z*-2.30**, Scheme 2.14). In this series, reactions with *Z*-crotyl–B(pin) ***Z*-2.15**, furnished products with uniformly high enantioselectivities for the (*R*)-enantiomer of product (≥96:4 er, see Schemes 2.9 and 2.12). When the same experiments were carried out with ***E*-2.15** there was a more distinct switch in

enantioselectivity. **Z-2.30** (*o*-Me, CF_3) was isolated in 44:56 enantioselectivity, **Z-2.66** (*o*-Me, CF_2H) was isolated in 9:91 enantioselectivity and **Z-2.69** (*o*-Me, CFH_2) was isolated in 4:96 enantioselectivity in favor of the (*S*)-enantiomer. The observed preference for the formation of the (*S*)-enantiomer of the product with sterically more hindered substrates suggests that transformations with ***E*-2.15** are sensitive to the sterics of the substrate, implying that electrostatic attractions in the transition state may be less dominant than in reactions with ***Z*-2.15**. The exact origin of this reversal of enantioselectivity will be explored in full detail below. A final case worth noting is the reaction with benzyl-substituted trifluoromethyl ketone. When ***Z*-2.55** was generated with **Z-2.15** the product was obtained with moderate *Z* selectivity (79:21 *Z*:*E*, Scheme 2.9), yet when ***E*-2.15** was utilized the product was obtained with perfect *Z* selectivity (>98:2 *Z*:*E*), this result underscores a trend which has been observed on several occasions. That, in general, reactions of trifluoromethyl ketones with *E*-crotyl–B(pin) are slightly less enantioselective, but more *Z*-selective.

2.4.4 Reactions with rac-α-Methyl-Allyl–B(pin)

In order to investigate if these selectivity fluctuations between transformations with *E*- and *Z*-crotyl–B(pin) are due to isomerization events caused by 1,3-borotropic shifts we decided to explore the reaction outcome with ***rac*-2.81** (Scheme 2.15). Depending on the regioselectivity of the reaction with ***rac*-2.81** with trifluoroacetophenone **2.1**, we would be able to deduce if 1,3-borotropic shift was occurring during the course of the reaction.

Scheme 2.15. Diastereo- and Enantioselective Additions with α-Methyl-Allyl–B(pin)

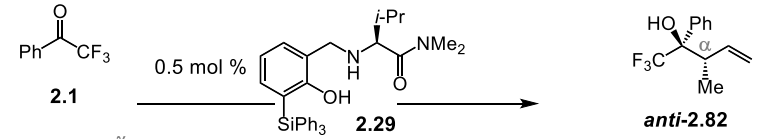

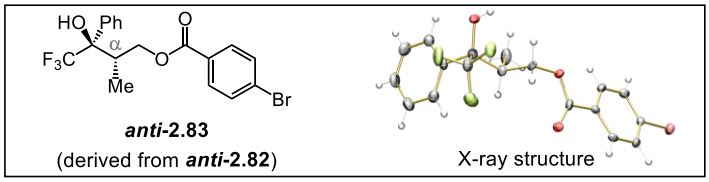

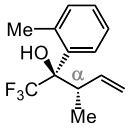

***anti*-2.84**
3 h, 97% conv., 85% yield,
≥98:2 α:γ, 68:32 *anti:syn,*
92:8 er

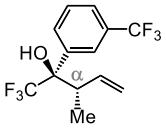

***anti*-2.85**
3 h, ≥98% conv, 86% yield,
≥98:2 α:γ, 84:16 *anti:syn,*
88:12 er

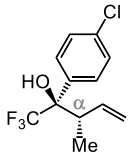

***anti*-2.86**
1.5 h, 95% conv, 82% yield,
≥98:2 α:γ, 81:19 *anti:syn,*
94:6 er

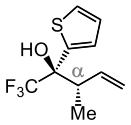

***anti*-2.87**
1.5 h, ≥98% conv, 79% yield,
≥98:2 α:γ, 79:21 *anti:syn,*
85:15 er

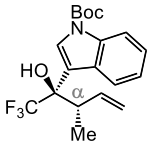

***anti*-2.88**
1.5 h, ≥98% conv, 97% yield,
≥98:2 α:γ, 78:22 *anti:syn,*
78:22 er

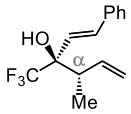

***anti*-2.89**
1.5 h, ≥98% conv, 95% yield,
≥98:2 α:γ, 88:12 *anti:syn,*
87:13 er

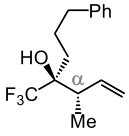

***anti*-2.90**
3 h, ≥98% conv, 97% yield,
≥98:2 α:γ, 75:25 *anti:syn,*
86:14 er

When we utilized ***rac*-2.81** in the reaction, we found that the transformation was still α-selective, which in this case generated the branched regioisomer of the product, ***anti*-2.82** (Scheme 2.15). If 1,3-borotropic shifts were occurring in this transformation, we

would expect to see the linear regioisomer, **2.22**.[19] However, we were surprised to find that the transformation proceeded with higher diastereoselectivity than we had expected. Previous studies utilizing α-branched allyl–B(pin) reagents required the reagent to be enantiomerically enriched to achieve high diastereoselectivity.[20] In this transformation, however, when ***rac*-2.81** was utilized in reactions with trifluoromethyl ketone **2.1**, the product, ***anti*-2.82** (absolute and relative stereochemistry confirmed by X-ray structure of ***anti*-2.83**), was isolated in 85:15 dr and 92:8 er.[21] We found that the sterically hindered *ortho*-methyl trifluoroacetophenone reacted with lower diastereoselectivity (68:32 dr, ***anti*-2.84**, Scheme 2.15), though the enantioselectivity remained high (92:8 er). *Meta*- and *para*-substituted electrophiles also reacted with satisfactory diastereoselectivities and enantioselectivities. *Meta*-trifluoromethyl ***anti*-2.85** was isolated in high yield and 84:16 dr and 88:12 er. Similarly, *para*-chloro-substituted ***anti*-2.86**, was synthesized in 81:19 dr and 94:6 er. Heteroaryl-substituted electrophiles were also amenable to the reaction conditions as evidenced by ***anti*-2.87** (generated in 79:21 dr and 85:15 er) and ***anti*-2.88** (generated in 78:22 dr and 78:22 er), though with diminished diastereo- and enantioselectivities. Alkenyl substrates were also compatible with the reaction conditions and furnished products in 88:12 dr and 87:13 er (***anti*-2.89**, Scheme 2.15). Lastly, alkyl-substituted ***anti*-2.90** could also accessed in moderate diastereo- and enantioselectivity (75:25 dr and 86:14 er).

(19) Note: for the reasoning behind this experiment, see Chapter 1 for further details.
(20) See: (a) Silverio, D. L.; Torker, S.; Pilyugina, T.; Vieira, E. M.; Snapper, M. L.; Haeffner, F.; Hoveyda, A. H. *Nature* **494**, 216–221; (b) van der Mei, F. W.; Miyamoto, H.; Silverio, D. L.; Hoveyda, A. H. *Angew. Chem., Int. Ed.* **2016**, *55*, 4701–4706.
(21) We believe that this is due to each enantiomer of reagent preferentially forming the same diastereomer, with varying degrees of selectivity. See the experimental section for further details.

2.4.5 Illustrating the Utility of the Product through Catalytic Z-Selective Cross-Metathesis

Recent work in our laboratory has unveiled that, with certain highly reactive olefin metathesis catalysts, catalyst lifetime can be prolonged by utilizing *Z*-methyl substituted internal olefins rather than terminal olefins.[22] These findings, in part, prompted us to develop methods which can access *Z*-methyl-substituted alkenes directly. In order to highlight the utility of these products, we have utilized them in tandem with catalytic olefin metathesis, as demonstrated in Scheme 2.16.

(22) For some examples, see: (a) Koh, M. J.; Nguyen, T. T.; Lam, J. K.; Torker, S.; Hyvl, J.; Shrock, R. R.; Hoveyda, A H. *Nature* **2017**, *542*, 80–85; (b) Xu, C.; Shen, X.; Hoveyda, A. H. *J. Am. Chem. Soc.* **2017**, *139*, 10919–10928.

Scheme 2.16. *Z*-Methyl-Substituted Alkenes as Efficient Cross Partners in Olefin Metathesis

A In Combination with *Z*-Selective, Molybdenum-Catalyzed Cross-Metathesis

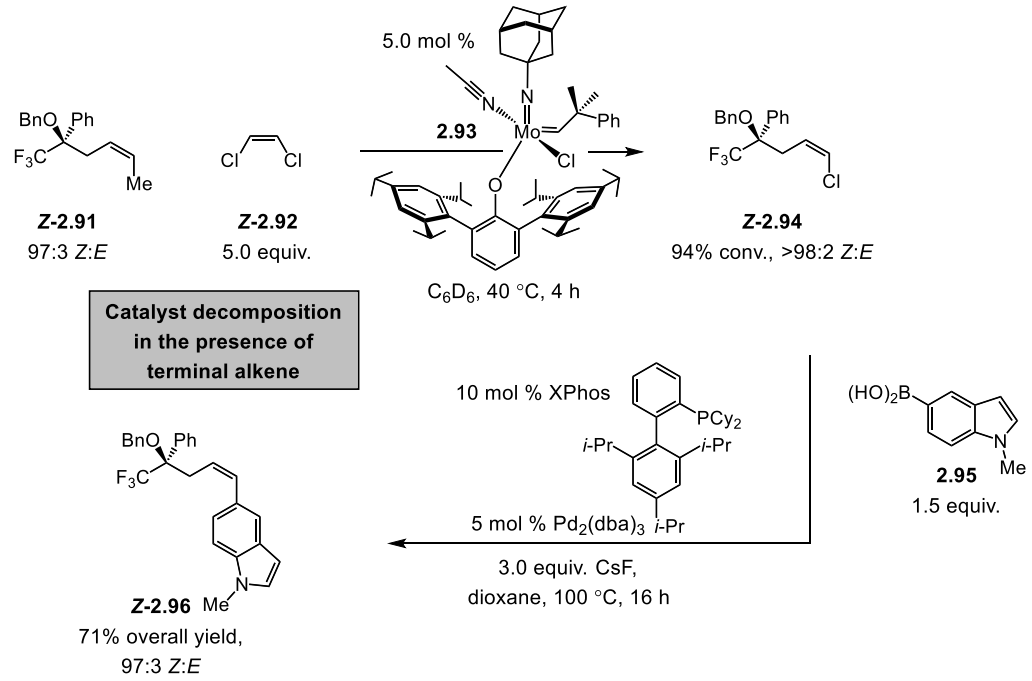

B In Combination with *Z*-Selective, Ru-Dithiolate-Catalyzed Cross-Metathesis

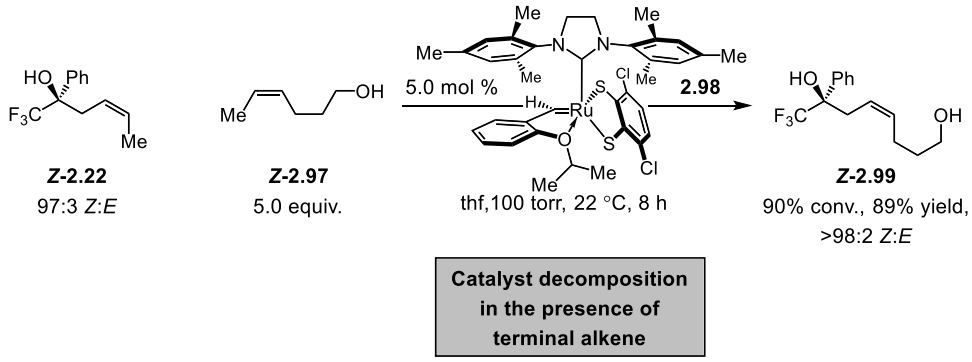

We were able to carry out a catalytic, *Z*-selective molybdenum-catalyzed cross metathesis between benzyl-protected ***Z*-2.91** and *cis*-dichloro-ethylene ***Z*-2.92**, to access *Z*-chloro-substituted ***Z*-2.94** in >98% *Z* selectivity. We were then able to further functionalize this product by carrying out a palladium-catalyzed Suzuki cross-coupling reaction to generate *Z*-indole substituted ***Z*-2.96** in 71% yield over two steps and 97:3 *Z*:*E* selectivity, as demonstrated in Scheme 2.16 A.

Ruthenium-dithiolate catalysts are also susceptible to catalyst decomposition in the presence of terminal olefins. However by utilizing ***Z*-2.22**, as shown in Scheme 2.16 B, in the presence of 5.0 mol % of **2.98** and 5.0 equivalents of cross partner ***Z*-2.97**, we were able to synthesize ***Z*-2.99** in 89% yield and 98% *Z* selectivity. In both of these examples, if terminal olefin is used instead of *Z*-methyl-substituted internal olefin, we observe low conversions to product, likely due to catalyst decomposition.

2.5. Mechanistic Nuances in the Aminophenol Promoted Crotyl Additions to Trifluoromethyl Ketones

2.5.1 Comparison of Z- and E-Crotyl–B(pin)

As has been briefly discussed earlier, during our studies of this transformation, we found that *E*- and Z-crotyl–B(pin) perform very differently in this reaction. For example, we observed that reactions with *E*-crotyl–B(pin) proceed much more sluggishly in comparison to reactions with *Z*-crotyl–B(pin). Specifically, reactions with ***E*-2.15** require 2.5 mol % **2.29**, 5.0 mol % $Zn(OMe)_2$, and 24 hours, whereas the analogues reaction with ***Z*-2.15** can be carried out with 0.5 mol% **2.29**, 5.0 mol % $Zn(OMe)_2$ and is complete within 1.5 hours (Scheme 2.17 A). We also observed, that regardless of the olefin isomer of the crotyl–Boron reagent employed (***E*-2.15** or ***Z*-2.15**), only the *Z* isomer of the product (***Z*-2.22**) was formed. Initially, we suspected that 1,3-borotropic shift might play a role in these two distinct reagents converging to a common intermediate. However, our experiments with ***rac*-2.81** preclude the involvement of 1,3-borotropic shifts in this particular transformation.

Scheme 2.17. Contrasting Reactivity Profiles between *E*- and *Z*-Crotyl–B(pin)

A Reactions with Trifluoroacetophenone

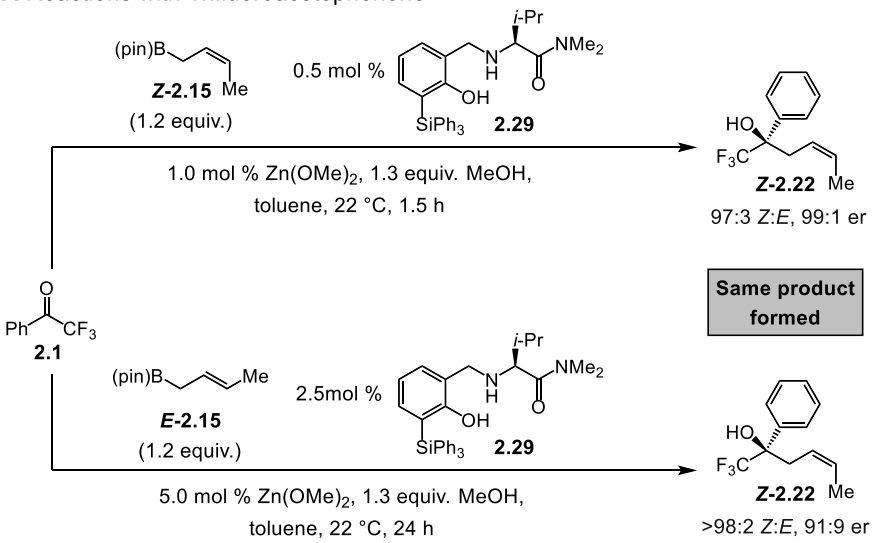

B Reactions with Other Fluoroalkyl Ketones

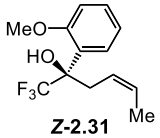

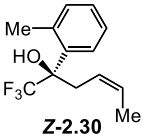

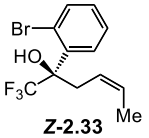

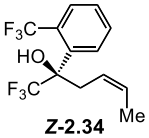

with:	***Z*-2.31**	***Z*-2.30**	***Z*-2.33**	***Z*-2.34**
***Z*-Crotyl-B(pin)**	98:2 *Z*:*E*, **>99**:1 er	96:4 *Z*:*E*, **98**:2 er	90:10 *Z*:*E*, **98**:2 er	88:12 *Z*:*E*, **98**:2 er
***E*-Crotyl-B(pin)**	98:2 *Z*:*E*, **85**:15 er	83:17 *Z*:*E*, 44:**56** er	96:4 *Z*:*E*, 24:**76** er	>98:2 *Z*:*E*, 6:**94** er

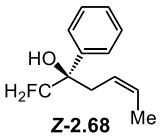

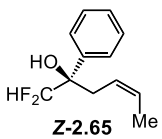

with:	***Z*-2.68**	***Z*-2.65**
***Z*-Crotyl-B(pin)**	78:22 *Z*:*E*, **95**:5 er	91:9 *Z*:*E*, **98.5**:1.5 er
***E*-Crotyl-B(pin)**	>98:2 *Z*:*E*, 9:**91** er	>98:2 *Z*:*E*, 22:**78** er

Sense of enantioselectivity substrate dependent

Moreover, when other substrate classes were investigated with ***E*-2.15**, we observed a particularly unusual phenomenon, where occasionally there would be a reversal of enantioselectivity (Scheme 2.17 B). This was particularly evident in a series of substrates with *ortho*-substituents (Scheme 2.17 B, **Z-2.30**, **Z-2.31**, **Z-2.33**, and **Z-2.34**). As the size

of the substituent increased (OMe < Me < Br < CF_3)[23], the formation of the (*R*)-enantiomer of the product decreased, and eventually reversed, favoring formation of the (*S*)-enantiomer of the product. For example, in the case of trifluoroacetophenone, both reagents produced the (*R*)-enantiomer of the product in high enantioselectivity. However, when *o*-CF_3-trifluoroacetophenone was subjected to the reaction conditions, *Z*-crotyl–B(pin) yielded the (*R*)-enantiomer of the product in 98:2 er, while *E*-crotyl–B(pin) produced the (*S*)-enantiomer of the product in 6:94 er (***Z*-2.34**, Scheme 2.17 B). A similar reversal of enantioselectivity was observed with mono- and difluoroacetophenone. Impressively, when monofluoroacetophenone was subjected to the reaction conditions, *Z*-crotyl–B(pin) yielded the (*R*)-enantiomer of the product in 95:5 er, while *E*-crotyl–B(pin) produced the (*S*)-enantiomer of the product in 9:91 er (***Z*-2.68**, Scheme 2.17 B). We were puzzled by these findings and set out to investigate the nature of these enantioselectivity fluctuations.

As was detailed in Chapter 1, we propose that when *E*- and *Z*-crotyl–B(pin) are subjected to the reaction conditions, we form two distinct diastereomeric chiral allylboron species, as depicted in Scheme 2.18.

(23) Interestingly, there could also be an electronic effect in action. However, due to the transition states for this transformation (found later in this chapter), we believe that the sterics of these substituents is the origin for these selectivity fluctuations.

Scheme 2.18. Generation of Diastereomeric Intermediates

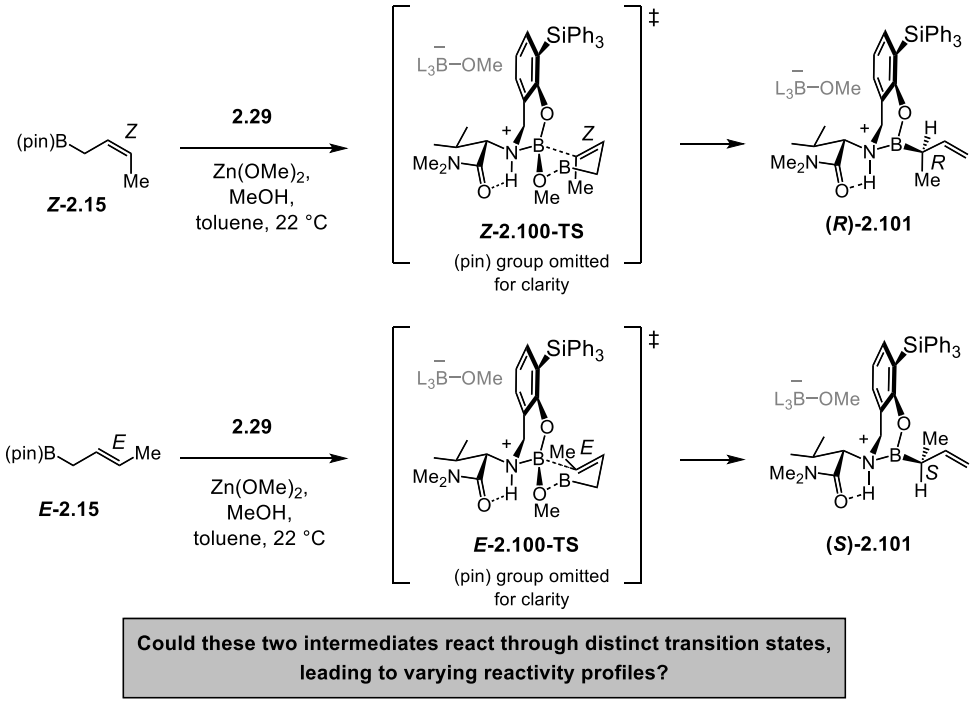

As is the case with diastereomeric intermediates, it is entirely possible that these two complexes, **(*R*)-2.101** and **(*S*)-2.101** (generated from ***Z*-2.15** and ***E*-2.15**, respectively) react through different transition states, giving rise to the selectivity fluctuations that we have previously observed. We decided that the best way to probe this system would be to carry out density functional theory computations to find the lowest energy transition states for each diastereomeric complex. We hoped that through analyzing these transition states we would be able to rationalize our experimentally observed results.

2.5.2 Density Functional Theory Analysis to Probe Possible Transition States

We set out to investigate the various transition states by which **(*R*)-2.101** and **(*S*)-2.101** (generated from ***Z*-2.15** and ***E*-2.15**, respectively) can engage in reaction with trifluoroacetophenone (**2.1**), with the goal of understanding the differences in selectivity

between *Z*- and *E*-crotyl–B(pin). In both cases, every possible six-membered ring transition state was investigated for both possible rotamers of the triphenylsilyl group. In both cases (i.e. for **(*R*)-2.101** and **(*S*)-2.101**), we have identified the lowest energy transition state for each isomer of interest. In order to rationalize the enantioselectivity of the transformation, we identified the lowest energy transition state that generates the major enantiomer of the major product (**(*R*)-*Z*-2.22**, Scheme 2.19) as well as the minor enantiomer of the major product (**(*S*)-*Z*-2.22**, Scheme 2.19). Similarly, to gauge the *Z* selectivity of the transformation, we identified the lowest energy transition state that accessed the *E* isomer of the product, regardless of which enantiomer was formed, which happened to be **(*R*)-*E*-2.22**. The results for our computational investigations into reactions that occur via the intermediacy of **(*R*)-2.101** can be found in Scheme 2.19.[24]

(24) For a full account of the computational studies, see the Experimental section.

Scheme 2.19. Transition State Analysis for Pathways from *Z*-Crotyl–B(pin)

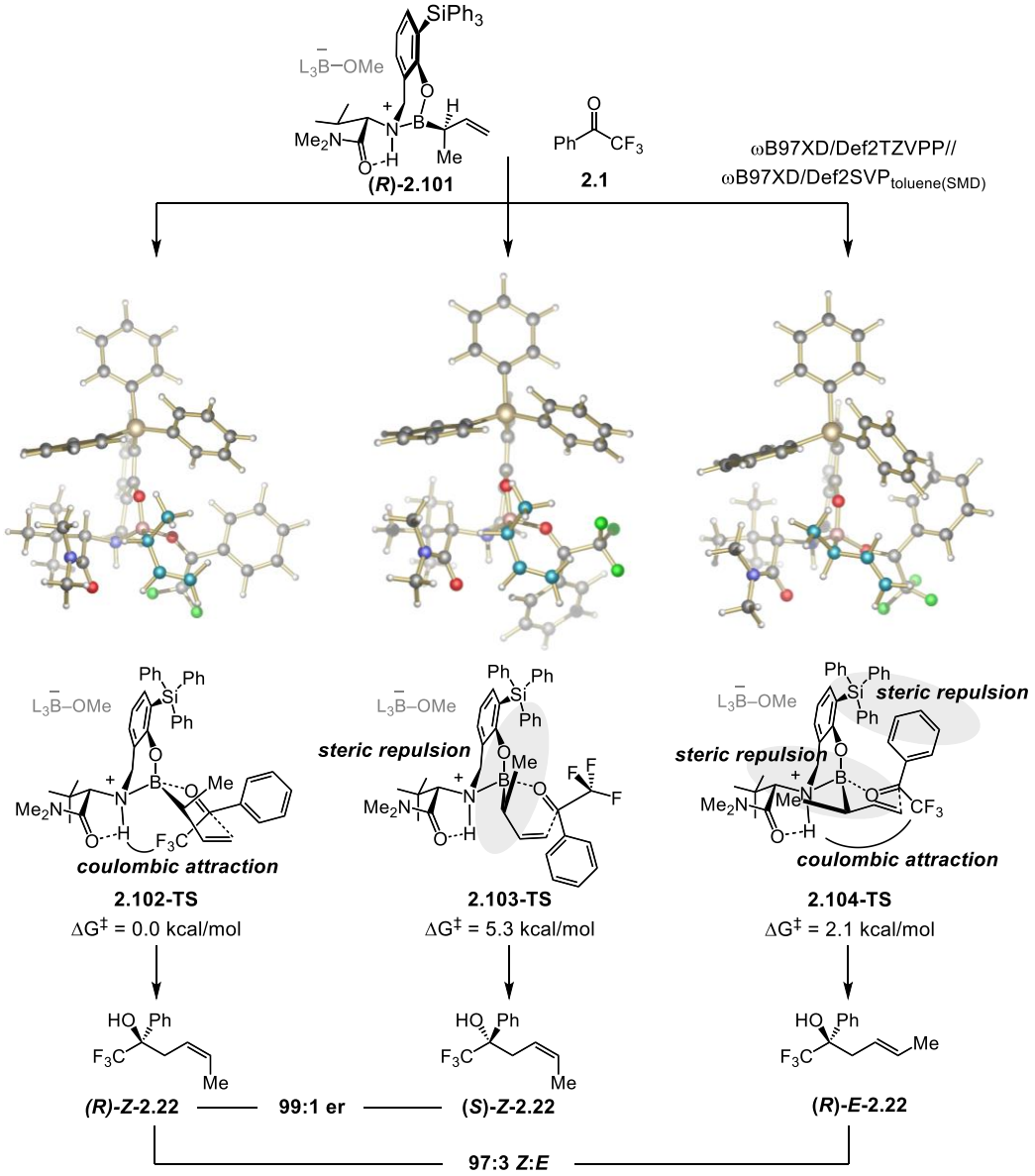

We found that the lowest energy transition state for this reaction, **2.102-TS**, produced the experimentally observed major enantiomer of the product, **(*R*)-*Z*-2.22**. There were two notable features of this transition state. The first was that, similar to the previously reported allyl additions to trifluoromethyl ketones, there seems to be a driving force to situate the trifluoromethyl moiety proximal to the ammonium group. This led us to believe that the electrostatic/coulombic attraction, that we had previously proposed, is operative.

The second interesting feature of transition state **2.102-TS** is that there is a steric preference to place the methyl group in the pseudo-axial position of the six-membered ring, an interesting occurrence which gives rise to the high *Z* selectivity of this transformation. Though this preference may seem counterintuitive, due to the inclination for placing substituents on cyclohexane rings in the equatorial positions, it becomes logical once one considers the other operative transition states. For example, in transition state **2.104-TS**, the lowest energy transition state which furnishes the *E* olefin isomer of product (**(*R*)-*E*-2.22**) has the methyl group located in the pseudo-equatorial position of the six-membered ring transition state. The consequence of this mode of reaction, is that this induces a *syn*-pentane interaction between the methyl group and the backbone of the aminophenol ligand, causing transition state **2.104-TS** to be 2.1 kcal/mol higher in energy than **2.102-TS**, a number which falls in line with the experimentally observed 97:3 *Z*:*E* ratio. We also found that the location of the methyl substituent plays a role in the high enantioselectivity of the transformation, as supported by transition state **2.103-TS**, the lowest energy transition state, which generates the minor enantiomer **(*S*)-*Z*-2.22**. In this transition state, the absence of a coulombic attraction between the trifluoromethyl group and the ammonium ion, in addition to the steric repulsion between the methyl unit and the oxygen of the aminophenol ligand, cause **2.103-TS** to be 5.3 kcal/mol higher in energy than **2.102-TS**. Again, the energetic difference between these two transition states (5.3 kcal/mol) falls in line with the experimentally observed enantioselectivity of 99:1 er. With these transition states in hand we can now rationalize the data found in Table 2.1

Table 2.1. Dependence of Aminophenol Structure on Stereoselectivity with *Z*-Crotyl–B(pin)

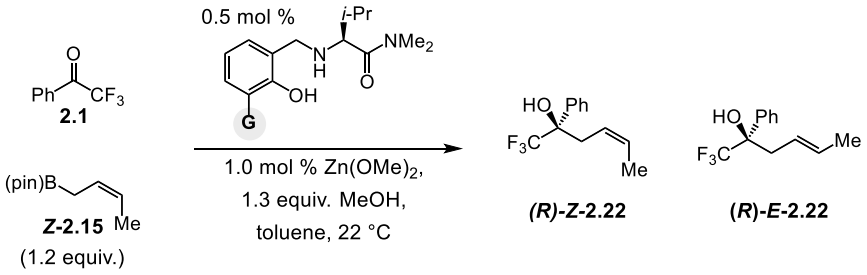

Entry	G	time (h)	conv (%)	yield (%)	α:γ	*Z*:*E*	er
1	SiPh3 (**2.29**)	1.5	>98	87	>98:2	97:3	99:1
2	*t*-Bu (**2.10**)	12	>98	85	>98:2	83:17	98:2
3	H (**2.25**)	48	45	32	>98:2	84:16	97:3

During our screening of aminophenol ligands we observed that the triphenylsilyl-substituted aminophenol (**2.29**) was uniquely *Z*-selective. For example, when aminophenol **2.29** was utilized in reactions at 22 °C, the transformation proceeded with 97% *Z* selectivity (Table 2.1). However, when a *tert*-butyl or non-substituted aminophenol was utilized (**2.10** and **2.25**, respectively), the *Z* selectivity of the transformation was much lower, i.e. 83% and 84%, respectively.[25] After performing our computational investigations, we were able to rationalize that the high *Z* selectivity of the triphenylsilyl group originates from the steric repulsion between the triphenylsilyl group and the phenyl group of trifluoroacetophenone, pictured in **2.104-TS** (Scheme 2.19). This steric repulsion disfavors **2.104-TS** over transition state **2.102-TS**, leading to high *Z* selectivity. However, when that substituent becomes smaller, for example when **G** = *t*-Bu or H, the steric repulsion which disfavors

(25) Note: We believe that the diminished efficiency of the H-substituted aminophenol is due to the ability of the aminophenol to form an inactive dimer with a boron atom. A bulky substituent on the aryl ring of the aminophenol, such as a *t*-Bu or $SiPh_3$ group, prevents this, consequently increasing the efficiency of the reaction.

2.104-TS over **2.102-TS** lessens, causing transition state **2.104-TS** to be more competitive, leading to lowered *Z* selectivity in the transformation.

Scheme 2.20. Transition State Analysis for Pathways from *E*-Crotyl–B(pin)

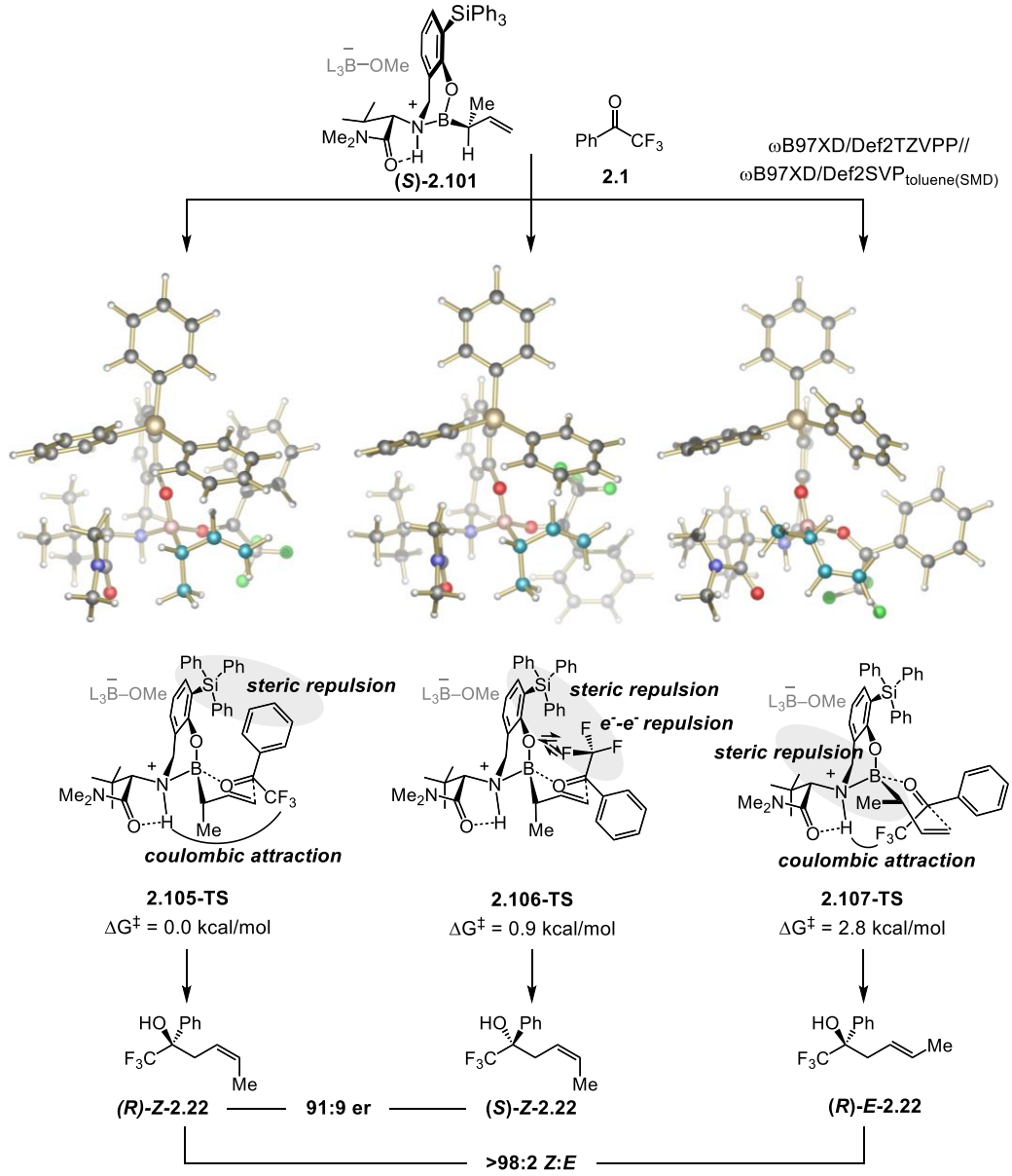

The same computational analysis was carried out for transition states arising from reactions with *E*-crotyl–B(pin) (***E*-2.15**), which proceed through diastereomeric intermediate **(*S*)-2.101**. As shown in Scheme 2.20, the three lowest energy transition states

that were found. As we had previously observed (in Scheme 2.19), there was again a preference to place the methyl group in the pseudo-axial position of the six-membered ring transition state. However, due to **(*S*)-2.101** being a diastereomer of **(*R*)-2.101**, the pseudo-axial placement of the methyl unit leads to completely different six-membered ring transition states (cf. **2.102-TS**, Scheme 2.19 and **2.105-TS**, Scheme 2.20). The lowest energy transition state in this scenario again positioned the trifluoromethyl moiety towards the ammonium group, suggesting that an electrostatic interaction is the driving force for high enantioselectivity. However, in this transition state the phenyl group of the substrate is the located more closely to the triphenylsilyl moiety of the aminophenol. This steric interaction could explain why reactions with *Z*-crotyl–B(pin), which do not encounter this steric clash (see **2.102-TS**, Scheme 2.19), are more enantioselective than the equivalent reaction with *E*-crotyl–B(pin). Another plausible explanation for this discrepancy in enantioselectivity is that the trifluoromethyl group in transition state **2.102-TS** is much closer to the ammonium group, allowing for a stronger electrostatic/coulombic attraction, leading to higher enantioselectivity.[26] In the lowest energy transition state which generates the minor enantiomer, **2.106-TS**, placement of the trifluoromethyl unit in the pseudo-axial position of the six-membered ring transition state generates electron-electron repulsion between the lone pairs of the fluorine atoms and the aryl-oxide arm of the aminophenol in addition to eliminating the electrostatic attraction. This causes transition state **2.106-TS** to be 0.9 kcal/mol higher in energy than **2.105-TS**, which corresponds with the 91:9

(26) Note: The energy of an ion-dipole electrostatic interaction is proportional to the inverse squared distance between the two charges in question. I.e., the further the two charges, the weaker the attraction. For further details, see: Anslyn, E. V.; Dougherty, D. A. *Modern Physical Organic Chemistry*, 1st ed.; University Science Books: **2005**.

enantiomeric ratio which was experimentally observed. In order to generate the *E* olefin isomer of the product, the methyl unit has to be placed in the pseudo-equatorial position, as shown in **2.107-TS**. As was described earlier, this establishes a *syn*-pentane interaction between the methyl group and the aminophenol backbone, causing transition state **2.107-TS**, to be 2.8 kcal/mol higher in energy than **2.105-TS**, which is in agreement with the experimentally observed >98% *Z* selectivity of reactions with *E*-crotyl–B(pin). With the computed transition states responsible for *Z* selectivity in hand (i.e. **2.105-TS** and **2.107-TS**), we were able to rationalize the trends summarized in Table 2.2.

Table 2.2. Dependence of Aminophenol Structure on Stereoselectivity with *E*-Crotyl–B(pin)

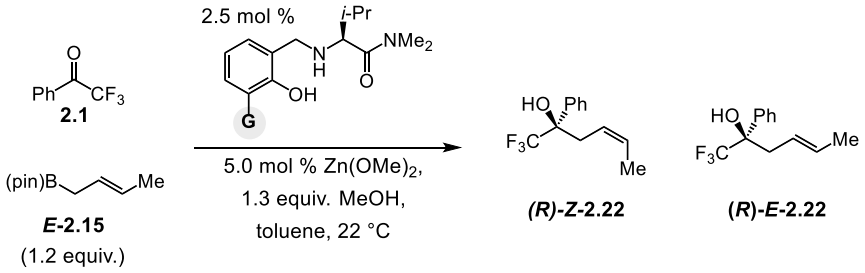

Entry	G	time (h)	conv (%)	yield (%)	α:γ	*Z*:*E*	er
1	SiPh3 (**2.29**)	24	>98	86	>98:2	>98:2	91:9
2	*t*-Bu (**2.10**)	24	>98	84	>98:2	97:3	93:7
3	H (**2.25**)	24	71	60	>98:2	96:4	89:11

Whereas we had previously observed a drastic effect of the aminophenol structure on the *Z* selectivity of the transformation when *Z*-crotyl–B(pin) was utilized (Table 2.1), the same effect was not observed when *E*-crotyl–B(pin) was employed. In reactions with *E*-crotyl–B(pin) (Table 2.2), *Z* selectivity was high regardless of the structure of the catalyst. This is likely due to the fact that the transition state which is responsible for the formation of the *E* olefin isomer of product, **2.107-TS**, is not heavily influenced by the sterics of the aminophenol ligand. One could visualize that transition state **2.107-TS** would

not become lower in energy if the triphenylsilyl moiety was replaced with a smaller group, such as *tert*-butyl or a hydrogen atom. Similarly, the transition state responsible for the formation of the *Z* olefin isomer of product, **2.105-TS**, would not be disfavored by reducing the steric size of the aminophenol ligand. Hence, it follows that the sterics of the aminophenol ligand would not influence the *Z* selectivity of the transformation with *E*-crotyl–B(pin).

2.5.3 Effect of Substrate on Enantioselectivity of the Transformation

With the knowledge obtained from the aforementioned density functional theory computations, we set out to comprehend the enantioselectivity fluctuations in key substrate classes with both *E*- and *Z*-crotyl–B(pin). As was discussed earlier, we had observed a peculiar reversal of enantioselectivity with *ortho*-substituted substrates (see Scheme 2.21 A for some illustrative examples). When we consider the transition states which are operative in reactions which utilize *Z*-crotyl–B(pin), as shown in Scheme 2.21 B, it becomes evident that the increased sterics of a large *ortho*-substituent, such as a trifluoromethyl moiety, would not impact the sense of enantioselectivity of the transformation. However there are two key differences in transition state **2.110-TS**, which is accessed when *E*-crotyl–B(pin) is used. The first is the distance of the trifluoromethyl group from the ammonium group, which results in a weakened electrostatic attraction between the two groups. The second difference is the fact that the aryl ring of the substrate is located much more proximal to the triphenylsilyl group of the aminophenol. It follows that due to the weaker coulombic attraction, if the steric size of the aryl group is increased, say through the inclusion of a large *ortho*-substituent, that the sense of enantioselectivity

becomes controlled through steric factors.[27] In other words, when **G** is large (**2.110-TS**, Scheme 2.21 C), the reaction proceeds under steric control, resulting in transition state **2.111-TS** being the lowest energy transition state, resulting in the opposite enantiomer of product being formed.

Scheme 2.21. *Z*- and *E*-Crotyl–B(pin) in Reactions with *o*-Substituted Electrophiles

A Pertinent results with *ortho*-substituted trilfuoromethyl ketones

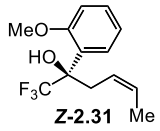

***Z*-2.31**

***Z*-Crotyl–B(pin):** 98:2 *Z*:*E*, **>99**:1 er

***E*-Crotyl–B(pin):** 98:2 *Z*:*E*, **85**:15 er

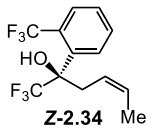

***Z*-2.34**

***Z*-Crotyl–B(pin):** 88:12 *Z*:*E*, **98**:2 er:

***E*-Crotyl–B(pin):** >98:2 *Z*:*E*, 6:**94** er

B Transition states from *Z*-crotyl–B(pin): same sense of enantioselectivity

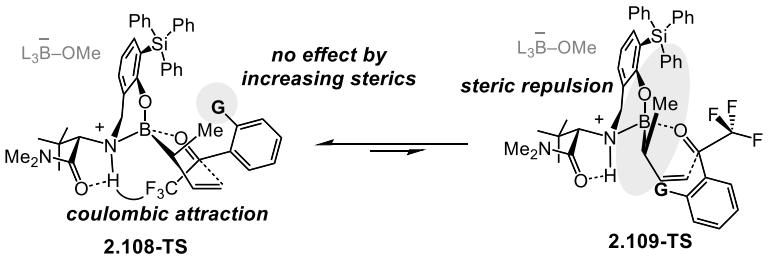

C Transition states from *E*-crotyl–B(pin): reversal of enantioselectivity

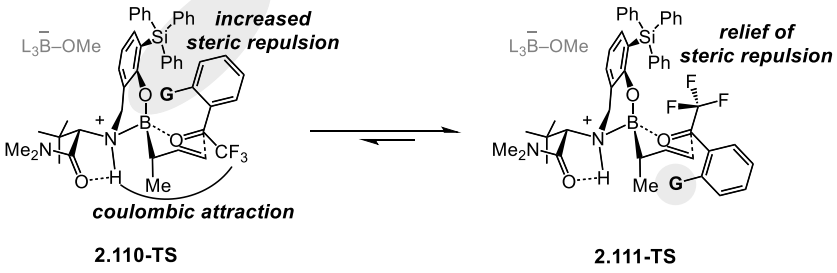

We also believe that a similar rationale applies to the reversal of enantioselectivity in reactions with mono- and difluoromethyl ketones, as shown in Scheme 2.22 A. In these cases we again observed that *Z*- and *E*-crotyl–B(pin) produce opposite enantiomers of the

(27) Note: While this trend is also true for **G** = Br, it is possible that an *ortho*-CF_3 group could also participate in an electrostatic attraction with the ammonium group, which could contribute to the reversal of enantioselectivity.

product. Using what we have learned, we believe that the main reason for this phenomenon is the weaker coulombic attraction in the transition states accessed from *E*-crotyl–B(pin).

Scheme 2.22. *Z*- and *E*-Crotyl–B(pin) in Reactions with Mono-/Difluoro- Ketones

A Pertinent results with mono- and difluoro-alkyl ketones

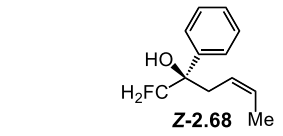

***Z*-2.68**

***Z*-Crotyl–B(pin)**	***E*-Crotyl–B(pin):**
78:22 *Z*:*E*, **95**:5 er	>98:2 *Z*:*E*, 9:**91** er

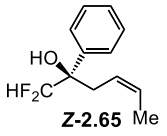

***Z*-2.65**

***Z*-Crotyl–B(pin):**	***E*-Crotyl–B(pin):**
91:9 *Z*:*E*, **98.5**:1.5 er	>98:2 *Z*:*E*, 22:**78** er

B Transition states from *Z*-crotyl–B(pin): same sense of enantioselectivity

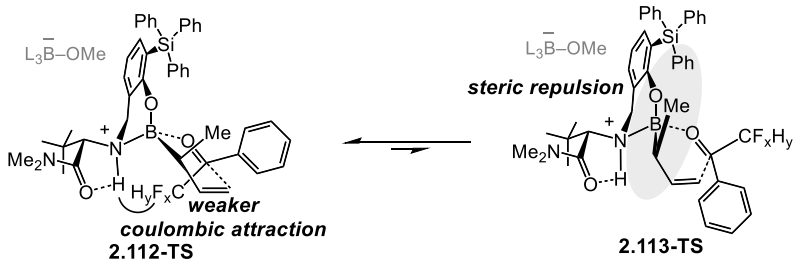

2.112-TS **2.113-TS**

C Transition states from *E*-crotyl–B(pin): reversal of enantioselectivity

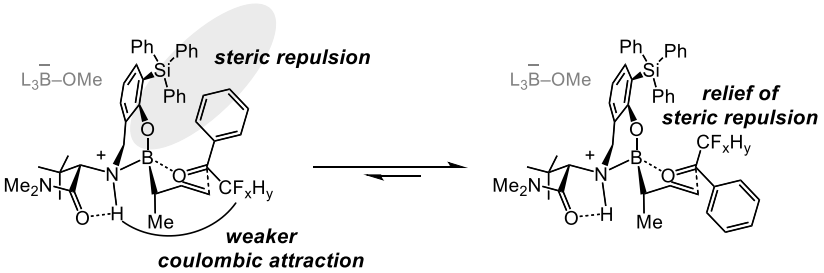

2.114-TS **2.115-TS**

As shown in Scheme 2.22 B, due to the proximity of the fluoroalkyl group to the ammonium group it is possible for the weaker coulombic attraction to still be the dominant factor in the enantioselectivity of the transformation. However, in transition state **2.114-TS** (Scheme 2.22 C), accessed from *E*-crotyl–B(pin), the fluoroalkyl group is once again further from the ammonium group. This weakens the coulombic attraction to such a degree that the steric repulsion between the substrate and the triphenylsilyl group overcomes the electrostatic attraction, making **2.115-TS** the more favored transition state. For these

substrate classes, it appears that due to the different transition states by which *E*- and *Z*-crotyl–B(pin) react, the enantioselectivity of reactions with *Z*-crotyl–B(pin) is controlled by electrostatic factors, whereas in reactions with *E*-crotyl–B(pin) steric control is likely to be the driving force behind enantioselectivity.

2.6. Conclusions

In summary, we have developed the first catalytic, enantioselective crotyl additions to mono-, di-, and trifluoromethyl ketones. The scope was shown to be broad and general with respect to electrophiles as well as a variety of allyl boron reagents. In order to rationalize and appreciate unusual selectivity profiles, density functional theory computations were carried out to model the differences between reactions with *E*- and *Z*-crotyl–B(pin). The knowledge gained from these studies not only allowed us to rationalize the observed experimental outcomes, but also served as the basis for the studies in the forthcoming chapter: the first aminophenol-promoted enantioselective reactions with aldehydes.

2.7. *Experimental Section*

2.7.1. *General*

Infrared (IR) spectra were recorded on a Bruker FT-IR Alpha (ATR mode) spectrophotometer, ν_{max} in cm^{-1}. Bands are characterized as broad (br), strong (s), medium (m), and weak (w). ^{1}H NMR spectra were recorded on a Varian Unity INOVA 400 (400 MHz), 500 (500 MHz), or 600 (600 MHz) spectrometer. Chemical shifts are reported in ppm from tetramethylsilane with the solvent resonance as the internal standard ($CDCl_3$: δ 7.26 ppm). Data are reported as follows: chemical shift, multiplicity (s = singlet, d = doublet, t = triplet, q = quartet, p = pentet, br s = broad singlet, m = multiplet, app. = apparent), coupling constant (Hz) and integration. ^{13}C NMR spectra were recorded on a Varian Unity INOVA 400 (100 MHz), 500 (125 MHz), or 600 (150 MHz) spectrometer with complete proton decoupling. Chemical shifts are reported in ppm from tetramethylsilane with the solvent resonance as the internal standard ($CDCl_3$: δ 77.16 ppm). ^{19}F NMR spectra were recorded on a Varian Unity INOVA 400 (376 MHz) spectrometer. Chemical shifts are reported in ppm with $C_6H_5CF_3$ as an external standard ($C_6H_5CF_3$: –63.72 ppm). Data are reported as follows: chemical shift, multiplicity, coupling constants (Hz), and integration. High-resolution mass spectrometry was performed on a JEOL AccuTOF DART (positive mode) at the Mass Spectrometry Facility, Boston College. Enantiomeric ratios were determined by high-performance liquid chromatography (HPLC) with a Shimadzu chromatograph (Chiral Technologies Chiralcel OD-H (4.6 x 250 mm), Chiralcel OJ-H (4.6 x 250 mm), Chiralcel OZ-H (4.6 x

250 mm), Chiralpak AD-H (4.6 x 250 mm), Chiralpak AS-H (4.6 x 250 mm)) in comparison with authentic racemic materials. Specific rotations were measured using either an Atago AP-300 Automated Polarimeter or a Rudolph Research Analytical Autopol IV Polarimeter. Unless otherwise noted, all reactions were carried out with distilled and degassed solvents under an atmosphere of dry N_2 in oven- (135 °C) or flame-dried glassware with standard dry box or vacuum-line techniques. Solvents were purified under a positive pressure of dry argon by a modified Innovative Technologies purification system: toluene was purified through a copper oxide and alumina column. Dimethoxy ethane was freshly distilled from a sodium and benzophenone ketyl solution. $CDCl_3$ was purchased from Cambridge Isotope Laboratories and store over activated 4Å molecular sieves prior to use. All work-up and purification procedures were carried out with reagent grade solvents (purchased from Fisher Scientific) in air.

Reagents:

Benzoyl chloride was purchased from Sigma-Aldrich and used as received.

Benzyl bromide was purchased from Sigma-Aldrich and used as received.

Bis(pinacolato)diboron was purchased from Frontier Scientific, Inc. and recrystallized from pentane.

4-Bromobenzoyl chloride was purchased from Sigma-Aldrich and used as received.

(*E*)-But-2-en-1-yl methyl carbonate was synthesized according to literature procedure.[1]

2-Buten-1-ol (95:5 trans:cis, 96%) was purchased from Alfa Aesar and used as received.

---

(1) Hu, T.; Corey, E. J. *Org Lett.* **2002**, *4*, 2441–2443.

3-Buten-2-ol, 97% was purchased from Sigma-Aldrich and used as received.

***rac-2*-(But-3-en-2-yl)-4,4,5,5-tetramethyl-1,3,2-dioxaborolane** was synthesized according to literature procedure.[2]

(*R*)-2-(But-3-en-2-yl)-4,4,5,5-tetramethyl-1,3,2-dioxaborolane was synthesized utilizing literature procedure.[3] See below for details.

(*S*)-2-(But-3-en-2-yl)-4,4,5,5-tetramethyl-1,3,2-dioxaborolane was synthesized utilizing literature procedure.[3] See below for details.

Cesium fluoride was purchased from Strem and used as received.

2-Cinnamyl-4,4,5,5-tetramethyl-1,3,2-dioxaborolane was synthesized according to literature procedure.[4]

Copper(II) trifluoromethanesulfonate was purchased from Strem and used as received.

***cis*-Crotylboronic acid pinacol ester, 97%** was purchased from Sigma-Aldrich and used as received.

***trans*-Crotylboronic acid pinacol ester, 95%** was purchased from Sigma-Aldrich and used as received.

(*Z*)-2-(Dec-2-en-1-yl)-4,4,5,5-tetramethyl-1,3,2-dioxaborolane was synthesized according to literature procedure e.[5]

***cis*-1,2-Dichloroethylene** was purchased from Sigma-Aldrich and used as received.

---

(2) Fandrick, K. R.; Fandrick, D. R.; Gao, J. J.; Reeves, J. T.; Tan, Z.; Li, W.; Song, J. J.; Lu, B.; Yee, N. K., Senanayake, C. H. *Org. Lett.* **2010**, *12*, 3748–3751.

(3) Guzman-Martinez, A.; Hoveyda, A. H. *J. Am. Chem. Soc.* **2010**, *132*, 10634–10637.

(4) Zhang, P.; Roundtree, I. A.; Morken, J. P. *Org. Lett*. **2012**, *14*, 1416–1419.

(5) Ely, R. J.; Morken, J. P. *Org. Synth.* **2011**, *88*, 342–352.

(Difluoromethyl)trimethylsilane was purchased from Oakwood and used as received.

4-Dimethylaminopyridine was purchased from Oakwood and used as received.

1-Ethynyl-4-methoxybenzene was purchased from Combi-Blocks and used as received.

1-Ethynyl-4-(trifluoromethyl)benzene was purchased from Aldrich and used as received.

***cis*-4-Hexenol** was purchased from Alfa Aesar and distilled over CaH prior to use.

Imidazolinium salts NHC1 and NHC2 were synthesized according to literature procedures.[6]

Methanol was purchased from Acros (99.8% anhydrous) and used as received.

1-Methylindole-5-boronic acid was purchased from Combi-Blocks and used as received.

Methyl (*E*)-3-(4-methoxyphenyl)acrylate was purchased from Combi-Blocks and used as received.

Methyl (*E*)-3-(4-(trifluoromethyl)phenyl)acrylate was purchased from Combi-Blocks and used as received.

4-Nitrobenzoyl chloride was purchased from Aldrich and used as received.

Sodium borohydride was purchased from Aldrich and used as received.

Sodium methoxide was purchased from Strem and used as received.

Sodium perborate tetrahydrate was purchased from Aldrich and used as received.

Triethylamine was purchased from Sigma-Aldrich and used as received.

---

(6) (a) Lee, Y.; Akiyama, K.; Gillingham, D. G.; Brown, M. K.; Hoveyda A. H. *J. Am. Chem. Soc.* **2008***, 130,* 446–447. (b) Akiyama, K.; Gao, F.; Hoveyda, A. H. *Angew. Chem., Int. Ed.* **2010**, *49*, 419–423. (c) Gao, F.; Carr, J. L.; Hoveyda, A. H. *Angew. Chem., Int. Ed.* **2012**, *51*, 6613–6617.

Trimethyl(trifluoromethyl)silane was purchased from Oakwood and used as received.

Tris(dibenzylideneacetone)dipalladium(0) was purchased from Strem and used as received.

XPhos was purchased from Sigma-Aldrich and used as received.

Zinc methoxide was purchased from Sigma-Aldrich and used as received.

Aminophenol Compounds:

Aminophenols 1 & 2 (ap1 & ap2, respectively) were synthesized according to literature procedure.[7]

Aminophenol 3 (ap3) was synthesized according to literature procedure.[8]

Metathesis Complexes:

Molybdenum-1 (Mo-1) was synthesized according to literature procedure.[9]

Ruthenium-1 (Ru-1) was synthesized according to literature procedure.[10]

---

(7) Silverio, D. L.; Torker, S.; Pilyugina, T.; Vieira, E. M.; Snapper, M. L.; Haeffner, F.; Hoveyda, A. H. *Nature* **2013**, *494*, 216–221.

(8) Lee, K.; Silverio, D.L.; Torker, S.; Haeffner, F.; Robbins, D. W.; van der Mei, F. W.; Hoveyda, A. H. *Nat. Chem.* **2016**, *8*, 768.

(9) Lam, J. K.; Zhu, C.; Bukhryakov, K. V.; Müller, P.; Hoveyda A.; Schrock, R. R. *J. Am. Chem. Soc.* **2016**, *138*, 15774–15783.

(10) Koh, M. J.; Khan., R. K. M.; Torker, S.; Yu, M.; Mikus, M. S.; Hoveyda, A. H. *Nature* **2015**, *517*, 181–186.

Substrates:

Chart S2.1: Supplementary information numbering for ketone substrates.

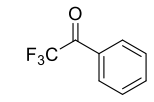

S-3a

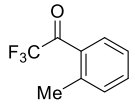

S-3b

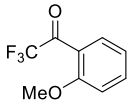

S-3c

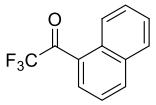

S-3d

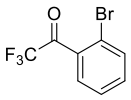

S-3e

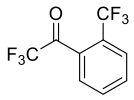

S-3f

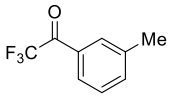

S-3g

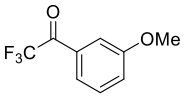

S-3h

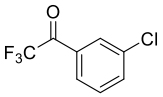

S-3i

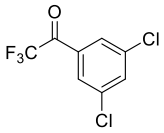

S-3j

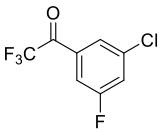

S-3k

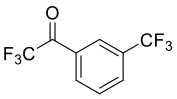

S-3l

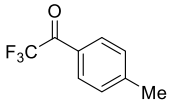

S-3m

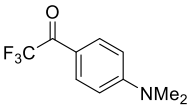

S-3n

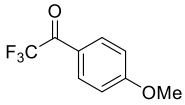

S-3o

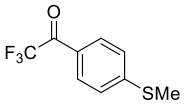

S-3p

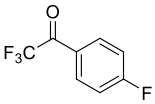

S-3q

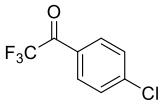

S-3r

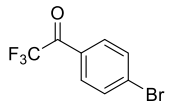

S-3s

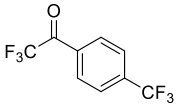

S-3t

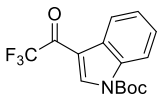

S-7

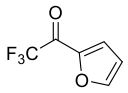

S-8a

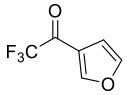

S-8b

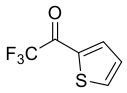

S-9a

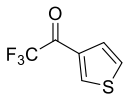

S-9b

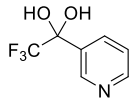

S-10

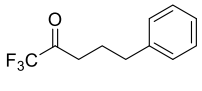

S-11a

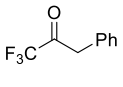

S-11b

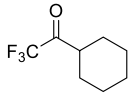

S-11c

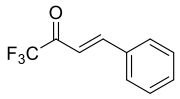

S-12a

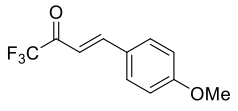

S-12b

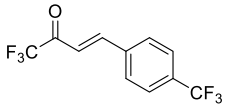

S-12c

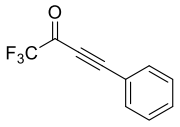

S-13a

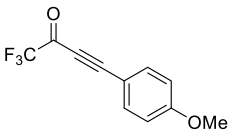

S-13b

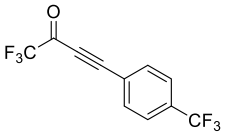

S-13c

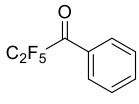

S-14

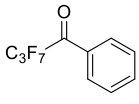

S-15

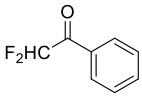

S-16a

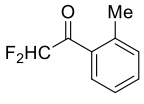

S-16b

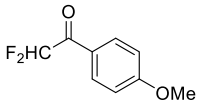

S-16c

S-17a

S-17b

S-17c

2,2,2,-Trifluoroacetophenone (S-3a) was purchased from Oakwood and distilled under vacuum over calcium chloride prior to use.

2,2,2-Trifluoro-1-(*o*-tolyl)ethan-1-one (S-3b) was synthesized according to literature procedure[11] using Knochel's procedure[12] to generate the requisite Grignard reagent. Analytical data are fully consistent with those reported previously.[13]

2,2,2-Trifluoro-1-(2-methoxyphenyl)ethan-1-one (**S-3c)** was purchased from Oakwood and used as received.

2,2,2-Trifluoro-1-(naphthalen-1-yl)ethan-1-one (S-3d) was purchased from Oakwood and used as received.

1-(2-Bromophenyl)-2,2,2-trifluoroethan-1-one (S-3e) was synthesized according to literature procedure.[14,15] **IR (neat):** 1730 (m), 1586 (m), 1433 (m), 1203 (s), 1184 (s), 1141 (s), 933 (s), 741 (s), 682 (s), 605 (m) cm^{-1}; **^{1}H NMR (600 MHz, $CDCl_3$):** δ 7.78 – 7.72 (m, 1H), 7.69 (ddq, *J* = 5.6, 2.9, 1.4 Hz, 1H), 7.50 – 7.42 (m, 2H); **^{13}C NMR (150 MHz, $CDCl_3$):** δ 182.3 (q, *J* = 36.5 Hz), 135.1, 134.1, 132.4, 130.0, 127.5, 121.8, 115.7 (q, *J* = 292 Hz); **^{19}F NMR (564 MHz, $CDCl_3$):** δ –74.06 (s, 3F); **HRMS (DART):** Calcd for $C_8H_5BrF_3O$ $[M+H]^+$: 252.9476; Found: 252.9483.

2,2,2-Trifluoro-1-(2-(trifluoromethyl)phenyl)ethan-1-one (S-3f) was purchased from Combi-Blocks and used as received.

---

(11) Shaw, D. A.; Tuominen, T. C. *Synth. Commun*. **1985**, *15*, 1291–1297.
(12) Krasovskiy, A.; Knochel, P. *Angew. Chem., Int. Ed.* **2004**, *43*, 3333–3336.
(13) Chong, J. M. and Mar, E. K. *J. Org. Chem.* **1991**, *56*, 893–896.
(14) Singh, R. P.; Cao, G.; Kirchmeier, R. L.; Shreeve, J M. *J. Org. Chem.* **1999**, *64*, 2873–2876.
(15) Trost, B. M.; Debien, L. *J. Am. Chem. Soc.* **2015**, *137*, 11606–11609.

2,2,2-Trifluoro-1-(*m*-tolyl)ethan-1-one (S-3g) was purchased from Oakwood and used as received.

2,2,2-Trifluoro-1-(3-methoxyphenyl)ethan-1-one (S-3h) was purchased from Oakwood and used as received.

1-(3-Chlorophenyl)-2,2,2-trifluoroethan-1-one (S-3i) was purchased from Oakwood and used as received.

1-(3,5-Dichlorophenyl)-2,2,2-trifluoroethan-1-one (S-3j) was purchased from Oakwood and used as received.

1-(3-Chloro-5-fluorophenyl)-2,2,2-trifluoroethan-1-one (S-3k) was purchased from Oakwood and used as received.

2,2,2-Trifluoro-1-(3-(trifluoromethyl)phenyl)ethan-1-one (S-3l) was purchased from Sigma-Aldrich and used as received.

2,2,2-Trifluoro-1-(*p*-tolyl)ethan-1-one (S-3m) was purchased from Oakwood and used as received.

1-(4-(Dimethylamino)phenyl)-2,2,2-trifluoroethan-1-one (S-3n) was purchased from Sigma-Aldrich as orange-yellow solid, dissolved in hot hexanes (HPLC grade, Fisher) and filtered through a hot glass frit to remove dark orange solids. The fritted disc was washed with HPLC grade hexanes and minimal dichloromethane (Fisher, reagent grade) to recover maximum amount of **S-3n**. Concentration in vacuo affords **S-3n** as a bright yellow solid.

2,2,2-Trifluoro-1-(4-methoxyphenyl)ethan-1-one (S-3o) was purchased from Oakwood and used as received.

2,2,2-Trifluoro-1-(4-(methylthio)phenyl)ethan-1-one (S-3p) was purchased from Oakwood and used as received.

2,2,2-Trifluoro-1-(4-fluorophenyl)ethan-1-one (S-3q) was purchased from Oakwood and used as received.

1-(4-Chlorophenyl)-2,2,2-trifluoroethan-1-one (S-3r) was purchased from Oakwood and used as received.

1-(4-Bromophenyl)-2,2,2-trifluoroethan-1-one (S-3s) was purchased from Matrix and used as received.

2,2,2-Trifluoro-1-(4-(trifluoromethyl)phenyl)ethan-1-one (S-3t) was purchased from Oakwood and used as received.

***tert*-Butyl 3-(2,2,2-trifluoroacetyl)-1H-indole-1-carboxylate (S-7)** was synthesized through Boc protection of the free indole (purchased from Sigma-Aldrich, and used as received) **IR (neat):** 1736 (m), 1685 (s), 1540 (m), 1447 (m), 1370 (s), 1359 (s), 1151 (s), 1127 (s), 1106 (s) 752 (s), 732 (s) cm^{-1}; **^{1}H NMR (600 MHz, $CDCl_3$):** δ 8.46 – 8.43 (m, 1H), 8.39 – 8.34 (m, 1H), 8.19 – 8.14 (m, 1H), 7.48 – 7.40 (m, 2H), 1.74 (s, 9H); **^{13}C NMR (150 MHz, $CDCl_3$):** δ 176.3 (q, J = 35.9 Hz), 148.5, 135.5 (q, J = 5.0 Hz), 127.3, 126.6, 125.3, 122.5, 116.6 (q, J = 290.8 Hz), 115.3, 113.1, 86.6, 28.1; **^{19}F NMR (564 MHz, $CDCl_3$):** δ –73.80 (s, 3F); **HRMS (DART):** Calcd for $C_{15}H_{15}F_3O_3N$ $[M+H]^+$: 314.1004; Found: 314.1001.

2,2,2-Trifluoro-1-(furan-2-yl)ethan-1-one (S-8a) was synthesized according to literature procedure.[16]

2,2,2-Trifluoro-1-(furan-3-yl)ethan-1-one (S-8b) was synthesized according to literature procedure.[16]

2,2,2-Trifluoro-1-(thiophen-2-yl)ethan-1-one (S-9a) was purchased from Sigma-Aldrich and used as received.

2,2,2-Trifluoro-1-(thiophen-3-yl)ethan-1-one (S-9b) was synthesized according to literature procedure.[16]

2,2,2-Trifluoro-1-(pyridin-3-yl)ethane-1,1-diol (S-10) was synthesized according to literature procedure. After silica gel chromatography, the product was isolated as the derived monohydrate.[14] **IR (neat):** 3376 (br, s), 1429 (w), 1277 (m), 1179 (s), 716 (m) cm^{-1}; **^{1}H NMR (400 MHz, d_6-DMSO):** δ 8.75 (s, 1H), 8.61 (dt, J = 4.8, 1.7 Hz, 1H), 7.97 – 7.92 (m, 1H), 7.83 (s, 2H), 7.49 – 7.42 (m, 1H); **^{13}C NMR (100 MHz, d_6-DMSO):** δ 150.1, 148.5, 135.3, 134.2, 123.3 (q, J = 286.9 Hz), 123.0, 91.9 (q, J = 31.9 Hz); **^{19}F NMR (376 MHz, d_6-DMSO):** δ –83.2 (s, 3F); **HRMS (DART):** Calcd for $C_7H_7F_3ON$ $[M+H-H_2O]^+$: 194.0429; Found: 194.0430.

1,1,1-Trifluoro-5-phenylpentan-2-one (S-11a) was synthesized according to literature procedure.[7] Analytical data are fully consistent with those reported previously.[17]

1,1,1-Trifluoro-3-phenylpropan-2-one (S-11b) was purchased from Oakwood and used as received.

---

(16) Lee, K.; Silverio, D.L.; Torker, S.; Haeffner, F.; Robbins, D. W.; van der Mei, F. W.; Hoveyda, A. H. *Nat. Chem.* **2016**, *8*, 768.

(17) Bonnet-Delpon, D.; Camvillau, C.; Charpentier-Morize, M.; Jacquot, R.; Mesureur, D.; Ourevitch, M. *J. Org. Chem.* **1988**, *53*, 754–759.

1-Cyclohexyl-2,2,2-trifluoroethan-1-one (S-11c) was purchased from Oakwood and used as received.

(*E*)-1,1,1-Trifluoro-4-phenylbut-3-en-2-one (S-12a) was synthesized according to literature procedure.[18] Analytical data are fully consistent with those reported previously.[18]

(*E*)-1,1,1-Trifluoro-4-(4-methoxyphenyl)but-3-en-2-one (S-12b) was synthesized according to literature procedure.[14] Analytical data are fully consistent with those reported previously.[19]

(*E*)-1,1,1-Trifluoro-4-(4-(trifluoromethyl)phenyl)but-3-en-2-one (S-12c) was synthesized according to literature procedure.[14] Analytical data are fully consistent with those reported previously.[20]

1,1,1-Trifluoro-4-phenylbut-3-yn-2-one (S-13a) was synthesized according to literature procedure.[14]

1,1,1-Trifluoro-4-(4-methoxyphenyl)but-3-yn-2-one (S-13b) was synthesized according to literature procedure.[21] Analytical data are fully consistent with those reported previously.[22]

1,1,1-Trifluoro-4-(4-(trifluoromethyl)phenyl)but-3-yn-2-one (S-13c) was synthesized according to literature procedure.[21] **IR (neat):** 2206 (m), 1708 (m), 1433 (m), 1320 (s),

---

(18) Kawana, Y.; Kaneko, N.; Mukaiyama, T. *Bull. Chem. Soc. Jpn.* **2006**, *79*, 1133–1145.

(19) Mlostoń, G.; Grzelak, P.; Heimgartner, H. *Journal of Fluorine Chemistry* **2016**, *190*, 56–60.

(20) Wang, Y.; Han, J.; Chen, J.; Cao, W. *Tetrahedron* **2015**, *71*, 8256–8262.

(21) Sasaki, S.; Ikekame, Y.; Tanayama, M.; Yamauchi, T.; Higashiyama, K. *Synlett* **2012**, *23*, 2699–2703.

(22) Kelly, C.B.; Mercadante, M.A.; Hamlin, T.A.; Fletcher, M.H.; Leadbeater, N.H. *J. Org. Chem.* **2012**, *77*, 8131–8141.

1129 (s), 1107 (s), 843 (s), 727 (s), **^{1}H NMR (400 MHz, $CDCl_3$):** δ 7.79 (dd, *J* = 7.8, 1.0 Hz, 2H), 7.73 – 7.63 (m, 2H); **^{13}C NMR (100 MHz, $CDCl_3$):** δ 167.2 (q, *J* = 42.7 Hz), 134.1, 134.0 (q, peak overlapped at 134.1), 126.0 (q, *J* = 3.8 Hz), 123.4 (q, *J* = 272.7 Hz), 122.0, 114.9 (q, *J* = 288.2 Hz), 97.3, 84.0; **^{19}F NMR (376 MHz, $CDCl_3$):** –63.35 (s, 3F), –77.88 (s, 3F); **HRMS (DART):** Calcd for $C_{11}H_5F_6O$ $[M+H]^+$: 267.02446; Found: 267.02556.

2,2,3,3,3-Pentafluoro-1-phenylpropan-1-one (S-14) was purchased from Matrix and used as received.

2,2,3,3,4,4,4-Heptafluoro-1-phenylbutan-1-one (S-15) was purchased from Alfa Aesar and used as received.

2,2-Difluoro-1-phenylethan-1-one (S-16a) was purchased from Alfa Aesar and used as received.

2,2-Difluoro-1-(*o*-tolyl)ethan-1-one (S-16b) was synthesized from the corresponding aldehyde utilizing a method developed for difluoromethyl additions to ketones[23] followed by Swern oxidation of the resulting alcohol.[24] **IR (neat):** 1703 (s), 1601 (w), 1457 (w), 1235 (w), 1147 (m), 1120 (s), 1054 (s), 965 (m), 758 (m), 724 (m) cm^{-1}; **^{1}H NMR (400 MHz, $CDCl_3$):** δ 7.97 – 7.79 (m, 1H), 7.50 (td, *J* = 7.5, 1.4 Hz, 1H), 7.40 – 7.29 (m, 2H), 6.27 (t, *J* = 53.8 Hz, 1H), 2.58 (s, 3H); **^{13}C NMR (100 MHz, $CDCl_3$):** δ 189.8 (t, *J* = 24.4 Hz), 141.6, 133.5, 132.7, 131.0, 130.4 (t, *J* = 4.1 Hz), 126.0, 110.9 (t, *J* = 254.3 Hz),

(23) Chen, D.; Ni, C.; Zhao, Y.; Cai, X.; Li. X.; Xiao, P.; Hu. J. *Angew. Chem., Int. Ed.* **2016**, *55*, 12632–12636.

(24) Trost, B. M.; Debien, L. *J. Am. Chem. Soc.* **2015**, *137*, 11606–11609.

21.8; **^{19}F NMR (376 MHz, $CDCl_3$):** δ –122.73 (dd, *J* = 53.8, 1.8 Hz, 2F); **HRMS(DART):** Calcd for $C_9H_9F_2O$ $[M+H]^+$: 171.0621; Found: 171.0629.

2,2-Difluoro-1-(4-methoxyphenyl)ethan-1-one (S-16c) was synthesized according to literature procedure.[25]

2-Fluoro-1-phenylethan-1-one (S-17a) was synthesized according to literature procedure.[26]

2-Fluoro-1-(*o*-tolyl)ethan-1-one (S-17b) was synthesized by fluorination of the corresponding, commercially available, α–bromo ketone through literature procedure.[22] The analytical data was fully consistent with the literature.[27]

2-Fluoro-1-(4-methoxyphenyl)ethan-1-one (S-17c) was synthesized by fluorination of the corresponding, commercially available, α–bromo ketone through a previously reported literature procedure.[22] The analytical data was fully consistent with the literature.[23]

2.7.2. *Catalytic Enantioselective Additions to Fluoroketones*

General Procedure for Catalytic Enantioselective Crotyl Additions:

In a N_2-filled glovebox, an oven-dried vial (8 mL) equipped with a stir bar was charged with aminophenol (0.01 mmol), zinc methoxide (2.6 mg, 0.02 mmol) and toluene (1.74 g) to prepare a pre-catalyst solution, which was allowed to stir at 22 °C for 15 min. In another vial (8 mL) equipped with a stir bar, trifluoroketone (0.2 mmol) was weighed

(25) Konno, T.; Takehana, T.; Mishima, M.; Ishihara, T. *J. Org. Chem.* **2006**, *71*, 3545–3550.
(26) Wei, Z.-L.; Li, Z.-Y.; Lin, G.-Q. *Tetrahedron* **1998**, *54*, 13059–13072.
(27) Yang, Q.; Mao, L.-L.; Yang, B.; Yang, S.-D. *Org. Lett.* **2014**, *16*, 3460-3463.

out and *cis*-crotylboronic acid pinacol ester (46 mg, 52 μL, 0.24 mmol), MeOH (8.3 mg, 11 μL, 0.26 mmol), the aminophenol/zinc methoxide solution (174 mg) and toluene (696 mg) were added. This latter vial was sealed with a screw cap and electrical tape then removed from the glovebox. The solution was allowed to stir outside of the glovebox for 1.5 h at 22 °C (unless otherwise noted) to afford trifluoroketone (>98% conv), as monitored by analysis of the ^{19}F NMR spectrum of the unpurified mixture, which was purified through silica gel chromatography.

Procedure for Gram-Scale Catalytic Enantioselective Crotyl Additions:

A vial (40 mL) was equipped with a stir bar. Aminophenol **ap-03** (62.5 mg, 0.125 mmol), zinc methoxide (32.5 mg, 0.25 mmol), **S-10** (966 mg, 5 mmol), *cis*-crotylboronic acid pinacol ester (1.15 g, 6.0 mmol), MeOH (275 μL, 6.5 mmol), and toluene (25 mL) were added, in that order. The vial was sealed with a septum and the solution was allowed to stir at 60 °C for 36 h leading to >98% conv according to ^{19}F NMR analysis. The crude mixture was then purified by silica gel chromatography (hexanes:ethyl acetate, 10:1) to afford ***Z*-2.53** as colorless oil (1.064 g, 4.6 mmol, 92% yield).

2.7.3. *Analytical Data for New Compounds*

(*R*,*Z*)-1,1,1-Trifluoro-2-phenylhex-4-en-2-ol (*Z*-2.22): IR (neat): 3500 (br, m), 3030 (w), 2919 (w), 2862 (w), 1660 (w), 1450 (w), 1272 (w), 1156 (s), 1020 (w), 700 (m) cm^{-1}; **^{1}H NMR (400 MHz, $CDCl_3$):** δ 7.58 (d, *J* = 8.0 Hz, 2H), 7.43 – 7.35 (m, 3H), 5.80 – 5.72 (m, 1H), 5.24 – 5.18 (m, 1H), 3.00 – 2.89 (m, 2H), 2.54 (1H, s), 1.76 (d, *J* = 8.8 Hz, 3H); **^{13}C NMR (100 MHz, $CDCl_3$):** δ 137.1, 130.9, 128.4, 128.3, 126.4, 125.4 (q, *J* = 283.9 Hz), 121.5, 76.4 (q, *J* = 27.4 Hz), 33.1, 13.1; **^{19}F NMR (376 MHz, $CDCl_3$):** δ –

80.2 (s, 3F); **HRMS (DART):** Calcd for $C_{12}H_{12}F_3$ $[M+H-H_2O]^+$: 213.0891; Found: 213.0896; **Specific Rotation:** $[\alpha]^{21.9}_D$ +57.1° (*c* 1.63, $CHCl_3$) for a 99:1 er sample. Enantiomeric purity was determined by HPLC analysis in comparison with authentic racemic material (Chiralpak AS-H, 99:1 hexanes:*i*-PrOH, 0.3 mL/min, 220 nm): t_R: 24.2 min (major) and 26.8 min (minor).

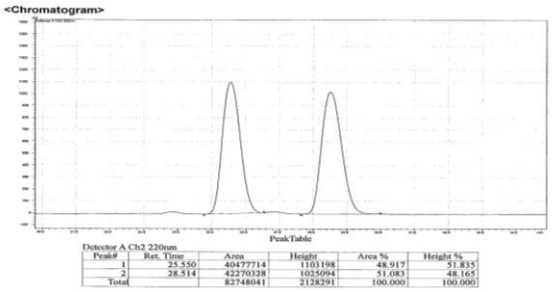

Peak#	Ret. Time	Area	Height	Area %	Height %
1	25.550	40477714	1103198	48.917	51.835
2	28.514	42270328	1025094	51.083	48.165
Total		82748041	2128291	100.000	100.000

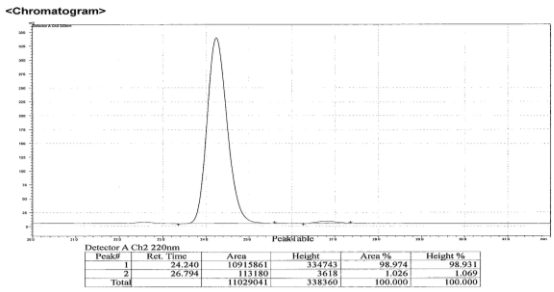

Peak#	Ret. Time	Area	Height	Area %	Height %
1	24.240	10915861	334743	98.974	98.931
2	26.794	113180	3618	1.026	1.069
Total		11029041	338360	100.000	100.000

Peak #	Ret. Time	Area	Area %	Peak #	Ret. Time	Area	Area %
1	25.550	40477714	48.917	1	24.240	10915861	98.974
2	28.514	42270328	51.083	2	26.794	113180	1.026

(*R*,*Z*)-1,1,1-Trifluoro-2-(*o*-tolyl)hex-4-en-2-ol (*Z*-2.30): IR (neat): 3545 (br, m), 3028 (w), 2927 (w), 1489 (w), 1372 (w), 1216 (s), 759 (m) cm^{-1}; **^{1}H NMR (400 MHz, $CDCl_3$):** δ 7.44 (d, *J* = 7.2 Hz, 1H), 7.24 – 7.17 (m, 3H), 5.82 – 5.74 (m, 1H), 5.31 – 5.25 (m, 1H), 3.15 – 2.91 (m, 2H), 2.58 (s, 3H), 2.55 (s, 1H), 1.69 (d, *J* = 6.8 Hz, 3H); **^{13}C NMR (100 MHz, $CDCl_3$):** δ 138.5, 134.5, 133.4, 131.3, 128.8, 128.7, 126.1 (q, *J* = 283.9 Hz), 125.7, 122.1, 78.6 (q, *J* = 28.1 Hz), 33.8, 23.1, 13.3; **^{19}F NMR (376 MHz, $CDCl_3$):** δ –79.3 (s, 3F); **HRMS (DART):** Calcd for $C_{13}H_{14}F_3$ $[M+H-H_2O]^+$: 227.1047; Found: 227.1047; **Specific Rotation:** $[\alpha]^{21.3}_D$ +19.0° (*c* 2.10, $CHCl_3$) for a >99:1 er sample. Enantiomeric purity was determined by HPLC analysis in comparison with authentic racemic material (Chiralcel OJ-H, 98:2 hexanes:i-PrOH, 0.3 mL/min, 220 nm): t_R: 27.4 min (major) and 32.6 min (minor).

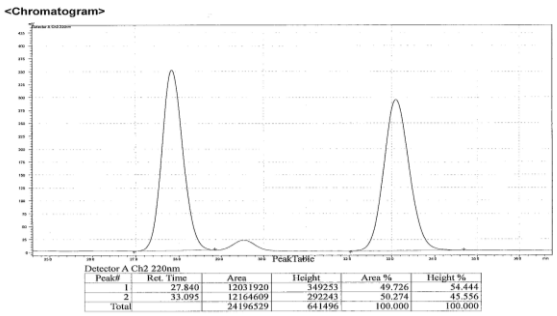

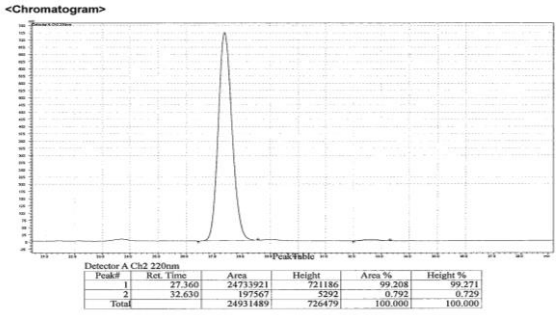

Peak #	Ret. Time	Area	Area %	Peak #	Ret. Time	Area	Area %
1	27.840	12031920	49.726	1	27.360	24733921	99.208
2	33.095	12164609	50.274	2	32.630	197567	0.792

(*R*,*Z*)-1,1,1-Trifluoro-2-(2-methoxyphenyl)hex-4-en-2-ol (*Z*-2.31): IR (neat): 3456 (br, m), 3031 (w), 2923 (w), 1603 (w), 1181 (m), 1155 (s), 1023 (w), 796 (m) cm $^{-1}$; **^{1}H NMR (400 MHz, $CDCl_3$):** δ 7.35 – 7.21 (m, 2H), 7.01 – 6.97 (m, 2H), 6.08 (s, 1H), 5.91 – 5.52 (m, 1H), 5.35 – 5.29 (m, 1H), 3.90 (s, 3H), 3.04 – 2.98 (m, 1H), 2.82 – 2.77 (m, 1H), 1.67 (d, *J* = 6.8 Hz, 3H); **^{13}C NMR (100 MHz, $CDCl_3$):** δ 158.8, 130.3, 130.1, 127.1, 125.9 (q, *J* = 283.9 Hz), 123.4, 123.3, 121.3, 112.6, 78.8 (q, *J* = 28.1 Hz), 56.3, 31.2, 13.2; **^{19}F NMR (376 MHz, $CDCl_3$):** δ –78.5 (s, 3F); **HRMS (DART):** Calcd for $C_{13}H_{14}F_3O$ $[M+H–H_2O]^+$: 243.0996; Found: 243.1005; **Specific Rotation:** $[\alpha]^{21.3}_D$ –26.7° (*c* 2.12, $CHCl_3$) for a >99:1 er sample. Enantiomeric purity was determined by HPLC analysis in comparison with authentic racemic material (Chiralcel OJ-H, 99.5:0.5 hexanes:i-PrOH, 0.1 mL/min, 220 nm): t_R: 99.4 min (minor) and 108.8 min (major).

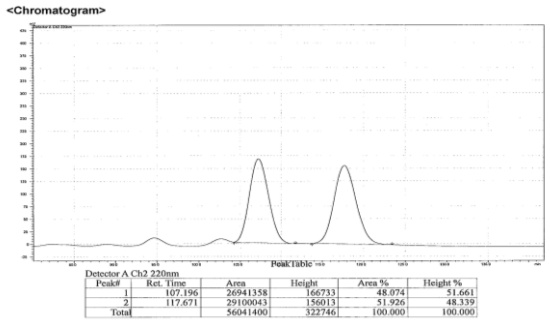

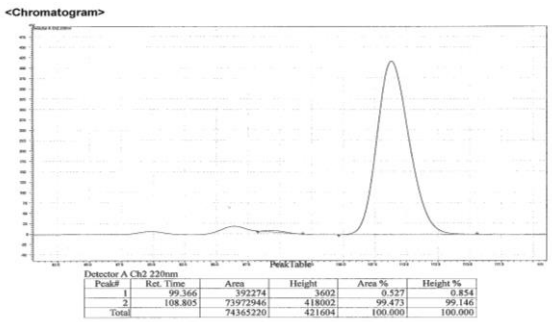

Peak #	Ret. Time	Area	Area %	Peak #	Ret. Time	Area	Area %
1	107.196	26941358	48.074	1	99.366 min	392274	0.527
2	117.671	29100043	51.926	2	108.805 min	73972946	99.473

(*R*,*Z*)-1,1,1-Trifluoro-2-(naphthalen-1-yl)hex-4-en-2-ol (*Z*-2.32): IR (neat): 3528 (br, m), 3030 (w), 2924 (w), 1654 (w), 1511 (s), 1268 (w), 1157 (m), 862 (w), 640 (m) cm^{-1}; **^{1}H NMR (400 MHz, $CDCl_3$):** δ 8.90 (d, *J* = 8.4 Hz, 1H), 7.88 – 7.85 (m, 2H), 7.67 (d, *J* = 7.2 Hz, 1H), 7.53 – 7.43 (m, 3H), 5.80 – 5.72 (m, 1H), 5.36 – 5.30 (m, 1H), 3.37 – 3.12 (m, 2H), 2.90 (s, 1H), 1.69 – 1.67 (m, 3H); **^{13}C NMR (100 MHz, $CDCl_3$):** δ 135.0, 134.2, 132.4, 132.3, 131.4, 130.6, 129.2, 127.4, 127.3, 126.1 (q, *J* = 286.2 Hz), 126.0, 125.6, 124.5, 123.1, 122.1, 79.5 (q, *J* = 28.0 Hz), 34.2, 13.3; **^{19}F NMR (376 MHz, $CDCl_3$):** δ –77.9 (s, 3F); **HRMS (DART):** Calcd for $C_{16}H_{14}F_3$ $[M+H–H_2O]^+$: 263.1047; Found: 263.1047; **Specific Rotation:** $[\alpha]^{21.3}_D$ –19.1° (*c* 2.19, $CHCl_3$) for a 97:3 er sample. Enantiomeric purity was determined by HPLC analysis in comparison with authentic racemic material (Chiralcel OJ-H, 98:2 hexanes:*i*-PrOH, 0.3 mL/min, 220 nm): t_R: 74.2 min (major) and 85.0 min (minor).

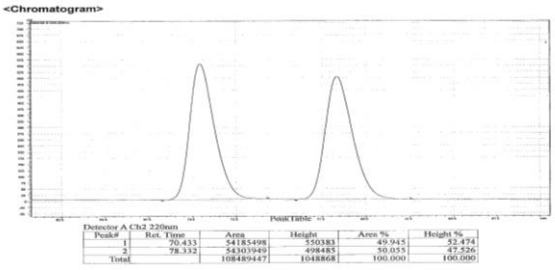

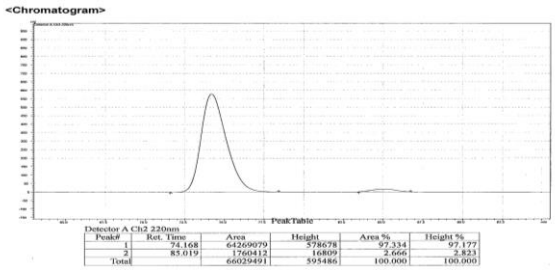

Peak #	Ret. Time	Area	Area %	Peak #	Ret. Time	Area	Area %
1	70.433	54185498	49.945	1	74.168	64269079	97.334
2	78.332	54303949	50.055	2	85.019	1760412	2.666

(*R*,*Z*)-2-(2-Bromophenyl)-1,1,1-trifluorohex-4-en-2-ol (*Z*-2.33): IR (neat): 3522 (br, m), 3029 (w), 2924 (w), 1466 (w), 1161 (s), 1018 (w), 755 (m); **^{1}H NMR (400 MHz, $CDCl_3$):** δ 7.68 – 7.62 (m, 2H), 7.35 – 7.31 (m, 1H), 7.20 – 7.16 (m, 1H), 5.73 – 5.65 (m, 1H), 5.28 – 5.21 (m, 1H), 3.63 (s, 1H), 3.48 – 3.42 (m, 1H), 3.01 – 2.95 (m, 1H), 1.69 – 1.67 (m, 3H); **^{13}C NMR (100 MHz, $CDCl_3$):** δ 136.0, 134.9, 131.6, 130.3, 129.9, 127.5, 125.5 (q, J = 283.9 Hz), 122.2, 121.2, 78.7 (q, J = 28.0 Hz), 32.3, 13.4; **^{19}F NMR (376 MHz, $CDCl_3$):** δ –78.5 (s, 3F); **HRMS (DART):** Calcd for $C_{12}H_{11}F_3Br$ $[M+H–H_2O]^+$: 290.9996; Found: 291.0005; **Specific Rotation:** $[\alpha]^{21.1}_D$ +18.5° (*c* 2.70, $CHCl_3$) for a 97:3 er sample. Enantiomeric purity was determined by HPLC analysis in comparison with authentic racemic material (Chiralpak AS-H, 98:2 hexanes:*i*-PrOH, 0.2 mL/min, 220 nm): t_R: 45.0 min (major) and 48.4 min (minor).

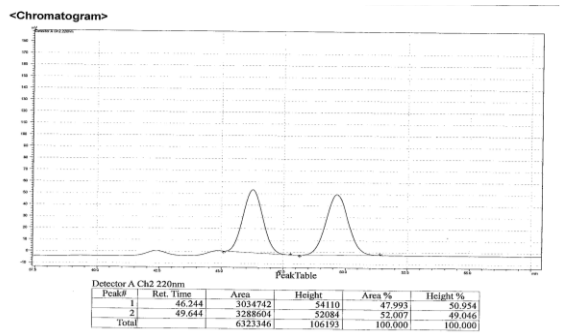

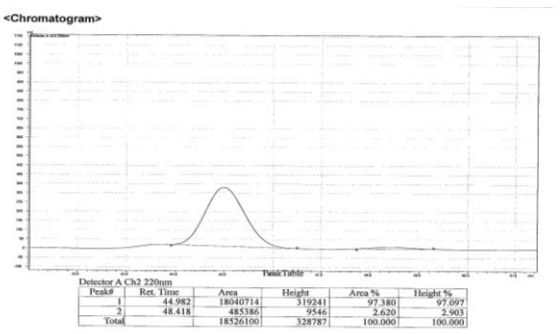

Peak #	Ret. Time	Area	Area %	Peak #	Ret. Time	Area	Area %
1	46.244	3034741	47.993	1	44.982	18040714	97.380
2	49.644	3288604	52.007	2	48.418	485386	2.620

(*R*,*Z*)-1,1,1-Trifluoro-2-(2-(trifluoromethyl)phenyl)hex-4-en-2-ol (*Z*-2.34): IR (neat): 3557 (br, m), 3031 (w), 2927 (w), 1494 (w), 1302 (w), 1285 (m), 1137 (s), 768 (m) cm^{-1}; **^{1}H NMR (400 MHz, $CDCl_3$):** δ 7.86 (d, *J* = 8.0 Hz, 1H), 7.60 – 7.52 (m, 2H), 7.47 – 7.43 (m, 1H), 5.82 – 5.73 (m, 1H), 5.18 – 5.11 (m, 1H), 3.04 – 2.92 (m, 2H), 2.90 – 2.89 (m, 1H), 1.67 – 1.64 (m, 3H); **^{13}C NMR (100 MHz, $CDCl_3$):** δ 136.8, 132.1, 131.5, 130.1, 129.8 (q, *J* = 9.2 Hz), 129.6, 129.5, 129.2, 128.7, 128.6, 128.5, 128.4, 128.3, 126.7, 124.3 (q, *J* = 271.7 Hz), 123.9, 121.0, 78.4 (q, *J* = 28.1 Hz), 35.5, 13.2; **^{19}F NMR (376 MHz, $CDCl_3$):** δ –55.1 (s, 3F), –78.4 (s, 3F); **HRMS (DART):** Calcd for $C_{13}H_{16}F_6NO$ $[M+NH_4]^+$: 316.1136; Found: 316.1139; **Specific Rotation:** $[\alpha]^{21.3}_D$ +32.2° (*c* 1.55, $CHCl_3$) for a 97:3 er sample. Enantiomeric purity was determined by HPLC analysis in comparison with authentic racemic material (Chiralpak AS-H, 99:1 hexanes:*i*-PrOH, 0.3 mL/min, 220 nm): t_R: 18.3 min (major) and 20.8 min (minor).

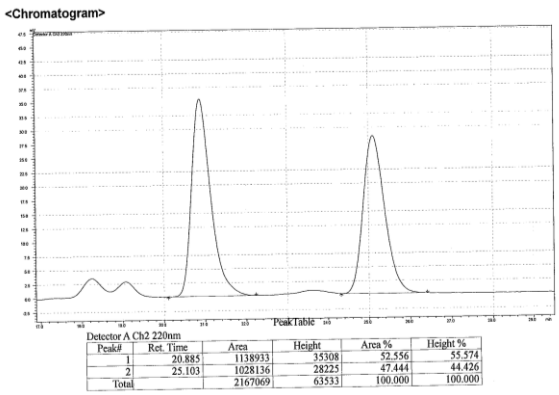

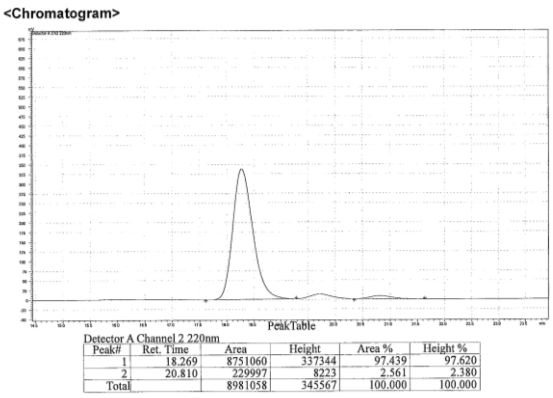

Peak #	Ret. Time	Area	Area %	Peak #	Ret. Time	Area	Area %
1	20.885	1138933	52.556	1	18.269	8751060	97.439
2	25.103	1028136	47.444	2	20.810	229997	2.561

(*R*,*Z*)-1,1,1-Trifluoro-2-(*m*-tolyl)hex-4-en-2-ol (*Z*-2.35): IR (neat): 3527 (br, m), 3029 (w), 2925 (w), 1270 (w), 1167 (m), 1146 (m), 1027 (w), 724 (m) cm^{-1}; **^{1}H NMR (400 MHz, $CDCl_3$):** δ 7.38 – 7.34 (m, 2H), 7.27 (t, *J* = 7.2 Hz, 1H), 7.16 (d, *J* = 7.2 Hz, 1H), 5.78 – 5.69 (m, 1H), 5.23 – 5.16 (m, 1H), 2.97 – 2.86 (m, 2H), 2.52 (s, 1H), 2.37 (s, 3H), 1.67 – 1.65 (m, 3H); **^{13}C NMR (100 MHz, $CDCl_3$):** δ 137.9, 137.0, 130.9, 129.2, 128.1, 127.1, 125.5 (q, *J* = 284.6 Hz), 123.5, 121.6, 76.3 (q, *J* = 28.1 Hz), 33.1, 21.6, 13.3; **^{19}F NMR (376 MHz, $CDCl_3$):** δ –80.1 (s, 3F); **HRMS (DART):** Calcd for $C_{13}H_{14}F_3$ $[M+H–H_2O]^+$: 227.1047; Found: 227.1046; **Specific Rotation:** $[\alpha]^{21.1}_D$ +52.4° (*c* 2.82, $CHCl_3$) for a 99:1 er sample. Enantiomeric purity was determined by HPLC analysis in comparison with authentic racemic material (Chiralcel OJ-H, 98:2 hexanes:*i*-PrOH, 0.3 mL/min, 220 nm): t_R: 32.3 min (major) and 40.2 min (minor).

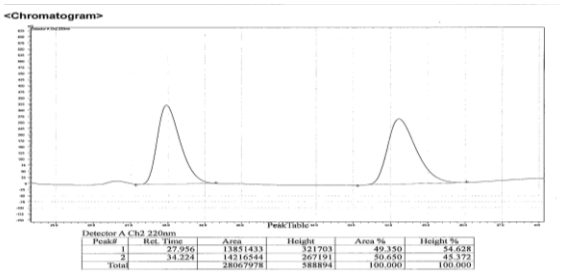

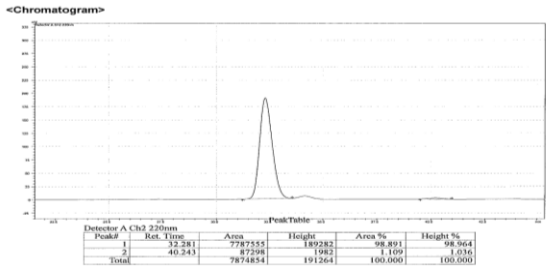

Peak #	Ret. Time	Area	Area %	Peak #	Ret. Time	Area	Area %
1	27.956	13851433	49.350	1	32.281	7787555	98.891
2	34.224	1421654	50.650	2	40.243	87298	1.109

(*R*,*Z*)-2-(3-Chlorophenyl)-1,1,1-trifluorohex-4-en-2-ol (*Z*-2.36): IR (neat): 3539 (br, m), 3030 (w), 2925 (w), 1598 (w), 1162 (s), 999 (w), 661 (w) cm^{-1}; **^{1}H NMR (400 MHz, $CDCl_3$):** δ 7.61 (s, 1H), 7.46 – 7.47 (m, 1H), 7.37 – 7.32 (m, 1H), 5.84 – 5.75 (m, 1H), 5.23 – 5.16 (m, 1H), 2.98 – 2.85 (m, 2H), 2.59 (s, 1H), 1.69 – 1.66 (m, 3H); **^{13}C NMR (100 MHz, $CDCl_3$):** δ 139.2, 134.5, 131.5, 129.5, 128.7, 126.9, 125.1 (q, J = 286.2 Hz), 124.6, 120.9, 76.1 (q, J = 28.1 Hz), 33.2, 13.1; **^{19}F NMR (376 MHz, $CDCl_3$):** δ –80.0 (s, 3F); **HRMS (DART):** Calcd for $C_{12}H_{11}F_3Cl$ $[M+H–H_2O]^+$: 247.0501; Found: 247.0501; **Specific Rotation:** $[\alpha]^{22.3}_D$ +22.8° (*c* 2.11, $CHCl_3$) for a 98:2 er sample. Enantiomeric purity was determined by HPLC analysis in comparison with authentic racemic material (Chiralpak AD-H, 98:2 hexanes:*i*-PrOH, 0.3 mL/min, 220 nm): t_R: 22.8 min (minor) and 25.7 min (major).

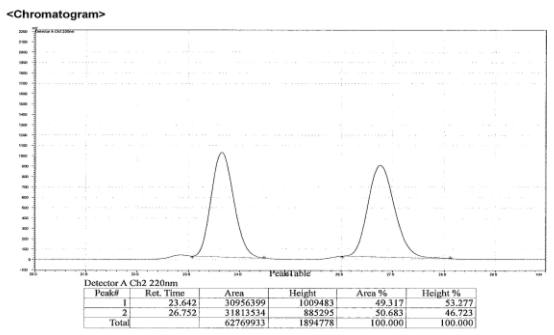

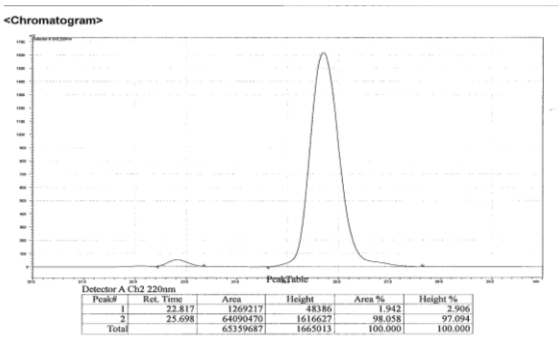

Peak #	Ret. Time	Area	Area %	Peak #	Ret. Time	Area	Area %
1	23.642	30956399	49.317	1	22.817	1269217	1.942
2	26.752	31813534	50.683	2	25.698	64090470	98.058

(*R*,*Z*)-2-(3,5-Dichlorophenyl)-1,1,1-trifluorohex-4-en-2-ol (*Z*-2.37): IR (neat): 3531 (br, m), 3094 (w), 3029 (w), 1656 (w), 1590 (w), 1568 (w), 1162 (s), 800 (m), 699 (w) cm^{-1}; **^{1}H NMR (400 MHz, $CDCl_3$):** δ 7.47 (s, 2H), 7.37 (s, 1H), 5.85 – 5.77 (m, 1H), 5.21 – 5.15 (m, 1H), 2.96 – 2.78 (m, 2H), 2.63 (s, 1H), 1.66 (d, *J* = 7.2 Hz, 3H); **^{13}C NMR (100 MHz, $CDCl_3$):** δ 140.8, 135.3, 132.2, 128.9, 125.5, 125.0 (q, *J* = 286.2 Hz), 120.6, 76.1 (q, *J* = 28.1 Hz), 33.3, 13.3; **^{19}F NMR (376 MHz, $CDCl_3$):** δ –79.9 (s, 3F); **HRMS (DART):** Calcd for $C_{12}H_{10}F_3Cl_2$ $[M+H–H_2O]^+$: 281.0111; Found: 281.0111; **Specific Rotation:** $[\alpha]^{22.3}_D$ +30.4° (*c* 2.30, $CHCl_3$) for a 96:4 er sample. Enantiomeric purity was determined by HPLC analysis in comparison with authentic racemic material (Chiralpak AD-H, 98:2 hexanes:*i*-PrOH, 0.3 mL/min, 220 nm): t_R: 18.7 min (minor) and 21.9 min (major).

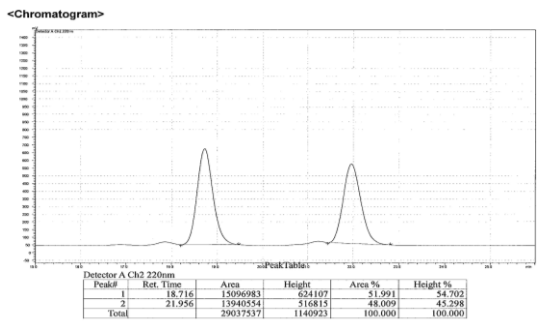

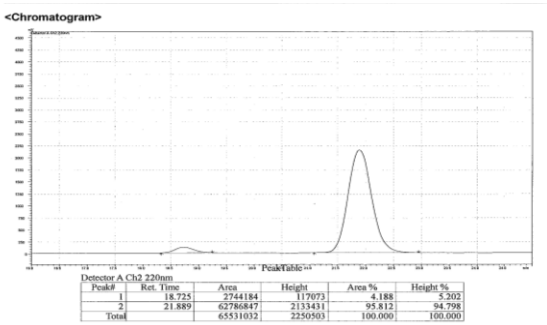

Peak #	Ret. Time	Area	Area %	Peak #	Ret. Time	Area	Area %
1	18.716	15096983	51.991	1	18.725	2744184	4.188
2	21.956	13940554	48.009	2	21.889	62786847	95.812

(*R*,*Z*)-2-(3-Chloro-5-fluorophenyl)-1,1,1-trifluorohex-4-en-2-ol (*Z*-2.38): IR (neat): 3531 (br, m), 3099 (w), 3031 (w), 2927 (w), 1609 (w), 1589 (m), 1438 (m), 1173 (s), 1141 (m), 859 (m) cm^{-1}; **^{1}H NMR (400 MHz, $CDCl_3$):** δ 7.38 (s, 1H), 7.21 (d, *J* = 10.0 Hz, 1H), 7.12 – 7.09 (m, 1H), 5.85 – 5.77 (m, 1H), 5.21 – 5.15 (m, 1H), 2.96 – 2.80 (m, 2H), 2.62 (s, 1H), 1.68 – 1.66 (m, 3H); **^{13}C NMR (100 MHz, $CDCl_3$):** δ 162.7 (d, *J* = 248.2 Hz), 141.2 (d, *J* = 8.4 Hz), 135.3 (d, *J* = 9.8 Hz), 132.1, 125.1 (q, *J* = 284.6 Hz), 122.9 (q, *J* = 1.5 Hz), 120.7, 116.7, 116.4, 112.9, 112.6, 76.1 (q, *J* = 28.8 Hz), 33.4, 13.3; **^{19}F NMR (376 MHz, $CDCl_3$):** δ –80.0 (s, 3F), -111.2 (t, *J* = 8.3 Hz, 1F); **HRMS (DART):** Calcd for $C_{12}H_{10}F_4ClO$ $[M+H–H_2O]^+$: 283.0512; Found: 283.0513; **Specific Rotation:** $[\alpha]^{22.3}_D$ +38.3° (*c* 2.50, $CHCl_3$) for a 97:3 er sample. Enantiomeric purity was determined by HPLC analysis in comparison with authentic racemic material (Chiralpak AD-H, 98:2 hexanes:*i*-PrOH, 0.3 mL/min, 220 nm): t_R: 19.7 min (minor) and 23.2 min (major).

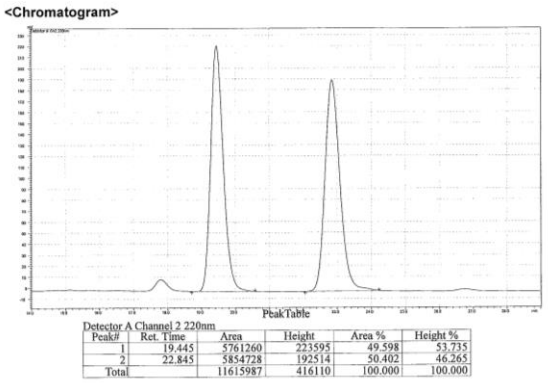

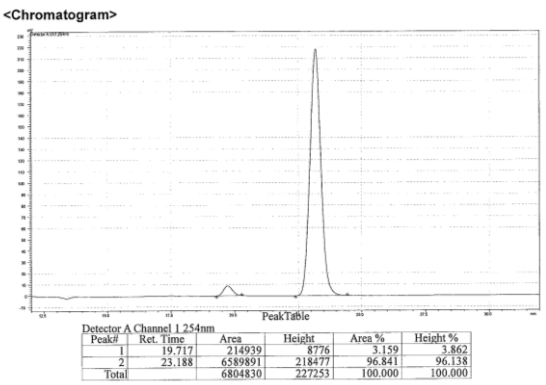

Peak #	Ret. Time	Area	Area %	Peak #	Ret. Time	Area	Area %
1	19.445	5761260	49.598	1	19.717	214939	3.159
2	22.845	5854728	50.402	2	23.188	6589891	96.841

(*R*,*Z*)-1,1,1-Trifluoro-2-(3-(trifluoromethyl)phenyl)hex-4-en-2-ol (*Z*-2.39): IR (neat): 3530 (br, m), 3031 (w), 1618 (w), 1615 (m), 1570 (s), 816 (m) cm^{-1}; **^{1}H NMR (400 MHz, $CDCl_3$):** δ 7.87 (s, 1H), 7.76 (d, *J* = 8.0 Hz, 1H), 7.63 (d, *J* = 8.0 Hz, 1H), 7.53 (t, *J* = 8.0 Hz, 1H), 5.83 – 5.75 (m, 1H), 5.22 – 5.15 (m, 1H), 3.01 – 2.89 (m, 2H), 2.64 (s, 1H), 1.67 (d, *J* = 6.4 Hz, 3H); **^{13}C NMR (100 MHz, $CDCl_3$):** δ 138.4, 131.9, 131.0 (q, *J* = 32.7 Hz), 130.0, 128.9, 125.6 (q, *J* = 4.7 Hz), 125.3 (q, *J* = 283.9 Hz), 123.7 (q, *J* = 4.7 Hz), 122.8, 120.9, 76.3 (q, *J* = 28.1 Hz), 33.3, 13.3; **^{19}F NMR (376 MHz, $CDCl_3$):** δ –63.6 (s, 3F), –80.8 (s, 3F); **HRMS (DART)** Calcd for $C_{13}H_{11}F_6$ $[M+H–H_2O]^+$: 281.0764; Found: 281.0768; **Specific Rotation:** $[\alpha]^{22.1}_D$ +30.4° (*c* 2.30, $CHCl_3$) for a 98:2 er sample. Enantiomeric purity was determined by HPLC analysis in comparison with authentic racemic material (Chiralpak AD-H, 99:1 hexanes:*i*-PrOH, 0.2 mL/min, 220 nm): t_R: 39.0 min (minor) and 44.7 min (major).

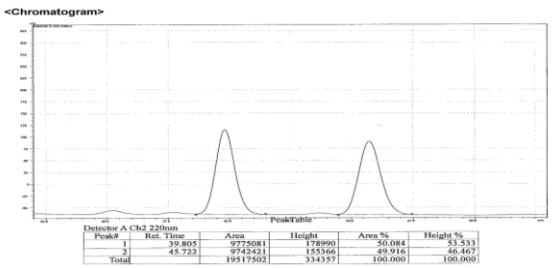

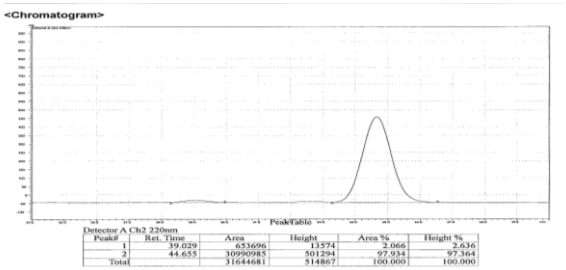

Peak #	Ret. Time	Area	Area %	Peak #	Ret. Time	Area	Area %
1	39.805	9775081	50.084	1	39.029	653696	2.066
2	45.722	9742421	49.916	2	44.655	30990985	97.934

(*R*,*Z*)-1,1,1-Trifluoro-2-(*p*-tolyl)hex-4-en-2-ol (*Z*-2.40): IR (neat): 3535 (br, m), 3031 (w), 2921 (w), 2851 (w), 1516 (w), 1219 (w), 1153 (s), 813 (m), 727 (m) cm^{-1}; **^{1}H NMR (400 MHz, $CDCl_3$):** δ 7.45 (d, *J* = 8.0 Hz, 2H), 7.20 (d, *J* = 8.0 Hz, 2H), 5.78 – 5.70 (m, 1H), 5.24 – 5.17 (m, 1H), 2.97 – 2.86 (m, 2H), 2.49 (s, 1H), 2.37 (s, 3H), 1.68 – 1.66 (m, 3H); **^{13}C NMR (100 MHz, $CDCl_3$):** δ 138.5, 134.2, 130.9, 129.2, 126.5, 125.6 (q, *J* = 284.6 Hz), 121.8, 76.5 (q, *J* = 28.1 Hz), 33.1, 21.2, 13.3; **^{19}F NMR (376 MHz, $CDCl_3$):** δ –80.4 (s, 3F); **HRMS (DART):** Calcd for $C_{13}H_{14}F_3$ $[M+H–H_2O]^+$: 227.1047; Found: 227.1046; **Specific Rotation:** $[\alpha]^{21.1}_D$ +54.9° (*c* 1.60, $CHCl_3$) for a >99:1 er sample. Enantiomeric purity was determined by HPLC analysis in comparison with authentic racemic material (Chiralpak AS-H, 99:1 hexanes:*i*-PrOH, 0.3 mL/min, 220 nm): t_R: 21.9 min (major) and 25.7 min (minor).

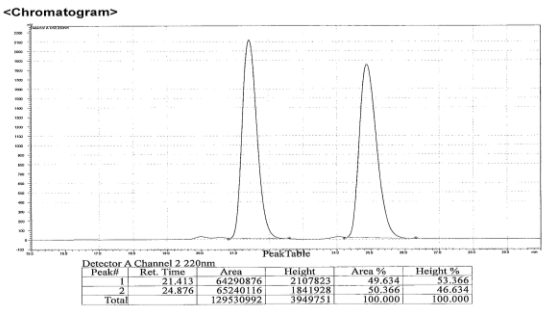

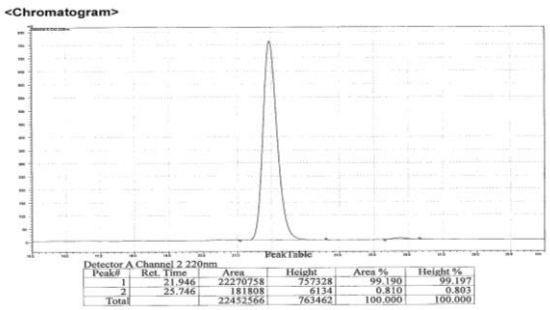

Peak #	Ret. Time	Area	Area %	Peak #	Ret. Time	Area	Area %
1	21.413	64290876	49.634	1	21.946	22270758	99.190
2	24.876	65240116	50.366	2	25.746	181808	0.810

(*R*,*Z*)-2-(4-(Dimethylamino)phenyl)-1,1,1-trifluorohex-4-en-2-ol (*Z*-2.41): IR (neat): 3526 (br, m), 3027 (w), 1662 (m), 1328 (m), 1155 (s), 1124 (s), 1022 (w), 801 (w) cm^{-1}; **^{1}H NMR (400 MHz, $CDCl_3$):** δ 7.41 (d, *J* = 8.8 Hz, 2H), 6.75 – 6.72 (m, 2H), 5.78 – 5.69 (m, 1H), 5.28 – 5.22 (m, 1H), 2.98 (s, 6H), 2.91 (d, *J* = 8.0 Hz, 2H), 2.48 (s, 1H), 1.68 (d, *J* = 6.4 Hz, 3H); **^{13}C NMR (100 MHz, $CDCl_3$):** δ 150.5, 130.5, 127.5, 125.8 (q, *J* = 283.8 Hz), 124.3, 122.2, 111.9, 76.3 (q, *J* = 28.1 Hz), 40.4, 32.8, 13.3; **^{19}F NMR (376 MHz, $CDCl_3$):** δ –80.8 (s, 3F); **HRMS (DART):** Calcd for $C_{14}H_{19}F_3ON$ $[M+H]^+$: 274.1418; Found: 274.1420; **Specific Rotation:** $[\alpha]^{21.8}_D$ +48.6° (*c* 2.30, $CHCl_3$) for a >99:1 er sample. Enantiomeric purity was determined by HPLC analysis in comparison with authentic racemic material (Chiralpak AD-H, 98:2 hexanes:*i*-PrOH, 0.8 mL/min, 220 nm): t_R: 18.5 min (major) and 28.5 min (minor).

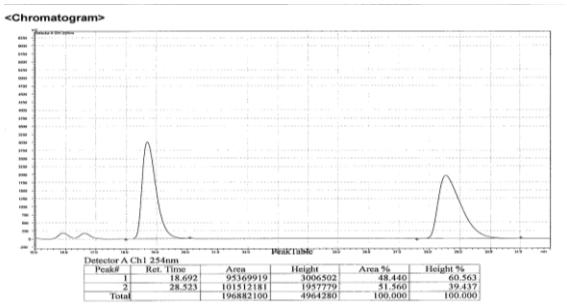

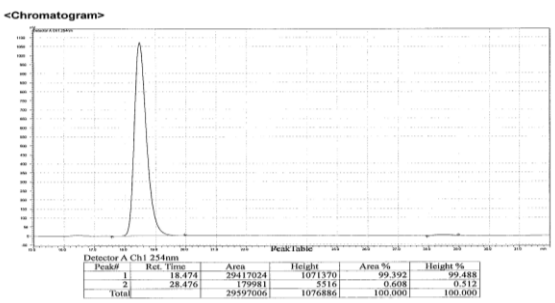

Peak #	Ret. Time	Area	Area %	Peak #	Ret. Time	Area	Area %
1	18.692	95369919	48.440	1	18.474	29417024	99.392
2	28.523	101512181	51.560	2	28.476	179981	0.608

(*R*,*Z*)-1,1,1-Trifluoro-2-(4-methoxyphenyl)hex-4-en-2-ol (*Z*-2.42): IR (neat): 3484 (br, m), 2938 (w), 2841 (w), 2862 (w), 1612 (w), 1515 (m), 1252 (m), 1154 (s), 999 (m), 829 (m), 752 (m), cm^{-1}; **^{1}H NMR (400 MHz, $CDCl_3$):** δ 7.48 (d, *J* = 8.8 Hz, 2H), 6.94 – 6.90 (m, 2H), 5.78 – 5.70 (m, 1H), 5.24 – 5.17 (m, 1H), 3.82 (s, 3H), 2.96 – 2.86 (m, 2H), 2.49 (s, 1H), 1.67 (d, *J* = 8.0 Hz, 3H); **^{13}C NMR (100 MHz, $CDCl_3$):** δ 159.8, 130.9, 129.2, 127.9, 125.6 (q, *J* = 283.8 Hz), 121.8, 113.7, 76.3 (q, *J* = 28.1 Hz), 55.4, 33.1, 13.3; **^{19}F NMR (376 MHz, $CDCl_3$):** δ –80.6 (s, 3F); **HRMS (DART):** Calcd for $C_{13}H_{14}F_3O$ $[M+H–H_2O]^+$: 243.0996; Found: 243.0999; **Specific Rotation:** $[\alpha]^{21.8}_D$ +33.1° (*c* 2.29, $CHCl_3$) for a >99:1 er sample. Enantiomeric purity was determined by HPLC analysis in comparison with authentic racemic material (Chiralpak AD-H, 98:2 hexanes:*i*-PrOH, 0.8 mL/min, 220 nm): t_R: 13.7 min (major) and 17.3 min (minor).

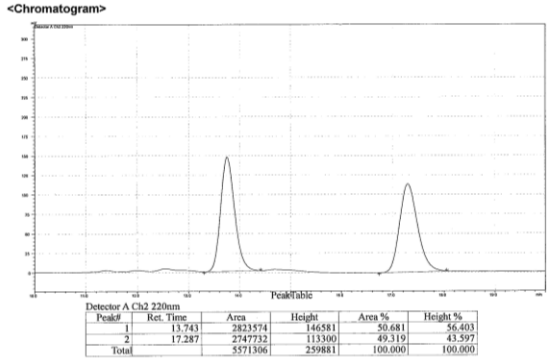

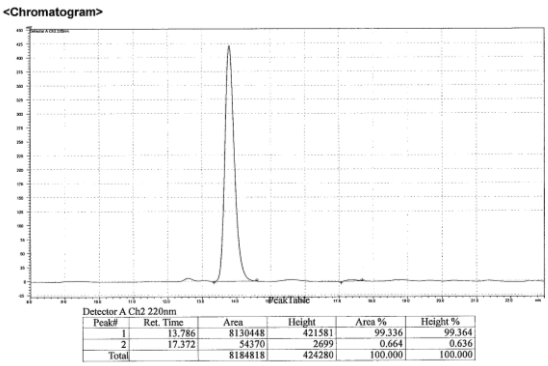

Peak #	Ret. Time	Area	Area %	Peak #	Ret. Time	Area	Area %
1	13.743	2823574	50.681	1	13.786	8130448	99.336
2	17.287	2747732	49.319	2	17.372	54370	0.664

(*R*,*Z*)-1,1,1-Trifluoro-2-(4-(methylthio)phenyl)hex-4-en-2-ol (*Z*-2.43): IR (neat): 3513 (br, m), 3027 (w), 2923 (w), 1599 (w), 1496 (w), 1158 (s), 738 (m) cm^{-1}; **^{1}H NMR (400 MHz, $CDCl_3$):** δ 7.46 (d, *J* = 8.8 Hz, 2H), 7.26 – 7.23 (m, 2H), 5.78 – 5.69 (m, 1H), 5.21 – 5.15 (m, 1H), 2.95 – 2.84 (m, 2H), 2.53 (s, 1H), 2.48 (s, 3H), 1.66 – 1.64 (m, 3H); **^{13}C NMR (100 MHz, $CDCl_3$):** δ 139.3, 133.8, 131.1, 127.1, 126.1, 125.5 (q, *J* = 283.8 Hz), 121.5, 76.4 (q, *J* = 28.1 Hz), 33.1, 15.5, 13.2; **^{19}F NMR (376 MHz, $CDCl_3$):** δ –80.4 (s, 3F); **HRMS (DART):** Calcd for $C_{13}H_{16}F_3OS$ $[M+H]^+$: 277.0873; Found: 277.0883; **Specific Rotation:** $[\alpha]^{21.1}_D$ +44.4° (*c* 2.70, $CHCl_3$) for a >99:1 er sample. Enantiomeric purity was determined by HPLC analysis in comparison with authentic racemic material (Chiralpak AS-H, 98:2 hexanes:*i*-PrOH, 0.3 mL/min, 220 nm): t_R: 31.7 min (major) and 39.0 min (minor).

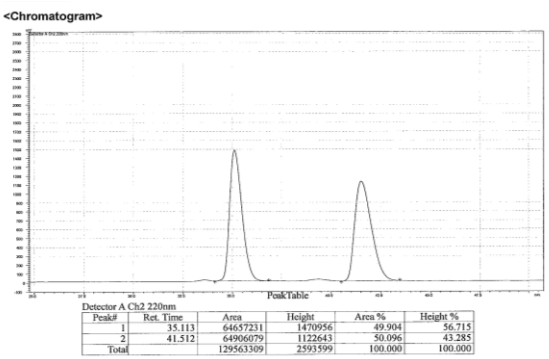

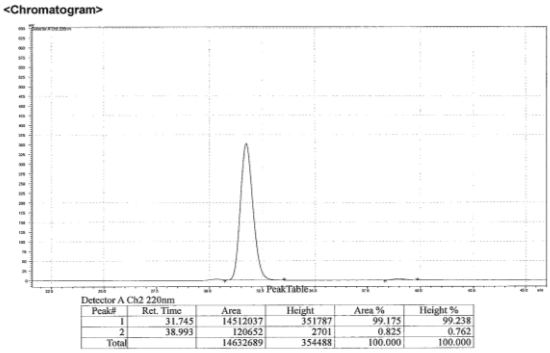

Peak #	Ret. Time	Area	Area %	Peak #	Ret. Time	Area	Area %
1	35.113	64657231	49.904	1	31.745	14512037	99.238
2	41.512	64906079	50.096	2	38.993	120652	0.762

(*R*,*Z*)-1,1,1-Trifluoro-2-(4-fluorophenyl)hex-4-en-2-ol (*Z*-2.44): IR (neat): 3520 (br, m), 3032 (w), 2924 (w), 1606 (w), 1502 (w), 1155 (s), 833 (m) cm^{-1}; **^{1}H NMR (400 MHz, $CDCl_3$):** δ 7.57 – 7.53 (m, 2H), 7.11 – 7.05 (m, 2H), 5.81 – 5.72 (m, 1H), 5.22 – 5.15 (m, 1H), 2.97 – 2.85 (m, 2H), 2.53 (s, 1H), 1.67 – 1.65 (m, 3H); **^{13}C NMR (100 MHz, $CDCl_3$):** δ 164.1, 161.7, 132.9, 131.4, 128.5 (d, J = 1.2 Hz), 128.5 (d, J = 1.2 Hz), 125.3 (q, J = 283.8 Hz), 121.3, 115.4, 115.2, 76.2 (q, J = 28.0 Hz), 33.3, 13.2; **^{19}F NMR (376 MHz, $CDCl_3$):** δ –80.4 (s, 3F), –114.8 (s, 1F); **HRMS (DART):** Calcd for $C_{12}H_{11}F_4$ $[M+H–H_2O]^+$: 231.0796; Found: 231.0807; **Specific Rotation:** $[\alpha]^{21.1}_D$ +28.5° (*c* 2.19, $CHCl_3$) for a >99:1 er sample. Enantiomeric purity was determined by HPLC analysis in comparison with authentic racemic material (Chiralpak AS-H, 99:1 hexanes:*i*-PrOH, 0.3 mL/min, 220 nm): t_R: 23.8 min (major) and 27.5 min (minor).

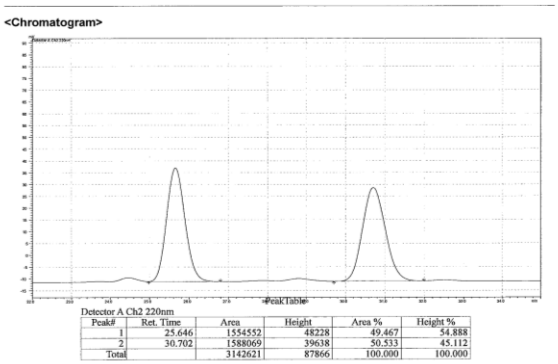

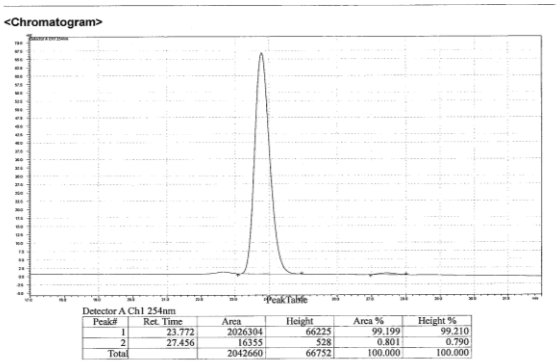

Peak #	Ret. Time	Area	Area %	Peak #	Ret. Time	Area	Area %
1	25.646	1554552	49.467	1	23.772	2026304	99.199
2	30.702	1588069	50.533	2	27.456	16355	0.801

(*R*,*Z*)-2-(4-Chlorophenyl)-1,1,1-trifluorohex-4-en-2-ol (*Z*-2.45): IR (neat): 3539 (br, m), 3029 (w), 2918 (w), 1598 (w), 1494 (m), 1155 (s), 1094 (m) cm^{-1}; **^{1}H NMR (400 MHz, $CDCl_3$):** δ 7.51 (d, *J* = 8.4 Hz, 2H), 7.37 (d, *J* = 8.4 Hz, 2H), 5.81 – 5.73 (m, 1H), 5.21 – 5.15 (m, 1H), 2.97 – 2.84 (m, 2H), 2.55 (s, 1H), 1.66 (d, *J* = 6.4 Hz, 3H); **^{13}C NMR (100 MHz, $CDCl_3$):** δ 135.8, 134.8, 131.5, 128.6, 128.2, 125.4 (q, *J* = 284.6 Hz), 121.2, 76.3 (q, *J* = 28.1 Hz), 33.2, 13.3; **^{19}F NMR (376 MHz, $CDCl_3$):** δ –80.3 (s, 3F); **HRMS (DART):** Calcd for $C_{12}H_{11}F_3Cl$ $[M+H–H_2O]^+$: 247.0501; Found: 247.0510; **Specific Rotation:** $[\alpha]^{22.1}_D$ +46.7° (*c* 1.58, $CHCl_3$) for a 99:1 er sample. Enantiomeric purity was determined by HPLC analysis in comparison with authentic racemic material (Chiralpak AD-H, 98:2 hexanes:*i*-PrOH, 0.3 mL/min, 220 nm): t_R: 28.1 min (major) and 32.5 min (minor).

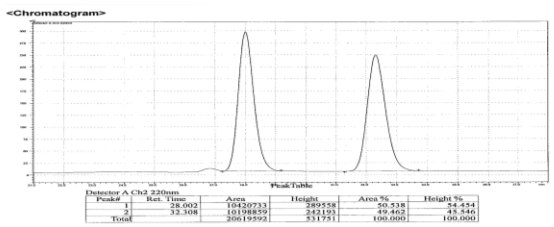

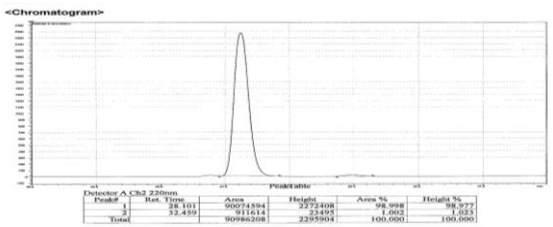

Peak #	Ret. Time	Area	Area %	Peak #	Ret. Time	Area	Area %
1	28.002	10420733	50.538	1	28.101	90074594	98.998
2	32.308	10198859	49.462	2	32.459	911614	1.002

(*R*,*Z*)-2-(4-Bromophenyl)-1,1,1-trifluorohex-4-en-2-ol (*Z*-2.46): IR (neat): 3532 (br, m), 3029 (w), 2921 (w), 1489 (w), 1159 (s), 1076 (w), 819 (w), 687 (w) cm^{-1}; **^{1}H NMR (400 MHz, $CDCl_3$):** δ 7.53 – 7.50 (m, 2H), 7.45 – 7.42 (m, 2H), 5.82 – 5.74 (m, 1H), 5.23 – 5.16 (m, 1H), 2.94 – 2.82 (m, 2H), 2.57 (s, 1H), 1.68 – 1.66 (m, 3H); **^{13}C NMR (100 MHz, $CDCl_3$):** δ 136.2, 131.4, 131.3, 128.3, 125.1 (q, J = 284.6 Hz), 122.9, 121.0, 76.2 (q, J = 28.1 Hz), 33.0, 13.1; **^{19}F NMR (376 MHz, $CDCl_3$):** δ –80.3 (s, 3F); **HRMS (DART):** Calcd for $C_{12}H_{11}F_3Br$ $[M+H–H_2O]^+$: 290.9996; Found: 290.9990; **Specific Rotation:** $[\alpha]^{22.3}_D$ +35.6° (*c* 2.52, $CHCl_3$) for a >99:1 er sample. Enantiomeric purity was determined by HPLC analysis in comparison with authentic racemic material (Chiralpak AD-H, 98:2 hexanes:*i*-PrOH, 0.3 mL/min, 220 nm): t_R: 30.4 min (major) and 37.7 min (minor).

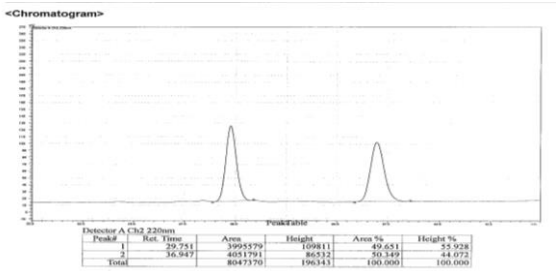

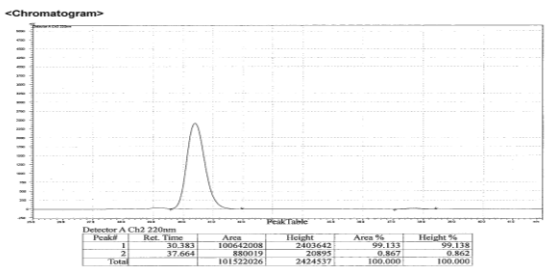

Peak #	Ret. Time	Area	Area %	Peak #	Ret. Time	Area	Area %
1	29.751	3995579	49.651	1	30.383	100642008	99.133
2	36.947	4051791	50.349	2	37.664	880019	0.867

(*R*,*Z*)-1,1,1-Trifluoro-2-(4-(trifluoromethyl)phenyl)hex-4-en-2-ol (*Z*-2.47): IR (neat): 3540 (br, m), 3032 (w), 2925 (w), 1662 (w), 1443 (w), 1326 (s), 1161 (m), 1126 (m), 1069 (m), 835 (m) cm^{-1}; **^{1}H NMR (400 MHz, $CDCl_3$):** δ 7.71 – 7.63 (m, 4H), 5.80 – 5.72 (m, 1H), 5.20 – 5.13 (m, 1H), 2.99 – 2.87 (m, 2H), 2.64 (s, 1H), 1.65 – 1.63 (m, 3H); **^{13}C NMR (100 MHz, $CDCl_3$):** δ 141.3, 134.4, 131.8, 131.3 (q, *J* = 31.9 Hz), 128.2, 127.2, 125.3 (q, *J* = 283.8 Hz), 125.4 (q, *J* = 3.8 Hz), 122.8, 121.9, 120.9, 120.1, 76.4 (q, *J* = 28.1 Hz), 33.4, 13.2; **^{19}F NMR (376 MHz, $CDCl_3$):** δ –63.6 (s, 3F), –80.0 (s, 3F); **HRMS (DART):** Calcd for $C_{13}H_{11}F_6$ $[M+H–H_2O]^+$: 281.0764; Found: 281.0771; **Specific Rotation:** $[\alpha]^{21.1}_D$ +33.6° (*c* 3.68, $CHCl_3$) for a 99:1 er sample. Enantiomeric purity was determined by HPLC analysis in comparison with authentic racemic material (Chiralpak AS-H, 99:1 hexanes:*i*-PrOH, 0.3 mL/min, 220 nm): t_R: 22.4 min (major) and 26.3 min (minor).

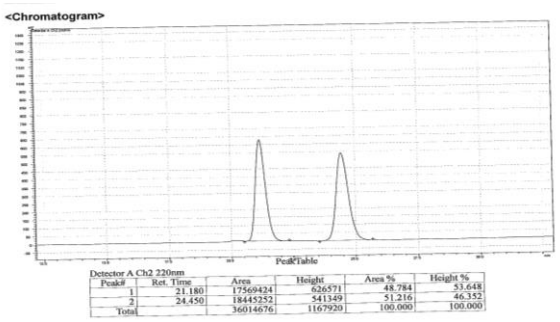

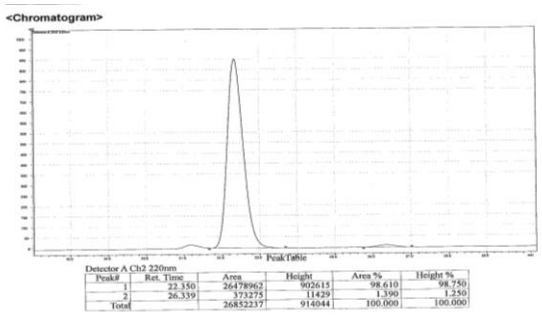

Peak #	Ret. Time	Area	Area %	Peak #	Ret. Time	Area	Area %
1	21.180	17569424	48.784	1	22.350	26478962	98.610
2	24.450	18445252	51.216	2	26.339	373275	1.390

***tert*-Butyl (*R*,*Z*)-3-(1,1,1-trifluoro-2-hydroxyhex-4-en-2-yl)-1H-indole-1-carboxylate (*Z*-2.48): IR (neat):** 3485 (br, m), 2979 (w), 1736 (m), 1452 (m), 1370 (m), 1152 (s), 1079 (m), 747 (m) cm^{-1}; **^{1}H NMR (400 MHz, $CDCl_3$):** δ 8.17 (d, *J* = 8.0 Hz, 1H), 7.82 (d, *J* = 8.0 Hz, 1H), 7.68 (s, 1H), 7.34 – 7.22 (m, 1H), 5.79 – 5.71 (m, 1H), 5.34 – 5.27

(m, 1H); 3.09 – 2.97 (m, 2H), 2.67 (s, 1H), 1.69 – 1.67 (m, 12H); **^{13}C NMR (100 MHz, $CDCl_3$):** δ 149.6, 136.0, 131.0, 128.1, 127.5 (q, *J* = 284.6 Hz), 125.6, 124.7, 123.0, 121.7, 121.6, 117.6, 115.4, 84.4, 75.6 (q, *J* = 27.3 Hz), 32.5, 28.3, 13.3; **^{19}F NMR (376 MHz, $CDCl_3$):** δ –80.4 (s, 3F); **HRMS (DART):** Calcd for $C_{19}H_{21}F_3O_2N$ $[M+H–H_2O]^+$: 352.1524; Found: 352.1509; **Specific Rotation:** $[\alpha]^{21.8}_D$ +25.8° (*c* 2.90, $CHCl_3$) for a 99:1 er sample. Enantiomeric purity was determined by HPLC analysis in comparison with authentic racemic material (Chiralpak AD-H, 98:2 hexanes:*i*-PrOH, 0.5 mL/min, 220 nm): t_R: 15.1 min (minor) and 17.3 min (major).

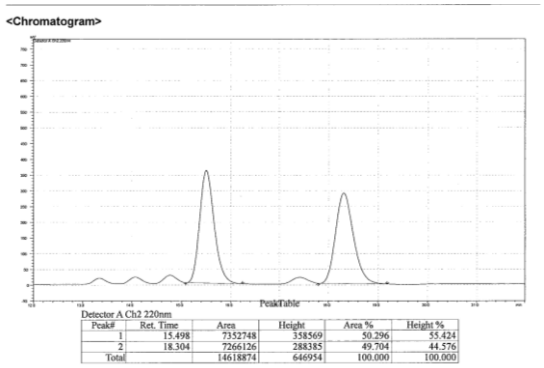

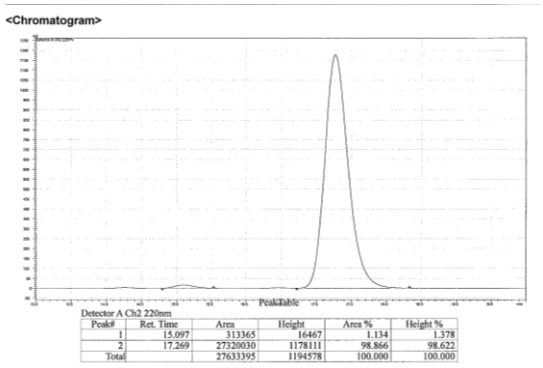

Peak #	Ret. Time	Area	Area %	Peak #	Ret. Time	Area	Area %
1	15.498	7352748	50.296	1	15.097	313365	1.134
2	18.304	7266126	49.704	2	17.269	27320030	98.866

(*R*,*Z*)-1,1,1-Trifluoro-2-(furan-2-yl)hex-4-en-2-ol (*Z*-2.49): IR (neat): 3512 (br, m), 2925 (w), 1276 (m), 1175(s), 1149 (s), 1016 (m), 742 (s), 720 (m) cm^{-1}; **^{1}H NMR (400 MHz, $CDCl_3$):** δ 7.45 (dd, *J* = 1.8, 0.8 Hz, 1H), 6.46 (dd, *J* = 3.3, 0.7 Hz, 1H), 6.42 – 6.38 (m, 1H), 5.76 – 5.71 (m, 1H), 5.31 – 5.21 (m, 1H), 2.95 – 2.81 (m, 2H), 2.79 (s, 1H), 1.67 (dd, *J* = 6.9, 1.0 Hz, 3H); **^{13}C NMR (100 MHz, $CDCl_3$):** δ 150.1, 143.2, 130.4, 124.7 (q, *J* = 283.8 Hz), 121.5, 110.1, 109.5, 74.7 (q, *J* = 29.6 Hz), 31.1, 13.2; **^{19}F NMR (376 MHz, $CDCl_3$):** δ –80.6 (s, 3F); **HRMS (DART):** Calcd for $C_{10}H_{10}F_3O_1$ $[M+H–H_2O]^+$: 203.0683; Found: 203.0693; **Specific Rotation:** $[\alpha]^{20.0}_D$ +24.9° (*c* 1.00, $CHCl_3$)

for a 85:15 er sample. Enantiomeric purity was determined by HPLC analysis in comparison with authentic racemic material (Chiralpak AZ-H, 99:1 hexanes:*i*-PrOH, 0.5 mL/min, 220 nm): t_R: 46.4 min (minor) and 52.6 min (major).

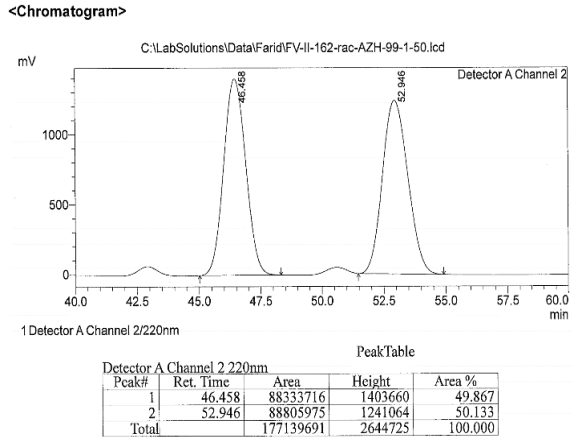

PeakTable

Detector A Channel 2 220nm

Peak#	Ret. Time	Area	Height	Area %
1	46.458	88333716	1403660	49.867
2	52.946	88805975	1241064	50.133
Total		177139691	2644725	100.000

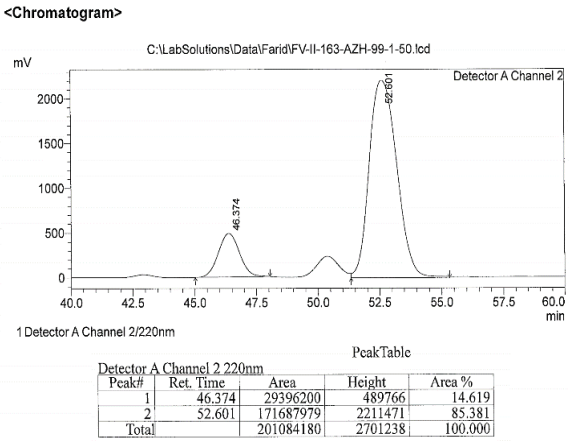

PeakTable

Detector A Channel 2 220nm

Peak#	Ret. Time	Area	Height	Area %
1	46.374	29396200	489766	14.619
2	52.601	171687979	2211471	85.381
Total		201084180	2701238	100.000

Peak #	Ret. Time	Area	Area %	Peak #	Ret. Time	Area	Area %
1	46.458	88333716	49.867	1	46.374	29396200	14.619
2	52.946	88805975	50.133	2	52.601	171687979	85.381

(*R*,*Z*)-1,1,1-Trifluoro-2-(furan-3-yl)hex-4-en-2-ol (*Z*-2.50): IR (neat): 3539 (br, m), 2924 (w), 1504 (w), 1214 (s), 1076 (m), 1023 (m), 876 (m), 799 (m), 601 (m) cm^{-1}; **^{1}H NMR (400 MHz, $CDCl_3$):** δ 7.56 (s, 1H), 7.42 (t, *J* = 1.6 Hz, 1H), 6.43 (s, 1H), 5.81 – 5.71 (m, 1H), 5.35 – 5.28 (m, 1H), 2.87 – 2.66 (m, 2H), 2.44 (s, 1H), 1.65 (d, *J* = 6.4 Hz, 3H); **^{13}C NMR (100 MHz, $CDCl_3$):** δ 143.7, 141.3, 130.8, 125.5 (q, *J* = 283.1 Hz), 123.9, 121.6, 109.1, 74.0 (q, *J* = 29.6 Hz), 33.2, 13.3; **^{19}F NMR (376 MHz, $CDCl_3$):** δ –81.65 (s, 3F); **HRMS (DART):** Calcd for $C_{10}H_{10}F_3O_1$ $[M+H–H_2O]^+$: 203.0683; Found: 203.0682; **Specific Rotation:** $[\alpha]^{20.0}_D$ +25.3° (*c* 0.95, $CHCl_3$) for a 99:1 er sample. Enantiomeric purity was determined by HPLC analysis in comparison with authentic racemic material (Chiralpak AZ-H, 99:1 hexanes:*i*-PrOH, 0.5 mL/min, 220 nm): t_R: 59.0 min (minor) and 61.7 min (major).

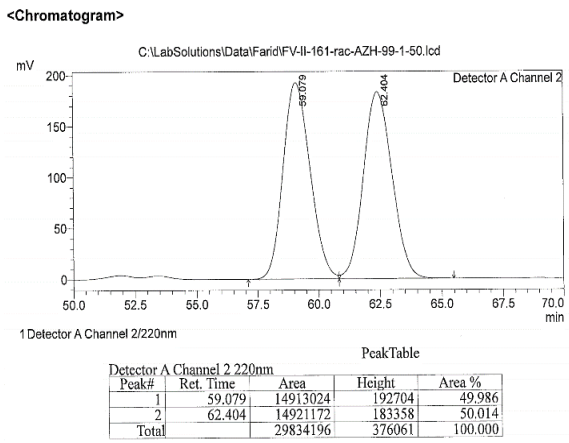

PeakTable

Detector A Channel 2 220nm

Peak#	Ret. Time	Area	Height	Area %
1	59.079	14913024	192704	49.986
2	62.404	14921172	183358	50.014
Total		29834196	376061	100.000

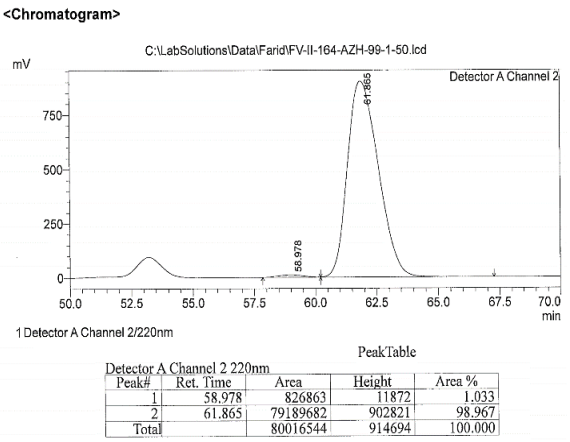

PeakTable

Detector A Channel 2 220nm

Peak#	Ret. Time	Area	Height	Area %
1	58.978	826863	11872	1.033
2	61.865	79189682	902821	98.967
Total		80016544	914694	100.000

Peak #	Ret. Time	Area	Area %	Peak #	Ret. Time	Area	Area %
1	59.079	14913024	49.986	1	58.978	826863	1.033
2	62.404	14921172	50.014	2	61.865	79189682	98.967

(*S*,*Z*)-1,1,1-Trifluoro-2-(thiophen-2-yl)hex-4-en-2-ol (*Z*-2.51): IR (neat): 3519 (br, m), 3029 (w), 2920 (w), 1407 (w), 1275 (w), 1166 (s), 745 (m) cm $^{-1}$; **^{1}H NMR (400 MHz, $CDCl_3$):** δ 7.36 – 7.34 (m, 1H), 7.14 – 7.13 (m, 1H), 7.06 – 7.04 (m, 1H), 5.86 – 5.77 (m, 1H), 5.34 – 5.27 (m, 1H), 3.02 – 2.83 (m, 2H), 2.79 (s, 1H), 1.69 – 1.67 (m, 3H); **^{13}C NMR (100 MHz, $CDCl_3$):** δ 141.4, 131.4, 127.1, 126.1, 125.7, 124.8 (q, J = 283.9 Hz), 121.0, 76.1 (q, J = 28.0 Hz), 34.1, 13.1; **^{19}F NMR (376 MHz, $CDCl_3$):** δ –81.3 (s, 3F); **HRMS (DART):** Calcd for $C_{10}H_{10}F_3S$ $[M+H–H_2O]^+$: 219.0455; Found: 219.0464; **Specific Rotation:** $[\alpha]^{21.1}_D$ +41.6° (*c* 1.80, $CHCl_3$) for a 98:2 er sample. Enantiomeric purity was determined by HPLC analysis in comparison with authentic racemic material (Chiralpak AS-H, 99:1 hexanes:*i*-PrOH, 0.3 mL/min, 220 nm): t_R: 28.7 min (major) and 33.7 min (minor).

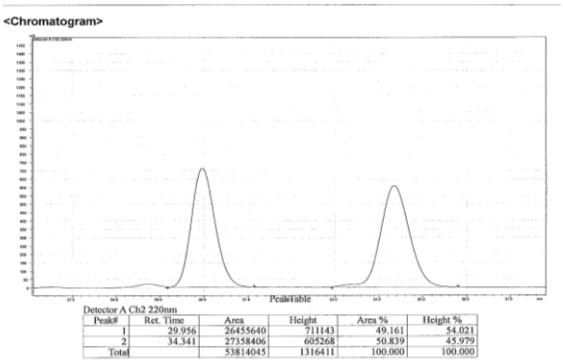

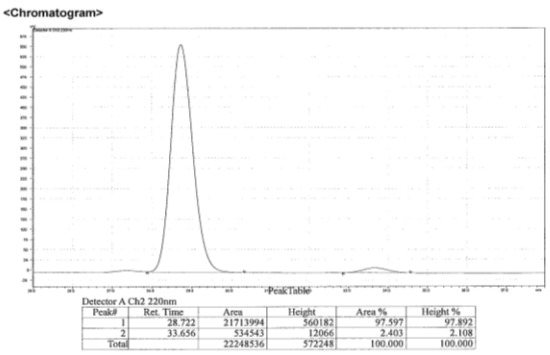

Peak #	Ret. Time	Area	Area %	Peak #	Ret. Time	Area	Area %
1	29.956	26455640	49.161	1	28.722	21713994	97.597
2	34.341	27358406	50.839	2	33.656	534543	2.403

(*R*,*Z*)-1,1,1-Trifluoro-2-(thiophen-3-yl)hex-4-en-2-ol (*Z*-2.52): IR (neat): 3519 (br, m), 3029 (w), 2923 (w), 1440 (w), 1214 (w), 1154 (m), 711 (w) cm^{-1}; **^{1}H NMR (400 MHz, $CDCl_3$):** δ 7.40 – 7.39 (m, 1H), 7.33 – 7.31 (m, 1H), 7.12 (d, *J* = 4.8 Hz, 1H), 5.78 – 5.69 (m, 1H), 5.25 – 5.19 (m, 1H), 2.91 – 2.76 (m, 2H), 2.56 (s, 1H), 1.64 – 1.61 (m, 3H); **^{13}C NMR (100 MHz, $CDCl_3$):** δ 139.0, 130.9, 126.2, 126.1, 125.1 (q, *J* = 283.9 Hz), 123.8, 121.6, 76.0 (q, *J* = 28.0 Hz), 33.6, 13.2; **^{19}F NMR (376 MHz, $CDCl_3$):** δ –80.8 (s, 3F); **HRMS (DART):** Calcd for $C_{10}H_{10}F_3S$ $[M+H–H_2O]^+$: 219.0455; Found: 219.0464; **Specific Rotation:** $[\alpha]^{21.1}_D$ +35.7° (*c* 1.40, $CHCl_3$) for a >99:1 er sample. Enantiomeric purity was determined by HPLC analysis in comparison with authentic racemic material (Chiralpak AS-H, 98:2 hexanes:*i*-PrOH, 0.3 mL/min, 220 nm): t_R: 23.9 min (major) and 26.6 min (minor).

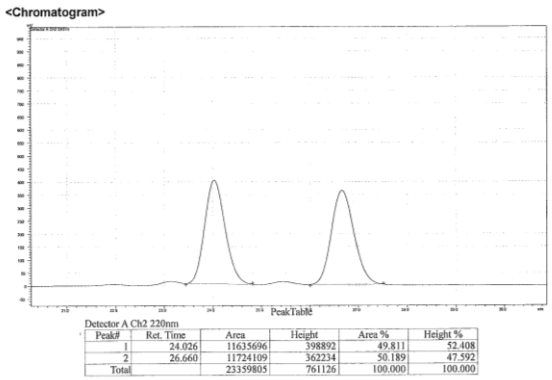

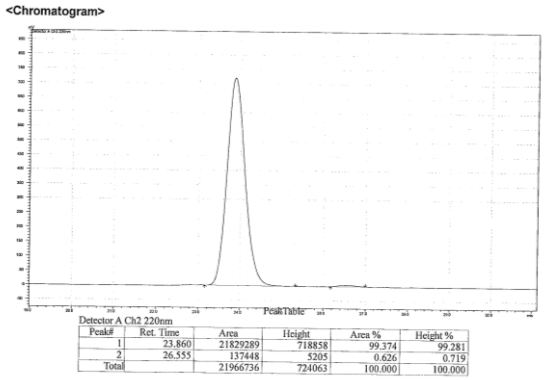

Peak #	Ret. Time	Area	Area %	Peak #	Ret. Time	Area	Area %
1	24.026	11635696	49.811	1	23.860	21829289	99.374
2	26.660	11724109	50.189	2	26.555	137448	0.626

(*R*,*Z*)-1,1,1-Trifluoro-2-(pyridin-3-yl)hex-4-en-2-ol (*Z*-2.53): IR (neat): 3031 (w), 2923 (w), 2859 (w), 1596 (w), 1582 (w), 1424 (w), 1270 (w), 1158 (s), 720 (m) cm^{-1}; **^{1}H NMR (400 MHz, $CDCl_3$):** δ 8.76 (d, *J* = 2.4 Hz, 1H), 8.54 – 8.52 (m, 1H), 7.94 – 7.92 (m, 1H), 7.33 – 7.30 (m, 1H), 5.70 – 5.62 (m, 1H), 5.23 – 5.16 (m, 1H), 4.65 (s, 1H), 2.91 (d, *J* = 7.2 Hz, 2H), 1.58 – 1.56 (m, 3H); **^{13}C NMR (100 MHz, $CDCl_3$):** δ 149.2, 148.0, 135.2, 133.6, 130.7, 125.5 (q, *J* = 284.6 Hz), 123.4, 123.3, 121.2, 75.6 (q, *J* = 28.1 Hz), 32.9, 13.2; **^{19}F NMR (376 MHz, $CDCl_3$):** δ –80.3 (s, 3F); **HRMS (DART):** Calcd for $C_{11}H_{13}F_3NO$ $[M+H]^+$: 232.0949; Found: 232.0952; **Specific Rotation:** $[\alpha]^{20.5}_D$ +15.9° (*c* 1.89, $CHCl_3$) for a 97:3 er sample. Enantiomeric purity was determined by HPLC analysis in comparison with authentic racemic material (Chiralpak AS-H, 95:5 hexanes:*i*-PrOH, 0.5 mL/min, 254 nm): t_R: 23.3 min (major) and 37.2 min (minor).

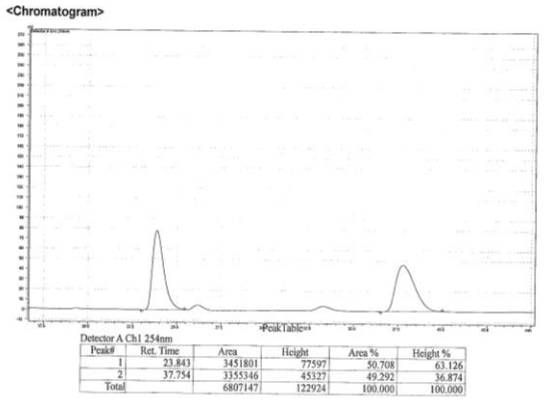

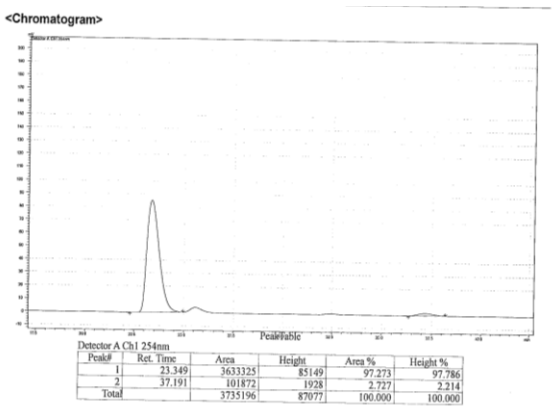

Peak #	Ret. Time	Area	Area %	Peak #	Ret. Time	Area	Area %
1	23.843	3451801	50.708	1	23.349	3633325	97.273
2	37.754	3355346	49.292	2	37.191	101872	2.727

(*S*,*Z*)-1-Phenyl-4-(trifluoromethyl)oct-6-en-4-ol (*Z*-2.54): IR (neat): 3466 (br, m), 3027 (w), 2925 (w), 2856 (w), 1496 (w), 1453 (w), 1161 (s), 750 (m), 699 (m) cm^{-1}; **^{1}H NMR (400 MHz, $CDCl_3$):** δ 7.31 – 7.28 (m, 2H), 7.22 – 7.18 (m, 3H), 5.79 – 5.72 (m, 1H), 5.46 – 5.39 (m, 1H), 2.66 – 2.63 (m, 2H), 2.56 – 2.38 (m, 2H), 2.08 (s, 1H), 1.82 – 1.69 (m, 4H), 1.65 (d, *J* = 8.0 Hz, 3H); **^{13}C NMR (100 MHz, $CDCl_3$):** δ 141.8, 129.8, 128.6, 128.5, 126.6 (q, *J* = 285.1 Hz), 126.1, 122.2, 75.2 (q, *J* = 27.0 Hz), 36.3, 33.7, 31.1, 29.8, 24.7, 13.1; **^{19}F NMR (376 MHz, $CDCl_3$):** δ –80.51 (s, 3F); **HRMS (DART):** Calcd for $C_{15}H_{20}F_3O$ $[M+H]^+$: 273.1466; Found: 273.1464; **Specific Rotation:** $[\alpha]^{20.0}_D$ – 1.50° (*c* 0.70, $CHCl_3$) for a 96:4 er sample. Enantiomeric purity was determined by HPLC analysis in comparison with authentic racemic material (Chiralcel OD-H, 99:1 hexanes:*i*-PrOH, 0.6 mL/min, 220 nm): t_R: 19.5 min (major) and 28.6 min (minor).

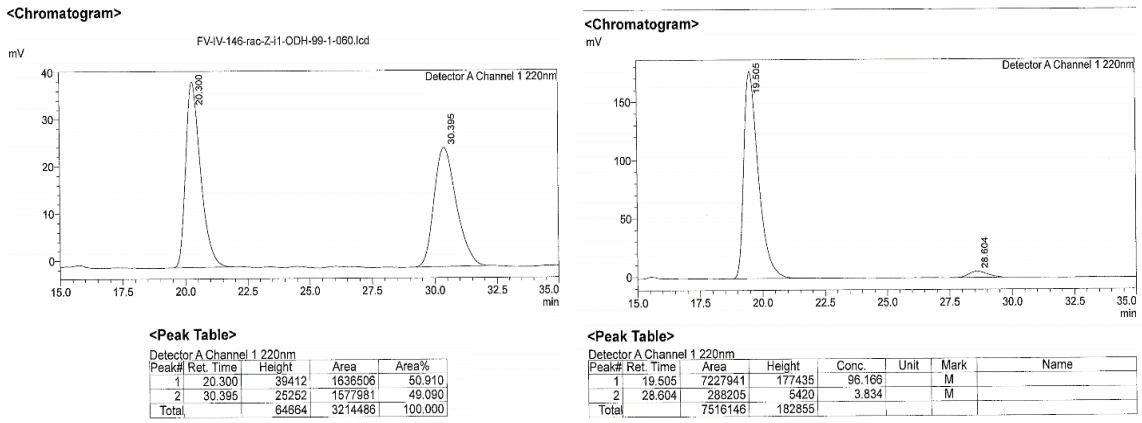

Peak #	Ret. Time	Area	Area %	Peak #	Ret. Time	Area	Area %
1	20.300	1636506	50.910	1	19.505	7227941	96.166
2	30.395	1577981	49.090	2	28.604	288205	3.834

(*R*,*Z*)-2-Benzyl-1,1,1-trifluorohex-4-en-2-ol (*Z*-2.55): IR (neat): 3529 (br, m), 3032 (w), 2918 (w), 2849 (w), 1497 (w), 1455 (w), 1165 (s), 709 (m) cm $^{-1}$; **^{1}H NMR (400 MHz, $CDCl_3$):** δ 7.34 – 7.24 (m, 5H), 5.78 – 5.70 (m, 1H), 5.46 – 5.39 (m, 1H), 3.15 – 2.86 (m, 2H), 2.49 – 2.34 (m, 2H), 2.24 (s, 1H), 1.46 (d, *J* = 7.2 Hz, 3H); **^{13}C NMR (100 MHz, $CDCl_3$):** δ 134.6, 131.1, 130.4, 128.4, 127.3, 126.5 (q, *J* = 285.4 Hz), 122.3, 75.1 (q, *J* = 25.8 Hz), 39.6, 31.0, 12.8; **^{19}F NMR (376 MHz, $CDCl_3$):** δ –80.0 (s, 3F); **HRMS (DART):** Calcd for $C_{13}H_{16}F_3O$ $[M+H]^+$: 245.1153; Found: 245.1158; **Specific Rotation:** $[\alpha]^{19.9}_D$ –20.4° (*c* 1.21, $CHCl_3$) for a 96:4 er sample. Enantiomeric purity was determined by HPLC analysis in comparison with authentic racemic material (Chiralcel OD-H, 99:1 hexanes:*i*-PrOH, 0.2 mL/min, 220 nm): t_R: 48.4 min (major) and 56.6 min (minor).

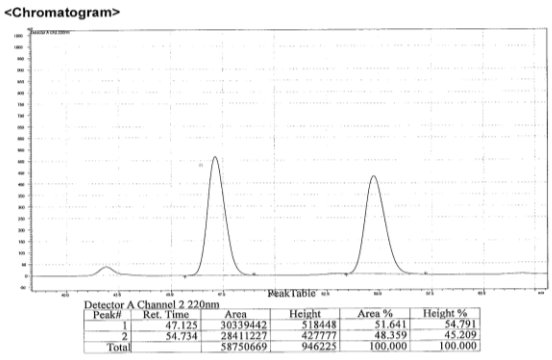

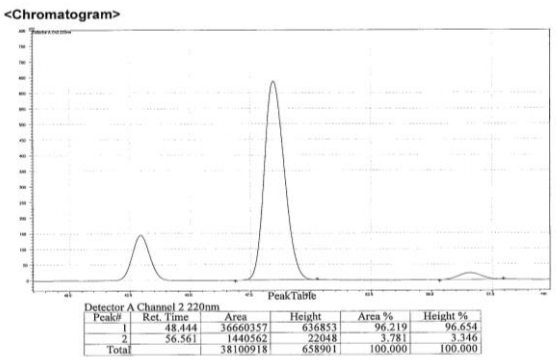

Peak #	Ret. Time	Area	Area %	Peak #	Ret. Time	Area	Area %
1	47.125	30339442	51.641	1	48.444	36660357	96.219
2	54.734	28411227	48.359	2	56.561	1440562	3.781

(*R*,*Z*)-2-Cyclohexyl-1,1,1-trifluorohex-4-en-2-ol (*Z*-2.56): IR (neat): 3537 (br, m), 2928 (w), 2856 (w), 1454 (w), 1159 (m), 771 (w), cm^{-1}; **^{1}H NMR (400 MHz, $CDCl_3$):** δ 5.82 – 5.74 (m, 1H), 5.48 – 5.41 (m, 1H), 2.58 – 2.34 (m, 2H), 2.21 (s, 1H), 1.92 – 1.64 (m, 9H), 1.29 – 1.08 (m, 5H); **^{13}C NMR (100 MHz, $CDCl_3$):** δ 130.3, 126.9 (q, J = 286.9 Hz), 122.5, 76.7 (t, J = 25.1 Hz), 43.2, 29.1, 27.1, 26.8, 26.7, 26.5, 13.1; **^{19}F NMR (376 MHz, $CDCl_3$):** δ –75.4 (m, 3F); **HRMS (DART):** Calcd for $C_{12}H_{18}F_3$ $[M+H–H_2O]^+$: 219.1360; Found: 219.1368; **Specific Rotation:** $[\alpha]^{20.8}_D$ +6.43° (*c* 2.02, $CHCl_3$) for a 90:10 er sample. Enantiomeric purity was determined by HPLC analysis in comparison with authentic racemic material (Chiralpak AD-H, hexanes, 0.1 mL/min, 254 nm): t_R: 45.8 min (minor) and 49.6 min (major).[28]

(28) Note: the optical rotation and enantiomeric ratio were determined for the corresponding benzoate derivative.

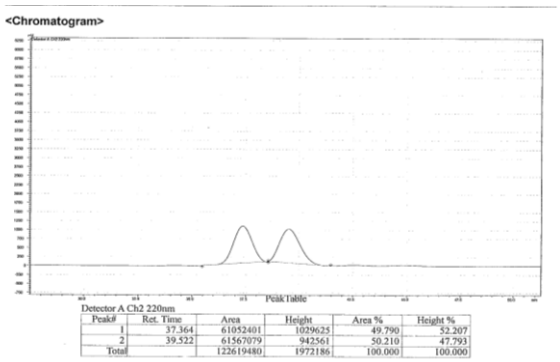

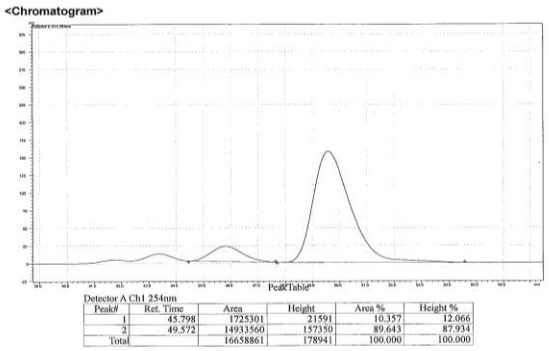

Peak #	Ret. Time	Area	Area %	Peak #	Ret. Time	Area	Area %
1	37.364	61052401	49.790	1	45.798	1725301	10.357
2	39.522	61567079	50.210	2	49.572	14933560	89.643

(*R*,1*E*,5*Z*)-1-Phenyl-3-(trifluoromethyl)hepta-1,5-dien-3-ol (*Z*-2.57): IR (neat): 3477 (br, m), 3029 (w), 2923 (w), 1449 (w), 1167 (s), 1138 (s), 970 (m), 749 (m), 690 (m) cm^{-1}; **^{1}H NMR (400 MHz, $CDCl_3$):** δ 7.42 – 7.24 (m, 5H), 6.85 (d, *J* = 16.0 Hz, 1H), 6.20 (d, *J* = 16.0 Hz, 1H), 5.82 – 5.73 (m, 1H), 5.45 – 5.38 (m, 1H), 2.76 – 2.54 (m, 2H), 2.30 (s, 1H), 1.67 – 1.65 (m, 3H); **^{13}C NMR (100 MHz, $CDCl_3$):** δ 135.8, 133.2, 130.4, 128.8, 128.5, 126.9, 125.5 (q, *J* = 283.8 Hz), 125.0, 121.5, 75.9 (q, *J* = 27.3 Hz), 32.5, 13.2; **^{19}F NMR (376 MHz, $CDCl_3$):** δ –80.4 (s, 3F); **HRMS (DART):** Calcd for $C_{14}H_{14}F_3$ $[M+H–H_2O]^+$: 239.1047; Found: 239.1056; **Specific Rotation:** $[\alpha]^{21.1}_D$ +119.0° (*c* 2.13, $CHCl_3$) for a 99:1 er sample. Enantiomeric purity was determined by HPLC analysis in comparison with authentic racemic material (Chiralpak AS-H, 99:1 hexanes:*i*-PrOH, 0.3 mL/min, 220 nm): t_R: 31.6 min (major) and 34.7 min (minor).

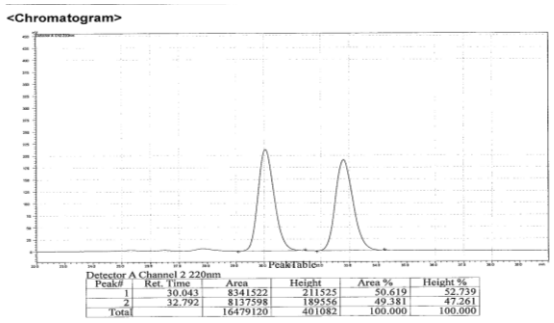

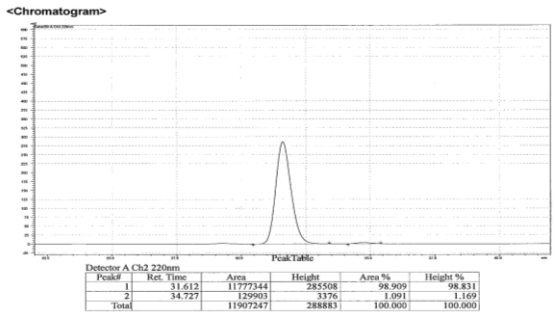

Peak #	Ret. Time	Area	Area %	Peak #	Ret. Time	Area	Area %
1	30.043	8341522	50.619	1	31.612	11777344	98.909
2	32.792	8137598	49.381	2	34.727	129903	1.091

(*R*,1*E*,5*Z*)-1-(4-Methoxyphenyl)-3-(trifluoromethyl)hepta-1,5-dien-3-ol (*Z*-2.58): IR (neat): 3466 (br, m), 2958 (w), 1607 (w), 1512 (s), 1248 (s), 1139 (s), 1032 (m), 817 (w) cm^{-1}; **^{1}H NMR (400 MHz, $CDCl_3$):** δ 7.41 – 7.30 (m, 2H), 6.92 – 6.82 (m, 2H), 6.79 (d, *J* = 16.0 Hz, 1H), 6.06 (dd, *J* = 16.0, 0.7 Hz, 1H), 5.84 – 5.67 (m, 1H), 5.42 (dddd, *J* = 9.0, 2.8, 1.9, 1.0 Hz, 1H), 3.82 (s, 3H), 2.73 (dd, *J* = 14.5, 8.0 Hz, 1H), 2.56 (dd, *J* = 14.6, 7.1 Hz, 1H), 2.26 (s, 1H), 1.82 – 1.61 (m, 3H); **^{13}C NMR (100 MHz, $CDCl_3$):** 159.9, 132.5, 130.2, 128.6, 128.2, 125.5 (q, *J*=284 Hz), 122.7, 121.7, 114.2, 75.9 (q, *J* = 28.0 Hz), 55.4, 32.5, 13.2; **^{19}F NMR (376 MHz, $CDCl_3$):** δ –81.5 (s, 3F); **HRMS (DART):** Calcd for $C_{15}H_{16}F_3O$ $[M+H–H_2O]^+$: 269.1153; Found: 269.1159; **Specific Rotation:** $[\alpha]^{25.0}_D$ +80.65° (*c* 1.28, $CHCl_3$) for a 99:1 er sample. Enantiomeric purity was determined by HPLC analysis in comparison with authentic racemic material (Chiralpak AS-H, 99:1 hexanes:*i*-PrOH, 0.3 mL/min, 254 nm): t_R: 54.9 min (major) and 74.8 min (minor).

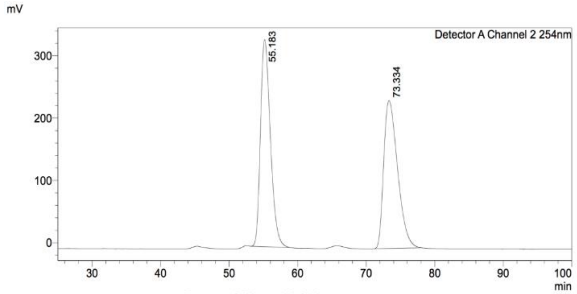

Detector A Channel 2 254nm

Peak#	Ret. Time	Area	Area%
1	55.183	33401982	49.986
2	73.334	33421035	50.014
Total		66823017	100.000

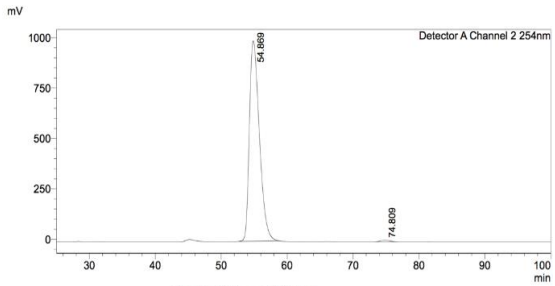

Detector A Channel 2 254nm

Peak#	Ret. Time	Area	Area%
1	54.869	104613229	99.244
2	74.809	796696	0.756
Total		105409926	100.000

Peak #	Ret. Time	Area	Area %	Peak #	Ret. Time	Area	Area %
1	55.183	33401982	49.986	1	54.869	104513229	99.244
2	73.334	33421035	50.014	2	74.809	796696	0.756

(*R*,1*E*,5*Z*)-3-(Trifluoromethyl)-1-(4-(trifluoromethyl)phenyl)hepta-1,5-dien-3-ol (*Z*-2.59): IR (neat): 3494 (br, m), 2924 (w), 1618 (w), 1324 (s), 1167 (s), 1126 (s), 1017

(m), 819 (w) cm^{-1}; **^{1}H NMR (400 MHz, $CDCl_3$):** δ 7.60 (d, *J* = 8.3 Hz, 2H), 7.54 – 7.41 (m, 2H), 6.91 (d, *J* = 16.0 Hz, 2H), 6.30 (d, *J* = 16.0 Hz, 1H), 5.94 – 5.65 (m, 1H), 5.40 (ddddd, *J* = 9.9, 8.1, 6.3, 1.8, 0.9 Hz, 1H), 2.75 (dd, *J* = 14.7, 7.9 Hz, 1H), 2.64 – 2.49 (m, 1H), 2.34 (s, 1H), 1.67 (d, *J* = 6.9 Hz, 3H); **^{13}C NMR (100 MHz, $CDCl_3$):** δ 139.3, 131.9, 130.8, 130.2 (q, *J* = 32.6 Hz), 127.7, 127.1, 125.2 (q, *J* = 285.6 Hz), 124.2 (q, *J* = 271.9 Hz), 125.8 (q, *J* = 3.8 Hz), 121.2, 75.8 (q, *J* = 28.2 Hz), 32.5, 13.2; **^{19}F NMR (376 MHz, $CDCl_3$):** δ –62.6 (s, 3F), –80.4 (s, 3F); **HRMS (DART):** Calcd for $C_{15}H_{13}F_6$ $[M+H–H_2O]^+$: 307.0921; Found: 307.0911; **Specific Rotation:** $[\alpha]^{26.6}_D$ +17.37° (*c* 1.15, $CHCl_3$) for a 99:1 er sample. Enantiomeric purity was determined by HPLC analysis in comparison with authentic racemic material (Chiralpak AS-H, 99:1 hexanes:*i*-PrOH, 0.3 mL/min, 254 nm): t_R: 31.6 min (major) and 34.7 min (minor).

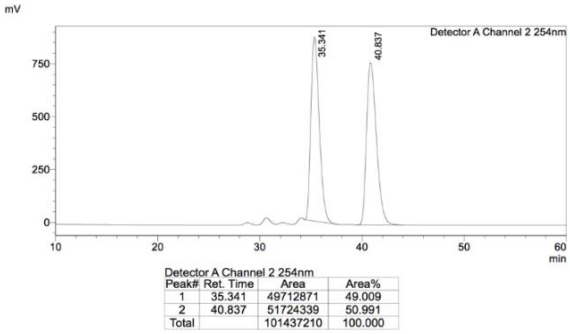

Detector A Channel 2 254nm

Peak#	Ret. Time	Area	Area%
1	35.341	49712871	49.009
2	40.837	51724339	50.991
Total		101437210	100.000

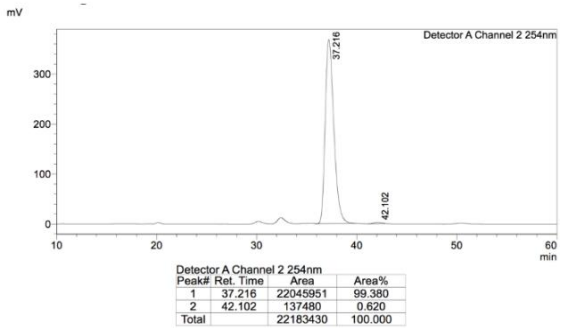

Detector A Channel 2 254nm

Peak#	Ret. Time	Area	Area%
1	37.216	22045951	99.380
2	42.102	137480	0.620
Total		22183430	100.000

Peak #	Ret. Time	Area	Area %	Peak #	Ret. Time	Area	Area %
1	35.341	49712871	49.009	1	37.216	22045951	99.380
2	40.837	51724339	50.991	2	42.102	137480	0.620

(*R*,*Z*)-1-Phenyl-3-(trifluoromethyl)hept-5-en-1-yn-3-ol (*Z*-2.60): IR (neat): 3457 (br, m), 3028 (w), 2927 (w), 2235 (w), 1599 (w), 1275 (m), 1018 (m), 757 (w) cm^{-1}; **^{1}H NMR (400 MHz, $CDCl_3$):** δ 7.46 – 7.44 (m, 2H), 7.38 – 7.29 (m, 3H), 5.87 – 5.79 (m, 2H), 5.69 – 5.62 (m, 2H), 2.77 – 2.66 (m, 2H), 2.64 (s, 1H), 1.71 – 1.69 (m, 3H); **^{13}C NMR (100 MHz, $CDCl_3$):** δ 132.1, 130.0, 129.4, 128.5, 124.1 (q, *J* = 283.9 Hz), 121.9, 121.3,

87.5, 83.7, 71.9 (q, J = 31.2 Hz), 33.1, 13.3; **^{19}F NMR (376 MHz, $CDCl_3$):** δ –82.0 (m, 3F); **HRMS (DART):** Calcd for $C_{14}H_{14}F_3O$ $[M+H–H_2O]^+$: 255.0996; Found: 255.1006; **Specific Rotation:** $[\alpha]^{21.3}_D$ +38.9° (*c* 1.64, $CHCl_3$) for a 81:19 er sample. Enantiomeric purity was determined by HPLC analysis in comparison with authentic racemic material (Chiralpak AS-H, 99:1 hexanes:*i*-PrOH, 0.3 mL/min, 220 nm): t_R: 33.9 min (minor) and 36.3 min (major).

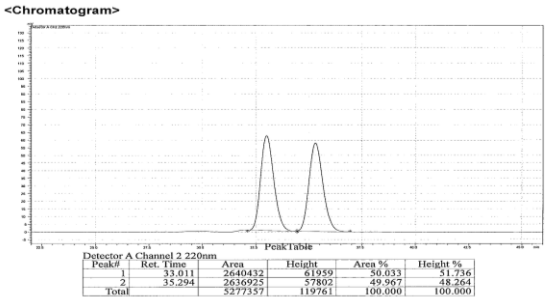

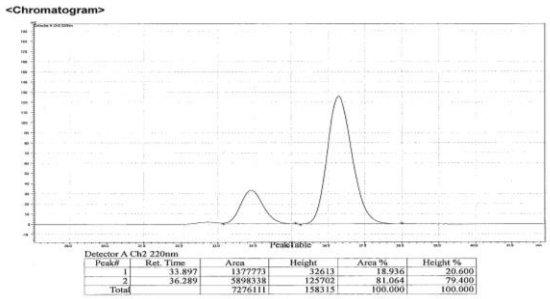

Peak #	Ret. Time	Area	Area %	Peak #	Ret. Time	Area	Area %
1	33.011	2640432	50.033	1	33.897	1377773	18.936
2	35.294	2636925	49.967	2	36.289	5898338	81.064

(*R*,*Z*)-1-(4-Methoxyphenyl)-3-(trifluoromethyl)hept-5-en-1-yn-3-ol (*Z*-2.61): IR (neat): 3446 (br, m), 2922 (w), 1606 (w), 1510 (m), 1275 (m), 1174 (s), 832 (w) cm^{-1}; **^{1}H NMR (400 MHz, $CDCl_3$):** δ 7.43 – 7.32 (m, 2H), 6.98 – 6.75 (m, 2H), 5.83 (dqt, J = 10.9, 6.7, 1.5 Hz, 1H), 5.76 – 5.58 (m, 1H), 3.82 (s, 3H), 2.78 – 2.65 (m, 2H), 2.63 (d, J = 0.8 Hz, 1H), 1.71 (ddt, J = 6.8, 1.7, 0.8 Hz, 3H); **^{13}C NMR (100 MHz, $CDCl_3$):** δ 160.4, 133.6, 129.8, 124.1 (q, J = 284.9 Hz), 122.0, 114.1, 113.3, 87.5, 82.4, 71.9 (q, J = 31.2 Hz), 55.4, 33.2, 13.3; **^{19}F NMR (376 MHz, $CDCl_3$):** δ –82.0 (m, 3F); **HRMS (DART):** Calcd for $C_{15}H_{16}F_3O_2$ $[M+H]^+$: 285.1102; Found: 285.1091; **Specific Rotation:** $[\alpha]^{26.7}_D$ – 18.8° (*c* 1.06, $CHCl_3$) for a 82:18 er sample. Enantiomeric purity was determined by

HPLC analysis in comparison with authentic racemic material (Chiralpak AD-H, 98:2 hexanes:*i*-PrOH, 0.3 mL/min, 254 nm): t_R: 63.5 min (minor) and 73.3 min (major).

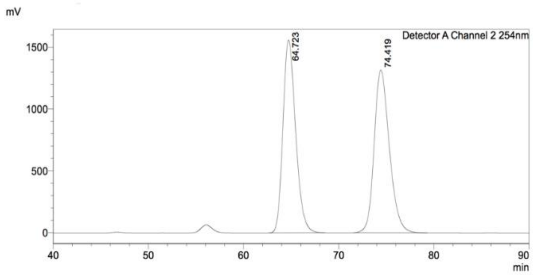

Detector A Channel 2 254nm

Peak#	Ret. Time	Area	Area%
1	64.723	144625148	49.688
2	74.419	146440346	50.312
Total		291065494	100.000

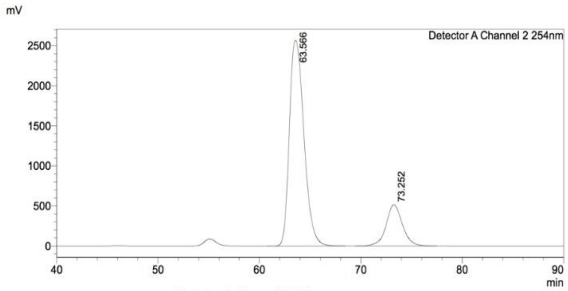

Detector A Channel 2 254nm

Peak#	Ret. Time	Area	Area%
1	63.566	255660259	81.633
2	73.252	57522537	18.367
Total		313182797	100.000

Peak #	Ret. Time	Area	Area %	Peak #	Ret. Time	Area	Area %
1	64.723	144625148	49.688	1	63.566	255660259	81.633
2	74.419	146440346	50.312	2	73.252	57522537	18.367

(*R*,*Z*)-3-(trifluoromethyl)-1-(4-(trifluoromethyl)phenyl)hept-5-en-1-yn-3-ol (*Z*-2.62): **IR (neat):** 3441 (br, m), 2925 (w), 1616 (w), 1332 (s), 1276 (w), 1171 (m), 1129 (m), 843 (w) cm^{-1}; **^{1}H NMR (400 MHz, $CDCl_3$):** δ 7.84 – 7.41 (m, 5H), 5.86 (ddt, *J* = 10.9, 6.8, 1.5 Hz, 1H), 5.69 – 5.50 (m, 1H), 2.89 – 2.67 (m, 2H), 2.65 (s, 1H), 1.85 – 1.61 (m, 3H); **^{13}C NMR (100 MHz, $CDCl_3$):** δ 159.9, 132.5, 130.2, 128.6, 128.2, 125.5 (q, *J* = 284.0 Hz), 122.7, 121.7, 114.2, 75.9 (q, *J* = 28.0 Hz), 55.4, 32.5, 13.2; **^{19}F NMR (376 MHz, $CDCl_3$):** δ –64.0 (m, 3F), –81.9 (m, 3F); **HRMS (DART):** Calcd for $C_{15}H_{13}F_6O$ $[M+H]^+$: 323.0871; Found: 323.0869; **Specific Rotation:** $[\alpha]^{26.7}_D$ –18.6° (*c* 1.07, $CHCl_3$) for a 85:15 er sample. Enantiomeric purity was determined by HPLC analysis in comparison with authentic racemic material (Chiralpak AS-H, 99:1 hexanes:*i*-PrOH, 0.3 mL/min, 254 nm): t_R: 32.0 min (minor) and 37.4 min (major).

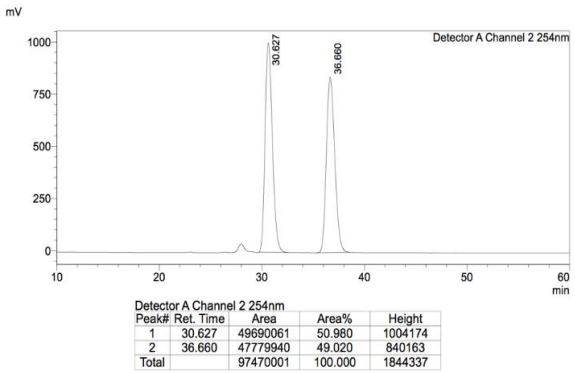

Detector A Channel 2 254nm

Peak#	Ret. Time	Area	Area%	Height
1	30.627	49690061	50.980	1004174
2	36.660	47779940	49.020	840163
Total		97470001	100.000	1844337

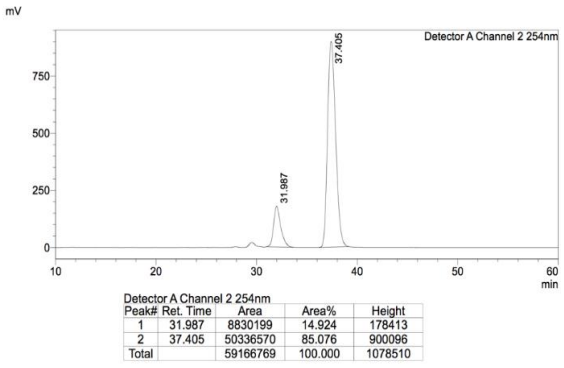

Detector A Channel 2 254nm

Peak#	Ret. Time	Area	Area%	Height
1	31.987	8830199	14.924	178413
2	37.405	50336570	85.076	900096
Total		59166769	100.000	1078510

Peak #	Ret. Time	Area	Area %	Peak #	Ret. Time	Area	Area %
1	30.627	49690061	50.980	1	31.987	8830199	14.924
2	36.660	47779940	49.020	2	37.405	50336570	85.076

(*R*,*Z*)-1,1,1,2,2-Pentafluoro-3-phenylhept-5-en-3-ol (*Z*-2.72): IR (neat): 3538 (br, m), 3031 (w), 2927 (w), 1497 (w), 1339 (w), 1214 (m), 1174 (m), 750 (w) cm^{-1}; **^{1}H NMR (400 MHz, $CDCl_3$):** δ 7.55 (d, *J* = 8.4 Hz, 2H), 7.41 – 7.33 (m, 3H), 5.79 – 5.70 (m, 1H), 5.11 – 5.03 (m, 1H), 3.11 – 2.89 (m, 2H), 2.54 (s, 1H), 1.67 (d, *J* = 6.8 Hz, 3H); **^{13}C NMR (100 MHz, $CDCl_3$):** δ 137.2, 131.6, 128.5, 128.4, 126.6, 121.5, 121.1-120.4 (m), 118.2-116.8 (m), 115.3-114.2 (m), 112.6-111.5 (m), 108.2-107.1 (m), 76.7 (q, *J* = 23.5 Hz), 33.3, 13.3; **^{19}F NMR (376 MHz, $CDCl_3$):** δ –78.1 (s, 3F), –121.7 (m, 3F); **HRMS (DART):** Calcd for $C_{13}H_{12}F_5$ $[M+H–H_2O]^+$: 263.0859; Found: 263.0852; **Specific Rotation:** $[\alpha]^{22.1}_D$ +35.7° (*c* 1.90, $CHCl_3$) for a >99:1 er sample. Enantiomeric purity was determined by HPLC analysis in comparison with authentic racemic material (Chiralpak AD-H, 99:1 hexanes:*i*-PrOH, 0.2 mL/min, 220 nm): t_R: 34.4 min (minor) and 37.8 min (major).

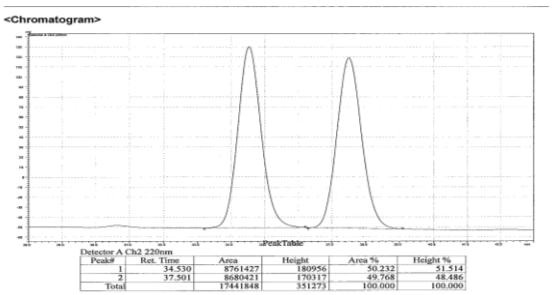

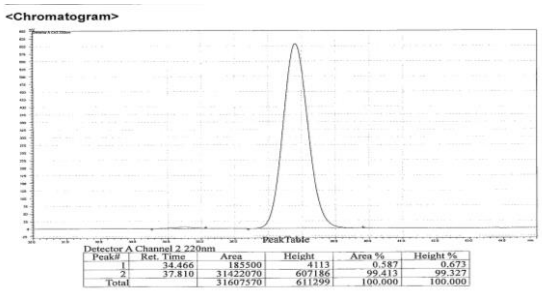

Peak #	Ret. Time	Area	Area %	Peak #	Ret. Time	Area	Area %
1	34.530	8761427	50.232	1	34.466	185500	0.587
2	37.504	8680421	49.768	2	37.810	31422070	99.413

(*R*,*Z*)-1,1,1,2,2,3,3-Heptafluoro-4-phenyloct-6-en-4-ol (*Z*-2.73): IR (neat): 3544 (br, m), 3031 (w), 2923 (w), 1339 (w), 1211 (m), 1117 (m), 723 (w), cm^{-1}; **^{1}H NMR (400 MHz, $CDCl_3$):** δ 7.57 (d, *J* = 8.4 Hz, 2H), 7.42 – 7.33 (m, 3H), 5.79 – 5.72 (m, 1H), 5.11 – 5.04 (m, 1H), 3.14 – 2.89 (m, 2H), 2.59 (s, 1H), 1.67 (d, *J* = 7.2 Hz, 3H); **^{13}C NMR (100 MHz, $CDCl_3$):** δ 137.2, 131.7, 128.5, 128.3, 126.7, 121.4, 119.8 – 118.4 (m), 116.9 – 115.8 (m), 113.8 – 112.4 (m), 110.9 – 109.7 (m), 108.2 – 107.1 (m), 77.2 (q, *J* = 24.1 Hz), 33.6, 13.3; **^{19}F NMR (376 MHz, $CDCl_3$):** δ –80.9 – –80.0 (m, 3F), –116.6 – –119.1 (m, 2F), –121.0 – –124.7 (m, 2F); **HRMS (DART):** Calcd for $C_{14}H_{12}F_7$ $[M+H–H_2O]^+$: 313.0827; Found: 313.0820; **Specific Rotation:** $[\alpha]^{22.1}_D$ +38.2° (*c* 2.70, $CHCl_3$) for a 99:1 er sample. Enantiomeric purity was determined by HPLC analysis in comparison with authentic racemic material (Chiralpak AD-H, 98:2 hexanes:*i*-PrOH, 0.5 mL/min, 220 nm): t_R: 9.8 min (minor) and 10.7 min (major).

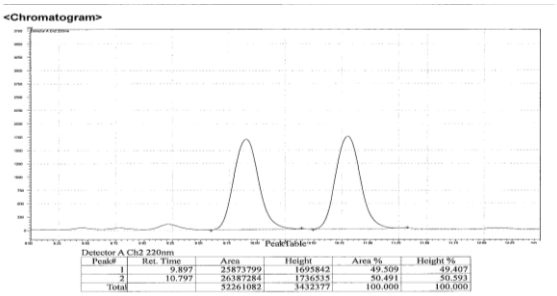

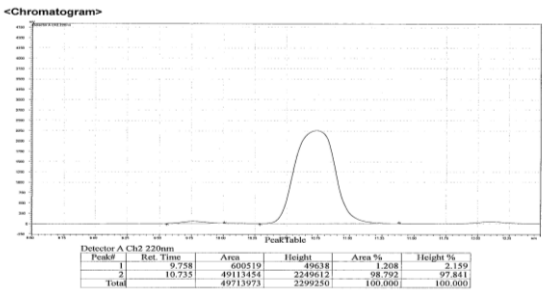

Peak #	Ret. Time	Area	Area %	Peak #	Ret. Time	Area	Area %
1	9.897 min	25873799	49.509	1	9.758 min	600519	1.208
2	10.797	26387284	50.491	2	10.735	49113454	98.792

(*R*,*Z*)-1,1-Difluoro-2-phenylhex-4-en-2-ol (*Z*-2.65): IR (neat): 3540 (br, m), 3028 (w), 2924 (w), 2858 (w), 1589 (w), 1449 (w), 1066 (s), 699 (s), 609 (m), 569 (w) cm^{-1}; **^{1}H NMR (400 MHz, $CDCl_3$):** δ 7.51 – 7.29 (m, 5H), 5.76 (t, *J* = 56.4 Hz, 1H), 5.72 – 5.64 (m, 1H), 5.27 – 5.21 (m, 1H), 2.86 – 2.75 (m, 2H), 2.41 (s), 1.64 – 1.62 (m, 3H); **^{13}C NMR (100 MHz, $CDCl_3$):** δ 139.1, 130.0, 128.5, 128.2, 126.4, 122.4, 116.9 (t, *J* = 248.2 Hz), 76.1 (t, *J* = 21.2 Hz), 32.6 (t, *J* = 2.3 Hz), 13.2; **^{19}F NMR (376 MHz, $CDCl_3$):** δ –129.5 – –132.1 (m, 2F); **HRMS (DART):** Calcd for $C_{12}H_{13}F_2$ $[M+H–H_2O]^+$: 195.0985; Found: 195.0993; **Specific Rotation:** $[\alpha]^{20.8}_D$ +32.8° (*c* 1.89, $CHCl_3$) for a 98.5:1.5 er sample. Enantiomeric purity was determined by HPLC analysis in comparison with authentic racemic material (Chiralpak AZ-H, 99:1 hexanes:*i*-PrOH, 0.2 mL/min, 254 nm): t_R: 57.9 min (minor) and 71.0 min (major).

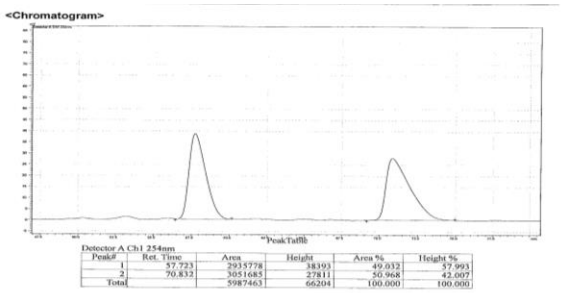

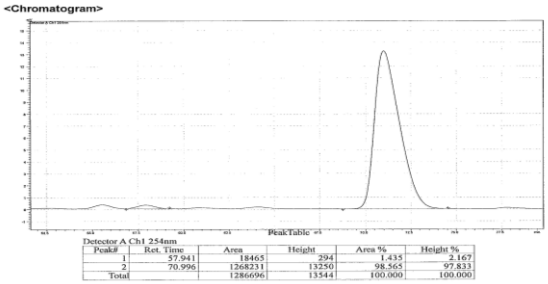

Peak #	Ret. Time	Area	Area %	Peak #	Ret. Time	Area	Area %
1	57.723	2935778	49.032	1	57.941	18465	1.435
2	70.832	3051685	50.968	2	70.996	1268231	98.565

(*R*,*Z*)-1,1-Difluoro-2-(*o*-tolyl)hex-4-en-2-ol (*Z*-2.66): IR (neat): 3552 (br, m), 2925 (m), 2858 (w), 1491 (w), 1150 (w), 1069 (s), 761 (w), 753 (s) cm^{-1}; **^{1}H NMR (400 MHz, $CDCl_3$):** δ 7.40 (dd, *J* = 7.5, 2.3 Hz, 1H), 7.25 – 7.13 (m, 3H), 5.98 (t, *J* = 56.3, 1H), 5.69 (dddd, *J* = 10.9, 8.6, 6.9, 5.3 Hz, 1H), 5.29 (q, *J* = 8.7 Hz, 1H), 3.05 – 2.77 (m, 2H), 2.55 (s, 3H), 2.37 (s, 1H), 1.70 – 1.59 (m, 3H); **^{13}C NMR (100 MHz, $CDCl_3$):** δ 137.1, 136.5, 133.1, 129.9, 128.2, 127.9, 125.8, 122.8, 116.5 (*t*, *J* = 246 Hz), 77.9 (*t*, *J* = 21 Hz), 32.5, 22.7, 13.2; **^{19}F NMR (376 MHz, $CDCl_3$):** δ –128.98 – –131.72 (m, 2F); **HRMS (DART):** Calcd for $C_{13}H_{15}F_2$ $[M+H–H_2O]^+$: 209.1142; Found: 209.1151; **Specific Rotation:** $[\alpha]^{20.0}_D$ –19.64° (*c* 1.02, $CHCl_3$) for a 91:9 er sample of the (*S*)-enantiomer. Enantiomeric purity was determined by HPLC analysis in comparison with authentic racemic material (Chiralpak AZ-H, 99:1 hexanes:*i*-PrOH, 1.0 mL/min, 220 nm): t_R: 7.8 min (minor) and 9.9 min (major).

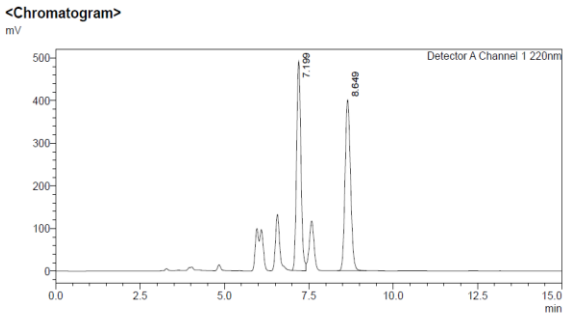

<Peak Table>
Detector A Channel 1 220nm

Peak#	Ret. Time	Area	Height	Conc.	Unit	Mark	Name
1	7.199	4454415	491379	49.452		M	
2	8.649	4553191	401065	50.548		M	
Total		9007606	892444				

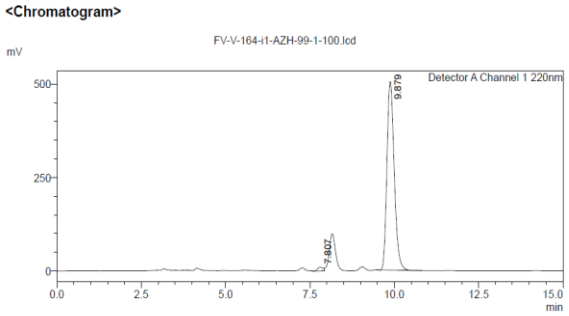

<Peak Table>
Detector A Channel 1 220nm

Peak#	Ret. Time	Height	Area	Area%
1	7.807	10701	126250	1.633
2	9.879	504216	7605808	98.367
Total		514918	7732058	100.000

Peak #	Ret. Time	Area	Area %	Peak #	Ret. Time	Area	Area %
1	7.199 min	4454415	49.452	1	7.807 min	126250	1.633
2	8.649 min	4553191	50.548	2	9.879 min	7605808	98.367

(*R*,*Z*)-1,1-Difluoro-2-(4-methoxyphenyl)hex-4-en-2-ol (*Z*-2.67): IR (neat): 3470 (br, m), 3028 (w), 2960 (w), 2935 (w), 1611 (m), 1463 (s), 1250 (s), 1180 (m), 1066 (s), 1035 (s), 832 (m) cm $^{-1}$; **^{1}H NMR (400 MHz, CDCl$_3$):** δ 7.54 – 7.38 (m, 2H), 6.92 (d, *J* = 8.9 Hz, 2H), 5.76 – 5.65 (m, 1H), 5.72 (*t*, *J* = 56.7, 1H), 5.33 – 5.18 (m, 1H), 3.82 (s, 3H), 2.89 – 2.68 (m, 2H), 2.32 (s, 1H), 1.70 – 1.62 (m, 3H); **^{13}C NMR (100 MHz, CDCl$_3$):** δ 159.4, 131.0, 129.8, 127.6, 122.5, 117.0 (t, *J* = 249Hz), 113.8, 75.8 (t, *J* = 21 Hz), 55.3, 32.5, 13.2; **^{19}F NMR (376 MHz, CDCl$_3$):** δ –128.59 – –131.49 (m, 2F); **HRMS (DART):** Calcd for $C_{13}H_{15}F_2O$ $[M+H–H_2O]^+$: 225.1091; Found: 225.1082; **Specific Rotation:** $[\alpha]^{20.0}_D$ –26.24° (*c* 1.14, $CHCl_3$) for a 81:19 er sample of the (*S*)-enantiomer. Enantiomeric purity was determined by HPLC analysis in comparison with authentic racemic material (Chiralcel OJ-H, 99:1 hexanes:*i*-PrOH, 1.0 mL/min, 220 nm): t_R: 46.8 min (major) and 76.1 min (minor).

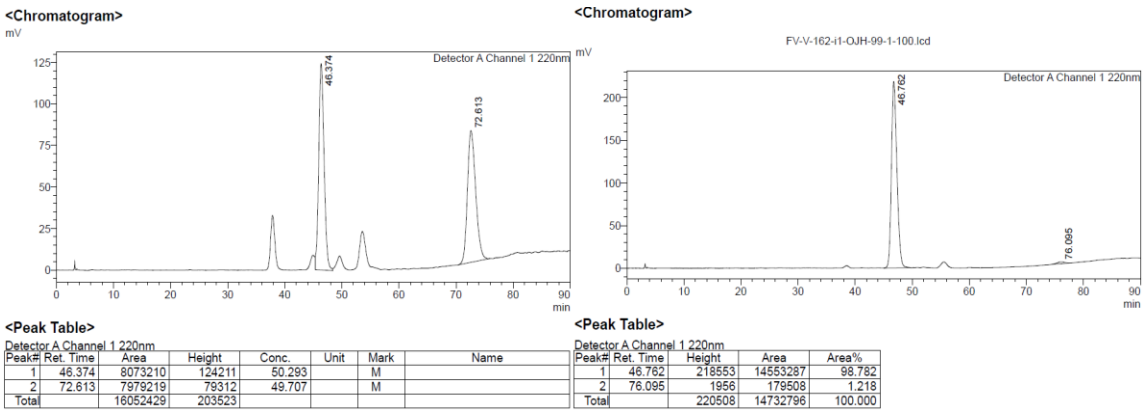

<Peak Table>
Detector A Channel 1 220nm

Peak#	Ret. Time	Area	Height	Conc.	Unit	Mark	Name
1	46.374	8073210	124211	50.293		M	
2	72.613	7979219	79312	49.707		M	
Total		16052429	203523				

<Peak Table>
Detector A Channel 1 220nm

Peak#	Ret. Time	Height	Area	Area%
1	46.762	218553	14553287	98.782
2	76.095	1956	179508	1.218
Total		220508	14732796	100.000

Peak #	Ret. Time	Area	Area %	Peak #	Ret. Time	Area	Area %
1	46.374	8073210	50.293	1	46.762	14553287	98.782
2	72.613	7979219	49.707	2	76.095	179508	1.218

(***R*,*Z*)-1-Fluoro-2-phenylhex-4-en-2-ol (*Z*-2.68): IR (neat):** 3566 (br, m), 3026 (w), 2953 (w), 2921 (w), 1448 (w), 1070 (w), 700 (m) cm^{-1}; **^{1}H NMR (400 MHz, $CDCl_3$):** δ 7.48 – 7.23 (m, 5H), 5.69 – 5.5.61 (m, 1H), 5.30 – 5.24 (m, 1H), 4.52 (d, *J* = 48.4 Hz, 2H), 2.82 – 2.63 (m, 2H), 2.43 (s, 1H), 1.61 (d, *J* = 7.2 Hz, 3H); **^{13}C NMR (100 MHz, $CDCl_3$):** δ 141.9, 129.0, 128.5, 127.6, 125.7, 123.6, 88.6 (d, *J* = 176.8 Hz), 75.8 (d, *J* = 17.5 Hz), 35.4, 13.2; **^{19}F NMR (376 MHz, $CDCl_3$):** δ –225.6 (t, *J* = 47.4 Hz, 2F); **HRMS (DART):** Calcd for $C_{12}H_{14}F$ $[M+H–H_2O]^+$: 177.1079; Found: 177.1085; **Specific Rotation:** $[\alpha]^{22.3}_D$ +19.7° (*c* 1.45, $CHCl_3$) for a 95:5 er sample. Enantiomeric purity was determined by HPLC analysis in comparison with authentic racemic material (Chiralpak AZ-H, 98:2 hexanes:*i*-PrOH, 0.3 mL/min, 254 nm): t_R: 29.7 min (minor) and 36.6 min (major).

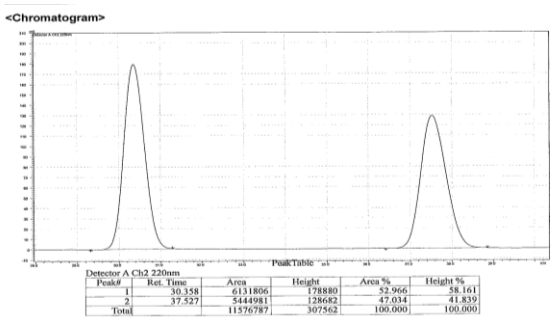

Peak#	Ret. Time	Area	Height	Area %	Height %
1	30.358	6131806	178880	52.966	58.161
2	37.527	5444981	128682	47.034	41.839
Total		11576787	307562	100.000	100.000

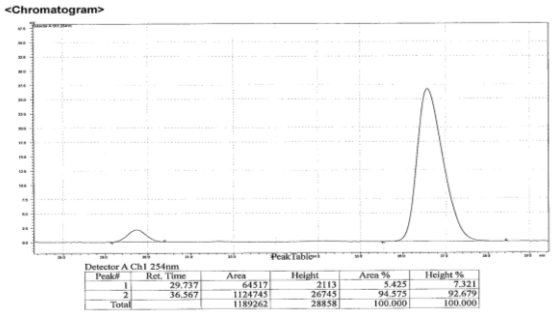

Peak#	Ret. Time	Area	Height	Area %	Height %
1	29.737	64517	2113	5.425	7.321
2	36.567	1124745	26745	94.575	92.679
Total		1189262	28858	100.000	100.000

Peak #	Ret. Time	Area	Area %	Peak #	Ret. Time	Area	Area %
1	30.358	6131806	52.966	1	29.737	64517	5.425
2	37.527	5444981	47.034	2	36.567	1124745	94.575

(*R*,*Z*)-1-Fluoro-2-(*o*-tolyl)hex-4-en-2-ol (*Z*-2.69): IR (neat): 3557 (br, m), 3461 (br), 3021 (m), 2957 (m), 2930 (m), 1490 (m), 1058 (m), 1013 (s), 733 (s), cm^{-1}; **^{1}H NMR (400 MHz, $CDCl_3$):** δ 7.42 – 7.34 (m, 1H), 7.22 – 7.14 (m, 3H), 5.70 – 5.58 (m, 1H), 5.33 – 5.24 (m, 1H), 4.82 – 4.51 (m, 2H), 2.87 – 2.78 (m, 2H), 2.58 (d, *J* = 0.8 Hz, 3H), 2.44 (t, *J* = 1.6 Hz, 1H), 1.62 (ddd, *J* = 6.9, 1.8, 0.9 Hz, 3H); **^{13}C NMR (100 MHz, $CDCl_3$):** δ 139.0 (d, *J* = 3.2 Hz), 136.4, 133.0, 128.6, 127.8, 127.2(d, *J* = 1.0 Hz), 125.8, 123.9, 87.6 (d, *J* = 176.1 Hz), 77.3 (d, *J* = 17.6 Hz), 34.3, 22.5, 13.1; **^{19}F NMR (376 MHz, $CDCl_3$):** δ –225.58 (t, *J* = 47.7 Hz, 1F); **HRMS (ESI+):** Calcd for $C_{13}H_{16}F$ $[M+H-H_2O]^+$: 191.1236; Found: 191.1241; **Specific Rotation:** $[\alpha]^{20.0}_D$ –9.34° (*c* 0.92, $CHCl_3$) for a 96:4 er sample of the (*S*)-enantiomer. Enantiomeric purity was determined by HPLC analysis in comparison with authentic racemic material (Chiralpak AZ-H, 99:1 hexanes:*i*-PrOH, 1.0 mL/min, 220 nm): t_R: 8.9 min (minor) and 10.5 min (major).

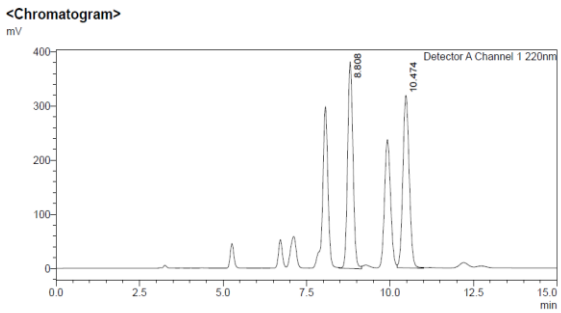

<Peak Table>
Detector A Channel 1 220nm

Peak#	Ret. Time	Area	Height	Conc.	Unit	Mark	Name
1	8.808	4213275	382079	49.826		M	
2	10.474	4242698	318426	50.174		M	
Total		8455972	700504				

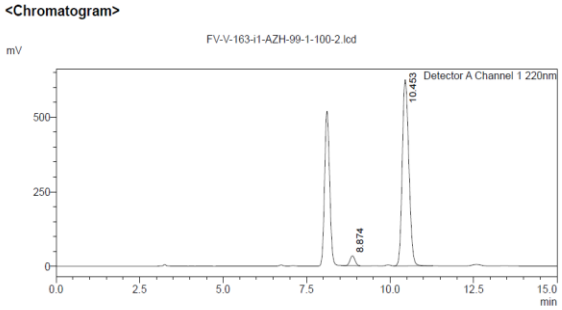

<Peak Table>
Detector A Channel 1 220nm

Peak#	Ret. Time	Height	Area	Area%
1	8.874	32937	336490	3.742
2	10.453	625036	8655835	96.258
Total		657973	8992325	100.000

Peak #	Ret. Time	Area	Area %	Peak #	Ret. Time	Area	Area %
1	8.808 min	4213275	49.826	1	8.874 min	336490	3.742
2	10.474	4242698	50.174	2	10.453	8655835	96.258

(*R*,*Z*)-1-Fluoro-2-(4-methoxyphenyl)hex-4-en-2-ol (*Z*-2.70): IR (neat): 3494 (br, m), 3019 (w), 2953 (w), 1611 (m), 1512 (s), 1462 (m), 1248 (s), 1032 (s), 802 (m), cm^{-1}; **^{1}H NMR (400 MHz, $CDCl_3$):** δ 7.42 – 7.35 (m, 2H), 6.96 – 6.86 (m, 2H), 5.64 (dqt, *J* = 10.9, 6.8, 1.5 Hz, 1H), 5.27 (ddddd, *J* = 10.8, 7.8, 6.9, 1.8, 0.7 Hz, 1H), 4.57 – 4.33 (m, 2H), 3.81 (s, 3H), 2.87 – 2.53 (m, 2H), 2.34 (s, 1H), 1.68 – 1.57 (m, 3H); **^{13}C NMR (100 MHz, $CDCl_3$):** δ 159.0, 133.9, 128.8, 126.9, 123.7, 113.8, 88.6 (d, *J* = 177.9 Hz), 75.5 (d, *J* = 18.0 Hz), 55.3, 35.3, 13.1; **^{19}F NMR (376 MHz, $CDCl_3$):** δ –224.29 (t, *J* = 47.9 Hz, 1F); **HRMS (ESI+):** Calcd for $C_{13}H_{16}FO$ $[M+H–H_2O]^+$: 207.1185; Found: 207.1185; **Specific Rotation:** $[\alpha]^{20.0}_D$ –22.11° (*c* 1.04, $CHCl_3$) for a 91:9 er sample of the (*S*)-enantiomer. Enantiomeric purity was determined by HPLC analysis in comparison with authentic racemic material (Chiralcel OJ-H, 99:1 hexanes:*i*-PrOH, 1.0 mL/min, 220 nm): t_R: 44.3 min (major) and 69.9 min (minor).

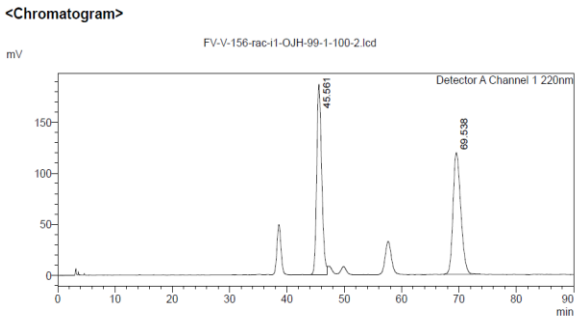

<Peak Table>
Detector A Channel 1 220nm

Peak#	Ret. Time	Height	Area	Area%
1	45.561	186431	11314987	50.288
2	69.538	119100	11185164	49.712
Total		305531	22500151	100.000

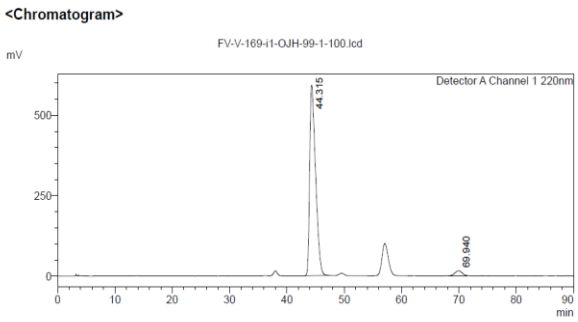

<Peak Table>
Detector A Channel 1 220nm

Peak#	Ret. Time	Height	Area	Area%
1	44.315	593145	42479677	96.884
2	69.940	15807	1366254	3.116
Total		608952	43845931	100.000

Peak #	Ret. Time	Area	Area %	Peak #	Ret. Time	Area	Area %
1	45.561	11314987	50.288	1	44.315	42479677	96.884
2	69.538	11185164	49.712	2	69.940	1366254	3.116

(*R*,*Z*)-1,1,1-Trifluoro-2-(4-methoxyphenyl)dodec-4-en-2-ol (*Z*-2.76): IR (neat): 3458 (br, m), 2925 (s), 2854 (m), 1612(m), 1514 (s), 1220 (s), 1155 (s), 1101 (m), 1035 (m), 828 (m) cm^{-1}; **^{1}H NMR (400 MHz, $CDCl_3$):** δ 7.70 (d, *J* = 9.2 Hz, 2H), 6.94 – 6.90 (m, 2H), 5.69 – 5.62 (m, 1H). 5.20 – 5.13 (m, 1H), 3.82 (s, 3H), 2.95 – 2.85 (m, 2H), 2.48 (s, 1H), 2.09 – 2.04 (m, 2H), 1.35 – 1.25(m, 10H), 0.89 (t, *J* = 7.2 Hz, 3H); **^{13}C NMR (100 MHz, $CDCl_3$):** δ 159.8, 137.2, 129.2, 128.0, 125.6 (q, *J* = 283.8 Hz), 120.5, 113.8, 76.2 (q, *J* = 28.1 Hz), 55.4, 33.4, 31.9, 29.6, 29.4, 29.3, 27.7, 22.8, 14.2; **^{19}F NMR (376 MHz, $CDCl_3$):** δ –80.79 (s, 3F); **HRMS (DART):** Calcd for $C_{19}H_{26}F_3O$ $[M+H–H_2O]^+$: 327.1935; Found: 327.1934; **Specific Rotation:** $[\alpha]^{20.0}_D$ +29.95° (*c* 1.56, $CHCl_3$) for a >99:1 er sample. Enantiomeric purity was determined by HPLC analysis in comparison with authentic racemic material (Chiralpak AD-H, 99:1 hexanes:*i*-PrOH, 0.3 mL/min, 220 nm): t_R: 30.0 min (major) and 43.3 min (minor).

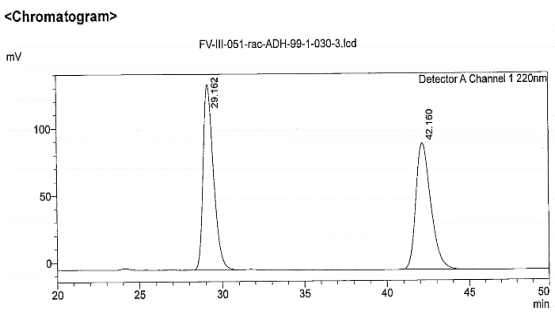

<Peak Table>
Detector A Channel 1 220nm

Peak#	Ret. Time	Height	Area	Area%
1	29.162	138262	6046523	50.399
2	42.160	94336	5950670	49.601
Total		232598	11997193	100.000

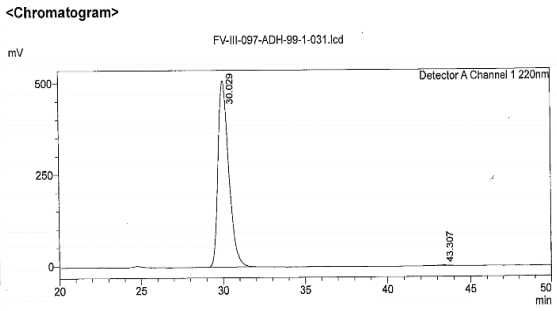

<Peak Table>
Detector A Channel 1 220nm

Peak#	Ret. Time	Height	Area	Area%
1	30.029	509577	23237991	99.655
2	43.307	1696	80350	0.345
Total		511274	23318341	100.000

Peak #	Ret. Time	Area	Area %	Peak #	Ret. Time	Area	Area %
1	29.162	6046523	50.399	1	30.029	2327991	99.655
2	42.160	5950670	49.601	2	43.307	80350	0.345

(*R*,*Z*)-2-(4-Chlorophenyl)-1,1,1-trifluorododec-4-en-2-ol (*Z*-2.77): IR (neat): 3538 (br, m), 2924 (s), 2854 (m), 1494 (m), 1267 (m), 1160 (s), 1095 (s), 1013 (m), 823 (m), 734 (w) cm^{-1}; **^{1}H NMR (400 MHz, $CDCl_3$):** δ 7.50 (d, *J* = 8.4 Hz, 2H), 7.39 – 7.35 (m, 2H), 5.71 – 5.64 (m, 1H), 5.16 – 5.10 (m, 1H), 2.95 – 2.83 (m, 2H), 2.52 (s, 1H), 2.07 – 2.01 (m, 2H), 1.34 – 1.27 (m, 10H), 0.89 (t, *J* = 7.2 Hz, 3H); **^{13}C NMR (100 MHz, $CDCl_3$):** δ 137.7, 135.8, 134.8, 128.6, 128.2, 125.4 (q, *J* = 283.8 Hz), 119.9, 76.1 (q, *J* = 28.1 Hz), 33.6, 31.9, 29.5, 29.4, 29.3, 27.7, 22.8, 14.2; **^{19}F NMR (376 MHz, $CDCl_3$):** δ –80.50 (s, 3F); **HRMS (DART):** Calcd for $C_{18}H_{23}ClF_3$ $[M+H–H_2O]^+$: 331.1440; Found: 331.1449; **Specific Rotation:** $[\alpha]^{20.0}_D$ +25.20° (*c* 0.34, $CHCl_3$) for a >99:1 er sample. Enantiomeric purity was determined by HPLC analysis in comparison with authentic racemic material (Chiralpak AD-H, 99:1 hexanes:*i*-PrOH, 0.3 mL/min, 220 nm): t_R: 20.1 min (major) and 25.9 min (minor).

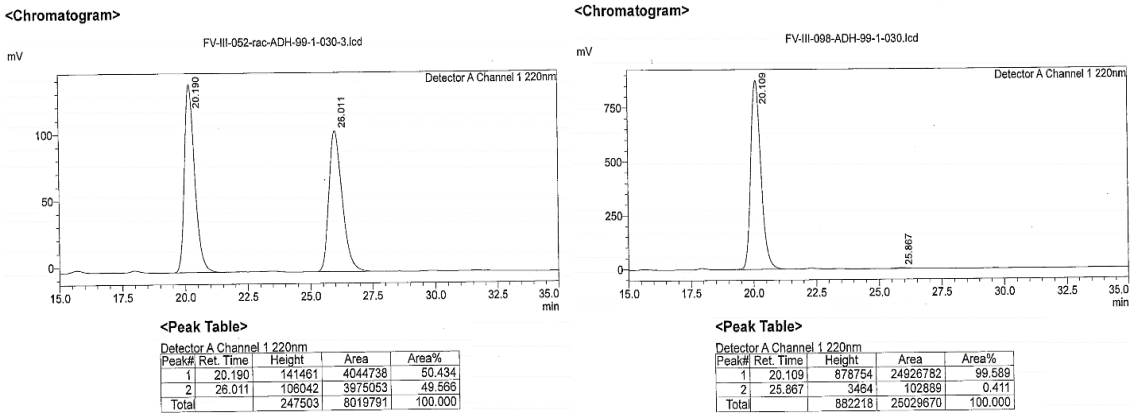

Peak #	Ret. Time	Area	Area %	Peak #	Ret. Time	Area	Area %
1	20.190	4044738	50.434	1	20.109	24926782	99.589
2	26.011	3975053	49.566	2	25.867	102889	0.411

(*S*,*Z*)-1,1,1-Trifluoro-2-(thiophen-2-yl)dodec-4-en-2-ol (*Z*-2.78): IR (neat): 3544 (br, m), 2925 (s), 2855 (m), 1464 (w), 1436 (w), 1275 (m), 1170 (s), 720 (m), 702 (s) cm^{-1}; **^{1}H NMR (400 MHz, $CDCl_3$):** δ 7.35 – 7.33 (m, 1H), 7.12 – 7.11 (m, 1H), 7.05 – 7.02 (m, 1H), 5.75 – 5.68 (m, 1H), 5.28 – 5.21 (m, 1H), 2.99 – 2.81 (m, 2H), 2.75 (s, 1H), 2.08 – 2.03 (m, 2H), 1.35 – 1.23 (m, 10H), 0.89 (t, *J* = 6.8 Hz, 3H); **^{13}C NMR (100 MHz, $CDCl_3$):** δ 137.8, 127.3, 126.3, 125.92, 125.90, 124.9 (q, *J* = 283.8 Hz), 119.9, 76.1 (q, *J* = 28.8 Hz), 34.6, 31.9, 29.6, 29.4, 29.3, 27.7, 22.8, 14.2; **^{19}F NMR (376 MHz, $CDCl_3$):** δ –81.57(s, 3F); **HRMS (DART):** Calcd for $C_{16}H_{22}F_3S$ $[M+H–H_2O]^+$: 303.1394; Found: 303.1408; **Specific Rotation:** $[\alpha]^{20.0}_D$ +28.39° (*c* 0.50, $CHCl_3$) for a 98:2 er sample. Enantiomeric purity was determined by HPLC analysis in comparison with authentic racemic material (Chiralpak AD-H, 99:1 hexanes:*i*-PrOH, 0.3 mL/min, 220 nm): t_R: 23.6 min (major) and 27.9 min (minor).

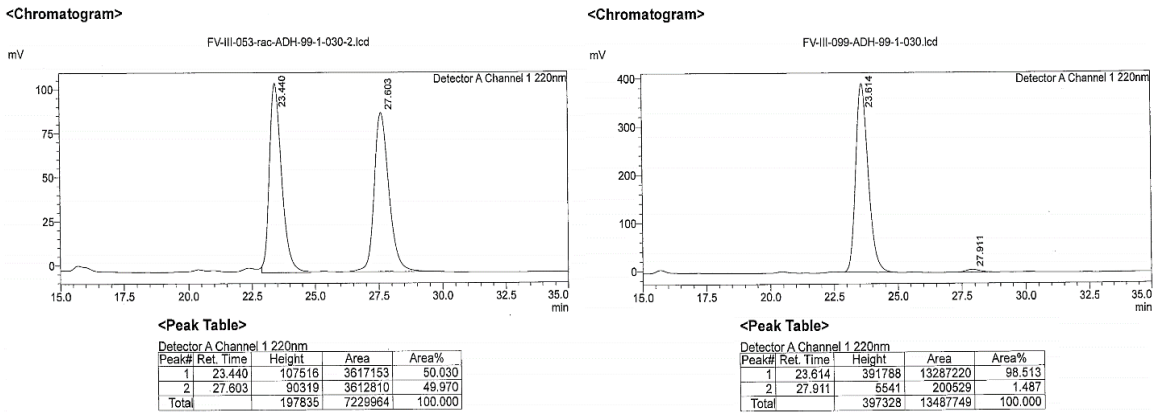

Peak #	Ret. Time	Area	Area %	Peak #	Ret. Time	Area	Area %
1	23.440	3617153	50.030	1	23.614	13287220	98.513
2	27.603	3612810	49.970	2	27.911	200529	1.487

(*R*,*Z*)-1,1,1-Trifluoro-2,5-diphenylpent-4-en-2-ol (*Z*-2.79): IR (neat): 3541(br, m), 3027 (w), 2924 (w), 1493 (w), 1449 (w), 1271 (m), 1154 (s), 763 (m), 699 (s) cm^{-1}; **^{1}H NMR (400 MHz, $CDCl_3$):** δ 7.54 (d, *J* = 7.2 Hz, 2H), 7.43 – 7.36 (m, 5H), 7.31 – 7.21 (m, 3H), 6.62 (d, *J* = 11.6 Hz, 1H), 5.43 (app dt, *J* = 14.4, 7.2 Hz, 1H), 3.24 – 3.16 (m, 2H), 2.50 (s, 1H); **^{13}C NMR (100 MHz, $CDCl_3$):** δ 136.4, 136.2, 134.4, 128.65, 128.60, 128.5, 128.4, 127.3, 126.6, 125.4 (q, *J* = 283.8 Hz), 123.2, 76.2 (q, *J* = 28.1 Hz), 34.2; **^{19}F NMR (376 MHz, $CDCl_3$):** δ –80.64 (s, 3F); **HRMS (DART):** Calcd for $C_{17}H_{14}F_3$ $[M+H–H_2O]^+$: 275.1047; Found: 275.1052; **Specific Rotation:** $[\alpha]^{20.0}_D$ –29.76° (*c* 2.4, $CHCl_3$) for a 85:15 er sample. Enantiomeric purity was determined by HPLC analysis in comparison with authentic racemic material (Chiralcel OD-H, 99:1 hexanes:*i*-PrOH, 1.0 mL/min, 220 nm): t_R: 14.6 min (major) and 21.7 min (minor).

<Chromatogram>

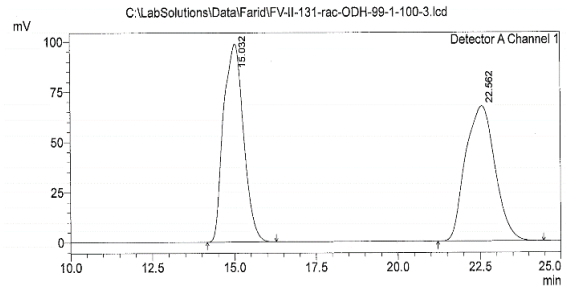

PeakTable

Detector A Channel 1 254nm

Peak#	Ret. Time	Area	Height	Area %
1	15.032	4211988	98683	49.998
2	22.562	4212381	67317	50.002
Total		8424368	166000	100.000

<Chromatogram>

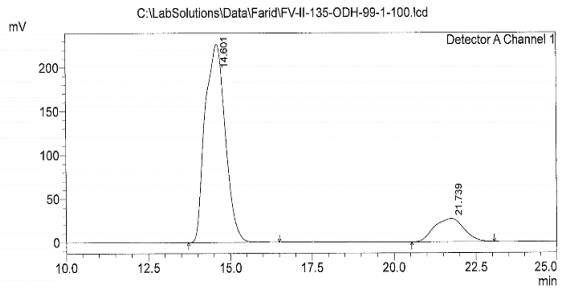

PeakTable

Detector A Channel 1 254nm

Peak#	Ret. Time	Area	Height	Area %
1	14.601	9753841	226857	85.381
2	21.739	1669999	26683	14.619
Total		11423840	253540	100.000

Peak #	Ret. Time	Area	Area %	Peak #	Ret. Time	Area	Area %
1	15.032	4211988	49.998	1	14.601	9753841	85.381
2	22.562	4212381	50.002	2	21.739	1669999	14.619

(*R*)-1,1,1-Trifluoro-5-methyl-2-phenylhex-4-en-2-ol (*Z*-2.80): IR (neat): 3518 (br, m), 2938 (w), 2918 (w), 2851 (w), 1449 (w), 1271 (w), 1157 (s), 701 (m) cm $^{-1}$; **^{1}H NMR (400 MHz, $CDCl_3$):** δ 7.60-7.58 (m, 2H), 7.43-7.37 (m, 3H), 4.96-4.92 (m, 1H), 2.96-2.85 (m, 2H), 2.58 (s, 3H), 1.70 (d, *J* = 7.2 Hz, 3H); **^{13}C NMR (100 MHz, $CDCl_3$):** δ 139.8, 137.6, 128.5, 128.6, 126.6, 125.6 (q, *J* = 283.8 Hz), 115.5, 76.4 (q, *J* = 27.3 Hz), 34.5, 26.2, 18.3; **^{19}F NMR (376 MHz, $CDCl_3$):** δ –80.0 (s, 3F); **HRMS (DART):** Calcd for $C_{13}H_{14}F_3$ $[M+H–H_2O]^+$: 227.1047; Found: 227.1053; **Specific Rotation:** $[\alpha]^{21.8}_D$ +39.9° (*c* 1.70, $CHCl_3$) for a 89:11 er sample. Enantiomeric purity was determined by HPLC analysis in comparison with authentic racemic material (Chiralpak AS-H, 99:1 hexanes:*i*-PrOH, 0.2 mL/min, 220 nm): t_R: 32.0 min (major) and 33.9 min (minor).

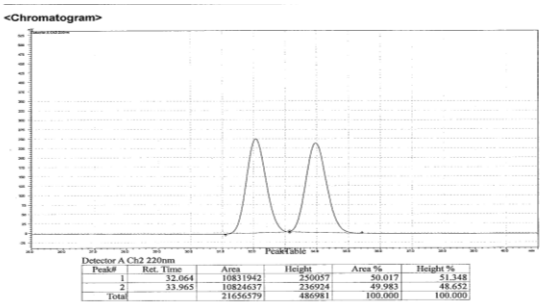

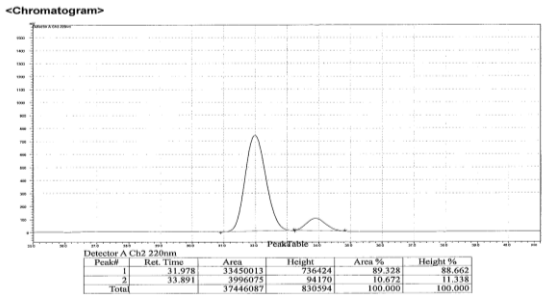

Peak #	Ret. Time	Area	Area %	Peak #	Ret. Time	Area	Area %
1	32.064	10831942	51.348	1	31.978	33450013	89.328
2	33.965	10824637	48.652	2	33.891	3996075	10.672

(2*R*,3*S*)-1,1,1-Trifluoro-3-methyl-2-phenylpent-4-en-2-ol (*anti*-2.82): IR (neat): 3548 (br, m), 2980 (w), 2926 (w), 1451 (w), 1376 (w), 1263 (m), 1158 (s), 760 (w), 714 (m), 707 (m) cm^{-1}; **^{1}H NMR (400 MHz, $CDCl_3$):** δ 7.63 – 7.48 (m, 2H), 7.48 – 7.29 (m, 3H), 6.21 – 5.98 (m, 1H), 5.46 – 5.12 (m, 2H), 3.14 (p, *J* = 7.1 Hz, 1H), 2.60 (s, 1H), 0.80 (d, *J* = 7.0 Hz, 3H); **^{13}C NMR (100 MHz, $CDCl_3$):** δ 137.1, 136.9, 128.2, 128.1, 125.6, 125.6 (q, *J* = 287.5 Hz), 118.0, 78.6 (q, *J* = 26.7 Hz), 42.1, 13.52; **^{19}F NMR (376 MHz, $CDCl_3$):** δ –74.49 (s, 3F); **HRMS (DART):** Calcd for $C_{12}H_{12}F_3$ $[M+H–H_2O]^+$: 213.0891; Found: 213.0895; **Specific Rotation:** $[\alpha]^{20.0}_D$ +22.39° (*c* 1.15, $CHCl_3$) for a 93:7 er sample. Enantiomeric purity was determined by HPLC analysis in comparison with authentic racemic material (Chiralpak AS-H, 99:1 hexanes:*i*-PrOH, 0.3 mL/min, 220 nm): t_R: 47.6 min (major) and 51.4 min (minor).

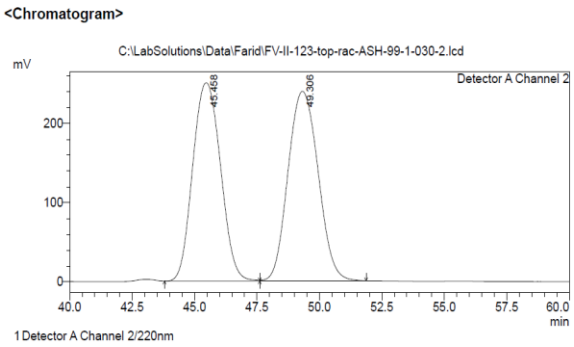

PeakTable

Detector A Channel 2 220nm

Peak#	Ret. Time	Area	Height	Area %
1	45.458	19426843	250350	49.141
2	49.306	20106291	239413	50.859
Total		39533135	489763	100.000

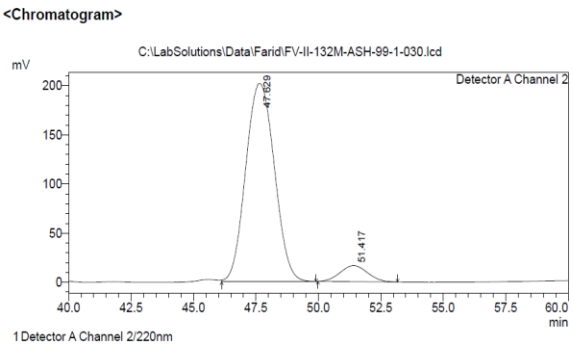

PeakTable

Detector A Channel 2 220nm

Peak#	Ret. Time	Area	Height	Area %
1	47.629	16156853	201607	92.870
2	51.417	1240376	16307	7.130
Total		17397229	217914	100.000

Peak #	Ret. Time	Area	Area %	Peak #	Ret. Time	Area	Area %
1	45.458	19426843	49.141	1	47.629	16156853	92.870
2	49.306	20106291	50.859	2	51.417	1240376	7.130

(2*R*,3*S*)-1,1,1-Trifluoro-3-methyl-2-(*o*-tolyl)pent-4-en-2-ol (*anti*-2.84): IR (neat): 3538 (br, m), 2984 (w), 1490 (w), 1459 (w), 1256 (m), 1158 (s), 758 (m), 729 (m), 708 (w) cm^{-1}; **^{1}H NMR (400 MHz, $CDCl_3$) for a 69:31 mixture of diastereomers:** δ 7.52 – 7.48 (m, 1.2H), 7.23 – 7.16 (m, 4.2H), 6.15 (**major**, dddt, *J* = 15.4, 11.3, 6.9, 2.4 Hz, 1H), 5.77 – 5.64 (**minor**, m, .4H), 5.43 – 5.29 (**major**, m, 2H), 5.19 – 5.10 (**minor**, m, .8H), 3.47 – 3.34 (**major**, m, 1H), 3.27 (**minor**, p, *J* = 7.1 Hz, .4H), 2.64 (**major**, s, 1H), 2.60 (**minor**, s, .4H), 2.58 (s, 4.2H), 1.21 (**minor**, dq, *J* = 6.9, 1.7 Hz, 1.2H), 0.89 (**major**, d, *J* = 7.0 Hz, 3H); **^{13}C NMR (100 MHz, $CDCl_3$) for a 69:31 mixture of diastereomers:** δ 137.8, 137.8, 137.5, 137.2, 137.1, 135.2, 134.6, 133.6, 133.4, 128.2, 128.2, 127.7 (q, *J* = 2.5 Hz), 127.6, 126.1 (q, *J* = 287.0 Hz), 125.8, 125.6, 118.8, 118.1, 81.30 (q, *J* = 26.7 Hz), 43.7, 41.6, 23.3, 14.18 (q, *J* = 2.5 Hz), 13.2; **^{19}F NMR (376 MHz, $CDCl_3$):** δ –72.15 (minor, s, 1.2F), –73.89 (major, br s, 3F); **HRMS (DART):** Calcd for $C_{13}H_{14}F_3$ $[M+H–H_2O]^+$: 227.1047; Found: 227.1058; **Specific Rotation:** $[\alpha]^{20.0}_D$ +25.57° (*c* 1.51, $CHCl_3$) for a 69:31 dr, 93:7 er sample. Enantiomeric purity was determined by

HPLC analysis in comparison with authentic racemic material (Chiralcel OD-H, 99:1 hexanes:*i*-PrOH, 0.3 mL/min, 220 nm): t_R: 15.6 min (minor) and 16.5 min (major).

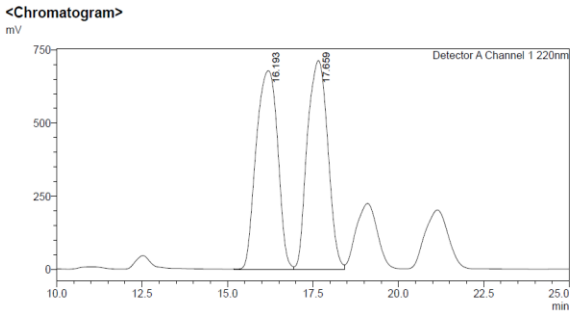

<Peak Table>
Detector A Channel 1 220nm

Peak#	Ret. Time	Area	Height	Conc.	Unit	Mark	Name
1	16.193	29767437	678303	50.017		M	
2	17.659	29747376	712540	49.983		V M	
Total		59514813	1390843				

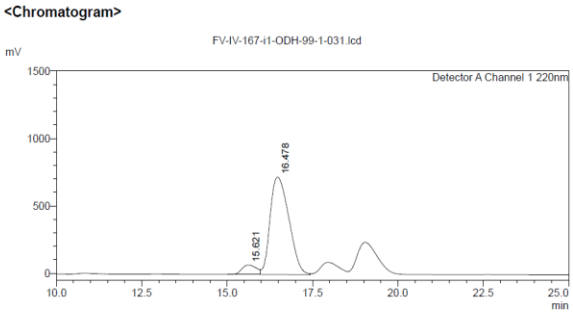

<Peak Table>
Detector A Channel 1 220nm

Peak#	Ret. Time	Height	Area	Area%
1	15.621	70821	2091836	7.027
2	16.478	723347	27677006	92.973
Total		794168	29768842	100.000

Peak #	Ret. Time	Area	Area %	Peak #	Ret. Time	Area	Area %
1	16.193	29767437	50.017	1	15.621	2091836	7.027
2	17.659	29747376	49.983	2	16.478	27677006	92.973

(2*R*,3*S*)-1,1,1-Trifluoro-3-methyl-2-(3-(trifluoromethyl)phenyl)pent-4-en-2-ol (*anti*-2.85): IR (neat): 3545 (br, w), 2985 (w), 1327 (s), 1260 (m), 1158 (s), 1158 (s), 1128 (s), 1076 (s), 801 (m), 723 (m) cm^{-1}; **^{1}H NMR (400 MHz, $CDCl_3$):** δ 7.86 (s, 1H), 7.75 (d, *J* = 8.0 Hz, 1H), 7.63 (d, *J* = 7.6 Hz, 1H), 7.53 (t, *J* = 7.9 Hz, 1H), 6.16 – 5.99 (m, 1H), 5.45 – 5.25 (m, 2H), 3.16 (app t, *J* = 7.0 Hz, 1H), 2.69 (s, 1H), 0.79 (d, *J* = 7.0 Hz, 3H); **^{13}C NMR (100 MHz, $CDCl_3$):** δ 138.3, 136.6, 131.0 (q, *J* = 32.5 Hz), 129.3, 129.0, 125.5 (q, *J* = 287.5 Hz), 125.3 (q, *J* = 3.7 Hz), 124.1 (q, *J* = 272.3 Hz), 123.0 (dd, *J* = 3.9, 1.5 Hz), 118.9 , 78.6 (q, *J* = 27.0 Hz), 42.0, 13.5; **^{19}F NMR (376 MHz, $CDCl_3$):** –63.59 (s, 3F), –74.74 (s, 3F); **HRMS (DART):** Calcd for $C_{13}H_{11}F_6$ $[M+H–H_2O]^+$: 281.0764; Found: 281.0773; **Specific Rotation:** $[\alpha]^{20.0}_D$ +20.45° (*c* 1.89, $CHCl_3$) for a 86:14 dr, 87:13 er sample. Enantiomeric purity was determined by HPLC analysis in comparison with authentic racemic material (Chiralpak AD-H, 99:1 hexanes:*i*-PrOH, 0.3 mL/min, 220 nm): t_R: 19.4 min (minor) and 21.1 min (major).

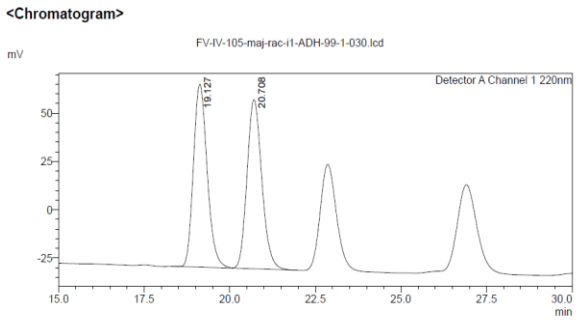

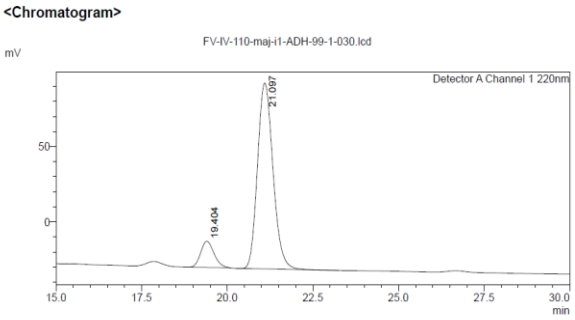

<Peak Table>
Detector A Channel 1 220nm

Peak#	Ret. Time	Height	Area	Area%
1	19.127	94689	2638290	49.979
2	20.708	87685	2640539	50.021
Total		182374	5278829	100.000

<Peak Table>
Detector A Channel 1 220nm

Peak#	Ret. Time	Height	Area	Area%
1	19.404	17380	470847	10.813
2	21.097	123510	3883785	89.187
Total		140890	4354633	100.000

Peak #	Ret. Time	Area	Area %	Peak #	Ret. Time	Area	Area %
1	19.127	2638290	49.979	1	19.404	470847	10.813
2	20.708	2640539	50.021	2	21.097	3883785	89.187

(2*R*,3*S*)-2-(4-Chlorophenyl)-1,1,1-trifluoro-3-methylpent-4-en-2-ol (*anti*-2.86): IR (neat): 3545 (br, m), 2984 (w), 1494 (m), 1263 (m), 1158 (s), 1096 (m), 1016 (m), 913 (m), 847 (w), 818 (m) cm^{-1}; **^{1}H NMR (400 MHz, $CDCl_3$):** δ 7.53 – 7.48 (m, 2H), 7.40 – 7.35 (m, 2H), 6.14 – 5.98 (m, 1H), 5.39 – 5.24 (m, 2H), 3.10 (p, *J* = 7.0 Hz, 1H), 2.61 (d, *J* = 0.8 Hz, 1H), 0.80 (d, *J* = 7.0 Hz, 3H); **^{13}C NMR (100 MHz, $CDCl_3$):** δ 136.8, 135.7, 134.4, 128.6, 127.4, 125.6 (q, *J* = 287.6 Hz), 118.6, 78.58 (q, *J* = 27.0 Hz), 42.0, 13.57; **^{19}F NMR (376 MHz, $CDCl_3$):** δ –75.10 (s, 3F); **HRMS (DART):** Calcd for $C_{12}H_{11}ClF_3$ $[M+H–H_2O]^+$: 247.0501; Found: 247.0501; **Specific Rotation:** $[\alpha]^{20.0}_D$ +31.9° (*c* 1.52, $CHCl_3$) for a 81:19 dr, 95:5 er sample. Enantiomeric purity was determined by HPLC analysis in comparison with authentic racemic material (Chiralpak AZ-H, 99:1 hexanes:*i*-PrOH, 0.3 mL/min, 220 nm): t_R: 19.1 min (major) and 24.4 min (minor).

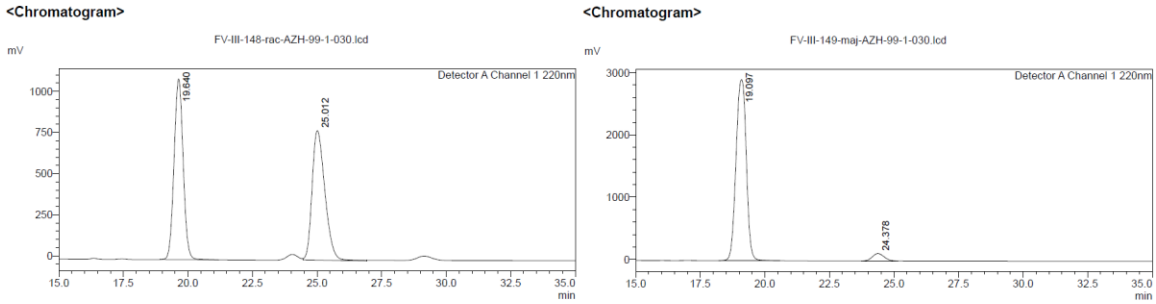

<Peak Table>
Detector A Channel 1 220nm

Peak#	Ret. Time	Height	Area	Area%
1	19.640	1097880	26853184	49.713
2	25.012	786564	27163518	50.287
Total		1884444	54016702	100.000

<Peak Table>
Detector A Channel 1 220nm

Peak#	Ret. Time	Height	Area	Area%
1	19.097	2907065	80214718	95.402
2	24.378	120334	3865693	4.598
Total		3027398	84080411	100.000

Peak #	Ret. Time	Area	Area %	Peak #	Ret. Time	Area	Area %
1	19.640	26853184	49.713	1	19.097	80214718	95.402
2	25.012	27163518	50.287	2	24.378	3865693	4.598

(2*S*,3*S*)-1,1,1-Trifluoro-3-methyl-2-(thiophen-2-yl)pent-4-en-2-ol (*anti*-2.87): IR (neat): 3531 (br, m), 2982 (w), 1458 (w), 1436 (w), 1263 (m), 1165 (s), 1079 (w), 833 (w), 707 (s) cm^{-1}; **^{1}H NMR (400 MHz, $CDCl_3$):** δ 7.33 (dd, *J* = 5.1, 1.2 Hz, 1H), 7.11 (dt, *J* = 3.7, 1.0 Hz, 1H), 7.05 (dd, *J* = 5.1, 3.7 Hz, 1H), 5.94 – 5.81 (m, 1H), 5.29 – 5.22 (m, 2H), 3.06 – 2.95 (m, 1H), 2.78 (s, 1H), 1.02 (d, *J* = 7.1, 3H); **^{13}C NMR (150 MHz, $CDCl_3$):** δ 140.8, 137.0, 127.2, 125.6, 125.2 (q, *J* = 1.3 Hz), 125.1 (q, *J* = 286.7 Hz), 118.4, 78.6 (q, *J* = 28.5 Hz), 44.1, 14.5; **^{19}F NMR (376 MHz, $CDCl_3$):** δ –77.12 (s, 3F); **HRMS (DART):** Calcd for $C_{10}H_{10}F_3S$ $[M+H–H_2O]^+$: 219.0455; Found: 219.0453; **Specific Rotation:** $[\alpha]^{20.0}_D$ +10.9° (*c* 0.26, $CHCl_3$) for a 79:21 dr, 86:14 er sample. Enantiomeric purity was determined by HPLC analysis in comparison with authentic racemic material (Chiralcel OJ-H, 99:1 hexanes:*i*-PrOH, 0.3 mL/min, 220 nm): t_R: 24.0 min (major) and 27.1 min (minor).

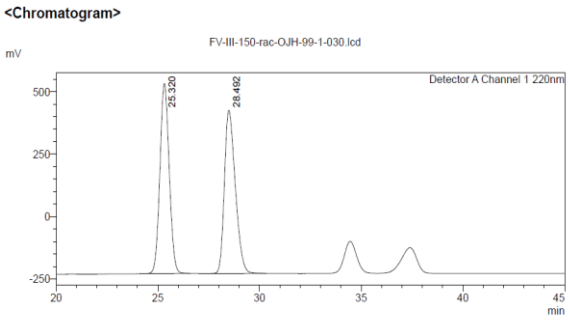

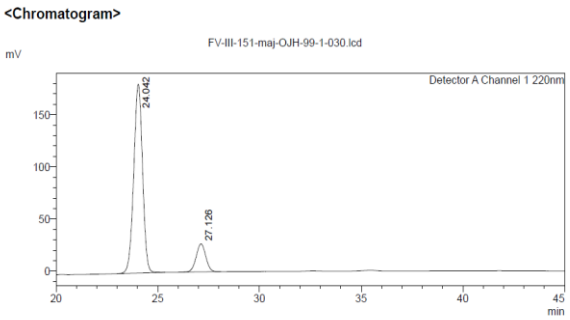

<Peak Table>
Detector A Channel 1 220nm

Peak#	Ret. Time	Height	Area	Area%
1	25.320	760459	24154794	49.869
2	28.492	653247	24281764	50.131
Total		1413706	48436558	100.000

<Peak Table>
Detector A Channel 1 220nm

Peak#	Ret. Time	Height	Area	Area%
1	24.042	181168	5448495	86.049
2	27.126	26938	883389	13.951
Total		208106	6331884	100.000

Peak #	Ret. Time	Area	Area %	Peak #	Ret. Time	Area	Area %
1	25.320	24154794	49.869	1	24.042	5448495	86.049
2	28.492	24281764	50.131	2	27.126	883389	13.951

(3*S*,4*S*,*E*)-4-Methyl-1-phenyl-3-(trifluoromethyl)hexa-1,5-dien-3-ol (*anti*-2.89): IR (neat): 3539 (br, m), 2941 (w), 1497 (w), 1284 (w), 1251 (m), 1143 (s), 1005 (m), 972 (m), 748 (m), 691 (w) cm^{-1}; **^{1}H NMR (400 MHz, $CDCl_3$):** δ 7.46 – 7.41 (m, 2H), 7.39 – 7.33 (m, 2H), 7.30 (d, *J* = 7.2 Hz, 1H), 6.89 (d, *J* = 16.0 Hz, 1H), 6.26 (d, *J* = 16.0 Hz, 1H), 5.89 – 5.75 (m, 1H), 5.30 – 5.19 (m, 2H), 2.79 (p, *J* = 7.2 Hz, 1H), 2.37 (s, 1H), 1.18 (d, *J* = 7.0, 3H); **^{13}C NMR (100 MHz, Methylene Chloride-*d*$_2$):** δ 137.8, 136.2, 133.9, 129.0, 128.7, 127.2, 126.0 (q, *J* = 286.8 Hz), 123.7, 118.5, 77.6 (q, *J* = 26.9 Hz), 43.7, 15.2; **^{19}F NMR (376 MHz, $CDCl_3$):** δ –77.43 (s, 3F); **HRMS (DART):** Calcd for $C_{14}H_{14}F_3$ $[M+H–H_2O]^+$: 239.1047; Found: 239.1054; **Specific Rotation:** $[\alpha]^{20.0}_D$ +105.3° (*c* 2.25, $CHCl_3$) for a 88.5:11.5 dr, 87:13 er sample. Enantiomeric purity was determined by HPLC analysis in comparison with authentic racemic material (Chiralcel OJ-H, 99:1 hexanes:*i*-PrOH, 0.3 mL/min, 220 nm): t_R: 45.0 min (major) and 50.3 min (minor).

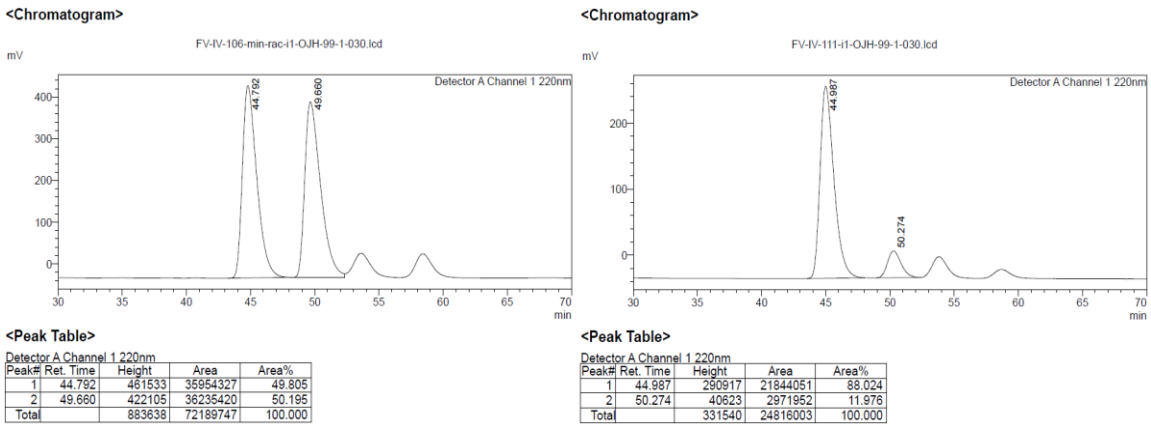

Peak #	Ret. Time	Area	Area %	Peak #	Ret. Time	Area	Area %
1	44.792	35954327	49.805	1	44.987	21844051	88.024
2	49.660	36235420	50.195	2	50.274	2971952	11.976

(3*S*,4*S*)-3-Methyl-7-phenyl-4-(trifluoromethyl)hept-1-en-4-ol (*anti*-2.90): IR (neat): 3549 (br, m), 2962 (w), 1496 (w), 1454 (w), 1239 (m), 1156 (s), 924 (m), 749 (m), 699 (w) cm^{-1}; **^{1}H NMR (400 MHz, $CDCl_3$) for a 74:26 mixture of diastereomers:** δ 7.29 (ddt, *J* = 7.8, 6.7, 1.1 Hz, 2.66H), 7.23 – 7.15 (m, 4H), 5.92 – 5.81 (**major,** m, 1H), 5.81 – 5.72 (**minor,** m, .33H), 5.21 – 5.12 (m, 2.66H), 2.75 – 2.50 (m, 4H), 2.27 (**minor,** s, .33H), 2.05 (**major,** s, 1H), 1.89 – 1.63 (m, 5.32H), 1.11 (**minor**, dq, *J* = 7.2, 1.6 Hz, 1H), 1.08 (**major**, dq, *J* = 7.0, 1.1 Hz, 3H); **^{13}C NMR (100 MHz, $CDCl_3$) for a 74:26 mixture of diastereomers:** δ 141.8, 141.7, 138.1, 138.0, 128.5, 128.5, 126.7 (q, *J* = 287 Hz), 126.6 (q, *J* = 288 Hz), 126.1, 126.0, 118.5, 117.7, 76.6 (q, *J* = 25.6 Hz), 76.1 (q, *J* = 25.5 Hz), 43.7, 41.8, 36.3, 36.2, 32.1, 31.9, 24.5, 24.3, 15.0, 14.1; **^{19}F NMR (376 MHz, $CDCl_3$):** δ –75.15 (**minor**, s, 1F), –75.67 (**major**, s, 3F); **HRMS (DART):** Calcd for $C_{15}H_{18}F_3$ $[M+H–H_2O]^+$: 255.1360; Found: 255.1352; **Specific Rotation:** $[\alpha]^{20.0}_D$ –6.15° (*c* 2.52, $CHCl_3$) for a 74:26 dr, 87:13 er sample. Enantiomeric purity was determined by HPLC analysis in comparison with authentic racemic material (Chiralpak AZ-H, 99:1 hexanes:*i*-PrOH, 0.3 mL/min, 220 nm): t_R: 20.4 min (minor) and 22.2 min (major).

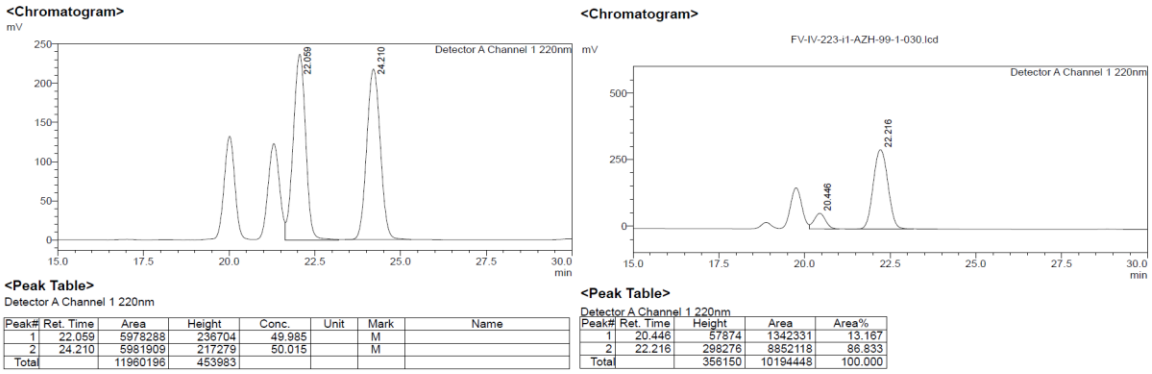

Peak #	Ret. Time	Area	Area %	Peak #	Ret. Time	Area	Area %
1	22.059	5978288	49.985	1	20.446	1342331	13.167
2	24.210	5981909	50.015	2	22.216	8852118	86.833

2.7.4. *Transformations Involving Z-Selective Cross-Metathesis*

(*R*,*Z*)-(2-(Benzyloxy)-1,1,1-trifluorohex-4-en-2-yl)benzene (*Z*-2.91): Sodium hydride (60 wt % in oil, 26 mg, 0.65 mmol) was added to an 8 dram vial equipped with stir bar. The vial was sealed with a septum, placed under vacuum, and back-filled with nitrogen (3 times). DMF (2.5 mL) was added and the resulting suspension was allowed to cool to 0 °C. A solution of ***Z*-2.22** (100 mg, 0.43 mmol) in DMF (2 mL) was added drop-wise. The mixture was allowed to warm to 22 °C and benzyl bromide (62 µL, 0.52 mmol) was added drop-wise after which the mixture was allowed to stir for 14 h at 80 °C. The reaction was then quenched with water and washed with ethyl acetate (3 x 5 mL). The organic layers were dried over $MgSO_4$ and the volatiles were removed in vacuo. The resulting pale yellow oil was purified by silica gel chromatography (100% hexanes) to afford ***Z*-2.91** as colorless oil (110 mg, 0.34 mmol, 80% yield). **IR (neat):** 3031 (w), 1497 (w), 1449 (m), 1263 (m), 1150 (s), 1059 (m), 733 (m), 695 (s), 668 (m) cm^{-1}; **^{1}H NMR (600 MHz, $CDCl_3$):** δ 7.60 (d, *J* = 7.5 Hz, 2H), 7.45 – 7.36 (m, 7H), 7.33 (td, *J* = 7.1, 1.8 Hz, 1H), 5.59 (dddd, *J* = 11.9, 7.0, 4.5, 2.6 Hz, 1H), 5.44 (dt, *J* = 11.4, 6.8 Hz,

1H), 4.72 – 4.53 (m, 2H), 3.09 (ddd, *J* = 126.3, 16.4, 6.5 Hz, 2H), 1.64 (d, *J* = 6.3 Hz, 3H); **^{13}C NMR (150 MHz, $CDCl_3$):** δ 138.0, 136.1, 128.6, 128.5, 128.3, 127.7, 127.6, 127.6, 127.3, 125.7 (q, *J* = 288 Hz, outer peaks overlap with the signals at δ 128.6 and 122.9), 122.9, 81.7 (q, *J* = 26.4 Hz), 66.2, 30.6, 13.2; **^{19}F NMR (564 MHz, $CDCl_3$):** δ –74.77 (s, 3F); **HRMS (DART):** Calcd for $C_{19}H_{23}F_3ON$ $[M+NH_4]^+$: 338.1732; Found: 338.1741; **Specific Rotation:** $[\alpha]^{20.0}_D$ –5.63° (*c* 1.42, $CHCl_3$) for a 99:1 er sample.

(*R*,*Z*)-5-(4-(Benzyloxy)-5,5,5-trifluoro-4-phenylpent-1-en-1-yl)-1-methyl-1H-indole (*Z*-2.96): First, ***Z*-2.91** was dried by azeotropic distillation with anhydrous benzene (3 x 0.1 mL), and was then weighed in a N_2-filled glovebox (10 mg, 0.031 mmol) and placed in an oven-dried 2 dram vial that contained a stir bar. *cis*-1,2-Dichloroethylene (15.4 mg, 0.16 mmol) was added along with a solution of **2.93** in benzene (0.1M, 16 μL, 0.0016 mmol). The vial was then sealed and allowed to stir at 40 °C for 4 h. At this time, the reaction was quenched by the addition of "wet" diethyl ether. The volatiles were then removed in vacuo and the resulting dark red oil was passed through a plug of silica gel to afford a mixture containing >98:2 *Z*:*E* alkenyl chloride (***Z*-2.94**), unreacted starting material, and terphenol ligand. This mixture was directly subjected to the subsequent cross-coupling reaction.

In a N_2-filled glovebox, alkenyl chloride (***Z*-2.94**, 10.2 mg, 0.03 mmol) was weighed out into a 2 dram vial containing a stir bar. A solution of boronic acid **2.95** (7.9 mg, 0.045 mmol), $Pd_2(dba)_3$ (1.4 mg, 0.0015 mmol), xphos (1.4 mg, 0.003 mmol) and CsF (13.7 mg, 0.09 mmol) in dioxane (300 μL) was added. The vial was sealed, brought out of the glovebox and allowed to stir at 100 °C for 16 h. After the solution was allowed to cool to 22 °C, the mixture was diluted with 5 mL diethyl ether and washed with 5 mL

of a 1M solution of NaOH. The layers were separated and the aqueous phase was washed with 5 mL of Et_2O. The resulting orange oil was purified by silica gel chromatography (10:1 pentane:diethyl ether → 1:1 pentane:diethyl ether), affording ***Z*-2.96** as colorless oil (10.8 mg, 0.025 mmol, 80% overall yield, 2 steps) in >98:2 *Z*:*E* selectivity. **IR (neat):** 3029 (w), 2925 (w), 1489 (m), 1448 (m), 1245 (m), 1169 (s), 1064 (m), 718 (s), 699 (s) cm^{-1}; **^{1}H NMR (400 MHz, $CDCl_3$):** δ 7.62 – 7.56 (m, 2H), 7.55 – 7.52 (m, 1H), 7.43 – 7.35 (m, 7H), 7.34 – 7.29 (m, 2H), 7.15 (dd, *J* = 8.5, 1.6 Hz, 1H), 7.08 (d, *J* = 3.1 Hz, 1H), 6.66 (dt, *J* = 11.8, 2.1 Hz, 1H), 6.51 (dd, *J* = 3.1, 0.9 Hz, 1H), 5.61 (dt, *J* = 12.3, 6.6 Hz, 1H), 4.65 – 4.48 (m, 2H), 3.81 (s, 3H), 3.46 (dddd, *J* = 88.2, 17.0, 6.5, 1.9 Hz, 2H); **^{13}C NMR (100 MHz, $CDCl_3$):** δ 138.0, 136.1, 135.9, 133.1, 129.5, 128.6, 128.5, 128.4, 128.3, 125.7 (q, *J* = 289.0 Hz). 127.9, 127.8, 127.6, 127.4, 122.9, 122.1, 121.1, 109.2, 101.3, 81.5 (q, *J* = 26.4 Hz), 66.2, 33.0, 30.8; **^{19}F NMR (376 MHz, $CDCl_3$):** δ –74.44 (s, 3F); **HRMS (DART):** Calcd for $C_{27}H_{25}F_3ON$ $[M+H]^+$: 436.1888; Found: 436.1893; **Specific Rotation:** $[\alpha]^{20.0}_D$ –40.70° (*c* 0.504, $CHCl_3$) for a 99:1 er sample.

(*R*,*Z*)-8,8,8-Trifluoro-7-phenyloct-4-ene-1,7-diol (*Z*-2.99): In a N_2-filled glovebox, ***Z*-2.22** (23.0 mg, 0.1 mmol) was weighed out into an oven dried 2 dram vial equipped with stir a bar. *cis*-4-Hexenol(***Z*-2.97**) (30 mg, 0.3 mmol, 3.0 equiv) was added followed by a solution of **2.98** (3.8 mg, 0.005 mmol) in 150 µL thf. The vial was placed under 100 torr vacuum (generated from a diaphragm pump) and allowed to stir at 22 °C for 8 h. The vessel was removed from the glovebox and the reaction was quenched by the addition of "wet" acetonitrile. Removal of the volatiles in vacuo and purification of the resulting black oil by silica gel chromatography (4:1 pentane:diethyl ether → 1:1 pentane:diethyl ether) afforded ***Z*-2.99** as yellow oil (24.5 mg, 0.089 mmol, 89% yield) in >98:2 *Z*:*E*

selectivity. **IR (neat):** 3330 (br, s), 2938 (w), 1449 (w), 1266 (m), 1151 (s), 1072 (m), 1013 (m), 716 (m), 700 (s) cm^{-1}; **^{1}H NMR (400 MHz, $CDCl_3$):** δ 7.65 – 7.54 (m, 2H), 7.47 – 7.29 (m, 3H), 5.54 (dddd, *J* = 12.6, 6.1, 3.2, 1.3 Hz, 1H), 5.15 (td, *J* = 10.2, 5.8 Hz, 1H), 4.04 (s, 1H), 3.80 – 3.59 (m, 2H), 3.17 – 2.78 (m, 2H), 2.50 – 1.99 (m, 2H), 1.81 – 1.62 (m, 2H), 1.60 – 1.50 (m, 1H); **^{13}C NMR (125 MHz, $CDCl_3$):** δ 137.2, 134.4, 128.4, 128.3, 126.7, 125.7 (q, *J* = 285 Hz), 122.3, 76.3 (q, *J* = 27.9 Hz), 61.5, 33.1, 31.1, 23.4; **^{19}F NMR (376 MHz, $CDCl_3$):** δ –80.67 (s, 3F); **HRMS (ESI+):** Calcd for $C_{14}H_{17}O_2F_3Na$ $[M+Na]^+$: 297.1078; Found: 297.1075; **Specific Rotation:** $[\alpha]^{20.0}_D$ +81.38° (*c* 0.78, $CHCl_3$) for a 99:1 er sample.

2.7.5. *Determination of Relative and Absolute Stereochemistry*

Ethenolysis of *Z*-2.22

Scheme S2.2. Ethenolysis of ***Z*-2.22** to Determine Absolute Stereochemistry

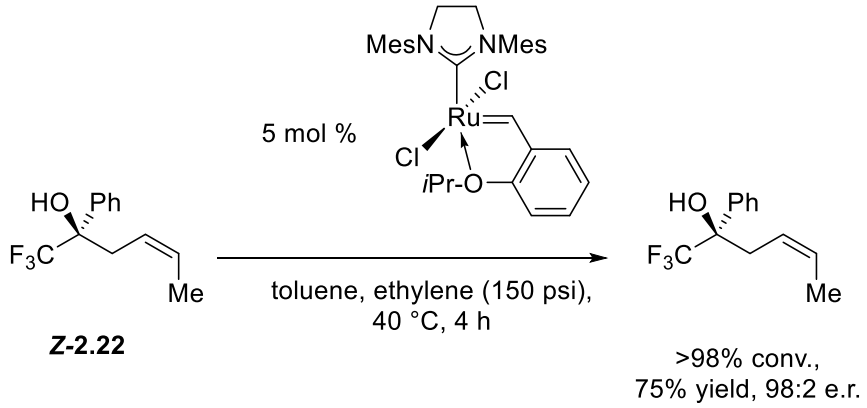

To determine the absolute stereochemistry of ***Z*-2.22** it was converted to a product with known absolute stereochemistry. To do so, the olefin was cleaved utilizing olefin metathesis[29] to generate the corresponding allyl addition product (see Scheme S1). HPLC

29. Marx, V. M.; Sullivan, A. H.; Melaimi, M.; Virgil, S. C.; Keitz, B. K.; Weinberger, D. S.; Bertrand, G.; Grubbs, R. H. *Angew. Chem., Int. Ed.* **2015**, *54*, 1919.

analysis was performed and the trace was compared to the trace in a previous report.[16] The absolute stereochemistry was determined to be (*R*). Enantiomeric purity was determined by HPLC analysis in comparison with authentic racemic material (Chiralpak AS-H, 98:2 hexanes:*i*-PrOH, 0.5 mL/min, 220 nm): t_R: 13.1 (major) and 14.4 min (minor).

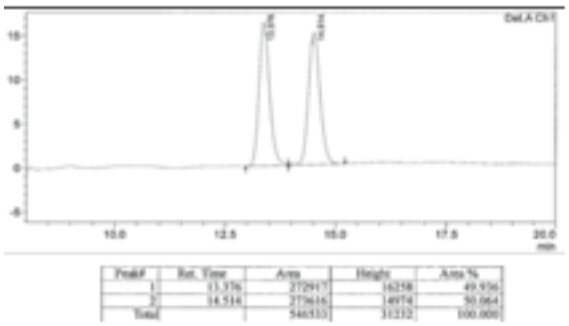

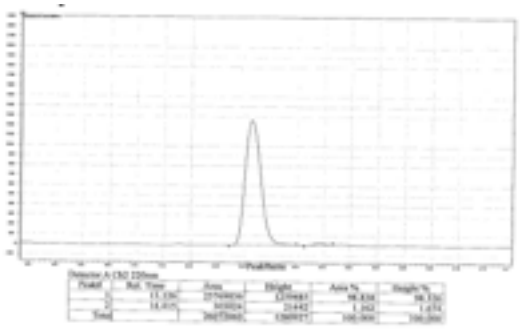

	Ret. Time	Area	Area %	Peak #	Ret. Time	Area	Area %
1	13.376	272917	49.936	1	13.126	25769036	98.838
2	14.514	273616	50.064	2	14.415	303024	1.162

Determination of absolute stereochemistry of *Z*-2.68

Scheme S2.3. Synthesis of **2.71**

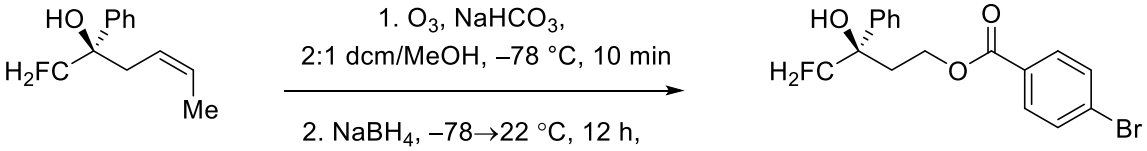

(*R*)-4-Fluoro-3-hydroxy-3-phenylbutyl 4-bromobenzoate (2.71): An 8 dram vial equipped with a stir bar was charged with ***Z*-2.68** (0.1 mmol, 19.4 mg), $NaHCO_3$ (67 mg, 8.0 mmol), 5 mL methanol and 10 mL dichloromethane. The vial was allowed to cool to –78 °C and a stream of ozone was introduced through the solution until it turned light blue. The ozone generator was then shut-off and oxygen was allowed to bubble through the solution until the color disappeared. $NaBH_4$ (30.0 equiv., 30 mmol, 113 mg) was then

added to the solution. The reaction mixture was then allowed to warm to 22 °C and allowed to stir for 12 h. The reaction was quenched by addition of water (after cooling to 0 °C). The organic layer was then removed and the aqueous layer was extracted with EtOAc (3 x 10 mL). The combined organic layers were dried over $MgSO_4$ and filtered. The resulting solution was then concentrated and the residue was treated with 4-bromobenzoyl chloride (1.5 equiv., 0.15 mmol, 33 mg), DMAP (0.2 equiv., 0.02 mmol, 2.4mg), 700 μL dichloromethane and Et_3N (2.0 equiv., 0.4 mmol, 55 μL). The reaction was allowed to stir for 3 hours at 22 °C. The reaction mixture was concentrated and the pale yellow solid was purified by silica gel chromatography (gradient elution, hexanes → 1:1 hexanes:diethyl ether), to afford **2.71** (14.3 mg, 0.039 mmol, 39% yield over 2 steps), as a white solid. **Melting Point:** 81–82 °C; **IR (neat):** 3489 (br, m), 2957 (w), 1714 (s), 1509 (m), 1272 (s), 1117 (m), 1104 (m), 1012 (s), 756 (s), 701 (m) cm^{-1}; **^{1}H NMR (400 MHz, $CDCl_3$):** δ 7.67 – 7.64 (m, 2H), 7.53 – 7.47 (m, 4H), 7.38 – 7.34 (m, 2H), 7.29 – 7.25 (m, 1H), 4.59 – 4.51 (m, 1H), 4.47 – 4.31 (m, 3H), 2.79 (s, 1H), 2.43 (t, *J* = 6.8 Hz, 2H); **^{13}C NMR (150 MHz, $CDCl_3$):** δ 165.9, 140.8 (d, *J* = 3.0 Hz), 131.7, 131.1, 128.9, 128.7, 128.2, 127.8, 125.4, 89.2 (d, *J* = 178.2 Hz), 75.1 (d, *J* = 18.5 Hz), 61.2, 36.4; **^{19}F NMR (376 MHz, $CDCl_3$):** δ –224.1 (t, *J* = 47.4 Hz, 1F); **HRMS (DART):** Calcd for $C_{17}H_{15}BrFO_2$ $[M+H–H_2O]^+$: 349.0239; Found: 349.0245; **Specific Rotation:** $[\alpha]^{20.0}_D$ +7.63° (*c* 0.64, $CHCl_3$) for a 95:5 er sample.

Determination of absolute stereochemistry of the *E*-isomer of 2.68

Scheme S2.4. *Z* and *E* Alkene Isomers Contain *R* and *S* Stereocenters

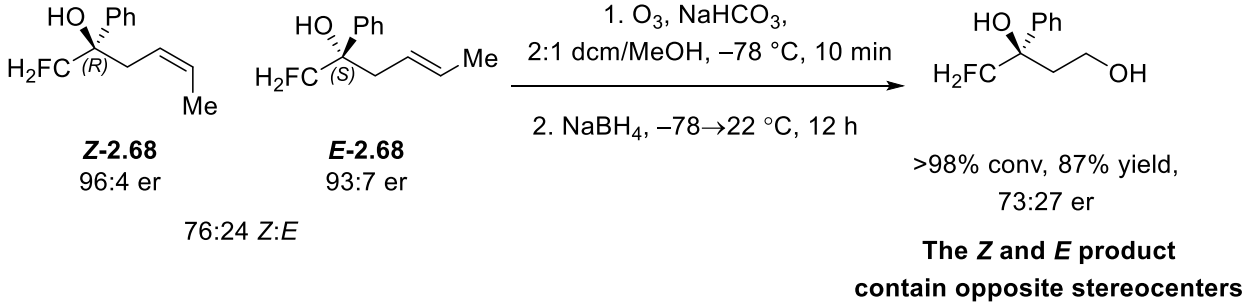

***Z*-2.68** 96:4 er

***E*-2.68** 93:7 er

76:24 *Z*:*E*

>98% conv, 87% yield, 73:27 er

The *Z* and *E* product contain opposite stereocenters

See above for the details of the oxidative cleavage procedure.

HPLC traces for the starting material: The enantiomeric purity was determined by HPLC analysis in comparison with authentic racemic material (Chiralcel OD-H, 98:2 hexanes:*i*-PrOH, 1.0 mL/min, 220 nm): t_R: 8.8 min (minor, *E* isomer), 9.2 (major, *E* isomer), 9.8 (major, *Z* isomer) and 10.2 min (minor, *Z* isomer).

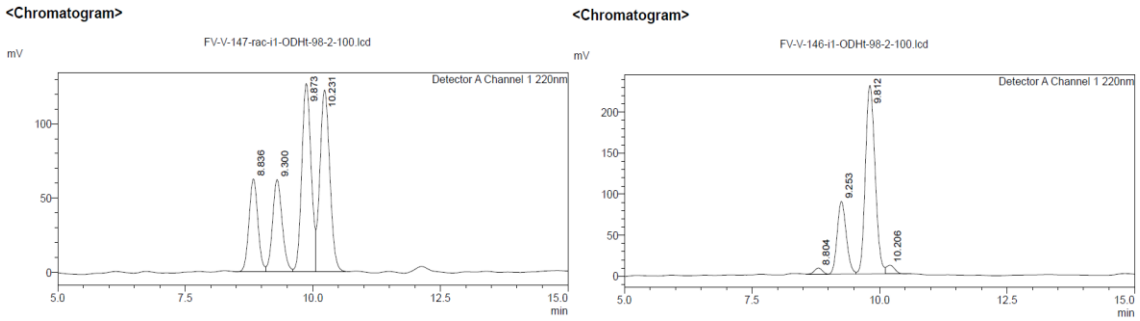

<Peak Table>
Detector A Channel 1 220nm

Peak#	Ret. Time	Height	Area	Area%
1	8.836	62321	758586	15.676
2	9.300	61898	814361	16.828
3	9.873	126476	1616126	33.396
4	10.231	122120	1650155	34.100
Total		372816	4839229	100.000

<Peak Table>
Detector A Channel 1 220nm

Peak#	Ret. Time	Height	Area	Area%
1	8.804	7406	78067	1.793
2	9.253	88415	1106433	25.405
3	9.812	229407	3049096	70.012
4	10.206	10546	121520	2.790
Total		335774	4355116	100.000

Peak	Ret. Time	Area	Area %	Peak #	Ret. Time	Area	Area %
1	8.836 min	758586	15.676	1	8.804 min	78067	1.793
2	9.300 min	814361	16.828	2	9.253 min	1106433	25.405
3	9.873 min	1616126	33.396	3	9.812 min	3049096	70.012
4	10.231 min	1650155	34.100	4	10.206 min	121520	2.790

(*R*)-4-Fluoro-3-phenylbutane-1,3-diol: IR (neat): 3359 (br, s), 2955 (w), 2895 (w), 1493 (w), 1447 (m), 1049 (s), 1015 (s), 763 (m), 701 (s) cm^{-1}; **^{1}H NMR (400 MHz,**

$CDCl_3$): δ 7.51 – 7.45 (m, 2H), 7.44 – 7.36 (m, 2H), 7.34 – 7.27 (m, 1H), 4.46 (d, *J* = 47.8 Hz, 2H), 3.92 (s, 1H), 3.85 – 3.60 (m, 2H), 2.33 (dddd, *J* = 14.9, 9.4, 4.3, 1.2 Hz, 1H), 2.14 (s, 1H), 2.08 (dddd, *J* = 14.9, 5.1, 3.4, 0.8 Hz, 1H); **^{13}C NMR (100 MHz, $CDCl_3$):** δ 141.7 (d, *J* = 3.8 Hz), 128.6, 127.6, 125.6, 89.1 (d, *J* = 178.6 Hz), 77.1 (d, *J* = 17.9 Hz), 59.7, 38.1; **^{19}F NMR (376 MHz, $CDCl_3$):** δ –224.24 (t, *J* = 47.8 Hz, 1F); **HRMS (ESI+):** Calcd for $C_{10}H_{13}F_1O_2Na$ $[M+Na]^+$: 207.0797; Found: 207.0787; **Specific Rotation:** $[\alpha]^{20.0}{}_D$ +19.7° (*c* 0.72, $CHCl_3$) for a 73:27 er sample. The enantiomeric purity was determined by HPLC analysis in comparison with authentic racemic material (Chiralpak AZ-H, 90:10 hexanes:*i*-PrOH, 1.0 mL/min, 220 nm): t_R: 11.0 min (major) and 12.4 min (minor).

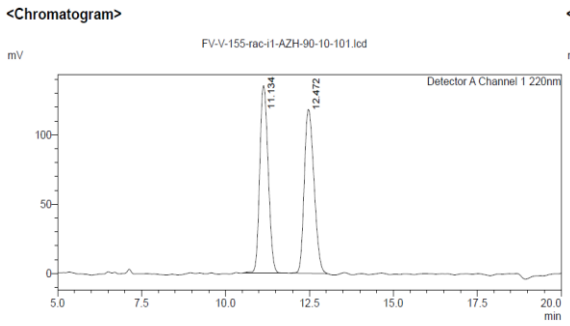

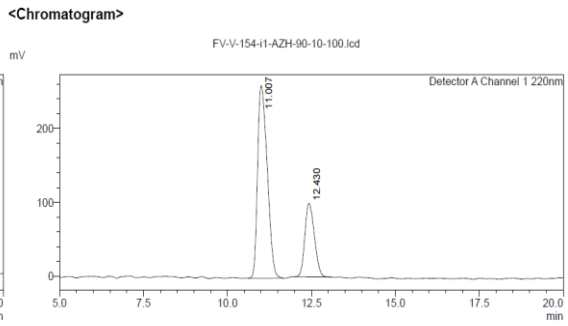

<Peak Table>
Detector A Channel 1 220nm

Peak#	Ret. Time	Height	Area	Area%
1	11.134	135028	2337300	49.588
2	12.472	118283	2376172	50.412
Total		253311	4713472	100.000

<Peak Table>
Detector A Channel 1 220nm

Peak#	Ret. Time	Height	Area	Area%
1	11.007	260486	5182030	72.582
2	12.430	99667	1957474	27.418
Total		360153	7139504	100.000

Peak #	Ret. Time	Area	Area %	Peak #	Ret. Time	Area	Area %
1	11.134	2337300	49.588	1	11.007	5182030	72.582
2	12.472	2376172	50.412	2	12.430	1957474	27.418

Determination of absolute and relative stereochemistry of *anti*-2.82 (synthesis of *anti*-2.83)

Scheme S2.5. Synthesis of ***anti*-2.83**

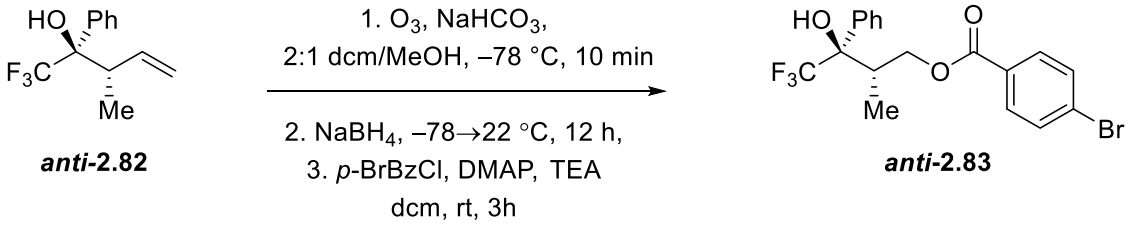

(2*S*,3*R*)-4,4,4-Trifluoro-3-hydroxy-2-methyl-3-phenylbutyl 4-bromobenzoate (*anti*-2.83): The same procedure as above was followed. **Melting Point:** 100 – 103 °C; **IR (neat):** 3459 (br, m), 2922 (w), 1708 (s), 1590 (m), 1270 (s), 1155 (s), 1103 (m), 1012 (m), 757 (m) cm^{-1}; **^{1}H NMR (400 MHz, $CDCl_3$):** δ 7.86 – 7.83 (m, 2H), 7.63 – 7.57 (m, 4H), 7.44 – 7.35 (m, 3H), 4.68 – 4.50 (m, 2H), 3.23 (s, 1H), 2.82 – 2.75 (m, 1H), 0.97 (d, *J* = 7.2 Hz, 3H); **^{13}C NMR (100 MHz, $CDCl_3$):** δ 165.7, 137.1, 132.1, 131.1, 128.7, 128.67, 128.63, 125.9 (q, *J* = 285.3 Hz), 125.7, 79.5 (q, *J* = 23.5 Hz), 66.93, 66.91, 38.3, 12.6; **^{19}F NMR (376 MHz, $CDCl_3$):** δ –75.76 (s); **HRMS (DART):** Calcd for $C_{18}H_{15}BrF_3O_2$ $[M+H–H_2O]^+$: 399.0207; Found: 399.0204; **Specific Rotation:** $[\alpha]^{20.0}_D$ +21.9° (*c* 0.67, $CHCl_3$) for a 93:7 er sample.

2.7.6. *Enantiomerically Enriched α-Methyl Allyl–B(pin) Compounds*

Scheme S2.6. Synthesis of **(*R*)**- and **(*S*)-2.81**

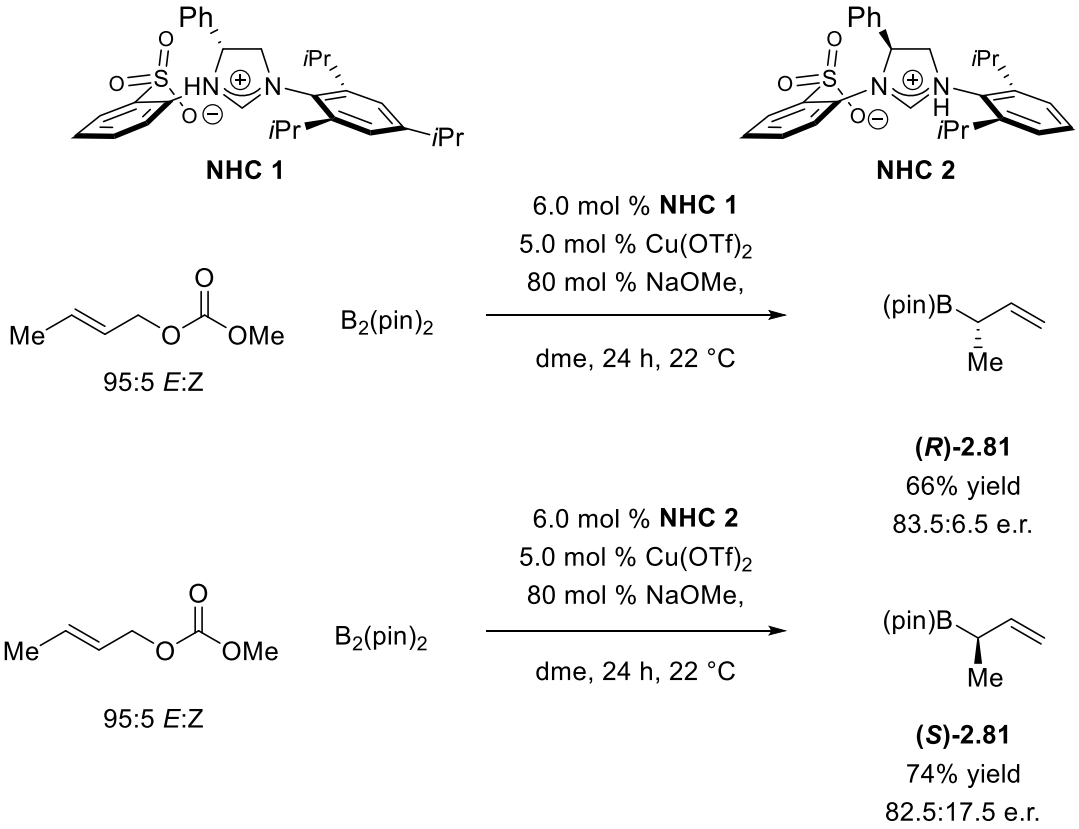

The requisite allylic carbonate was prepared according to literature procedure.[30] Commercially available crotyl alcohol was used (95:5 *E:Z*). The allylic boronates were synthesized by a reported NHC-Cu catalyzed boron allylic substitution.[6] Analytical data for the products were fully consistent with literature values.[19]

Determination of enantiomeric ratio and absolute stereochemistry of (*R*)-2.81: Specific Rotation: $[\alpha]^{20.0}_{D}$ +9.8° (*c* 1.39, $CHCl_3$) for a 83.5:16.5 er sample [literature: $[\alpha]^{14.3}_{D}$ –15.6° (*c* 1.34, $CHCl_3$) for a 2.5:97.5 er sample].[19] Enantiomeric purity was determined by HPLC analysis of the *p*-nitrobenzoyl derivative of the corresponding

30. Ito, H.; Ito, S.; Sasaki, Y.; Matsuura, K.; Sawamura, M. *J. Am. Chem. Soc*. **2007**, *129*, 14856.

alcohol obtained after oxidation (sodium perborate) of the allyl boronate. Commercially available racemic 3-buten-2-ol was used for the racemic sample, after *p*-nitrobenzoyl protection (Chiralcel OZ-H, 99.5:0.5 hexanes:*i*-PrOH, 0.5 mL/min, 220 nm): t_R: 25.5 min (minor) and 28.2 min (major).

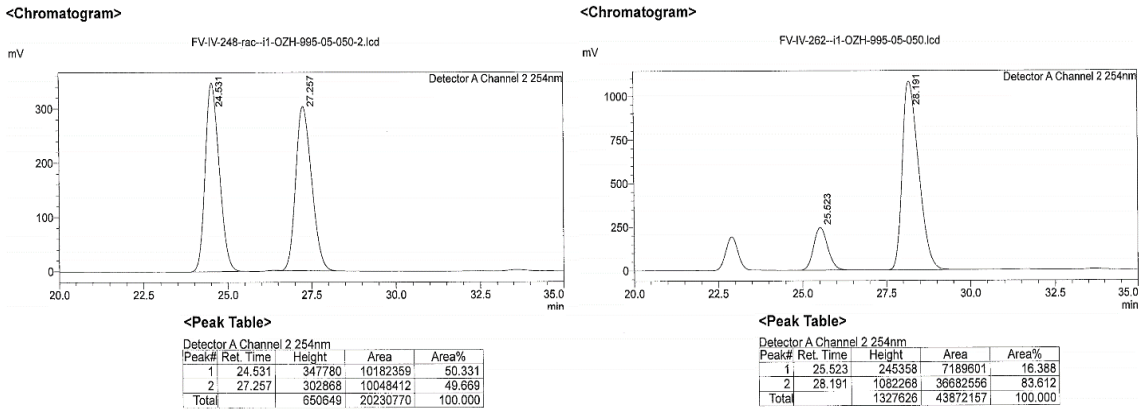

Peak #	Ret. Time	Area	Area %	Peak #	Ret. Time	Area	Area %
1	24.531	10182359	50.331	1	25.523	7189601	16.388
2	27.257	10048412	49.669	2	28.191	36682556	83.612

Determination of enantiomeric ratio and absolute stereochemistry of (*S*)-2.81: **Specific Rotation:** $[\alpha]^{20.0}_D$ –8.7° (*c* 1.38, $CHCl_3$) for a 17.5:82.5 er sample [literature: $[\alpha]^{14.3}_D$ –15.6° (*c* 1.34, $CHCl_3$) for a 2.5:97.5 er sample].[19] Enantiomeric purity was determined by HPLC analysis of the *p*-nitrobenzoyl derivative of the corresponding alcohol obtained after oxidation (sodium perborate) of the allyl boronate. Commercially available racemic 3-buten-2-ol was used for the racemic sample, after *p*-nitrobenzoyl protection (Chiralcel OZ-H, 99.5:0.5 hexanes:*i*-PrOH, 0.5 mL/min, 220 nm): t_R: 25.5 min (major) and 28.4 min (minor).

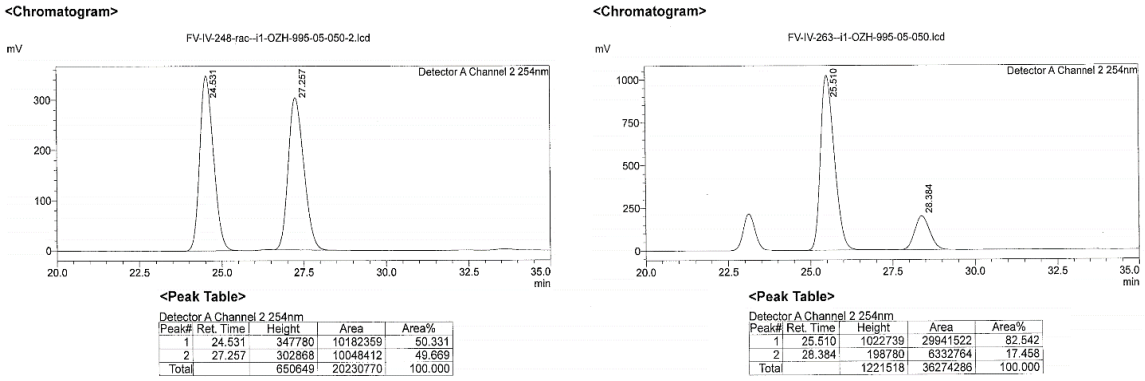

Peak #	Ret. Time	Area	Area %	Peak #	Ret. Time	Area	Area %
1	24.531	10182359	50.331	1	25.510	29941522	82.542
2	27.257	10048412	49.669	2	28.384	6332764	17.458

Reactions with (*R*)-2.81 and (*S*)-2.81:

Scheme S2.7. Reactions with **(*R*)**- and **(*S*)**-2.81

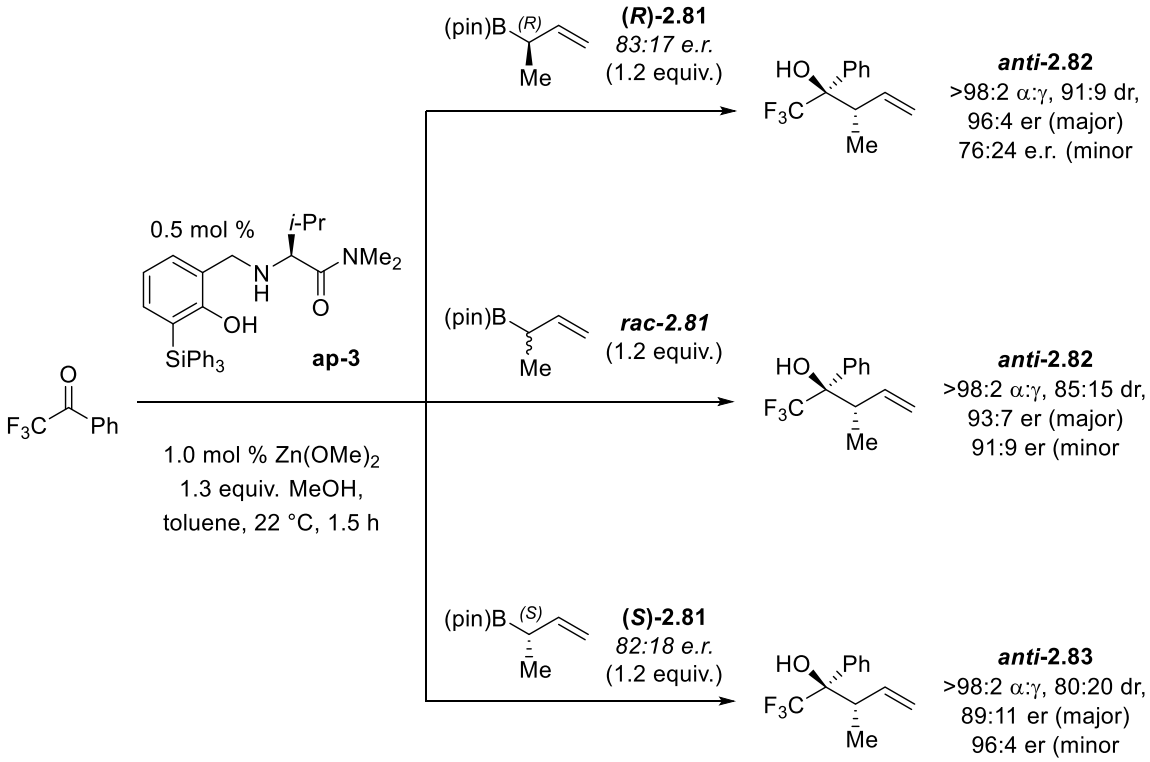

HPLC Data for reactions with (*R*)-2.81: The enantiomeric purity was determined by HPLC analysis in comparison with authentic racemic material (Chiralcel OJ-H, 99:1 hexanes:*i*-PrOH, 0.6 mL/min, 220 nm): t_R: 15.5 min (major) and 23.8 min (minor).

<Chromatogram>

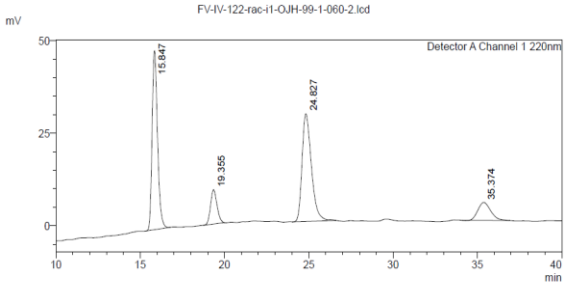

<Peak Table>

Detector A Channel 1 220nm

Peak#	Ret. Time	Height	Area	Area%
1	15.847	48361	1083578	40.137
2	19.355	9244	244806	9.068
3	24.827	29082	1114905	41.298
4	35.374	4838	256398	9.497
Total		91524	2699687	100.000

<Chromatogram>

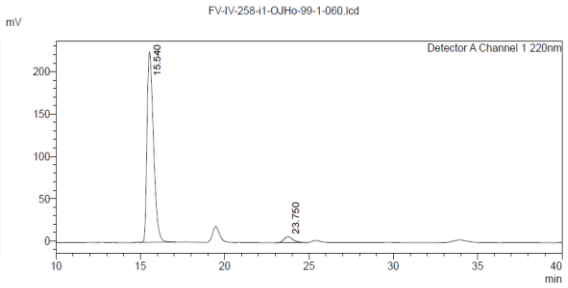

<Peak Table>

Detector A Channel 1 220nm

Peak#	Ret. Time	Height	Area	Area%
1	15.540	224418	5944052	96.101
2	23.750	6786	241171	3.899
Total		231204	6185223	100.000

Peak #	Ret. Time	Area	Area %	Peak #	Ret. Time	Area	Area %
1	15.847	1083578	49.288	1	15.540	5944052	96.101
2	24.827	1114905	50.712	2	23.750	241171	3.899

HPLC Data for reactions with (*S*)-2.81: The enantiomeric purity was determined by HPLC analysis in comparison with authentic racemic material (Chiralcel OJ-H, 99:1 hexanes:*i*-PrOH, 0.6 mL/min, 220 nm): t_R: 15.3 min (major) and 24.0 min (minor).

<Chromatogram>

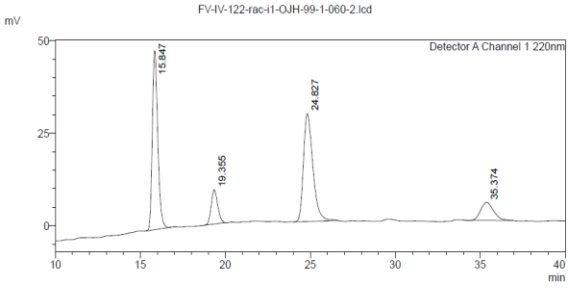

<Peak Table>

Detector A Channel 1 220nm

Peak#	Ret. Time	Height	Area	Area%
1	15.847	48361	1083578	40.137
2	19.355	9244	244806	9.068
3	24.827	29082	1114905	41.298
4	35.374	4838	256398	9.497
Total		91524	2699687	100.000

<Chromatogram>

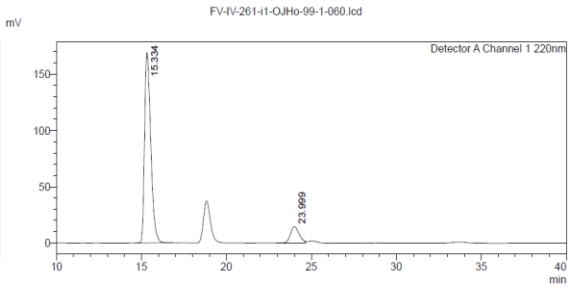

<Peak Table>

Detector A Channel 1 220nm

Peak#	Ret. Time	Height	Area	Area%
1	15.334	168905	4234108	88.830
2	23.999	14685	532407	11.170
Total		183590	4766515	100.000

Peak #	Ret. Time	Area	Area %	Peak #	Ret. Time	Area	Area %
1	15.847	1083578	49.288	1	15.334	4234108	88.830
2	24.827	1114905	50.712	2	23.999	532407	11.170

2.7.7. *DFT Analysis of Transition States*

DFT calculations were performed with the Gaussian 09 suite of programs[31] employing the dispersion corrected ωB97XD functional.[32] The Def2SVP[33] basis set and the SMD[34] solvation model (toluene) was used for geometry optimization and frequency calculation. The nature of all stationary points was checked through vibrational analysis. Single point electronic energy (ΔE_{sp}) calculations applying the ωB97XD functional and the Def2TZVPP[22] basis set in solution with the SMD solvation model were performed on the geometries obtained with the Def2SVP basis set. The single point electronic energies (ΔE_{sp}) at the Def2TZVPP level were corrected by addition of thermal corrections to the Gibbs free energy (ΔG_{corr}) obtained at the corresponding Def2SVP level. Tables of electronic and free energies and single point energies are given below.

---

(31) Frisch, M. J.; Trucks, G. W.; Schlegel, H. B.; Scuseria, G. E.; Robb, M. A.; Cheeseman, J. R.; Scalmani, G.; Barone, V.; Mennucci, B.; Petersson, G. A.; Nakatsuji, H.; Caricato, M.; Li, X.; Hratchian, H. P.; Izmaylov, A. F.; Bloino, J.; Zheng, G.; Sonnenberg, J. L.; Hada, M.; Ehara, M.; Toyota, K.; Fukuda, R.; Hasegawa, J.; Ishida, M.; Nakajima, T.; Honda, Y.; Kitao, O.; Nakai, H.; Vreven, T.; Montgomery Jr., J. A.; Peralta, J. E.; Ogliaro, F.; Bearpark, M.; Heyd, J. J.; Brothers, E.; Kudin, K. N.; Staroverov, V. N.; Kobayashi, R.; Normand, J.; Raghavachari, K.; Rendell, A.; Burant, J. C.; Iyengar, S. S.; Tomasi, J.; Cossi, M.; Rega, N.; Millam, J. M.; Klene, M.; Knox, J. E.; Cross, J. B.; Bakken, V.; Adamo, C.; Jaramillo, J.; Gomperts, R.; Stratmann, R. E.; Yazyev, O.; Austin, A. J.; Cammi, R.; Pomelli, C.; Ochterski, J. W.; Martin R. L.; Morokuma, K.; Zakrzewski, V. G.; Voth, G. A.; Salvador, P.; J. J. Dannenberg, J. J.; Dapprich, S.; Daniels, A. D.; Farkas, Ö.; Foresman, J. B.; Ortiz, J. V.; Cioslowski, J.; Fox, D. J., Gaussian 09, Revision D.01, Gaussian, Inc., Wallingford CT, 2009.

(32) Chai, J.-D.; Head-Gordon, M. *Phys. Chem. Chem. Phys.* **2008**, *10*, 6615–6620.

(33) Weigend, F.; R. Ahlrichs, R. *Phys. Chem. Chem. Phys*. **2005**, *7*, 3297–3305.

(34) Marenich, A. V.; Cramer, C. J.; Truhlar, D. G. *J. Phys. Chem. B* **2009**, *113*, 6378–6396.

Transition States from Reaction with *Z*-Crotyl–B(pin) (*Z*-2.15)

Scheme S2.8. Generation of Intermediate **(*R*)-2.101** from ***Z*-2.15**

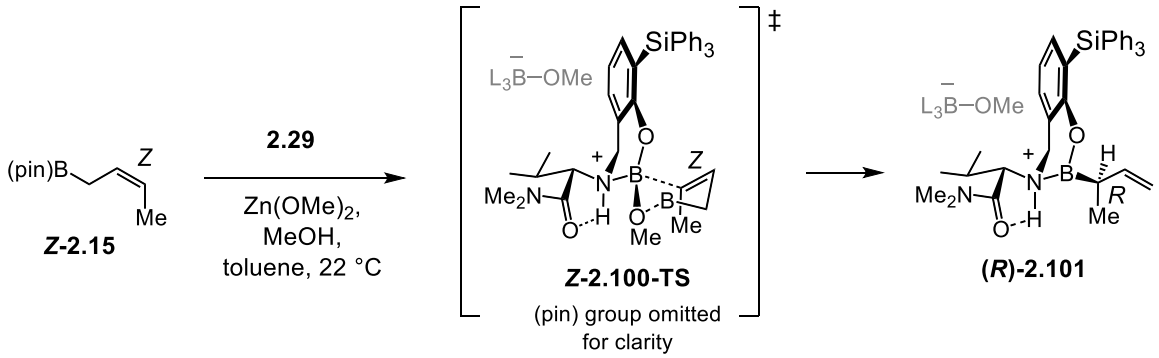

For the chiral intermediate (Scheme S2.8) generated in this pathway, all possible chair and boat transition states were evaluated. Additionally, due to the staggered structure of the phenyl rings on the triphenylsilyl group, both rotamers of every transition state were analyzed. As can be seen in the located transition state structures for this pathway (Scheme S2.9), the driving force for high *Z*-selectivity originates from a steric preference for placing the methyl group pseudo-axially in the 6-membered ring transition state. This is likely due to the fact that placement of this methyl group in the pseudo-equatorial position generates *syn*-pentane or eclipsing interactions with the backbone of the aminophenol complex. Additionally, enantiotopic facial selectivity comes from preferential placement of the trifluoromethyl group in close proximity to the ammonium group on the complex. This electrostratic interaction has been discussed at length in the corresponding allylation of these substrates.[35] In general the boat-like transition states are much higher in energy than their corresponding chair-like transition states.

(35) Lee, K.; Silverio, D.L.; Torker, S.; Haeffner, F.; Robbins, D. W.; van der Mei, F. W.; Hoveyda, A. H. *Nat. Chem.* **2016**, *8*, 768.

Scheme S2.9: Transition state structures accessed from *Z*-Crotyl–B(pin).

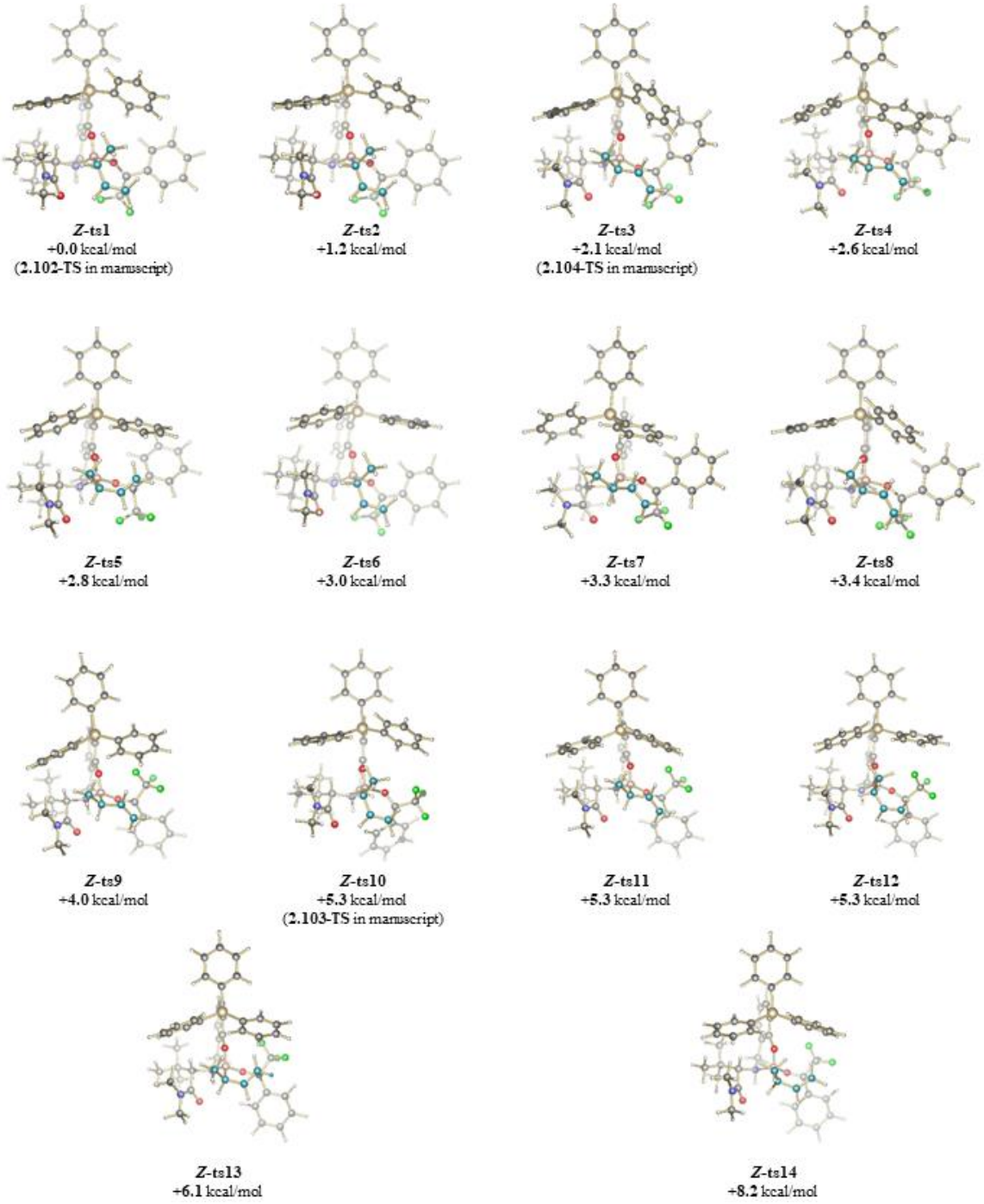

***Table S2.1*: *Z*-Crotyl–B(pin) pathway transition state energies and Gibbs free energies calculated with ωB97XD/Def2SVP, calculations were carried out in toluene with the SMD solvation model.**

TS	Product	E [Hartree]	ΔE [kcal/mol]	G [Hartree]	ΔG [kcal/mol]	ΔG_{corr} [kcal/mol]	Freq [cm^{-1}]
***Z*-ts1**	(*Z*)-*R*-3a	-2690.799983	0.0	-2690.017716	0.0	0.0	-160.669
***Z*-ts2**	(*Z*)-*R*-3a	-2690.799851	0.1	-2690.01585	1.2	1.1	-178.3144
***Z*-ts3**	(*E*)-*R*-3a	-2690.796943	1.9	-2690.01207	3.5	1.6	-126.4984
***Z*-ts4**	(*E*)-*R*-3a	-2690.795037	3.1	-2690.011384	4.0	0.9	-125.5145
***Z*-ts5**	(*Z*)-*R*-3a	-2690.794726	3.3	-2690.011736	3.8	0.5	-88.049
***Z*-ts6**	(*Z*)-*R*-3a	-2690.798066	1.2	-2690.012885	3.0	1.8	-206.9677
***Z*-ts7**	(*E*)-*R*-3a	-2690.793762	3.9	-2690.01173	3.8	-0.1	-213.4408
***Z*-ts8**	(*E*)-*R*-3a	-2690.795929	2.5	-2690.011442	3.9	1.4	-202.3365
***Z*-ts9**	(*E*)-*S*-3a	-2690.793443	4.1	-2690.010294	4.7	0.6	-190.9625
***Z*-ts10**	(*Z*)-*S*-3a	-2690.791827	5.1	-2690.007837	6.2	1.1	-171.1397
***Z*-ts11**	(*E*)-*S*-3a	-2690.791817	5.1	-2690.008099	6.0	0.9	-160.974
***Z*-ts12**	(*Z*)-*S*-3a	-2690.787894	7.6	-2690.007512	6.4	-1.2	-245.8888
***Z*-ts13**	(*Z*)-*S*-3a	-2690.789515	6.6	-2690.006908	6.8	0.2	-182.5052
***Z*-ts14**	(*Z*)-*S*-3a	-2690.787151	8.1	-2690.003514	8.9	0.9	-202.8154

***Table S2.2*: *Z*-Crotyl–B(pin) pathway transition state single point energies calculated with ωB97XD/Def2TZVPP, calculations were carried out in toluene with the SMD solvation model.**

Transition State	Resulting Product Isomer	E_{sp} [Hartree]	ΔE_{sp} [kcal/mol]	ΔG_{sp} [kcal/mol]
***Z*-ts1**	(*Z*)-*R*-3a	-2693.494925	0.0	0.0
***Z*-ts2**	(*Z*)-*R*-3a	-2693.494824	0.1	1.2
***Z*-ts3**	(*E*)-*R*-3a	-2693.49418	0.5	2.1
***Z*-ts4**	(*E*)-*R*-3a	-2693.492202	1.7	2.6
***Z*-ts5**	(*Z*)-*R*-3a	-2693.491187	2.3	2.8
***Z*-ts6**	(*Z*)-*R*-3a	-2693.492995	1.2	3.0
***Z*-ts7**	(*E*)-*R*-3a	-2693.489361	3.5	3.3
***Z*-ts8**	(*E*)-*R*-3a	-2693.491777	2.0	3.4
***Z*-ts9**	(*E*)-*S*-3a	-2693.489421	3.5	4.0
***Z*-ts10**	(*Z*)-*S*-3a	-2693.488199	4.2	5.3
***Z*-ts11**	(*E*)-*S*-3a	-2693.487908	4.4	5.3
***Z*-ts12**	(*Z*)-*S*-3a	-2693.483644	7.1	5.9
***Z*-ts13**	(*Z*)-*S*-3a	-2693.485487	5.9	6.1
***Z*-ts14**	(*Z*)-*S*-3a	-2693.483179	7.4	8.2

Transition States from Reaction with *E*-Crotyl–B(pin) (*E*-2.15)

Scheme S2.10. Generation of Intermediate **(*S*)-2.101** from ***E*-2.15**

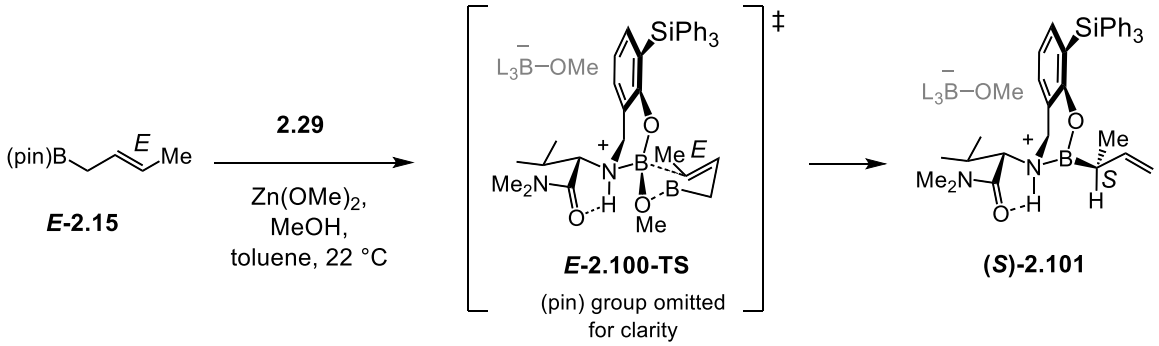

For the chiral intermediate (Scheme S2.10) in this pathway, all possible chair and boat transition state were also evaluated. Additionally, due to the staggered structure of the phenyl rings on the triphenylsilyl group, both rotamers of every transition state were analyzed. As can be seen in the located transition state structures for this pathway (Scheme S2.11), the driving force for high *Z*-selectivity again originates from a steric preference for placing the methyl group pseudo-axially in the 6-membered ring transition state. However, to do so for this complex, the carbon-carbon bond forming step must go through a completely different chair transition state (see ***Z*-ts1**, Scheme S2.9 and ***E*-ts1**, Scheme S2.11) due to this intermediate having the opposite configuration at that carbon. This has profound impacts on the enantioselectivity of the transformation with the *E*-crotyl-B(pin) reagent, as well as why in some cases the product is obtained with the opposite sense of enantioselectivity. The reason for this phenomenon could be that in ***E*-ts1** the trifluoromethyl group is located much further away from the ammonium group, weakening the electrostatic attraction and subsequently lowering enantioselectivity. This effect can further be seen when very sterically demanding *o*-substituted substrates are used. In these cases, the steric pressure of these groups overwhelms the stabilization

gained from the electrostatic interaction, causing the substrate to bind with the phenyl ring pointing down (as shown in ***E*-ts2**, Scheme S2.11). As seen previously, the boat-like transition states are much higher in energy than their corresponding chair-like transition states.

Scheme S10: Transition state structures accessed from *E*-Crotyl–B(pin).

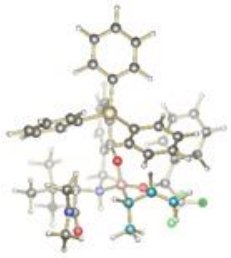

***E*-ts1**
+0.0 kcal/mol
(**2.105-TS** in manuscript)

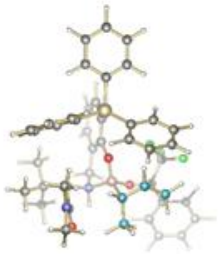

***E*-ts2**
+0.9 kcal/mol
(**2.106-TS** in manuscript)

***E*-ts3**
+1.5 kcal/mol

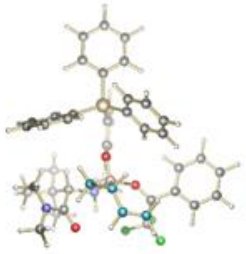

***E*-ts4**
+2.8 kcal/mol
(**2.107-TS** in manuscript)

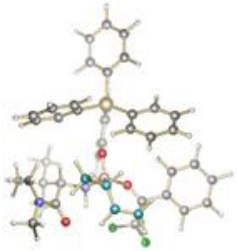

***E*-ts5**
+4.2 kcal/mol

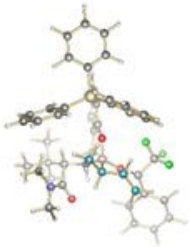

***E*-ts6**
+5.6 kcal/mol

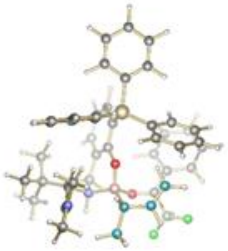

***E*-ts7**
+8.0 kcal/mol

***E*-ts8**
+8.3 kcal/mol

***E*-ts9**
+8.9 kcal/mol

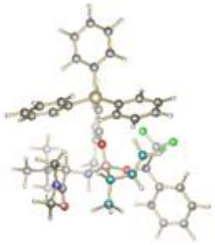

***E*-ts10**
+9.5 kcal/mol

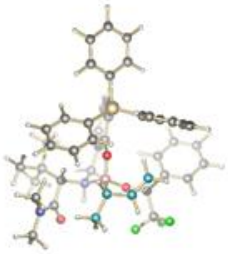

***E*-ts11**
+10.0 kcal/mol

***E*-ts12**
+10.5 kcal/mol

***Table S2.3*: *E*-Crotyl–B(pin) pathway transition state energies and Gibbs free energies calculated with ωB97XD/Def2SVP, calculations were carried out in toluene with the SMD solvation model**

TS	Product	E [Hartree]	ΔE [kcal/mol]	G [Hartree]	ΔG [kcal/mol]	ΔG_{corr} [kcal/mol]	Freq [cm^{-1}]
***E*-ts1**	(*Z*)-*R*-3a	-2690.796277	0.0	-2690.012583	0.0	0.0	-48.2638
***E*-ts2**	(*Z*)-*S*-3a	-2690.793805	1.6	-2690.012441	0.1	-1.5	-184.2725
***E*-ts3**	(*Z*)-*R*-3a	-2690.795336	0.6	-2690.010308	1.4	0.8	-153.5039
***E*-ts4**	(*E*)-*R*-3a	-2690.790148	3.8	-2690.009451	2.0	-1.9	-215.1569
***E*-ts5**	(*E*)-*R*-3a	-2690.790619	3.6	-2690.007578	3.1	-0.4	-262.8373
***E*-ts6**	(*Z*)-*S*-3a	-2690.790418	3.7	-2690.005434	4.5	0.8	-240.6652
***E*-ts7**	(*E*)-*R*-3a	-2690.781883	9.0	-2689.999544	8.2	-0.9	-99.3569
***E*-ts8**	(*E*)-*S*-3a	-2690.781243	9.4	-2689.999002	8.5	-0.9	-222.253
***E*-ts9**	(*E*)-*S*-3a	-2690.783163	8.2	-2689.998282	9.0	0.7	-224.706
***E*-ts10**	(*E*)-*S*-3a	-2690.779786	10.3	-2689.997323	9.6	-0.8	-128.6955
***E*-ts11**	(*E*)-*R*-3a	-2690.782824	8.4	-2689.997204	9.7	1.2	-160.8634
***E*-ts12**	(*E*)-*S*-3a	-2690.778148	11.4	-2689.996311	10.2	-1.2	-182.8265

***Table S2.4*: *E*-Crotyl–B(pin) pathway transition state single point energies calculated with ωB97XD/Def2TZVPP, calculations were carried out in toluene with the SMD solvation model.**

Transition State	Resulting Product Isomer	E_{sp} [Hartree]	ΔE_{sp} [kcal/mol]	ΔG_{sp} [kcal/mol]
***E*-ts1**	(*Z*)-*R*-3a	-2693.492677	0.0	0.0
***E*-ts2**	(*Z*)-*S*-3a	-2693.488967	2.3	0.9
***E*-ts3**	(*Z*)-*R*-3a	-2693.491636	0.7	1.5
***E*-ts4**	(*E*)-*R*-3a	-2693.485266	4.7	2.8
***E*-ts5**	(*E*)-*R*-3a	-2693.48528	4.6	4.2
***E*-ts6**	(*Z*)-*S*-3a	-2693.485033	4.8	5.6
***E*-ts7**	(*E*)-*R*-3a	-2693.478606	8.8	8.0
***E*-ts8**	(*E*)-*S*-3a	-2693.477975	9.2	8.3
***E*-ts9**	(*E*)-*S*-3a	-2693.479692	8.1	8.9
***E*-ts10**	(*E*)-*S*-3a	-2693.476354	10.2	9.5
***E*-ts11**	(*E*)-*R*-3a	-2693.478704	8.8	10.0
***E*-ts12**	(*E*)-*S*-3a	-2693.47406	11.7	10.5

2.7.8. *Crystallographic Data*

Crystallographic Data for (*R*,*Z*)-1,1,1-Trifluoro-2-(pyridine-3-yl)hex-4-en-2-ol (*Z*-2.53)

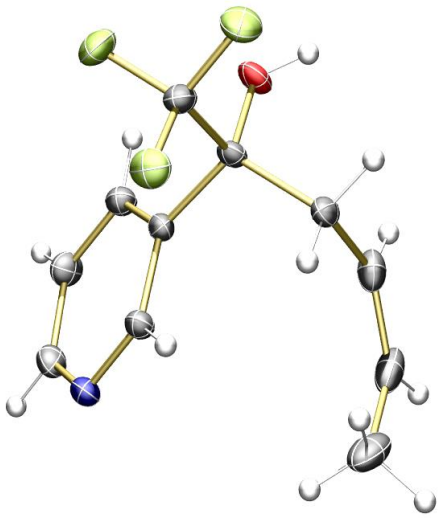

Table S2.5. Crystal data and structure refinement for $C_{11}H_{12}F_3NO$

Identification code	C11H12F3NO	
Empirical formula	C11 H12 F3 N O	
Formula weight	231.22	
Temperature	100(2) K	
Wavelength	0.71073 Å	
Crystal system	Triclinic	
Space group	P-1	
Unit cell dimensions	a = 9.2081(17) Å	□= 64.322(4)°.
	b = 10.881(2) Å	□= 85.777(4)°.
	c = 12.396(2) Å	□ = 86.065(4)°.
Volume	1115.3(4) $Å^3$	
Z	4	
Density (calculated)	1.377 Mg/m^3	
Absorption coefficient	0.122 mm^{-1}	
F(000)	480	
Crystal size	0.600 x 0.170 x 0.150 mm^3	
Theta range for data collection	1.825 to 28.324°.	
Index ranges	-12<=h<=12, -12<=k<=14, 0<=l<=16	

Reflections collected	5569
Independent reflections	5569 [R(int) = ?]
Completeness to theta = 25.242°	100.0 %
Absorption correction	Semi-empirical from equivalents
Max. and min. transmission	0.7457 and 0.5883
Refinement method	Full-matrix least-squares on F^2
Data / restraints / parameters	5569 / 0 / 298
Goodness-of-fit on F^2	1.037
Final R indices [I>2sigma(I)]	R1 = 0.0401, wR2 = 0.0989
R indices (all data)	R1 = 0.0493, wR2 = 0.1046
Extinction coefficient	na
Largest diff. peak and hole	0.359 and -0.291 e.$Å^{-3}$

Table S2.6. Atomic coordinates ($x10^4$) and equivalent isotropic displacement parameters ($Å^2x10^3$) for $C_{11}H_{12}F_3NO$. U(eq) is defined as one third of the trace of the orthogonalized U^{ij} tensor

	x	y	z	U(eq)
F(1)	4026(1)	8025(1)	8853(1)	29(1)
F(2)	3629(1)	5872(1)	9598(1)	31(1)
F(3)	5467(1)	6679(1)	8346(1)	30(1)
O(1)	3193(1)	6010(1)	7347(1)	24(1)
N(1)	-406(1)	8923(1)	8140(1)	19(1)
C(1)	2033(2)	11265(2)	4878(2)	33(1)
C(2)	2061(2)	9972(2)	4719(2)	28(1)
C(3)	2751(2)	8788(2)	5351(1)	25(1)
C(4)	3679(2)	8448(2)	6411(1)	20(1)
C(5)	3100(2)	7203(1)	7533(1)	17(1)
C(6)	1517(2)	7420(1)	7901(1)	16(1)
C(7)	981(2)	8676(1)	7854(1)	18(1)
C(8)	-1324(2)	7894(2)	8519(1)	21(1)
C(9)	-895(2)	6604(2)	8614(2)	24(1)
C(10)	544(2)	6367(2)	8295(1)	20(1)
C(11)	4055(2)	6937(2)	8592(1)	22(1)
F(4)	10037(1)	1510(1)	9159(1)	30(1)
F(5)	10404(1)	3482(1)	7679(1)	29(1)
F(6)	8711(1)	3279(1)	9043(1)	27(1)
O(2)	9082(1)	1704(1)	7023(1)	23(1)
N(2)	5772(1)	5520(1)	6322(1)	20(1)
C(12)	3759(2)	2010(2)	8795(2)	35(1)
C(13)	4506(2)	1386(2)	8028(2)	30(1)
C(14)	5930(2)	1123(2)	7910(2)	26(1)
C(15)	7106(2)	1399(1)	8550(1)	19(1)
C(16)	8271(2)	2339(1)	7664(1)	17(1)
C(17)	7590(2)	3681(1)	6752(1)	16(1)
C(18)	6478(2)	4398(1)	7097(1)	18(1)
C(19)	6181(2)	5986(2)	5152(1)	22(1)

C(20)	7300(2)	5376(2)	4725(1)	24(1)
C(21)	8019(2)	4199(2)	5538(1)	20(1)
C(22)	9358(2)	2656(2)	8389(1)	21(1)

Table S2.7. Bond lengths [Å] and angles [°] for $C_{11}H_{12}F_3NO$

F(1)-C(11)	1.3534(19)
F(2)-C(11)	1.3383(18)
F(3)-C(11)	1.3517(17)
O(1)-C(5)	1.4104(18)
O(1)-H(1O)	0.84(2)
N(1)-C(7)	1.3417(19)
N(1)-C(8)	1.343(2)
C(1)-C(2)	1.501(2)
C(1)-H(1A)	0.9800
C(1)-H(1B)	0.9800
C(1)-H(1C)	0.9800
C(2)-C(3)	1.328(2)
C(2)-H(2)	0.9500
C(3)-C(4)	1.514(2)
C(3)-H(3)	0.9500
C(4)-C(5)	1.553(2)
C(4)-H(4A)	0.9900
C(4)-H(4B)	0.9900
C(5)-C(6)	1.5277(19)
C(5)-C(11)	1.545(2)
C(6)-C(10)	1.395(2)
C(6)-C(7)	1.3987(19)
C(7)-H(7)	0.9500
C(8)-C(9)	1.389(2)
C(8)-H(8)	0.9500
C(9)-C(10)	1.394(2)
C(9)-H(9)	0.9500
C(10)-H(10)	0.9500
F(4)-C(22)	1.3446(17)
F(5)-C(22)	1.3483(18)
F(6)-C(22)	1.3488(18)
O(2)-C(16)	1.4084(17)
O(2)-H(2O)	0.83(2)

N(2)-C(18)	1.3423(19)
N(2)-C(19)	1.346(2)
C(12)-C(13)	1.495(3)
C(12)-H(12A)	0.9800
C(12)-H(12B)	0.9800
C(12)-H(12C)	0.9800
C(13)-C(14)	1.334(2)
C(13)-H(13)	0.9500
C(14)-C(15)	1.507(2)
C(14)-H(14)	0.9500
C(15)-C(16)	1.551(2)
C(15)-H(15A)	0.9900
C(15)-H(15B)	0.9900
C(16)-C(17)	1.5334(19)
C(16)-C(22)	1.542(2)
C(17)-C(21)	1.396(2)
C(17)-C(18)	1.398(2)
C(18)-H(18)	0.9500
C(19)-C(20)	1.383(2)
C(19)-H(19)	0.9500
C(20)-C(21)	1.399(2)
C(20)-H(20)	0.9500
C(21)-H(21)	0.9500

C(5)-O(1)-H(1O)	107.7(15)
C(7)-N(1)-C(8)	117.91(12)
C(2)-C(1)-H(1A)	109.5
C(2)-C(1)-H(1B)	109.5
H(1A)-C(1)-H(1B)	109.5
C(2)-C(1)-H(1C)	109.5
H(1A)-C(1)-H(1C)	109.5
H(1B)-C(1)-H(1C)	109.5
C(3)-C(2)-C(1)	128.29(16)
C(3)-C(2)-H(2)	115.9
C(1)-C(2)-H(2)	115.9

C(2)-C(3)-C(4)	126.96(15)
C(2)-C(3)-H(3)	116.5
C(4)-C(3)-H(3)	116.5
C(3)-C(4)-C(5)	111.20(12)
C(3)-C(4)-H(4A)	109.4
C(5)-C(4)-H(4A)	109.4
C(3)-C(4)-H(4B)	109.4
C(5)-C(4)-H(4B)	109.4
H(4A)-C(4)-H(4B)	108.0
O(1)-C(5)-C(6)	107.79(11)
O(1)-C(5)-C(11)	107.32(11)
C(6)-C(5)-C(11)	108.37(12)
O(1)-C(5)-C(4)	111.44(13)
C(6)-C(5)-C(4)	112.95(11)
C(11)-C(5)-C(4)	108.77(12)
C(10)-C(6)-C(7)	117.21(13)
C(10)-C(6)-C(5)	121.04(12)
C(7)-C(6)-C(5)	121.74(12)
N(1)-C(7)-C(6)	123.85(13)
N(1)-C(7)-H(7)	118.1
C(6)-C(7)-H(7)	118.1
N(1)-C(8)-C(9)	122.70(14)
N(1)-C(8)-H(8)	118.6
C(9)-C(8)-H(8)	118.6
C(8)-C(9)-C(10)	118.77(14)
C(8)-C(9)-H(9)	120.6
C(10)-C(9)-H(9)	120.6
C(9)-C(10)-C(6)	119.53(13)
C(9)-C(10)-H(10)	120.2
C(6)-C(10)-H(10)	120.2
F(2)-C(11)-F(3)	107.08(12)
F(2)-C(11)-F(1)	106.80(13)
F(3)-C(11)-F(1)	106.65(12)
F(2)-C(11)-C(5)	112.52(13)
F(3)-C(11)-C(5)	111.52(13)

F(1)-C(11)-C(5)	111.92(12)
C(16)-O(2)-H(2O)	107.6(15)
C(18)-N(2)-C(19)	117.74(13)
C(13)-C(12)-H(12A)	109.5
C(13)-C(12)-H(12B)	109.5
H(12A)-C(12)-H(12B)	109.5
C(13)-C(12)-H(12C)	109.5
H(12A)-C(12)-H(12C)	109.5
H(12B)-C(12)-H(12C)	109.5
C(14)-C(13)-C(12)	127.80(16)
C(14)-C(13)-H(13)	116.1
C(12)-C(13)-H(13)	116.1
C(13)-C(14)-C(15)	125.62(16)
C(13)-C(14)-H(14)	117.2
C(15)-C(14)-H(14)	117.2
C(14)-C(15)-C(16)	112.09(13)
C(14)-C(15)-H(15A)	109.2
C(16)-C(15)-H(15A)	109.2
C(14)-C(15)-H(15B)	109.2
C(16)-C(15)-H(15B)	109.2
H(15A)-C(15)-H(15B)	107.9
O(2)-C(16)-C(17)	107.91(12)
O(2)-C(16)-C(22)	106.91(11)
C(17)-C(16)-C(22)	109.24(12)
O(2)-C(16)-C(15)	112.11(12)
C(17)-C(16)-C(15)	112.00(11)
C(22)-C(16)-C(15)	108.53(12)
C(21)-C(17)-C(18)	117.62(13)
C(21)-C(17)-C(16)	120.96(13)
C(18)-C(17)-C(16)	121.37(13)
N(2)-C(18)-C(17)	123.67(14)
N(2)-C(18)-H(18)	118.2
C(17)-C(18)-H(18)	118.2
N(2)-C(19)-C(20)	123.01(14)
N(2)-C(19)-H(19)	118.5

C(20)-C(19)-H(19)	118.5
C(19)-C(20)-C(21)	118.79(14)
C(19)-C(20)-H(20)	120.6
C(21)-C(20)-H(20)	120.6
C(17)-C(21)-C(20)	119.12(14)
C(17)-C(21)-H(21)	120.4
C(20)-C(21)-H(21)	120.4
F(4)-C(22)-F(5)	106.94(12)
F(4)-C(22)-F(6)	106.90(13)
F(5)-C(22)-F(6)	106.55(12)
F(4)-C(22)-C(16)	111.21(12)
F(5)-C(22)-C(16)	112.17(13)
F(6)-C(22)-C(16)	112.71(12)

Symmetry transformations used to generate equivalent atoms:

Table S2.8. Anisotropic displacement parameters ($Å^2x10^3$) for $C_{11}H_{12}F_3NO$. The anisotropic displacement factor exponent takes the form: $-2p^2[h^2a^{*2}U^{11} + ... + 2hka^*b^*U^{12}]$

	U^{11}	U^{22}	U^{33}	U^{23}	U^{13}	U^{12}
F(1)	31(1)	32(1)	29(1)	-16(1)	-10(1)	3(1)
F(2)	23(1)	31(1)	24(1)	2(1)	-2(1)	5(1)
F(3)	13(1)	37(1)	32(1)	-10(1)	-4(1)	5(1)
O(1)	19(1)	18(1)	36(1)	-16(1)	5(1)	2(1)
N(1)	18(1)	19(1)	20(1)	-8(1)	-2(1)	6(1)
C(1)	35(1)	25(1)	32(1)	-6(1)	-4(1)	2(1)
C(2)	31(1)	31(1)	19(1)	-7(1)	-4(1)	-5(1)
C(3)	30(1)	26(1)	21(1)	-12(1)	1(1)	-4(1)
C(4)	18(1)	18(1)	21(1)	-7(1)	2(1)	0(1)
C(5)	14(1)	14(1)	21(1)	-6(1)	-2(1)	2(1)
C(6)	14(1)	16(1)	16(1)	-7(1)	-3(1)	3(1)
C(7)	17(1)	15(1)	19(1)	-6(1)	-2(1)	1(1)
C(8)	14(1)	25(1)	24(1)	-10(1)	-1(1)	4(1)
C(9)	16(1)	21(1)	32(1)	-9(1)	1(1)	-3(1)
C(10)	18(1)	14(1)	27(1)	-8(1)	-2(1)	2(1)
C(11)	15(1)	22(1)	24(1)	-6(1)	0(1)	4(1)
F(4)	24(1)	28(1)	32(1)	-7(1)	-11(1)	6(1)
F(5)	18(1)	32(1)	35(1)	-12(1)	2(1)	-7(1)
F(6)	26(1)	32(1)	29(1)	-19(1)	-3(1)	0(1)
O(2)	27(1)	17(1)	25(1)	-10(1)	4(1)	7(1)
N(2)	19(1)	16(1)	24(1)	-9(1)	0(1)	2(1)
C(12)	19(1)	43(1)	33(1)	-6(1)	-3(1)	-3(1)
C(13)	27(1)	26(1)	27(1)	0(1)	-8(1)	-12(1)
C(14)	31(1)	19(1)	25(1)	-7(1)	-3(1)	-7(1)
C(15)	18(1)	15(1)	20(1)	-4(1)	0(1)	1(1)
C(16)	16(1)	16(1)	19(1)	-9(1)	1(1)	3(1)
C(17)	15(1)	14(1)	20(1)	-8(1)	0(1)	-1(1)
C(18)	18(1)	16(1)	20(1)	-8(1)	1(1)	1(1)
C(19)	23(1)	17(1)	22(1)	-5(1)	-4(1)	1(1)

C(20)	25(1)	24(1)	18(1)	-5(1)	3(1)	-2(1)
C(21)	19(1)	21(1)	22(1)	-10(1)	2(1)	1(1)
C(22)	15(1)	21(1)	23(1)	-8(1)	1(1)	1(1)

Table S2.9. Hydrogen coordinates ($x10^4$) and isotropic displacement parameters ($Å^2x10^3$) for $C_{11}H_{12}F_3NO$

	x	y	z	U(eq)
H(1O)	4020(20)	5970(20)	7030(20)	35
H(1A)	2742	11173	5464	49
H(1B)	1056	11439	5166	49
H(1C)	2285	12029	4109	49
H(2)	1515	10005	4085	33
H(3)	2651	8079	5113	30
H(4A)	3676	9248	6594	24
H(4B)	4696	8242	6204	24
H(7)	1639	9395	7606	21
H(8)	-2307	8056	8731	26
H(9)	-1570	5896	8890	29
H(10)	860	5494	8346	24
H(2O)	9150(20)	870(20)	7470(20)	35
H(12A)	4408	1931	9416	53
H(12B)	2864	1531	9174	53
H(12C)	3515	2975	8298	53
H(13)	3892	1148	7570	36
H(14)	6228	728	7375	31
H(15A)	7585	523	9084	23
H(15B)	6658	1835	9055	23
H(18)	6207	4074	7926	22
H(19)	5678	6770	4594	27
H(20)	7575	5749	3894	29
H(21)	8788	3759	5267	24

Table S2.10. Torsion angles [°] for $C_{11}H_{12}F_3NO$.

C(1)-C(2)-C(3)-C(4)	0.7(3)
C(2)-C(3)-C(4)-C(5)	122.87(18)
C(3)-C(4)-C(5)-O(1)	63.81(16)
C(3)-C(4)-C(5)-C(6)	-57.71(17)
C(3)-C(4)-C(5)-C(11)	-178.08(12)
O(1)-C(5)-C(6)-C(10)	16.52(18)
C(11)-C(5)-C(6)-C(10)	-99.33(16)
C(4)-C(5)-C(6)-C(10)	140.08(14)
O(1)-C(5)-C(6)-C(7)	-163.35(13)
C(11)-C(5)-C(6)-C(7)	80.80(16)
C(4)-C(5)-C(6)-C(7)	-39.79(19)
C(8)-N(1)-C(7)-C(6)	1.6(2)
C(10)-C(6)-C(7)-N(1)	-1.5(2)
C(5)-C(6)-C(7)-N(1)	178.35(13)
C(7)-N(1)-C(8)-C(9)	-0.6(2)
N(1)-C(8)-C(9)-C(10)	-0.4(3)
C(8)-C(9)-C(10)-C(6)	0.5(2)
C(7)-C(6)-C(10)-C(9)	0.4(2)
C(5)-C(6)-C(10)-C(9)	-179.47(14)
O(1)-C(5)-C(11)-F(2)	-59.06(16)
C(6)-C(5)-C(11)-F(2)	57.09(15)
C(4)-C(5)-C(11)-F(2)	-179.76(12)
O(1)-C(5)-C(11)-F(3)	61.28(15)
C(6)-C(5)-C(11)-F(3)	177.44(11)
C(4)-C(5)-C(11)-F(3)	-59.41(15)
O(1)-C(5)-C(11)-F(1)	-179.33(12)
C(6)-C(5)-C(11)-F(1)	-63.18(15)
C(4)-C(5)-C(11)-F(1)	59.98(16)
C(12)-C(13)-C(14)-C(15)	0.5(3)
C(13)-C(14)-C(15)-C(16)	-122.92(17)
C(14)-C(15)-C(16)-O(2)	-66.49(16)
C(14)-C(15)-C(16)-C(17)	54.98(16)
C(14)-C(15)-C(16)-C(22)	175.65(12)

O(2)-C(16)-C(17)-C(21)	-11.24(18)
C(22)-C(16)-C(17)-C(21)	104.65(15)
C(15)-C(16)-C(17)-C(21)	-135.09(14)
O(2)-C(16)-C(17)-C(18)	166.04(13)
C(22)-C(16)-C(17)-C(18)	-78.07(16)
C(15)-C(16)-C(17)-C(18)	42.19(18)
C(19)-N(2)-C(18)-C(17)	-1.1(2)
C(21)-C(17)-C(18)-N(2)	2.5(2)
C(16)-C(17)-C(18)-N(2)	-174.85(13)
C(18)-N(2)-C(19)-C(20)	-1.1(2)
N(2)-C(19)-C(20)-C(21)	1.7(2)
C(18)-C(17)-C(21)-C(20)	-1.8(2)
C(16)-C(17)-C(21)-C(20)	175.62(13)
C(19)-C(20)-C(21)-C(17)	-0.2(2)
O(2)-C(16)-C(22)-F(4)	-60.33(15)
C(17)-C(16)-C(22)-F(4)	-176.85(12)
C(15)-C(16)-C(22)-F(4)	60.79(15)
O(2)-C(16)-C(22)-F(5)	59.38(15)
C(17)-C(16)-C(22)-F(5)	-57.14(15)
C(15)-C(16)-C(22)-F(5)	-179.51(11)
O(2)-C(16)-C(22)-F(6)	179.64(11)
C(17)-C(16)-C(22)-F(6)	63.12(16)
C(15)-C(16)-C(22)-F(6)	-59.24(15)

Symmetry transformations used to generate equivalent atoms:

Table S2.11. Hydrogen bonds for $C_{11}H_{12}F_3NO$ [Å and °].

D-H...A	d(D-H)	d(H...A)	d(D...A)	<(DHA)
O(1)-H(1O)...N(2)	0.84(2)	1.91(2)	2.7396(17)	168(2)
O(2)-H(2O)...N(1)#1	0.83(2)	1.94(2)	2.7501(17)	165(2)

Symmetry transformations used to generate equivalent atoms:
#1 x+1,y-1,z

Crystallographic Data for (*R*)-4-Fluoro-3-hydroxy-3-phenylbutyl 4-bromobenzoate (2.71)

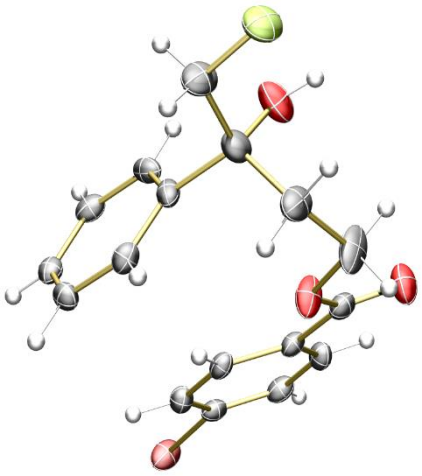

Table S2.12. Crystal data and structure refinement for $C_{17}H_{16}BrFO_3$

Identification code	C17H16BrFO3	
Empirical formula	C17 H16 Br F O3	
Formula weight	367.21	
Temperature	100(2) K	
Wavelength	0.71073 Å	
Crystal system	Orthorhombic	
Space group	$P2_12_12_1$	
Unit cell dimensions	a = 5.7041(7) Å	a= 90°.
	b = 7.4617(9) Å	b= 90°.
	c = 35.703(5) Å	g = 90°.
Volume	1519.6(3) $Å^3$	
Z	4	
Density (calculated)	1.605 Mg/m^3	
Absorption coefficient	2.726 mm^{-1}	
F(000)	744	
Crystal size	0.380 x 0.320 x 0.070 mm^3	
Theta range for data collection	2.282 to 28.316°.	
Index ranges	-7<=h<=7, -9<=k<=9, -47<=l<=47	
Reflections collected	26774	
Independent reflections	3780 [R(int) = 0.0549]	
Completeness to theta = 25.242°	99.9 %	

Absorption correction	Semi-empirical from equivalents
Max. and min. transmission	0.7457 and 0.5828
Refinement method	Full-matrix least-squares on F^2
Data / restraints / parameters	3780 / 1 / 203
Goodness-of-fit on F^2	1.113
Final R indices [I>2sigma(I)]	R1 = 0.0389, wR2 = 0.0901
R indices (all data)	R1 = 0.0434, wR2 = 0.0918
Absolute structure parameter	0.074(15)
Extinction coefficient	na
Largest diff. peak and hole	0.810 and -0.568 e.$Å^{-3}$

Table S2.13. Atomic coordinates ($x10^4$) and equivalent isotropic displacement parameters ($Å^2x10^3$) for $C_{17}H_{16}BrFO_3$. U(eq) is defined as one third of the trace of the orthogonalized U^{ij} tensor

	x	y	z	U(eq)
Br(1)	-599(1)	10657(1)	2553(1)	34(1)
F(1)	5040(5)	1644(4)	4849(1)	39(1)
O(1)	-513(7)	8610(5)	4425(1)	38(1)
O(2)	2983(7)	7587(5)	4250(1)	33(1)
O(3)	1807(7)	3422(6)	4415(1)	40(1)
C(1)	-111(7)	9883(5)	3053(1)	22(1)
C(2)	-1815(8)	10240(6)	3315(1)	25(1)
C(3)	-1442(7)	9713(6)	3683(1)	24(1)
C(4)	634(8)	8867(5)	3785(1)	20(1)
C(5)	2310(7)	8491(6)	3516(1)	20(1)
C(6)	1958(7)	8998(6)	3145(1)	22(1)
C(7)	941(8)	8367(6)	4188(1)	24(1)
C(8)	3350(11)	6905(8)	4628(1)	41(1)
C(9)	4998(9)	5341(6)	4616(1)	32(1)
C(10)	4280(10)	3785(6)	4368(1)	29(1)
C(11)	5557(11)	2087(6)	4474(1)	33(1)
C(12)	4714(8)	4087(5)	3949(1)	23(1)
C(13)	6811(8)	4826(6)	3814(1)	23(1)
C(14)	7147(7)	5067(6)	3432(1)	22(1)
C(15)	5423(8)	4573(5)	3182(1)	21(1)
C(16)	3372(8)	3805(6)	3312(1)	25(1)
C(17)	3028(7)	3562(6)	3691(1)	24(1)

Table S2.14. Bond lengths [Å] and angles [°] for $C_{17}H_{16}BrFO_3$.

Br(1)-C(1)	1.898(4)
F(1)-C(11)	1.408(5)
O(1)-C(7)	1.199(6)
O(2)-C(7)	1.321(6)
O(2)-C(8)	1.457(5)
O(3)-C(10)	1.446(7)
O(3)-H(3O)	0.86(3)
C(1)-C(2)	1.373(6)
C(1)-C(6)	1.391(6)
C(2)-C(3)	1.389(6)
C(2)-H(2)	0.9500
C(3)-C(4)	1.391(6)
C(3)-H(3)	0.9500
C(4)-C(5)	1.385(6)
C(4)-C(7)	1.496(5)
C(5)-C(6)	1.391(6)
C(5)-H(5)	0.9500
C(6)-H(6)	0.9500
C(8)-C(9)	1.499(7)
C(8)-H(8A)	0.9900
C(8)-H(8B)	0.9900
C(9)-C(10)	1.517(6)
C(9)-H(9A)	0.9900
C(9)-H(9B)	0.9900
C(10)-C(11)	1.510(7)
C(10)-C(12)	1.533(6)
C(11)-H(11A)	0.9900
C(11)-H(11B)	0.9900
C(12)-C(17)	1.387(6)
C(12)-C(13)	1.402(6)
C(13)-C(14)	1.390(6)
C(13)-H(13)	0.9500
C(14)-C(15)	1.379(6)

C(14)-H(14)	0.9500
C(15)-C(16)	1.384(6)
C(15)-H(15)	0.9500
C(16)-C(17)	1.380(6)
C(16)-H(16)	0.9500
C(17)-H(17)	0.9500

C(7)-O(2)-C(8)	115.9(4)
C(10)-O(3)-H(3O)	104(5)
C(2)-C(1)-C(6)	122.2(4)
C(2)-C(1)-Br(1)	118.4(3)
C(6)-C(1)-Br(1)	119.3(3)
C(1)-C(2)-C(3)	118.6(4)
C(1)-C(2)-H(2)	120.7
C(3)-C(2)-H(2)	120.7
C(2)-C(3)-C(4)	120.5(4)
C(2)-C(3)-H(3)	119.8
C(4)-C(3)-H(3)	119.8
C(5)-C(4)-C(3)	119.8(4)
C(5)-C(4)-C(7)	122.5(4)
C(3)-C(4)-C(7)	117.7(4)
C(4)-C(5)-C(6)	120.4(4)
C(4)-C(5)-H(5)	119.8
C(6)-C(5)-H(5)	119.8
C(1)-C(6)-C(5)	118.4(4)
C(1)-C(6)-H(6)	120.8
C(5)-C(6)-H(6)	120.8
O(1)-C(7)-O(2)	123.9(4)
O(1)-C(7)-C(4)	124.0(4)
O(2)-C(7)-C(4)	112.0(4)
O(2)-C(8)-C(9)	109.6(4)
O(2)-C(8)-H(8A)	109.7
C(9)-C(8)-H(8A)	109.7
O(2)-C(8)-H(8B)	109.7
C(9)-C(8)-H(8B)	109.7

H(8A)-C(8)-H(8B)	108.2
C(8)-C(9)-C(10)	116.3(4)
C(8)-C(9)-H(9A)	108.2
C(10)-C(9)-H(9A)	108.2
C(8)-C(9)-H(9B)	108.2
C(10)-C(9)-H(9B)	108.2
H(9A)-C(9)-H(9B)	107.4
O(3)-C(10)-C(11)	106.5(4)
O(3)-C(10)-C(9)	109.8(4)
C(11)-C(10)-C(9)	111.4(4)
O(3)-C(10)-C(12)	107.3(4)
C(11)-C(10)-C(12)	106.9(4)
C(9)-C(10)-C(12)	114.4(4)
F(1)-C(11)-C(10)	109.6(4)
F(1)-C(11)-H(11A)	109.8
C(10)-C(11)-H(11A)	109.8
F(1)-C(11)-H(11B)	109.8
C(10)-C(11)-H(11B)	109.8
H(11A)-C(11)-H(11B)	108.2
C(17)-C(12)-C(13)	118.4(4)
C(17)-C(12)-C(10)	119.6(4)
C(13)-C(12)-C(10)	122.0(4)
C(14)-C(13)-C(12)	120.3(4)
C(14)-C(13)-H(13)	119.8
C(12)-C(13)-H(13)	119.8
C(15)-C(14)-C(13)	120.3(4)
C(15)-C(14)-H(14)	119.9
C(13)-C(14)-H(14)	119.9
C(14)-C(15)-C(16)	119.7(4)
C(14)-C(15)-H(15)	120.2
C(16)-C(15)-H(15)	120.2
C(17)-C(16)-C(15)	120.3(4)
C(17)-C(16)-H(16)	119.8
C(15)-C(16)-H(16)	119.8
C(16)-C(17)-C(12)	121.0(4)

C(16)-C(17)-H(17)	119.5
C(12)-C(17)-H(17)	119.5

Symmetry transformations used to generate equivalent atoms:

Table S2.15. Anisotropic displacement parameters ($Å^2x10^3$) for $C_{17}H_{16}BrFO_3$. The anisotropic displacement factor exponent takes the form: $-2p^2[h^2a^{*2}U^{11} + ... + 2hka^*b^*U^{12}]$

	U^{11}	U^{22}	U^{33}	U^{23}	U^{13}	U^{12}
Br(1)	50(1)	28(1)	23(1)	2(1)	-11(1)	5(1)
F(1)	52(2)	39(2)	25(1)	11(1)	-6(1)	0(1)
O(1)	41(2)	50(2)	24(2)	0(1)	6(2)	10(2)
O(2)	42(2)	41(2)	17(2)	-2(1)	-7(1)	18(2)
O(3)	30(2)	63(3)	26(2)	4(2)	0(2)	-7(2)
C(1)	28(2)	17(2)	20(2)	0(2)	-5(2)	-3(2)
C(2)	24(2)	20(2)	32(2)	-2(2)	-8(2)	4(2)
C(3)	19(2)	26(2)	28(2)	-4(2)	3(2)	2(2)
C(4)	23(2)	16(2)	20(2)	-3(1)	-4(2)	2(2)
C(5)	17(2)	19(2)	24(2)	-4(2)	-3(2)	3(2)
C(6)	19(2)	24(2)	23(2)	-4(2)	-1(2)	0(2)
C(7)	30(2)	19(2)	23(2)	-3(2)	-3(2)	0(2)
C(8)	62(3)	48(3)	13(2)	-3(2)	-10(2)	25(3)
C(9)	48(3)	31(3)	17(2)	2(2)	-5(2)	2(2)
C(10)	34(2)	33(2)	20(2)	4(2)	0(2)	0(2)
C(11)	46(3)	32(2)	21(2)	6(2)	-8(2)	1(3)
C(12)	29(2)	20(2)	19(2)	4(2)	4(2)	9(2)
C(13)	22(2)	24(2)	22(2)	-4(2)	-6(2)	2(2)
C(14)	17(2)	25(2)	24(2)	1(2)	3(2)	1(2)
C(15)	26(2)	19(2)	20(2)	1(1)	-2(2)	5(2)
C(16)	24(2)	20(2)	30(2)	-1(2)	-9(2)	3(2)
C(17)	17(2)	22(2)	34(2)	4(2)	4(2)	1(2)

Table S2.16. Hydrogen coordinates ($x10^4$) and isotropic displacement parameters ($Å^2x10^3$) for $C_{17}H_{16}BrFO_3$

	x	y	z	U(eq)
H(3O)	1650(120)	3320(90)	4653(8)	59
H(2)	-3221	10836	3245	31
H(3)	-2613	9933	3866	29
H(5)	3709	7883	3584	24
H(6)	3103	8747	2959	27
H(8A)	1832	6527	4737	49
H(8B)	4014	7862	4788	49
H(9A)	5196	4886	4875	38
H(9B)	6547	5777	4531	38
H(11A)	5067	1097	4307	40
H(11B)	7267	2262	4445	40
H(13)	8007	5164	3985	27
H(14)	8570	5573	3343	27
H(15)	5643	4760	2921	26
H(16)	2195	3442	3140	29
H(17)	1616	3027	3777	29

Table S2.17. Torsion angles [°] for $C_{17}H_{16}BrFO_3$

C(6)-C(1)-C(2)-C(3)	0.6(6)
Br(1)-C(1)-C(2)-C(3)	-178.5(3)
C(1)-C(2)-C(3)-C(4)	1.0(6)
C(2)-C(3)-C(4)-C(5)	-2.2(6)
C(2)-C(3)-C(4)-C(7)	178.9(4)
C(3)-C(4)-C(5)-C(6)	1.8(6)
C(7)-C(4)-C(5)-C(6)	-179.3(4)
C(2)-C(1)-C(6)-C(5)	-1.0(6)
Br(1)-C(1)-C(6)-C(5)	178.1(3)
C(4)-C(5)-C(6)-C(1)	-0.2(6)
C(8)-O(2)-C(7)-O(1)	3.9(7)
C(8)-O(2)-C(7)-C(4)	-174.6(4)
C(5)-C(4)-C(7)-O(1)	-177.0(5)
C(3)-C(4)-C(7)-O(1)	2.0(6)
C(5)-C(4)-C(7)-O(2)	1.6(6)
C(3)-C(4)-C(7)-O(2)	-179.5(4)
C(7)-O(2)-C(8)-C(9)	151.5(4)
O(2)-C(8)-C(9)-C(10)	-56.9(6)
C(8)-C(9)-C(10)-O(3)	-42.8(5)
C(8)-C(9)-C(10)-C(11)	-160.5(4)
C(8)-C(9)-C(10)-C(12)	78.0(6)
O(3)-C(10)-C(11)-F(1)	-59.9(5)
C(9)-C(10)-C(11)-F(1)	59.9(6)
C(12)-C(10)-C(11)-F(1)	-174.4(4)
O(3)-C(10)-C(12)-C(17)	-15.6(6)
C(11)-C(10)-C(12)-C(17)	98.3(5)
C(9)-C(10)-C(12)-C(17)	-137.8(5)
O(3)-C(10)-C(12)-C(13)	166.7(4)
C(11)-C(10)-C(12)-C(13)	-79.4(5)
C(9)-C(10)-C(12)-C(13)	44.5(6)
C(17)-C(12)-C(13)-C(14)	1.8(6)
C(10)-C(12)-C(13)-C(14)	179.5(4)
C(12)-C(13)-C(14)-C(15)	-0.3(6)

C(13)-C(14)-C(15)-C(16)	-1.3(6)
C(14)-C(15)-C(16)-C(17)	1.2(6)
C(15)-C(16)-C(17)-C(12)	0.3(6)
C(13)-C(12)-C(17)-C(16)	-1.8(6)
C(10)-C(12)-C(17)-C(16)	-179.6(4)

Symmetry transformations used to generate equivalent atoms:

Table S2.18. Hydrogen bonds for $C_{17}H_{16}BrFO_3$ [Å and °].

D-H...A	d(D-H)	d(H...A)	d(D...A)	<(DHA)
O(3)-H(3O)...F(1)#1	0.86(3)	2.00(4)	2.816(5)	158(7)

Symmetry transformations used to generate equivalent atoms:
#1 x-1/2,-y+1/2,-z+1

Crystallographic Data for (2S,3R)-4,4,4-Trifluoro-3-hydroxy-2-methyl-3-phenylbutyl 4-bromobenzoate (anti-2.83)

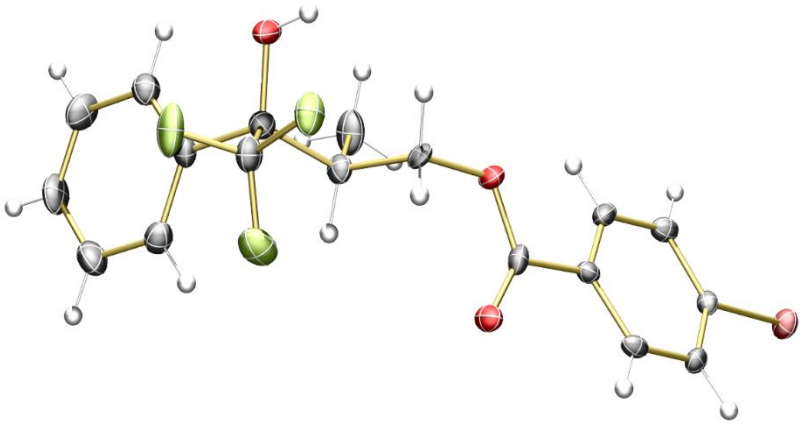

Table S2.19. Crystal data and structure refinement for $C_{18}H_{16}BrF_3O_3$

Identification code	C18H16BrF3O3	
Empirical formula	C18 H16 Br F3 O3	
Formula weight	417.22	
Temperature	100(2) K	
Wavelength	1.54178 Å	
Crystal system	Orthorhombic	
Space group	$P2_12_12_1$	
Unit cell dimensions	a = 5.8607(4) Å	a= 90°.
	b = 7.7375(12) Å	b= 90°.
	c = 37.867(2) Å	g = 90°.
Volume	1717.1(3) $Å^3$	
Z	4	
Density (calculated)	1.614 Mg/m^3	
Absorption coefficient	3.689 mm^{-1}	
F(000)	840	
Crystal size	0.360 x 0.080 x 0.050 mm^3	
Theta range for data collection	2.334 to 66.944°.	
Index ranges	-6<=h<=6, -9<=k<=9, -45<=l<=45	
Reflections collected	23263	
Independent reflections	3033 [R(int) = 0.0619]	
Completeness to theta = 66.944°	99.6 %	
Absorption correction	Semi-empirical from equivalents	

Max. and min. transmission	0.7528 and 0.5912
Refinement method	Full-matrix least-squares on F^2
Data / restraints / parameters	3033 / 1 / 229
Goodness-of-fit on F^2	1.285
Final R indices [I>2sigma(I)]	R1 = 0.0427, wR2 = 0.0984
R indices (all data)	R1 = 0.0439, wR2 = 0.0986
Absolute structure parameter	0.024(8)
Extinction coefficient	na
Largest diff. peak and hole	0.721 and -1.106 e.Å^{-3}

Table 2.20. Atomic coordinates ($x10^4$) and equivalent isotropic displacement parameters ($Å^2x10^3$) for $C_{18}H_{16}BrF_3O_3$. U(eq) is defined as one third of the trace of the orthogonalized U^{ij} tensor.

	x	y	z	U(eq)
Br(1)	-1076(1)	11312(1)	5154(1)	23(1)
F(1)	8909(8)	335(5)	6108(1)	28(1)
F(2)	5897(8)	-35(5)	6425(1)	34(1)
F(3)	9213(9)	-723(5)	6629(1)	35(1)
O(1)	2392(7)	3546(6)	5837(1)	21(1)
O(2)	5666(8)	5047(6)	5857(1)	21(1)
O(3)	10704(8)	2734(7)	6528(1)	25(1)
C(1)	388(11)	9332(8)	5346(2)	15(1)
C(2)	2512(12)	9543(9)	5509(2)	20(2)
C(3)	3523(11)	8066(9)	5652(2)	20(2)
C(4)	2453(10)	6464(9)	5627(2)	16(1)
C(5)	374(10)	6303(9)	5457(2)	17(1)
C(6)	-665(12)	7756(8)	5313(2)	18(1)
C(7)	3456(12)	4860(9)	5785(2)	18(2)
C(8)	6813(10)	3541(9)	6013(2)	19(1)
C(9)	6733(11)	3609(10)	6417(2)	20(1)
C(10)	7279(16)	5438(9)	6546(2)	34(2)
C(11)	8424(12)	2300(9)	6589(2)	19(2)
C(12)	8096(13)	464(10)	6441(2)	24(2)
C(13)	8033(12)	2254(9)	6992(2)	20(1)
C(14)	6000(14)	1651(8)	7134(2)	25(2)
C(15)	5672(14)	1641(10)	7499(2)	33(2)
C(16)	7375(14)	2289(10)	7718(2)	32(2)
C(17)	9373(14)	2904(10)	7576(2)	32(2)
C(18)	9709(13)	2881(9)	7211(2)	24(2)

Table S21. Bond lengths [Å] and angles [°] for $C_{18}H_{16}BrF_3O_3$

Br(1)-C(1)	1.902(6)
F(1)-C(12)	1.354(8)
F(2)-C(12)	1.347(9)
F(3)-C(12)	1.333(8)
O(1)-C(7)	1.209(8)
O(2)-C(7)	1.332(9)
O(2)-C(8)	1.468(8)
O(3)-C(11)	1.397(8)
O(3)-H(3O)	0.85(3)
C(1)-C(6)	1.372(9)
C(1)-C(2)	1.398(9)
C(2)-C(3)	1.396(9)
C(2)-H(2)	0.9500
C(3)-C(4)	1.392(9)
C(3)-H(3A)	0.9500
C(4)-C(5)	1.383(8)
C(4)-C(7)	1.499(9)
C(5)-C(6)	1.391(10)
C(5)-H(5)	0.9500
C(6)-H(6)	0.9500
C(8)-C(9)	1.533(8)
C(8)-H(8A)	0.9900
C(8)-H(8B)	0.9900
C(9)-C(10)	1.531(10)
C(9)-C(11)	1.559(9)
C(9)-H(9)	1.0000
C(10)-H(10A)	0.9800
C(10)-H(10B)	0.9800
C(10)-H(10C)	0.9800
C(11)-C(12)	1.538(9)
C(11)-C(13)	1.544(9)
C(13)-C(18)	1.376(10)
C(13)-C(14)	1.388(11)

C(14)-C(15)	1.396(9)
C(14)-H(14)	0.9500
C(15)-C(16)	1.391(11)
C(15)-H(15)	0.9500
C(16)-C(17)	1.374(11)
C(16)-H(16)	0.9500
C(17)-C(18)	1.393(10)
C(17)-H(17)	0.9500
C(18)-H(18)	0.9500

C(7)-O(2)-C(8)	116.2(5)
C(11)-O(3)-H(3O)	111(6)
C(6)-C(1)-C(2)	123.1(6)
C(6)-C(1)-Br(1)	118.5(5)
C(2)-C(1)-Br(1)	118.5(5)
C(3)-C(2)-C(1)	116.9(6)
C(3)-C(2)-H(2)	121.6
C(1)-C(2)-H(2)	121.6
C(4)-C(3)-C(2)	120.8(6)
C(4)-C(3)-H(3A)	119.6
C(2)-C(3)-H(3A)	119.6
C(5)-C(4)-C(3)	120.5(6)
C(5)-C(4)-C(7)	117.2(6)
C(3)-C(4)-C(7)	122.2(6)
C(4)-C(5)-C(6)	119.7(7)
C(4)-C(5)-H(5)	120.1
C(6)-C(5)-H(5)	120.1
C(1)-C(6)-C(5)	119.0(6)
C(1)-C(6)-H(6)	120.5
C(5)-C(6)-H(6)	120.5
O(1)-C(7)-O(2)	124.0(6)
O(1)-C(7)-C(4)	124.0(6)
O(2)-C(7)-C(4)	111.9(6)
O(2)-C(8)-C(9)	111.0(5)
O(2)-C(8)-H(8A)	109.4

C(9)-C(8)-H(8A)	109.4
O(2)-C(8)-H(8B)	109.4
C(9)-C(8)-H(8B)	109.4
H(8A)-C(8)-H(8B)	108.0
C(10)-C(9)-C(8)	110.1(6)
C(10)-C(9)-C(11)	109.6(6)
C(8)-C(9)-C(11)	112.0(5)
C(10)-C(9)-H(9)	108.4
C(8)-C(9)-H(9)	108.4
C(11)-C(9)-H(9)	108.4
C(9)-C(10)-H(10A)	109.5
C(9)-C(10)-H(10B)	109.5
H(10A)-C(10)-H(10B)	109.5
C(9)-C(10)-H(10C)	109.5
H(10A)-C(10)-H(10C)	109.5
H(10B)-C(10)-H(10C)	109.5
O(3)-C(11)-C(12)	106.4(6)
O(3)-C(11)-C(13)	108.1(5)
C(12)-C(11)-C(13)	108.6(6)
O(3)-C(11)-C(9)	112.5(6)
C(12)-C(11)-C(9)	111.7(5)
C(13)-C(11)-C(9)	109.4(5)
F(3)-C(12)-F(2)	107.3(6)
F(3)-C(12)-F(1)	105.8(6)
F(2)-C(12)-F(1)	105.8(6)
F(3)-C(12)-C(11)	112.4(5)
F(2)-C(12)-C(11)	113.7(6)
F(1)-C(12)-C(11)	111.2(6)
C(18)-C(13)-C(14)	119.8(6)
C(18)-C(13)-C(11)	118.9(6)
C(14)-C(13)-C(11)	121.2(6)
C(13)-C(14)-C(15)	120.2(7)
C(13)-C(14)-H(14)	119.9
C(15)-C(14)-H(14)	119.9
C(16)-C(15)-C(14)	119.3(7)

C(16)-C(15)-H(15)	120.3
C(14)-C(15)-H(15)	120.3
C(17)-C(16)-C(15)	120.2(7)
C(17)-C(16)-H(16)	119.9
C(15)-C(16)-H(16)	119.9
C(16)-C(17)-C(18)	120.2(7)
C(16)-C(17)-H(17)	119.9
C(18)-C(17)-H(17)	119.9
C(13)-C(18)-C(17)	120.2(7)
C(13)-C(18)-H(18)	119.9
C(17)-C(18)-H(18)	119.9

Symmetry transformations used to generate equivalent atoms:

Table S2.22. Anisotropic displacement parameters ($Å^2x10^3$) for $C_{18}H_{16}BrF_3O_3$. The anisotropic displacement factor exponent takes the form: $-2p^2[h^2a^{*2}U^{11} + ... + 2hka^*b^*U^{12}]$

	U^{11}	U^{22}	U^{33}	U^{23}	U^{13}	U^{12}
Br(1)	25(1)	18(1)	26(1)	2(1)	-5(1)	3(1)
F(1)	37(2)	28(2)	19(2)	-2(2)	0(2)	9(2)
F(2)	39(3)	29(2)	33(2)	-3(2)	0(2)	-15(2)
F(3)	59(3)	23(2)	24(2)	2(2)	-8(2)	12(2)
O(1)	17(2)	18(2)	27(2)	4(2)	-1(2)	0(2)
O(2)	13(2)	24(2)	25(2)	6(2)	-3(2)	0(2)
O(3)	14(2)	39(3)	21(2)	3(2)	1(2)	0(2)
C(1)	15(3)	14(3)	15(3)	1(2)	1(3)	4(2)
C(2)	20(4)	20(3)	20(3)	-5(3)	1(3)	-5(3)
C(3)	14(4)	28(4)	18(3)	1(3)	-2(3)	0(3)
C(4)	15(3)	18(3)	15(3)	0(3)	1(2)	-4(3)
C(5)	17(3)	17(3)	17(3)	-4(3)	2(2)	-6(3)
C(6)	18(4)	20(3)	14(3)	-1(2)	-4(3)	-2(3)
C(7)	21(4)	20(4)	14(3)	1(3)	-3(3)	6(3)
C(8)	12(3)	21(3)	23(3)	4(3)	-4(2)	5(3)
C(9)	21(3)	18(3)	21(3)	2(3)	0(3)	4(3)
C(10)	53(5)	19(4)	29(4)	1(3)	-6(4)	6(4)
C(11)	20(4)	20(3)	18(3)	-1(3)	-1(3)	-2(3)
C(12)	29(4)	24(4)	17(3)	0(3)	-2(3)	1(3)
C(13)	26(4)	18(3)	17(3)	3(3)	-2(3)	0(3)
C(14)	27(4)	24(4)	24(3)	0(3)	-5(3)	-2(3)
C(15)	33(4)	38(5)	27(3)	7(3)	8(3)	1(4)
C(16)	43(5)	39(5)	13(3)	1(3)	3(3)	6(4)
C(17)	34(5)	41(4)	21(4)	-8(3)	-6(3)	2(4)
C(18)	26(4)	25(4)	22(3)	0(3)	1(3)	2(3)

Table S2.23. Hydrogen coordinates ($x10^4$) and isotropic displacement parameters ($Å^2x10^3$) for $C_{18}H_{16}BrF_3O_3$.

	x	y	z	U(eq)
H(3O)	11010(150)	2720(100)	6309(8)	30
H(2)	3234	10641	5522	24
H(3A)	4957	8155	5767	24
H(5)	-340	5205	5439	20
H(6)	-2081	7660	5192	21
H(8A)	8423	3512	5933	22
H(8B)	6060	2470	5929	22
H(9)	5152	3308	6495	24
H(10A)	7223	5468	6804	51
H(10B)	8808	5768	6466	51
H(10C)	6155	6249	6450	51
H(14)	4827	1243	6982	30
H(15)	4300	1196	7597	39
H(16)	7156	2307	7966	38
H(17)	10530	3347	7726	38
H(18)	11098	3300	7115	29

Table S2.24. Torsion angles [°] for $C_{18}H_{16}BrF_3O_3$

C(6)-C(1)-C(2)-C(3)	-2.3(10)
Br(1)-C(1)-C(2)-C(3)	179.2(5)
C(1)-C(2)-C(3)-C(4)	0.8(9)
C(2)-C(3)-C(4)-C(5)	0.7(10)
C(2)-C(3)-C(4)-C(7)	-178.4(6)
C(3)-C(4)-C(5)-C(6)	-0.6(9)
C(7)-C(4)-C(5)-C(6)	178.5(6)
C(2)-C(1)-C(6)-C(5)	2.4(10)
Br(1)-C(1)-C(6)-C(5)	-179.1(5)
C(4)-C(5)-C(6)-C(1)	-0.9(9)
C(8)-O(2)-C(7)-O(1)	-0.7(9)
C(8)-O(2)-C(7)-C(4)	-179.8(5)
C(5)-C(4)-C(7)-O(1)	-15.7(9)
C(3)-C(4)-C(7)-O(1)	163.4(6)
C(5)-C(4)-C(7)-O(2)	163.4(5)
C(3)-C(4)-C(7)-O(2)	-17.5(9)
C(7)-O(2)-C(8)-C(9)	-91.4(7)
O(2)-C(8)-C(9)-C(10)	-43.7(7)
O(2)-C(8)-C(9)-C(11)	-165.9(5)
C(10)-C(9)-C(11)-O(3)	-55.1(7)
C(8)-C(9)-C(11)-O(3)	67.4(7)
C(10)-C(9)-C(11)-C(12)	-174.7(6)
C(8)-C(9)-C(11)-C(12)	-52.2(8)
C(10)-C(9)-C(11)-C(13)	65.1(7)
C(8)-C(9)-C(11)-C(13)	-172.4(6)
O(3)-C(11)-C(12)-F(3)	68.5(7)
C(13)-C(11)-C(12)-F(3)	-47.6(8)
C(9)-C(11)-C(12)-F(3)	-168.3(6)
O(3)-C(11)-C(12)-F(2)	-169.3(5)
C(13)-C(11)-C(12)-F(2)	74.6(7)
C(9)-C(11)-C(12)-F(2)	-46.1(8)
O(3)-C(11)-C(12)-F(1)	-50.0(7)
C(13)-C(11)-C(12)-F(1)	-166.1(6)

C(9)-C(11)-C(12)-F(1)	73.2(8)
O(3)-C(11)-C(13)-C(18)	10.4(9)
C(12)-C(11)-C(13)-C(18)	125.4(7)
C(9)-C(11)-C(13)-C(18)	-112.5(7)
O(3)-C(11)-C(13)-C(14)	-171.9(6)
C(12)-C(11)-C(13)-C(14)	-56.9(8)
C(9)-C(11)-C(13)-C(14)	65.2(8)
C(18)-C(13)-C(14)-C(15)	-1.5(10)
C(11)-C(13)-C(14)-C(15)	-179.2(7)
C(13)-C(14)-C(15)-C(16)	1.9(11)
C(14)-C(15)-C(16)-C(17)	-1.1(12)
C(15)-C(16)-C(17)-C(18)	-0.1(12)
C(14)-C(13)-C(18)-C(17)	0.3(11)
C(11)-C(13)-C(18)-C(17)	178.1(7)
C(16)-C(17)-C(18)-C(13)	0.5(12)

Symmetry transformations used to generate equivalent atoms:

Table S2.25. Hydrogen bonds for $C_{18}H_{16}BrF_3O_3$ [Å and °]

D-H...A	d(D-H)	d(H...A)	d(D...A)	<(DHA)
O(3)-H(3O)...O(1)#1	0.85(3)	2.06(4)	2.866(6)	158(8)

Symmetry transformations used to generate equivalent atoms:
#1 x+1,y,z

2.7.9. *NMR Spectra (^{1}H, ^{13}C, ^{19}F)*

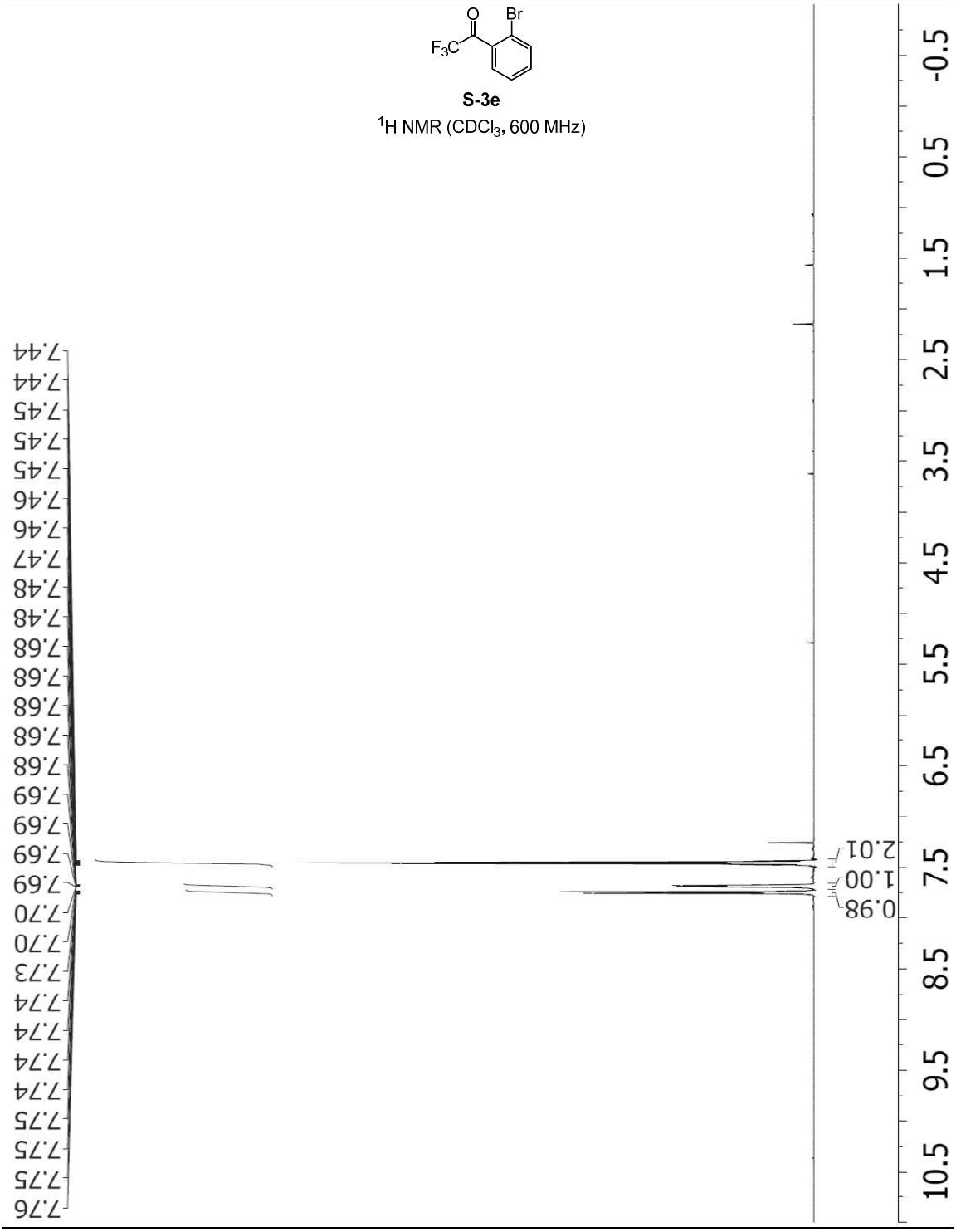

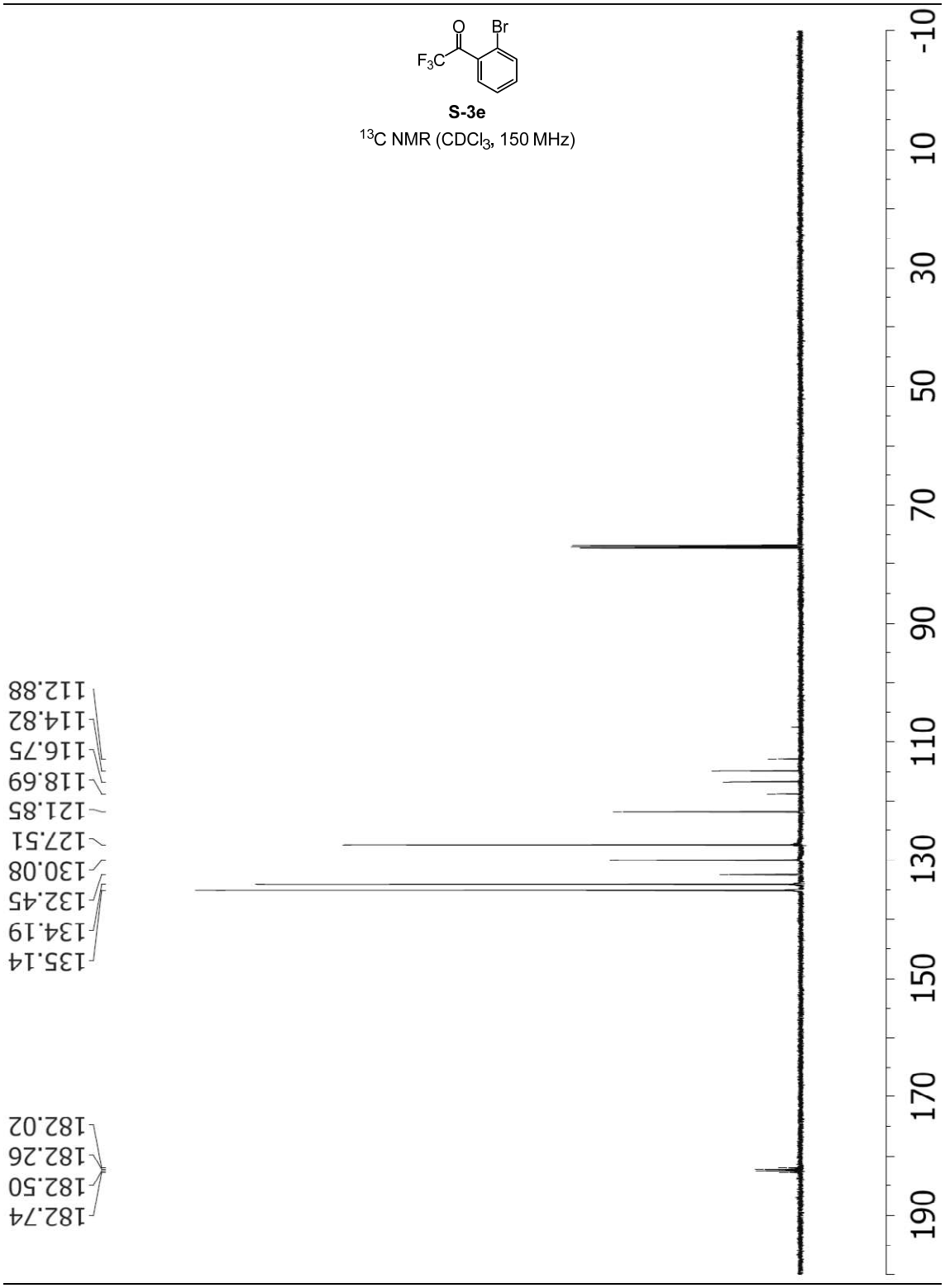
O
Br
F3C
S-3e
13C NMR (CDCl3, 150 MHz)
182.74
182.50
182.26
182.02
135.14
134.19
132.45
130.08
127.51
121.85
118.69
116.75
114.82
112.88
-10
10
30
50
70
90
110
130
150
170
190

S-3e

^{19}F NMR ($CDCl_3$, 564 MHz)

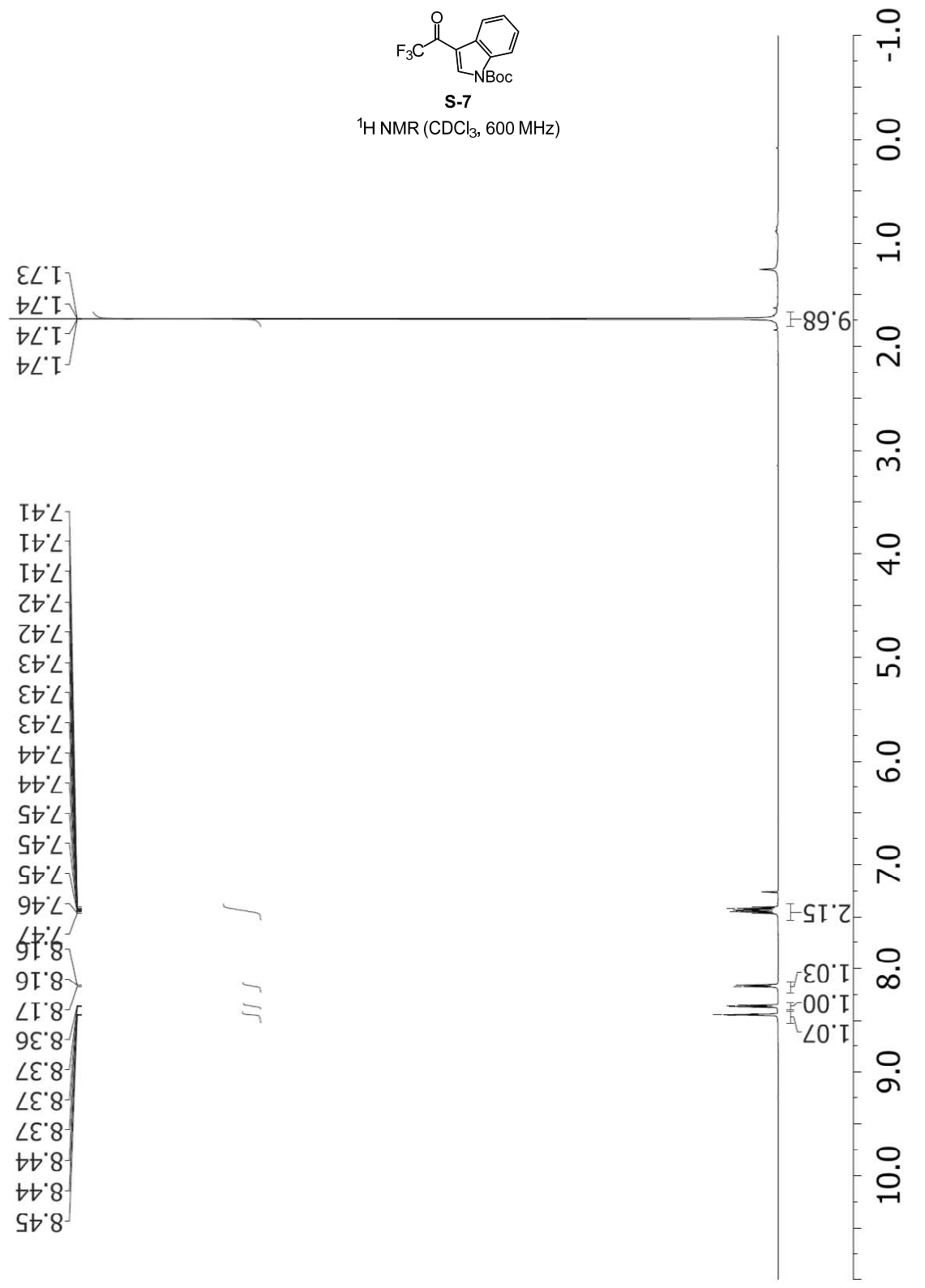

S-7

^{1}H NMR ($CDCl_3$, 600 MHz)

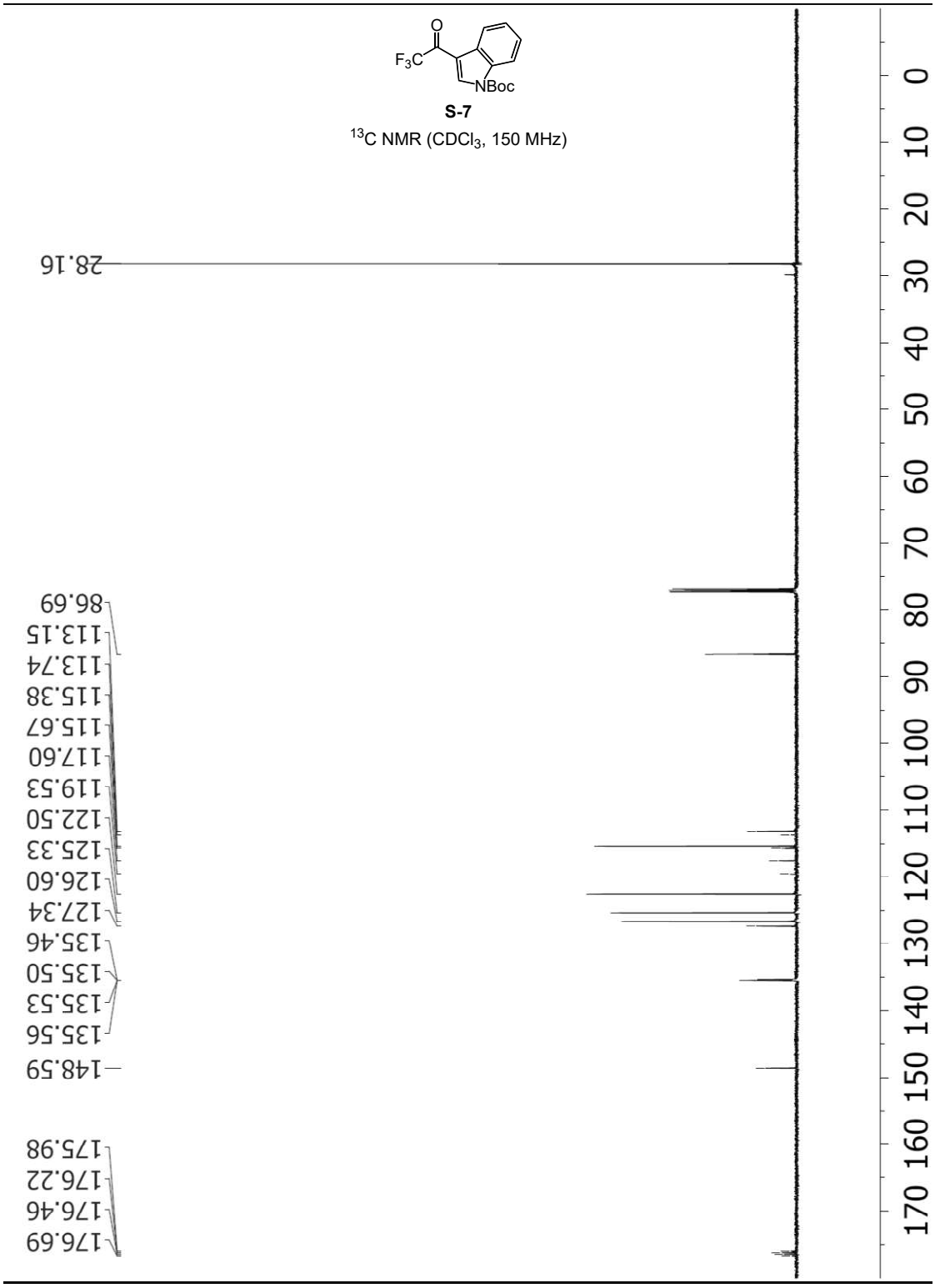

S-7

^{13}C NMR ($CDCl_3$, 150 MHz)

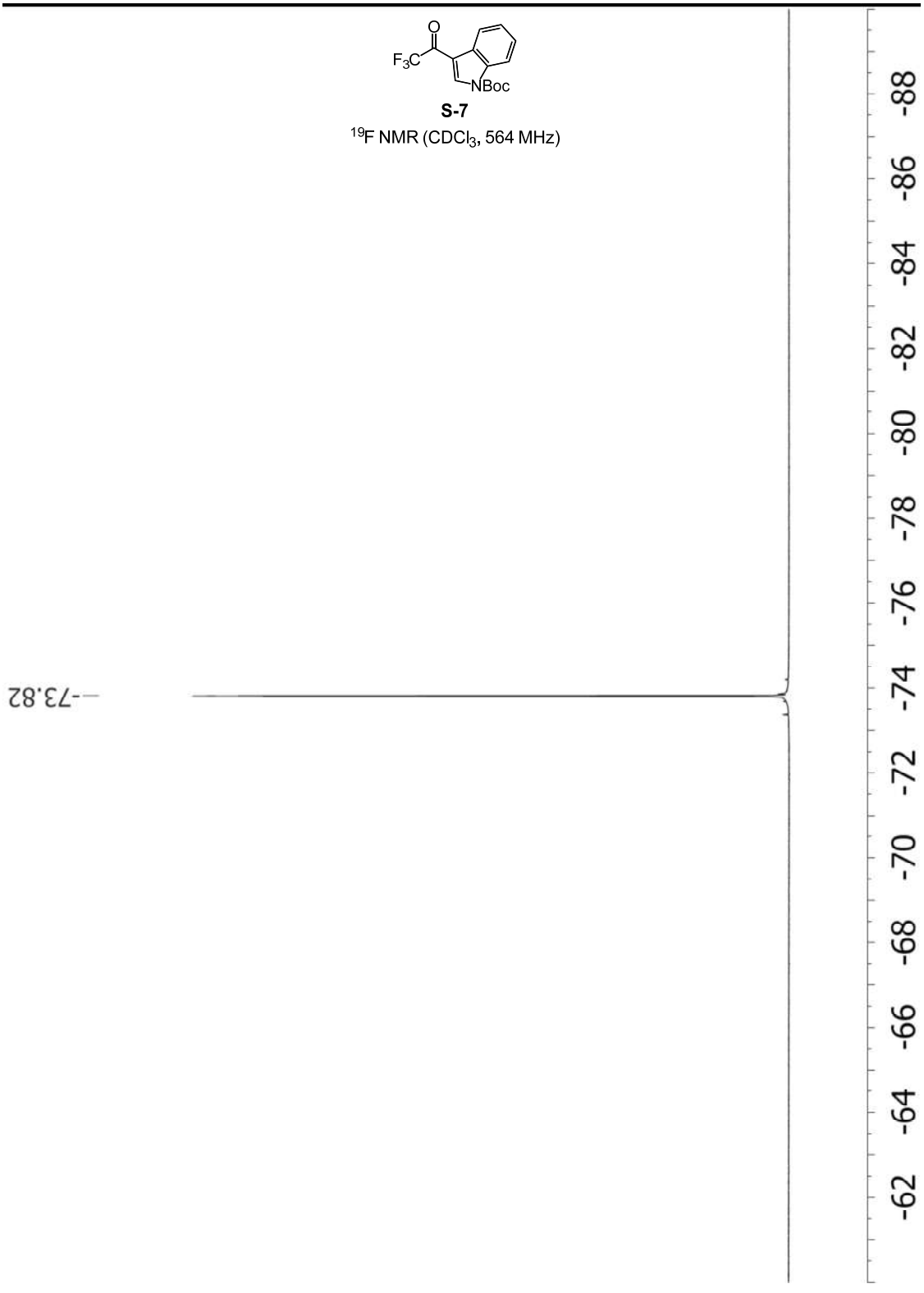

S-7

^{19}F NMR ($CDCl_3$, 564 MHz)

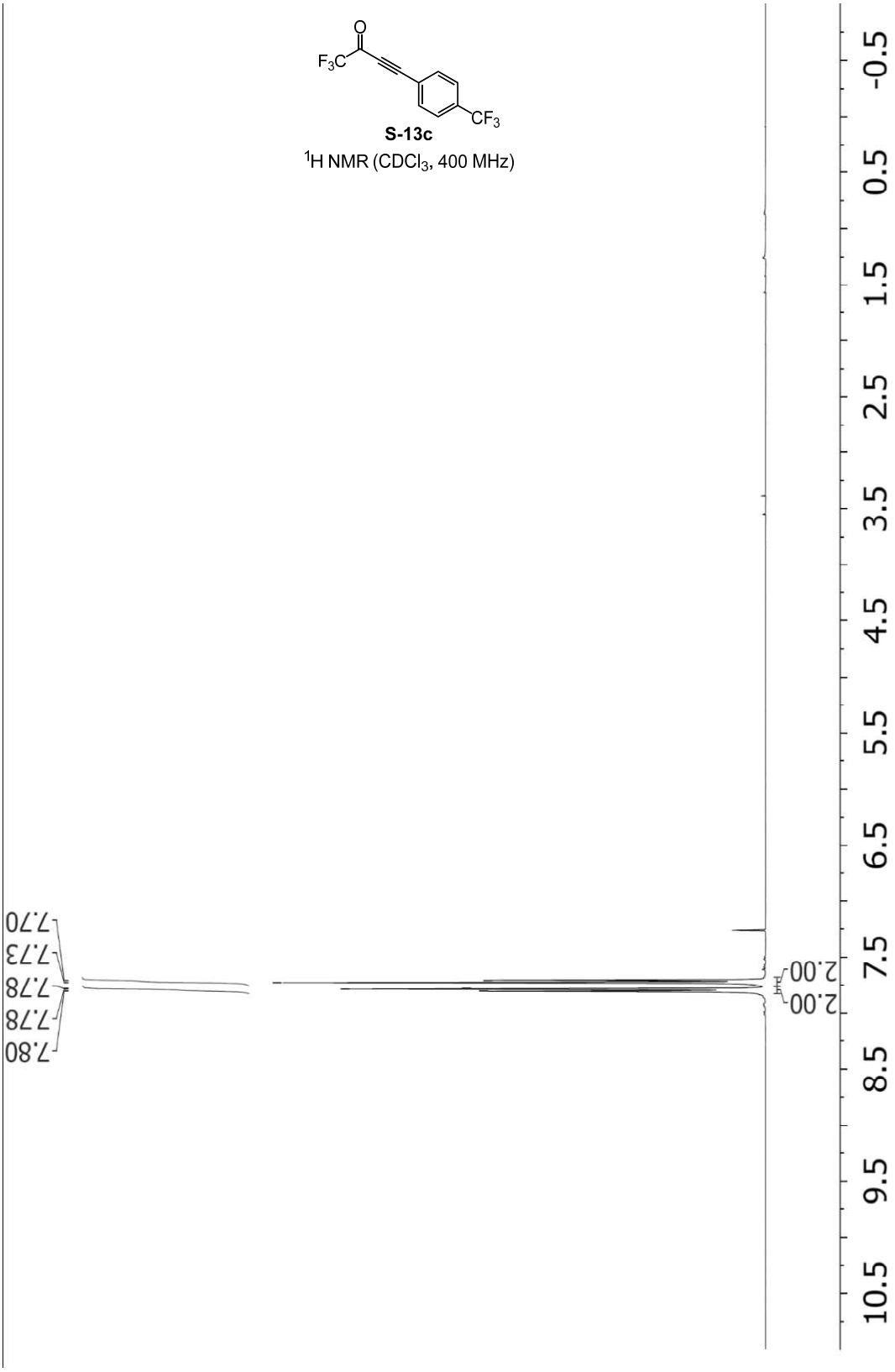
O
F3C
CF3
S-13c
1H NMR (CDCl3, 400 MHz)
7.70
7.73
7.78
7.78
7.80
2.00
2.00
-0.5
0.5
1.5
2.5
3.5
4.5
5.5
6.5
7.5
8.5
9.5
10.5

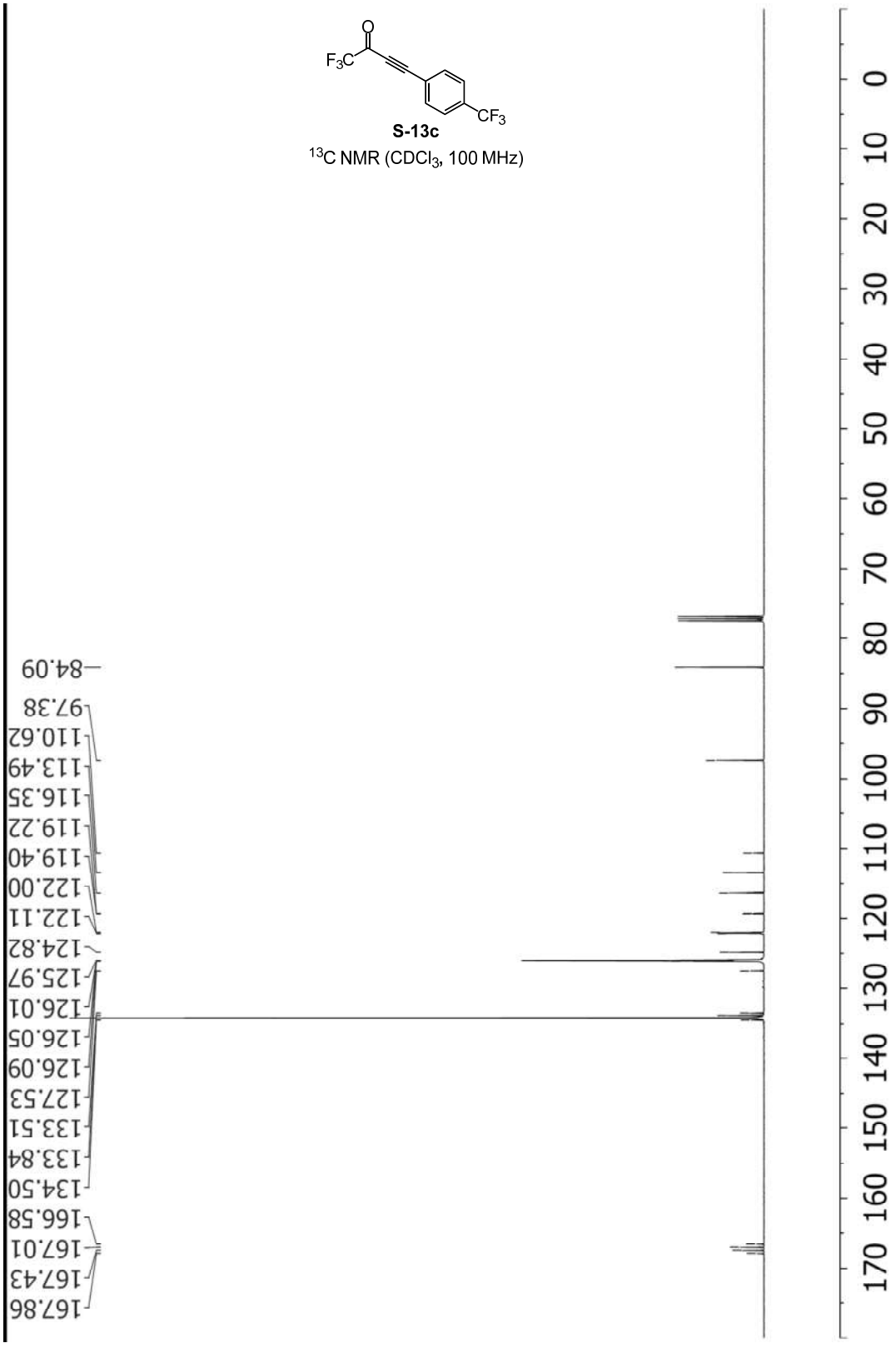
F3C
O
CF3
S-13c
13C NMR (CDCl3, 100 MHz)
84.09
97.38
110.62
113.49
116.35
119.22
119.40
122.00
122.11
124.82
125.97
126.01
126.05
126.09
127.53
133.51
133.84
134.50
166.58
167.01
167.43
167.86
0
10
20
30
40
50
60
70
80
90
100
110
120
130
140
150
160
170

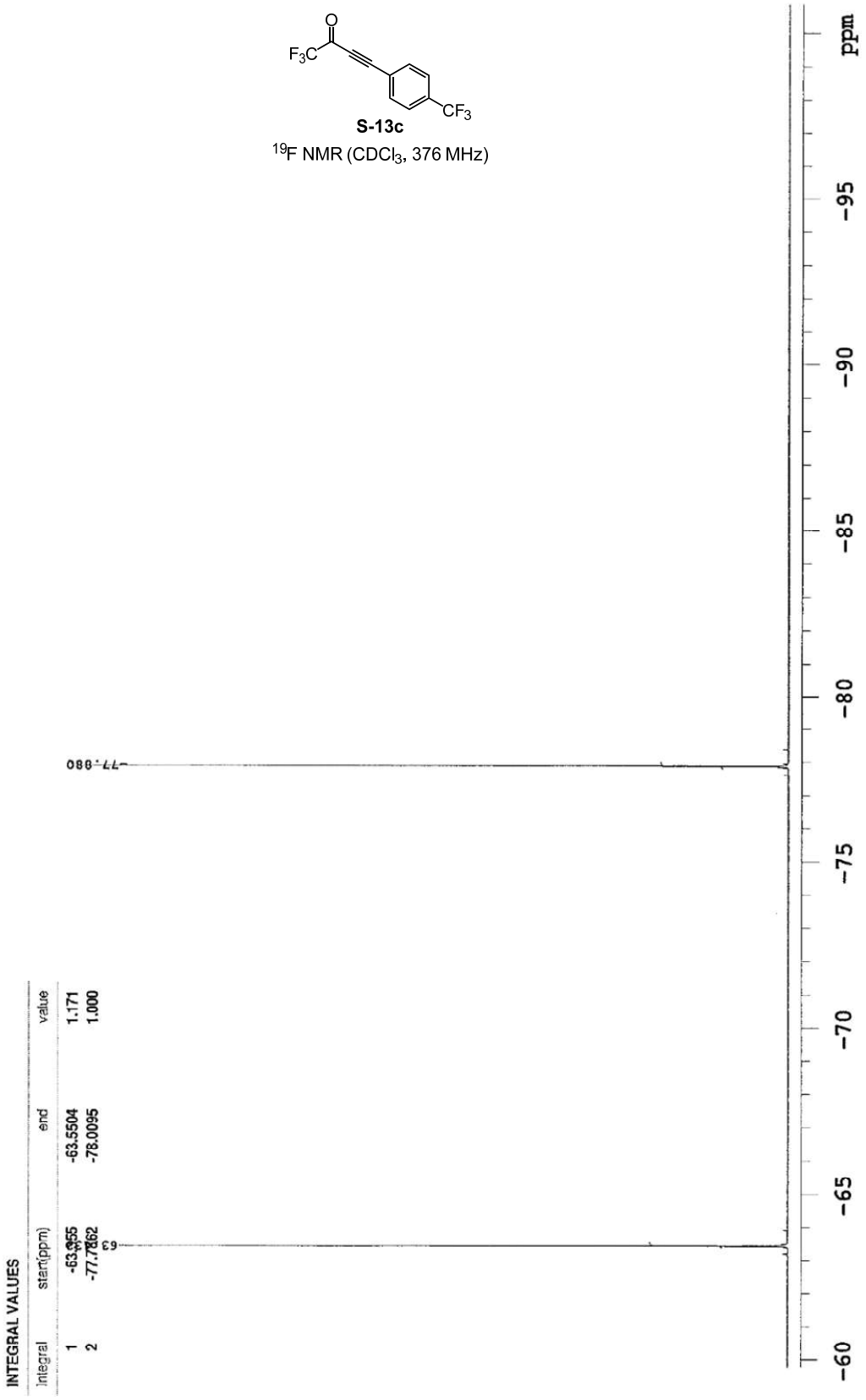
O
F3C
CF3
S-13c
19F NMR (CDCl3, 376 MHz)
INTEGRAL VALUES
Integral
start(ppm)
end
value
1
-63.5505
-63.5504
1.171
2
-77.7862
-78.0095
1.000
-77.880
-63
-60
-65
-70
-75
-80
-85
-90
-95
ppm

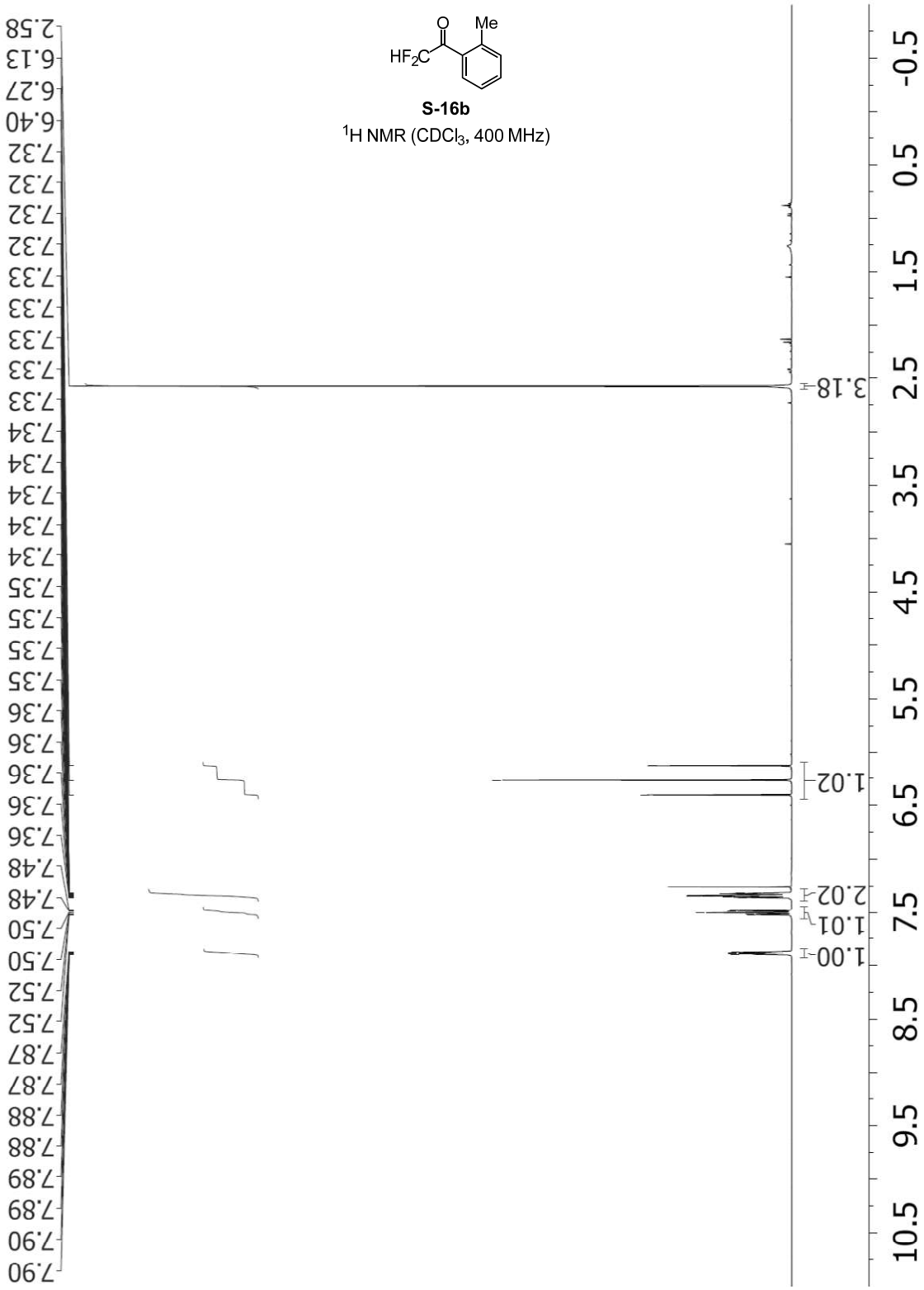
O
Me
HF2C
S-16b
1H NMR (CDCl3, 400 MHz)
3.18
1.02
2.02
1.01
1.00

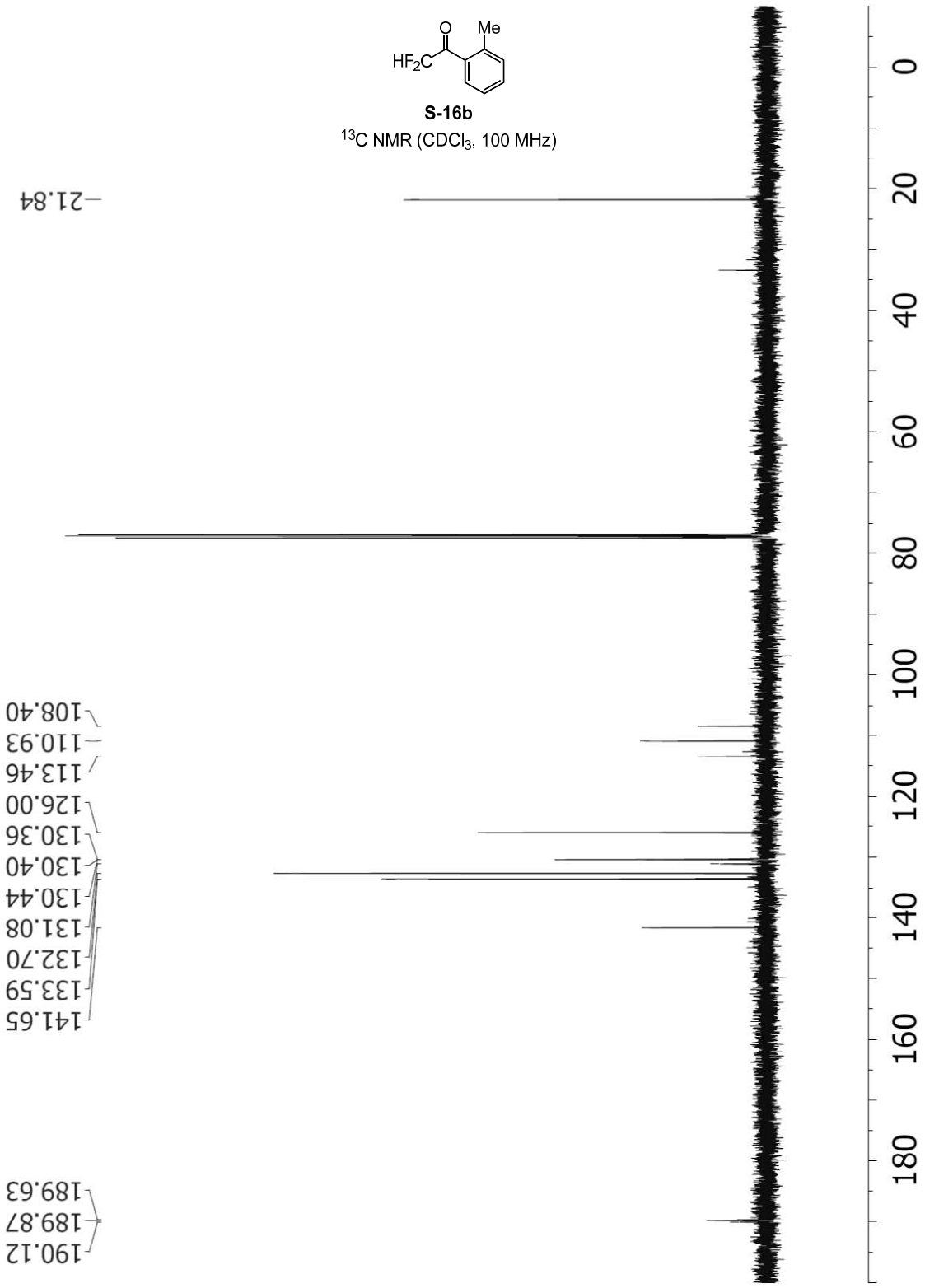
O
Me
HF2C
S-16b
13C NMR (CDCl3, 100 MHz)
21.84
108.40
110.93
113.46
126.00
130.36
130.40
130.44
131.08
132.70
133.59
141.65
189.63
189.87
190.12
0
20
40
60
80
100
120
140
160
180

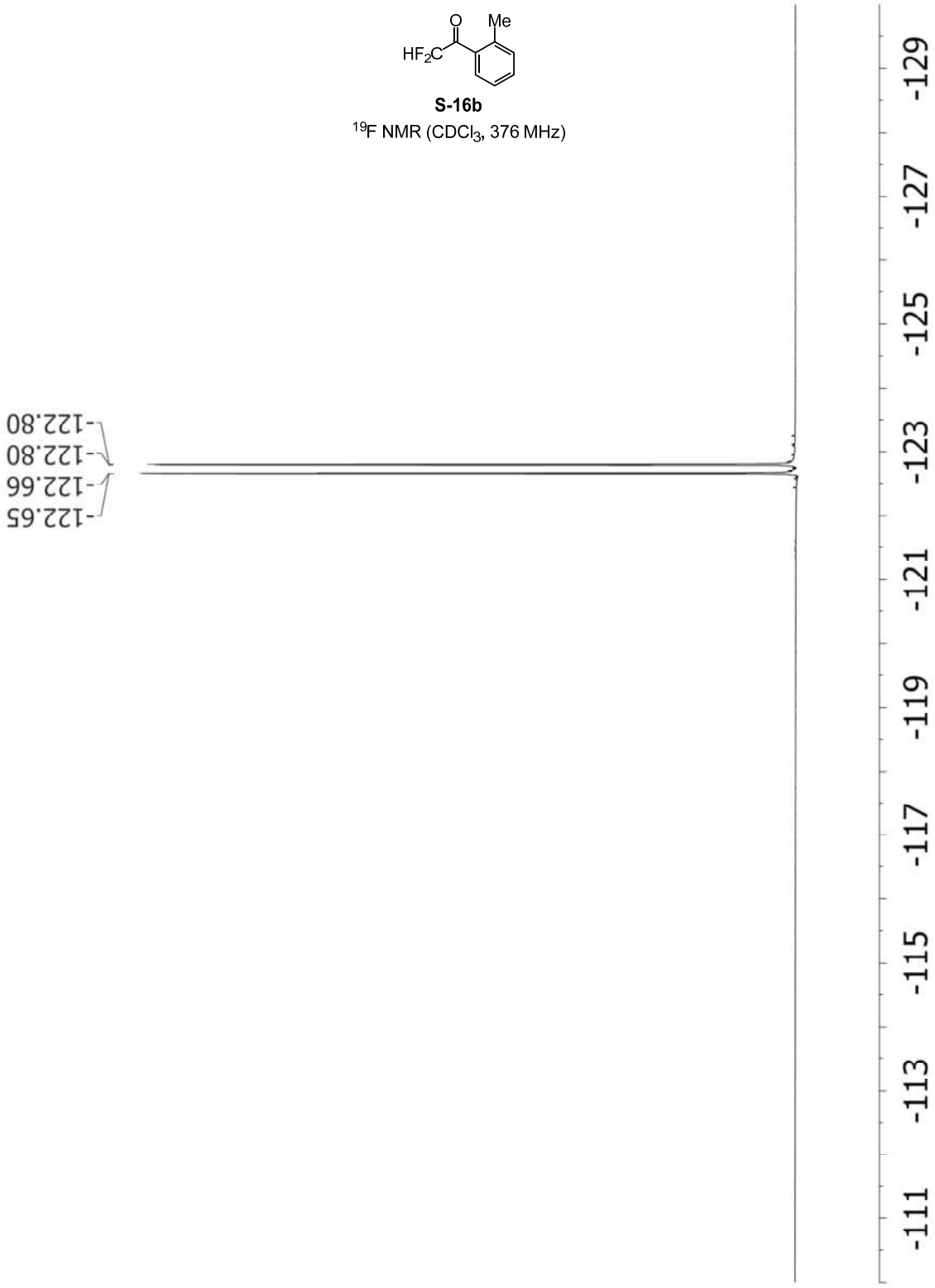

S-16b

^{19}F NMR ($CDCl_3$, 376 MHz)

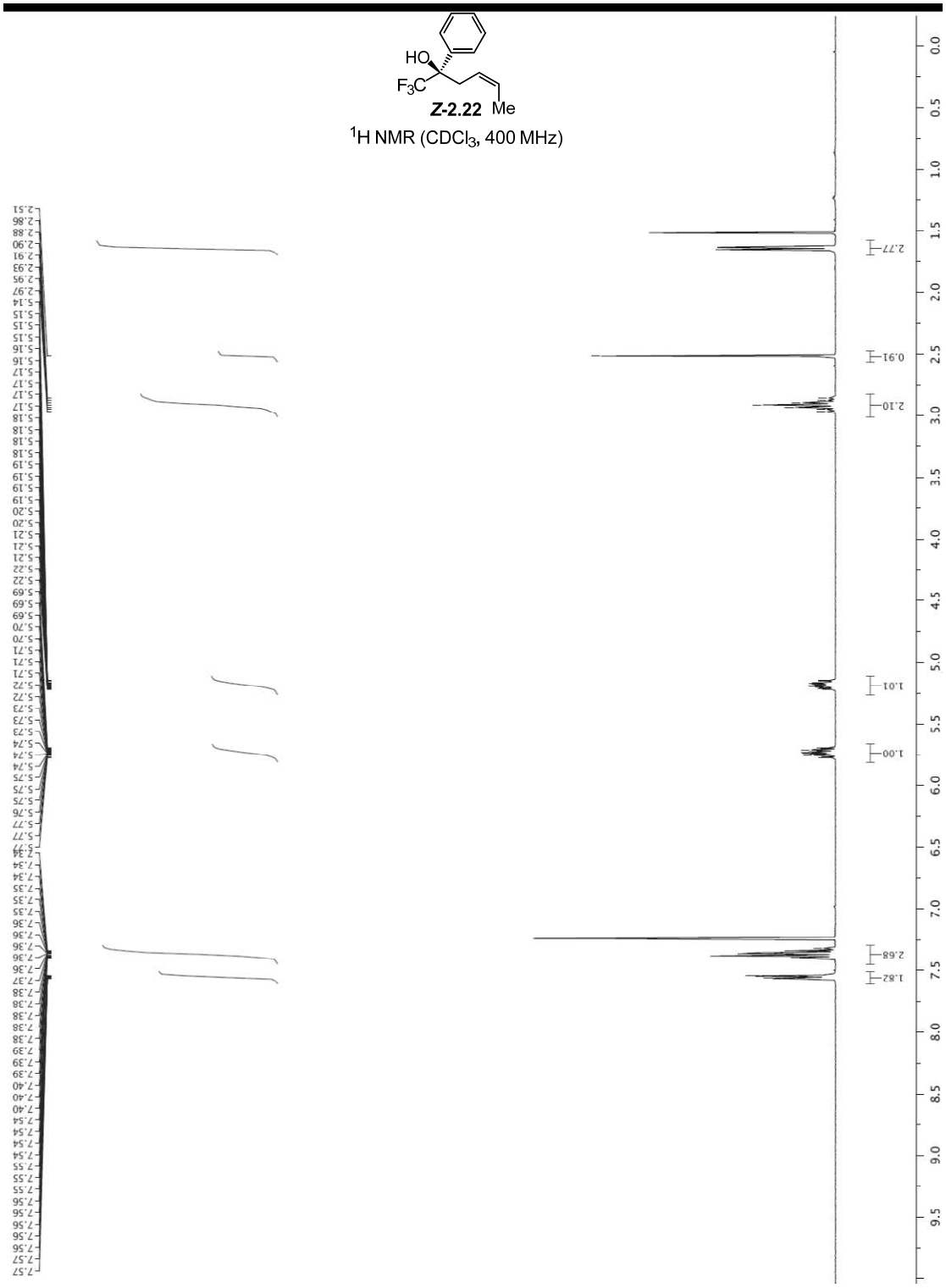
HO
F3C
Me
Z-2.22
1H NMR (CDCl3, 400 MHz)
2.77
0.91
2.10
1.01
1.00
2.68
1.82

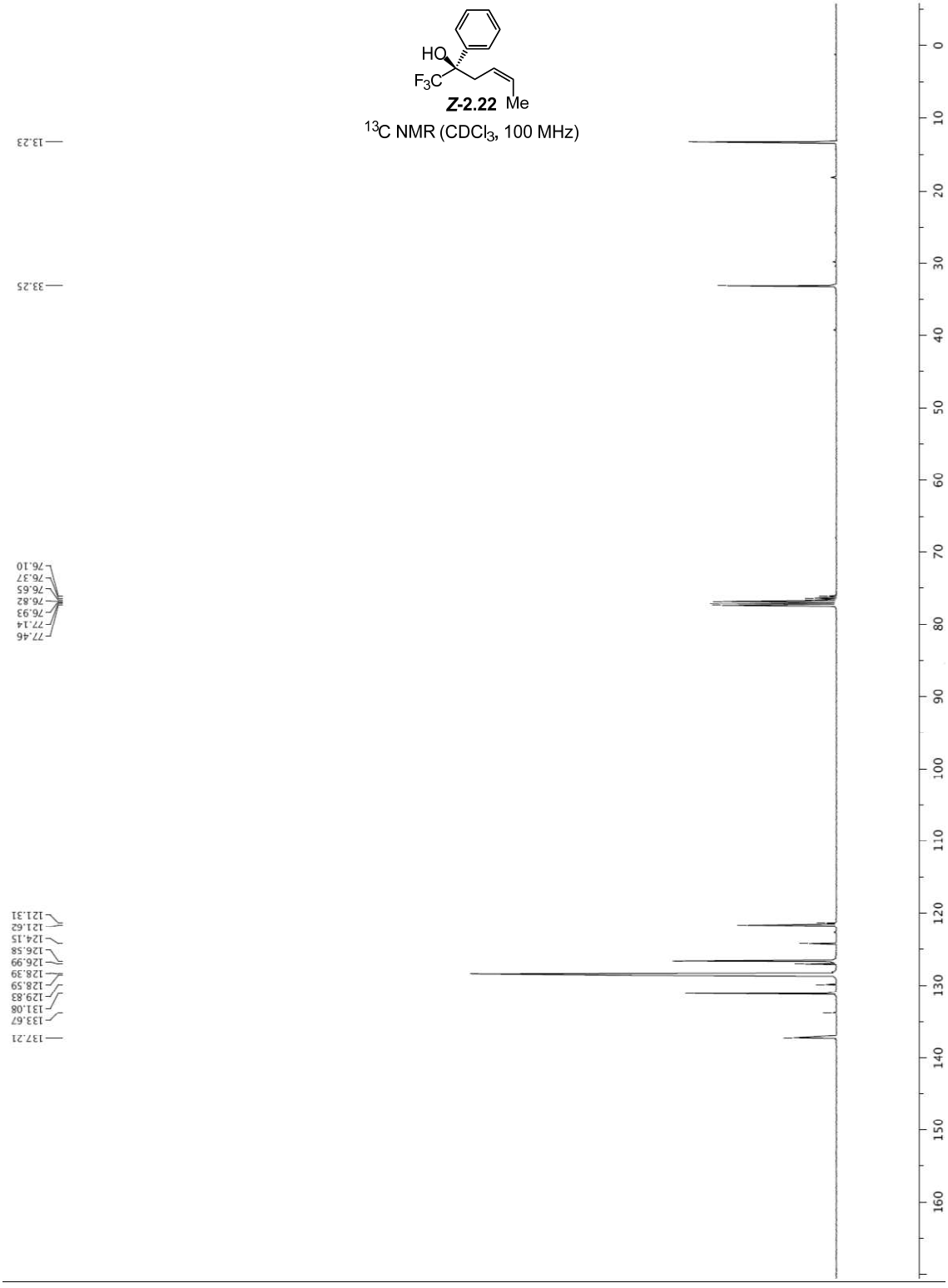
HO
F3C
Me
Z-2.22
13C NMR (CDCl3, 100 MHz)
13.23
33.25
76.10
76.37
76.65
76.82
76.93
77.14
77.46
121.31
121.62
124.15
126.58
126.99
128.39
128.59
129.83
131.08
133.67
137.21

***Z*-2.22**

^{19}F NMR ($CDCl_3$, 376 MHz)

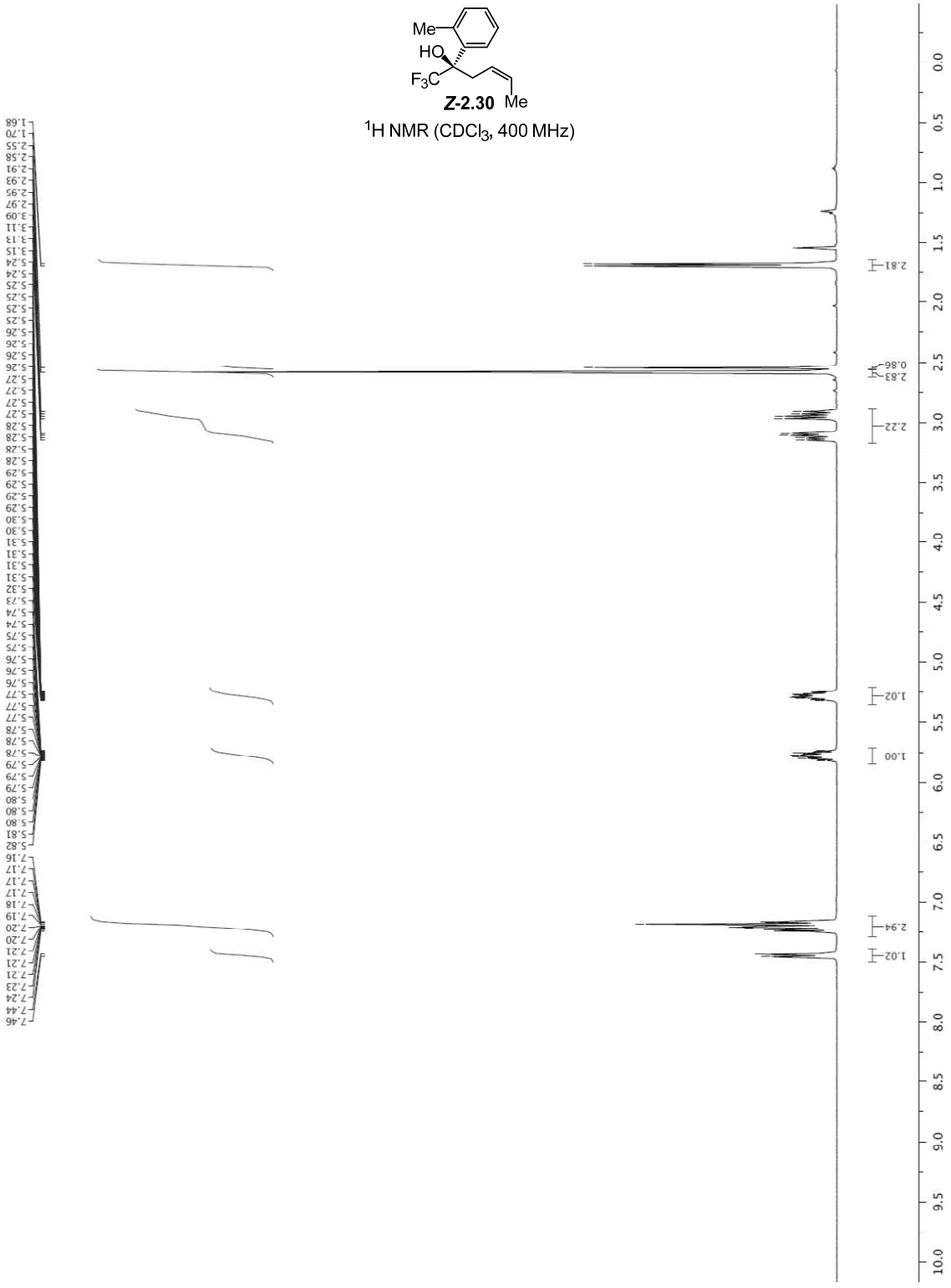
Me
HO
F3C
Me
Z-2.30
1H NMR (CDCl3, 400 MHz)
2.81
0.86
2.83
2.22
1.02
1.00
2.94
1.02

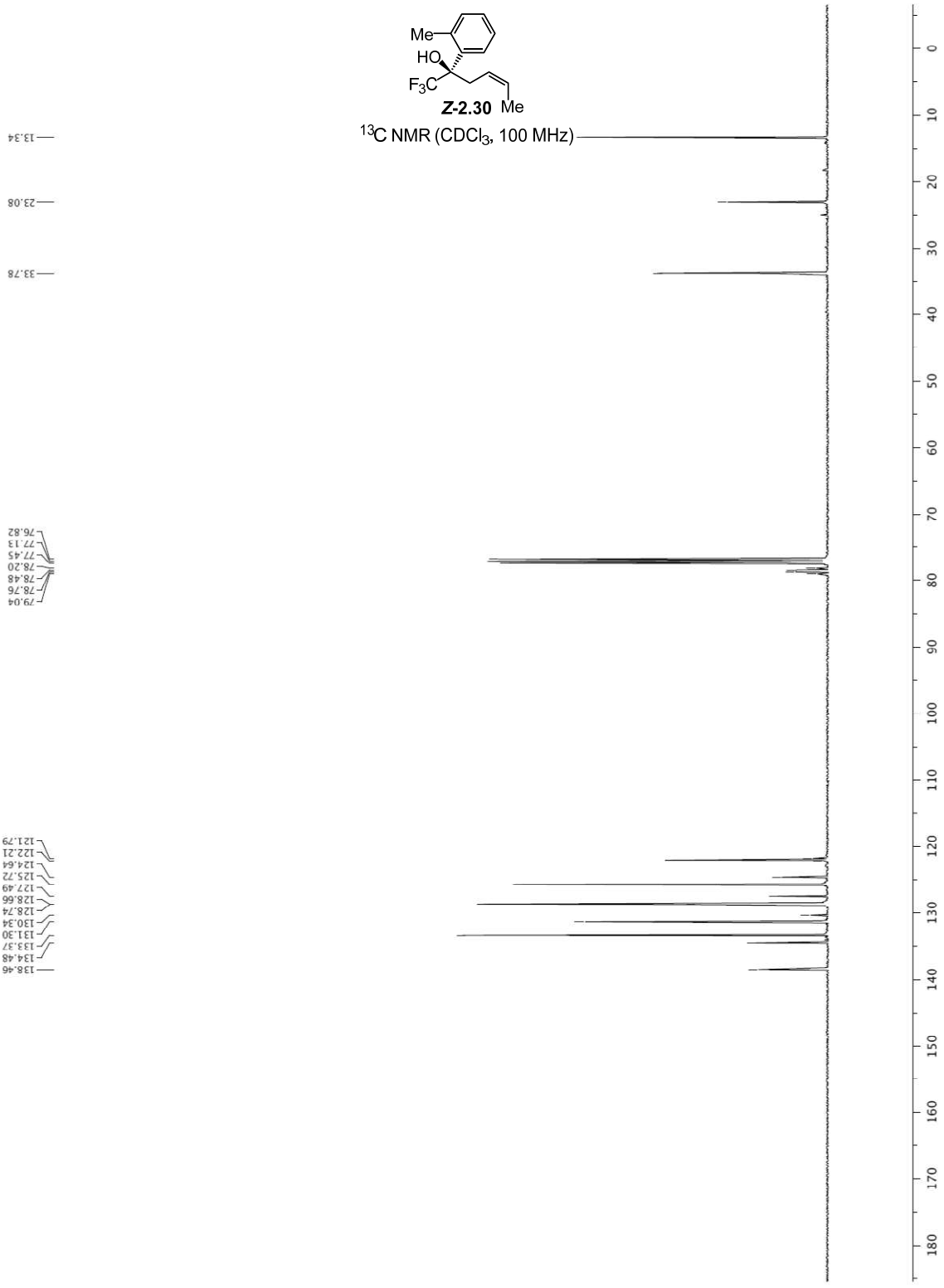
Me
HO
F3C
Z-2.30 Me
13C NMR (CDCl3, 100 MHz)
13.34
23.08
33.78
76.82
77.13
77.45
78.20
78.48
78.76
79.04
121.79
122.21
124.64
125.72
127.49
128.66
128.74
130.34
131.30
133.37
134.48
138.46

***Z*-2.30**

^{19}F NMR ($CDCl_3$, 376 MHz)

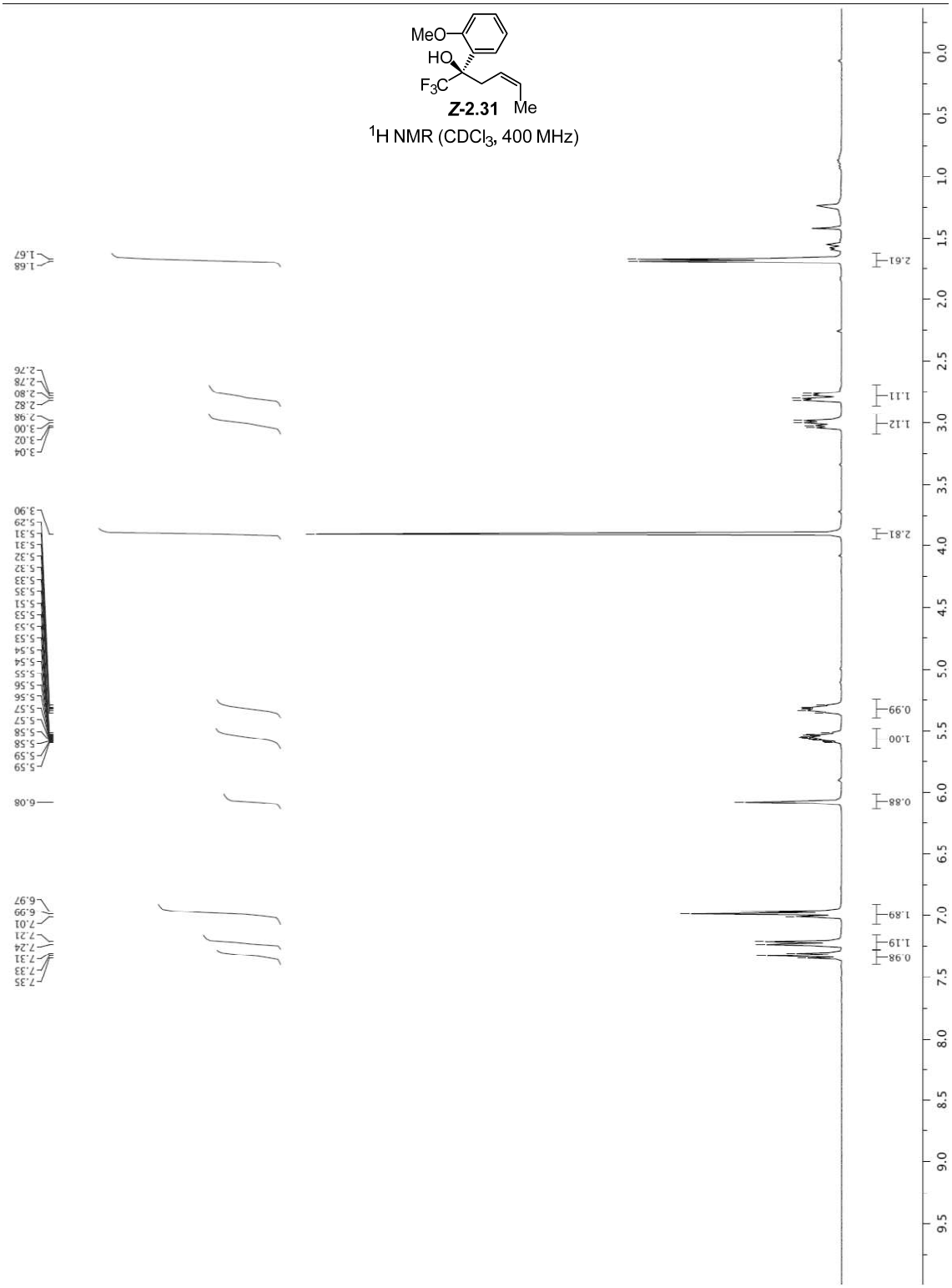
MeO
HO
F3C
Me
Z-2.31
1H NMR (CDCl3, 400 MHz)

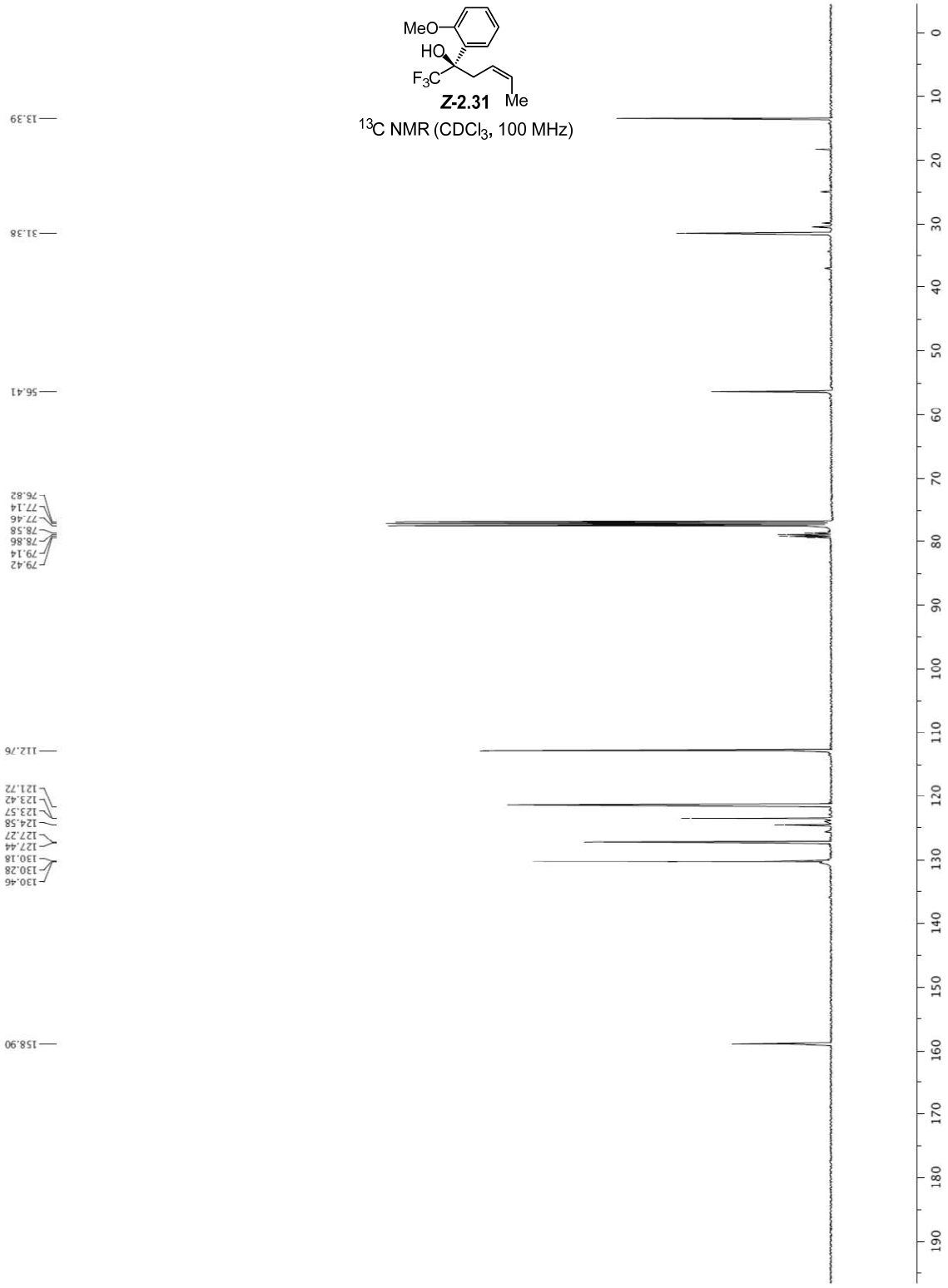
MeO
HO
F3C
Me
Z-2.31
13C NMR (CDCl3, 100 MHz)
13.39
31.38
56.41
76.82
77.14
77.46
78.58
78.86
79.14
79.42
112.76
121.72
123.42
123.57
124.58
127.27
127.44
130.18
130.28
130.46
158.90

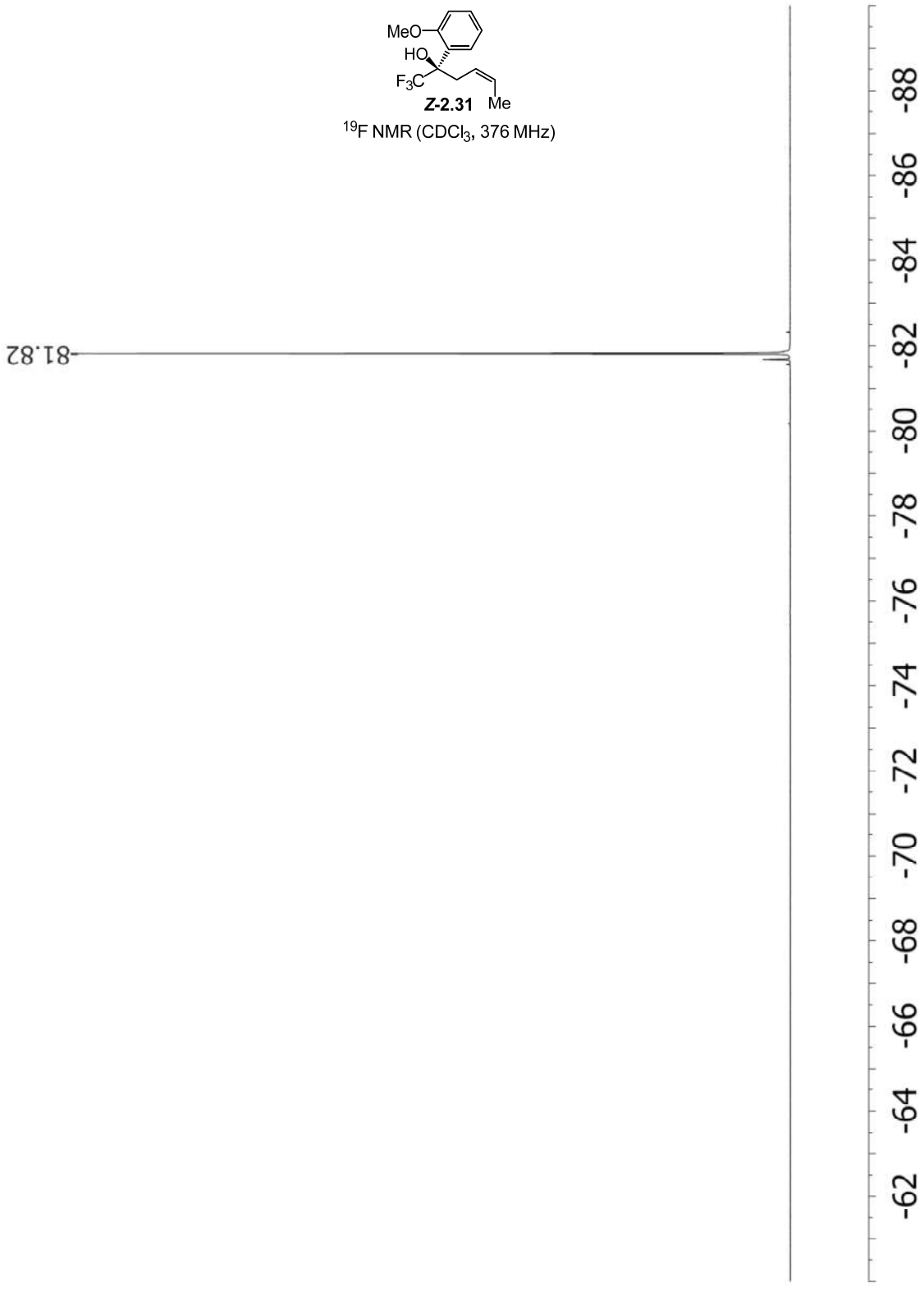
MeO
HO
F3C
Me
Z-2.31
19F NMR (CDCl3, 376 MHz)
-81.82
-62
-64
-66
-68
-70
-72
-74
-76
-78
-80
-82
-84
-86
-88

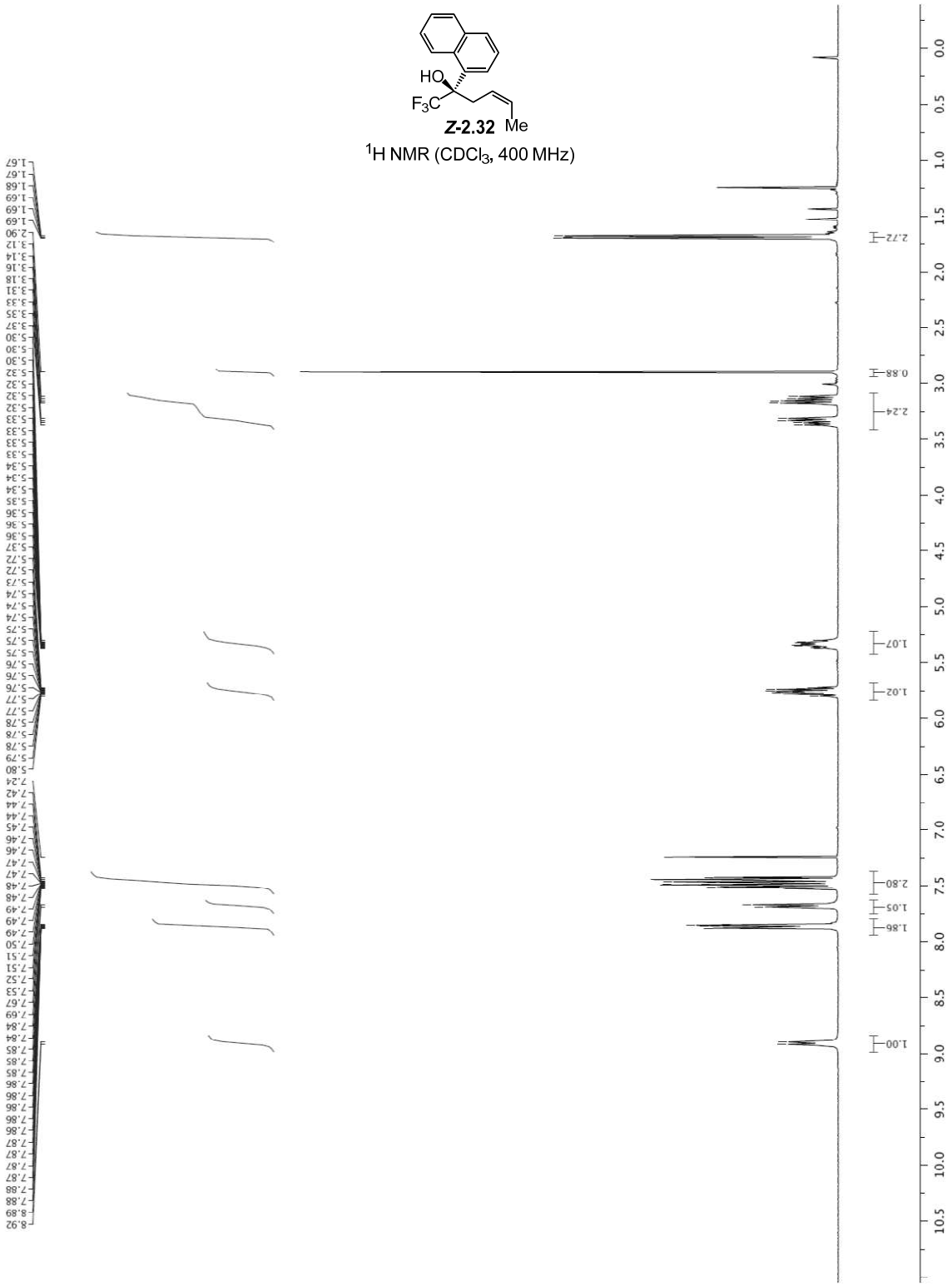
HO
F3C
Me
Z-2.32
1H NMR (CDCl3, 400 MHz)
2.72
0.88
2.24
1.07
1.02
2.80
1.05
1.86
1.00

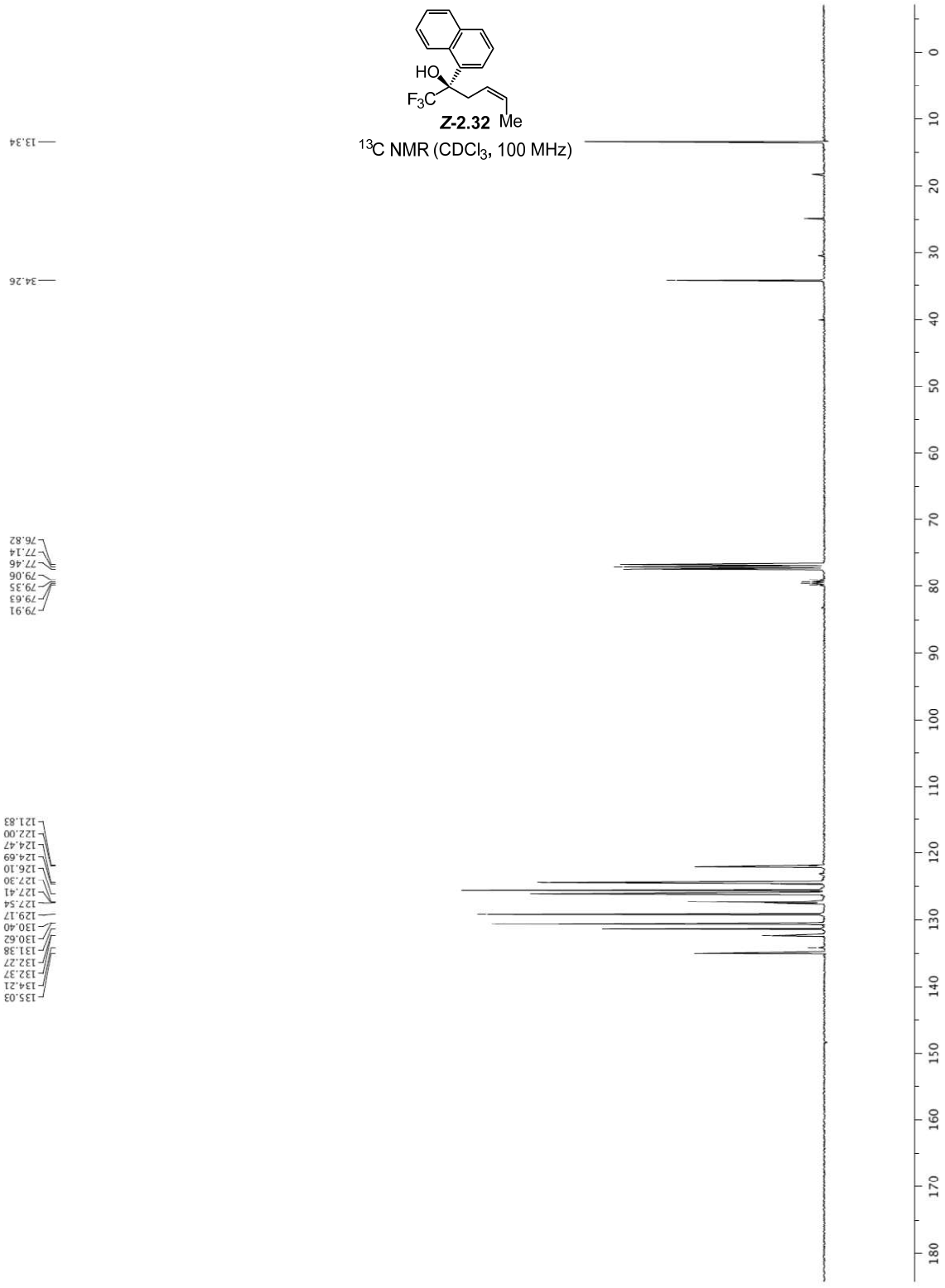
HO
F3C
Z-2.32 Me
13C NMR (CDCl3, 100 MHz)
13.34
34.26
76.82
77.14
77.46
79.06
79.35
79.63
79.91
121.83
122.00
124.47
124.69
126.10
127.30
127.41
127.54
129.17
130.40
130.62
131.38
132.27
132.37
134.21
135.03
0
10
20
30
40
50
60
70
80
90
100
110
120
130
140
150
160
170
180


HO
F3C
Me
Z-2.32
19F NMR (CDCl3, 376 MHz)
-77.98
-62
-64
-66
-68
-70
-72
-74
-76
-78
-80
-82
-84
-86
-88

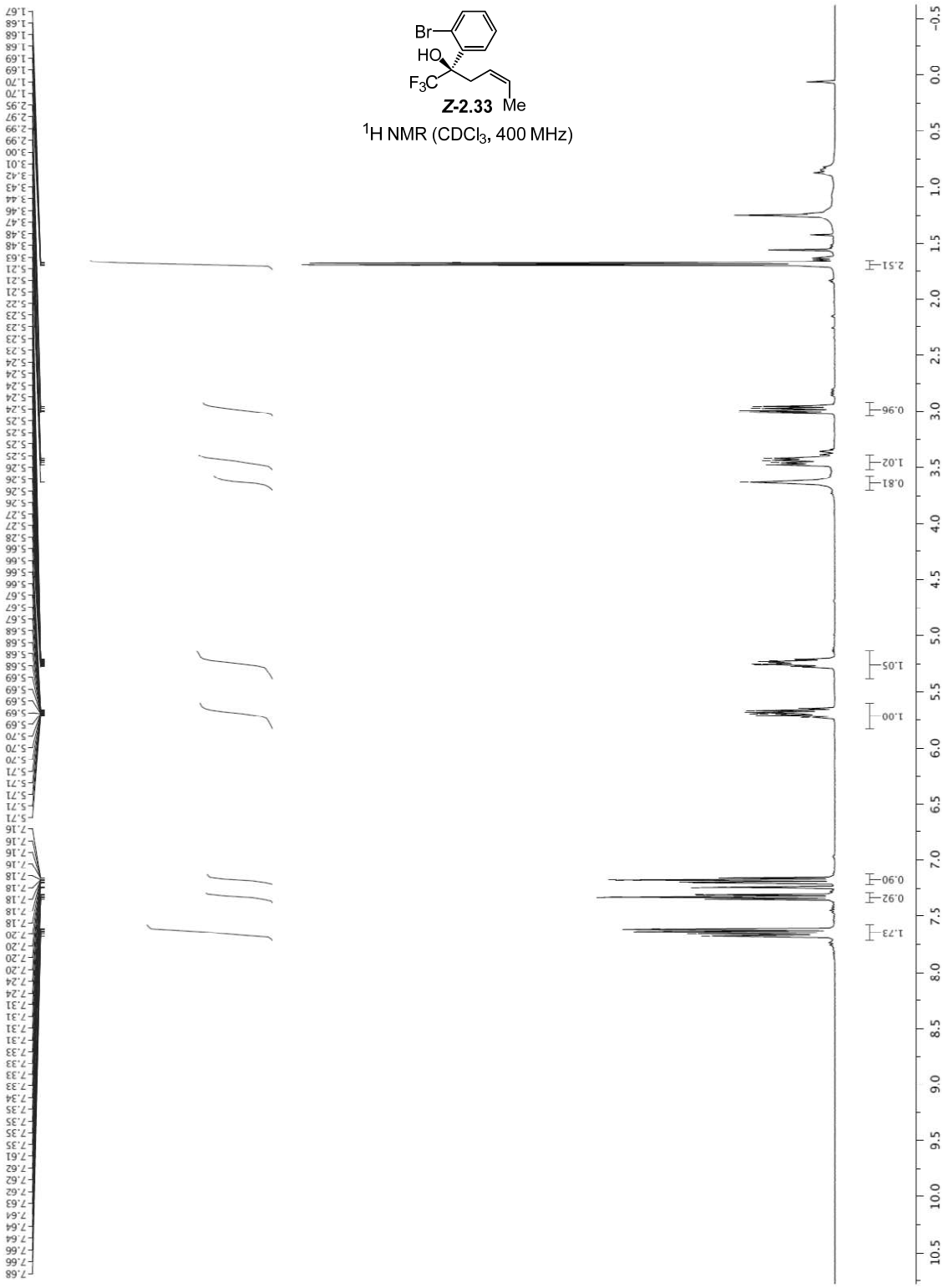
Br
HO
F3C
Me
Z-2.33
1H NMR (CDCl3, 400 MHz)
2.51
0.96
1.02
0.81
1.05
1.00
0.90
0.92
1.73

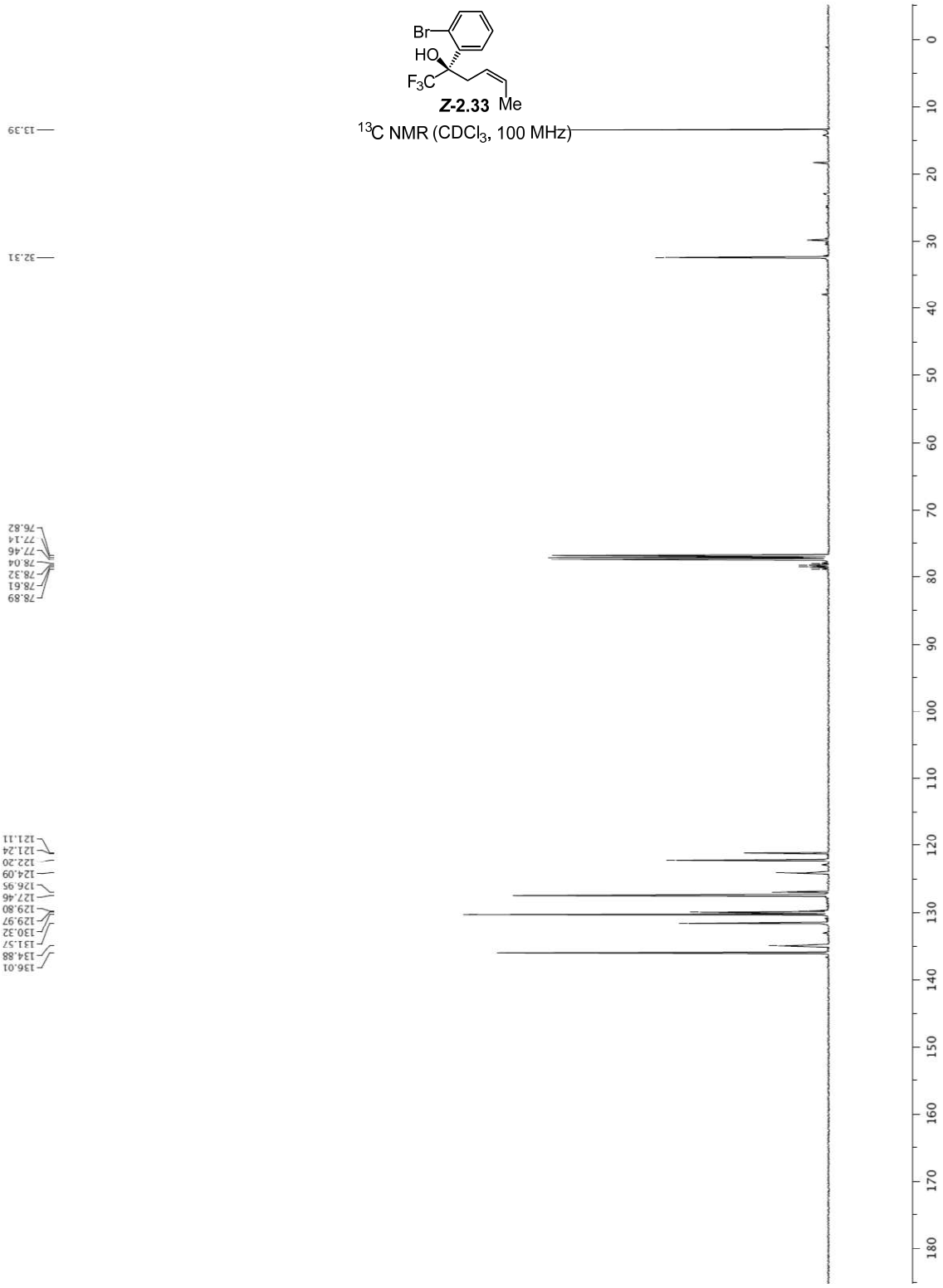
Br
HO
F3C
Me
Z-2.33
13C NMR (CDCl3, 100 MHz)
13.39
32.31
76.82
77.14
77.46
78.04
78.32
78.61
78.89
121.11
121.24
122.20
124.09
126.95
127.46
129.80
129.97
130.32
131.57
134.88
136.01

***Z*-2.33**

^{19}F NMR ($CDCl_3$, 376 MHz)

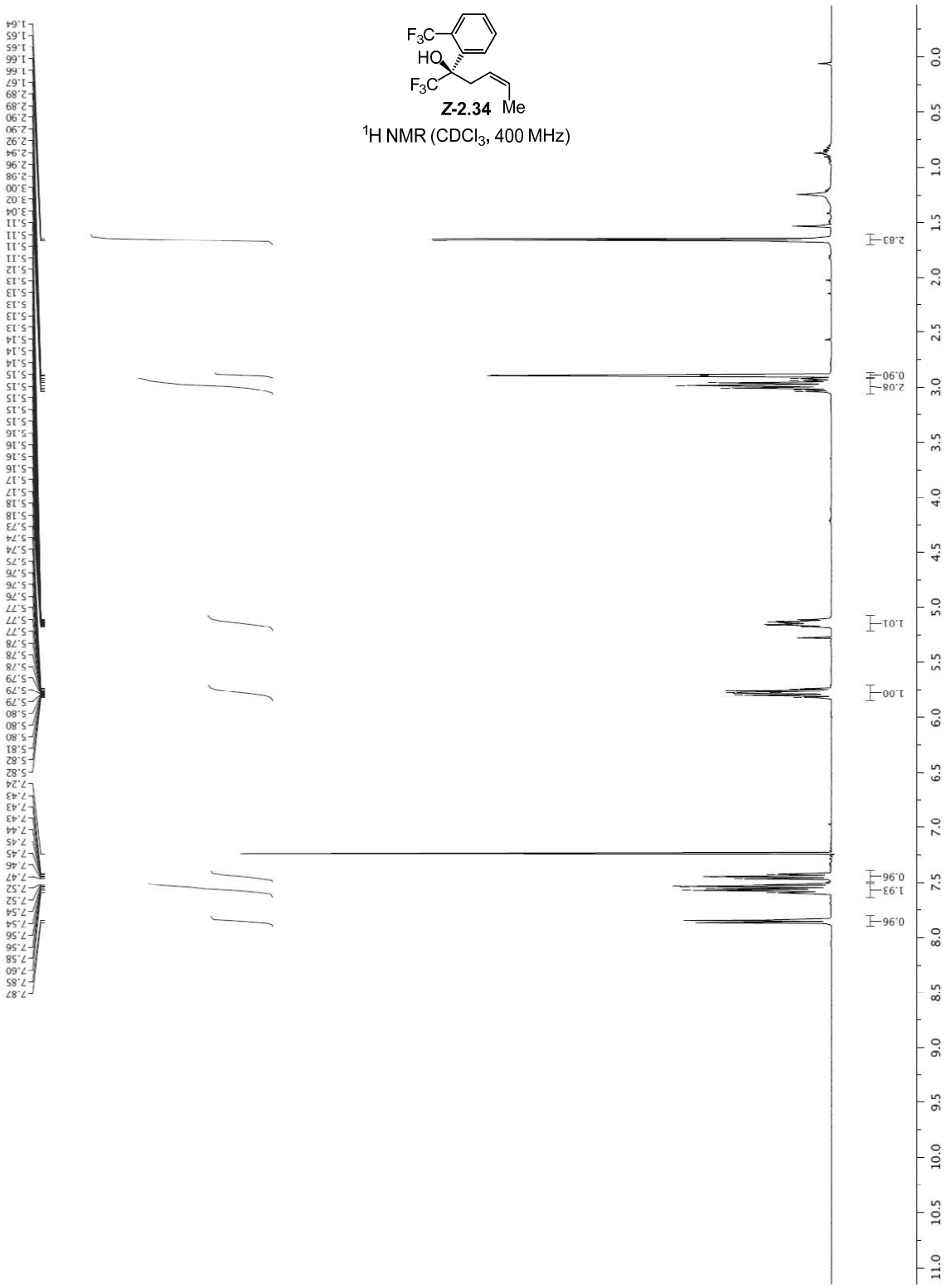
F3C
HO
F3C
Me
Z-2.34
1H NMR (CDCl3, 400 MHz)

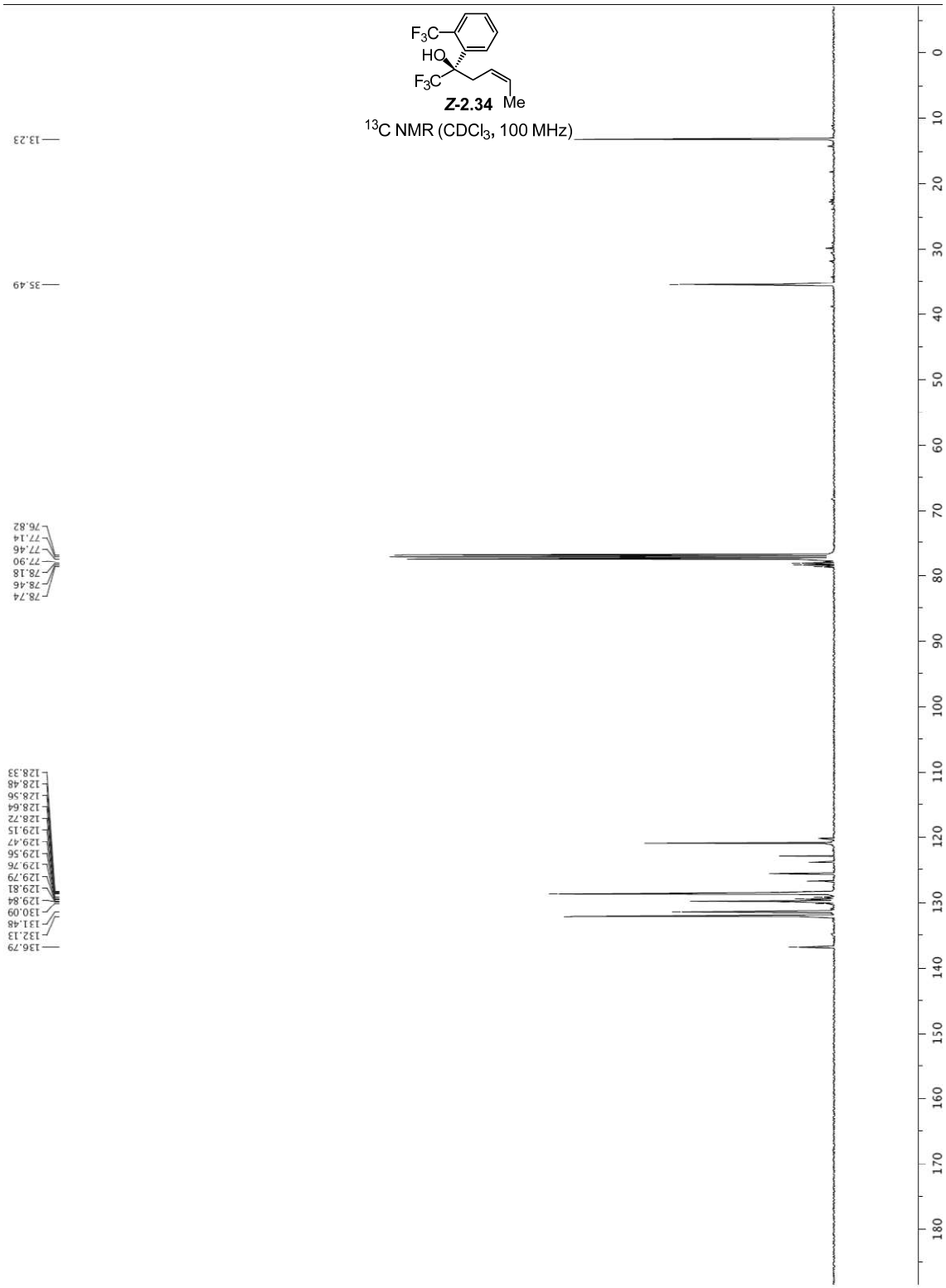
F3C
HO
F3C
Me
Z-2.34
13C NMR (CDCl3, 100 MHz)
13.23
35.49
76.82
77.14
77.46
77.90
78.18
78.46
78.74
128.33
128.48
128.56
128.64
128.72
129.15
129.47
129.56
129.76
129.79
129.81
129.84
130.09
131.48
132.13
136.79

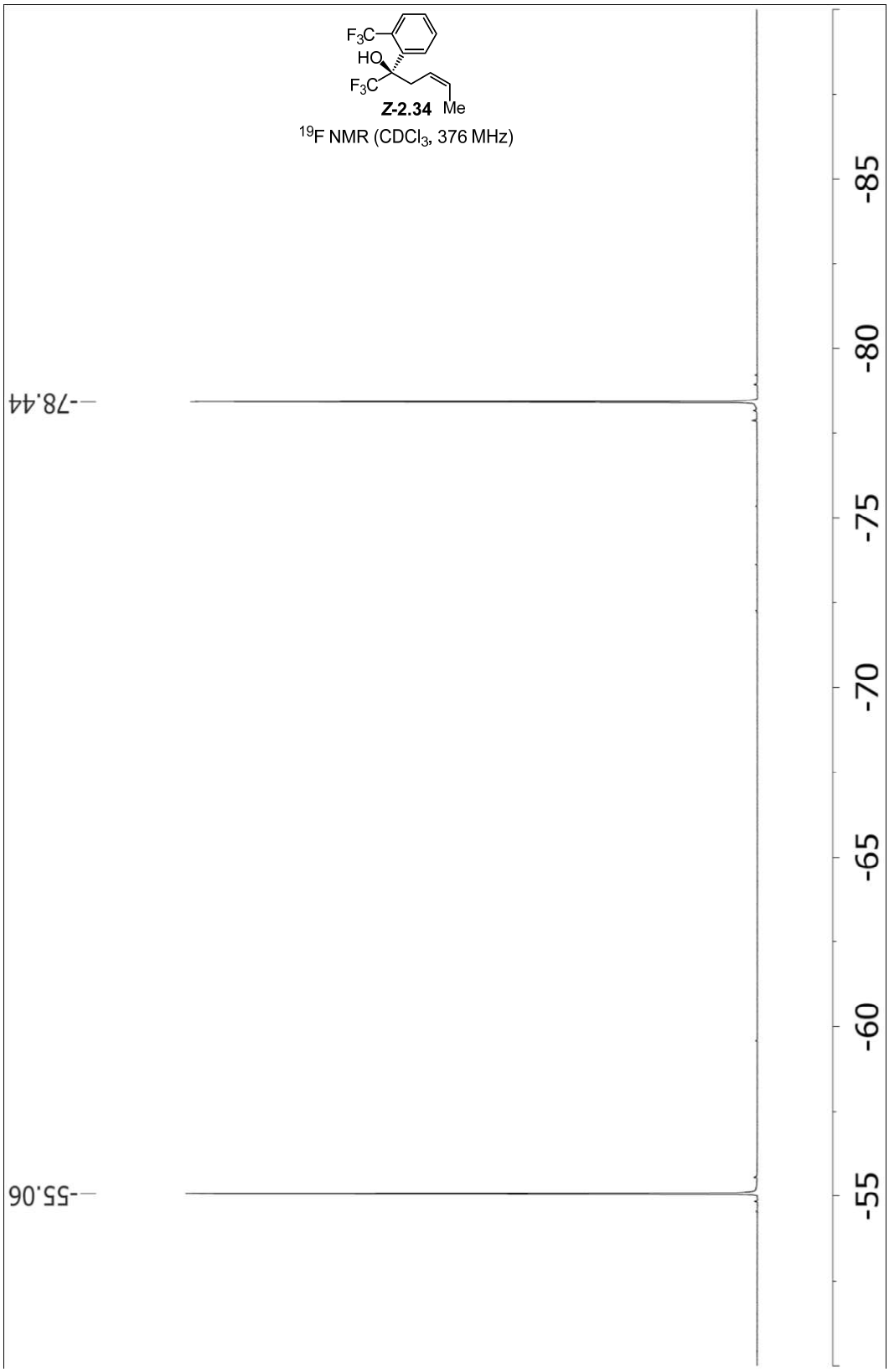

***Z*-2.34**

^{19}F NMR ($CDCl_3$, 376 MHz)

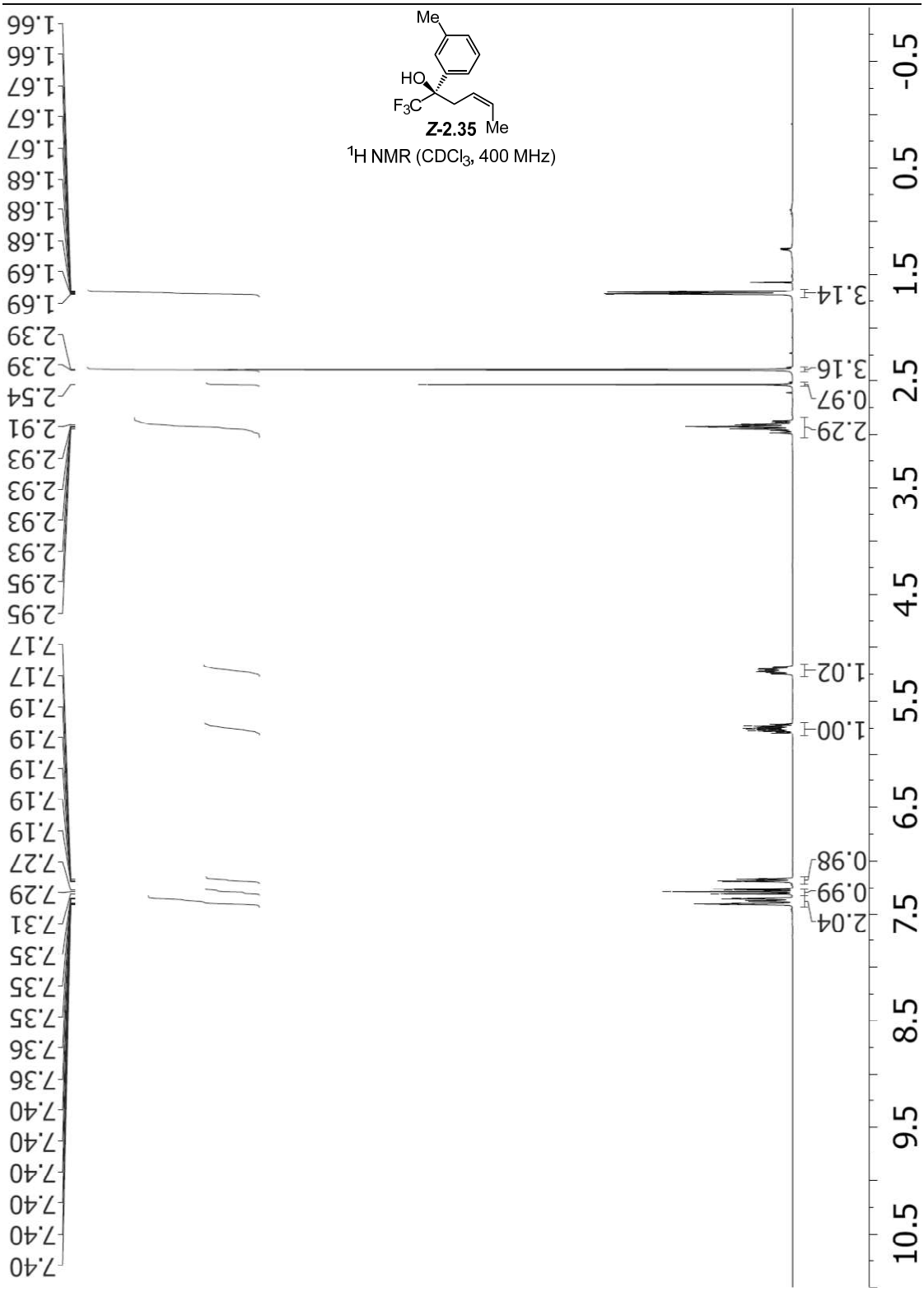
Me
HO
F3C
Me
Z-2.35
1H NMR (CDCl3, 400 MHz)

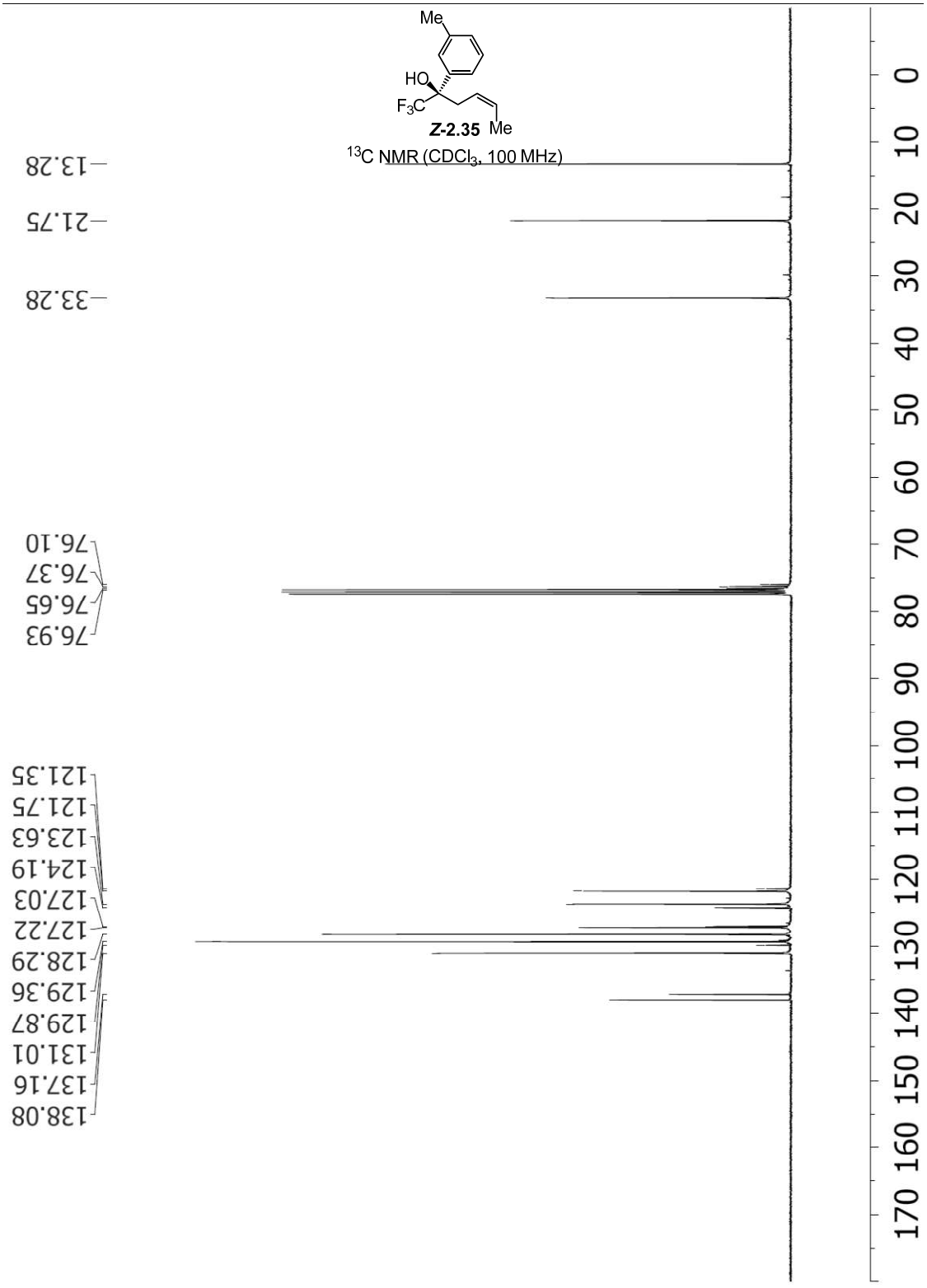
Me
HO
F3C
Z-2.35 Me
13C NMR (CDCl3, 100 MHz)
13.28
21.75
33.28
76.10
76.37
76.65
76.93
121.35
121.75
123.63
124.19
127.03
127.22
128.29
129.36
129.87
131.01
137.16
138.08
0 10 20 30 40 50 60 70 80 90 100 110 120 130 140 150 160 170

***Z*-2.35**

^{19}F NMR ($CDCl_3$, 376 MHz)

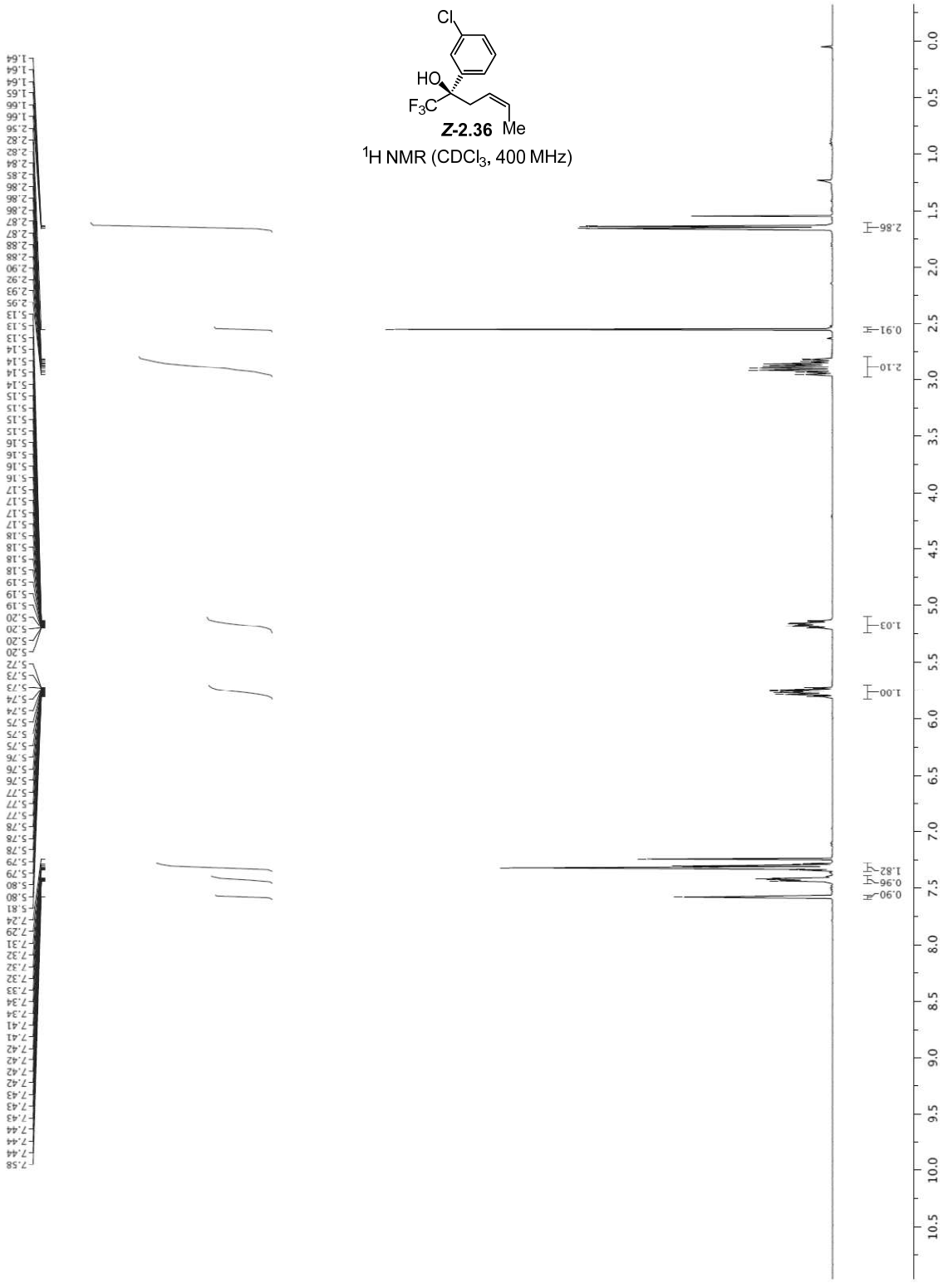
Cl
HO
F3C
Me
Z-2.36
1H NMR (CDCl3, 400 MHz)
2.86
0.91
2.10
1.03
1.00
1.82
0.96
0.90

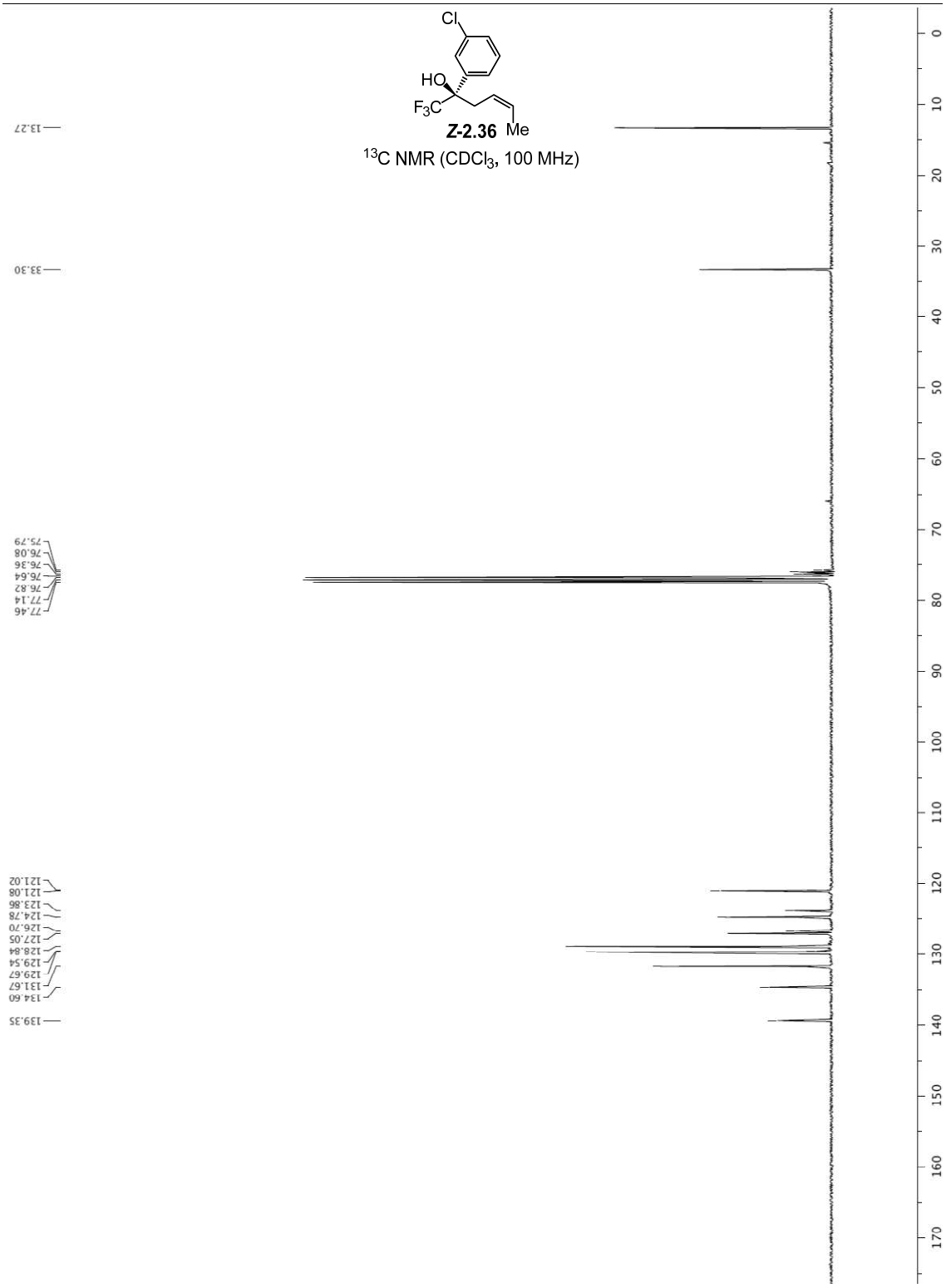
Cl
HO
F3C
Me
Z-2.36
13C NMR (CDCl3, 100 MHz)
13.27
33.30
75.79
76.08
76.36
76.64
76.82
77.14
77.46
121.02
121.08
123.86
124.78
126.70
127.05
128.84
129.54
129.67
131.67
134.60
139.35
0
10
20
30
40
50
60
70
80
90
100
110
120
130
140
150
160
170

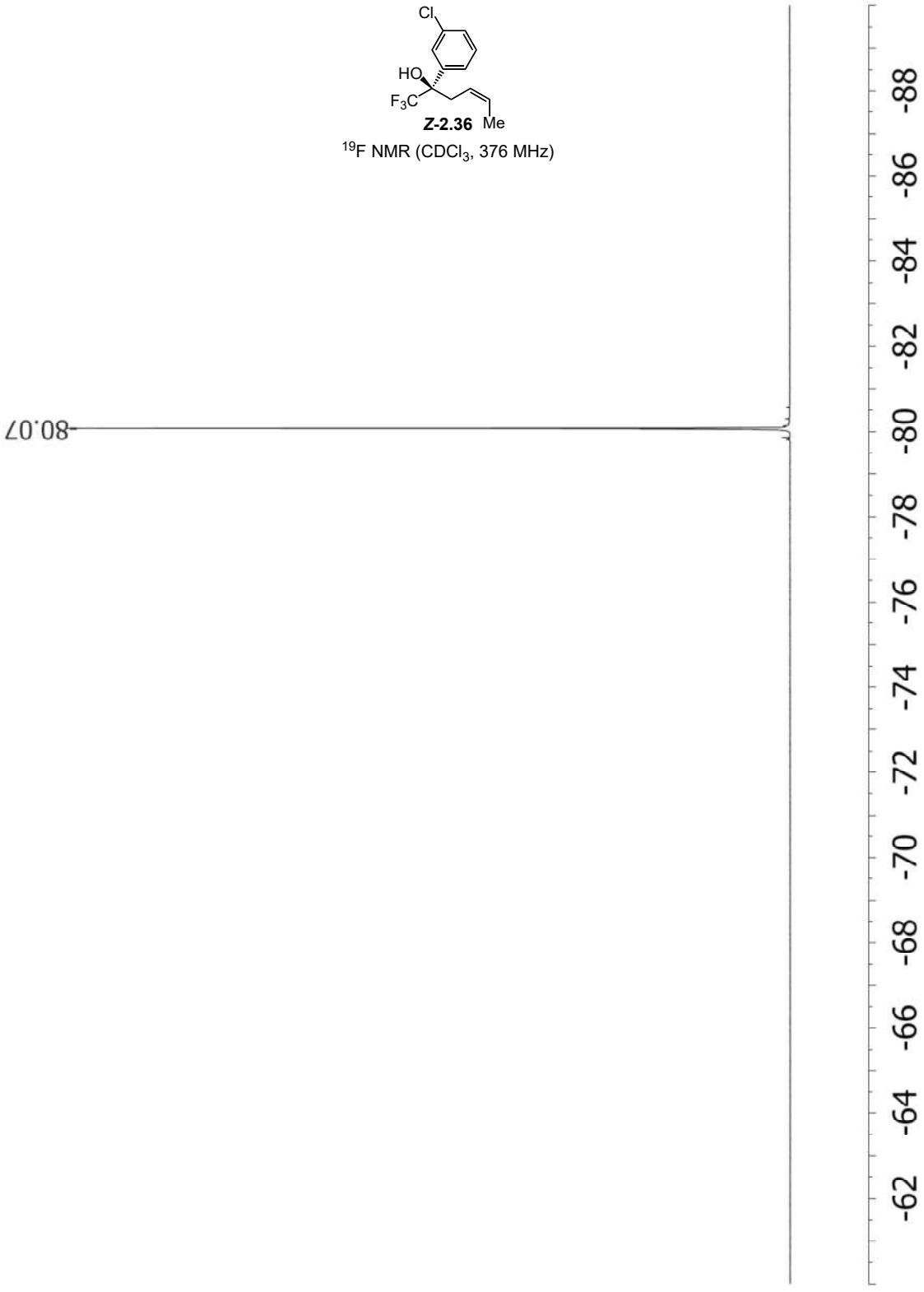
Cl
HO
F3C
Me
Z-2.36
19F NMR (CDCl3, 376 MHz)
-80.07
-62
-64
-66
-68
-70
-72
-74
-76
-78
-80
-82
-84
-86
-88

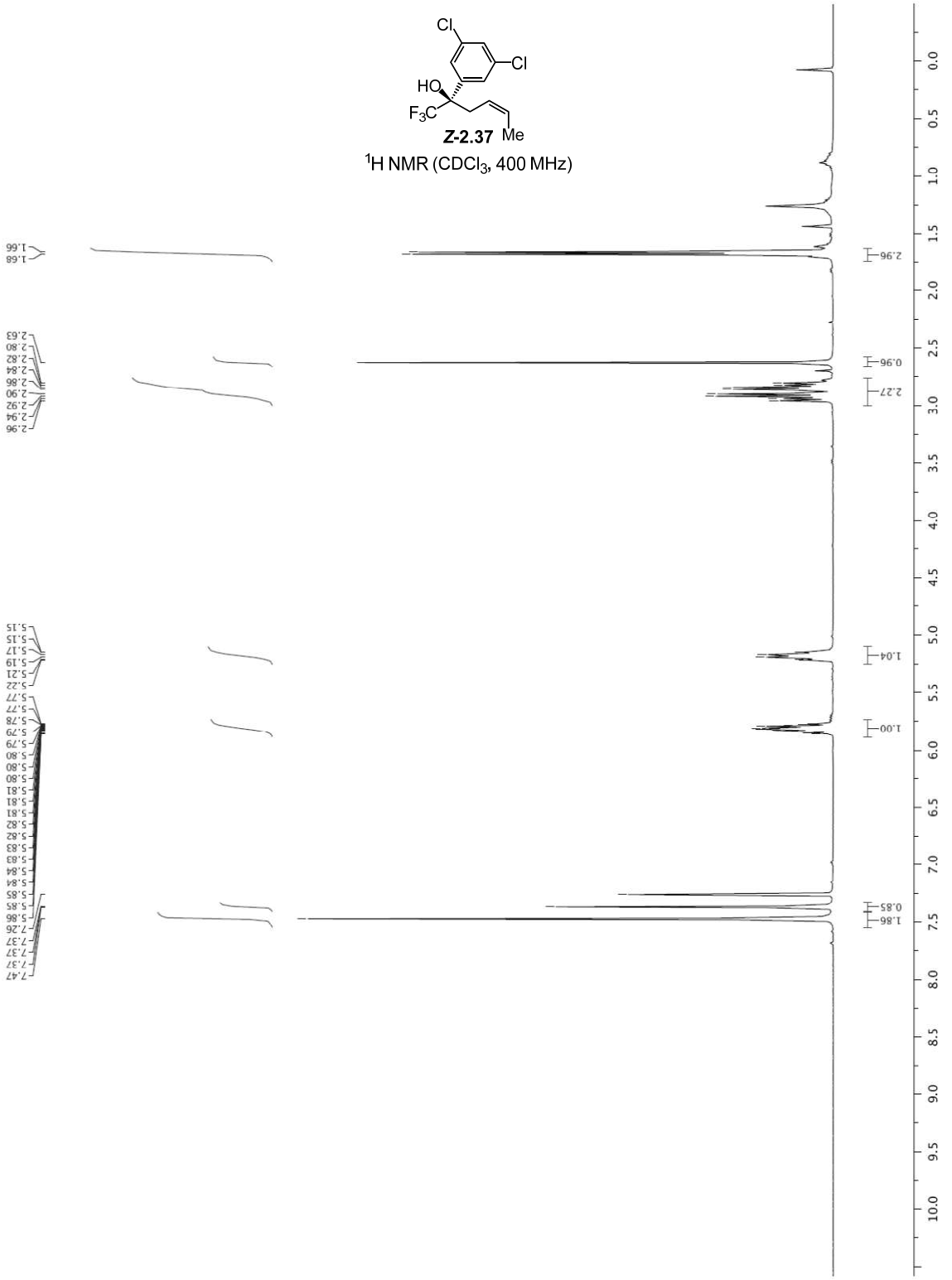
Cl
Cl
HO
F3C
Me
Z-2.37
1H NMR (CDCl3, 400 MHz)

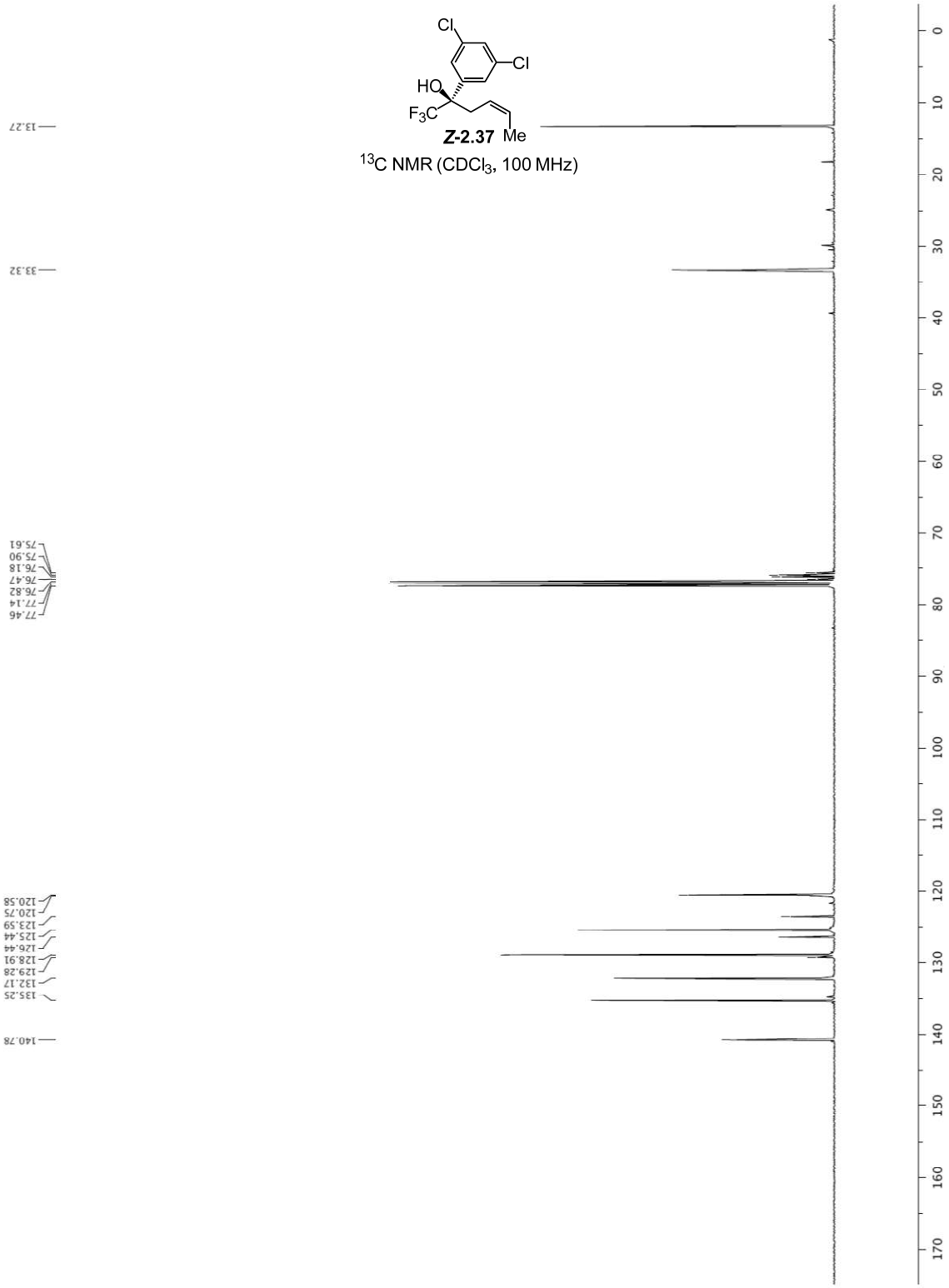
Cl
Cl
HO
F3C
Me
Z-2.37
13C NMR (CDCl3, 100 MHz)
13.27
33.32
75.61
75.90
76.18
76.47
76.82
77.14
77.46
120.58
120.75
123.59
125.44
126.44
128.91
129.28
132.17
135.25
140.78
0
10
20
30
40
50
60
70
80
90
100
110
120
130
140
150
160
170

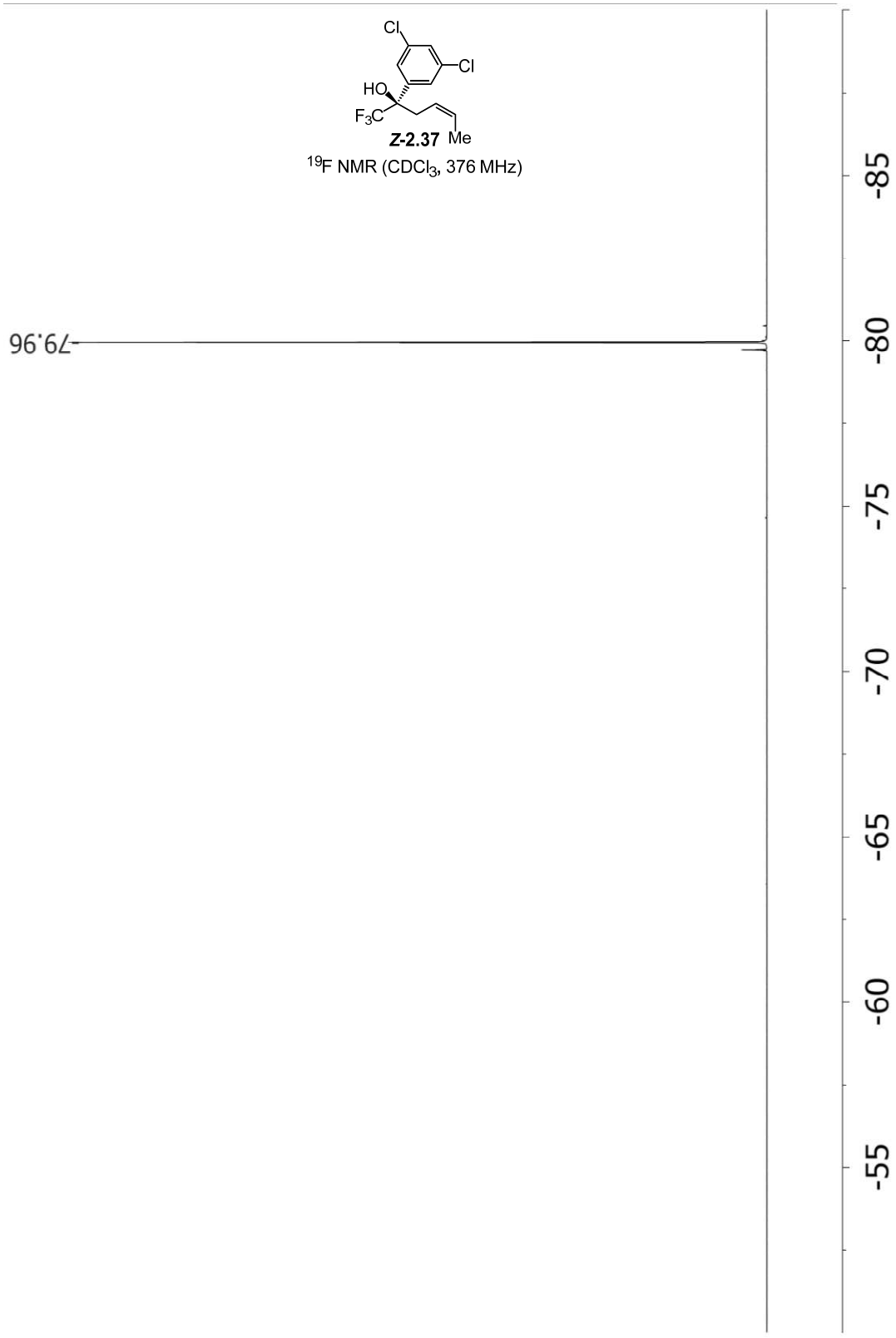

***Z*-2.37**

^{19}F NMR ($CDCl_3$, 376 MHz)

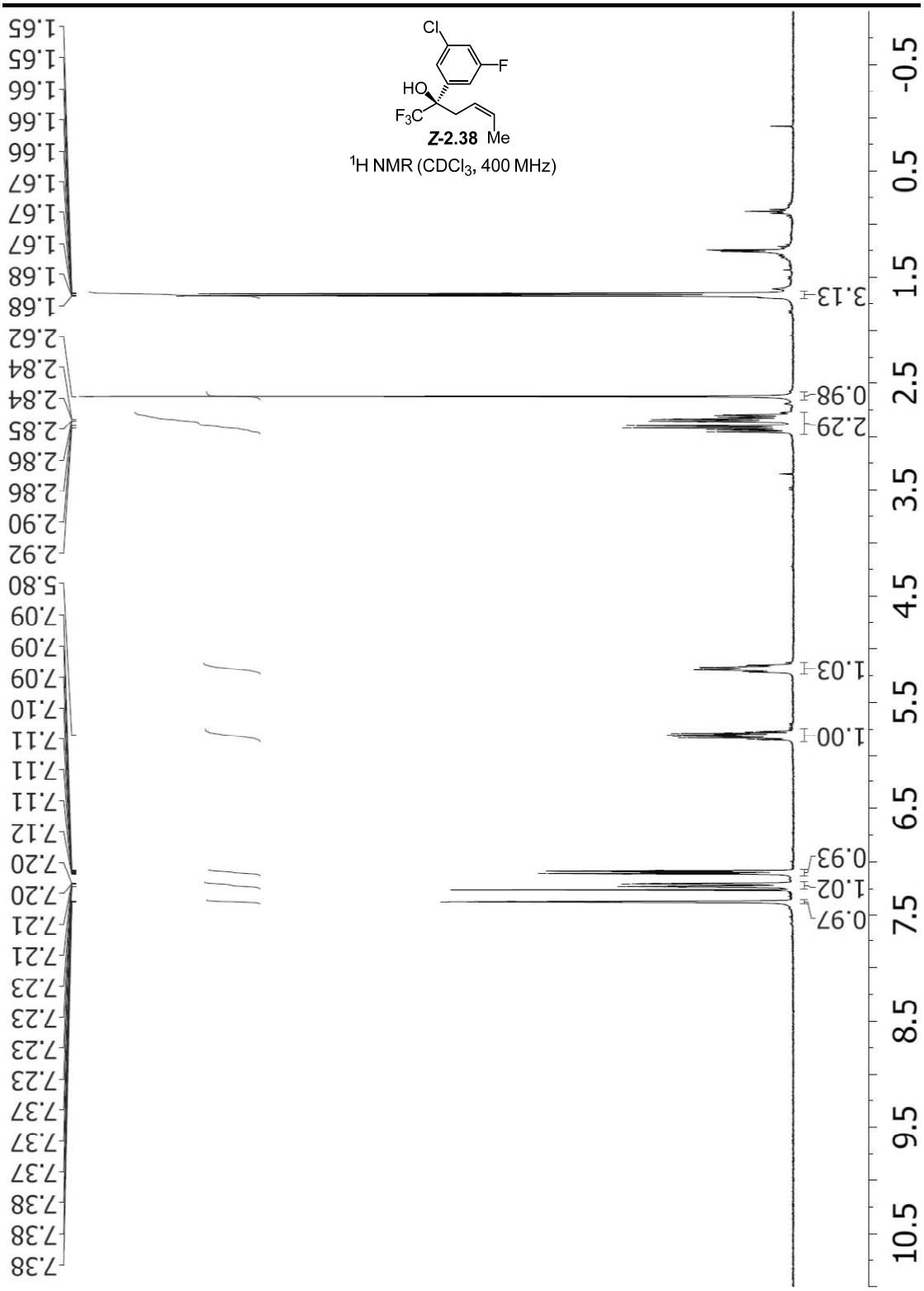
Cl
F
HO
F3C
Me
Z-2.38
1H NMR (CDCl3, 400 MHz)
3.13
0.98
2.29
1.03
1.00
0.93
1.02
0.97

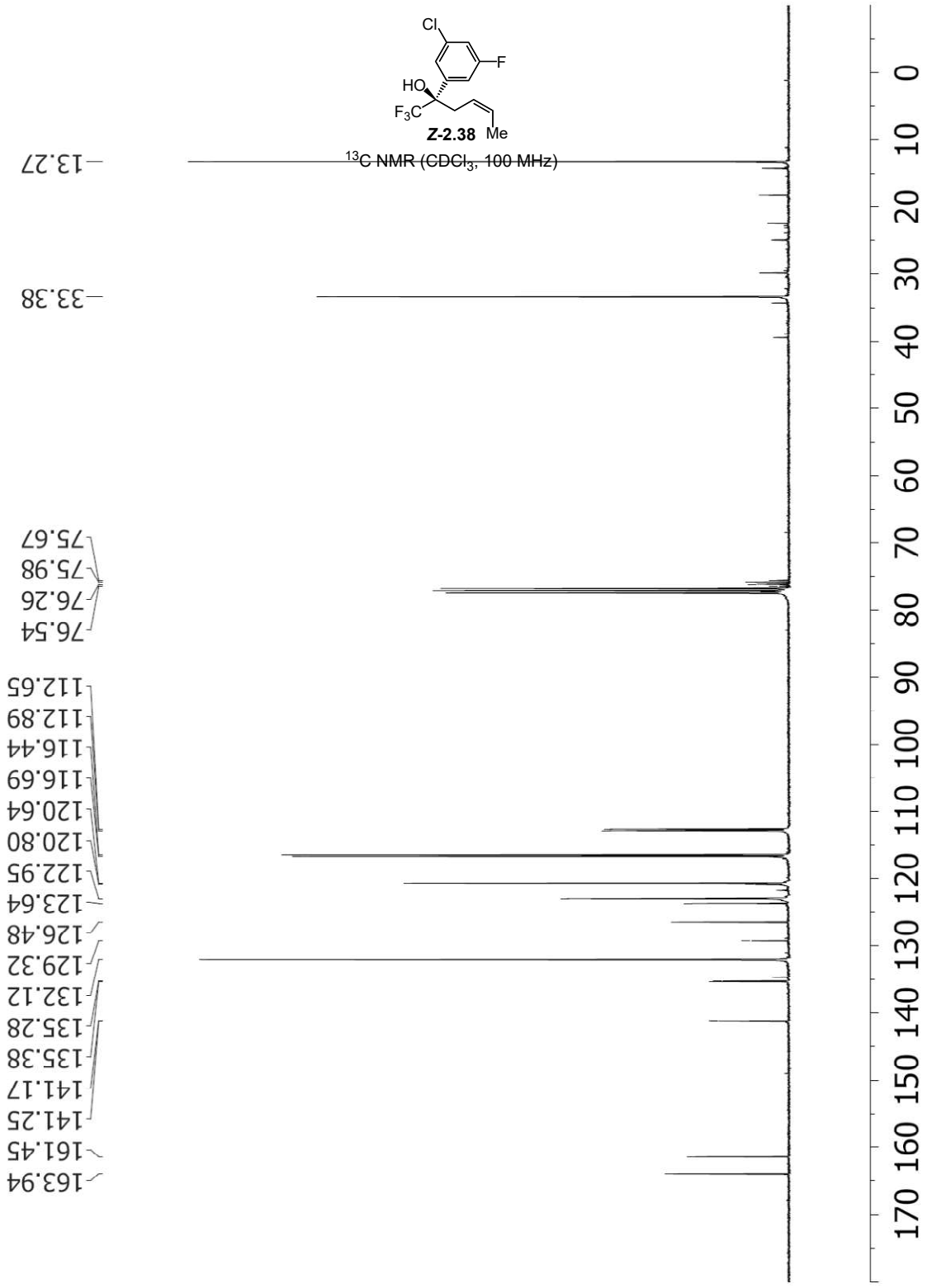
Cl
F
HO
F3C
Me
Z-2.38
13C NMR (CDCl3, 100 MHz)
13.27
33.38
75.67
75.98
76.26
76.54
112.65
112.89
116.44
116.69
120.64
120.80
122.95
123.64
126.48
129.32
132.12
135.28
135.38
141.17
141.25
161.45
163.94
0
10
20
30
40
50
60
70
80
90
100
110
120
130
140
150
160
170

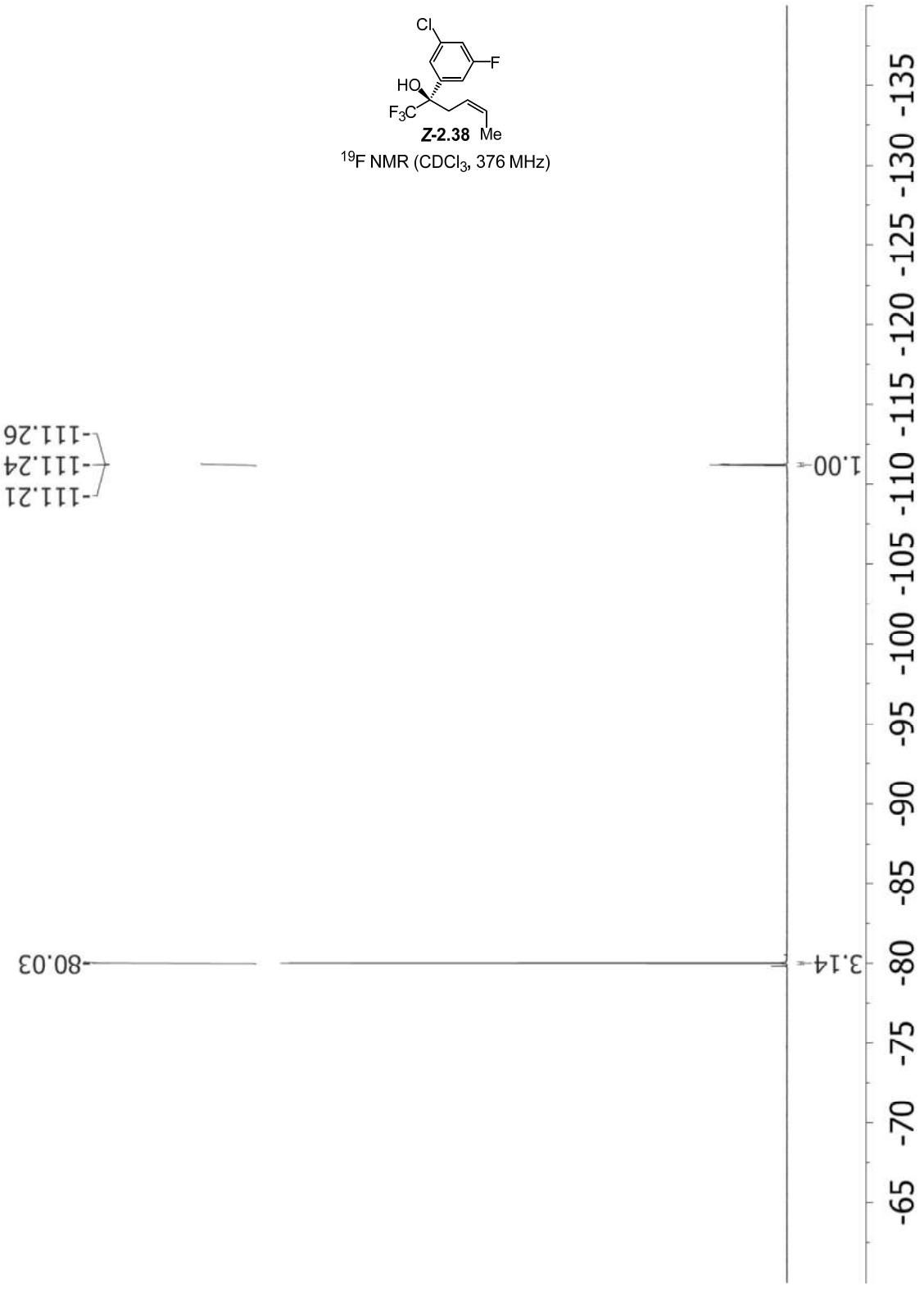
Cl
F
HO
F3C
Me
Z-2.38
19F NMR (CDCl3, 376 MHz)
-111.26
-111.24
-111.21
-80.03
1.00
3.14
-65 -70 -75 -80 -85 -90 -95 -100 -105 -110 -115 -120 -125 -130 -135

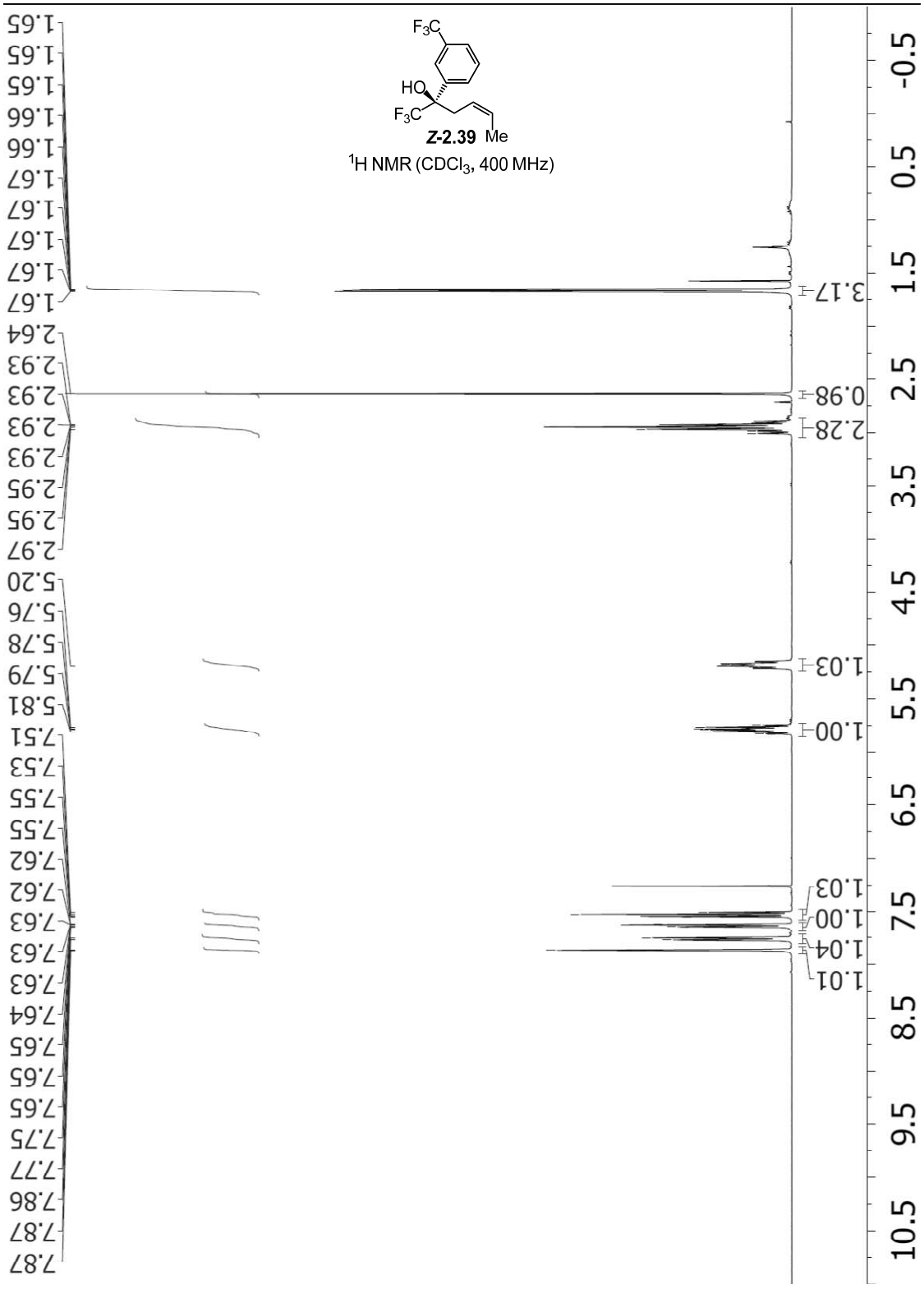
F3C
HO
F3C
Z-2.39 Me
1H NMR (CDCl3, 400 MHz)

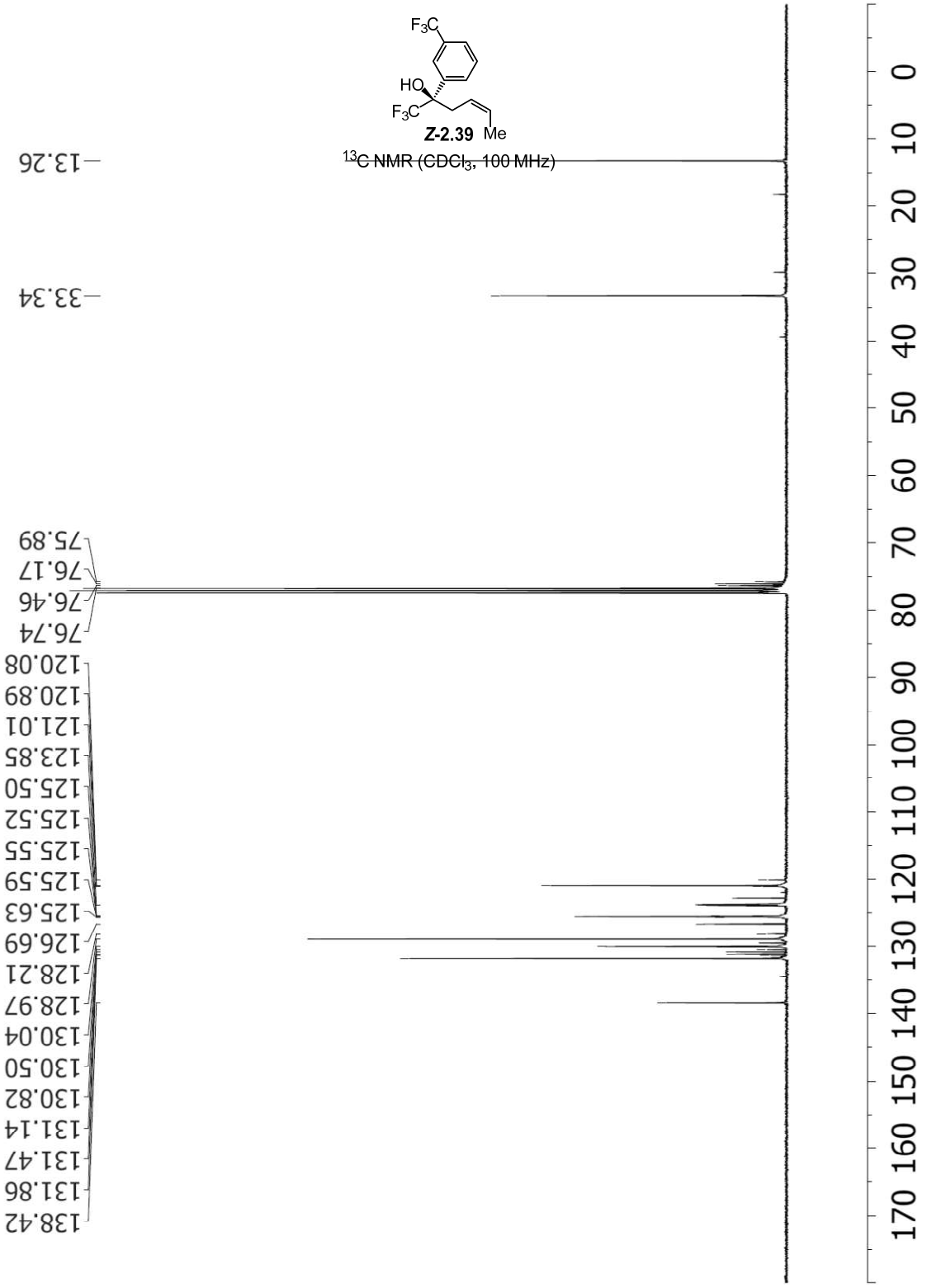
F3C
HO
F3C
Z-2.39 Me
13C NMR (CDCl3, 100 MHz)
13.26
33.34
75.89
76.17
76.46
76.74
120.08
120.89
121.01
123.85
125.50
125.52
125.55
125.59
125.63
126.69
128.21
128.97
130.04
130.50
130.82
131.14
131.47
131.86
138.42
0
10
20
30
40
50
60
70
80
90
100
110
120
130
140
150
160
170


F3C
HO
F3C
Z-2.39 Me
19F NMR (CDCl3, 376 MHz)
-80.12
-63.58
-61
-63
-65
-67
-69
-71
-73
-75
-77
-79
-81
-83
-85
-87
-89

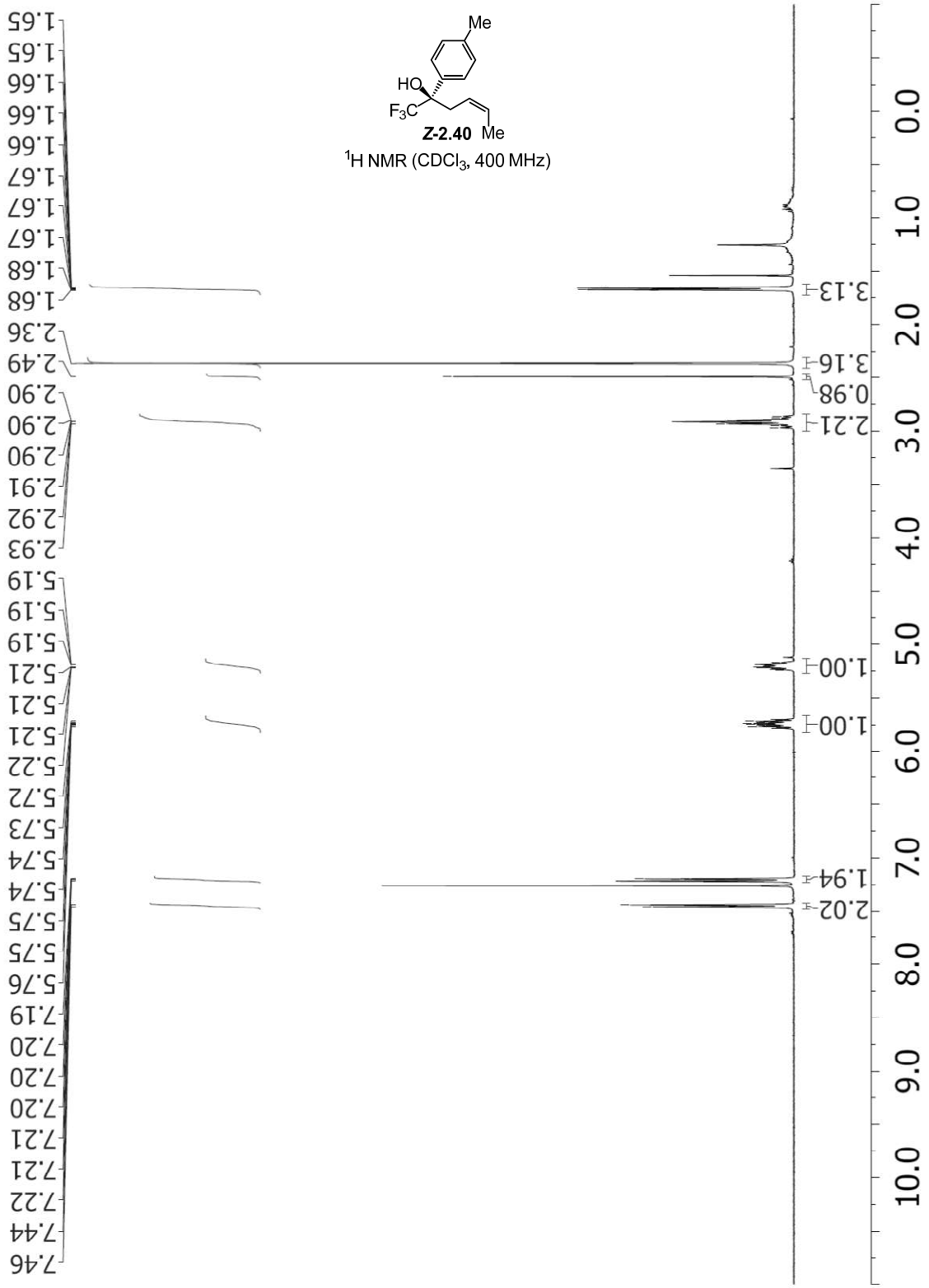
Me
HO
F3C
Z-2.40 Me
1H NMR (CDCl3, 400 MHz)
1.65
1.65
1.66
1.66
1.66
1.67
1.67
1.67
1.68
1.68
2.36
2.49
2.90
2.90
2.90
2.91
2.92
2.93
5.19
5.19
5.19
5.21
5.21
5.21
5.22
5.72
5.73
5.74
5.74
5.75
5.75
5.76
7.19
7.20
7.20
7.20
7.21
7.21
7.22
7.44
7.46
3.13
3.16
0.98
2.21
1.00
1.00
1.94
2.02
0.0
1.0
2.0
3.0
4.0
5.0
6.0
7.0
8.0
9.0
10.0

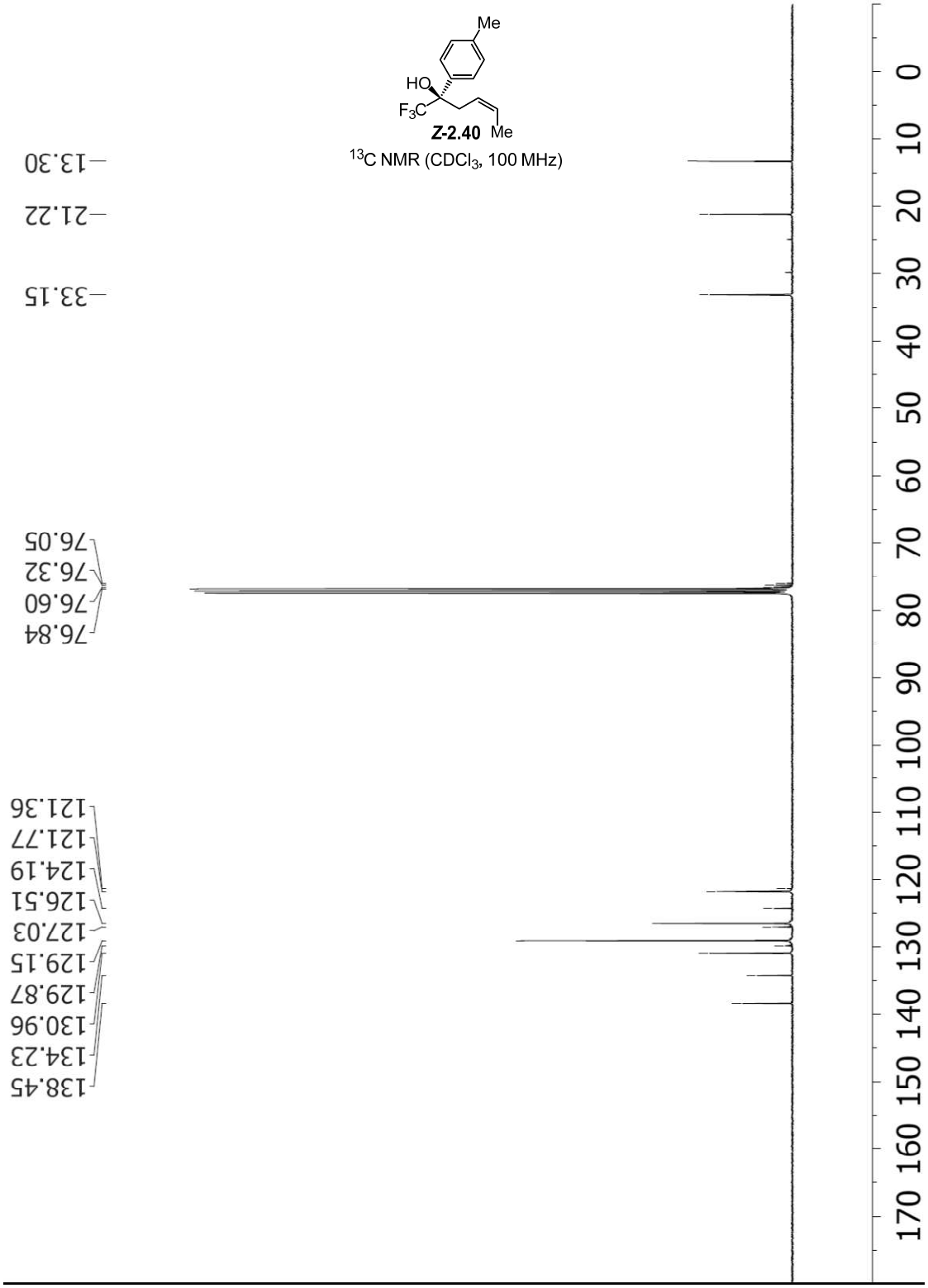
Me
HO
F3C
Z-2.40
Me
13C NMR (CDCl3, 100 MHz)
13.30
21.22
33.15
76.05
76.32
76.60
76.84
121.36
121.77
124.19
126.51
127.03
129.15
129.87
130.96
134.23
138.45
0
10
20
30
40
50
60
70
80
90
100
110
120
130
140
150
160
170

Z-2.40

^{19}F NMR ($CDCl_3$, 376 MHz)

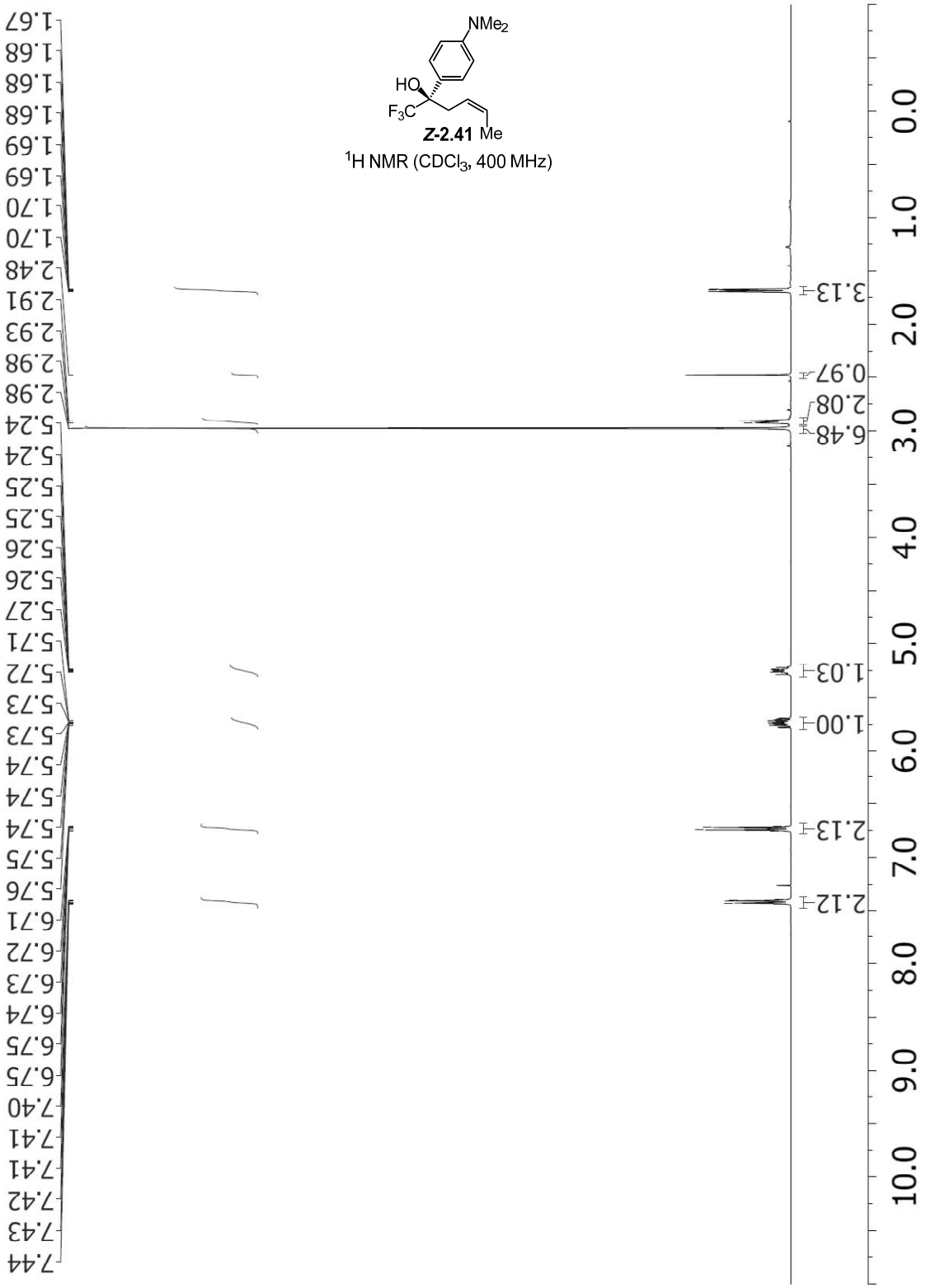
NMe2
HO
F3C
Z-2.41 Me
1H NMR (CDCl3, 400 MHz)
3.13
0.97
2.08
6.48
1.03
1.00
2.13
2.12

NMe2
HO
F3C
Z-2.41 Me
13C NMR (CDCl3, 100 MHz)
13.30
32.82
40.44
75.94
76.22
76.50
76.78
111.92
121.54
122.20
124.31
124.38
127.22
127.52
130.06
130.45
150.46
0
10
20
30
40
50
60
70
80
90
100
110
120
130
140
150
160
170

***Z*-2.41**

^{19}F NMR ($CDCl_3$, 376 MHz)

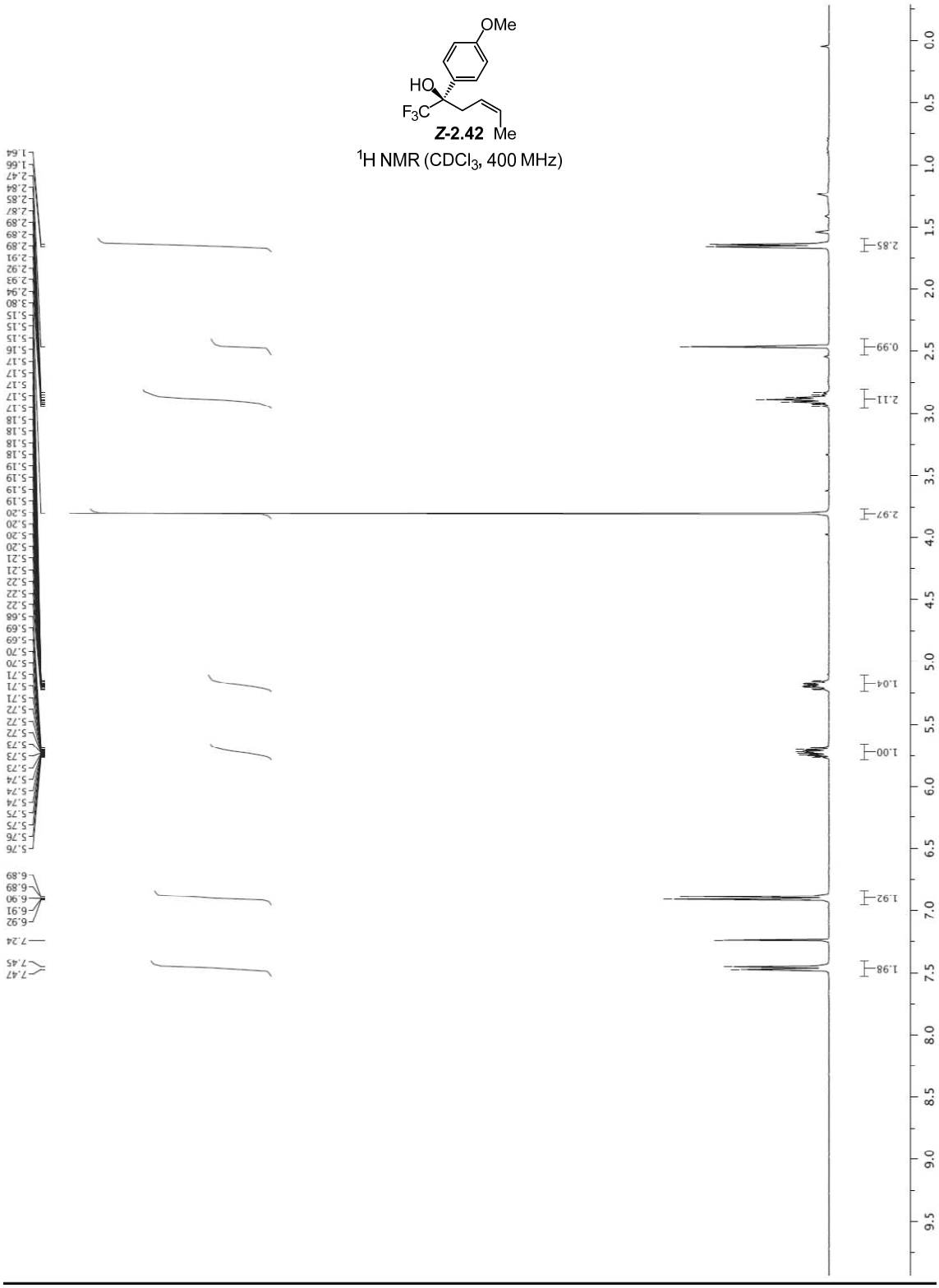
OMe
HO
F3C
Me
Z-2.42
1H NMR (CDCl3, 400 MHz)

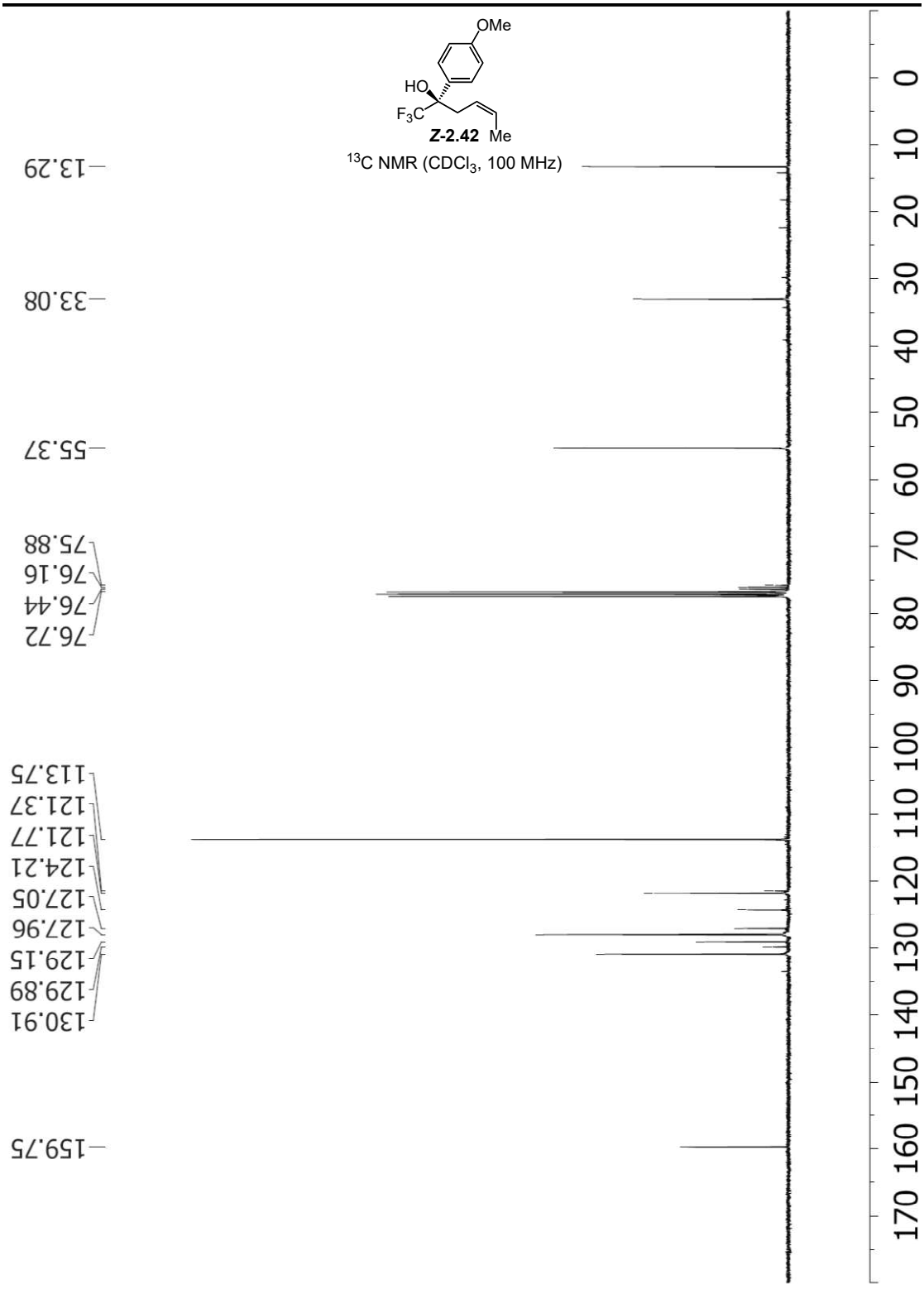
OMe
HO
F3C
Me
Z-2.42
13C NMR (CDCl3, 100 MHz)
13.29
33.08
55.37
75.88
76.16
76.44
76.72
113.75
121.37
121.77
124.21
127.05
127.96
129.15
129.89
130.91
159.75
0
10
20
30
40
50
60
70
80
90
100
110
120
130
140
150
160
170

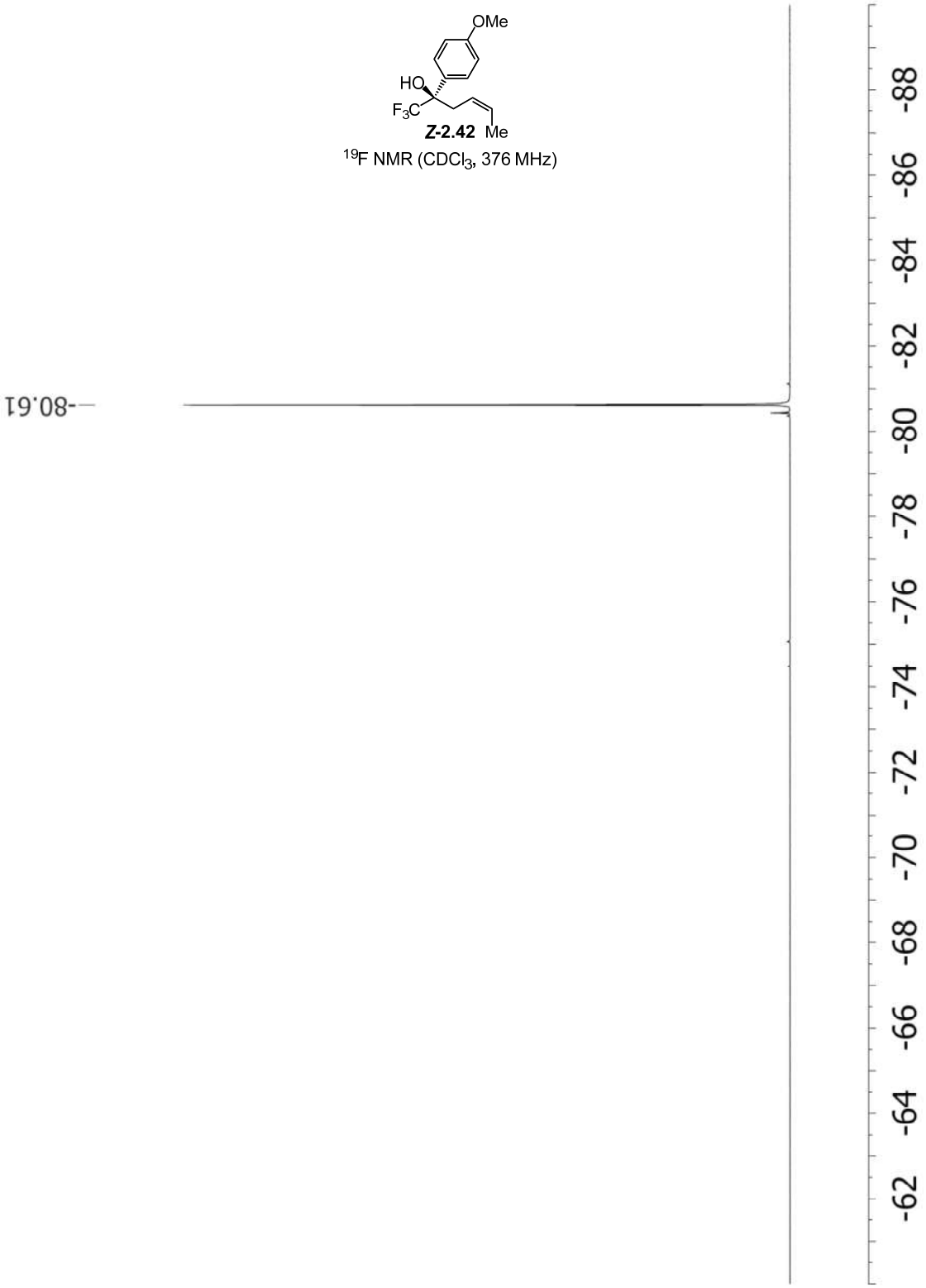

***Z*-2.42**

^{19}F NMR ($CDCl_3$, 376 MHz)

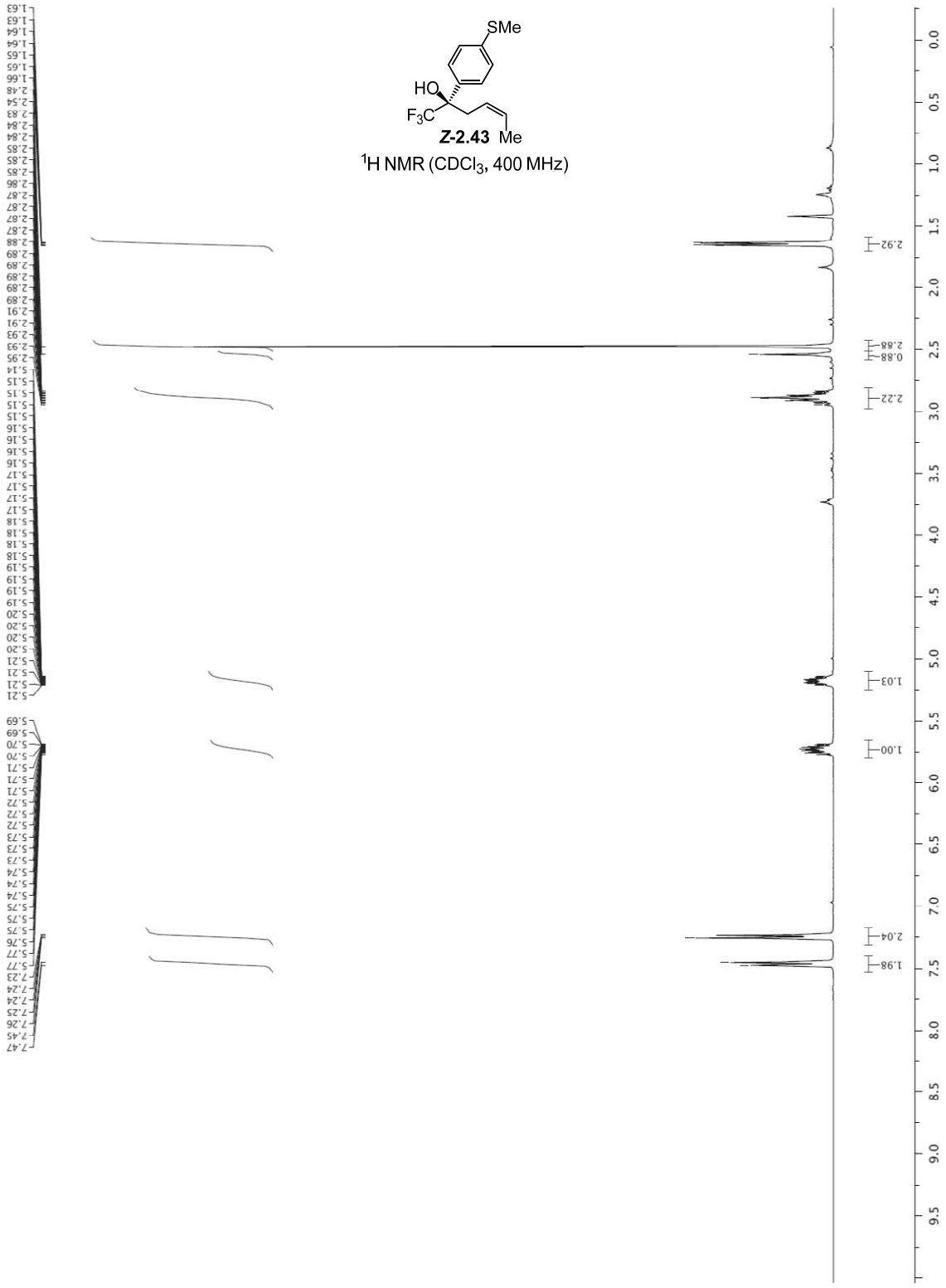
SMe
HO
F3C
Me
Z-2.43
1H NMR (CDCl3, 400 MHz)
2.92
0.88
2.88
2.22
1.03
1.00
2.04
1.98

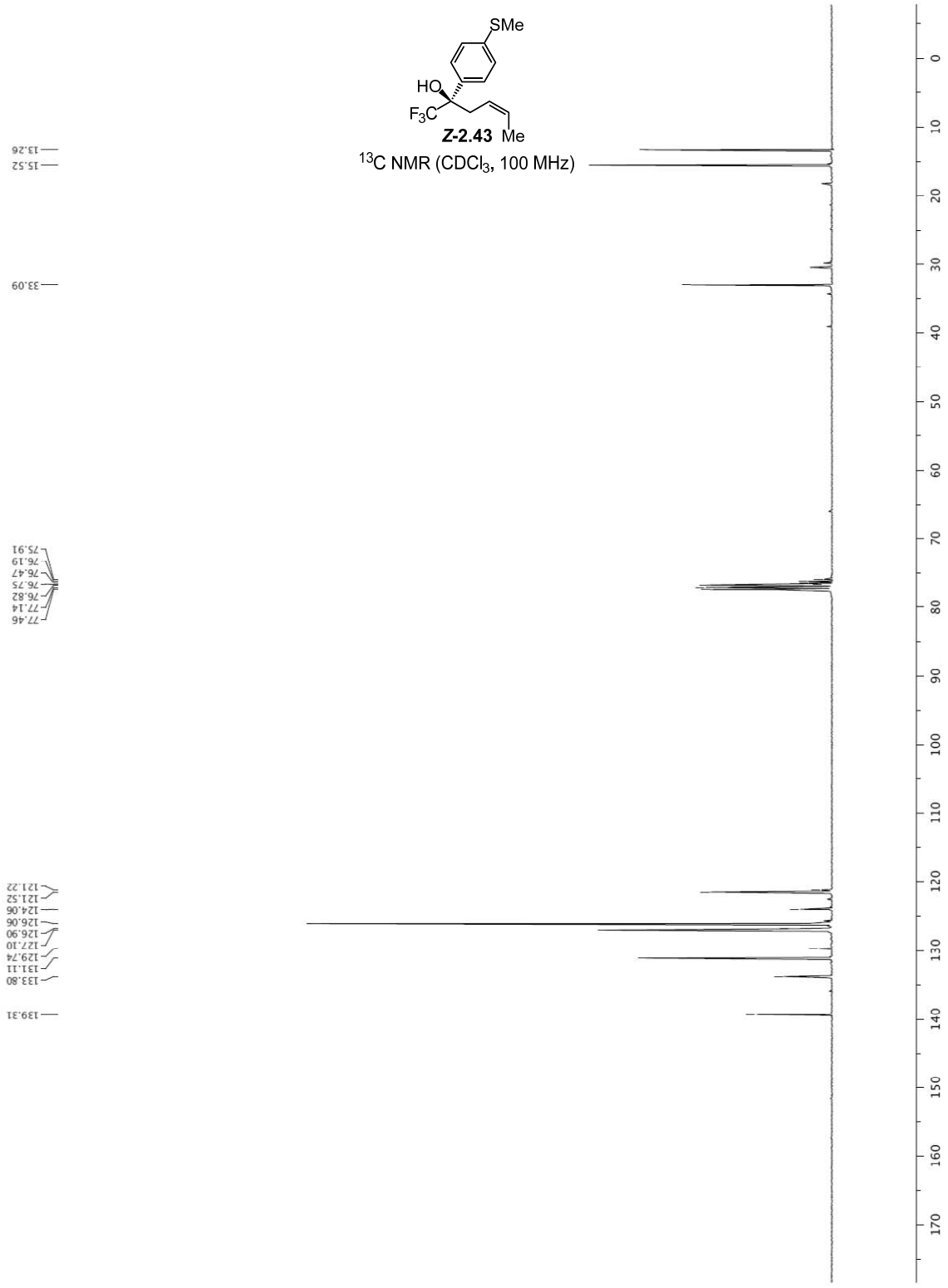
SMe
HO
F3C
Me
Z-2.43
13C NMR (CDCl3, 100 MHz)
13.26
15.52
33.09
75.91
76.19
76.47
76.75
76.82
77.14
77.46
121.22
121.52
124.06
126.06
126.90
127.10
129.74
131.11
133.80
139.31

***Z*-2.43**

^{19}F NMR ($CDCl_3$, 376 MHz)

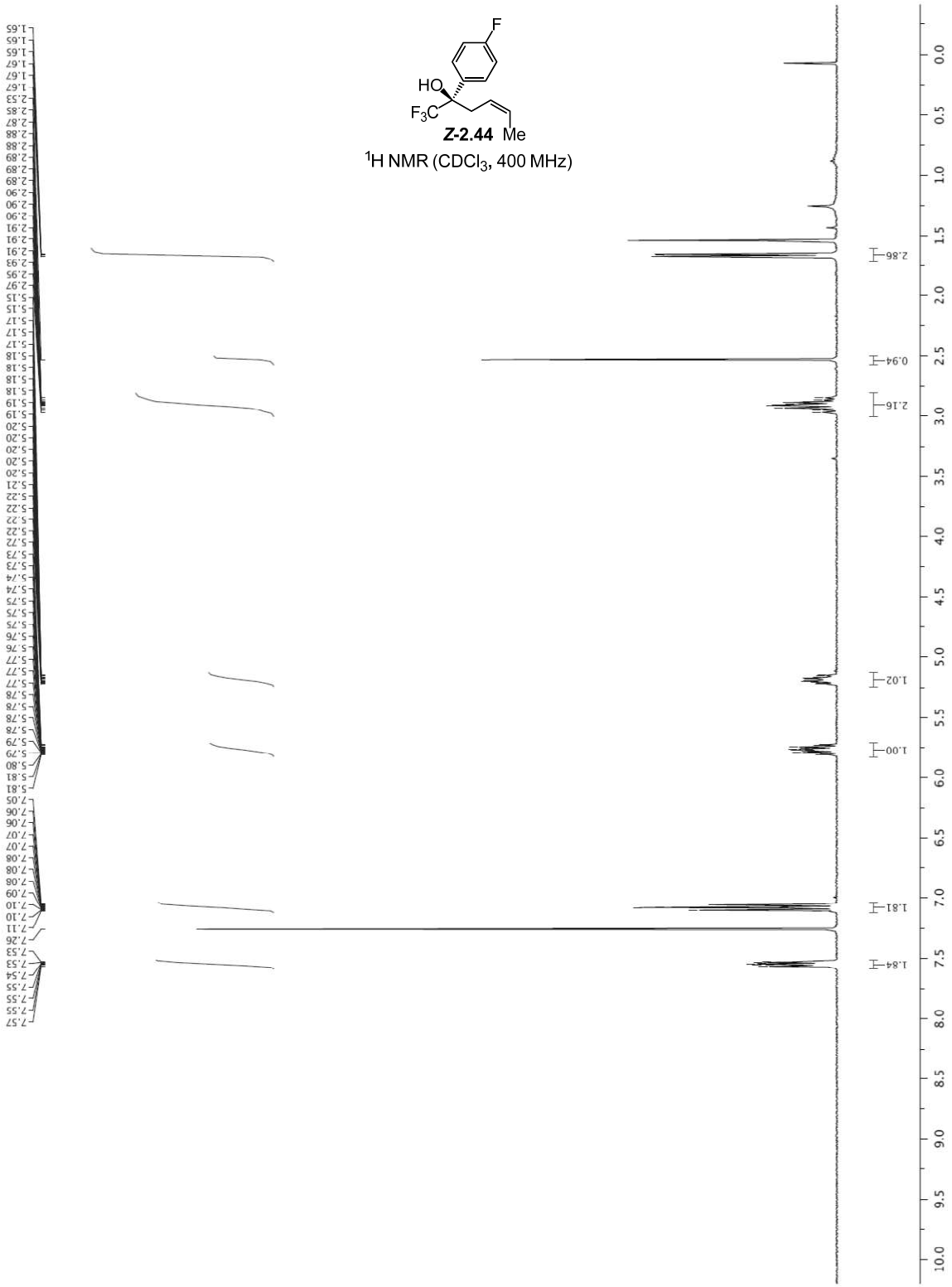
F
HO
F3C
Z-2.44 Me
1H NMR (CDCl3, 400 MHz)
2.86
0.94
2.16
1.02
1.00
1.81
1.84

F
HO
F3C
Z-2.44 Me
13C NMR (CDCl3, 100 MHz)
13.28
33.29
75.82
76.11
76.39
76.67
115.24
115.45
121.18
121.33
124.02
126.87
128.56
128.66
129.70
131.38
133.01
161.69
164.15
0
10
20
30
40
50
60
70
80
90
100
110
120
130
140
150
160
170

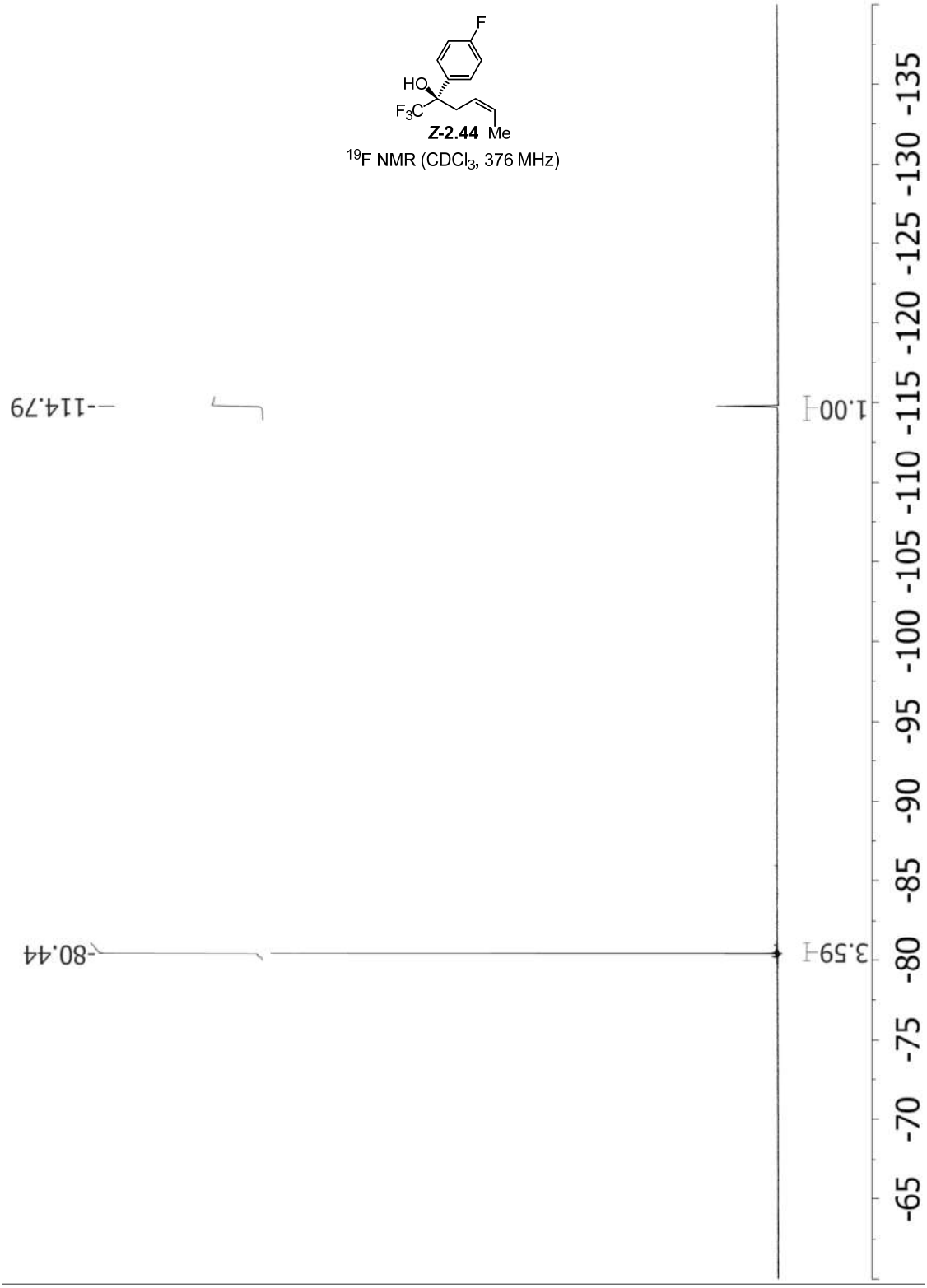
F
HO
F3C
Z-2.44 Me
19F NMR (CDCl3, 376 MHz)
-114.79
-80.44
1.00
3.59
-65 -70 -75 -80 -85 -90 -95 -100 -105 -110 -115 -120 -125 -130 -135

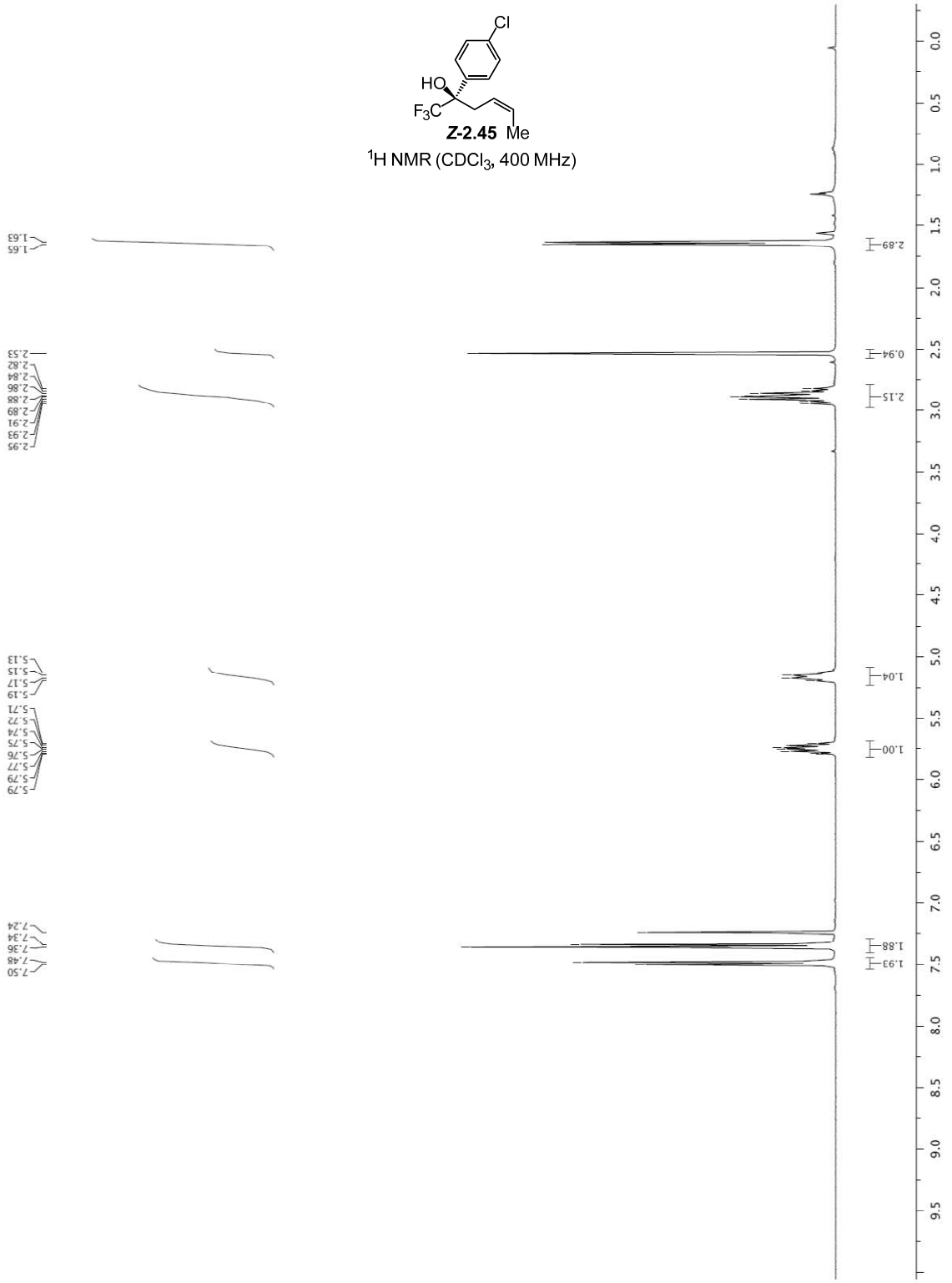
Cl
HO
F3C
Me
Z-2.45
1H NMR (CDCl3, 400 MHz)
1.63
1.65
2.53
2.82
2.84
2.86
2.88
2.89
2.91
2.93
2.95
5.13
5.15
5.17
5.19
5.71
5.72
5.74
5.75
5.76
5.77
5.79
5.79
7.24
7.34
7.36
7.48
7.50
2.89
0.94
2.15
1.04
1.00
1.88
1.93
0.0
0.5
1.0
1.5
2.0
2.5
3.0
3.5
4.0
4.5
5.0
5.5
6.0
6.5
7.0
7.5
8.0
8.5
9.0
9.5

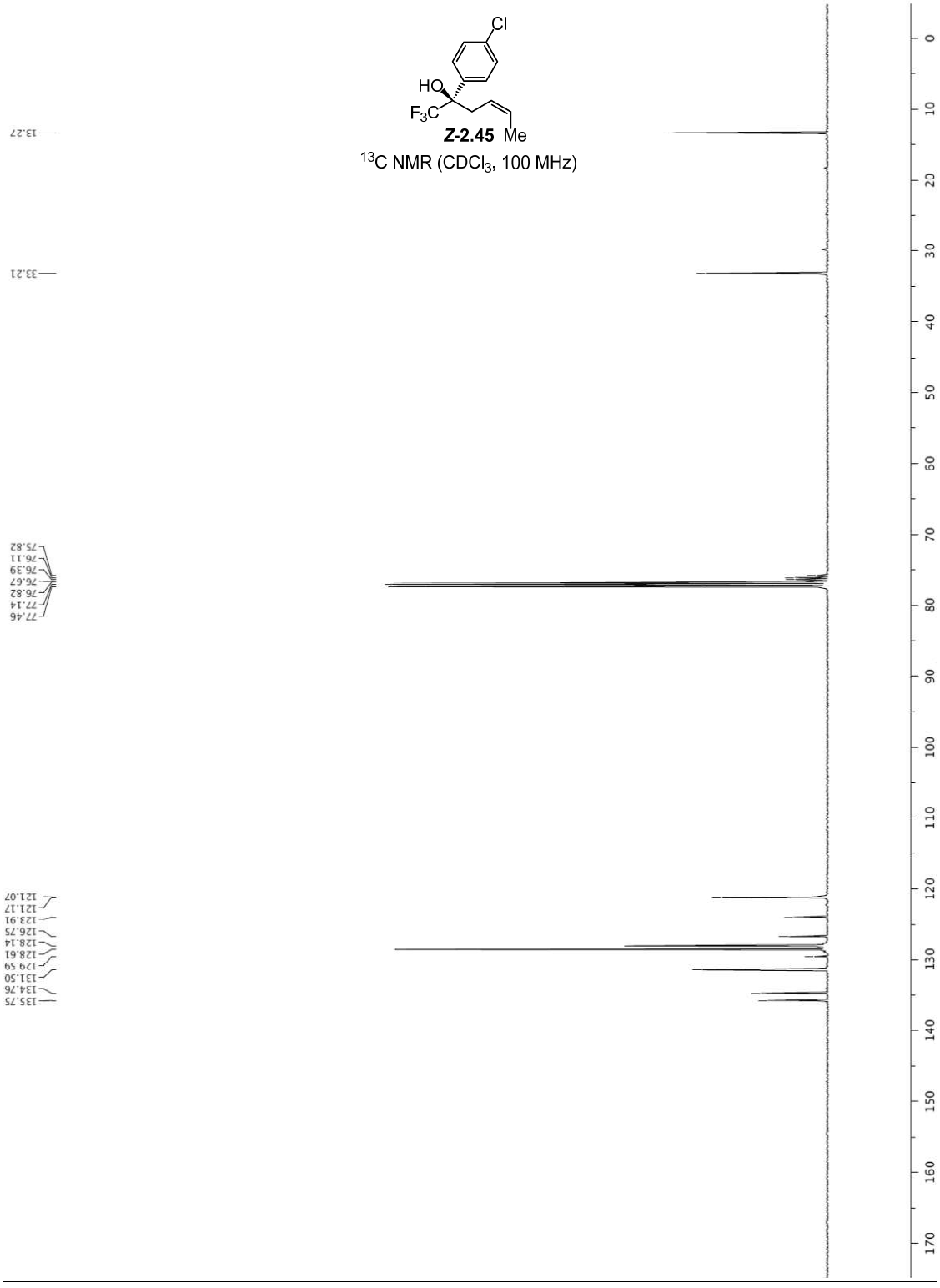
Cl
HO
F3C
Me
Z-2.45
13C NMR (CDCl3, 100 MHz)
13.27
33.21
75.82
76.11
76.39
76.67
76.82
77.14
77.46
121.07
121.17
123.91
126.75
128.14
128.61
129.59
131.50
134.76
135.75
0
10
20
30
40
50
60
70
80
90
100
110
120
130
140
150
160
170

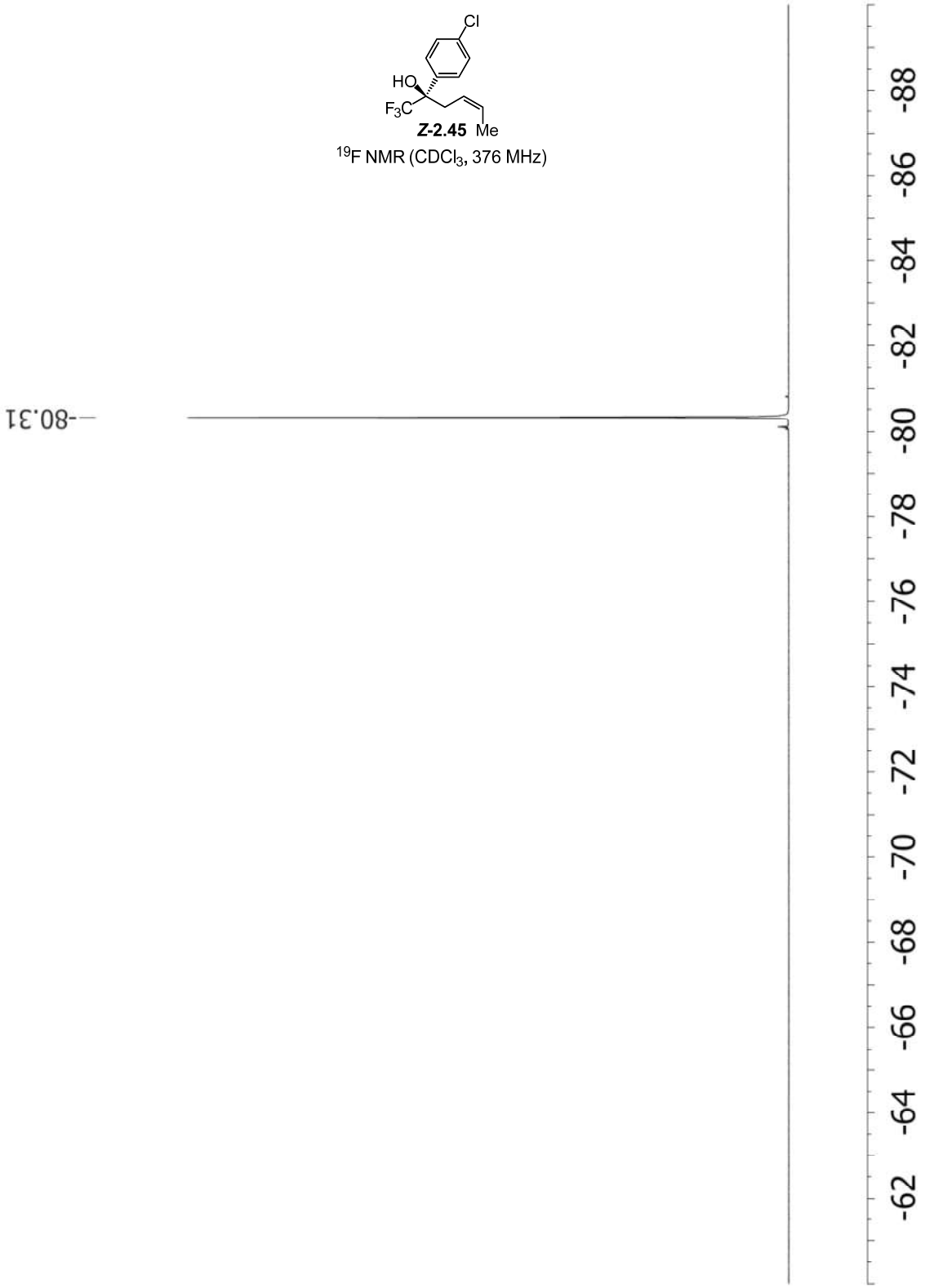

***Z*-2.45**

^{19}F NMR ($CDCl_3$, 376 MHz)

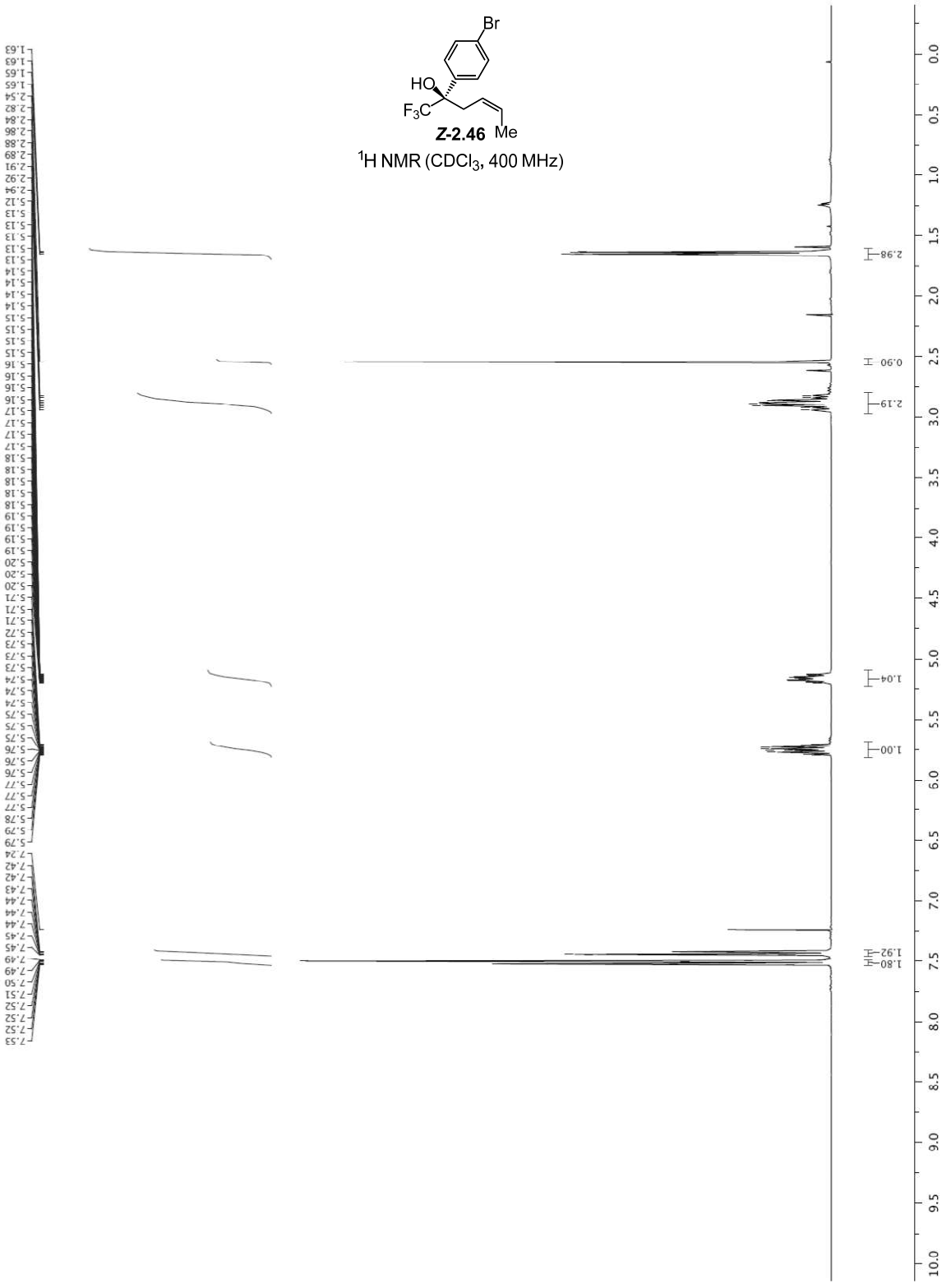
Br
HO
F3C
Me
Z-2.46
1H NMR (CDCl3, 400 MHz)
2.98
0.90
2.19
1.04
1.00
1.92
1.80

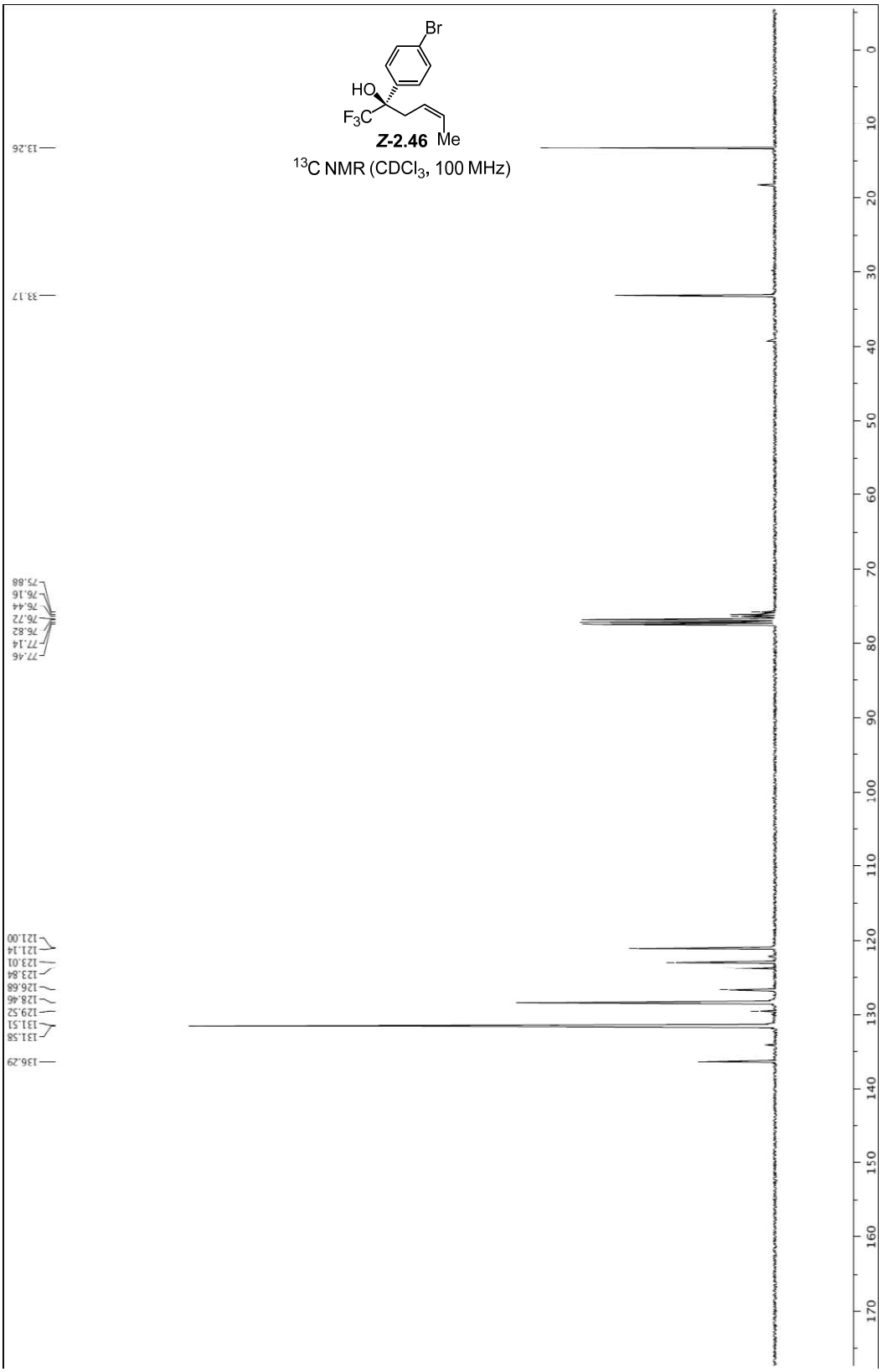
Br
HO
F3C
Me
Z-2.46
13C NMR (CDCl3, 100 MHz)
13.26
33.17
75.88
76.16
76.44
76.72
76.82
77.14
77.46
121.00
121.14
123.01
123.84
126.68
128.46
129.52
131.51
131.58
136.29

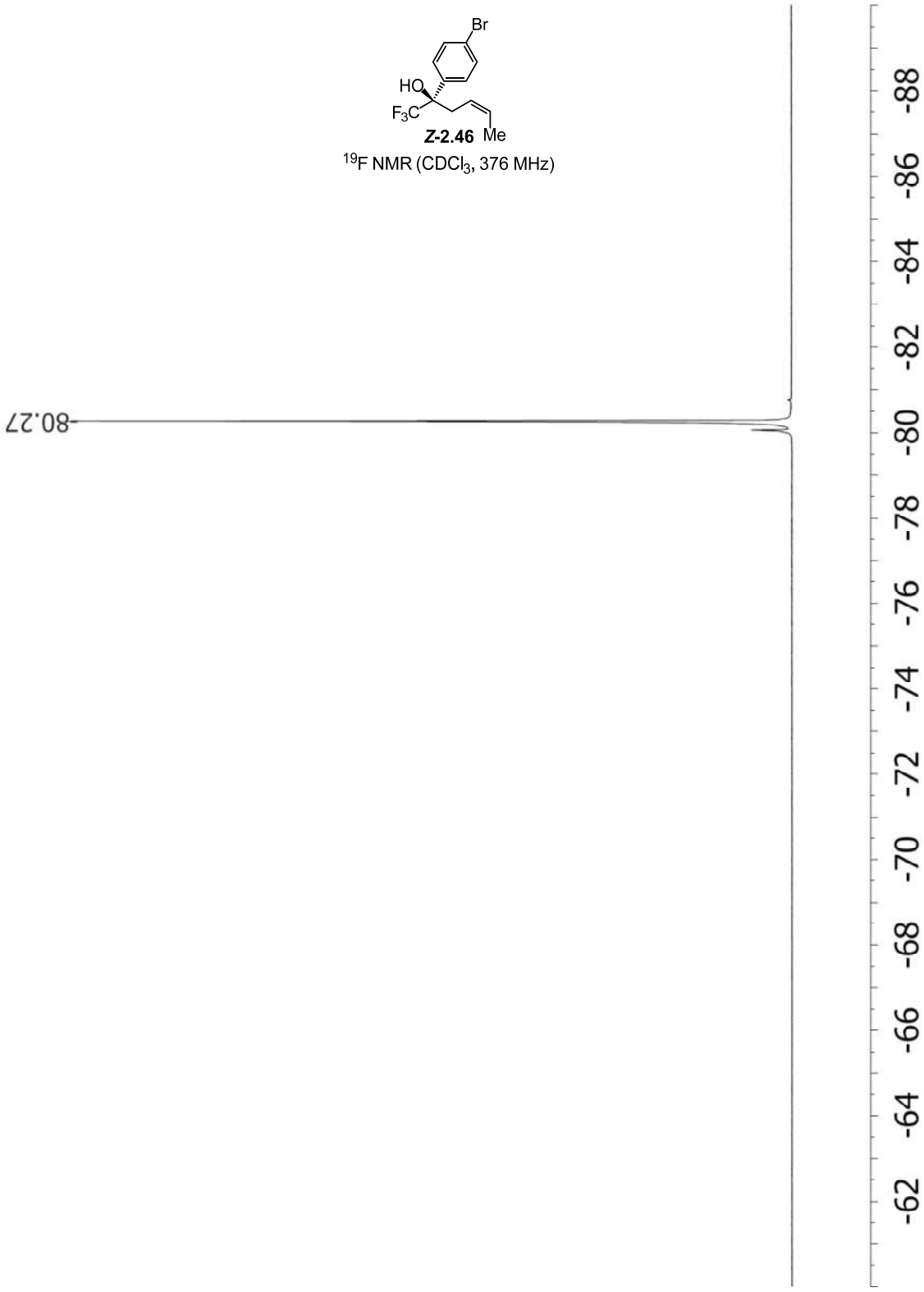

Z-2.46

^{19}F NMR ($CDCl_3$, 376 MHz)

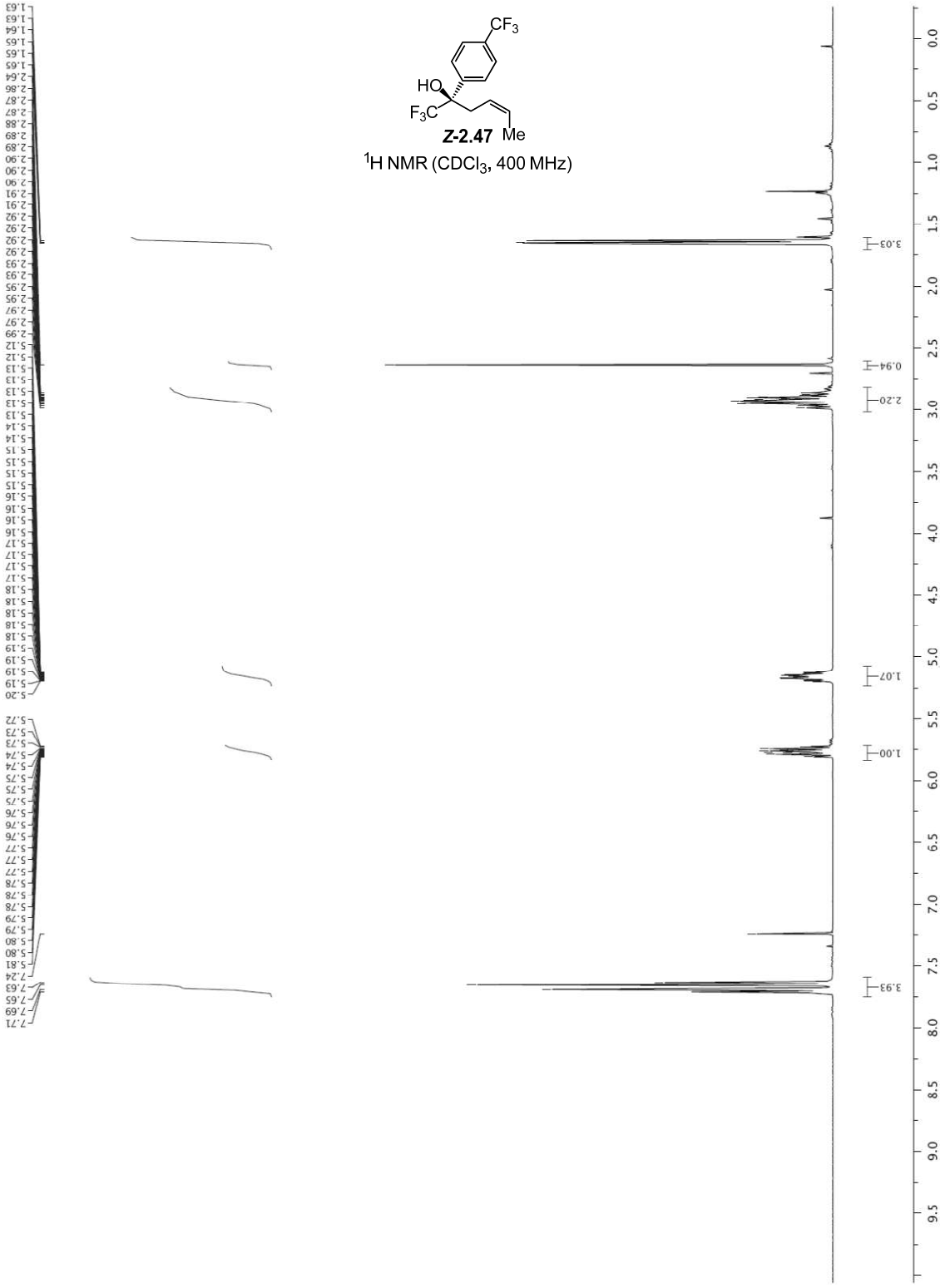
CF3
HO
F3C
Me
Z-2.47
1H NMR (CDCl3, 400 MHz)
3.03
0.94
2.20
1.07
1.00
3.93

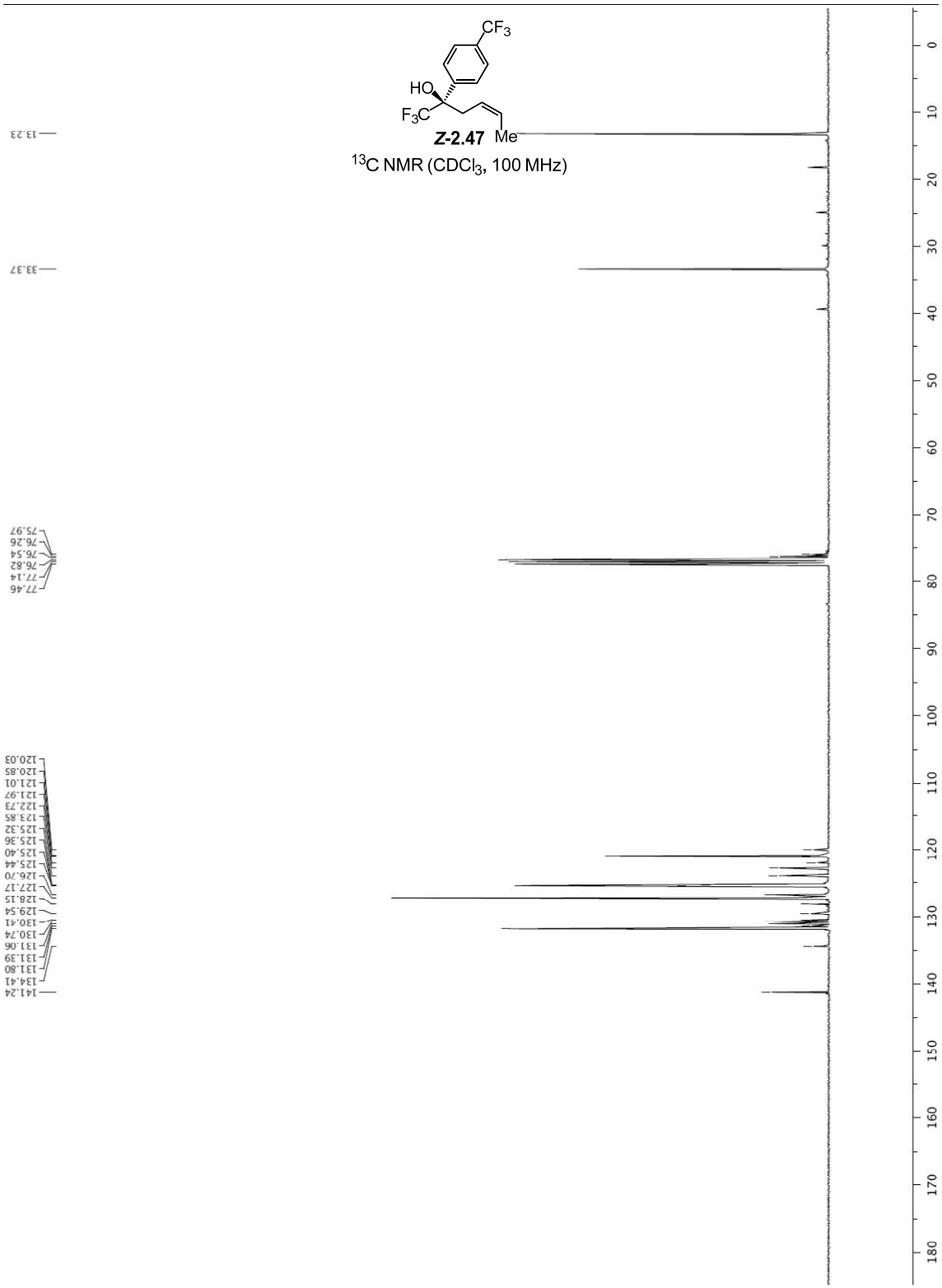
CF3
HO
F3C
Me
Z-2.47
13C NMR (CDCl3, 100 MHz)
13.23
33.37
75.97
76.26
76.54
76.82
77.14
77.46
120.03
120.85
121.01
121.97
122.73
123.85
125.32
125.36
125.40
125.44
126.70
127.17
128.15
129.54
130.41
130.74
131.06
131.39
131.80
134.41
141.24
0
10
20
30
40
50
60
70
80
90
100
110
120
130
140
150
160
170
180

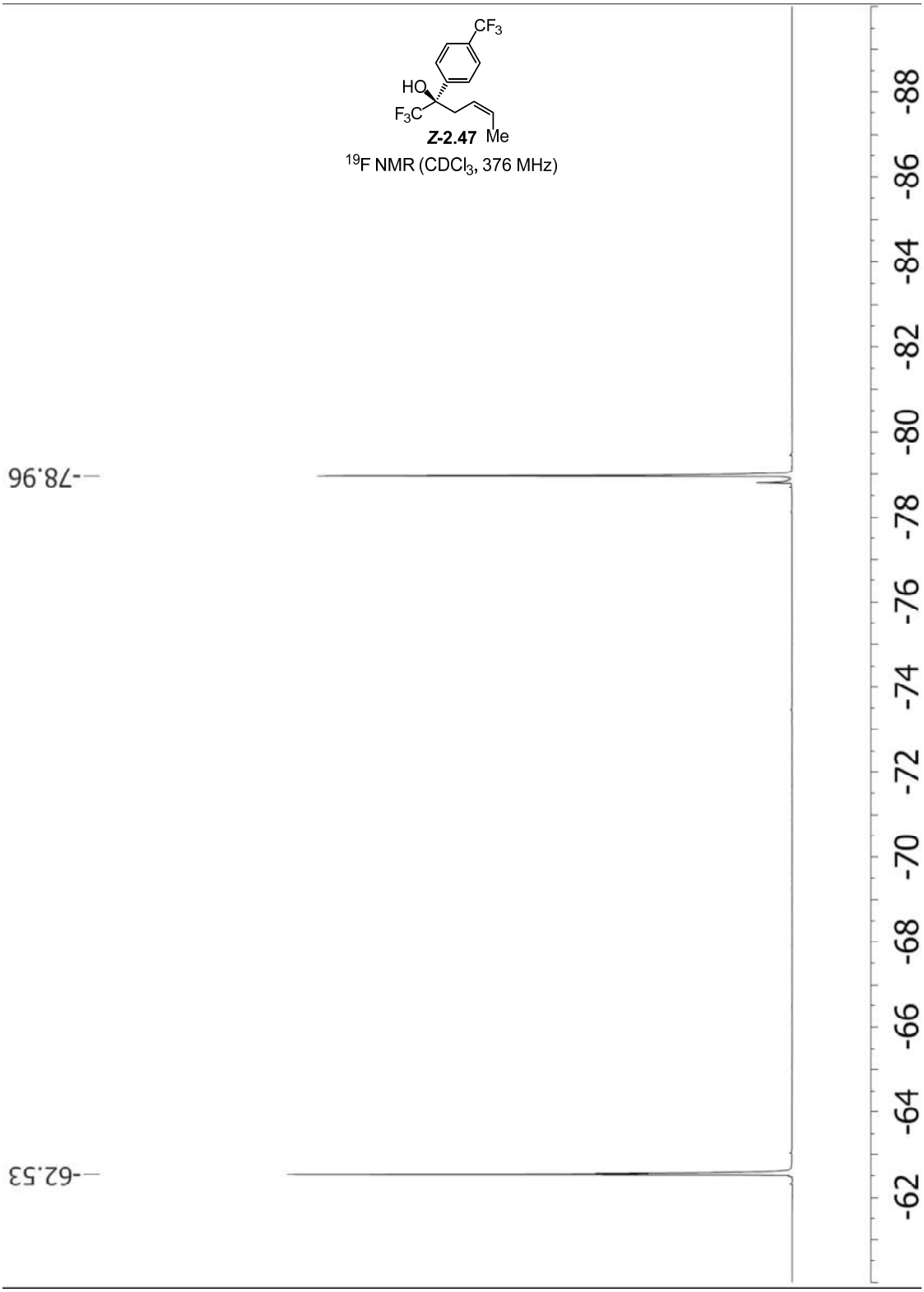

***Z*-2.47**

^{19}F NMR ($CDCl_3$, 376 MHz)

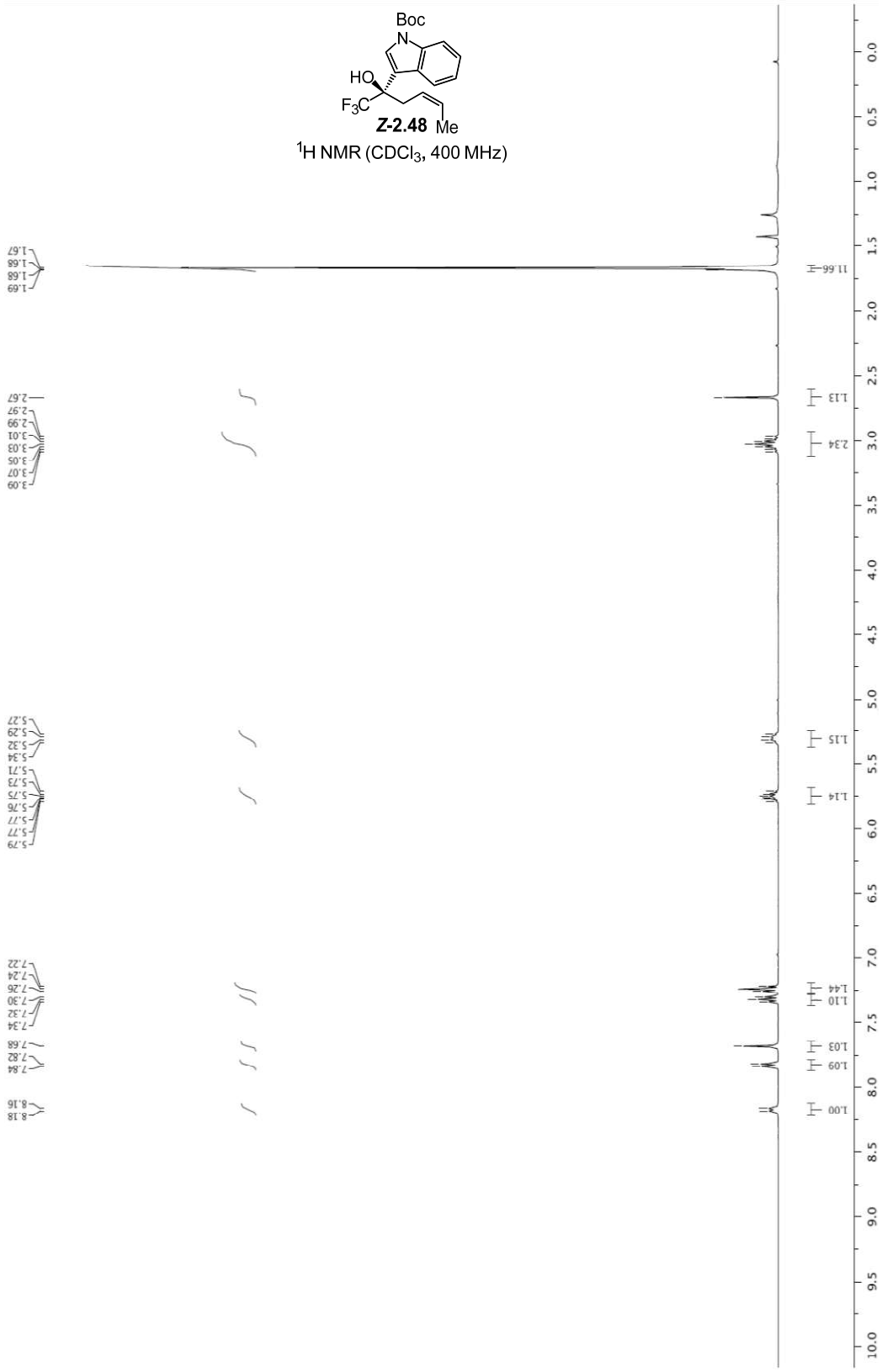
Boc
N
HO
F3C
Me
Z-2.48
1H NMR (CDCl3, 400 MHz)

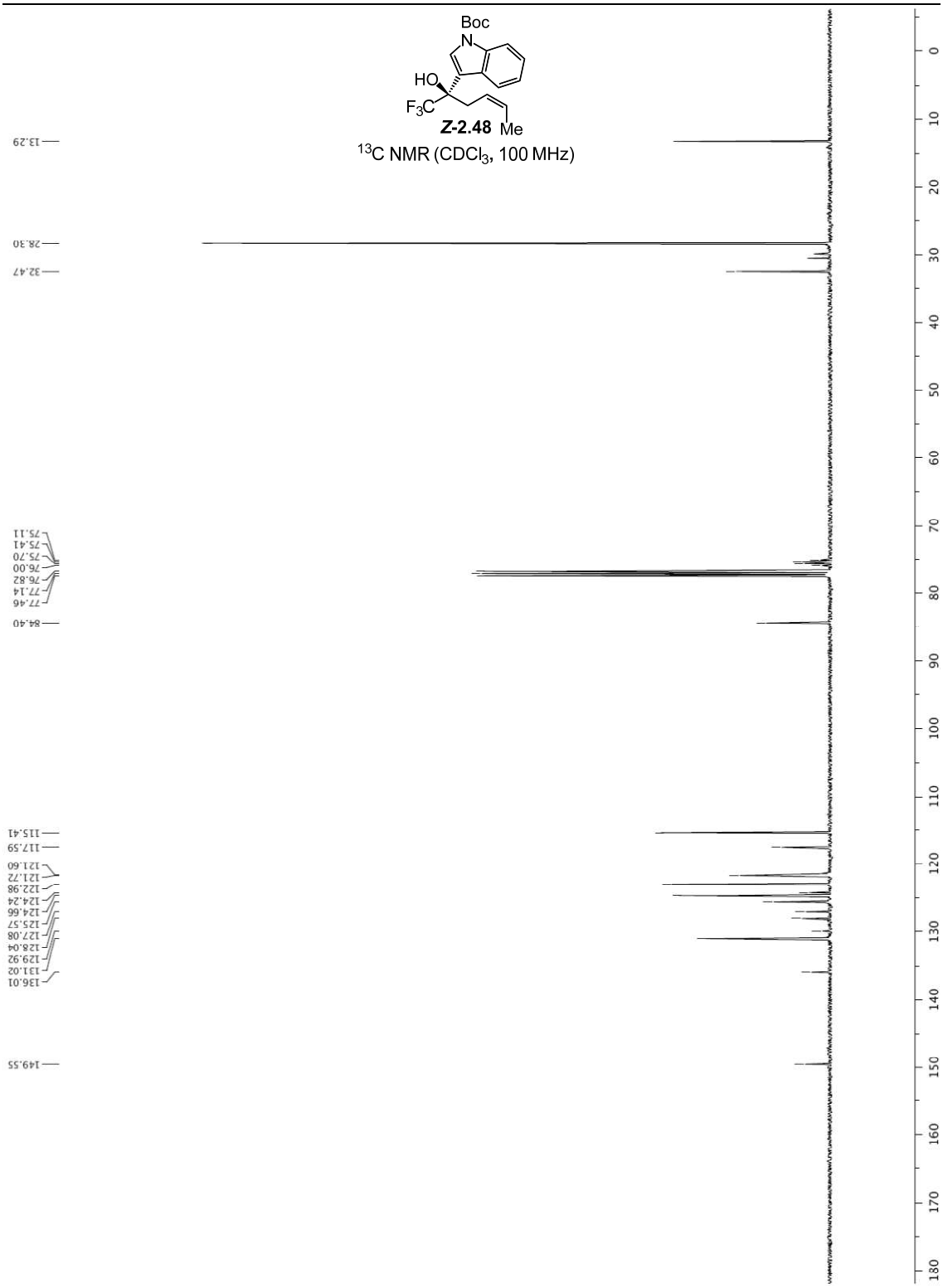
Boc
N
HO
F3C
Me
Z-2.48
13C NMR (CDCl3, 100 MHz)
13.29
28.30
32.47
75.11
75.41
75.70
76.00
76.82
77.14
77.46
84.40
115.41
117.59
121.60
121.72
122.98
124.24
124.66
125.57
127.08
128.04
129.92
131.02
136.01
149.55

***Z*-2.48**

^{19}F NMR ($CDCl_3$, 376 MHz)

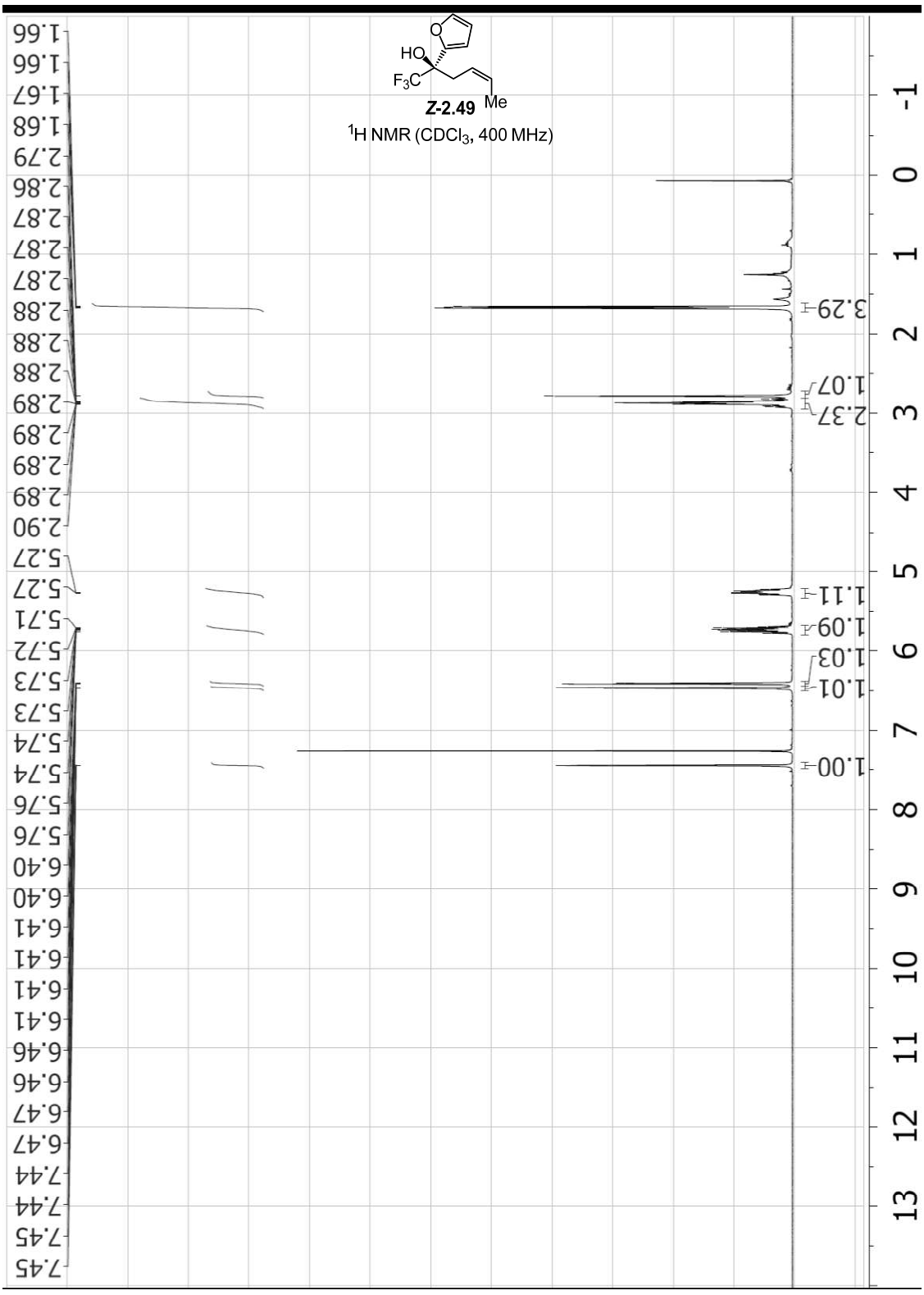
HO
F3C
Me
Z-2.49
1H NMR (CDCl3, 400 MHz)
3.29
1.07
2.37
1.11
1.09
1.03
1.01
1.00

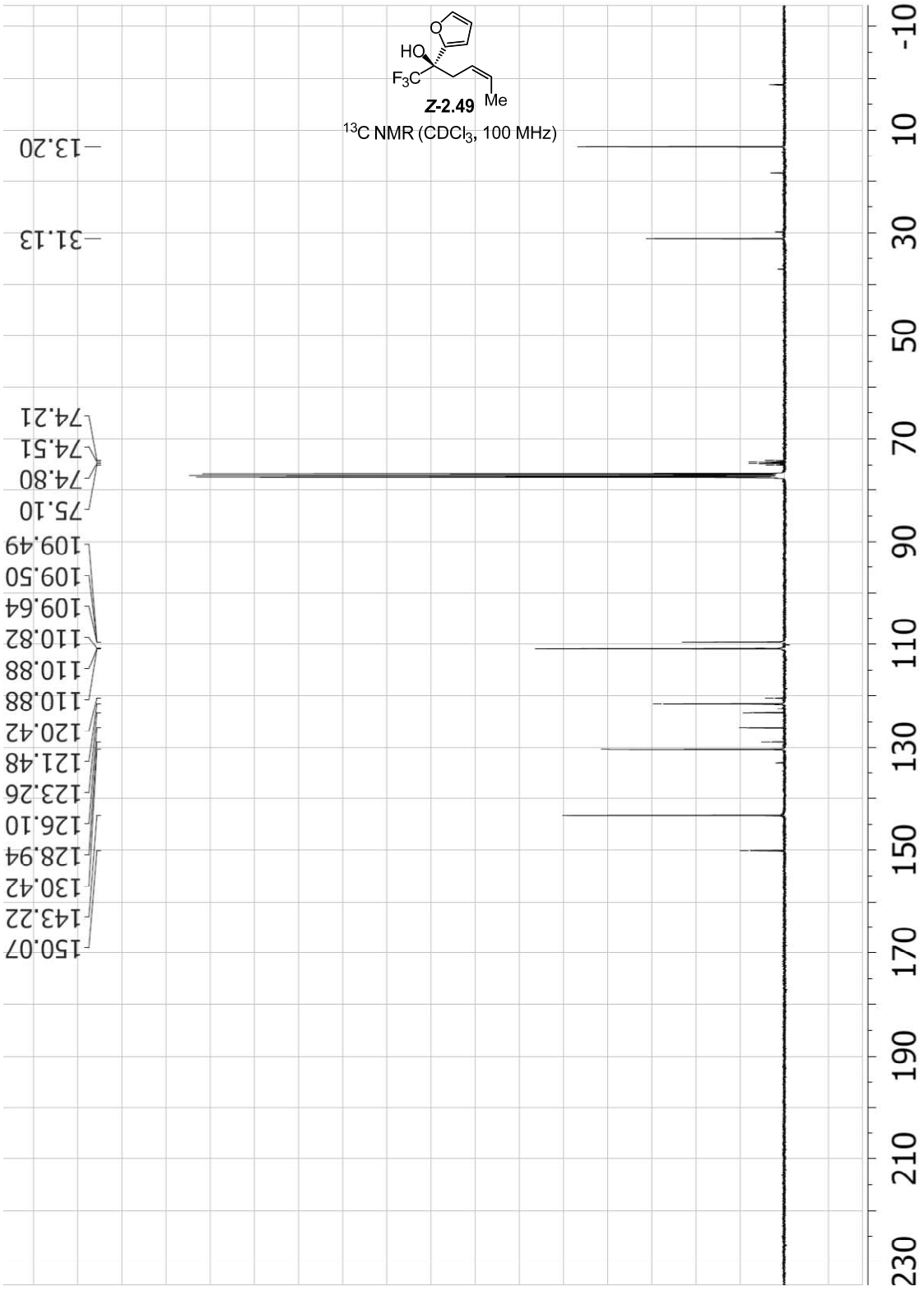
HO
F3C
Me
Z-2.49
13C NMR (CDCl3, 100 MHz)
13.20
31.13
74.21
74.51
74.80
75.10
109.49
109.50
109.64
110.82
110.88
110.88
120.42
121.48
123.26
126.10
128.94
130.42
143.22
150.07
-10
10
30
50
70
90
110
130
150
170
190
210
230

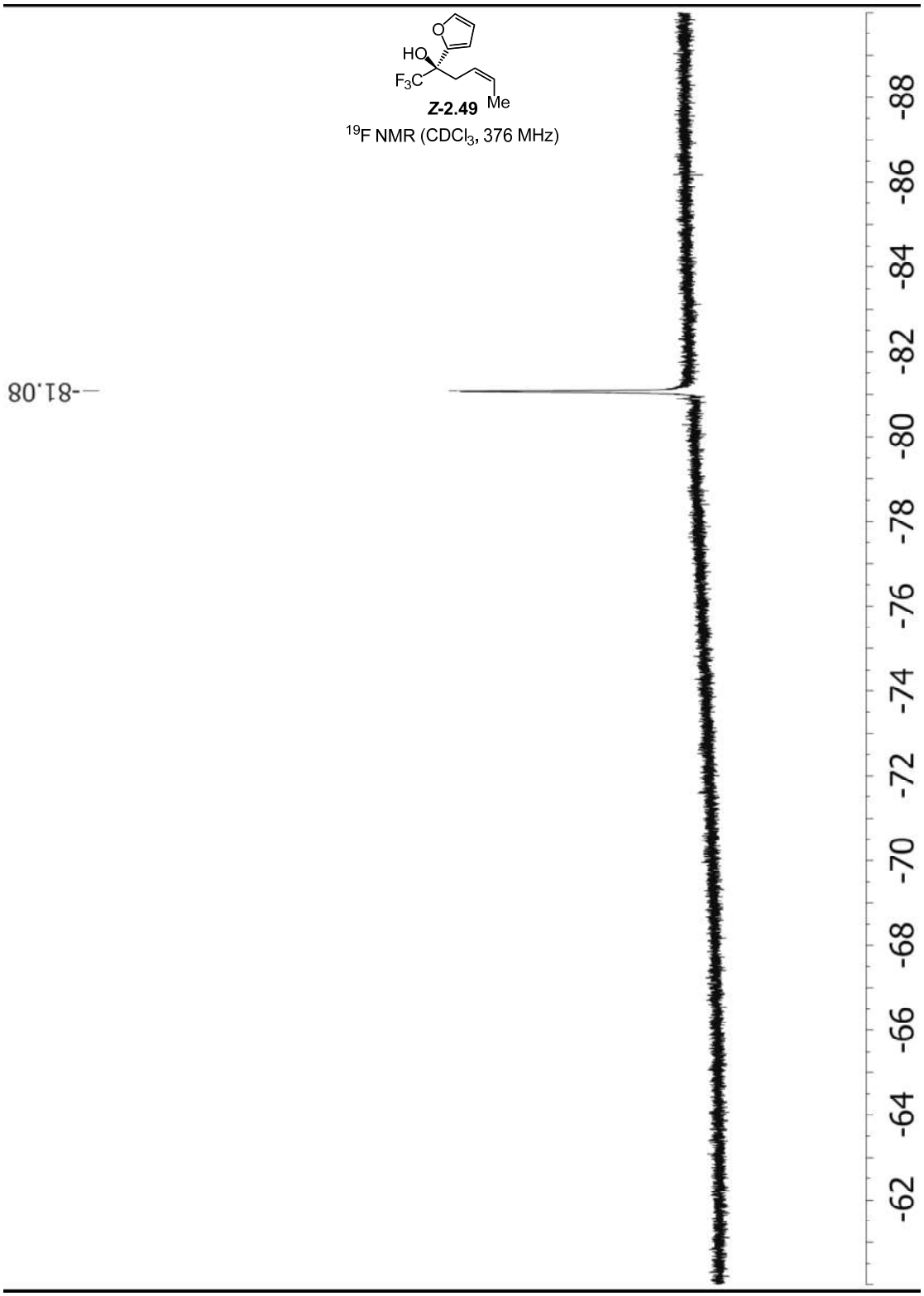
HO
F3C
Me
Z-2.49
19F NMR (CDCl3, 376 MHz)
-81.08
-62
-64
-66
-68
-70
-72
-74
-76
-78
-80
-82
-84
-86
-88

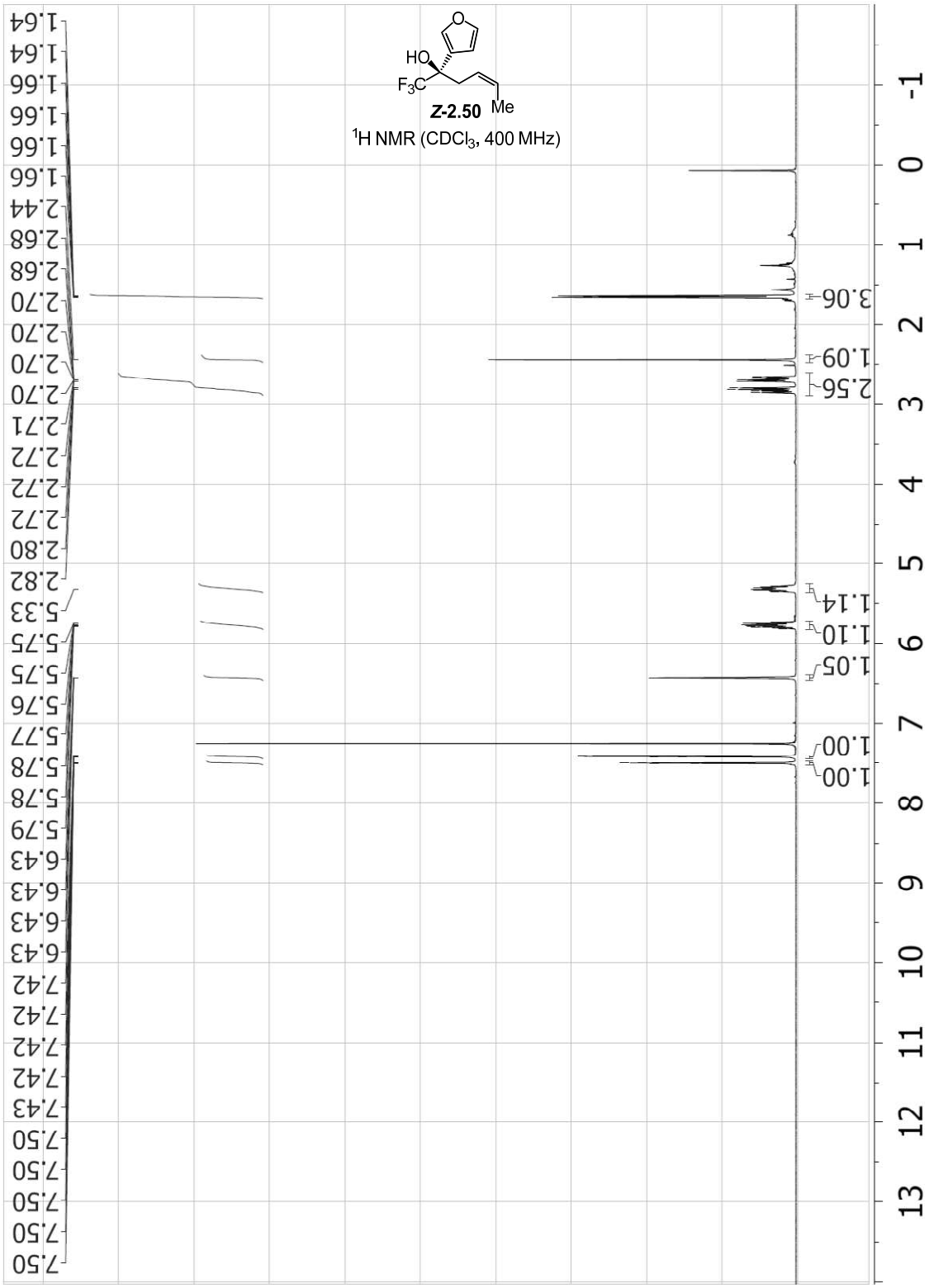
HO
F3C
Me
Z-2.50
1H NMR (CDCl3, 400 MHz)
3.06
1.09
2.56
1.14
1.10
1.05
1.00
1.00

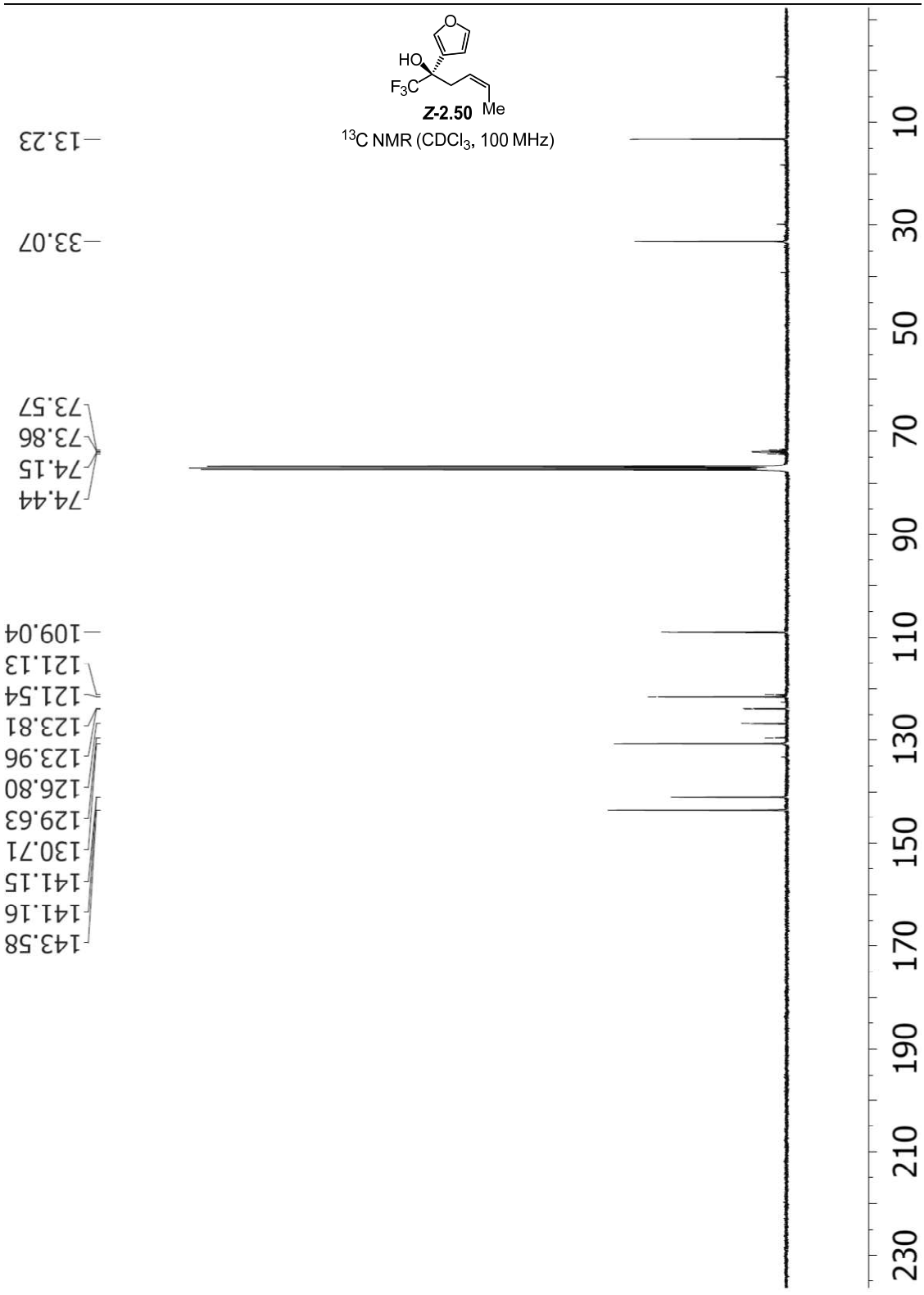
HO
F3C
Me
Z-2.50
13C NMR (CDCl3, 100 MHz)
13.23
33.07
73.57
73.86
74.15
74.44
109.04
121.13
121.54
123.81
123.96
126.80
129.63
130.71
141.15
141.16
143.58
10
30
50
70
90
110
130
150
170
190
210
230

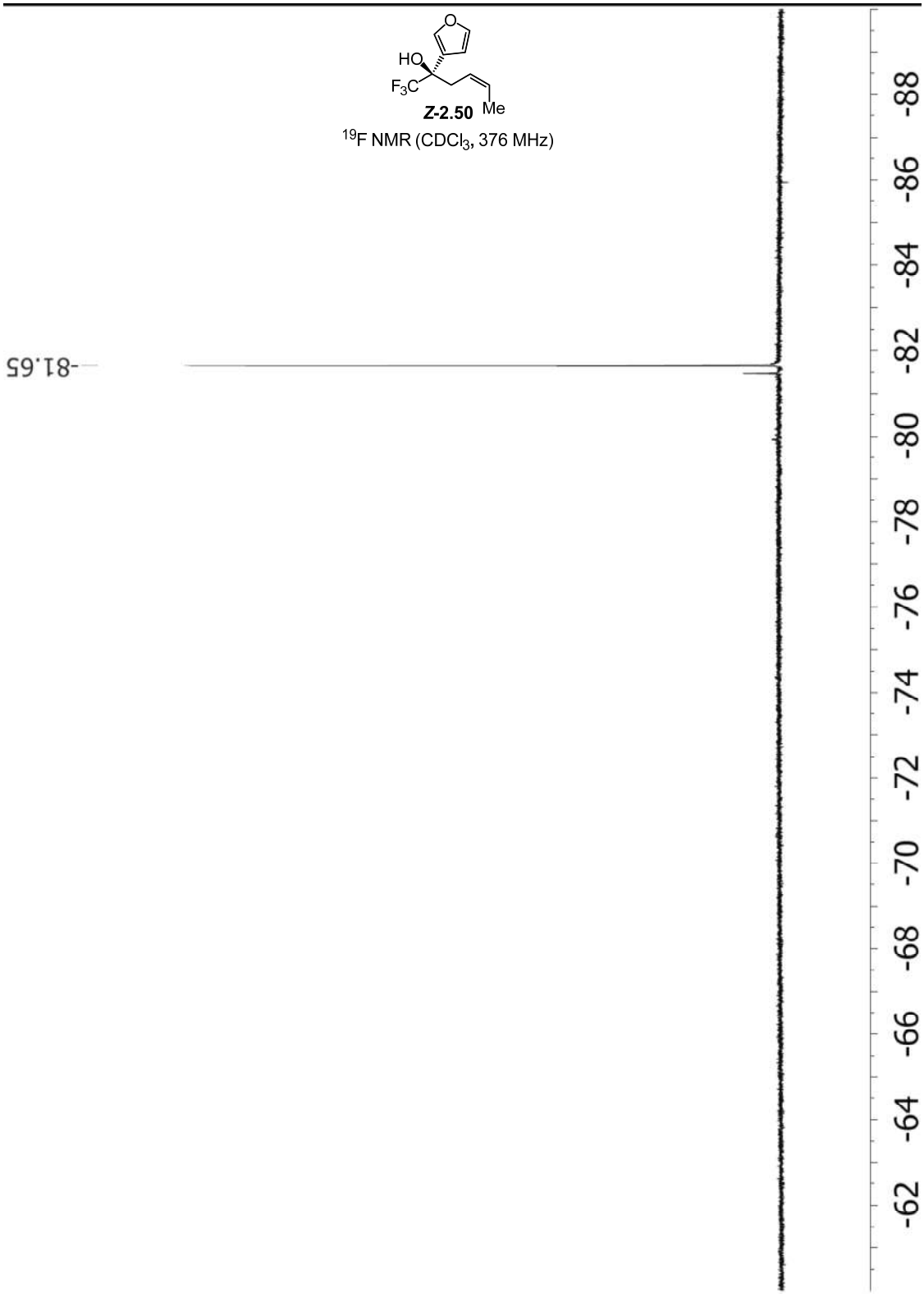
HO
F3C
Me
Z-2.50
19F NMR (CDCl3, 376 MHz)
-81.65
-62
-64
-66
-68
-70
-72
-74
-76
-78
-80
-82
-84
-86
-88

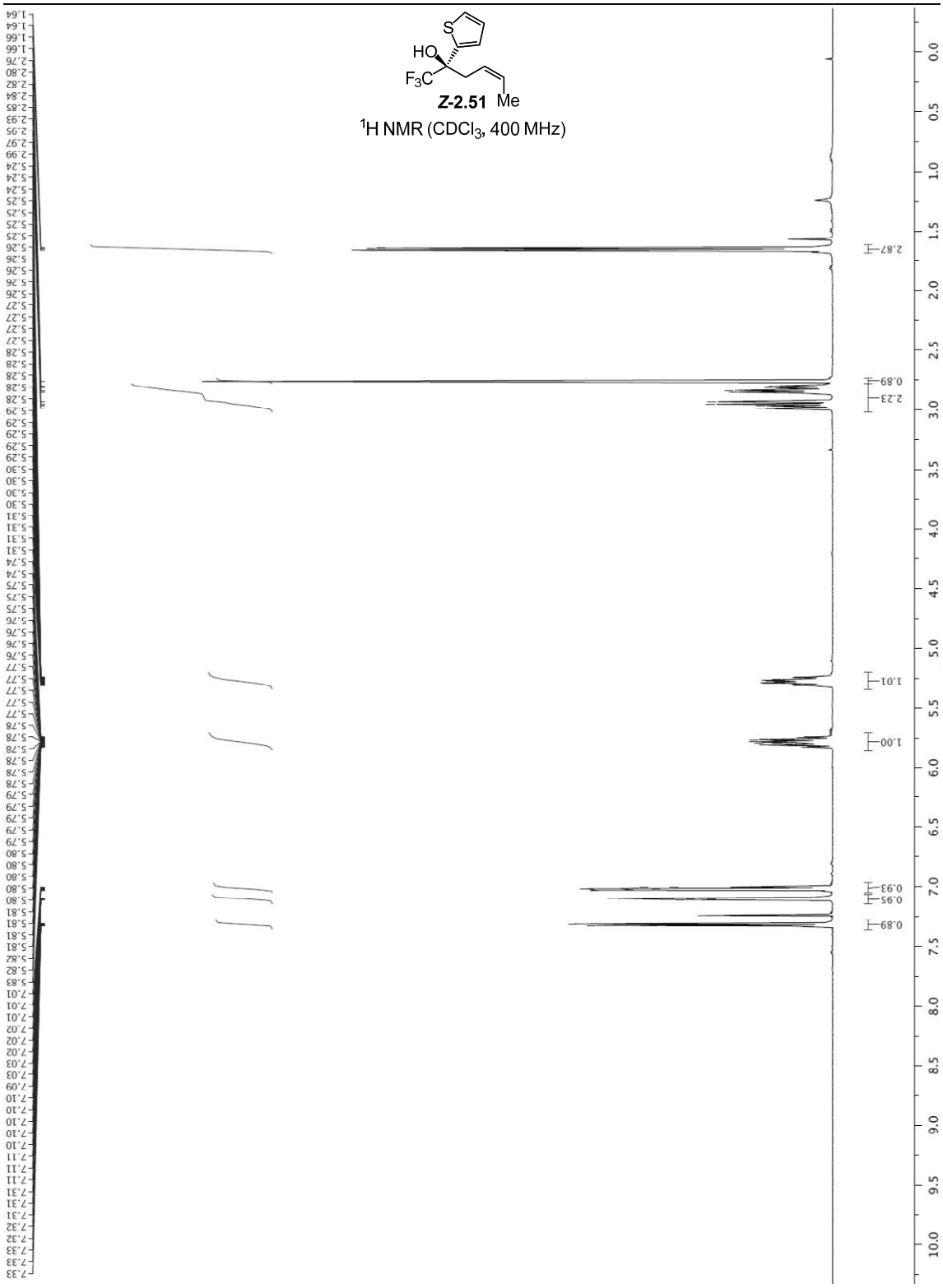
HO
S
F3C
Me
Z-2.51
1H NMR (CDCl3, 400 MHz)
2.87
0.89
2.23
1.01
1.00
0.93
0.95
0.89

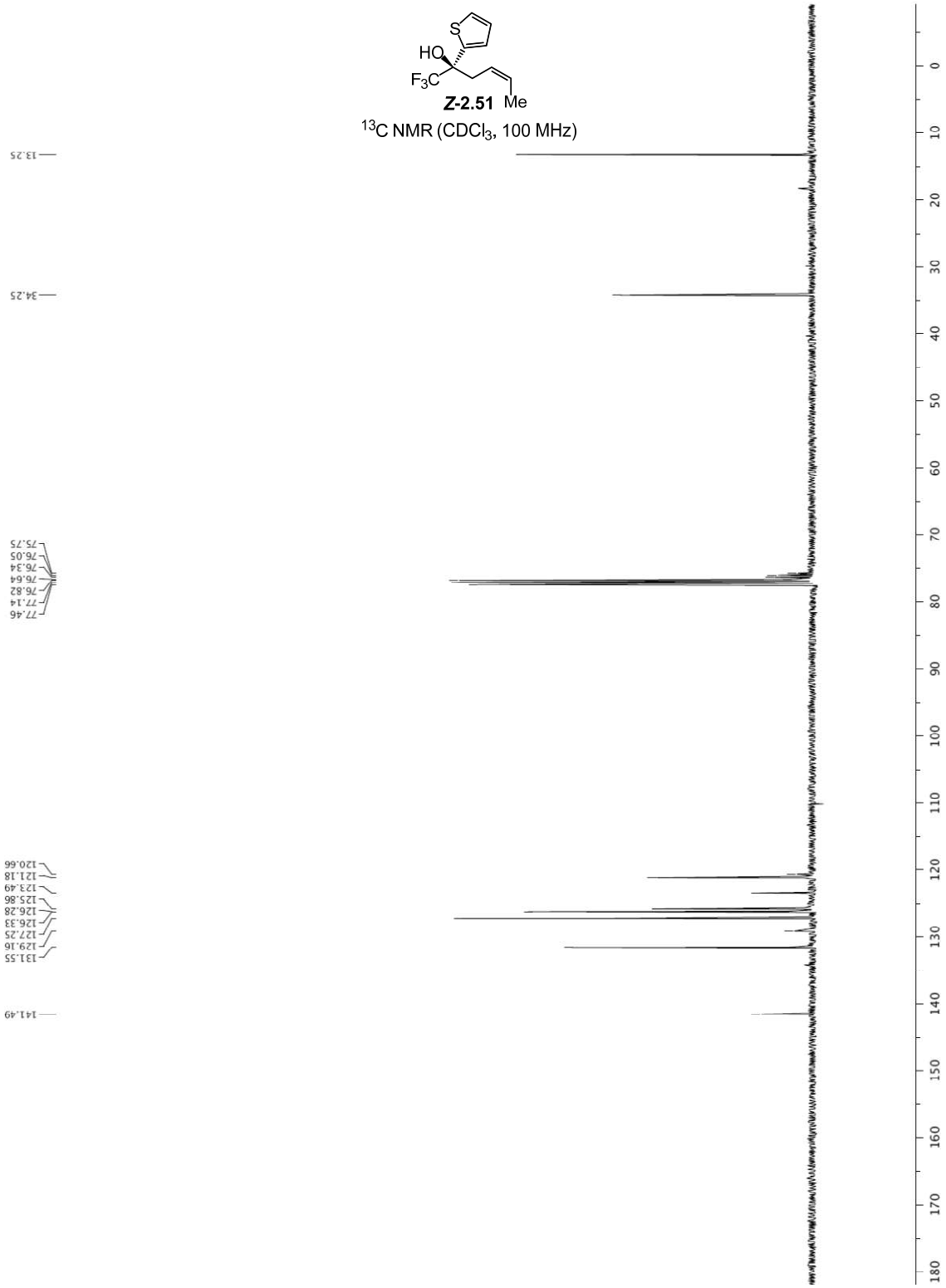
HO
F3C
S
Me
Z-2.51
13C NMR (CDCl3, 100 MHz)
13.25
34.25
75.75
76.05
76.34
76.64
76.82
77.14
77.46
120.66
121.18
123.49
125.86
126.28
126.33
127.25
129.16
131.55
141.49

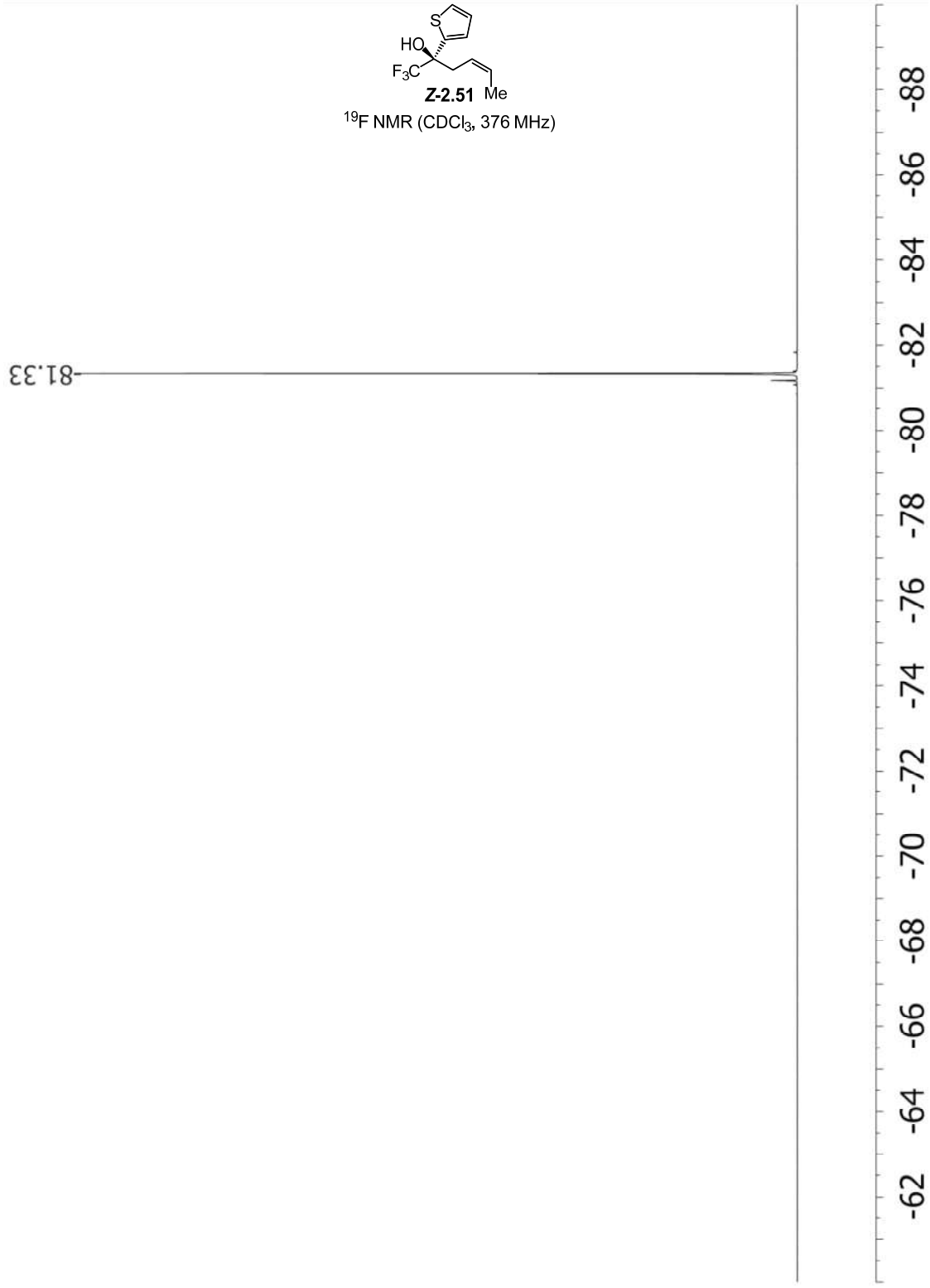

***Z*-2.51**

^{19}F NMR ($CDCl_3$, 376 MHz)

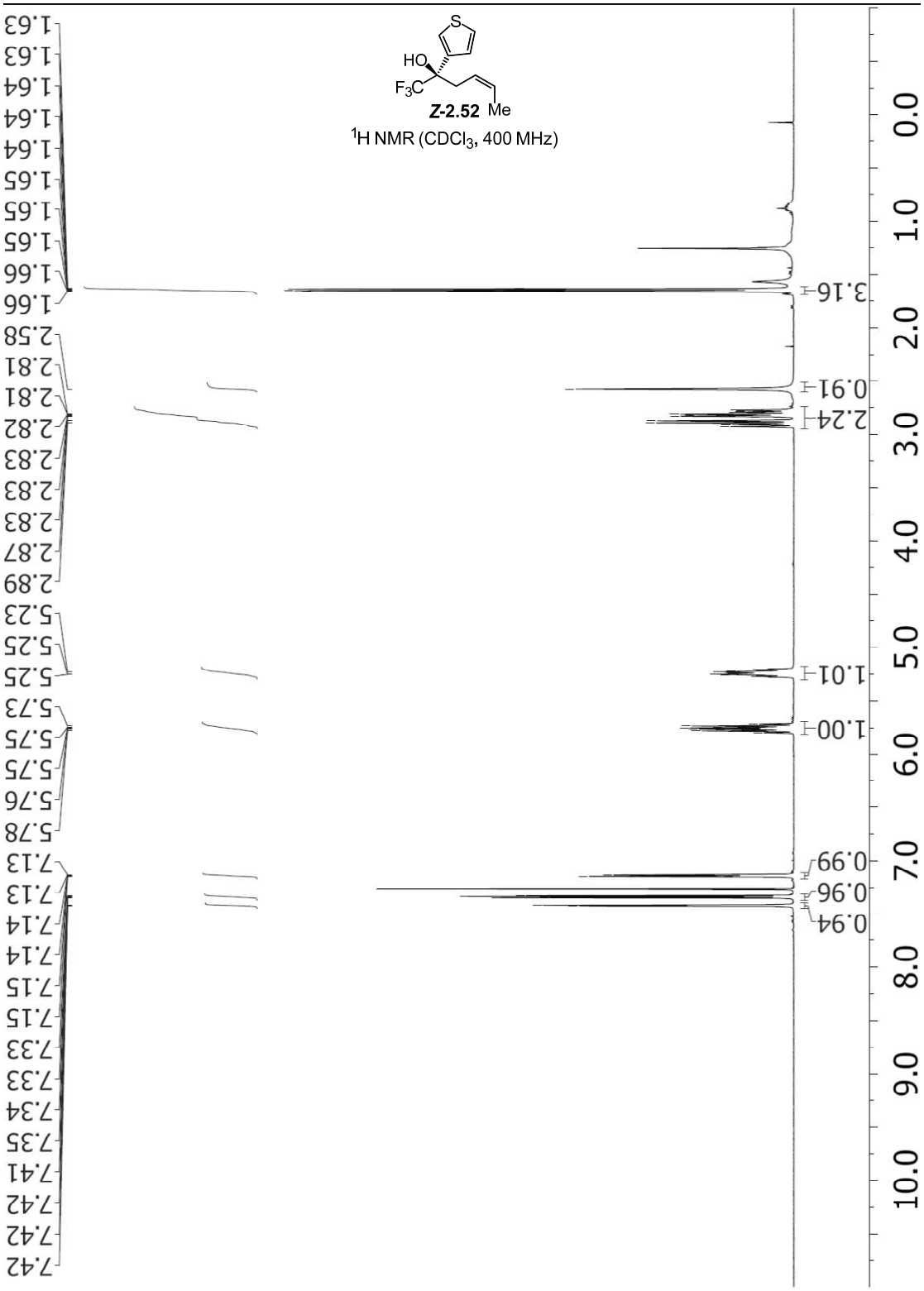
S
HO
F3C
Z-2.52 Me
1H NMR (CDCl3, 400 MHz)
3.16
0.91
2.24
1.01
1.00
0.99
0.96
0.94
0.0
1.0
2.0
3.0
4.0
5.0
6.0
7.0
8.0
9.0
10.0

Z-2.52
13C NMR (CDCl3, 100 MHz)
13.22
33.56
75.54
75.83
76.12
76.41
121.06
121.55
123.83
123.90
126.07
126.24
126.74
129.57
130.90
139.03

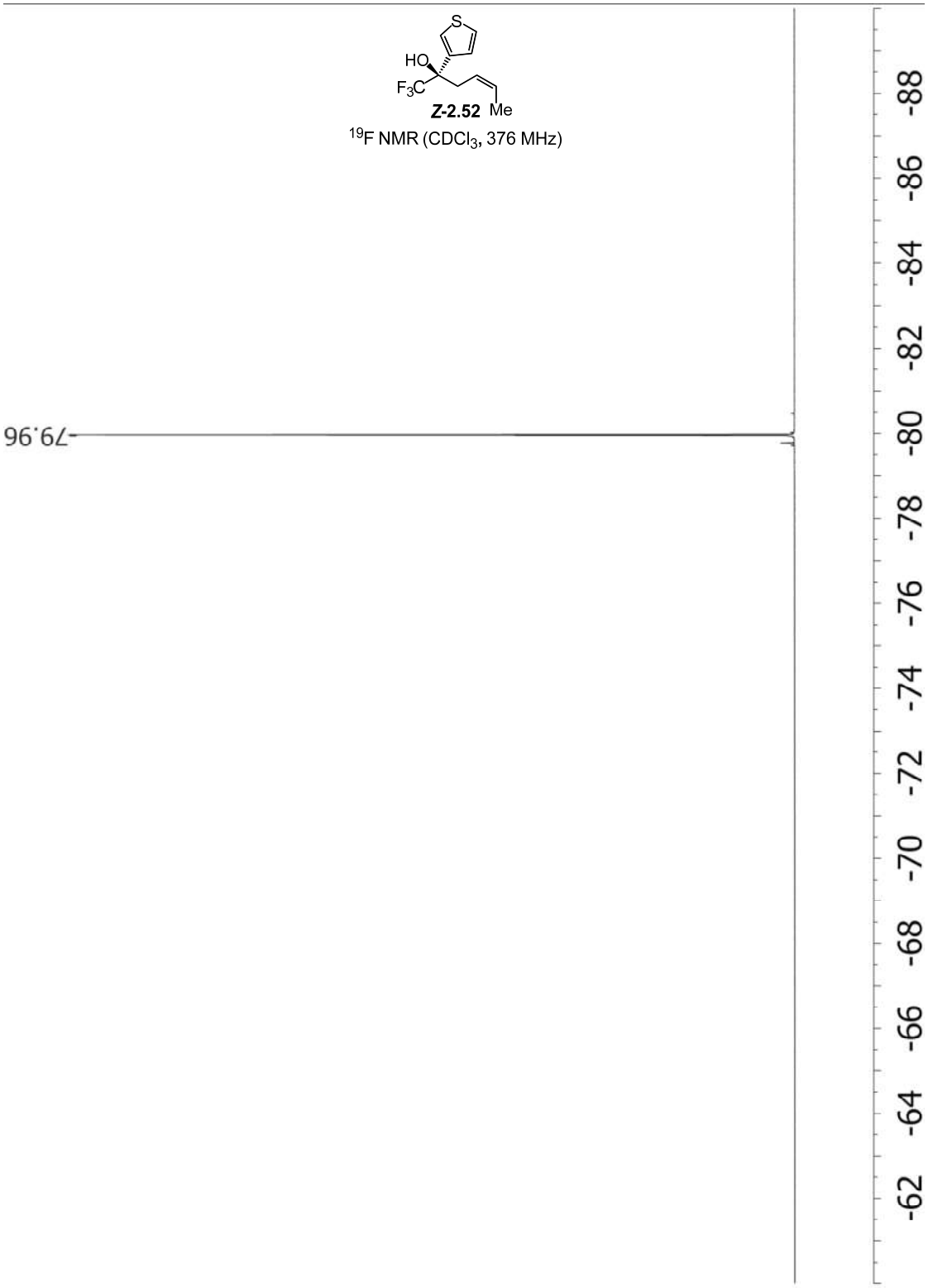

***Z*-2.52**

^{19}F NMR ($CDCl_3$, 376 MHz)

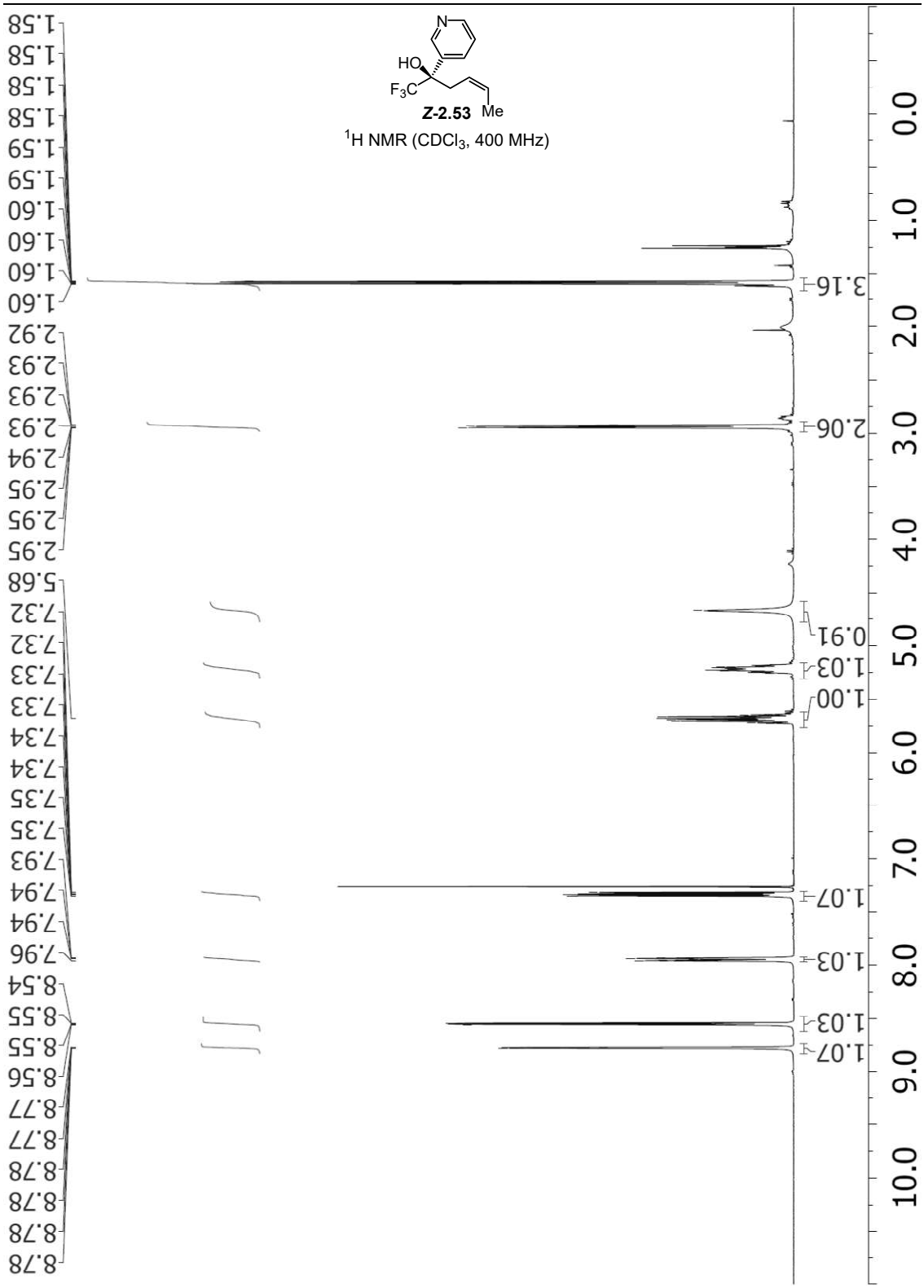
N
HO
F3C
Me
Z-2.53
1H NMR (CDCl3, 400 MHz)
3.16
2.06
0.91
1.03
1.00
1.07
1.03
1.03
1.07

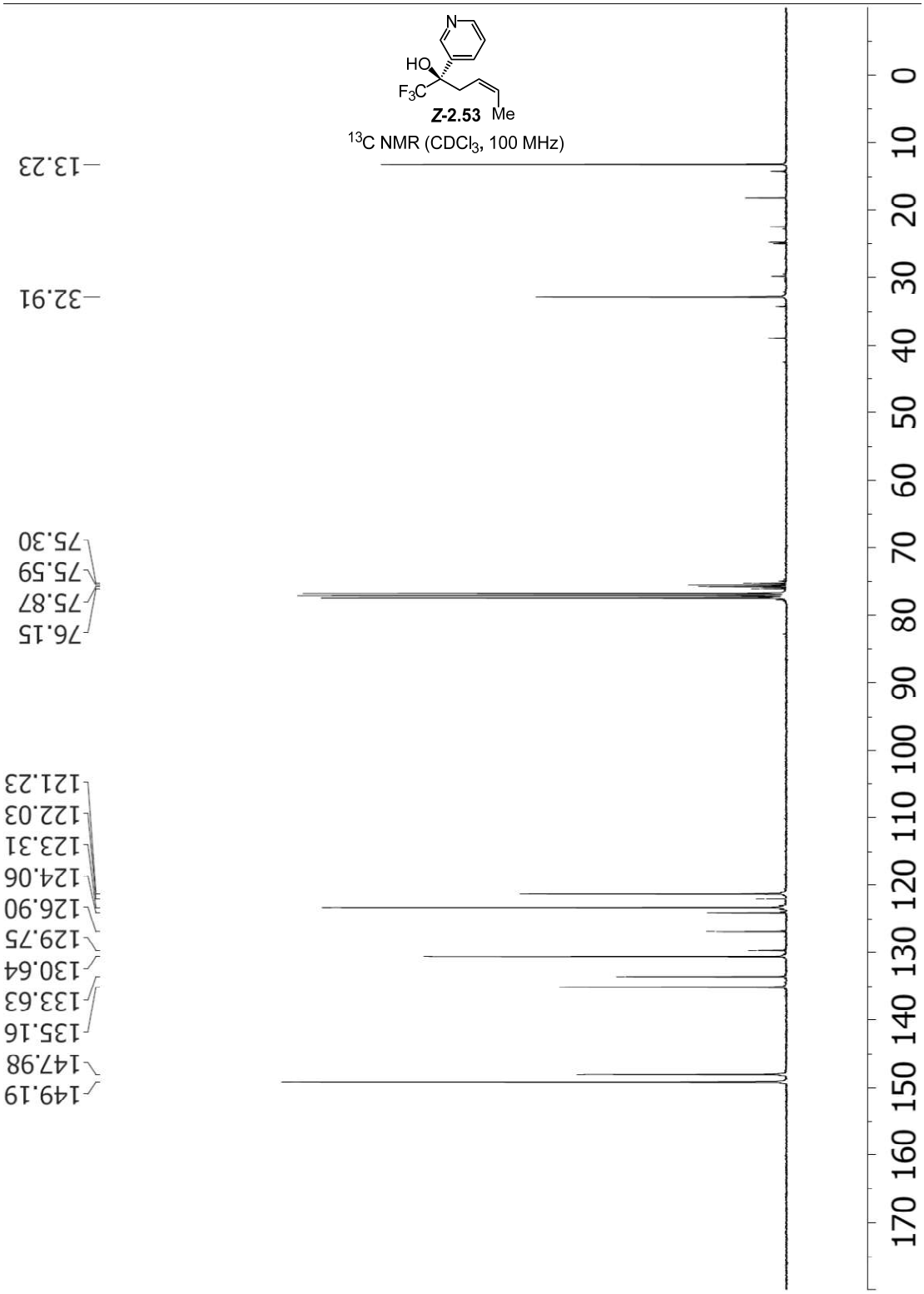
Z-2.53
13C NMR (CDCl3, 100 MHz)
13.23
32.91
75.30
75.59
75.87
76.15
121.23
122.03
123.31
124.06
126.90
129.75
130.64
133.63
135.16
147.98
149.19

***Z*-2.53**

^{19}F NMR ($CDCl_3$, 376 MHz)

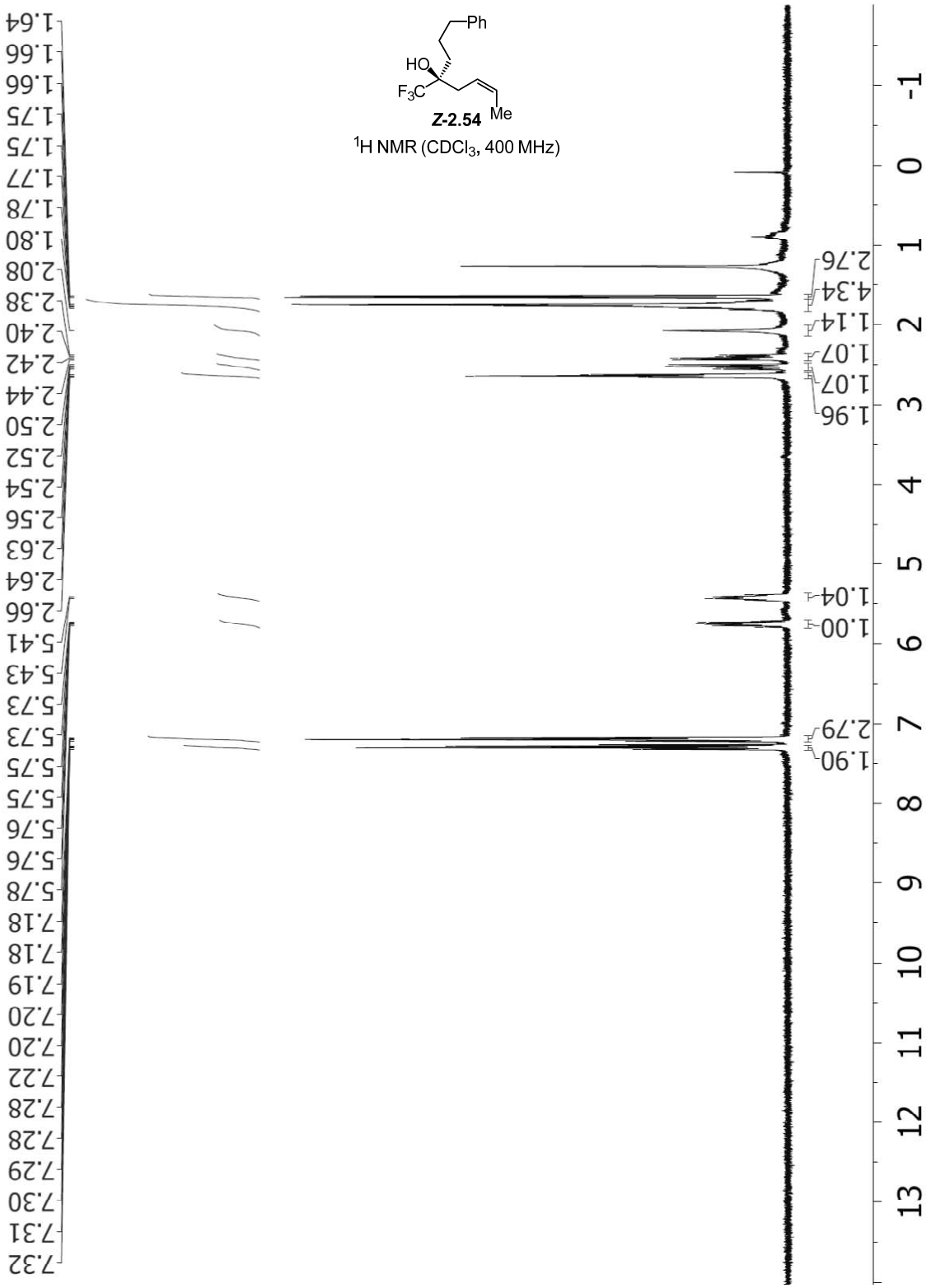
Ph
HO
F3C
Me
Z-2.54
1H NMR (CDCl3, 400 MHz)

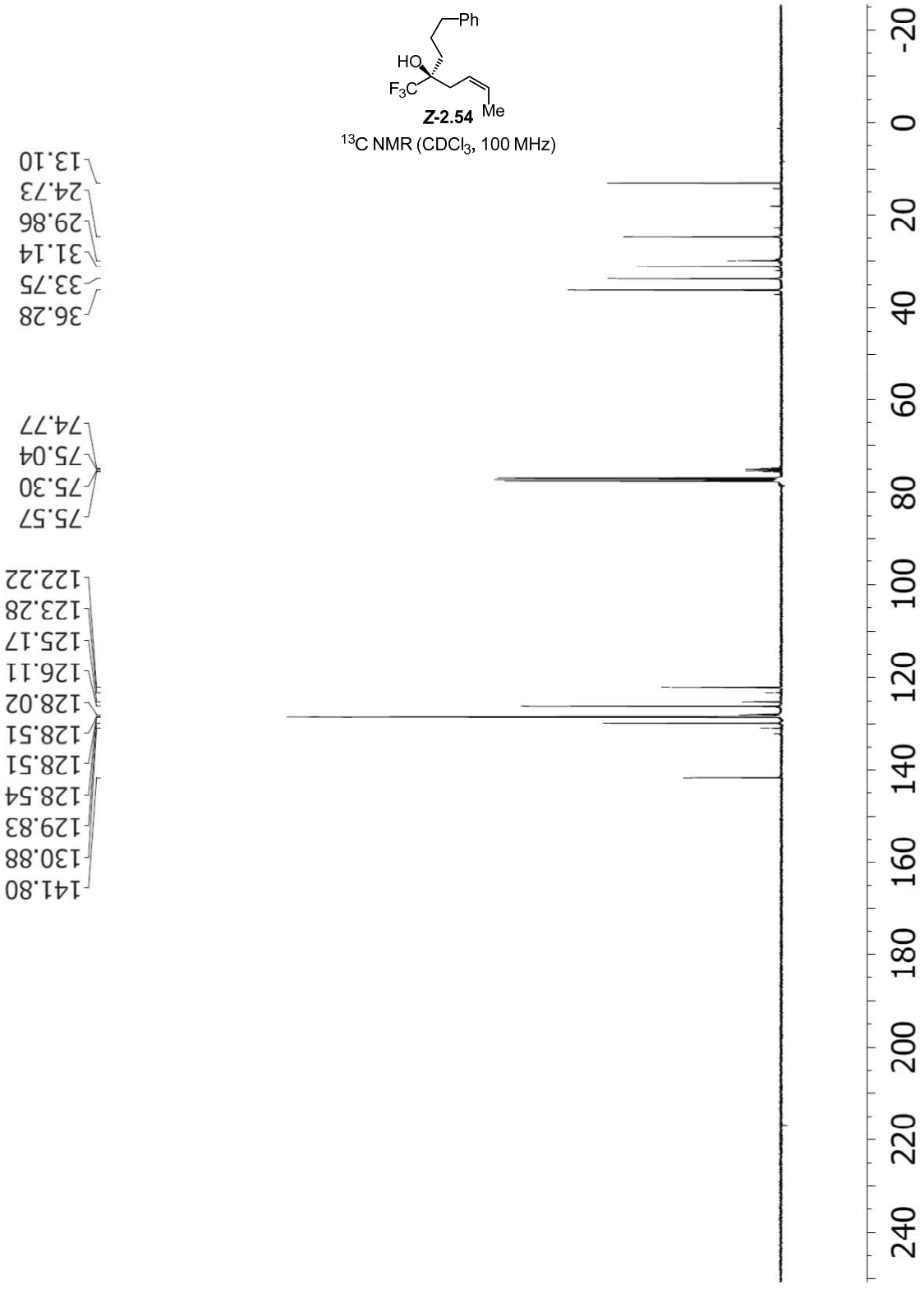
Ph
HO
F3C
Me
Z-2.54
13C NMR (CDCl3, 100 MHz)
13.10
24.73
29.86
31.14
33.75
36.28
74.77
75.04
75.30
75.57
122.22
123.28
125.17
126.11
128.02
128.51
128.51
128.54
129.83
130.88
141.80
-20
0
20
40
60
80
100
120
140
160
180
200
220
240

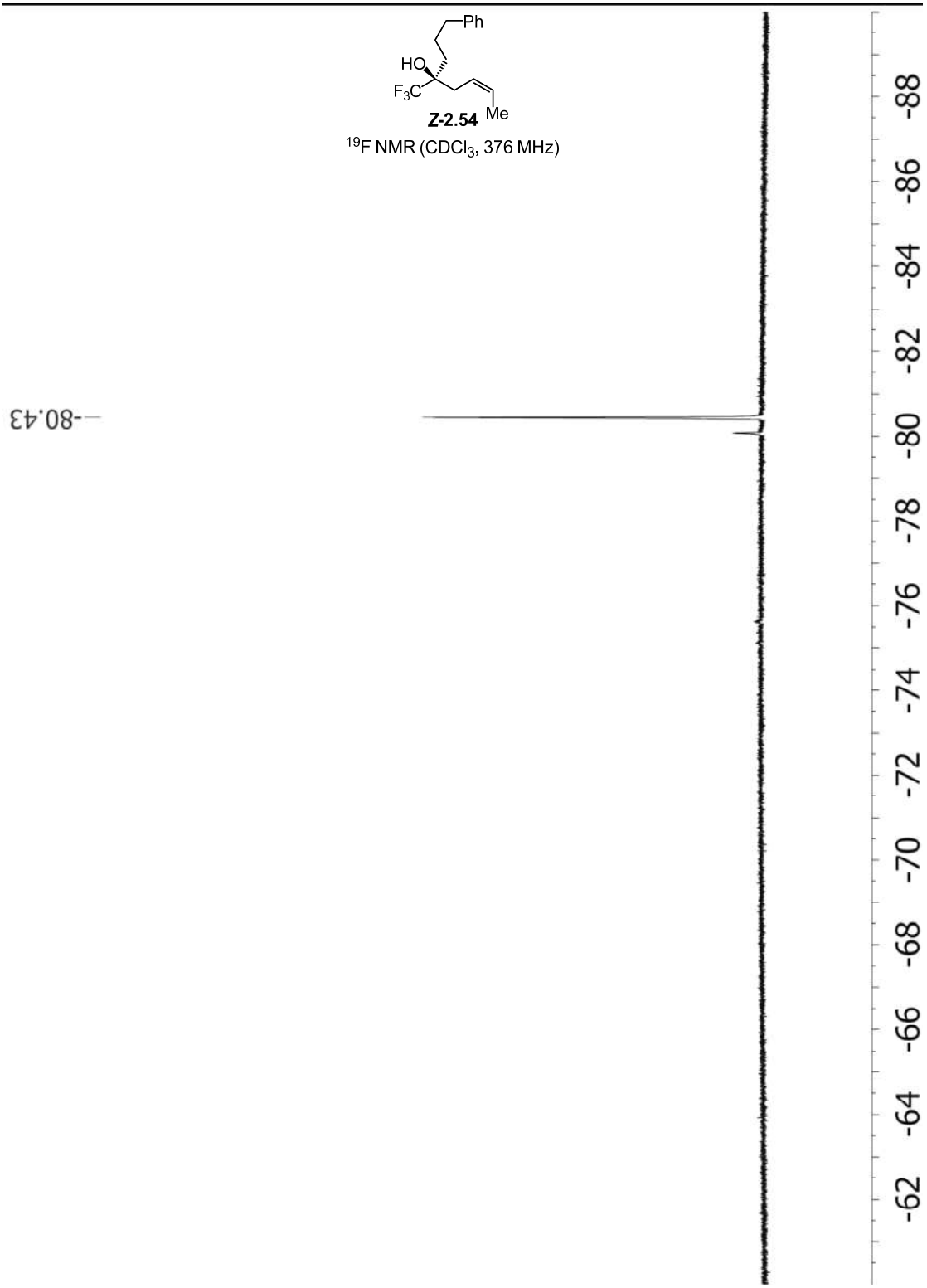
Ph
HO
F3C
Me
Z-2.54
19F NMR (CDCl3, 376 MHz)
-80.43
-62
-64
-66
-68
-70
-72
-74
-76
-78
-80
-82
-84
-86
-88

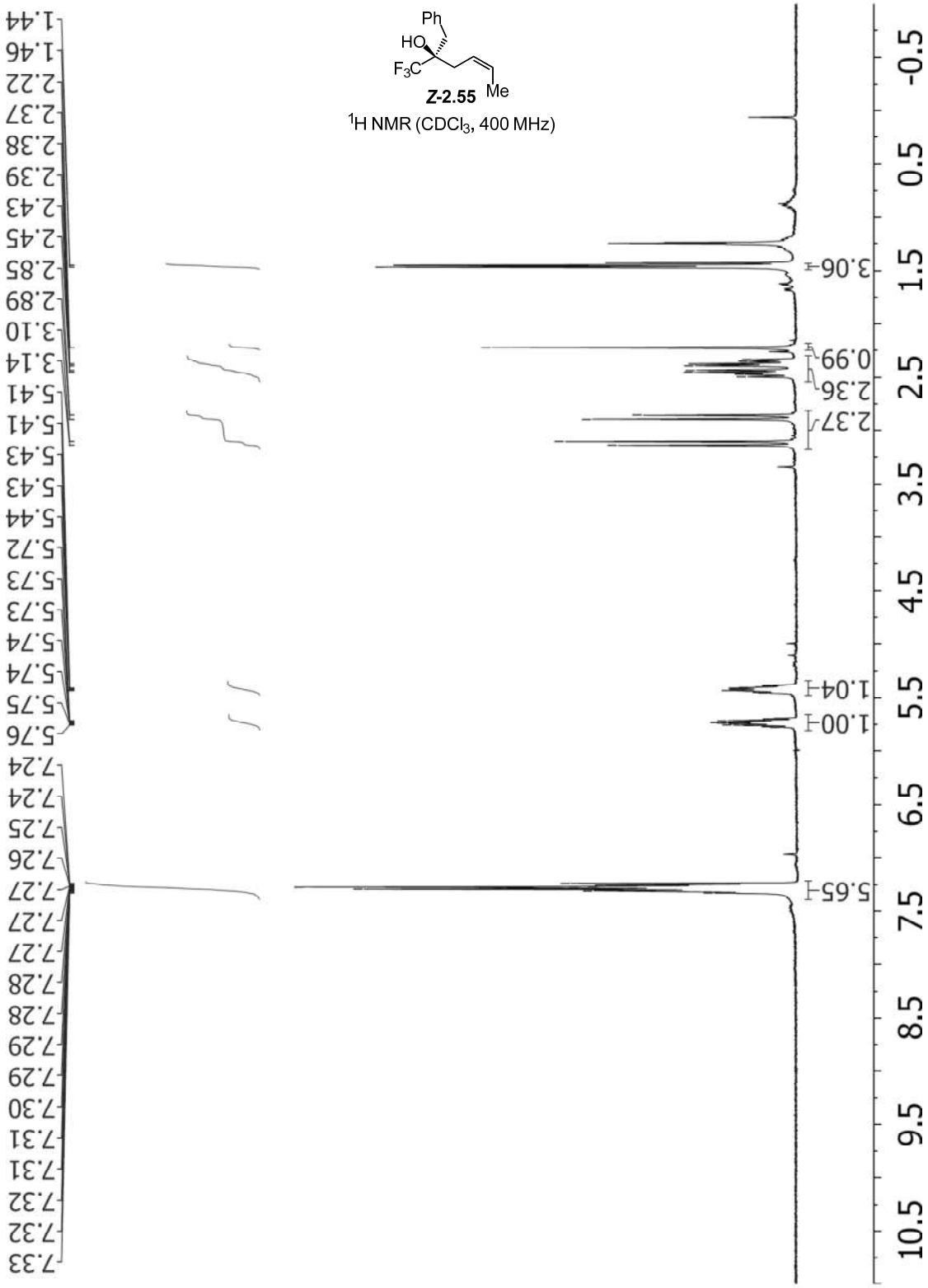
Ph
HO
F3C
Me
Z-2.55
1H NMR (CDCl3, 400 MHz)
3.06
0.99
2.36
2.37
1.04
1.00
5.65

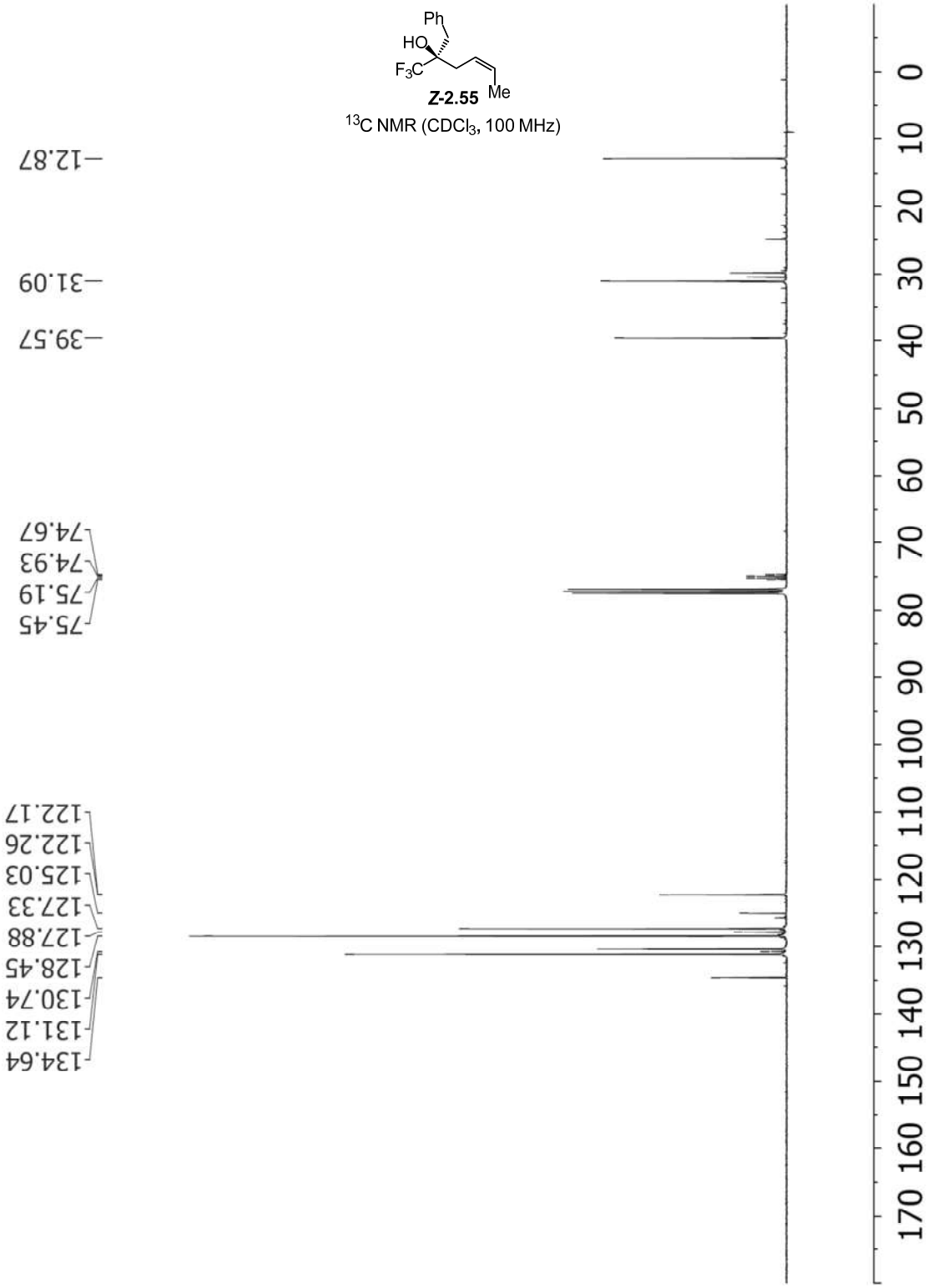
Ph
HO
F3C
Me
Z-2.55
13C NMR (CDCl3, 100 MHz)
12.87
31.09
39.57
74.67
74.93
75.19
75.45
122.17
122.26
125.03
127.33
127.88
128.45
130.74
131.12
134.64
0
10
20
30
40
50
60
70
80
90
100
110
120
130
140
150
160
170


Ph
HO
F3C
Me
Z-2.55
19F NMR (CDCl3, 376 MHz)
-80.03
-62
-64
-66
-68
-70
-72
-74
-76
-78
-80
-82
-84
-86
-88

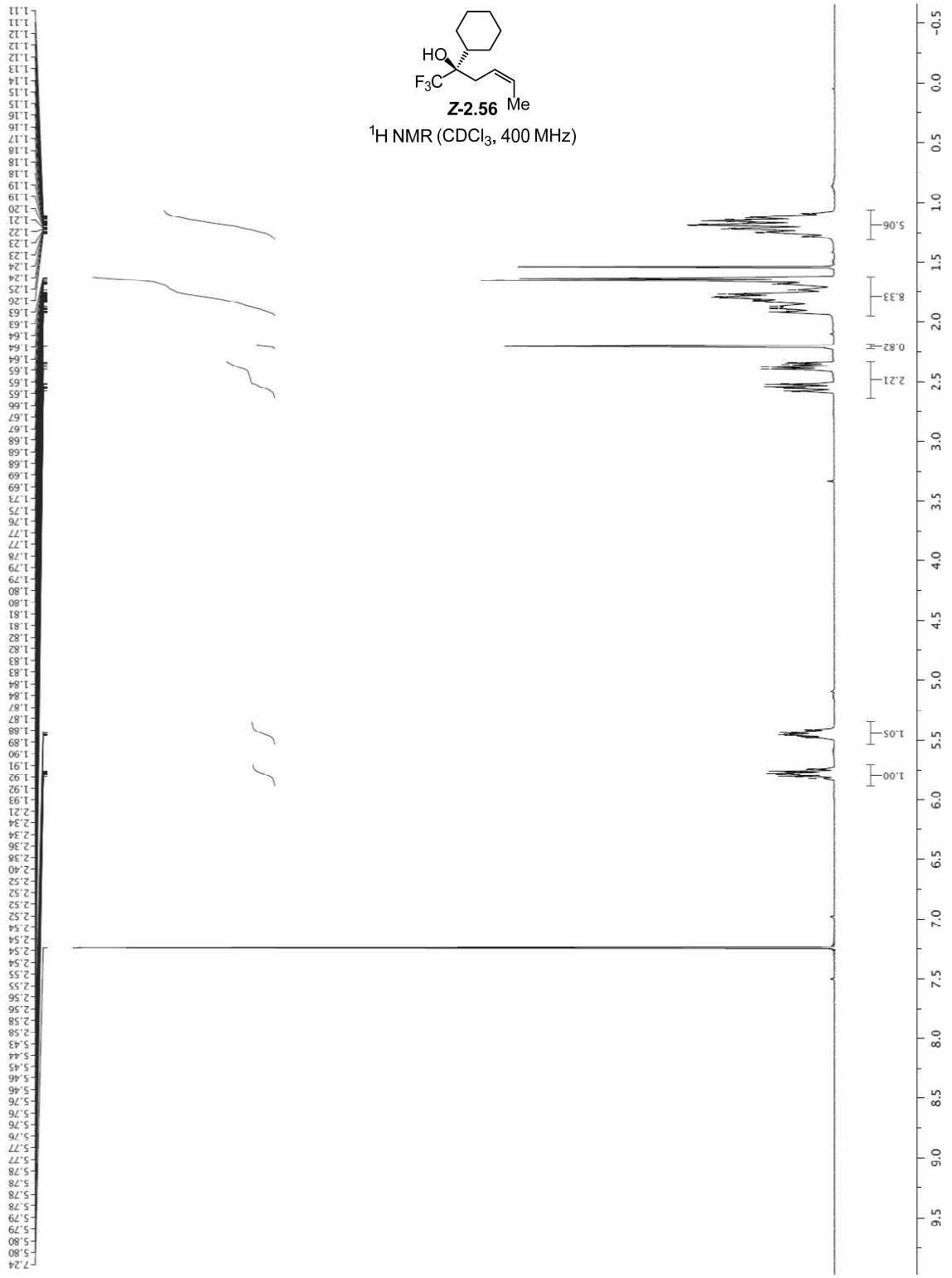
HO
F3C
Me
Z-2.56
1H NMR (CDCl3, 400 MHz)
5.06
8.33
0.82
2.21
1.05
1.00

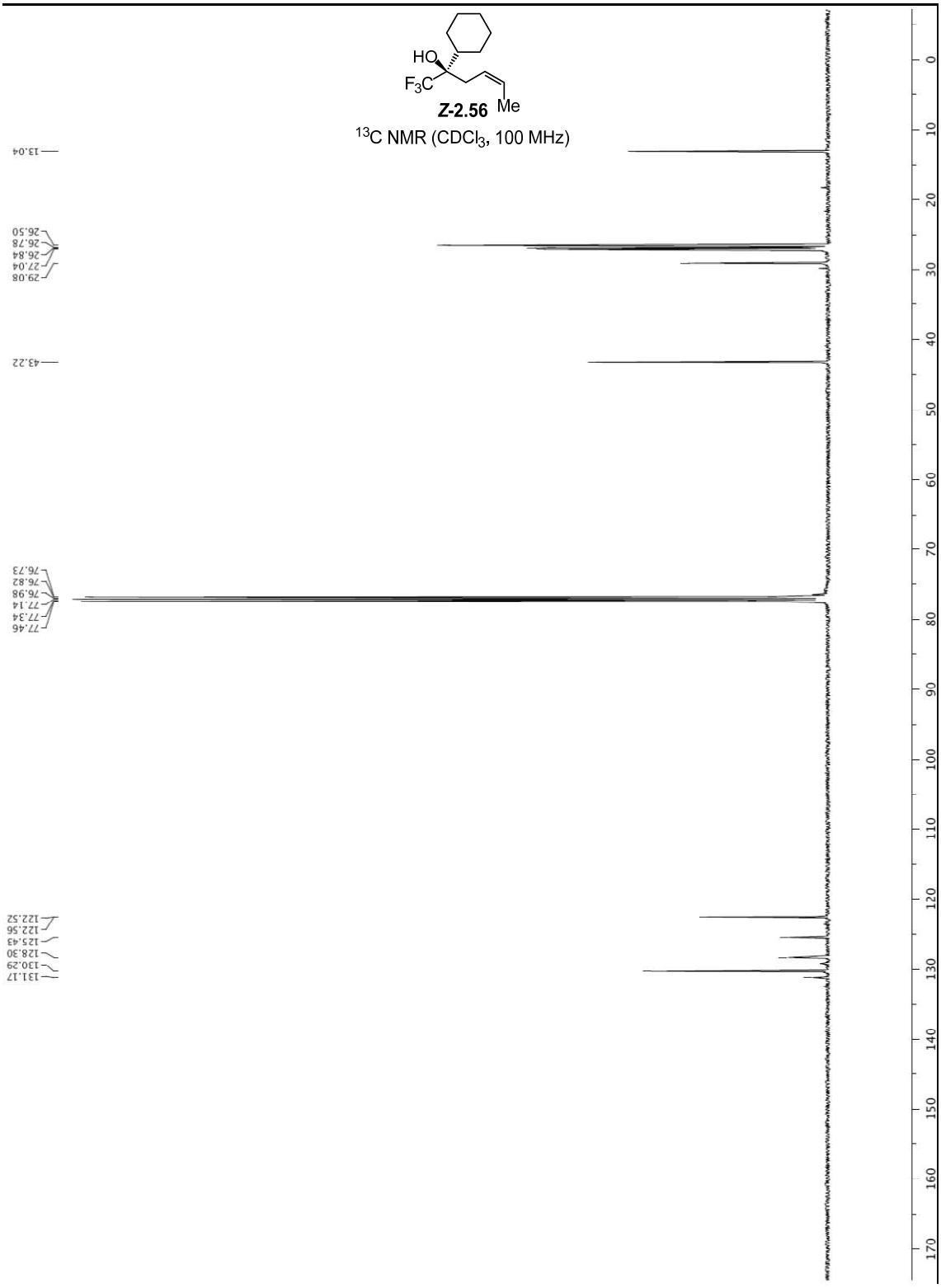
HO
F3C
Me
Z-2.56
13C NMR (CDCl3, 100 MHz)
13.04
26.50
26.78
26.84
27.04
29.08
43.22
76.73
76.82
76.98
77.14
77.34
77.46
122.52
122.56
125.43
128.30
130.29
131.17

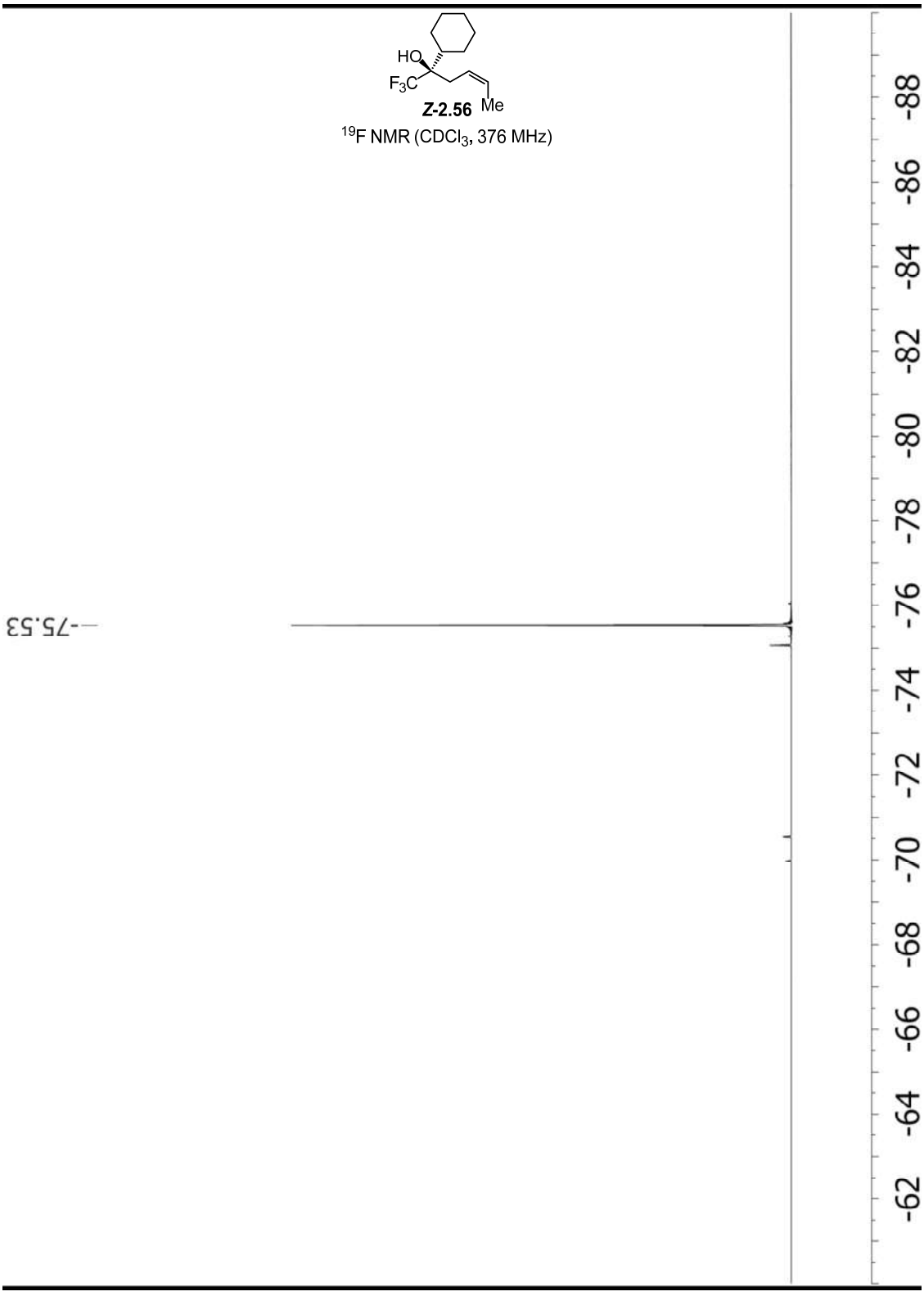
HO
F3C
Me
Z-2.56
19F NMR (CDCl3, 376 MHz)
-75.53
-62
-64
-66
-68
-70
-72
-74
-76
-78
-80
-82
-84
-86
-88

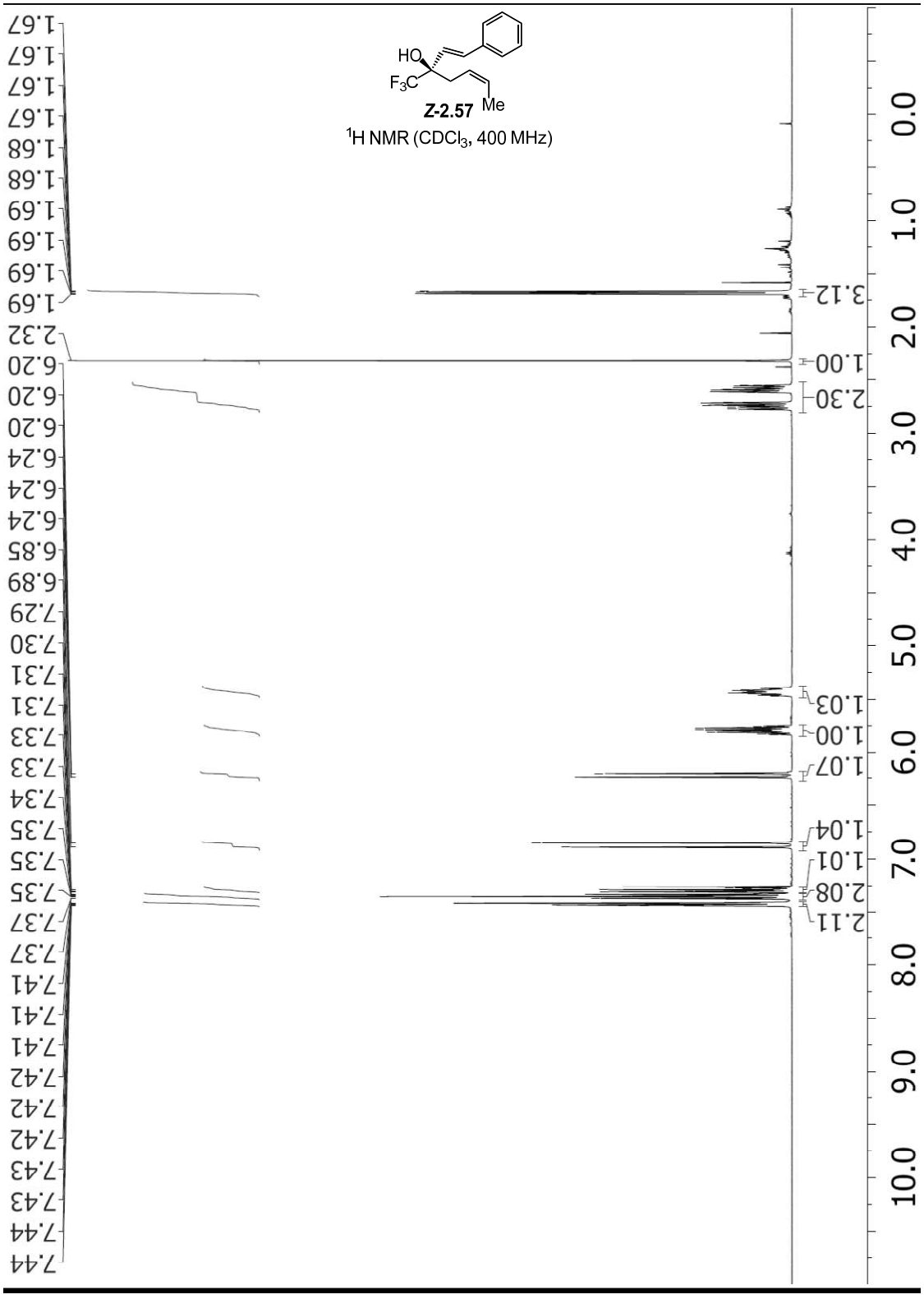
HO
F3C
Me
Z-2.57
1H NMR (CDCl3, 400 MHz)
3.12
1.00
2.30
1.03
1.00
1.07
1.04
1.01
2.08
2.11

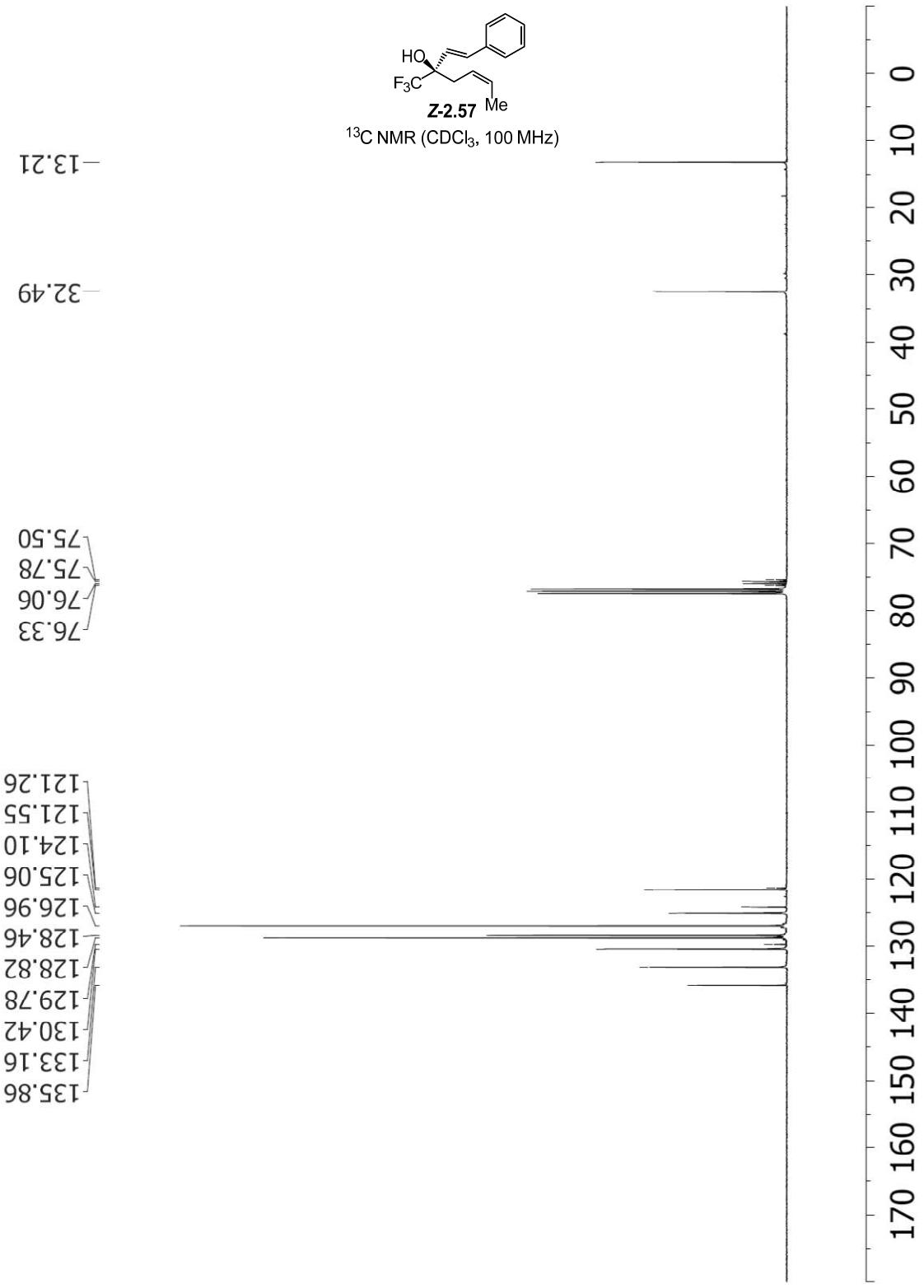
HO
F3C
Me
Z-2.57
13C NMR (CDCl3, 100 MHz)
13.21
32.49
75.50
75.78
76.06
76.33
121.26
121.55
124.10
125.06
126.96
128.46
128.82
129.78
130.42
133.16
135.86
0 10 20 30 40 50 60 70 80 90 100 110 120 130 140 150 160 170


HO
F3C
Me
Z-2.57
19F NMR (CDCl3, 376 MHz)
-81.47
-62
-64
-66
-68
-70
-72
-74
-76
-78
-80
-82
-84
-86
-88

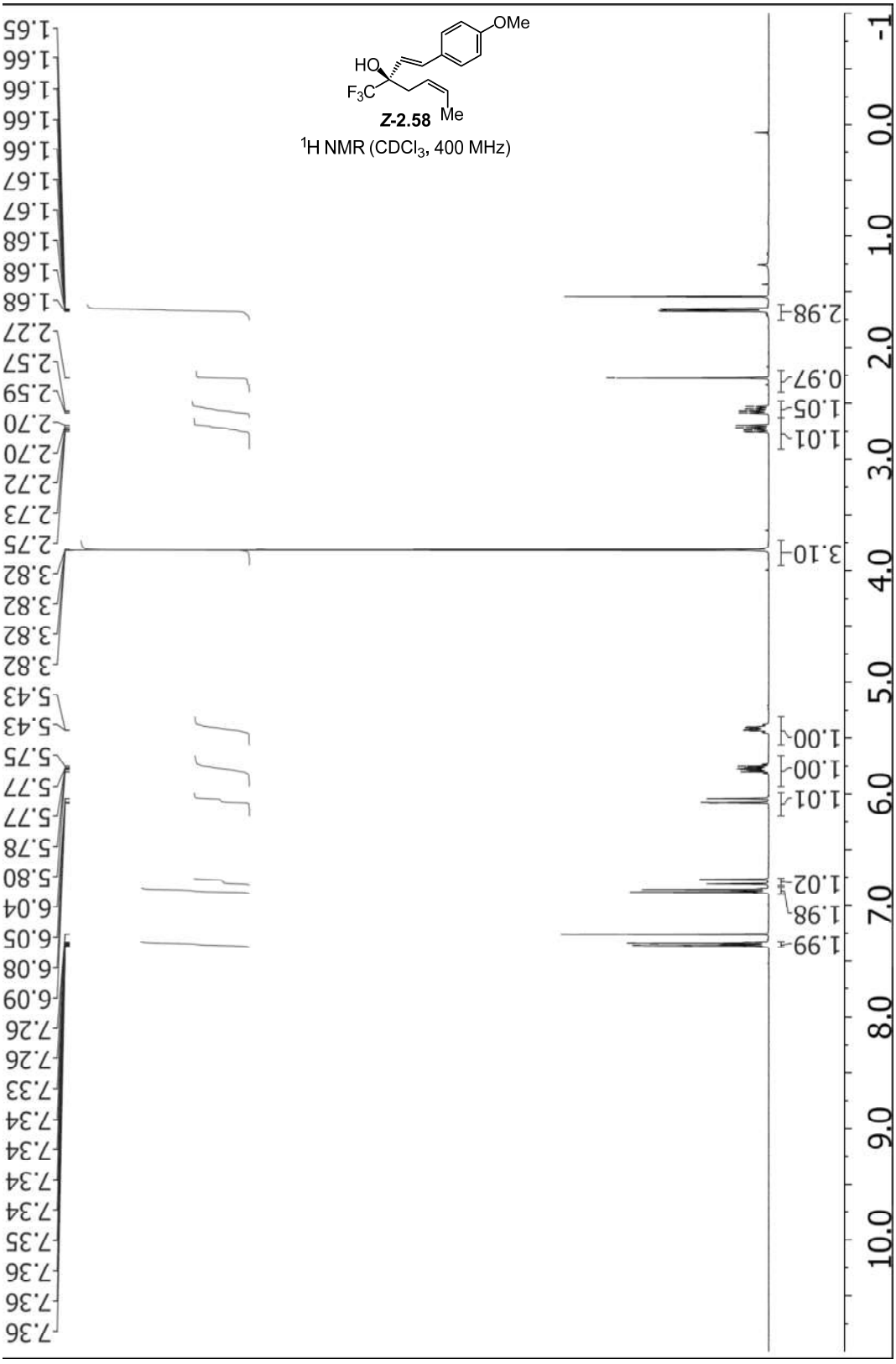
OMe
HO
F3C
Me
Z-2.58
1H NMR (CDCl3, 400 MHz)

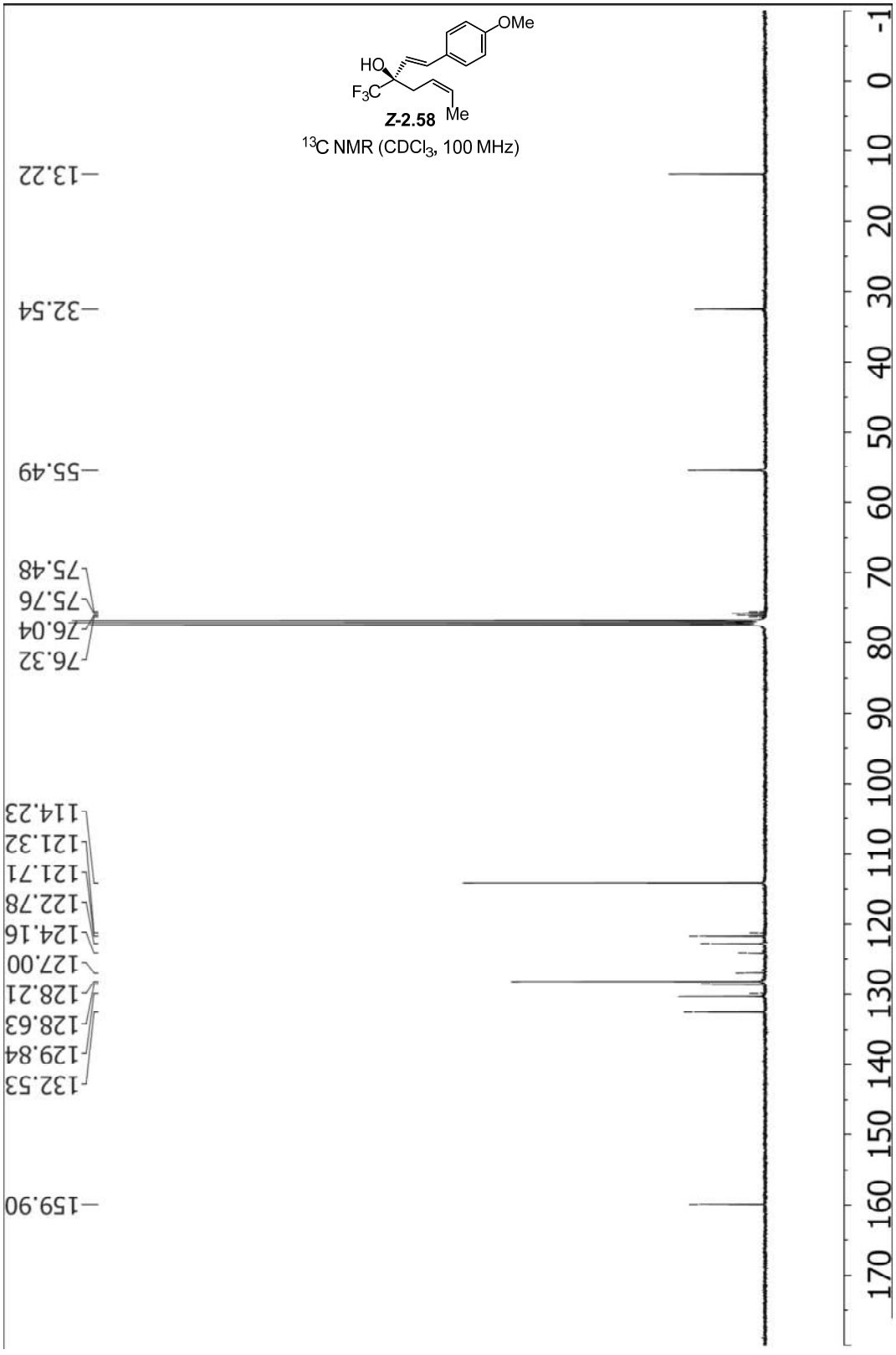
OMe
HO
F3C
Me
Z-2.58
13C NMR (CDCl3, 100 MHz)
13.22
32.54
55.49
75.48
75.76
76.04
76.32
114.23
121.32
121.71
122.78
124.16
127.00
128.21
128.63
129.84
132.53
159.90

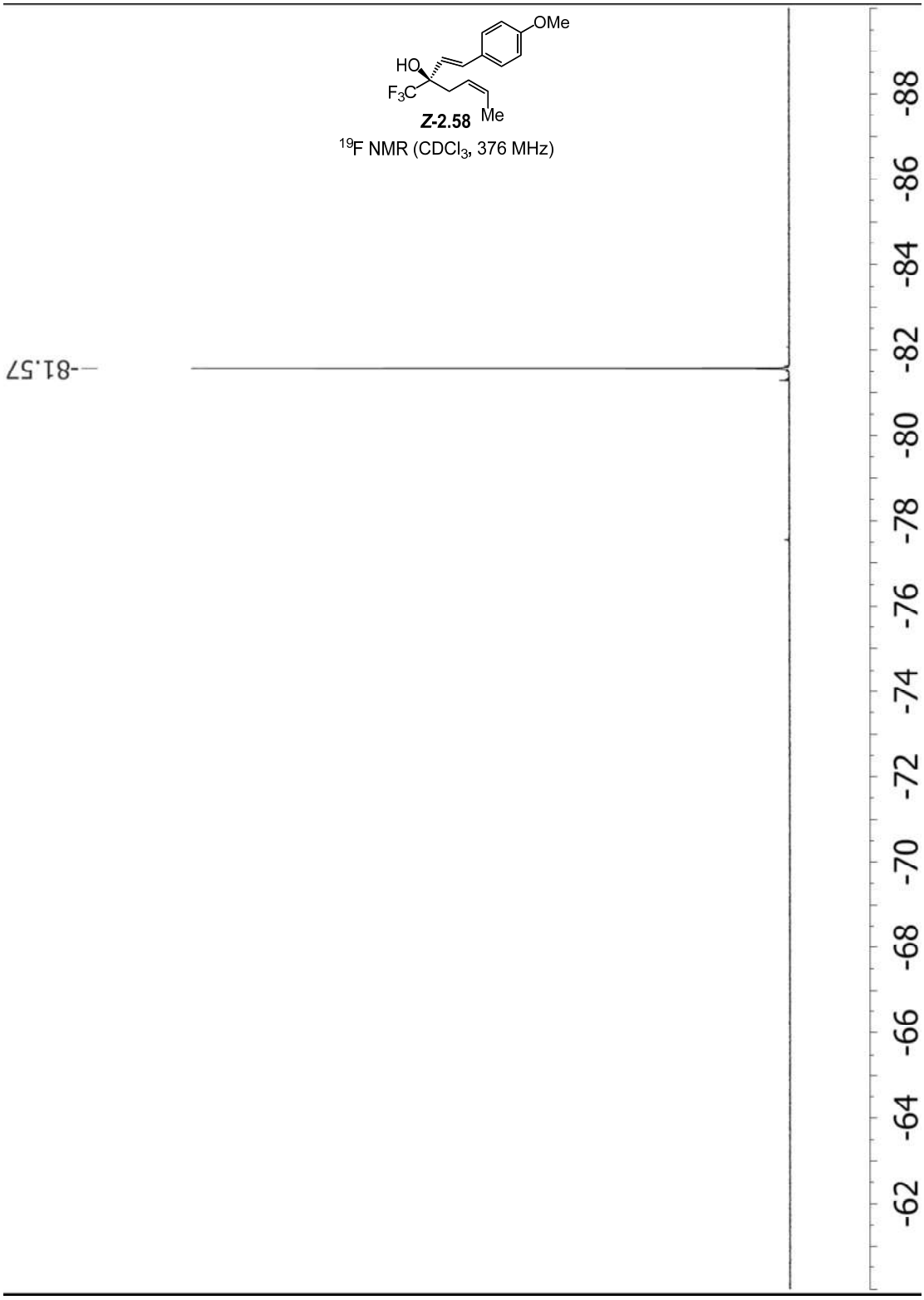
OMe
HO
F3C
Me
Z-2.58
19F NMR (CDCl3, 376 MHz)
-81.57
-62
-64
-66
-68
-70
-72
-74
-76
-78
-80
-82
-84
-86
-88

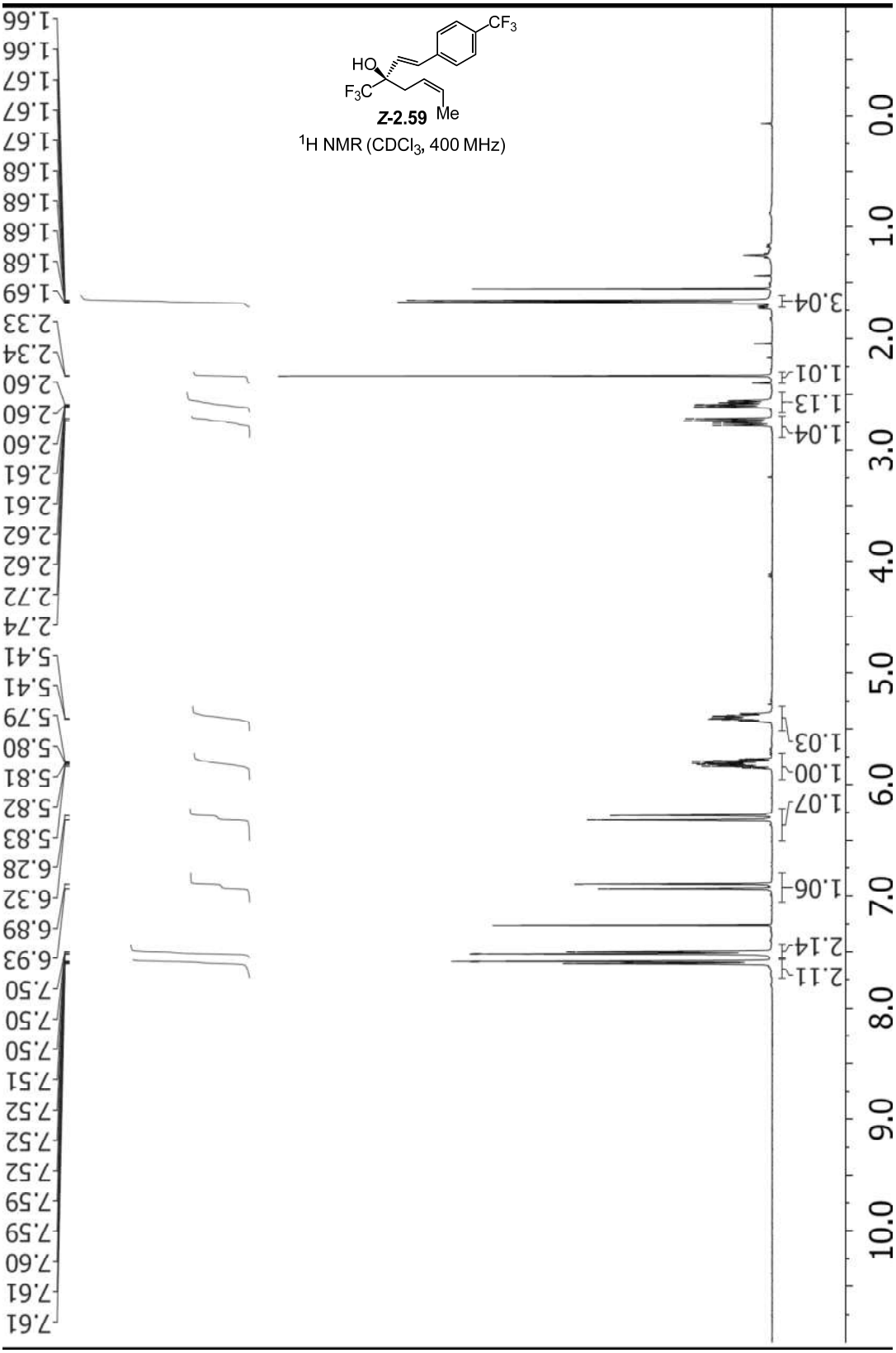
CF3
HO
F3C
Me
Z-2.59
1H NMR (CDCl3, 400 MHz)

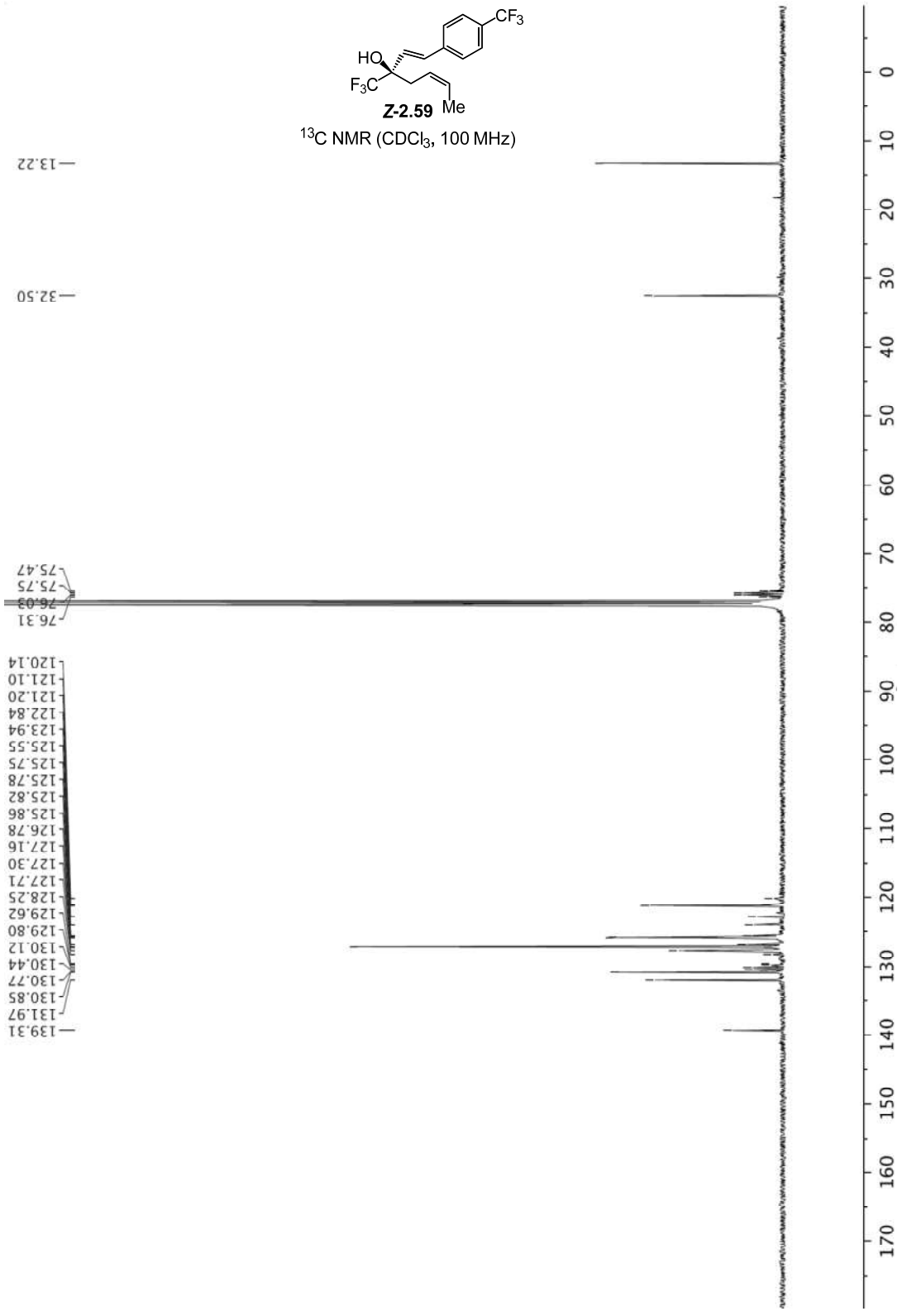
CF3
HO
F3C
Me
Z-2.59
13C NMR (CDCl3, 100 MHz)
13.22
32.50
75.47
75.75
76.03
76.31
120.14
121.10
121.20
122.84
123.94
125.55
125.75
125.78
125.82
125.86
126.78
127.16
127.30
127.71
128.25
129.62
129.80
130.12
130.44
130.77
130.85
131.97
139.31
0
10
20
30
40
50
60
70
80
90
100
110
120
130
140
150
160
170

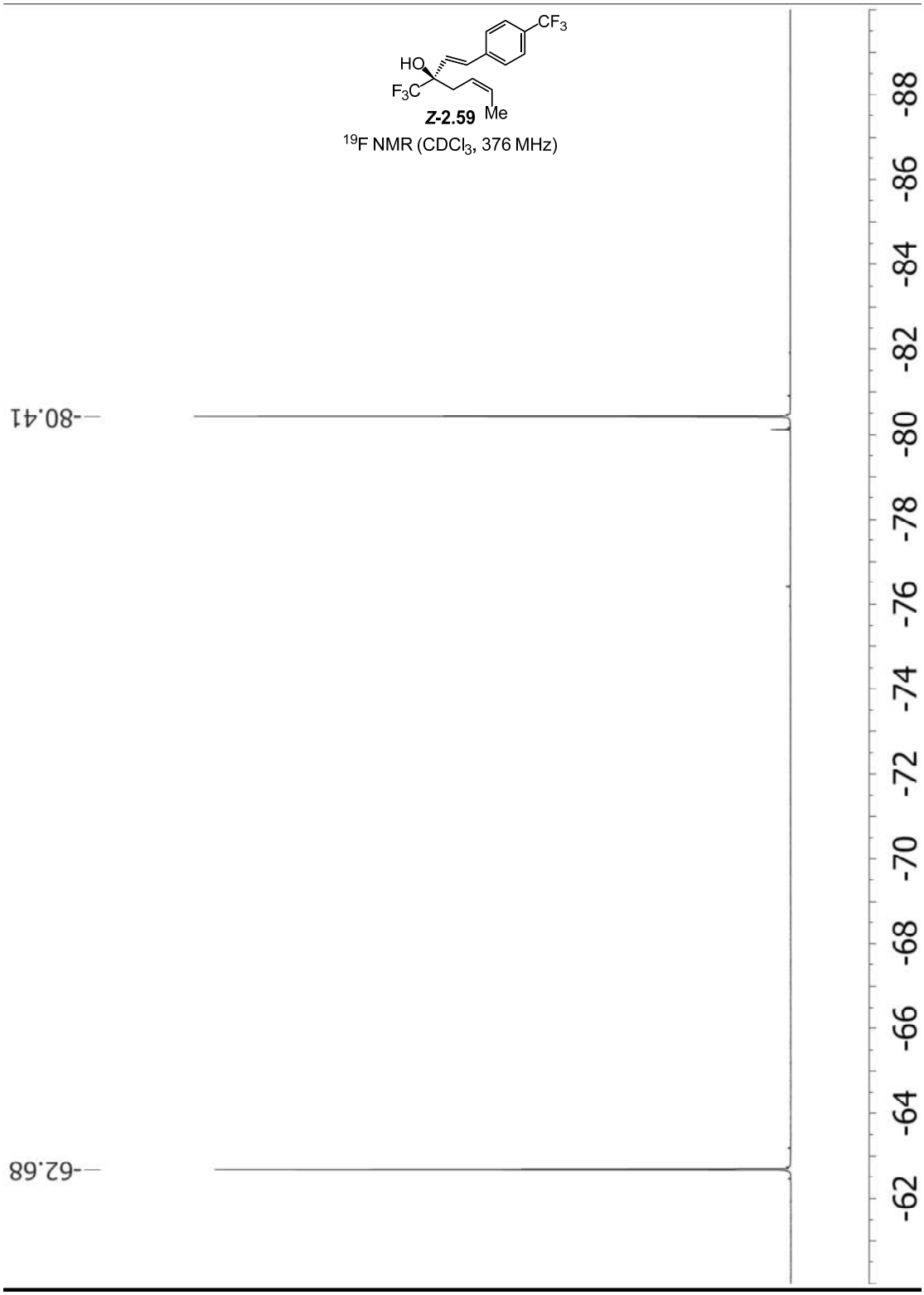
CF3
HO
F3C
Me
Z-2.59
19F NMR (CDCl3, 376 MHz)
-80.41
-62.68
-62
-64
-66
-68
-70
-72
-74
-76
-78
-80
-82
-84
-86
-88

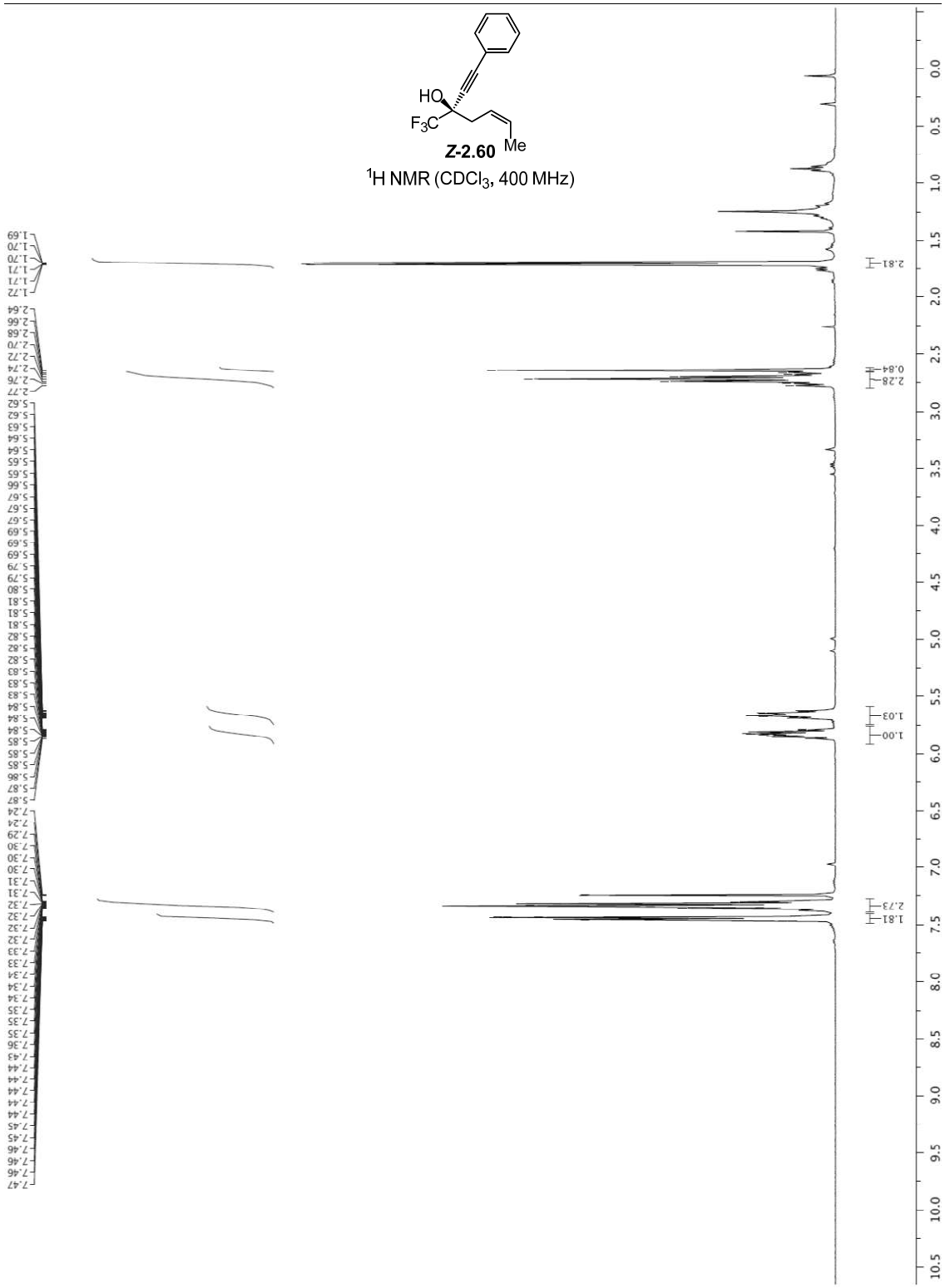
HO
F3C
Me
Z-2.60
1H NMR (CDCl3, 400 MHz)

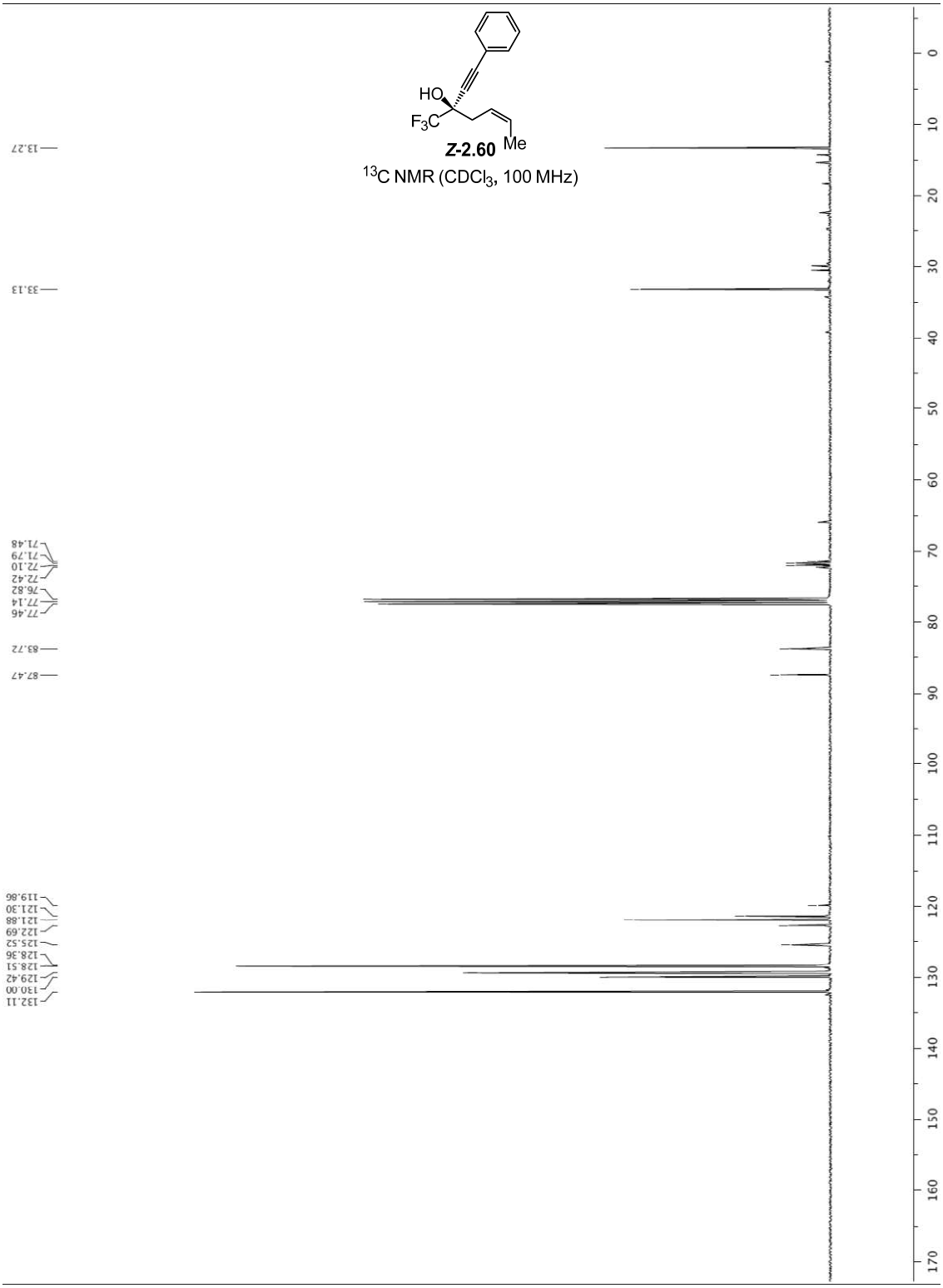
HO
F3C
Me
Z-2.60
13C NMR (CDCl3, 100 MHz)
13.27
33.13
71.48
71.79
72.10
72.42
76.82
77.14
77.46
83.72
87.47
119.86
121.30
121.88
122.69
125.52
128.36
128.51
129.42
130.00
132.11

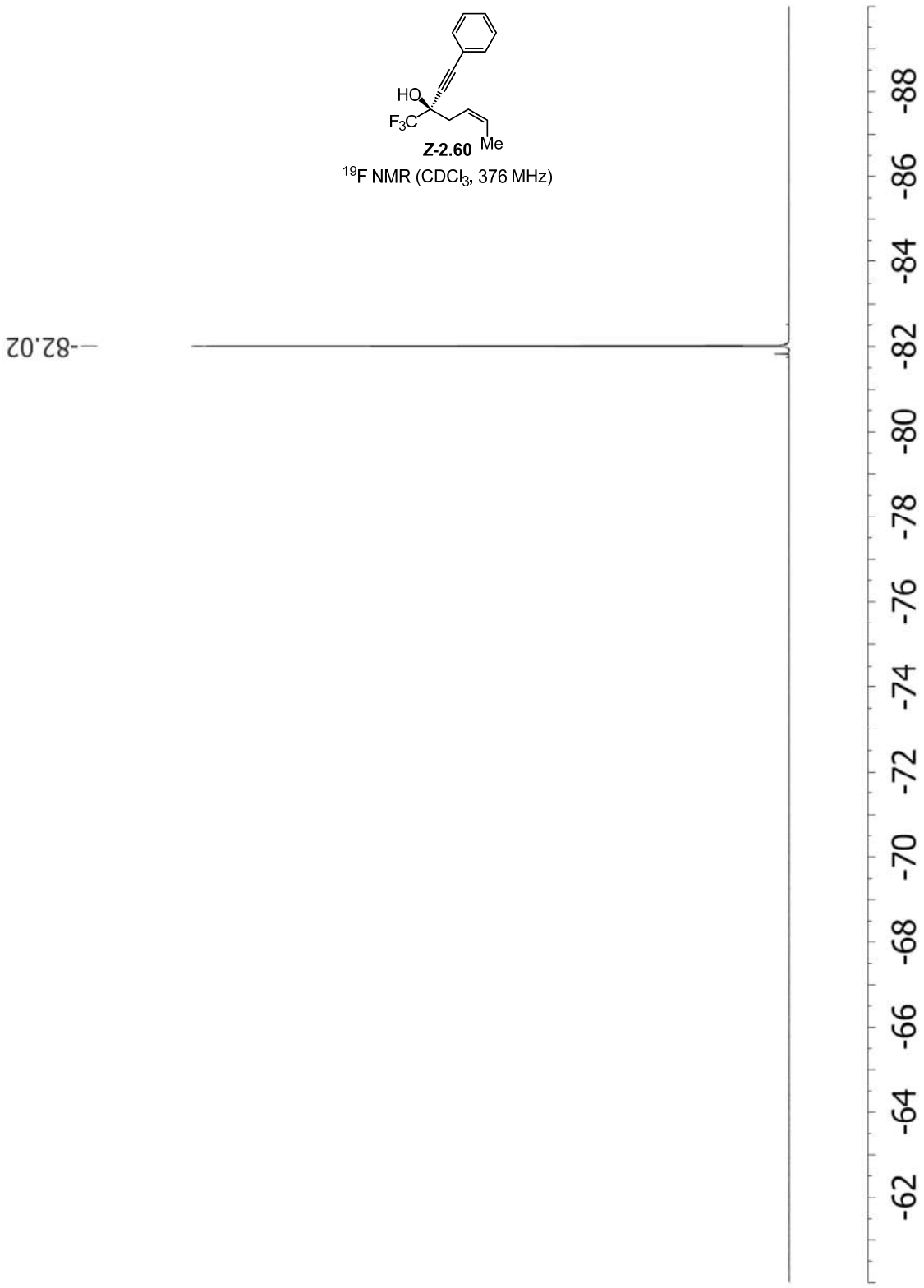

***Z*-2.60**

^{19}F NMR ($CDCl_3$, 376 MHz)

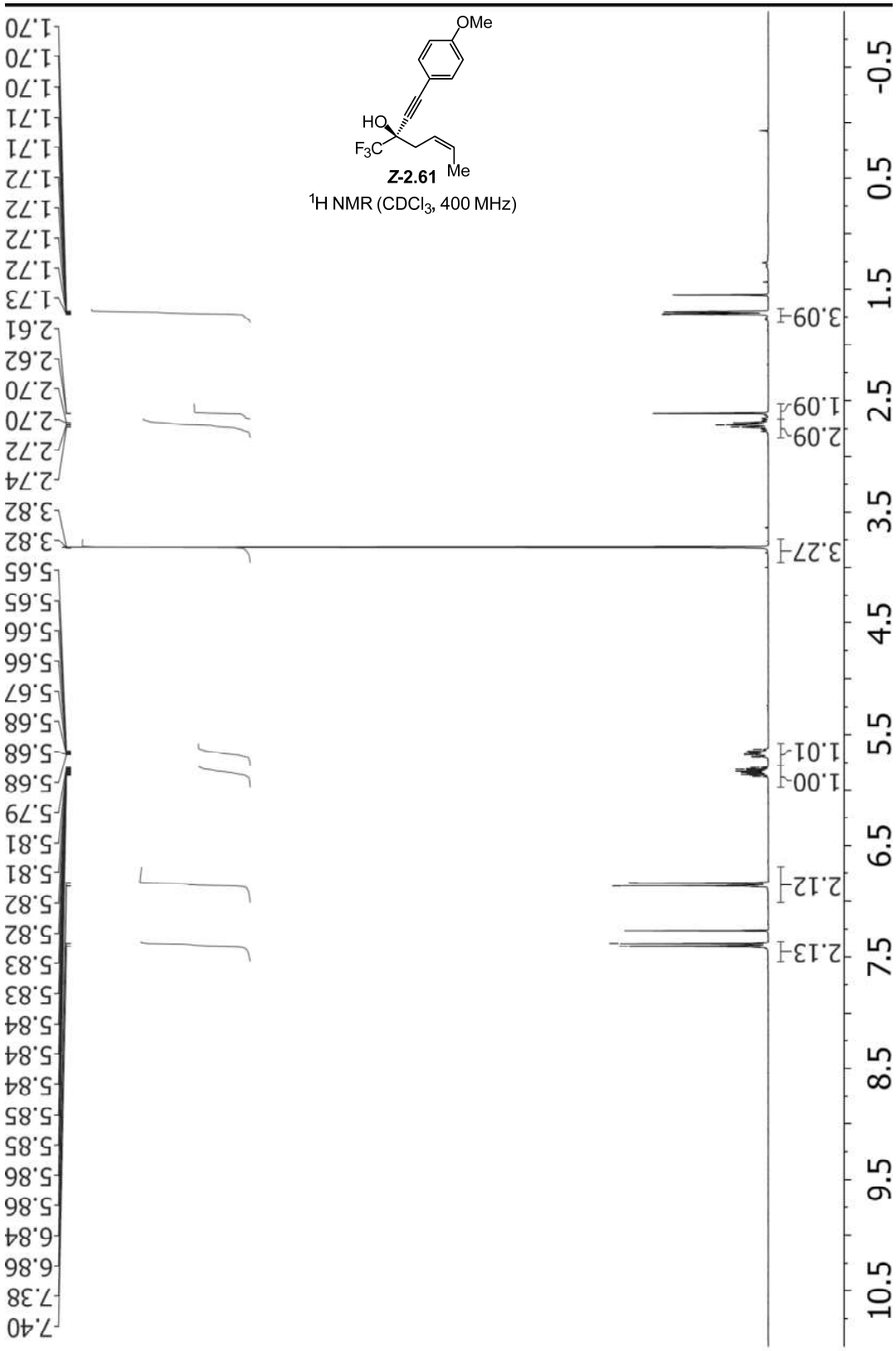
OMe
HO
F3C
Me
Z-2.61
1H NMR (CDCl3, 400 MHz)
3.09
1.09
2.09
3.27
1.01
1.00
2.12
2.13

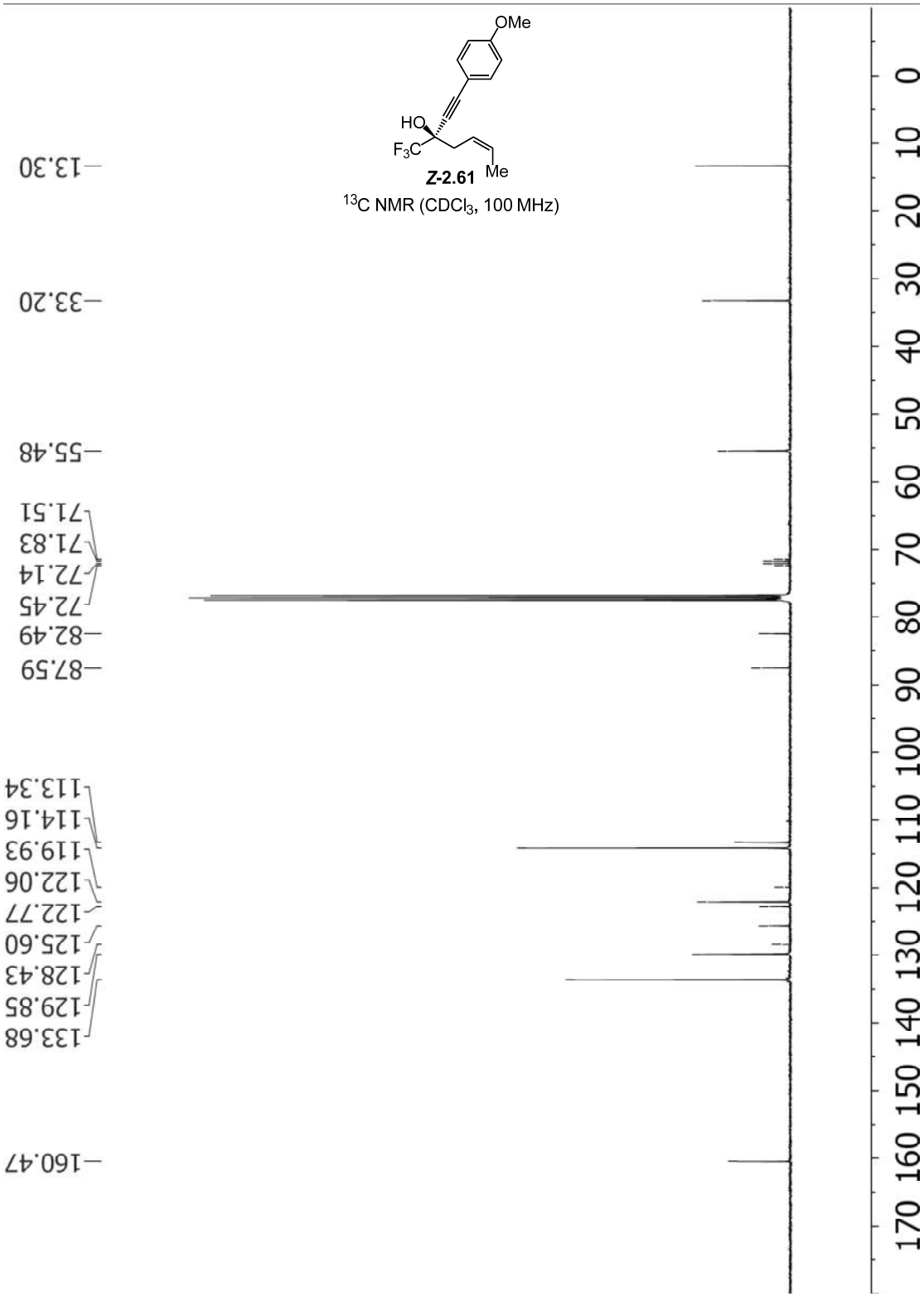
OMe
HO
F3C
Me
Z-2.61
13C NMR (CDCl3, 100 MHz)
13.30
33.20
55.48
71.51
71.83
72.14
72.45
82.49
87.59
113.34
114.16
119.93
122.06
122.77
125.60
128.43
129.85
133.68
160.47
0
10
20
30
40
50
60
70
80
90
100
110
120
130
140
150
160
170

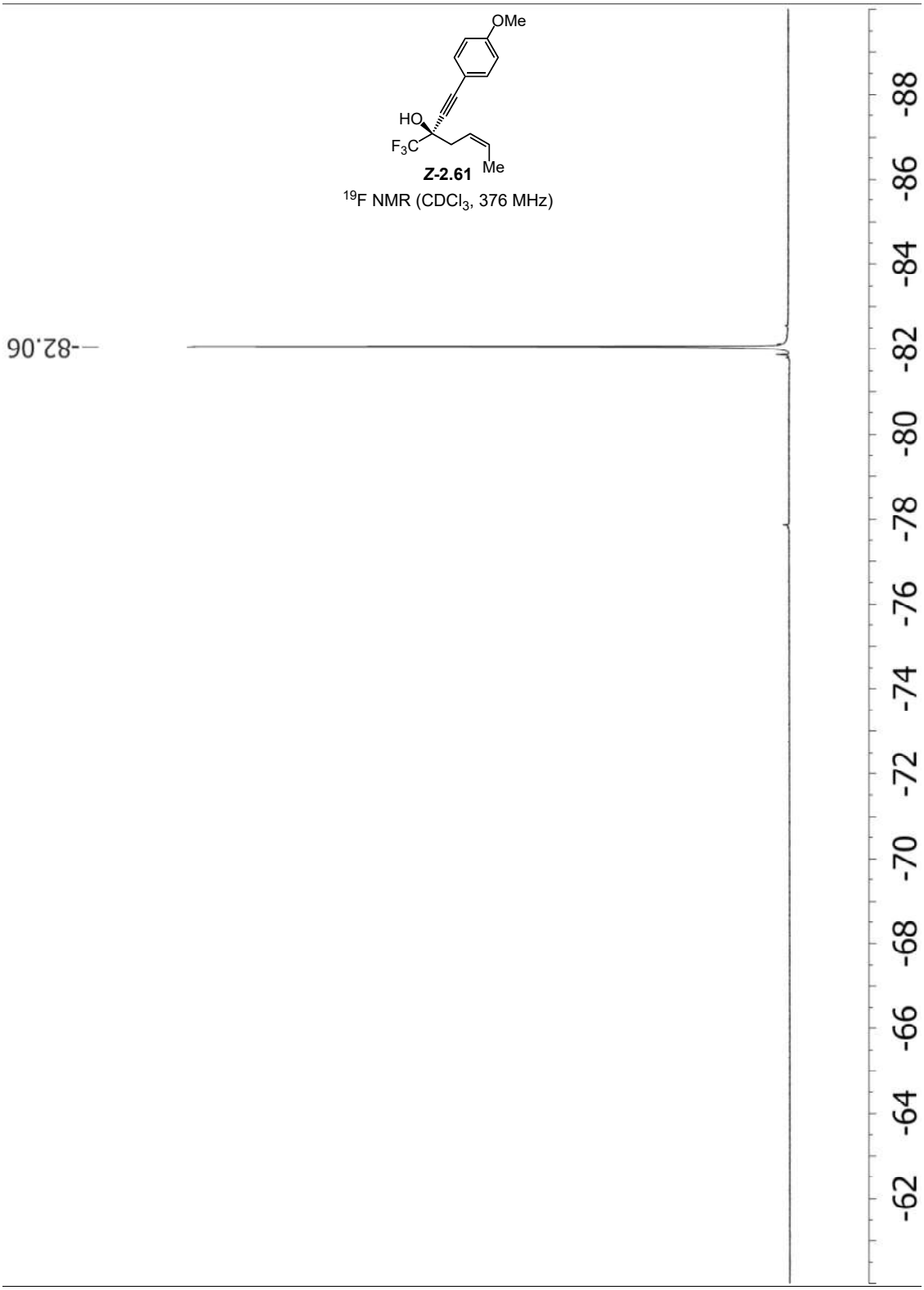

***Z*-2.61**

^{19}F NMR ($CDCl_3$, 376 MHz)

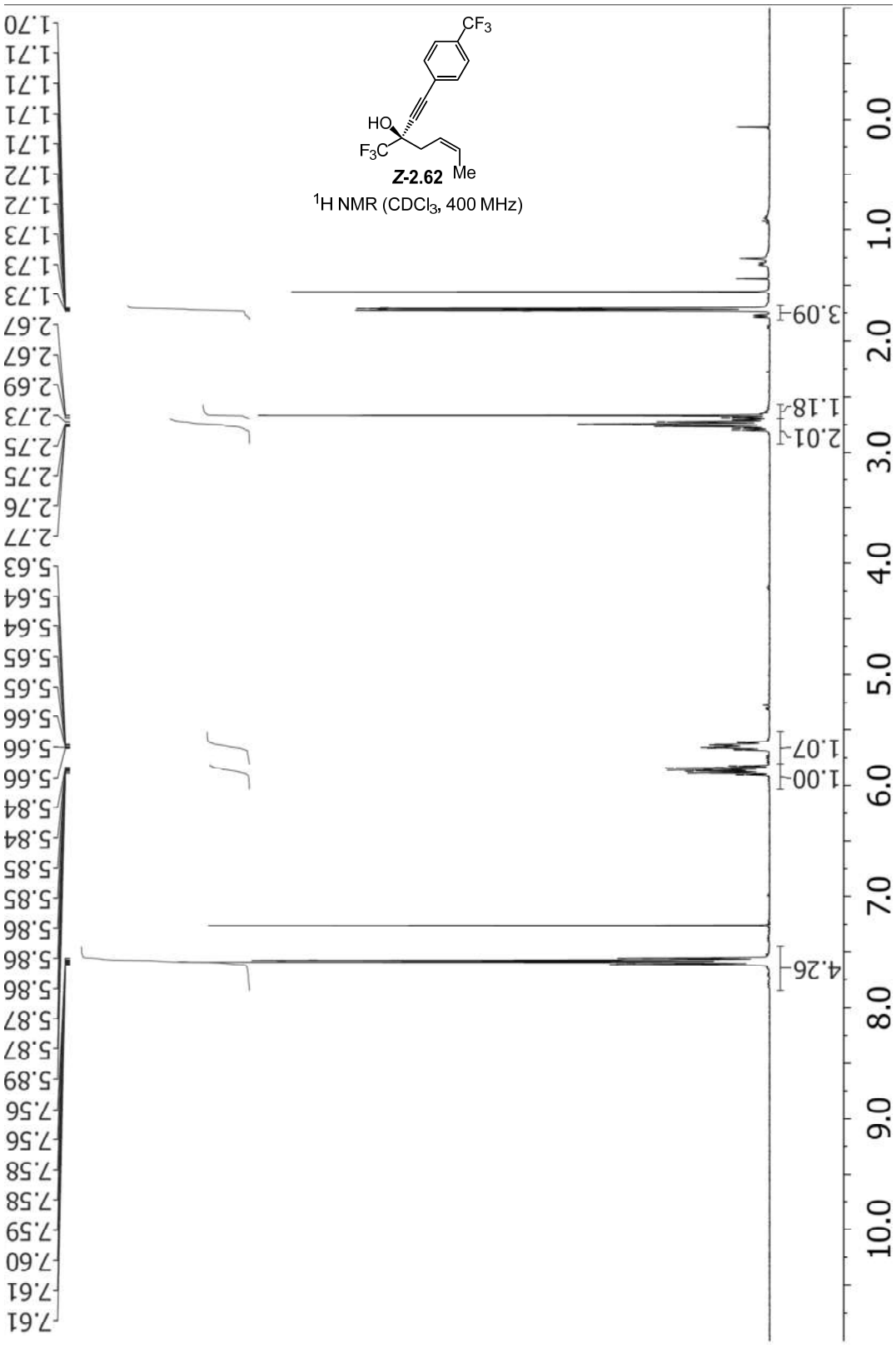
CF3
HO
F3C
Me
Z-2.62
1H NMR (CDCl3, 400 MHz)
3.09
1.18
2.01
1.07
1.00
4.26

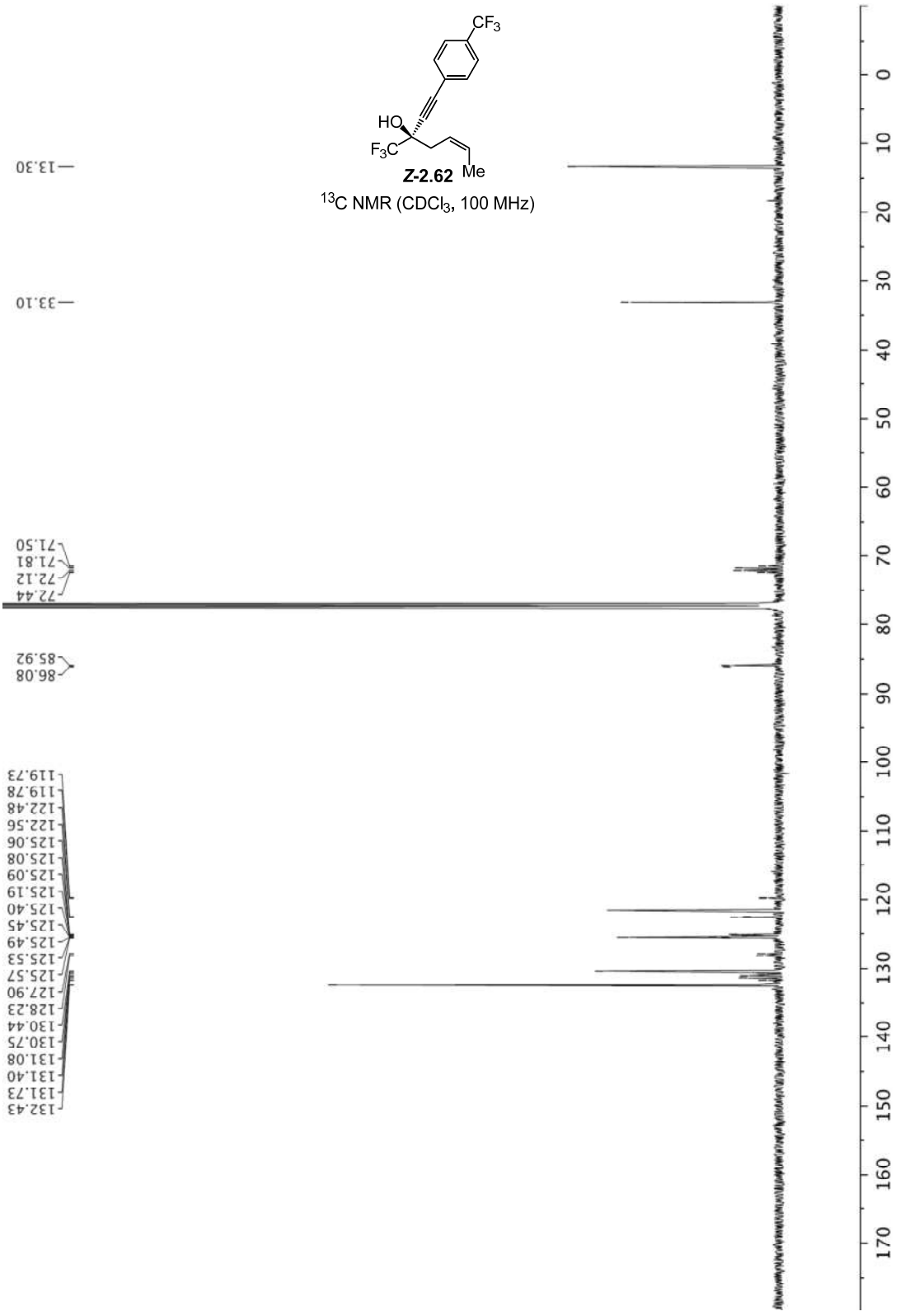
CF3
HO
F3C
Me
Z-2.62
13C NMR (CDCl3, 100 MHz)
13.30
33.10
71.50
71.81
72.12
72.44
85.92
86.08
119.73
119.78
122.48
122.56
125.06
125.08
125.09
125.19
125.40
125.45
125.49
125.53
125.57
127.90
128.23
130.44
130.75
131.08
131.40
131.73
132.43
0
10
20
30
40
50
60
70
80
90
100
110
120
130
140
150
160
170

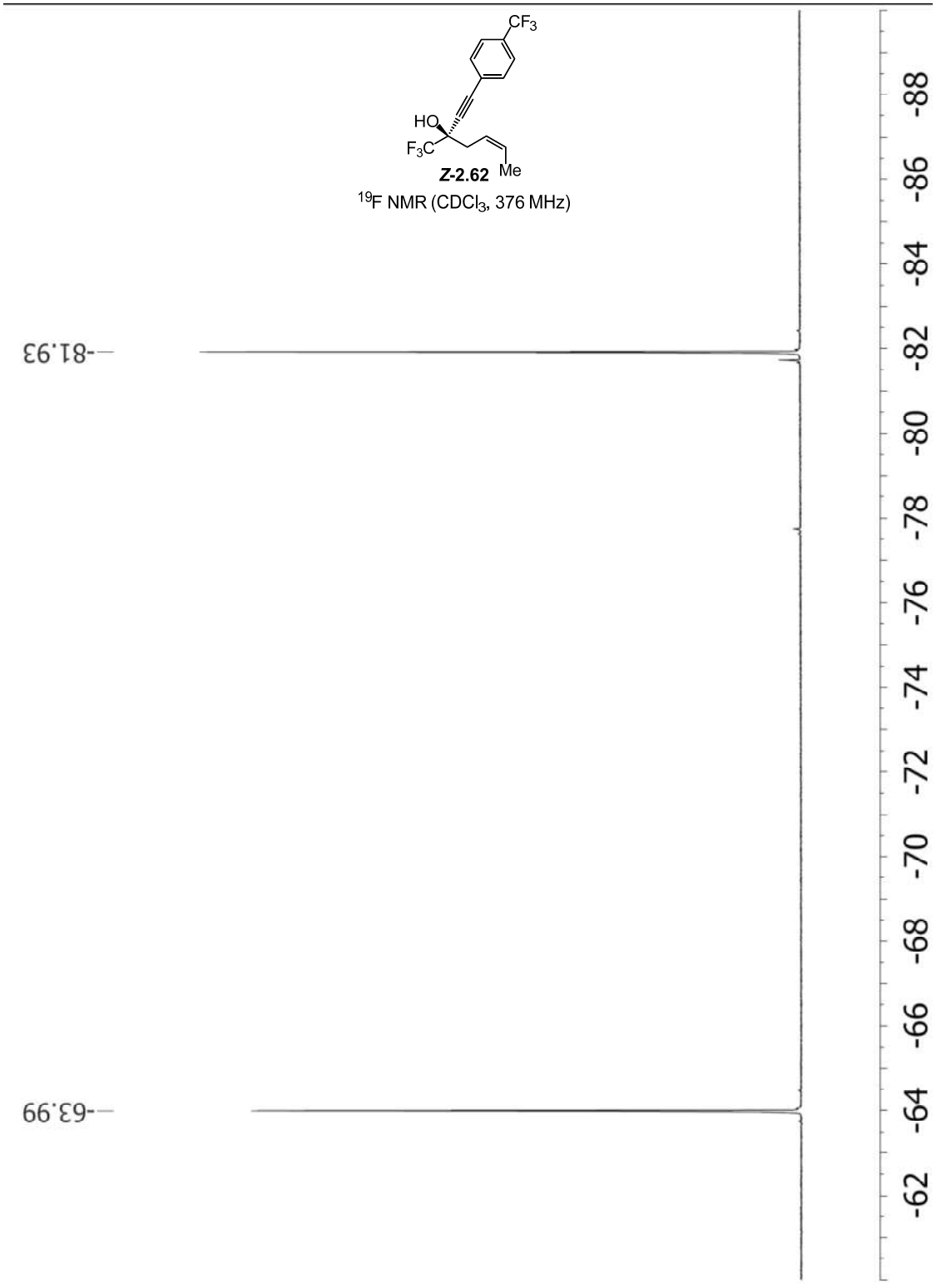
CF3
HO
F3C
Me
Z-2.62
19F NMR (CDCl3, 376 MHz)
-81.93
-63.99
-62
-64
-66
-68
-70
-72
-74
-76
-78
-80
-82
-84
-86
-88

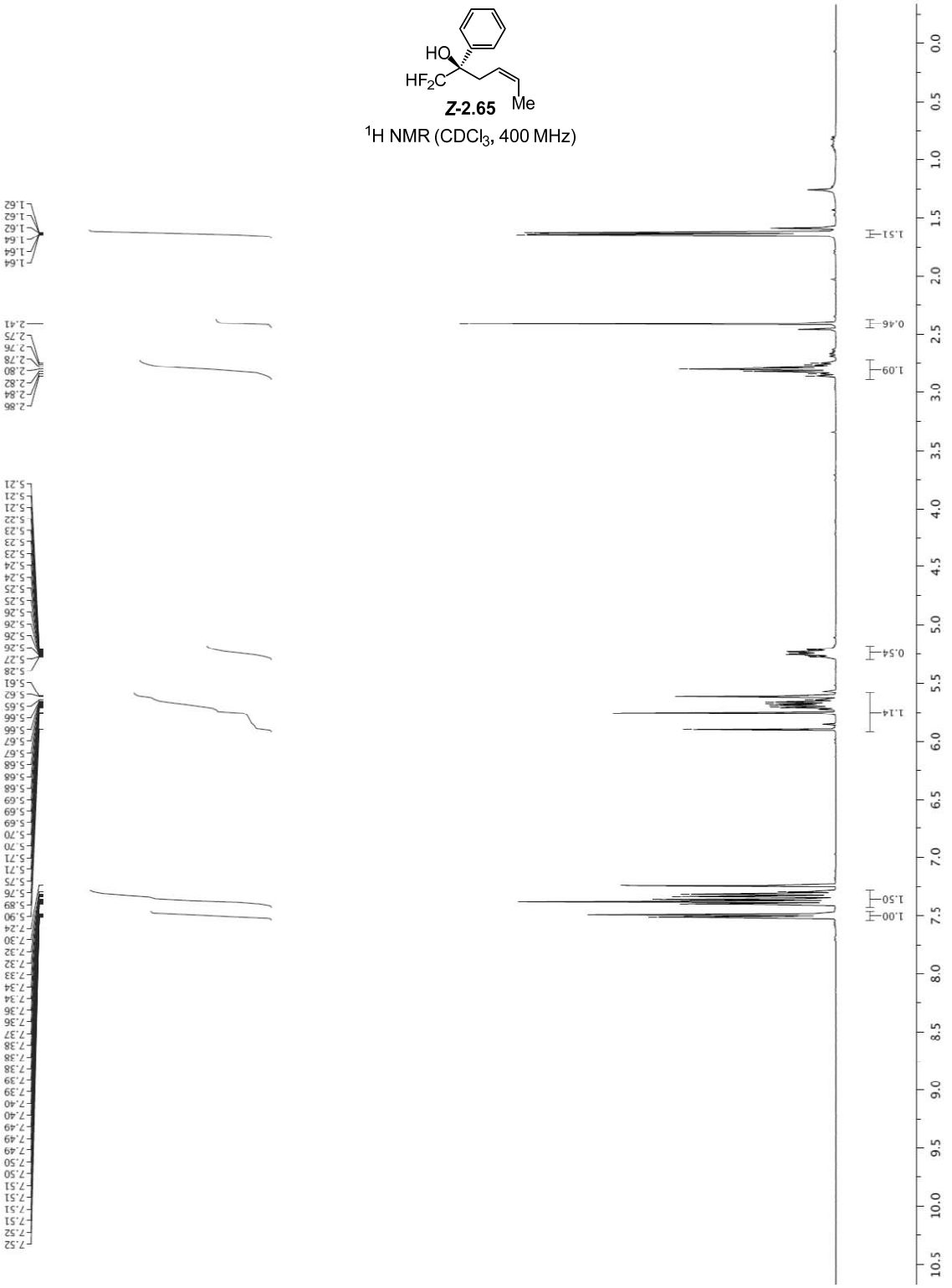
HO
HF2C
Me
Z-2.65
1H NMR (CDCl3, 400 MHz)

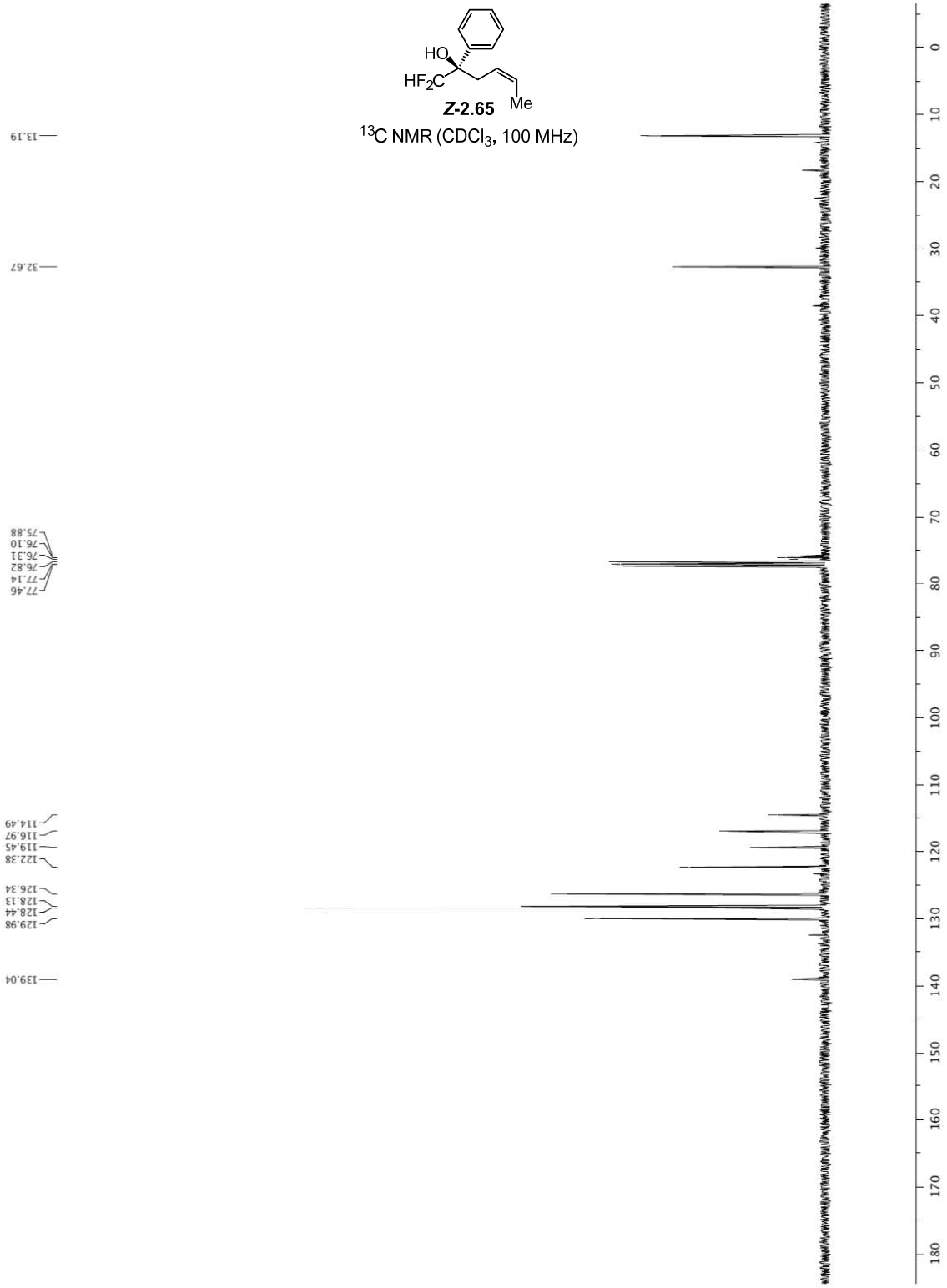
HO
HF2C
Me
Z-2.65
13C NMR (CDCl3, 100 MHz)
13.19
32.67
75.88
76.10
76.31
76.82
77.14
77.46
114.49
116.97
119.45
122.38
126.34
128.13
128.44
129.98
139.04

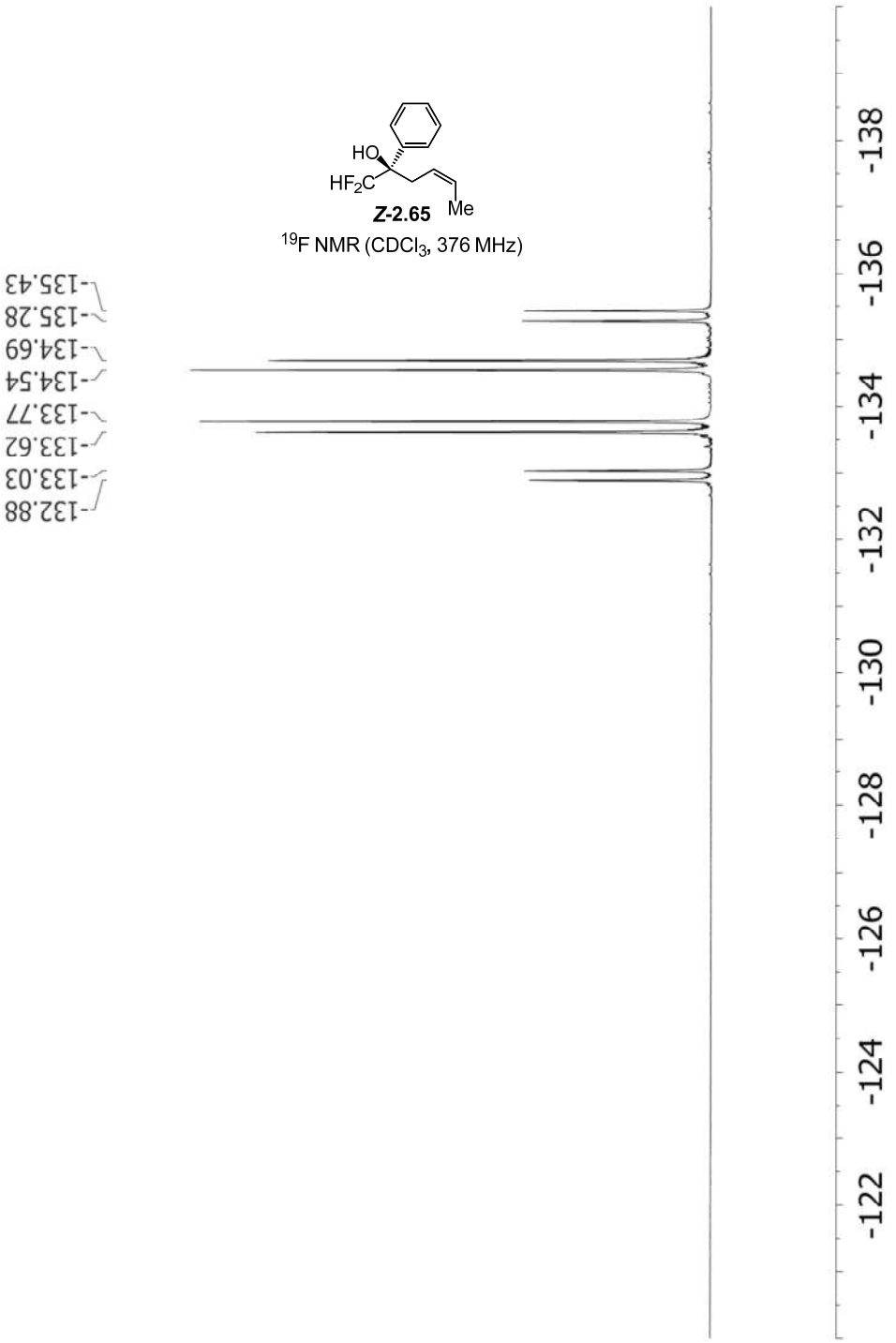
HO
HF2C
Me
Z-2.65
19F NMR (CDCl3, 376 MHz)
-135.43
-135.28
-134.69
-134.54
-133.77
-133.62
-133.03
-132.88
-122
-124
-126
-128
-130
-132
-134
-136
-138

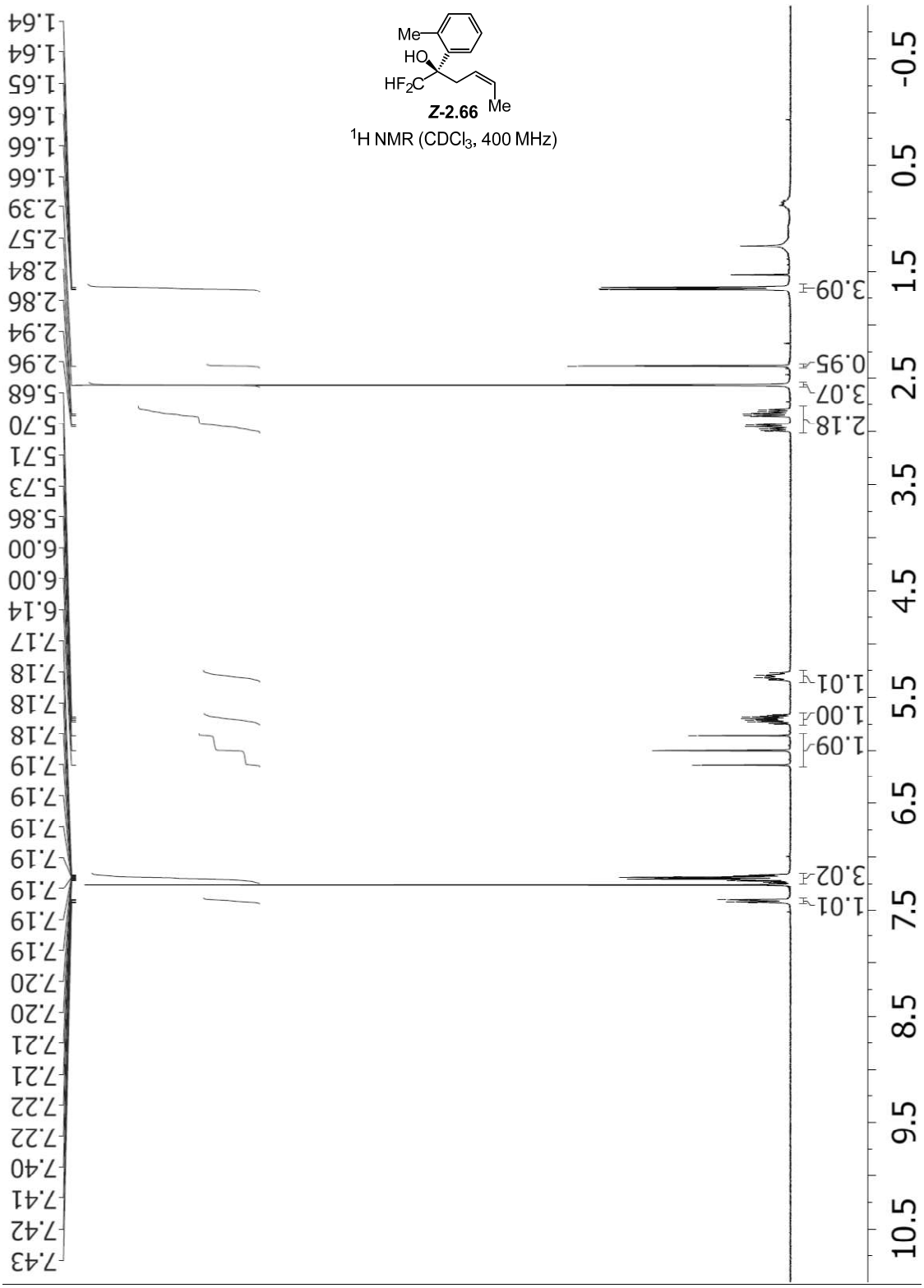
Me
HO
HF2C
Me
Z-2.66
1H NMR (CDCl3, 400 MHz)

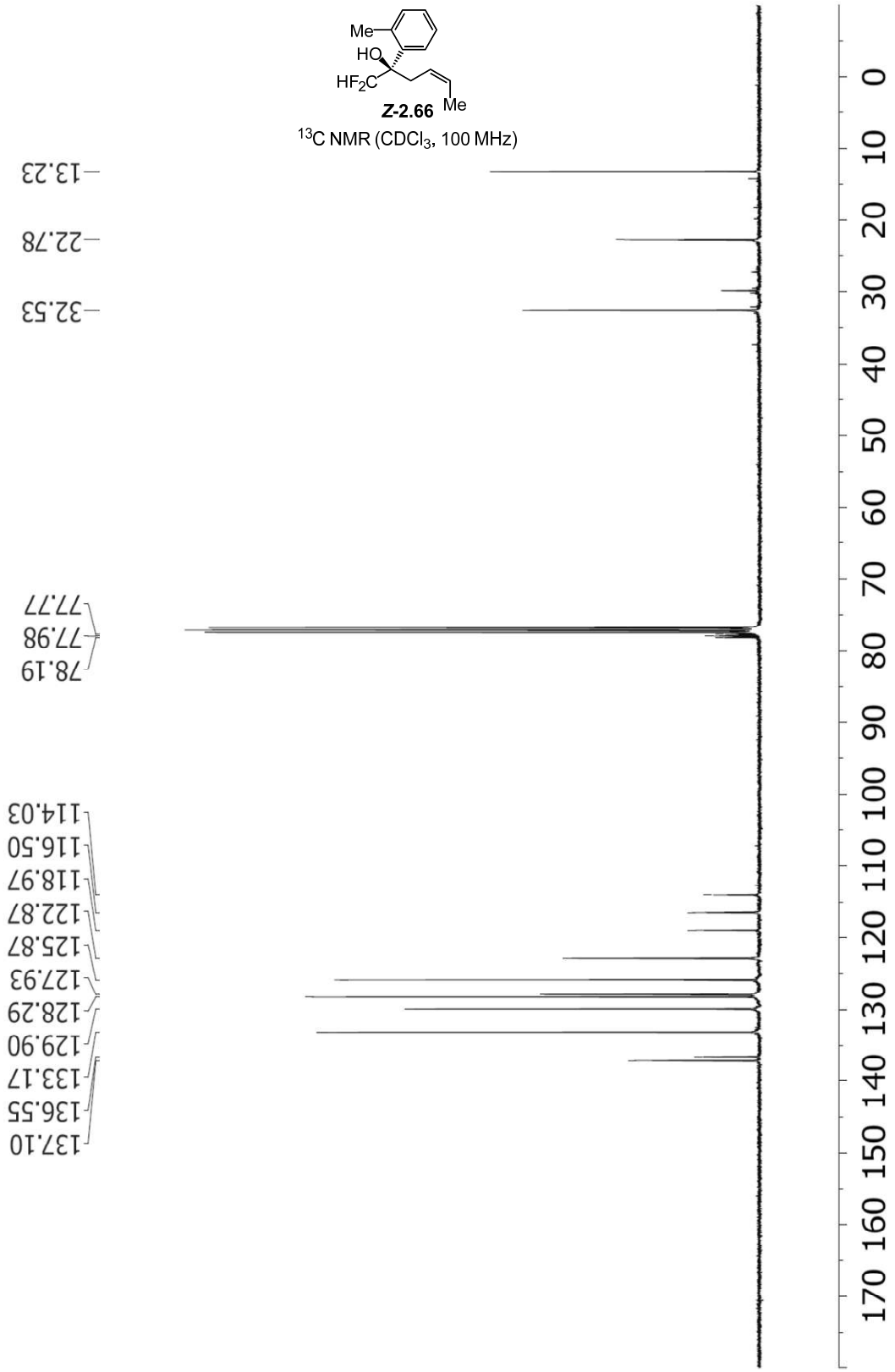
Me
HO
HF2C
Me
Z-2.66
13C NMR (CDCl3, 100 MHz)
13.23
22.78
32.53
77.77
77.98
78.19
114.03
116.50
118.97
122.87
125.87
127.93
128.29
129.90
133.17
136.55
137.10
0
10
20
30
40
50
60
70
80
90
100
110
120
130
140
150
160
170

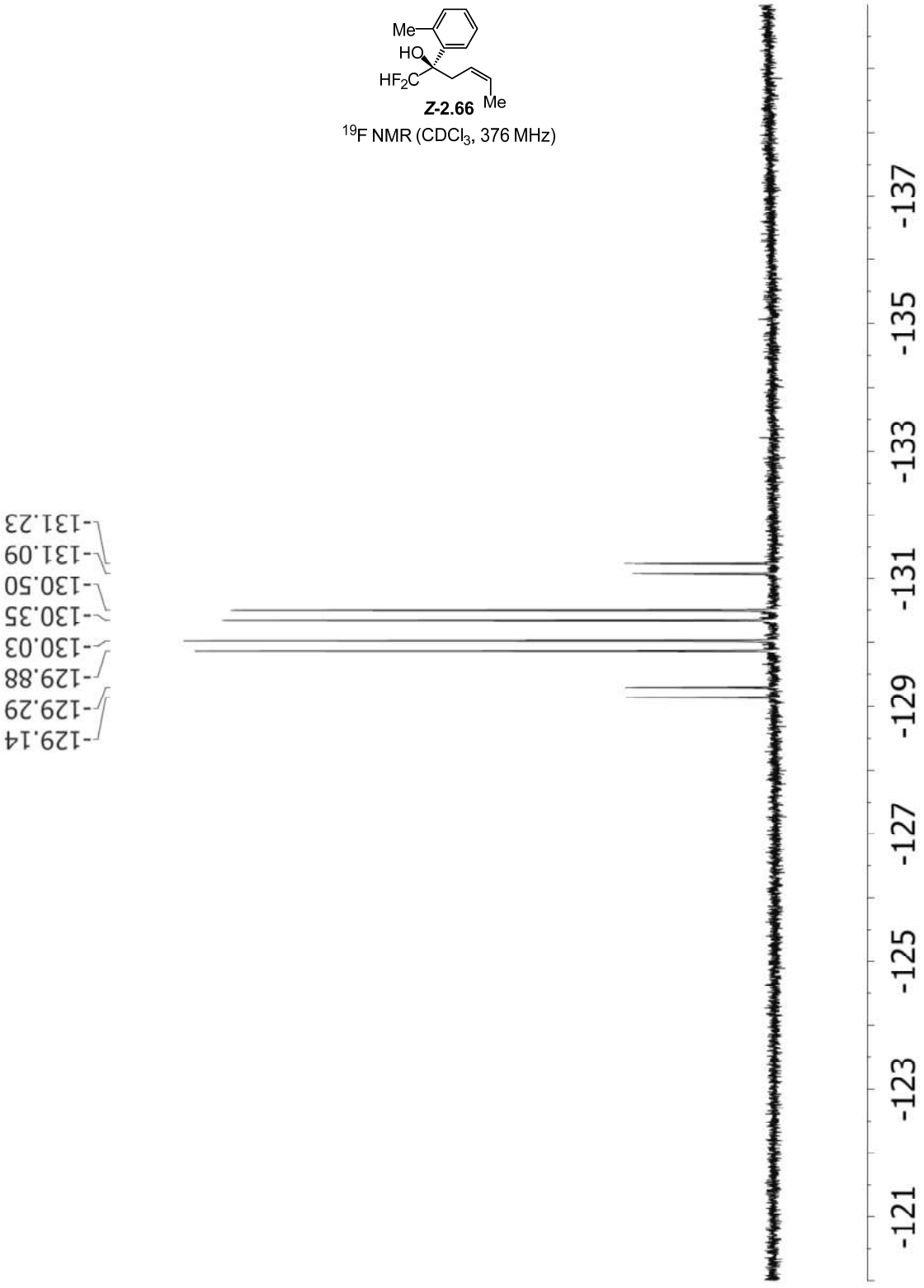
Me
HO
HF2C
Me
Z-2.66
19F NMR (CDCl3, 376 MHz)
-121
-123
-125
-127
-129
-131
-133
-135
-137
-129.14
-129.29
-129.88
-130.03
-130.35
-130.50
-131.09
-131.23

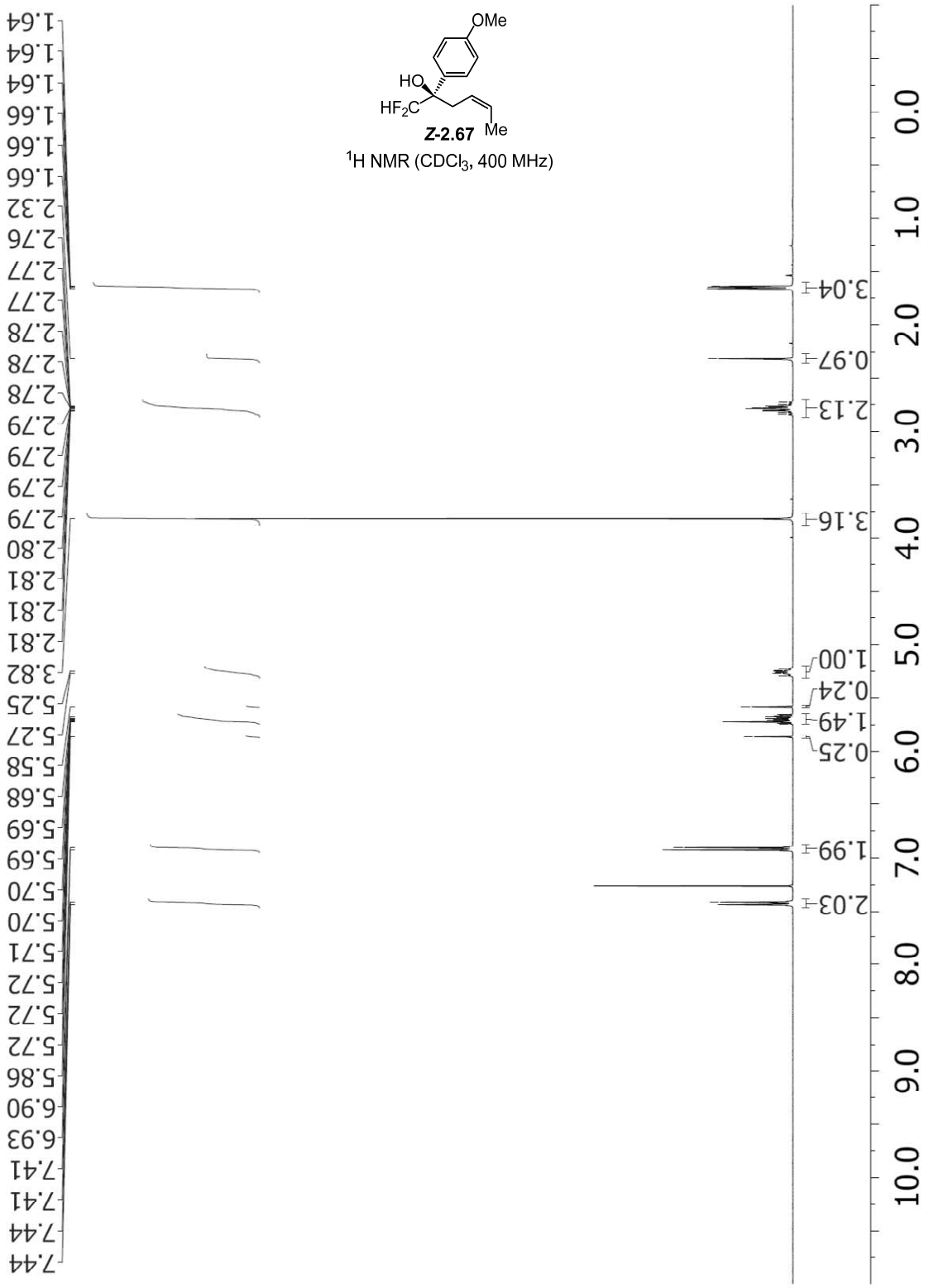
OMe
HO
HF2C
Me
Z-2.67
1H NMR (CDCl3, 400 MHz)

OMe
HO
HF2C
Me
Z-2.67
13C NMR (CDCl3, 100 MHz)
13.24
32.53
55.38
75.66
75.87
76.08
113.83
114.58
117.06
119.54
122.55
127.67
129.88
131.02
159.45
0
10
20
30
40
50
60
70
80
90
100
110
120
130
140
150
160
170

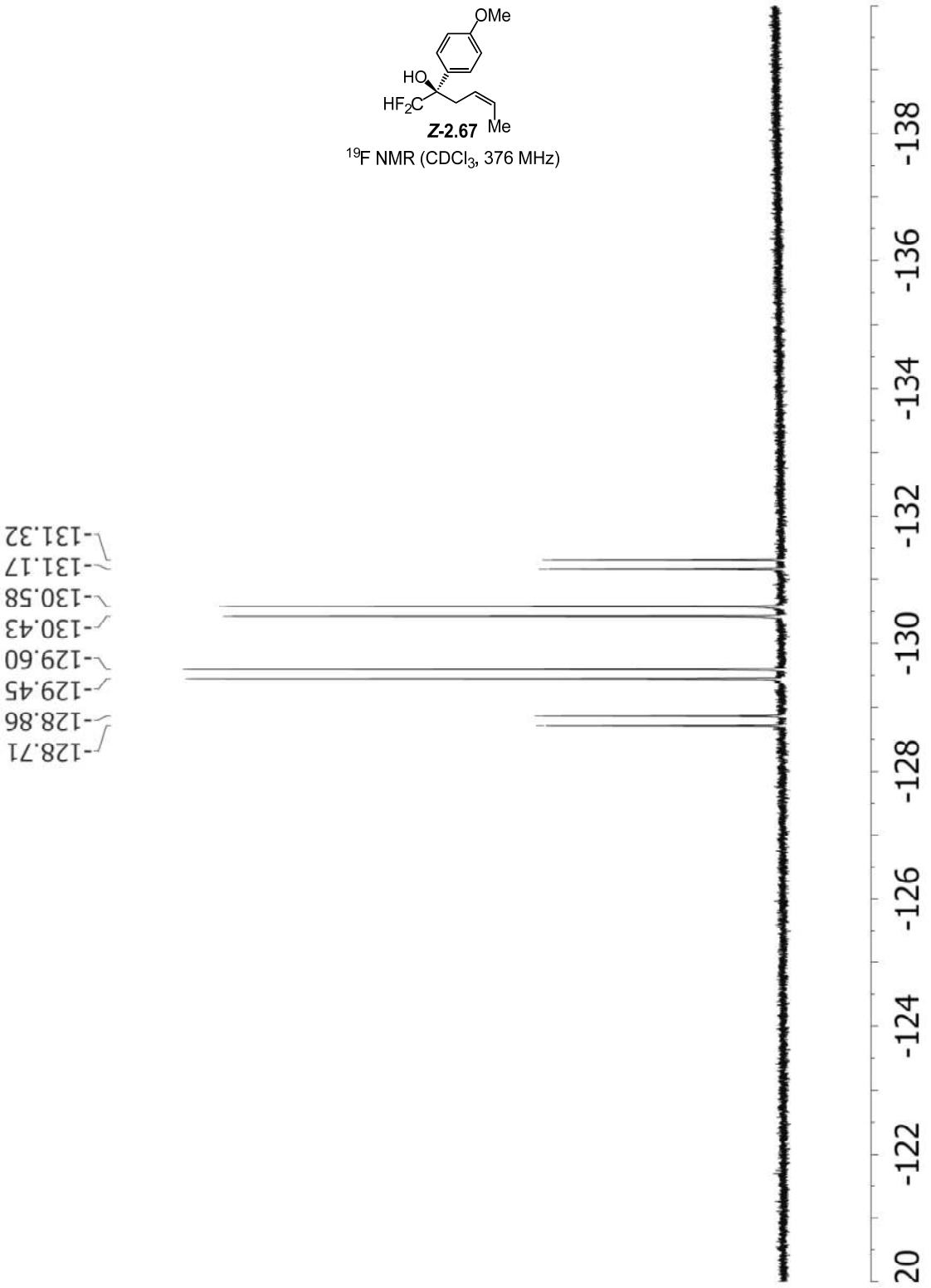
OMe
HO
HF2C
Me
Z-2.67
19F NMR (CDCl3, 376 MHz)
-131.32
-131.17
-130.58
-130.43
-129.60
-129.45
-128.86
-128.71
20
-122
-124
-126
-128
-130
-132
-134
-136
-138

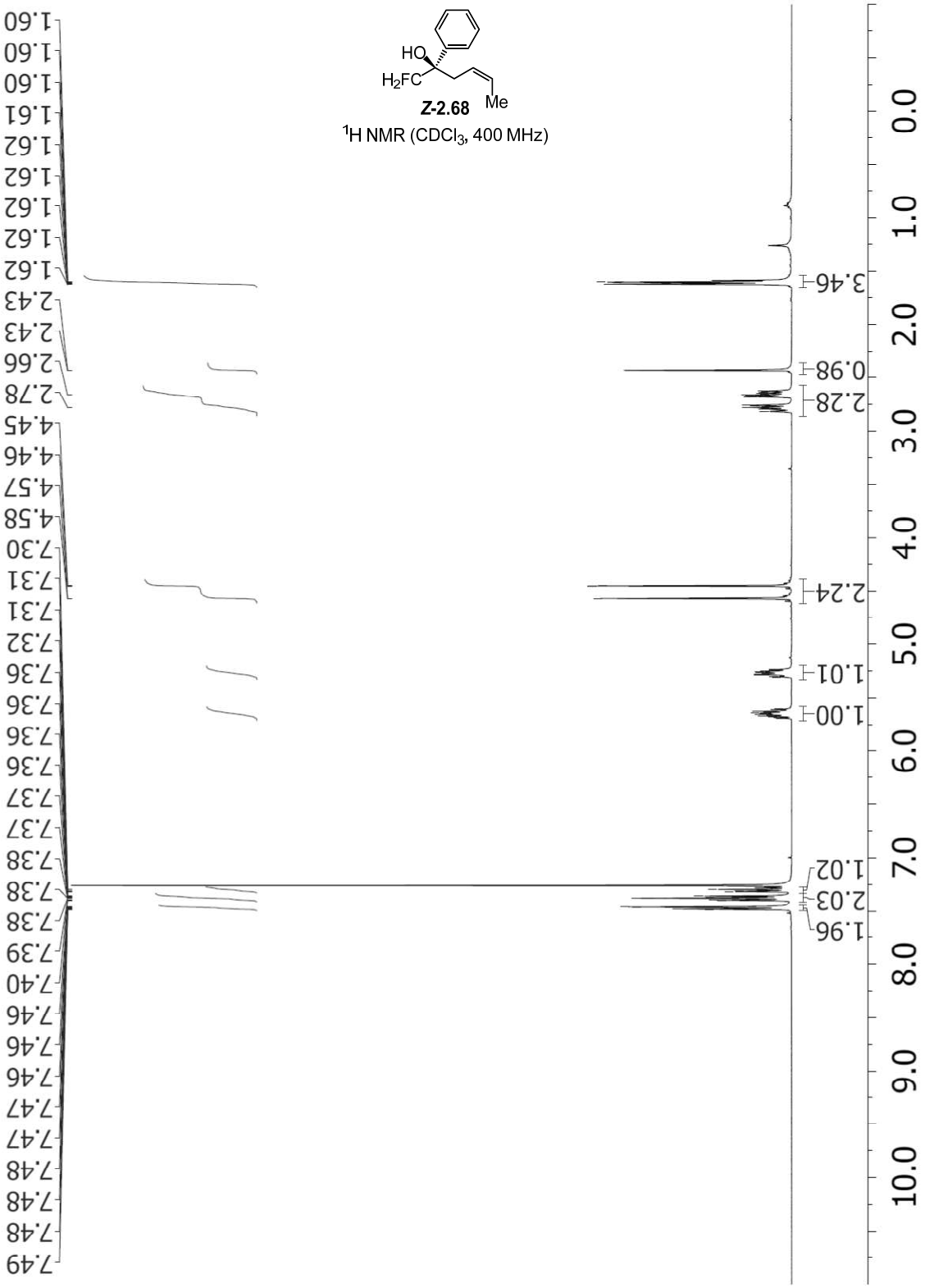
HO
H2FC
Me
Z-2.68
1H NMR (CDCl3, 400 MHz)
3.46
0.98
2.28
2.24
1.01
1.00
1.02
2.03
1.96

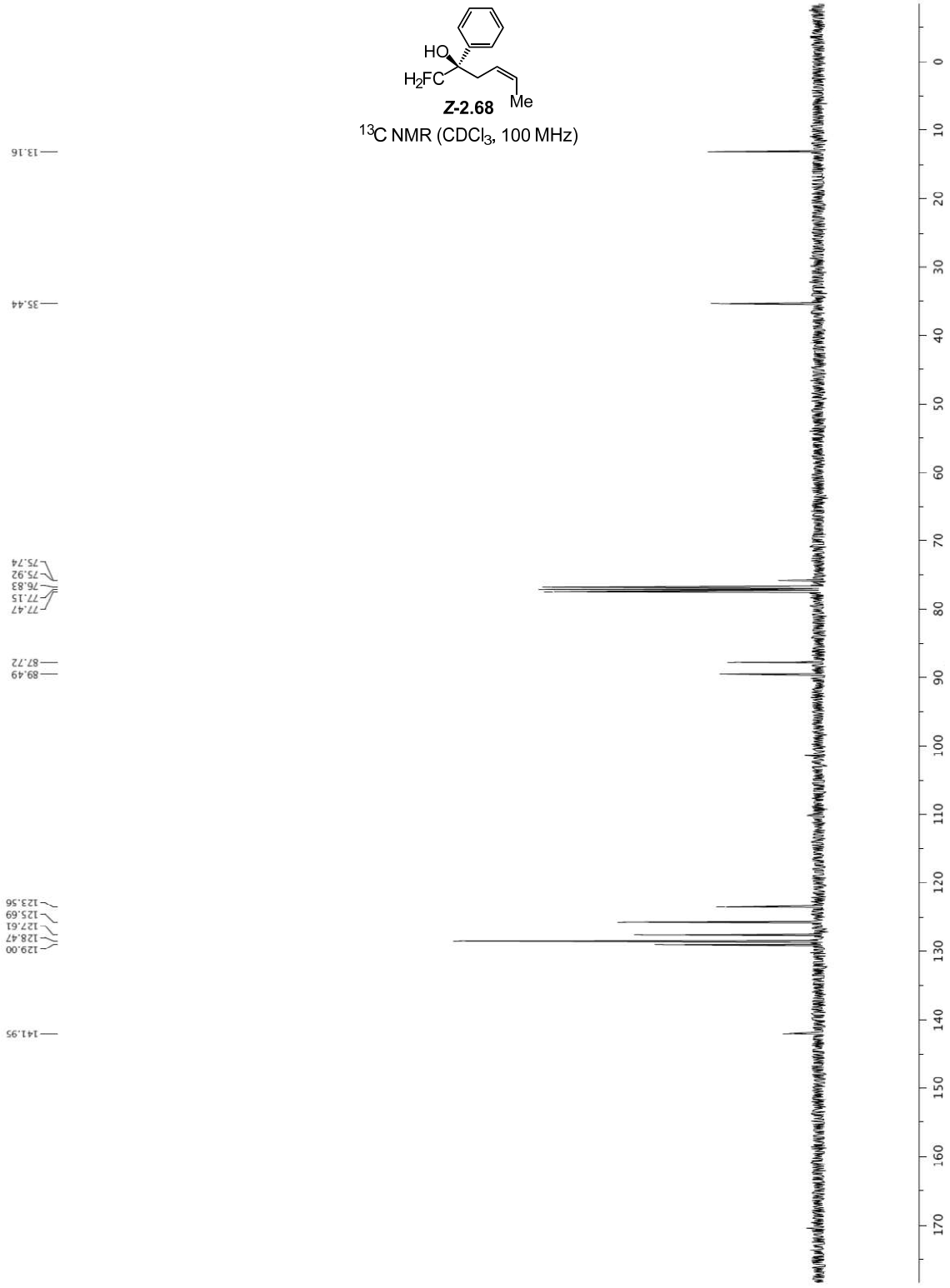
HO
H2FC
Me
Z-2.68
13C NMR (CDCl3, 100 MHz)
13.16
35.44
75.74
75.92
76.83
77.15
77.47
87.72
89.49
123.56
125.69
127.61
128.47
129.00
141.95

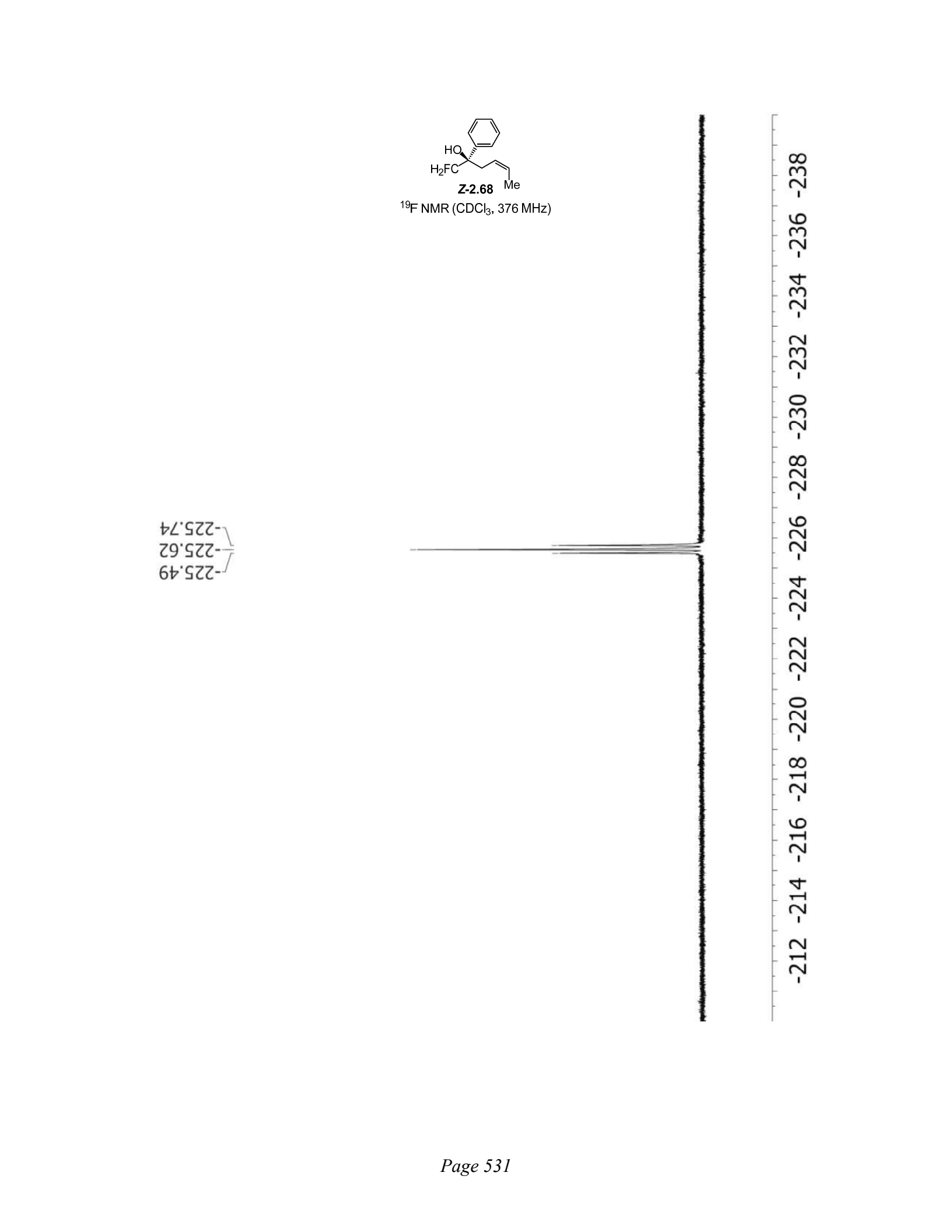
HO
H2FC
Me
Z-2.68
19F NMR (CDCl3, 376 MHz)
-225.49
-225.62
-225.74
-212 -214 -216 -218 -220 -222 -224 -226 -228 -230 -232 -234 -236 -238

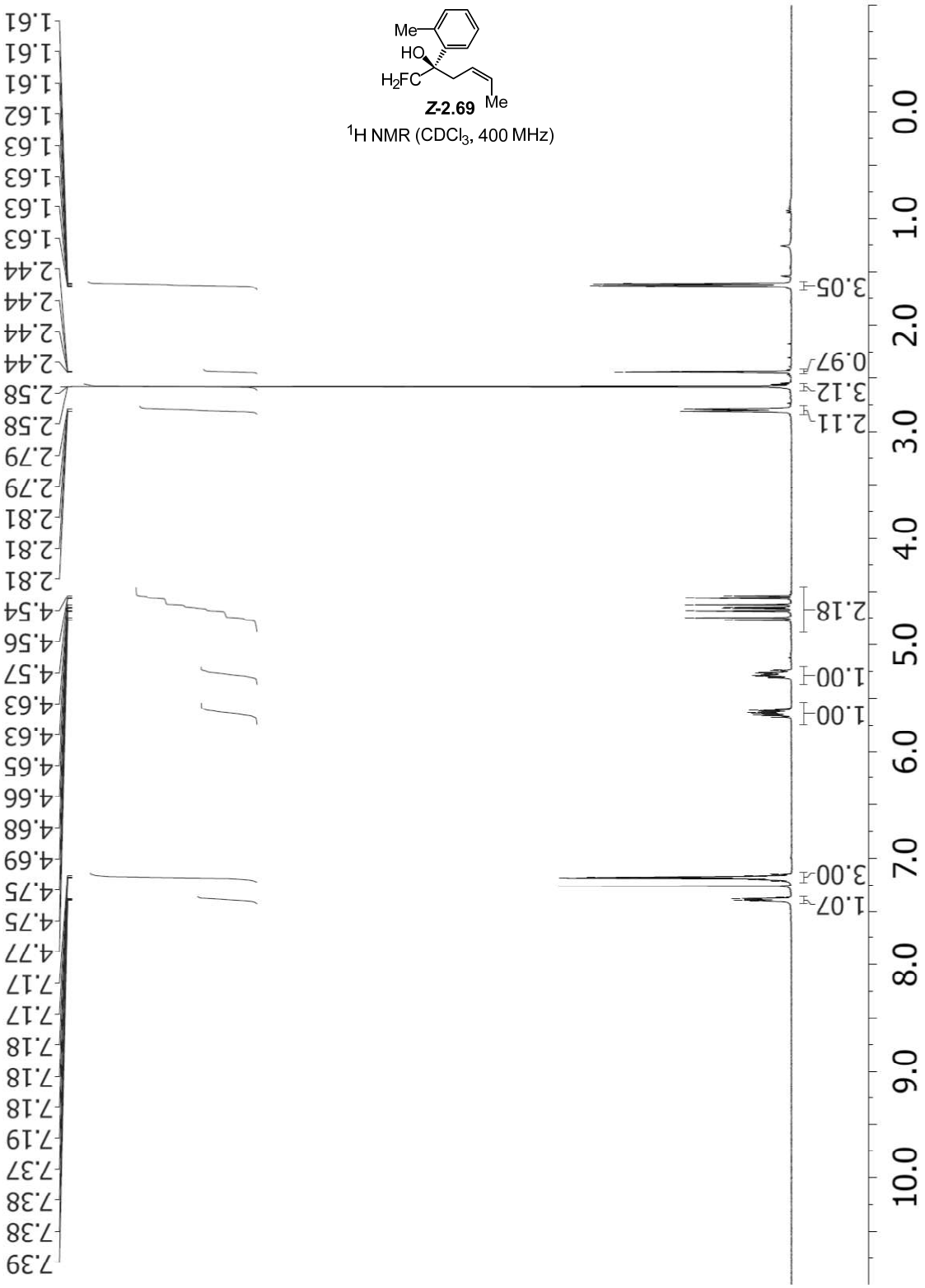
Me
HO
H2FC
Me
Z-2.69
1H NMR (CDCl3, 400 MHz)

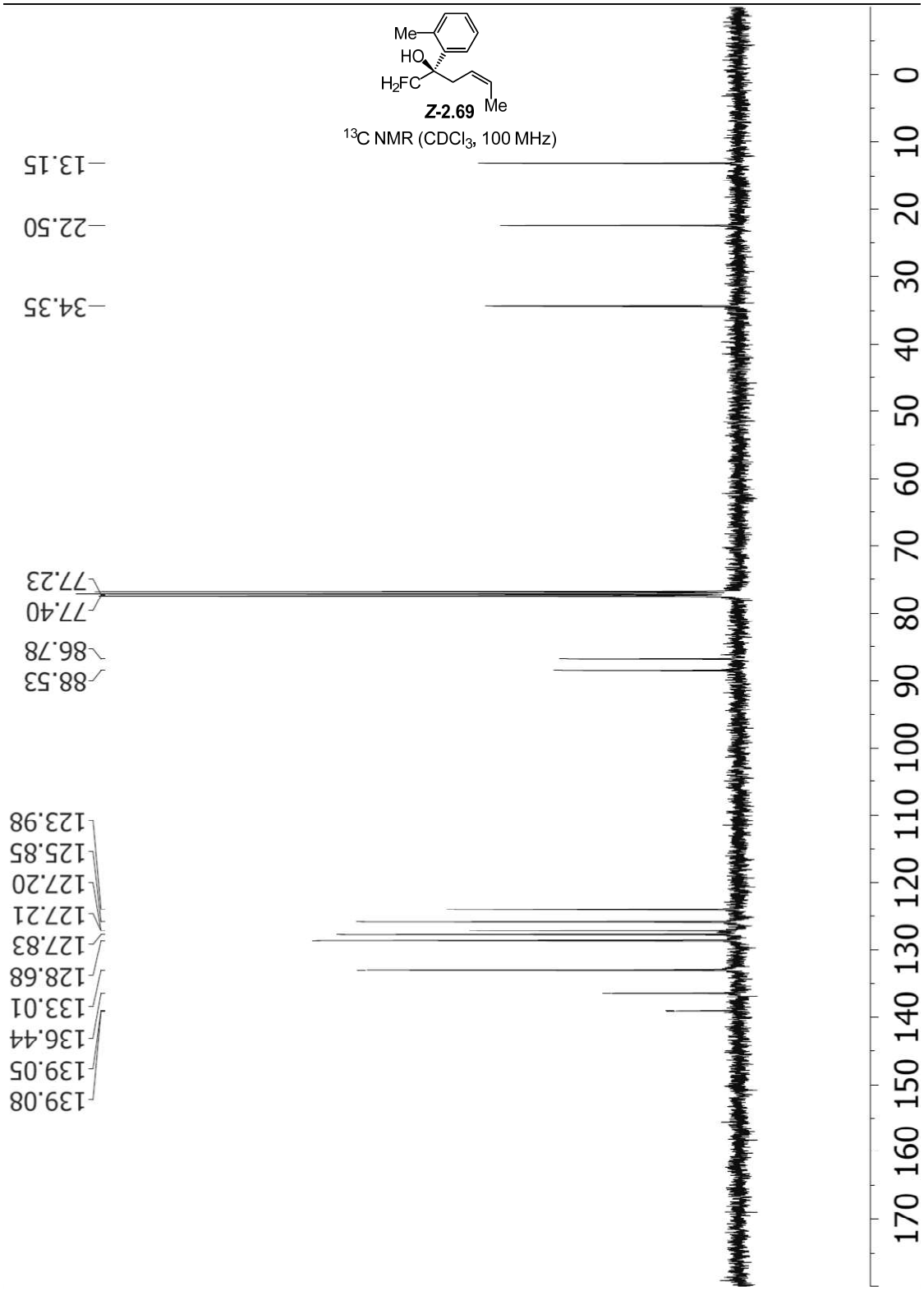
Me
HO
H2FC
Me
Z-2.69
13C NMR (CDCl3, 100 MHz)
13.15
22.50
34.35
77.23
77.40
86.78
88.53
123.98
125.85
127.20
127.21
127.83
128.68
133.01
136.44
139.05
139.08
0
10
20
30
40
50
60
70
80
90
100
110
120
130
140
150
160
170

***Z*-2.69**

^{19}F NMR ($CDCl_3$, 376 MHz)

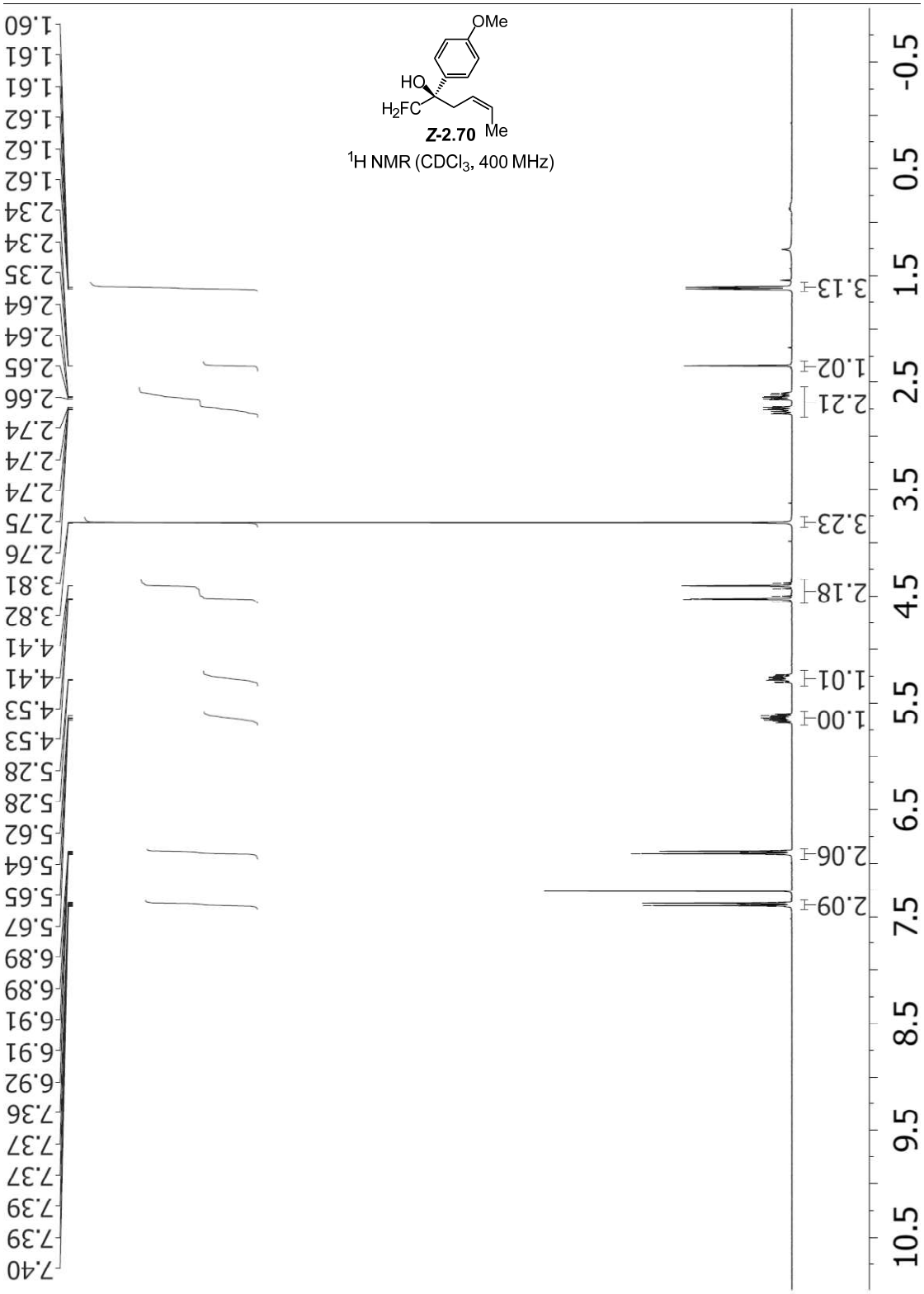
OMe
HO
H2FC
Me
Z-2.70
1H NMR (CDCl3, 400 MHz)

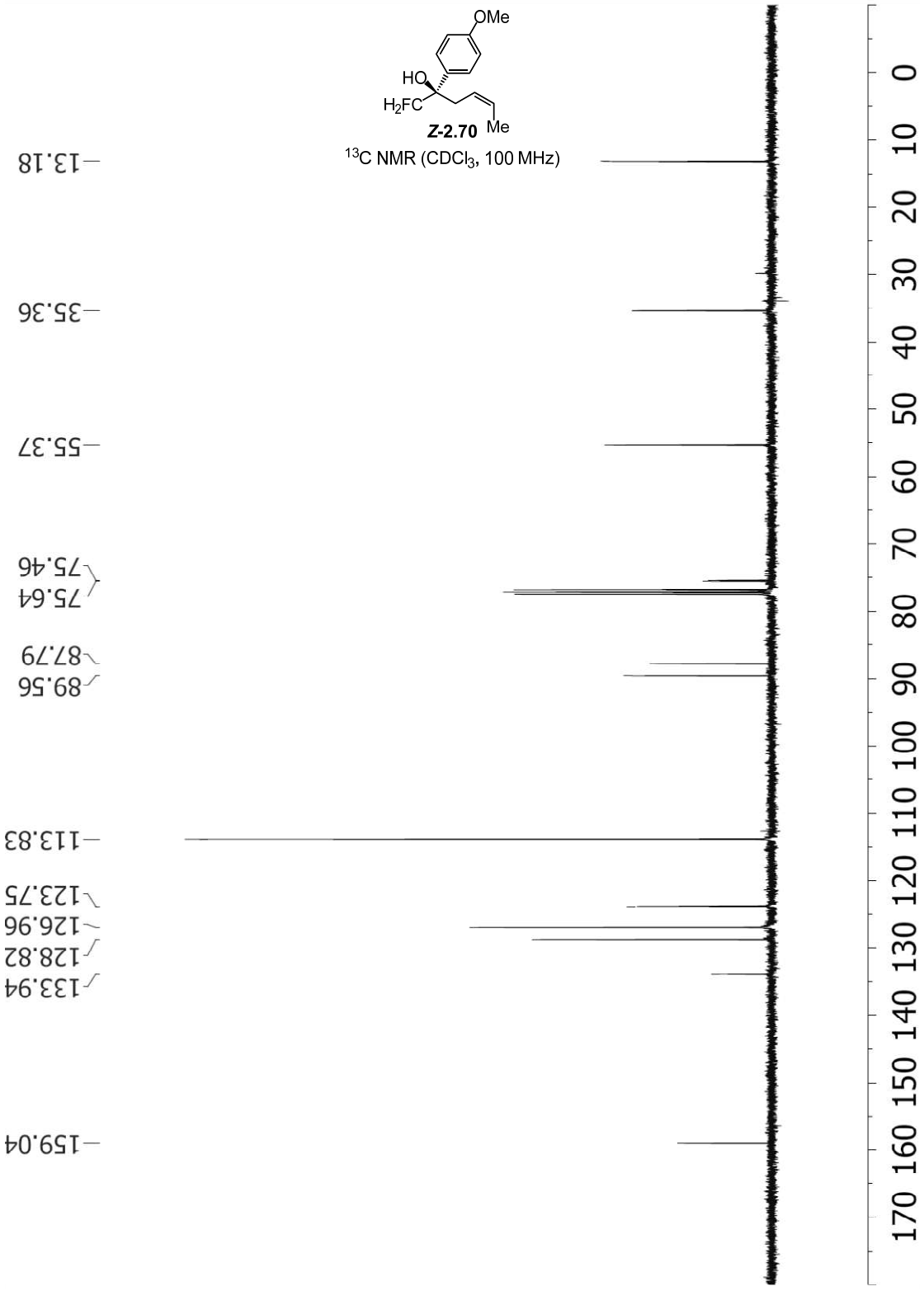
OMe
HO
H2FC
Me
Z-2.70
13C NMR (CDCl3, 100 MHz)
13.18
35.36
55.37
75.46
75.64
87.79
89.56
113.83
123.75
126.96
128.82
133.94
159.04
0 10 20 30 40 50 60 70 80 90 100 110 120 130 140 150 160 170

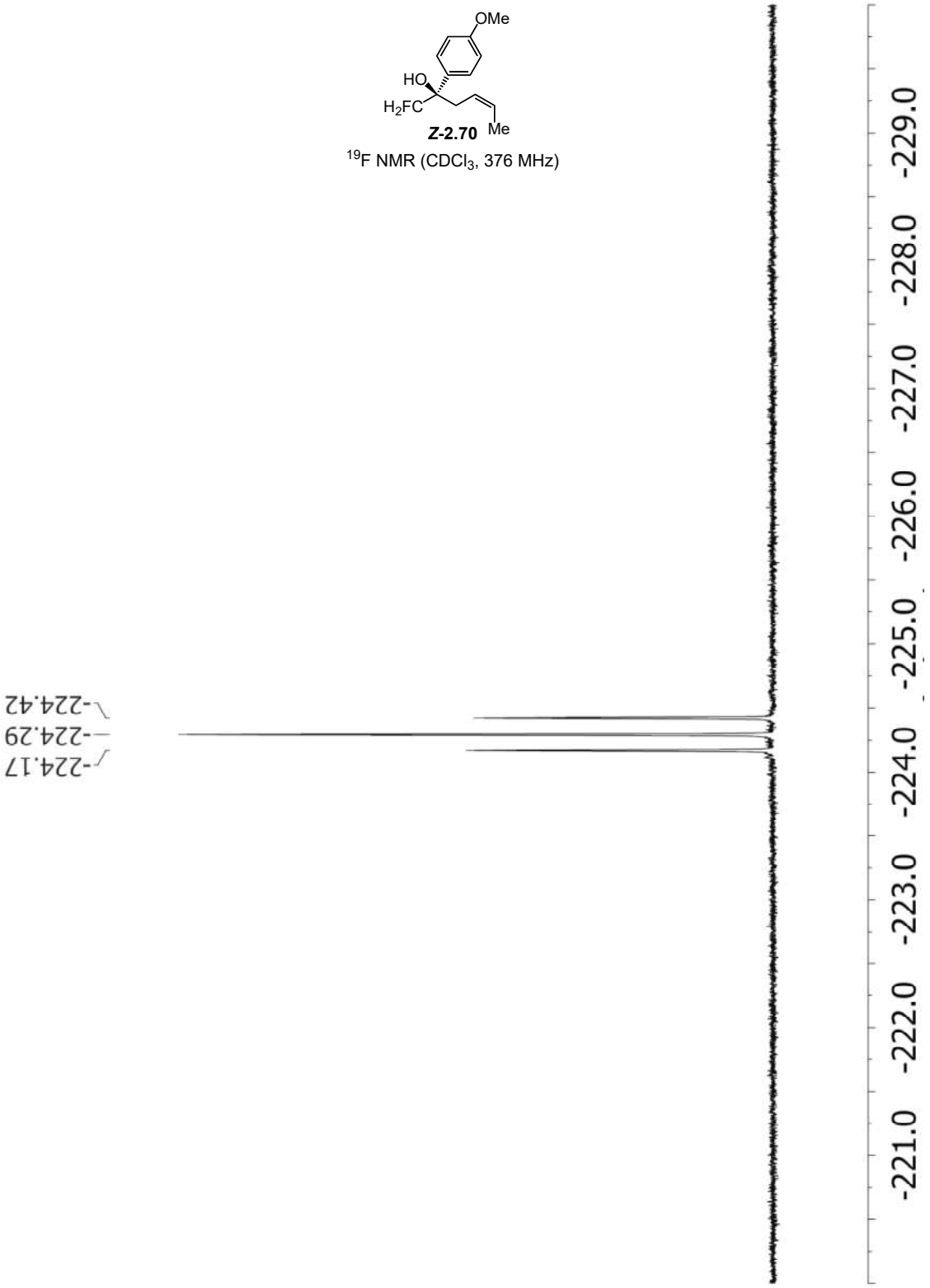
OMe
HO
H2FC
Me
Z-2.70
19F NMR (CDCl3, 376 MHz)
-224.42
-224.29
-224.17
-221.0
-222.0
-223.0
-224.0
-225.0
-226.0
-227.0
-228.0
-229.0

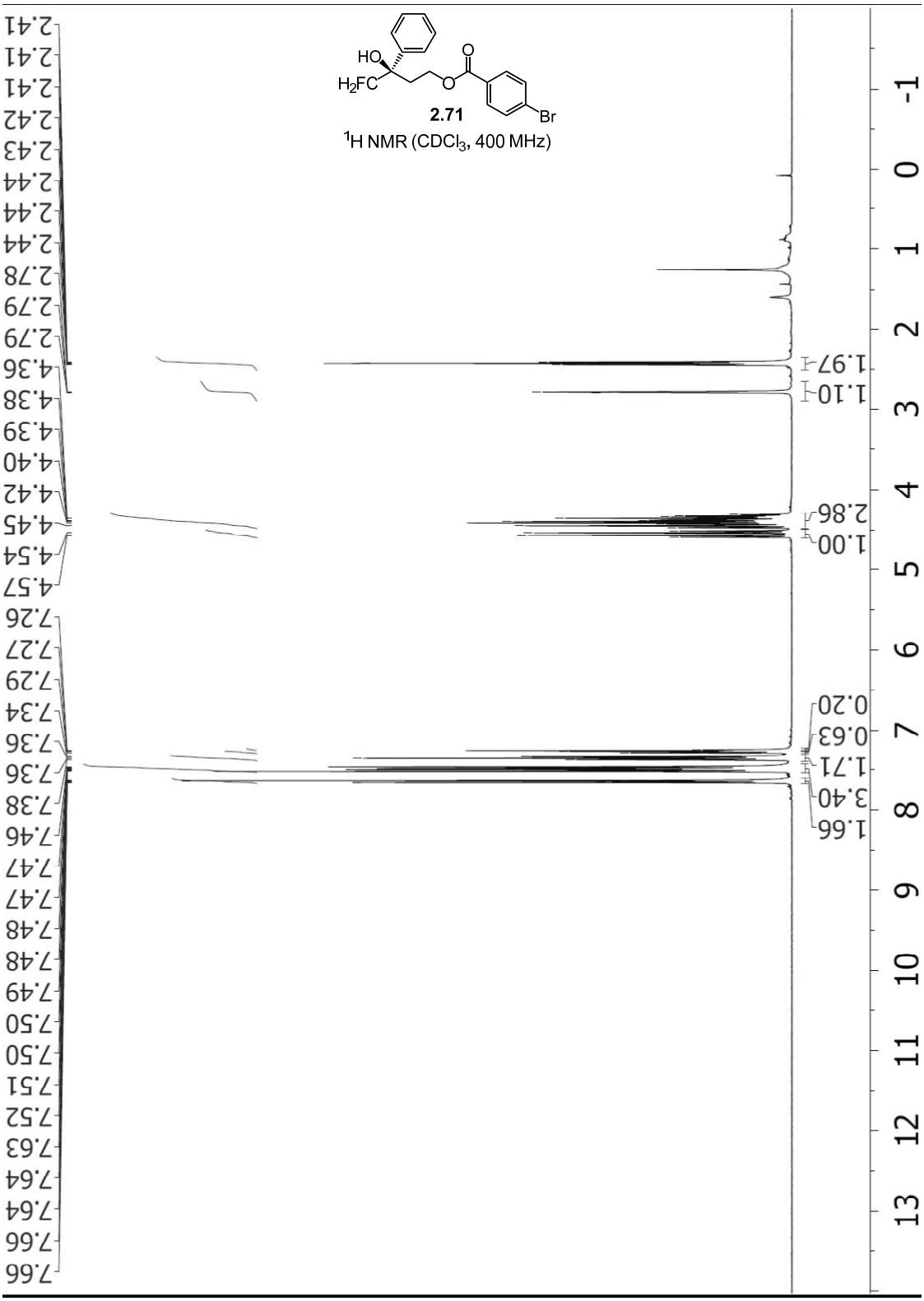
HO
H2FC
O
O
Br
2.71
1H NMR (CDCl3, 400 MHz)
1.97
1.10
2.86
1.00
0.20
0.63
1.71
3.40
1.66

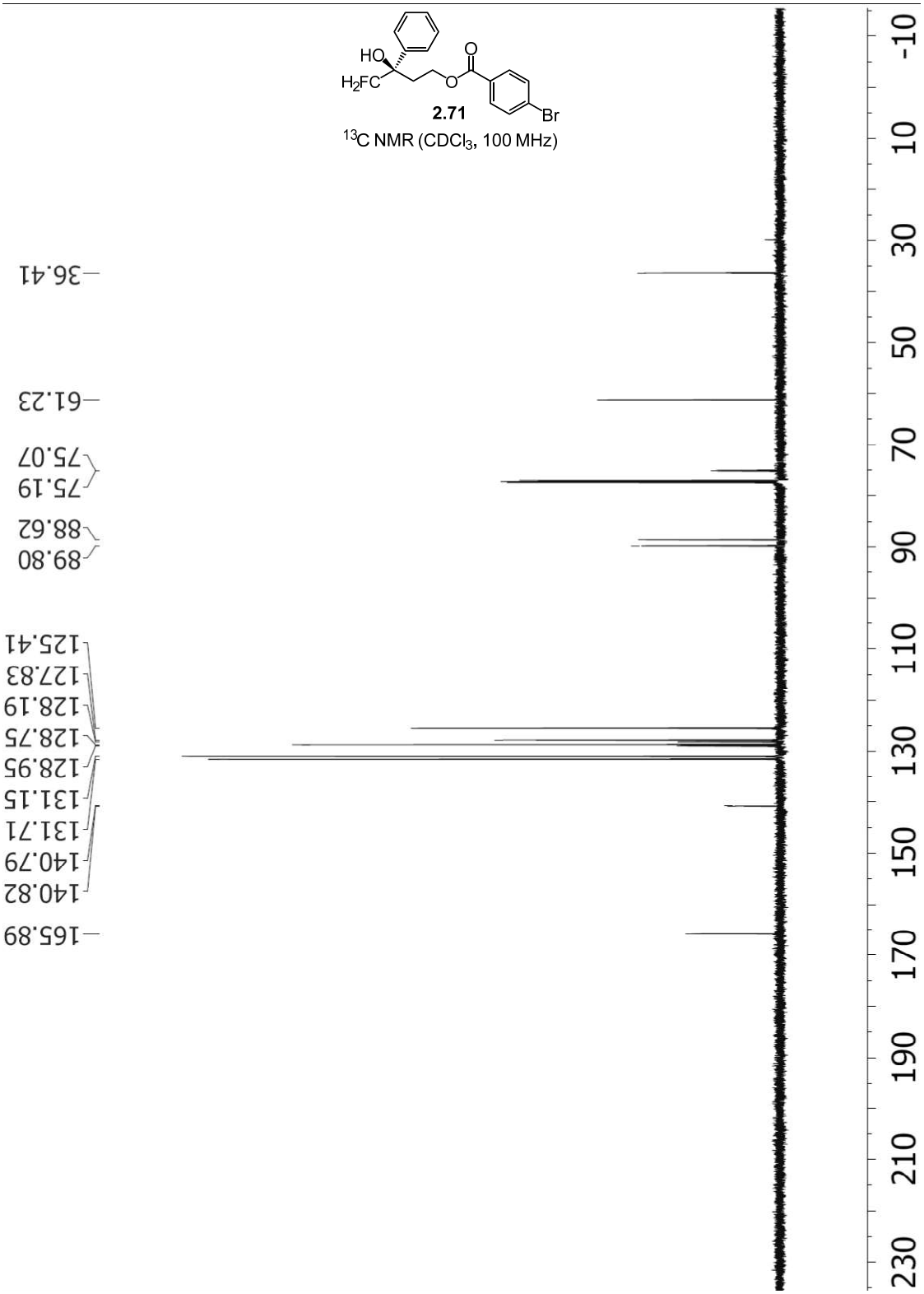
HO
H2FC
O
O
Br
2.71
13C NMR (CDCl3, 100 MHz)
36.41
61.23
75.07
75.19
88.62
89.80
125.41
127.83
128.19
128.75
128.95
131.15
131.71
140.79
140.82
165.89
-10
10
30
50
70
90
110
130
150
170
190
210
230

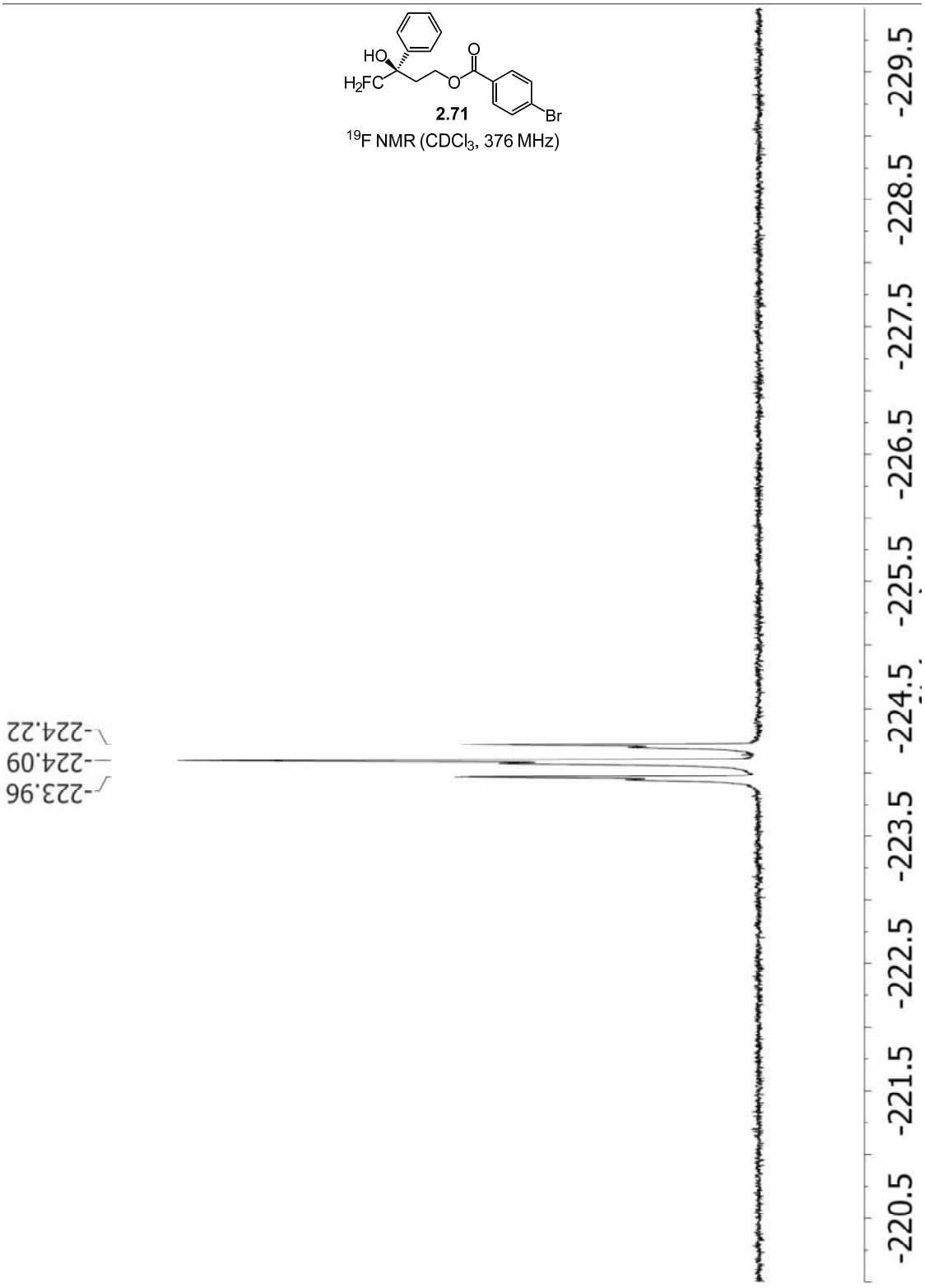
HO
H2FC
O
O
Br
2.71
19F NMR (CDCl3, 376 MHz)
-223.96
-224.09
-224.22
-220.5
-221.5
-222.5
-223.5
-224.5
-225.5
-226.5
-227.5
-228.5
-229.5

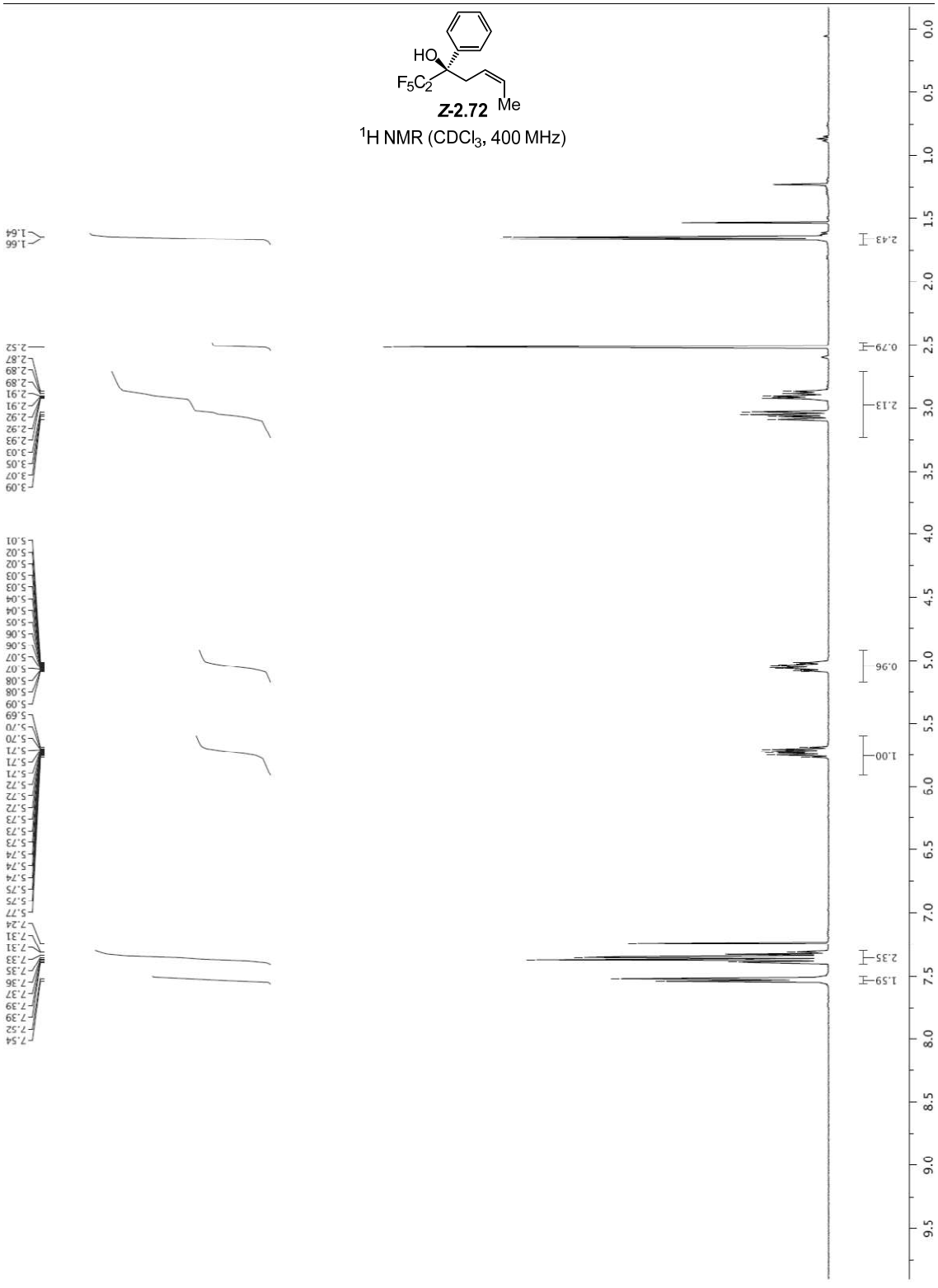
HO
F5C2
Me
Z-2.72
1H NMR (CDCl3, 400 MHz)

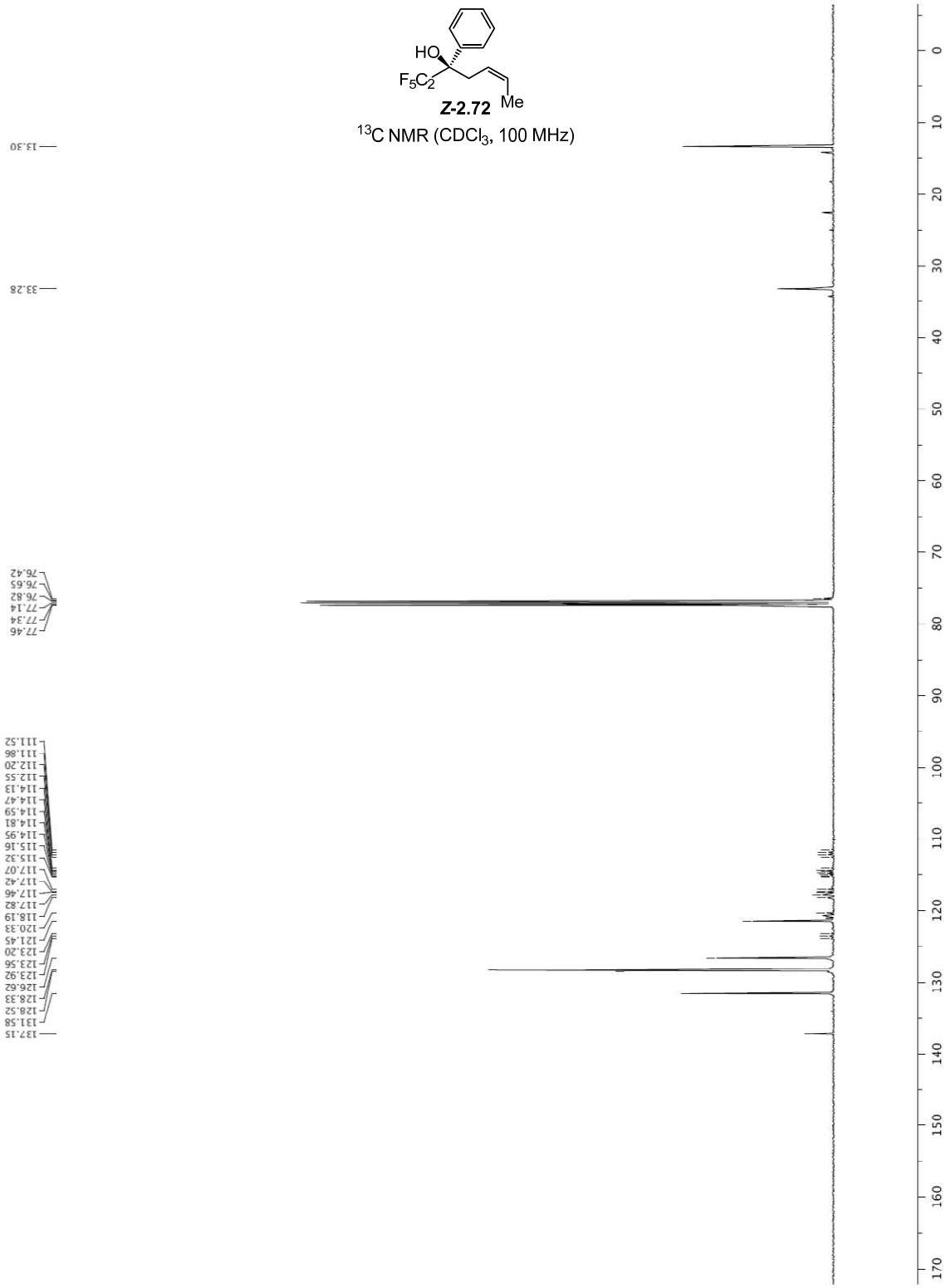
HO
F5C2
Me
Z-2.72
13C NMR (CDCl3, 100 MHz)
13.30
33.28
76.42
76.65
76.82
77.14
77.34
77.46
111.52
111.86
112.20
112.55
114.13
114.47
114.59
114.81
114.95
115.16
115.32
117.07
117.42
117.46
117.82
118.19
120.33
121.45
123.20
123.56
123.92
126.62
128.33
128.52
131.58
137.15
0
10
20
30
40
50
60
70
80
90
100
110
120
130
140
150
160
170

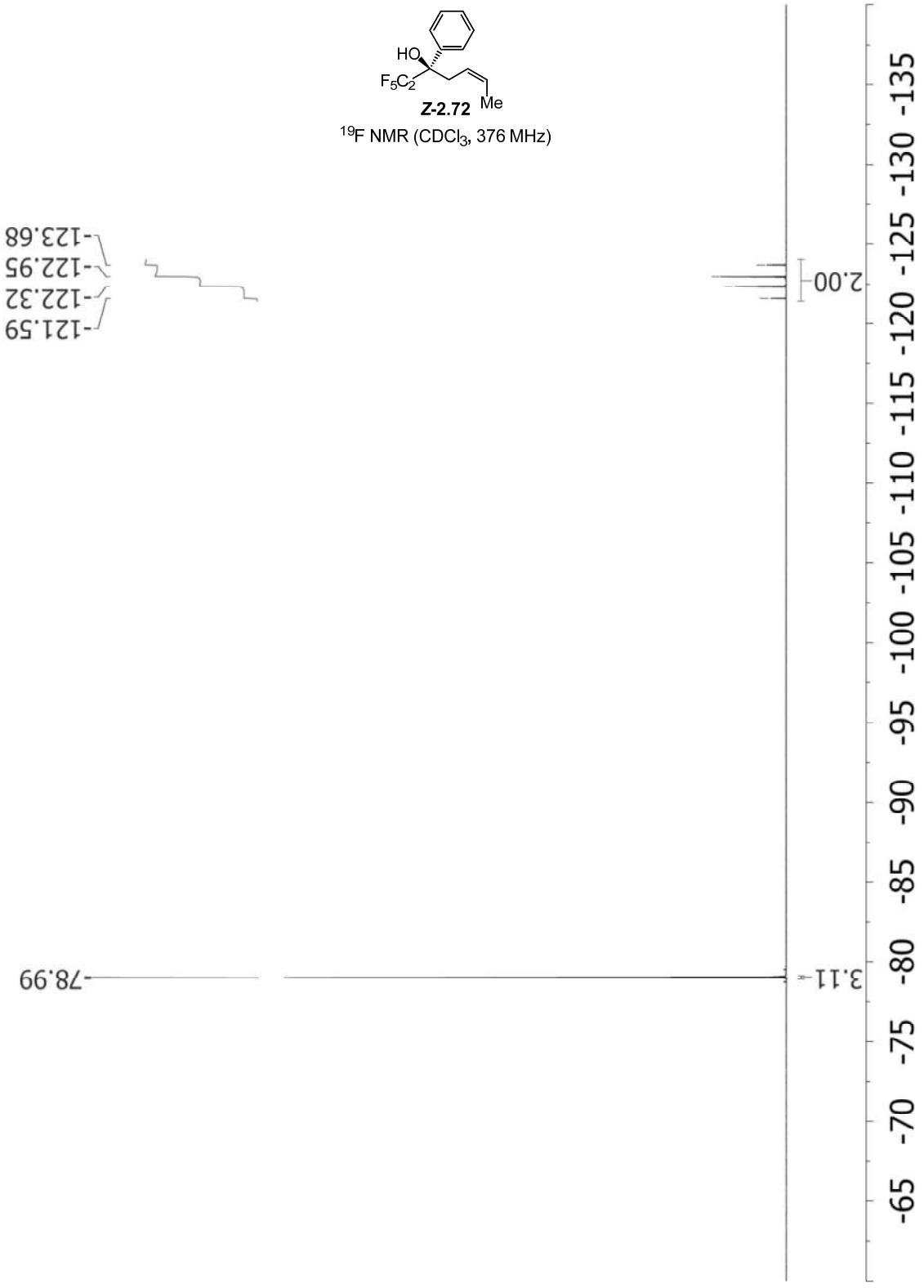
HO
F5C2
Me
Z-2.72
19F NMR (CDCl3, 376 MHz)
-123.68
-122.95
-122.32
-121.59
-78.99
2.00
3.11
-65 -70 -75 -80 -85 -90 -95 -100 -105 -110 -115 -120 -125 -130 -135

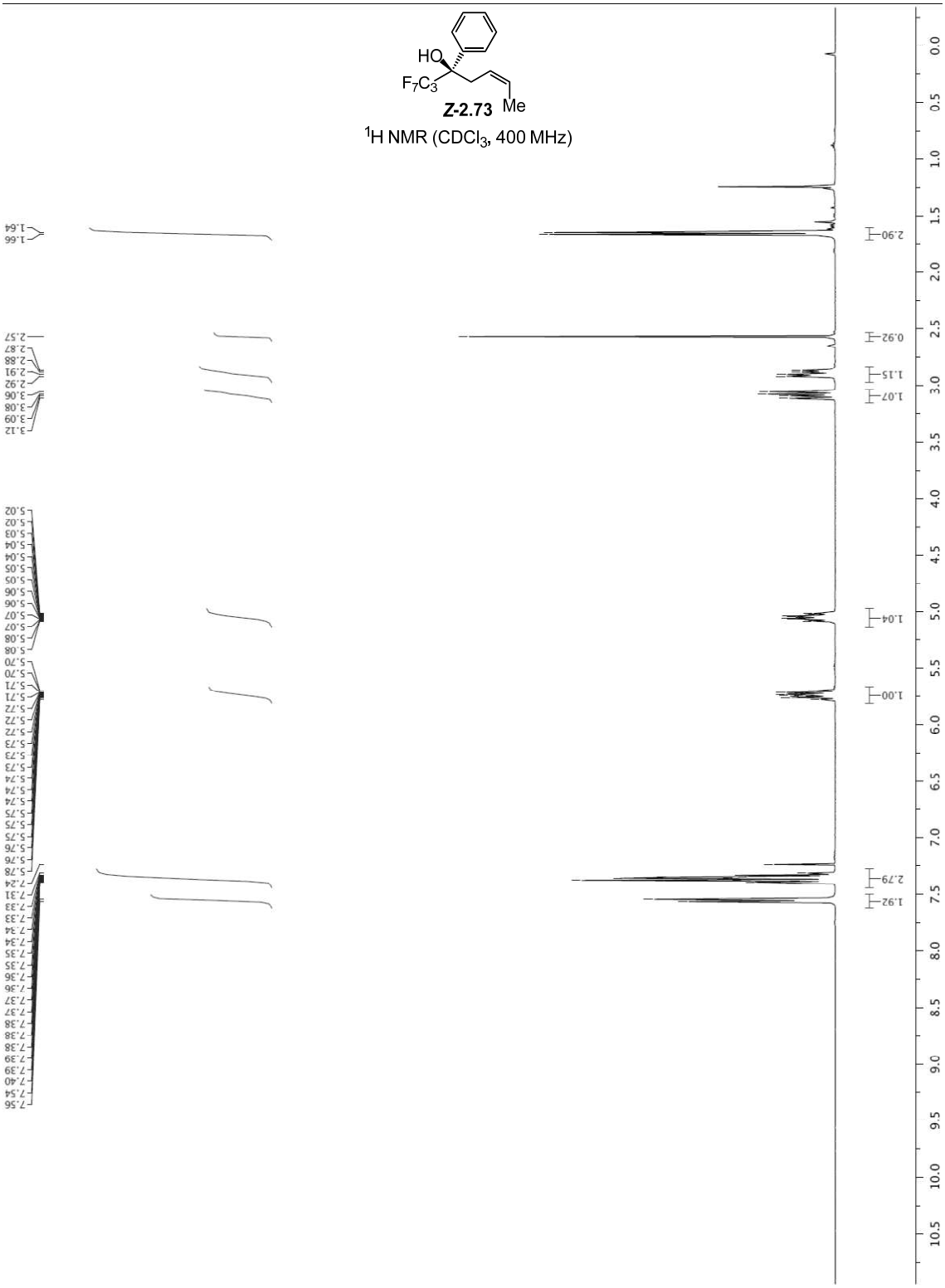
HO
F7C3
Me
Z-2.73
1H NMR (CDCl3, 400 MHz)

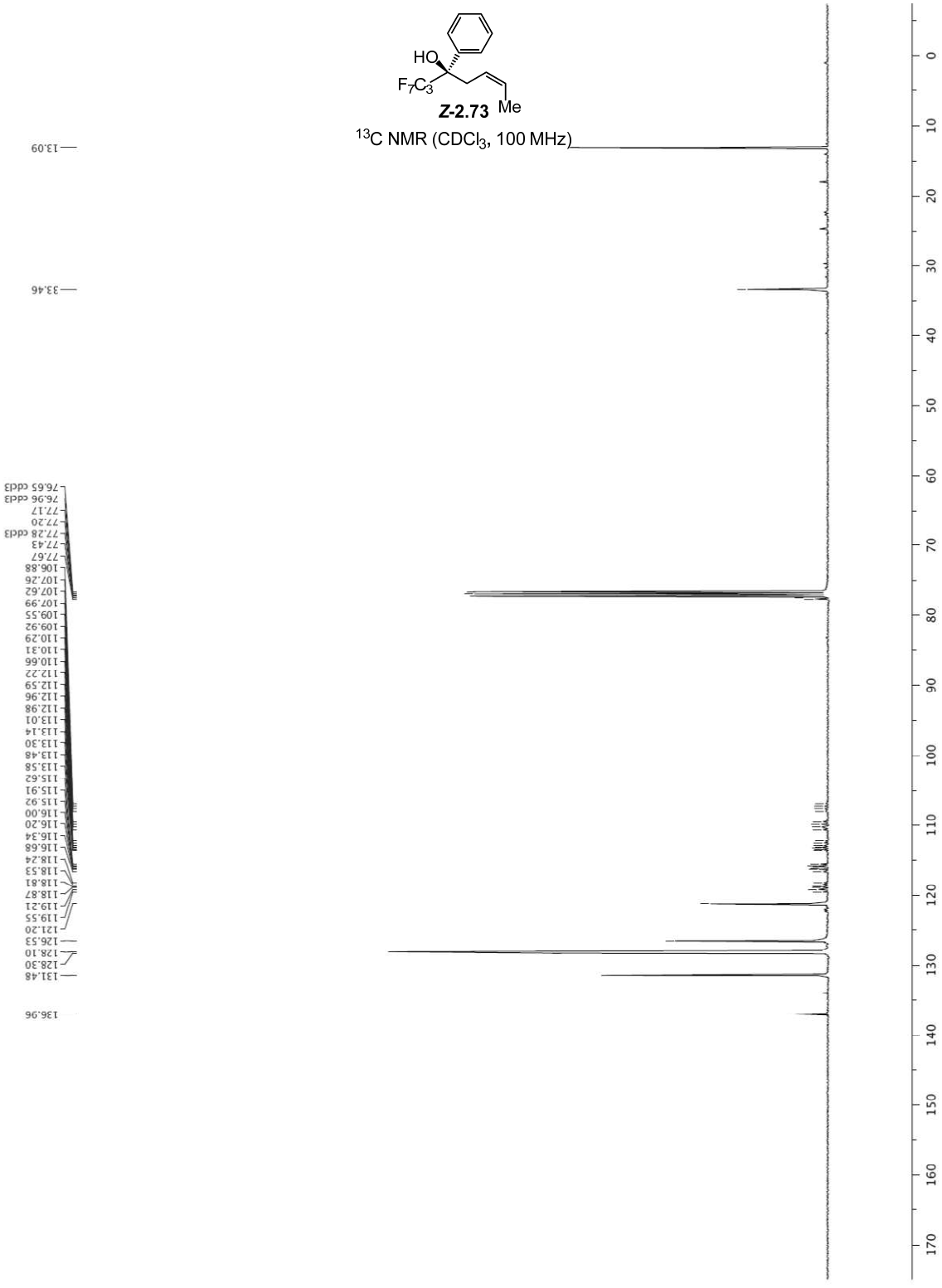
HO
F7C3
Me
Z-2.73
13C NMR (CDCl3, 100 MHz)
13.09
33.46
76.65 cdd3
76.96 cdd3
77.17
77.20
77.28 cdd3
77.43
77.67
106.88
107.26
107.62
107.99
109.55
109.92
110.29
110.31
110.66
112.22
112.59
112.96
112.98
113.01
113.14
113.30
113.48
113.58
115.62
115.91
115.92
116.00
116.20
116.34
116.68
118.24
118.53
118.61
118.87
119.21
119.55
121.20
126.53
128.10
128.30
131.48
136.96

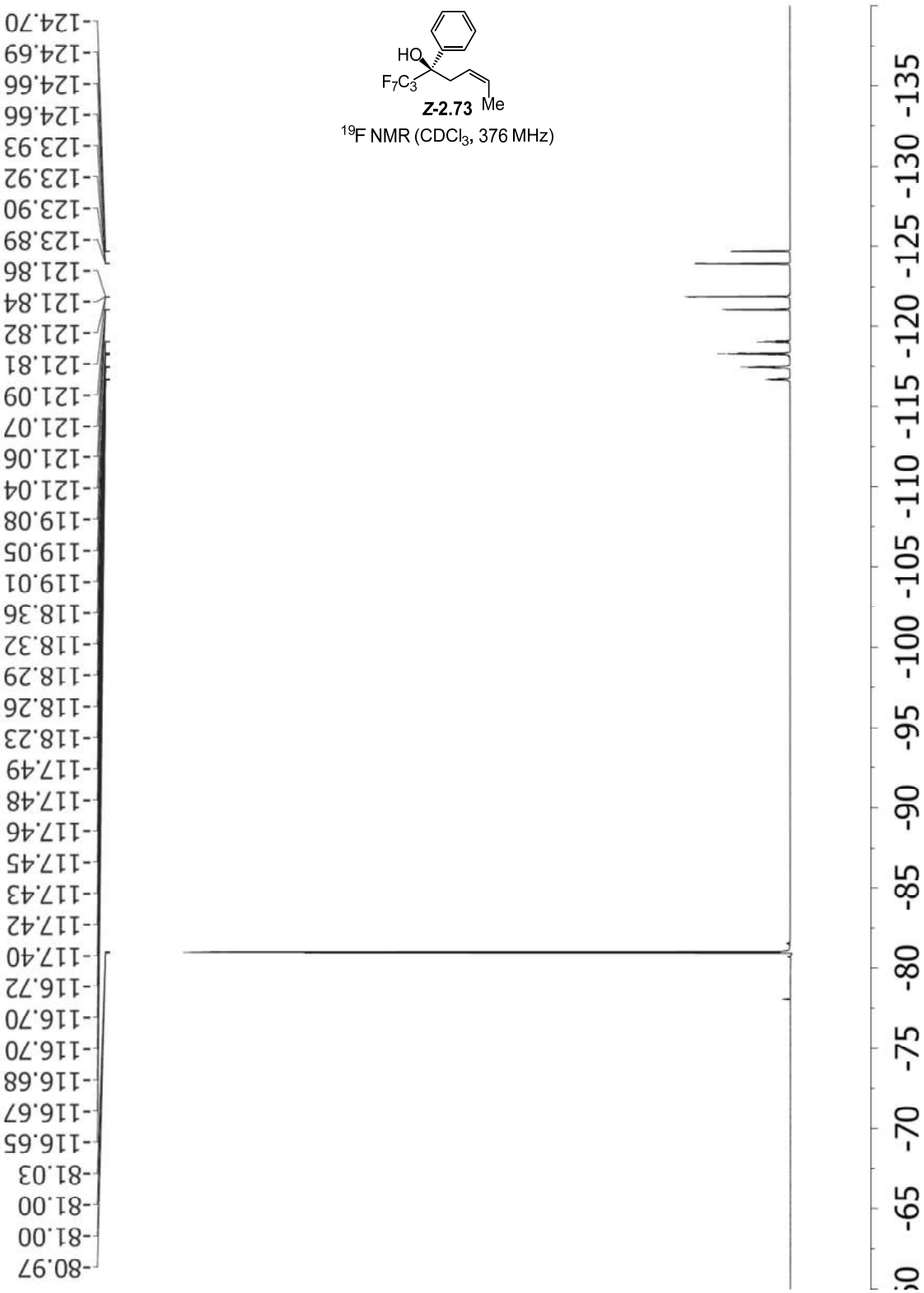

***Z*-2.73**

^{19}F NMR ($CDCl_3$, 376 MHz)

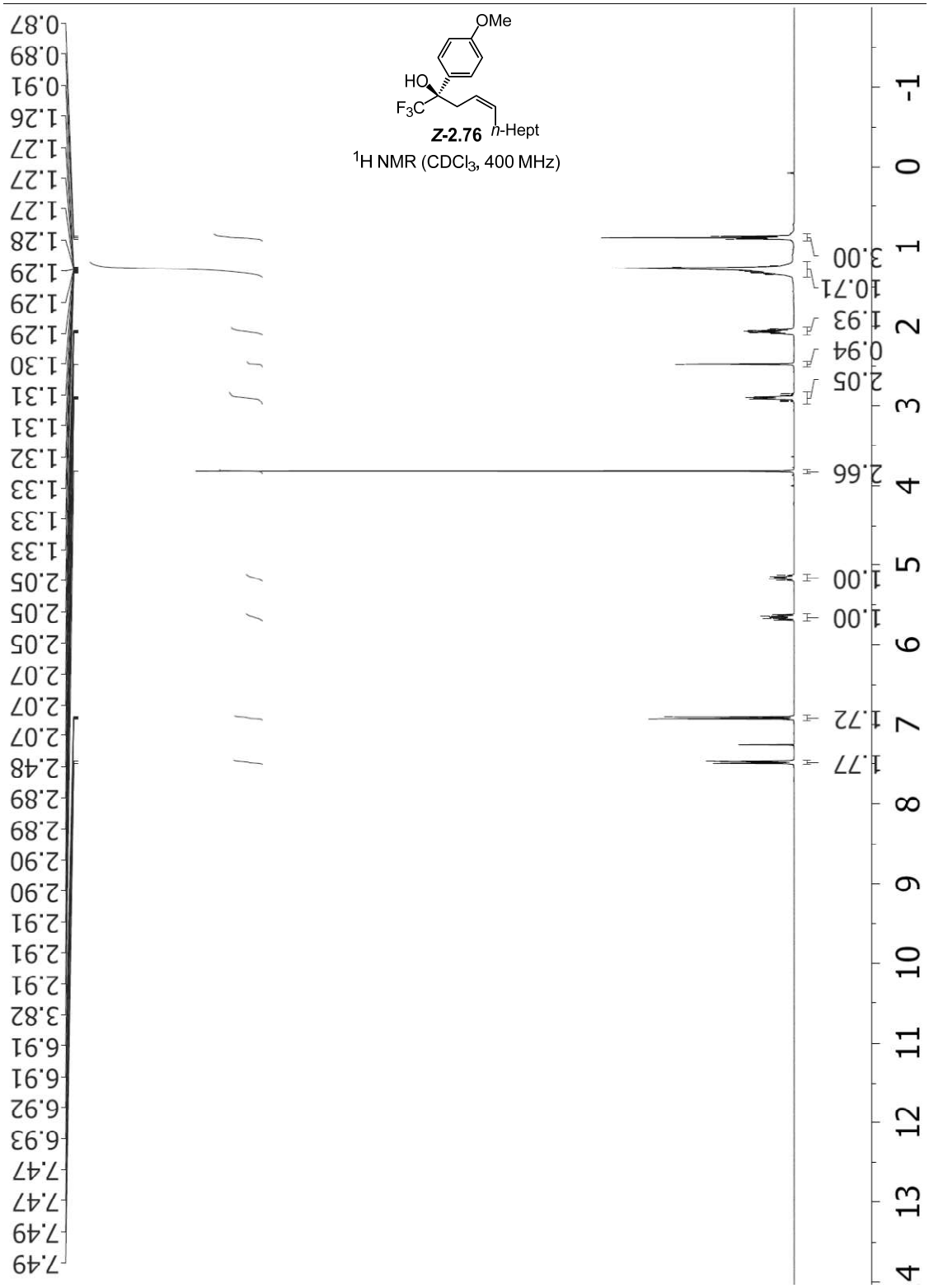
OMe
HO
F3C
Z-2.76 n-Hept
1H NMR (CDCl3, 400 MHz)

OMe
HO
F3C
n-Hept
Z-2.76
13C NMR (CDCl3, 100 MHz)
14.24
22.80
27.68
29.31
29.39
29.60
31.95
33.44
55.38
75.77
76.05
76.33
76.61
113.76
120.54
121.37
124.21
127.05
127.99
129.17
129.89
137.17
159.77
-10
10
30
50
70
90
110
130
150
170
190
210
230

***Z*-2.76**

^{19}F NMR ($CDCl_3$, 376 MHz)

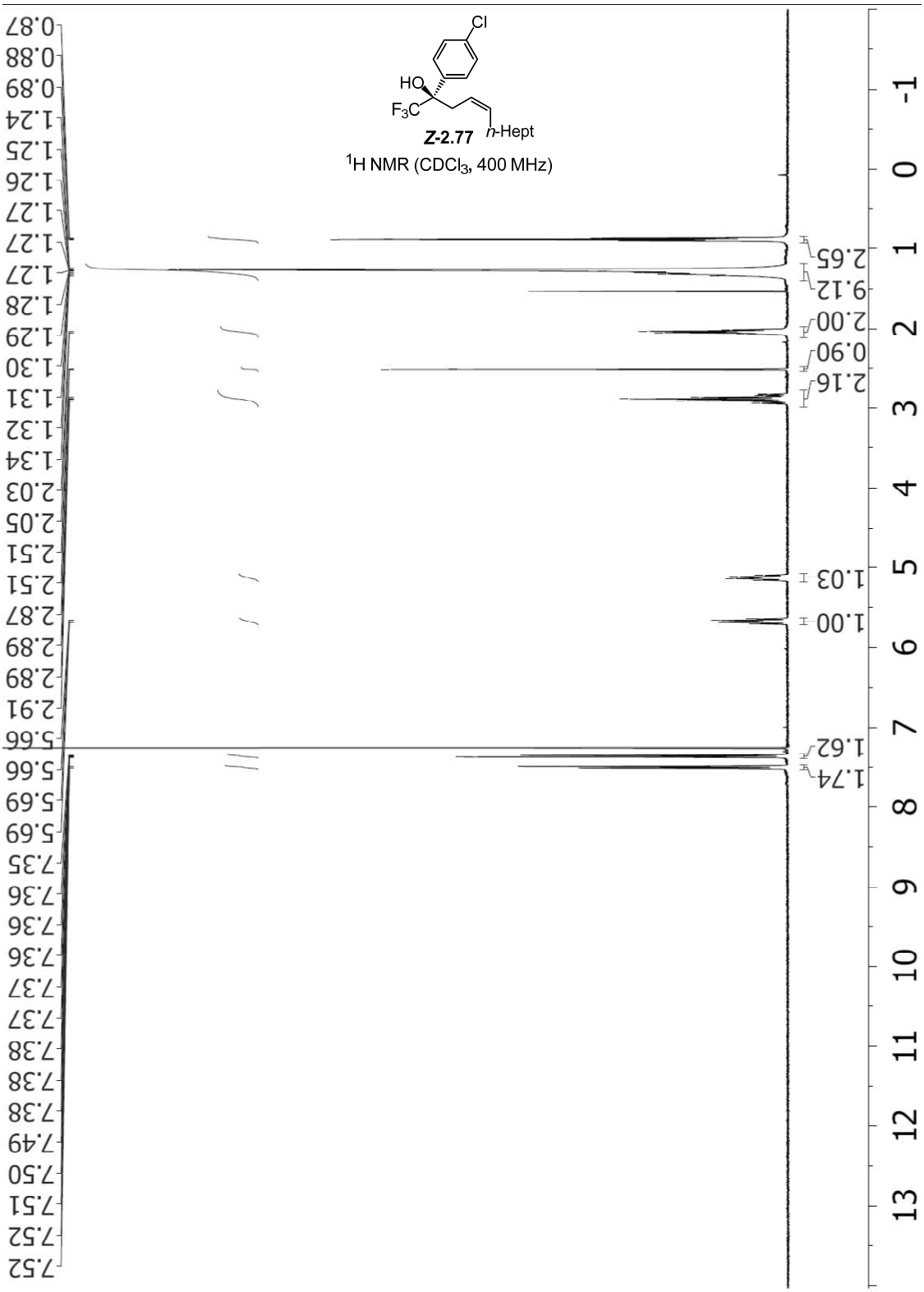
Cl
HO
F3C
Z-2.77
n-Hept
1H NMR (CDCl3, 400 MHz)
2.65
9.12
2.00
0.90
2.16
1.03
1.00
1.62
1.74

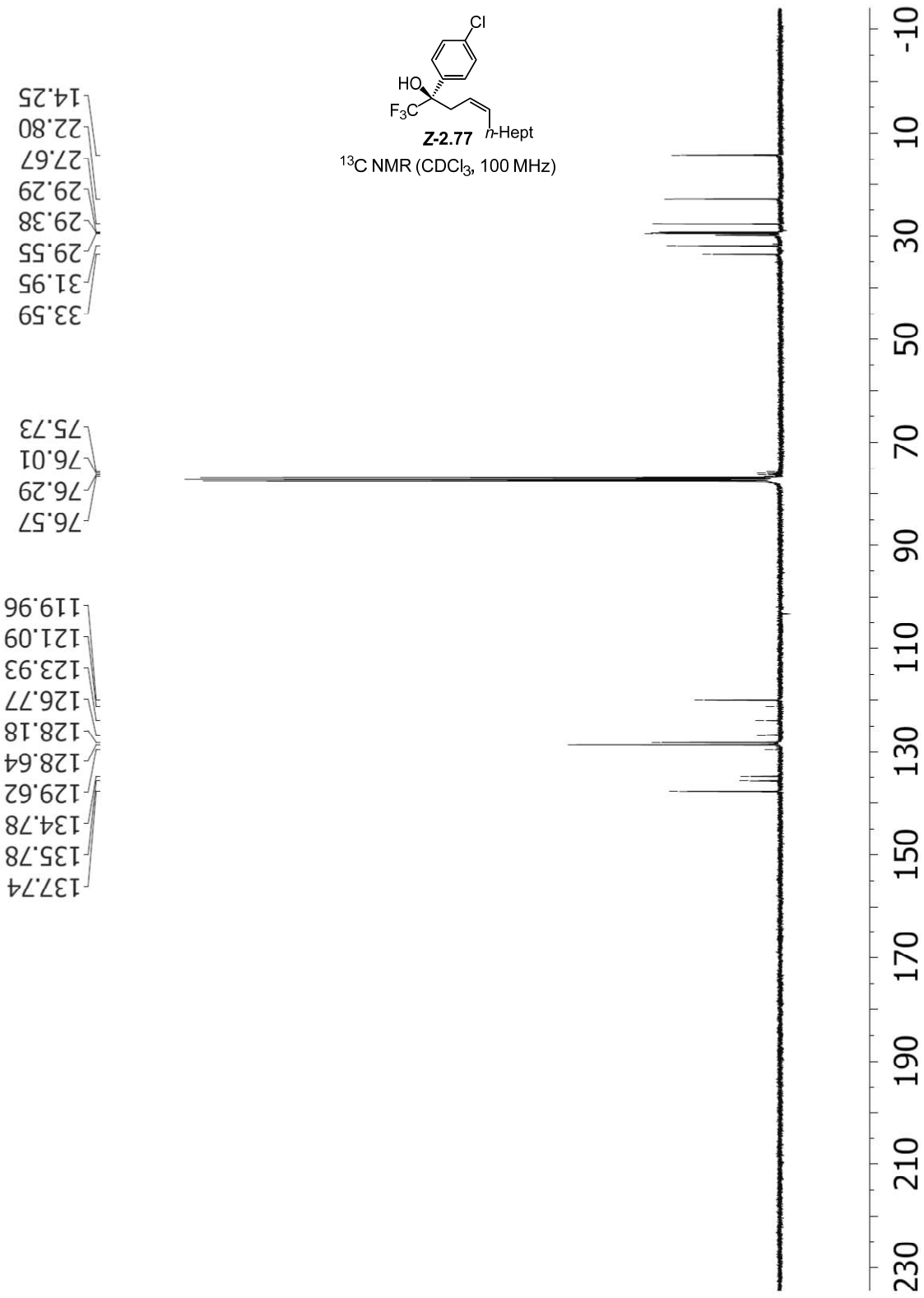
Cl
HO
F3C
Z-2.77
n-Hept
13C NMR (CDCl3, 100 MHz)
14.25
22.80
27.67
29.29
29.38
29.55
31.95
33.59
75.73
76.01
76.29
76.57
119.96
121.09
123.93
126.77
128.18
128.64
129.62
134.78
135.78
137.74
-10
10
30
50
70
90
110
130
150
170
190
210
230

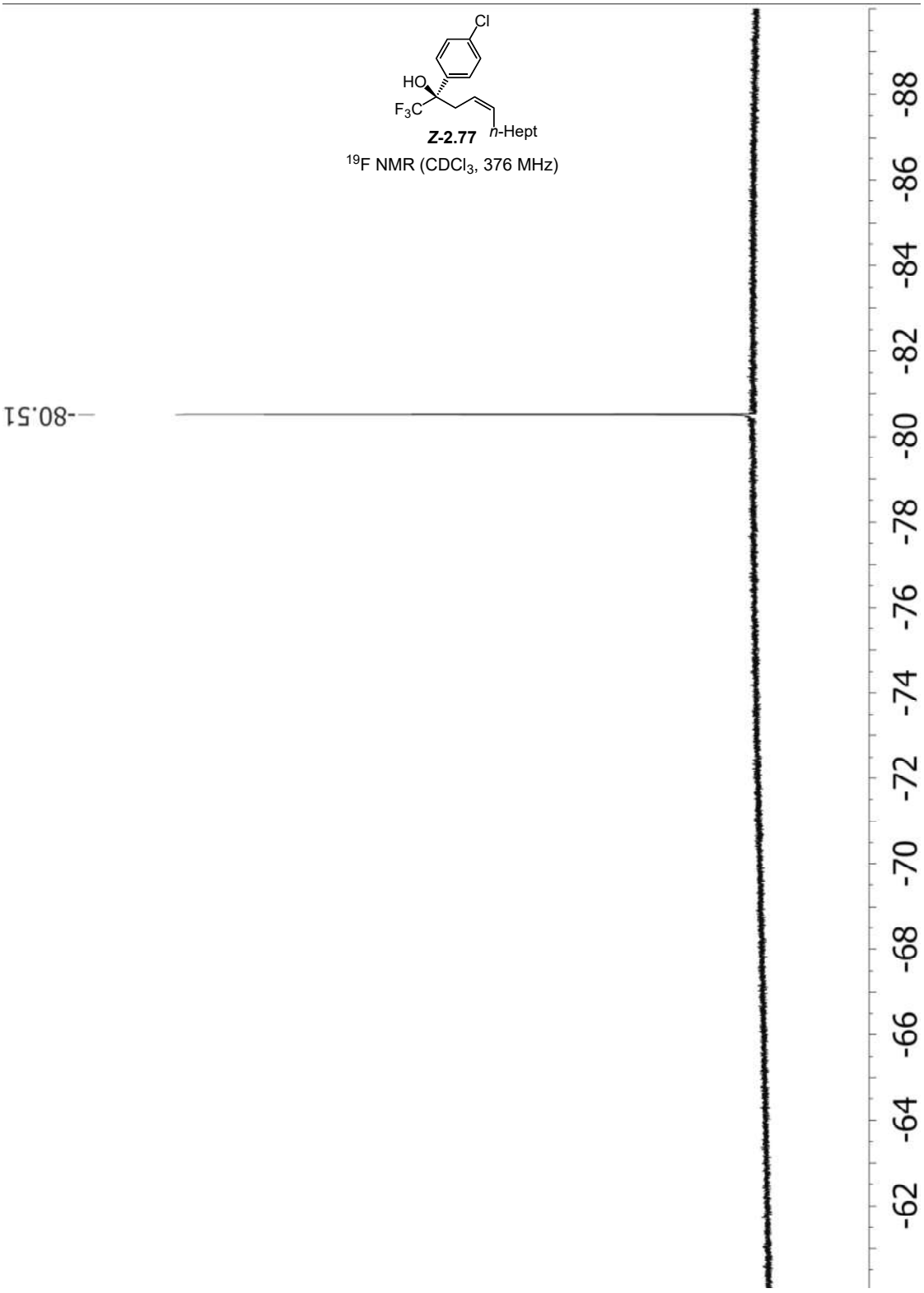
Cl
HO
F3C
Z-2.77
n-Hept
19F NMR (CDCl3, 376 MHz)
-80.51
-62
-64
-66
-68
-70
-72
-74
-76
-78
-80
-82
-84
-86
-88

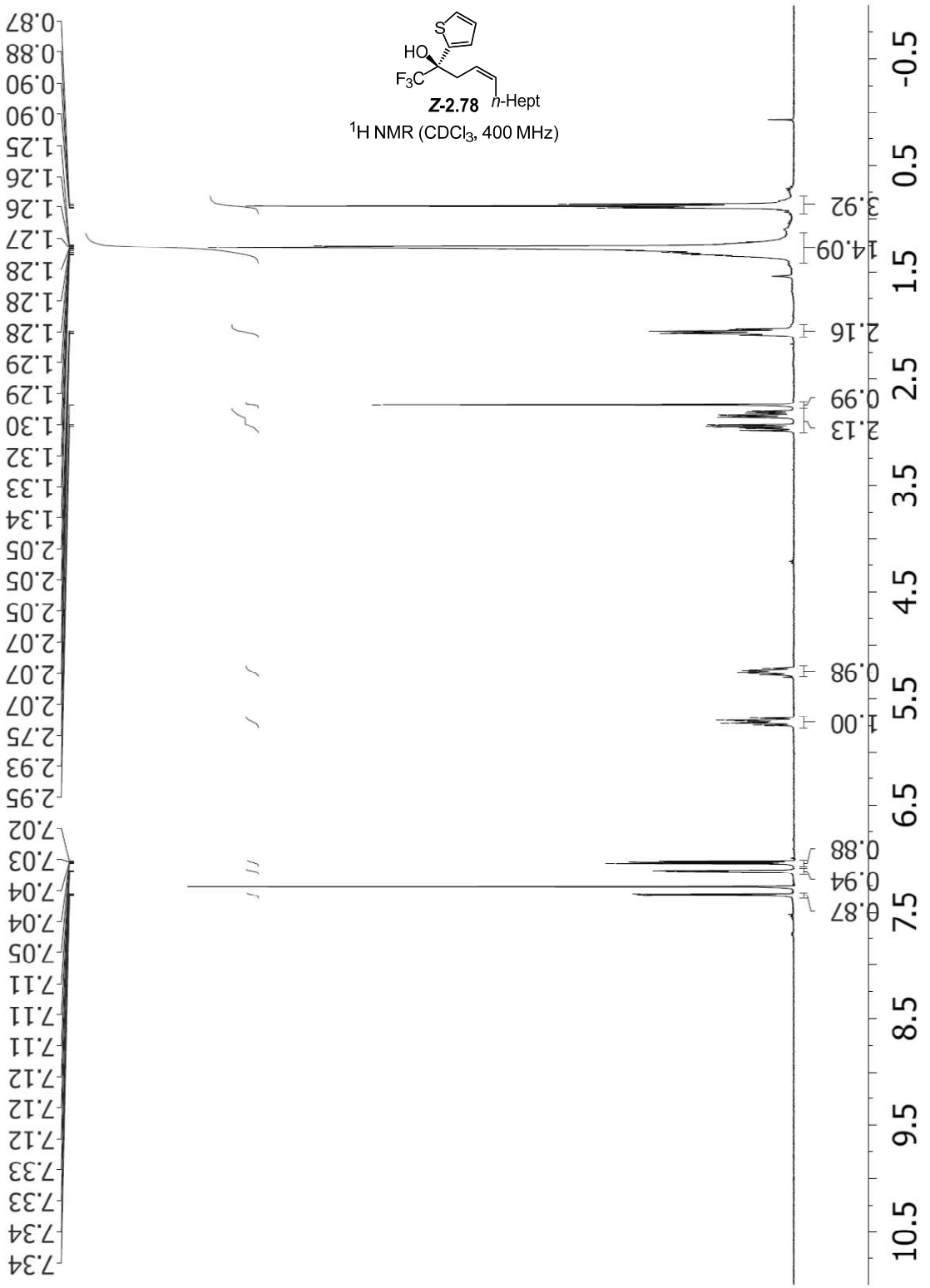
HO
F3C
S
Z-2.78 n-Hept
1H NMR (CDCl3, 400 MHz)

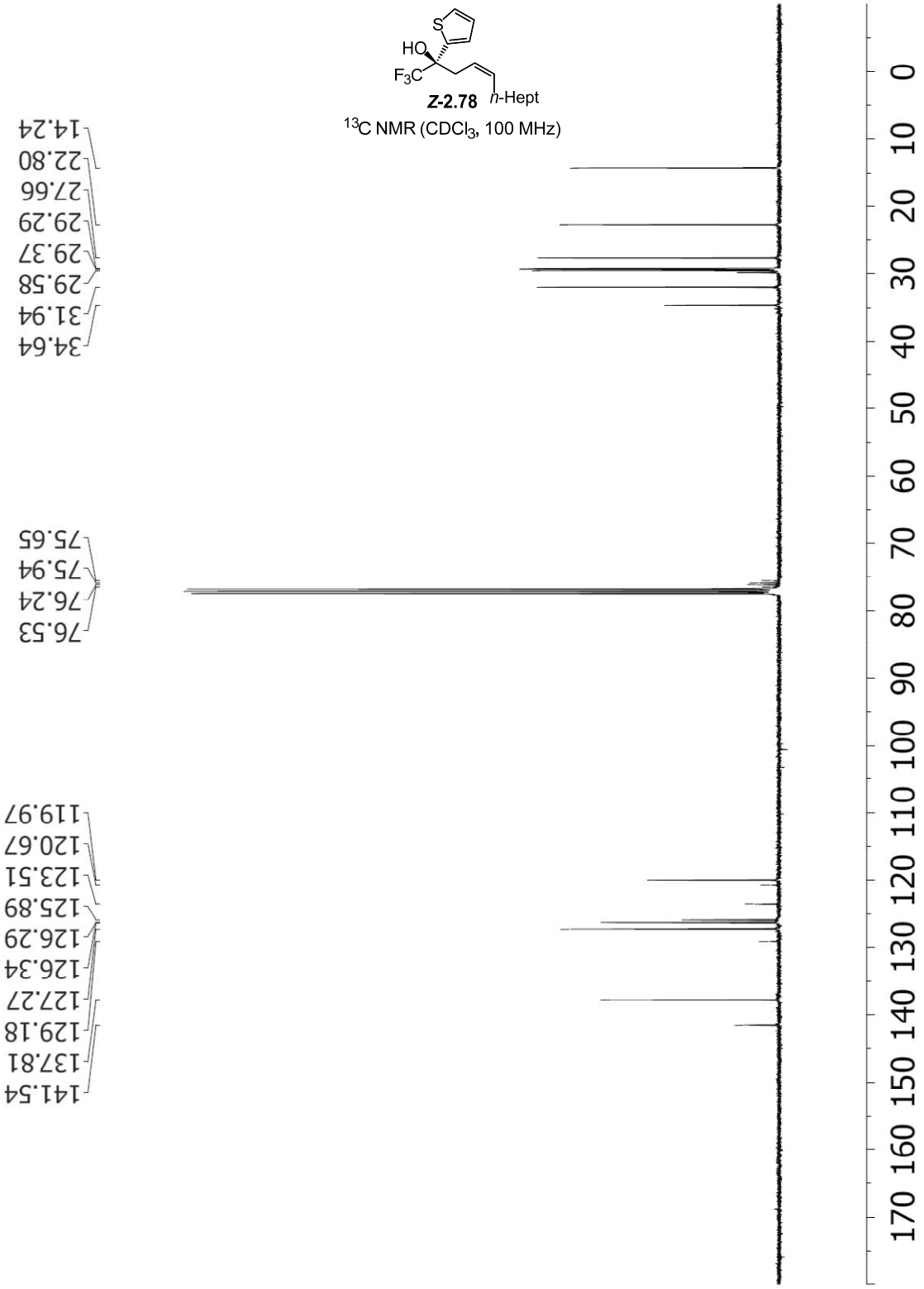
S
HO
F3C
Z-2.78 n-Hept
13C NMR (CDCl3, 100 MHz)
14.24
22.80
27.66
29.29
29.37
29.58
31.94
34.64
75.65
75.94
76.24
76.53
119.97
120.67
123.51
125.89
126.29
126.34
127.27
129.18
137.81
141.54
0 10 20 30 40 50 60 70 80 90 100 110 120 130 140 150 160 170


HO
F3C
S
Z-2.78
n-Hept
19F NMR (CDCl3, 376 MHz)
-81.58
-62
-64
-66
-68
-70
-72
-74
-76
-78
-80
-82
-84
-86
-88

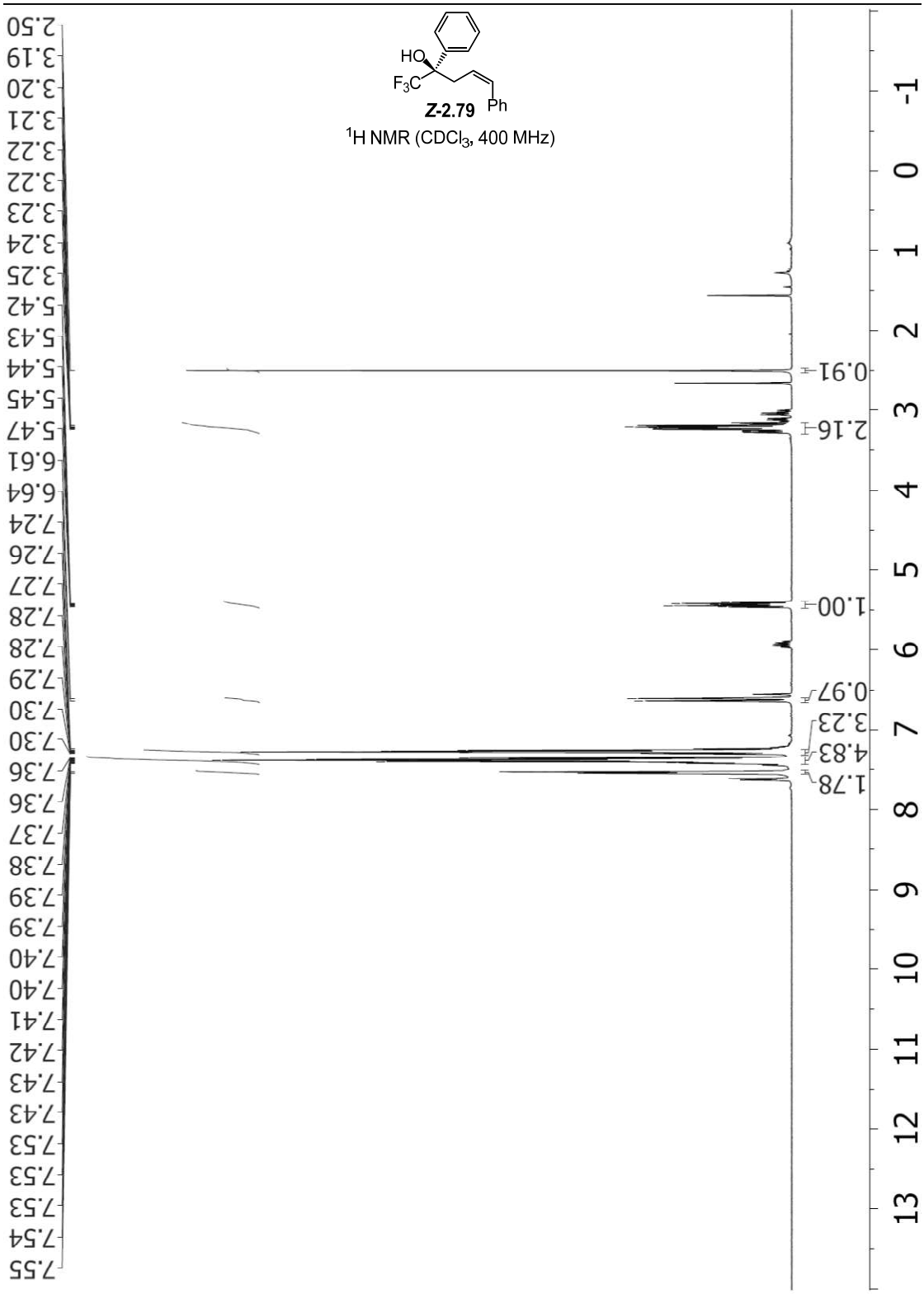
HO
F3C
Ph
Z-2.79
1H NMR (CDCl3, 400 MHz)
0.91
2.16
1.00
0.97
3.23
4.83
1.78

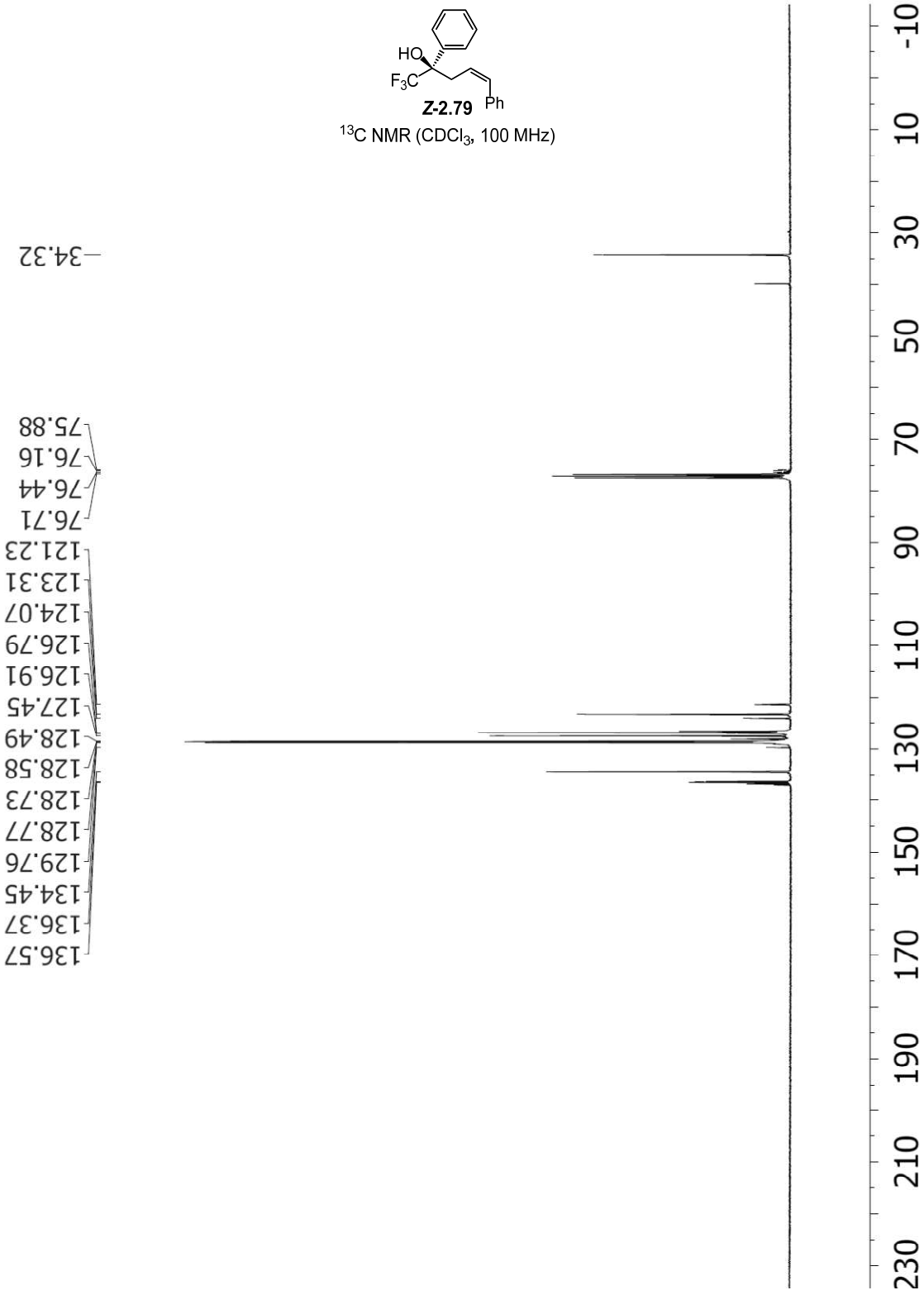
HO
F3C
Ph
Z-2.79
13C NMR (CDCl3, 100 MHz)
34.32
75.88
76.16
76.44
76.71
121.23
123.31
124.07
126.79
126.91
127.45
128.49
128.58
128.73
128.77
129.76
134.45
136.37
136.57
-10
10
30
50
70
90
110
130
150
170
190
210
230

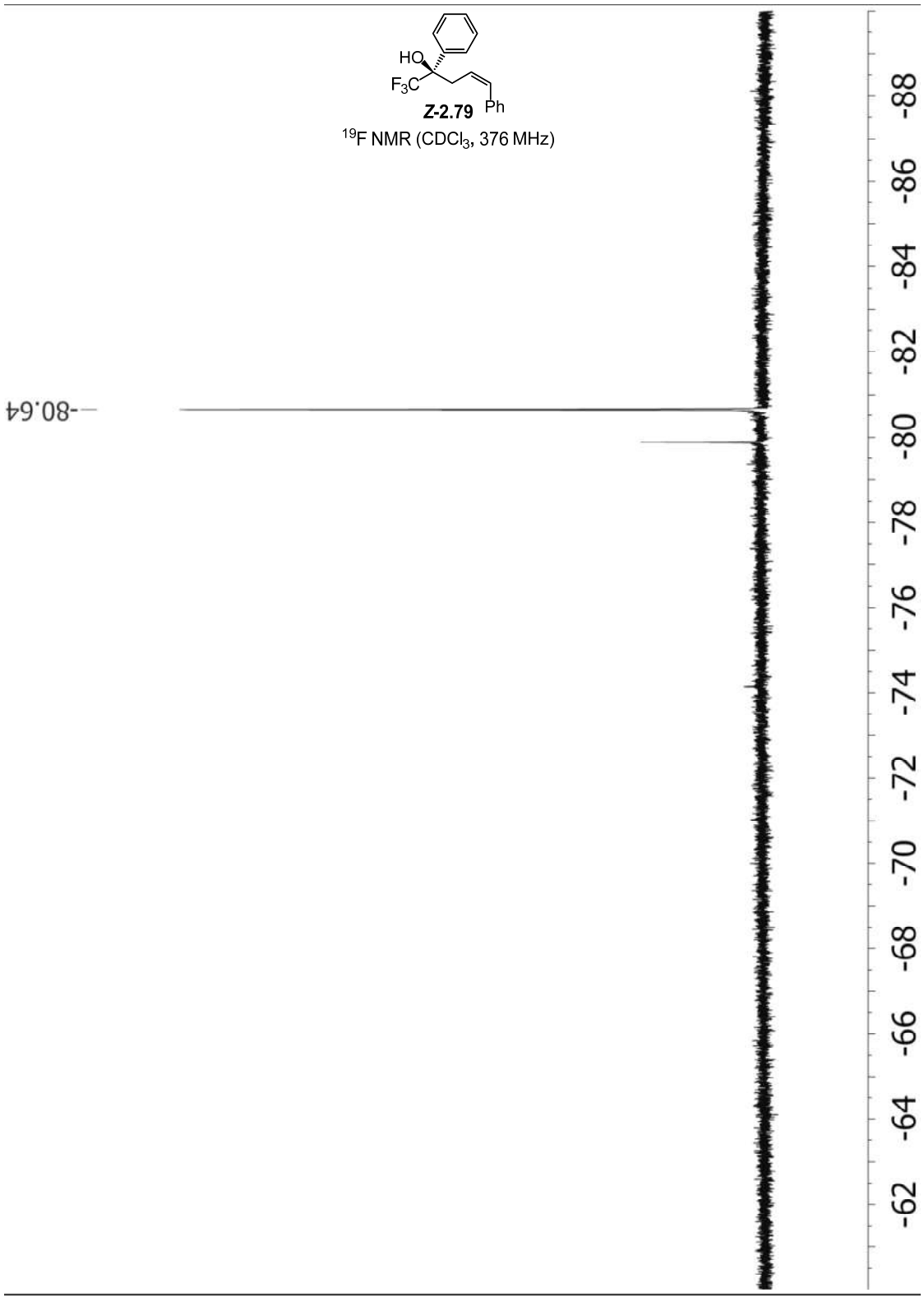
HO
F3C
Ph
Z-2.79
19F NMR (CDCl3, 376 MHz)
-80.64
-62
-64
-66
-68
-70
-72
-74
-76
-78
-80
-82
-84
-86
-88

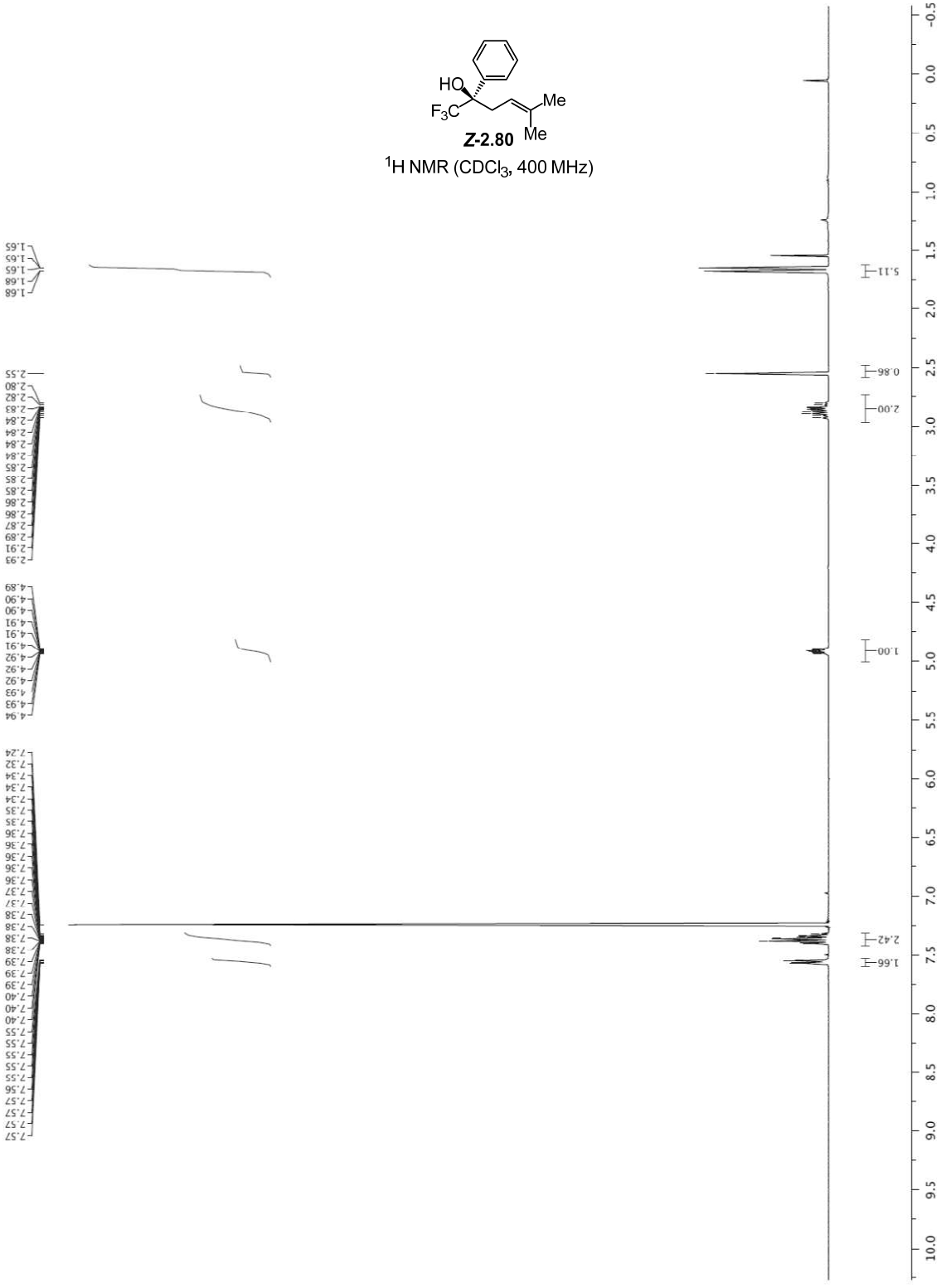
HO
F3C
Me
Me
Z-2.80
1H NMR (CDCl3, 400 MHz)

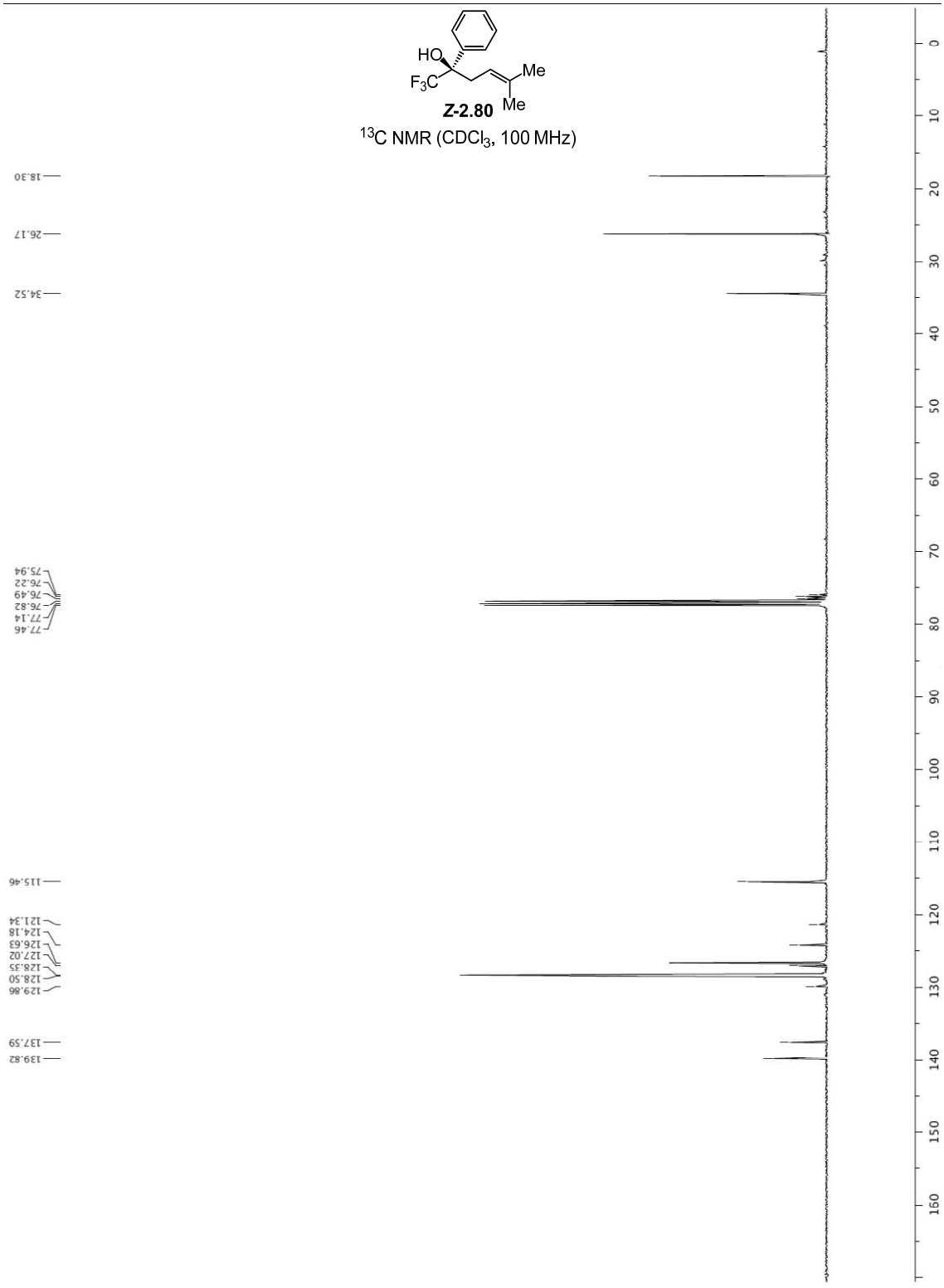
HO
F3C
Me
Me
Z-2.80
13C NMR (CDCl3, 100 MHz)
18.30
26.17
34.52
75.94
76.22
76.49
76.82
77.14
77.46
115.46
121.34
124.18
126.63
127.02
128.35
128.50
129.86
137.59
139.82


HO
F3C
Me
Me
Z-2.80
19F NMR (CDCl3, 376 MHz)
-80.05
-62
-64
-66
-68
-70
-72
-74
-76
-78
-80
-82
-84
-86
-88

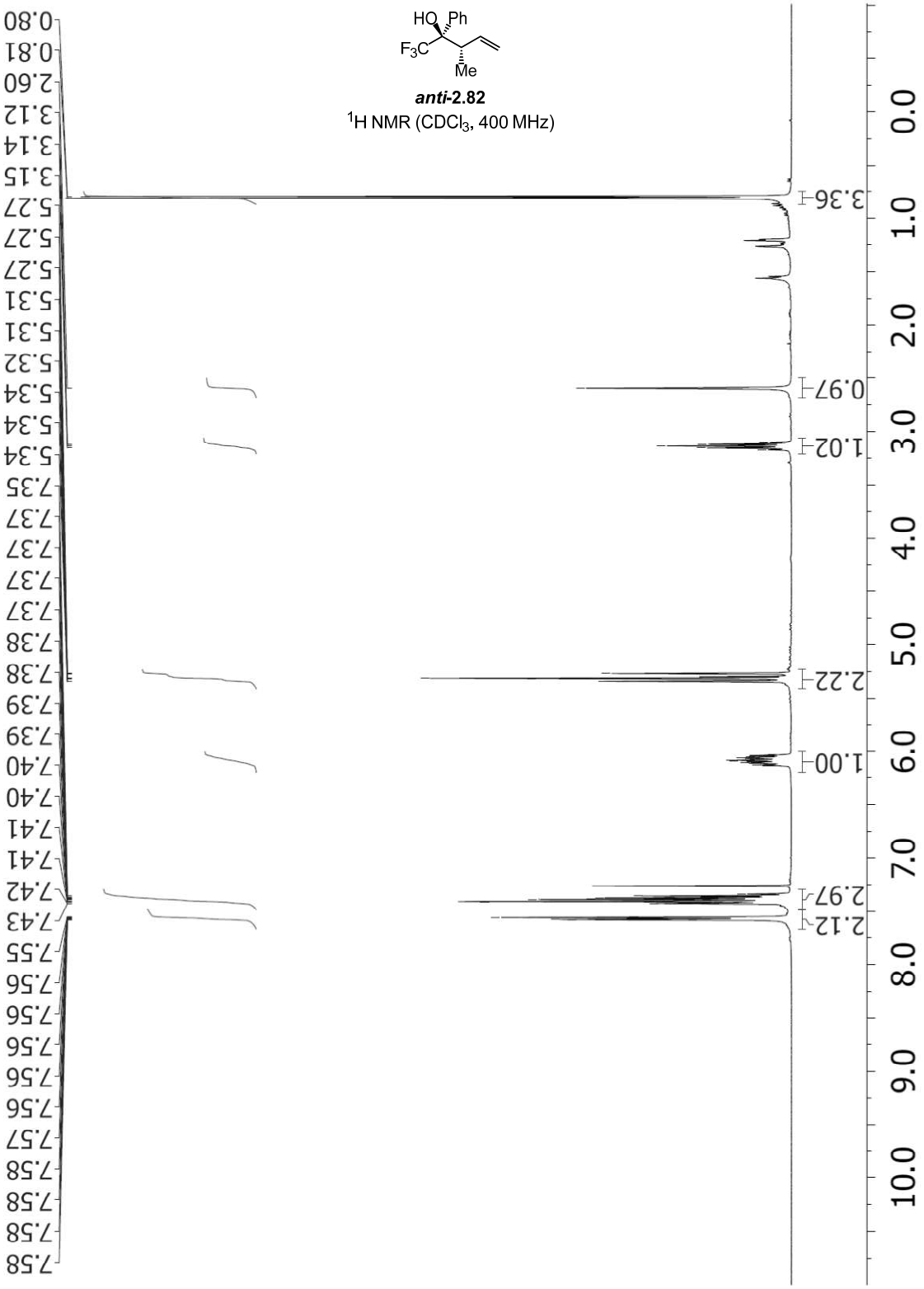
HO
Ph
F3C
Me
anti-2.82
1H NMR (CDCl3, 400 MHz)
3.36
0.97
1.02
2.22
1.00
2.97
2.12

HO
Ph
F3C
Me
anti-2.82
13C NMR (CDCl3, 100 MHz)
13.71
42.29
78.41
78.68
78.95
79.21
118.20
121.57
124.43
125.86
125.89
127.29
128.35
128.44
130.15
137.16
137.31
-10
10
30
50
70
90
110
130
150
170
190
210
230

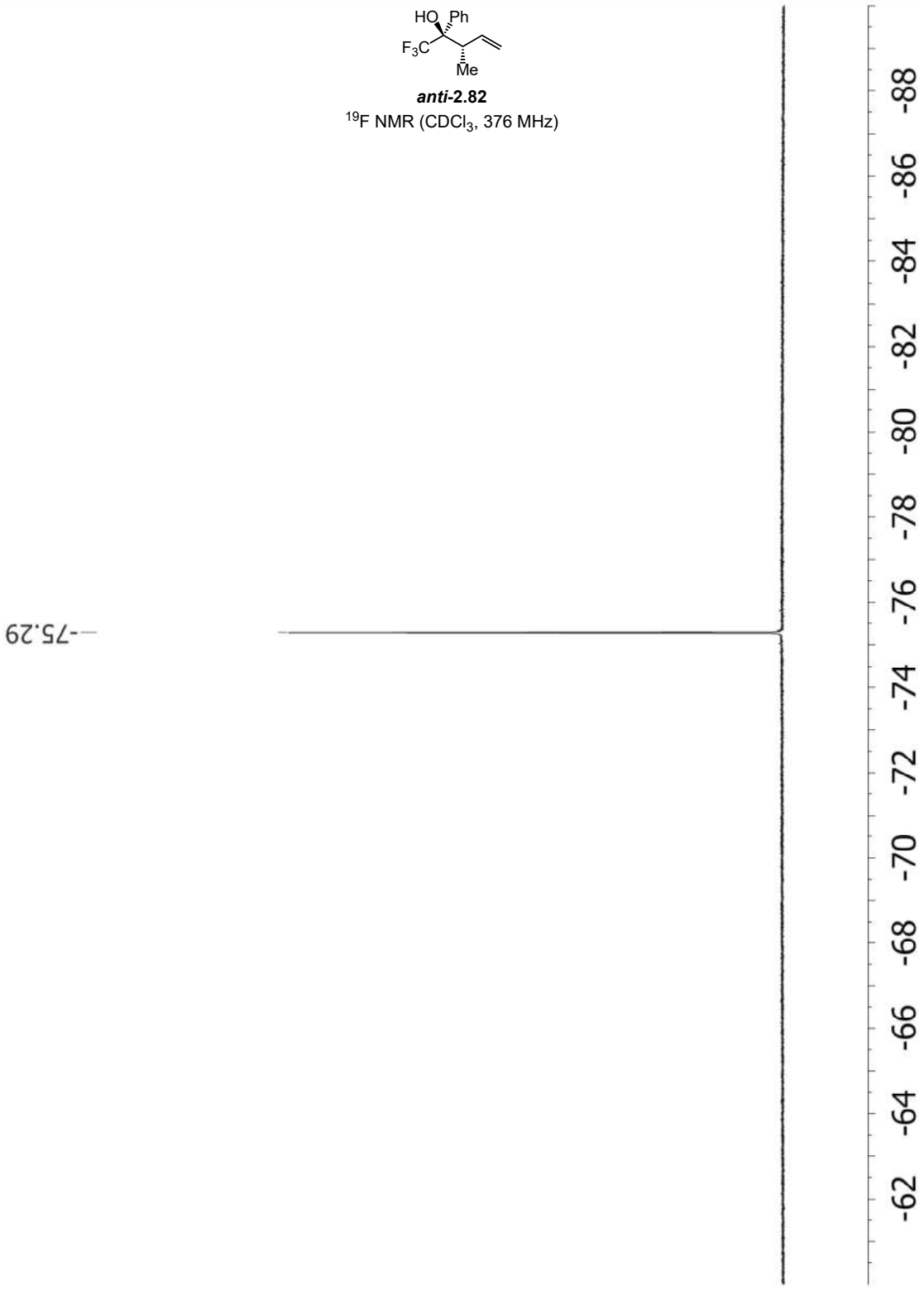
HO
Ph
F3C
Me
anti-2.82
19F NMR (CDCl3, 376 MHz)
-75.29
-62
-64
-66
-68
-70
-72
-74
-76
-78
-80
-82
-84
-86
-88

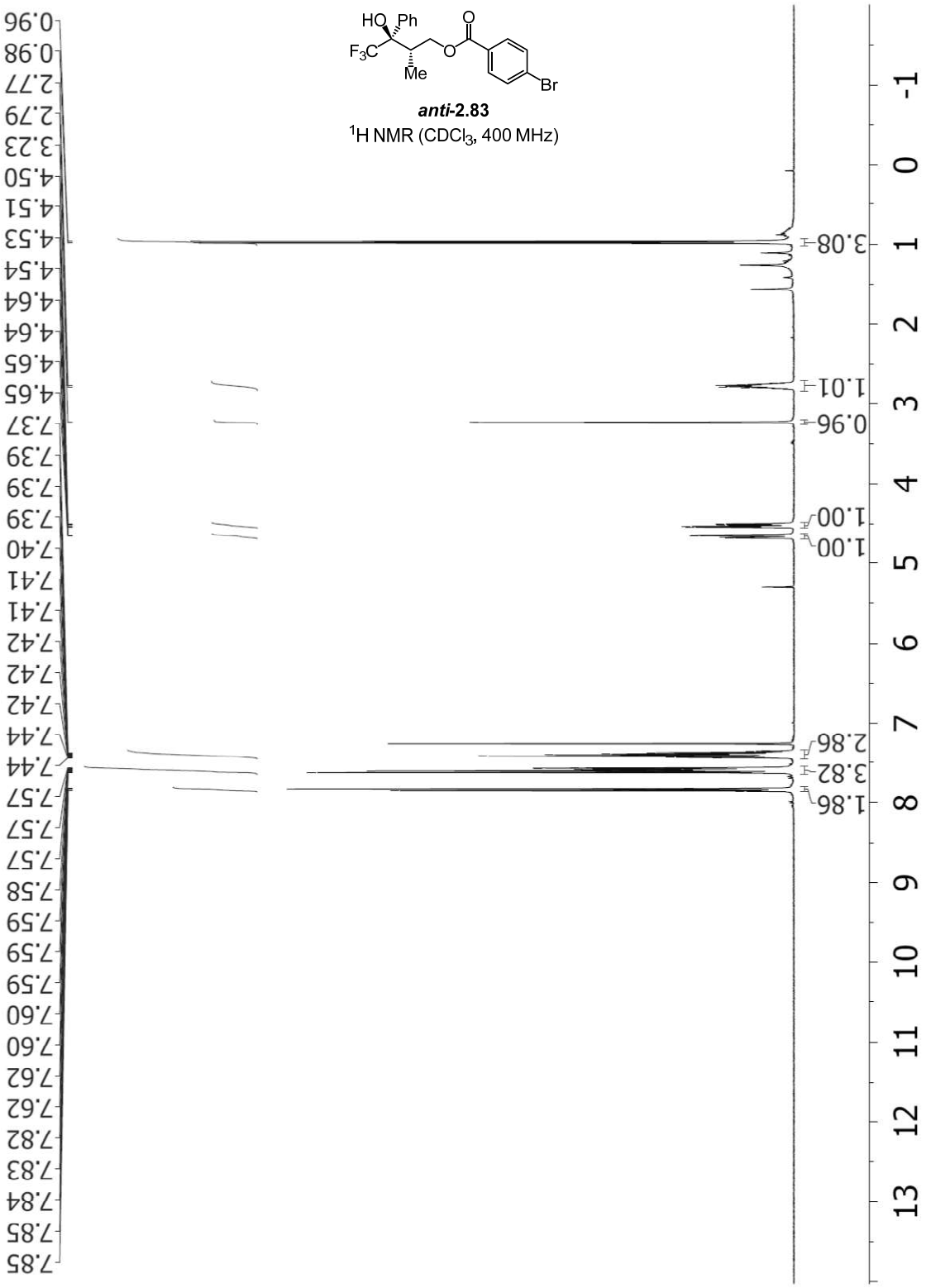
HO
Ph
F3C
O
O
Me
Br
anti-2.83
1H NMR (CDCl3, 400 MHz)
3.08
1.01
0.96
1.00
1.00
2.86
3.82
1.86

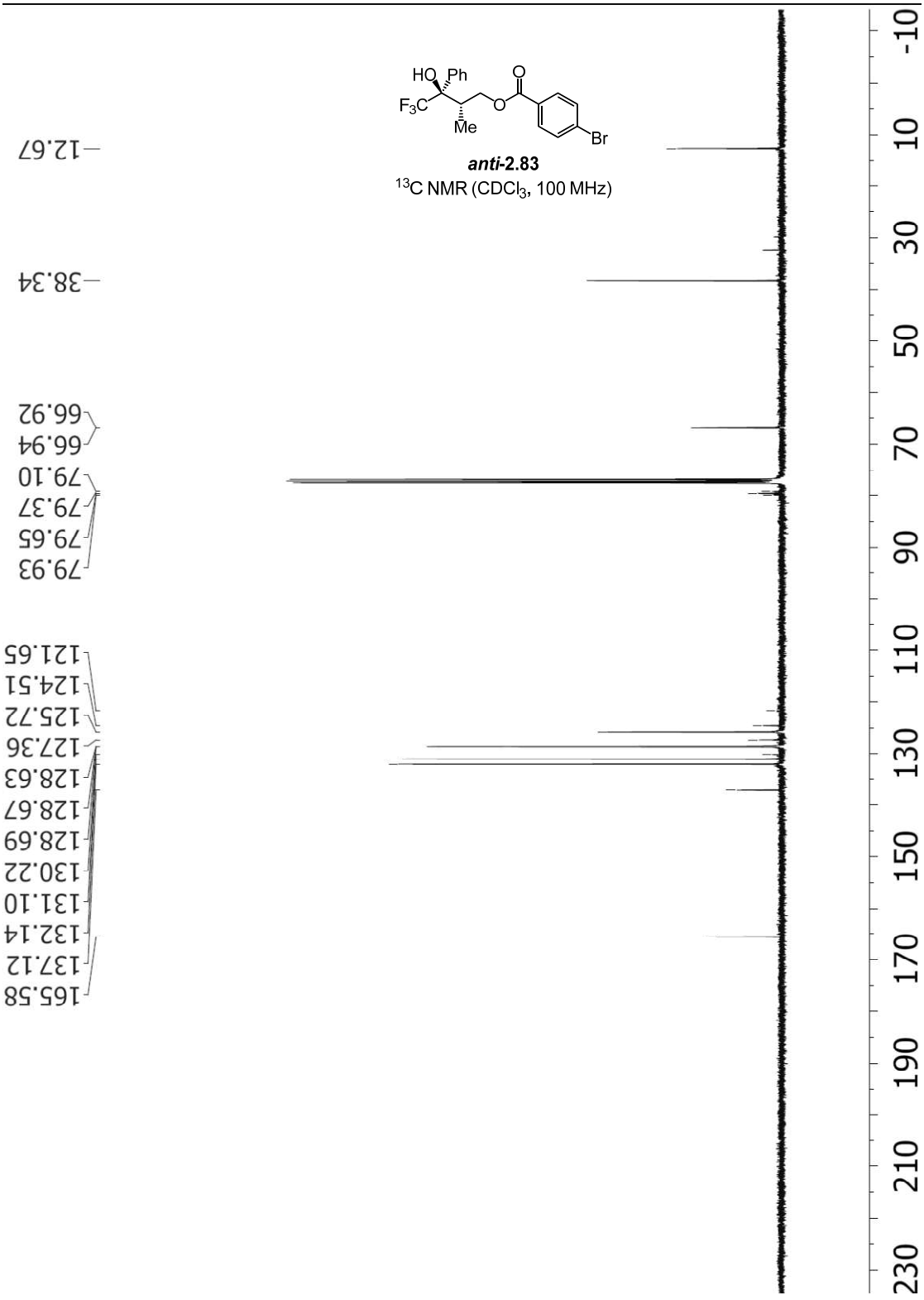
HO
Ph
F3C
Me
O
O
Br
anti-2.83
13C NMR (CDCl3, 100 MHz)
12.67
38.34
66.92
66.94
79.10
79.37
79.65
79.93
121.65
124.51
125.72
127.36
128.63
128.67
128.69
130.22
131.10
132.14
137.12
165.58
-10
10
30
50
70
90
110
130
150
170
190
210
230

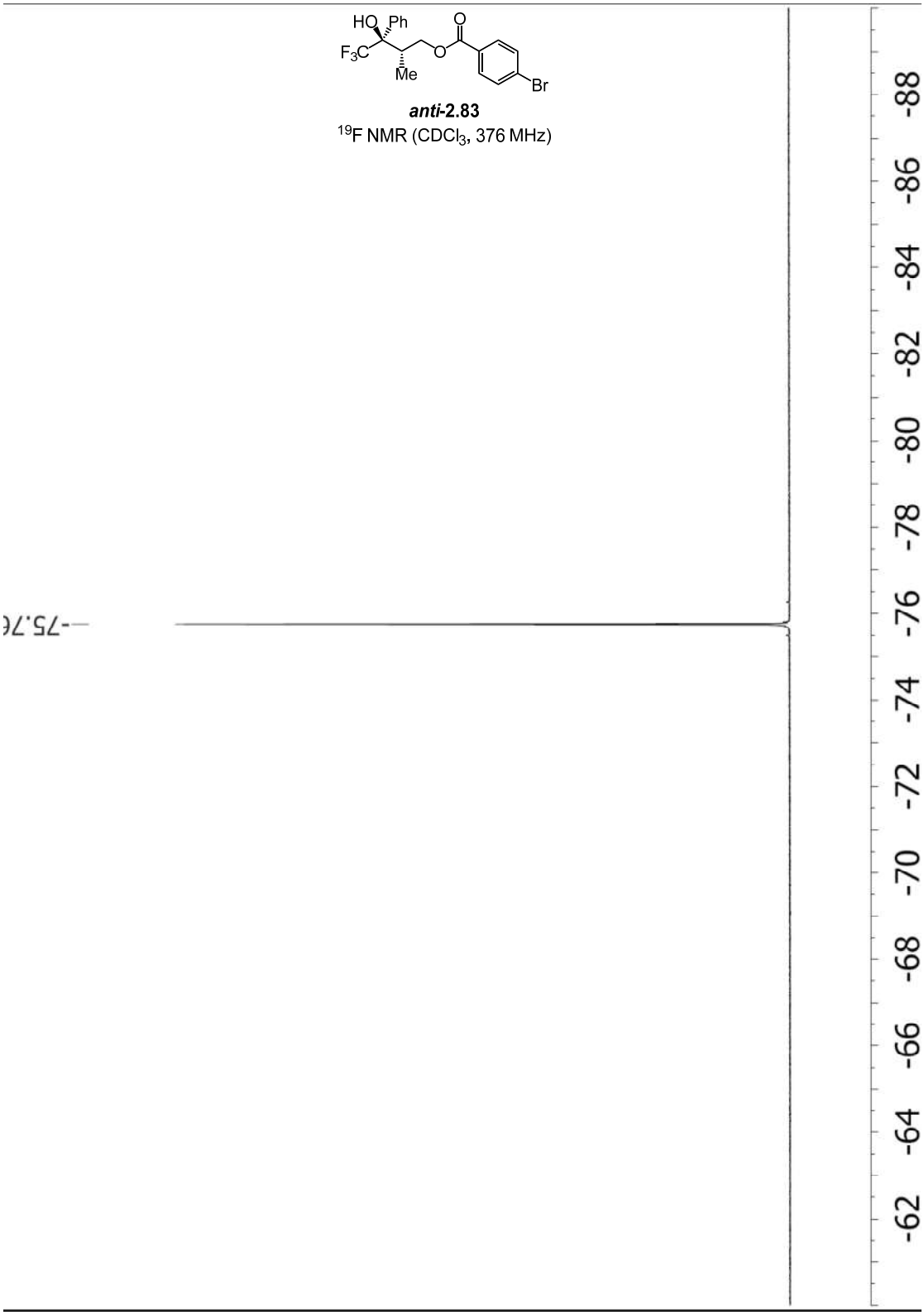
HO
Ph
O
F3C
O
Me
Br
anti-2.83
19F NMR (CDCl3, 376 MHz)
-75.76
-62
-64
-66
-68
-70
-72
-74
-76
-78
-80
-82
-84
-86
-88

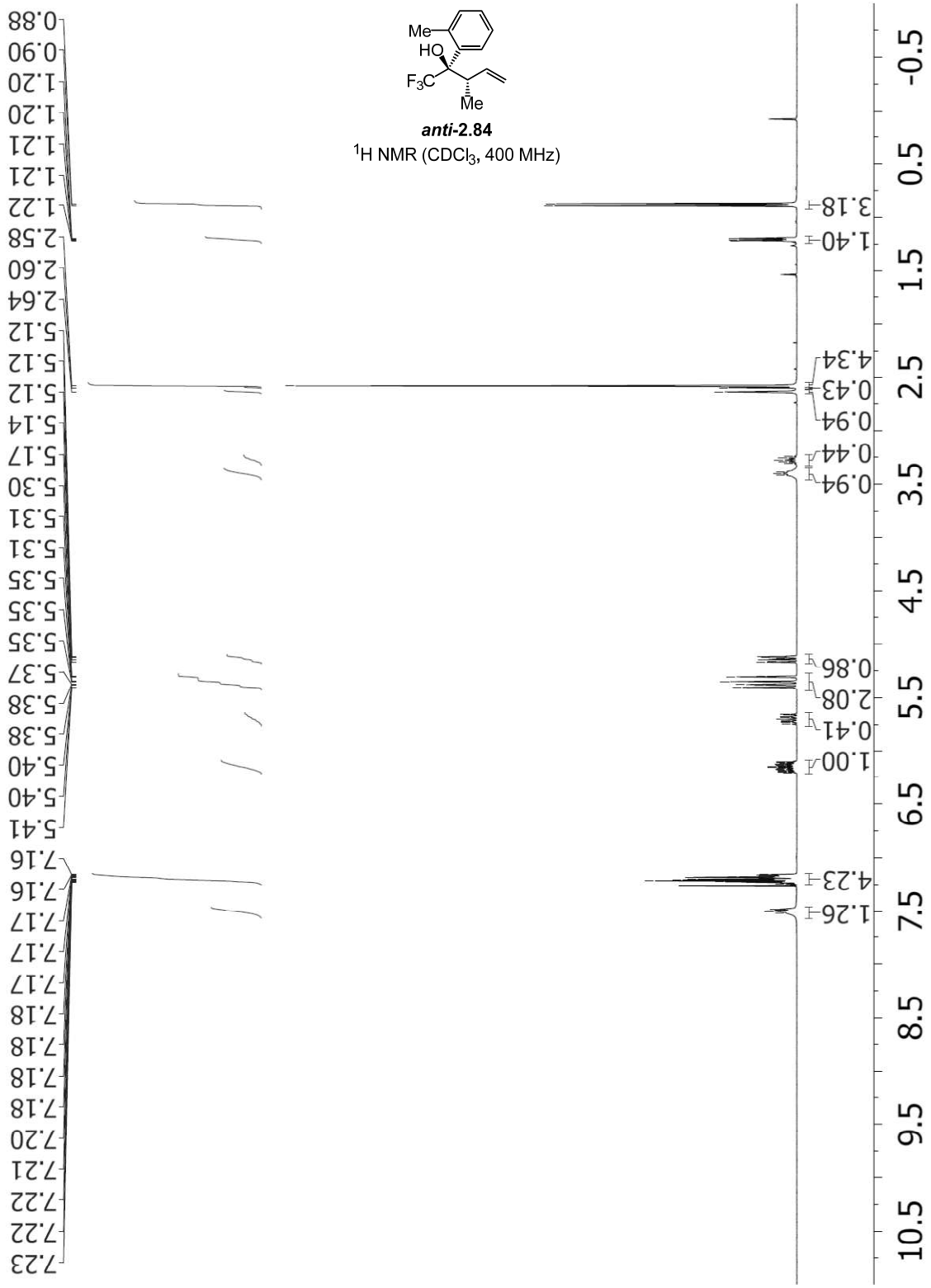
Me
HO
F3C
Me
anti-2.84
1H NMR (CDCl3, 400 MHz)

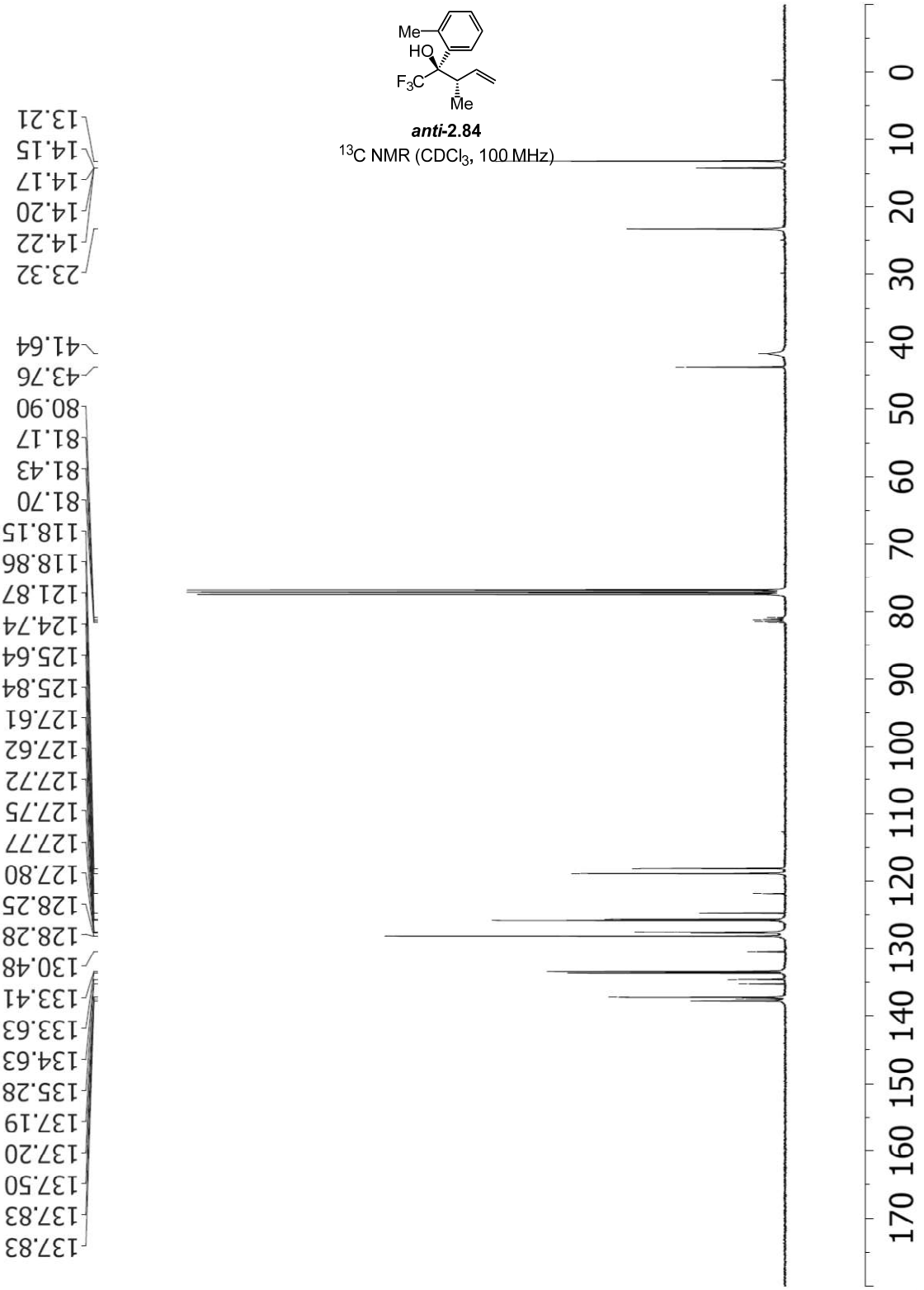
Me
HO
F3C
Me
anti-2.84
13C NMR (CDCl3, 100 MHz)
13.21
14.15
14.17
14.20
14.22
23.32
41.64
43.76
80.90
81.17
81.43
81.70
118.15
118.86
121.87
124.74
125.64
125.84
127.61
127.62
127.72
127.75
127.77
127.80
128.25
128.28
130.48
133.41
133.63
134.63
135.28
137.19
137.20
137.50
137.83
137.83
0
10
20
30
40
50
60
70
80
90
100
110
120
130
140
150
160
170

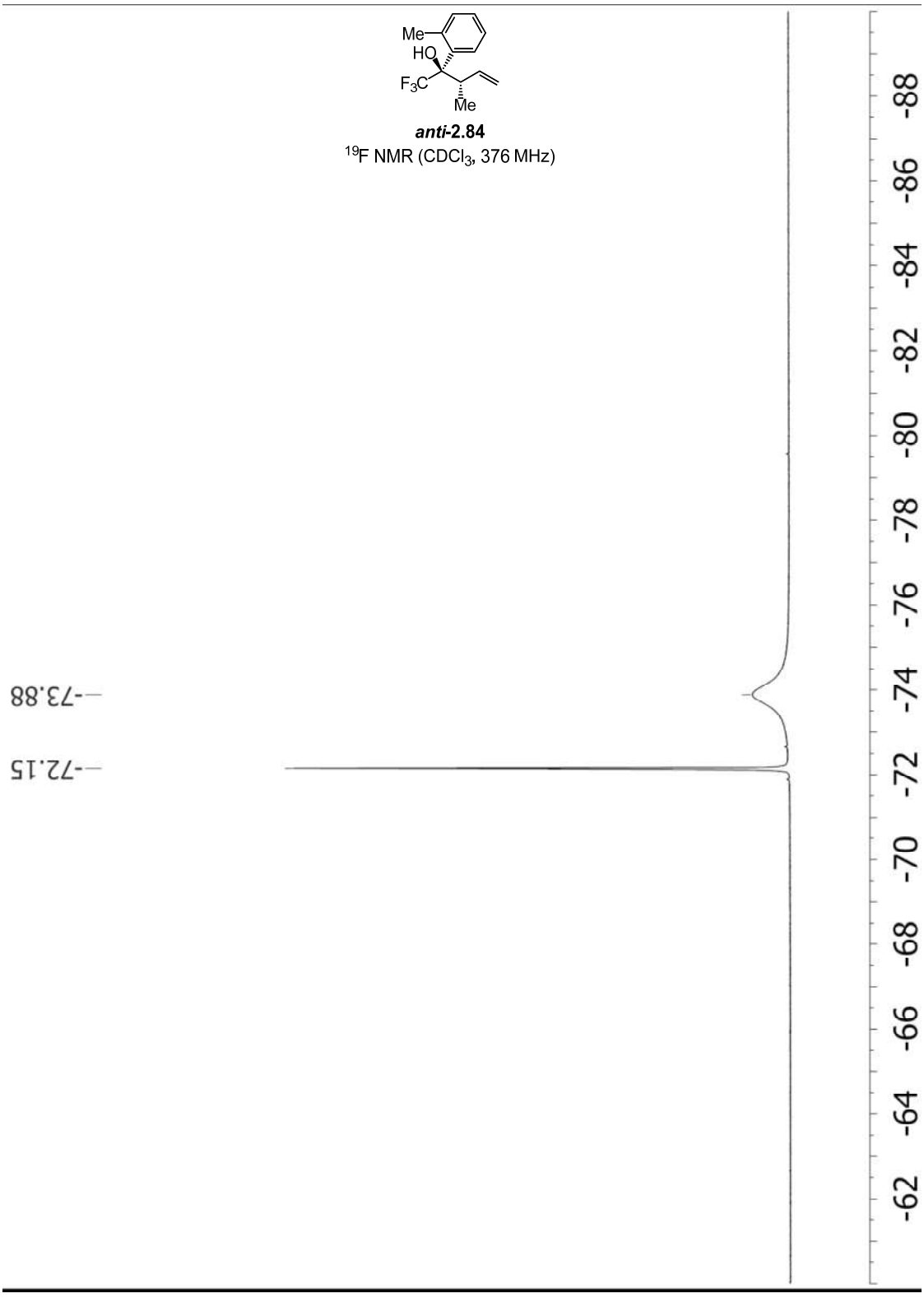
Me
HO
F3C
Me
anti-2.84
19F NMR (CDCl3, 376 MHz)
-73.88
-72.15
-62
-64
-66
-68
-70
-72
-74
-76
-78
-80
-82
-84
-86
-88

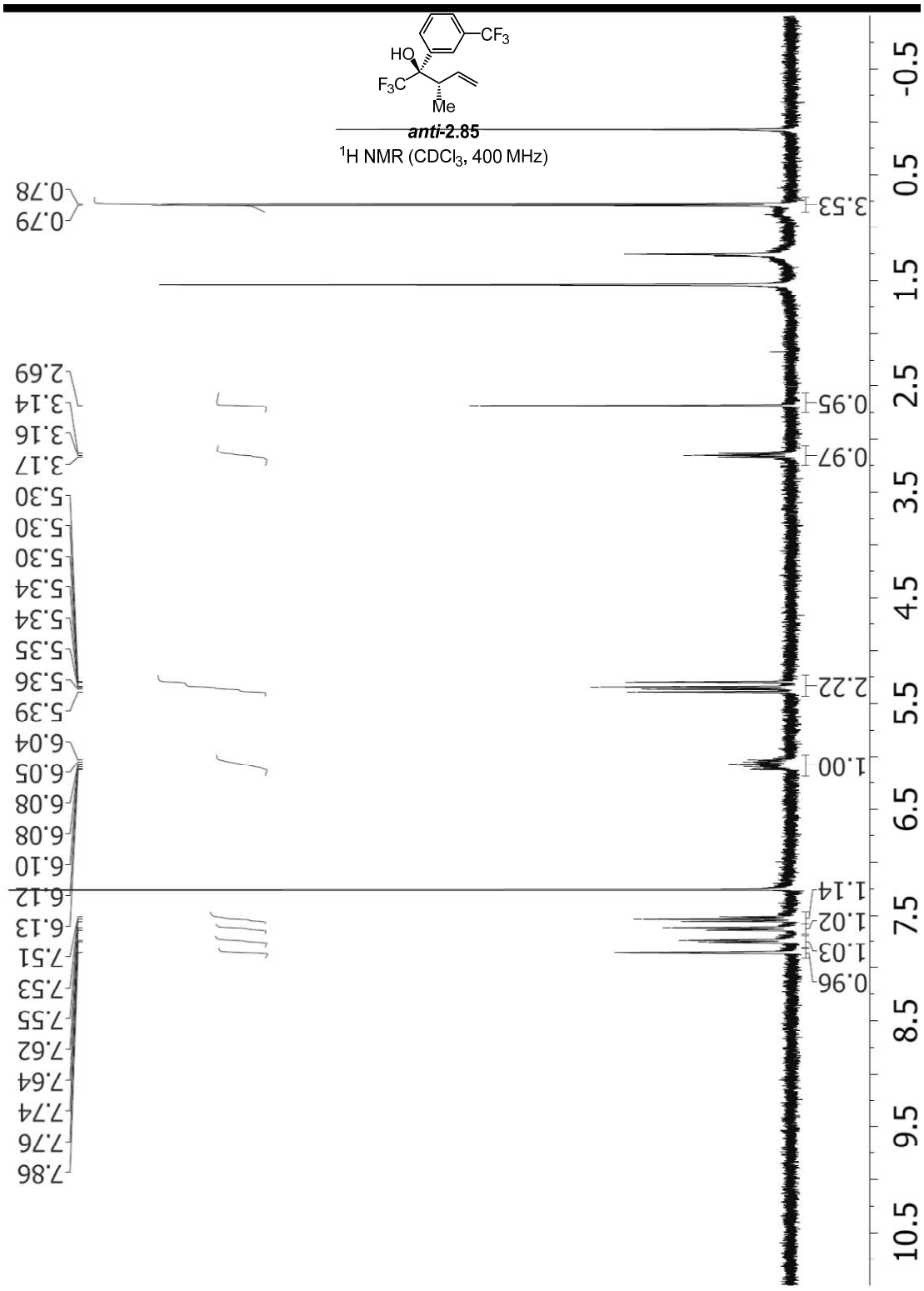
CF3
HO
F3C
Me
anti-2.85
1H NMR (CDCl3, 400 MHz)

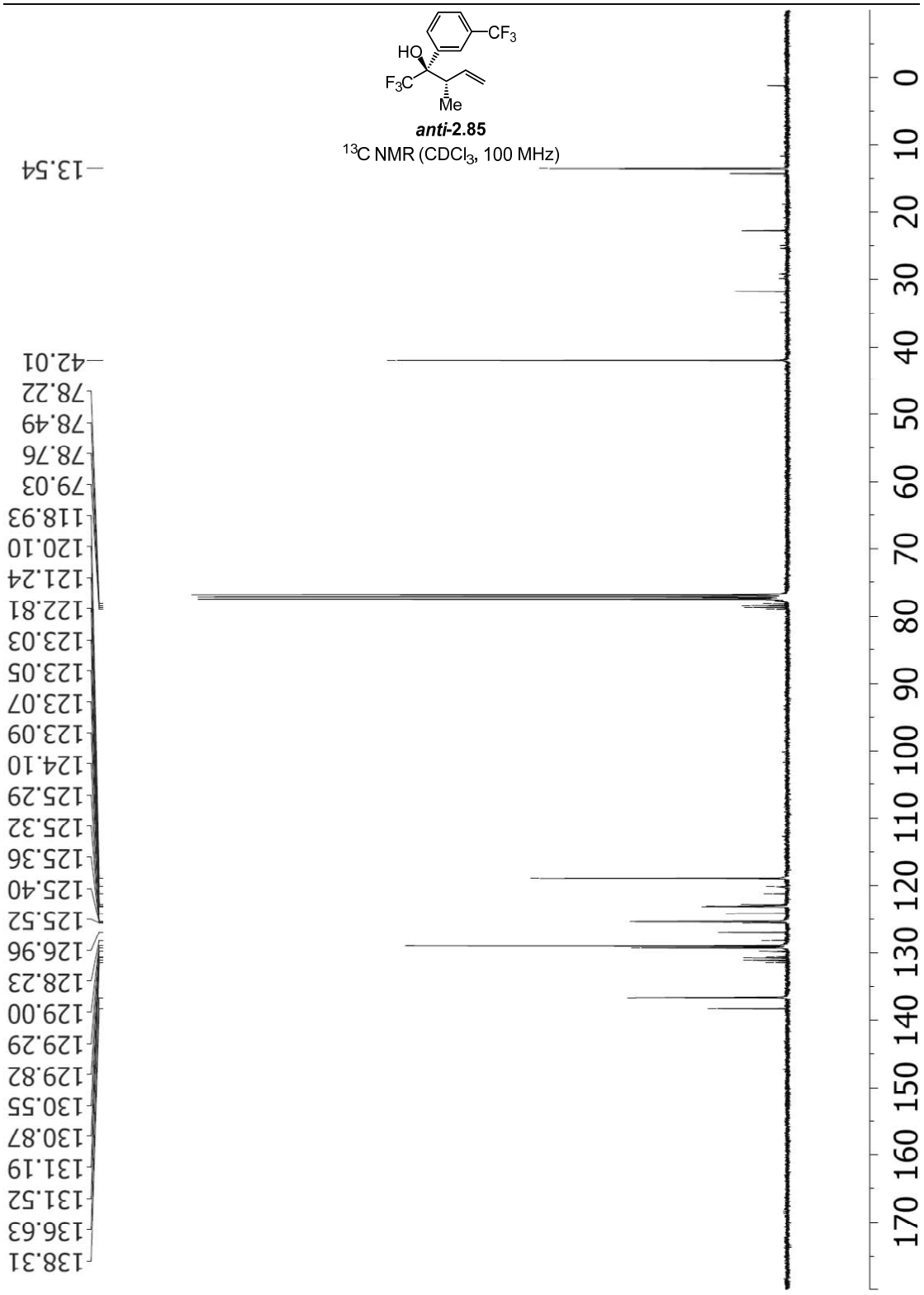
CF3
HO
F3C
Me
anti-2.85
13C NMR (CDCl3, 100 MHz)
13.54
42.01
78.22
78.49
78.76
79.03
118.93
120.10
121.24
122.81
123.03
123.05
123.07
123.09
124.10
125.29
125.32
125.36
125.40
125.52
126.96
128.23
129.00
129.29
129.82
130.55
130.87
131.19
131.52
136.63
138.31
0
10
20
30
40
50
60
70
80
90
100
110
120
130
140
150
160
170

***anti*-2.85**

^{19}F NMR ($CDCl_3$, 376 MHz)

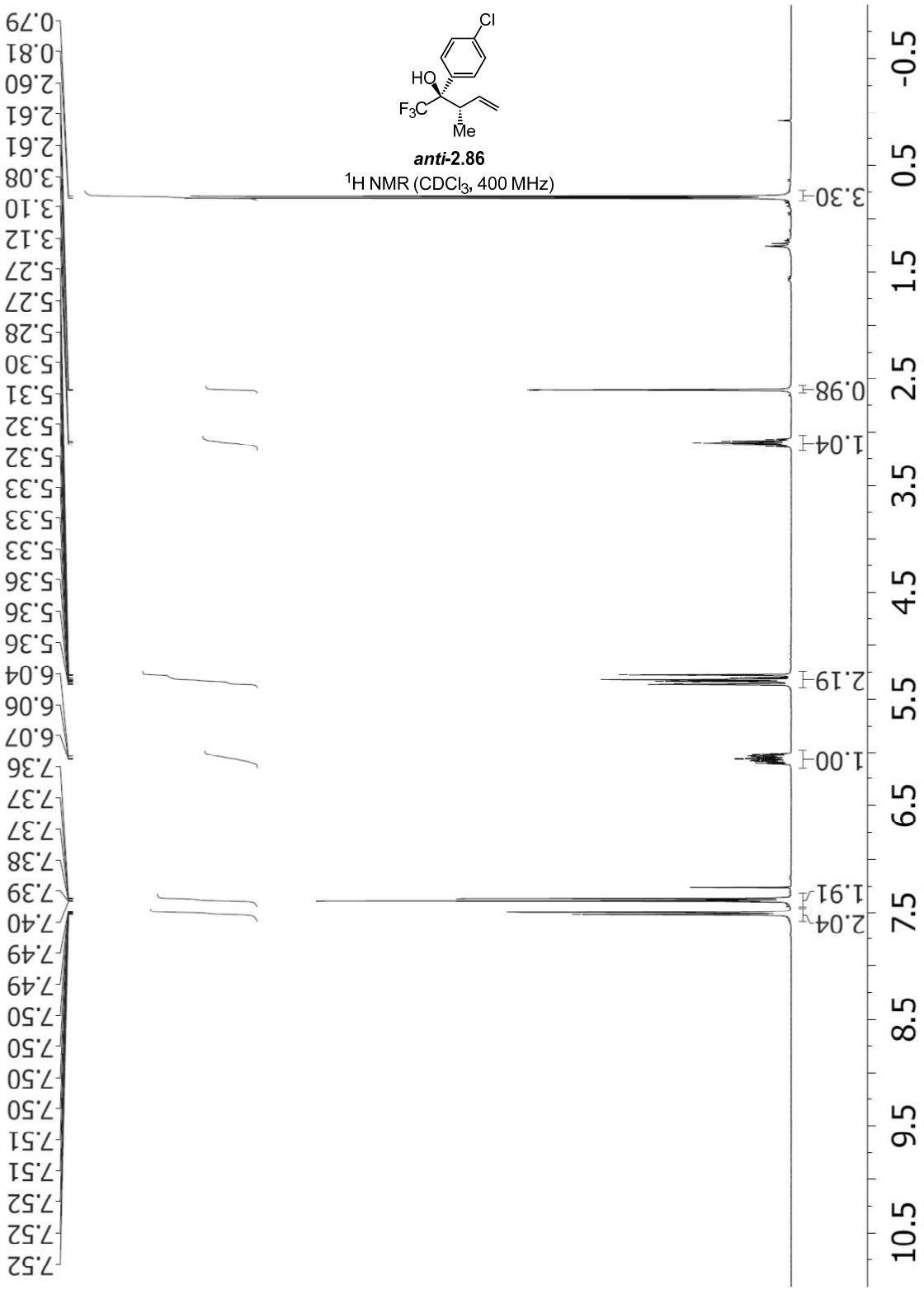
Cl
HO
F3C
Me
anti-2.86
1H NMR (CDCl3, 400 MHz)

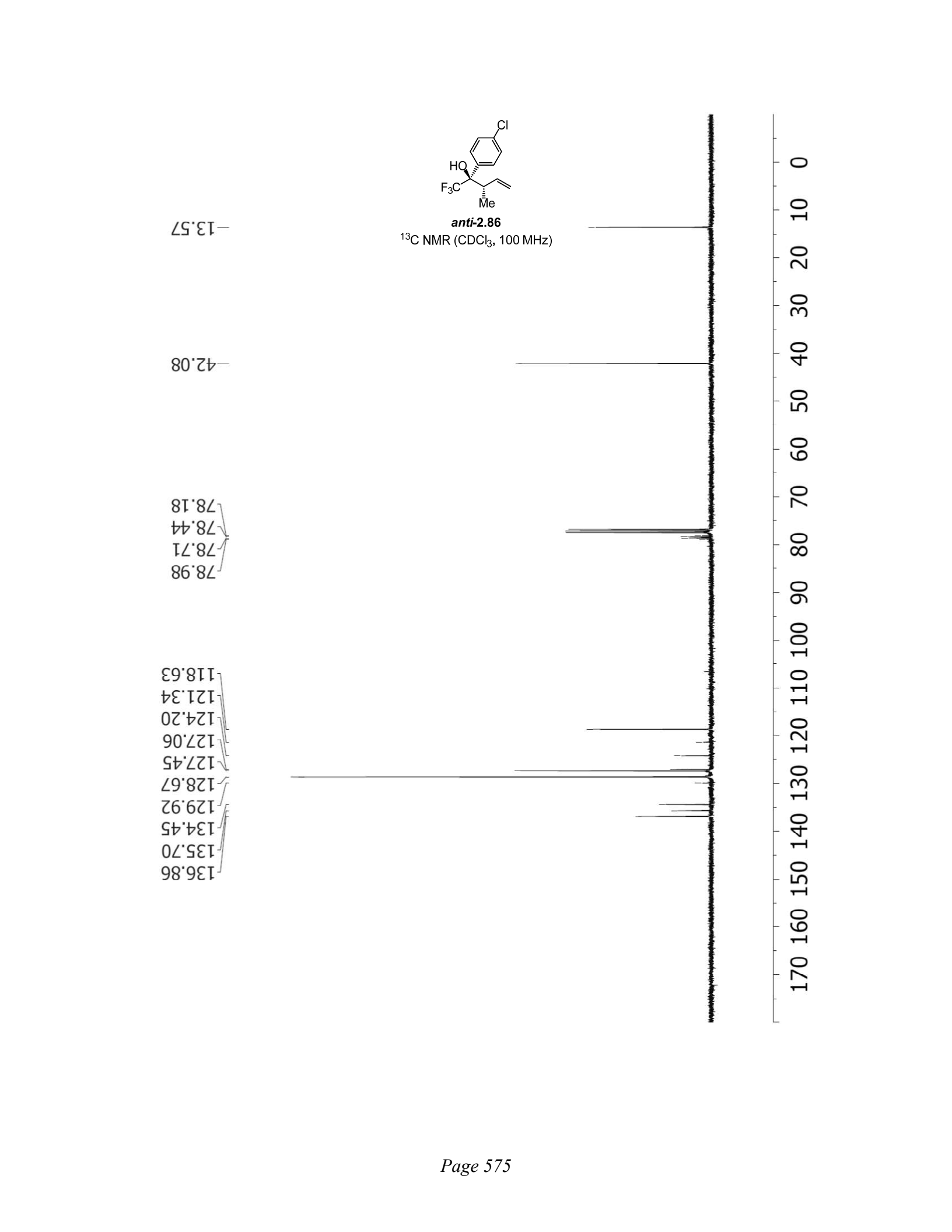
Cl
HO
F3C
Me
anti-2.86
13C NMR (CDCl3, 100 MHz)
13.57
42.08
78.18
78.44
78.71
78.98
118.63
121.34
124.20
127.06
127.45
128.67
129.92
134.45
135.70
136.86
0
10
20
30
40
50
60
70
80
90
100
110
120
130
140
150
160
170

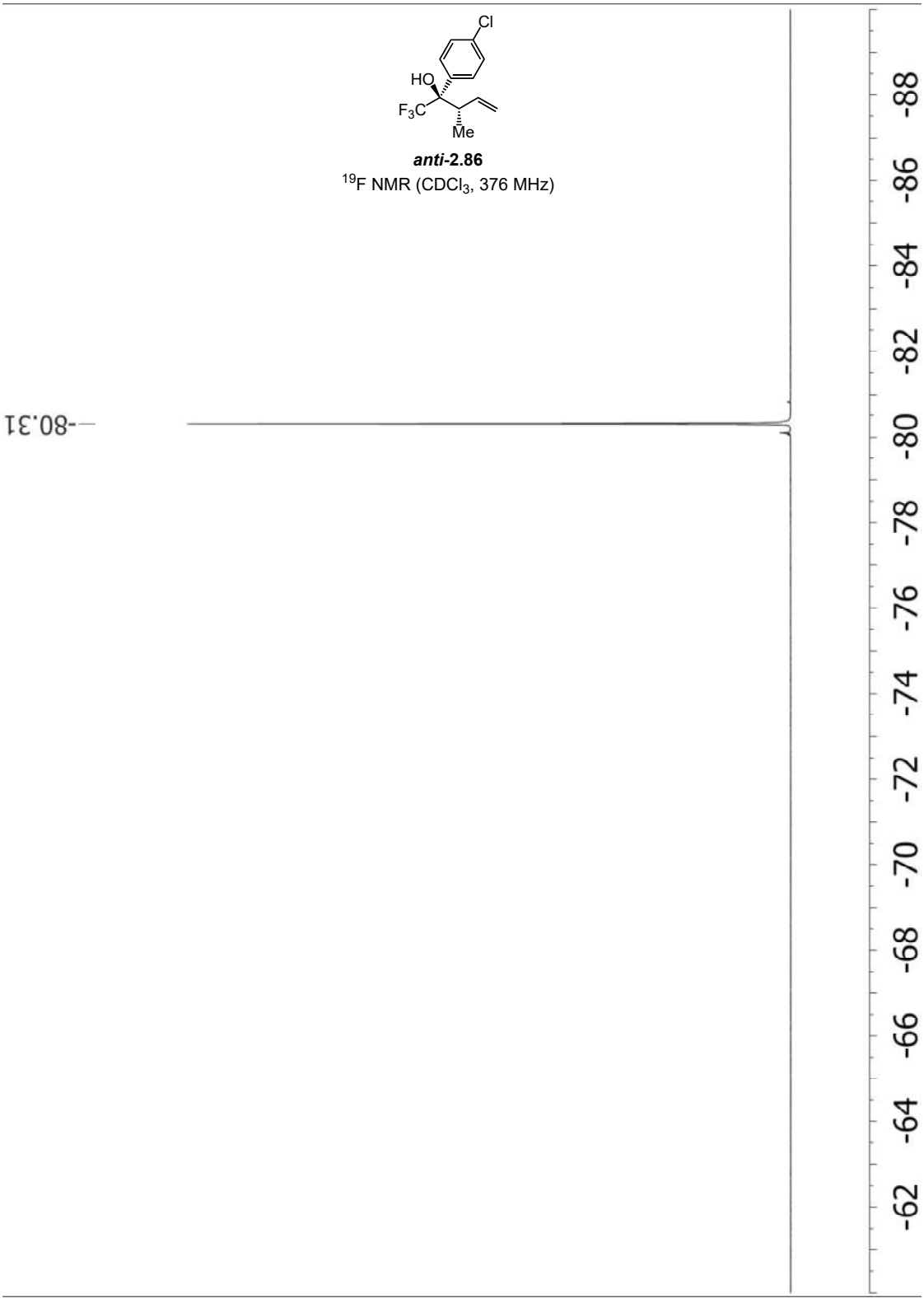

***anti*-2.86**

^{19}F NMR ($CDCl_3$, 376 MHz)

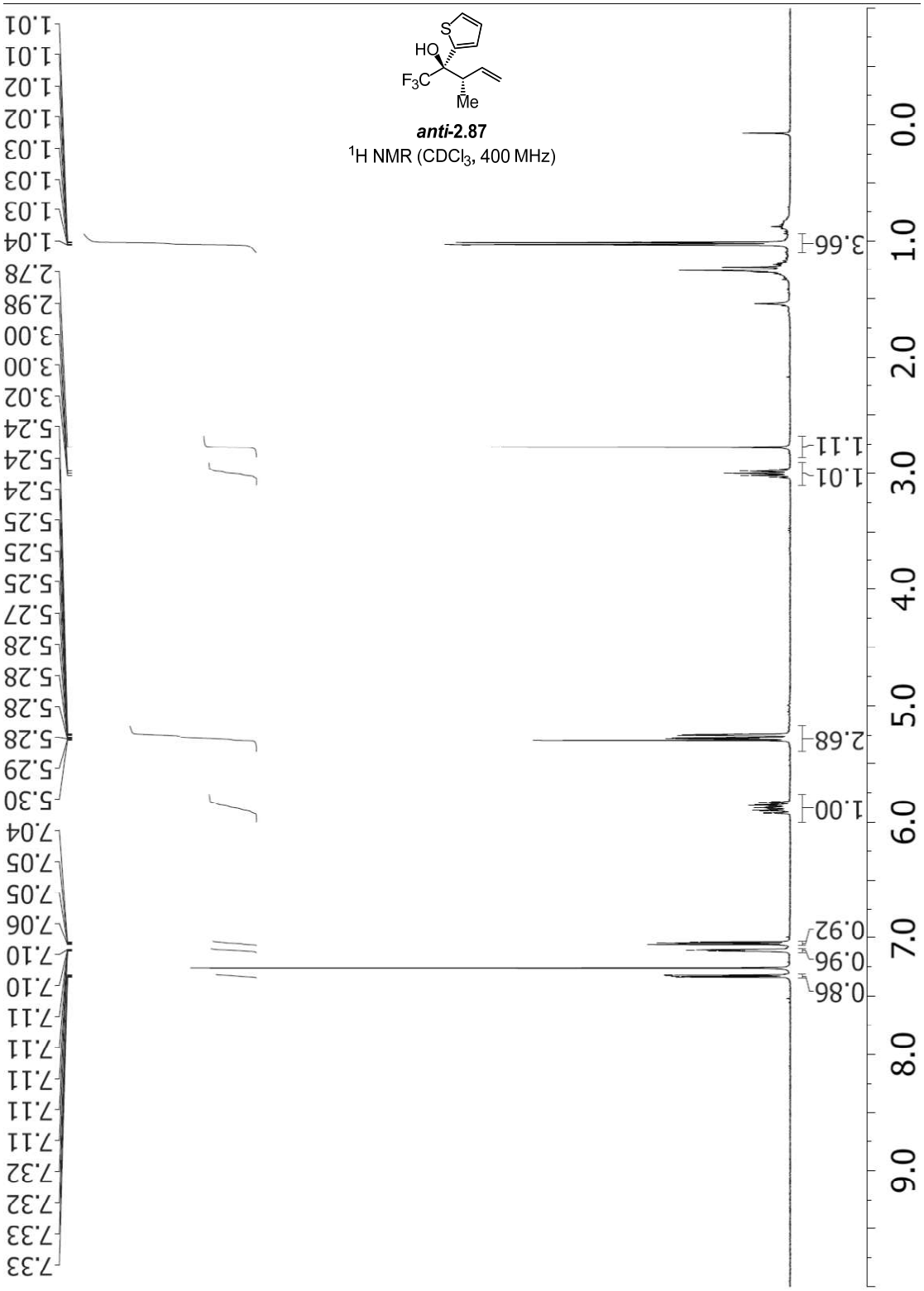
S
HO
F3C
Me
anti-2.87
1H NMR (CDCl3, 400 MHz)
3.66
1.11
1.01
2.68
1.00
0.92
0.96
0.86

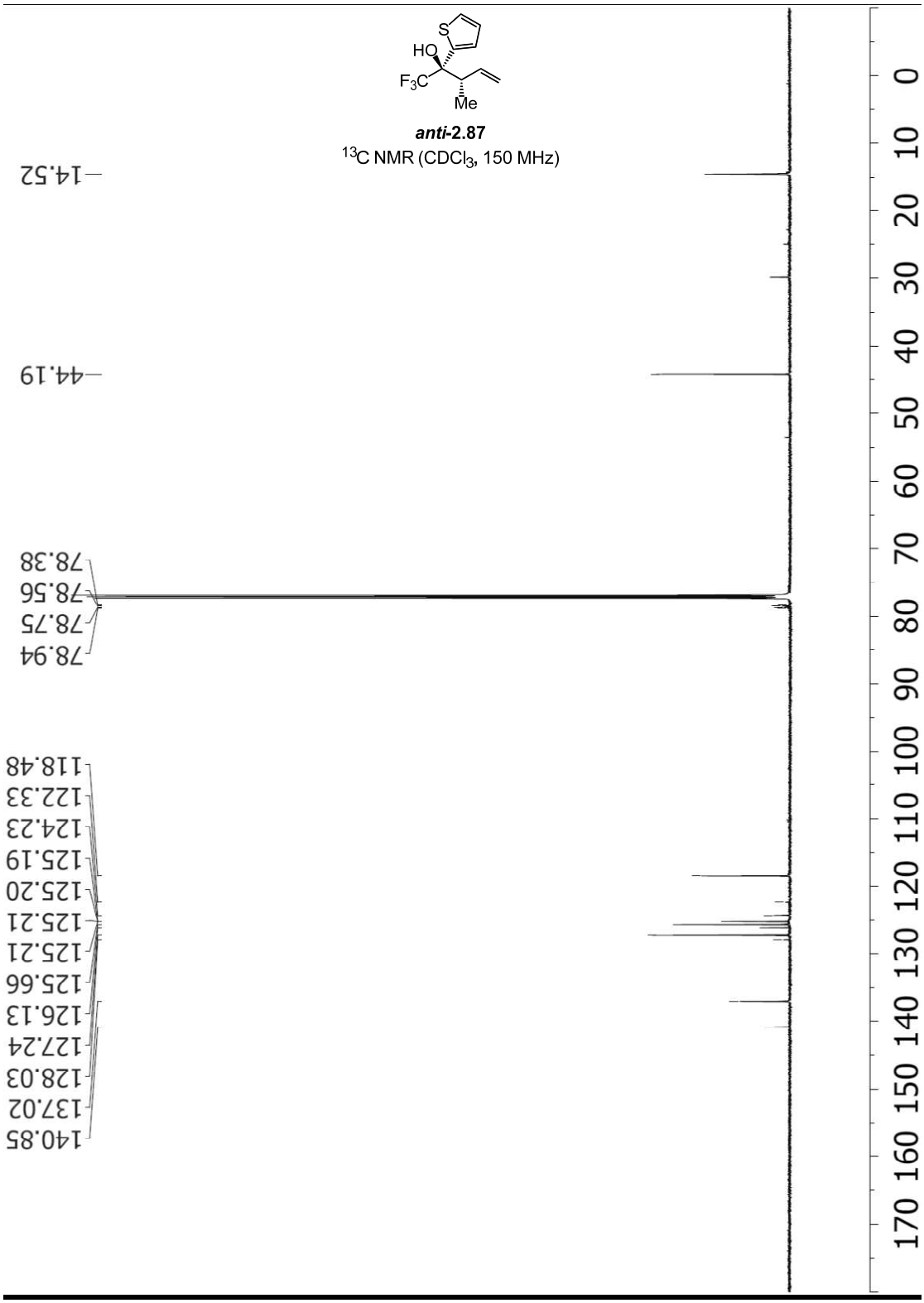
S
HO
F3C
Me
anti-2.87
13C NMR (CDCl3, 150 MHz)
14.52
44.19
78.38
78.56
78.75
78.94
118.48
122.33
124.23
125.19
125.20
125.21
125.21
125.66
126.13
127.24
128.03
137.02
140.85
0
10
20
30
40
50
60
70
80
90
100
110
120
130
140
150
160
170

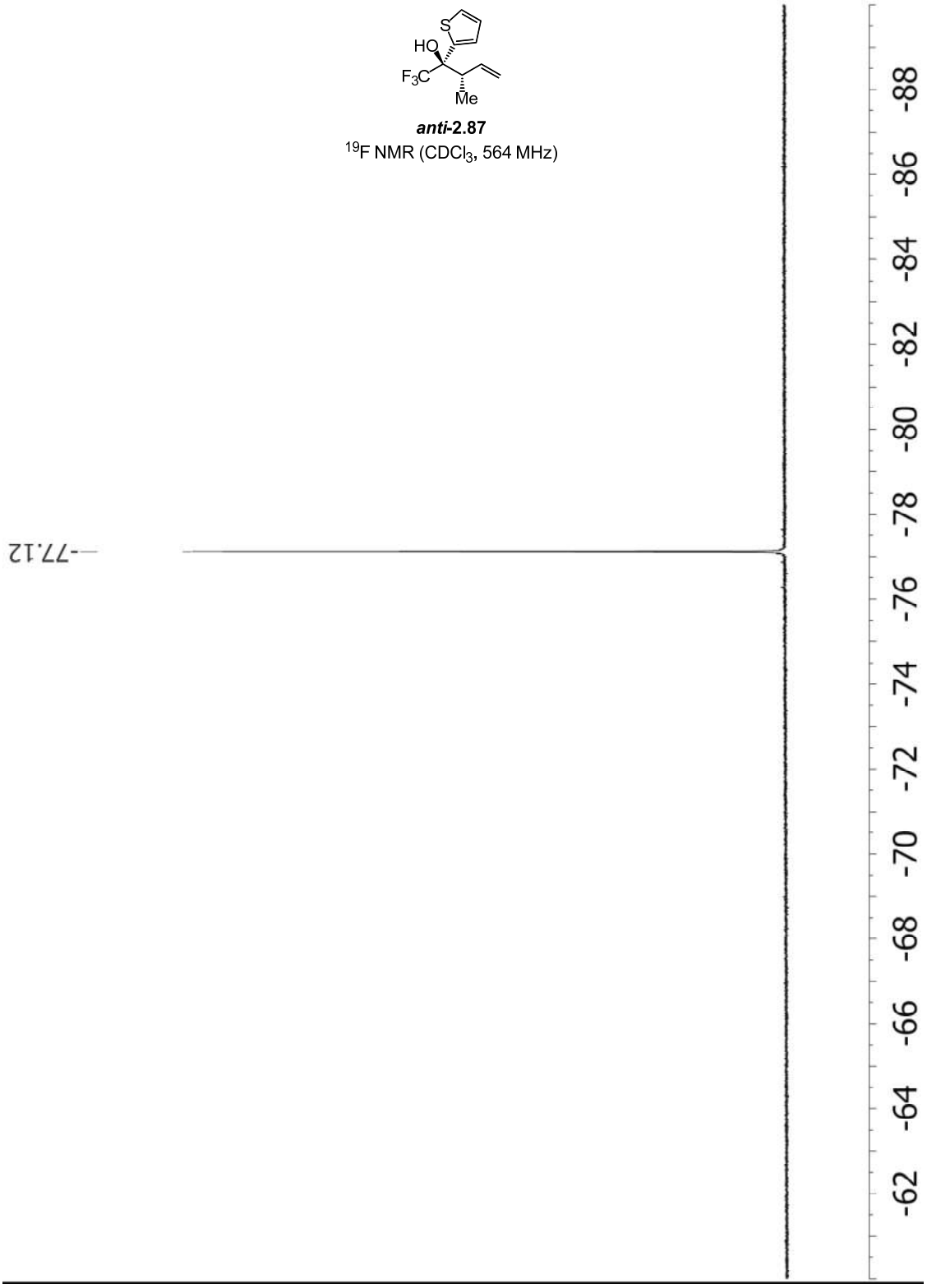

***anti*-2.87**

^{19}F NMR ($CDCl_3$, 564 MHz)

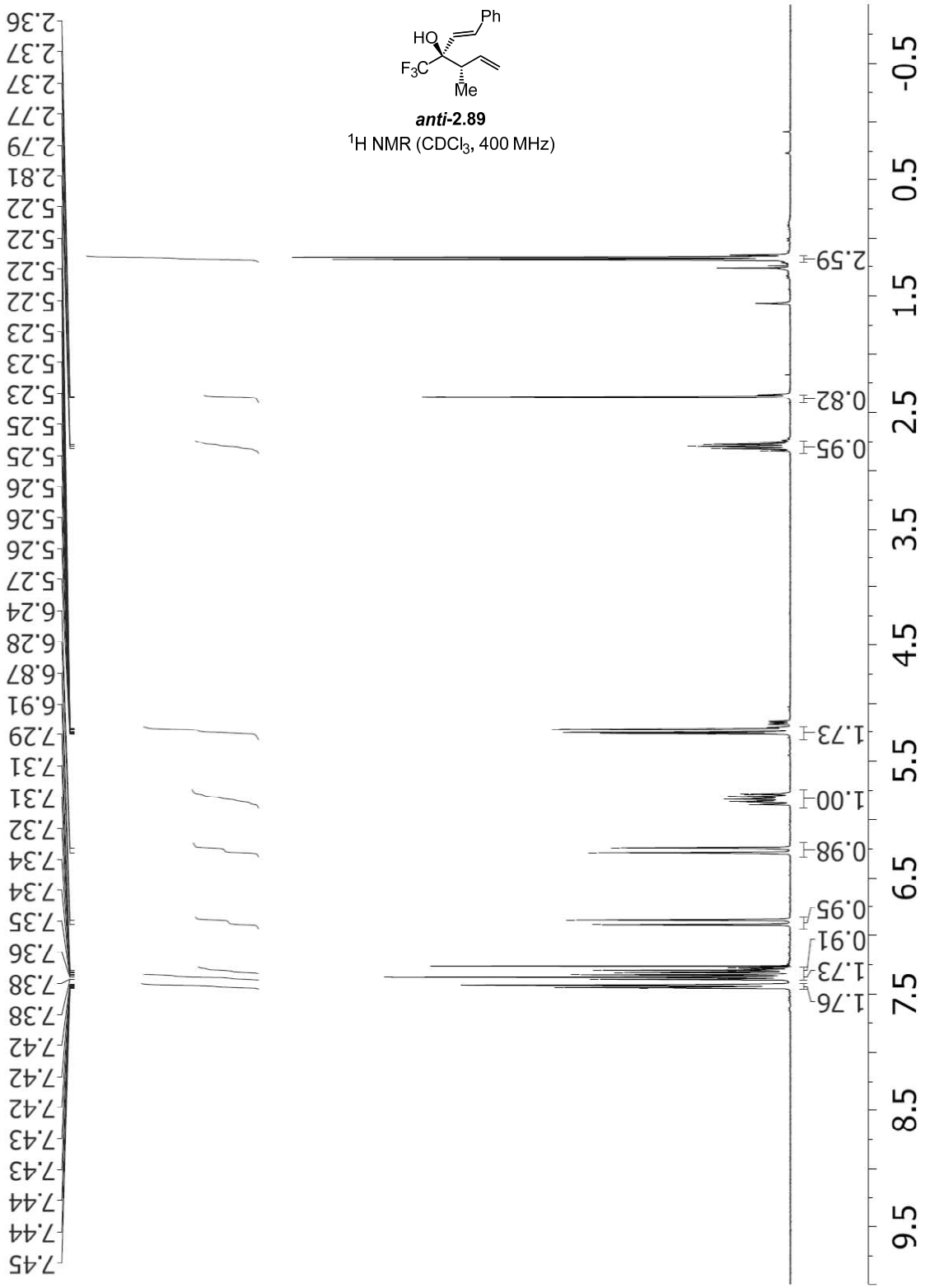
Ph
HO
F3C
Me
anti-2.89
1H NMR (CDCl3, 400 MHz)

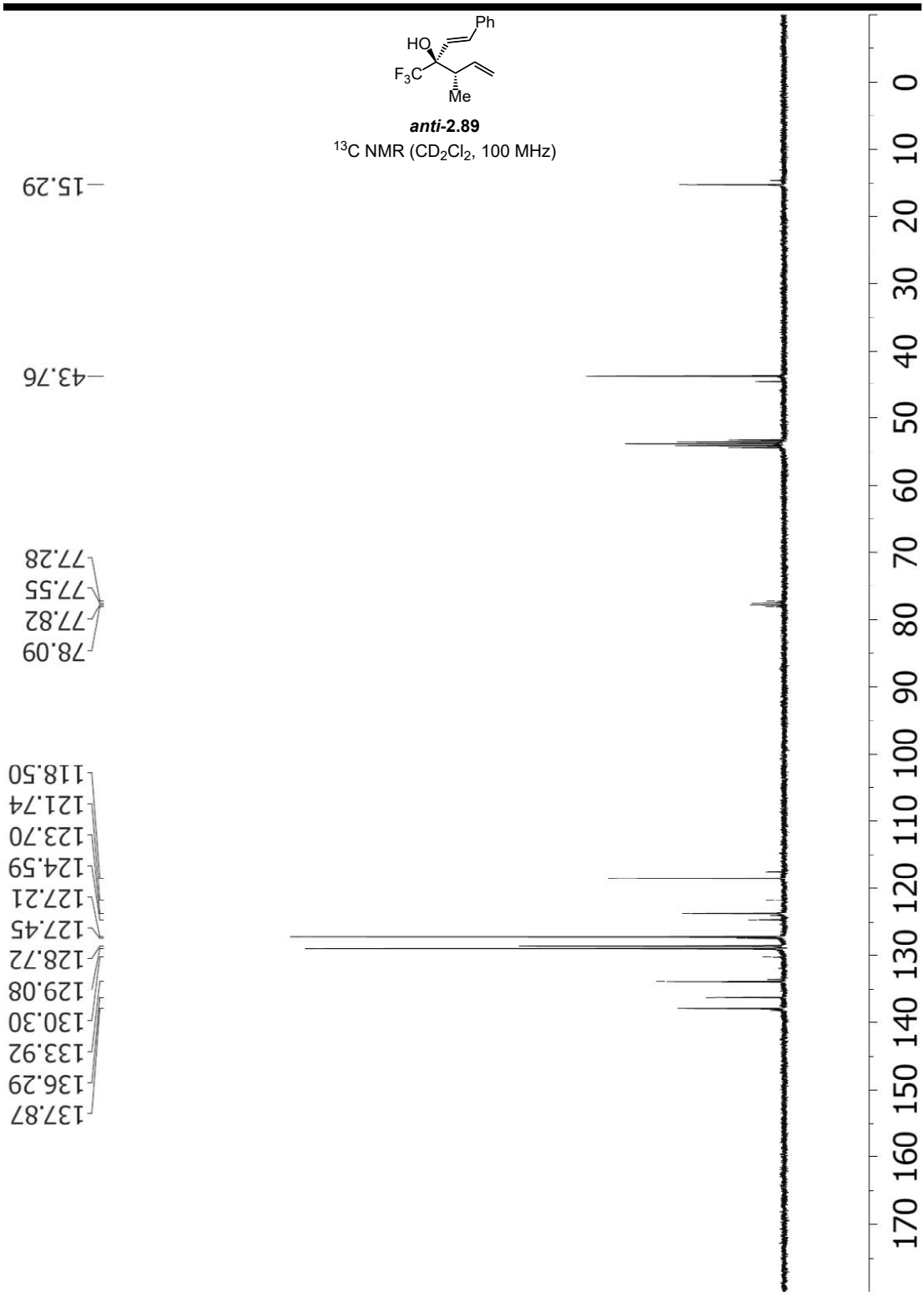
Ph
HO
F3C
Me
anti-2.89
13C NMR (CD2Cl2, 100 MHz)
15.29
43.76
77.28
77.55
77.82
78.09
118.50
121.74
123.70
124.59
127.21
127.45
128.72
129.08
130.30
133.92
136.29
137.87
0
10
20
30
40
50
60
70
80
90
100
110
120
130
140
150
160
170

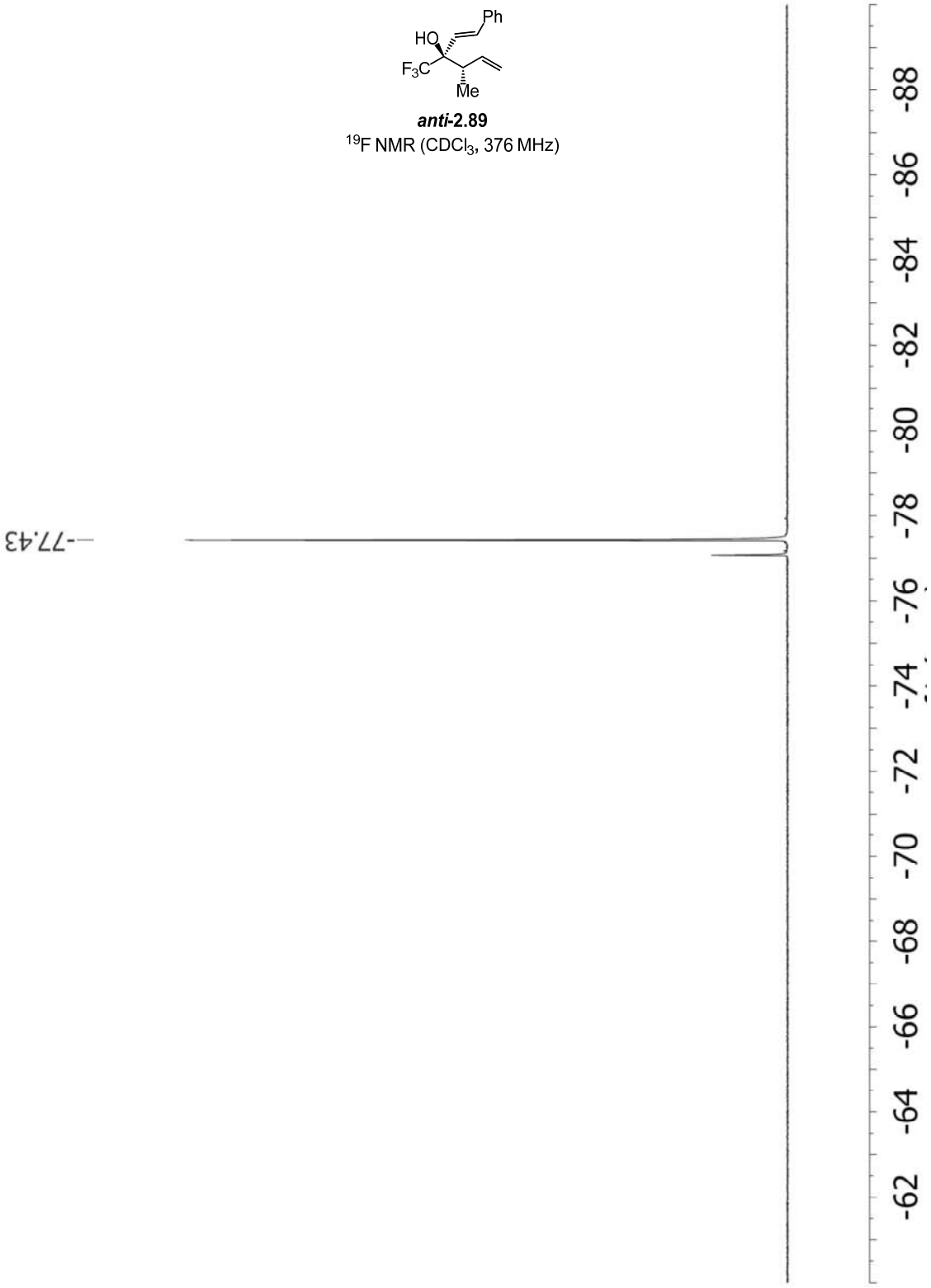

***anti*-2.89**

^{19}F NMR ($CDCl_3$, 376 MHz)

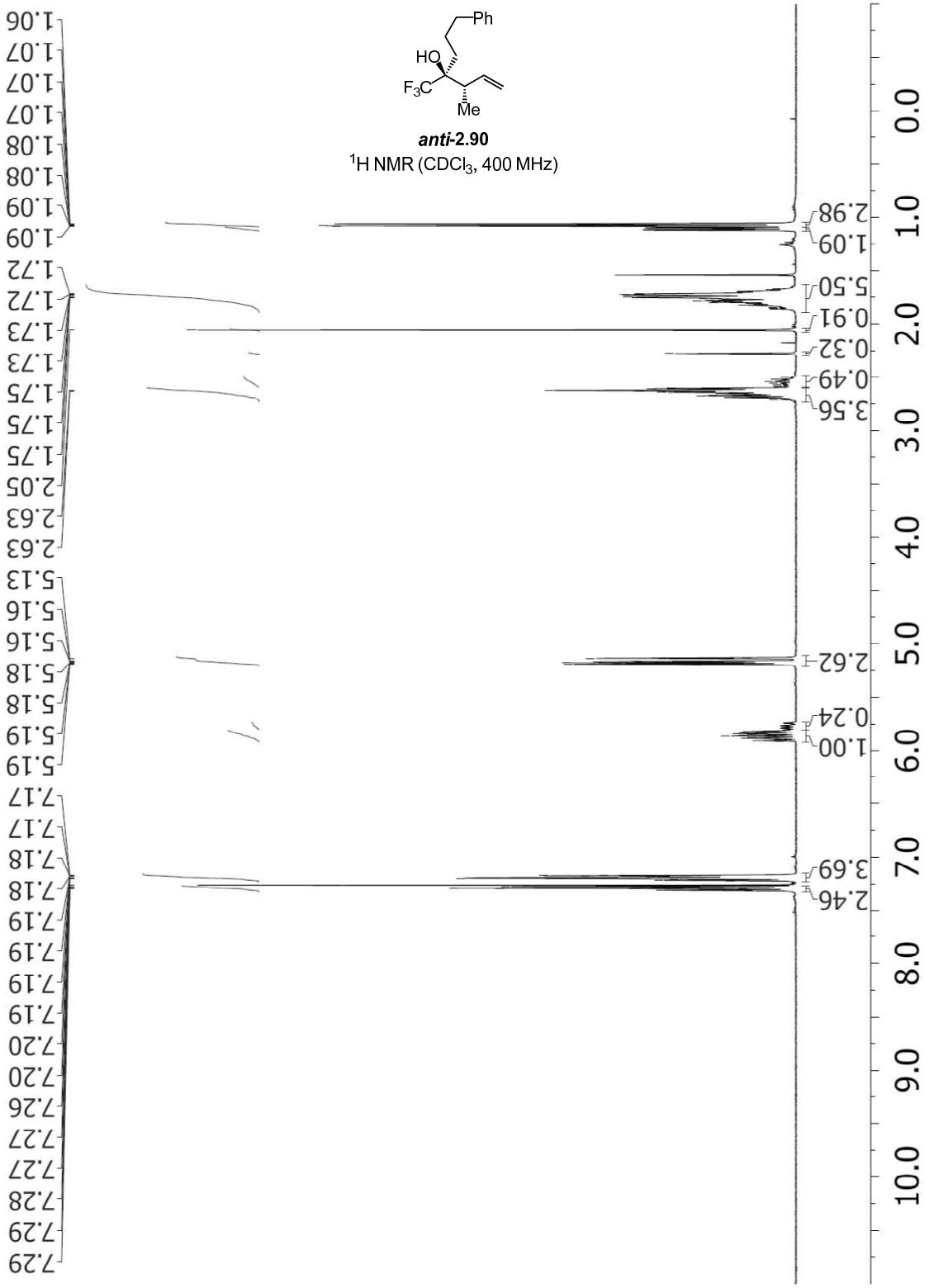
Ph
HO
F3C
Me
anti-2.90
1H NMR (CDCl3, 400 MHz)

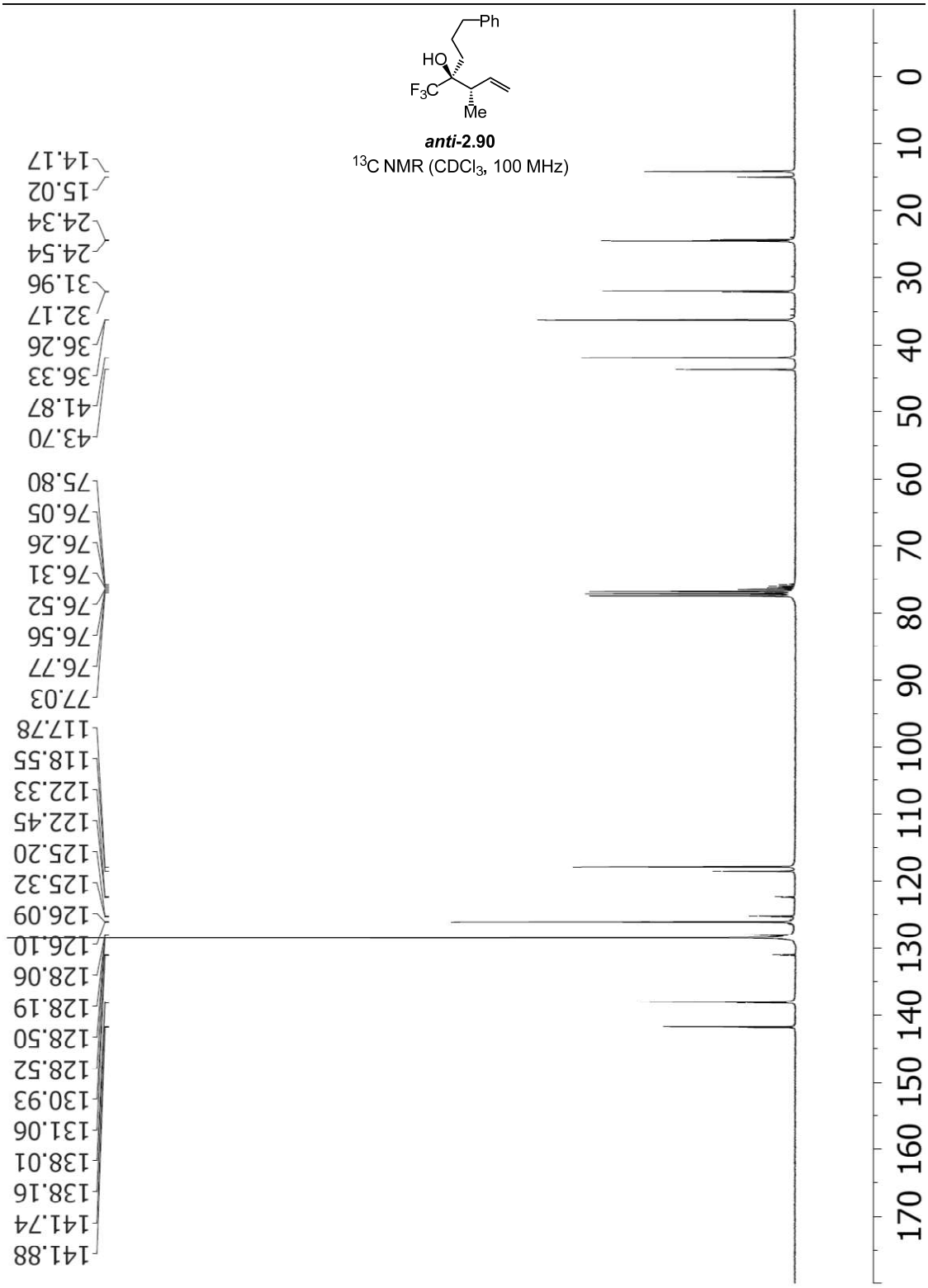
Ph
HO
F3C
Me
anti-2.90
13C NMR (CDCl3, 100 MHz)
14.17
15.02
24.34
24.54
31.96
32.17
36.26
36.33
41.87
43.70
75.80
76.05
76.26
76.31
76.52
76.56
76.77
77.03
117.78
118.55
122.33
122.45
125.20
125.32
126.09
126.10
128.06
128.19
128.50
128.52
130.93
131.06
138.01
138.16
141.74
141.88
0
10
20
30
40
50
60
70
80
90
100
110
120
130
140
150
160
170

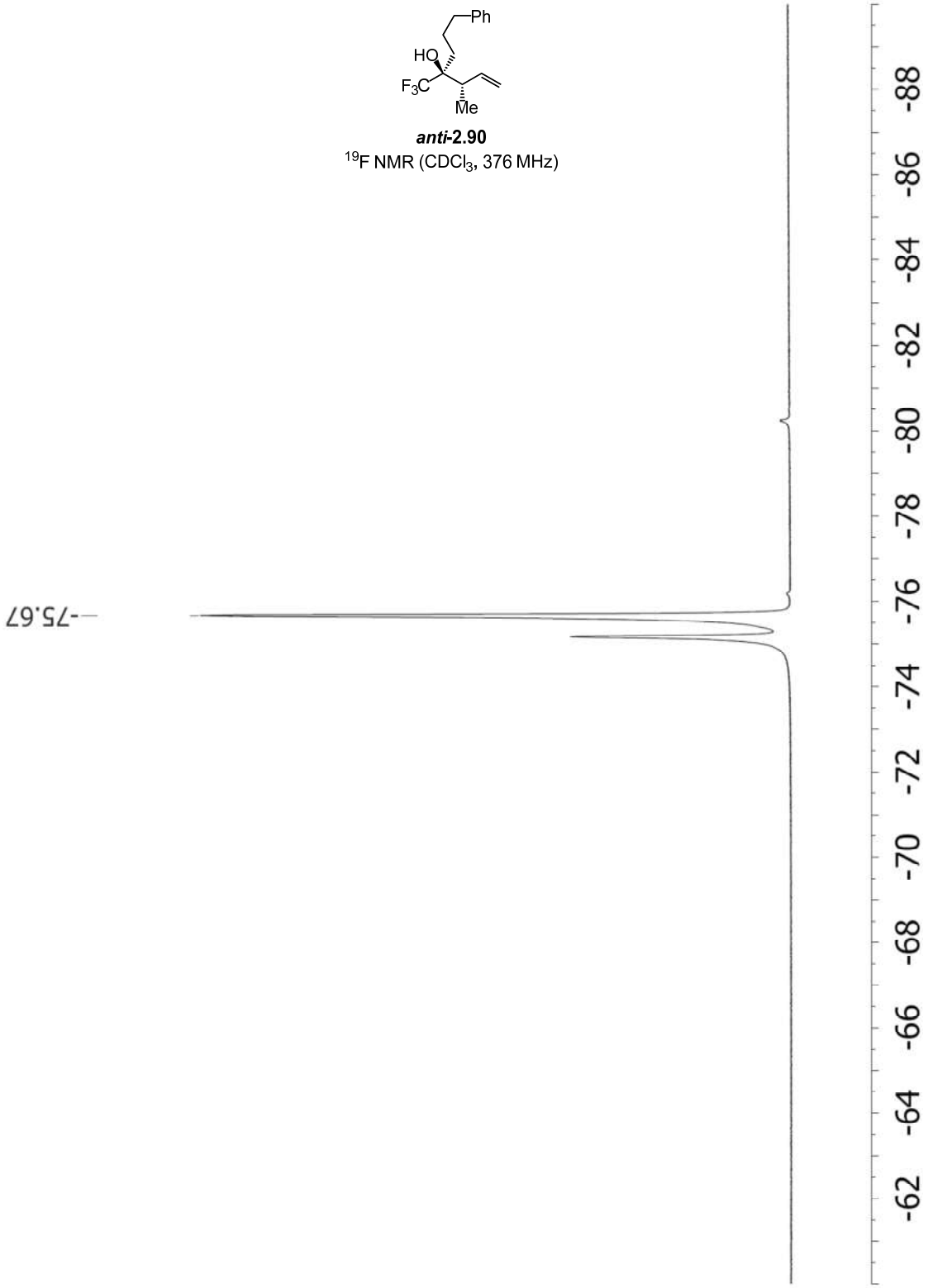

***anti*-2.90**

^{19}F NMR ($CDCl_3$, 376 MHz)

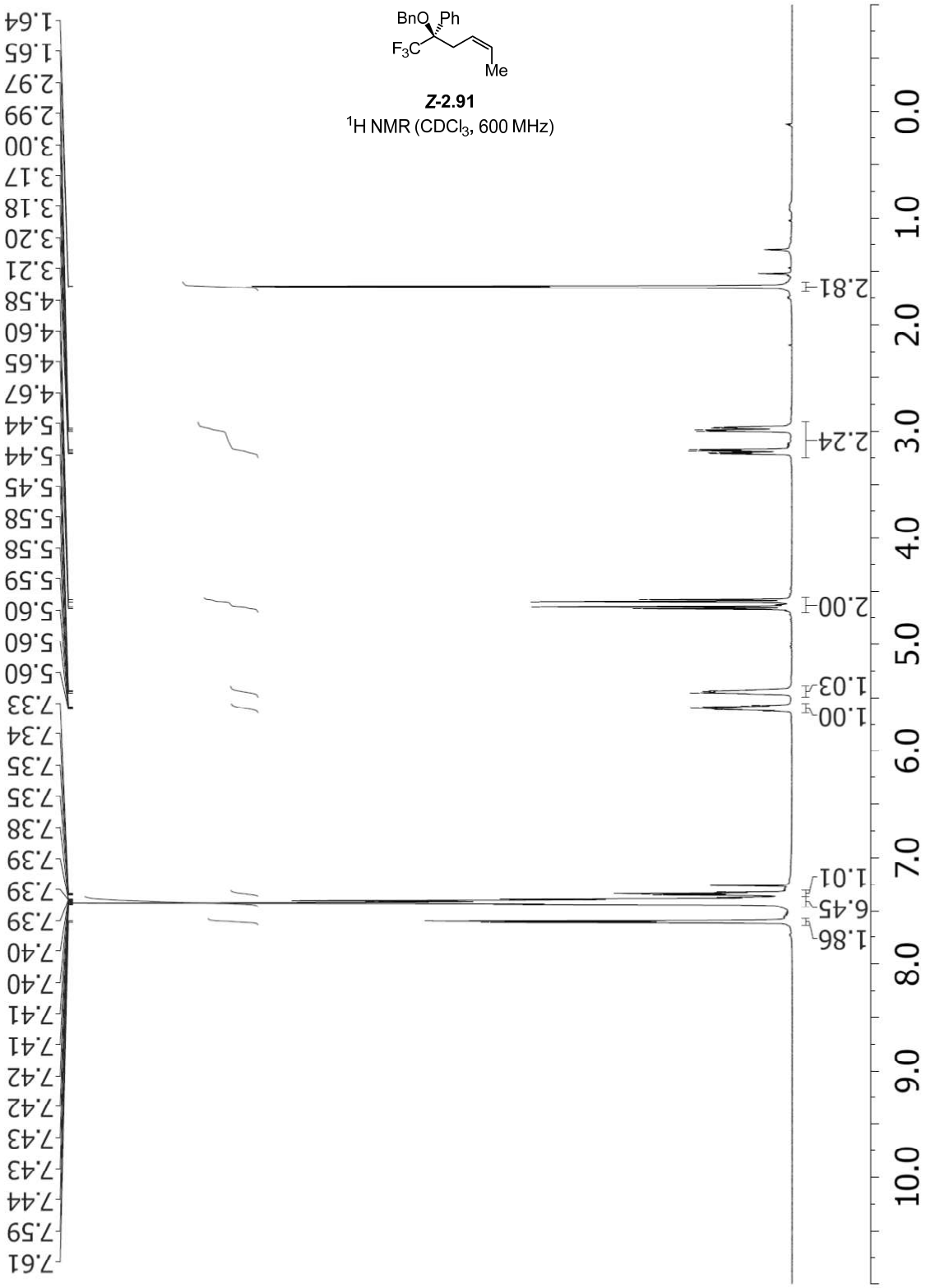
BnO
Ph
F3C
Me
Z-2.91
1H NMR (CDCl3, 600 MHz)
2.81
2.24
2.00
1.03
1.00
1.01
6.45
1.86

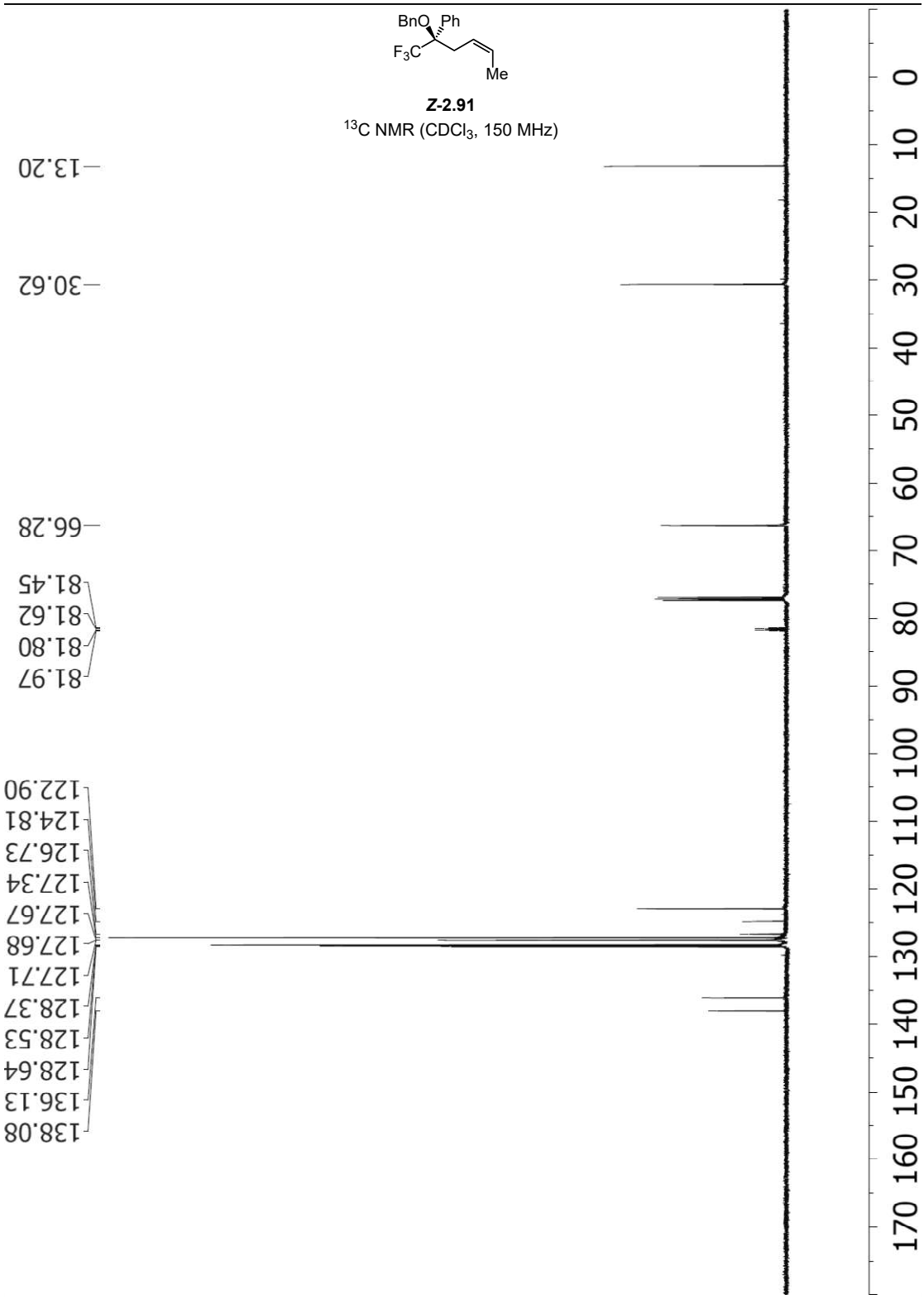
BnO
Ph
F3C
Me
Z-2.91
13C NMR (CDCl3, 150 MHz)
13.20
30.62
66.28
81.45
81.62
81.80
81.97
122.90
124.81
126.73
127.34
127.67
127.68
127.71
128.37
128.53
128.64
136.13
138.08
0
10
20
30
40
50
60
70
80
90
100
110
120
130
140
150
160
170


BnO
Ph
F3C
Me
Z-2.91
19F NMR (CDCl3, 564 MHz)
-74.78
-62
-64
-66
-68
-70
-72
-74
-76
-78
-80
-82
-84
-86
-88

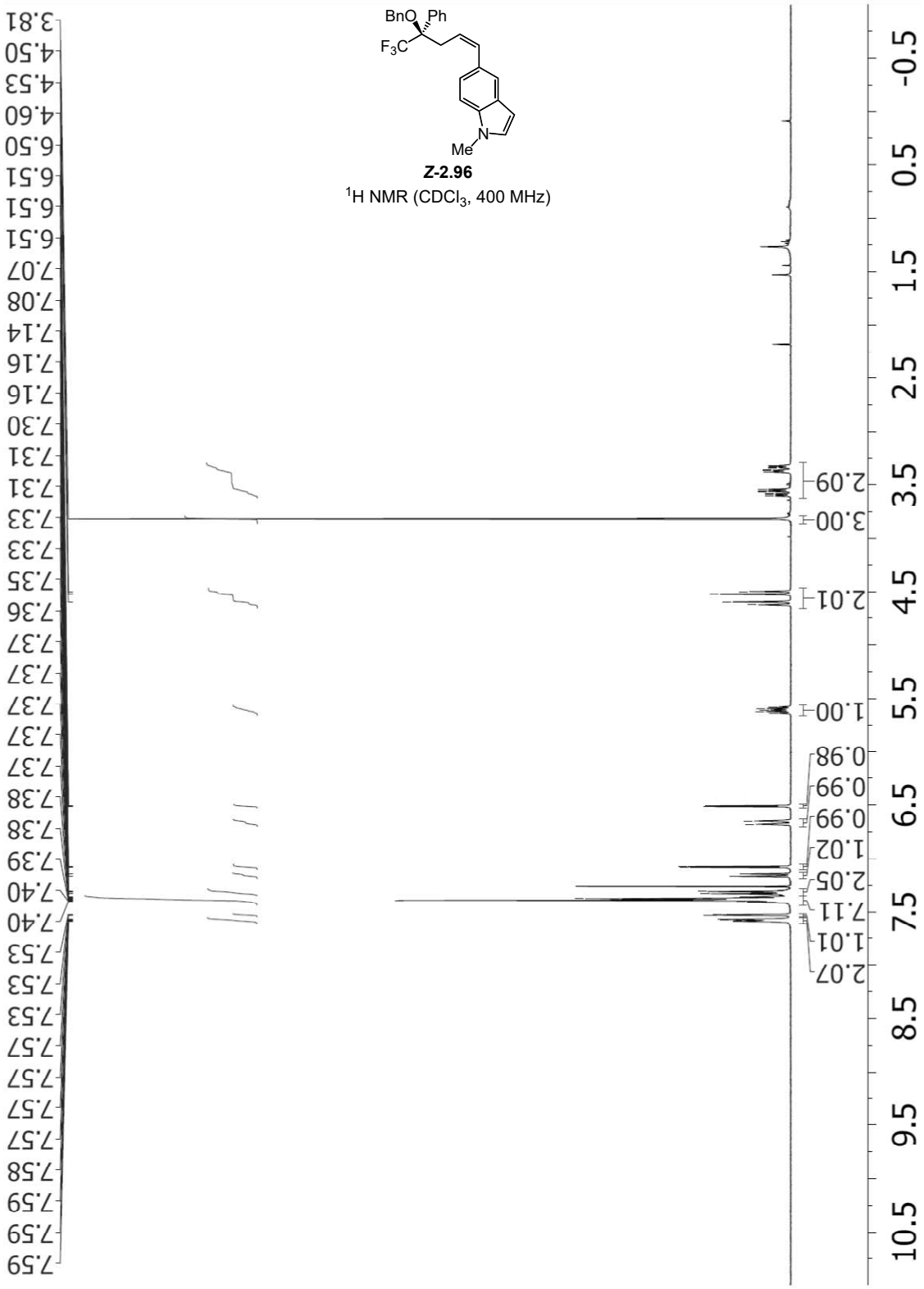
BnO
Ph
F3C
N
Me
Z-2.96
1H NMR (CDCl3, 400 MHz)

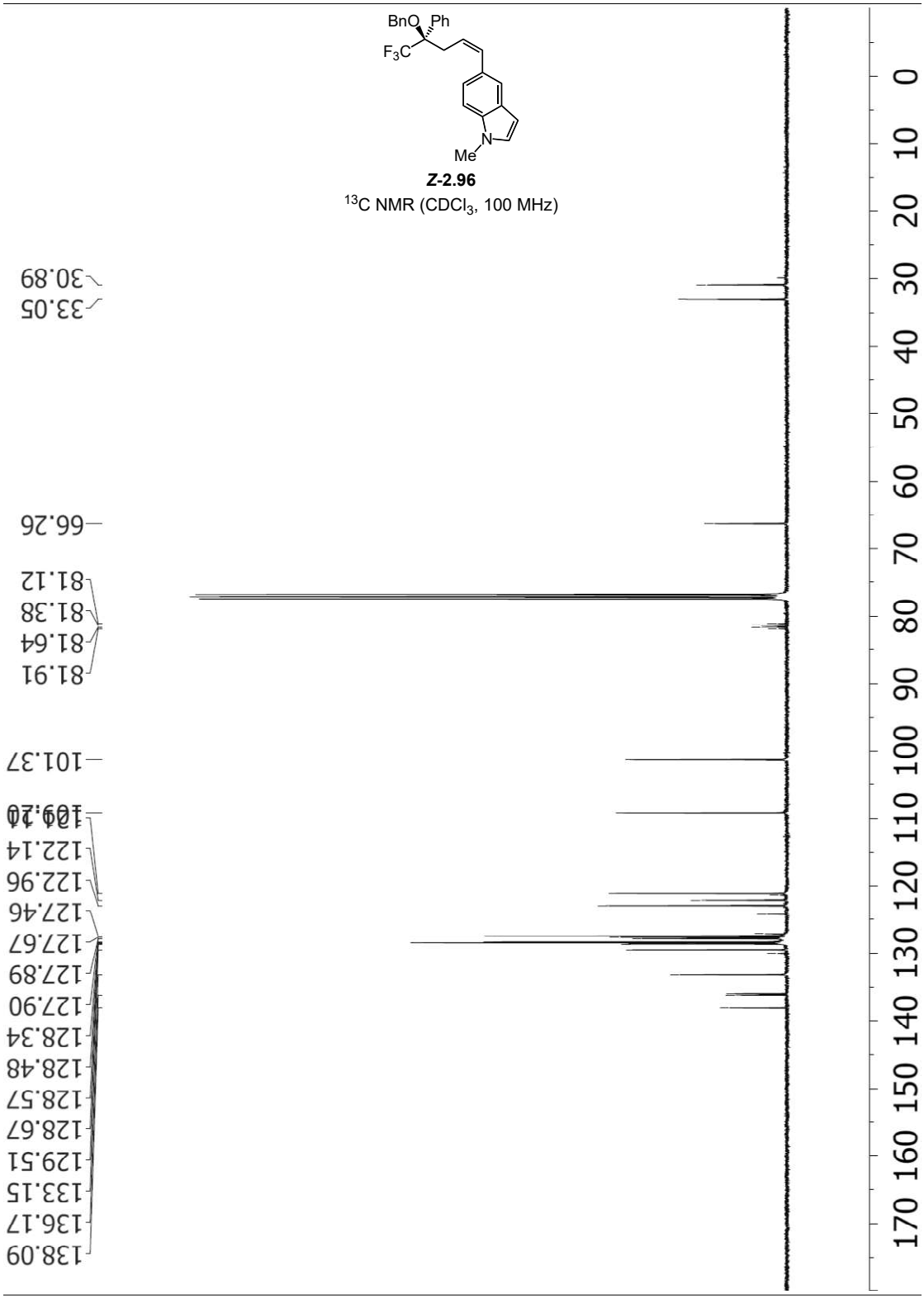
BnO
Ph
F3C
N
Me
Z-2.96
13C NMR (CDCl3, 100 MHz)
30.89
33.05
66.26
81.12
81.38
81.64
81.91
101.37
109.20
122.14
122.96
127.46
127.67
127.89
127.90
128.34
128.48
128.57
128.67
129.51
133.15
136.17
138.09
0
10
20
30
40
50
60
70
80
90
100
110
120
130
140
150
160
170

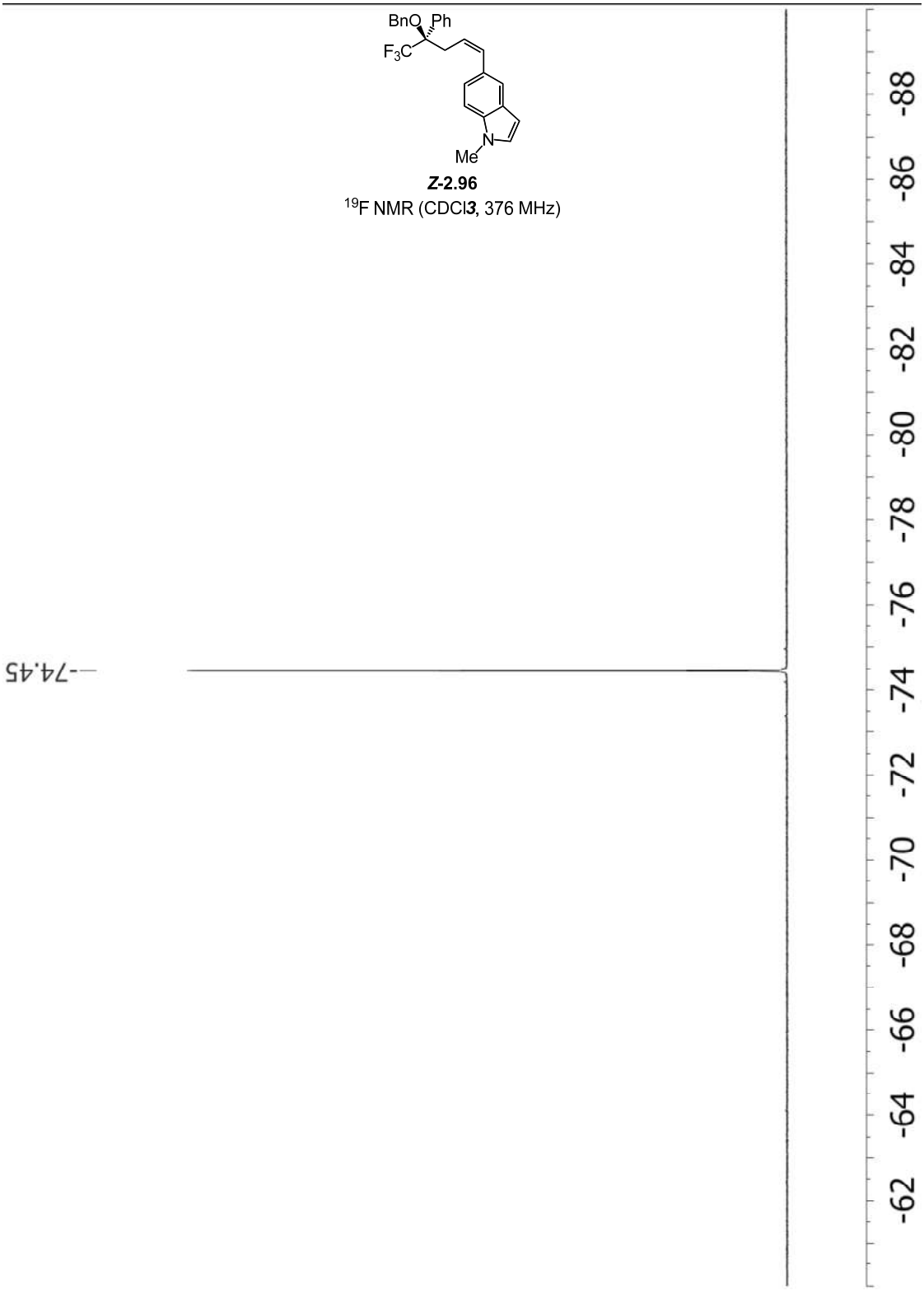

***Z*-2.96**

^{19}F NMR (CDCl**3**, 376 MHz)

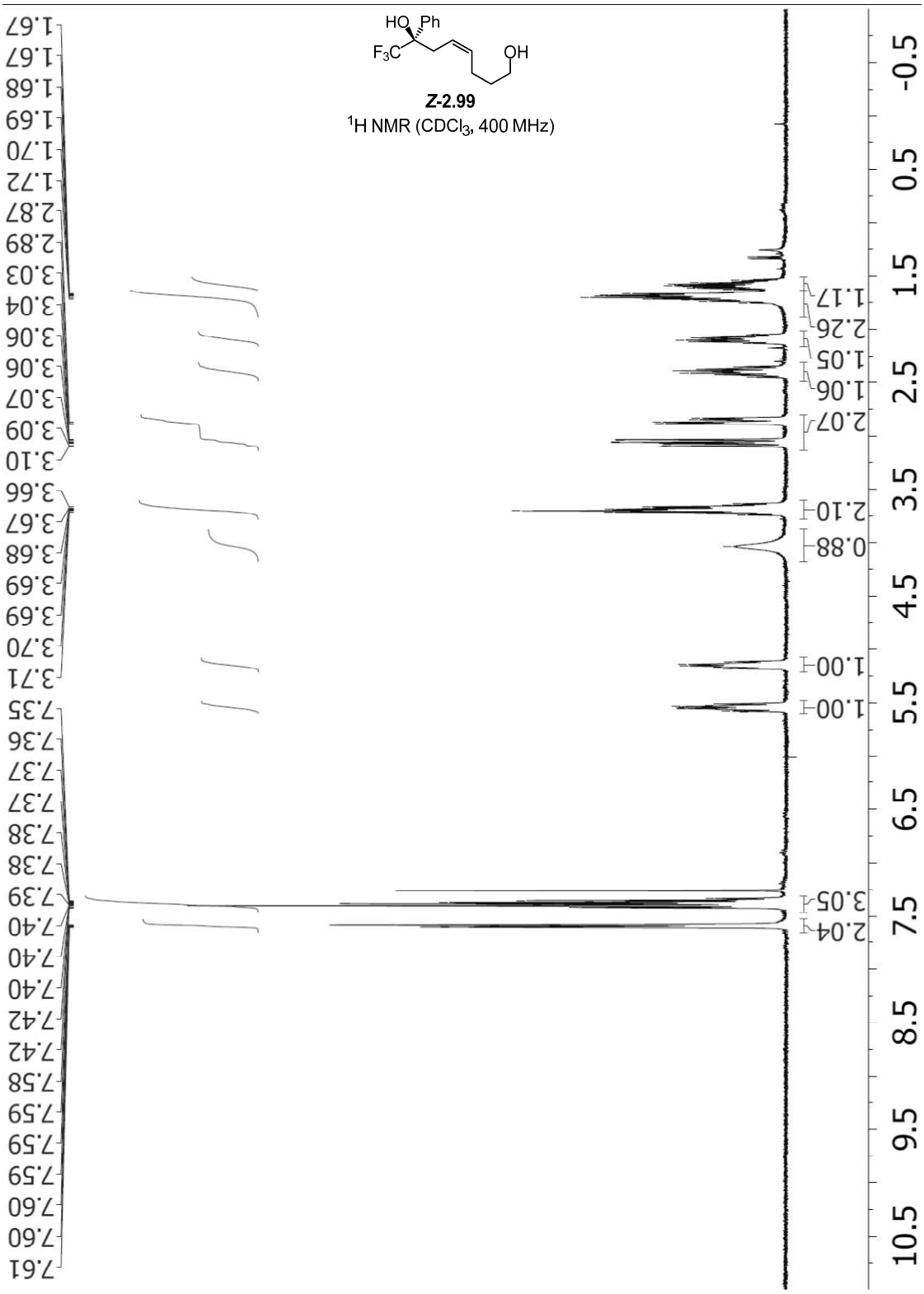
HO
Ph
F3C
OH
Z-2.99
1H NMR (CDCl3, 400 MHz)

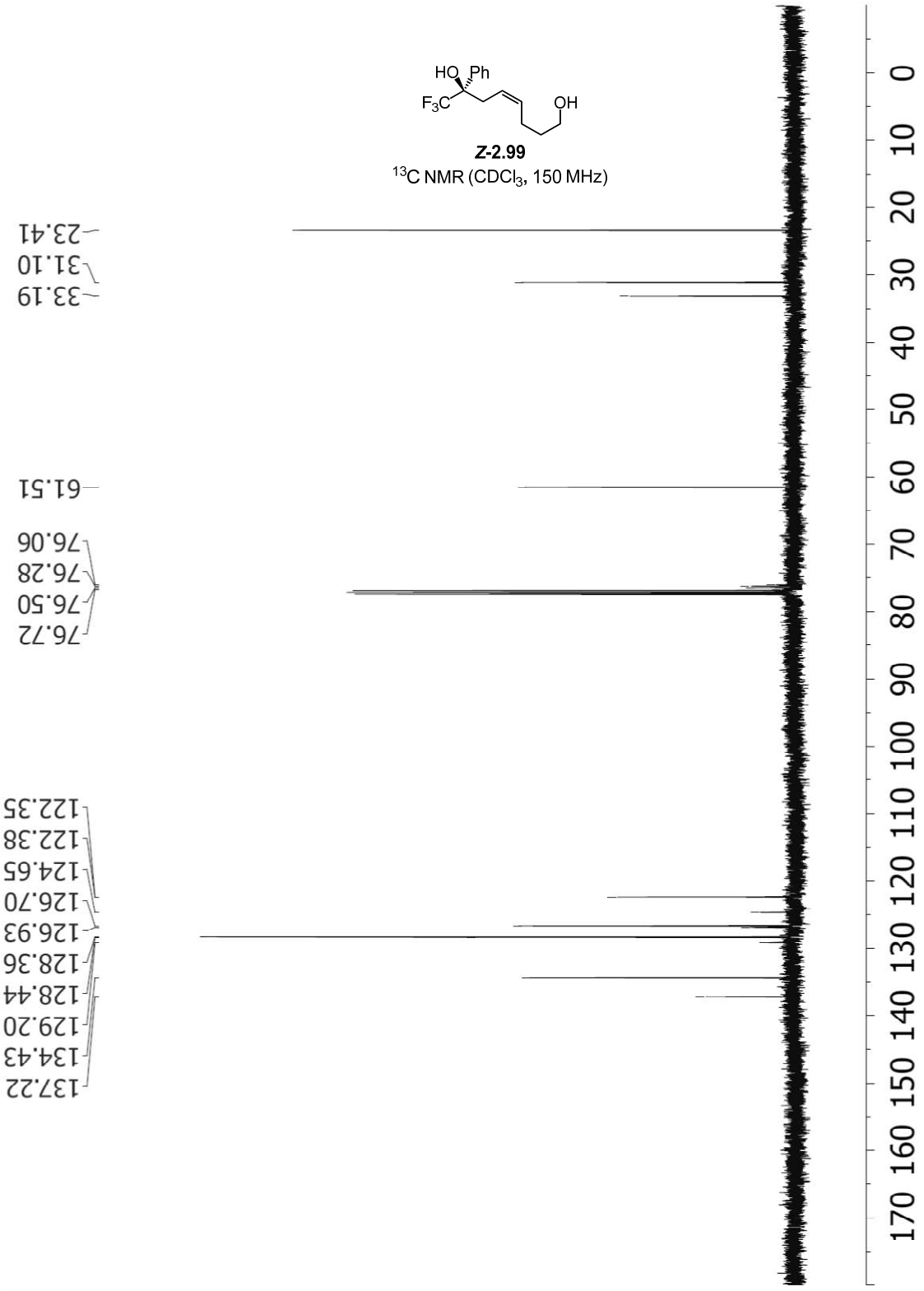
HO
Ph
F3C
OH
Z-2.99
13C NMR (CDCl3, 150 MHz)
23.41
31.10
33.19
61.51
76.06
76.28
76.50
76.72
122.35
122.38
124.65
126.70
126.93
128.36
128.44
129.20
134.43
137.22
0
10
20
30
40
50
60
70
80
90
100
110
120
130
140
150
160
170

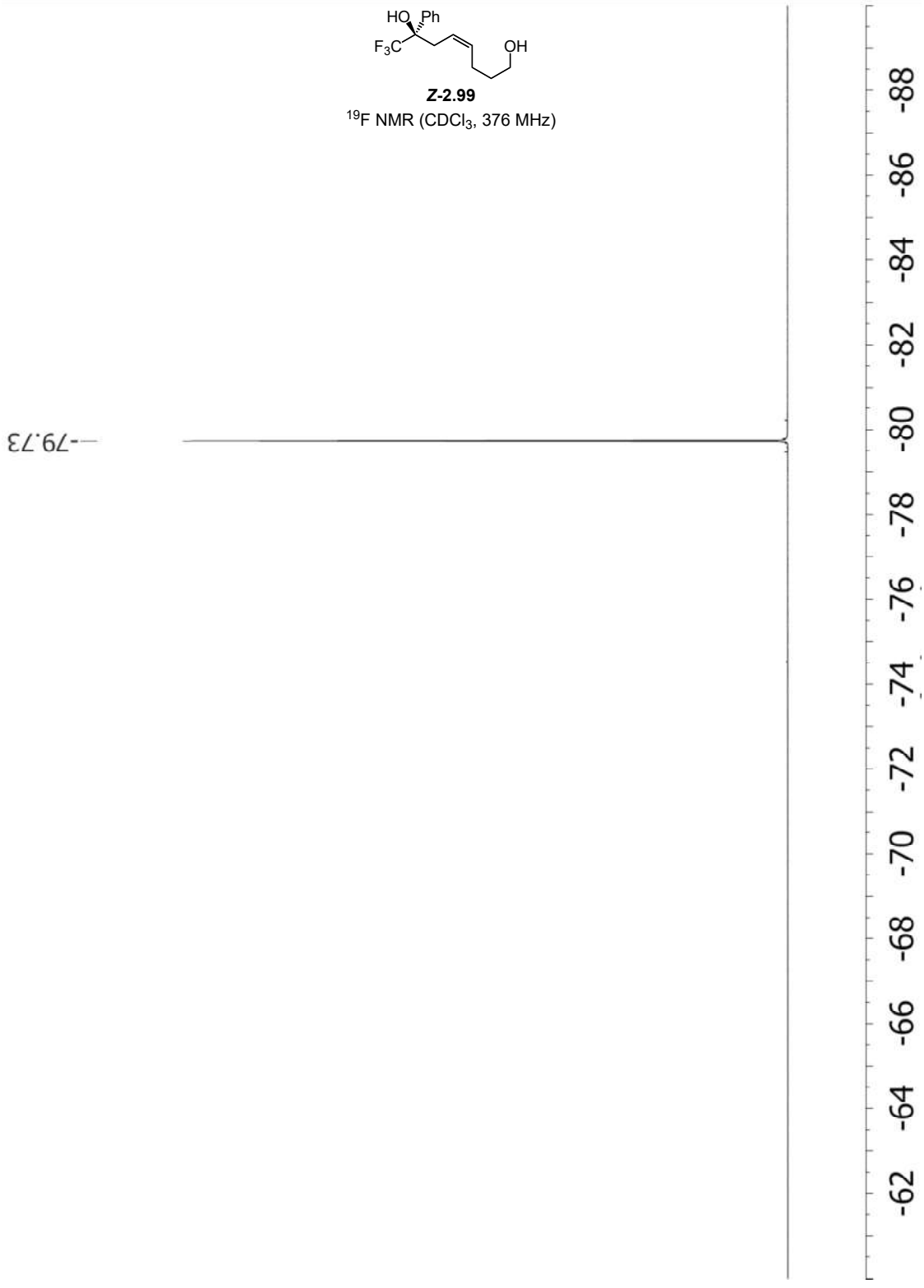

***Z*-2.99**

^{19}F NMR ($CDCl_3$, 376 MHz)

2.7.10. *DFT Calculation Structures*

104

Z-ts1 / electronic energy: -2690.79998320 a.u. / lowest freq: -160.67 cm-1

H	-4.977684	0.905583	-2.101905
C	2.355532	2.149309	-1.099390
C	4.668615	1.118619	0.569506
H	-3.782591	-1.178576	-1.662984
C	-3.887349	0.900399	-2.040816
Si	2.920227	0.719432	-0.017838
C	2.957709	-0.931616	-0.940497
C	-3.212359	-0.260522	-1.844441
H	-3.373621	1.817594	-2.334275
C	1.842067	0.458699	1.512129
C	-1.753162	-0.348911	-1.688757
H	3.390279	0.901827	2.945396
O	-0.015326	-0.025400	0.129163
C	-0.953403	0.743261	-2.403340
H	-1.418072	-1.330878	-2.050367
C	2.366967	0.543808	2.805868
C	0.523248	-0.007999	1.374283
B	-1.384193	-0.314648	-0.074976
C	1.618899	0.165387	3.923234
C	-0.209412	-0.474092	2.470840
H	-0.007924	-2.467042	-0.001991
H	2.045307	0.251048	4.924162
N	-1.725350	-1.597574	0.858254
H	-2.367663	-0.448505	2.478341
C	0.347165	-0.365003	3.747625
C	-1.542526	-1.139657	2.265639
H	-2.711196	-1.875658	0.735065
C	-0.983842	-2.817137	0.353642
O	-3.115664	-3.215346	-0.594511
C	-1.903254	-3.288868	-0.795863
H	1.190496	-3.104221	1.958448
H	-0.221762	-0.720800	4.611216
N	-1.389665	-3.761160	-1.945468
H	-0.037513	-3.038025	3.237486
H	-1.668805	-1.983743	2.948451
C	-2.303766	-4.274905	-2.951535
C	-0.001365	-3.684002	-2.356868
C	0.340607	-3.641433	2.405858
H	0.828731	-4.856499	0.043424

C	-0.720293	-4.005182	1.349083
C	-0.109144	-5.161249	0.531823
H	0.732390	-4.567928	2.850740
H	-0.792850	-5.558097	-0.231007
H	-2.535849	-3.746311	2.589584
C	-2.004739	-4.518285	2.013730
H	0.130231	-5.989281	1.214294
H	-2.713975	-4.919522	1.276902
H	-1.751758	-5.327026	2.715420
H	-1.205560	0.772910	-3.474163
H	0.123369	0.558787	-2.305107
H	-1.138868	1.741515	-1.983141
O	-2.224946	0.861547	0.464894
C	-3.358062	1.396117	0.289262
C	-3.421360	2.866607	0.228642
C	-2.240619	3.573017	0.515799
C	-2.237745	4.961859	0.513268
C	-4.598282	3.577660	-0.068626
C	-4.582243	4.966267	-0.081474
C	-3.406585	5.660142	0.209788
H	-5.523383	3.055547	-0.307364
H	-1.335098	3.021681	0.767912
H	-1.320081	5.501358	0.754727
H	-5.496572	5.512541	-0.319550
H	-3.403661	6.752198	0.204470
C	-4.581985	0.626753	0.856537
F	-5.732368	0.910699	0.272796
F	-4.404601	-0.690895	0.786346
F	-4.673658	0.950374	2.145676
C	4.982107	2.435638	0.948276
C	5.672128	0.144508	0.683141
C	6.941006	0.469737	1.163803
C	7.229492	1.780375	1.540831
C	6.247449	2.765186	1.430619
H	8.222998	2.036996	1.916103
H	6.470068	3.795787	1.716945
H	5.469512	-0.888296	0.386744
H	7.709004	-0.303611	1.239541
H	4.226469	3.222521	0.860650
C	1.194972	2.882278	-0.820757
C	3.135232	2.542844	-2.200711
C	2.751074	3.610963	-3.009813

C	1.584484	4.319484	-2.721066
C	0.809861	3.958327	-1.619760
H	-0.102855	4.512475	-1.387801
H	1.283958	5.159595	-3.351602
H	0.575706	2.594970	0.031877
H	4.068591	2.017791	-2.426321
H	3.369183	3.898059	-3.863684
C	3.095759	-2.119435	-0.199601
C	2.979417	-1.028605	-2.339777
C	3.287813	-3.349283	-0.829452
C	3.164067	-2.257770	-2.975953
C	3.332488	-3.418543	-2.222651
H	3.189318	-2.305967	-4.067285
H	3.494018	-4.377806	-2.720016
H	3.078537	-2.082162	0.894571
H	3.417170	-4.255205	-0.231964
H	2.863376	-0.129176	-2.950688
H	0.061184	-3.178488	-3.333018
H	0.434720	-4.689292	-2.460967
H	0.607447	-3.114504	-1.650119
H	-3.251084	-4.563360	-2.485026
H	-1.851668	-5.151732	-3.436056
H	-2.505922	-3.513219	-3.723165

104

Z-ts2 / electronic energy: -2690.79985092 a.u. / lowest freq: -178.31 cm-1

H	4.971143	-0.840945	-2.129033
C	-2.344637	-2.179170	-1.109158
C	-4.663394	-1.199244	0.581775
H	3.723348	1.223373	-1.723658
C	3.882499	-0.862614	-2.046998
Si	-2.922033	-0.770470	-0.007490
C	-2.984613	0.896215	-0.902290
C	3.177172	0.285321	-1.873608
H	3.388274	-1.799112	-2.311296
C	-1.841998	-0.513257	1.521104
C	1.719293	0.333655	-1.697811
H	-3.390494	-0.954093	2.954551
O	0.019706	-0.036842	0.140525
C	-2.370022	-0.588280	2.814259
C	-0.525729	-0.038755	1.381936
B	1.376551	0.300791	-0.075628
C	-1.629934	-0.187600	3.929207

C	0.193907	0.457163	2.473651
H	-0.058900	2.433885	-0.005970
H	-2.058245	-0.266083	4.929899
N	1.680271	1.600314	0.847457
H	2.353299	0.468308	2.467609
C	-0.365725	0.359350	3.750014
C	1.514271	1.144157	2.258551
H	2.659026	1.897882	0.719537
C	0.913690	2.802306	0.340565
O	3.032787	3.235549	-0.621378
C	1.818265	3.284533	-0.817056
H	-1.249591	3.061545	1.963202
H	0.194082	0.737372	4.610058
N	1.290598	3.741095	-1.966599
H	-0.010674	3.030076	3.233205
H	1.629751	1.992837	2.937581
C	2.189308	4.263732	-2.981861
C	-0.099909	3.647591	-2.365247
C	-0.406511	3.618448	2.399102
H	-0.932276	4.817496	0.037593
C	0.640309	3.992045	1.331941
C	0.007008	5.135905	0.514320
H	-0.812073	4.541568	2.838711
H	0.678003	5.535980	-0.257983
H	2.471919	3.764474	2.556755
C	1.922679	4.526594	1.984589
H	-0.234756	5.965258	1.194347
H	2.618789	4.938437	1.241224
H	1.662553	5.331834	2.687694
C	-4.956204	-2.526349	0.941015
C	-5.680417	-0.241808	0.715192
C	-6.941997	-0.593271	1.196614
C	-7.209788	-1.913580	1.554502
C	-6.214114	-2.882083	1.424332
H	-8.197588	-2.190480	1.930428
H	-6.420267	-3.920245	1.695193
H	-5.494366	0.798362	0.434447
H	-7.720468	0.167873	1.288165
H	-4.190255	-3.301323	0.837555
C	-1.254407	-2.988662	-0.764128
C	-3.049070	-2.487016	-2.285910
C	-2.653530	-3.540520	-3.108274

C	-1.553521	-4.322447	-2.756051
C	-0.860910	-4.051608	-1.577049
H	-0.008231	-4.673202	-1.295562
H	-1.243220	-5.151538	-3.396248
H	-0.707726	-2.782184	0.160317
H	-3.931907	-1.903503	-2.565208
H	-3.210509	-3.758462	-4.022448
C	-2.997884	1.026991	-2.299028
C	-3.160651	2.062681	-0.135493
C	-3.219404	2.263716	-2.907853
C	-3.385025	3.300963	-0.737806
C	-3.427812	3.401010	-2.129107
H	-3.543114	4.188018	-0.119509
H	-3.616780	4.365869	-2.605479
H	-2.844843	0.148505	-2.930897
H	-3.239412	2.336566	-3.997859
H	-3.149220	2.000550	0.957624
H	-0.166447	3.132083	-3.335897
H	-0.545066	4.648295	-2.475658
H	-0.698540	3.081337	-1.647398
H	1.728815	5.142287	-3.455490
H	2.382518	3.506950	-3.760534
H	3.141830	4.552070	-2.526190
C	0.939579	-0.791908	-2.384841
H	1.348466	1.301206	-2.063785
H	1.146112	-1.777518	-1.944130
H	1.186978	-0.839612	-3.456067
H	-0.140239	-0.627427	-2.284418
O	2.269417	-0.832964	0.459681
C	3.427676	-1.315135	0.276613
C	3.559435	-2.780778	0.232301
C	4.619455	-0.479866	0.819176
F	5.773066	-0.706789	0.214965
F	4.377346	0.826589	0.740553
F	4.750835	-0.787163	2.108630
C	4.799116	-3.445607	0.203995
C	4.839865	-4.834379	0.205426
C	2.372494	-3.533744	0.253224
C	2.424257	-4.920487	0.264398
C	3.657239	-5.573539	0.237200
H	5.737167	-2.894401	0.179466
H	5.804625	-5.343767	0.184505

H 1.414396 -3.015521 0.279397
H 1.498255 -5.497007 0.302683
H 3.697106 -6.664807 0.245444
104
Z-ts3 / electronic energy: -2690.79694315 a.u. / lowest freq: -126.50 cm-1
H 3.092009 3.333348 2.475020
C -2.669970 1.343860 1.304286
C -4.602436 -0.187102 -0.479033
H 1.049844 2.022543 2.280068
C 3.131824 2.299762 2.125416
Si -2.805150 -0.082693 0.081603
C -2.333040 -1.716344 0.912019
C 2.011922 1.545359 2.056852
H 4.121324 1.854273 1.992980
C -1.744216 -0.003851 -1.488131
C 1.956712 0.135436 1.618330
H -3.413248 -0.086702 -2.851984
O 0.241489 0.140646 -0.216547
C -2.327159 -0.155499 -2.751455
C -0.344159 -0.102350 -1.412755
B 1.635652 0.092021 -0.007189
C -1.557834 -0.427238 -3.886211
C 0.435306 -0.466097 -2.513808
H 1.020248 -2.516207 -0.017140
H -2.036889 -0.535363 -4.860715
N 2.270385 -1.077654 -0.939546
H 2.494208 0.187258 -2.577169
C -0.187491 -0.614379 -3.756517
C 1.909702 -0.712975 -2.344488
H 3.298752 -0.992510 -0.843642
C 2.041063 -2.478569 -0.419116
O 4.202213 -2.017670 0.425609
C 3.133879 -2.575366 0.679085
H 0.065476 -3.564139 -1.934004
H 0.413245 -0.890097 -4.627897
N 2.916472 -3.225503 1.835977
H 1.095329 -2.987490 -3.254806
H 2.254655 -1.485080 -3.034232
C 4.001023 -3.316243 2.799298
C 1.695338 -3.886337 2.249005
C 1.030558 -3.715269 -2.440213
H 1.176617 -5.144215 -0.176771

C	2.205098	-3.664353	-1.443501
C	2.147648	-4.996685	-0.670770
H	1.003265	-4.707874	-2.913165
H	2.946849	-5.094227	0.076419
H	3.752336	-2.675622	-2.694229
C	3.555823	-3.624109	-2.175082
H	2.275862	-5.820305	-1.387721
H	4.393994	-3.794328	-1.485629
H	3.577814	-4.418634	-2.935657
O	2.466280	1.258956	-0.593257
C	2.600919	2.479314	-0.306590
C	1.503433	3.451654	-0.419349
C	0.490227	3.168143	-1.349405
C	-0.535169	4.082004	-1.564294
C	1.489827	4.674433	0.272358
C	0.456117	5.575681	0.058692
C	-0.558865	5.280154	-0.854761
H	2.274941	4.914596	0.988521
H	0.517640	2.243674	-1.925912
H	-1.318149	3.850526	-2.288136
H	0.439233	6.517672	0.609400
H	-1.368401	5.994768	-1.015646
C	4.049910	2.962499	-0.571183
F	4.378325	4.047292	0.112717
F	4.926525	2.006509	-0.309134
F	4.123113	3.247367	-1.871072
C	-5.307060	0.983904	-0.806755
C	-5.258093	-1.417463	-0.636394
C	-6.569425	-1.478873	-1.109104
C	-7.250120	-0.306139	-1.432282
C	-6.617105	0.927860	-1.279235
H	-8.277364	-0.352907	-1.801477
H	-7.148431	1.850194	-1.525631
H	-4.741901	-2.347994	-0.384142
H	-7.062909	-2.446901	-1.222924
H	-4.827501	1.960240	-0.685189
C	-1.582078	2.226816	1.347204
C	-3.697457	1.523138	2.248108
C	-3.630827	2.535441	3.204835
C	-2.539088	3.402873	3.228648
C	-1.516841	3.249779	2.293429
H	-0.664601	3.934471	2.294689

H -2.489213 4.200431 3.973579
H -0.770038 2.108775 0.630950
H -4.571961 0.865387 2.235775
H -4.437623 2.650828 3.932304
C -2.447876 -1.901911 2.297456
C -1.939068 -2.817600 0.133146
C -2.187030 -3.140410 2.885071
C -1.685881 -4.061165 0.713141
C -1.812348 -4.225311 2.093155
H -1.401025 -4.908759 0.084148
H -1.620852 -5.198505 2.551393
H -2.745354 -1.065997 2.936914
H -2.288213 -3.261889 3.965981
H -1.842191 -2.707575 -0.951282
H 1.382570 -3.499422 3.230312
H 1.858620 -4.971351 2.342356
H 0.876525 -3.721072 1.546084
H 4.204821 -4.372337 3.033805
H 3.721884 -2.798711 3.730812
H 4.901983 -2.854960 2.384322
C 0.859320 -0.610159 2.395861
H 2.947957 -0.315711 1.773527
H -0.057611 -0.005278 2.434740
H 1.175565 -0.812407 3.429916
H 0.574151 -1.558579 1.930769

104

Z-ts4 / electronic energy: -2690.79503706 a.u. / lowest freq: -125.51 cm-1

H -2.269561 3.410432 -2.644160
C 2.388882 1.180220 -1.318731
C 4.673510 -0.128314 0.267757
H -0.523743 1.794217 -2.129212
C -2.533062 2.394731 -2.339286
Si 2.835727 -0.219298 -0.137447
C 2.476915 -1.933110 -0.855415
C -1.574496 1.477589 -2.085143
H -3.586453 2.108952 -2.401244
C 1.846342 -0.123335 1.474543
C -1.814297 0.088444 -1.633628
H 3.521100 -0.242394 2.829142
O -0.130499 0.068606 0.206686
C 2.432025 -0.264192 2.736342
C 0.442779 -0.147586 1.410689

B	-1.520610	0.078801	-0.011958
C	1.655434	-0.460515	3.882086
C	-0.351116	-0.425133	2.526383
H	-1.121675	-2.580503	0.141521
H	2.133833	-0.565472	4.857326
N	-2.234783	-0.990328	0.982585
H	-2.356737	0.373679	2.547373
C	0.274043	-0.571407	3.768094
C	-1.840112	-0.578637	2.367255
H	-3.252084	-0.820792	0.879948
C	-2.132977	-2.431582	0.539217
O	-4.237328	-1.814467	-0.348725
C	-3.230925	-2.491052	-0.558946
H	-0.262371	-3.665957	2.109242
H	-0.331996	-0.783990	4.653378
N	-3.089832	-3.246565	-1.663229
H	-1.197536	-2.859087	3.381376
H	-2.238560	-1.282655	3.099295
C	-4.190942	-3.303823	-2.610947
C	-1.938251	-4.040327	-2.041270
C	-1.233701	-3.650645	2.626608
H	-1.524094	-5.168601	0.432035
C	-2.401603	-3.539723	1.626808
C	-2.471064	-4.911785	0.928135
H	-1.324708	-4.599474	3.175217
H	-3.286482	-4.978454	0.195655
H	-3.846124	-2.356617	2.837590
C	-3.742886	-3.335586	2.349033
H	-2.656782	-5.683262	1.688985
H	-4.591435	-3.440481	1.659037
H	-3.850943	-4.099425	3.133491
O	-2.284906	1.330194	0.507882
C	-2.406916	2.540054	0.179323
C	-1.364562	3.543129	0.423133
C	-0.389322	3.233663	1.385085
C	0.530338	4.197562	1.781795
C	-1.390582	4.826724	-0.151950
C	-0.459442	5.777545	0.240390
C	0.496535	5.468449	1.211818
H	-2.129575	5.077725	-0.911866
H	-0.375819	2.251470	1.856941
H	1.271943	3.952102	2.543922

H	-0.479002	6.769998	-0.212949
H	1.217817	6.225618	1.525880
C	-3.896923	2.974842	0.222352
F	-4.175660	4.032757	-0.523636
F	-4.686688	1.977320	-0.141827
F	-4.165778	3.276547	1.493085
C	5.423005	1.039023	0.056624
C	5.327410	-1.243149	0.820777
C	6.677485	-1.189316	1.163365
C	7.403396	-0.016935	0.950658
C	6.775547	1.096229	0.394331
H	8.463178	0.026455	1.212970
H	7.341370	2.014028	0.218138
H	4.776866	-2.175092	0.982893
H	7.166828	-2.066760	1.592537
H	4.949947	1.919763	-0.386664
C	2.194710	2.467364	-0.794104
C	2.266467	1.015314	-2.706487
C	1.948881	2.090369	-3.537681
C	1.752475	3.359320	-2.994720
C	1.880549	3.546959	-1.618678
H	1.735838	4.537488	-1.183114
H	1.505248	4.202725	-3.643741
H	2.290596	2.635306	0.281984
H	2.407161	0.031022	-3.158598
H	1.853536	1.934058	-4.614553
C	3.082426	-2.357738	-2.049960
C	1.660578	-2.853640	-0.179141
C	2.849991	-3.631751	-2.568300
C	1.442494	-4.137404	-0.679437
C	2.026275	-4.525647	-1.884774
H	0.823976	-4.843220	-0.117939
H	1.857367	-5.529164	-2.282059
H	3.765734	-1.692291	-2.586369
H	3.329429	-3.934025	-3.502050
H	1.200038	-2.572228	0.771639
H	-1.637045	-3.780783	-3.067150
H	-2.182450	-5.113689	-2.014722
H	-1.080779	-3.865912	-1.387522
H	-4.420287	-4.354187	-2.845365
H	-3.917915	-2.788152	-3.545710
H	-5.075485	-2.823566	-2.182299

C -0.860270 -0.865478 -2.373818
H -2.870110 -0.171596 -1.805238
H 0.136993 -0.416024 -2.455799
H -1.223497 -1.067257 -3.392286
H -0.715615 -1.822128 -1.864811
104
Z-ts5 / electronic energy: -2690.79472578 a.u. / lowest freq: -88.05 cm-1
H -0.946930 3.429374 -2.538518
C 2.541094 0.929904 -1.265235
C 4.549770 -0.849516 0.230532
H -2.845498 1.925419 -2.742511
C -0.930368 2.450546 -2.055328
Si 2.727154 -0.610133 -0.191041
C 2.111788 -2.207542 -0.993393
C -1.964412 1.588297 -2.186002
H 0.003757 2.148426 -1.572770
C 1.766750 -0.394683 1.424381
C -2.000470 0.218758 -1.591837
H 3.443444 -0.544699 2.773185
O -0.194194 -0.164635 0.138375
C -1.077173 -0.713673 -2.406569
H -3.036313 -0.132997 -1.679503
C 2.357111 -0.454122 2.689847
C 0.367193 -0.277276 1.363250
B -1.551478 0.209765 -0.016230
C 1.583866 -0.417305 3.853680
C -0.431185 -0.303730 2.511632
H -1.537717 -2.381048 0.203425
H 2.063655 -0.459164 4.833011
N -2.422948 -0.658737 1.045796
H -2.318666 0.734871 2.587969
C 0.197912 -0.363210 3.758491
C -1.932781 -0.276049 2.404650
H -3.411597 -0.363474 0.968413
C -2.505291 -2.118027 0.648354
O -4.593798 -1.344951 -0.146120
C -3.651291 -2.095871 -0.393866
H -0.679770 -3.425533 2.174275
H -0.412387 -0.376664 4.666129
N -3.599510 -2.849690 -1.508225
H -1.523338 -2.600994 3.497788
H -2.389403 -0.917940 3.159184

C	-4.723812	-2.807205	-2.428018
C	-2.540693	-3.756572	-1.902220
C	-1.630144	-3.371414	2.726991
H	-2.156641	-4.900119	0.593048
C	-2.827572	-3.168544	1.776831
C	-3.057989	-4.538925	1.109247
H	-1.753489	-4.325975	3.259016
H	-3.896688	-4.537207	0.400038
H	-4.083934	-1.837540	3.040852
C	-4.106529	-2.824106	2.556600
H	-3.300062	-5.273678	1.890318
H	-4.993556	-2.844379	1.908807
H	-4.253375	-3.569317	3.352728
H	-1.470279	-0.869869	-3.422145
H	-0.959046	-1.690899	-1.924178
H	-0.071598	-0.281975	-2.489646
O	-1.732279	1.633859	0.576924
C	-1.840799	2.809615	0.130733
C	-0.847631	3.818191	0.512154
C	0.209403	3.409050	1.343258
C	1.143737	4.335387	1.786778
C	-0.941213	5.164443	0.112964
C	0.006646	6.079348	0.549732
C	1.045313	5.668799	1.389184
H	-1.746657	5.500685	-0.539846
H	0.281457	2.365203	1.650733
H	1.952004	4.014651	2.446314
H	-0.067672	7.123145	0.240135
H	1.780584	6.396909	1.738213
C	-3.297087	3.261429	-0.172722
F	-3.398582	4.075412	-1.215550
F	-4.073624	2.207622	-0.381755
F	-3.751633	3.899422	0.902713
C	5.509893	0.158180	0.053905
C	4.973811	-2.077744	0.767558
C	6.303969	-2.288497	1.124575
C	7.242725	-1.272012	0.944414
C	6.843904	-0.049212	0.407272
H	8.287795	-1.436195	1.217345
H	7.577001	0.747053	0.258010
H	4.253017	-2.889894	0.904834
H	6.612149	-3.251022	1.539469

H 5.220008 1.121477 -0.374795
C 2.664420 2.184649 -0.644974
C 2.342807 0.907440 -2.654113
C 2.277722 2.088213 -3.395059
C 2.409934 3.322249 -2.759609
C 2.598720 3.369134 -1.378935
H 2.692395 4.330706 -0.868736
H 2.362521 4.247570 -3.338520
H 2.819610 2.242747 0.436492
H 2.228966 -0.044242 -3.177344
H 2.122752 2.041969 -4.475425
C 2.556420 -2.619583 -2.260281
C 1.263436 -3.076811 -0.288652
C 2.133869 -3.826145 -2.819602
C 0.859725 -4.296687 -0.829842
C 1.281492 -4.667914 -2.106278
H 0.221368 -4.965903 -0.246811
H 0.962822 -5.620144 -2.536767
H 3.260867 -2.001137 -2.824165
H 2.487952 -4.119067 -3.810718
H 0.923912 -2.806862 0.714949
H -2.241834 -3.540624 -2.938579
H -2.888070 -4.800674 -1.854446
H -1.654307 -3.658357 -1.272290
H -5.492240 -2.133327 -2.037849
H -5.150325 -3.814754 -2.552427
H -4.387406 -2.446337 -3.412967
104
Z-ts6 / electronic energy: -2690.79806558 a.u. / lowest freq: -206.97 cm-1
H -4.730772 1.419561 -2.061461
C 2.377916 2.115155 -0.832716
C 4.782515 0.723901 0.447137
H -3.856028 -0.824822 -1.607902
C -3.654815 1.248001 -1.996707
Si 2.974601 0.504639 -0.057117
C 2.909048 -1.042190 -1.142241
C -3.157148 -0.004118 -1.807151
H -3.006873 2.068280 -2.310574
C 1.964049 0.150711 1.499133
C -1.728705 -0.295785 -1.660829
H 3.587450 0.376394 2.899762
O 0.037995 -0.110482 0.150180

C	2.529859	0.128234	2.777369
C	0.601094	-0.173750	1.382117
B	-1.356168	-0.251915	-0.041816
C	1.776404	-0.215752	3.902468
C	-0.150485	-0.589957	2.484876
H	-0.313330	-2.602631	-0.049292
H	2.235926	-0.217116	4.892253
N	-1.837004	-1.487964	0.893410
H	-2.278939	-0.257694	2.512387
C	0.448100	-0.591173	3.747509
C	-1.564647	-1.063559	2.298095
H	-2.856009	-1.614375	0.799824
C	-1.308928	-2.804419	0.363503
O	-3.526244	-2.885901	-0.466113
C	-2.352427	-3.148917	-0.727898
H	0.860751	-3.387117	1.908780
H	-0.136344	-0.907945	4.616013
N	-1.987215	-3.719284	-1.890393
H	-0.312875	-3.141474	3.214718
H	-1.807781	-1.876041	2.987608
C	-3.028872	-4.098466	-2.830176
C	-0.632330	-3.878415	-2.379915
C	-0.043545	-3.797847	2.381883
H	0.207015	-5.084677	0.021773
C	-1.173433	-4.016130	1.358826
C	-0.753013	-5.249173	0.534271
H	0.227874	-4.767105	2.824837
H	-1.503899	-5.548041	-0.209199
H	-2.912981	-3.508753	2.637470
C	-2.493391	-4.350997	2.068634
H	-0.616921	-6.100043	1.216890
H	-3.265080	-4.680248	1.359785
H	-2.322257	-5.169447	2.783917
C	5.406837	1.979171	0.502545
C	5.542328	-0.405208	0.800476
C	6.870584	-0.284570	1.203578
C	7.471376	0.973731	1.255193
C	6.737928	2.105053	0.902565
H	8.514401	1.071393	1.565500
H	7.205399	3.091910	0.934915
H	5.092534	-1.401670	0.754384
H	7.441992	-1.176312	1.472216

H	4.852174	2.879206	0.223764
C	2.159400	3.194977	0.041130
C	2.230740	2.347496	-2.207431
C	1.884983	3.608506	-2.694789
C	1.697876	4.671573	-1.812964
C	1.837619	4.462430	-0.440923
H	1.700853	5.289382	0.260374
H	1.446973	5.663631	-2.196072
H	2.258720	3.050859	1.121516
H	2.380192	1.537366	-2.924358
H	1.772929	3.763887	-3.770224
C	3.391011	-1.061776	-2.460975
C	2.534357	-2.270031	-0.570215
C	3.466255	-2.250158	-3.188557
C	2.637833	-3.465549	-1.280923
C	3.093198	-3.457134	-2.599107
H	2.367870	-4.409886	-0.800228
H	3.175336	-4.391807	-3.158754
H	3.745447	-0.140967	-2.931400
H	3.843294	-2.235357	-4.213762
H	2.182574	-2.297932	0.465175
H	-0.536146	-3.389252	-3.361963
H	-0.382823	-4.944094	-2.499595
H	0.102731	-3.424111	-1.711969
H	-2.750985	-5.044521	-3.315749
H	-3.152250	-3.328291	-3.610014
H	-3.980906	-4.223903	-2.304585
C	-0.773730	0.637380	-2.408977
H	-1.541531	-1.329839	-1.979523
H	-0.777990	1.659673	-2.005623
H	-1.033919	0.690083	-3.477168
H	0.254219	0.265976	-2.320192
O	-2.056571	1.009087	0.469524
C	-3.135312	1.650548	0.259738
C	-3.049174	3.117496	0.142222
C	-4.427127	1.036776	0.869881
F	-5.542232	1.358653	0.235674
F	-4.362440	-0.293685	0.908387
F	-4.516462	1.469094	2.125445
C	-4.184222	3.948069	0.177348
C	-4.041696	5.324544	0.055590
C	-1.775321	3.690229	-0.019474

C -1.647033 5.066838 -0.145857
C -2.776421 5.885791 -0.111368
H -5.184463 3.536359 0.299239
H -4.926706 5.962459 0.087793
H -0.886362 3.055643 -0.041295
H -0.656888 5.503942 -0.273752
H -2.668070 6.967426 -0.214283
104
Z-ts7 / electronic energy: -2690.79376230 a.u. / lowest freq: -213.44 cm-1
H -3.071633 2.917328 -2.569699
C 2.261223 1.448401 -1.294232
C 4.705762 0.647971 0.393858
H -0.948289 1.748568 -2.329597
C -3.056275 1.872582 -2.252742
Si 2.940778 0.181027 -0.069532
C 2.948816 -1.578510 -0.762688
C -1.883829 1.194019 -2.170356
H -4.011212 1.341884 -2.235303
C 1.885919 0.144313 1.498664
C -1.744633 -0.196502 -1.711247
H 3.475880 0.446655 2.924629
O 0.006521 -0.184632 0.119421
C 2.411376 0.235960 2.790463
C 0.513591 -0.126197 1.371588
B -1.388356 -0.140113 -0.090372
C 1.603354 0.047886 3.915352
C -0.305157 -0.368279 2.479766
H -0.663048 -2.659085 0.201004
H 2.030664 0.127243 4.916466
N -2.053632 -1.239724 0.918253
H -2.403479 0.130215 2.448714
C 0.258938 -0.270074 3.755190
C -1.753974 -0.741059 2.296349
H -3.078341 -1.224922 0.784536
C -1.705405 -2.663412 0.542152
O -3.834432 -2.480972 -0.469778
C -2.704059 -2.946084 -0.606585
H 0.262027 -3.510706 2.213960
H -0.366219 -0.456684 4.632937
N -2.341223 -3.661912 -1.688440
H -0.843975 -2.881725 3.447570
H -2.060331 -1.481894 3.035637

C	-3.339010	-3.929995	-2.710158
C	-1.039741	-4.239851	-1.956141
C	-0.714336	-3.668891	2.697576
H	-0.697710	-5.270960	0.543515
C	-1.849989	-3.763917	1.659736
C	-1.689776	-5.147754	1.001077
H	-0.653234	-4.617369	3.251234
H	-2.458381	-5.355710	0.244351
H	-3.480008	-2.782173	2.809814
C	-3.230270	-3.740846	2.334338
H	-1.785321	-5.920200	1.777510
H	-4.031803	-3.966463	1.617883
H	-3.257538	-4.506203	3.124109
C	5.175470	1.965321	0.273859
C	5.581985	-0.321446	0.910873
C	6.878714	0.013567	1.298078
C	7.325748	1.329117	1.172545
C	6.472147	2.304927	0.659711
H	8.343593	1.592273	1.469971
H	6.819793	3.335256	0.553518
H	5.250869	-1.359918	1.009083
H	7.546306	-0.755384	1.694000
H	4.523735	2.742629	-0.135163
C	1.689836	2.636790	-0.812426
C	2.323934	1.272742	-2.684870
C	1.831088	2.240343	-3.561114
C	1.266150	3.412651	-3.060910
C	1.196414	3.609973	-1.681834
H	0.753344	4.524206	-1.280406
H	0.884347	4.173796	-3.745364
H	1.626360	2.806218	0.266646
H	2.752996	0.360351	-3.104993
H	1.892091	2.077266	-4.639563
C	3.698039	-1.905327	-1.905281
C	2.263497	-2.619108	-0.115177
C	3.727871	-3.207231	-2.404966
C	2.307611	-3.927737	-0.596162
C	3.029568	-4.222684	-1.752391
H	1.788316	-4.726072	-0.059076
H	3.065129	-5.245649	-2.134188
H	4.289445	-1.136673	-2.411596
H	4.312877	-3.433506	-3.299436

H 1.702596 -2.410068 0.799899
H -0.722670 -3.969298 -2.974330
H -1.081628 -5.338384 -1.890055
H -0.275429 -3.879044 -1.263095
H -3.401760 -5.012903 -2.897471
H -3.062297 -3.428454 -3.651292
H -4.313863 -3.561159 -2.377320
C -0.621490 -0.912626 -2.477097
H -2.712523 -0.707948 -1.826404
H 0.271788 -0.276643 -2.524507
H -0.932990 -1.141582 -3.506999
H -0.310167 -1.843296 -1.994339
O -1.922087 1.184133 0.446233
C -2.733232 2.096302 0.097689
C -2.303306 3.495981 0.252096
C -4.217769 1.733333 0.361756
F -5.098052 2.468923 -0.293662
F -4.442498 0.452449 0.077678
F -4.421471 1.898379 1.669080
C -3.060953 4.588918 -0.204017
C -2.607611 5.882664 0.017303
C -1.100674 3.723105 0.941134
C -0.661968 5.021779 1.169423
C -1.410905 6.101885 0.703301
H -3.994572 4.434398 -0.744098
H -3.193079 6.728802 -0.346577
H -0.528064 2.872628 1.312257
H 0.268852 5.191421 1.713802
H -1.064550 7.122584 0.878670
104
Z-ts8 / electronic energy: -2690.79592900 a.u. / lowest freq: -202.34 cm-1
H 4.020249 -2.201293 -2.410125
C -2.195133 -1.934087 -1.256377
C -4.590220 -1.164578 0.476253
H 1.624712 -1.738822 -2.330139
C 3.660349 -1.215686 -2.108603
Si -2.851195 -0.653469 -0.039649
C -2.932257 1.089594 -0.774674
C 2.334240 -0.928186 -2.116497
H 4.401650 -0.416775 -2.025154
C -1.793464 -0.492999 1.518369
C 1.756510 0.357732 -1.705120

H	-3.324059	-0.993106	2.953601
O	0.025213	0.057785	0.130490
C	-2.304563	-0.624038	2.812714
C	-0.480896	-0.012773	1.383195
B	1.402180	0.286083	-0.079480
C	-1.542156	-0.272038	3.930292
C	0.274551	0.413789	2.479604
H	0.113669	2.557518	0.112294
H	-1.955176	-0.387372	4.933957
N	1.805817	1.547420	0.874851
H	2.432665	0.342214	2.456771
C	-0.271332	0.265613	3.757749
C	1.621001	1.057138	2.274596
H	2.805633	1.766544	0.733052
C	1.127132	2.826810	0.434630
O	3.235973	3.104978	-0.597587
C	2.025763	3.276511	-0.740569
H	-0.975318	3.268753	2.097665
H	0.306914	0.589649	4.627784
N	1.495917	3.814032	-1.855264
H	0.259085	2.990138	3.340184
H	1.771661	1.876174	2.980357
C	2.393250	4.274275	-2.900590
C	0.090639	4.035645	-2.130125
C	-0.063963	3.681925	2.555586
H	-0.474610	5.100480	0.306356
C	1.008369	3.988776	1.491514
C	0.514297	5.253060	0.761798
H	-0.342950	4.616607	3.063990
H	1.212391	5.604576	-0.010653
H	2.823152	3.483788	2.665522
C	2.357496	4.330088	2.141012
H	0.412864	6.065538	1.495602
H	3.083231	4.689956	1.398918
H	2.211775	5.126883	2.885887
C	-4.871776	-2.516156	0.738359
C	-5.619379	-0.227911	0.657296
C	-6.884487	-0.624807	1.091673
C	-7.142250	-1.969555	1.352647
C	-6.133576	-2.917049	1.174600
H	-8.132885	-2.282024	1.691614
H	-6.332930	-3.972928	1.372152

H	-5.437566	0.830900	0.452465
H	-7.673102	0.119962	1.222683
H	-4.093824	-3.273005	0.595973
C	-1.013385	-2.648246	-1.012386
C	-2.907030	-2.229148	-2.431352
C	-2.435769	-3.174438	-3.342602
C	-1.250691	-3.863439	-3.084929
C	-0.544030	-3.606599	-1.909960
H	0.373676	-4.157522	-1.686153
H	-0.886154	-4.610106	-3.794272
H	-0.447771	-2.450580	-0.101350
H	-3.855023	-1.723748	-2.639328
H	-3.001953	-3.382709	-4.253380
C	-3.075673	1.337237	-2.147821
C	-2.959546	2.194421	0.094686
C	-3.258884	2.632483	-2.634615
C	-3.148033	3.491562	-0.384800
C	-3.305016	3.712202	-1.753265
H	-3.185245	4.330010	0.315314
H	-3.460956	4.724756	-2.132874
H	-3.049740	0.508029	-2.859432
H	-3.377141	2.797690	-3.708043
H	-2.850044	2.039523	1.172561
H	-0.146909	3.649217	-3.131967
H	-0.145948	5.111167	-2.111614
H	-0.558246	3.525470	-1.413764
H	2.229589	5.346165	-3.092311
H	2.200588	3.721098	-3.833422
H	3.430509	4.115026	-2.591581
C	0.484136	0.674947	-2.504025
H	2.525884	1.133521	-1.834166
H	-0.200771	-0.185199	-2.498109
H	0.725581	0.915229	-3.550129
H	-0.071516	1.513566	-2.073867
O	2.201000	-0.877802	0.500369
C	3.206412	-1.593393	0.198445
C	3.063267	-3.058684	0.281550
C	4.562529	-0.945453	0.582620
F	5.616434	-1.466317	-0.020394
F	4.542958	0.364696	0.341954
F	4.706089	-1.111779	1.897296
C	4.045122	-3.956423	-0.172857

C 3.837714 -5.324608 -0.053471
C 1.890928 -3.555653 0.874282
C 1.693868 -4.925797 0.994052
C 2.662914 -5.811544 0.523544
H 4.960899 -3.592131 -0.637916
H 4.597335 -6.018913 -0.416687
H 1.152113 -2.856736 1.267374
H 0.782123 -5.303004 1.460327
H 2.506893 -6.888397 0.614970
104
Z-ts9 / electronic energy: -2690.79344338 a.u. / lowest freq: -190.96 cm-1
H 3.167742 -2.699970 -2.568442
C -2.426507 -2.102029 -0.934084
C -4.817941 -0.789277 0.502133
H 0.949589 -1.662953 -2.448402
C 3.049512 -1.677082 -2.205446
Si -3.011369 -0.572216 -0.002678
C -2.908632 1.038571 -0.990675
C 1.835816 -1.072950 -2.182392
H 3.964200 -1.100720 -2.043028
C -1.968650 -0.300846 1.552961
C 1.598383 0.298745 -1.696527
H -3.560671 -0.568754 2.982377
O -0.061212 -0.007508 0.184420
C 0.408187 0.929502 -2.431601
H 2.523819 0.877635 -1.835316
C -2.512947 -0.291558 2.840725
C -0.613892 0.054252 1.418669
B 1.306055 0.225277 -0.060868
C -1.755089 0.086291 3.952100
C 0.137411 0.512673 2.503813
H 0.374772 2.725263 -0.044864
H -2.200440 0.079316 4.948368
N 1.794672 1.460848 0.888263
H 2.274324 0.232154 2.492640
C -0.445006 0.512735 3.774313
C 1.536360 1.021385 2.294302
H 2.821526 1.524136 0.771742
C 1.376551 2.826175 0.391796
O 3.596294 2.672755 -0.427493
C 2.468011 3.101556 -0.679508
H -0.772332 3.547519 1.880279

H	0.138519	0.862236	4.630869
N	2.195896	3.765107	-1.815762
H	0.310528	3.090965	3.205074
H	1.763491	1.831267	2.989378
C	3.279718	3.983485	-2.761068
C	0.905132	4.250421	-2.263862
C	0.148403	3.829669	2.413997
H	0.087195	5.305278	0.178494
C	1.329686	3.998544	1.440044
C	1.060213	5.317891	0.690711
H	-0.043512	4.789187	2.916269
H	1.843838	5.565345	-0.037902
H	2.997705	3.263100	2.712549
C	2.661844	4.167622	2.186977
H	1.030544	6.136468	1.423663
H	3.471227	4.462466	1.504691
H	2.557333	4.959497	2.943910
H	0.668913	1.174510	-3.472005
H	0.031997	1.834439	-1.947043
H	-0.435984	0.229454	-2.446451
O	2.306436	-0.818448	0.473136
C	2.738970	-1.958594	0.129260
C	4.153038	-2.265776	0.402182
C	4.999515	-1.204714	0.768131
C	6.338151	-1.441439	1.045113
C	4.676307	-3.566442	0.305653
C	6.018257	-3.795203	0.587048
C	6.849364	-2.737933	0.956127
H	4.048131	-4.406716	0.011724
H	4.601941	-0.191018	0.826700
H	6.988498	-0.612647	1.330168
H	6.419008	-4.807625	0.514882
H	7.903261	-2.924142	1.172785
C	1.703444	-3.113986	0.115165
F	1.741820	-3.692176	1.315486
F	0.490470	-2.646213	-0.081878
F	1.953202	-4.043333	-0.800852
C	-5.538449	-1.971906	0.279778
C	-5.491751	0.287890	1.105554
C	-6.827076	0.182378	1.488039
C	-7.523039	-1.006483	1.264573
C	-6.877943	-2.081549	0.657120

H -8.571729 -1.091908 1.559083
H -7.419191 -3.012490 0.472627
H -4.968028 1.233720 1.276750
H -7.329253 1.032268 1.956176
H -5.054903 -2.825755 -0.201572
C -2.387170 -3.319816 -0.233379
C -2.009576 -2.106072 -2.272634
C -1.555236 -3.274765 -2.885348
C -1.520034 -4.470593 -2.169880
C -1.944517 -4.492578 -0.841656
H -1.922424 -5.426442 -0.275058
H -1.165960 -5.386679 -2.648393
H -2.695688 -3.356424 0.816237
H -2.033631 -1.183705 -2.857193
H -1.234492 -3.251630 -3.929889
C -3.391158 1.134467 -2.305237
C -2.435521 2.214286 -0.385275
C -3.358862 2.342139 -3.003692
C -2.426766 3.430338 -1.067123
C -2.873902 3.494599 -2.386997
H -2.081395 4.335958 -0.560638
H -2.864266 4.444610 -2.926533
H -3.815861 0.255604 -2.798780
H -3.733393 2.387248 -4.028983
H -2.076351 2.186343 0.647553
H 0.691161 3.847765 -3.264954
H 0.908855 5.349585 -2.325489
H 0.094284 3.944511 -1.599768
H 3.221320 3.255210 -3.586935
H 4.244397 3.870356 -2.257125
H 3.199080 4.996085 -3.180628

104

Z-ts10 / electronic energy: -2690.79182718 a.u. / lowest freq: -171.14 cm-1

H 4.284225 -1.762983 -2.714775
C -2.807870 -1.927773 -0.860264
C -4.906910 -0.470342 0.798499
H 3.500335 0.489829 -2.229404
C 3.221428 -1.577703 -2.541040
Si -3.150733 -0.358237 0.118560
C -2.993338 1.235022 -0.886782
C 2.769648 -0.323224 -2.291576
H 2.530328 -2.386065 -2.786660

C	-1.961745	-0.221505	1.580614
C	1.381195	0.025624	-1.953037
H	-3.439514	-0.411139	3.137847
O	-0.183711	-0.024805	0.037671
C	-2.380987	-0.254904	2.913940
C	-0.594849	-0.018982	1.331482
B	1.181428	-0.042271	-0.305005
C	-1.475813	-0.089731	3.965278
C	0.318213	0.202180	2.366240
H	0.390449	2.372735	0.088408
H	-1.822142	-0.128509	4.999562
N	1.917652	1.041333	0.662366
H	2.388979	-0.366943	2.123456
C	-0.136548	0.151744	3.686537
C	1.751761	0.525712	2.053079
H	2.928447	1.081639	0.468979
C	1.459126	2.441358	0.318934
O	3.500540	2.424883	-0.877684
C	2.318363	2.773754	-0.918999
H	-0.368984	3.132820	2.195083
H	0.572185	0.320643	4.502050
N	1.799828	3.427981	-1.970605
H	0.932564	2.671572	3.309341
H	2.160156	1.246481	2.765837
C	2.694961	3.816153	-3.049008
C	0.393133	3.697084	-2.206300
C	0.632460	3.409041	2.557969
H	0.250106	4.908961	0.336408
C	1.634414	3.571235	1.398621
C	1.280638	4.910974	0.722369
H	0.539377	4.368984	3.086577
H	1.964220	5.174072	-0.096360
H	3.434187	2.744843	2.394666
C	3.071788	3.672661	1.928175
H	1.346846	5.713651	1.470508
H	3.781463	3.937615	1.132899
H	3.117370	4.456552	2.698828
C	-5.358945	-1.690090	1.331766
C	-5.781393	0.626434	0.829597
C	-7.057890	0.513339	1.381652
C	-7.483827	-0.702442	1.913737
C	-6.631370	-1.806865	1.887895

H	-8.482968	-0.792193	2.346609
H	-6.962625	-2.763808	2.297899
H	-5.469419	1.586900	0.410529
H	-7.725471	1.378269	1.391806
H	-4.706873	-2.569012	1.310092
C	-3.578796	-2.247205	-1.991083
C	-1.843538	-2.854978	-0.438225
C	-1.650653	-4.055562	-1.121058
C	-2.409178	-4.343502	-2.254342
C	-3.374120	-3.435508	-2.690673
H	-3.979853	-3.661883	-3.571336
H	-2.256685	-5.282455	-2.791700
H	-4.365402	-1.565230	-2.328433
H	-1.232549	-2.643872	0.443505
H	-0.903189	-4.768427	-0.767271
C	-3.023007	1.276329	-2.288332
C	-2.935804	2.459540	-0.196997
C	-3.016712	2.491503	-2.975900
C	-2.938163	3.676943	-0.877924
C	-2.985848	3.694590	-2.272609
H	-2.912406	4.615670	-0.318678
H	-2.997551	4.646001	-2.809678
H	-3.059906	0.346682	-2.862021
H	-3.050032	2.496955	-4.068124
H	-2.909731	2.466233	0.897639
H	0.131292	3.366035	-3.222389
H	0.178171	4.773808	-2.126695
H	-0.255063	3.157405	-1.509976
H	2.363479	4.779076	-3.461296
H	2.686186	3.066072	-3.857069
H	3.717867	3.914975	-2.670762
C	0.298532	-0.840498	-2.606547
H	1.201600	1.076343	-2.221287
H	0.299162	-1.873775	-2.235646
H	0.436721	-0.866566	-3.697820
H	-0.694827	-0.428312	-2.391953
O	1.759735	-1.422999	0.034233
C	2.832742	-2.062208	-0.116696
C	2.562422	-3.568724	-0.379917
C	4.140388	-1.679171	0.480090
C	4.755350	-0.437268	0.258285
C	4.721154	-2.566156	1.405302

C 5.862943 -2.195840 2.110614
C 6.450334 -0.951996 1.898326
C 5.895284 -0.075573 0.964970
H 4.379211 0.248604 -0.498709
H 6.360811 0.892113 0.769314
H 4.277540 -3.538983 1.613151
H 6.291691 -2.893343 2.832286
H 7.349789 -0.669785 2.449084
F 1.535326 -3.735985 -1.195299
F 2.249063 -4.153773 0.779057
F 3.621705 -4.174045 -0.891004
104
Z-ts11 / electronic energy: -2690.79181739 a.u. / lowest freq: -160.97 cm-1
H -3.647735 -2.665231 2.389308
C 2.456592 -2.116488 1.160413
C 4.753992 -1.202306 -0.609212
H -1.276761 -2.073460 2.148244
C -3.349096 -1.646286 2.134453
Si 3.009971 -0.773874 -0.033417
C 3.057399 0.956827 0.744298
C -2.043571 -1.295067 2.042025
H -4.131893 -0.883976 2.130555
C 1.917783 -0.575788 -1.569514
C -1.568238 0.054949 1.684976
H 3.544014 -0.793348 -2.969681
O -0.048201 -0.352773 -0.265227
C -0.249009 0.361624 2.409381
H -2.354721 0.781044 1.937883
C 2.502287 -0.489061 -2.838908
C 0.572654 -0.178052 -1.455053
B -1.345536 0.102822 0.037383
C 1.802113 0.016430 -3.937259
C -0.102812 0.441626 -2.509262
H 0.078825 2.415254 0.013269
H 2.279334 0.065636 -4.917395
N -1.616893 1.465242 -0.823951
H -2.265928 0.373314 -2.476087
C 0.519152 0.518388 -3.757819
C -1.445418 1.068502 -2.256798
H -2.611175 1.700439 -0.674434
C -0.937116 2.700635 -0.288820
O -3.056015 2.865330 0.757631

C	-1.847675	3.052684	0.915017
H	1.119785	3.195334	-1.960997
H	-0.006174	0.991119	-4.592312
N	-1.337188	3.533680	2.061001
H	-0.137995	3.119146	-3.208556
H	-1.597542	1.935038	-2.902573
C	-2.250309	3.875537	3.138860
C	0.063556	3.740816	2.369903
C	0.228066	3.702305	-2.357279
H	0.679093	4.960068	-0.017330
C	-0.825276	3.938858	-1.257008
C	-0.316927	5.145805	-0.444472
H	0.550162	4.672393	-2.763169
H	-1.001672	5.441178	0.362388
H	-2.656935	3.530100	-2.445075
C	-2.179225	4.333632	-1.866047
H	-0.225795	6.008613	-1.119809
H	-2.895543	4.650373	-1.095631
H	-2.031141	5.177046	-2.557031
H	-0.421346	0.539603	3.481312
H	0.268005	1.231928	1.995747
H	0.447719	-0.482920	2.310710
O	-2.560673	-0.680145	-0.529908
C	-3.279085	-1.683825	-0.256647
C	-4.738638	-1.560129	-0.401798
C	-5.283011	-0.272279	-0.547598
C	-6.652305	-0.104239	-0.695006
C	-5.593352	-2.676108	-0.392753
C	-6.963519	-2.498692	-0.544608
C	-7.494706	-1.218134	-0.696303
H	-5.204586	-3.686420	-0.268386
H	-4.629079	0.600232	-0.532789
H	-7.067641	0.898628	-0.807618
H	-7.622875	-3.368374	-0.543261
H	-8.572027	-1.085741	-0.814664
C	-2.616389	-3.068719	-0.474306
F	-2.934102	-3.476257	-1.701466
F	-1.302572	-2.964386	-0.404971
F	-3.008322	-3.998427	0.387893
C	5.067770	-2.538583	-0.910679
C	5.754086	-0.233663	-0.783456
C	7.022009	-0.584870	-1.248269

C 7.311615 -1.915103 -1.548011
C 6.331740 -2.893672 -1.378025
H 8.304404 -2.191676 -1.910919
H 6.554988 -3.938732 -1.605305
H 5.548076 0.814735 -0.550018
H 7.788480 0.183813 -1.372716
H 4.313587 -3.320009 -0.774506
C 1.395642 -2.968389 0.829309
C 3.117926 -2.333052 2.381975
C 2.697329 -3.330726 3.260225
C 1.617001 -4.147706 2.923920
C 0.973785 -3.973889 1.699441
H 0.142457 -4.624427 1.416979
H 1.288585 -4.930861 3.611321
H 0.891409 -2.841575 -0.127918
H 3.987422 -1.727009 2.653035
H 3.220388 -3.478857 4.207795
C 3.213644 1.184177 2.120362
C 3.067459 2.079234 -0.103254
C 3.399009 2.470694 2.628038
C 3.253338 3.369082 0.397101
C 3.429645 3.566715 1.766281
H 3.276608 4.219318 -0.289152
H 3.586744 4.572929 2.161867
H 3.195167 0.345653 2.820052
H 3.529618 2.616350 3.702810
H 2.949549 1.944937 -1.182629
H 0.304648 3.242291 3.320241
H 0.279815 4.814990 2.479262
H 0.724864 3.335013 1.600800
H -2.204517 3.115977 3.936341
H -3.273614 3.929949 2.755534
H -1.965824 4.848049 3.566118
104
Z-ts12 / electronic energy: -2690.78789430 a.u. / lowest freq: -245.89 cm-1
H 3.987774 -2.105615 -2.421322
C -2.604234 -2.049459 -0.724129
C -4.911976 -0.473769 0.545117
H 3.732323 0.217034 -1.731072
C 2.990670 -1.680393 -2.290445
Si -3.102017 -0.388607 0.013411
C -2.939590 1.097648 -1.143204

C	2.834477	-0.364496	-1.976630
H	2.151087	-2.268422	-2.667112
C	-2.053361	-0.056278	1.549354
C	1.549747	0.279055	-1.711867
H	-3.672646	-0.168687	2.967433
O	-0.134944	0.083759	0.174787
C	-2.602437	0.009443	2.833474
C	-0.673848	0.176586	1.415872
B	1.250842	0.152276	-0.062785
C	-1.815662	0.306724	3.948882
C	0.118133	0.536873	2.509251
H	0.556239	2.636768	-0.079501
H	-2.263505	0.344936	4.943277
N	1.863993	1.312756	0.907527
H	2.210572	0.025284	2.495760
C	-0.465377	0.584319	3.778304
C	1.563486	0.893897	2.308729
H	2.891993	1.302247	0.809113
C	1.543538	2.695200	0.396267
O	3.783995	2.432828	-0.347501
C	2.685043	2.914528	-0.631823
H	-0.594758	3.439611	1.885540
H	0.150545	0.859987	4.639303
N	2.480527	3.608961	-1.763858
H	0.501905	3.066308	3.226359
H	1.878166	1.672885	3.007314
C	3.619949	3.861334	-2.631441
C	1.191617	3.969924	-2.324073
C	0.325646	3.758668	2.397855
H	0.298793	5.156662	0.093016
C	1.508495	3.887241	1.420173
C	1.257491	5.187982	0.632283
H	0.127053	4.740760	2.850959
H	2.058609	5.420465	-0.081666
H	3.156878	3.130050	2.694086
C	2.836828	4.044439	2.174274
H	1.204164	6.024569	1.343268
H	3.655376	4.334853	1.500892
H	2.735330	4.832578	2.935472
C	-5.601606	-1.687749	0.682676
C	-5.602671	0.713936	0.842947
C	-6.928951	0.689753	1.269928

C	-7.595102	-0.528862	1.404940
C	-6.929987	-1.717298	1.109299
H	-8.635955	-0.550734	1.736597
H	-7.447921	-2.674144	1.208269
H	-5.099737	1.679801	0.733451
H	-7.447638	1.625146	1.493057
H	-5.100608	-2.630949	0.449195
C	-2.410701	-3.120983	0.164774
C	-2.479939	-2.307962	-2.096743
C	-2.181066	-3.587678	-2.565739
C	-2.007798	-4.639266	-1.667166
C	-2.122679	-4.403631	-0.298001
H	-1.980370	-5.219552	0.414489
H	-1.781416	-5.643102	-2.034441
H	-2.485346	-2.954331	1.243867
H	-2.607124	-1.501983	-2.823250
H	-2.087236	-3.764620	-3.639845
C	-3.511383	1.092709	-2.425679
C	-2.343869	2.290337	-0.701127
C	-3.455750	2.217165	-3.249732
C	-2.307640	3.426412	-1.509914
C	-2.851865	3.388151	-2.793777
H	-1.867912	4.352820	-1.130781
H	-2.824667	4.275897	-3.430200
H	-4.029925	0.201794	-2.790773
H	-3.905068	2.184271	-4.244801
H	-1.920298	2.343013	0.306154
H	1.110660	3.556034	-3.341210
H	1.079151	5.062871	-2.384708
H	0.361488	3.564561	-1.740465
H	3.492660	4.840034	-3.113886
H	3.694355	3.089399	-3.415604
H	4.546223	3.860024	-2.047634
C	0.350604	-0.235286	-2.512361
H	1.659871	1.352519	-1.905319
H	0.082588	-1.267313	-2.259087
H	0.561398	-0.185097	-3.591392
H	-0.533278	0.380545	-2.303978
O	2.016534	-1.061336	0.431462
C	2.677076	-2.053478	-0.018485
C	1.791410	-3.303789	-0.265322
C	4.083211	-2.219535	0.405413

C 4.827514 -1.069843 0.720675
C 4.684941 -3.481261 0.533629
C 5.998570 -3.582883 0.983585
C 6.727275 -2.437410 1.294260
C 6.139237 -1.177516 1.157644
H 4.390629 -0.078335 0.597237
H 6.708009 -0.275321 1.389597
H 4.140438 -4.395443 0.301618
H 6.453953 -4.568741 1.091819
H 7.758919 -2.523980 1.641289
F 0.624219 -2.945056 -0.765964
F 1.581365 -3.889577 0.911451
F 2.343435 -4.195730 -1.081216
104
Z-ts13 / electronic energy: -2690.78951495 a.u. / lowest freq: -182.51 cm-1
H 1.948393 -3.214180 -1.981203
C -2.202268 -2.028414 -1.067552
C -4.727086 -0.933226 0.279138
H 3.240510 -1.203923 -2.357039
C 1.564635 -2.250038 -1.643115
Si -2.920164 -0.564204 -0.119962
C -2.893094 1.071909 -1.072173
C 2.249390 -1.106813 -1.899648
H 0.547813 -2.221615 -1.237764
C -1.987257 -0.251342 1.495137
C 1.790681 0.247896 -1.503749
H -3.682975 -0.468251 2.810827
O 0.011228 0.001852 0.261926
C 0.571265 0.662944 -2.354922
H 2.623005 0.938973 -1.686179
C -2.629359 -0.186531 2.735663
C -0.630699 0.115236 1.447805
B 1.390378 0.260173 0.102360
C -1.960187 0.253610 3.880347
C 0.034966 0.633093 2.561593
H 0.357130 2.699094 0.004908
H -2.478498 0.290273 4.840043
N 1.791421 1.532802 1.029671
H 2.166748 0.359253 2.703671
C -0.643141 0.686294 3.782127
C 1.444998 1.140073 2.431319
H 2.819862 1.627495 0.977346

C	1.343950	2.857414	0.456410
O	3.589860	2.783183	-0.291259
C	2.446518	3.122586	-0.601096
H	-0.869654	3.618372	1.853020
H	-0.130905	1.083634	4.662887
N	2.161505	3.686060	-1.788364
H	0.186717	3.251413	3.225552
H	1.625466	1.975958	3.109515
C	3.250153	3.925186	-2.721900
C	0.854482	4.069090	-2.285161
C	0.033599	3.942872	2.391226
H	0.007762	5.283938	0.071769
C	1.238672	4.080874	1.441810
C	0.963647	5.350225	0.611806
H	-0.185016	4.924155	2.837172
H	1.763666	5.579154	-0.105312
H	2.867665	3.455202	2.818904
C	2.539389	4.319696	2.224208
H	0.889495	6.207264	1.296259
H	3.370153	4.587587	1.557137
H	2.390486	5.152896	2.927368
H	0.855224	0.818824	-3.406156
H	0.110198	1.583490	-1.980757
H	-0.203740	-0.111988	-2.318936
O	2.327169	-0.781381	0.751627
C	2.670160	-1.961715	0.420901
C	4.096157	-2.242177	0.173768
C	4.979746	-1.151036	0.112388
C	6.331617	-1.360393	-0.121036
C	4.587597	-3.543914	-0.016526
C	5.943529	-3.744542	-0.250526
C	6.815625	-2.657713	-0.302533
H	3.921396	-4.405113	0.013734
H	4.600541	-0.137222	0.247658
H	7.014467	-0.509787	-0.159896
H	6.321947	-4.758170	-0.393247
H	7.879624	-2.821824	-0.485082
C	1.790454	-3.069212	1.071824
F	2.350993	-3.346421	2.249515
F	0.567311	-2.628548	1.293349
F	1.714818	-4.198260	0.377432
C	-5.274393	-2.221896	0.186642

C -5.571048 0.113572 0.690051
C -6.907447 -0.119686 1.007596
C -7.431100 -1.409555 0.912373
C -6.613219 -2.459944 0.499748
H -8.480504 -1.594068 1.153829
H -7.021034 -3.469948 0.415367
H -5.180344 1.133682 0.757907
H -7.546072 0.708445 1.323939
H -4.652088 -3.058302 -0.143338
C -1.899482 -3.197466 -0.349228
C -2.009483 -2.048406 -2.457491
C -1.529191 -3.187284 -3.104885
C -1.236941 -4.337151 -2.372519
C -1.423217 -4.340634 -0.990451
H -1.191898 -5.235329 -0.408043
H -0.864435 -5.231052 -2.878324
H -2.032668 -3.218831 0.736210
H -2.228782 -1.161767 -3.056287
H -1.384863 -3.176096 -4.187752
C -3.455114 1.184223 -2.354458
C -2.416223 2.247116 -0.469383
C -3.498216 2.407219 -3.024293
C -2.481109 3.478099 -1.121750
C -3.008411 3.559289 -2.410274
H -2.129993 4.381637 -0.615619
H -3.059428 4.521128 -2.925775
H -3.892395 0.307408 -2.840347
H -3.937357 2.464713 -4.022901
H -2.006601 2.207548 0.543283
H 0.695651 3.621477 -3.277592
H 0.783677 5.163381 -2.384730
H 0.046589 3.727694 -1.634679
H 3.157326 4.936351 -3.144015
H 3.211616 3.196350 -3.548236
H 4.210638 3.829889 -2.206853
104
Z-ts14 / electronic energy: -2690.78715131 a.u. / lowest freq: -202.82 cm-1
H 2.992887 -2.928286 -2.112976
C -2.243903 -2.151993 -1.233987
C -4.616065 -1.286966 0.433865
H 3.686325 -0.617683 -2.303714
C 2.317743 -2.128187 -1.803159

Si	-2.865566	-0.801582	-0.082171
C	-2.956798	0.921602	-0.867308
C	2.664705	-0.826964	-1.967058
H	1.296221	-2.407854	-1.525802
C	-1.835541	-0.587041	1.491684
C	1.809149	0.321677	-1.595117
H	-3.463146	-0.989248	2.848698
O	0.118256	-0.167223	0.223269
C	0.501202	0.336159	-2.412193
H	2.385192	1.230331	-1.805987
C	-2.437511	-0.622752	2.754665
C	-0.512654	-0.113738	1.420265
B	1.444033	0.280537	0.031802
C	-1.769830	-0.172714	3.896440
C	0.127211	0.450153	2.528299
H	-0.082318	2.427863	0.044887
H	-2.255931	-0.222108	4.872229
N	1.645295	1.613031	0.943578
H	2.290202	0.518852	2.596318
C	-0.508237	0.395575	3.771004
C	1.438615	1.167204	2.355349
H	2.625563	1.921020	0.839826
C	0.883924	2.801918	0.406524
O	3.021977	3.214436	-0.521871
C	1.810729	3.270965	-0.739930
H	-1.299816	3.083224	1.989158
H	-0.011406	0.824051	4.645968
N	1.306228	3.702974	-1.908516
H	-0.093952	3.071087	3.290000
H	1.502071	2.025866	3.027368
C	2.225079	4.169657	-2.932813
C	-0.091715	3.744332	-2.287087
C	-0.468124	3.646315	2.436849
H	-0.944607	4.875149	0.095811
C	0.604350	4.001284	1.388409
C	0.008266	5.160211	0.564985
H	-0.883625	4.576182	2.852291
H	0.690229	5.532559	-0.211862
H	2.419931	3.750157	2.637988
C	1.882992	4.518940	2.063334
H	-0.199007	6.001860	1.241494
H	2.591462	4.931277	1.331913

H	1.618996	5.321218	2.768345
H	0.705666	0.528128	-3.475834
H	-0.186352	1.105641	-2.044426
H	-0.029297	-0.622372	-2.329893
O	2.541097	-0.589586	0.671231
C	3.145015	-1.664581	0.364823
C	4.610738	-1.643086	0.215147
C	5.259630	-0.397108	0.217529
C	6.638867	-0.328182	0.077651
C	5.365257	-2.817696	0.062331
C	6.746418	-2.740000	-0.077717
C	7.384035	-1.499968	-0.070749
H	4.885073	-3.795829	0.047609
H	4.677953	0.519190	0.327628
H	7.137129	0.642693	0.084573
H	7.327461	-3.656350	-0.194529
H	8.468813	-1.444317	-0.182829
C	2.479512	-2.945859	0.947986
F	3.051306	-3.173034	2.128739
F	1.190257	-2.744286	1.150926
F	2.623576	-4.036127	0.204045
C	-4.894518	-2.631053	0.735940
C	-5.656818	-0.354487	0.560620
C	-6.928118	-0.746593	0.981447
C	-7.181864	-2.083319	1.283678
C	-6.162153	-3.027336	1.158891
H	-8.177408	-2.392180	1.611374
H	-6.357097	-4.077950	1.386584
H	-5.481500	0.698208	0.323144
H	-7.724560	-0.003760	1.069009
H	-4.109554	-3.387187	0.635238
C	-1.244883	-3.041061	-0.815499
C	-2.840699	-2.375858	-2.486463
C	-2.420792	-3.421580	-3.307310
C	-1.410348	-4.283531	-2.879762
C	-0.831278	-4.099860	-1.625021
H	-0.056771	-4.785004	-1.271529
H	-1.087983	-5.108764	-3.519094
H	-0.788371	-2.909969	0.165455
H	-3.663851	-1.740169	-2.825545
H	-2.895825	-3.574370	-4.279178
C	-3.113702	2.030250	-0.015872

C -3.026408 1.152166 -2.249817
C -3.362317 3.307490 -0.520480
C -3.273953 2.426802 -2.761783
C -3.454112 3.506420 -1.897804
H -3.335815 2.575218 -3.842364
H -3.660976 4.501829 -2.297664
H -3.069443 1.891155 1.068748
H -3.500729 4.145251 0.167310
H -2.890606 0.326236 -2.951406
H -0.220469 3.245656 -3.259028
H -0.436254 4.785645 -2.386237
H -0.733323 3.238876 -1.562032
H 1.861370 5.120981 -3.347980
H 2.291467 3.434694 -3.751767
H 3.219603 4.315096 -2.500509
104
E-ts1 / electronic energy: -2690.79627706 a.u. / lowest freq: -48.26 cm-1
H -2.190129 -3.295085 2.563576
C 1.885683 -1.087793 1.617453
C 4.331735 -0.667388 -0.214136
H -0.769345 -1.403826 2.062809
C -2.638460 -2.346916 2.260919
Si 2.588393 -0.069659 0.194905
C 2.730469 1.767001 0.629900
C -1.853720 -1.269028 2.030635
H -3.725964 -2.271200 2.327118
C 1.532847 -0.117223 -1.379003
C -2.341011 0.054710 1.590820
H 3.191173 -0.363683 -2.735683
O -0.459519 0.038490 -0.111595
C 2.121584 -0.157868 -2.647050
C 0.150641 0.129408 -1.320114
B -1.866553 0.114243 0.014878
C 1.381168 0.076511 -3.808819
C -0.591966 0.459369 -2.461413
H -0.680975 2.449955 -0.341109
H 1.863940 0.029692 -4.786303
N -2.351847 1.322913 -0.960594
H -2.713892 0.008350 -2.546842
C 0.037829 0.416448 -3.708129
C -2.041577 0.852222 -2.342980
H -3.367450 1.466084 -0.877100

C	-1.735281	2.648400	-0.551687
O	-3.751781	3.094967	0.574034
C	-2.530308	3.059376	0.695283
H	0.248658	3.378459	-2.296115
H	-0.535139	0.659375	-4.607188
N	-1.893947	3.382307	1.837878
H	-1.011965	3.003393	-3.487911
H	-2.294390	1.633528	-3.063228
C	-2.676522	3.906973	2.943495
C	-0.470881	3.254715	2.095085
C	-0.725568	3.698731	-2.690979
H	-0.411796	4.987434	-0.282191
C	-1.779461	3.846501	-1.576884
C	-1.385114	5.109813	-0.782409
H	-0.579525	4.675927	-3.173946
H	-2.133627	5.388836	-0.027780
H	-3.542662	3.203746	-2.748456
C	-3.165786	4.076235	-2.194097
H	-1.295596	5.957322	-1.476775
H	-3.912604	4.332899	-1.433357
H	-3.105437	4.905781	-2.914900
O	-2.632663	-1.114719	-0.583613
C	-2.565438	-2.347078	-0.308228
C	-1.388848	-3.197278	-0.573212
C	-0.590853	-2.861085	-1.676678
C	0.457932	-3.687251	-2.067083
C	-1.139622	-4.400527	0.110369
C	-0.088649	-5.217673	-0.280834
C	0.717399	-4.860860	-1.364823
H	-1.756821	-4.693705	0.957670
H	-0.816957	-1.974449	-2.263999
H	1.066047	-3.410589	-2.929924
H	0.104424	-6.144126	0.263119
H	1.541680	-5.509357	-1.668696
C	-3.954141	-3.032807	-0.390341
F	-4.020572	-4.160468	0.299266
F	-4.925665	-2.230852	0.014092
F	-4.160173	-3.313050	-1.677217
C	4.829224	-1.916934	0.186086
C	5.184542	0.174392	-0.950745
C	6.475537	-0.223995	-1.292358
C	6.947030	-1.474028	-0.890888

C 6.123462 -2.317626 -0.147672
H 7.961617 -1.785893 -1.149805
H 6.492773 -3.291818 0.181519
H 4.840068 1.166987 -1.257606
H 7.119598 0.446157 -1.866402
H 4.207883 -2.589928 0.782081
C 1.626413 -2.456870 1.435900
C 1.661617 -0.544738 2.892323
C 1.226623 -1.340159 3.953447
C 1.005292 -2.702636 3.759679
C 1.198493 -3.257905 2.494867
H 1.016121 -4.321699 2.328620
H 0.676351 -3.329968 4.591300
H 1.758690 -2.914799 0.451048
H 1.827298 0.519949 3.070856
H 1.065838 -0.892643 4.936873
C 3.424709 2.192763 1.776242
C 2.247043 2.755191 -0.241145
C 3.594762 3.547892 2.056248
C 2.429154 4.113295 0.023031
C 3.096272 4.512640 1.179447
H 2.058088 4.860434 -0.683027
H 3.243895 5.574235 1.390801
H 3.859921 1.457335 2.459357
H 4.135805 3.853119 2.954870
H 1.733284 2.460119 -1.159118
H -0.330478 2.872263 3.116761
H 0.041935 4.226573 2.019127
H 0.013154 2.548481 1.412876
H -2.189903 4.808892 3.343756
H -2.754668 3.161888 3.751764
H -3.683416 4.159697 2.596054
H -1.706352 0.811610 2.080480
C -3.821428 0.296001 1.885346
H -4.468522 -0.355796 1.284044
H -4.123072 1.327103 1.676984
H -4.039319 0.092316 2.944858

104

E-ts2 / electronic energy: -2690.79380474 a.u. / lowest freq: -184.27 cm-1

H -2.659044 -2.853852 2.252723
C 1.847912 -1.879750 1.474887
C 4.253408 -1.965080 -0.474173

H	-0.764855	-1.371311	1.959750
C	-2.827059	-1.786664	2.095756
Si	2.722653	-0.994594	0.057432
C	3.330443	0.732513	0.545227
C	-1.768956	-0.940952	1.987847
H	-3.844570	-1.422471	2.245581
C	1.620703	-0.712683	-1.459896
C	-1.876757	0.499006	1.700097
H	3.055754	-1.431486	-2.900553
O	-0.144512	0.066952	-0.086193
C	2.104591	-0.912863	-2.756498
C	0.385299	-0.053070	-1.328871
B	-1.471573	0.522616	0.093133
C	1.415095	-0.441676	-3.877180
C	-0.277671	0.504158	-2.428887
H	0.339148	2.425602	-0.239636
H	1.812752	-0.614928	-4.878604
N	-1.602667	1.863349	-0.827601
H	-2.424803	0.811023	-2.436898
C	0.248676	0.292333	-3.706579
C	-1.500237	1.365932	-2.234872
H	-2.524845	2.299377	-0.695541
C	-0.618485	2.929470	-0.399891
O	-2.413658	3.825748	0.826545
C	-1.235906	3.478419	0.894471
H	1.520495	3.278805	-2.118247
H	-0.260986	0.720867	-4.573969
N	-0.506888	3.575797	2.021878
H	0.190307	3.089409	-3.270385
H	-1.488996	2.213206	-2.924271
C	-1.106775	4.207182	3.184723
C	0.855026	3.112817	2.214351
C	0.612915	3.757055	-2.511573
H	1.267610	4.833877	-0.068713
C	-0.357231	4.136771	-1.378721
C	0.359249	5.225315	-0.552576
H	0.925721	4.671392	-3.037361
H	-0.288381	5.665329	0.219153
H	-2.208379	4.044177	-2.591914
C	-1.644615	4.743149	-1.955467
H	0.667490	6.042449	-1.220479
H	-2.318410	5.090658	-1.162129

H	-1.384335	5.605753	-2.587285
O	-2.586821	-0.339526	-0.524789
C	-3.091482	-1.482905	-0.298970
C	-4.558791	-1.602236	-0.381441
C	-5.299720	-0.437065	-0.648759
C	-6.682364	-0.493649	-0.758417
C	-5.234479	-2.825050	-0.220666
C	-6.619103	-2.872053	-0.328353
C	-7.344644	-1.711312	-0.596578
H	-4.691106	-3.742939	-0.003402
H	-4.782505	0.513467	-0.782156
H	-7.246711	0.415508	-0.973344
H	-7.135737	-3.824765	-0.200826
H	-8.432229	-1.756591	-0.683172
C	-2.223956	-2.708030	-0.694534
F	-2.478923	-2.942944	-1.982480
F	-0.938154	-2.456166	-0.569145
F	-2.496878	-3.814597	-0.012877
C	4.439030	-3.327616	-0.195254
C	5.264532	-1.298723	-1.189512
C	6.407135	-1.969135	-1.621514
C	6.567368	-3.325773	-1.339878
C	5.582164	-4.003110	-0.623591
H	7.463937	-3.853118	-1.673878
H	5.705590	-5.063697	-0.392576
H	5.164863	-0.231390	-1.408813
H	7.179783	-1.429303	-2.174020
H	3.688380	-3.878738	0.376191
C	1.285654	-3.149866	1.262139
C	1.738648	-1.327656	2.760893
C	1.113718	-2.020755	3.798206
C	0.570081	-3.283481	3.566466
C	0.651929	-3.844879	2.292049
H	0.218626	-4.828850	2.097743
H	0.079596	-3.827371	4.377040
H	1.327965	-3.607108	0.269683
H	2.138342	-0.332005	2.963726
H	1.045529	-1.568971	4.790464
C	4.069720	0.958156	1.719688
C	3.165324	1.814083	-0.334427
C	4.583571	2.219559	2.019665
C	3.696378	3.073242	-0.051988

C	4.397871	3.281622	1.133685
H	3.568805	3.890788	-0.766071
H	4.816131	4.265041	1.360639
H	4.271544	0.134380	2.410296
H	5.148444	2.370130	2.942551
H	2.627753	1.666490	-1.274269
H	0.923083	2.602249	3.186453
H	1.564576	3.955270	2.222949
H	1.169423	2.400010	1.446042
H	-0.409115	4.949429	3.600612
H	-1.324778	3.457648	3.962803
H	-2.038663	4.703965	2.897232
H	-1.029654	1.010548	2.186295
C	-3.217337	1.116723	2.095464
H	-4.056354	0.664657	1.548173
H	-3.250025	2.193964	1.901436
H	-3.409263	0.959758	3.168070

104

E-ts3 / electronic energy: -2690.79533621 a.u. / lowest freq: -153.50 cm-1

H	-1.911302	-3.319837	2.584940
C	2.458646	-1.285320	1.484435
C	4.448301	0.020727	-0.367756
H	-0.626996	-1.315221	2.152947
C	-2.425008	-2.406599	2.278434
Si	2.647973	0.075136	0.200522
C	2.302559	1.787404	0.929182
C	-1.718045	-1.264169	2.086116
H	-3.513863	-2.404071	2.364094
C	1.571953	-0.059421	-1.354965
C	-2.296865	0.004790	1.616028
H	3.258703	-0.169497	-2.694699
O	-0.448979	-0.051101	-0.110432
C	2.174315	-0.059442	-2.618993
C	0.173090	0.079959	-1.310541
B	-1.862258	-0.004888	0.015344
C	1.429802	0.095907	-3.790699
C	-0.575678	0.347330	-2.462490
H	-0.889928	2.372881	-0.178593
H	1.924728	0.077600	-4.763004
N	-2.397600	1.145923	-0.991284
H	-2.668209	-0.216284	-2.547647
C	0.064493	0.330579	-3.704015

C	-2.042815	0.667391	-2.359680
H	-3.424574	1.224677	-0.931259
C	-1.905221	2.516895	-0.562626
O	-4.102622	2.765675	0.238554
C	-2.916580	2.913490	0.526512
H	0.231256	3.126344	-2.129703
H	-0.517309	0.522531	-4.609709
N	-2.504530	3.389344	1.715817
H	-0.917514	2.821629	-3.448467
H	-2.334276	1.416795	-3.100311
C	-3.499156	3.852902	2.668107
C	-1.132041	3.545332	2.154082
C	-0.679923	3.497685	-2.620222
H	-0.560827	4.877627	-0.286953
C	-1.837252	3.683112	-1.621986
C	-1.512866	4.968193	-0.831075
H	-0.442301	4.470594	-3.074938
H	-2.302573	5.245075	-0.118782
H	-3.501340	3.025878	-2.929475
C	-3.155740	3.911075	-2.375339
H	-1.409707	5.803753	-1.537836
H	-3.967214	4.211900	-1.701142
H	-3.010901	4.713706	-3.114464
O	-2.616778	-1.254498	-0.509579
C	-2.517741	-2.482369	-0.210181
C	-1.346144	-3.314486	-0.545326
C	-0.600987	-2.952942	-1.677714
C	0.456720	-3.747748	-2.107082
C	-1.046876	-4.516929	0.118170
C	0.011213	-5.303516	-0.314280
C	0.772863	-4.916059	-1.418913
H	-1.624663	-4.829646	0.986281
H	-0.866694	-2.065013	-2.246629
H	1.028558	-3.451826	-2.988090
H	0.248764	-6.225797	0.218712
H	1.607061	-5.537859	-1.749856
C	-3.894628	-3.197248	-0.239767
F	-3.918908	-4.311950	0.474626
F	-4.871293	-2.407157	0.175567
F	-4.131619	-3.509069	-1.513383
C	5.060022	-1.225078	-0.590966
C	5.201894	1.177462	-0.617307

C 6.514889 1.095637 -1.082248
C 7.100345 -0.149281 -1.305482
C 6.370847 -1.312296 -1.056464
H 8.128648 -0.215105 -1.668714
H 6.828426 -2.290750 -1.220648
H 4.764687 2.163998 -0.442540
H 7.083148 2.010049 -1.267966
H 4.506940 -2.148440 -0.392182
C 1.547709 -2.342658 1.366805
C 3.319420 -1.277417 2.597716
C 3.244668 -2.266698 3.575812
C 2.315315 -3.299495 3.451010
C 1.474095 -3.339969 2.341448
H 0.758259 -4.156492 2.229647
H 2.257390 -4.079750 4.213424
H 0.883513 -2.388220 0.501797
H 4.074842 -0.492074 2.700453
H 3.922565 -2.239230 4.432021
C 2.214329 2.890357 0.060161
C 2.261919 2.039898 2.308743
C 2.126969 4.194262 0.548006
C 2.170849 3.342458 2.802972
C 2.114270 4.423018 1.924116
H 2.152048 3.513933 3.881779
H 2.056858 5.443027 2.311221
H 2.241632 2.732927 -1.022685
H 2.082696 5.034217 -0.149492
H 2.313473 1.210481 3.019037
H -1.013513 3.088927 3.148715
H -0.868827 4.611403 2.235274
H -0.417909 3.065010 1.479500
H -3.307505 4.906752 2.923950
H -3.452061 3.254921 3.591530
H -4.497485 3.762907 2.229348
H -1.693824 0.828715 2.031738
C -3.780672 0.166247 1.946330
H -4.401722 -0.563529 1.412986
H -4.168762 1.152703 1.678553
H -3.947967 0.018516 3.024029
104
E-ts4 / electronic energy: -2690.79014808 a.u. / lowest freq: -215.16 cm-1
H -4.535987 1.709946 -2.312720

C	2.394660	1.801330	-1.243076
C	4.726697	0.866695	0.487581
H	-3.674313	-0.592264	-2.077226
C	-3.471157	1.525399	-2.153234
Si	2.965045	0.462266	-0.045002
C	2.922202	-1.259706	-0.826490
C	-2.983117	0.259915	-2.062211
H	-2.788510	2.363273	-2.312137
C	1.886163	0.355311	1.504021
C	-1.572928	-0.019970	-1.778835
H	3.416862	0.783089	2.962329
O	0.064225	-0.107502	0.088093
C	2.374439	0.492191	2.806498
C	0.544103	-0.025234	1.351410
B	-1.323854	-0.173188	-0.148618
C	1.557200	0.249750	3.914502
C	-0.278771	-0.323516	2.440626
H	-0.302012	-2.579374	0.169263
H	1.954480	0.367320	4.924237
N	-1.886620	-1.347960	0.831960
H	-2.413197	-0.022566	2.363160
C	0.244896	-0.170772	3.727574
C	-1.681473	-0.825579	2.218925
H	-2.898959	-1.467284	0.665193
C	-1.345588	-2.716487	0.479231
O	-3.426968	-2.741278	-0.652837
C	-2.263398	-3.141576	-0.690418
H	0.636767	-3.249190	2.256286
H	-0.384124	-0.399499	4.592553
N	-1.811827	-3.957649	-1.659462
H	-0.600476	-2.809894	3.447896
H	-1.939745	-1.596250	2.945649
C	-2.756557	-4.459281	-2.641104
C	-0.424693	-4.276091	-1.932156
C	-0.321316	-3.558302	2.700642
H	0.007901	-5.173591	0.584400
C	-1.386240	-3.816917	1.613678
C	-1.006883	-5.183163	1.006556
H	-0.142546	-4.491443	3.254120
H	-1.711466	-5.527777	0.239012
H	-3.181306	-3.041731	2.673607
C	-2.790975	-3.963306	2.218811

H	-1.014925	-5.933759	1.809449
H	-3.522982	-4.287536	1.465550
H	-2.766900	-4.725342	3.011944
C	5.715418	-0.117882	0.635435
C	5.068247	2.196766	0.787645
C	6.348335	2.529946	1.226389
C	7.316375	1.535500	1.370259
C	6.999071	0.211151	1.072548
H	8.321880	1.795042	1.709956
H	7.756177	-0.569720	1.176077
H	4.323256	2.990174	0.671381
H	6.593619	3.570502	1.451830
H	5.488388	-1.161647	0.400710
C	1.213660	2.530952	-1.044894
C	3.176836	2.115974	-2.367377
C	2.777491	3.099605	-3.272397
C	1.591842	3.803250	-3.061410
C	0.813212	3.522846	-1.939062
H	-0.108452	4.081012	-1.753649
H	1.280610	4.577015	-3.766999
H	0.590003	2.317275	-0.176311
H	4.122785	1.593152	-2.539537
H	3.399045	3.324480	-4.142249
C	2.894806	-1.466730	-2.212993
C	2.973495	-2.392458	0.005439
C	2.934561	-2.753896	-2.752427
C	3.017616	-3.681102	-0.527549
C	3.003430	-3.863515	-1.911026
H	3.072614	-4.544818	0.140032
H	3.045113	-4.870379	-2.333188
H	2.841693	-0.611063	-2.891565
H	2.918095	-2.890137	-3.836307
H	2.993087	-2.268109	1.093004
H	-0.182561	-3.989497	-2.967347
H	-0.241641	-5.355684	-1.821309
H	0.257013	-3.737669	-1.269395
H	-2.539114	-5.517780	-2.844569
H	-2.674960	-3.899845	-3.588771
H	-3.778179	-4.361832	-2.260671
C	-0.926896	-1.080262	-2.676579
O	-1.986884	1.123462	0.374721
C	-3.018839	1.826442	0.169759

C -2.852440 3.293469 0.212669
C -4.370168 1.231543 0.644107
F -5.433140 1.787694 0.094276
F -4.435294 -0.080899 0.435282
F -4.427248 1.430856 1.962673
C -3.821727 4.195701 -0.259178
C -3.586834 5.562336 -0.185216
C -1.659808 3.785345 0.769028
C -1.437546 5.154715 0.847198
C -2.396964 6.044116 0.364673
H -4.745748 3.835056 -0.709181
H -4.336119 6.259419 -0.564284
H -0.922705 3.085982 1.164217
H -0.511698 5.528166 1.287959
H -2.219809 7.120132 0.420967
H -1.604428 -1.916855 -2.880620
H 0.006237 -1.460746 -2.239503
H -0.671062 -0.628471 -3.645702
H -0.998385 0.910853 -1.917236
104
E-ts5 / electronic energy: -2690.79061923 a.u. / lowest freq: -262.84 cm-1
H -4.372989 1.882271 -2.259118
C 2.323666 1.866464 -1.050565
C 4.786856 0.680318 0.429412
H -3.647736 -0.480053 -2.057708
C -3.322816 1.628755 -2.100520
Si 2.975716 0.419953 -0.029262
C 2.880336 -1.223034 -0.960690
C -2.908565 0.330961 -2.038314
H -2.589692 2.420180 -2.271113
C 1.948925 0.239660 1.547001
C -1.517617 -0.016585 -1.756897
H 3.489961 0.595622 3.014397
O 0.104923 -0.105855 0.124361
C 2.439679 0.341214 2.851367
C 0.589419 -0.072981 1.387716
B -1.287269 -0.139453 -0.115321
C 1.612861 0.115693 3.955508
C -0.242052 -0.362197 2.472384
H -0.405406 -2.617336 0.086849
H 2.012750 0.207217 4.966895
N -1.885764 -1.309146 0.848518

H	-2.360793	0.021783	2.385929
C	0.286266	-0.252666	3.761355
C	-1.660719	-0.809493	2.241336
H	-2.904857	-1.375663	0.689289
C	-1.432005	-2.702115	0.466726
O	-3.578463	-2.606499	-0.540759
C	-2.447789	-3.083152	-0.641461
H	0.576257	-3.179546	2.207778
H	-0.351468	-0.472280	4.622235
N	-2.119093	-3.939868	-1.625905
H	-0.640066	-2.845836	3.452136
H	-1.952390	-1.575987	2.959891
C	-3.163271	-4.373372	-2.538061
C	-0.779290	-4.352294	-1.994128
C	-0.354176	-3.548699	2.664014
H	-0.093385	-5.167590	0.535430
C	-1.447749	-3.801048	1.603484
C	-1.095729	-5.169453	0.987007
H	-0.120002	-4.496177	3.169949
H	-1.824644	-5.507960	0.240467
H	-3.221056	-3.008464	2.686470
C	-2.835298	-3.940037	2.248824
H	-1.088488	-5.919600	1.790283
H	-3.584324	-4.290442	1.524520
H	-2.785460	-4.681564	3.060102
C	5.562987	1.747580	-0.046335
C	5.418211	-0.279175	1.241797
C	6.763719	-0.165650	1.583561
C	7.513981	0.911109	1.109425
C	6.912807	1.864069	0.289997
H	8.570264	1.002570	1.372973
H	7.497480	2.703494	-0.093471
H	4.853139	-1.140122	1.613228
H	7.231202	-0.922444	2.217821
H	5.117214	2.502157	-0.699363
C	2.499212	3.179593	-0.581215
C	1.627851	1.690373	-2.255663
C	1.134315	2.780749	-2.973198
C	1.337522	4.076810	-2.500938
C	2.024771	4.274128	-1.303431
H	2.194829	5.286796	-0.929942
H	0.962821	4.933373	-3.066096

H 3.022681 3.358400 0.362936
H 1.460577 0.682378 -2.642622
H 0.598879 2.617671 -3.911913
C 3.289051 -1.329844 -2.299402
C 2.510553 -2.402943 -0.294797
C 3.301875 -2.560648 -2.956665
C 2.546595 -3.640014 -0.938218
C 2.932871 -3.720373 -2.276331
H 2.280551 -4.547975 -0.390283
H 2.960443 -4.687316 -2.784074
H 3.615759 -0.439441 -2.844725
H 3.619400 -2.616843 -4.000522
H 2.206871 -2.361251 0.755660
H -0.595791 -4.096130 -3.049330
H -0.655981 -5.439261 -1.876507
H -0.018128 -3.846196 -1.395983
H -2.998088 -5.428961 -2.795659
H -3.148614 -3.780028 -3.468491
H -4.144375 -4.260803 -2.065907
C -0.915111 -1.131245 -2.616472
O -1.921431 1.153735 0.390409
C -2.926221 1.897731 0.150657
C -2.692903 3.354500 0.169809
C -4.300990 1.357944 0.629987
F -5.342226 1.870248 -0.004933
F -4.368957 0.034534 0.505908
F -4.414942 1.648139 1.926050
C -3.732484 4.297649 0.254357
C -3.433932 5.653688 0.312307
C -1.358115 3.794370 0.124573
C -1.072804 5.151399 0.184071
C -2.107384 6.082667 0.279838
H -4.776579 3.990349 0.284279
H -4.243905 6.381533 0.385370
H -0.545763 3.068127 0.050858
H -0.034330 5.482797 0.158800
H -1.878972 7.149357 0.330654
H -1.634668 -1.933180 -2.816020
H -0.013867 -1.557521 -2.153793
H -0.618455 -0.721684 -3.593243
H -0.899443 0.882811 -1.905906
104

E-ts6 / electronic energy: -2690.79041777 a.u. / lowest freq: -240.67 cm-1

H	2.240828	-2.997069	-2.079195
C	-2.187431	-2.218709	-1.217195
C	-4.565438	-1.310961	0.397886
H	0.490588	-1.347486	-1.809210
C	2.508965	-1.946411	-1.953856
Si	-2.812451	-0.827751	-0.112922
C	-2.889430	0.843865	-1.000508
C	1.528450	-1.003508	-1.860418
H	3.542188	-1.677531	-2.175111
C	-1.815187	-0.543019	1.474436
C	1.773277	0.418464	-1.587830
H	-3.432750	-1.019543	2.821070
O	0.131769	-0.036533	0.228259
C	-2.418702	-0.620901	2.735327
C	-0.508546	-0.026551	1.421722
B	1.462003	0.420025	0.056569
C	-1.763405	-0.184008	3.889358
C	0.122002	0.513522	2.544843
H	-0.100642	2.446181	0.036404
H	-2.250824	-0.270157	4.861937
N	1.634275	1.731424	0.986821
H	2.285648	0.614274	2.622867
C	-0.511777	0.409827	3.784914
C	1.423756	1.253831	2.390101
H	2.600150	2.090702	0.917466
C	0.813672	2.884875	0.451280
O	2.938443	3.590818	-0.285359
C	1.759399	3.466820	-0.618942
H	-1.446843	2.913025	1.943422
H	-0.024026	0.820357	4.673330
N	1.306384	3.810553	-1.836018
H	-0.303427	3.056036	3.294468
H	1.470900	2.104687	3.075913
C	2.211045	4.464761	-2.765745
C	-0.031743	3.592851	-2.346474
C	-0.707566	3.574039	2.418501
H	-1.167445	4.717752	0.003071
C	0.369613	4.040707	1.422525
C	-0.299740	5.120317	0.546849
H	-1.244432	4.454361	2.801500
H	0.391559	5.575375	-0.176244

H	2.127956	3.983191	2.768499
C	1.540844	4.694391	2.168841
H	-0.665021	5.928675	1.196300
H	2.237945	5.192792	1.482749
H	1.146912	5.450894	2.864326
O	2.612615	-0.439919	0.593919
C	3.043824	-1.611597	0.341055
C	4.502743	-1.799757	0.228165
C	5.335903	-0.675322	0.343262
C	6.714648	-0.814439	0.243326
C	5.073533	-3.065663	0.010248
C	6.452437	-3.195487	-0.091855
C	7.274403	-2.072966	0.022129
H	4.447811	-3.952738	-0.092326
H	4.896816	0.307500	0.517748
H	7.356214	0.063263	0.339255
H	6.891244	-4.180047	-0.262298
H	8.357626	-2.181854	-0.061326
C	2.226555	-2.782946	0.955589
F	2.852229	-3.149300	2.073987
F	1.014745	-2.381381	1.291432
F	2.120090	-3.853186	0.179154
C	-4.798966	-2.624386	0.842173
C	-5.651013	-0.423241	0.372598
C	-6.921714	-0.827319	0.785077
C	-7.129974	-2.130559	1.232162
C	-6.064496	-3.031230	1.259854
H	-8.124431	-2.447820	1.554940
H	-6.222361	-4.056785	1.601810
H	-5.513223	0.601879	0.018918
H	-7.752889	-0.118847	0.754307
H	-3.979031	-3.349644	0.858379
C	-1.202276	-3.118914	-0.789227
C	-2.788787	-2.450207	-2.467246
C	-2.384898	-3.510517	-3.276676
C	-1.384098	-4.379930	-2.841565
C	-0.801366	-4.190070	-1.589827
H	-0.038855	-4.883757	-1.228439
H	-1.072996	-5.216155	-3.472188
H	-0.748035	-2.989307	0.192142
H	-3.602510	-1.806577	-2.813816
H	-2.864369	-3.668088	-4.245590

C -2.770608 1.005382 -2.389483
C -3.220747 1.980040 -0.239446
C -3.017329 2.236610 -2.999594
C -3.465866 3.213808 -0.842554
C -3.377707 3.340941 -2.229269
H -3.742903 4.074626 -0.229087
H -3.584043 4.301079 -2.707849
H -2.492615 0.156133 -3.018068
H -2.932036 2.331403 -4.084733
H -3.319519 1.894790 0.847566
H 0.030419 3.078759 -3.317850
H -0.552159 4.551488 -2.497444
H -0.636383 2.975799 -1.677591
H 1.752732 5.395362 -3.133461
H 2.413233 3.811140 -3.628980
H 3.154279 4.697040 -2.262451
H 0.932587 1.007633 -1.990580
C 3.124619 0.937374 -2.074998
H 3.956468 0.312008 -1.729170
H 3.341238 1.953033 -1.730239
H 3.156635 0.933770 -3.175504
104
E-ts7 / electronic energy: -2690.78188303 a.u. / lowest freq: -99.36 cm-1
H -0.689520 3.366694 -2.347572
C 2.276635 0.908885 -1.509614
C 4.339256 -0.596229 0.175020
H -2.806041 2.303411 -2.707603
C -0.884138 2.395745 -1.890522
Si 2.506337 -0.496259 -0.280460
C 2.043400 -2.220895 -0.903652
C -2.058512 1.767277 -2.110322
H -0.056897 1.908721 -1.374540
C 1.489617 -0.233205 1.297148
C -2.495672 0.454187 -1.549253
H 3.186311 -0.293762 2.625216
O -0.522861 -0.005873 0.046118
C -4.010830 0.332087 -1.772131
C 2.096104 -0.266253 2.557038
C 0.083361 -0.175428 1.254756
B -1.916174 0.279201 -0.024902
C 1.347141 -0.284178 3.736006
C -0.685020 -0.289798 2.421939

H	-1.286019	-2.239978	0.310407
H	1.846979	-0.301459	4.705904
N	-2.635283	-0.773068	0.996796
H	-2.651670	0.608932	2.564340
C	-0.037784	-0.330421	3.660034
C	-2.187025	-0.363436	2.357548
H	-3.659403	-0.688756	0.947971
C	-2.337752	-2.214757	0.608095
O	-4.495031	-2.330673	-0.317928
C	-3.300317	-2.496568	-0.551349
H	-0.398541	-3.303751	2.213319
H	-0.634961	-0.402643	4.573186
N	-2.836314	-2.911582	-1.745260
H	-1.448539	-2.651654	3.484298
H	-2.574902	-1.064049	3.101149
C	-3.796533	-3.293824	-2.766278
C	-1.445247	-3.054359	-2.132807
C	-1.379403	-3.409530	2.696761
H	-1.516483	-4.746873	0.294552
C	-2.529740	-3.362523	1.674683
C	-2.445816	-4.685418	0.882394
H	-1.394696	-4.384886	3.204735
H	-3.298879	-4.830029	0.204733
H	-4.037628	-2.395791	2.974130
C	-3.877342	-3.326156	2.409263
H	-2.448021	-5.528638	1.587437
H	-4.720207	-3.444185	1.718627
H	-3.906625	-4.149356	3.139108
O	-2.225847	1.687931	0.636424
C	-1.860183	2.849533	0.277722
C	-0.614056	3.480149	0.757944
C	0.000841	2.938638	1.894882
C	1.137283	3.531352	2.433944
C	-0.086263	4.653930	0.186906
C	1.048223	5.239964	0.729102
C	1.668598	4.676904	1.847469
H	-0.544826	5.100590	-0.694239
H	-0.431935	2.070089	2.382630
H	1.599003	3.096543	3.321933
H	1.456689	6.144144	0.274304
H	2.561599	5.143004	2.268995
C	-3.039210	3.814580	-0.040951

F	-2.777341	4.647780	-1.041756
F	-4.140242	3.145767	-0.336157
F	-3.274504	4.535528	1.052348
C	5.284779	0.353472	-0.240489
C	4.798937	-1.692998	0.926344
C	6.142998	-1.825046	1.267266
C	7.064721	-0.864069	0.850322
C	6.634025	0.222723	0.092641
H	8.121086	-0.969448	1.108313
H	7.352529	0.971805	-0.248117
H	4.097066	-2.468831	1.246457
H	6.475270	-2.686212	1.851706
H	4.974380	1.208101	-0.846691
C	2.552537	2.215916	-1.068624
C	1.907519	0.734732	-2.851474
C	1.847310	1.817435	-3.729637
C	2.157256	3.100234	-3.280645
C	2.501378	3.299904	-1.944152
H	2.732332	4.303285	-1.580203
H	2.124651	3.945078	-3.972675
H	2.817194	2.396624	-0.021635
H	1.652774	-0.257767	-3.229013
H	1.563718	1.656525	-4.772201
C	2.378768	-2.683646	-2.186931
C	1.510006	-3.152710	0.002687
C	2.158430	-4.010173	-2.558349
C	1.312097	-4.486794	-0.352894
C	1.627588	-4.916628	-1.640752
H	0.919882	-5.194569	0.381497
H	1.473540	-5.960113	-1.925205
H	2.847631	-2.010871	-2.909216
H	2.424721	-4.342835	-3.564351
H	1.268532	-2.837296	1.020992
H	-1.317093	-2.658263	-3.151292
H	-1.140261	-4.112383	-2.136793
H	-0.769018	-2.496126	-1.477958
H	-3.829235	-2.540344	-3.569633
H	-4.792437	-3.382740	-2.321034
H	-3.502331	-4.259668	-3.203319
H	-4.248950	0.518710	-2.830627
H	-4.552466	1.084547	-1.184127
H	-4.430881	-0.640992	-1.512499

H -1.963177 -0.326748 -2.124548
104
E-ts8 / electronic energy: -2690.78124301 a.u. / lowest freq: -222.25 cm-1
H 4.067859 -2.107887 -2.720124
C -2.502311 -1.563421 -1.231662
C -4.880833 -0.982990 0.655764
H 3.235916 0.206001 -2.577112
C 3.021290 -1.904216 -2.480971
Si -3.168873 -0.418809 0.110212
C -3.291885 1.379684 -0.463818
C 2.548343 -0.632866 -2.409580
H 2.318580 -2.737850 -2.546281
C -1.991921 -0.425037 1.590442
C 1.188033 -0.294706 -1.979618
H -3.431210 -0.752150 3.162941
O -0.253419 -0.097540 0.038530
C -2.383824 -0.546489 2.926086
C -0.635557 -0.172702 1.335077
B 1.103347 -0.150053 -0.322309
C -1.461330 -0.401328 3.966667
C 0.296065 0.027857 2.356471
H 0.319579 2.325878 0.176863
H -1.784582 -0.506425 5.003884
N 1.851266 0.949509 0.635695
H 2.379512 -0.475792 2.071770
C -0.134742 -0.097687 3.680184
C 1.716548 0.397805 2.022024
H 2.855129 0.986654 0.407575
C 1.399063 2.367041 0.365631
O 3.339265 2.278043 -0.996203
C 2.204536 2.749460 -0.896563
H -0.321400 3.059355 2.359141
H 0.580337 0.052750 4.493748
N 1.703947 3.607693 -1.801328
H 0.978860 2.448324 3.394465
H 2.118110 1.111790 2.742517
C 2.567079 4.060125 -2.878708
C 0.323671 4.038457 -1.911245
C 0.708094 3.247643 2.698369
H 0.306744 4.940315 0.670609
C 1.669477 3.428726 1.505162
C 1.361577 4.840108 0.964707

H	0.692914	4.175548	3.288445
H	1.997171	5.133262	0.119424
H	3.496325	2.441886	2.310511
C	3.139443	3.419992	1.954994
H	1.542197	5.567112	1.768992
H	3.810221	3.730932	1.141808
H	3.269408	4.129865	2.785421
C	-5.388554	-2.248309	0.323974
C	-5.686716	-0.129655	1.429744
C	-6.947047	-0.531727	1.868594
C	-7.430968	-1.796605	1.532645
C	-6.651342	-2.653122	0.757331
H	-8.420400	-2.112382	1.872049
H	-7.029302	-3.641245	0.484442
H	-5.328913	0.871632	1.690275
H	-7.558115	0.145296	2.470184
H	-4.794903	-2.931023	-0.290050
C	-2.048401	-2.841344	-0.865809
C	-2.412043	-1.196399	-2.581608
C	-1.889881	-2.072752	-3.533981
C	-1.448502	-3.338771	-3.151733
C	-1.531369	-3.723124	-1.813083
H	-1.185044	-4.711906	-1.504635
H	-1.045571	-4.029120	-3.896767
H	-2.088038	-3.155991	0.181886
H	-2.739577	-0.204941	-2.904105
H	-1.829670	-1.765898	-4.581117
C	-4.084666	1.728934	-1.570183
C	-2.659089	2.418328	0.238348
C	-4.214671	3.056201	-1.978102
C	-2.800996	3.750423	-0.152828
C	-3.570338	4.071357	-1.270663
H	-2.316475	4.544253	0.422112
H	-3.684389	5.113097	-1.579387
H	-4.626010	0.953482	-2.120624
H	-4.833987	3.301574	-2.844051
H	-2.062226	2.185421	1.125097
H	-0.044898	3.814486	-2.924036
H	0.236790	5.122703	-1.744441
H	-0.329644	3.522213	-1.203360
H	2.385571	5.128852	-3.061275
H	2.354459	3.507965	-3.810301

H 3.616915 3.906343 -2.610072
C 0.507675 0.816377 -2.783705
O 1.703918 -1.503400 0.088216
C 2.778838 -2.141449 -0.072238
C 2.508912 -3.669009 -0.131295
C 4.115917 -1.680225 0.391647
C 4.658049 -0.440713 0.020491
C 4.811674 -2.469355 1.325375
C 5.996309 -2.003391 1.890977
C 6.509394 -0.759863 1.533183
C 5.837023 0.019689 0.591159
H 4.186420 0.169784 -0.747899
H 6.239138 0.985438 0.279935
H 4.429865 -3.437760 1.646387
H 6.519140 -2.625361 2.619674
H 7.440547 -0.402083 1.976893
F 1.419978 -3.931435 -0.832594
F 2.303407 -4.109266 1.112429
F 3.528646 -4.332876 -0.652018
H 0.128103 0.402126 -3.728848
H 1.203963 1.622000 -3.043434
H -0.351845 1.236242 -2.243119
H 0.550887 -1.191939 -2.058616

104

E-ts9 / electronic energy: -2690.78316265 a.u. / lowest freq: -224.71 cm-1

H -4.274044 -2.012006 2.654966
C 2.825677 -1.750789 1.193302
C 4.867720 -0.737649 -0.818303
H -3.319548 0.257144 2.542336
C -3.212315 -1.861960 2.444616
Si 3.131584 -0.457588 -0.141187
C 3.019645 1.309442 0.532411
C -2.672639 -0.616083 2.388939
H -2.558567 -2.731842 2.537414
C 1.913161 -0.528590 -1.582942
C -1.288975 -0.349650 1.986692
H 3.342315 -0.864546 -3.162726
O 0.185246 -0.195084 -0.018364
C 2.297252 -0.652697 -2.921281
C 0.563798 -0.252494 -1.319399
B -1.177805 -0.185726 0.331960
C 1.372058 -0.494402 -3.957134

C	-0.363042	-0.015593	-2.337019
H	-0.275104	2.238501	-0.057415
H	1.687499	-0.606423	-4.995998
N	-1.865669	0.961519	-0.605302
H	-2.476318	-0.399359	-2.068750
C	0.056386	-0.155426	-3.662940
C	-1.760580	0.429975	-2.000698
H	-2.867140	1.053876	-0.377518
C	-1.340968	2.346416	-0.292441
O	-3.339906	2.325018	0.986050
C	-2.181447	2.747036	0.942149
H	0.487652	2.885687	-2.206719
H	-0.657793	0.020047	-4.472301
N	-1.680577	3.563549	1.883131
H	-0.831808	2.459203	-3.313262
H	-2.112252	1.181408	-2.709507
C	-2.563443	4.039968	2.933661
C	-0.285584	3.920514	2.055829
C	-0.499150	3.199158	-2.579125
H	-0.037213	4.817039	-0.495076
C	-1.485385	3.444753	-1.418242
C	-1.081991	4.814885	-0.837159
H	-0.359430	4.138123	-3.134084
H	-1.729475	5.146695	-0.015287
H	-3.338606	2.635279	-2.336872
C	-2.931456	3.567717	-1.920810
H	-1.162419	5.567538	-1.634196
H	-3.612171	3.891447	-1.120702
H	-2.974307	4.320764	-2.721592
C	5.249125	-2.034198	-1.206302
C	5.803349	0.297024	-0.964594
C	7.075000	0.048694	-1.483707
C	7.431579	-1.242395	-1.868938
C	6.515303	-2.285834	-1.729888
H	8.426425	-1.437597	-2.276206
H	6.791557	-3.300922	-2.024977
H	5.543099	1.316226	-0.665046
H	7.792368	0.866642	-1.584201
H	4.546108	-2.865906	-1.094710
C	1.726710	-2.623184	1.190101
C	3.770620	-1.886264	2.225439
C	3.609729	-2.835452	3.233827

C	2.505035	-3.686298	3.217667
C	1.568235	-3.583800	2.189860
H	0.713938	-4.263625	2.161180
H	2.381577	-4.439395	3.999616
H	0.981607	-2.560123	0.394140
H	4.659759	-1.247668	2.239906
H	4.356300	-2.919544	4.026992
C	3.151003	1.619112	1.894418
C	2.890703	2.378492	-0.372396
C	3.175632	2.943734	2.335668
C	2.915806	3.704363	0.062195
C	3.067397	3.989426	1.419788
H	2.833680	4.516541	-0.664657
H	3.099806	5.026270	1.763109
H	3.240939	0.815642	2.630544
H	3.290212	3.158669	3.400786
H	2.789304	2.176458	-1.443370
H	0.031744	3.649714	3.074495
H	-0.139972	5.002991	1.924007
H	0.364934	3.393361	1.353725
H	-2.356858	5.103027	3.123770
H	-2.395324	3.481152	3.870022
H	-3.608148	3.917826	2.631133
C	-0.554140	0.709086	2.813609
O	-1.833751	-1.503773	-0.104022
C	-2.923160	-2.119103	0.057523
C	-2.675336	-3.649980	0.124245
C	-4.245823	-1.632510	-0.417679
C	-4.746579	-0.367446	-0.074750
C	-4.970016	-2.422722	-1.327776
C	-6.143179	-1.934487	-1.898807
C	-6.615039	-0.667022	-1.569933
C	-5.913254	0.115272	-0.651362
H	-4.255536	0.244677	0.680253
H	-6.283211	1.100930	-0.363147
H	-4.620146	-3.410262	-1.626284
H	-6.689638	-2.557941	-2.608605
H	-7.537249	-0.291675	-2.017772
F	-1.587226	-3.916786	0.831056
F	-2.471296	-4.100747	-1.114388
F	-3.699964	-4.301216	0.649147
H	-0.196643	0.256307	3.749692

H -1.209629 1.543302 3.088971
H 0.326850 1.095219 2.282739
H -0.709428 -1.284279 2.061665
104
E-ts10 / electronic energy: -2690.77978583 a.u. / lowest freq: -128.70 cm-1
H 2.066154 -2.926304 -1.920938
C -1.768149 -2.148436 -1.309804
C -4.313322 -1.745491 0.364823
H 3.362305 -1.001658 -2.473414
C 1.736349 -1.947809 -1.570396
Si -2.670860 -0.965404 -0.158246
C -3.132009 0.697640 -0.930205
C 2.435998 -0.841462 -1.907760
H 0.769394 -1.886830 -1.069657
C -1.662687 -0.566799 1.396175
C 2.160179 0.571200 -1.511599
H -3.175146 -1.255543 2.770205
O 0.204370 0.154264 0.103111
C -2.214019 -0.746225 2.669399
C -0.410764 0.073380 1.317274
B 1.553012 0.597906 0.014645
C -1.579090 -0.276532 3.820855
C 0.194407 0.633336 2.449773
H -0.258800 2.477637 0.155961
H -2.029238 -0.438622 4.801684
N 1.629036 1.952227 0.926823
H 2.336470 0.915865 2.600435
C -0.396658 0.438631 3.700949
C 1.434762 1.479187 2.330252
H 2.555510 2.393062 0.858875
C 0.660090 3.006253 0.422083
O 2.496250 4.075850 -0.588036
C 1.377261 3.609735 -0.792943
H -1.595941 3.142598 1.982383
H 0.078008 0.868014 4.587483
N 0.789678 3.615229 -2.004356
H -0.374399 3.185434 3.266074
H 1.385567 2.338373 3.003644
C 1.448361 4.313492 -3.094667
C -0.487791 3.017055 -2.347180
C -0.794487 3.749652 2.426353
H -1.307760 4.768184 -0.070710

C	0.243089	4.189065	1.377255
C	-0.469859	5.223082	0.480022
H	-1.263872	4.645553	2.858913
H	0.209046	5.697159	-0.242773
H	2.016726	4.209439	2.702764
C	1.424733	4.885087	2.067047
H	-0.882717	6.024527	1.109035
H	2.109295	5.336368	1.339205
H	1.039888	5.680764	2.722840
O	2.535191	-0.349242	0.783028
C	2.961357	-1.509235	0.491569
C	4.405012	-1.707792	0.264355
C	5.272443	-0.662511	0.620320
C	6.643423	-0.802733	0.444837
C	4.931410	-2.894530	-0.272664
C	6.302476	-3.020965	-0.457837
C	7.159277	-1.979364	-0.098576
H	4.271969	-3.709451	-0.568555
H	4.864438	0.251031	1.054154
H	7.313946	0.007431	0.736677
H	6.706936	-3.939071	-0.887263
H	8.236280	-2.087620	-0.242029
C	2.169659	-2.682542	1.141941
F	2.698743	-2.838292	2.355711
F	0.890095	-2.399027	1.287127
F	2.274117	-3.836833	0.496134
C	-4.660309	-3.076414	0.087847
C	-5.253919	-0.952967	1.047939
C	-6.478198	-1.473944	1.459965
C	-6.796216	-2.804550	1.185856
C	-5.887678	-3.602575	0.494432
H	-7.756163	-3.216369	1.506184
H	-6.133964	-4.642388	0.266954
H	-5.033364	0.097509	1.260621
H	-7.189766	-0.838067	1.991787
H	-3.972041	-3.720880	-0.464202
C	-1.391714	-3.406258	-0.805836
C	-1.472110	-1.864642	-2.650962
C	-0.851651	-2.810349	-3.468261
C	-0.509497	-4.060837	-2.955403
C	-0.771618	-4.354993	-1.617390
H	-0.491954	-5.326255	-1.202905

H -0.031616 -4.804439 -3.597632
H -1.582298 -3.653018 0.242916
H -1.716560 -0.887019 -3.072491
H -0.637486 -2.570458 -4.512357
C -3.696545 0.805828 -2.212293
C -3.098580 1.855067 -0.135699
C -4.176809 2.025202 -2.690026
C -3.600082 3.072086 -0.597044
C -4.133421 3.161611 -1.881527
H -3.582863 3.950544 0.052898
H -4.529116 4.111249 -2.249173
H -3.792350 -0.078867 -2.847743
H -4.611005 2.083730 -3.690755
H -2.693452 1.796368 0.877837
H -0.396175 2.527964 -3.328187
H -1.279708 3.778964 -2.418080
H -0.799935 2.253533 -1.627878
H 0.749988 5.032742 -3.549227
H 1.769675 3.600059 -3.870074
H 2.324990 4.846063 -2.713503
H 1.326551 0.928223 -2.144392
C 3.434659 1.380901 -1.799565
H 3.373769 2.435861 -1.520465
H 3.673974 1.337973 -2.873431
H 4.293124 0.949738 -1.264433
104
E-ts11 / electronic energy: -2690.78282437 a.u. / lowest freq: -160.86 cm-1
H 0.536725 3.171964 -2.366682
C 3.023382 0.326634 -1.164894
C 4.008510 -2.282565 0.010493
H -1.703319 2.503139 -2.904161
C 0.101582 2.304936 -1.865413
Si 2.459540 -1.255802 -0.315781
C 1.199308 -2.245111 -1.318499
C -1.149693 1.894267 -2.179197
H 0.761814 1.716532 -1.226603
C 1.635814 -0.827700 1.333737
C -1.892818 0.740652 -1.589347
H 3.238444 -1.466330 2.629404
O -0.221711 -0.010556 0.121801
C -3.370355 0.782701 -2.006336
C 2.223961 -1.062133 2.580275

C	0.323860	-0.322729	1.320334
B	-1.497864	0.598537	-0.000413
C	1.537842	-0.802224	3.769762
C	-0.417600	-0.162843	2.493244
H	-2.154639	-1.846934	-0.075104
H	2.023502	-0.972408	4.732260
N	-2.479455	-0.100196	1.074486
H	-2.074837	1.216933	2.636018
C	0.214984	-0.378516	3.720205
C	-1.886097	0.156091	2.426320
H	-3.400420	0.378659	1.084123
C	-2.897881	-1.503865	0.655900
O	-4.974630	-0.366651	0.556404
C	-4.297894	-1.251897	0.036966
H	-0.849169	-2.928289	1.749644
H	-0.349267	-0.241116	4.646960
N	-4.763136	-2.005169	-0.975642
H	-1.477312	-2.274209	3.277667
H	-2.436505	-0.414935	3.178678
C	-6.131695	-1.776216	-1.407713
C	-3.961919	-2.821488	-1.866551
C	-1.699242	-2.949966	2.447649
H	-2.624063	-4.222182	0.249906
C	-3.031392	-2.650438	1.736282
C	-3.391607	-3.952461	0.990927
H	-1.748977	-3.960601	2.877929
H	-4.369571	-3.905624	0.497777
H	-4.067076	-1.412039	3.262571
C	-4.147820	-2.384718	2.758698
H	-3.441418	-4.768749	1.725341
H	-5.144099	-2.421472	2.296110
H	-4.115880	-3.163183	3.535545
O	-1.449688	2.067547	0.571062
C	-0.965907	3.145466	0.113103
C	0.278244	3.714742	0.653442
C	0.888594	3.067859	1.739435
C	2.013524	3.620422	2.340136
C	0.822401	4.920234	0.170480
C	1.947253	5.463233	0.774055
C	2.543421	4.817442	1.859912
H	0.373369	5.436528	-0.676976
H	0.466769	2.141185	2.126345

H	2.473982	3.115047	3.190882
H	2.364199	6.397628	0.394482
H	3.425281	5.253456	2.333953
C	-2.031266	4.142277	-0.433173
F	-1.625170	4.825685	-1.498353
F	-3.145953	3.505375	-0.751074
F	-2.312818	5.009897	0.535113
C	5.122234	-1.649761	0.591603
C	4.124716	-3.641287	-0.318963
C	5.301952	-4.346239	-0.064320
C	6.387851	-3.704047	0.527103
C	6.297234	-2.350618	0.854117
H	7.310341	-4.254660	0.725636
H	7.149580	-1.838587	1.306696
H	3.290977	-4.164180	-0.794170
H	5.372011	-5.402892	-0.333153
H	5.079951	-0.582823	0.833141
C	3.197768	1.499664	-0.415138
C	3.375049	0.357450	-2.524487
C	3.843775	1.527363	-3.120400
C	3.995926	2.687209	-2.359980
C	3.682708	2.668630	-1.001847
H	3.816216	3.566556	-0.395158
H	4.373419	3.601150	-2.824514
H	2.949502	1.505758	0.649328
H	3.296654	-0.547974	-3.132876
H	4.103668	1.530734	-4.181559
C	0.707603	-3.450778	-0.789421
C	0.689498	-1.818911	-2.553894
C	-0.230604	-4.217650	-1.481893
C	-0.249291	-2.579764	-3.251595
C	-0.704418	-3.786671	-2.721538
H	-0.623283	-2.229040	-4.216689
H	-1.428431	-4.391108	-3.273273
H	1.067386	-3.809449	0.180334
H	-0.583552	-5.160820	-1.057660
H	1.020468	-0.870417	-2.983778
H	-4.044560	-2.430941	-2.894171
H	-4.311986	-3.864605	-1.865428
H	-2.904856	-2.811825	-1.589679
H	-6.179262	-0.966940	-2.156368
H	-6.755247	-1.493633	-0.552637

H -6.522792 -2.698312 -1.857644
H -3.763173 -0.219166 -2.196873
H -3.497185 1.343253 -2.944067
H -4.018316 1.254747 -1.256659
H -1.416425 -0.163103 -2.016561
104
E-ts12 / electronic energy: -2690.77814775 a.u. / lowest freq: -182.83 cm-1
H 1.616167 -2.967541 -1.878310
C -2.075691 -2.334455 -1.026663
C -4.570532 -1.095939 0.137016
H 2.946692 -1.121331 -2.590430
C 1.414801 -1.980872 -1.457425
Si -2.747156 -0.757810 -0.239691
C -2.662538 0.825565 -1.271697
C 2.127346 -0.907805 -1.891835
H 0.509733 -1.866817 -0.860414
C -1.849326 -0.403511 1.389913
C 2.043254 0.502031 -1.419346
H -3.525864 -0.869063 2.664601
O 0.151392 0.103914 0.211636
C -2.497431 -0.502019 2.626317
C -0.528053 0.080642 1.388712
B 1.521160 0.487137 0.138657
C -1.866976 -0.134305 3.816725
C 0.078221 0.555233 2.555094
H 0.014823 2.520481 0.055872
H -2.386725 -0.240939 4.770349
N 1.681124 1.777270 1.105427
H 2.232253 0.629544 2.757807
C -0.593572 0.416633 3.771354
C 1.392922 1.282513 2.486145
H 2.650563 2.127790 1.100703
C 0.889458 2.950867 0.554103
O 3.028762 3.781347 0.032831
C 1.897148 3.594988 -0.414366
H -1.487677 2.901737 1.855831
H -0.117758 0.775232 4.688304
N 1.546799 3.918156 -1.671131
H -0.459536 3.019239 3.299774
H 1.404238 2.124725 3.184297
C 2.495653 4.640660 -2.500567
C 0.271628 3.649077 -2.302977

C	-0.800969	3.558446	2.410228
H	-1.077949	4.739280	-0.014471
C	0.346613	4.069169	1.520822
C	-0.272267	5.152158	0.611950
H	-1.381658	4.419404	2.772803
H	0.466036	5.640615	-0.039655
H	1.993738	4.021507	3.003156
C	1.432463	4.733027	2.380065
H	-0.713564	5.937566	1.242000
H	2.165305	5.276125	1.770075
H	0.956168	5.453013	3.062676
O	2.482927	-0.534449	0.808280
C	2.790075	-1.708873	0.410165
C	4.194078	-1.994275	0.037319
C	5.170057	-1.050091	0.387046
C	6.507555	-1.287794	0.090687
C	4.573310	-3.177668	-0.615490
C	5.910293	-3.401461	-0.920374
C	6.878406	-2.460002	-0.567016
H	3.825731	-3.916176	-0.905009
H	4.875641	-0.137498	0.906660
H	7.263968	-0.555266	0.377486
H	6.199159	-4.317919	-1.437934
H	7.928784	-2.643788	-0.802213
C	2.032462	-2.840541	1.163038
F	2.731353	-3.070373	2.274560
F	0.820472	-2.457510	1.520441
F	1.941247	-3.980089	0.491897
C	-4.927054	-2.290180	0.789090
C	-5.602371	-0.216969	-0.225154
C	-6.936308	-0.511571	0.061031
C	-7.265427	-1.693340	0.721176
C	-6.256009	-2.584941	1.085514
H	-8.309441	-1.923839	0.945881
H	-6.505738	-3.518015	1.595955
H	-5.371568	0.714874	-0.747556
H	-7.721813	0.186917	-0.236606
H	-4.155155	-3.013270	1.068995
C	-1.539268	-3.320307	-0.182095
C	-2.191668	-2.640200	-2.392740
C	-1.742518	-3.858879	-2.900411
C	-1.191778	-4.813985	-2.045818

C	-1.102268	-4.547082	-0.680944
H	-0.688597	-5.294024	0.000031
H	-0.846794	-5.771604	-2.443072
H	-1.450250	-3.126462	0.889242
H	-2.658240	-1.933140	-3.082067
H	-1.839517	-4.070194	-3.967878
C	-3.059293	2.012200	-0.626127
C	-2.381559	0.898792	-2.644015
C	-3.221741	3.205616	-1.328684
C	-2.542857	2.090632	-3.353928
C	-2.979891	3.242220	-2.702399
H	-2.336272	2.114487	-4.426625
H	-3.126159	4.169888	-3.260474
H	-3.279865	1.998902	0.446284
H	-3.556603	4.104623	-0.805670
H	-2.040519	0.013954	-3.184448
H	0.443922	3.179153	-3.283386
H	-0.288507	4.583047	-2.465600
H	-0.351036	2.972204	-1.712586
H	2.037115	5.574459	-2.861187
H	2.781353	4.033842	-3.374084
H	3.391009	4.876420	-1.917391
H	1.211313	0.983741	-1.967975
C	3.384496	1.174309	-1.757924
H	3.550003	2.132416	-1.258708
H	3.469935	1.340557	-2.842836
H	4.222542	0.525788	-1.467039

Chapter Three

Aminophenol Promoted α-, Z-, and Enantioselective Allyl Additions of Z-Allylborons to Aldehydes

3.1. Introduction

Allyl additions to aldehydes has been an extensively studied and well developed field in organic synthesis, due in part to the inherent value of enantioenriched homoallylic alcohols.[1] While this field has made tremendous strides in the past few decades, most of the work that has been carried out has revolved around simple allyl and crotyl addition of aldehydes, there are far fewer reports on additions involving more complex, substituted allylboron reagents.[2] Reports on α-selective additions of these allylboron reagents are scant, with only a handful of examples reported in the literature.[3] Our interest in this

(1) For a recent review on enantioselective synthesis of allyl groups to carbonyl compounds and imines, see: Yus, M.; González-Gómez, J. C.; Foubelo, F. *Chem. Rev.* **2011**, *111*, 7774–7854. For a recent review on diastereoselective methods for these transformations see: Yus, N.; González-Gómez, J. C.; Foubelo, F. *Chem. Rev.* **2013**, *113*, 5595–5698.

(2) For enantioselective examples utilizing terminal and/or internally-substituted allylboron reagents, see: (a) Denmark, S. E.; Wilson, T. W. *Angew. Chem., Int. Ed.* **2012**, *51*, 3236–3239. (b) Zbieg, J. R.; Yamaguchi, E.; McInturff, E. L.; Krische, M. J. *Science* **2012**, *336*, 324–327. (c) Miura, T.; Nishida, Y.; Morimoto, M.; Murakami, M. *J. Am. Chem. Soc.* **2013**, *135*, 11497–11500. (d) Chen, J. L-Y.; Scott, H. K.; Hesse, M. J.; Willis, C. L.; Aggarwal, V. K. *J. Am. Chem. Soc.* **2013**, *135*, 5316–5319. (e) Incerti-Pradillos, C. A.; Kabeshov, M. A.; Malkov, A. V. *Angew. Chem., Int. Ed.* **2013**, *52*, 5338–5341. (f) Feng, J.; Garza, V. J.; Krische, M. J. *J. Am. Chem. Soc.* **2014**, *136*, 8911–8914. For diastereoselective variants, see: (g) Loh, T.-P.; Hu, Q.-Y.; Chok, Y.-K.; Tan, K.-T. *Tetrahedron Lett.* **2001**, *42*, 9277–9280. (h) Nokami, J.; Nomiyama, K.; Shafi, S. M.; Kataoka, K. *Org. Lett.* **2004**, *6*, 1261–1264. (i) Schmidtmann, E. S.; Oestreich, M. *Angew. Chem., Int. Ed.* **2009**, *48*, 4634–4638. (j) Kliman, L. T.; Mlynarski, S. N.; Ferris, G. E.; Morken, J. P. *Angew. Chem., Int. Ed.* **2012**, *51*, 521–524. (k) Chen, M.; Roush, W. R. *Org. Lett.* **2013**, *15*, 1662–1665. (l) Yamamoto, E.; Takenouchi, Y.; Ozaki, T.; Miya, T.; Ito, H. *J. Am. Chem. Soc.* **2014**, *136*, 16515–16521. (m) Horino, Y.; Aimono, A.; Minoshima, N.; Abe, H. *Tetrahedron Lett.* **2016**, *57*, 3561–3564.

(3) (a) Kobayashi, S.; Endo, T.; Schneider, U.; Ueno, M. *Chem. Commun.*, **2010**, *46,* 1260–1262. (b) Kobayashi, S.; Endo, T.; Ueno, M. *Angew. Chem., Int. Ed.* **2011**, *50*, 12262–12265. (c) Kobayashi, S.; Endo, T.; Yoshino, T.; Schneider, U.; Ueno, M. *Chem. Asian. J.* **2013**, *8*, 2033–2045.

transformation also stems from the fact that while our aminophenol ligand has traditionally been a robust and broadly applicable system to catalyze enantioselective allyl additions to a variety of substrates (such as imines, methyl ketones and trifluoromethyl ketones), the analogous allyl additions to aldehydes have furnished products with low enantioselectivity.[4] The studies carried out in the previous chapter have led to insights which suggest that perhaps using *Z*-substituted allylboron reagents might enable these additions to occur enantioselectivity. Concurrently, recent work in molybdenum-catalyzed olefin metathesis in our laboratory has enabled the facile synthesis of *Z*-trifluoromethyl- and *Z*-chloro-substituted allylboron reagents in a single step from commercially available materials.[5] The studies herein have led to the first broadly applicable methods for the synthesis of enantioenriched *Z*-trifluoromethyl- and *Z*-chloro-substituted homoallylic alcohols.[6]

(4) (a) Silverio, D. L.; Torker, S.; Pilyugina, T.; Vieira, E. M.; Snapper, M. L., Haeffner, F.; Hoveyda, A. H. *Nature* **2013**, *494*, 216–221. (b) Wu, H.; Haeffner, F.; Hoveyda, A. H. *J. Am. Chem. Soc.* **2014**, *136*, 3780–3783. (c) van der Mei, F. W.; Miyamoto, H.; Silverio, D. L.; Hoveyda, A. H. *Angew. Chem., Int. Ed.* **2016**, *55*, 4701–4706. (d) Lee, K.; Silverio, D. L.; Torker, S.; Haeffner, F.; Robbins, D. W.; van der Mei, F. W.; Hoveyda, A. H. *Nat. Chem.* **2016**, *8*, 768–777. (e) Robbins, D. W.; Lee, K.; Silverio, D. L.; Volkov, A.; Torker, S.; Hoveyda, A. H. *Angew. Chem., Int. Ed.* **2016**, *55*, 9610–9614. (f) Mszar, N. W.; Mikus, M. S.; Torker, S.; Haeffner, F.; Hoveyda, A. H. *Angew. Chem., Int. Ed.* **2017**, *56*, 8736–8741. (g) van der Mei, F. W.; Qin, C.; Morrison, R. J.; Hoveyda, A. H.; *J. Am. Chem. Soc.* **2017**, *139*, 9053–9065.

(5) (a) Koh, M. J.; Nguyen, T. T.; Zhang, H.; Schrock, R. R.; Hoveyda, A. H. *Nature* **2016**, *531*, 459–465. (b) Koh, M. J.; Nguyen, T. T.; Lam, J. K.; Torker, S.; Hyvl, J.; Schrock, R. R.; Hoveyda, A. H. *Nature* **2017**, *542*, 80–85.

(6) There has been one seminal report on the synthesis of enantioenriched *Z*-nitrile-substituted homoallylic alcohols, see: Otsuka, Y.; Takada, H.; Yasuda, S.; Kumagai, N.; Shibasaki, M. *Chem. Asian. J.* **2013**, *8*, 354–358.

3.2. Background

3.2.1 State-of-the-Art in Trifluoromethyl-substituted Allyl Additions to Aldehydes

While trifluoromethyl-allyl additions to aldehydes are scarcely known there have been a few reports on the transformation. Of the few reports on additions of trifluoromethyl substituted allyl reagents, the majority pertained to methods that furnish the branched isomer. The Loh group, starting in 1997, has published several papers on the use of trifluoro-4-bromobut-2-ene and stoichiometric indium and tin for these types of additions.[7]

Scheme 3.1. Loh's Stoichiometric Indium Mediated CF_3-Allyl Addition

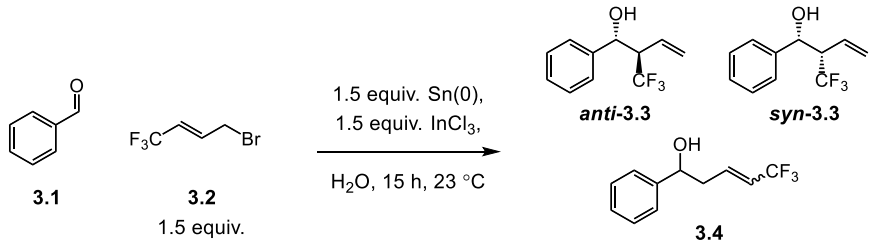

3.1 **3.2** 1.5 equiv. **3.4**

87% yield (γ),
91:9 γ:α, 95:5 *anti*:*syn*

Under the conditions reported by Loh and co-workers, an in situ generated trifluoromethyl-substituted allyl indium reagent, reacts with aldehydes to generate crotyl addition products (i.e. **3.3**, Scheme 3.1) with high regio- and diastereoselectivity. In some instances, they observe formation of the linear product (**3.4**) as a mixture of *E*:*Z* isomers. Additionally, the products are obtained as a racemic mixture, as the Loh group have not been able to develop an enantioselective variant of their protocol. The following report on

(7) (a) Loh, T.-P.; Li, X.-R. *Tetrahedron Lett.* **1997**, *38*, 869–872. (b) Loh, T.-P.; Li, X.-R. *Angew. Chem., Int. Ed.* **1997**, *36*, 980–982. (c) Loh, T.-P.; Li, X.-R. *Eur. J. Org. Chem.* **1999**, 1893–1899.

additions of CF_3-allyl groups to aldehydes, disclosed in 2011 by the Krische group (shown in Scheme 3.2), was the first enantioselective variant of this transformation.[8]

Scheme 3.2. Krische's Ir-Catalyzed Enantioselective CF_3-Allyl Addition to Aldehydes

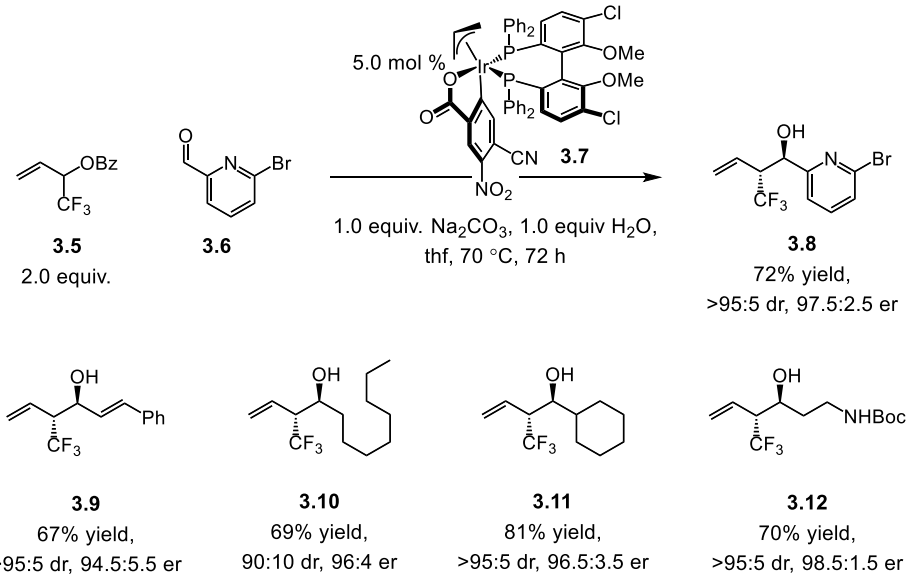

Krische *et al.* were able to utilize *racemic* trifluoromethyl-substituted allyl benzoate **3.5** as a trifluoromethyl-allyl source and carry out highly enantioselective and diastereoselective additions to a variety of aldehydes in the presence of their iridium-phosphine complex **3.7**. It was also reported that they can carry out the same transformation with the analogous alcohols (instead of aldehydes) through their transfer hydrogenation chemistry, however they do observe slightly diminished yields in some cases. In all reported examples, they form the *anti* diastereomer of the product with high (90:10 dr, **3.10**) to exceptional diastereoselectivities, however exceedingly long reaction times are required (72 h). In 2014, the Ramachandran group explored similar additions with a pinene-derived allylboron (Scheme 3.3).[9]

(8) Gao, X.; Zhang, Y. J.; Krische, M. J. *Angew. Chem., Int. Ed.* **2011**, *50*, 4173–4175.
(9) Li, G.; Gagare, P. D.; Ramachandran, P. V. *Tetrahedron* Lett. **2014**, 55, 1896–1898.

Scheme 3.3. Ramachandran's Enantioselective CF_3-Allyl Addition to Aldehydes

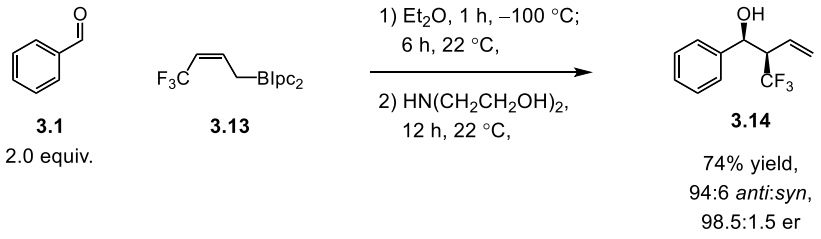

3.1
2.0 equiv.

3.13

3.14
74% yield,
94:6 *anti*:*syn*,
98.5:1.5 er

The Ramachandran group were able to generate **3.13** through hydroboration of the corresponding allene, which reacted with aldehydes to access the crotyl addition products (**3.14**) with high diastereoselectivities and enantioselectivities. Ramachandran's method generates the *syn* diastereomer of the product, making it complementary to the protocol developed by Krische *et al.* To date, there have been no protocols developed that can access the linear regioisomer of these products enantioselectively through an allyl addition. However, Loh *et al*. have reported an alternative strategy to access these products, as shown in Scheme 3.4.[10]

Scheme 3.4. Loh's Oxonia Cope Rearrangement

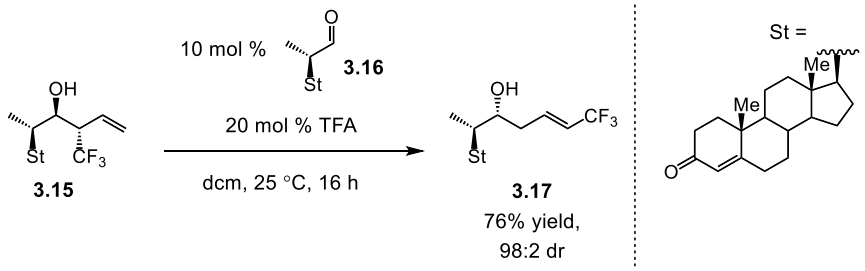

3.15

3.17
76% yield,
98:2 dr

Therein Loh and co-workers reported that, by the addition of a catalytic amount of aldehyde (**3.16**) and trifluoroacetic acid, the branched isomer of the product (**3.15**) can be isomerized to the corresponding linear regioisomer (**3.17**) through an oxonia-Cope rearrangement. While this provides access to the *E* olefin isomer of the linear product there

(10) Loh, T.-P.; Hu, Q.-Y.; Ma, L.-T. *Org. Lett.* **2002**, *4*, 2389–2391.

are no reports in the literature affording access to the *Z* isomer in an enantioselective or even racemic fashion. Additionally, these alkenyl–CF_3 moieties have been garnering much interest in the literature lately as highly useful precursors to 1,1-difluoroalkenes, compounds that are steadily gaining importance in the pharmaceutical industry.[11]

3.2.2 State-of-the-Art in Chloro-substituted Allyl Additions to Aldehydes

Another allyl addition to aldehydes that is relatively underdeveloped is the addition of chloro-substituted allyl groups to aldehydes. Since 1983 there have been a mere five reports on transformations with aldehydes involving chloro-substituted allyl groups.[12] The first reported methods to achieve this transformation were disclosed by Hoffmann *et al*., as depicted in Scheme 3.5.[13]

Scheme 3.5. Hoffmann's Synthesis of *Z*-Homoallylic Alcohols

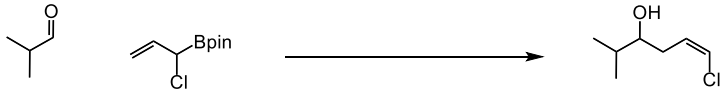

3.18 **3.19** **3.20**
82% yield,
95:5 *Z*:*E*

Hoffman *et al*. were able to utilize the *racemic α*-chloro-allyl–B(pin) reagent **3.19** for highly regio- and *Z*-selective additions to aldehydes, allowing access to racemic *Z*-chloro-substituted homoallylic alcohols, such as **3.20**. Subsequently, they were able to

(11) For recent methods which employ trifluoromethyl alkenes as precursors to difluoro-alkenes, see: (a) Huang, Y.; Hayashi, T. *J. Am. Chem. Soc.* **2016**, *138*, 12340–12343. (b) Xiao, T.; Li, L.; Zhou, L. *J. Org. Chem.* **2016**, *81*, 7908–7916. (c) Liu, Y.; Zhou, Y.; Zhao, Y., Qu, J. *Org. Lett.* **2017**, *19*, 946–949. (d) Lang, S. B.; Wiles, R. J.; Kelly, C. B.; Molander, G. A. *Angew. Chem., Int. Ed.* **2017**, *56*, 15073–15077. (e) Kojima, R.; Akiyama, S.; Ito, H. *Angew. Chem., Int. Ed.* **2018**, *57*, 7196–7199.
(12) Note: There have been five reports which can access the linear regiosiomer, see ref. 17 for methods which generate the branched, chlorohydrin product.
(13) (a) Hoffmann, R. W.; Landmann, B. *Tetrahedron Lett.* **1983**, *24*, 3209–3212. (b) Hoffmann, R. W.; Dresely, S. *Chem. Ber.* **1989**, *122*, 903–909. (c) Sturmer, R.; Hoffmann, R. W. *Synlett* **1990**, 759–760.

establish an enantioselective variant of the transformation by utilizing a chiral 1,2-dicyclohexyl-ethanediol boronic ester.[13c] This modification not only allowed for an extremely enantioselective reaction (≥92:8 er in all cases), it also improved the *Z* selectivity of the transformation (exclusive formation of the *Z* isomer). The next method affording access to linear, *Z*-chloro allylic alcohols was reported in 1993 by Junjappa *et al*., as shown in Scheme 3.6.[14]

Scheme 3.6. Junjappa's α-Addition of Chloroallyl Lithium

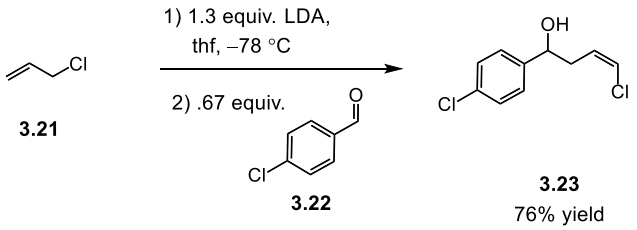

Junjappa and co-workers were able to treat allyl chloride (**3.21**) with LDA to form the *Z*-chloro-allyl lithium, which could be trapped by an aldehyde to form *Z*-chloro-homoallylic alcohols, such as **3.23**. Interestingly, they report that they can reverse the regioselectivity of the transformation, to form the isomeric chlorohydrin product, by including zinc(II) chloride in the first step of the transformation. Another attempt to render this class of transformations enantioselective was carried out by Roush & Chen in 2010.[15]

Scheme 3.7. Roush's Enantioselective Synthesis of *Z*-Homoallylic Alcohols

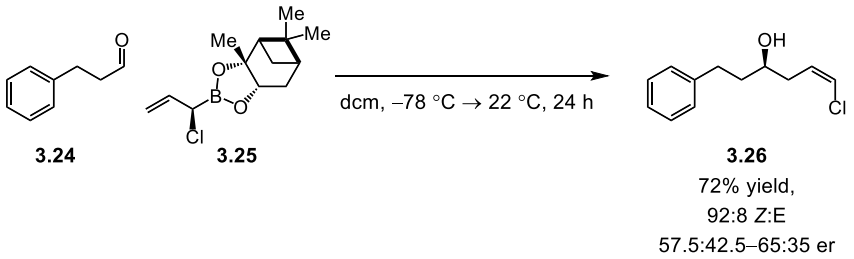

(14) Mallaiah, K.; Satyamarayana, J.; Ila, H.; Junjappa, H. *Tetrahedron Lett.* **1993**, *34*, 3145–3148.
(15) Chen, M.; Roush, W. R. *Org. Lett.* **2010**, *12*, 2706–2709.

Analogous to Hoffman *et al*., Roush & Chen were able to synthesize pinene-diol derived allylboron **3.25** for *Z*- and enantioselective chloro-allyl addition to hydrocinnamaldehyde (**3.24**). While they found that the product was isolated with high *Z* selectivity, they report that the enantioselectivity of the transformation was low and variable. The authors propose that the low enantioselectivity of the transformation is due to the inclination of **3.25** to isomerize under the reaction conditions, due to the acidity of the allylic proton. A result which lies in stark contrast to the results obtained Hoffman *et al.*, who were able to utilize a similar chiral allylboron reagent in order to obtain products with exceptional enantioselectivities. While there have been few reports on the synthesis of the aforementioned *Z*-chloro homoallylic alcohols, reports on the synthesis of the isomeric chlorohydrin products have been more numerous.[16,17] Despite the fact that *Z*-halogen-substituted homoallylic alcohols are quite common intermediates in natural product synthesis, there are no direct ways to access these products enantioselectively through allylation.[18] The current state-of-the-art in accessing these moieties has not

(16) (a) Hu, S.; Jayaraman, S.; Oehlschlager, A. C. *J. Org. Chem.* **1996**, *61*, 7513–7520. (b) Hertweck, C.; Boland, W. *Eur. J. Org. Chem.* **1998**, 2143–2148. (c) Bandini, M.; Cozzi, P. G.; Melchiorre, P.; Morganti, S.; Umani-Ronchi, A. *Org. Lett.* **2001**, *3*, 1153–1155.

(17) For examples of chlorohydrins in natural product synthesis synthesized through allyl additions, see: (a) Hu, S.; Jayaraman, S.; Oehlschlager, A. C. *J. Org. Chem.* **1999**, *64*, 2524–2526. (b) Hu, S.; Jayaraman, S.; Oehlschlager, A. C. *J. Org. Chem.* **1999**, *64*, 3719–3721. (c) Paterson, I.; Anderson, E. A.; Dalby, S. M.; Loiseleur, O. *Org. Lett.* **2005**, *7*, 4121–4124. (d) Fürstner, A.; Fenster, M. D. B.; Fasching, B.; Godbout, C.; Radkowski, K. *Angew. Chem., Int. Ed.* **2006**, *45*, 5510–5515. (e) Chung, W.-J.; Carlson, J. S.; Vanderwal, C. D. *J. Org. Chem.* **2014**, *79*, 2226–2241. (f) Landry, M. L.; Hu, D. X.; McKenna, G. M.; Burns, N. Z. *J. Am. Chem. Soc.* **2016**, *138*, 5150–5158.

(18) For examples of *Z*-halo-homoallylic alcohols in synthesis, see: (a) Yadav, J. S.; Dutta, P. J. *Org. Chem.* **2016**, *81*, 1786–1797. (b) Reddy, K. M.; Yamini, V.; Singarapu, K. K.; Ghosh, S. *Org. Lett.* **2014**, *16*, 2658–2660. (c) Kim, Y.; Singer, R. A.; Carreira, E. M. *Angew. Chem., Int. Ed.* **1998**, *37*, 1261–1263. (d) Smith, A. B., III; Ott, G. R. *J. Am. Chem. Soc.* **1998**, *120*, 3935–3948. (e) Nguyen, M. H.; Imanishi, M.; Kurogi, T.; Smith, A. N., III. *J. Am. Chem. Soc.* **2016**, *138*, 3675–3678. (f) Li, P.; Li, J.; Arikan, F.; Ahlbrecht, W.; Dieckmann, M.; Mench, D. *J. Org. Chem*. **2010**, *75*, 2429–2444. (g) Zhu, B.; Panek, J. S. *Org. Lett*. **2000**, *2*, 2575–2578. (h) Speed, A. W. H.; Mann, T. J.; O'Brien, R. V.; Schrock, R. R.; Hoveyda, A. H. *J. Am. Chem. Soc*. **2014**, *136*, 16136–16139. (i) Lei, H.; Yan, J.; Yu, J.; Liu, Y.; Wang, Z.; Xu, Z.; Ye, T. *Angew. Chem., Int. Ed*. **2014**, *53*, 6533–6537. (j) Adachi, Y.; Kamei, N.; Yokoshima, S.; Fukuyama, T. *Org. Lett*. **2011**, *13*,

changed from the traditional sequence of allylation, ozonolysis, followed by Stork-Zhao olefination. Thus we felt that being able to access these products directly and enantioselectively in one step would be useful to the synthetic community.

3.3. Utilizing Substituted Allylboron Reagents to Engender High Enantioselectivity in Allyl Additions to Aldehydes

While recent work in our laboratory has been able to utilize aminophenol ligands to promote a variety of enantioselective allyl additions to generate valuable products, we had never been able carry out this transformation on aldehydes.[4]

Scheme 3.8. Aminophenol Promoted Allyl Addition To Aldehydes

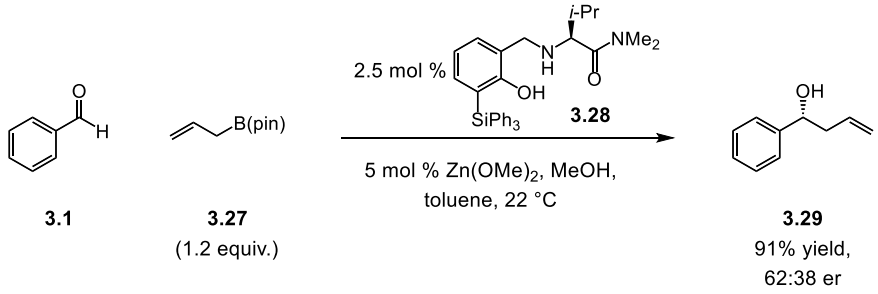

As shown in Scheme 3.8, when an aldehyde and allyl–B(pin) are subjected to 2.5 mol % of aminophenol ligand **3.28** and 5 mol % zinc(II) methoxide, the desired product is

4446–4449. (k) Mak, S. Y. F; Curtis, N. R.; Payne, A. N.; Congreve, M. S.; Wildsmith, A. J.; Francis, C. L.; Davies, J. E.; Pascu, S. I.; Burton, J. W.; Holmes, A. B. *Chem. Eur. J.* **2008**, *14*, 2867–2885. (l) Franke, J.; Bock, M.; Dehn, R.; Fohrer, J.; Mhaske, S. B.; Migliorini, A.; Kanakis, A. A.; Jansen, R.; Herrmann, J.; Müller, R.; Kirschning, A. *Chem. Eur. J.* **2015**, *21*, 4272–4284. (m) Muñoz, D. M.; Passey, S. C.; Simpson, T. J.; Willis, C. L.; Campbell, J. B.; Rosser, R. *Aust. J. Chem.* **2004**, *57*, 645–649. (n) Wang, X.; Porco, J. A., Jr. *J. Am. Chem. Soc.* **2003**, *125*, 6040–6041. (o) Holmes, M. T.; Britton, R. *Chem. Eur. J.* **2013**, *19*, 12649–12652. (p) LeClair, C. A.; Boxer, M. B.; Thomas, C. J.; Maloney, D. J. *Tetrahedron Lett.* **2010**, *51*, 6852–6855. (q) Stork, G.; Zhao, K. *J. Am. Chem. Soc.* **1990**, *112*, 5875–5876. (r) Crimmins, M. T.; Debaillie, A. C. *Org. Lett.* **2003**, *5*, 3009–3011. (s) Hillier, M. C.; Price, A. T.; Meyers, A. I. *J. Org. Chem.* **2001**, *66*, 6037–6045. (t) Yoshikawa, Y.; Yamakawa, M.; Kobayashi, T.; Murai, K.; Arisawa, M.; Sumimoto, M.; Fujioka, H. *Eur. J. Org. Chem.* **2017**, 2715–2718. (u) Crimmins, M. T.; Tabet, E. A. *J. Am. Chem. Soc.* **2000**, *122*, 5473–5476.

formed in high yield but low enantioselectivity (62:38 er). Initially, this was a rather surprising result, as in the past we had been able to carry out enantioselective allyl additions to methyl ketones, a substrate class were enantiotopic differentiation of the substrate is more challenging than it is in aldehydes.[4e] Due to this finding we were led to believe that the issue may lie in a highly competitive, un-catalyzed background reaction, as allyl–B(pin) compounds are known to react with aldehydes at, or below, room temperature.[19] To probe this we decided to investigate the regioselectivity of the transformation through the use of deuterated allyl–B(pin).

Scheme 3.9. d_2-Labeling Experiments Reveal an α-Selective Transformation

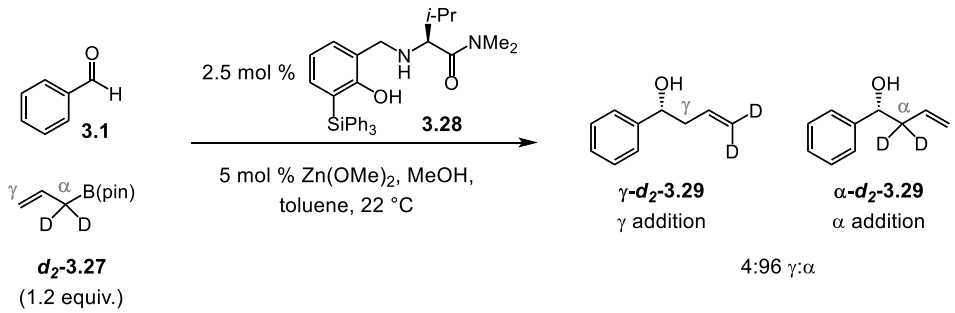

The rationale behind this experiment was that aminophenol catalyzed allyl additions proceed with α selectivity, whereas any background processes proceed with γ selectivity (for example, when the reaction is carried out with NaO*t*-Bu and no aminophenol, the product is obtained with 95:5 γ:α selectivity). When we carried out the experiment with ***d*₂-3.27** we found that, under the reaction conditions, the product was obtained with high α selectivity (4:96 γ:α selectivity). This suggested that the origin of the poor enantioselectivity may not be a highly competitive background reaction; rather, that the aminophenol ligand has poor differentiation between the enantiotopic faces of the

(19) Roush, W. R.; Adam, M. A.; Walts, A. E.; Harris, D. J. *J. Am. Chem. Soc.* **1986**, *108*, 3422–3434.

aldehyde. This realization came concurrently with the discovery of two viable transition states in crotyl additions to trifluoromethyl ketones, previously described in Chapter 2. As shown in Scheme 3.10 A, the transition state for the crotyl addition to trifluoromethyl ketones depends on which olefin isomer of crotyl–B(pin) is used for the reaction. When *Z*-crotyl–B(pin) is used, the lowest energy transition state is **(*R*)-TS-3.30**, whereas when *E*-crotyl–B(pin) is used **(*S*)-TS-3.31** is the lowest energy transition state for the reaction. These two distinct transition states occur through two different chair-like transition states due to a driving force to place the methyl substituent in the psuedo-axial position (for a more in-depth discussion, see Chapter 2). However, due to the coulombic/electrostatic attraction between the trifluoromethyl unit and the proton, the addition to the substrate still occurs to the same enantiotopic face, regardless of which olefin isomer of reagent is utilized.

Scheme 3.10. Low Enantioselectivity Due to Poor Catalyst Control

A. Crotylation of CF_3-Ketones: Transition State Control Through Methyl Group

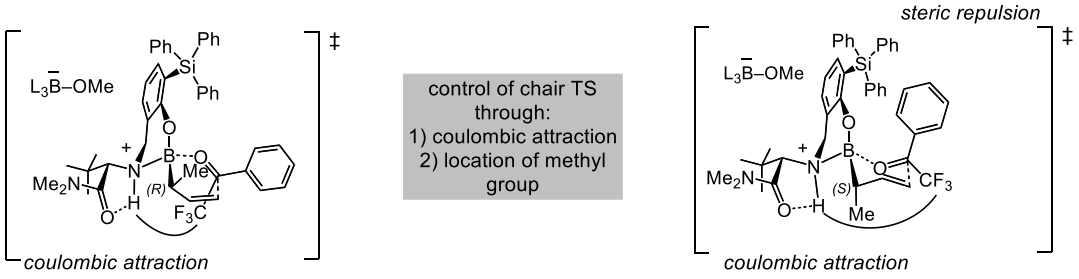

(*R*)-TS-3.30 **(*S*)-TS-3.31**

B. Allylation of Aldehydes: Competitive Transition States Lead to Low Enantioselectivity

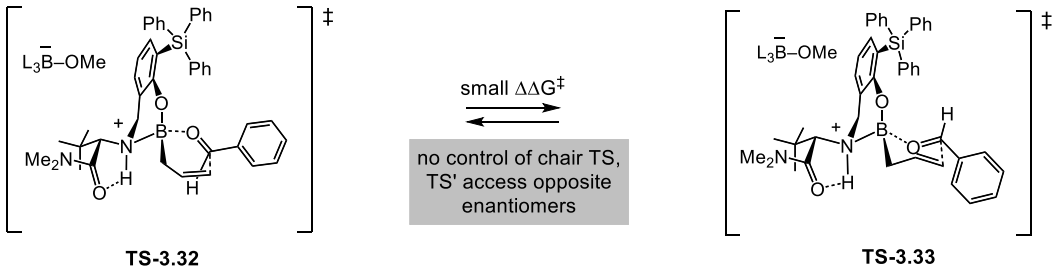

TS-3.32 **TS-3.33**

However, when we now consider these two distinct chair-like transition states in the case of allylation of aldehydes, there are two critical alterations. First, without the presence of a methyl substituent on the six-membered ring transition state, there is no control of which chair-like transition state is favored (**TS-3.32** and **TS-3.33,** Scheme 3.10 B). Additionally, in the absence of a coulombic/electrostatic attraction (due to the absence of a trifluoromethyl unit in aldehydes), differentiation of the enantiotopic faces of the substrate becomes entirely dependent on steric control. In **(*S*)-TS-3.31**, the electrostatic attraction overcame the steric repulsion between the aryl ring of the substrate and the triphenylsilyl moiety on the aminophenol, in **TS-3.33**, due to the lack of an electrostatic attraction, steric repulsion becomes the dominant force. This causes the aldehyde to bind in a way that places the phenyl group pseudo-equatorially, thereby minimizing steric interaction with the triphenylsilyl group on the aminophenol. This allows for two competitive transition states for C–C bond formation where the addition occurs on opposing enantiotopic faces of the substrate, furnishing a product with low enantioselectivity.

Scheme 3.11. Increasing Enantioselectivity by Controlling the Chair Transition States

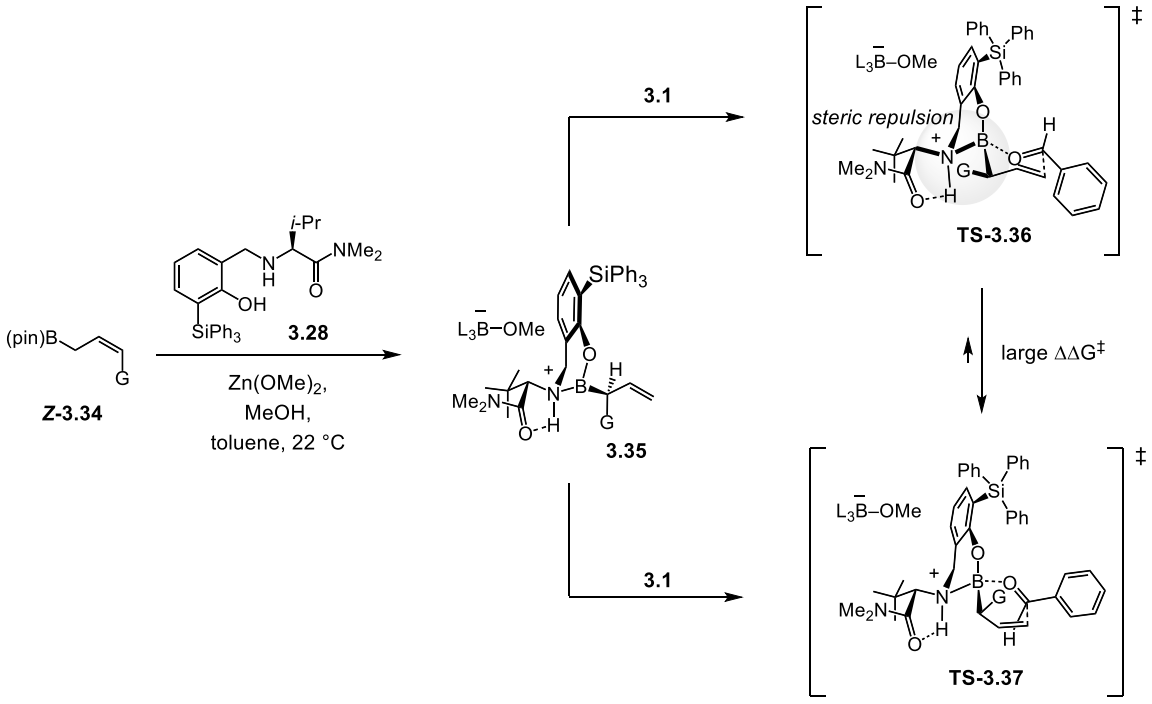

Utilizing insights obtained through our previous investigations, we envisioned that, perhaps by utilizing a substituted allylboron reagent, such as **Z-3.34**, we could favor which chair-like transition state is energetically favored (Scheme 3.11). After generation of the diastereomeric intermediate **3.35** from the initial allyl transfer, the aldehyde would likely bind in one of two ways, as shown in **TS-3.36** and **TS-3.37**. However, due to the additional substituent on the six-membered ring transition state, the aldehyde binding in the mode shown in **TS-3.36** is accompanied by the generation of a *syn*-pentane interaction between the G group and the backbone of the aminophenol. We hoped that this interaction would be enough to differentiate these two transition states and lead to a highly enantioselective addition to aldehydes.

Scheme 3.12. *Z*-Crotyl–B(pin) in Aminophenol Promoted Crotyl Additions to Aldehydes

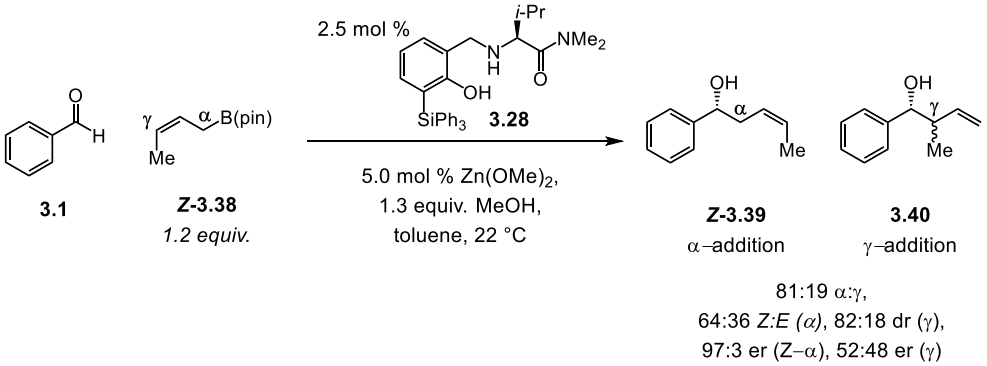

What we found was that although the reaction was very efficient, the regioselectivity and diastereoselectivity of the transformation were low. However, when we checked the enantioselectivities of the product we found that indeed the *Z* isomer of the α-addition product was generated in high enantioselectivity (97:3 er). At this stage, we hypothesized that perhaps background reaction with this reagent could be problematic and decided to explore less reactive allylboron reagents.

3.4. Development of Aminophenol Promoted CF_3-Allyl Additions to Aldehydes

3.4.1 Initial Result for CF_3-Allyl Additions to Aldehydes

During our search for a less reactive allylboron source our group disclosed a protocol for the catalytic, Z-selective cross metathesis of alkenyl–CF_3 groups. Therein we reported the first synthesis of Z-CF_3-allyl–B(pin) through molybdenum-catalyzed cross methathesis.[5b] When we attempted to use this reagent in allylation of aldehydes, we found that there was no discernible reaction, even at elevated temperatures. This reagent was an intriguing candidate to utilize in aminophenol promoted allyl additions due to the low

reactivity of the reagent coupled with the value of the product. Our first attempt at utilizing this reagent in a catalytic, enantioselective transformation is shown in Scheme 3.13.

Scheme 3.13. Initial Result for CF_3-Allyl Additions to Aldehydes

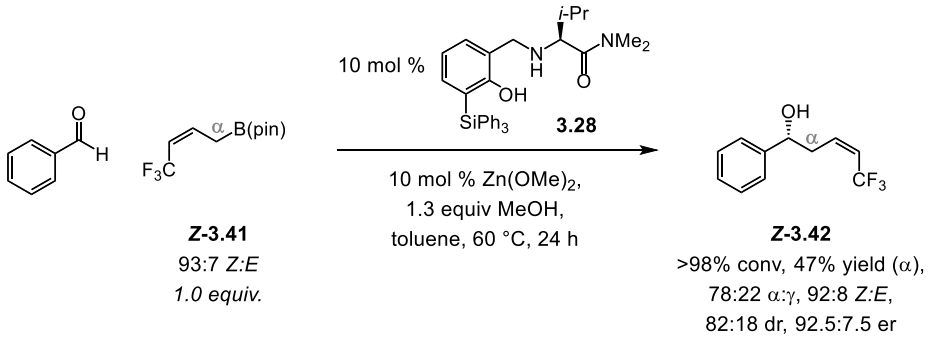

***Z*-3.41**
93:7 *Z:E*
1.0 equiv.

***Z*-3.42**
>98% conv, 47% yield (α),
78:22 α:γ, 92:8 *Z:E*,
82:18 dr, 92.5:7.5 er

Due to the supposed inertness of the reagent, high catalyst loadings and elevated temperatures were used to see if any reaction would take place. What we found was that, in the presence of aldehydes, there was full conversion to product with moderate regioselectivity and high *Z* and enantioselectivity.

3.4.2 Screening of Conditions Towards a Highly Selective Transformation

In order to optimize the selectivities of the transformation we first turned to screening of aminophenol ligands, as shown in Scheme 3.14. Interestingly, what we found was that the substituent on the aryl ring of the aminophenol was critical in achieving a selective transformation. When aminophenols bearing a small substituent, such as **3.43** or **3.44** were employed in the transformation, the regioselectivities and enantioselectivities were significantly diminished. With respect to the regioselectivity of the transformation, we believe that the larger triphenylsilyl group hinders chelation of the zinc methoxide to the aminophenol aryloxide, slowing down 1,3-borotropic shift (see Chapter 1 for a full discussion on the factors involving 1,3-borotropic shift), thereby making the reaction more

α-selective. Unfortunately, increasing the size of the triphenylsilyl group on the aminophenol was synthetically cumbersome, so other modifications of the aminophenol were investigated.

Scheme 3.14. Reaction Optimization Through Aminophenol Screening

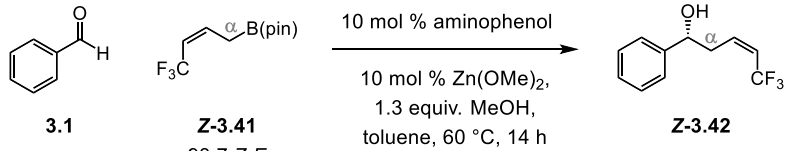

3.1

***Z*-3.41**
93:7 *Z*:*E*
1.0 equiv.

***Z*-3.42**

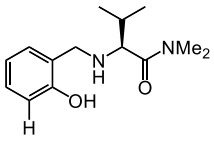

3.43
89% conv, 76% yield,
43:57 α:γ, 75:25 *Z*:*E*,
87:13 dr, 38:62 er

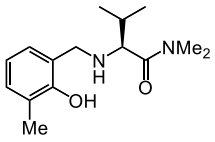

3.44
>94% conv, 69% yield,
42:58 α:γ, 73:27 *Z*:*E*,
87:13 dr, 28:72 er

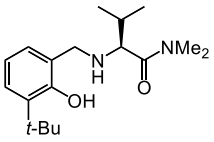

3.45
98% conv, 83% yield,
51:49 α:γ, 80:20 *Z*:*E*,
83:17 dr, 57:43 er

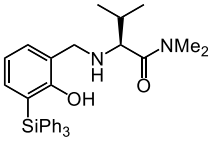

3.28
>98% conv, 47% yield (α),
78:22 α:γ, 92:8 *Z*:*E*,
82:18 dr, 92.5:7.5 er

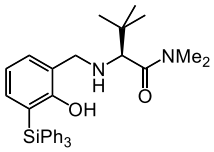

3.46
>98% conv, 82% yield (α),
85:15 α:γ, 95:5 *Z*:*E*,
84:16 dr, 95:5 er

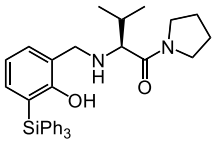

3.47
>98% conv, 42% yield (α),
79:21 α:γ, 93:7 *Z*:*E*,
84:16 dr, 93.5:7.5 er

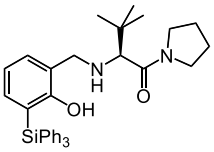

3.48
97% conv, 87% yield (α),
88:12 α:γ, 95:5 *Z*:*E*,
86:14 dr, 92:8 er

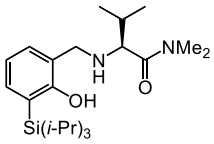

3.49
>98% conv, 57% yield (α),
60:40 α:γ, 67:33 *Z*:*E*,
81:19 dr, 81:19 er

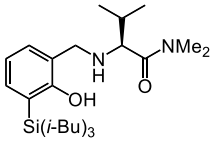

3.50
>98% conv, 56% yield (α),
53:47 α:γ, 74:26 *Z*:*E*,
81:19 dr, 86:14 er

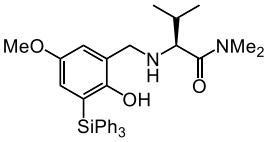

3.51
>98% conv, 53% yield (α),
76:24 α:γ, 90:10 *Z*:*E*,
82:18 dr, 89:11 er

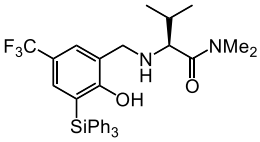

3.52
91% conv, 80% yield (α),
81:19 α:γ, 92.5:7.5 *Z*:*E*,
86:14 dr, 89.5:10.5 er

We next turned to modification of the amino acid residue of the aminophenol ligand. What we found was that, for reasons that are as-of-yet not well understood, utilizing the sterically larger *tert*-leucine derived aminophenol ligand (**3.46**) further improved the

regio-, *Z*, and enantioselectivity of the transformation to 85:15 α:γ, 95:5 *Z*:*E*, and 95:5 er. Modification of the amide group, i.e. **3.47** and **3.48**, did not considerably improve the selectivity of the transformation. Trialkylsilyl substituted aryl oxides, such as the tri-iso-propyl silyl or tri-isobutyl silyl groups on **3.49** and **3.50**, respectively, were found to react with lower regioselectivity, suggesting that the high α selectivity of triphenylsilyl-substituted aminophenols might not simply be due to the sterics of the triphenylsilyl group. To investigate this, electronically modified aminophenols **3.51** and **3.52** were synthesized. They were found to be similarly α-selective, but less enantioselective. At this stage we determined that aminophenol **3.46** was optimal ligand for the transformation and we turned to investigating other reaction conditions. During reaction optimization, it was found that the reaction proceeded to completion within two hours at 4 °C and that the catalyst and zinc(II) methoxide loadings could be lowered to 1.0 and 5.0 mol %, respectively, as shown in Scheme 3.15.

Scheme 3.15. Effect of Temperature on Selectivity of the Transformation

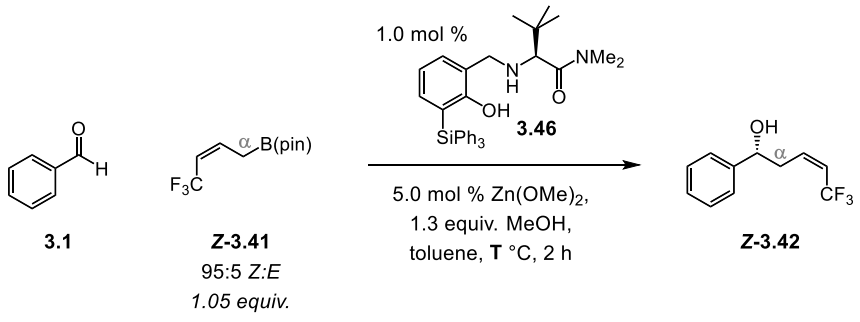

3.1

***Z*-3.41**
95:5 *Z*:*E*
1.05 equiv.

***Z*-3.42**

T = 22 °C
>98% conv, 86% yield (α),
87:13 α:γ, 94:6 *Z*:*E*,
94:6 er

T = 4 °C
>98% conv, 88% yield (α),
95:5 α:γ, 94:6 *Z*:*E*,
95:5 er

Lastly, we found that cooling the reaction to 4 °C could further improve the regioselectivity of the transformation to 95:5 α:γ selectivity. With the results shown in

Scheme 3.15 (88% yield, 95:5 α:γ, 94:6 *Z*:*E*, and 95:5 er), we set out to examine the generality of the protocol.

3.4.3 Scope of the Catalytic, Enantioselective Protocol

A variety of aldehydes were subjected to the reaction conditions, which showed that the transformation was broadly applicable, as shown in Scheme 3.16. Sterically encumbered aldehydes, such as *o*-Me-substituted ***Z*-3.55** and *o*-Br-substituted ***Z*-3.56**, reacted efficiently and selectively. Similar results were also encountered when a variety of *meta*-substituted aldehydes were investigated (see: ***Z*-3.57** and ***Z*-3.58**). Electron-deficient *para*-substituted aldehydes reacted with high regioselectivities (>97:3 α:γ), *Z*:*E* selectivities (>95:5) and enantioselectivities (98:2 er), as shown by ***Z*-3.59** and ***Z*-3.60**. However, when the electron-rich *p*-OMe-substituted aldehyde was subjected to the reaction conditions (***Z*-3.61**), the regioselectivity of the transformation was greatly diminished to 71:29 α:γ.

Scheme 3.16. General Substrate Scope for CF_3-Allyl Additions to Aldehydes

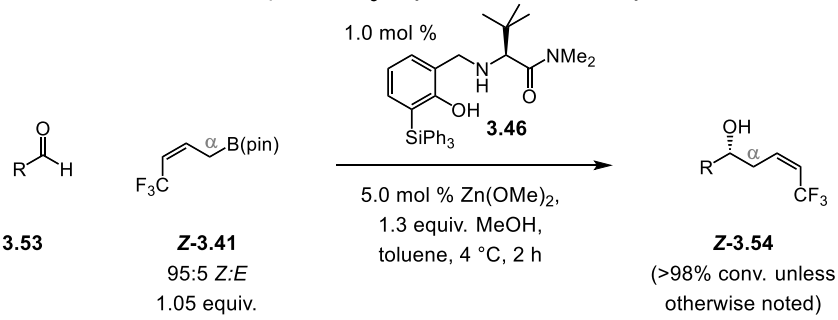

3.53

***Z*-3.41**
95:5 *Z:E*
1.05 equiv.

***Z*-3.54**
(>98% conv. unless otherwise noted)

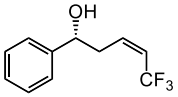

***Z*-3.42**
88% yield (α),
95:5 α:γ, 94:6 *Z:E*,
95:5 er

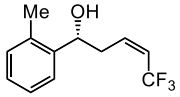

***Z*-3.55**
91% yield (α),
93:7 α:γ, 94:6 *Z:E*,
97:3 er

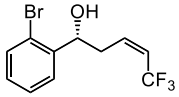

***Z*-3.56**
91% yield (α),
99:1 α:γ, 93:7 *Z:E*,
98:2 er

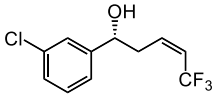

***Z*-3.57**
93% yield (α),
97:3 α:γ, 94:6 *Z:E*,
98:2 er

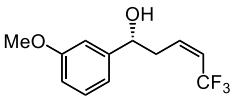

***Z*-3.58**
86% yield (α),
91:9 α:γ, 92:8 *Z:E*,
97:3 er

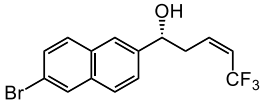

***Z*-3.59**
93% yield (α),
97:3 α:γ, 95:5 *Z:E*,
98:2 er

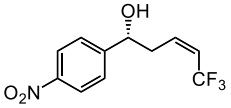

***Z*-3.60**
98% yield (α),
>98:2 α:γ, 98:2 *Z:E*,
98:2 er

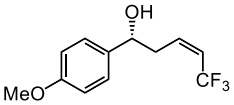

***Z*-3.61**
76% yield (96% α),
71:29 α:γ, 91:9 *Z:E*,
91:9 er

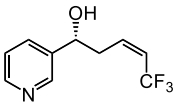

***Z*-3.62**
89% yield (α),
98:2 α:γ, 91:9 *Z:E*,
92.5:7.5 er

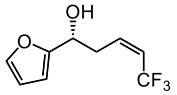

***Z*-3.63**
82% yield (α),
91:9 α:γ, 81:19 *Z:E*,
93:7 er

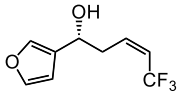

***Z*-3.64**
35% yield (α),
73:27 α:γ, 85:15 *Z:E*,
93.5:6.5 er

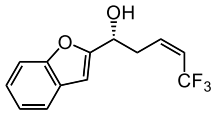

***Z*-3.65**
97% conv, 94% yield (α),
99:1 α:γ, 87:13 *Z:E*,
94:6 er

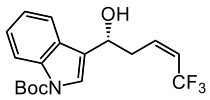

***Z*-3.66**
90% conv, 75% yield (α),
83:17 α:γ, 91:9 *Z:E*,
94:6 er

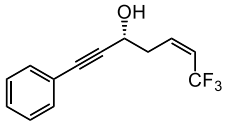

***Z*-3.67**
93% yield (α),
>98:2 α:γ, 83:17 *Z:E*,
97:3 er

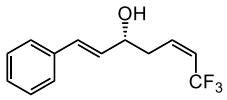

***Z*-3.68**
71% yield (α),
79:21 α:γ, 86:14 *Z:E*,
87.5:12.5 er

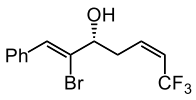

***Z*-3.69**
93% yield (α),
97:3 α:γ, 90:10 *Z:E*,
98.5:1.5 er

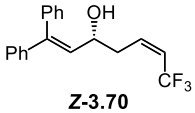

***Z*-3.70**
98% conv, 78% yield (α),
92:8 α:γ, 92:8 *Z:E*,
92:8 er

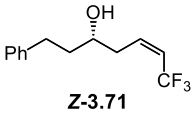

***Z*-3.71**
65% yield (α),
70:30 α:γ, 83:17 *Z:E*,
82:18 er

Ultimately, this observation was consistent for all electron-rich aldehydes (see: ***Z*-3.64**, ***Z*-3.66**, ***Z*-3.68**, and ***Z*-3.71**), an outcome which will be discussed in detail below. Hetero-aryl aldehydes were also tolerated in the reaction, as evidenced by ***Z*-3.62**. However, when smaller hetero-aryl substrates were utilized, the *Z* selectivity of the transformation eroded, as shown by ***Z*-3.63** and ***Z*-3.64** (81:19 and 85:15 *Z*:*E*, respectively), a phenomenon which is currently not well understood. Larger five-membered-ring heteroaryl substrates (***Z*-3.65** and ***Z*-3.66**) reacted with slightly improved *Z*:*E* selectivities, suggesting that the size of the substrate could be the origin of the low *Z*:*E* selectivity for ***Z*-3.63** and ***Z*-3.64**. Alkynyl-substituted aldehyde (***Z*-3.67**) reacted with exceptional regio- and enantioselectivity (>98:2 α:γ and 97:3 er), but furnished a product with low *Z* selectivity, presumably due to the small size of the substrate. The slightly more electron-rich alkenyl substrate (***Z*-3.68**) reacted with lower regioselectivity (79:21 α:γ), low *Z* selectivity (86:14 *Z*:*E*) and enantioselectivity (87.5:12.5 er). However, when trisubstituted alkenyl substrates were explored (see: ***Z*-3.69** and ***Z*-3.70**), the selectivities improved greatly. Lastly hydrocinnamaldehyde ***Z*-3.71** reacted similarly to cinnamaldehyde ***Z*-3.68**, yielding products with low regio-, *Z*, and enantioselectivity. Clearly, the limitation to the current method is that electron rich aldehydes (see: ***Z*-3.61**, ***Z*-3.64**, ***Z*-3.66**, ***Z*-3.68**, and ***Z*-3.71**) react with low regioselectivity. In aminophenol-zinc catalyzed reactions with substituted allylboron reagents, the regioselectivity of the transformation depends on the rate of 1,3-bororopic shift versus C–C bond formation, as shown in Scheme 3.17.

Scheme 3.17. Exploiting the Kinetics of 1,3-Borotropic Shift to Improve Regioselectivity

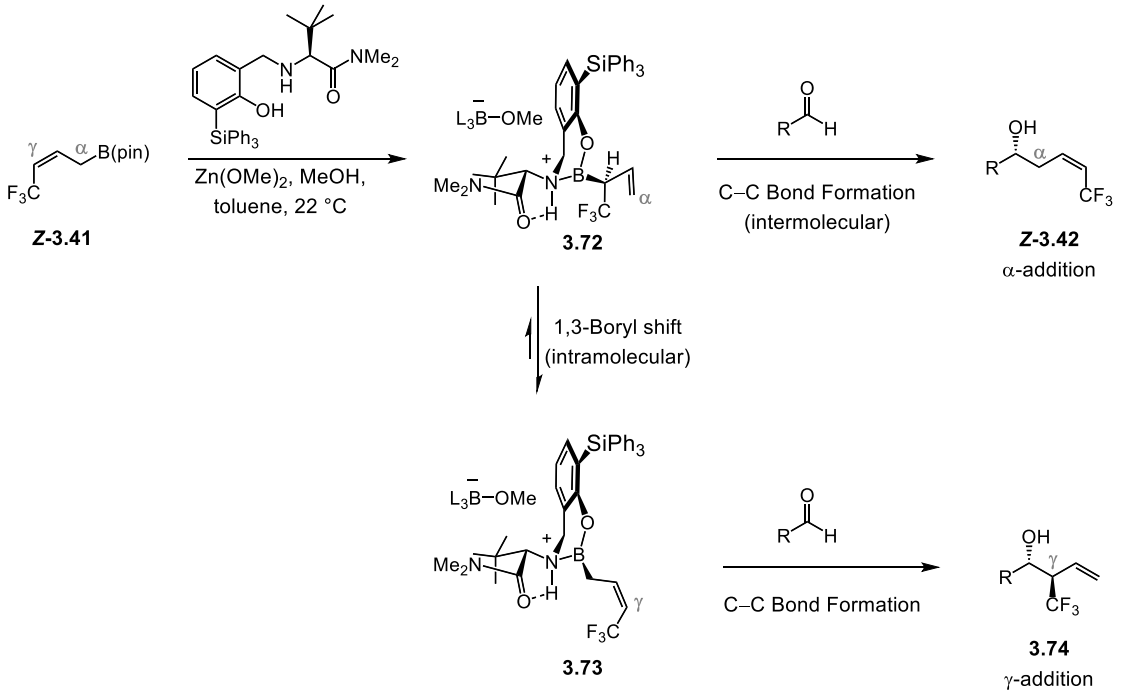

As has been discussed in great detail in Chapters 1 and 2, when a substituted allyl is used, such as ***Z*-3.41**, the initial allyl transfer onto the chiral aminophenol-boron-methoxide complex produces a diastereomeric intermediate, **3.72**. At this point, C–C bond formation can occur (producing α-addition product ***Z*-3.42**), provided addition to the substrate is more facile than 1,3-borotropic shift, which accesses intermediate **3.73** (ultimately producing γ-addition product **3.74**). In other words, regioselectivity depends on the competition between direct C–C bond formation versus 1,3-borotropic shift. Thus, it follows that more electron rich substrates react with diminished regioselectivity, as 1,3-borotropic shift becomes more competitive. One important observation to make note of, however, is that direct C–C bond formation is an intermolecular process depending on the concentration of the aldehyde and **3.72**. Whereas 1,3-borotropic shift is an intramolecular process depending solely on the concentration of **3.72**. Therefore we hypothesized that if

an excess of aldehyde reagent is used, the rate of direct C–C bond formation should be enhanced, while the rate of 1,3-borotropic shift should remain unchanged. The consequences of this hypothesis are shown in Scheme 3.18.

Scheme 3.18. Modified Reaction Conditions for Electron Rich Substrates

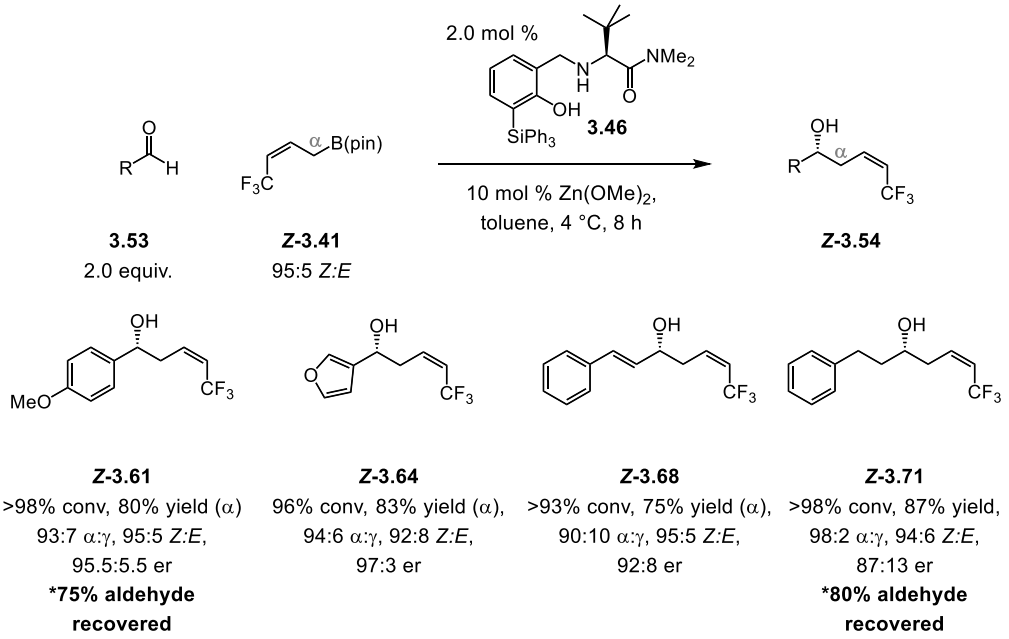

3.53
2.0 equiv.

***Z*-3.41**
95:5 *Z*:*E*

***Z*-3.54**

***Z*-3.61**
>98% conv, 80% yield (α)
93:7 α:γ, 95:5 *Z*:*E*,
95.5:5.5 er
***75% aldehyde recovered**

***Z*-3.64**
96% conv, 83% yield (α),
94:6 α:γ, 92:8 *Z*:*E*,
97:3 er

***Z*-3.68**
>93% conv, 75% yield (α),
90:10 α:γ, 95:5 *Z*:*E*,
92:8 er

***Z*-3.71**
>98% conv, 87% yield,
98:2 α:γ, 94:6 *Z*:*E*,
87:13 er
***80% aldehyde recovered**

When excess aldehyde was used, in addition to a few other small changes (no methanol, and 8 hours of reaction time), we found that the regioselectivity of the transformation was greatly improved for electron rich aldehydes. Additionally, we found that for these electron rich aldehydes, the reaction can turn over without the need for methanol. In these cases, not using methanol was found to make the transformation more enantioselective. It is also noteworthy that during the reaction conditions there is little to no decomposition of the aldehydes, allowing for the recovery of up to 80% of the unreacted aldehydes (Scheme 3.18, see ***Z*-3.61** and ***Z*-3.71***)*. Regrettably, we found that while methanol was not required for the aforementioned electron rich aldehydes, sterically hindered aldehydes do require methanol for high reaction efficiency.

Scheme 3.19. Sterically Hindered Electron Rich Substrates

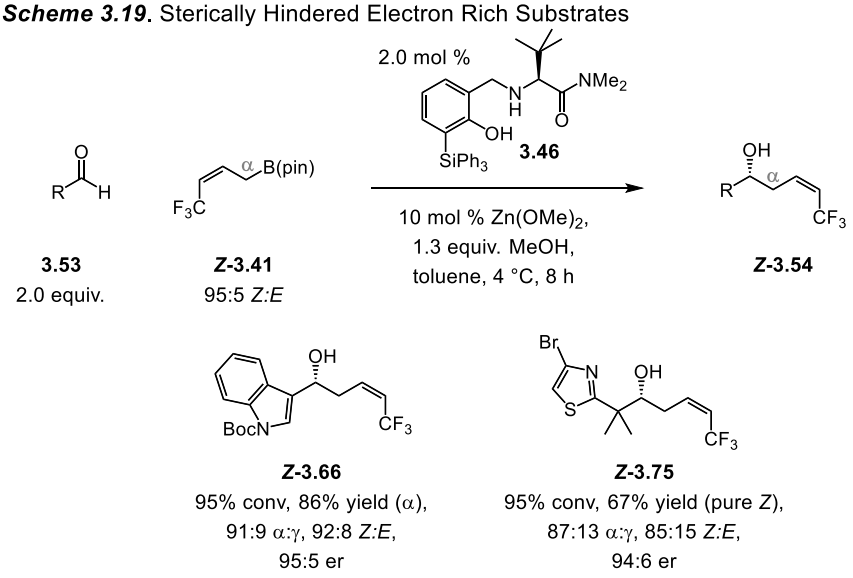

***Z*-3.66**
95% conv, 86% yield (α),
91:9 α:γ, 92:8 *Z*:*E*,
95:5 er

***Z*-3.75**
95% conv, 67% yield (pure *Z*),
87:13 α:γ, 85:15 *Z*:*E*,
94:6 er

While the 3-Boc-indole and bromothiazole substrates did benefit from utilizing 2 equivalents of aldehyde during the reaction, it was found that in the absence of methanol the reaction did not proceed efficiently (53% conversion and 18% conversion in 8 hours, respectively). In these cases we found that utilizing an excess of aldehyde in addition to 1.3 equivalents of methanol afforded the products with high efficiency and selectivity, see Scheme 3.19 (***Z*-3.66** and ***Z*-3.75**). At this stage, we were interested in expanding the scope of the protocol in regard to the substituted allylboron reagent we used.

3.4.4 Expanding to Enantioselective Chloro-Allyl Additions to Aldehydes

As suggested by the introduction of this chapter, we quickly realized the potential utility of this transformation if halogen-substituted allylboron reagents could be used. Thus, we set out to develop a transformation which utilizes a *Z*-chloro-substituted allylboron reagent to generate *Z*-chloro-substituted homoallylic alcohols, which can serve as powerful intermediates towards more complex *Z*-substituted homoallylic alcohols. Our first attempts

at subjecting *Z*-chloro-substituted allyl–B(pin) (***Z*-3.77**) to our reactions are shown in Scheme 3.20.

Scheme 3.20. Initial Result for Chloro-Allyl Addition to Aldehydes

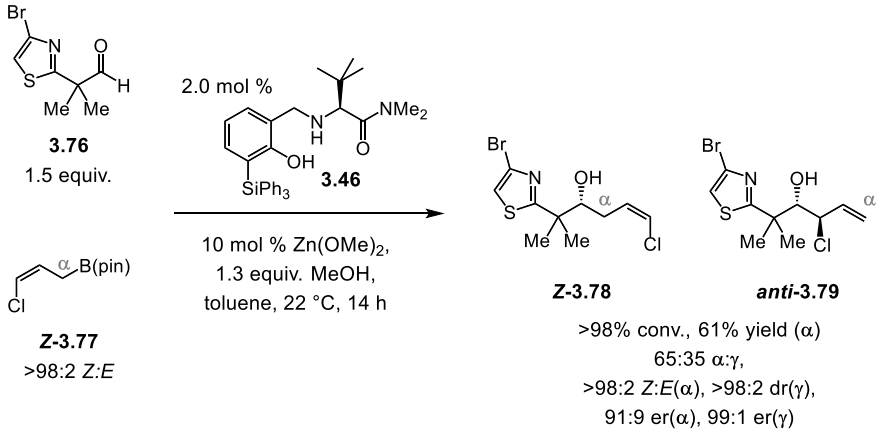

When aldehyde **3.76** and allylboron reagent ***Z*-3.77** were subjected to the reaction conditions, we found that the desired product, homoallylic alcohol ***Z*-3.78**, was generated in high *Z* and enantioselectivity. Unfortunately, even when a slight excess of aldehyde was employed, the transformation proceeded with low regioselectivity favoring the linear, α-addition product. At this stage, we turned to aminophenol ligand screening in hopes of increasing the regio- and enantioselectivity of the transformation. Lastly, while carrying out the optimization of this reaction on aldehyde **3.76** may seem like a strange choice, the product of this transformation (***Z*-3.78**) will serve as an intermediate in the total synthesis of mycothiazole. The aminophenol screening data, shown in Scheme 3.21, shows that the regioselectivity of the transformation is highly dependent on the aminophenol structure.

Scheme 3.21. Aminophenol Screening for Chloro-Allyl Addition to Aldehydes

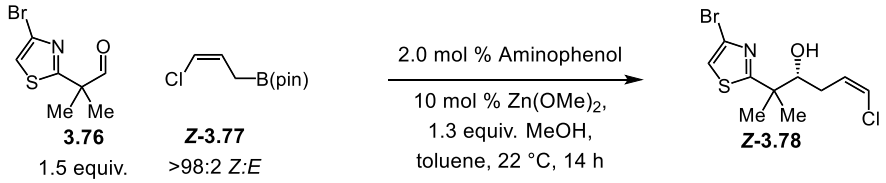

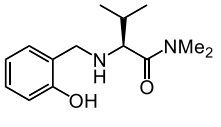

3.43
94% conv., 23% yield(α)
23:77 α:γ,
>*98:2 Z*:*E*(α), 90:10 dr(γ),
67:33 er(α), 92:8 er(γ)

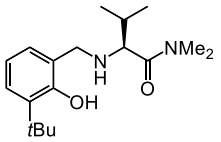

3.45
>98% conv., 34% yield(α)
36:64 α:γ,
>*98:2 Z*:*E*(α), 95:5 dr(γ),
72:28 er(α), 95:5 er(γ)

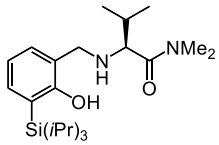

3.49
>98% conv., 43% yield(α)
44:56 α:γ,
>*98:2 Z*:*E*(α), 94:6 dr(γ),
88:12 er(α), 94:6 er(γ)

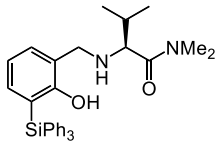

3.28
>98% conv., 60% yield(α)
63:37 α:γ,
>*98:2 Z*:*E*(α), >98:2 dr(γ),
86.5:13.5 er(α), 99:1 er(γ)

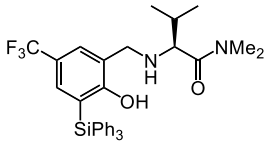

3.51
>98% conv., 68% yield(α)
68:32 α:γ,
>*98:2 Z*:*E*(α), >98:2 dr(γ),
87:13 er(α), 98:2 er(γ)

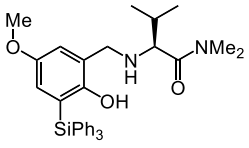

3.50
>98% conv., 66% yield(α)
66:34 α:γ,
>*98:2 Z*:*E*(α), >98:2 dr(γ),
86:14 er(α), 97:3 er(γ)

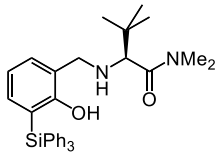

3.46
>98% conv., 61% yield(α)
65:35 α:γ,
>*98:2 Z*:*E*(α), >98:2 dr(γ),
91:9 er(α), 99:1 er(γ)

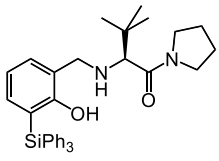

3.48
>98% conv., 72% yield(α)
72:38 α:γ,
>*98:2 Z*:*E*(α), >98:2 dr(γ),
91.5:8.5 er(α), 99:1 er(γ)

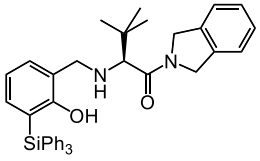

3.80
>98% conv., 79% yield(α)
80:20 α:γ,
>*98:2 Z*:*E*(α), >98:2 dr(γ),
92.5:7.5 er(α), 98:2 er(γ)

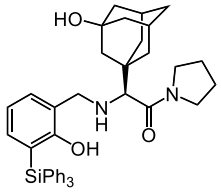

3.81
>98% conv., 88% yield(α)
92:8 α:γ,
>*98:2 Z*:*E*(α), >98:2 dr(γ),
93:7 er(α), n.d. er(γ)

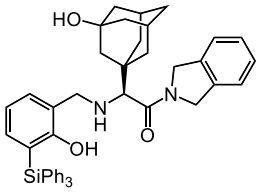

3.82
>98% conv., 95% yield(α)
95:5 α:γ,
>*98:2 Z*:*E*(α), >98:2 dr(γ),
94:6 er(α), n.d. er(γ)

When the substituent *ortho* to the phenol of the aminophenol is small, i.e. R = H (**3.43**) or R = *t*-Bu (**3.45**) the transformation became more γ-selective (23:77 and 36:64 α:γ, respectively). However, we were pleased to see that in this case the γ-addition product was

generated with high diastereo- and enantioselectivity.[20] Moving to the larger triisopropyl-silyl substituted aminophenol (**3.49**) improved the regioselectivity slightly to 44:56 α:γ, nonetheless the best regioselectivity was observed with the original triphenyl-silyl moiety (**3.28**, 63:27 α:γ). To probe whether or not the electronic attributes of the aryl ring on the aminophenol impact the rate of 1,3-borotropic shift and thus affect the regioselectivity of the transformation, electronically deactivated *para*-CF_3-substituted aminophenol **3.51** and electronically activated *para*-OMe-substituted aminophenol **3.50** were subjected to the reaction conditions. We found that in this case there was little to no effect of the electronic attributes of the aryl ring on the reaction outcome. We then turned to modifying the aminophenol residue and amide group to optimize the reaction selectivities. We found that utilizing the sterically larger *tert*-leucine amino acid again improved the α selectivity and enantioselectivity of the transformation, though to a much lesser degree than it did in the case of the CF_3-substituted allylboron reagent utilized previously. Increasing the steric bulk of the amide group to a pyrrolidine amide improved the regioselectivity further from 63:35 to 72:38 α:γ selectivity (**3.48**). Further increasing the size of the amide group to an isoindolene substituted amide (**3.80**) yielded even greater regioselectivity and slightly increased the enantioselectivity of the transformation (80:20 α:γ and 92.5:2.5 er). At this point we wondered if we could use an even larger amino acid residue to improve the regioselectivity further. We found that a hydroxy-adamantyl-derived amino acid was inexpensive and available from several commercial sources. When we utilized this residue to synthesize new aminophenol ligands (**3.81** and **3.82**) we found that these ligands are able

(20) This is likely due to the fact that there is no background reaction in the absence of aminophenol, <5% conversion, 14 h.

to catalyze a highly α-selective transformation, allowing us to access the desired regioisomer with 95:5 α:γ selectivity and 94:6 enantioselectivity (**3.82**).

Scheme 3.22. Effect of Equivalents of Aldehyde on Selectivity of Reaction

A Excess Aldehyde is Required for High α Selectivity

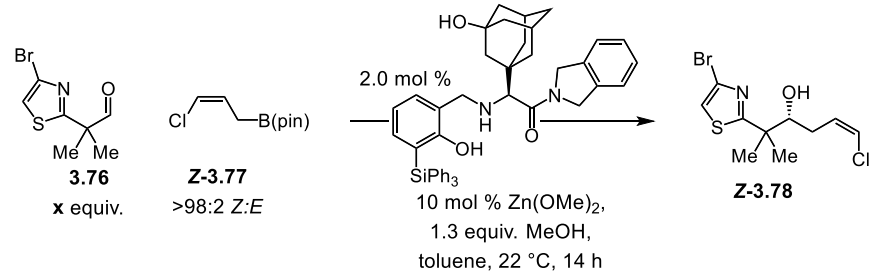

1.5 equiv.
>98% conv., 95% yield(α)
95:5 α:γ, >*98:2 Z:E*(α),
94:6 er(α)

1.0 equiv.
98% conv., 53% yield(α)
80:20 α:γ, >98:2 *Z*:*E*(α),
93:7 er(α)

B Modifying the Reaction Conditions to Access the Other Regioisomer

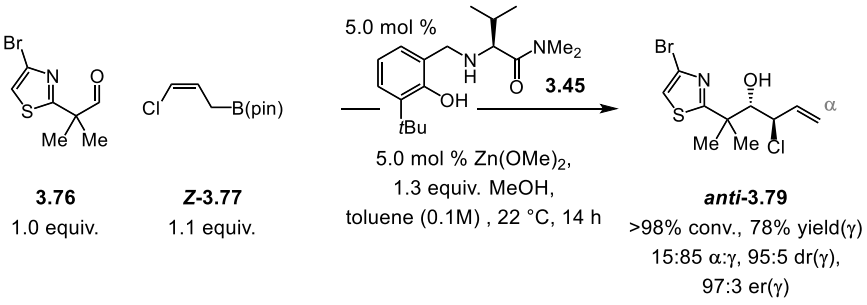

Lastly, to ensure that 1.5 equivalents of aldehyde **3.76** were indeed necessary for the approach to be highly α-selective, the reaction was carried out with one equivalent of aldehyde, as shown in Scheme 3.22 A. We found that when only one equivalent of aldehyde was employed that, unsurprisingly, the regioselectivity of the transformation dropped to 80:20 α:γ, due to the rate of C–C bond formation being slower. This observation, coupled with the aminophenol screening data shown in Scheme 3.21, led us to conclude that perhaps, by making a few strategic modifications to the reaction conditions, we could selectively access the other regioisomer of product. The results, summarized in Scheme

3.22 B, show that indeed we can access the other regioisomer in synthetically useful yield and selectivities (78% yield, 95:5 diastereoselectivity, and 97:3 enantioselectivity). While this is a promising result, future work will revolve around optimizing this result further. Remarkably, this is the first example of an aminophenol promoted reaction that can access the both regioisomers of product by simple modification of the reaction conditions. In regard to the reaction conditions that access the α-addition product, since the excess aldehyde is not consumed and easily recovered, we decided that using 1.5 equivalents of aldehyde was acceptable. With the newly designed aminophenol ligand and these conditions in hand we went on to show the generality and broad applicability of the protocol.

3.4.5 Scope of the Catalytic, Enantioselective Chloro-Allyl Addition

With the optimal conditions in hand (*Z*-Cl-allyl–B(pin), 2.0 mol % **3.82**, 10 mol % $Zn(OMe)_2$, 1.3 equivalents of methanol) we set out to show the broad applicability of the protocol. We found that a variety of aryl substrates were well tolerated under this conditions, generally reacting with exclusive α selectivity, as illustrated in Scheme 3.23. Since the reaction was optimized with a bulky, electron rich, alkyl aldehyde, the regioselectivity with more reactive aryl aldehydes was not an issue. When we explored the transformation with electron poor aldehydes, such as the *para*-ketone- (***Z*-3.86**) and *para*-trifluoromethyl-substituted (***Z*-3.87**) benzaldehydes, we observed that while the reaction efficiency, regio- and *Z* selectivity remained high, the products were obtained with diminished enantioselectivity (88:12 and 87:13 er, respectively). Unusually, when electron rich aldehydes such as *para*-methoxy-benzaldehyde (***Z*-3.88**) or *para*-thiomethyl-

substituted benzaldehyde (***Z*-3.89**) were subjected to the reaction conditions, we observed that they *also* reacted with moderate enantioselectivity (89:11 and 90:10 er, respectively), similar to the electron poor substrates. However, when the *meta*- and *para*-subtituted piperonal was utilized in the reaction (***Z*-3.90**), the high enantioselectivity was again regained. Lastly, while these trends could lead one to assume that the electronically deactivated difluoronitrile substituted benzaldehyde (***Z*-3.91**) would also react with low enantioselectivity, we found that the product was obtained in high enantioselectivity (94:6 er). This suggests that the two *ortho*-substituted fluorine atoms increase size of the substrate enough to overcome the reduced enantioselectivity found in *para*-substituted substrates.

Scheme 3.23. Scope for Aromatic Substrates

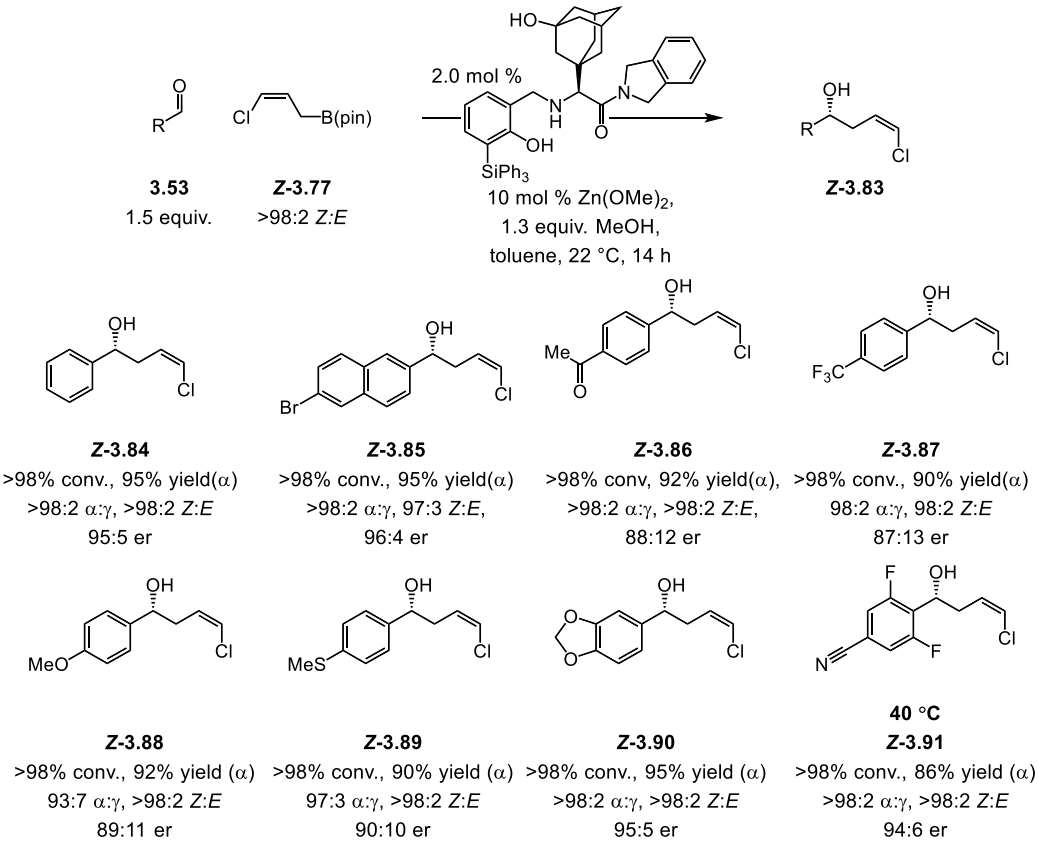

As detailed in Scheme 3.24, the scope of the protocol in regards to heteroaromatic substrates is broad and general. As can be seen, 3-pyridyl carboxaldehyde (***Z*-3.92**) reacted efficiently and with high enantioselectivity. 2-Benzofuryl carboxaldyhyde, on the other hand, reacted with moderate enantioselectivity. Likely due to the ability of the oxygen heteroatom to participate in a competing electrostatic interaction with the ammonium group of the catalyst complex, diminishing enantioselectivity. When the hetero atom is moved to the 3 position, as in ***Z*-3.94** and ***Z*-3.95**, the high enantioselectivity returned (93:7 and 96:4 er, respectively).

Scheme 3.24. Heteroaromatic Substrates in the Transformation

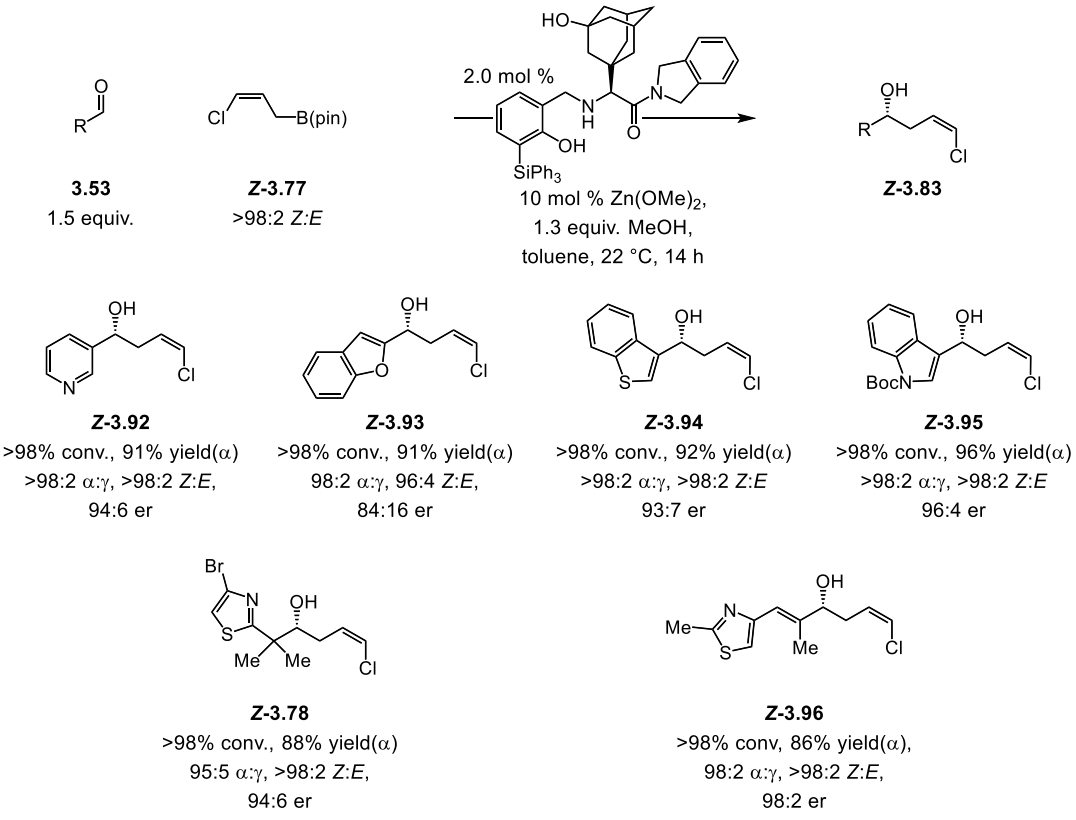

Heterocycles with more than one heteroatom are also tolerated in the reaction conditions as evidenced by thiazoles **Z-3.78** and **Z-3.96** (a potential intermediate in the synthesis of epothilones A and C). When sterically smaller alkyl (***Z*-3.97**), alkenyl (***Z*-3.98**)

or alkynyl (***Z*-3.99**) were subjected to the reaction conditions, we found that the enantioselectivity of the transformation was moderate (~80:20 er). While this was disappointing, it was not surprising, as differentiation of the enantiotopic faces of the aldehyde becomes much more challenging.

Scheme 3.25. Alkyl, Alkenyl, and Alkynyl Substrates in the Transformation

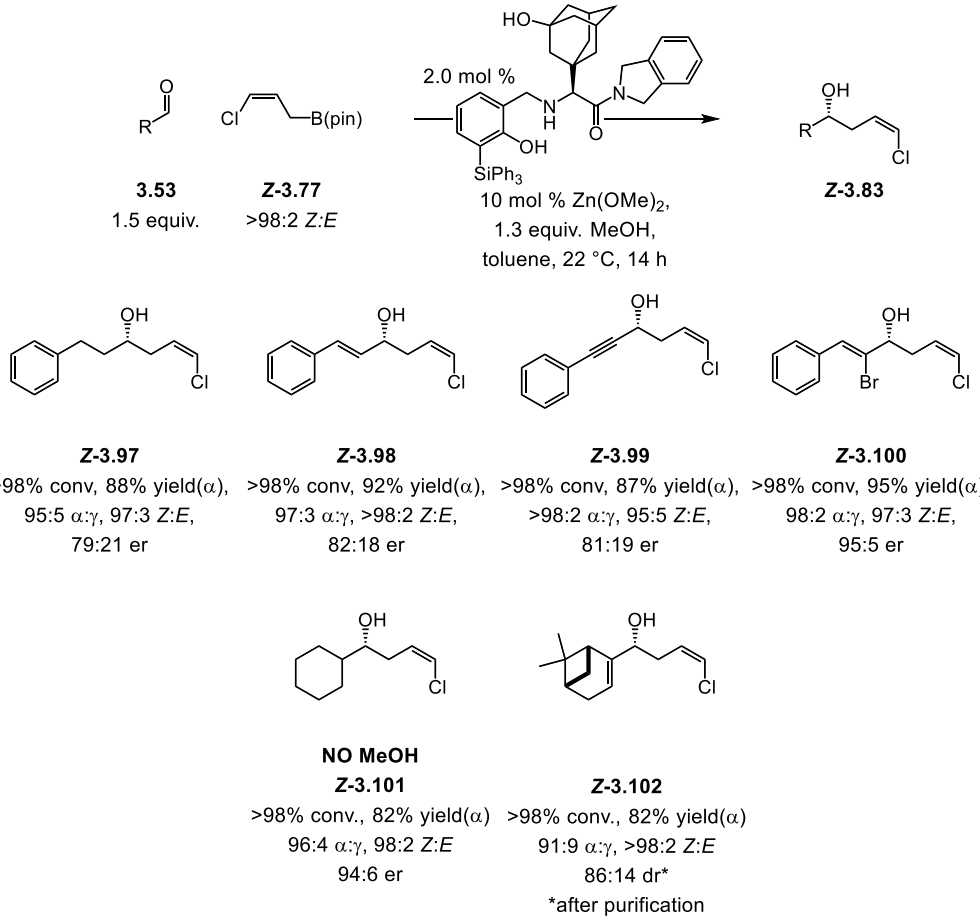

The enantioselectivity of the transformation could be regained when the size of the substrate was increased, for example α-bromo-cinnamaldehyde (***Z*-3.100**) and cyclohexyl carboxaldehyde (***Z*-3.101**) reacted to form products with high enantioselectivity (95:5 and 94:6 er, respectively). Lastly, the protocol also tolerated substrates which already contain stereocenters such as myrtenal ***Z*-3.102** (86:14 dr). After establishing the generality of the

protocol, we set out to demonstrate the potential utility and impact of the method by carrying out a highly convergent, catalytic synthesis of a small molecule.

3.5. A Convergent, Catalytic Approach to Mycothiazole

The driving force for the development of this protocol was that we felt that it would be a compelling way to introduce a *Z*-homoallylic alcohol into a molecule enantioselectively. We quickly found mycothiazole, a polyketide heterocycle isolated from a marine sponge, and thought that it would make for a challenging candidate to utilize this method.[21] We were intrigued by its structure, because it contained two challenging-to-synthesize *Z*-alkenes: a *Z*-diene and a *Z*-skipped diene. Currently, there is only one reported synthesis of this potent HIF-1 inhibitory natural product, which requires 20 steps (longest linear sequence) and furnished the final product in 0.66% overall yield.[22,23] Our retrosynthetic strategy for convergently assembling mycothiazole is depicted in Scheme 3.26.

(21) (a) Crews, P.; Kakou, Y.; Quiñoà, E. *J. Am. Chem. Soc.* **1988**, *110*, 4365–4368. (b) Sonnenschein, R. N.; Johnson, T. A.; Tenney, K.; Valeriote, F. A.; Crews, P. *J. Nat. Prod.* **2006**, *69*, 145–147.
(22) Wang, L.; Hale, K. J. *Org. Lett.* **2015**, *17*, 4200–4203.
(23) There had previously been two reported syntheses of the incorrect structure of mycothiazole. See: (a) Sugiyama, H.; Yokokawa, F.; Shioiri, T. *Org. Lett.* **2000**, *2*, 2149–2152. (b) Le Flohic, A.; Meyer, C.; Cossy, J. *Org. Lett.* **2005**, *7*, 339–342.

Scheme 3.26. Mycothiazole: Retrosynthetic Strategy

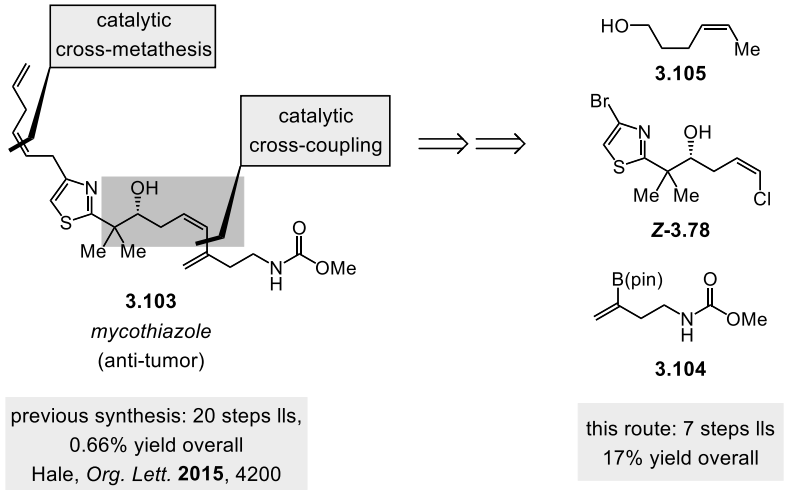

We planned to deconstruct mycothiazole into three simple fragments, which could be assembled through methods developed in our lab. We envisioned that a late stage ruthenium-catalyzed cross-metathesis developed in our lab could install the pendant primary alcohol, which would serve as a masked alkene after dehydration, to install the Z-skipped diene moiety of mycothiazole. Prior to that, the Z-diene would be installed through a palladium-catalyzed Suzuki cross-coupling reaction between a 1,1-disubstituted alkenyl–B(pin) reagent (**3.104**) with a Z-chloro-substituted homoallylic alcohol (**Z-3.78**), which would be synthesized through the newly developed aminophenol catalyzed chloro-allyl addition to the derived aldehyde.[24] This would allow us to rapidly assemble mycothiazole in a convergent way utilizing protocols which tolerate free hydroxyl groups, averting the need for any protection and deprotection of the secondary alcohol. The synthesis of two key fragments utilized in the synthesis of mycothiazole are shown in Scheme 3.27

(24) For the synthesis of the aldehyde see Ref 23 (b).

Scheme 3.27. Mycothiazole: Synthesis of the Coupling Partners

A Synthesis of *Z*-Chloro-Allyl-B(pin) through Molybdenum-Catalyzed Olefin Metathesis

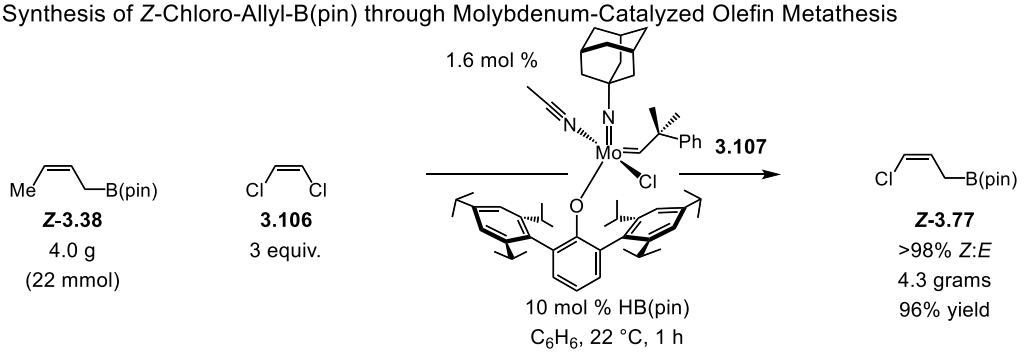

B Copper-Catalyzed Proto-Boryl Addition to Allenes: Access to Alkenyl–B(pin) Compounds

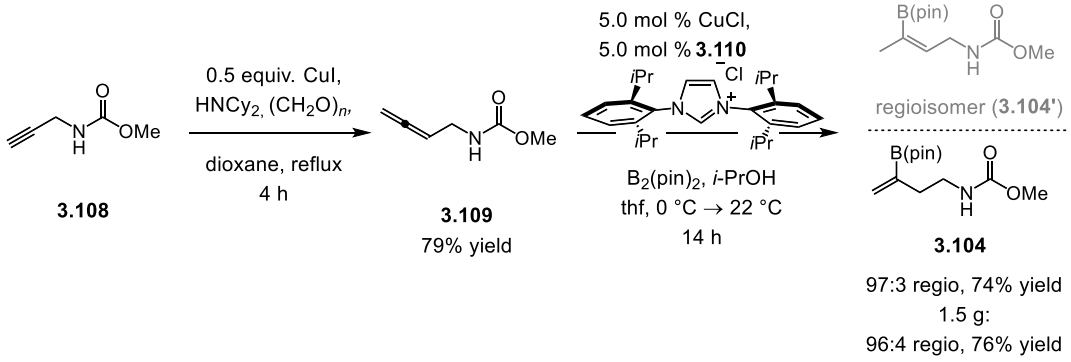

Recent work in our laboratories has revolved around the development and use of molybdenum-chloride alkylidenes as highly efficient and reactive catalysts for stereoretentive cross-metathesis reactions.[5] We have been able to utilize these protocols in the highly efficient and *Z*-selective synthesis of a variety of allylboron reagents, such as ***Z*-3.77**. As shown in Scheme 3.27 A, we have been able to synthesize this reagent in high selectivity and yield on four gram scale utilizing only 1.6 mol % of the requisite Mo catalyst (**3.107**). One point worth further elaboration is the inclusion of 10 mol % of HB(pin) in the reaction mixture, an additive which might seem obscure at the onset. However, what recent work in our laboratory has shown is that, HB(pin) can *in situ* react with any free hydroxyl groups (by-products of the synthesis of **Z-3.38**) and/or water, compounds which are able

to decompose the molybdenum catalyst.[25] Through the use of a catalytic amount of HB(pin) we are able to effectively remove any potentially harmful acidic protons from the reaction mixture, enabling us to drop the catalyst loading from 5.0 mol % to 1.6 mol %, which is almost a seventy percent reduction in catalyst loading.

We found that an efficient way to synthesize alkenyl–B(pin) fragment **3.104** would be through a site-selective proto-boryl addition to carbamate-containing allene **3.109** through another protocol developed in our laboratory.[26] The synthesis of this fragment begins from Moc-protected propargyl amine (**3.108**), readily available in one step from commercially available materials in quantitative yield.[27] The required allene was then synthesized in 79% yield by utilizing a modified Crabbé homologation developed by Ma *et al*.[28,29] When the allene was subjected to the previously developed proto-boryl addition conditions (with MeOH instead of *i*PrOH), we found that the transformation proceeded with 92:8 regioselectivity for the desired isomer. However, due to the mechanism of copper-catalyzed proto-boryl addition, we rationalized that utilizing a sterically hindered alcohol should result in protonation at the desired, internal position. Indeed, when isopropanol was utilized in the reaction, the regioselectivity improved to 97:3 and we could obtain the desired 1,1-disubstituted alkenyl–B(pin) in 74% yield. We were also able to carry out the method on a gram scale with little to no deterioration of selectivity or

(25) This work is as-of-yet unpublished, for more details see the thesis of Thach T. Nguyen (Chapter 4).
(26) Meng, F.; Jung, B.; Haeffner, F.; Hoveyda, A. H. *Org. Lett.* **2013**, *15*, 1414–1417.
(27) Teller, H.; Corbet, M.; Mantilli, L.; Gopakumar, G.; Goddard, R.; Thiel, W.; Fürstner, A. *J. Am. Chem. Soc.* **2012**, *134*, 15331–15342.
(28) For the original reports on this transformation, see: (a) Crabbé, P.; Fillion, H.; André, D.; Luche, J.-L. *J. Chem. Soc., Chem. Commun.* **1979**, 859–860; (b) Searles, S.; Li, Y.; Nassim, B.; Lopes, M.-T. R.; Tran, P. T.; Crabbé, P. *J. Chem. Soc., Perkin Trans. 1*, **1984**, 747–751.
(29) Kuang, J.; Ma, S. *J. Org. Chem.* **2009**, *74*, 1763–1765.

efficiency. With these reagents in hand, we could begin synthesis on the core of mycothiazole, the route of which is shown in Scheme 3.28.

Scheme 3.28. A Multi-Catalytic, Convergent Approach to Mycothiazole

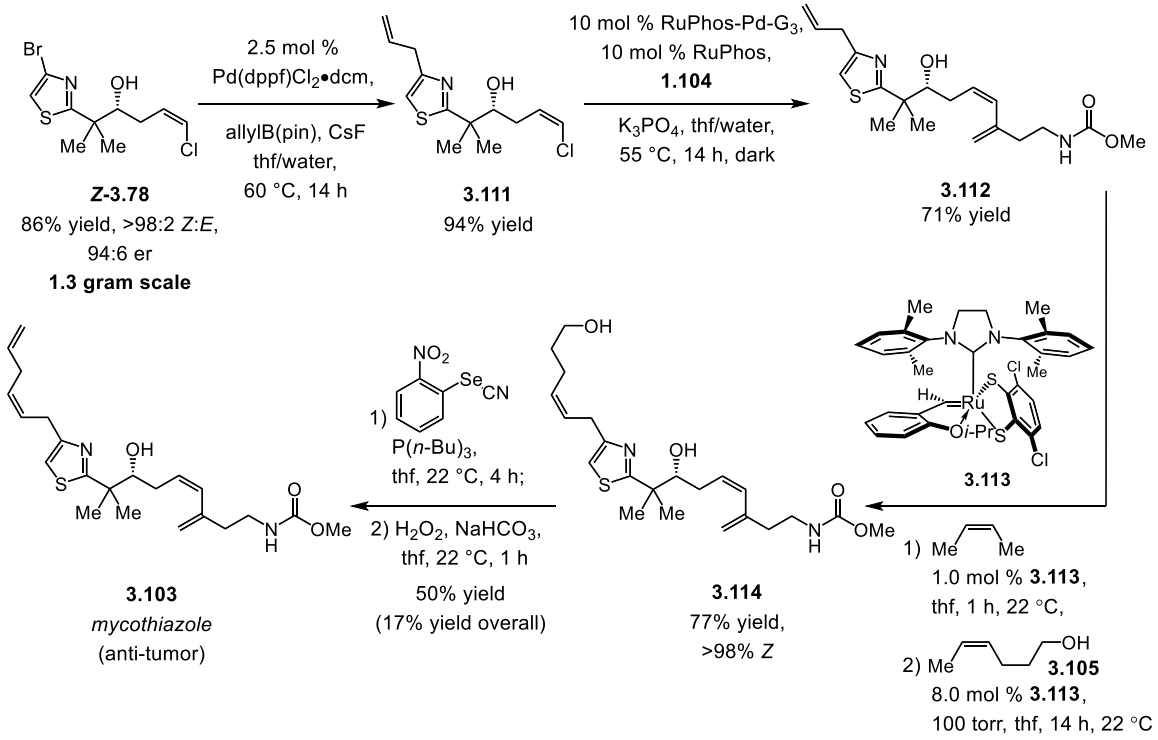

The starting point of this synthesis involves aldehyde **3.76**, which has previously been synthesized by Cossy *et al*. in two steps from commercially available materials in 78% overall yield. Aldehyde **3.76** was then subjected to aminophenol-promoted chloro-allyl addition to access *Z*-chloro-homoallylic alcohol ***Z*-3.78** (Scheme 3.24) in high yield, regio-, *Z* and enantioselectivity. A chemoselective, palladium-catalyzed Suzuki cross-coupling reaction with allyl–B(pin) was then carried out in order to install an allyl group, which would serve as a handle for the subsequent cross-metathesis reaction. By utilizing Pd(dppf)Cl_2•dcm and cesium fluoride as a base, this reaction proceeds with exclusive chemoselectivity for the aryl bromide, furnishing the desired product (**3.111**) in 94% yield. The following step, a Suzuki cross-coupling reaction to install the *Z*-diene was then carried

out, by the use of a ligand and precatalyst developed in the Buchwald lab. It was found that the Buchwald ligand systems were uniquely effective in enabling the oxidative addition of the alkenyl-chloride to take place. Utilizing this system at low temperatures allowed us to access this sensitive *Z*-diene (**3.112**) with no isomerization of the double bond (to the *E*-diene) in 71% yield. We found that at elevated temperatures, i.e. temperatures ≥65 °C, we observed the formation of significant amounts of the *E*-diene. In order to access the skipped diene moiety we opted to use an olefin metathesis/elimination sequence. A new class of ruthenium carbenes developed in our lab enables highly *Z*-selective cross-metathesis with the functional group compatibility that is accompanied by ruthenium-based cross metathesis.[30] However, since we have discovered that these catalysts can decompose in the presence of terminal olefins, leading to low reaction efficiency. To circumvent this decomposition pathway, colleagues in our laboratory have developed a method to *in situ* cap terminal olefins, to produce *Z*-internal olefins, by adding an excess of *cis*-2-butene to the reaction.[31] This strategy allows catalyst lifetime to be prolonged, enabling an efficient and *Z*-selective transformation. Thus, in order to carry out the desired transformation, we had to utilize the two step approach illustrated in Scheme 3.28, **3.112** → **3.114**. We were able to access compound **3.114**, in 77% yield and exclusive *Z* selectivity by utilizing 9.0 mol % of Ru complex **3.113** and commercially available *Z*-hexenol **3.105**. In order to eliminate the alcohol and generate the required skipped diene we were able to utilize a

(30) (a) Khan, R. K. M.; Torker, S.; Hoveyda, A. H. *J. Am. Chem. Soc.* **2013**, *135*, 10258–10261; (b) Koh, M. J.; Khan, R. K. M.; Torker, S.; Hoveyda, A. H. *Angew. Chem., Int. Edi.* **2014**, 1968–1972; (c) Koh, M. J.; Khan, R. K. M.; Torker, S.; Yu, M.; Mikus, M. S.; Hoveyda, A. H. *Nature* **2015**, *517*, 181–186.
(31) Xu, C.; Shen, X.; Hoveyda, A. H. *J. Am. Chem. Soc.* **2017**, *139*, 10919–10928.

Grieco elimination, generating mycothiazole in 50% yield and 17% overall yield over seven steps.[32]

3.6. Conclusion

For many years allyl additions to aldehydes catalyzed by the aminophenol ligand were challenging and never produced products with acceptable levels of enantioselectivity. However through mechanistic understanding gained from the studies carried out in Chapter 2, we were able to rationalize the possible mechanistic underpinnings responsible for the poor enantioselectivity. By utilizing *Z*-substituted and less reactive allylboron reagents we were able to catalyze the first aminophenol promoted allyl additions to aldehydes. Additionally, due to the α selectivity of aminophenol promoted allyl additions, we were able to develop a method that generates enantioenriched *Z*-trifluoromethyl-homoallylic alcohols and *Z*-chloro-homoallylic alcohols with high efficiency and in high yield, *Z* and enantioselectivity. To highlight the utility of these products we were able to synthesis mycothiazole in 7 steps and 17% overall yield, a drastic improvement over the only previous total synthesis (20 steps, 0.66% overall yield). Additionally, due to our understanding of 1,3-borotropic shift, we have been able to modify the reaction conditions and invert the regioselectivity of the transformation. This allows us to access the γ-addition product with high diastereoselectivity and enantioselectivity. This example marks the first case of an aminophenol promoted allyl addition which can access both regioisomers of the

(32) Trost, B. M.; Probst, G. D.; Schoop, A. *J. Am. Chem. Soc.* **1998**, *120*, 9228–9236.

product with high levels of selectivity and further work will be carried out to improve the selectivities of the γ-selective protocol.

3.7. *Experimental Section*

3.7.1. *General*

Infrared (IR) spectra were recorded on a Bruker FT-IR Alpha (ATR mode) spectrophotometer, ν_{max} in cm^{-1}. Bands are characterized as broad (br), strong (s), medium (m), and weak (w). ^{1}H NMR spectra were recorded on a Varian Unity INOVA 400 (400 MHz), 500 (500 MHz), or 600 (600 MHz) spectrometer. Chemical shifts are reported in ppm from tetramethylsilane with the solvent resonance as the internal standard ($CDCl_3$: δ 7.26 ppm). Data are reported as follows: chemical shift, multiplicity (s = singlet, d = doublet, t = triplet, q = quartet, p = pentet, br s = broad singlet, m = multiplet, app. = apparent), coupling constant (Hz) and integration. ^{13}C NMR spectra were recorded on a Varian Unity INOVA 400 (100 MHz), 500 (125 MHz), or 600 (150 MHz) spectrometer with complete proton decoupling. Chemical shifts are reported in ppm from tetramethylsilane with the solvent resonance as the internal standard ($CDCl_3$: δ 77.16 ppm). ^{19}F NMR spectra were recorded on a Varian Unity INOVA 400 (376 MHz) spectrometer. Chemical shifts are reported in ppm with $C_6H_5CF_3$ as an external standard ($C_6H_5CF_3$: –63.72 ppm). Data are reported as follows: chemical shift, multiplicity, coupling constants (Hz), and integration. High-resolution mass spectrometry was performed on a JEOL AccuTOF DART (positive mode) at the Mass Spectrometry Facility, Boston College. Enantiomeric ratios were determined by high-performance liquid chromatography (HPLC) with a Shimadzu chromatograph (Chiral Technologies Chiralcel OD-H (4.6 x 250 mm), Chiralcel OJ-H (4.6 x 250 mm), Chiralcel OZ-H (4.6 x

250 mm), Chiralpak AD-H (4.6 x 250 mm), Chiralpak AS-H (4.6 x 250 mm)) in comparison with authentic racemic materials. Specific rotations were measured using either an Atago AP-300 Automated Polarimeter or a Rudolph Research Analytical Autopol IV Polarimeter. Unless otherwise noted, all reactions were carried out with distilled and degassed solvents under an atmosphere of dry N_2 in oven- (135 °C) or flame-dried glassware with standard dry box or vacuum-line techniques. Solvents were purified under a positive pressure of dry argon by a modified Innovative Technologies purification system: toluene was purified through a copper oxide and alumina column. Dimethoxy ethane was freshly distilled from a sodium and benzophenone ketyl solution. $CDCl_3$ was purchased from Cambridge Isotope Laboratories and store over activated 4Å molecular sieves prior to use. All work-up and purification procedures were carried out with reagent grade solvents (purchased from Fisher Scientific) in air.

Reagents:

Aldehydes were purchased from commercial sources. Liquid aldehydes were distilled over CaH prior to use. Crystalline aldehydes were purified with silica gel column chromatography prior to use.

Allylboronic acid pinacol ester was purchased from Frontier and distilled over CaH prior to use.

1,3-Bis(2,6-diisopropylphenyl)imidazolium chloride was purchased from Strem and used as received.

[1,1′-Bis(diphenylphosphino)ferrocene]dichloropalladium(II), complex with dichloromethane was purchased from Sigma-Aldrich and used as received.

Bis(pinacolato)diboron was purchased from Frontier Scientific and recrystallized from pentane.

(2*S*)-[(*tert*-Butoxycarbonyl)amino](3-hydroxytricyclo[3.3.1.13,7]decan-1-yl)ethanoic acid was purchased from ArkPharm and used as received.

Calcium Hydride was purchased from Strem and used as received.

Cesium fluoride was purchased from Sigma-Aldrich and used as received.

1-Chloro-3-methyl-2-butene was purchased from Alfa Aesar and used as received.

Copper(I) chloride was purchased from Strem and used as received.

Copper(I) iodide was purchased from Strem and used as received.

***cis*-Crotylboronic acid pinacol ester, 97% (*Z*-1a)** was purchased from Sigma-Aldrich and distilled over CaH prior to use.

2,4-Dibromothiazole was purchased from Combi-Blocks and used as received.

***cis*-1,2-Dichloroethylene** was purchased from TCI and distilled over CaH prior to use.

Dicyclohexylamine was purchased from Sigma-Aldrich and used as received.

2-Dicyclohexylphosphino-2′,6′-diisopropoxybiphenyl (RuPhos) was purchased from Strem and used as received.

(2-Dicyclohexylphosphino-2′,6′-diisopropoxy-1,1′-biphenyl)[2-(2′-amino-1,1′-biphenyl)]palladium(II) methanesulfonate (RuPhos-Pd-G3) was purchased from Strem and used as received.

***N*-(3-Dimethylaminopropyl)-*N*′-ethylcarbodiimide hydrochloride (EDC•HCl)** was purchased from Advanced ChemTech and used as received.

4-Dimethylaminopyridine was purchased from Oakwood and used as received.

***Z*-Hexafluoro-2-butene** was purchased from Synquest and used as received.

***cis*-4-Hexenol** was purchased from Alfa Aesar and used as received.

Hydrochloric acid (4M in dioxane) was purchased from Acros and used as received.

1-Hydroxybenzotriazole hydrate was purchased from Oakwood and used as received.

Isoindoline hydrochloride was purchased from Combi-Blocks and used as received.

2,6-Lutidine was purchased from Sigma-Aldrich and used as received.

Magnesium Sulfate was purchased from Fisher Scientific and used as received.

Magnesium turnings were purchased from Sigma-Aldrich and used as received.

Methanol was purchased from Acros (99.8% anhydrous) and used as received.

Methyl chloroformate was purchased Sigma-Aldrich and used as received.

4-Nitrobenzoyl chloride was purchased from Sigma-Aldrich and used as received.

Osmium tetroxide (4 wt % in H_2O) was purchased from Strem and used as received.

Paraformaldehyde was purchased from Sigma-Aldrich and used as received.

Pinacolborane was purchased from Oakwood and distilled over CaH prior to use.

Potassium phosphate tribasic (K_3PO_4) was purchased from Fisher Scientific and dried under vacuum at 60 °C overnight prior to use.

Propargyl amine was purchased from Combi-Blocks and used as received.

Sodium borohydride was purchased from Aldrich and used as received.

Sodium periodate was purchased from Alfa Aesar and used as received.

Sodium *tert*-Butoxide was purchased from Strem and used as received.

Triethylamine was purchased from Sigma-Aldrich and used as received.

Zinc methoxide was purchased from Sigma-Aldrich and used as received.

Aminophenol Compounds:

Aminophenols were synthesized according to literature procedure.[1]

Metathesis Complexes:

Molybdenum-1 (3.107) was synthesized according to literature procedure.[2]

Ruthenium-1 (3.113) was synthesized according to literature procedure.[3]

3.7.2. *Catalytic Enantioselective CF_3-Allyl Additions to Aldehydes*

General Procedure for Catalytic Enantioselective Allyl Additions with CF_3-Substituted Allyl–B(pin)

In a N_2-filled glovebox, a stock solution of aminophenol and zinc(II) methoxide was prepared. An oven-dried vial (8 mL) equipped with a stir bar was charged with aminophenol (2.6 mg, 0.005 mmol), zinc methoxide (3.2 mg, 0.025 mmol) and toluene (2.0 mL). The freshly prepared stock solution was allowed to stir at 22 °C for 15 min. In another vial (8 mL) a stock solution of aldehyde **3.1** was prepared. Aldehyde **3.1** (106 mg, 1.0 mmol) was weighed out and dissolved in toluene (1.0 mL). A third oven-dried vial (8 mL) was charged with the aldehyde stock solution (100 μL, 0.1 mmol) and the aminophenol/zinc(II) methoxide stock solution (400 μL). A stir bar was added to the reaction mixture followed by MeOH (5 μL, 0.13 mmol). The vial was then sealed with a septa-cap, brought out of the glovebox and cooled to 4 °C. After 5 minutes of cooling, *Z*-CF_3-allyl–B(pin) (25 mg, 0.105 mmol) was added via micro-syringe. The reaction was

(1) (a) Silverio, D. L.; Torker, S.; Pilyugina, T.; Vieira, E. M.; Snapper, M. L.; Haeffner, F.; Hoveyda, A. H. *Nature* **2013**, *494*, 216–221; (b) Lee, K.; Silverio, D. L.; Torker, S.; Haeffner, F.; Robbins, D. W.; van der Mei, F. W.; Hoveyda, A. H. *Nat. Chem.* **2016**, *8*, 768–777; (c) Robbins, D. W.; Lee, K.; Silverio, D. L.; Volkov, A.; Torker, S.; Hoveyda, A. H. *Angew. Chem., Int. Ed.* **2016**, *55*, 9610–9614.
(2) Lam, J. K.; Zhu, C.; Bukhryakov, K. V.; Müller, P.; Hoveyda A.; Schrock, R. R. *J. Am. Chem. Soc.* **2016**, *138*, 15774–15783.
(3) Koh, M. J.; Khan., R. K. M.; Torker, S.; Yu, M.; Mikus, M. S.; Hoveyda, A. H. *Nature* **2015**, *517*, 181–186.

then allowed to stir at 4 °C for 2 hours. The reaction was then quenched by the addition of MeOH (1.5 mL) and allowed to stir for 0.5 h at 22 °C. The reaction mixture was then concentrated and the resulting opaque oil was purified by silica gel column chromatography (30 mL 10:1 hexanes:Et_2O → 4:1 hexanes:Et_2O), to afford a 94:6 *Z*:*E* mixture of ***Z*-3.42** (19.2 mg, 0.089 mmol, 89% yield), as colorless oil.

3.7.3. *Analytical Data for New Compounds*

(*R*,*Z*)-5,5,5-Trifluoro-1-phenylpent-3-en-1-ol (*Z*-3.42): IR (neat): 3375 (br, w), 2920 (w), 1671 (w), 1454 (w), 1418 (w), 1274 (m), 1226 (m), 1195 (m), 1112 (s), 1051 (m), 698 (s) cm^{-1}; **^{1}H NMR (400 MHz, $CDCl_3$):** δ 7.41 – 7.28 (m, 5H), 6.10 (dt, *J* = 11.7, 7.6 Hz, 1H), 5.70 (dqt, *J* = 11.9, 8.5, 1.8 Hz, 1H), 4.80 (dd, *J* = 7.6, 5.5 Hz, 1H), 2.86 – 2.68 (m, 2H), 1.99 (s, 1H); **^{13}C NMR (100 MHz, $CDCl_3$):** δ 143.4, 138.6 (q, *J* = 5.4 Hz), 128.8, 128.2, 125.9, 123.3 (q, *J* = 271.8 Hz), 120.4 (q, *J* = 33.4 Hz), 73.6, 37.7; **^{19}F NMR (376 MHz, $CDCl_3$):** δ –57.97 (3F, dt, *J* = 8.5, 2.2 Hz); **HRMS (DART):** Calcd for $C_{11}H_{10}F_3$ $[M+H–H_2O]^+$: 199.0735; Found: 199.0741; **Specific Rotation:** $[\alpha]^{20.0}_D$ +34.97° (*c* 0.74, $CHCl_3$) for a 95:5 er sample. Enantiomeric purity was determined by HPLC analysis in comparison with authentic racemic material (Chiralpak AD-H, 99.5:0.5 hexanes:*i*-PrOH, 1.0 mL/min, 220 nm): t_R: 68.8 min (major) and 64.1 min (minor).

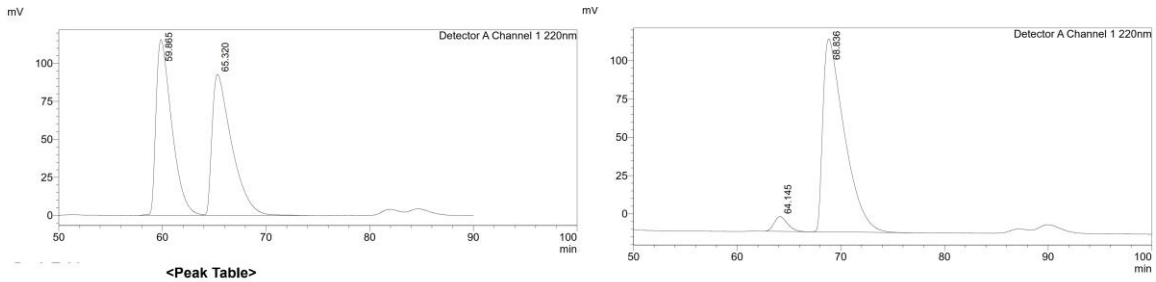

<Peak Table>
Detector A Channel 1 220nm

Peak#	Ret. Time	Height	Area	Area%
1	59.865	115796	12218876	49.924
2	65.320	92858	12256231	50.076
Total		208653	24475107	100.000

<Peak Table>
Detector A Channel 1 220nm

Peak#	Ret. Time	Area	Height	Conc.
1	64.145	856550	9611	4.501
2	68.836	18174970	125917	95.499
Total		19031520	135528	

Peak #	Ret. Time	Area	Area %	Peak #	Ret. Time	Area	Area %
1	59.865 min	12218876	49.924	1	64.145 min	856550	4.501
2	65.320 min	12256231	50.076	2	68.836 min	18174970	95.499

(*R*,*Z*)-5,5,5-Trifluoro-1-(o-tolyl)pent-3-en-1-ol (*Z*-3.55): IR (neat): 3365 (br, m), 2930 (w), 1670 (w), 1488 (w), 1461 (m), 1275 (m), 1228 (m), 1119 (s), 1049 (m), 758 (m), 729 (m) cm^{-1}; **^{1}H NMR (400 MHz, $CDCl_3$):** δ 7.50 (dd, *J* = 7.6, 1.5 Hz, 1H), 7.29 – 7.12 (m, 3H), 6.19 (dtd, *J* = 11.7, 7.7, 0.7 Hz, 1H), 5.78 – 5.65 (m, 1H), 5.05 (ddd, *J* = 8.0, 5.1, 3.2 Hz, 1H), 2.77 – 2.66 (m, 2H), 2.34 (s, 3H), 1.79 (d, *J* = 3.4 Hz, 1H); **^{13}C NMR (100 MHz, $CDCl_3$):** δ 141.6, 139.0 (q, *J* = 5.4 Hz), 134.5, 130.7, 127.8, 126.6, 125.2, 123.3 (q, *J* = 271.8 Hz), 120.3 (q, *J* = 33.4 Hz), 69.9, 36.5, 19.0; **^{19}F NMR (376 MHz, $CDCl_3$):** δ –59.09 (3F, dt, *J* = 8.4, 2.2 Hz); **HRMS (DART):** Calcd for $C_{12}H_{12}F_3$ $[M+H-H_2O]^+$: 213.0891; Found: 213.0886; **Specific Rotation:** $[\alpha]^{20.0}_D$ +59.9° (*c* 0.95, $CHCl_3$) for a 97:3 er sample. Enantiomeric purity was determined by HPLC analysis in comparison with authentic racemic material (Chiralcel OD-H, 99:1 hexanes:*i*-PrOH, 1.0 mL/min, 254 nm): t_R: 31.3 min (major) and 22.7 min (minor).

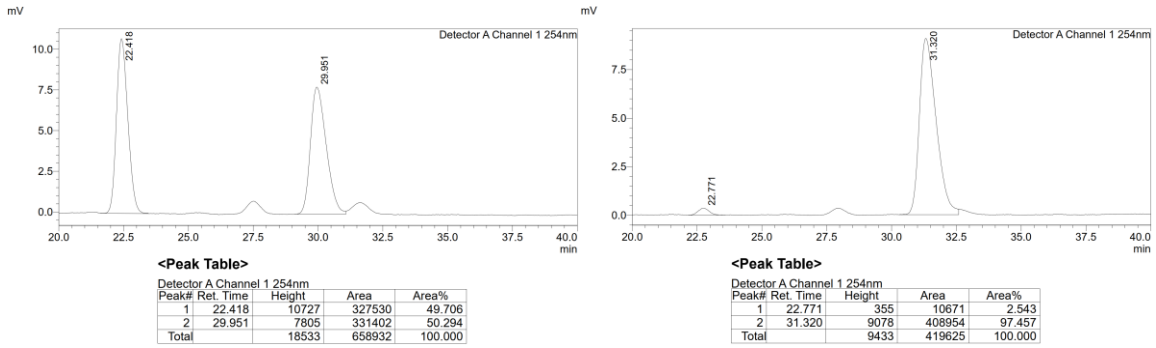

Peak #	Ret. Time	Area	Area %	Peak #	Ret. Time	Area	Area %
1	22.418 min	327530	49.706	1	22.771 min	10671	2.543
2	29.951 min	331402	50.294	2	31.320 min	408954	97.457

(*R*,*Z*)-1-(2-Bromophenyl)-5,5,5-trifluoropent-3-en-1-ol (*Z*-3.56): IR (neat): 3385 (br, m), 1671 (w), 1468 (w), 1419 (m), 1275 (m), 1224 (m), 1196 (m), 1117 (s), 1062 (m), 1045 (m), 1022 (m), 756 (m) cm^{-1}; **^{1}H NMR (400 MHz, $CDCl_3$):** δ 7.57 (dd, *J* = 7.8, 1.8 Hz, 1H), 7.54 (dd, *J* = 8.0, 1.2 Hz, 1H), 7.36 (tdd, *J* = 7.8, 1.2, 0.5 Hz, 1H), 7.16 (ddd, *J* = 7.9, 7.3, 1.7 Hz, 1H), 6.18 (dt, *J* = 11.7, 7.5 Hz, 1H), 5.78 – 5.68 (dqt, *J* = 12.0, 8.4, 1.8 Hz, 1H), 5.21 (dt, *J* = 8.0, 4.0 Hz, 1H), 2.89 – 2.79 (m, 1H), 2.79 – 2.67 (m, 1H), 2.02 (d, *J* = 3.7 Hz, 1H); **^{13}C NMR (100 MHz, $CDCl_3$):** δ 142.22, 138.27 (q, *J* = 5.4 Hz), 132.97, 129.43, 127.99, 123.21 (q, *J* = 271.7 Hz), 121.92, 120.68 (q, *J* = 33.5 Hz), 71.90, 36.01; **^{19}F NMR (376 MHz, $CDCl_3$):** δ –58.22 (3F, dt, *J* = 8.5, 2.1 Hz); **HRMS (DART):** Calcd for $C_{11}H_9BrF_3$ $[M+H–H_2O]^+$: 276.984; Found: 276.9834; **Specific Rotation:** $[\alpha]^{20.0}_D$ +59.6° (*c* 1.25, $CHCl_3$) for a 98:2 er sample. Enantiomeric purity was determined by HPLC analysis in comparison with authentic racemic material (Chiralpak AZ-H, 98:2 hexanes:*i*-PrOH, 1.0 mL/min, 220 nm): t_R: 8.7 min (major) and 10.2 min (minor).

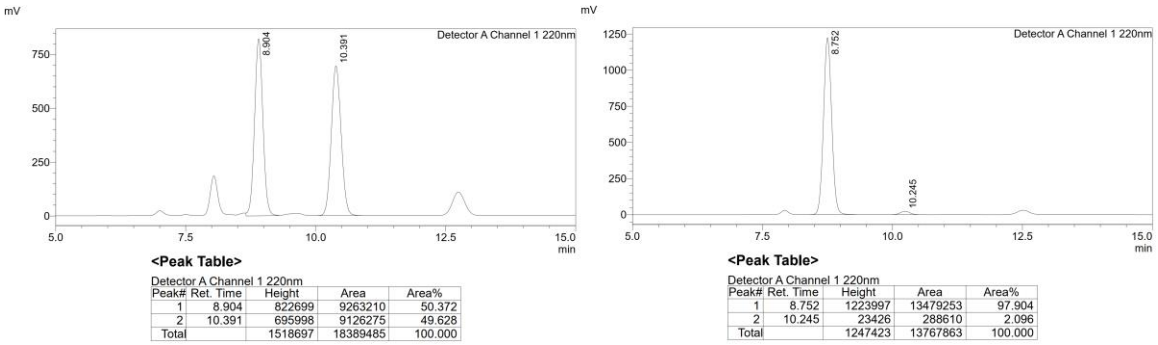

Peak #	Ret. Time	Area	Area %	Peak #	Ret. Time	Area	Area %
1	8.904 min	9263210	50.372	1	8.752 min	13479253	97.904
2	10.391 min	9126275	49.628	2	10.245 min	288610	2.096

(*R*,*Z*)-1-(3-Chlorophenyl)-5,5,5-trifluoropent-3-en-1-ol (*Z*-3.57): IR (neat): 3354 (br, m), 1671 (w), 1598 (w), 1576 (w), 1419 (m), 1276 (m), 1227 (m), 1197 (m), 1120 (s), 788 (m), 698 (m) cm^{-1}; **^{1}H NMR (400 MHz, $CDCl_3$):** δ 7.40 – 7.34 (m, 1H), 7.35 – 7.19 (m, 3H), 6.09 (dt, *J* = 11.7, 7.6 Hz, 1H), 5.77 – 5.67 (m, 1H), 4.87 – 4.74 (m, 1H), 2.77 – 2.72 (m, 2H), 1.93 (d, *J* = 3.6 Hz, 2H); **^{13}C NMR (100 MHz, $CDCl_3$):** δ 145.42, 138.02 (q, *J* = 5.3 Hz), 134.74, 130.09, 128.27, 126.07, 123.99, 123.2 (q, *J* = 270.0 Hz) 120.85 (q, *J* = 33.5 Hz), 72.90, 37.65; **^{19}F NMR (376 MHz, $CDCl_3$):** δ –58.26 (3F, dt, *J* = 8.5, 2.1 Hz); **HRMS (DART):** Calcd for $C_{11}H_9F_3Cl$ $[M+H–H_2O]^+$: 233.0345; Found: 233.0353; **Specific Rotation:** $[\alpha]^{20.0}_D$ +24.55° (*c* 1.00, $CHCl_3$) for a 98:2 er sample. Enantiomeric purity was determined by HPLC analysis in comparison with authentic racemic material (Chiralcel OJ-H, 98:2 hexanes:*i*-PrOH, 1.0 mL/min, 220 nm): t_R: 23.3 min (major) and 20.1 min (minor).

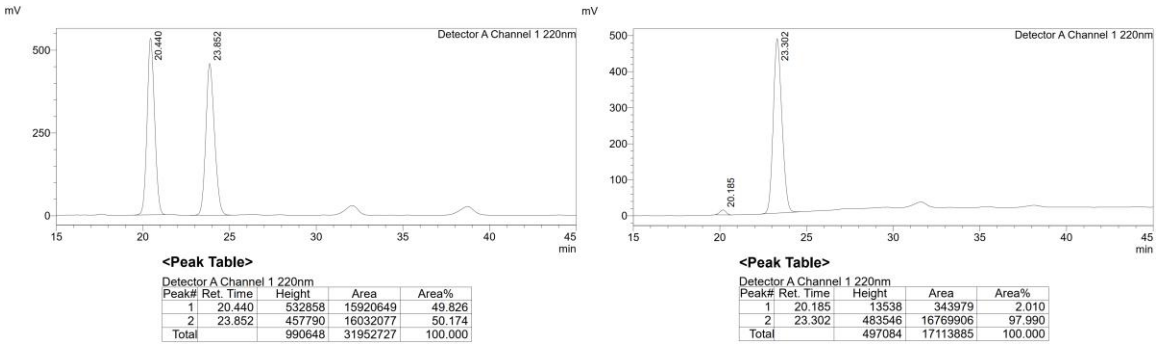

Peak #	Ret. Time	Area	Area %	Peak #	Ret. Time	Area	Area %
1	20.440 min	15920649	49.826	1	20.185 min	343979	2.010
2	23.852 min	16032077	50.174	2	23.302 min	16769906	97.990

(*R*,*Z*)-5,5,5-Trifluoro-1-(3-methoxyphenyl)pent-3-en-1-ol (*Z*-3.58): IR (neat): 3406 (br, m), 1602 (w), 1587 (w), 1488 (w), 1419 (w), 1268 (m), 1118 (s), 1043 (m), 871 (w), 699 (w) cm^{-1}; **^{1}H NMR (400 MHz, $CDCl_3$):** δ 7.33 – 7.26 (m, 1H), 6.99 – 6.90 (m, 2H), 6.89 – 6.80 (m, 1H), 6.10 (dt, *J* = 11.7, 7.6 Hz, 1H), 5.77 – 5.63 (m, 1H), 4.81 – 4.77 (m, 1H), 3.82 (d, *J* = 0.9 Hz, 3H), 2.83 – 2.72 (m, 2H), 1.89 (d, *J* = 3.5 Hz, 1H); **^{13}C NMR (100 MHz, $CDCl_3$):** δ 160.0, 145.1, 138.6 (q, *J* = 5.4 Hz), 129.9, 123.3 (q, *J* = 271.8 Hz), 120.4 (q, *J* = 33.4 Hz), 118.1, 113.5, 111.4, 73.5, 55.4, 37.6; **^{19}F NMR (376 MHz, $CDCl_3$):** δ –58.25 (3F, dt, *J* = 8.5, 2.2 Hz); **HRMS (DART):** Calcd for $C_{12}H_{12}F_3O$ $[M+H–H_2O]^+$: 229.084; Found: 229.085; **Specific Rotation:** $[\alpha]^{20.0}_D$ +15.2° (*c* 1.39, $CHCl_3$) for a 97:3 er sample. Enantiomeric purity was determined by HPLC analysis in comparison with authentic racemic material (Chiralcel OJ-H, 98:2 hexanes:*i*-PrOH, 1.0 mL/min, 220 nm): t_R: 30.9 min (major) and 32.6 min (minor).

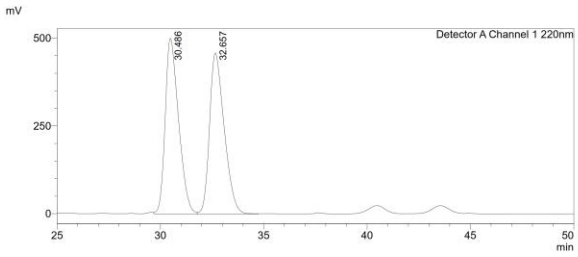

<Peak Table>
Detector A Channel 1 220nm

Peak#	Ret. Time	Height	Area	Area%
1	30.486	500336	22474231	49.830
2	32.657	458433	22627254	50.170
Total		958769	45101485	100.000

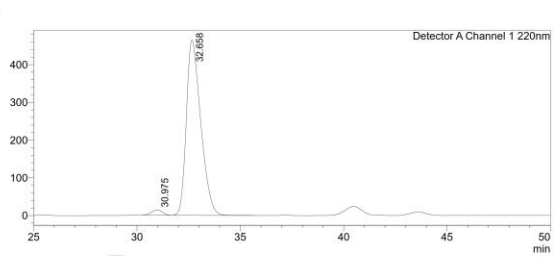

<Peak Table>
Detector A Channel 1 220nm

Peak#	Ret. Time	Height	Area	Area%
1	30.975	13666	490854	2.139
2	32.658	464694	22462335	97.861
Total		478360	22953190	100.000

Peak #	Ret. Time	Area	Area %	Peak #	Ret. Time	Area	Area %
1	30.486 min	22474231	49.830	1	30.975 min	490854	2.139
2	32.657 min	22627254	50.170	2	32.658 min	22462335	97.861

(*R*,*Z*)-1-(6-Bromonaphthalen-2-yl)-5,5,5-trifluoropent-3-en-1-ol (*Z*-3.59): IR (neat): 3367 (br, m), 1671 (w), 1591 (w), 1418 (w), 1275 (m), 1228 (w), 1118 (s), 1062 (m), 877 (m), 807 (m) cm^{-1}; **^{1}H NMR (400 MHz, $CDCl_3$):** δ 8.02 – 7.98 (m, 1H), 7.78 – 7.72 (m, 2H), 7.69 (d, *J* = 8.7 Hz, 1H), 7.56 (dd, *J* = 8.7, 2.0 Hz, 1H), 7.49 (dd, *J* = 8.5, 1.8 Hz, 1H), 6.11 (dt, *J* = 11.7, 7.6 Hz, 1H), 5.76 – 7.66 (m, 1H), 4.96 (dd, *J* = 7.3, 5.7 Hz, 1H), 2.91 – 2.78 (m, 2H), 2.11 (s, 1H); **^{13}C NMR (100 MHz, $CDCl_3$):** δ 141.24, 138.27 (q, *J* = 5.4 Hz), 134.27, 131.76, 129.92, 129.89, 129.75, 127.80, 124.89, 124.63, 123.2 (q, *J* = 270 Hz), 120.7 (q, *J* = 33.3 Hz), 120.22, 73.47, 37.54; **^{19}F NMR (376 MHz, $CDCl_3$):** δ –59.13 (3F ,dt, *J* = 8.4, 2.2 Hz); **HRMS (DART):** Calcd for $C_{15}H_{11}BrF_3$ $[M+H–H_2O]^+$: 326.9996; Found: 327.0002; **Specific Rotation:** $[\alpha]^{20.0}_D$ +21.9° (*c* 1.50, $CHCl_3$) for a 98:2 er sample. Enantiomeric purity was determined by HPLC analysis in comparison with authentic racemic material (Chiralcel OD-H, 98:2 hexanes:*i*-PrOH, 1.0 mL/min, 254 nm): t_R: 57.9 min (major) and 29.2 min (minor).

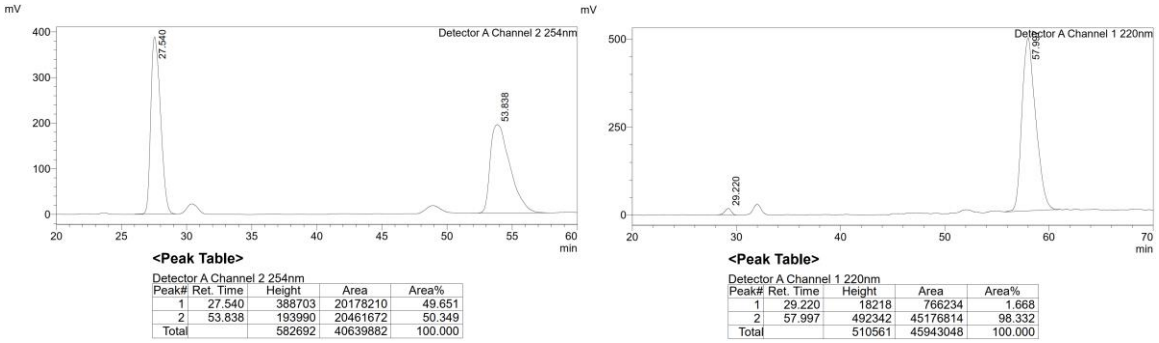

Peak #	Ret. Time	Area	Area %	Peak #	Ret. Time	Area	Area %
1	27.540 min	20178210	49.651	1	29.220 min	766234	1.668
2	53.838 min	20461672	50.349	2	57.997 min	45176814	98.332

(*R*,*Z*)-5,5,5-Trifluoro-1-(4-nitrophenyl)pent-3-en-1-ol (*Z*-3.60): IR (neat): 3444 (br, m), 1671 (w), 1605 (w), 1519 (s), 1418 (w), 1346 (s), 1276 (m), 1226 (m), 1198 (m), 1118 (s), 1013 (m), 856 (m) cm^{-1}; **^{1}H NMR (400 MHz, $CDCl_3$):** δ 8.33 – 8.11 (m, 1H), 7.61 – 7.43 (m, 1H), 6.10 (dt, *J* = 11.7, 7.7 Hz, 1H), 5.79 – 5.69 (m, 1H), 4.97 (t, *J* = 6.3 Hz, 1H), 2.79 – 2.74 (m, 1H), 2.24 (s, 1H); **^{13}C NMR (100 MHz, $CDCl_3$):** δ 150.5, 147.6, 137.3 (q, *J* = 5.4 Hz), 126.6, 123.9, 123.0 (q, *J* = 271.9 Hz), 121.3 (q, *J* = 33.5 Hz), 72.5, 37.7; **^{19}F NMR (376 MHz, $CDCl_3$):** δ –58.27 (3F, dt, *J* = 8.5, 2.1 Hz); **HRMS (DART):** Calcd for $C_{11}H_{11}F_3NO_3$ $[M+H]^+$: 262.0691; Found: 262.0694; **Specific Rotation:** $[\alpha]^{20.0}_D$ +16.9° (*c* 1.21, $CHCl_3$) for a 98:2 er sample. Enantiomeric purity was determined by HPLC analysis in comparison with authentic racemic material (Chiralpak AZ-H, 98:2 hexanes:*i*-PrOH, 1.0 mL/min, 254 nm): t_R: 23.6 min (major) and 22.0 min (minor).

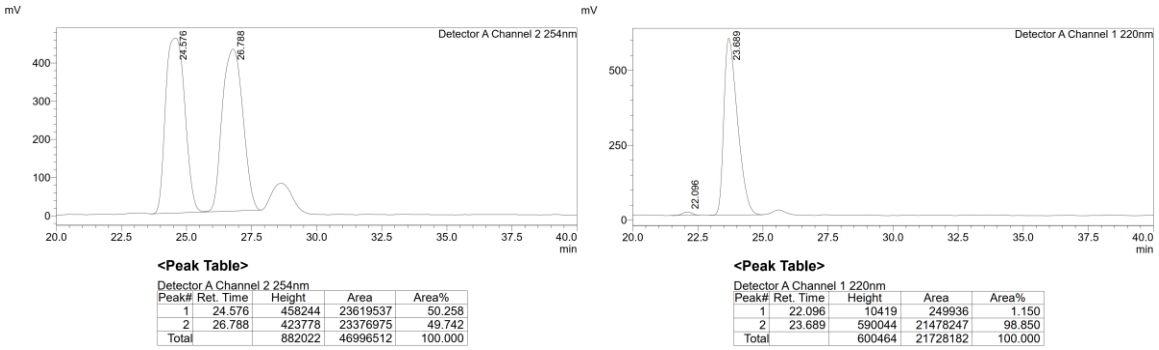

<Peak Table>
Detector A Channel 2 254nm

Peak#	Ret. Time	Height	Area	Area%
1	24.576	458244	23619537	50.258
2	26.788	423778	23376975	49.742
Total		882022	46996512	100.000

<Peak Table>
Detector A Channel 1 220nm

Peak#	Ret. Time	Height	Area	Area%
1	22.096	10419	249936	1.150
2	23.689	590044	21478247	98.850
Total		600464	21728182	100.000

Peak #	Ret. Time	Area	Area %	Peak #	Ret. Time	Area	Area %
1	24.576 min	23619537	50.258	1	22.096 min	249936	1.150
2	26.788 min	23376975	49.742	2	23.689 min	21478247	98.850

(*R*,*Z*)-5,5,5-Trifluoro-1-(4-methoxyphenyl)pent-3-en-1-ol (*Z*-3.61): IR (neat): 3415 (br, m), 2916 (w), 1670 (w), 1612 (w), 1513 (m), 1418 (w), 1247 (m), 1176 (m), 1118 (s), 1034 (m), 833 (m) cm^{-1}; **^{1}H NMR (400 MHz, $CDCl_3$):** δ 7.36 – 7.20 (m, 2H), 6.94 – 6.85 (m, 2H), 6.08 (dt, *J* = 11.7, 7.6 Hz, 1H), 5.73 – 5.63 (m, 1H), 4.75 (ddd, *J* = 8.2, 5.4, 3.2 Hz, 1H), 3.81 (s, 3H), 2.89 – 2.63 (m, 2H), 1.89 (d, *J* = 3.3 Hz, 1H); **^{13}C NMR (100 MHz, $CDCl_3$):** δ 159.5, 138.7 (q, *J* = 5.4 Hz), 135.5, 127.1, 123.2 (q, *J* = 271.7 Hz), 120.2 (q, *J* = 33.4 Hz), 114.1, 73.2, 55.4, 37.6; **^{19}F NMR (376 MHz, $CDCl_3$):** δ –58.27 (dt, *J* = 8.5, 2.2 Hz); **HRMS (DART):** Calcd for $C_{12}H_{12}F_3O$ $[M+H–H_2O]^+$: 229.084; Found: 229.085; **Specific Rotation:** $[\alpha]^{20.0}_D$ +32.9° (*c* 0.9, $CHCl_3$) for a 95.5:9.5 er sample. Enantiomeric purity was determined by HPLC analysis in comparison with authentic racemic material (Chiralcel OZ-H, 98:2 hexanes:*i*-PrOH, 1.0 mL/min, 220 nm): t_R: 14.9 min (major) and 17.7 min (minor).

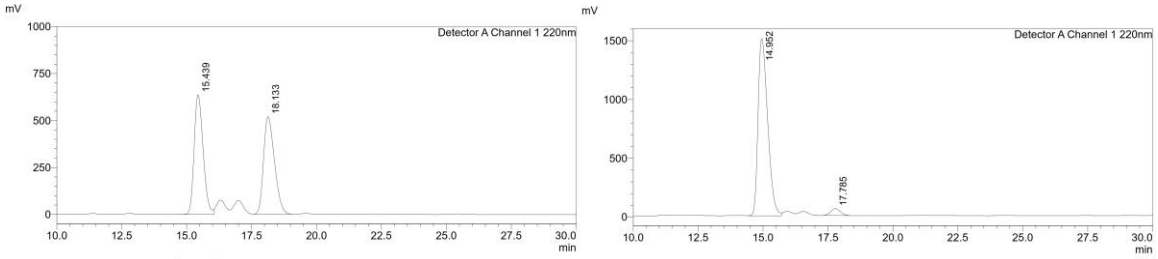

<Peak Table>
Detector A Channel 1 220nm

Peak#	Ret. Time	Height	Area	Area%
1	15.439	636721	15348205	50.272
2	18.133	519008	15182406	49.728
Total		1155728	30530611	100.000

<Peak Table>
Detector A Channel 1 220nm

Peak#	Ret. Time	Height	Area	Area%
1	14.952	1508602	38649704	96.232
2	17.785	58503	1513218	3.768
Total		1567105	40162922	100.000

Peak #	Ret. Time	Area	Area %	Peak #	Ret. Time	Area	Area %
1	15.439 min	15348205	50.272	1	14.952 min	38649704	96.232
2	18.133 min	15182406	49.728	2	17.785 min	1513218	3.768

(*R*,*Z*)-5,5,5-Trifluoro-1-(pyridin-3-yl)pent-3-en-1-ol (*Z*-3.62): IR (neat): 3192 (br, m), 2917 (w), 1671 (w), 1422 (m), 1320 (m), 1277 (m), 1118 (s), 1070 (m), 1029 (w), 714 (m) cm^{-1}; **^{1}H NMR (400 MHz, $CDCl_3$):** δ 8.56 – 8.31 (m, 2H), 7.72 (dt, *J* = 7.9, 2.1 Hz, 1H), 7.28 (ddd, *J* = 7.9, 4.9, 0.9 Hz, 1H), 6.10 (dt, *J* = 11.7, 7.6 Hz, 1H), 5.76 – 5.65 (m, 1H), 4.84 (dd, *J* = 7.4, 5.6 Hz, 1H), 3.82 (s, 1H), 2.83 – 2.68 (m, 2H); **^{13}C NMR (100 MHz, $CDCl_3$):** δ 149.0, 147.4, 139.3, 137.8 (q, *J* = 5.2 Hz), 133.9, 123.8, 123.1 (q, *J* = 271.8 Hz), 120.8 (q, *J* = 34.0 Hz), 70.9, 37.6; **^{19}F NMR (376 MHz, $CDCl_3$):** δ –58.31 (3F, dt, *J* = 8.4, 2.1 Hz); **HRMS (DART):** Calcd for $C_{10}H_{11}F_3NO$ $[M+H]^+$: 218.0793; Found: 218.0793; **Specific Rotation:** $[\alpha]^{20.0}_D$ +46.1° (*c* 0.54, $CHCl_3$) for a 93:7 er sample. Enantiomeric purity was determined by HPLC analysis in comparison with authentic racemic material (Chiralpak AZ-H, 95:5 hexanes:*i*-PrOH, 1.0 mL/min, 254 nm): t_R: 31.9 min (major) and 27.0 min (minor).

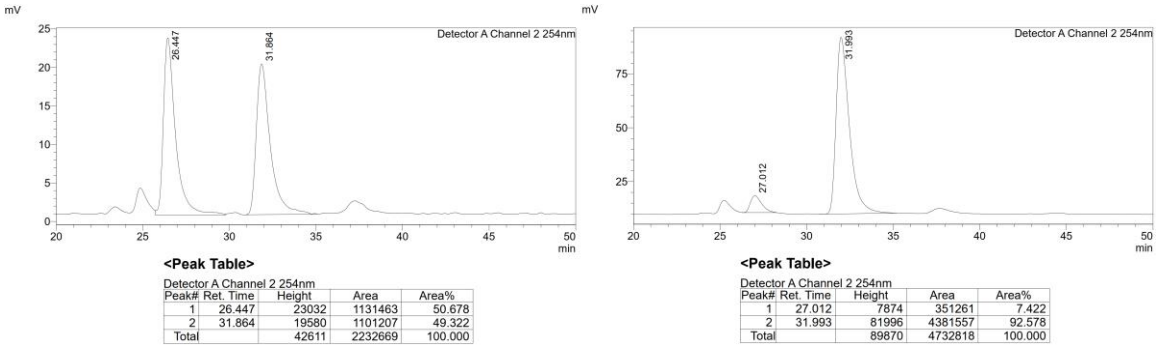

Peak #	Ret. Time	Area	Area %	Peak #	Ret. Time	Area	Area %
1	26.447 min	1131463	50.678	1	27.012 min	351261	7.422
2	31.864 min	1101207	49.322	2	31.993 min	4381557	92.578

(*R*,*Z*)-5,5,5-Trifluoro-1-(furan-2-yl)pent-3-en-1-ol (*Z*-3.63): IR (neat): 3373 (br, m), 1672 (w), 1420 (w), 1329 (m), 1278 (m), 1118 (s), 1011 (m), 740 (m) cm^{-1}; **^{1}H NMR (400 MHz, $CDCl_3$):** δ 7.39 (dd, *J* = 1.8, 0.8 Hz, 1H), 6.35 (dd, *J* = 3.2, 1.8 Hz, 1H), 6.27 (dt, *J* = 3.2, 0.7 Hz, 1H), 6.10 (dt, *J* = 11.7, 7.4 Hz, 1H), 5.79 – 5.66 (m, 1H), 4.84 – 4.78 (m, 1H), 2.93 – 2.83 (m, 2H), 2.04 (d, *J* = 5.2 Hz, 1H); **^{13}C NMR (100 MHz, $CDCl_3$):** δ 155.3, 142.5, 137.8 (q, *J* = 5.5 Hz), 123.2 (q, *J* = 270 Hz), 120.6 (q, *J* = 33.5 Hz), 110.4, 106.6, 66.8, 37.6; **^{19}F NMR (376 MHz, $CDCl_3$):** δ –58.43 (3F, dt, *J* = 8.5, 2.3 Hz); **HRMS (DART):** Calcd for $C_9H_8F_3O$ $[M+H–H_2O]^+$: 189.0527.0891; Found: 189.0532; **Specific Rotation:** $[\alpha]^{20.0}_D$ +10.9° (*c* 0.74, $CHCl_3$) for a 93:7 er sample. Enantiomeric purity was determined by HPLC analysis in comparison with authentic racemic material (Chiralcel OJ-H, 98:2 hexanes:*i*-PrOH, 1.0 mL/min, 220 nm): t_R: 20.3 min (major) and 19.0 min (minor).

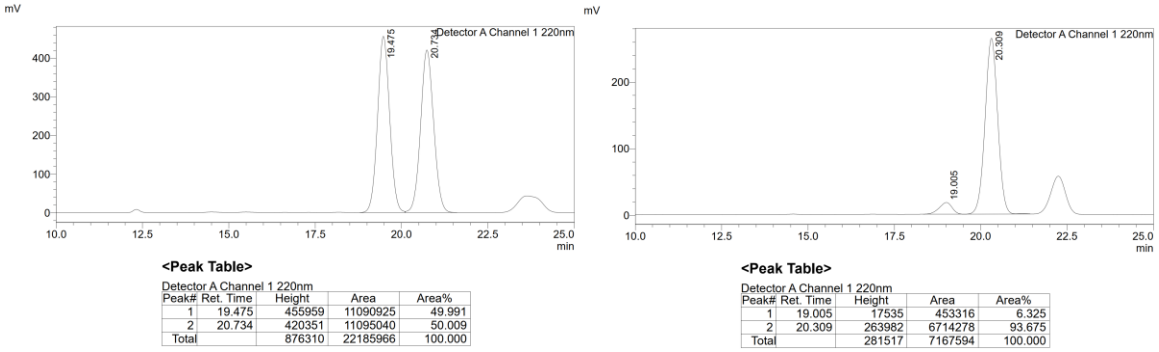

<Peak Table>
Detector A Channel 1 220nm

Peak#	Ret. Time	Height	Area	Area%
1	19.475	455959	11090925	49.991
2	20.734	420351	11095040	50.009
Total		876310	22185966	100.000

<Peak Table>
Detector A Channel 1 220nm

Peak#	Ret. Time	Height	Area	Area%
1	19.005	17535	453316	6.325
2	20.309	263982	6714278	93.675
Total		281517	7167594	100.000

Peak #	Ret. Time	Area	Area %	Peak #	Ret. Time	Area	Area %
1	19.475 min	11090925	49.991	1	19.005 min	453316	6.325
2	20.734 min	11095040	50.009	2	20.309 min	6714278	93.675

(*R*,*Z*)-5,5,5-Trifluoro-1-(furan-3-yl)pent-3-en-1-ol (*Z*-3.64): IR (neat): 3375 (br, m), 2922 (w), 1672 (w), 1504 (w), 1420 (w), 1278 (m), 1229 (m), 1198 (m), 1119 (s), 1020 (m), 874 (m), 798 (m) cm^{-1}; **^{1}H NMR (400 MHz, $CDCl_3$):** δ 7.44 – 7.38 (m, 2H), 6.41 (dd, *J* = 1.8, 1.0 Hz, 1H), 6.10 (dt, *J* = 11.8, 7.5 Hz, 1H), 5.79 – 5.64 (m, 1H), 4.80 (td, *J* = 6.5, 4.2 Hz, 1H), 2.86 – 2.69 (m, 2H), 1.79 (d, *J* = 4.4 Hz, 1H); **^{13}C NMR (100 MHz, $CDCl_3$):** δ 143.8, 139.3, 138.2 (q, *J* = 5.4 Hz), 128.1, 123.2 (q, *J* = 271.7 Hz), 120.5 (q, *J* = 33.5 Hz), 108.4, 66.1, 36.4; **^{19}F NMR (376 MHz, $CDCl_3$):** δ –58.35 (3F, dt, *J* = 8.5, 2.3 Hz); **HRMS (DART):** Calcd for $C_9H_8F_3O$ $[M+H–H_2O]^+$: 189.0527; Found: 189.0526; **Specific Rotation:** $[\alpha]^{20.0}_D$ +17.2° (*c* 0.2, $CHCl_3$) for a 97:3 er sample. Enantiomeric purity was determined by HPLC analysis in comparison with authentic racemic material (Chiralpak AD-H, 98:2 hexanes:*i*-PrOH, 1.0 mL/min, 220 nm): t_R: 22.4 min (major) and 21.3 min (minor).

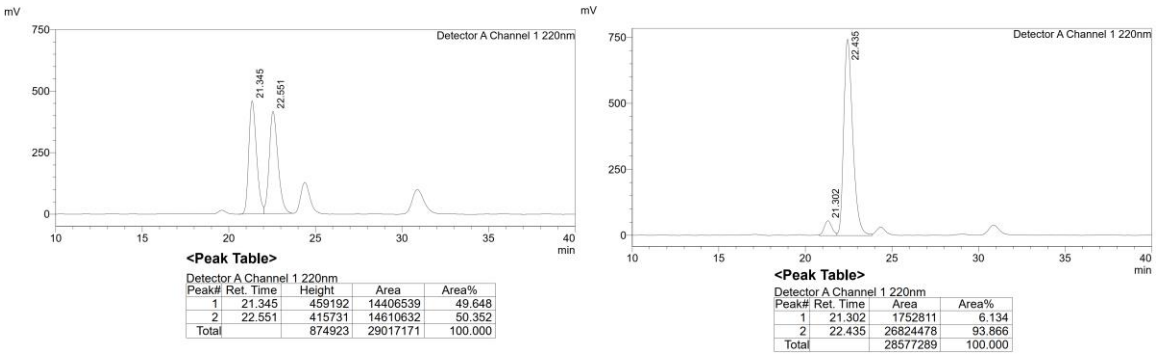

Peak #	Ret. Time	Area	Area %	Peak #	Ret. Time	Area	Area %
1	21.345 min	14406539	49.648	1	21.302 min	1752811	6.134
2	22.551 min	14610632	50.352	2	22.435 min	26824478	93.866

(*R*,*Z*)-1-(Benzofuran-2-yl)-5,5,5-trifluoropent-3-en-1-ol (*Z*-3.65): IR (neat): 3364 (br, m), 1672 (w), 1454 (m), 1420 (w), 1278 (m), 1253 (m), 1229 (m), 1120 (s), 1072 (m), 880 (w), 810 (m), 750 (m) cm^{-1}; **^{1}H NMR (400 MHz, $CDCl_3$):** δ 7.56 (dd, *J* = 7.8, 1.1 Hz, 1H), 7.47 (dd, *J* = 8.1, 0.9 Hz, 1H), 7.32 – 7.27 (m, 1H), 7.24 (td, *J* = 7.5, 1.2 Hz, 1H), 6.66 (s, 1H), 6.15 (dt, *J* = 11.7, 7.4 Hz, 1H), 5.83 – 5.67 (m, 1H), 4.96 (dt, *J* = 7.1, 5.5 Hz, 1H), 3.05 – 2.92 (m, 2H), 2.22 (d, *J* = 5.3 Hz, 1H); **^{13}C NMR (100 MHz, $CDCl_3$):** δ 157.8, 154.9, 137.4 (q, *J* = 5.4 Hz), 128.0, 124.6, 123.2 (q, *J* = 271.8 Hz), 123.1, 121.3, 120.9 (q, *J* = 33.5 Hz), 111.4, 103.3, 67.3, 34.2; **^{19}F NMR (376 MHz, $CDCl_3$):** δ –58.37 (3F, dt, *J* = 8.5, 2.2 Hz); **HRMS (ESI+):** Calcd for $C_{13}H_{10}F_3O$ $[M+H–H_2O]^+$: 239.068374; Found: 239.068298; **Specific Rotation:** $[\alpha]^{20.0}_D$ +11.3° (*c* 1.14, $CHCl_3$) for a 95:5 er sample. Enantiomeric purity was determined by HPLC analysis in comparison with authentic racemic material (Chiralcel OZ-H, 98:2 hexanes:*i*-PrOH, 1.0 mL/min, 254 nm): t_R: 14.7 min (major) and 11.7 min (minor).

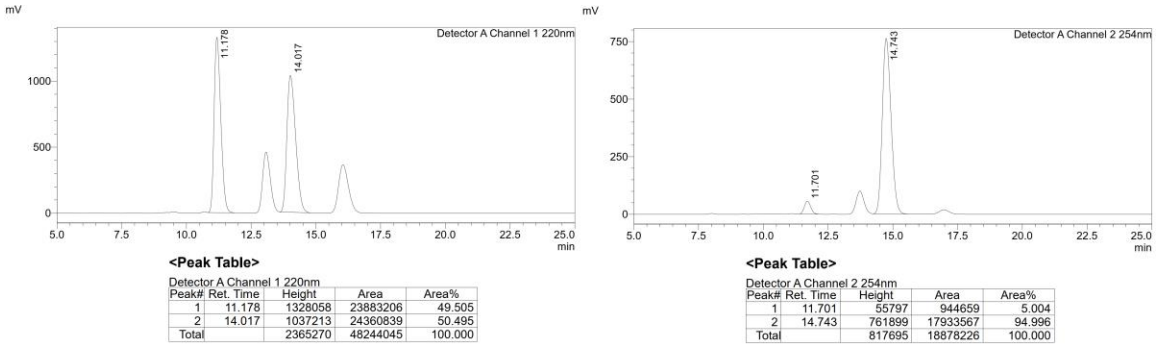

<Peak Table>
Detector A Channel 1 220nm

Peak#	Ret. Time	Height	Area	Area%
1	11.178	1328058	23883206	49.505
2	14.017	1037213	24360839	50.495
Total		2365270	48244045	100.000

<Peak Table>
Detector A Channel 2 254nm

Peak#	Ret. Time	Height	Area	Area%
1	11.701	55797	944659	5.004
2	14.743	761899	17933567	94.996
Total		817695	18878226	100.000

Peak #	Ret. Time	Area	Area %	Peak #	Ret. Time	Area	Area %
1	11.178 min	23883206	49.505	1	11.701 min	944659	5.004
2	14.017 min	24360839	50.495	2	14.743 min	17933567	94.996

***tert*-Butyl (*R*,*Z*)-3-(5,5,5-trifluoro-1-hydroxypent-3-en-1-yl)-1H-indole-1-carboxylate (*Z*-3.66): IR (neat):** 3409 (br, m), 2981 (w), 1734 (s), 1453 (s), 1371 (s), 1271 (m), 1256 (m), 1225 (m), 1154 (s), 1139 (s), 1120 (s), 1089 (m), 766 (w), 746 (m) cm^{-1}; **^{1}H NMR (400 MHz, $CDCl_3$):** δ 8.16 (d, *J* = 8.3 Hz, 1H), 7.68 – 7.63 (m, 1H), 7.57 (s, 1H), 7.35 (ddd, *J* = 8.4, 7.2, 1.3 Hz, 1H), 7.28 – 7.24 (m, 1H), 6.18 (dt, *J* = 11.7, 7.5 Hz, 1H), 5.79 – 5.68 (m, 1H), 5.09 (td, *J* = 6.3, 3.1 Hz, 1H), 2.99 – 2.94 (m, 2H), 1.95 (d, *J* = 3.6 Hz, 1H), 1.68 (s, 9H); **^{13}C NMR (150 MHz, $CDCl_3$):** δ 149.7, 138.5 (q, *J* = 5.4 Hz), 136.0, 128.3, 124.9, 123.32 (q, *J* = 271.8 Hz, one peak overlapping at 120.62), 122.9, 122.7, 120.5 (q, *J* = 33.5 Hz), 119.6, 115.6, 84.1, 67.1, 35.9, 28.3; **^{19}F NMR (376 MHz, $CDCl_3$):** δ –58.21 (dd, *J* = 8.4, 1.6 Hz); **HRMS (DART):** Calcd for $C_{18}H_{19}F_3NO_2$ $[M+H–H_2O]^+$: 338.1368; Found: 338.1371; **Specific Rotation:** $[\alpha]^{20.0}_D$ +20.8° (*c* 0.77, $CHCl_3$) for a 94:6 er sample. Enantiomeric purity was determined by HPLC analysis in comparison with authentic racemic material (Chiralpak AD-H, 98:2 hexanes:*i*-PrOH, 1.0 mL/min, 220 nm): t_R: 19.8 min (major) and 19.0 min (minor).

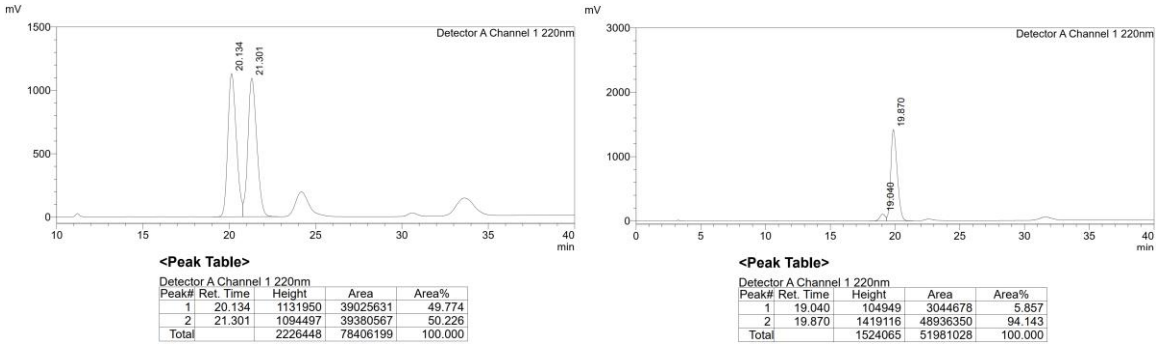

Peak #	Ret. Time	Area	Area %	Peak #	Ret. Time	Area	Area %
1	20.134 min	39025631	49.774	1	19.040 min	3044678	5.857
2	21.301 min	39380567	50.226	2	19.870 min	48936350	94.143

(*R*,*Z*)-7,7,7-Trifluoro-1-phenylhept-5-en-1-yn-3-ol (*Z*-3.67): IR (neat): 3359 (br, m), 1672 (w), 1492 (w), 1419 (w), 1277 (m), 1228 (m), 1120 (s), 1041 (m), 966 (m), 756 (m), 722 (m) cm^{-1}; **^{1}H NMR (400 MHz, $CDCl_3$):** δ 7.46 – 7.39 (m, 2H), 7.37 – 7.29 (m, 3H), 6.25 (dt, *J* = 11.8, 7.5 Hz, 1H), 5.89 – 5.70 (m, 1H), 4.74 (app q, *J* = 5.9 Hz, 1H), 2.86 – 2.82 (m, 2H), 1.96 (d, *J* = 5.3 Hz, 1H); **^{13}C NMR (100 MHz, $CDCl_3$):** δ 172.1, 137.1 (q, *J* = 5.4 Hz), 131.8, 128.8, 128.4, 123.2 (q, *J* = 271.9 Hz), 121.1 (q, *J* = 33.6 Hz), 88.4, 86.1, 61.7, 36.5; **^{19}F NMR (376 MHz, $CDCl_3$):** δ –59.26 (3F, dt, *J* = 8.5, 2.1 Hz); **HRMS (DART):** Calcd for $C_{13}H_{10}F_3$ $[M+H–H_2O]^+$: 223.0735; Found: 223.0735; **Specific Rotation:** $[\alpha]^{20.0}_D$ –3.4° (*c* 1.1, $CHCl_3$) for a 97:3 er sample. Enantiomeric purity was determined by HPLC analysis in comparison with authentic racemic material (Chiralpak AY-3, 99:1 hexanes:*i*-PrOH, 1.0 mL/min, 254 nm): t_R: 16.7 min (major) and 15.5 min (minor).

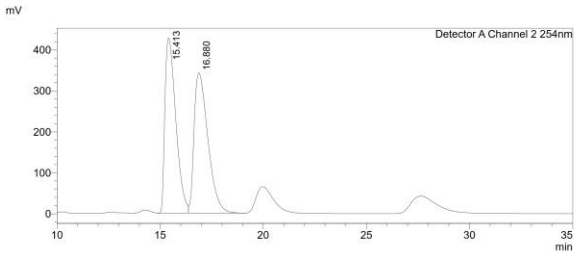

<Peak Table>
Detector A Channel 2 254nm

Peak#	Ret. Time	Height	Area	Area%
1	15.413	427350	15667125	49.536
2	16.880	342258	15960613	50.464
Total		769608	31627738	100.000

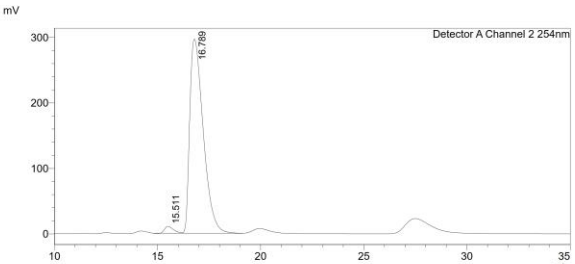

<Peak Table>
Detector A Channel 2 254nm

Peak#	Ret. Time	Area	Height	Conc.
1	15.511	312897	10524	2.267
2	16.789	13489402	296461	97.733
Total		13802299	306985	

Peak #	Ret. Time	Area	Area %	Peak #	Ret. Time	Area	Area %
1	15.413 min	15667125	49.536	1	15.511 min	312897	2.267
2	16.880 min	15960613	50.464	2	16.789 min	13489402	97.733

(*R*,1*E*,5*Z*)-7,7,7-Trifluoro-1-phenylhepta-1,5-dien-3-ol (*Z*-3.68): IR (neat): 3361 (br, m), 1670 (w), 1418 (w), 1275 (m), 1227 (m), 1193 (m), 1118 (s), 1071 (m), 1043 (m), 966 (m), 750 (m), 693 (m) cm^{-1}; **^{1}H NMR (400 MHz, $CDCl_3$):** 7.42 – 7.30 (m, 4H), 7.29 – 7.23 (m, 1H), 6.63 (dd, *J* = 15.9, 1.2 Hz, 1H), 6.23 (dd, *J* = 15.9, 6.6 Hz, 1H), 6.16 (dt, *J* = 11.7, 7.6 Hz, 1H), 5.79 – 5.68 (m, 1H), 4.44 (app q, *J* = 6.5 Hz, 1H), 2.72 – 2.64 (m, 2H), 1.71 (s, 1H); **^{13}C NMR (100 MHz, $CDCl_3$):** 138.2 (q, *J* = 5.3 Hz), 136.3, 131.4, 130.9, 128.8, 128.1, 126.7, 123.2 (q, *J* = 271.8 Hz), 120.5 (q, *J* = 33.4 Hz), 71.9, 35.9; **^{19}F NMR (564 MHz, $CDCl_3$):** δ –58.20 (3F, dt, *J* = 8.5, 2.4 Hz); **HRMS (DART):** Calcd for $C_{13}H_{12}F_3$ $[M+H–H_2O]^+$: 225.0891; Found: 225.088; **Specific Rotation:** $[\alpha]^{20.0}_D$ –14.3° (*c* 0.25, $CHCl_3$) for a 97:3 er sample. Enantiomeric purity was determined by HPLC analysis in comparison with authentic racemic material (Chiralcel OD-H, 98:2 hexanes:*i*-PrOH, 1.0 mL/min, 220 nm): t_R: 33.0 min (major) and 68.4 min (minor).

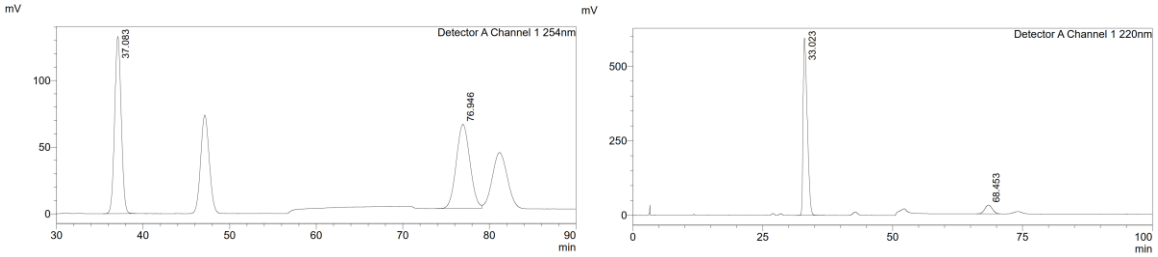

<Peak Table>
Detector A Channel 1 254nm

Peak#	Ret. Time	Height	Area	Area%
1	37.083	132889	7009204	50.208
2	76.946	63165	6951068	49.792
Total		196054	13960272	100.000

<Peak Table>
Detector A Channel 1 220nm

Peak#	Ret. Time	Height	Area	Area%
1	33.023	594760	32907283	91.776
2	68.453	29193	2948934	8.224
Total		623953	35856217	100.000

Peak #	Ret. Time	Area	Area %	Peak #	Ret. Time	Area	Area %
1	37.083 min	7009204	50.208	1	33.023 min	32907283	91.776
2	76.946 min	6951068	49.792	2	68.453 min	2948934	8.224

(*R*,1*Z*,5*Z*)-2-Bromo-7,7,7-trifluoro-1-phenylhepta-1,5-dien-3-ol (*Z*-3.69): IR (neat): 3386 (br, m), 1672 (w), 1429 (w), 1446 (w), 1418 (w), 1276 (m), 1228 (m), 1195 (m), 1119 (s), 1074 (m), 1050 (m), 754 (m), 693 (m) cm^{-1}; **^{1}H NMR (400 MHz, $CDCl_3$):** δ 7.66 – 7.58 (m, 2H), 7.43 – 7.32 (m, 3H), 7.12 (s, 1H), 6.12 (dt, *J* = 11.7, 7.6 Hz, 1H), 5.83 – 5.71 (m, 1H), 4.43 – 4.37 (m, 1H), 2.89 – 2.76 (m, 2H), 2.22 (d, *J* = 5.8 Hz, 1H); **^{13}C NMR (100 MHz, $CDCl_3$):** δ 137.3 (q, *J* = 5.4 Hz), 134.7, 129.2, 128.9, 128.5, 128.3, 128.3, 123.2 (q, *J* = 271.9 Hz), 120.9 (q, *J* = 33.6 Hz), 76.5, 34.7; **^{19}F NMR (376 MHz, $CDCl_3$):** δ –58.24 (3F, dt, *J* = 8.5, 2.1 Hz); **HRMS (ESI+):** Calcd for $C_{13}H_{11}BrF_3$ $[M+H–H_2O]^+$: 302.999620; Found: 302.999298; **Specific Rotation:** $[\alpha]^{20.0}_D$ –10.9° (*c* 1.37, $CHCl_3$) for a 98.5:1.5 er sample. Enantiomeric purity was determined by HPLC analysis in comparison with authentic racemic material (Chiralcel OJ-H, 98:2 hexanes:*i*-PrOH, 1.0 mL/min, 254 nm): t_R: 41.0 min (major) and 38.6 min (minor).

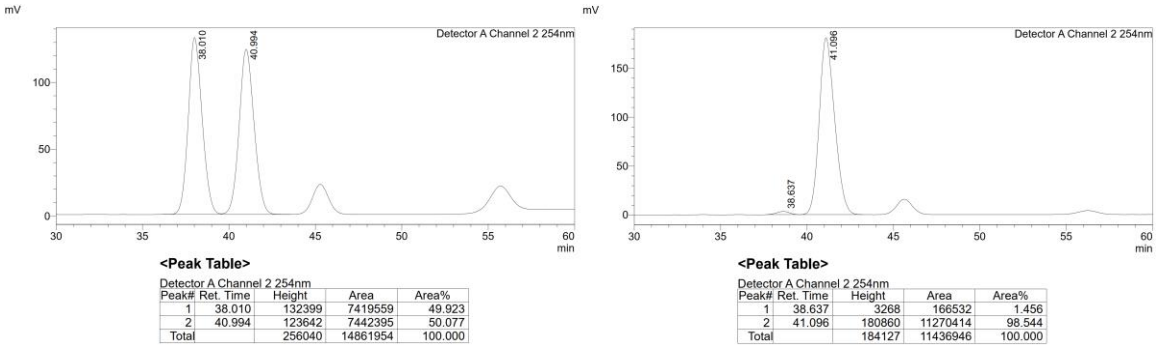

Peak #	Ret. Time	Area	Area %	Peak #	Ret. Time	Area	Area %
1	38.010 min	7419559	49.923	1	38.673 min	166532	1.456
2	40.994 min	7442395	50.077	2	41.096 min	11270414	98.544

(*R*,*Z*)-7,7,7-Trifluoro-1,1-diphenylhepta-1,5-dien-3-ol (*Z*-3.70): IR (neat): 3343 (br, m), 3057 (w), 3024 (w), 1670 (w), 1493 (w), 1444 (w), 1275 (m), 1228 (m), 1197 (m), 1119 (s), 1030 (m), 764 (m), 730 (w), 699 (m) cm^{-1}; **^{1}H NMR (400 MHz, $CDCl_3$):** δ 7.44 – 7.33 (m, 3H), 7.33 – 7.16 (m, 7H), 6.16 – 6.01 (m, 2H), 5.75 – 5.65 (m, 1H), 4.41 – 4.22 (m, 1H), 2.67 – 2.63 (m, 2H), 1.66 (s, 1H); **^{13}C NMR (100 MHz, $CDCl_3$):** δ 144.7, 141.4, 139.0, 138.3 (q, *J* = 5.4 Hz), 129.6, 129.6, 128.5, 128.3, 128.0, 127.8, 127.6, 123.2 (q, *J* = 271.8 Hz), 120.3 (q, *J* = 33.4 Hz), 68.6, 36.3; **^{19}F NMR (376 MHz, $CDCl_3$):** δ –58.06 (3F, dt, *J* = 8.3, 2.0 Hz); **HRMS (DART):** Calcd for $C_{19}H_{16}F_3$ $[M+H–H_2O]^+$: 301.1204; Found: 301.1199; **Specific Rotation:** $[\alpha]^{20.0}_D$ +22.7° (*c* 1.76, $CHCl_3$) for a 92:8 er sample. Enantiomeric purity was determined by HPLC analysis in comparison with authentic racemic material (Chiralcel OD-H, 98:2 hexanes:*i*-PrOH, 1.0 mL/min, 220 nm): t_R: 35.7 min (major) and 27.4 min (minor).

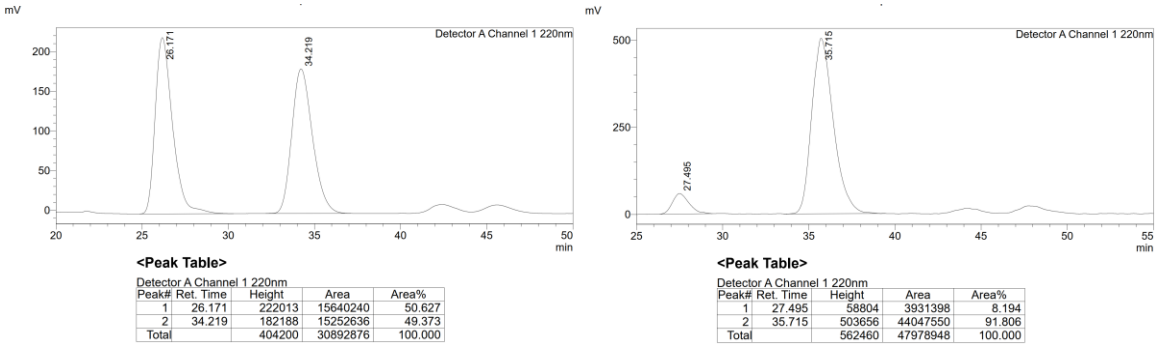

Peak #	Ret. Time	Area	Area %	Peak #	Ret. Time	Area	Area %
1	26.171 min	15640240	50.627	1	27.495 min	3931398	8.194
2	34.219 min	15252636	49.373	2	35.715 min	44047550	91.806

(*S*,*Z*)-7,7,7-Trifluoro-1-phenylhept-5-en-3-ol (*Z*-3.71): IR (neat): 3390 (br, m), 2921 (w), 1670 (w), 1496 (w), 1454 (w), 1418 (w), 1275 (m), 1227 (m), 1117 (s), 1083 (m), 1055 (m), 747(w), 699 (m) cm^{-1}; **^{1}H NMR (400 MHz, $CDCl_3$):** δ δ 7.33 – 7.27 (m, 2H), 7.22 – 7.19 (m, 3H), 6.13 (dt, *J* = 11.7, 7.7 Hz, 1H), 5.72 (dqt, *J* = 12.0, 8.5, 1.8 Hz, 1H), 3.76 (tq, *J* = 7.3, 5.1 Hz, 1H), 2.86 – 2.75 (m, 1H), 2.75 – 2.64 (m, 1H), 2.59 – 2.44 (m, 2H), 1.88 – 1.75 (m, 2H), 1.43 (d, *J* = 5.2 Hz, 1H); **^{13}C NMR (100 MHz, $CDCl_3$):** δ 141.6, 138.9 (q, *J* = 5.4 Hz), 128.6, 128.5, 126.1, 123.3 (q, *J* = 271.7 Hz), 120.4 (q, *J* = 33.3 Hz), 70.3, 38.8, 36.2, 32.0; **^{19}F NMR (376 MHz, $CDCl_3$):** δ –58.05 (3F, dt, *J* = 8.4, 2.2 Hz); **HRMS (DART):** Calcd for $C_{13}H_{14}F_3$ $[M+H–H_2O]^+$: 227.1048; Found: 227.1039; **Specific Rotation:** $[\alpha]^{20.0}_D$ –11.6° (*c* 0.25, $CHCl_3$) for a 87:13 er sample. Enantiomeric purity was determined by HPLC analysis in comparison with authentic racemic material (Chiralcel OD-H, 92:2 hexanes:*i*-PrOH, 1.0 mL/min, 220 nm): t_R: 37.2 min (major) and 59.0 min (minor).

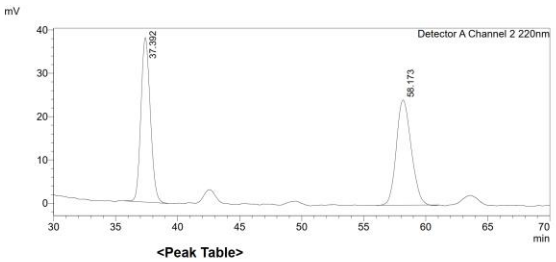

<Peak Table>
Detector A Channel 2 220nm

Peak#	Ret. Time	Height	Area	Area%
1	37.392	37988	2007374	49.762
2	58.173	24297	2026611	50.238
Total		62285	4033985	100.000

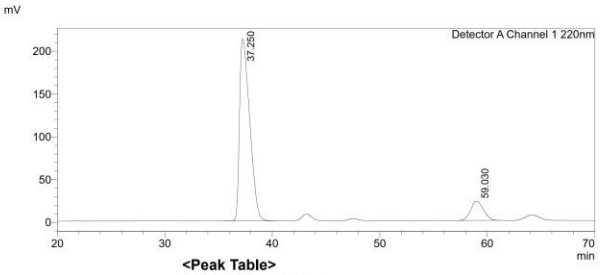

<Peak Table>
Detector A Channel 1 220nm

Peak#	Ret. Time	Height	Area	Area%
1	37.250	213221	13997478	88.166
2	59.030	22397	1878879	11.834
Total		235619	15876357	100.000

Peak #	Ret. Time	Area	Area %	Peak #	Ret. Time	Area	Area %
1	37.392 min	2007374	49.762	1	37.250 min	13997478	88.166
2	58.173 min	2026611	50.238	2	59.030 min	1878879	11.834

(*R*,*Z*)-2-(4-Bromothiazol-2-yl)-7,7,7-trifluoro-2-methylhept-5-en-3-ol (*Z*-3.75): The title compound was purified by preparative thin layer chromatography. **IR (neat):** 3422 (br, m), 3030 (w), 2972 (w), 2932 (w), 1670 (w), 1466 (m), 1416 (w), 1277 (w), 1258 (m), 1234 (m), 1211 (m), 1119 (s), 1082 (m), 1052 (m) cm^{-1}; **^{1}H NMR (600 MHz, $CDCl_3$):** δ 7.15 (s, 1H), 6.24 (dt, *J* = 11.7, 7.5 Hz, 1H), 5.73 – 5.63 (m, 1H), 3.81 (ddd, *J* = 10.9, 6.5, 2.5 Hz, 1H), 3.70 (d, *J* = 6.5 Hz, 1H), 2.58 (ddd, *J* = 15.2, 7.2, 2.6 Hz, 1H), 2.24 – 2.16 (m, 1H), 1.44 (d, *J* = 14.6 Hz, 6H); **^{13}C NMR (100 MHz, $CDCl_3$):** δ 179.8, 140.1 (q, *J* = 5.3 Hz), 124.3, 123.3 (q, *J* = 270 Hz), 119.6 (q, *J* = 33.3 Hz), 116.0, 77.6, 45.3, 30.9, 26.8, 23.8; **^{19}F NMR (376 MHz, $CDCl_3$):** δ –58.13 (dt, *J* = 8.5, 2.1 Hz); **HRMS (DART):** Calcd for $C_{11}H_{14}BrF_3NSO$ $[M+H]^+$: 343.9932; Found: 343.9927; **Specific Rotation:** $[\alpha]^{20.0}_D$ +14.8° (*c* 0.33, $CHCl_3$) for a 94:6 er sample. Enantiomeric purity was determined by HPLC analysis in comparison with authentic racemic material (Chiralpak AZ-H, 98:2 hexanes:*i*-PrOH, 1.0 mL/min, 220 nm): t_R: 7.3 min (major) and 6.9 min (minor).

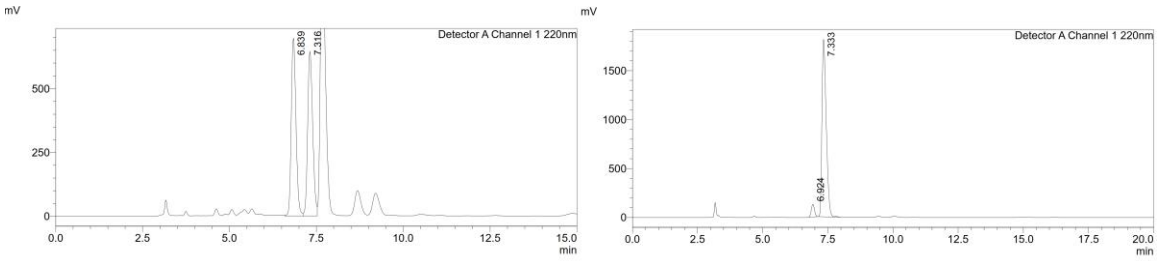

<Peak Table>
Detector A Channel 1 220nm

Peak#	Ret. Time	Height	Area	Area%
1	6.839	695196	6449893	49.714
2	7.316	642916	6524108	50.286
Total		1338112	12974001	100.000

<Peak Table>
Detector A Channel 1 220nm

Peak#	Ret. Time	Height	Area	Area%
1	6.924	130402	1089601	5.033
2	7.333	1811504	20561508	94.967
Total		1941906	21651109	100.000

Peak #	Ret. Time	Area	Area %	Peak #	Ret. Time	Area	Area %
1	6.839 min	6449893	49.714	1	6.924 min	1089601	5.033
2	7.316 min	6524108	50.286	2	7.333 min	20561508	94.967

3.7.4. *Determination of Absolute Stereochemistry*

Scheme S3.1. Determination of Absolute Stereochemistry

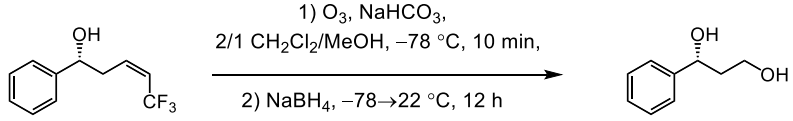

***Z*-3.42**
94:6 Z:E,
95:5 er

S3.1
57% yield

(*R*)-1-phenylpropane-1,3-diol (S3.1): An 8 dram vial equipped with a stir bar was charged with ***Z*-3.42** (0.07 mmol, 15.2 mg), NaHCO3 (47 mg, .56 mmol), 5 mL methanol and 10 mL dichloromethane. The vial was allowed to cool to –78 °C and a stream of ozone was introduced through the solution until it turned light blue. The ozone generator was then shut-off and oxygen was allowed to bubble through the solution until the color disappeared. $NaBH_4$ (2.1 mmol, 80 mg) was then added to the solution. The reaction mixture was then allowed to warm to 22 °C and allowed to stir for 12 h. The reaction was quenched by addition of water (after cooling to 0 °C). The organic layer was then removed and the aqueous layer was extracted with EtOAc (3 x 10 mL). The combined organic layers were dried over MgSO4 and filtered. The crude residue was purified by

silica gel column chromatography (gradient elution 1:0 hexanes:EtOAc → 0:1 hexanes:EtOAc) to afford **S3.1** (6.1 mg, 0.04 mmol, 57% yield) as colorless oil. The analytical data for this compound was fully consistent with those reported previously.[4] **Specific Rotation:** $[\alpha]^{20.0}_{D}$ +36.8° (*c* 0.61, $CHCl_3$) [literature: $[\alpha]^{24}_{D}$ +65.1° (*c* 1.05, $CHCl_3$)].[4]

3.7.5. *Catalytic Enantioselective Cl-Allyl Additions to Aldehydes*

Procedure for the Synthesis of *Z*-Cl-Allyl–B(pin)

Scheme S3.2. Synthesis of *Z*-Cl-Allyl-B(pin)

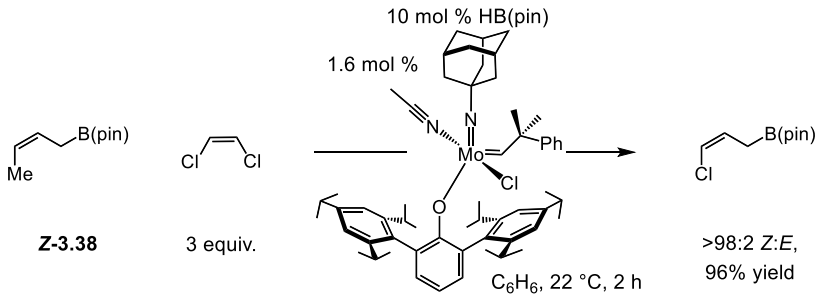

(*Z*)-2-(3-Chloroallyl)-4,4,5,5-tetramethyl-1,3,2-dioxaborolane (*Z*-3.77). In a N_2-filled glovebox, *Z*-crotyl–B(pin) (***Z*-3.38**) (4.0 g, 21.9 mmol) and *cis*-dichloroethylene (6.4g, 66 mmol) were added to an oven-dried 40 mL vial equipped with stir bar. Pinacolborane (320 μL, 2.2 mmol) was then added to the reaction mixture (note: upon stirring the reaction mixture bubbles gently). The reaction mixture was then sealed with a cap and allowed to stir 22 °C for 10 min. A solution of molybdenum catalyst (333 mg, 0.35 mmol) in benzene (3.5 mL) was then then slowly added to the reaction mixture. The vial was then capped and the resulting black solution was then allowed to stir at 22 °C for 2 h.

(4) Denmark, S. E.; Bui, T. *J. Org. Chem.* **2005**, *70*, 10190–10193.

The vial was removed from the glovebox and the volatiles were removed. The unpurified black oil was then purified by short path distillation affording a >98:2 *Z*:*E* mixture of ***Z*-3.77** (4.3 g, 21 mmol, 96% yield), as colorless oil.

Representative General Procedure for Catalytic Enantioselective Allyl Additions with *Z*-Cl-Substituted Allyl–B(pin)

In a N_2-filled glovebox, a stock solution of aminophenol and zinc(II) methoxide was prepared. An oven-dried vial (8 mL) equipped with a stir bar was charged with aminophenol (**3.82**) (5.5 mg, 0.008 mmol), zinc methoxide (5.1 mg, 0.04 mmol) and toluene (2.0 mL). The freshly prepared stock solution was allowed to stir at 22 °C for 15 min. In another vial (8 mL), aldehyde **3.1** (15.9 mg, 0.15 mmol) was weighed out. The aminophenol/zinc(II) methoxide stock solution was then added by syringe (500 μL). *Z*-Chloro-allyl–B(pin) (***Z*-3.77**) (20.2 mg, 0.1 mmol), was then added to the reaction followed by MeOH (5 μL, 0.13 mmol). A stir bar was added to the reaction mixture and the vial was then sealed with a cap and brought out of the glovebox. The reaction was then allowed to stir at 22 °C for 14 hours. The reaction was then quenched by the addition of MeOH (1.5 mL) and allowed to stir for 0.5 h at 22 °C. The reaction mixture was then concentrated and the resulting opaque oil was purified by silica gel column chromatography (30 mL 10:1 hexanes:Et_2O → 4:1 hexanes:Et_2O), to afford a >98:2 *Z*:*E* mixture of ***Z*-3.84** (17.7 mg, 0.097 mmol, 97% yield), as colorless oil.

General Procedure for Gram Scale Catalytic Enantioselective Allyl Additions with *Z*-Cl-Substituted Allyl–B(pin)

In a N_2-filled glovebox, an oven-dried round bottom flask (25 mL) equipped with a stir bar was charged with aminophenol (**3.82**) (69 mg, 0.1 mmol), zinc methoxide (64 mg, 0.5 mmol) and toluene (25 mL). The reaction mixture was allowed to stir at 22 °C for 15

min. Aldehyde **3.76** (1.76 g, 7.5 mmol) was then added to the round bottom flask, followed by ***Z*-3.77** (1.01 g, 5.0 mmol) and MeOH (260 μL, 6.5 mmol). The round bottom flask was sealed with a septa, brought out of the glovebox and allowed to stir at 22 °C for 14 h. The reaction mixture was then concentrated and the resulting opaque oil was purified by silica gel column chromatography (30 mL 10:1 hexanes:Et_2O → 4:1 hexanes:Et_2O), to afford a >98:2 *Z*:*E* mixture of ***Z*-3.84** (1.32 g, 4.3 mmol, 86% yield), as colorless oil. The unreacted aldehyde (**3.76**) was collected and further purified by short path distillation to afford **3.76** (570 mg, 2.4 mmol, 97% recovered) as colorless oil.

3.7.6. *Analytical Data for New Compounds*

(*R*,*Z*)-2-(4-Bromothiazol-2-yl)-6-chloro-2-methylhex-5-en-3-ol (*Z*-3.78): IR (neat): 3421 (br, m), 2968 (m), 2931 (w), 1630 (w), 1465 (s), 1387 (m), 1366 (m), 1257 (s), 1081 (s), 1050 (s), 885 (m), 838 (m), 748 (s) cm^{-1}; **^{1}H NMR (400 MHz, $CDCl_3$):** δ 7.14 (s, 1H), 6.09 (dt, *J* = 7.1, 1.5 Hz, 1H), 5.95 (q, *J* = 7.0 Hz, 1H), 3.82 (ddd, *J* = 10.2, 6.3, 2.7 Hz, 1H), 3.52 (dd, *J* = 6.3, 0.6 Hz, 1H), 2.56 – 2.47 (m, 1H), 2.15 (dddd, *J* = 14.8, 10.2, 6.6, 1.5 Hz, 1H), 1.46 (d, *J* = 5.7 Hz, 6H); **^{13}C NMR (150 MHz, $CDCl_3$):** 179.9, 128.9, 124.3, 119.5, 116.0, 77.5, 45.3, 30.1, 26.7, 24.0; **HRMS (DART):** Calcd for $C_{10}H_{14}BrClNOS$ $[M+H]^+$: 309.9668; Found: 309.9673; **Specific Rotation:** $[\alpha]^{24.5}$ +13.3° (*c* 1.0, $CHCl_3$) for a 94:6 er sample. Enantiomeric purity was determined by HPLC analysis in comparison with authentic racemic material (Chiralcel OD-H, 98:2 hexanes:*i*-PrOH, 1.0 mL/min, 220 nm): t_R: 10.4 min (major) and 11.6 min (minor).

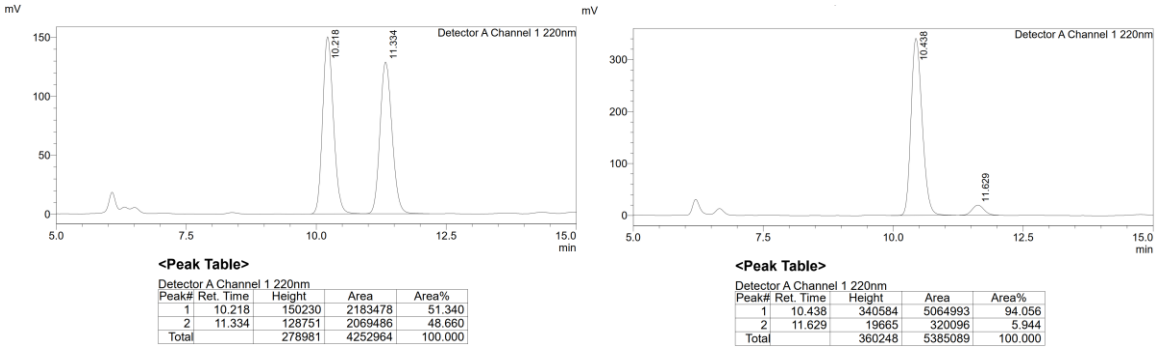

Peak #	Ret. Time	Area	Area %	Peak #	Ret. Time	Area	Area %
1	10.218 min	2183478	51.340	1	10.438 min	5064993	94.056
2	11.334 min	2069486	48.660	2	11.629 min	320096	5.944

(R,Z)-4-chloro-1-phenylbut-3-en-1-ol (*Z*-3.84): IR (neat): 3366 (br, m), 1630 (w), 1453 (w), 1335 (w), 1307 (w), 1053 (m), 743 (m), 699 (s) cm^{-1}; **^{1}H NMR (400 MHz, $CDCl_3$):** δ 7.41 – 7.34 (m, 4H), 7.32 – 7.27 (m, 1H), 6.14 (dt, *J* = 7.1, 1.6 Hz, 1H), 5.84 (q, *J* = 7.1 Hz, 1H), 4.82 (ddd, *J* = 7.6, 5.6, 3.5 Hz, 1H), 2.86 – 2.60 (m, 2H), 1.90 (d, *J* = 3.5 Hz, 1H); **^{13}C NMR (150 MHz, $CDCl_3$):** δ 143.7, 128.6, 127.9, 127.6, 125.9, 120.4, 73.3, 36.8; **HRMS (DART):** Calcd for $C_{10}H_{10}Cl$ $[M+H–H_2O]^+$: 165.0471; Found: 165.0469; **Specific Rotation:** $[\alpha]^{24.56}$ +46.6° (*c* 1.0, $CHCl_3$) for a 95:5 er sample. Enantiomeric purity was determined by HPLC analysis in comparison with authentic racemic material (Chiralpak AZ-H, 99:9 hexanes:*i*-PrOH, 1.0 mL/min, 220 nm): t_R: 28.8 min (major) and 25.3 min (minor).

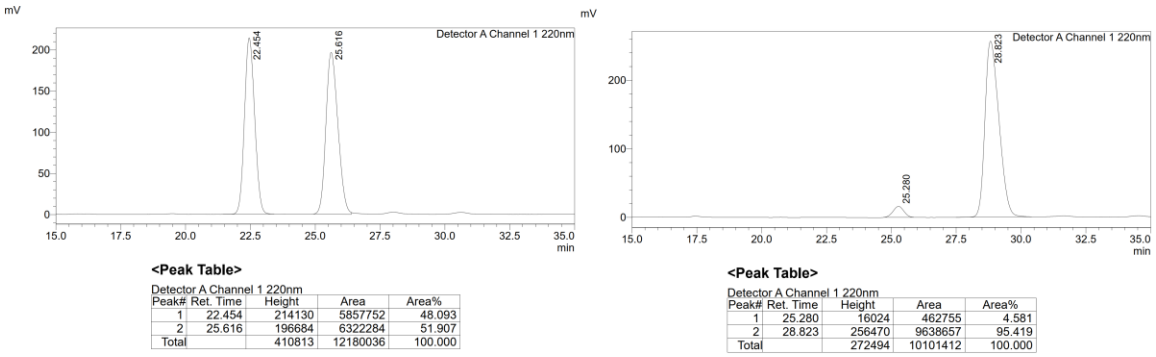

Peak #	Ret. Time	Area	Area %	Peak #	Ret. Time	Area	Area %
1	22.454 min	5857752	48.093	1	25.280 min	462755	4.581
2	25.616 min	6322284	51.907	2	28.823 min	9638657	95.419

(*R*,*Z*)-1-(6-bromonaphthalen-2-yl)-4-chlorobut-3-en-1-ol (*Z*-3.85): IR (neat): 3387 (br, m), 1630 (m), 1590 (m), 1497 (m), 1463 (w), 1337 (m), 1314 (m), 1161 (m), 1127 (m), 1061 (s), 877 (s), 805 (s), 746 (s), 475 (s) cm^{-1}; **^{1}H NMR (400 MHz, $CDCl_3$):** δ 7.99 (d, *J* = 1.9 Hz, 1H), 7.77 (d, *J* = 1.1 Hz, 1H), 7.74 (d, *J* = 8.6 Hz, 1H), 7.69 (d, *J* = 8.7 Hz, 1H), 7.55 (dd, *J* = 8.7, 2.0 Hz, 1H), 7.51 (dd, *J* = 8.5, 1.7 Hz, 1H), 6.15 (dt, *J* = 7.1, 1.5 Hz, 1H), 5.83 (q, *J* = 7.1 Hz, 1H), 4.96 (td, *J* = 6.8, 2.9 Hz, 1H), 2.85 – 2.71 (m, 2H), 2.13 (d, *J* = 3.2 Hz, 1H); **^{13}C NMR (150 MHz, $CDCl_3$):** 141.6, 134.2, 131.7, 129.8, 129.7, 129.7, 127.6, 127.2, 125.0, 124.6, 120.8, 120.0, 73.2, 36.6; **HRMS (DART):** Calcd for $C_{14}H_{11}BrCl$ $[M+H–H_2O]^+$: 292.9733; Found: 292.9737; **Specific Rotation:** $[\alpha]^{24.6}_D$ +13.5° (*c* 1.97, $CHCl_3$) for a 96:4 er sample. Enantiomeric purity was determined by HPLC analysis in comparison with authentic racemic material (Chiralcel OJ-H, 96:5 hexanes:*i*-PrOH, 1.0 mL/min, 220 nm): t_R: 74.7 min (major) and 55.5 min (minor).

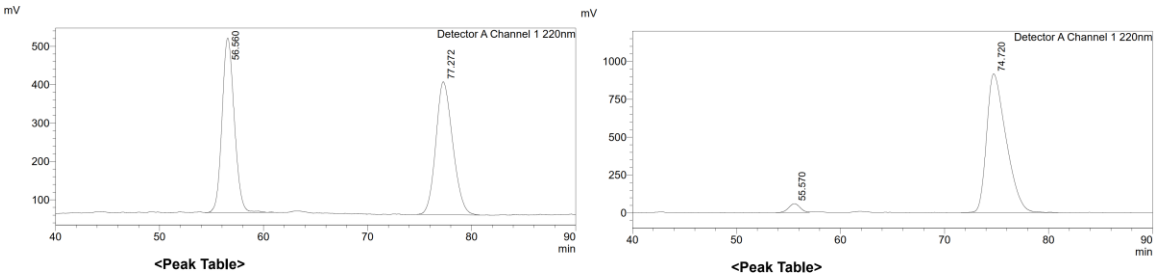

<Peak Table>
Detector A Channel 1 220nm

Peak#	Ret. Time	Height	Area	Area%
1	56.560	454327	37160771	48.726
2	77.272	346013	39103354	51.274
Total		800341	76264126	100.000

<Peak Table>
Detector A Channel 1 220nm

Peak#	Ret. Time	Height	Area	Area%
1	55.570	58400	4473795	3.615
2	74.720	915368	119267933	96.385
Total		973769	123741727	100.000

Peak #	Ret. Time	Area	Area %	Peak #	Ret. Time	Area	Area %
1	56.560 min	37160771	48.726	1	55.570 min	4473795	3.615
2	77.272 min	39103354	51.274	2	74.720 min	119267933	96.385

(*R*,*Z*)-1-(4-(4-chloro-1-hydroxybut-3-en-1-yl)phenyl)ethan-1-one (*Z*-3.86): IR (neat): 3424 (br, m), 1671 (w), 1630 (w), 1607 (s), 1412 (m), 1359 (s), 1304 (m), 1268 (s), 1065 (m), 853 (m), 752 (m), 722 (m) cm^{-1}; **^{1}H NMR (400 MHz, $CDCl_3$):** δ 7.95 (d, *J* = 8.3 Hz, 1H), 7.47 (d, *J* = 8.3 Hz, 1H), 6.16 (dt, *J* = 7.1, 1.5 Hz, 1H), 5.82 (q, *J* = 7.1 Hz, 1H), 4.90 (td, *J* = 6.4, 3.2 Hz, 1H), 2.74 – 2.69 (m, 2H), 2.60 (s, 3H), 2.10 (d, *J* = 3.8 Hz, 1H); **^{13}C NMR (100 MHz, $CDCl_3$):** δ 197.9, 149.0, 136.6, 128.7, 126.9, 126.0, 121.0, 72.7, 36.7, 26.7; **HRMS (DART):** Calcd for $C_{12}H_{14}O_2Cl$ $[M+H]^+$: 225.06768; Found: 225.06659; **Specific Rotation:** $[\alpha]^{20.0}_D$ +21.4° (*c* 1.33, $CHCl_3$) for a 88:12 er sample. Enantiomeric purity was determined by HPLC analysis in comparison with authentic racemic material (Chiralpak AD-H, 95:5 hexanes:*i*-PrOH, 1.0 mL/min, 220 nm): t_R: 22.0 min (major) and 23.8 min (minor).

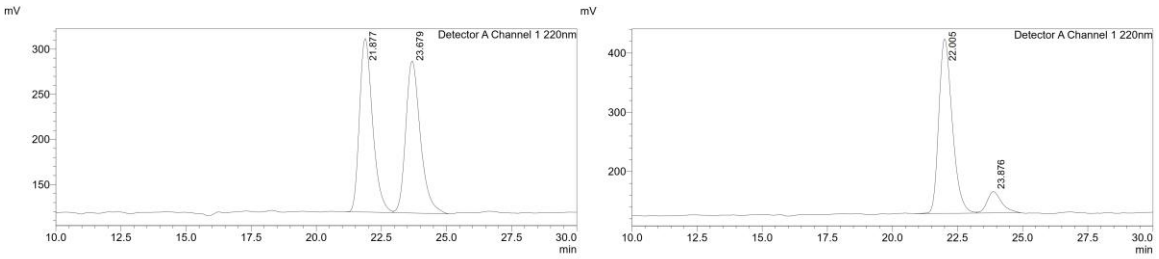

<Peak Table>
Detector A Channel 1 220nm

Peak#	Ret. Time	Height	Area	Area%
1	21.877	192221	6743165	50.457
2	23.679	168437	6621097	49.543
Total		360658	13364263	100.000

<Peak Table>
Detector A Channel 1 220nm

Peak#	Ret. Time	Height	Area	Area%
1	22.005	294635	10588026	88.248
2	23.876	35971	1410016	11.752
Total		330606	11998042	100.000

Peak #	Ret. Time	Area	Area %	Peak #	Ret. Time	Area	Area %
1	21.877 min	6743165	50.457	1	22.005 min	10588026	88.248
2	23.679 min	6621097	49.543	2	23.876 min	1410016	11.752

(*R*,*Z*)-4-Chloro-1-(4-(trifluoromethyl)phenyl)but-3-en-1-ol (*Z*-3.87): IR (neat): 3359 (br, m), 1621 (w), 1418 (w), 1322 (s), 1162 (m), 1109 (s), 1065 (s), 1015 (m), 842 (m), 753 (m), 737 (m), 710 (m), 607 (m) cm^{-1}; **^{1}H NMR (400 MHz, $CDCl_3$):** δ 7.67 – 7.56 (m, 2H), 7.55 – 7.44 (m, 2H), 6.17 (dt, *J* = 7.1, 1.5 Hz, 1H), 5.82 (q, *J* = 7.2 Hz, 1H), 4.90 (td, *J* = 6.5, 3.6 Hz, 1H), 2.83 – 2.60 (m, 2H), 2.01 (d, *J* = 3.6 Hz, 1H); **^{13}C NMR (100 MHz, $CDCl_3$):** δ 147.6, 130.1(q, *J* = 32.4 Hz), 126.8, 126.2, 125.6 (q, *J* = 3.8 Hz), 124.2 (q, *J* = 271 Hz), 121.2, 72.7, 36.8; **^{19}F NMR (376 MHz, $CDCl_3$):** δ –62.53 (s, 3F); **HRMS (DART):** Calcd for $C_{11}H_9F_3Cl$ $[M+H–H_2O]^+$: 233.03394; Found: 233.03349; **Specific Rotation:** $[\alpha]^{20.0}_D$ +20.7° (*c* 1.48, $CHCl_3$) for a 87:13 er sample. Enantiomeric purity was determined by HPLC analysis in comparison with authentic racemic material (Chiralpak AD-H, 98:2 hexanes:*i*-PrOH, 1.0 mL/min, 220 nm): t_R: 14.1 min (major) and 14.9 min (minor).

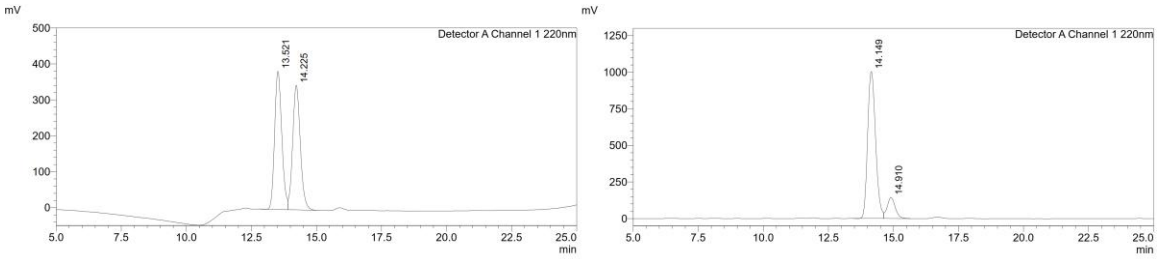

<Peak Table>
Detector A Channel 1 220nm

Peak#	Ret. Time	Height	Area	Area%
1	13.521	384543	7375322	50.767
2	14.225	346780	7152534	49.233
Total		731323	14527855	100.000

<Peak Table>
Detector A Channel 1 220nm

Peak#	Ret. Time	Height	Area	Area%
1	14.149	1005231	21314367	87.247
2	14.910	143842	3115505	12.753
Total		1149073	24429872	100.000

Peak #	Ret. Time	Area	Area %	Peak #	Ret. Time	Area	Area %
1	13.521 min	7375322	50.767	1	14.149 min	21314367	87.247
2	14.225 min	7152534	49.233	2	14.910 min	3115505	12.753

(*R*,*Z*)-4-chloro-1-(4-methoxyphenyl)but-3-en-1-ol (*Z*-3.88): IR (neat): 3407 (br, m), 1611 (m), 1512 (s), 1463 (w), 1441 (w), 1303 (m), 1246 (s), 1175 (m), 1034 (s), 832 (m), 746 (m) cm^{-1}; **^{1}H NMR (600 MHz, $CDCl_3$):** δ 7.31 – 7.28 (m, 2H), 6.91 – 6.87 (m, 2H), 6.12 (dt, *J* = 7.1, 1.5 Hz, 1H), 5.80 (q, *J* = 7.1 Hz, 1H), 4.75 (ddd, *J* = 7.8, 5.6, 2.3 Hz, 1H), 3.81 (s, 3H), 2.73 (dddd, *J* = 14.8, 7.6, 7.0, 1.5 Hz, 1H), 2.65 (dddd, *J* = 14.7, 7.1, 5.6, 1.6 Hz, 1H), 1.95 (d, *J* = 3.1 Hz, 1H); **^{13}C NMR (150 MHz, $CDCl_3$):** δ 159.3, 135.9, 127.7, 127.2, 120.3, 114.0, 72.9, 55.4, 36.7; **HRMS (DART):** Calcd for $C_{11}H_{12}OCl$ $[M+H–H_2O]^+$: 195.05712; Found: 195.05662; **Specific Rotation:** $[\alpha]^{20.0}_D$ +28.1° (*c* 1.00, $CHCl_3$) for a 89:11 er sample. Enantiomeric purity was determined by HPLC analysis in comparison with authentic racemic material (Chiralcel OD-H, 98:2 hexanes:*i*-PrOH, 1.0 mL/min, 220 nm): t_R: 27.0 min (major) and 29.1 min (minor).

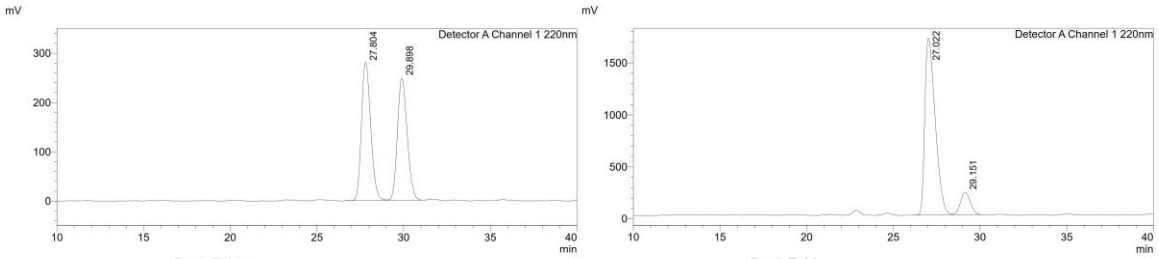

<Peak Table>
Detector A Channel 1 220nm

Peak#	Ret. Time	Height	Area	Area%
1	0.119	387	8733	0.043
2	27.804	280734	10380801	51.528
3	29.898	248125	9756582	48.429
Total		529246	20146116	100.000

<Peak Table>
Detector A Channel 1 220nm

Peak#	Ret. Time	Height	Area	Area%
1	27.022	1702650	71138610	89.010
2	29.151	217974	8783690	10.990
Total		1920624	79922300	100.000

Peak #	Ret. Time	Area	Area %	Peak #	Ret. Time	Area	Area %
1	27.804 min	10380801	51.528	1	27.022 min	71138610	89.010
2	29.898 min	9756582	48.429	2	29.151 min	8783690	10.990

(R,*Z*)-4-Chloro-1-(4-(methylthio)phenyl)but-3-en-1-ol (*Z*-3.89): IR (neat): 3377 (br, m), 2920 (m), 1630 (m), 1599 (m), 1494 (s), 1435 (m), 1406 (m), 1300 (m), 1092 (s), 1055 (s), 1014 (m), 968 (m), 821 (m), 749 (s), 729 (s), 712 (s) cm^{-1}; **^{1}H NMR (400 MHz, $CDCl_3$):** δ 7.38 – 7.10 (m, 4H), 6.14 (dt, *J* = 7.1, 1.6 Hz, 1H), 5.81 (q, *J* = 7.1 Hz, 1H), 4.78 (ddd, *J* = 7.4, 5.5, 3.4 Hz, 1H), 2.85 – 2.59 (m, 2H), 2.49 (s, 3H), 1.91 (d, *J* = 2.1 Hz, 1H); **^{13}C NMR (100 MHz, $CDCl_3$):** δ 140.6, 138.0, 127.4, 126.8, 126.4, 120.5, 72.9, 36.7, 16.0; **HRMS (DART):** Calcd for $C_{11}H_{12}SCl$ $[M+H-H_2O]^+$: 211.03428; Found: 211.03309; **Specific Rotation:** $[\alpha]^{20.0}_D$ +16.0° (*c* 1.35, $CHCl_3$) for a 90:10 er sample. Enantiomeric purity was determined by HPLC analysis in comparison with authentic racemic material (Chiralpak AZ-H, 98:2 hexanes:*i*-PrOH, 1.0 mL/min, 220 nm): t_R: 26.9 min (major) and 25.2 min (minor).

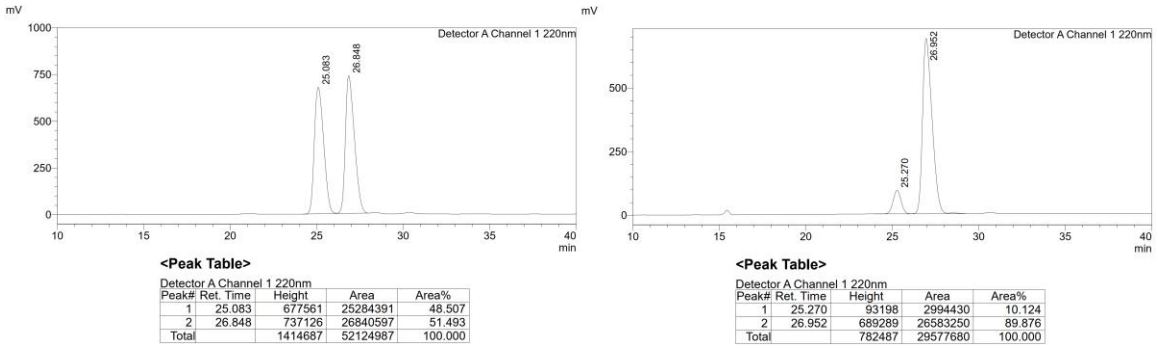

Peak #	Ret. Time	Area	Area %	Peak #	Ret. Time	Area	Area %
1	25.083 min	25284391	48.507	1	25.270 min	2994430	10.124
2	26.848 min	26840597	51.493	2	26.952 min	26583250	89.876

(R,Z)-1-(benzo[d][1,3]dioxol-5-yl)-4-chlorobut-3-en-1-ol (*Z*-3.90): IR (neat): 3384 (br, m), 2894 (w), 1738 (m), 1503 (m), 1487 (s), 1442 (m), 1365 (w), 1321 (w), 1244 (s), 1095 (w), 1039 (s), 933 (m), 747 (m) cm^{-1}; **^{1}H NMR (400 MHz, $CDCl_3$):** δ 6.89 (dd, *J* = 1.7, 0.5 Hz, 1H), 6.82 (ddd, *J* = 7.9, 1.7, 0.5 Hz, 1H), 6.78 (dd, *J* = 7.9, 0.5 Hz, 1H), 6.13 (dt, *J* = 7.2, 1.6 Hz, 1H), 5.96 (s, 2H), 5.80 (q, *J* = 7.1 Hz, 1H), 4.73 (ddd, *J* = 7.7, 5.6, 3.3 Hz, 1H), 2.77 – 2.57 (m, 2H), 1.85 (d, *J* = 3.3 Hz, 1H); **^{13}C NMR (100 MHz, $CDCl_3$):** δ 147.9, 147.2, 137.8, 127.5, 120.4, 119.3, 108.2, 106.4, 101.1, 73.2, 36.8; **HRMS (DART):** Calcd for $C_{11}H_{10}O_2Cl$ $[M+H-H_2O]^+$: 209.03638; Found: 209.03521; **Specific Rotation:** $[\alpha]^{20.0}_D$ +16.9° (*c* 1.40, $CHCl_3$) for a 95:5 er sample. Enantiomeric purity was determined by HPLC analysis in comparison with authentic racemic material (Chiralpak AZ-H, 98:2 hexanes:*i*-PrOH, 1.0 mL/min, 220 nm): t_R: 37.9 min (major) and 35.5 min (minor).

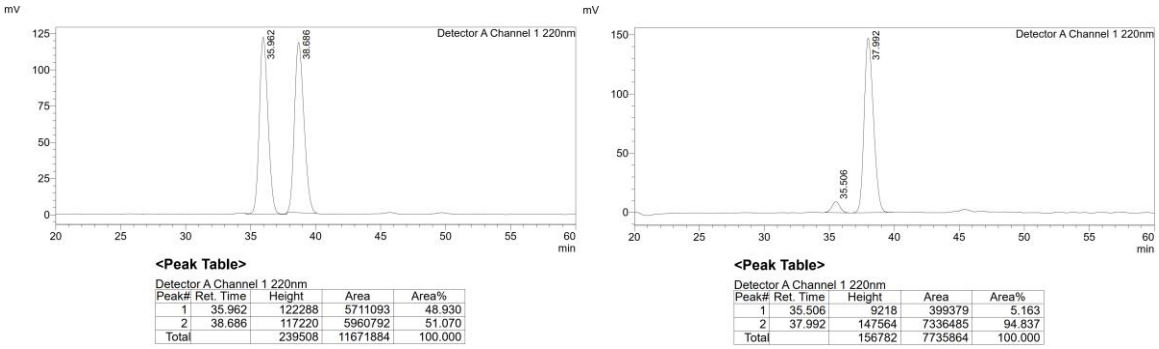

Peak #	Ret. Time	Area	Area %	Peak #	Ret. Time	Area	Area %
1	35.962 min	5711093	48.930	1	35.506 min	399379	5.163
2	38.686 min	5960792	51.070	2	37.992 min	7336485	94.837

(*R*,*Z*)-4-(4-chloro-1-hydroxybut-3-en-1-yl)-3,5-difluorobenzonitrile (*Z*-3.91): IR (neat): 3443 (br, m), 2237 (w), 1626 (m), 1573 (s), 1423 (s), 1320 (s), 1203 (m), 1190 (m), 1048 (s), 1018 (s), 971 (m), 863 (s), 755 (m), 727 (m), 710 (m) cm^{-1}; **^{1}H NMR (400 MHz, $CDCl_3$):** δ 7.25 – 7.18 (m, 1H), 6.17 (dt, *J* = 7.2, 1.5 Hz, 1H), 5.81 (q, *J* = 7.2 Hz, 1H), 5.18 (dt, *J* = 8.8, 7.1 Hz, 1H), 2.98 – 2.79 (m, 1H), 2.35 (dt, *J* = 8.8, 1.9 Hz, 1H); **^{13}C NMR (100 MHz, $CDCl_3$):** δ 160.8 (dd, *J* = 252.2, 9.2 Hz), 125.7, 124.8 (t, *J* = 16.4 Hz), 121.9, 116.4 (t, *J* = 3.5 Hz), 116.1 (dd, *J* = 21, 9.0 Hz), 113.2 (t, *J* = 12.6 Hz), 65.3, 34.6; **^{19}F NMR (376 MHz, $CDCl_3$):** δ –110.74 (d, *J* = 6.7 Hz). **HRMS (DART):** Calcd for $C_{11}H_9NOF_2Cl$ $[M+H]^+$: 244.03352; Found: 244.03341; **Specific Rotation:** $[\alpha]^{20.0}_D$ +25.1° (*c* 1.25, $CHCl_3$) for a 94:6 er sample. Enantiomeric purity was determined by HPLC analysis in comparison with authentic racemic material (Chiralpak AD-H, 95:5 hexanes:*i*-PrOH, 1.0 mL/min, 220 nm): t_R: 14.5 min (major) and 12.6 min (minor).

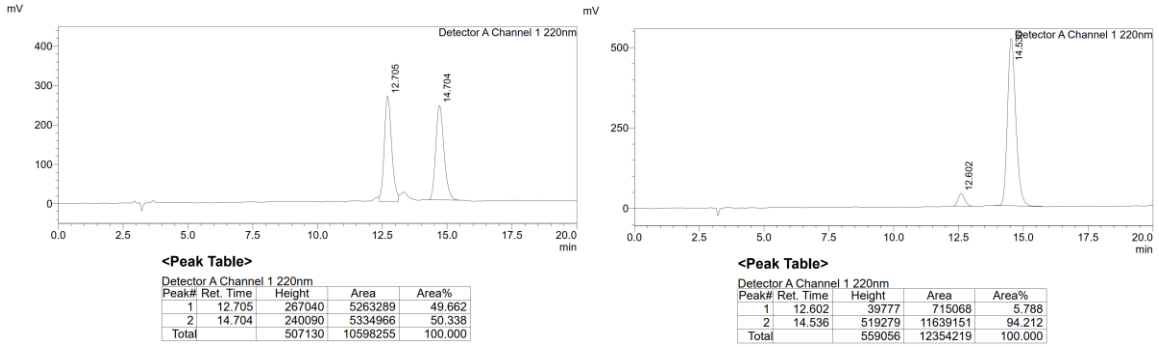

Peak #	Ret. Time	Area	Area %	Peak #	Ret. Time	Area	Area %
1	12.705 min	5263289	49.662	1	12.602 min	715068	5.788
2	14.704 min	5334966	50.338	2	14.536 min	11639151	94.212

(R,Z)-4-chloro-1-(pyridin-3-yl)but-3-en-1-ol (*Z*-3.92): IR (neat): 3184 (br, s), 2916 (br, m), 2854 (br, m), 1630 (w), 1594 (w), 1580 (w), 1480 (w), 1427 (m), 1339 (w), 1314 (w), 1071 (m), 1028 (m), 748 (m), 712 (s) cm^{-1}; **^{1}H NMR (400 MHz, $CDCl_3$):** 8.60 (d, *J* = 2.3 Hz, 1H), 8.54 (dd, *J* = 4.9, 1.7 Hz, 1H), 7.74 (dddd, *J* = 7.9, 2.3, 1.7, 0.6 Hz, 1H), 7.35 – 7.27 (m, 1H), 6.18 (dt, *J* = 7.2, 1.5 Hz, 1H), 5.83 (q, *J* = 7.2 Hz, 1H), 4.94 – 4.85 (m, 1H), 2.89 – 2.62 (m, 2H), 2.18 (s, 1H); **^{13}C NMR (150 MHz, $CDCl_3$):** δ 148.9, 147.6, 139.4, 133.8, 126.8, 123.6, 121.0, 70.8, 36.7; **HRMS (DART):** Calcd for $C_9H_{11}ClNO$ $[M+H]^+$: 184.0529; Found: 184.053; **Specific Rotation:** $[\alpha]^{20.0}_D$ +28.8° (*c* 1.27, $CHCl_3$) for a 94:6 er sample. Enantiomeric purity was determined by HPLC analysis in comparison with authentic racemic material (Chiralpak AZ-H, 97:3 hexanes:*i*-PrOH, 1.0 mL/min, 254 nm): t_R: 146.1 min (major) and 112.0 min (minor).

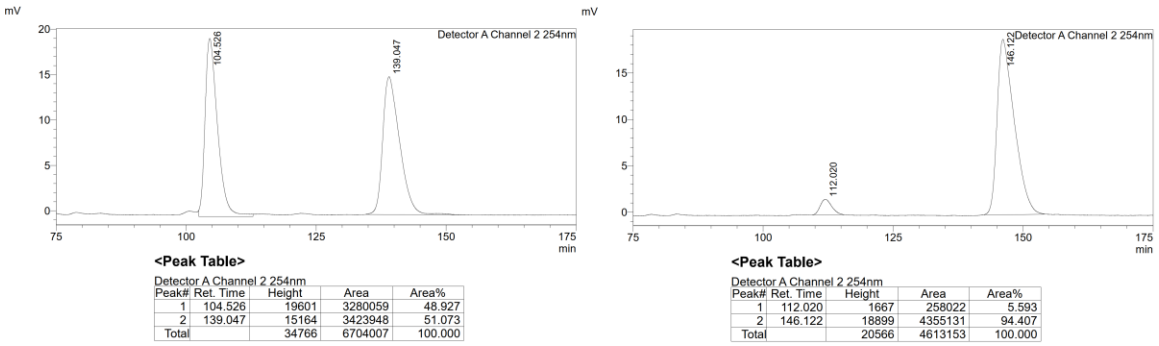

Peak #	Ret. Time	Area	Area %	Peak #	Ret. Time	Area	Area %
1	104.526 min	3280059	48.927	1	112.020 min	258022	5.593
2	139.047 min	3423948	51.073	2	146.122 min	4355131	94.407

(R,Z)-1-(benzofuran-2-yl)-4-chlorobut-3-en-1-ol (*Z*-3.93): IR (neat): 3370 (br, m), 1631 (w), 1454 (s), 1333 (m), 1254 (s), 1171 (m), 1068 (m), 1007 (m), 808 (m), 750 (s); **^{1}H NMR (400 MHz, $CDCl_3$):** δ 7.55 (ddd, *J* = 7.5, 1.5, 0.7 Hz, 1H), 7.47 (dd, *J* = 8.2, 0.9 Hz, 1H), 7.31 – 7.26 (m, 1H), 7.23 (td, *J* = 7.4, 1.1 Hz, 1H), 6.67 (s, 1H), 6.19 (dt, *J* = 7.2, 1.6 Hz, 1H), 5.89 (q, *J* = 7.1 Hz, 1H), 5.02 – 4.92 (m, 1H), 3.05 – 2.83 (m, 2H), 2.12 (d, *J* = 5.4 Hz, 1H); **^{13}C NMR (150 MHz, $CDCl_3$):** δ 158.3, 154.9, 128.1, 126.6, 124.4, 123.0, 121.2, 121.0, 111.4, 103.0, 67.1, 33.4; **HRMS (DART):** Calcd for $C_{11}H_{14}BrF_3NSO$ $[M+H–H_2O]^+$: 205.042; Found: 205.041; **Specific Rotation:** $[\alpha]^{25.2}_D$ +10.0° (*c* 1.0, $CHCl_3$) for a 84:16 er sample. Enantiomeric purity was determined by HPLC analysis in comparison with authentic racemic material (Chiralcel OJ-H, 99:1 hexanes:*i*-PrOH, 1.0 mL/min, 220 nm): t_R: 106.6 min (major) and 120.8 min (minor).

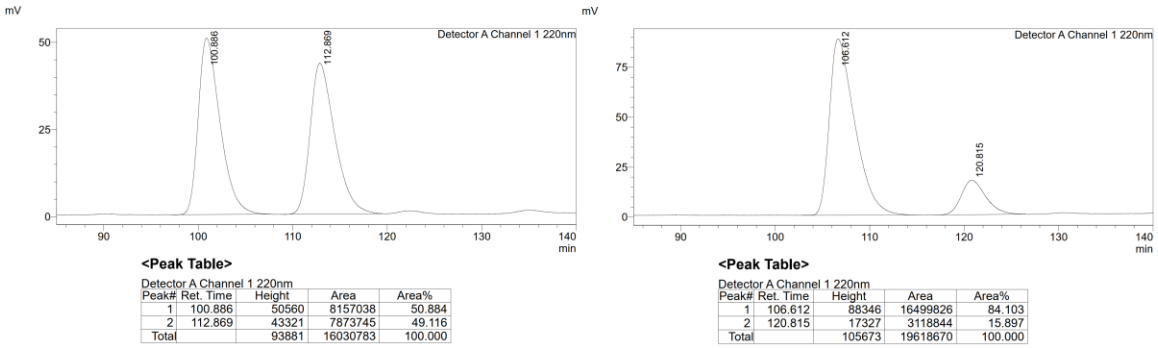

Peak #	Ret. Time	Area	Area %	Peak #	Ret. Time	Area	Area %
1	100.886 min	8157038	50.884	1	106.612 min	16499826	84.103
2	112.869 min	7873745	49.116	2	120.815 min	3118844	15.897

(R,*Z*)-1-(benzo[b]thiophen-3-yl)-4-chlorobut-3-en-1-ol (*Z*-3.94): IR (neat): 3378 (br, m), 1630 (w), 1459 (w), 1427 (m), 1339 (w), 1309 (w), 1256 (w), 1094 (w), 1066 (m), 1047 (m), 1021 (m), 761 (s), 732 (s), 713 (m) cm^{-1}; **^{1}H NMR (600 MHz, $CDCl_3$):** δ 7.95 – 7.90 (m, 1H), 7.90 – 7.84 (m, 1H), 7.44 (s, 1H), 7.39 (dddd, *J* = 21.0, 8.2, 7.1, 1.3 Hz, 2H), 6.19 (dt, *J* = 7.1, 1.6 Hz, 1H), 5.93 (q, *J* = 7.1 Hz, 1H), 5.23 (dddd, *J* = 7.9, 5.0, 4.1, 0.9 Hz, 1H), 2.95 (dddd, *J* = 15.0, 7.0, 5.1, 1.6 Hz, 1H), 2.87 (dddd, *J* = 14.9, 7.7, 6.9, 1.5 Hz, 1H), 1.99 (d, *J* = 4.1 Hz, 1H); **^{13}C NMR (150 MHz, $CDCl_3$):** δ 141.0, 138.7, 137.2, 127.5, 124.6, 124.3, 123.1, 122.6, 122.3, 120.7, 68.8, 35.1; **HRMS (DART):** Calcd for $C_{12}H_{10}SCl$ $[M+H-H_2O]^+$: 221.01863; Found: 221.01796; **Specific Rotation:** $[\alpha]^{20.0}_D$ +29.6° (*c* 1.1, $CHCl_3$) for a 93:7 er sample. Enantiomeric purity was determined by HPLC analysis in comparison with authentic racemic material (Chiralcel OD-H, 96:4 hexanes:*i*-PrOH, 1.0 mL/min, 220 nm): t_R: 46.5 min (major) and 22.6 min (minor).

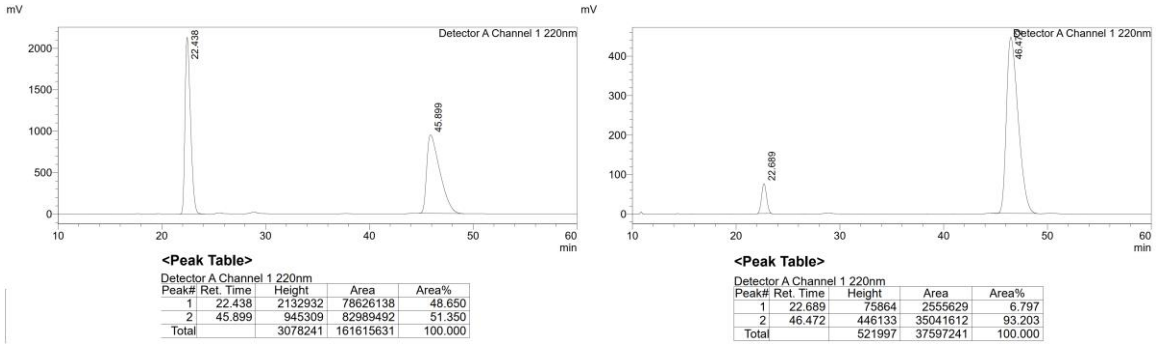

Peak #	Ret. Time	Area	Area %	Peak #	Ret. Time	Area	Area %
1	22.438 min	78626138	48.650	1	22.689 min	2555629	6.797
2	45.899 min	82989492	51.350	2	46.472 min	35041612	93.203

tert-Butyl (*R*,*Z*)-3-(4-chloro-1-hydroxybut-3-en-1-yl)-1H-indole-1-carboxylate (*Z*-3.95): IR (neat): 3421 (br, w), 2979 (w), 1732 (s), 1452 (s), 1370 (s), 1255 (m), 1224 (m), 1156 (s), 1090 (m), 1056 (w), 1019 (w), 856 (w), 766 (m), 746 (s) cm^{-1}; **^{1}H NMR (500 MHz, $CDCl_3$):** δ 8.15 (d, *J* = 5.9 Hz, 1H), 7.68 (d, *J* = 7.8 Hz, 1H), 7.58 (s, 1H), 7.33 (d, *J* = 8.1 Hz, 1H), 7.25 (t, *J* = 7.5 Hz, 1H), 6.17 (dd, *J* = 7.2, 1.4 Hz, 1H), 5.97 – 5.87 (m, 1H), 5.08 (t, *J* = 6.7 Hz, 1H), 3.03 – 2.77 (m, 2H), 2.08 (s, 1H), 1.67 (s, 9H); **^{13}C NMR (125 MHz, $CDCl_3$):** δ 149.7, 135.9, 128.5, 127.7, 127.5, 124.9, 124.5, 123.2, 123.0, 122.8, 122.5, 122.4, 120.6, 120.4, 119.9, 119.6, 115.5, 83.9, 67.2, 66.7, 35.1, 28.3, 28.2 (extra peaks were observed due to rotamers); **HRMS (DART):** Calcd for $C_{17}H_{19}NO_2Cl$ $[M+H-H_2O]^+$: 304.10988; Found: 304.10987; **Specific Rotation:** $[\alpha]^{20.0}_D$ +19.5° (*c* 1.35, $CHCl_3$) for a 96:4 er sample. Enantiomeric purity was determined by HPLC analysis in comparison with authentic racemic material (Chiralcel OD-H, 98:2 hexanes:*i*-PrOH, 1.0 mL/min, 220 nm): t_R: 17.9 min (major) and 20.3 min (minor).

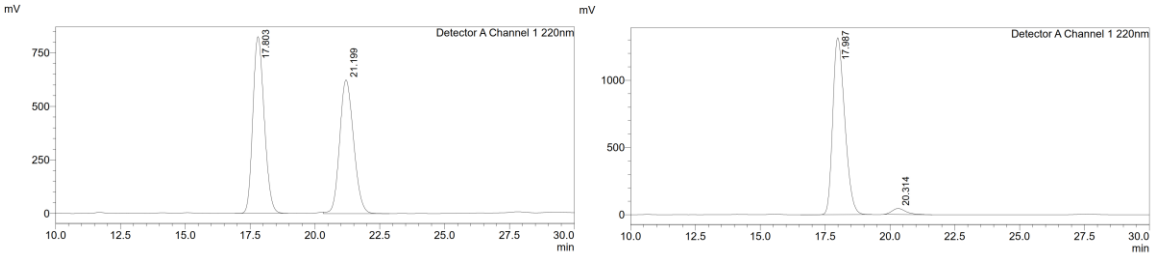

<Peak Table>
Detector A Channel 1 220nm

Peak#	Ret. Time	Height	Area	Area%
1	17.803	824805	25116671	51.727
2	21.199	624208	23439094	48.273
Total		1449013	48555765	100.000

<Peak Table>
Detector A Channel 1 220nm

Peak#	Ret. Time	Height	Area	Area%
1	17.987	1315424	42194991	96.228
2	20.314	44349	1653955	3.772
Total		1359773	43848946	100.000

Peak #	Ret. Time	Area	Area %	Peak #	Ret. Time	Area	Area %
1	17.803 min	25116671	51.727	1	17.987 min	42194991	96.228
2	21.199 min	23439094	48.273	2	20.314 min	1653955	3.772

(*R*,1*E*,5*Z*)-6-Chloro-2-methyl-1-(2-methylthiazol-4-yl)hexa-1,5-dien-3-ol (*Z*-3.96): **IR (neat):** 3282 (br, s), 2921 (m), 1630 (w), 1507 (m), 1438 (m), 1306 (m), 1188 (s), 1046 (s), 879 (m), 746 (s) cm^{-1}; **^{1}H NMR (400 MHz, $CDCl_3$):** δ 6.94 (s, 1H), 6.12 (ddd, *J* = 7.1, 1.8, 1.3 Hz, 1H), 5.85 (q, *J* = 7.0 Hz, 1H), 4.28 (t, *J* = 6.5 Hz, 1H), 2.70 (s, 2H), 2.67 – 2.51 (m, 2H), 2.41 (s, 1H), 2.04 (d, *J* = 1.3 Hz, 3H); **^{13}C NMR (100 MHz, $CDCl_3$):** δ 164.8, 152.6, 141.4, 127.7, 120.1, 119.4, 115.8, 76.3, 33.1, 19.2, 14.3; **HRMS (DART):** Calcd for $C_{11}H_{14}NOSCl$ $[M+H]^+$: 243.04791; Found: 243.04791; **Specific Rotation:** $[\alpha]^{25.0}_D$ +13.9° (*c* 1.44, $CHCl_3$) for a 98:2 er sample. Enantiomeric purity was determined by HPLC analysis in comparison with authentic racemic material (Chiralpak AZ-H, 94:6 hexanes:*i*-PrOH, 1.0 mL/min, 220 nm): t_R: 18.8 min (major) and 15.9 min (minor).

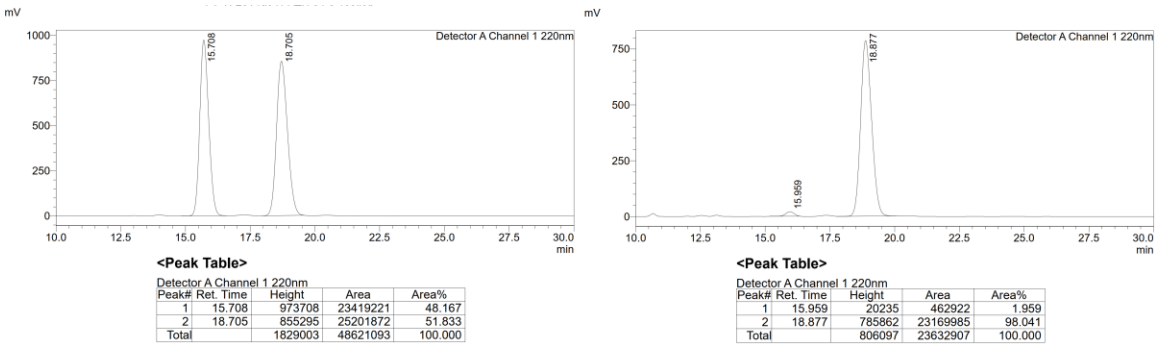

Peak #	Ret. Time	Area	Area %	Peak #	Ret. Time	Area	Area %
1	15.708 min	23419221	48.167	1	15.959 min	462922	1.959
2	18.705 min	25201872	51.833	2	18.877 min	23169985	98.041

(S,*Z*)-6-Chloro-1-phenylhex-5-en-3-ol (*Z*-3.97): IR (neat): 3356 (br, m), 2924 (m), 1630 (m), 1495 (w), 1453 (m), 1331 (w), 1081 (m), 1046 (m), 1030 (m), 931 (w), 861 (m), 744 (s), 696 (s) cm^{-1}; **^{1}H NMR (400 MHz, $CDCl_3$):** δ 7.37 – 7.27 (m, 2H), 7.20 (ddt, *J* = 10.6, 6.4, 1.6 Hz, 3H), 6.17 (dt, *J* = 7.1, 1.6 Hz, 1H), 5.87 (q, *J* = 7.2 Hz, 1H), 3.83 – 3.72 (m, 1H), 2.81 (ddd, *J* = 13.8, 8.4, 6.6 Hz, 1H), 2.76 – 2.65 (m, 1H), 2.51 – 2.42 (m, 2H), 1.90 – 1.78 (m, 2H), 1.46 (d, *J* = 4.9 Hz, 1H); **^{13}C NMR (100 MHz, $CDCl_3$):** δ 141.9, 128.5, 128.5, 127.7, 126.0, 120.4, 70.3, 38.7, 35.2, 32.1; **HRMS (DART):** Calcd for $C_{11}H_{14}BrF_3NSO$ $[M+H-H_2O]^+$: 193.0784; Found: 193.0783; **Specific Rotation:** $[\alpha]^{21.5}_D$ –27.4° (*c* 1.82, $CHCl_3$) for a 79:21 er sample. Enantiomeric purity was determined by HPLC analysis in comparison with authentic racemic material (Chiralcel OD-H, 98:2 hexanes:*i*-PrOH, 1.0 mL/min, 220 nm): t_R: 29.1 min (major) and 46.9 min (minor).

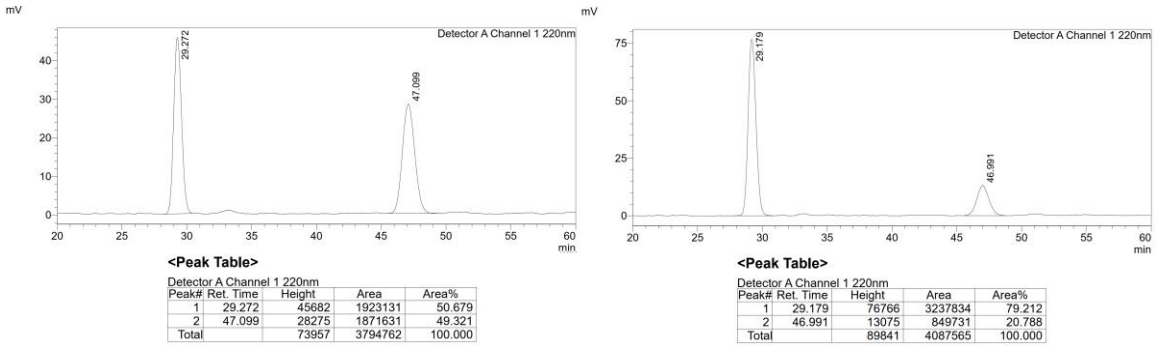

Peak #	Ret. Time	Area	Area %	Peak #	Ret. Time	Area	Area %
1	29.727 min	1923131	50.679	1	29.179 min	3237834	79.212
2	47.099 min	1871631	49.321	2	46.991 min	849731	20.788

(*R*,1*E*,5*Z*)-6-Chloro-1-phenylhexa-1,5-dien-3-ol (*Z*-3.98): IR (neat): 3342 (br, m), 3026 (w), 1630 (w), 1493 (w), 1448 (w), 1306 (w), 1100 (w), 1029 (m), 965 (s), 750 (s), 714 (m), 692 (s) cm^{-1}; **^{1}H NMR (600 MHz, $CDCl_3$):** δ 7.39 (d, *J* = 7.2 Hz, 2H), 7.33 (t, *J* = 7.7 Hz, 2H), 7.25 (t, *J* = 7.3 Hz, 1H), 6.62 (d, *J* = 15.9 Hz, 1H), 6.25 (dd, *J* = 15.9, 6.5 Hz, 1H), 6.18 (dt, *J* = 7.2, 1.6 Hz, 1H), 5.90 (q, *J* = 7.1 Hz, 1H), 4.44 (dddd, *J* = 11.5, 6.8, 4.7, 2.3 Hz, 1H), 2.70 – 2.57 (m, 2H), 1.68 (d, *J* = 3.9 Hz, 1H); **^{13}C NMR (150 MHz, $CDCl_3$):** δ 136.5, 131.3, 131.0, 128.7, 127.9, 127.2, 126.6, 120.6, 71.8, 35.1; **HRMS (DART):** Calcd for $C_{12}H_{12}Cl$ $[M+H–H_2O]^+$: 191.0628; Found: 191.0621; **Specific Rotation:** $[\alpha]^{25.7}_D$ +9.9° (*c* 1.0, $CHCl_3$) for a 82:18 er sample. Enantiomeric purity was determined by HPLC analysis in comparison with authentic racemic material (Chiralpak AZ-H, 99:1 hexanes:*i*-PrOH, 1.0 mL/min, 220 nm): t_R: 35.9 min (major) and 39.0 min (minor).

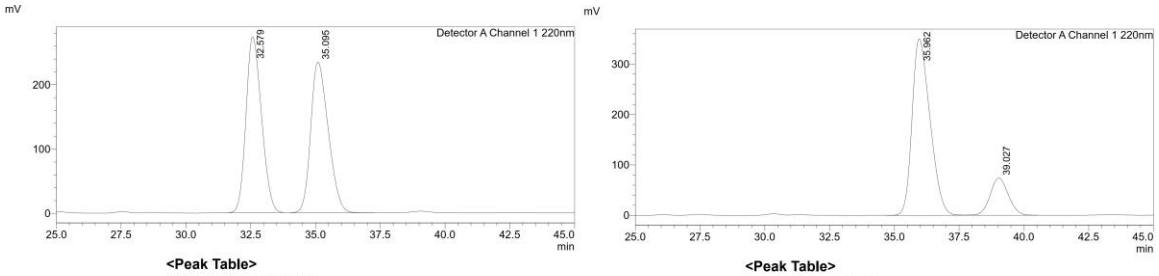

Peak #	Ret. Time	Area	Area %	Peak #	Ret. Time	Area	Area %
1	32.579 min	11421984	50.793	1	35.962 min	16856632	82.407
2	35.095 min	11065389	49.207	2	39.027 min	3598651	17.593

(*R,Z*)-6-Chloro-1-phenylhex-5-en-1-yn-3-ol (*Z*-3.99): IR (neat): 3330 (br, m), 1632 (w), 1489 (m), 1442 (w), 1326 (w), 1308 (w), 1043 (m), 754 (s), 690 (s) cm^{-1}; **^{1}H NMR (400 MHz, $CDCl_3$):** δ 7.47 – 7.40 (m, 2H), 7.36 – 7.27 (m, 3H), 6.24 (dt, *J* = 7.2, 1.6 Hz, 1H), 6.00 (q, *J* = 7.1 Hz, 1H), 4.72 (q, *J* = 6.1 Hz, 1H), 2.85 – 2.70 (m, 2H), 1.95 (dd, *J* = 5.7, 0.7 Hz, 1H); **^{13}C NMR (100 MHz, $CDCl_3$):** δ 131.8, 128.7, 128.4, 126.4, 122.4, 121.2, 89.1, 85.5, 61.7, 35.7; **HRMS (DART):** Calcd for $C_{12}H_{10}Cl$ $[M+H–H_2O]^+$: 189.0471; Found: 180.0469; **Specific Rotation:** $[\alpha]^{21.1}_D$ +17.4° (*c* 1.52, $CHCl_3$) for a 81:19 er sample. Enantiomeric purity was determined by HPLC analysis in comparison with authentic racemic material (Chiralcel OZ-H, 98:2 hexanes:*i*-PrOH, 1.0 mL/min, 220 nm): t_R: 14.1 min (major) and 15.0 min (minor).

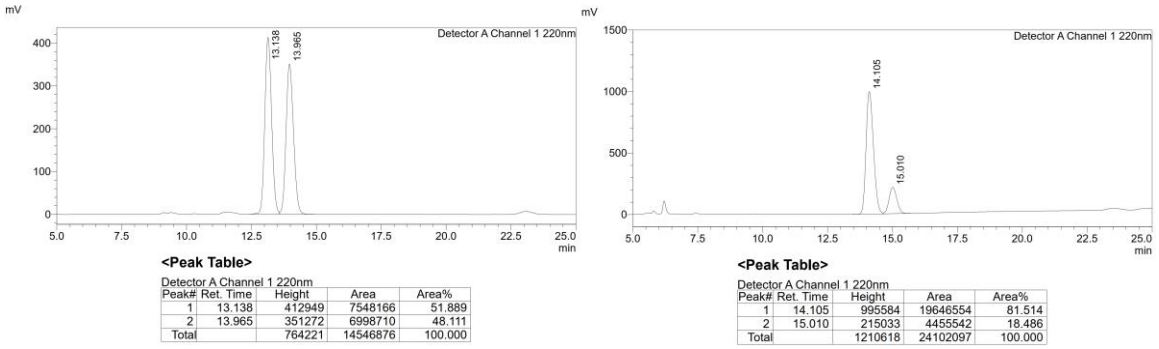

Peak #	Ret. Time	Area	Area %	Peak #	Ret. Time	Area	Area %
1	13.138 min	7548166	51.889	1	14.105 min	19646554	81.514
2	13.965 min	6998710	48.111	2	15.010 min	4455542	18.486

(*R*,1*Z*,5*Z*)-2-Bromo-6-chloro-1-phenylhexa-1,5-dien-3-ol (*Z*-3.100): IR (neat): 3381 (br, m), 1631 (w), 1491 (w), 1445 (w), 1338 (w), 1303 (w), 1275 (w), 1050 (m), 1030 (m), 920 (w), 867 (w), 752 (s), 717 (s) cm^{-1}; **^{1}H NMR (400 MHz, $CDCl_3$):** δ 7.72 – 7.53 (m, 2H), 7.43 – 7.29 (m, 3H), 7.09 (s, 1H), 6.20 (dt, *J* = 7.1, 1.5 Hz, 1H), 5.86 (q, *J* = 7.1 Hz, 1H), 4.40 (q, *J* = 6.3 Hz, 1H), 2.76 (tt, *J* = 7.0, 1.6 Hz, 2H), 2.18 (d, *J* = 6.0 Hz, 1H); **^{13}C NMR (100 MHz, $CDCl_3$):** δ 134.9, 129.2, 128.9, 128.7, 128.4, 128.3, 126.5, 121.0, 76.4, 33.8; **HRMS (DART):** Calcd for $C_{12}H_{11}BrCl$ $[M+H–H_2O]^+$: 268.9733; Found: 268.9736; **Specific Rotation:** $[\alpha]^{25.3}_D$ –31.4° (*c* 2.4, $CHCl_3$) for a 95:5 er sample. Enantiomeric purity was determined by HPLC analysis in comparison with authentic racemic material (Chiralcel OZ-H, 98:2 hexanes:*i*-PrOH, 1.0 mL/min, 220 nm): t_R: 11.1 min (major) and 12.5 min (minor).

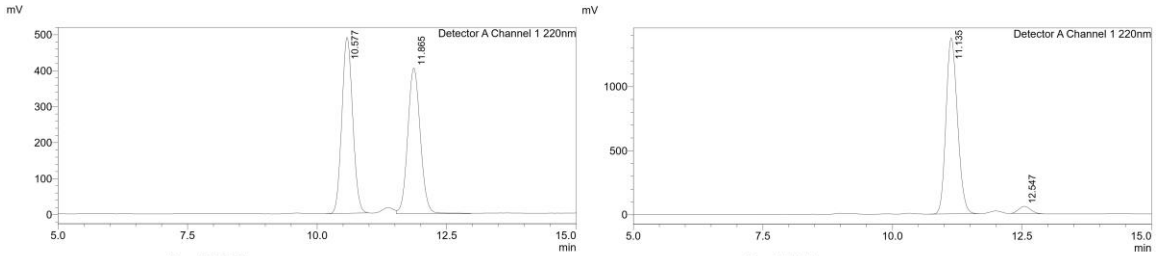

<Peak Table>
Detector A Channel 1 220nm

Peak#	Ret. Time	Height	Area	Area%
1	10.577	489192	7137557	50.882
2	11.865	405090	6890042	49.118
Total		894282	14027599	100.000

<Peak Table>
Detector A Channel 1 220nm

Peak#	Ret. Time	Height	Area	Area%
1	11.135	1372907	21193634	95.878
2	12.547	56580	911046	4.122
Total		1429488	22104680	100.000

Peak #	Ret. Time	Area	Area %	Peak #	Ret. Time	Area	Area %
1	10.577 min	7137557	50.882	1	11.135 min	21193634	95.878
2	11.865 min	6890042	49.118	2	12.547 min	911046	4.122

(*R*,*Z*)-4-Chloro-1-cyclohexylbut-3-en-1-ol (*Z*-3.101): IR (neat): 3361 (br, m), 2922 (s), 2851 (s), 1449 (m), 1334 (w), 1102 (w), 1086 (w), 1059 (w), 1036 (m), 892 (w), 860 (w), 748 (m), 714 (m) cm^{-1}; **^{1}H NMR (400 MHz, $CDCl_3$):** δ 6.14 (dt, *J* = 7.1, 1.6 Hz, 1H),

5.90 (q, *J* = 7.1 Hz, 1H), 3.53 – 3.42 (m, 1H), 2.47 (dddd, *J* = 15.0, 6.9, 4.0, 1.7 Hz, 1H), 2.43 – 2.32 (m, 1H), 1.87 (dtt, *J* = 12.2, 3.3, 1.8 Hz, 1H), 1.83 – 1.73 (m, 2H), 1.69 (dddd, *J* = 13.9, 8.0, 3.9, 2.3 Hz, 2H), 1.42 (d, *J* = 5.0 Hz, 1H), 1.40 – 0.96 (m, 6H); **^{13}C NMR (100 MHz, $CDCl_3$):** δ 128.6, 119.9, 75.3, 43.5, 32.2, 29.2, 28.0, 26.5, 26.3, 26.2; **HRMS (DART):** Calcd for $C_{10}H_{16}Cl$ $[M+H-H_2O]^+$: 171.09350; Found: 171.09304; **Specific Rotation:** $[\alpha]^{20.0}_D$ +8.1° (*c* 1.1, $CHCl_3$) for a 94:6 er sample. Enantiomeric purity was determined by HPLC analysis of the *p*-nitrobenzoyl derived product in comparison with authentic racemic material (Chiralpak AS-H, 99:1 hexanes:*i*-PrOH, 1.0 mL/min, 220 nm): t_R: 9.7 min (major) and 11.7 min (minor).

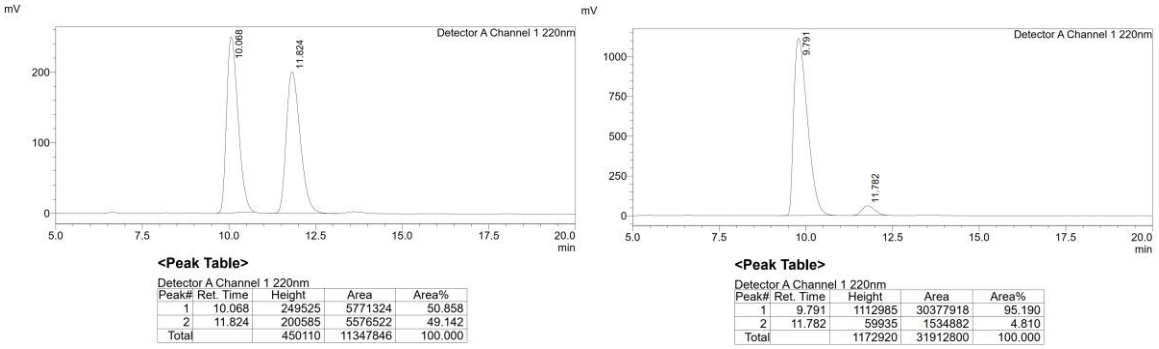

<Peak Table>
Detector A Channel 1 220nm

Peak#	Ret. Time	Height	Area	Area%
1	10.068	249525	5771324	50.858
2	11.824	200585	5576522	49.142
Total		450110	11347846	100.000

<Peak Table>
Detector A Channel 1 220nm

Peak#	Ret. Time	Height	Area	Area%
1	9.791	1112985	30377918	95.190
2	11.782	59935	1534882	4.810
Total		1172920	31912800	100.000

Peak #	Ret. Time	Area	Area %	Peak #	Ret. Time	Area	Area %
1	10.068 min	5771324	50.858	1	9.791 min	30377918	95.190
2	11.824 min	5576522	49.142	2	11.782 min	1534882	4.810

(*R*,*Z*)-4-Chloro-1-((1*R*,5*S*)-6,6-dimethylbicyclo[3.1.1]hept-2-en-2-yl)but-3-en-1-ol (*Z*-3.102): IR (neat): 3366 (br, m), 2985 (m), 2914 (s), 2831 (m), 1630 (m), 1467 (m), 1381 (m), 1045 (s), 964 (m), 868 (m), 749 (s), 717 (s), 695 (s) cm^{-1}; **^{1}H NMR (400 MHz, $CDCl_3$):** δ 6.12 (dt, *J* = 7.1, 1.7 Hz, 1H), 5.85 (q, *J* = 7.0 Hz, 1H), 5.49 (dq, *J* = 3.6, 1.8 Hz, 1H), 4.14 – 4.08 (m, 1H), 2.50 – 2.18 (m, 6H), 2.11 (dq, *J* = 6.2, 2.8 Hz, 1H), 1.44 (d, *J* = 4.0 Hz, 1H), 1.31 (s, 3H), 1.16 (d, *J* = 8.7 Hz, 1H), 0.83 (s, 3H); **^{13}C NMR (100**

MHz, $CDCl_3$): δ 149.8, 128.0, 119.8, 118.2, 73.7, 42.2, 41.0, 37.9, 32.7, 31.9, 31.2, 26.3, 21.4; **HRMS (DART):** Calcd for $C_{13}H_{18}Cl$ $[M+H-H_2O]^+$: 209.10915; Found: 209.10986; **Specific Rotation:** $[\alpha]^{21.3}_D$ –30.8° (*c* 1.62, $CHCl_3$) for a 87:13 dr, >98:2 er sample.

3.7.7. *Synthesis of Mycothiazole*

Scheme S3.3. Synthesis of Alkenyl-B(pin) **3.104**

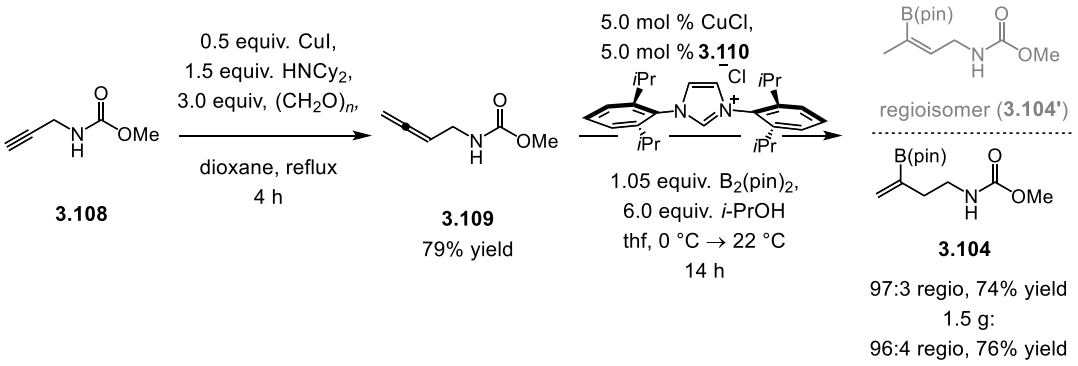

Methyl buta-2,3-dien-1-ylcarbamate (3.109). Copper iodide (952 mg, 5.0 mmol) and paraformaldehyde (900 mg, 30 mmol) were added to a flame-dried round bottom flask equipped with stir bar and a reflux condenser. Dioxane (45 mL) was then added and the resulting reaction mixture was allowed to stir at 22 °C. A solution of Moc-protected propargyl amine[5] (**3.108**) (1.0 g, 8.8 mmol) in dioxane (5 mL) was then added, followed by dicyclohexylamine (5.0 mL, 25 mmol). The reaction was then heated to reflux and allowed to stir for 4 h. The reaction was then allowed to cool to 22 °C and diluted with water (50 mL) and diethyl ether (100 mL). The aqueous layer was removed and extracted with diethyl ether (3 x 10 mL). The combined organic layers were dried over magnesium sulfate, filtered and concentrated onto silica gel. The resulting powder was then purified

(5) This compound has been previously synthesized in quantitative yield in 1 step from commercially available starting materials, see: Teller, H.; Corbet, M.; Mantilli, L; Gopakumar, G.; Goddard, G.; Thiel, W.; Fμürstner, A. *J. Am. Chem. Soc.* **2012**, *134*, 15331–15342.

using silica gel column chromatography (9:1 hexanes/EtOAc) to afford allene **3.109** (880 mg, 79% yield) as pale yellow oil. **IR (neat):** 3327 (br, m), 2936 (w), 1704 (s), 1530 (s), 1462 (w), 1467 (m), 1261 (s), 1193 (w), 850 (w) cm^{-1}; **^{1}H NMR (400 MHz, $CDCl_3$):** δ 5.20 (p, *J* = 6.3 Hz, 1H), 4.90 – 4.73 (m, 3H), 3.78 (s, 2H), 3.67 (s, 3H); **^{13}C NMR (100 MHz, $CDCl_3$):** δ 207.9, 156.9, 88.3, 77.7, 52.3, 39.2; **HRMS (DART):** Calcd for $C_6H_{10}NO_2$ $[M+H]^+$: 128.0712; Found: 128.0718.

Methyl (3-(4,4,5,5-tetramethyl-1,3,2-dioxaborolan-2-yl)but-3-en-1-yl)carbamate (3.104). In a N_2-filled glovebox, copper chloride (38 mg, 0.39 mmol), NHC **3.110** (166 mg, 0.39 mmol) and NaO*t*Bu (300 mg, 3.13 mmol) were added to an oven-dried 100 mL round bottom flask equipped with stir bar. Anhydrous tetrahydrofuran (39 mL) was then added. The flask was sealed with a septa and allowed to stir at 22 °C for 2 h, after which $B_2(pin)_2$ (2.01 g, 7.9 mmol) and allene **3.109** (1.0 g, 7.8 mmol) were added. The vial was then sealed with a septa, brought out of the glovebox and cooled to 0 °C. Isopropanol (3.6 mL, 46.9 mmol) was then added dropwise to the reaction mixture. After the addition was complete, the ice bath was removed and the reaction was allowed to warm to 22 °C. After 14 h, the reaction was diluted with diethyl ether (50 mL) and passed through a plug of celite and silica gel. The resulting solution was then concentrated onto silica gel and purified by silica gel column chromatography (gradient elution, 10:1 → 4:1 hexanes/EtOAc) affording alkenyl-B(pin) **3.104** (1.5 g, 76% yield) as colorless oil. **IR (neat):** 3350 (br, w), 2977 (m), 1703 (s), 1526 (m), 1439 (m), 1371 (s), 1309 (s), 1249 (s), 1215 (s), 1192 (m), 1167 (m), 1139 (s), 854 (w), 832 (w) cm^{-1}; **^{1}H NMR (400 MHz, $CDCl_3$):** δ 5.88 (d, *J* = 3.3 Hz, 1H), 5.68 (s, 1H), 4.93 (s, 1H), 3.64 (s, 3H), 3.28 (q, *J* =

6.3 Hz, 2H), 2.34 (t, *J* = 6.5 Hz, 2H), 1.27 (s, 12H); **^{13}C NMR (100 MHz, $CDCl_3$):** 157.1, 132.1, 83.8, 51.9, 40.9, 35.6, 24.8; **HRMS (DART):** Calcd for $C_{12}H_{23}BNO_4$ $[M+H]^+$: 256.172; Found: 256.1733.

Scheme S3.4. Total Synthesis of Mycothiazole (**3.103**)

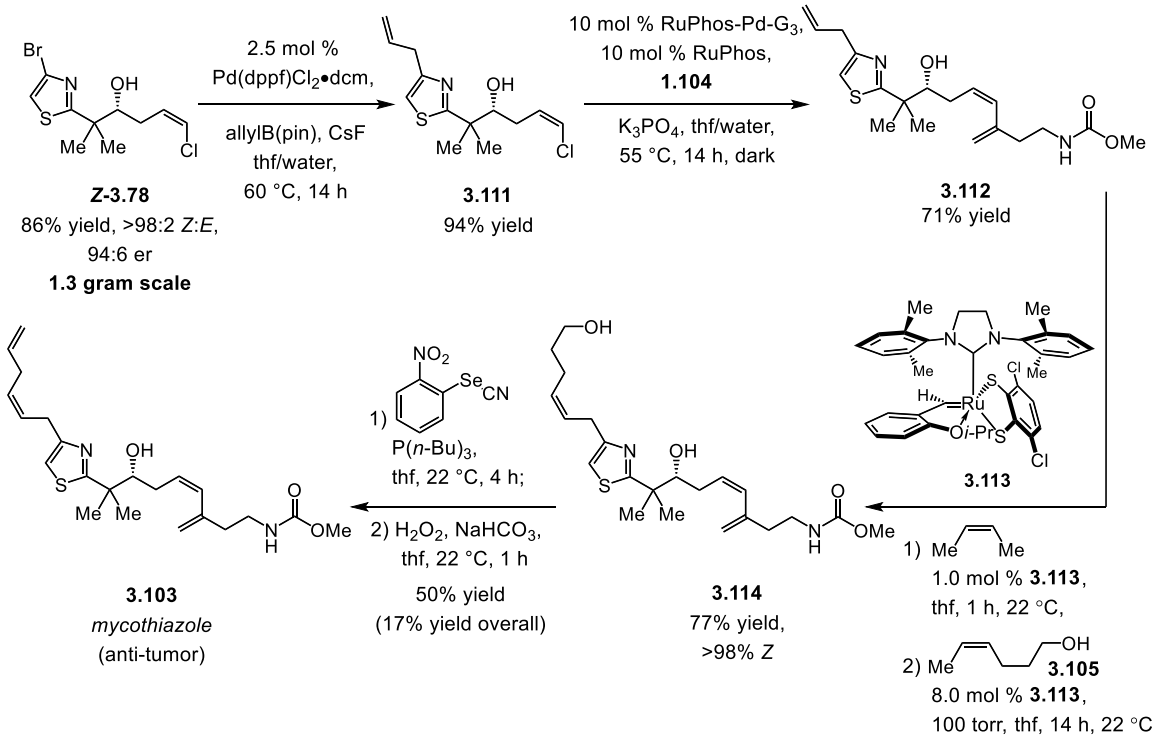

(*R,Z*)-2-(4-Allylthiazol-2-yl)-6-chloro-2-methylhex-5-en-3-ol (3.111): In a N_2-filled glovebox, aryl bromide **Z-3.78** (63 mg, 0.2 mmol) was added to an oven-dried 8 mL vial equipped with stir bar. Pd(dppf)Cl_2•dcm (4.1 mg, 0.005 mmol) was then added to the vial followed by tetrahydrofuran (2.0 mL). Allyl–B(pin) (134 mg, 0.8 mmol) and cesium fluoride (91 mg, 0.6 mmol) were then added. The vial was then sealed with a septa-cap and brought out of the glovebox. Water (200 μL) was then added and the vial was heated to 60 °C and allowed to stir for 14 h. The reaction was then allowed to cool to 22 °C, diluted with diethyl ether (4 mL) and filtered through a plug of silica gel. The unpurified

orange residue was purified by silica gel column chromatography (gradient elution 10:1 → 4:1 hexanes/Et_2O) to afford alkenyl-Cl **3.111** (51 mg, 94% yield) as light yellow oil. **IR (neat):** 3383 (br, m), 2963 (m), 2923 (s), 2854 (m), 1638 (w), 1519 (m), 1466 (m), 1426 (s), 1327 (m), 1051 (s), 993 (m), 916 (s), 747 (s) cm^{-1}; **^{1}H NMR (400 MHz, $CDCl_3$):** δ 6.79 (d, *J* = 1.0 Hz, 1H), 6.10 – 5.95 (m, 3H), 5.19 – 5.09 (m, 2H), 4.90 (d, *J* = 6.3 Hz, 1H), 3.75 (ddd, *J* = 10.3, 6.3, 2.8 Hz, 1H), 3.51 (dq, *J* = 6.8, 1.3 Hz, 2H), 2.59 – 2.46 (m, 1H), 2.13 (dddd, *J* = 14.8, 10.1, 6.3, 1.5 Hz, 1H), 1.45 (d, *J* = 19.0 Hz, 6H); **^{13}C NMR (100 MHz, $CDCl_3$):** 179.0, 154.8, 135.1, 129.4, 118.9, 117.0, 112.2, 77.8, 44.6, 35.9, 30.2, 27.5, 24.2; **HRMS (DART):** Calcd for $C_{13}H_{19}ClNOS$ $[M+H]^+$: 272.0876; Found: 272.0881; **Specific Rotation:** $[\alpha]^{21.5}_D$ +10.3° (*c* 2.58, $CHCl_3$) for a 94:6 er sample.

Methyl (*R*,*Z*)-(8-(4-Allylthiazol-2-yl)-7-hydroxy-8-methyl-3-methylenenon-4-en-1-yl)carbamate (3.112): In a N_2-filled glovebox, alkenyl-Cl **3.111** (500 mg, 1.84 mmol), alkenyl-B(pin) **3.104** (492 mg, 1.93 mmol), Ruphos-Pd-G_3 (150 mg, 0.18 mmol), Ruphos (84 mg, 0.18 mmol) and K_3PO_4 (1.2 g, 5.52 mmol) were added to an oven-dried 40 mL vial equipped with stir bar. Tetrahydrofuran (18 mL) was then added and the vial was sealed with a septa-cap and brought out of the glovebox. Water (1.8 mL) was added to the reaction mixture, the vial was then covered in aluminum foil, heated to 55 °C, and allowed to stir for 14 h. The reaction was then allowed to cool to 22 °C, diluted with diethyl ether (40 mL), and filtered through a plug of silica gel. The resulting unpurified yellow resulting residue was concentrated onto silica gel and purified on a Teledyne ISCO with a 24g RediSep Rf Gold column (gradient elution 1:0 → 0:1 hexanes/EtOAc),

affording diene **3.112** (480 mg, 71% yield) as yellow oil. **IR (neat):** 3340 (br, m), 2965 (m), 1703 (s), 1521 (s), 1466 (m), 1447 (m), 1385 (w), 1364 (w), 1268 (s), 1052 (m), 904 (m), 776 (w), 732 (w) cm^{-1}; **^{1}H NMR (400 MHz, $CDCl_3$):** δ 6.79 (s, 1H), 6.00 (ddt, *J* = 17.0, 10.2, 6.8 Hz, 1H), 5.87 (d, *J* = 11.6 Hz, 1H), 5.70 – 5.64 (m, 1H), 5.43 (s, 1H), 5.17 – 5.08 (m, 2H), 5.00 (s, 1H), 4.89 (d, *J* = 3.6 Hz, 1H), 4.87 (s, 1H), 3.78 (d, *J* = 9.9 Hz, 1H), 3.62 (s, 3H), 3.49 (d, *J* = 6.7 Hz, 2H), 3.37 – 3.10 (m, 2H), 2.45 – 2.19 (m, 4H), 1.41 (d, *J* = 17.9 Hz, 6H); **^{13}C NMR (100 MHz, $CDCl_3$):** δ 179.5, 157.2, 154.7, 142.5, 135.0, 131.0, 130.7, 117.0, 115.9, 112.3, 78.2, 51.9, 44.7, 39.5, 37.2, 35.9, 30.7, 26.8, 24.0; **HRMS (DART):** Calcd for $C_{19}H_{29}N_2O_3S$ $[M+H]^+$: 365.1899; Found: 365.1904; **Specific Rotation:** $[\alpha]^{23.9}_D$ –28.5° (*c* 2.45, $CHCl_3$) for a 94:6 er sample.

Methyl ((*R*,*Z*)-7-Hydroxy-8-(4-((Z)-6-hydroxyhex-2-en-1-yl)thiazol-2-yl)-8-methyl-3-methylenenon-4-en-1-yl)carbamate (3.114): In a N_2-filled glovebox, diene **3.112** (410 mg, 1.12 mmol) and a solution of *cis*-2-butene in tetrahydrofuran (28 wt %, 2.08 g, 10.4 mmol) were added to an oven-dried 40 mL vial equipped with a stir bar. A solution of ruthenium-complex **3.113** (10.7 mg, 0.014 mmol) in tetrahydrofuran (200 μL) was then added. The vial was sealed with a cap and allowed to stir at 22 °C for 1 h, after which the reaction mixture was concentrated to remove excess *cis*-2-butene. Alcohol **3.105** (730 μL, 6.24 mmol) was then added followed by a solution of ruthenium-complex **3.113** (86 mg, 0.08 mmol) in tetrahydrofuran (2 mL). The vial was then placed under vacuum (100 torr) for 2 h. The vacuum was then turned off and the vial was sealed with a cap. The resulting solution was then allowed to stir at 22 °C for 12 h. The reaction mixture was then concentrated onto silica gel and purified on a Teledyne ISCO with a 24g RediSep Rf

Gold column (gradient elution 1:0 → 9:1 dcm/MeOH), affording primary alcohol **3.114** (405 mg, 77% yield) as a dark oil containing ~5% of homocoupled thiazole. **IR (neat):** 3322 (br, m), 2934 (m), 1699 (s), 1520 (s), 1439 (m), 1385 (w), 1364 (w), 1271 (s), 1192 (m), 1144 (m), 1051 (s), 1014 (s), 899 (m), 775 (m), 734 (m) cm^{-1}; **^{1}H NMR (400 MHz, $CDCl_3$):** 6.79 (s, 1H), 5.87 (d, *J* = 11.5 Hz, 1H), 5.72 – 5.46 (m, 3H), 5.39 (s, 1H), 5.00 (s, 1H), 4.87 (s, 1H), 4.47 (d, *J* = 3.4 Hz, 1H), 3.81 (ddd, *J* = 10.3, 4.5, 2.5 Hz, 1H), 3.66 – 3.63 (m, 5H), 3.51 (d, *J* = 7.3 Hz, 2H), 3.21 (ddq, *J* = 33.6, 13.6, 6.6 Hz, 2H), 2.48 (s, 1H), 2.45 – 2.13 (m, 6H), 1.72 – 1.62 (m, 2H), 1.41 (d, *J* = 11.3 Hz, 6H); **^{13}C NMR (150 MHz, $CDCl_3$):** δ 179.6, 157.2, 155.2, 142.5, 131.1, 131.0, 130.5, 126.8, 116.0, 112.1, 78.2, 61.3, 51.9, 44.8, 39.5, 37.2, 32.0, 30.8, 29.6, 26.1, 24.1, 23.4; **HRMS (DART):** Calcd for $C_{22}H_{35}N_2O_4S$ $[M+H]^+$: 423.23120; Found: 423.23033; **Specific Rotation:** $[\alpha]^{20.0}_D$ –6.7° (*c* 1.9, $CHCl_3$) for a 94:6 er sample.

Mycothiazole [Methyl ((*R*,*Z*)-8-(4-((*Z*)-Hexa-2,5-dien-1-yl)thiazol-2-yl)-7-hydroxy-8-methyl-3-methylenenon-4-en-1-yl)carbamate] (3.104): Primary alcohol **3.114** (25 mg, 0.059 mmol) and *o*-NO_2-PhSeCN (41 mg, 0.18 mmol) were added to a vial equipped with a stir bar. Anhydrous tetrahydrofuran (590 µL) was then added, followed by dropwise addition of P*n*Bu_3 (45 µL, 0.18 mmol). The reaction was then allowed to stir at 22 °C for 3 h, after which $NaHCO_3$ (151 mg, 1.8 mmol) and H_2O_2 (30 wt % in water, 185 µL, 1.8 mmol) were added. After 1.5 h, the reaction was diluted with water (2 mL) and diethyl ether (2 mL) and the organic layer was removed. The aqueous layer was extracted with diethyl ether (3 x 1 mL). The combined organic layers were dried over magnesium sulfate, filtered and concentrated. The unpurified orange residue was purified by silica gel

column chromatography (gradient elution, 10:1 → 3:1 hexanes/EtOAc) to afford mycothiazole (12 mg, 50% yield) as light yellow oil. The analytical data was fully consistent with those found in the literature.[6] **IR (neat):** 3334 (br, m), 2923 (s), 2851 (m), 1705 (m), 1520 (s), 1465 (m), 1441 (m), 1269 (s), 1055 (m), 908 (m), 777 (w), 735 (w) cm^{-1}; **^{1}H NMR (400 MHz, $CDCl_3$):** δ 6.77 (s, 1H), 5.88 (d, *J* = 13.2 Hz, 1H), 5.88 – 5.76 (m, 1H), 5.76 – 5.64 (m, 2H), 5.64 – 5.55 (m, 1H), 5.42 (s, 1H), 5.10 – 4.97 (m, 3H), 4.92 – 4.84 (m, 2H), 3.78 (d, *J* = 10.0 Hz, 1H), 3.63 (s, 3H), 3.51 (d, *J* = 7.3 Hz, 2H), 3.37 – 3.11 (m, 2H), 2.88 (td, *J* = 6.8, 6.2, 1.7 Hz, 2H), 2.48 – 2.11 (m, 4H), 1.41 (d, *J* = 18.2 Hz, 6H); **^{13}C NMR (100 MHz, $CDCl_3$):** δ 179.6, 157.2, 155.1, 142.6, 136.5, 131.0, 130.7, 129.0, 126.8, 115.9, 115.1, 111.9, 78.2, 51.9, 44.7, 39.5, 37.3, 31.6, 30.7, 29.5, 26.8, 23.9. **HRMS (DART):** Calcd for $C_{22}H_{33}N_2O_3S$ $[M+H]^+$: 405.22064; Found: 405.22066; **Specific Rotation:** $[\alpha]^{20.0}_D$ –22.3° (*c* 0.2, $CHCl_3$) for a 94:6 er sample.

(6) Wang, L.; Hale, K. J. *Org. Lett.* **2015**, *17*, 4200–4203.

3.7.8. *NMR Spectra (^{1}H, ^{13}C, ^{19}F)*

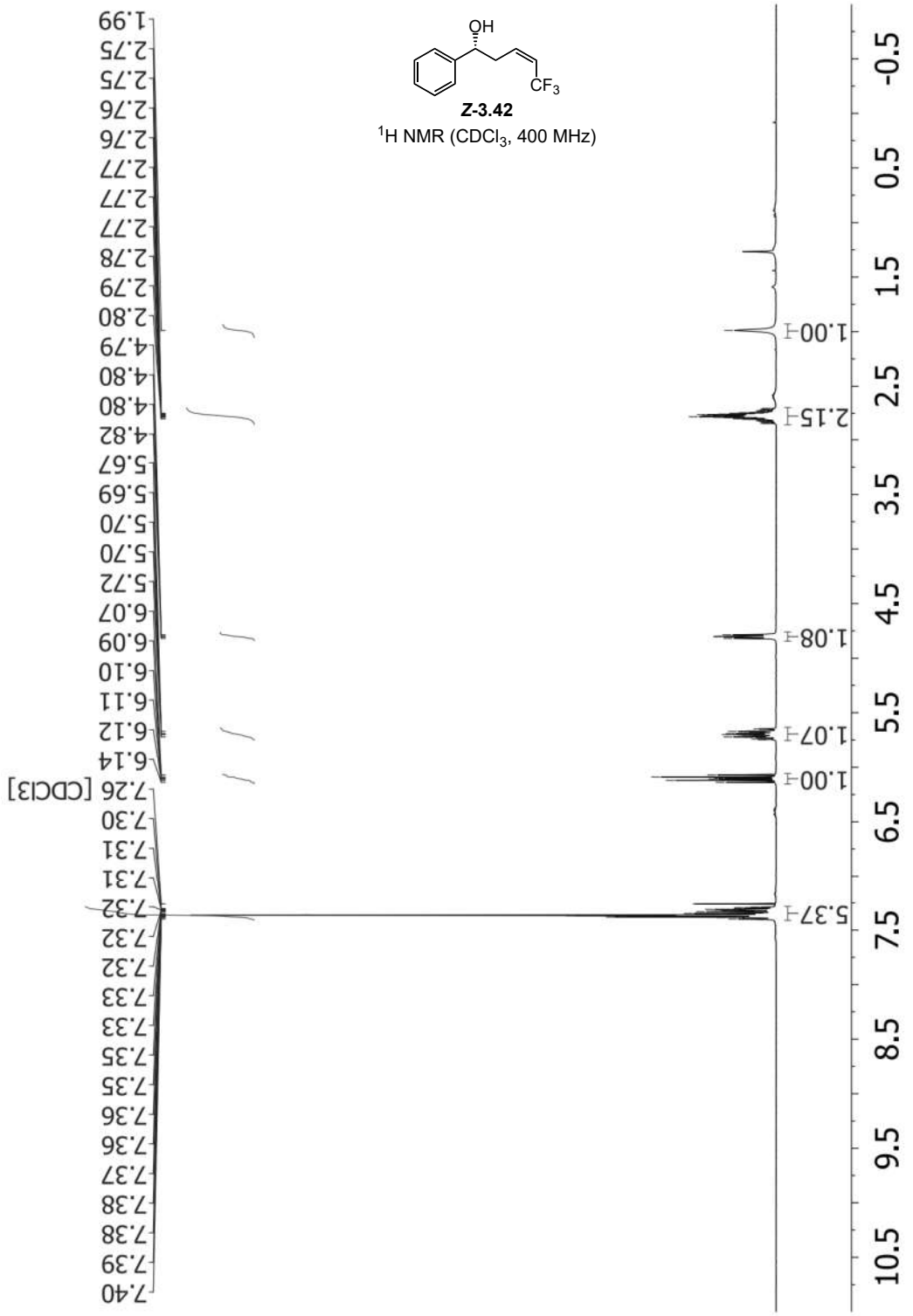

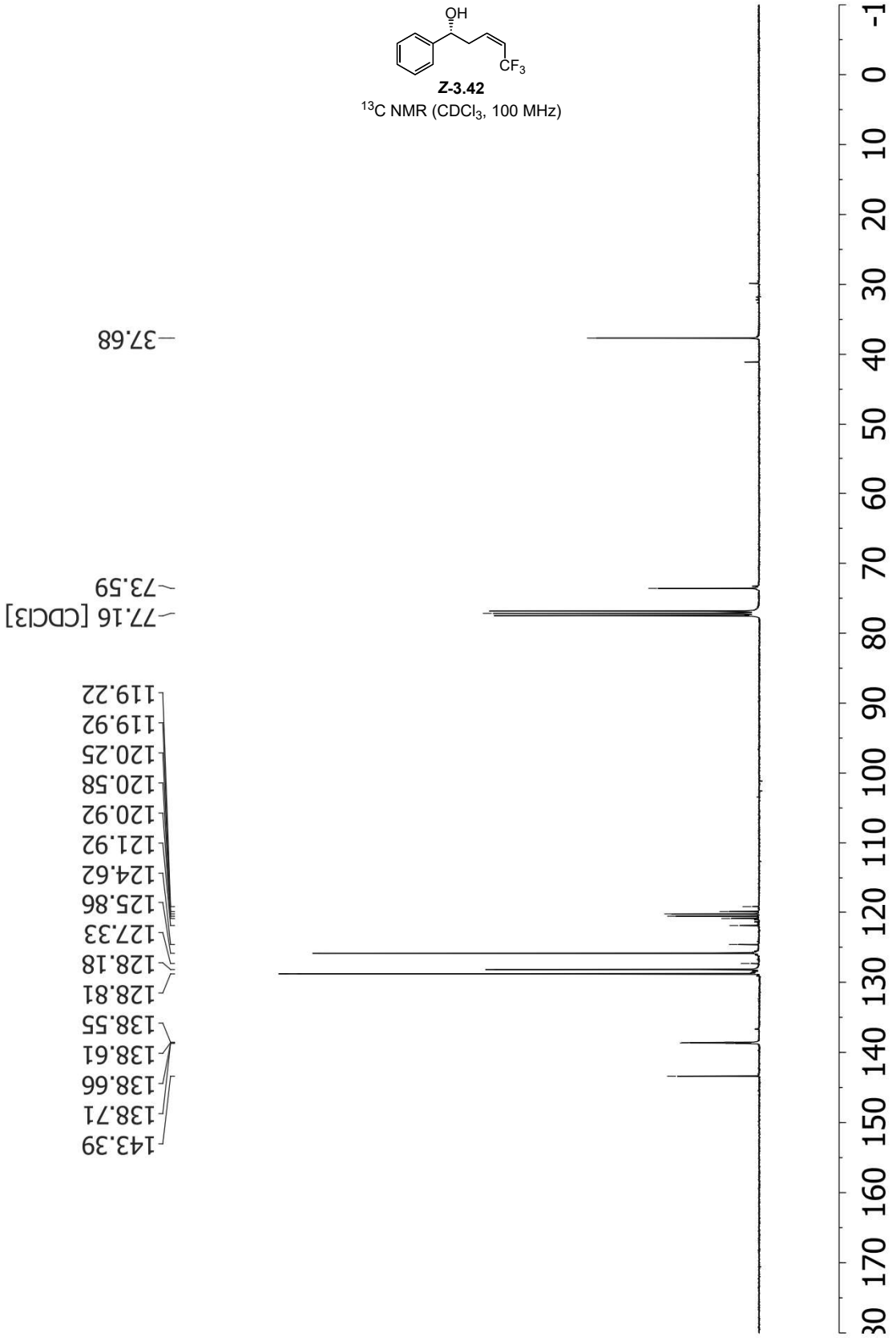
OH
CF3
Z-3.42
13C NMR (CDCl3, 100 MHz)
37.68
73.59
77.16 [CDCl3]
119.22
119.92
120.25
120.58
120.92
121.92
124.62
125.86
127.33
128.18
128.81
138.55
138.61
138.66
138.71
143.39

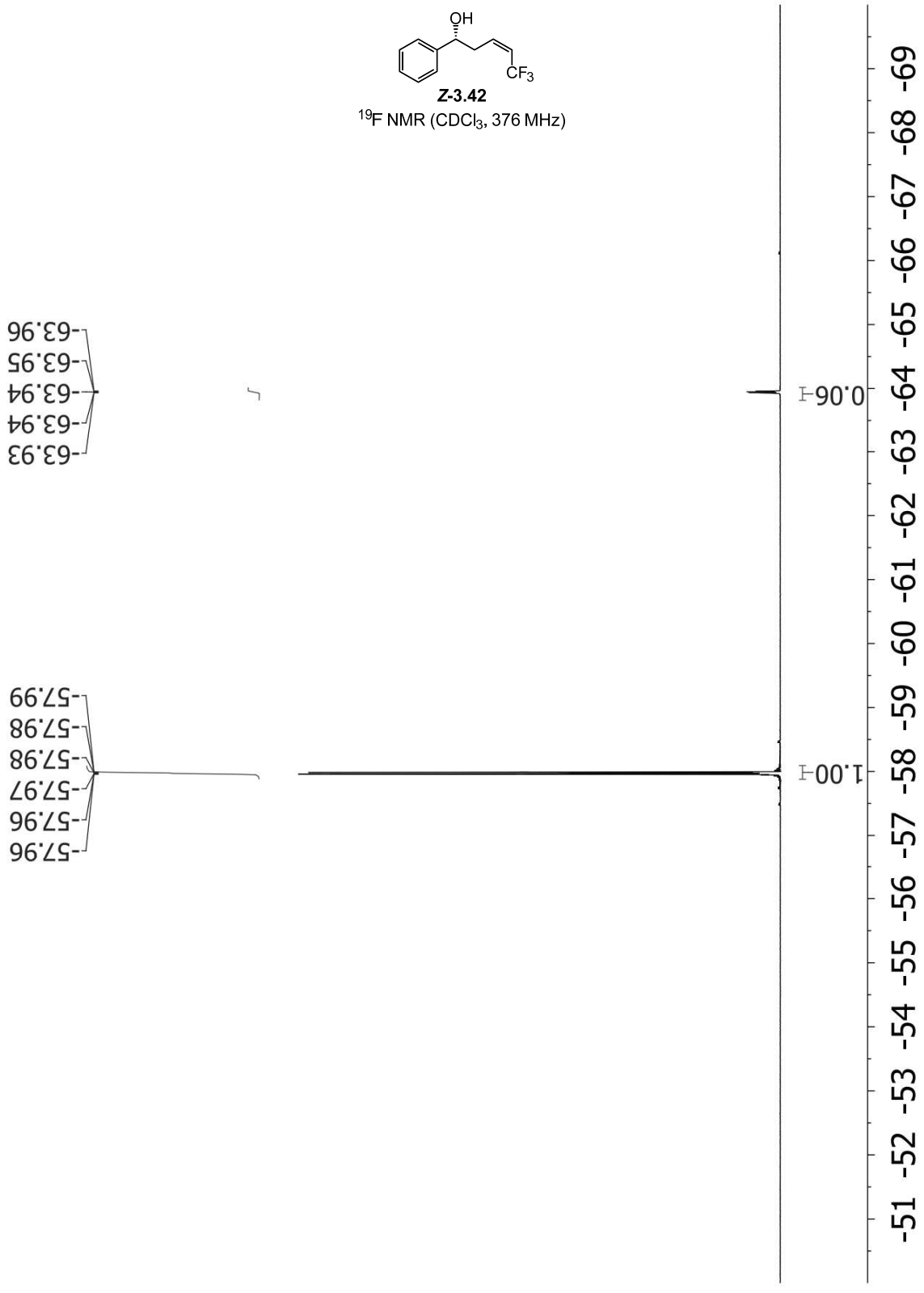
OH
CF3
Z-3.42
19F NMR (CDCl3, 376 MHz)
-63.96
-63.95
-63.94
-63.94
-63.93
-57.99
-57.98
-57.98
-57.97
-57.96
-57.96
0.06
1.00
-51 -52 -53 -54 -55 -56 -57 -58 -59 -60 -61 -62 -63 -64 -65 -66 -67 -68 -69

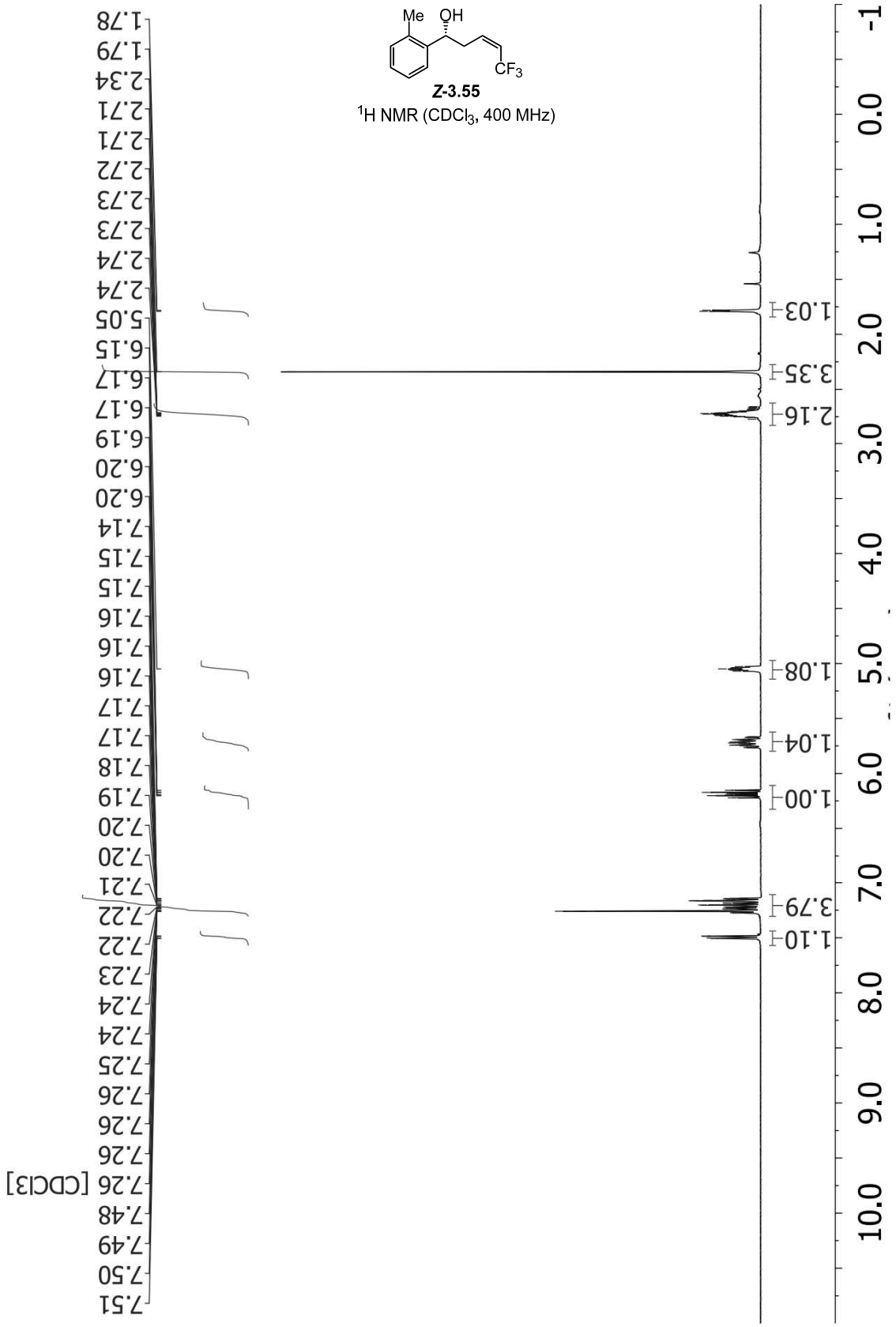
Me
OH
CF3
Z-3.55
1H NMR (CDCl3, 400 MHz)
1.03
3.35
2.16
1.08
1.04
1.00
3.79
1.10
[CDCl3]

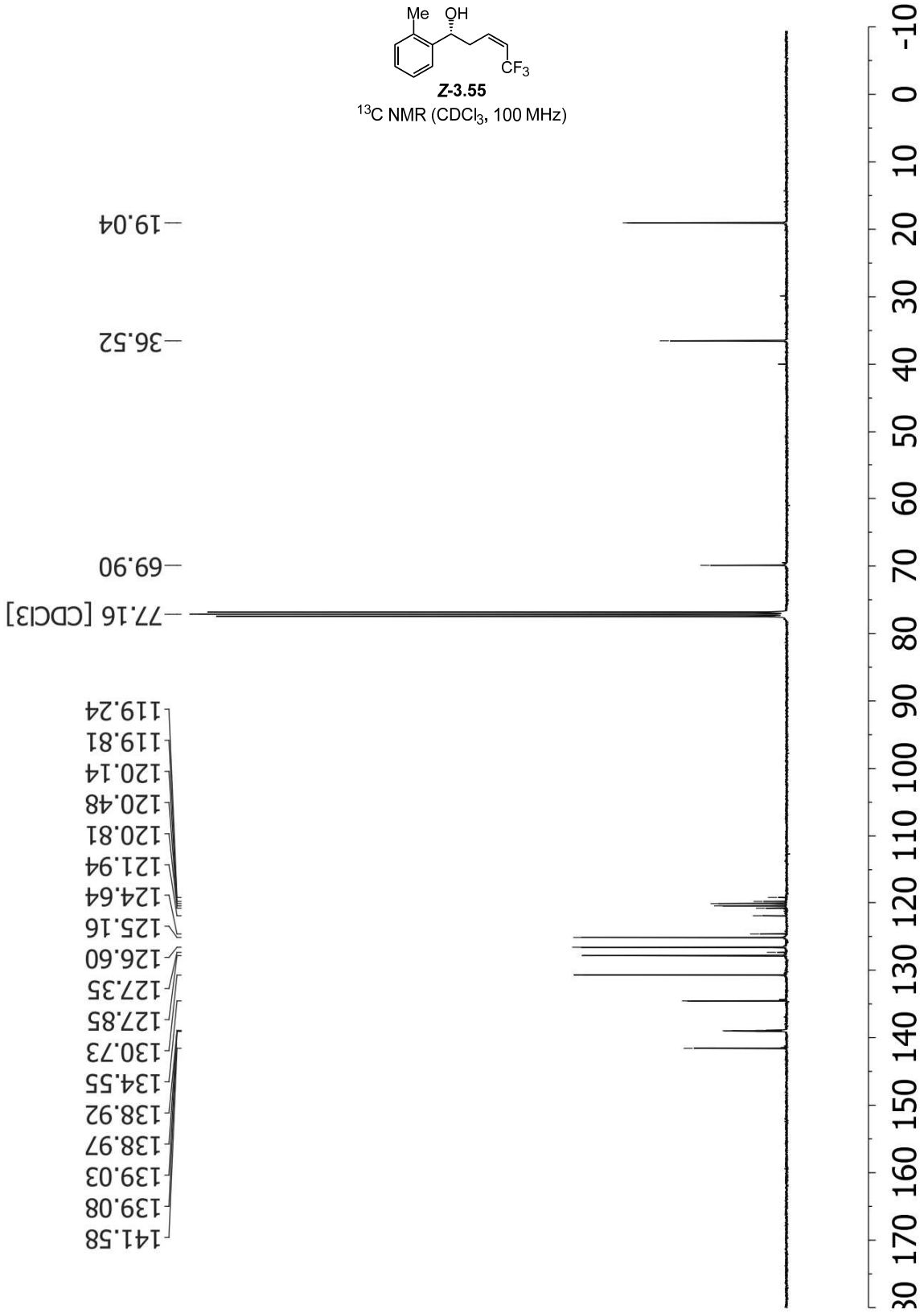
Me
OH
CF3
Z-3.55
13C NMR (CDCl3, 100 MHz)
19.04
36.52
69.90
77.16 [CDCl3]
119.24
119.81
120.14
120.48
120.81
121.94
124.64
125.16
126.60
127.35
127.85
130.73
134.55
138.92
138.97
139.03
139.08
141.58

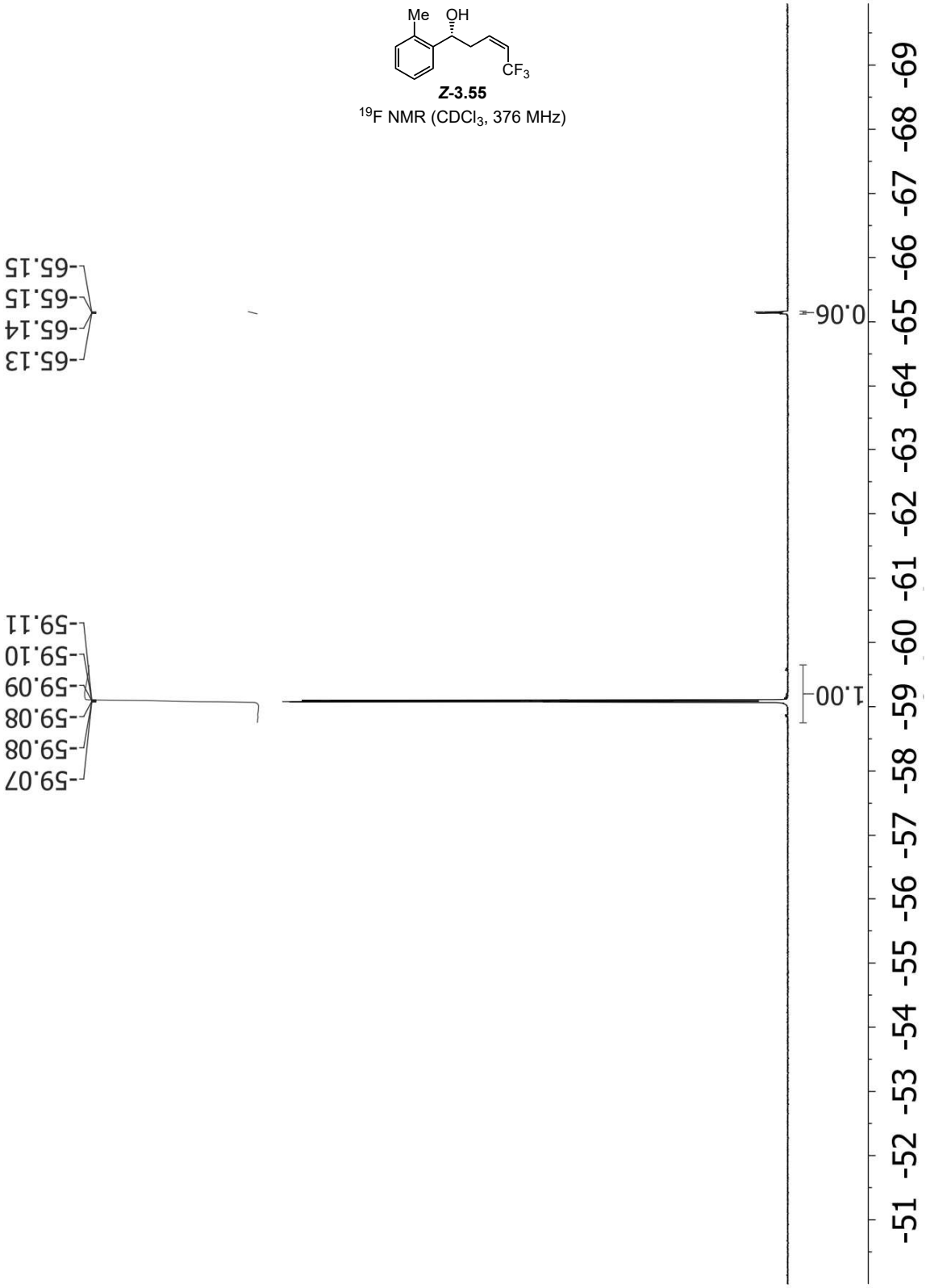
Me
OH
CF3
Z-3.55
19F NMR (CDCl3, 376 MHz)
-65.15
-65.15
-65.14
-65.13
-59.11
-59.10
-59.09
-59.08
-59.08
-59.07
0.06
1.00
-51 -52 -53 -54 -55 -56 -57 -58 -59 -60 -61 -62 -63 -64 -65 -66 -67 -68 -69

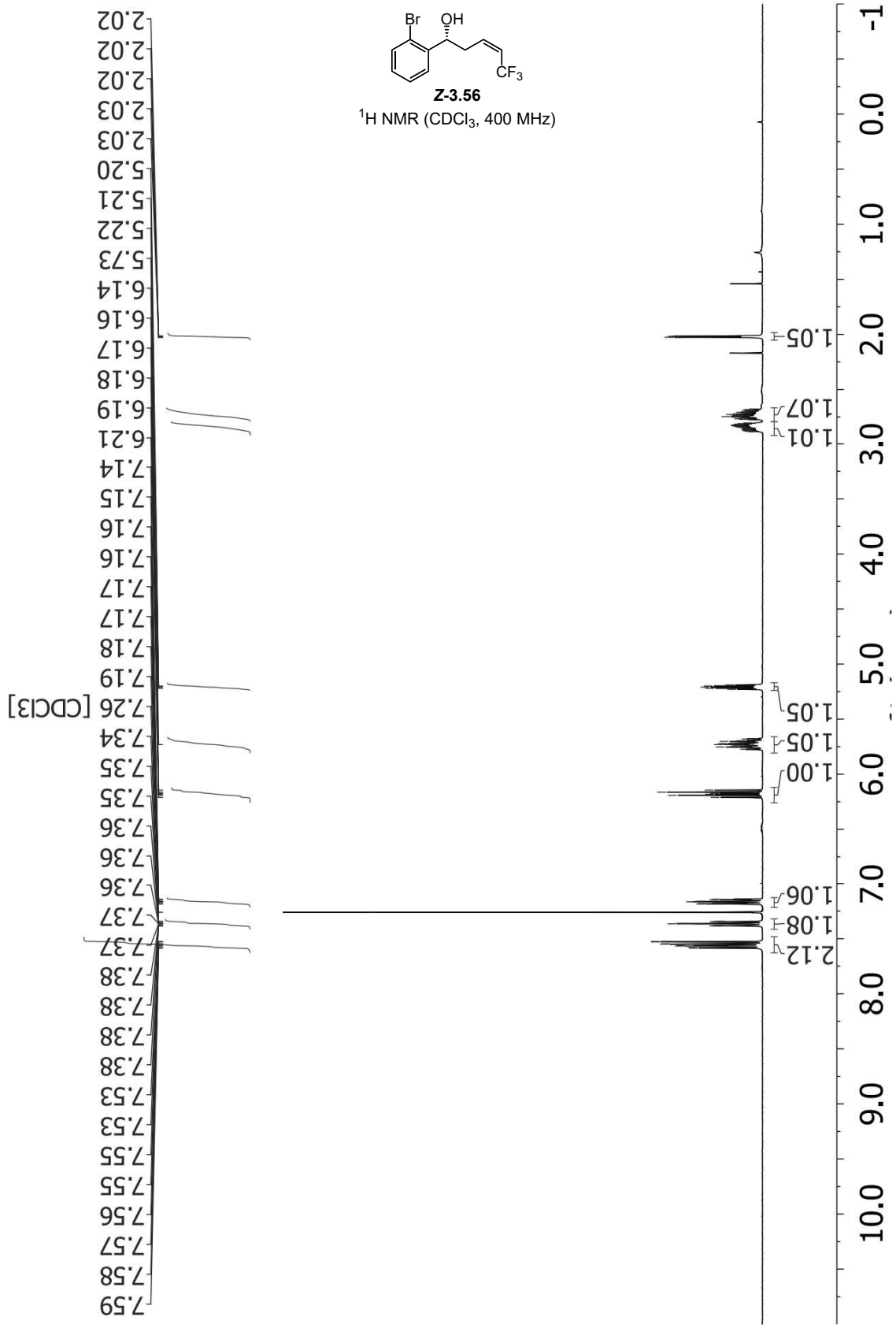
Br
OH
CF3
Z-3.56
1H NMR (CDCl3, 400 MHz)
[CDCl3]

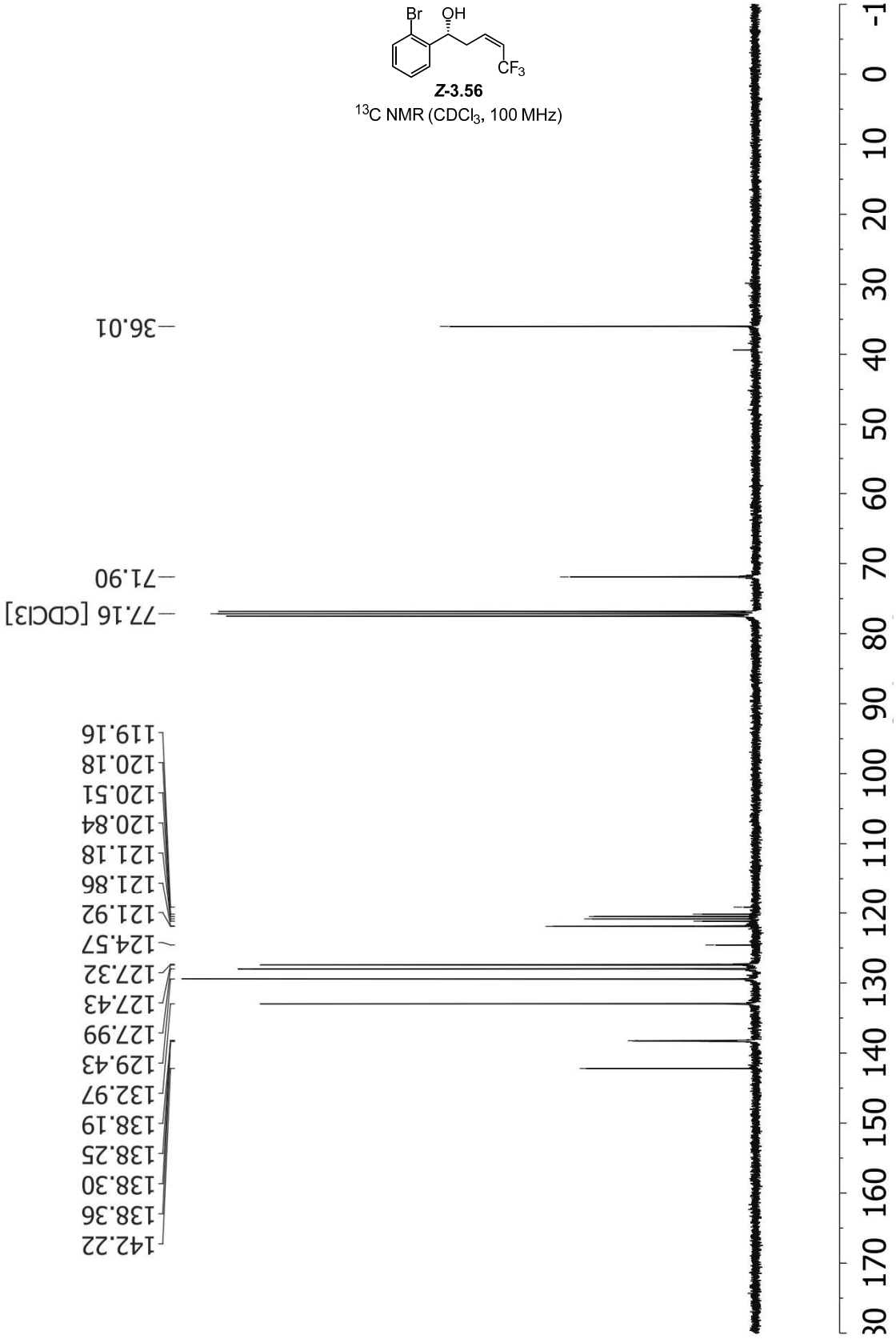
Br
OH
CF3
Z-3.56
13C NMR (CDCl3, 100 MHz)
36.01
71.90
77.16 [CDCl3]
119.16
120.18
120.51
120.84
121.18
121.86
121.92
124.57
127.32
127.43
127.99
129.43
132.97
138.19
138.25
138.30
138.36
142.22

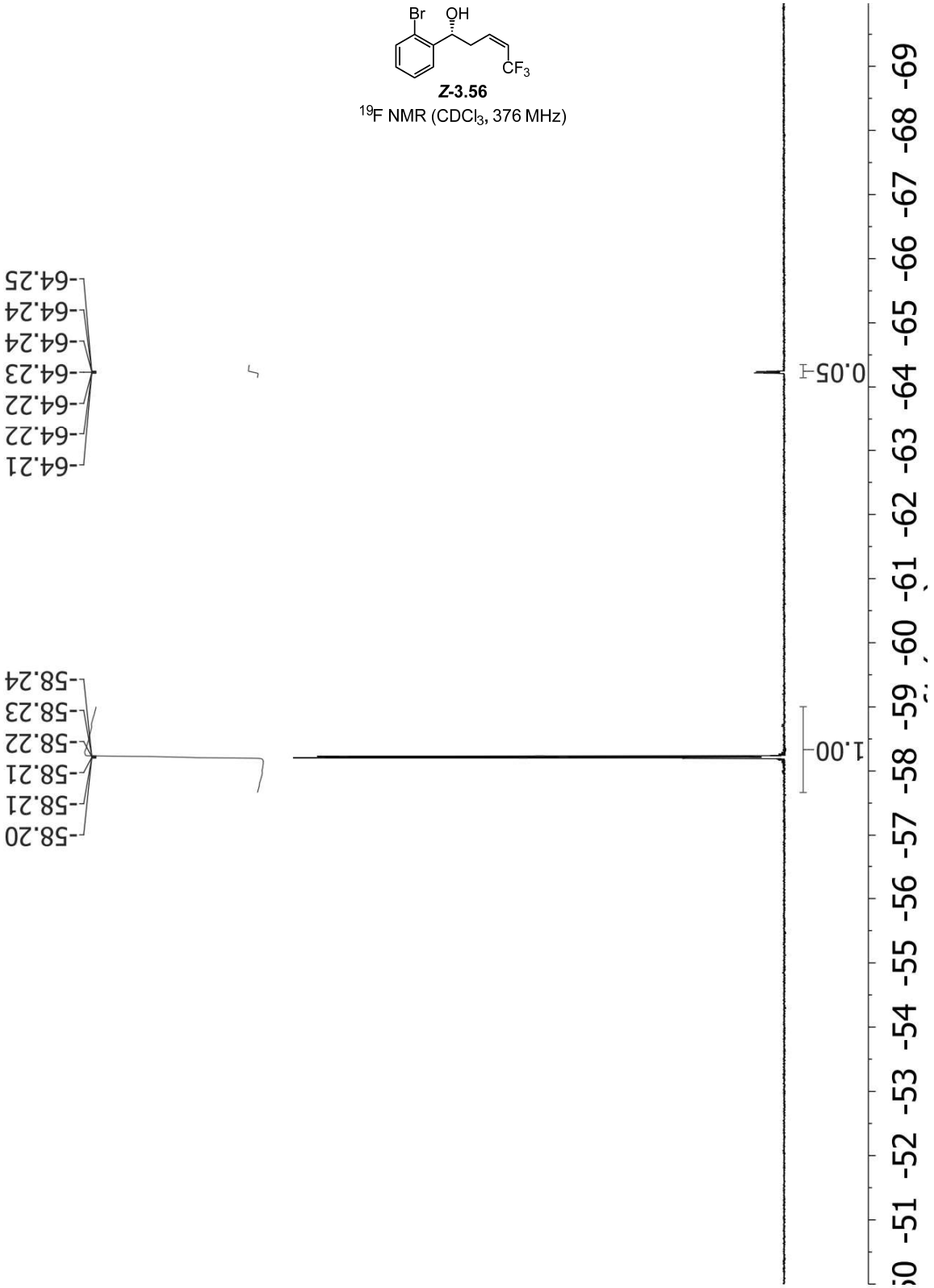
Br
OH
CF3
Z-3.56
19F NMR (CDCl3, 376 MHz)
-64.25
-64.24
-64.24
-64.23
-64.22
-64.22
-64.21
-58.24
-58.23
-58.22
-58.21
-58.21
-58.20
0.05
1.00
-50
-51
-52
-53
-54
-55
-56
-57
-58
-59
-60
-61
-62
-63
-64
-65
-66
-67
-68
-69

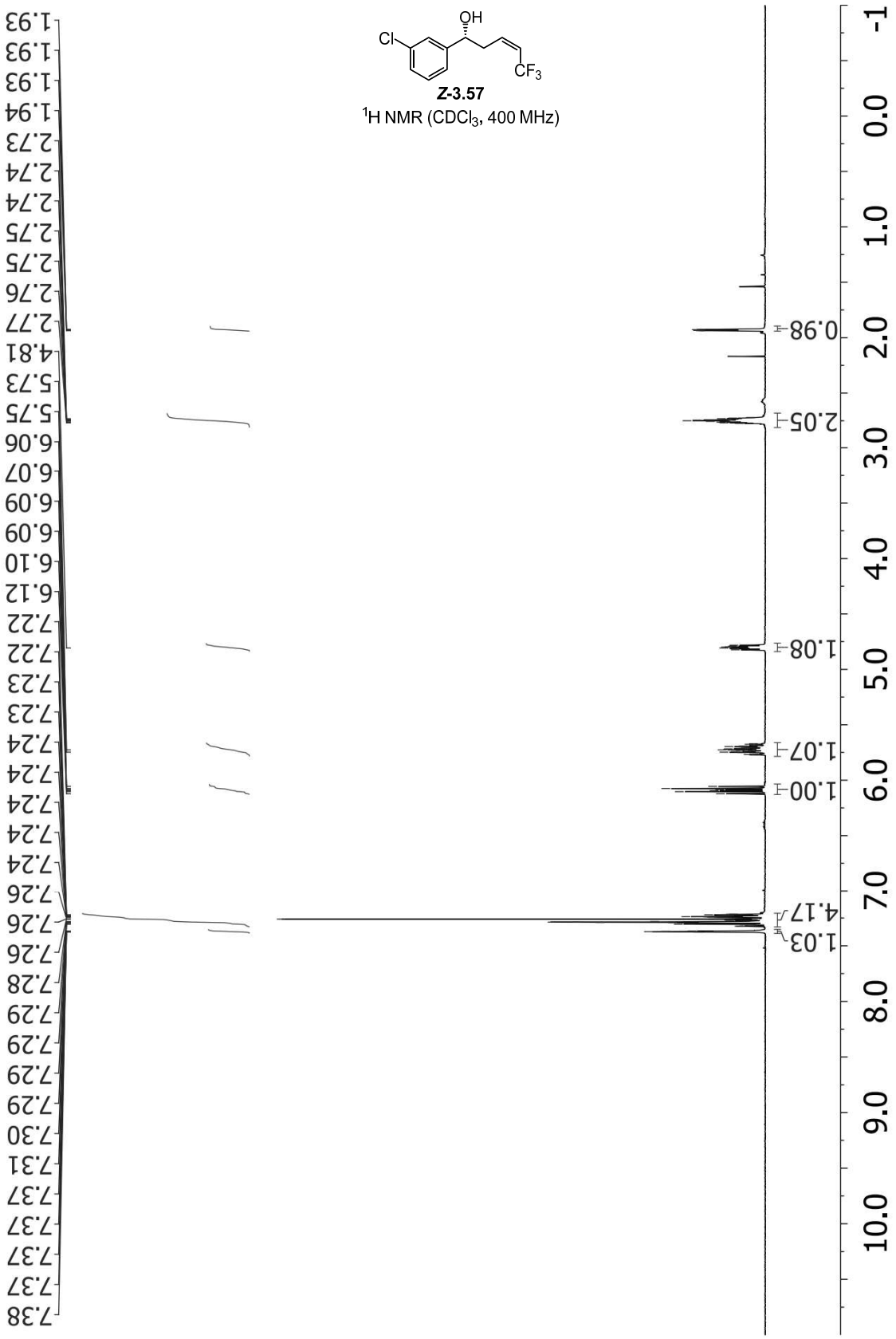
OH
Cl
CF3
Z-3.57
1H NMR (CDCl3, 400 MHz)
0.98
2.05
1.08
1.07
1.00
4.17
1.03

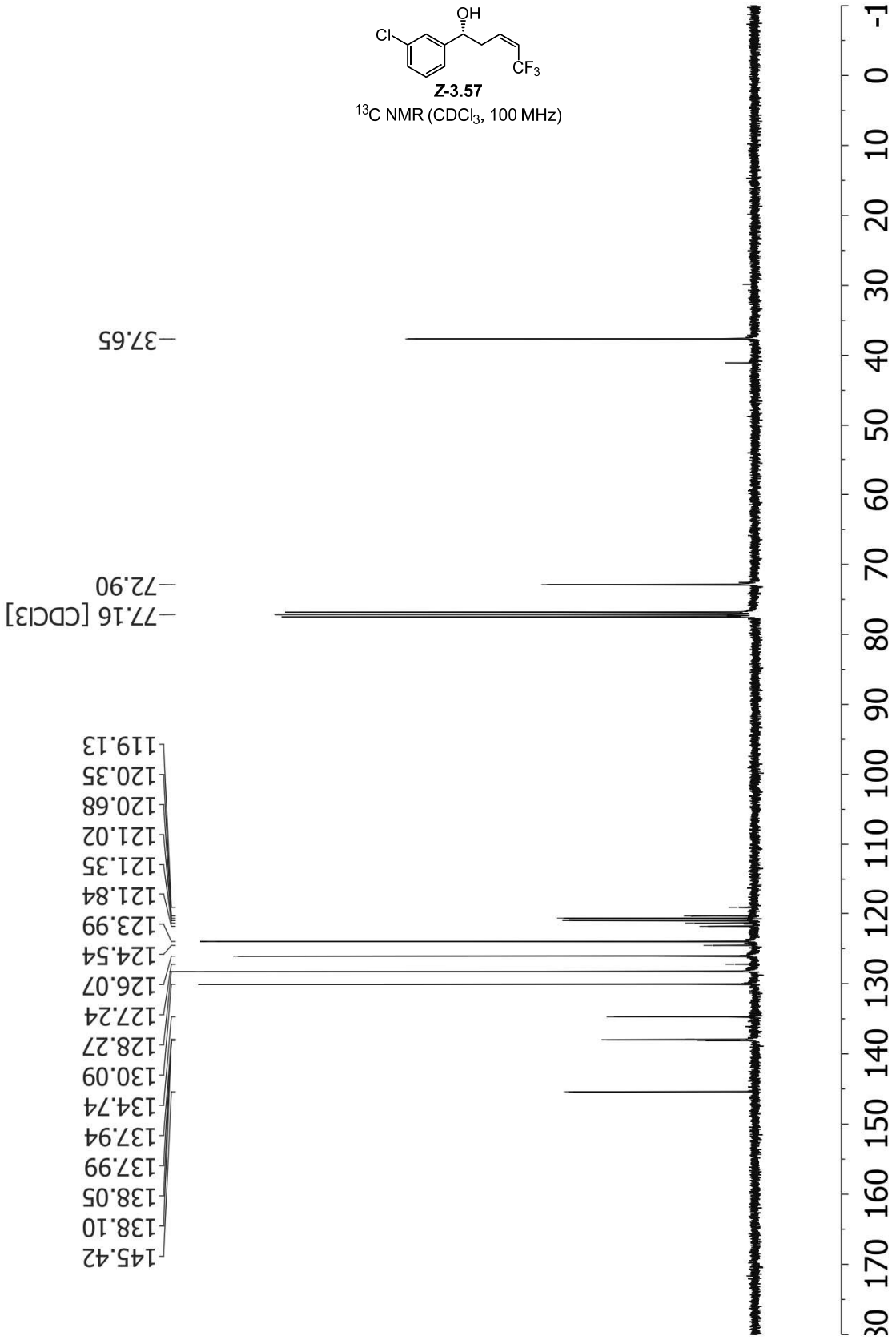
OH
Cl
CF3
Z-3.57
13C NMR (CDCl3, 100 MHz)
37.65
72.90
77.16 [CDCl3]
119.13
120.35
120.68
121.02
121.35
121.84
123.99
124.54
126.07
127.24
128.27
130.09
134.74
137.94
137.99
138.05
138.10
145.42

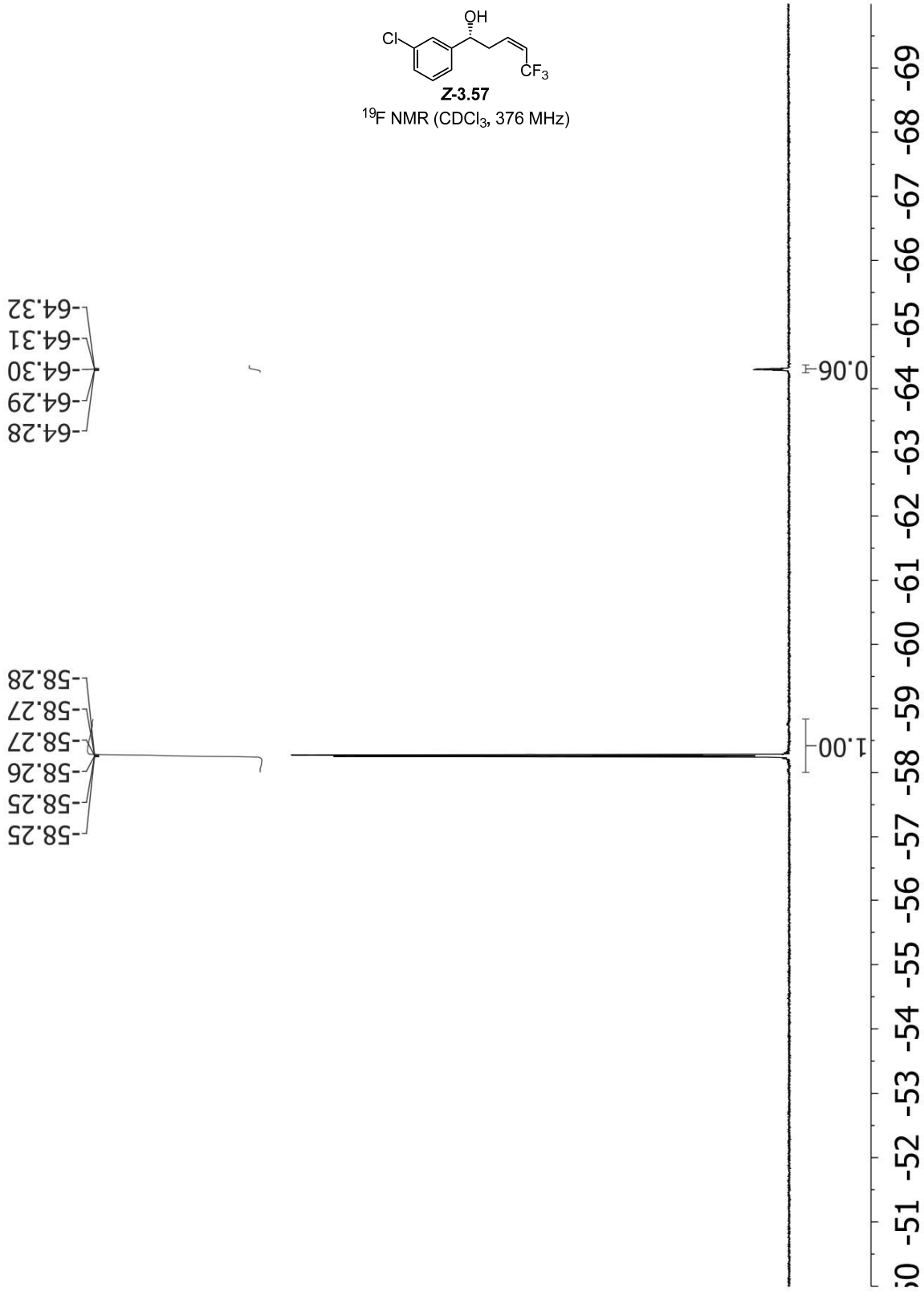
OH
Cl
CF3
Z-3.57
19F NMR (CDCl3, 376 MHz)
-58.25
-58.25
-58.26
-58.27
-58.27
-58.28
-58.28
-64.28
-64.29
-64.30
-64.31
-64.32
1.00
0.06
-50 -51 -52 -53 -54 -55 -56 -57 -58 -59 -60 -61 -62 -63 -64 -65 -66 -67 -68 -69

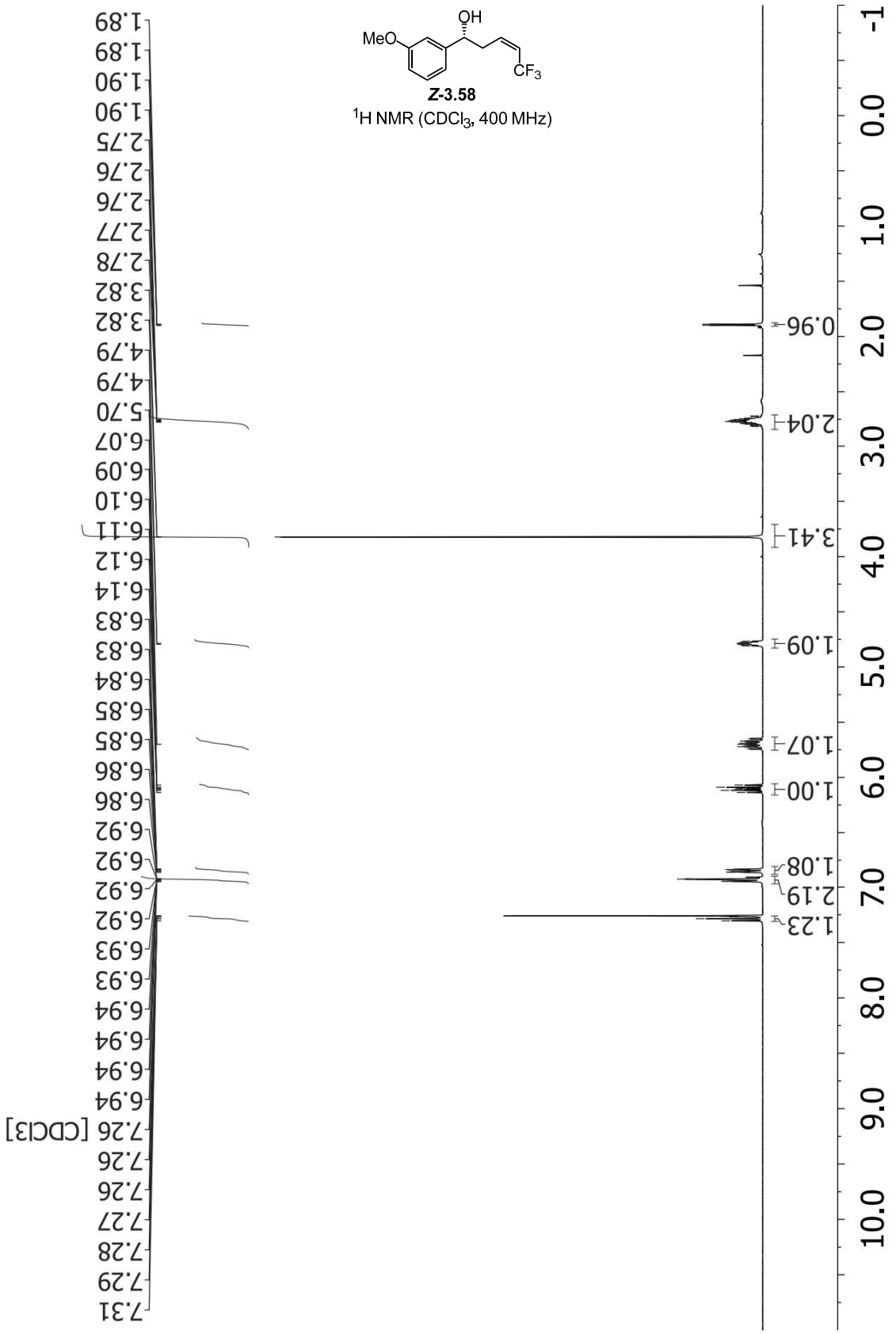
OH
MeO
CF3
Z-3.58
1H NMR (CDCl3, 400 MHz)
7.26 [CDCl3]
0.96
2.04
3.41
1.09
1.07
1.00
1.08
2.19
1.23

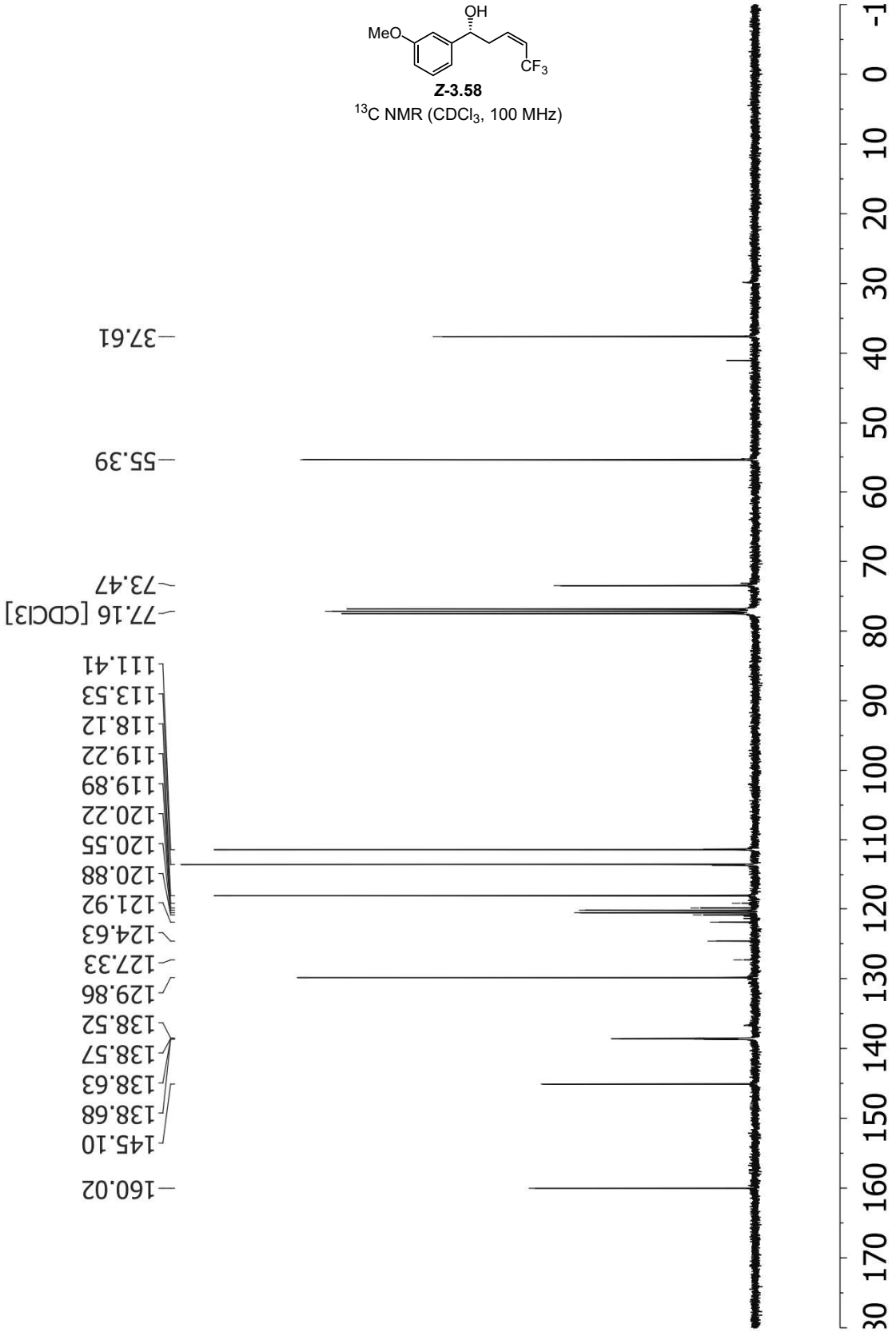
OH
MeO
CF3
Z-3.58
13C NMR (CDCl3, 100 MHz)
37.61
55.39
73.47
77.16 [CDCl3]
111.41
113.53
118.12
119.22
119.89
120.22
120.55
120.88
121.92
124.63
127.33
129.86
138.52
138.57
138.63
138.68
145.10
160.02
-10 0 10 20 30 40 50 60 70 80 90 100 110 120 130 140 150 160 170 180

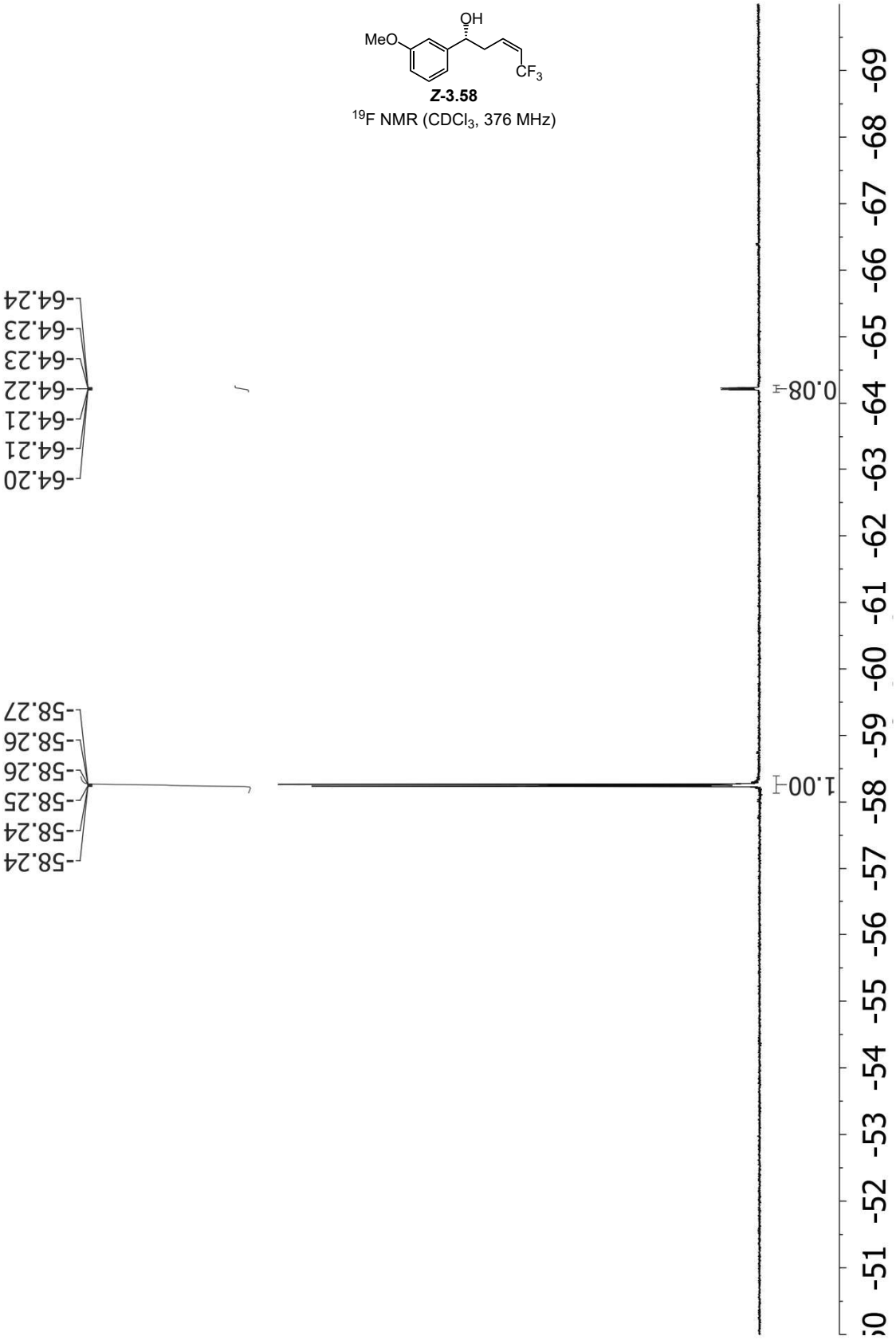
OH
MeO
CF3
Z-3.58
19F NMR (CDCl3, 376 MHz)
-58.24
-58.24
-58.25
-58.26
-58.26
-58.27
-64.20
-64.21
-64.21
-64.22
-64.23
-64.23
-64.24
1.00
0.08
-50
-51
-52
-53
-54
-55
-56
-57
-58
-59
-60
-61
-62
-63
-64
-65
-66
-67
-68
-69

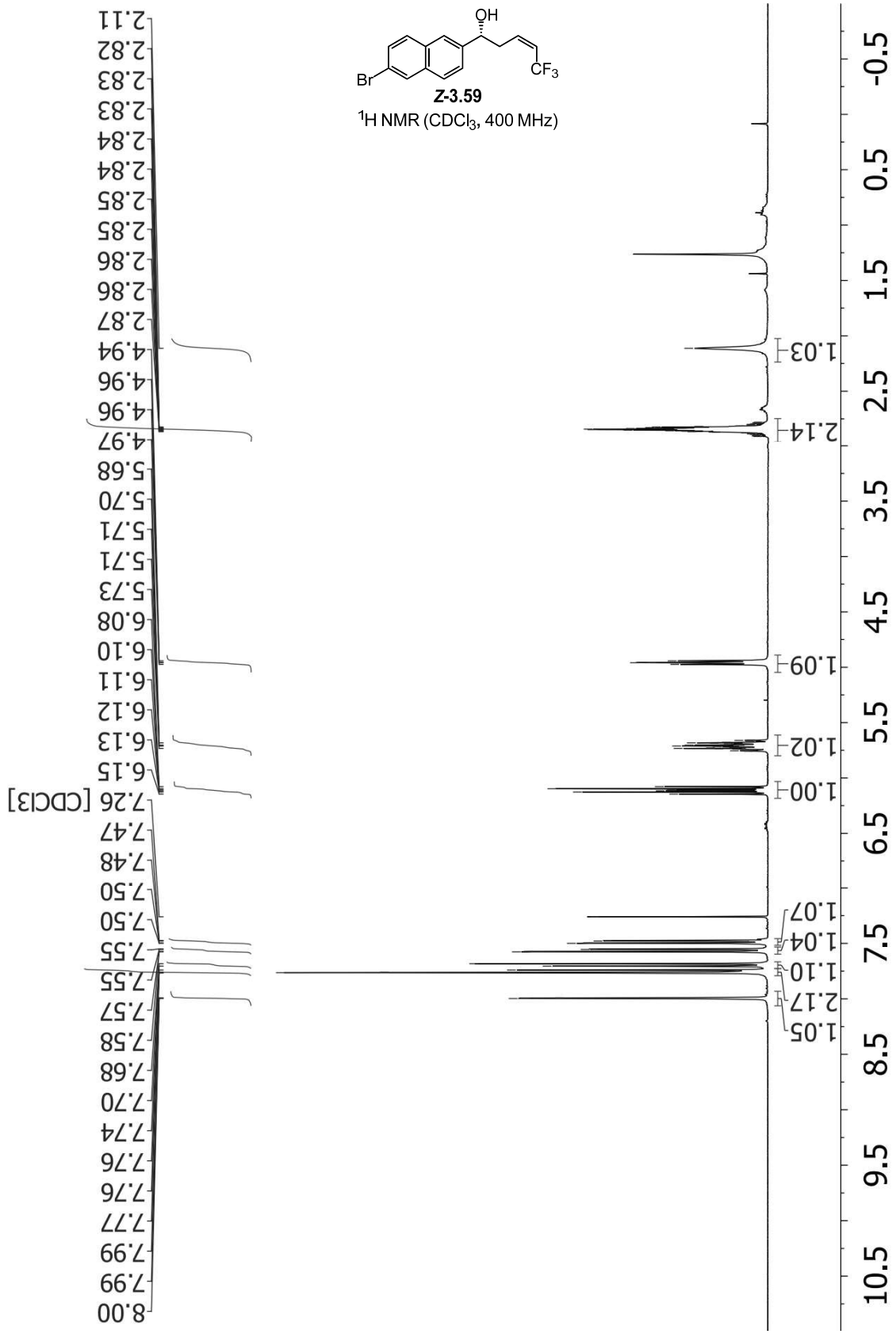
OH
Br
CF3
Z-3.59
1H NMR (CDCl3, 400 MHz)
[CDCl3]

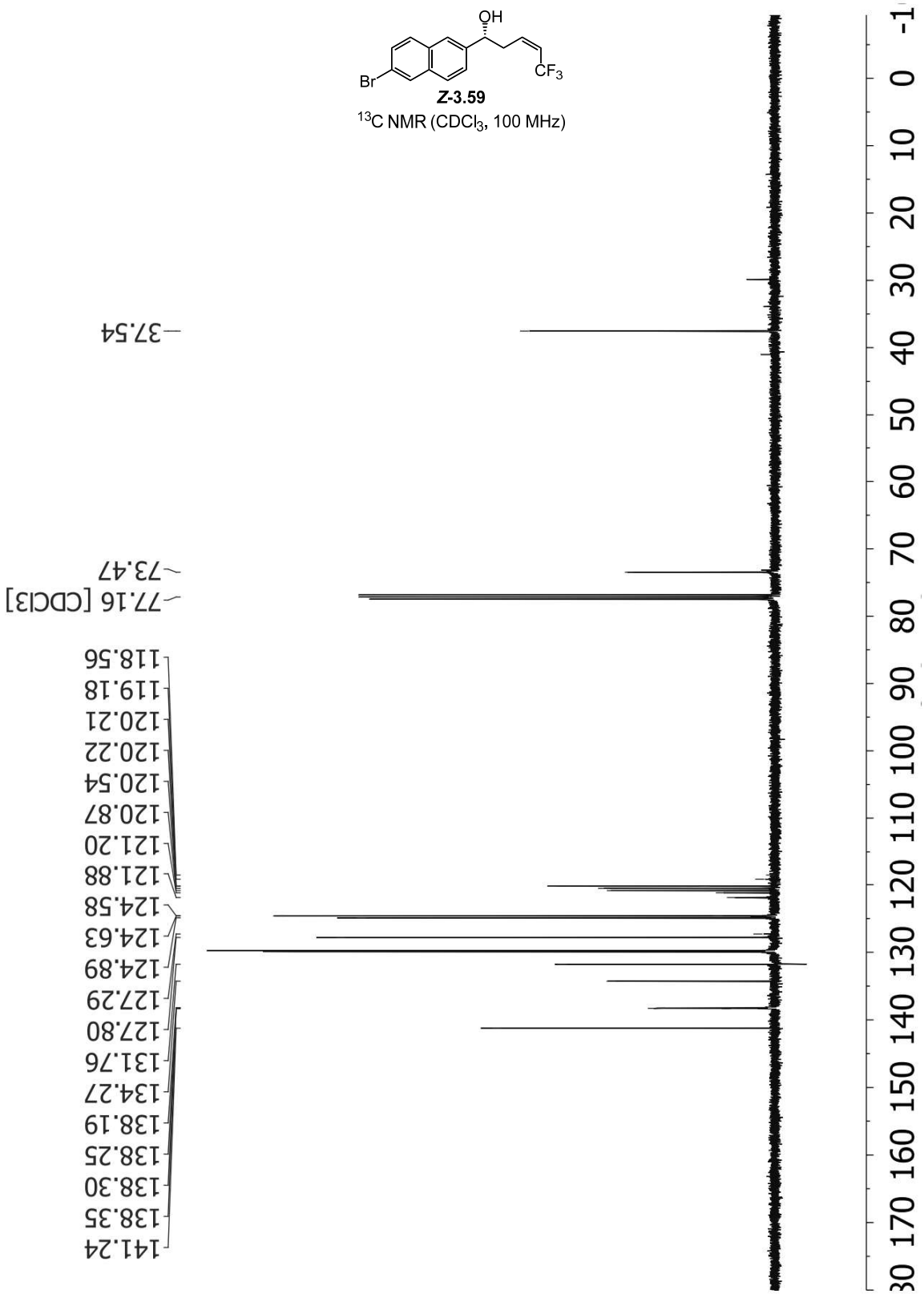
OH
Br
CF3
Z-3.59
13C NMR (CDCl3, 100 MHz)
37.54
73.47
77.16 [CDCl3]
118.56
119.18
120.21
120.22
120.54
120.87
121.20
121.88
124.58
124.63
124.89
127.29
127.80
131.76
134.27
138.19
138.25
138.30
138.35
141.24

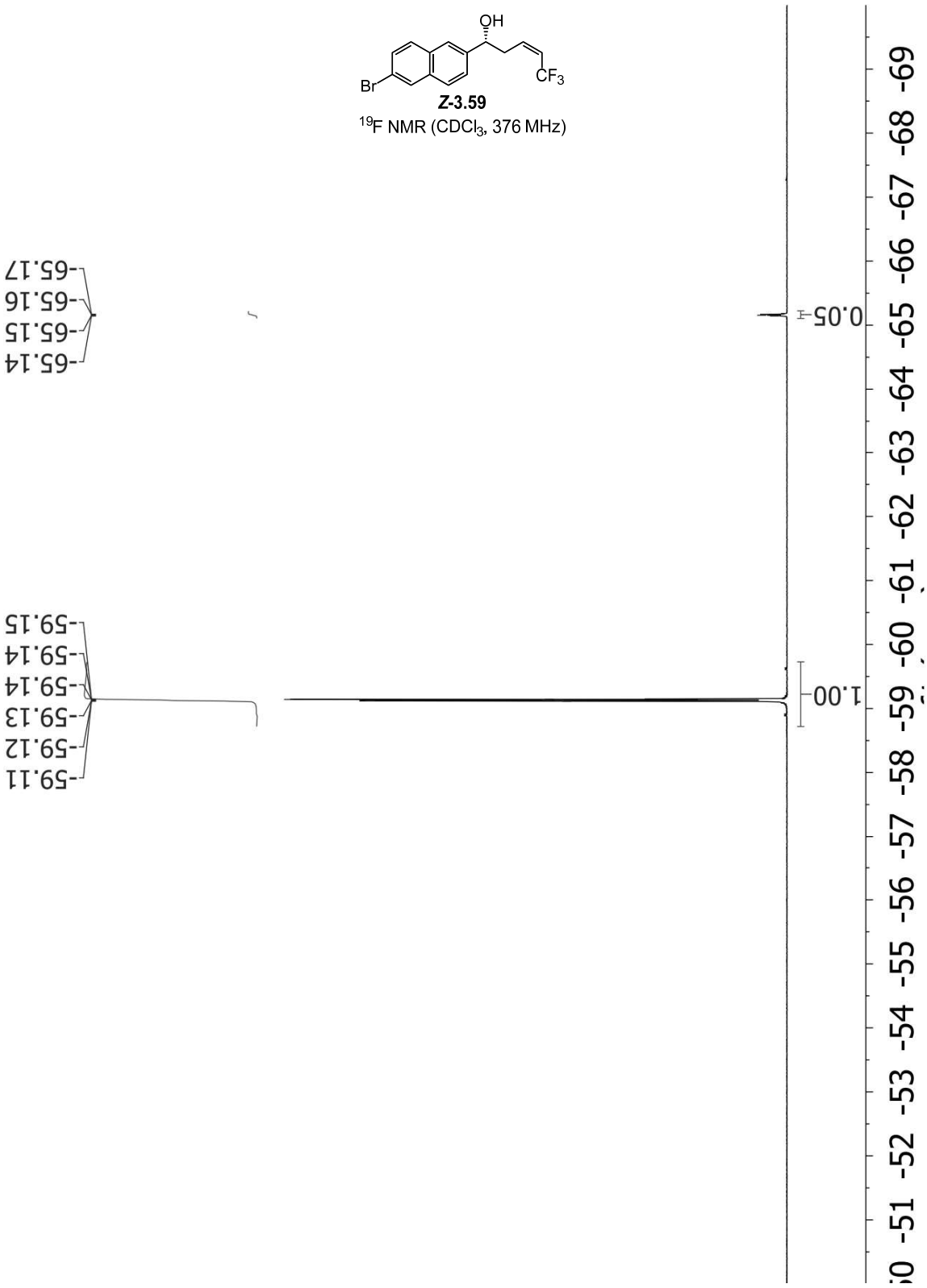
OH
Br
CF3
Z-3.59
19F NMR (CDCl3, 376 MHz)
-65.17
-65.16
-65.15
-65.14
-59.15
-59.14
-59.14
-59.13
-59.12
-59.11
0.05
1.00
-51 -52 -53 -54 -55 -56 -57 -58 -59 -60 -61 -62 -63 -64 -65 -66 -67 -68 -69

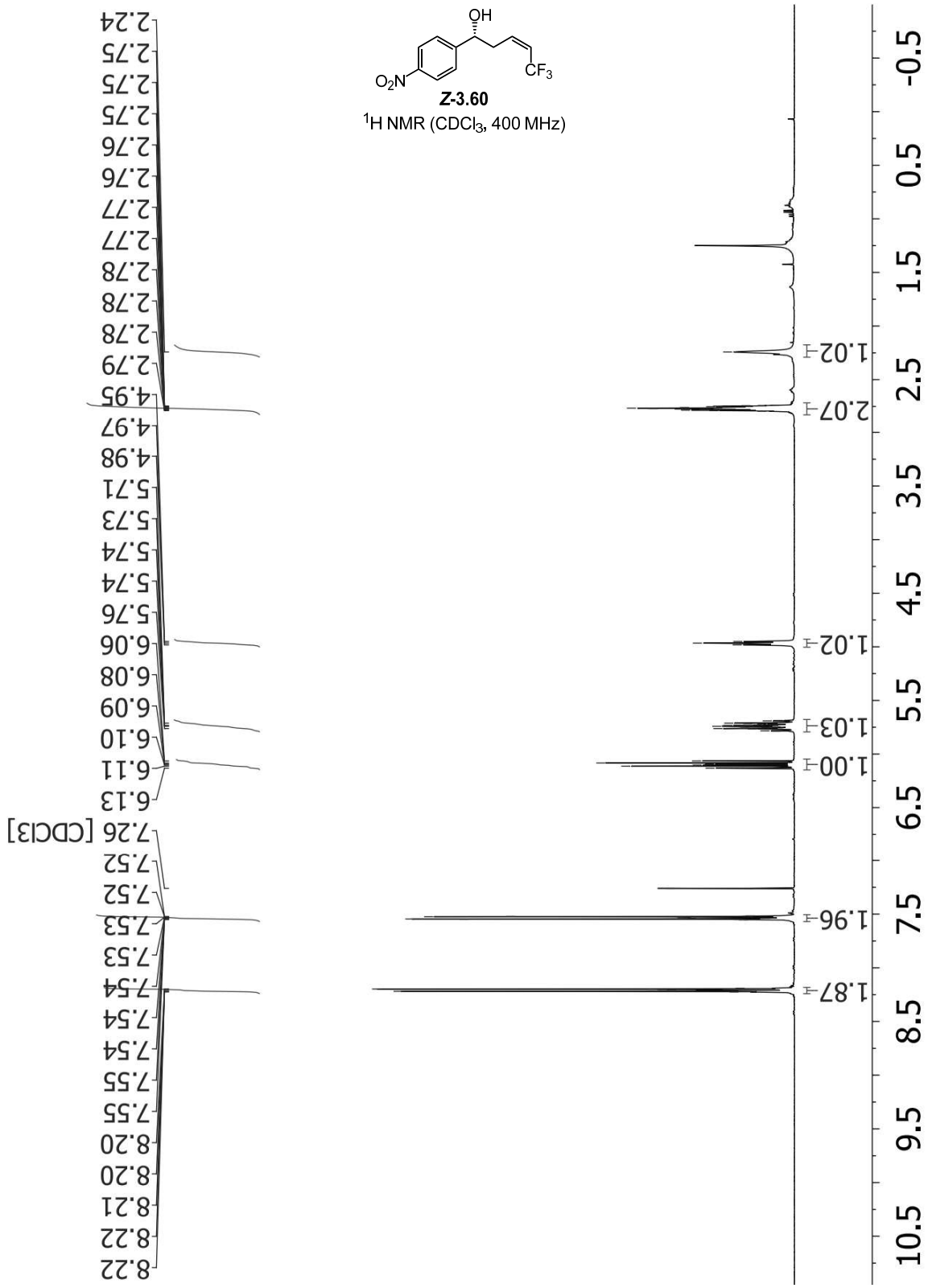
OH
O2N
CF3
Z-3.60
1H NMR (CDCl3, 400 MHz)
[CDCl3]

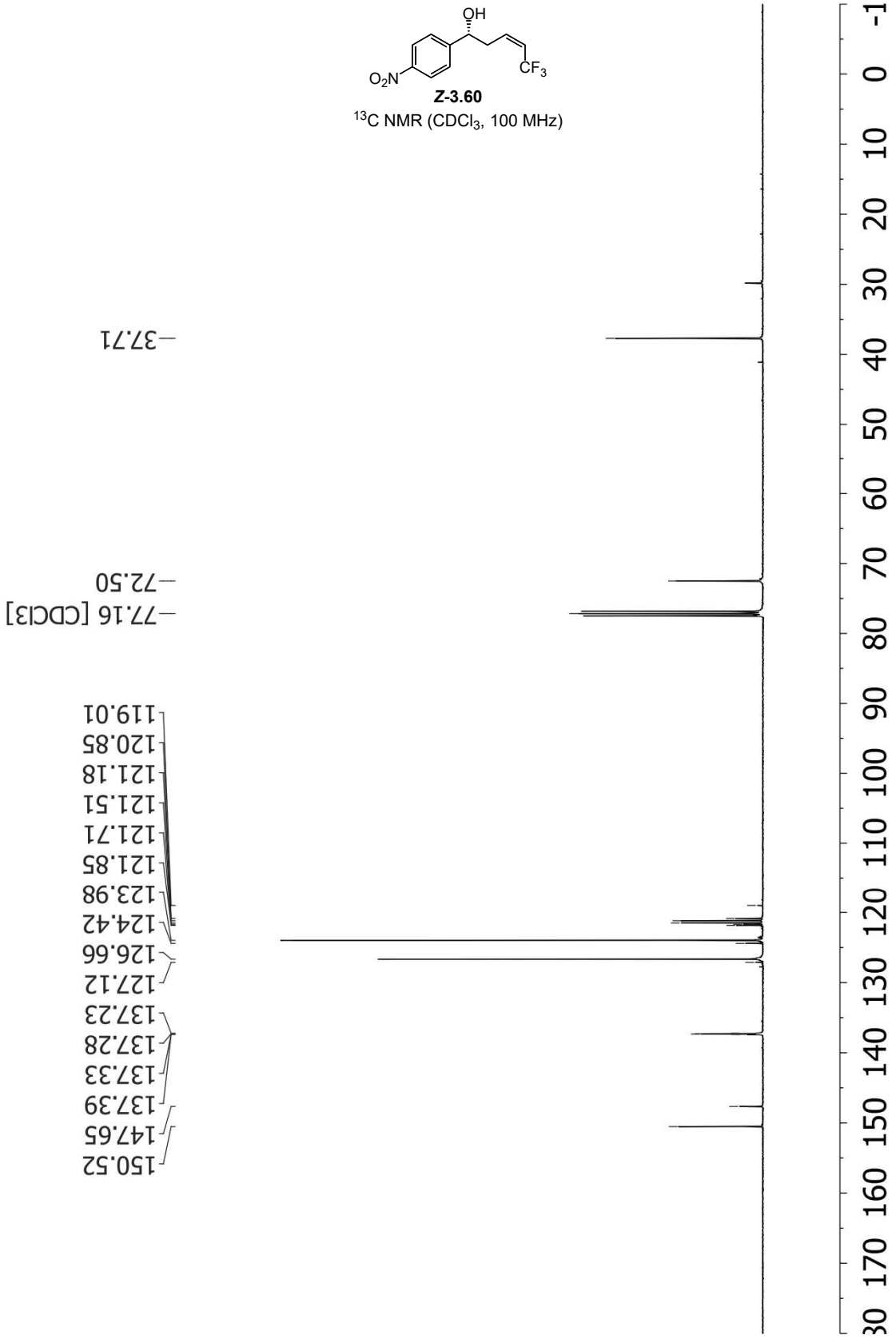
OH
O2N
CF3
Z-3.60
13C NMR (CDCl3, 100 MHz)
37.71
72.50
77.16 [CDCl3]
119.01
120.85
121.18
121.51
121.71
121.85
123.98
124.42
126.66
127.12
137.23
137.28
137.33
137.39
147.65
150.52

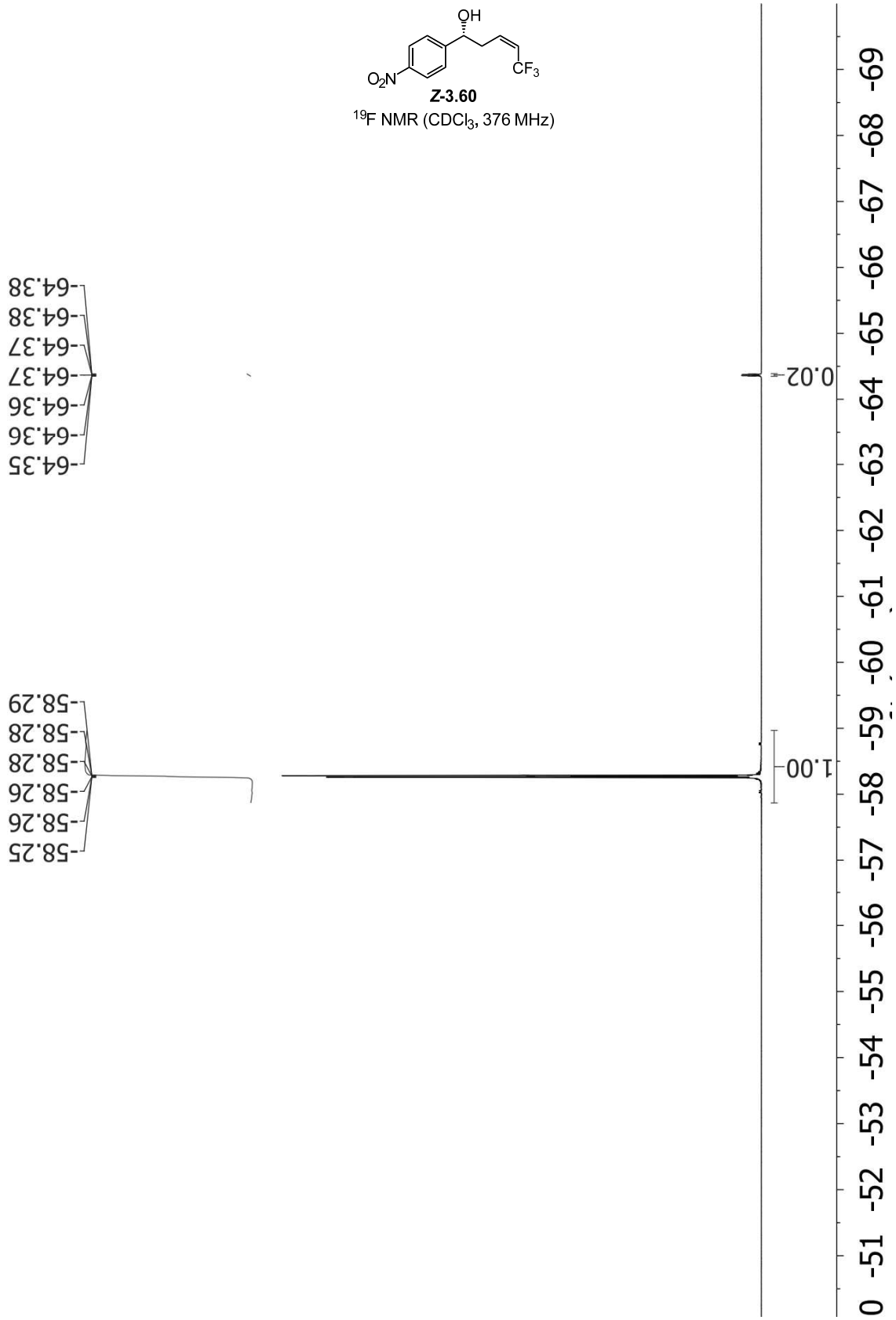
OH
O2N
CF3
Z-3.60
19F NMR (CDCl3, 376 MHz)
-64.38
-64.38
-64.37
-64.37
-64.36
-64.36
-64.35
-58.29
-58.28
-58.28
-58.26
-58.26
-58.25
0.02
1.00
0 -51 -52 -53 -54 -55 -56 -57 -58 -59 -60 -61 -62 -63 -64 -65 -66 -67 -68 -69

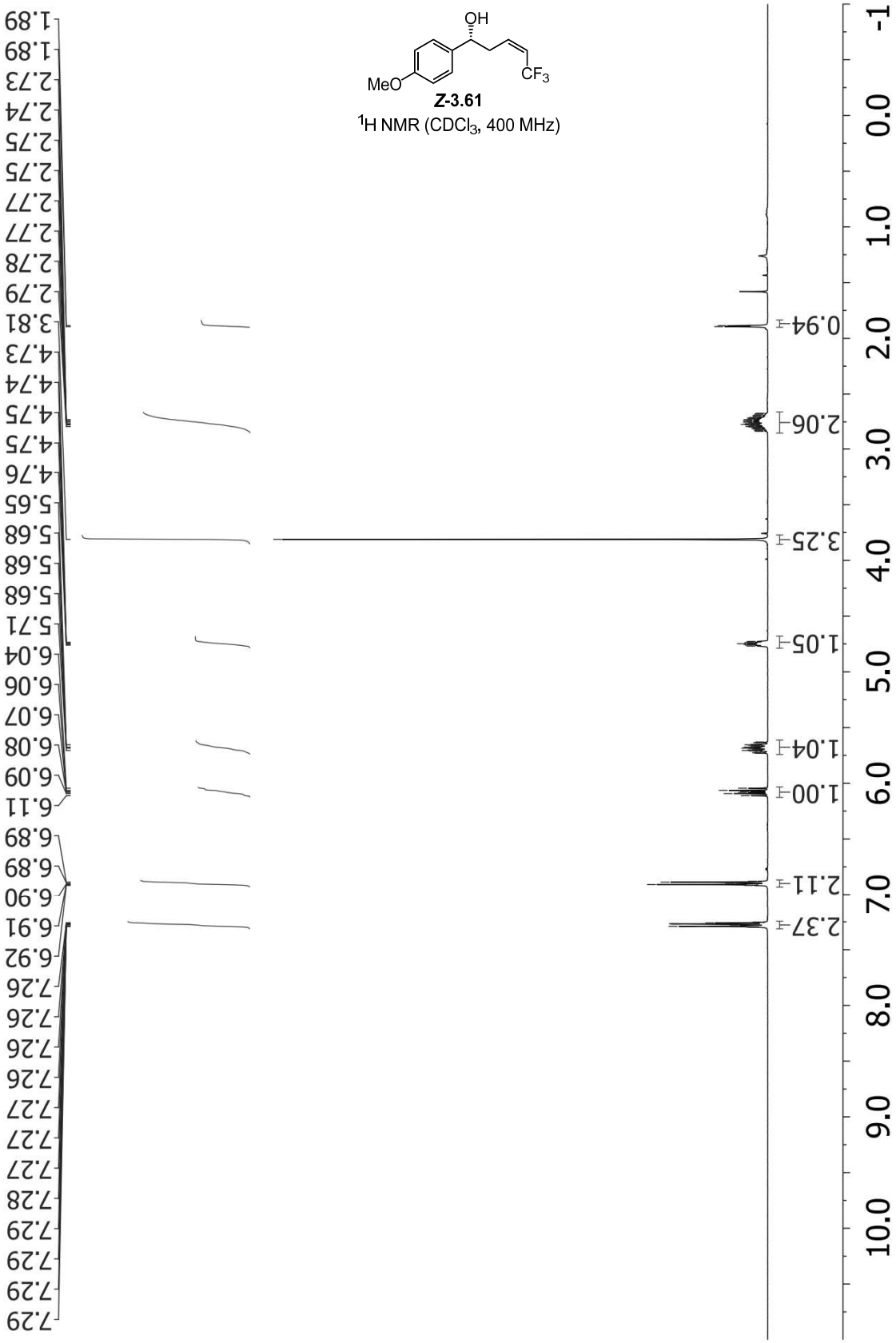
OH
MeO
CF3
Z-3.61
1H NMR (CDCl3, 400 MHz)

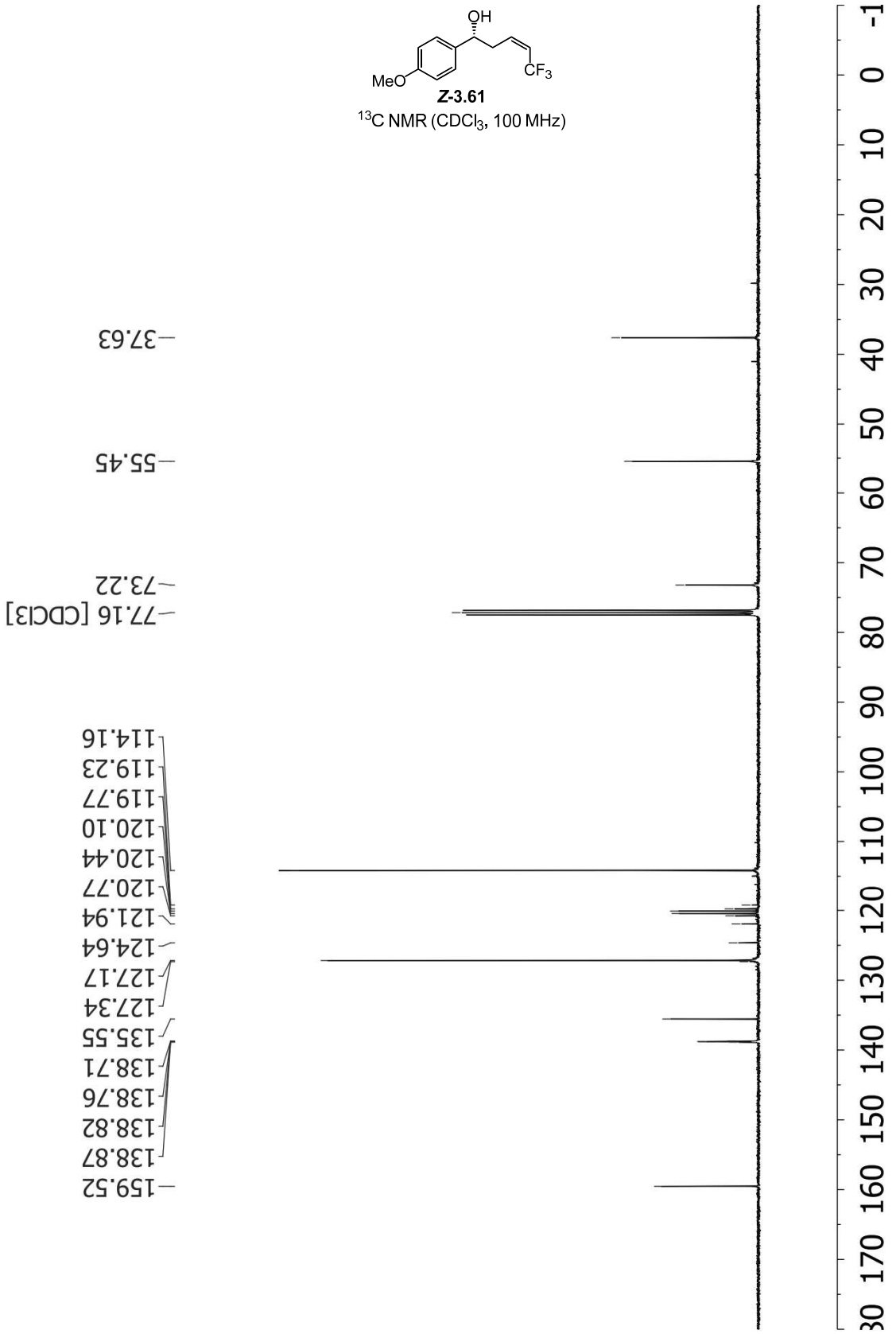
OH
MeO
CF3
Z-3.61
13C NMR (CDCl3, 100 MHz)
37.63
55.45
73.22
77.16 [CDCl3]
114.16
119.23
119.77
120.10
120.44
120.77
121.94
124.64
127.17
127.34
135.55
138.71
138.76
138.82
138.87
159.52

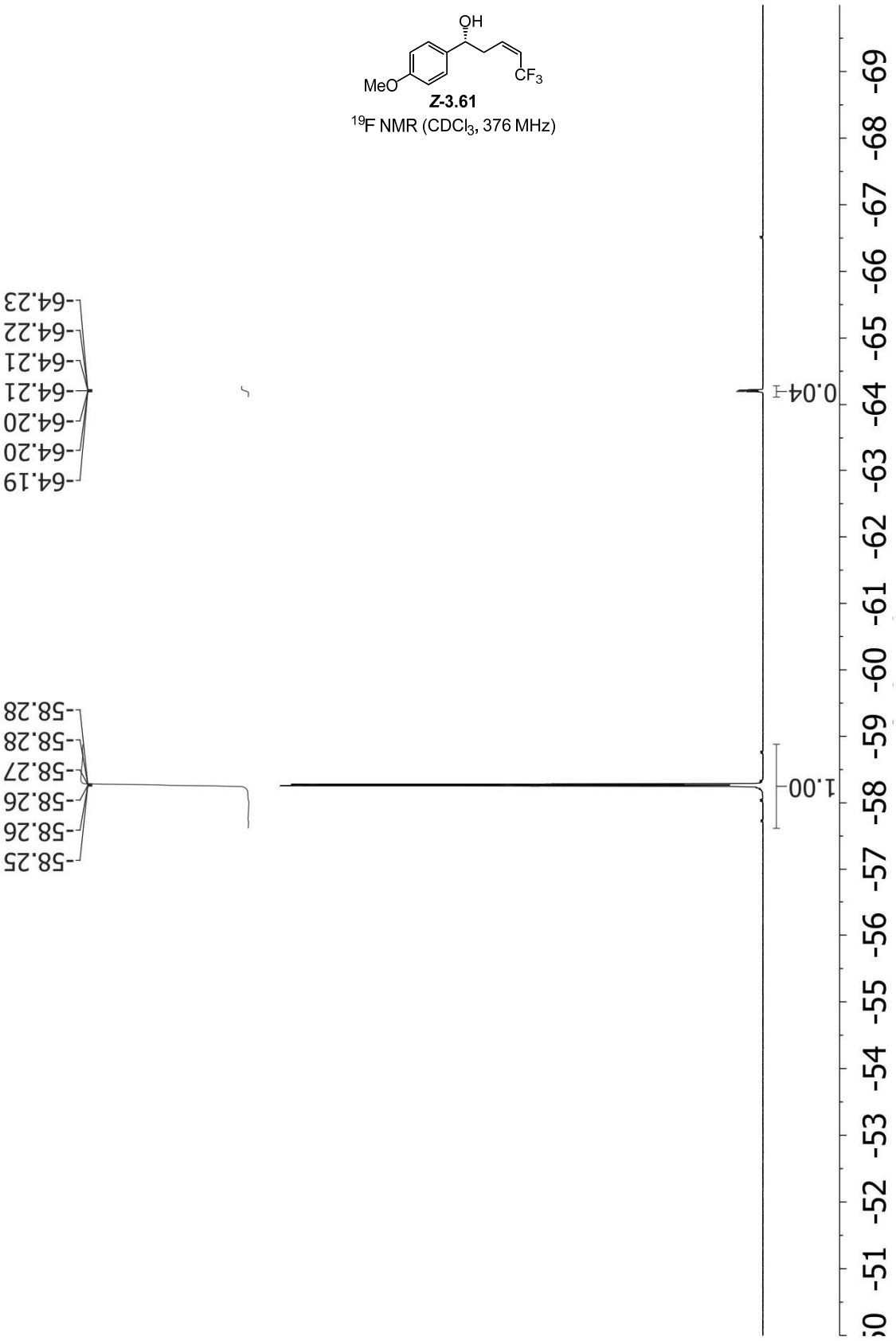
OH
MeO
CF3
Z-3.61
19F NMR (CDCl3, 376 MHz)
-64.23
-64.22
-64.21
-64.21
-64.20
-64.20
-64.19
-58.28
-58.28
-58.27
-58.26
-58.26
-58.25
0.04
1.00
-50
-51
-52
-53
-54
-55
-56
-57
-58
-59
-60
-61
-62
-63
-64
-65
-66
-67
-68
-69

OH
N
CF3
Z-3.62
1H NMR (CDCl3, 400 MHz)
2.74
2.74
2.75
2.75
2.76
2.76
2.77
2.77
2.78
4.82
4.84
4.84
4.86
5.70
5.70
5.71
5.73
6.07
6.09
6.10
6.11
6.12
6.14
7.26 [CDCl3]
7.27
7.27
7.28
7.28
7.28
7.29
7.30
7.30
7.70
7.71
7.71
7.72
7.73
7.73
8.42
8.42
8.43
8.43
8.45
8.46
2.05
1.01
1.10
1.08
1.00
1.10
1.08
2.19
-1
0.0
1.0
2.0
3.0
4.0
5.0
6.0
7.0
8.0
9.0
10.0

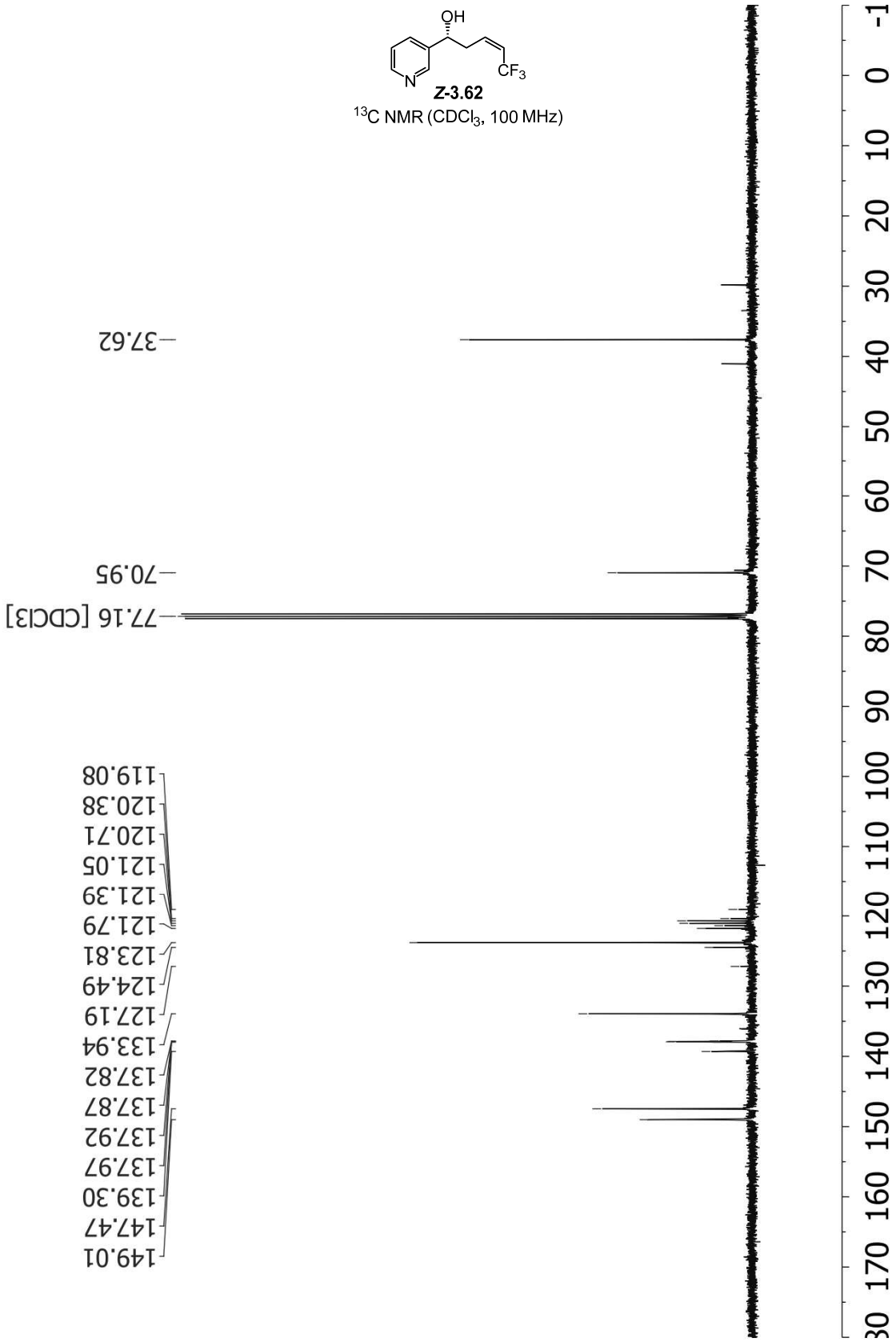
OH
N
CF3
Z-3.62
13C NMR (CDCl3, 100 MHz)
37.62
70.95
77.16 [CDCl3]
119.08
120.38
120.71
121.05
121.39
121.79
123.81
124.49
127.19
133.94
137.82
137.87
137.92
137.97
139.30
147.47
149.01

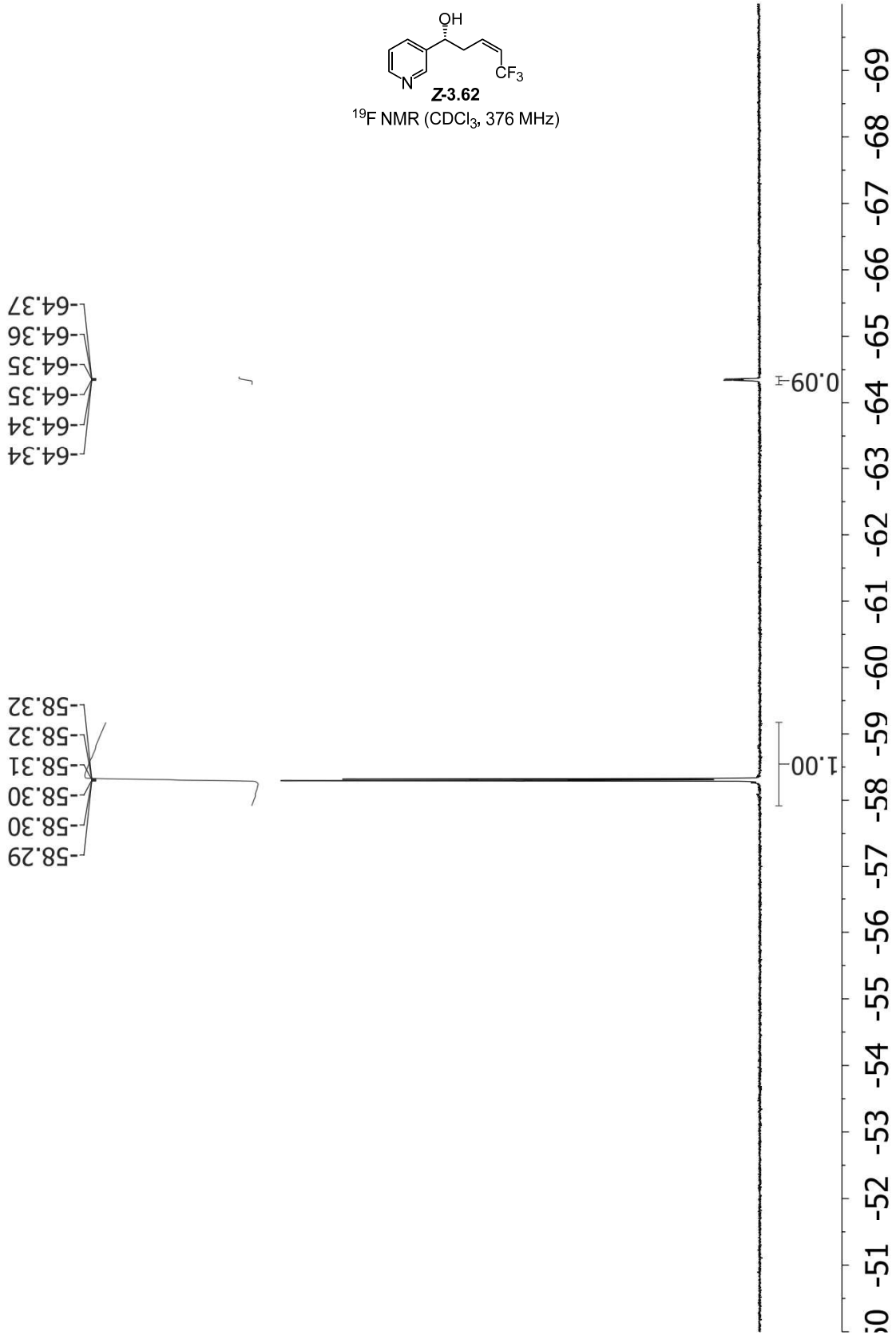
OH
N
CF3
Z-3.62
19F NMR (CDCl3, 376 MHz)
-58.29
-58.30
-58.30
-58.31
-58.32
-58.32
-64.34
-64.34
-64.35
-64.35
-64.36
-64.37
1.00
0.09
-50
-51
-52
-53
-54
-55
-56
-57
-58
-59
-60
-61
-62
-63
-64
-65
-66
-67
-68
-69

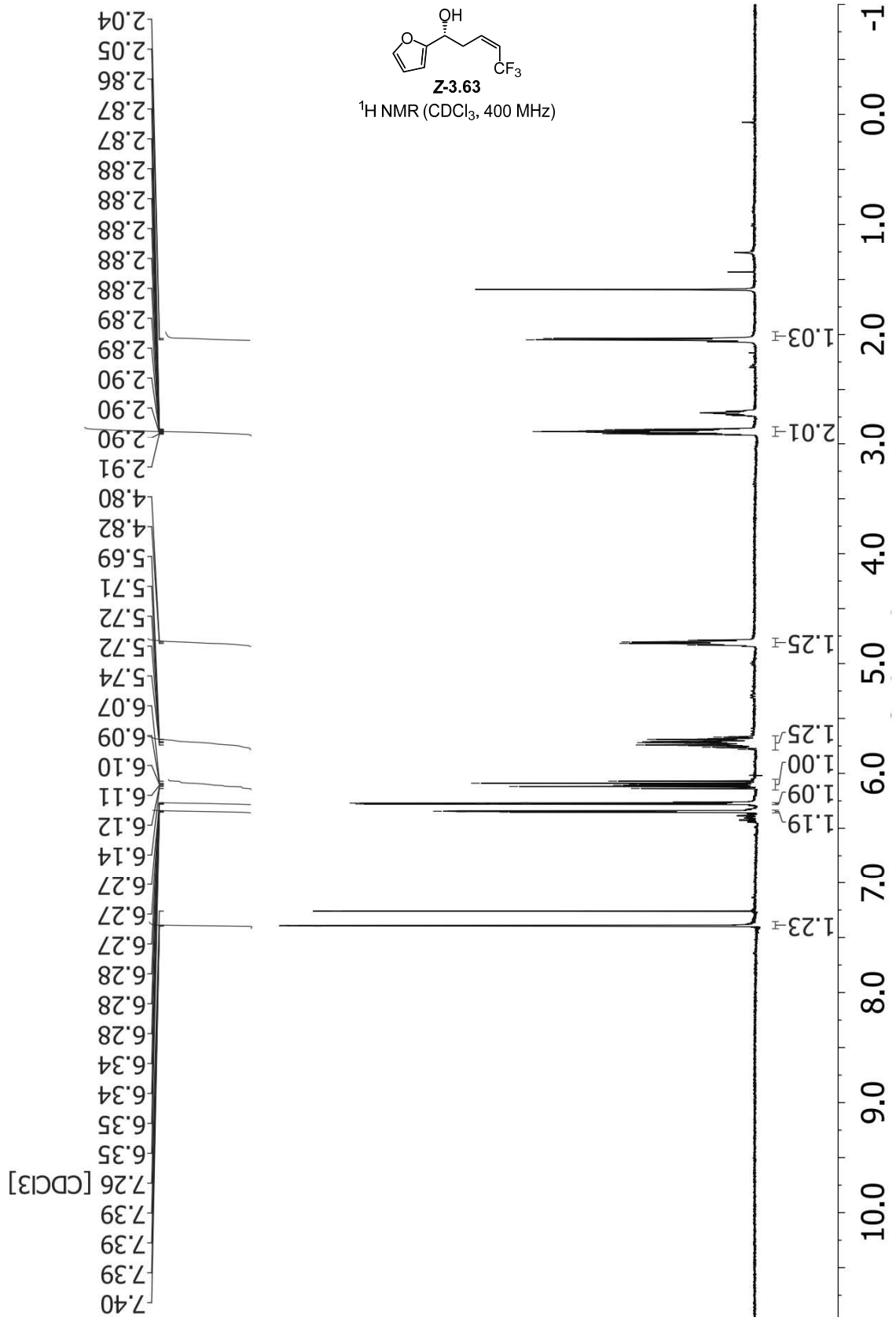
OH
O
CF3
Z-3.63
1H NMR (CDCl3, 400 MHz)
7.40
7.39
7.39
7.39
7.26 [CDCl3]
6.35
6.35
6.34
6.34
6.28
6.28
6.28
6.27
6.27
6.27
6.14
6.12
6.11
6.10
6.09
6.07
5.74
5.72
5.72
5.71
5.69
4.82
4.80
2.91
2.90
2.90
2.89
2.89
2.90
2.88
2.88
2.88
2.88
2.88
2.87
2.87
2.86
2.05
2.04
1.03
2.01
1.25
1.25
1.00
1.09
1.19
1.23
-1
0.0
1.0
2.0
3.0
4.0
5.0
6.0
7.0
8.0
9.0
10.0

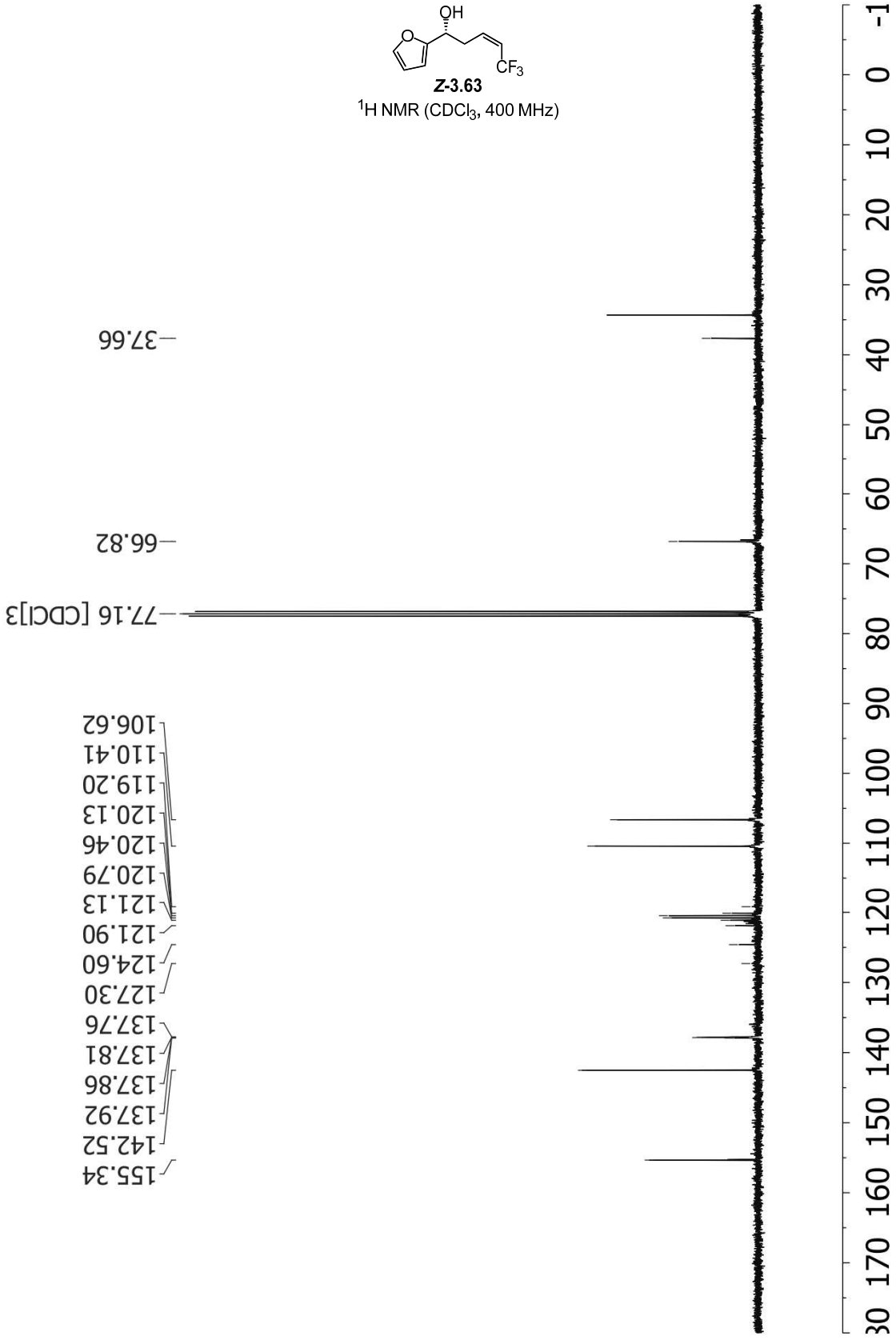
OH
CF3
Z-3.63
1H NMR (CDCl3, 400 MHz)
155.34
142.52
137.92
137.86
137.81
137.76
127.30
124.60
121.90
121.13
120.79
120.46
120.13
119.20
110.41
106.62
77.16 [CDCl]3
66.82
37.66

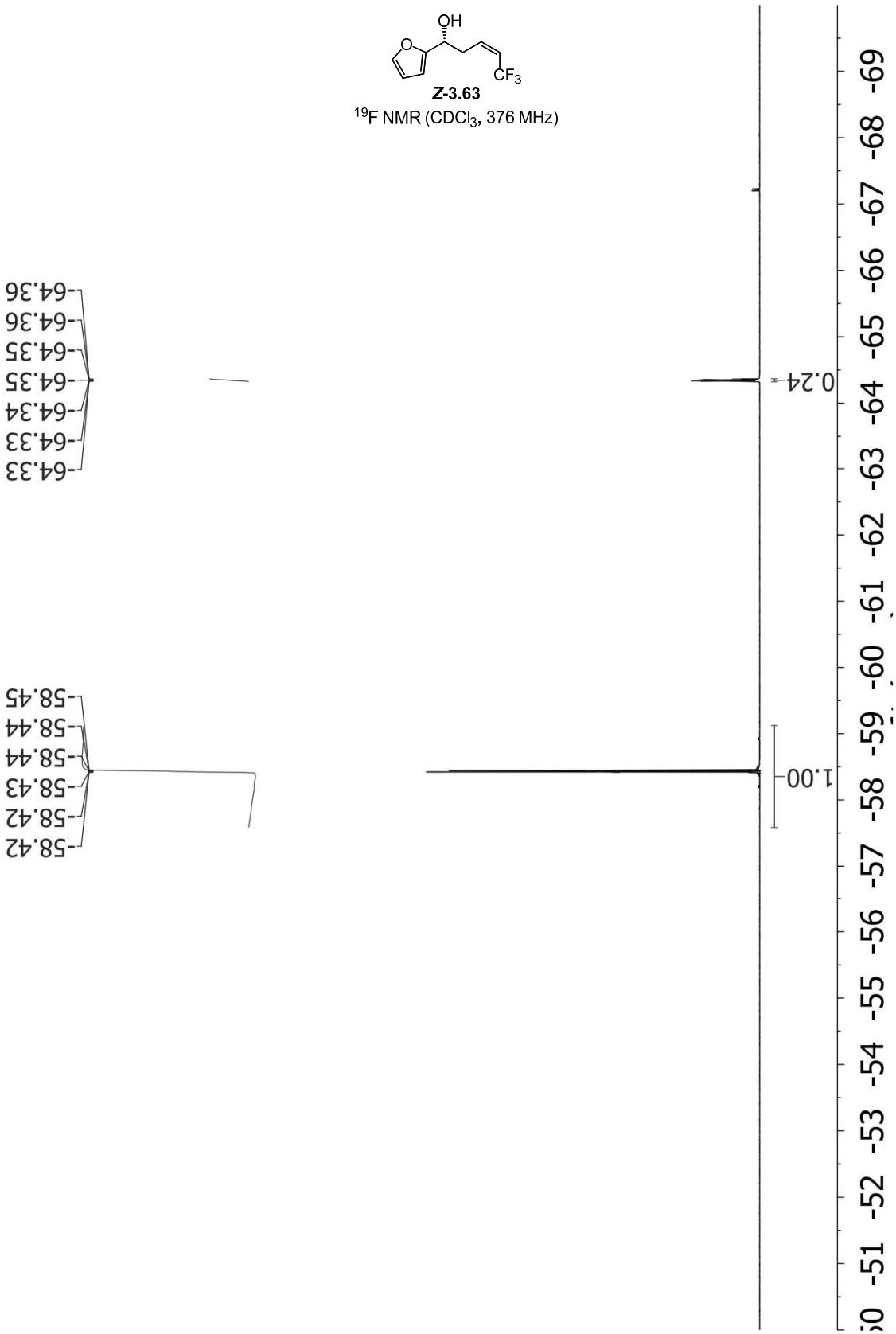
OH
O
CF3
Z-3.63
19F NMR (CDCl3, 376 MHz)
-64.36
-64.36
-64.35
-64.35
-64.34
-64.33
-64.33
-58.45
-58.44
-58.44
-58.43
-58.42
-58.42
0.24
1.00
-51
-52
-53
-54
-55
-56
-57
-58
-59
-60
-61
-62
-63
-64
-65
-66
-67
-68
-69

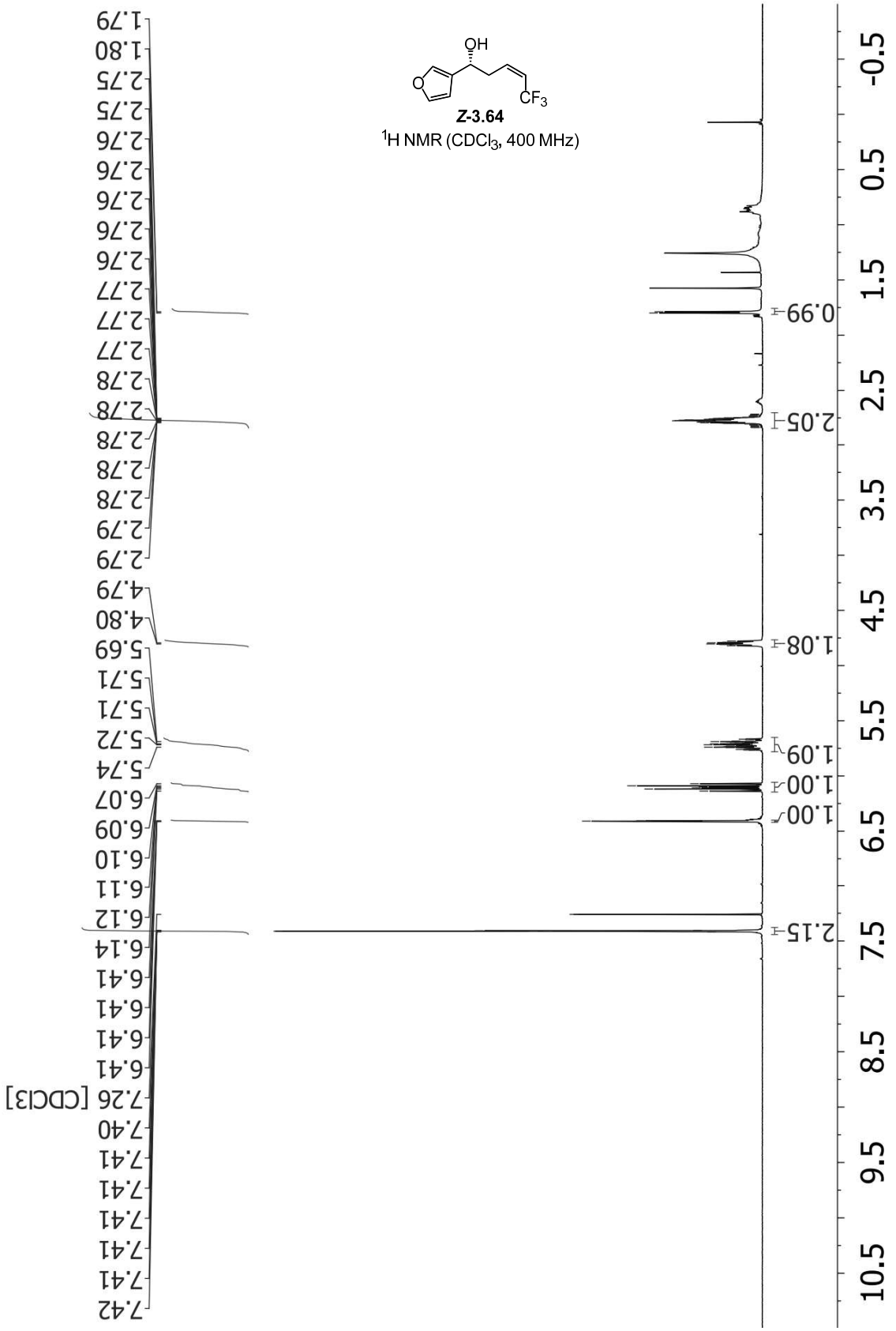
OH
O
CF3
Z-3.64
1H NMR (CDCl3, 400 MHz)
[CDCl3]

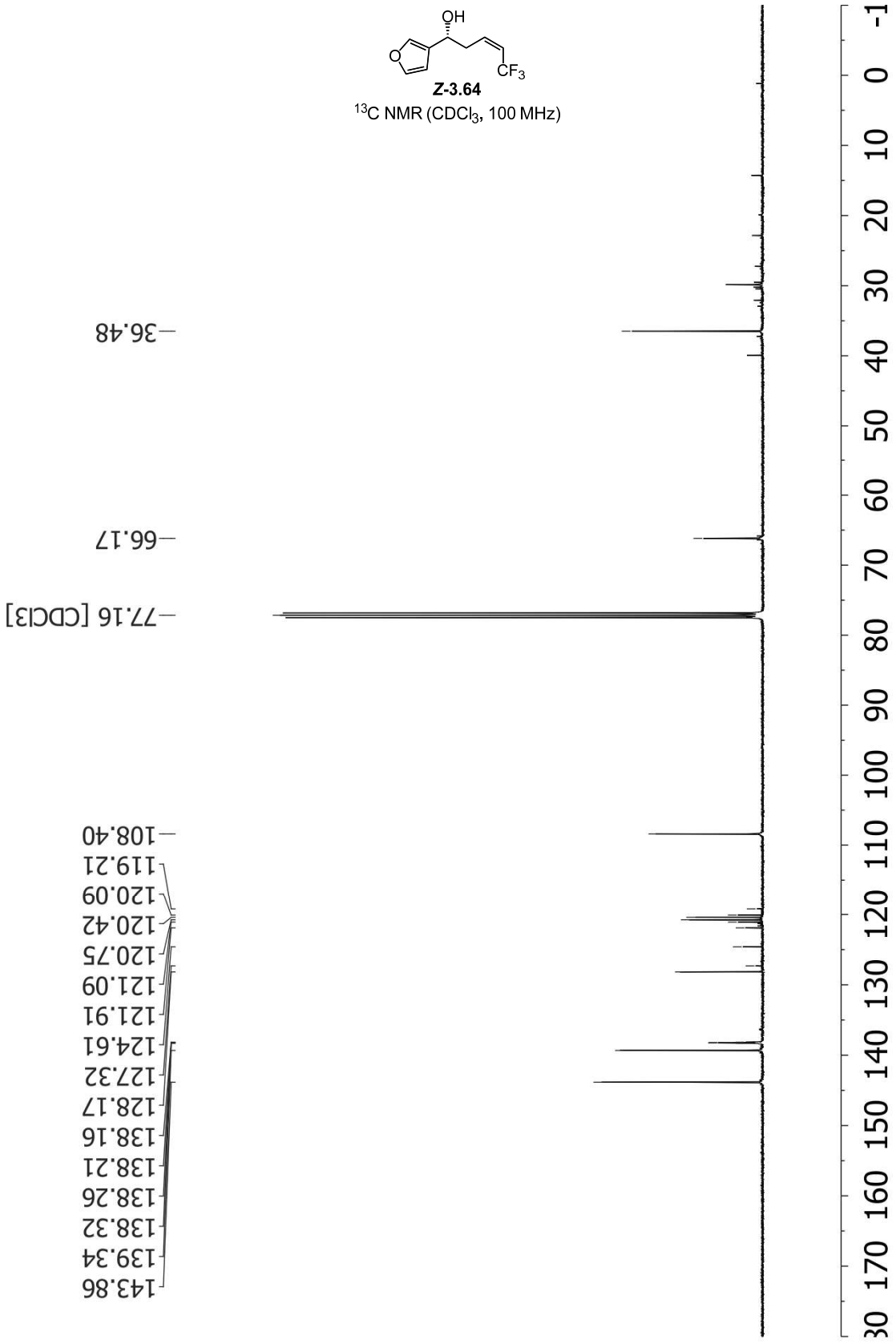
OH
CF3
Z-3.64
13C NMR (CDCl3, 100 MHz)
36.48
66.17
77.16 [CDCl3]
108.40
119.21
120.09
120.42
120.75
121.09
121.91
124.61
127.32
128.17
138.16
138.21
138.26
138.32
139.34
143.86

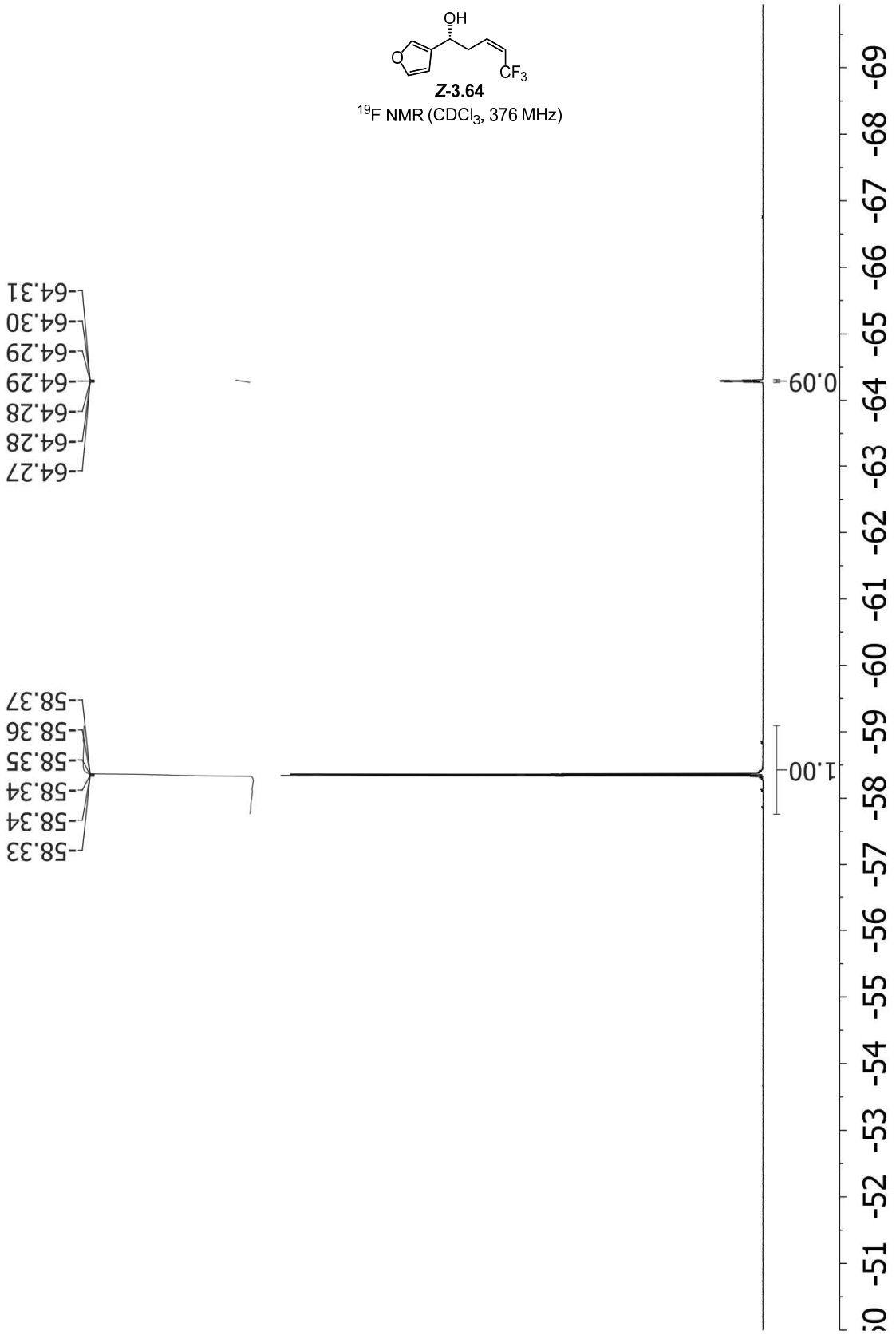
OH
CF3
Z-3.64
19F NMR (CDCl3, 376 MHz)
-58.33
-58.34
-58.34
-58.35
-58.36
-58.37
1.00
-64.27
-64.28
-64.28
-64.29
-64.29
-64.30
-64.31
0.09
-50 -51 -52 -53 -54 -55 -56 -57 -58 -59 -60 -61 -62 -63 -64 -65 -66 -67 -68 -69

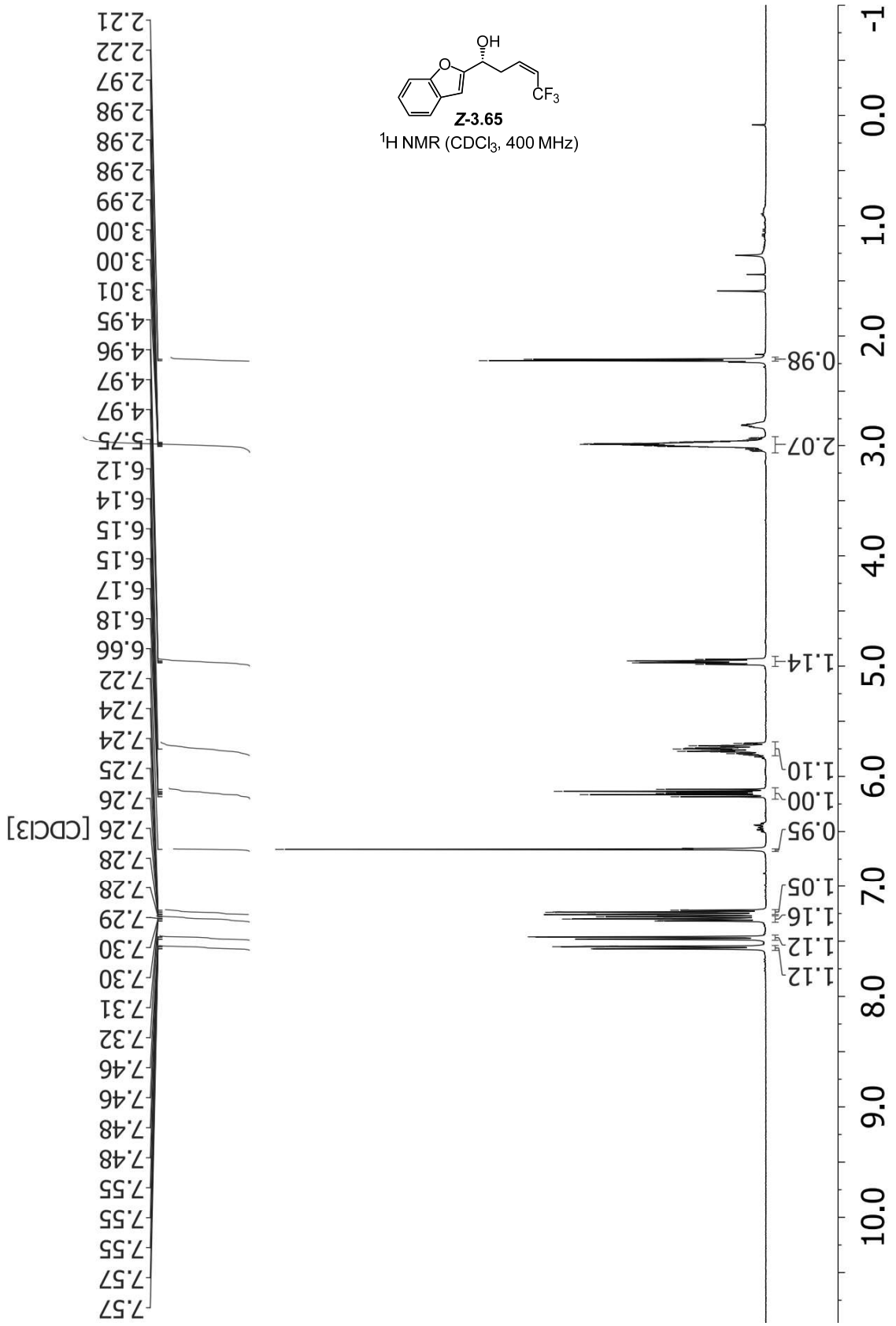
OH
O
CF3
Z-3.65
1H NMR (CDCl3, 400 MHz)
[CDCl3]
0.98
2.07
1.14
1.10
1.00
0.95
1.05
1.16
1.12
1.12

OH
O
CF3
Z-3.65
13C NMR (CDCl3, 100 MHz)
34.28
67.30
77.16 [CDCl3]
103.35
111.44
119.17
120.47
120.80
121.14
121.34
121.47
121.87
123.13
124.58
124.66
127.28
128.00
137.37
137.42
137.47
137.53
154.97
157.81
-1 0 10 20 30 40 50 60 70 80 90 100 110 120 130 140 150 160 170 180

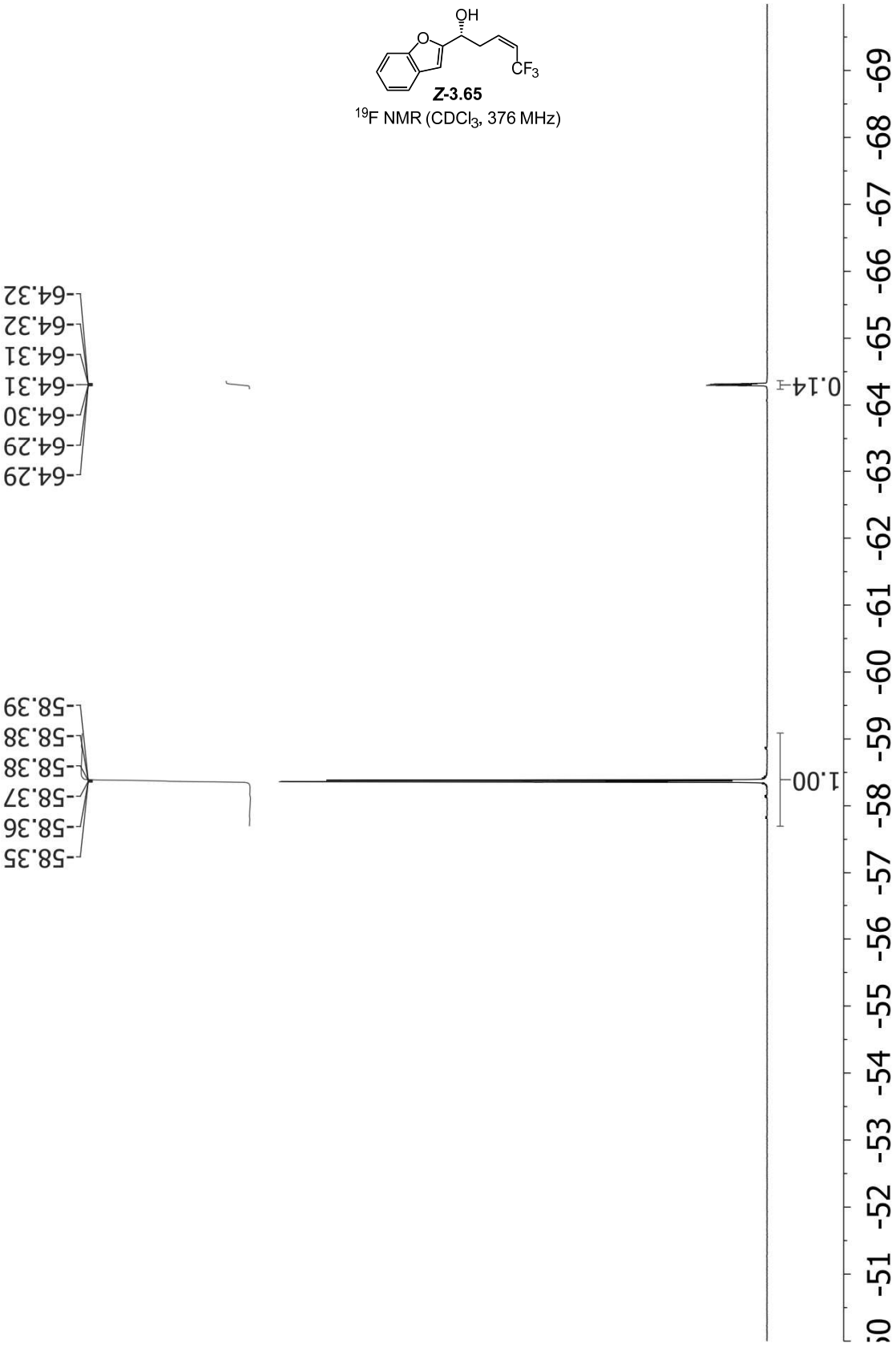
OH
O
CF3
Z-3.65
19F NMR (CDCl3, 376 MHz)
-64.32
-64.32
-64.31
-64.31
-64.30
-64.29
-64.29
-58.39
-58.38
-58.38
-58.37
-58.36
-58.35
0.14
1.00
-51
-52
-53
-54
-55
-56
-57
-58
-59
-60
-61
-62
-63
-64
-65
-66
-67
-68
-69

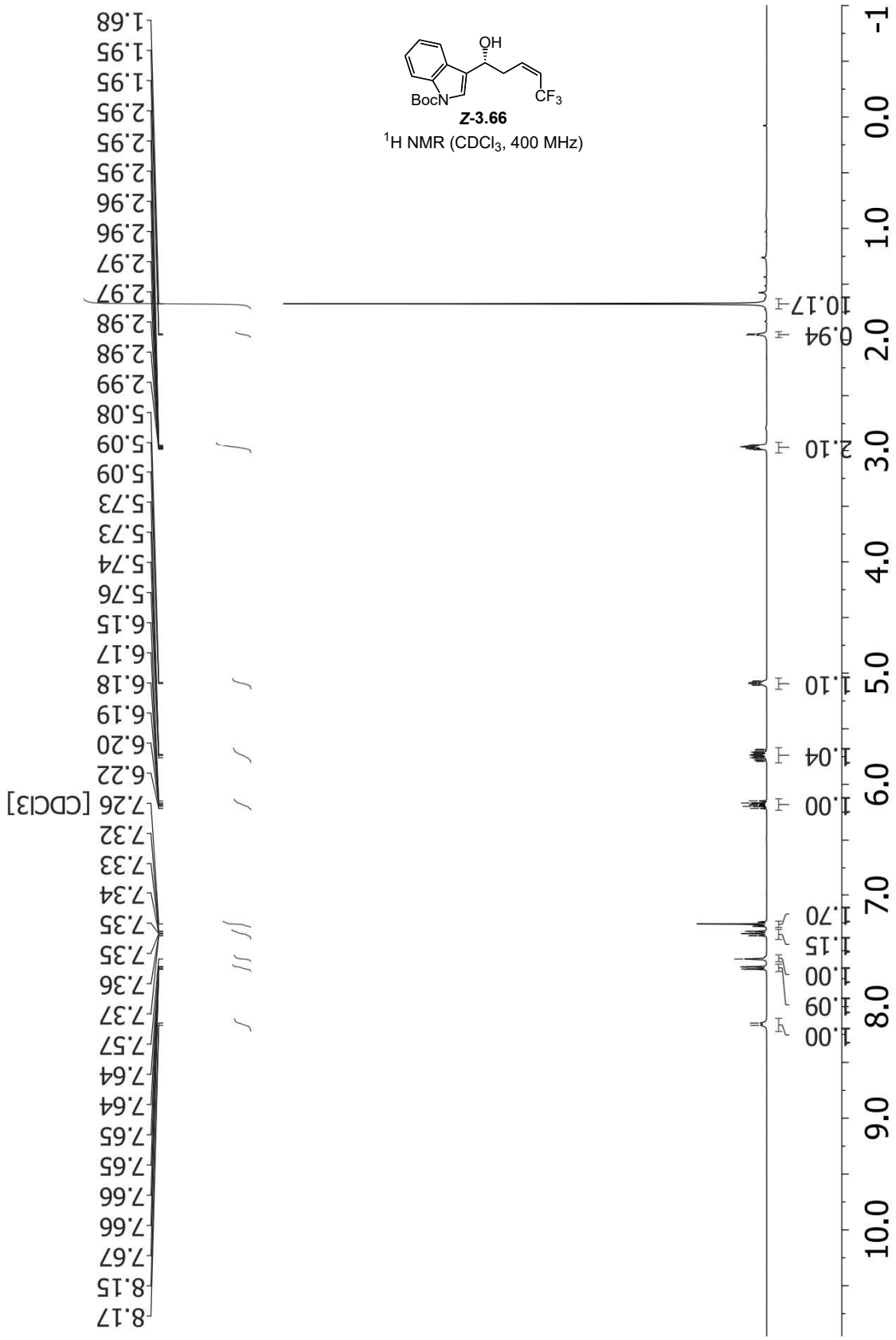
OH
BocN
CF3
Z-3.66
1H NMR (CDCl3, 400 MHz)
[CDCl3]

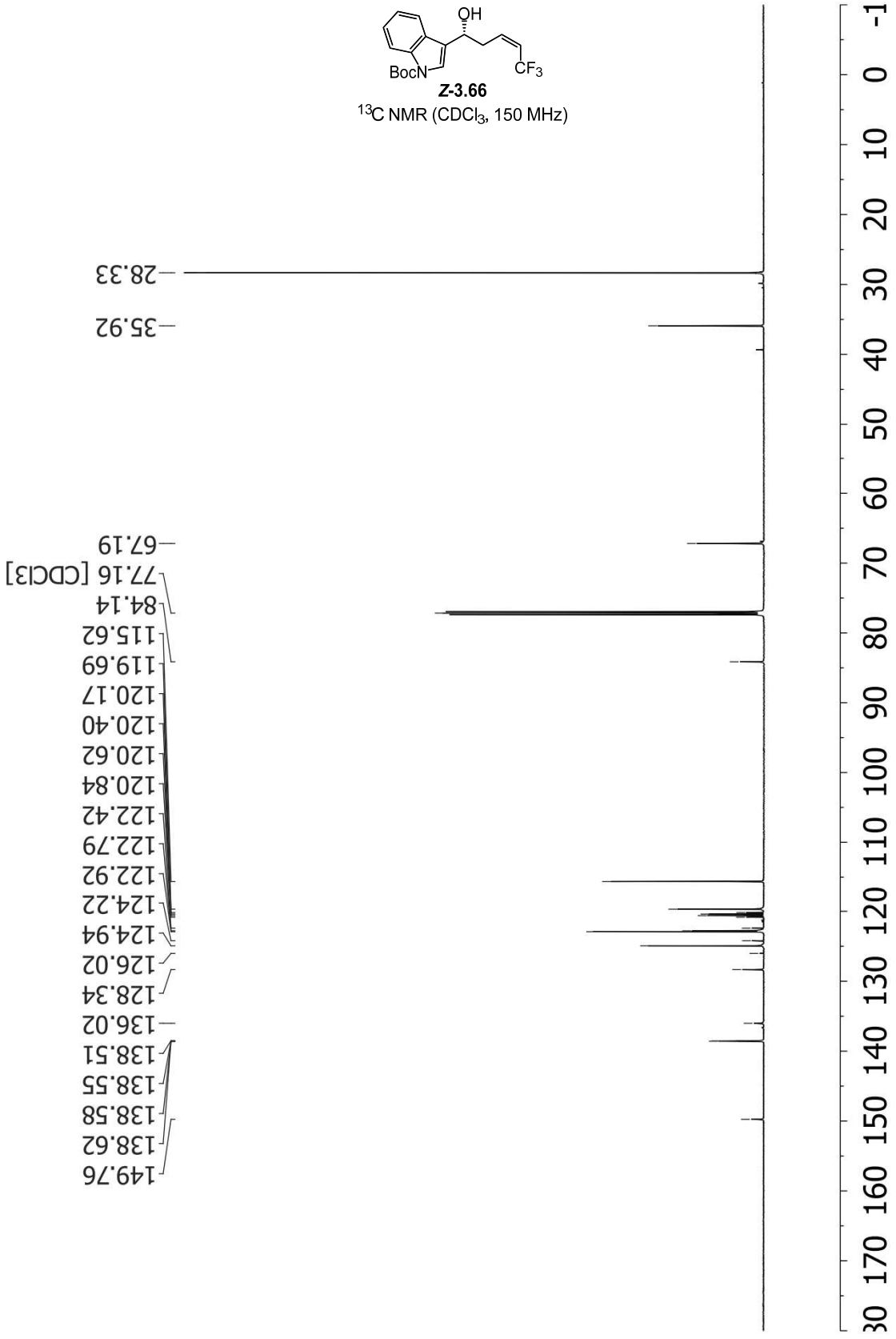
OH
BocN
CF3
Z-3.66
13C NMR (CDCl3, 150 MHz)
28.33
35.92
67.19
77.16 [CDCl3]
84.14
115.62
119.69
120.17
120.40
120.62
120.84
122.42
122.79
122.92
124.22
124.94
126.02
128.34
136.02
138.51
138.55
138.58
138.62
149.76

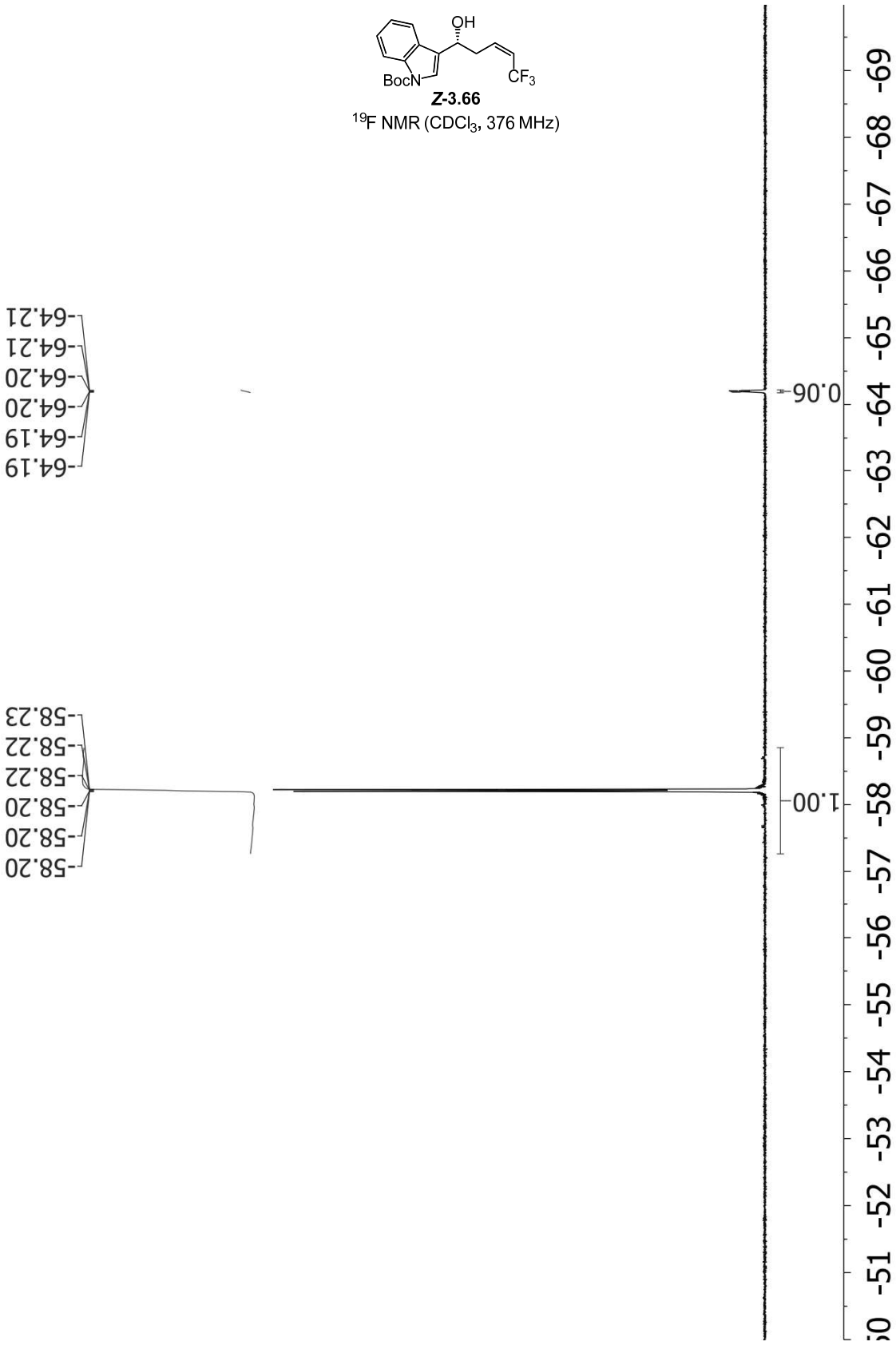
OH
BocN
CF3
Z-3.66
19F NMR (CDCl3, 376 MHz)
-58.20
-58.20
-58.22
-58.22
-58.23
-64.19
-64.19
-64.20
-64.20
-64.21
-64.21
1.00
0.06
-50
-51
-52
-53
-54
-55
-56
-57
-58
-59
-60
-61
-62
-63
-64
-65
-66
-67
-68
-69

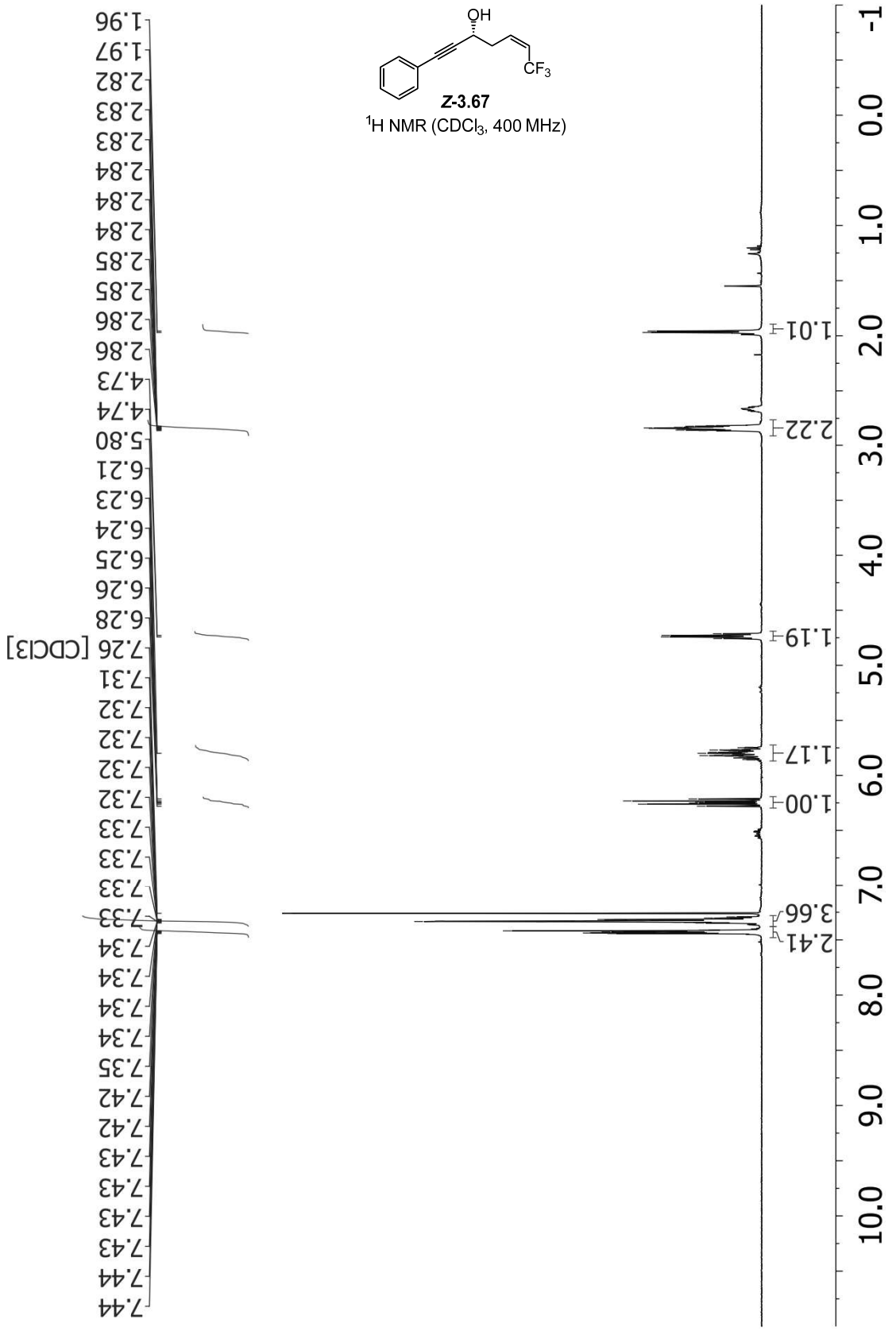
OH
CF3
Z-3.67
1H NMR (CDCl3, 400 MHz)
[CDCl3]

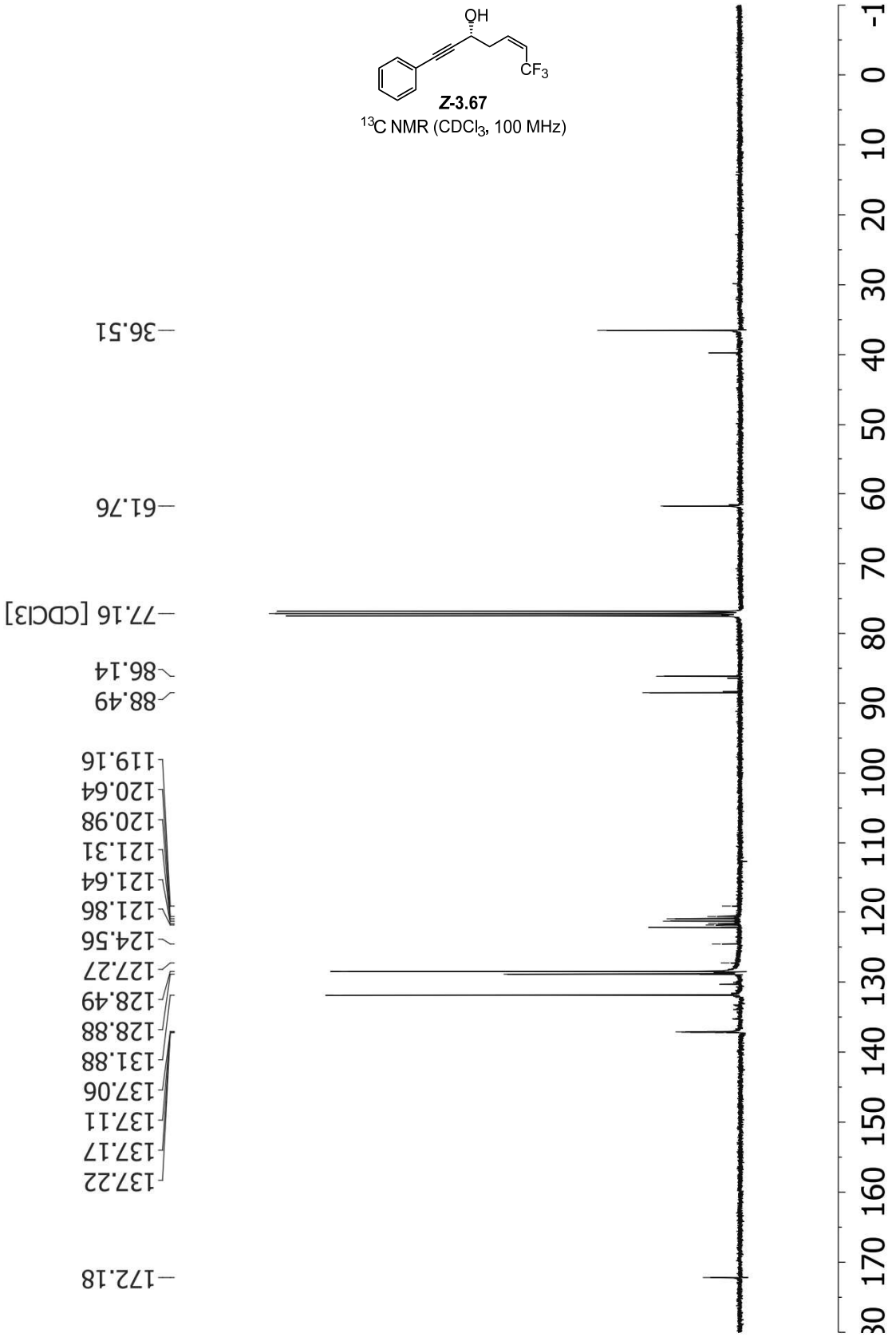
OH
CF3
Z-3.67
13C NMR (CDCl3, 100 MHz)
172.18
137.22
137.17
137.11
137.06
131.88
128.88
128.49
127.27
124.56
121.86
121.64
121.31
120.98
120.64
119.16
88.49
86.14
77.16 [CDCl3]
61.76
36.51

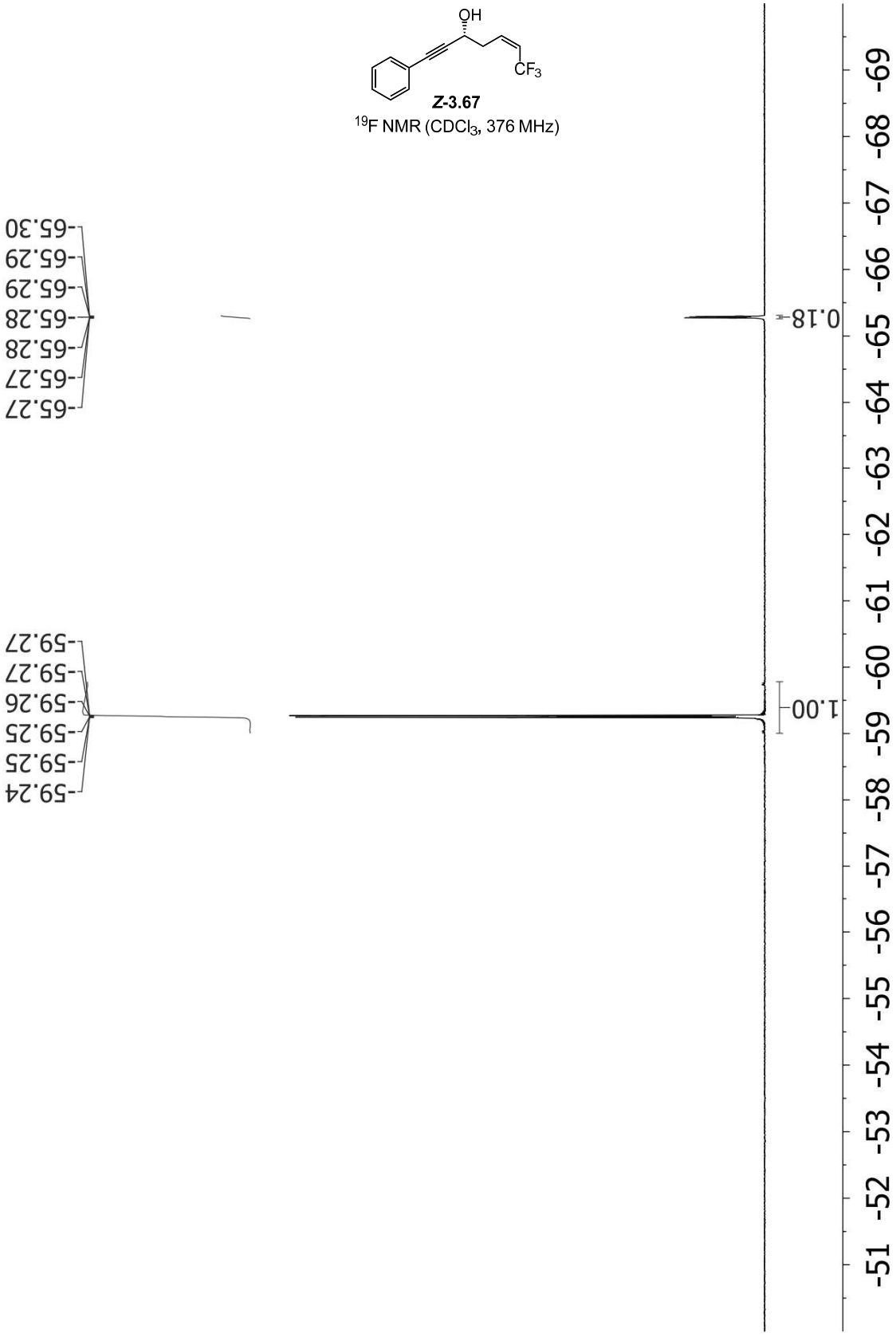
OH
CF3
Z-3.67
19F NMR (CDCl3, 376 MHz)
-65.30
-65.29
-65.29
-65.28
-65.28
-65.27
-65.27
-59.27
-59.27
-59.26
-59.25
-59.25
-59.24
0.18
1.00
-51 -52 -53 -54 -55 -56 -57 -58 -59 -60 -61 -62 -63 -64 -65 -66 -67 -68 -69

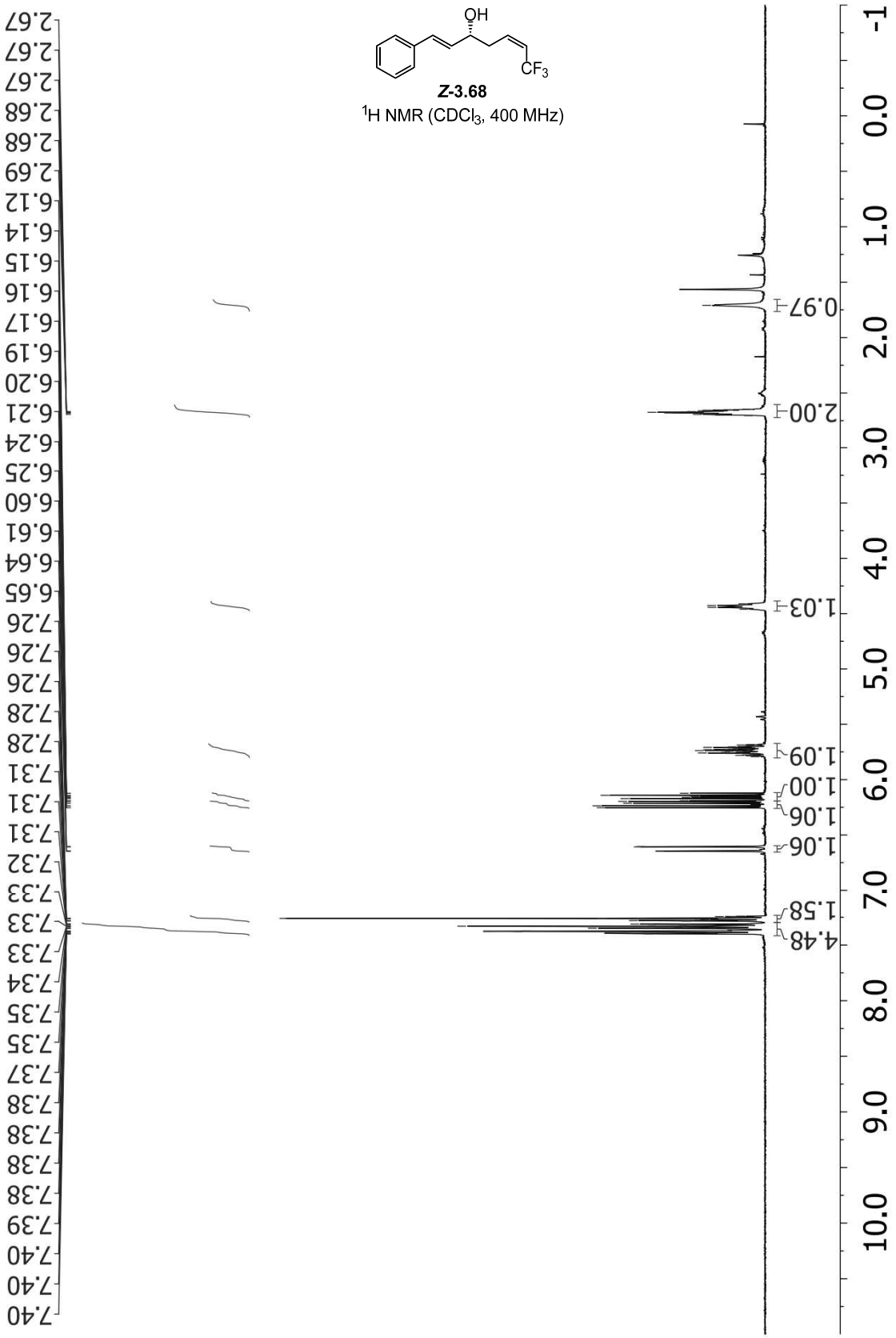
OH
CF3
Z-3.68
1H NMR (CDCl3, 400 MHz)
0.97
2.00
1.03
1.09
1.00
1.06
1.06
1.58
4.48

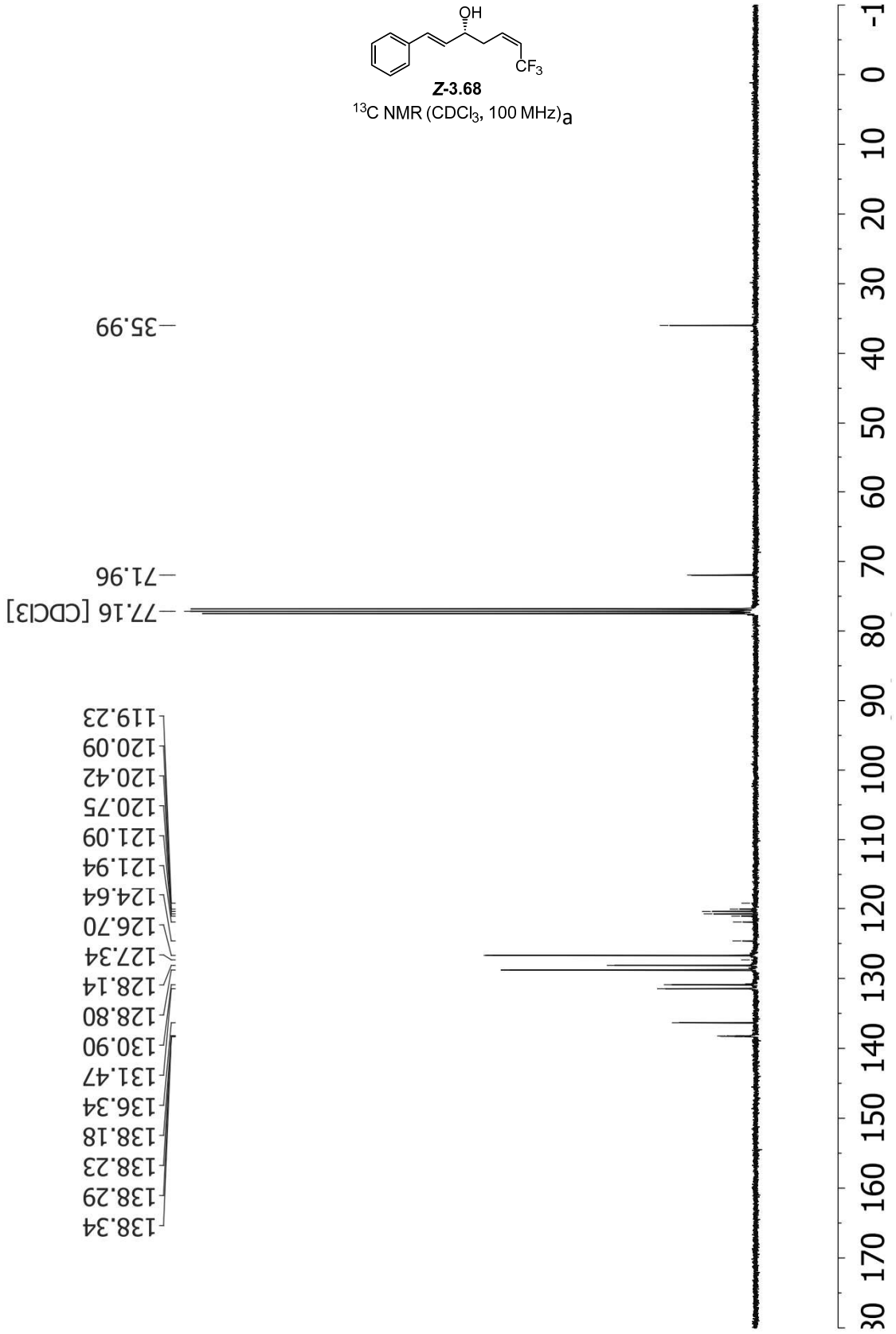
OH
CF3
Z-3.68
13C NMR (CDCl3, 100 MHz)a
35.99
71.96
77.16 [CDCl3]
119.23
120.09
120.42
120.75
121.09
121.94
124.64
126.70
127.34
128.14
128.80
130.90
131.47
136.34
138.18
138.23
138.29
138.34
-1
0
10
20
30
40
50
60
70
80
90
100
110
120
130
140
150
160
170
180

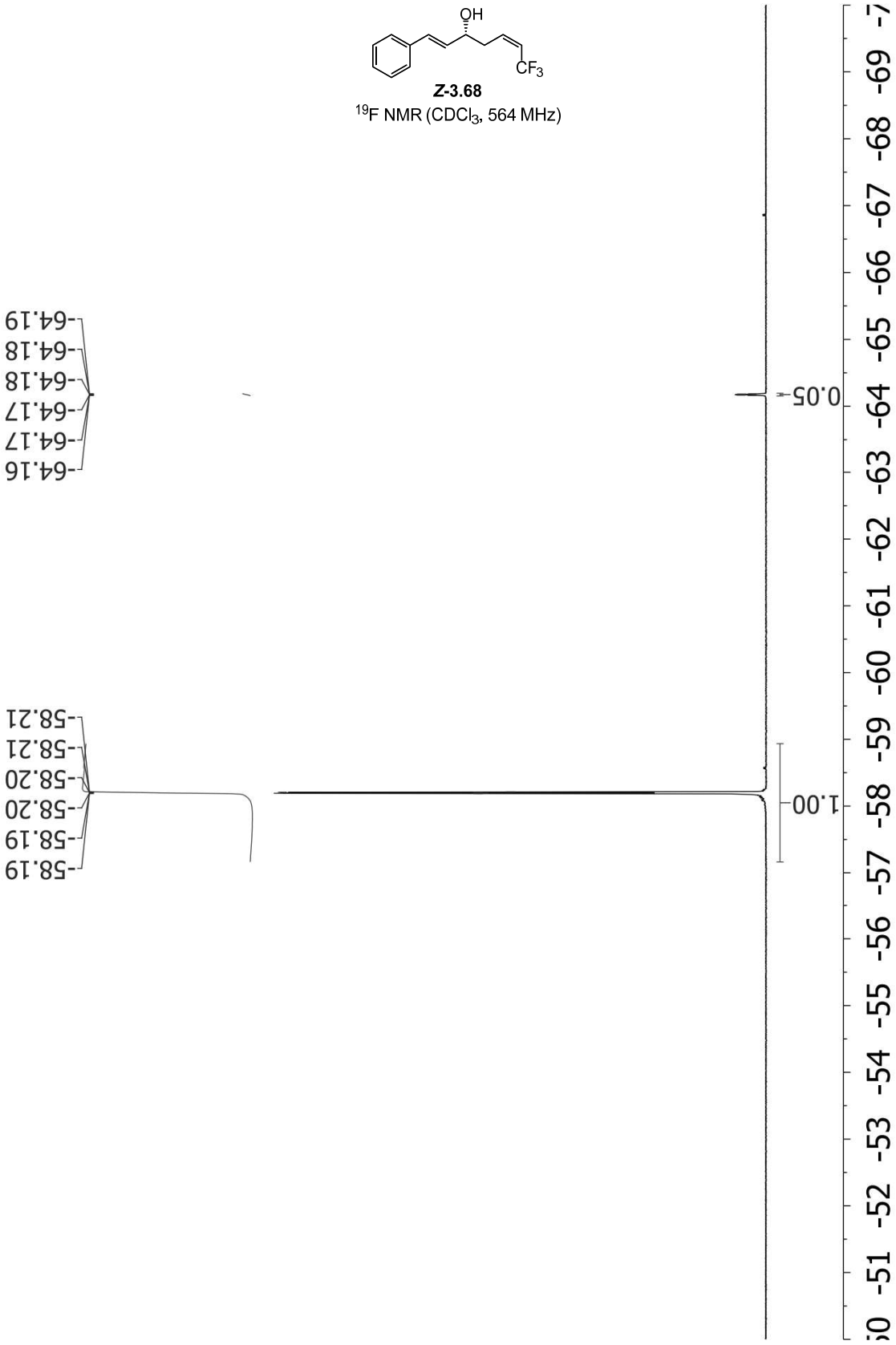
OH
CF3
Z-3.68
19F NMR (CDCl3, 564 MHz)
-58.19
-58.19
-58.20
-58.20
-58.21
-58.21
-64.16
-64.17
-64.17
-64.18
-64.18
-64.19
1.00
0.05
-51
-52
-53
-54
-55
-56
-57
-58
-59
-60
-61
-62
-63
-64
-65
-66
-67
-68
-69

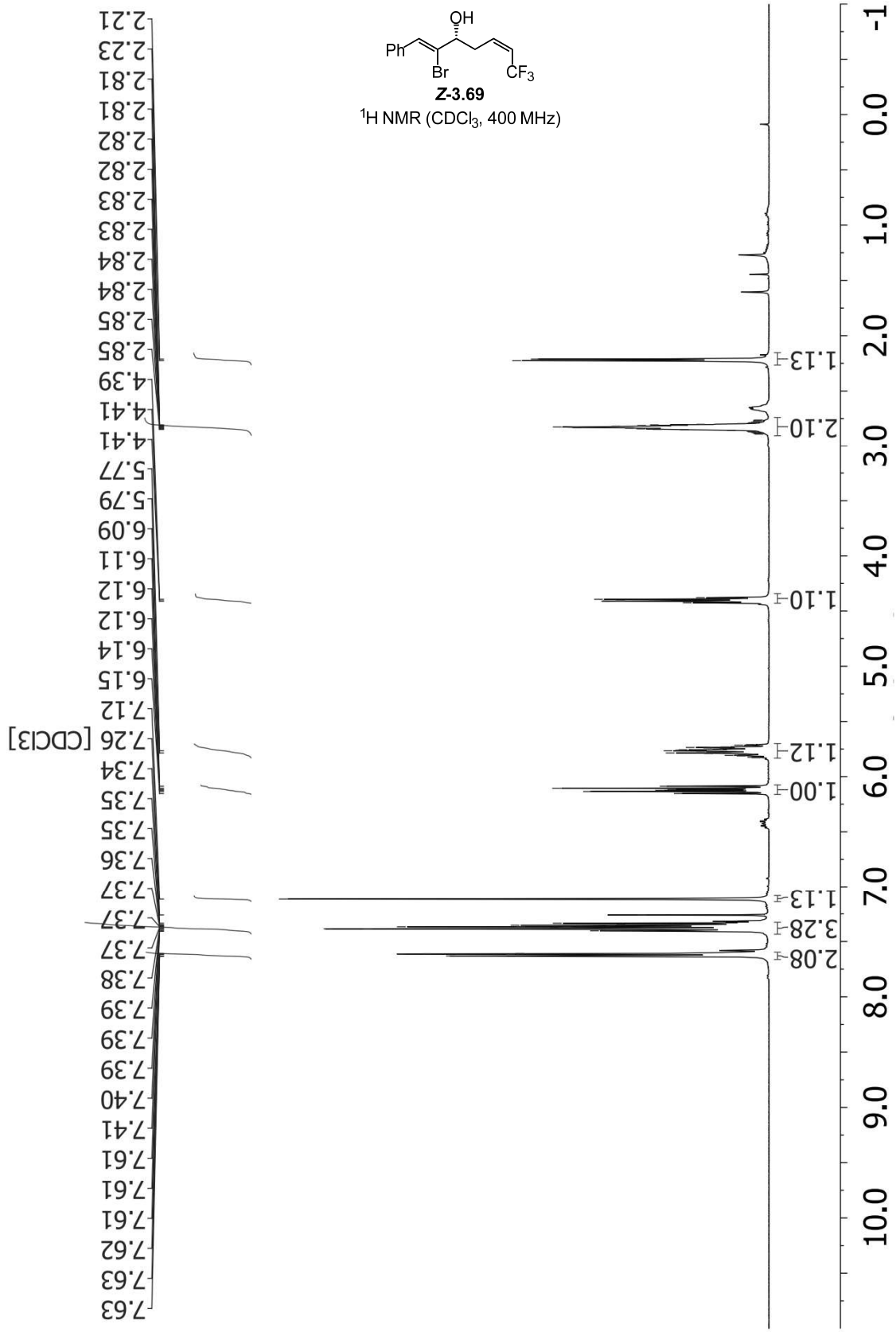
OH
Ph
Br
CF3
Z-3.69
1H NMR (CDCl3, 400 MHz)
[CDCl3]

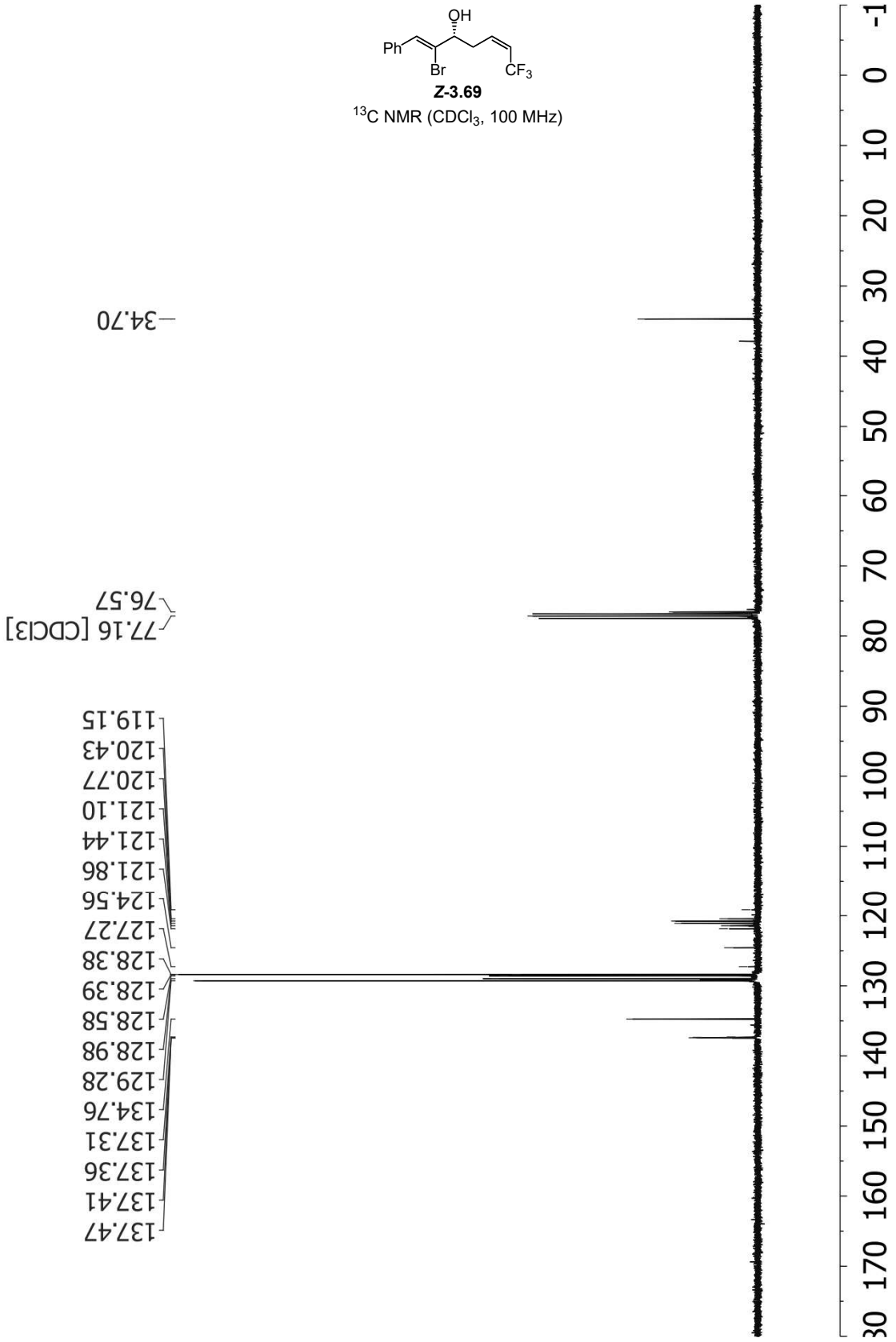
OH
Ph
Br
CF3
Z-3.69
13C NMR (CDCl3, 100 MHz)
34.70
77.16 [CDCl3]
76.57
119.15
120.43
120.77
121.10
121.44
121.86
124.56
127.27
128.38
128.39
128.58
128.98
129.28
134.76
137.31
137.36
137.41
137.47
-1
0
10
20
30
40
50
60
70
80
90
100
110
120
130
140
150
160
170

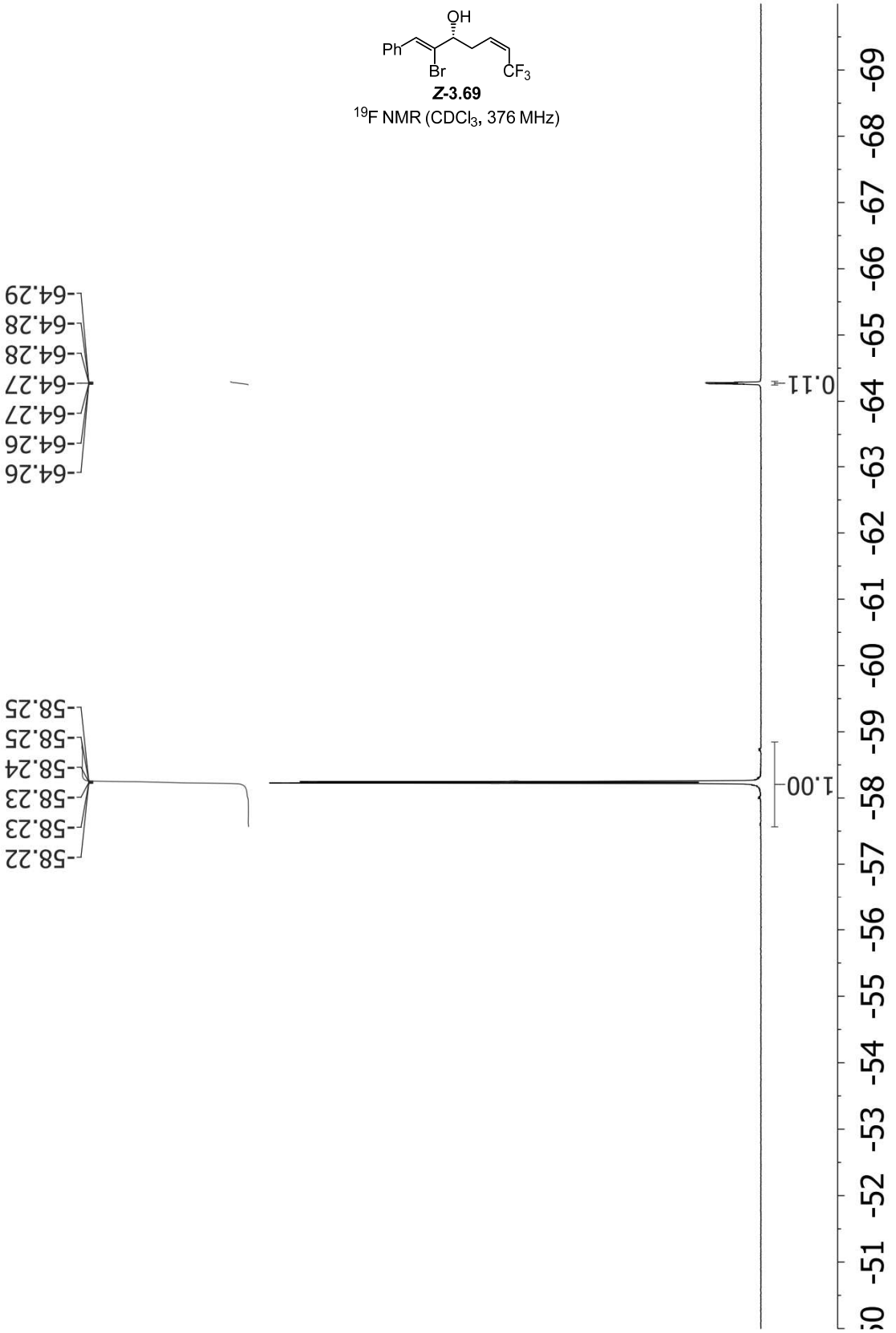
OH
Ph
Br
CF3
Z-3.69
19F NMR (CDCl3, 376 MHz)
-58.22
-58.23
-58.23
-58.24
-58.25
-58.25
-64.26
-64.26
-64.27
-64.27
-64.28
-64.28
-64.29
1.00
0.11
-51
-52
-53
-54
-55
-56
-57
-58
-59
-60
-61
-62
-63
-64
-65
-66
-67
-68
-69

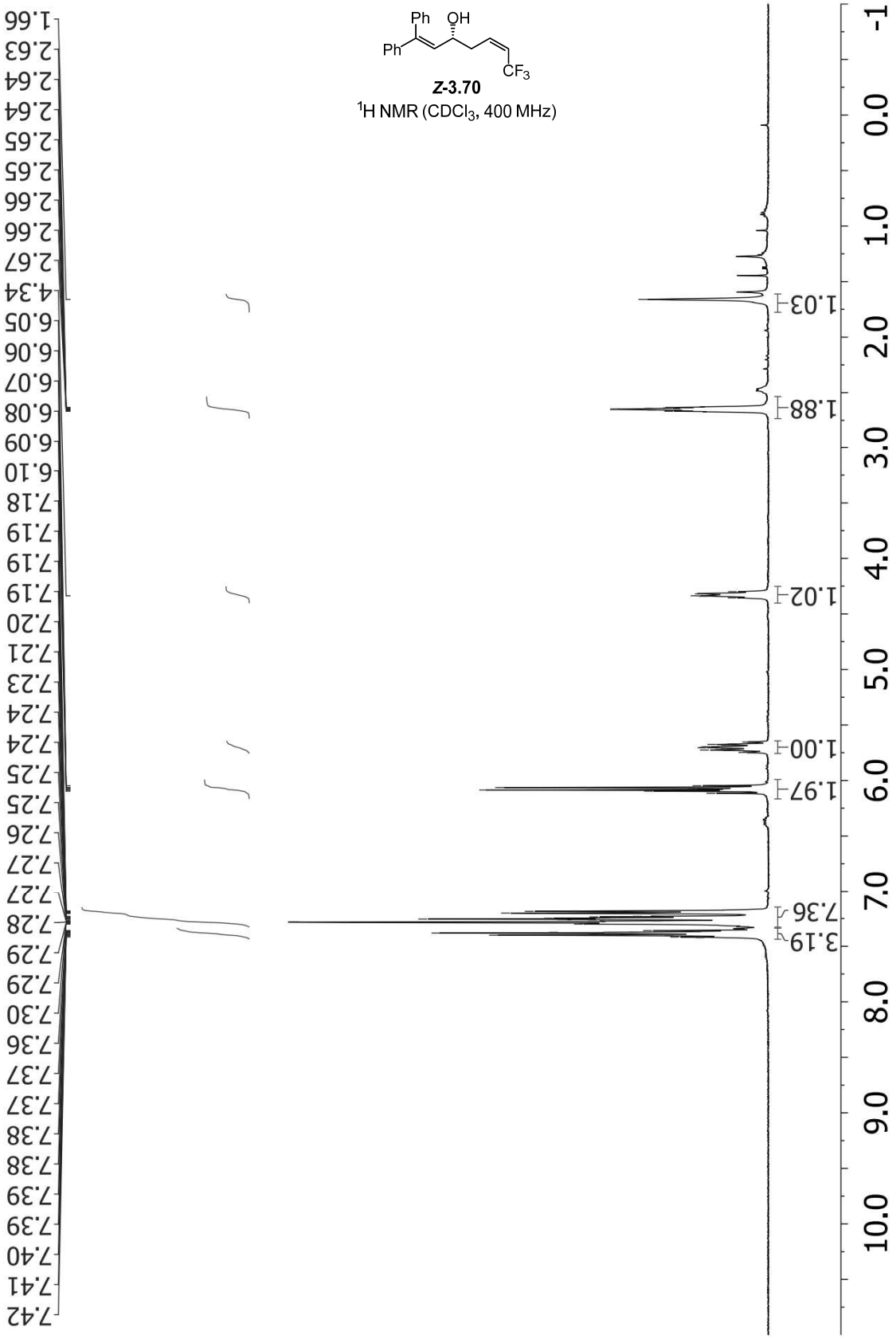
Ph
OH
Ph
CF3
Z-3.70
1H NMR (CDCl3, 400 MHz)
1.03
1.88
1.02
1.00
1.97
7.36
3.19

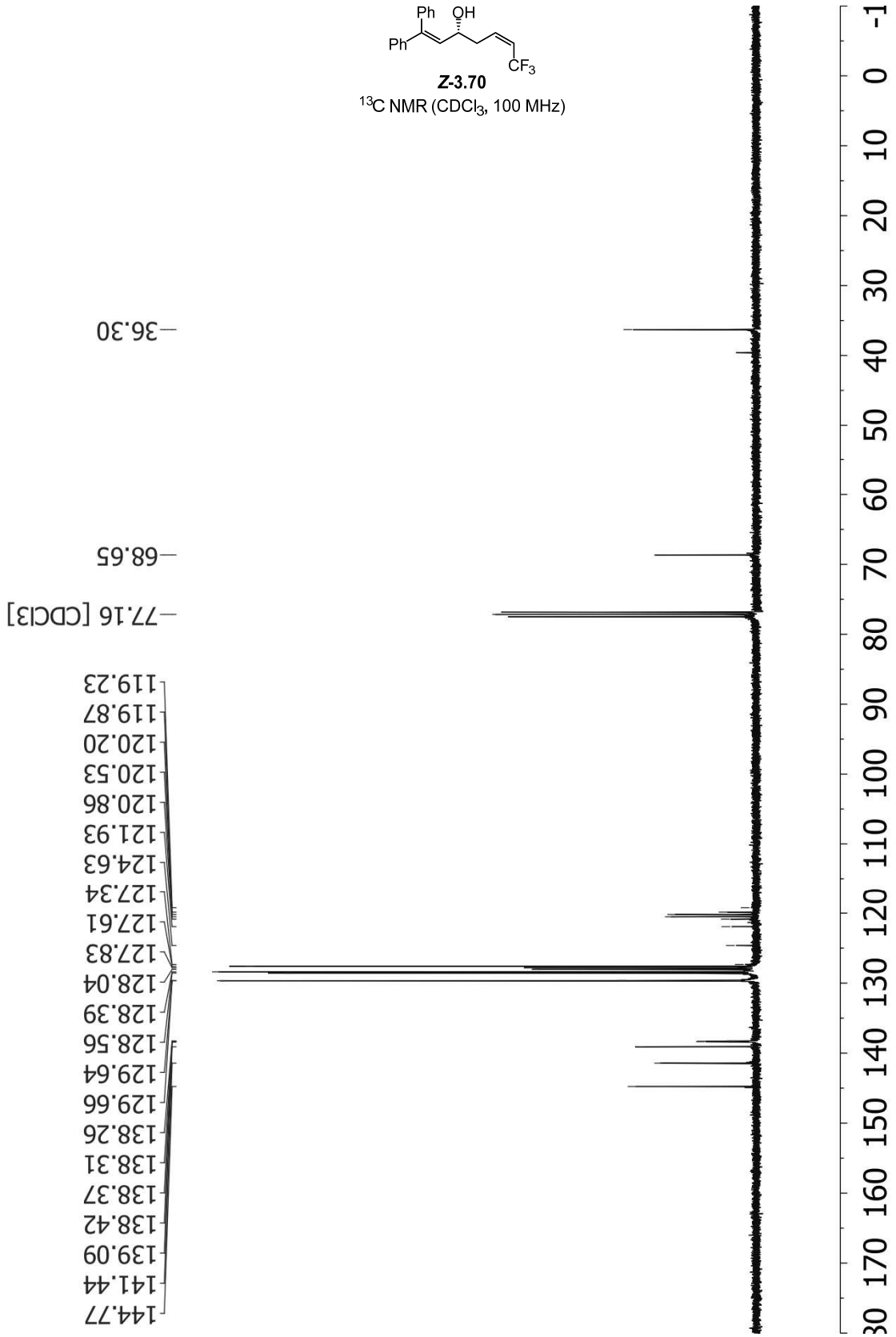
Ph
OH
Ph
CF3
Z-3.70
13C NMR (CDCl3, 100 MHz)
36.30
68.65
77.16 [CDCl3]
119.23
119.87
120.20
120.53
120.86
121.93
124.63
127.34
127.61
127.83
128.04
128.39
128.56
129.64
129.66
138.26
138.31
138.37
138.42
139.09
141.44
144.77

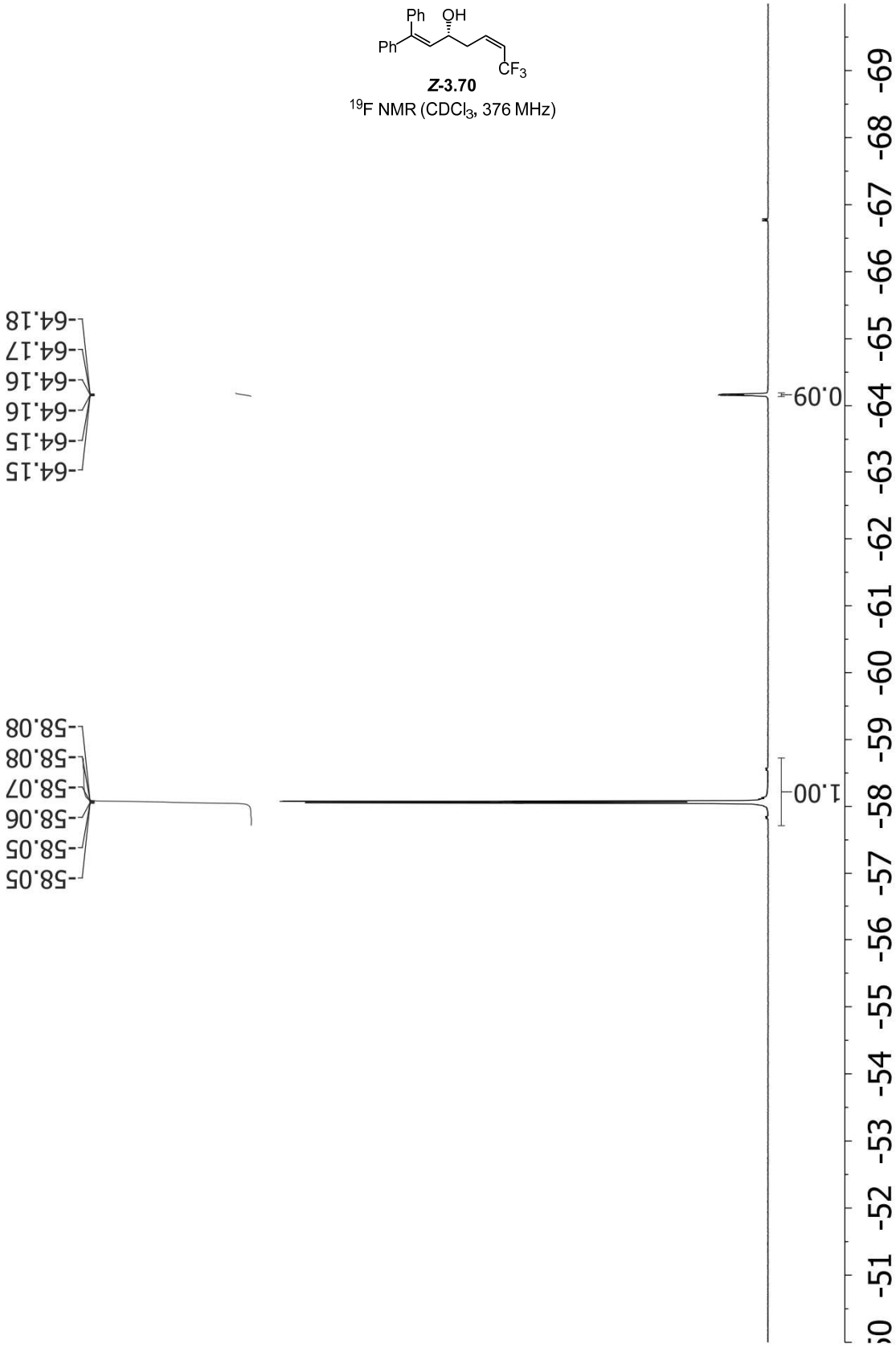
Ph
OH
Ph
CF3
Z-3.70
19F NMR (CDCl3, 376 MHz)
-64.18
-64.17
-64.16
-64.16
-64.15
-64.15
-58.08
-58.08
-58.07
-58.06
-58.05
-58.05
0.09
1.00
-51
-52
-53
-54
-55
-56
-57
-58
-59
-60
-61
-62
-63
-64
-65
-66
-67
-68
-69

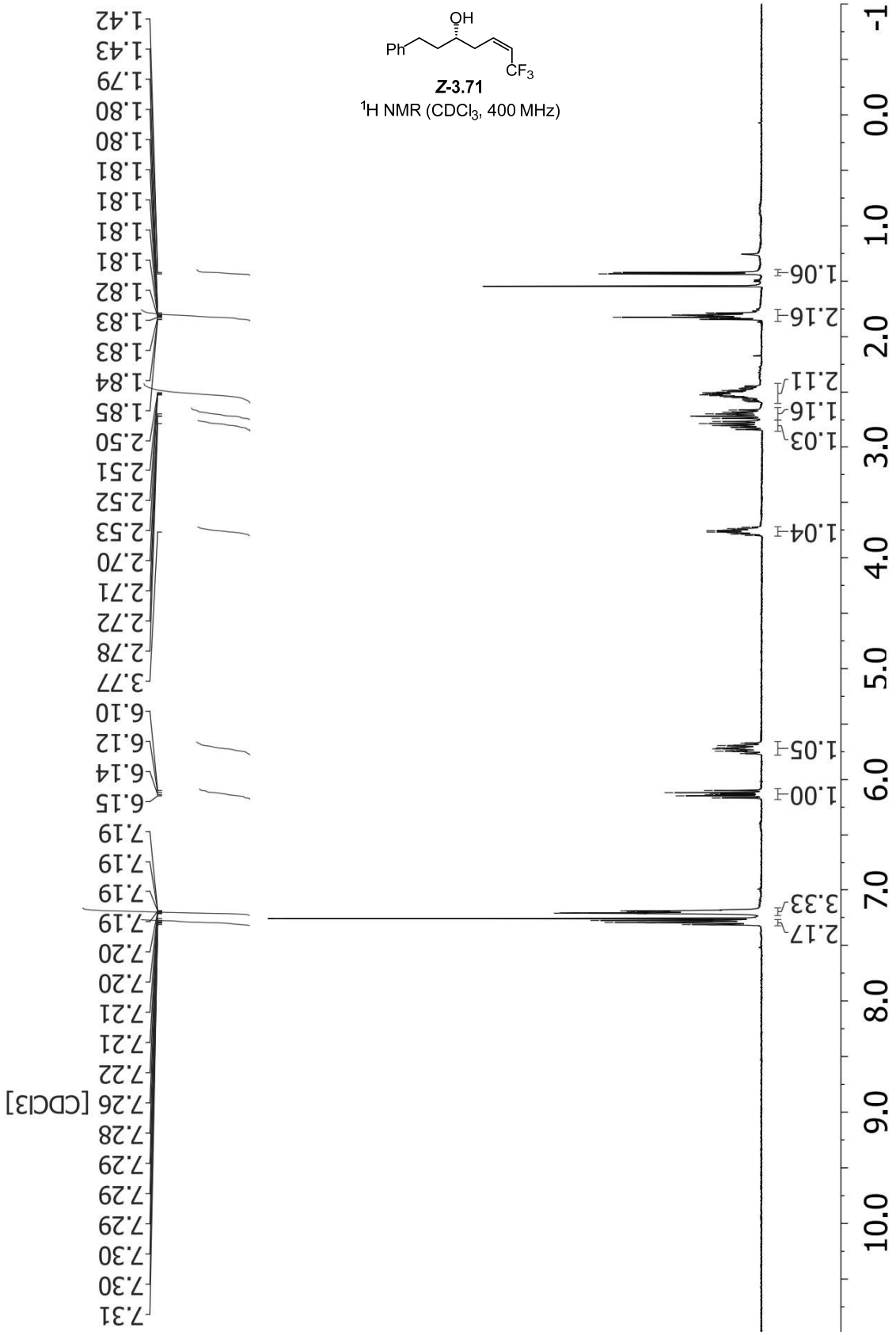
OH
Ph
CF3
Z-3.71
1H NMR (CDCl3, 400 MHz)
[CDCl3]

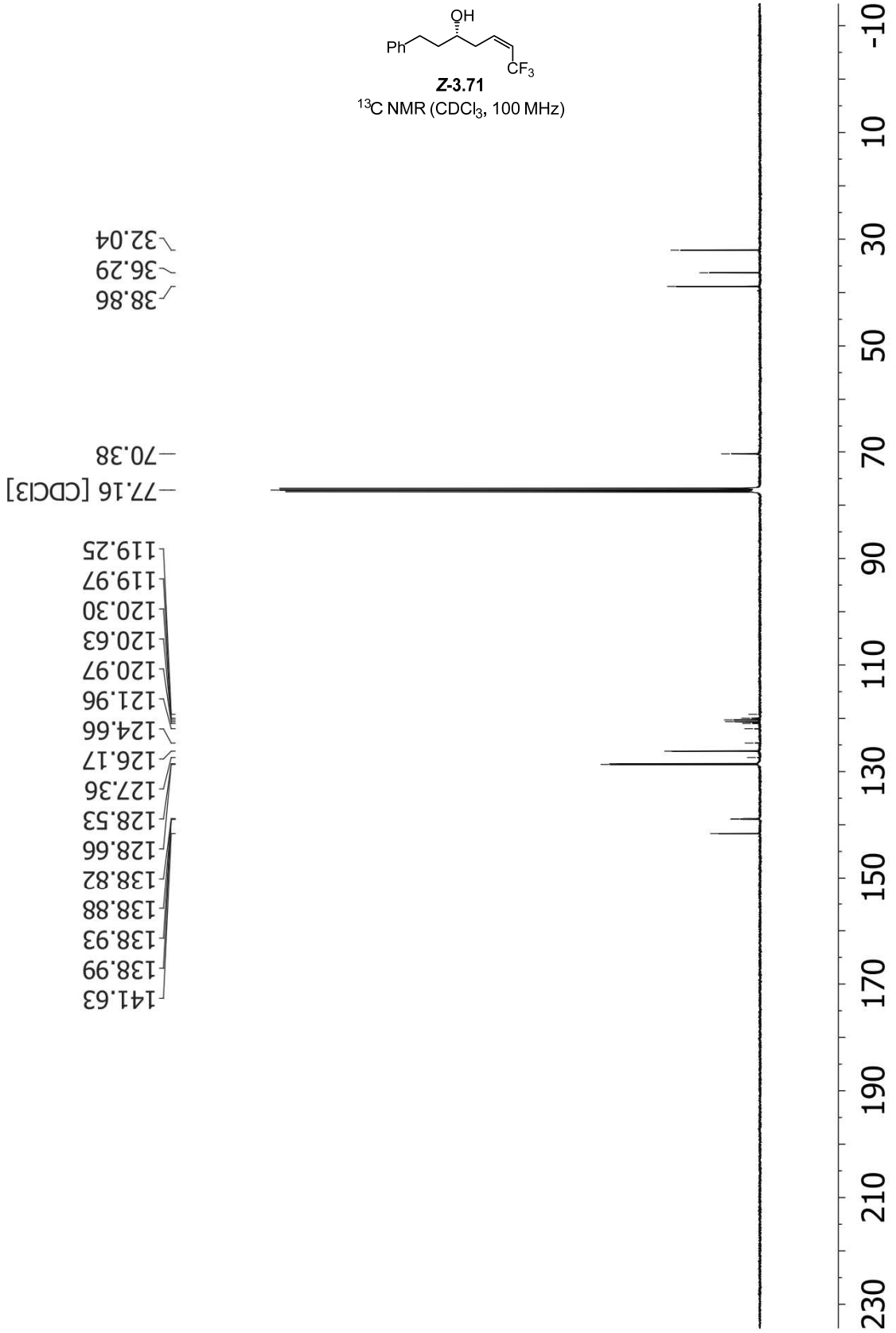
OH
Ph
CF3
Z-3.71
13C NMR (CDCl3, 100 MHz)
-10
10
30
50
70
90
110
130
150
170
190
210
230
32.04
36.29
38.86
70.38
77.16 [CDCl3]
119.25
119.97
120.30
120.63
120.97
121.96
124.66
126.17
127.36
128.53
128.66
138.82
138.88
138.93
138.99
141.63

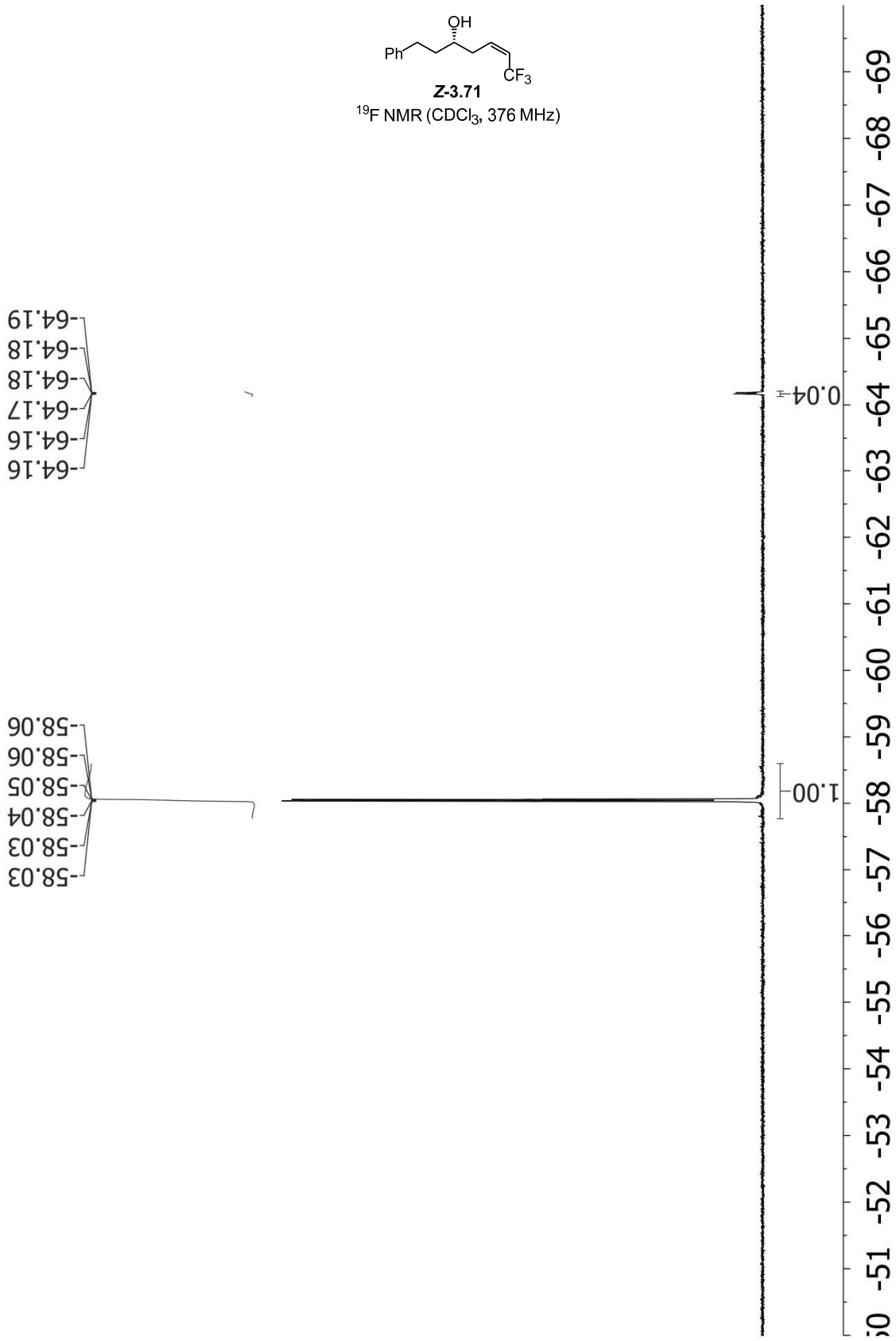
OH
Ph
CF3
Z-3.71
19F NMR (CDCl3, 376 MHz)
-58.03
-58.03
-58.04
-58.05
-58.06
-58.06
-64.16
-64.16
-64.17
-64.18
-64.18
-64.19
1.00
0.04
-50
-51
-52
-53
-54
-55
-56
-57
-58
-59
-60
-61
-62
-63
-64
-65
-66
-67
-68
-69

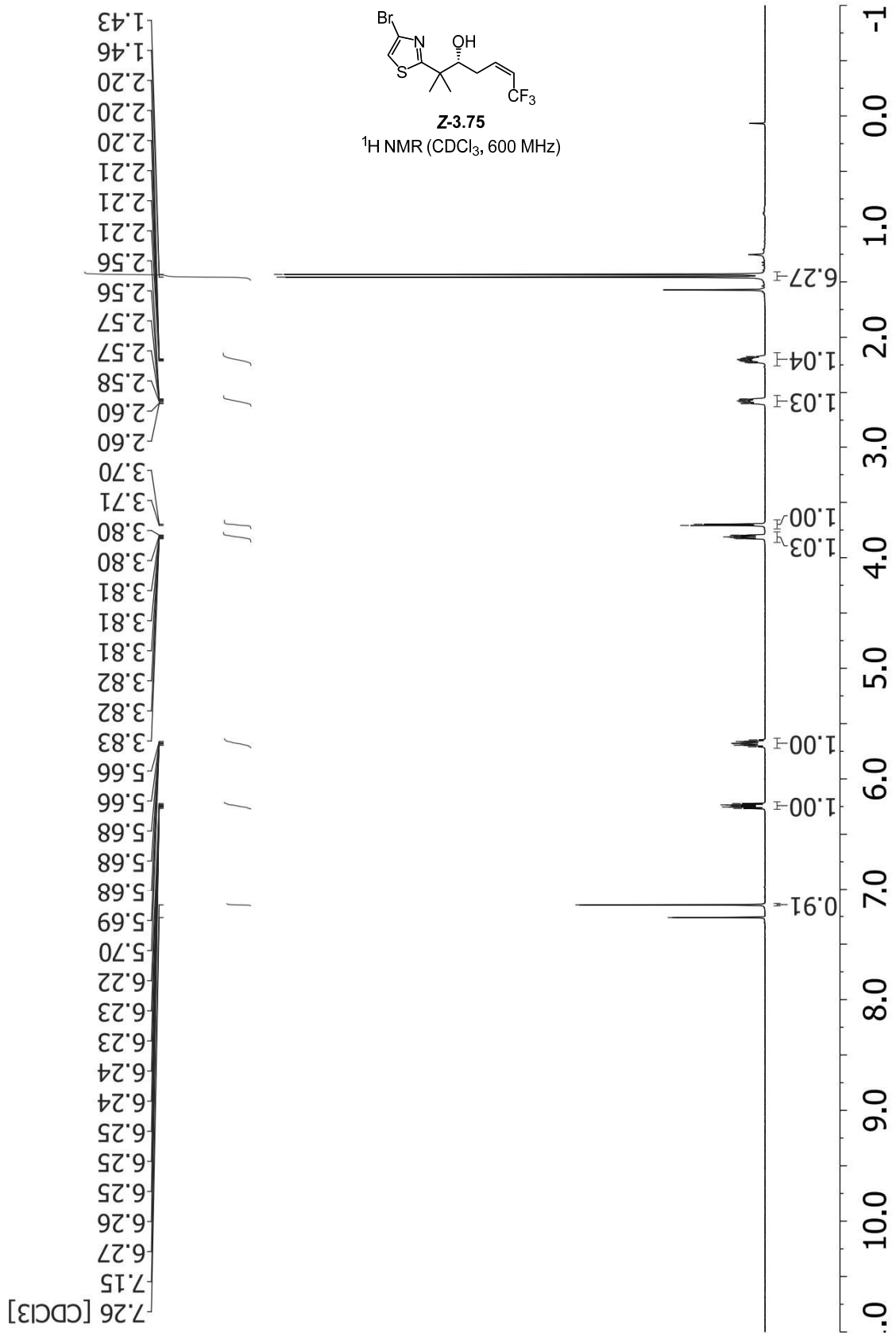
Br
N
OH
S
CF3
Z-3.75
1H NMR (CDCl3, 600 MHz)

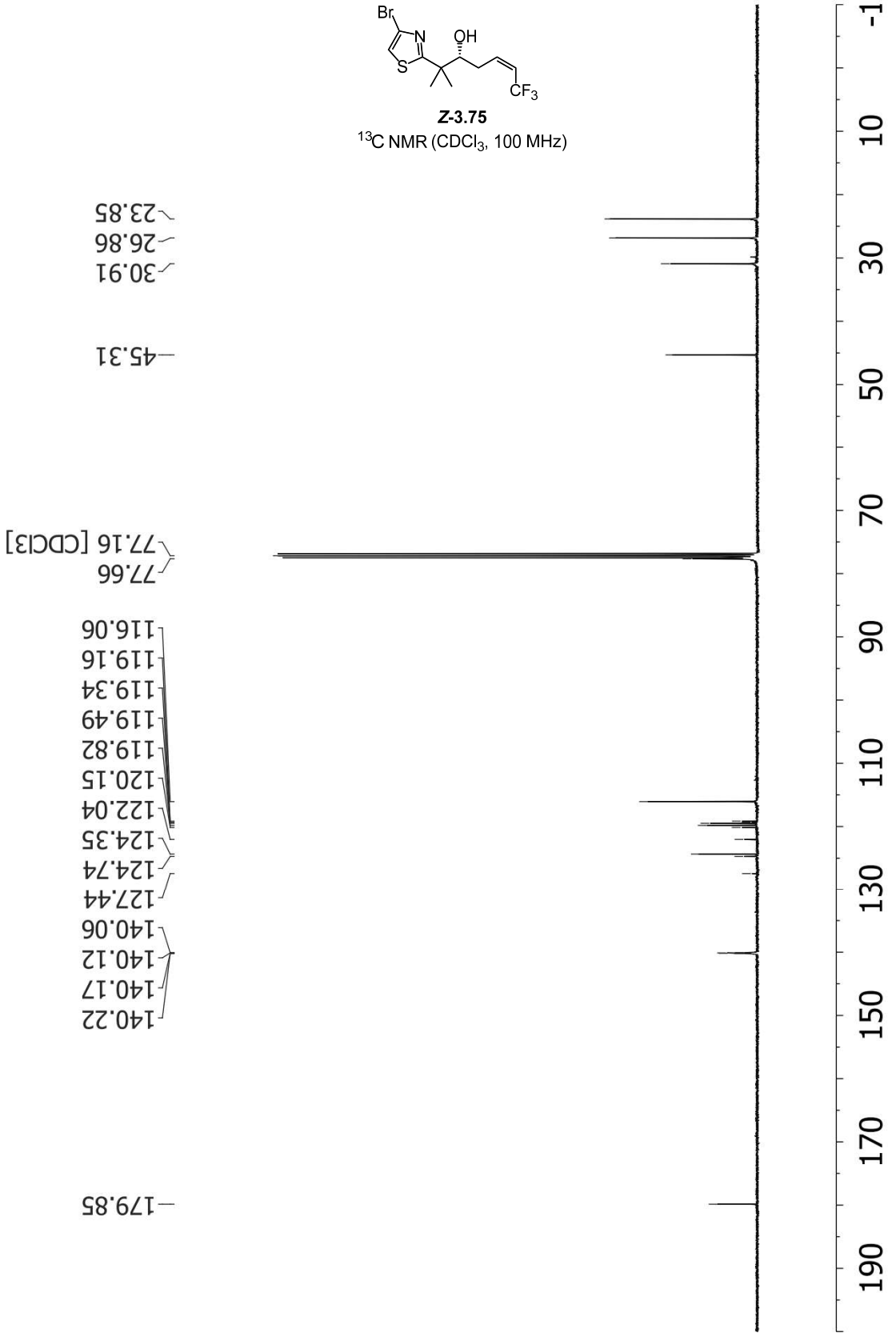
Br
N
OH
S
CF3
Z-3.75
13C NMR (CDCl3, 100 MHz)
23.85
26.86
30.91
45.31
77.16 [CDCl3]
77.66
116.06
119.16
119.34
119.49
119.82
120.15
122.04
124.35
124.74
127.44
140.06
140.12
140.17
140.22
179.85
-1
10
30
50
70
90
110
130
150
170
190

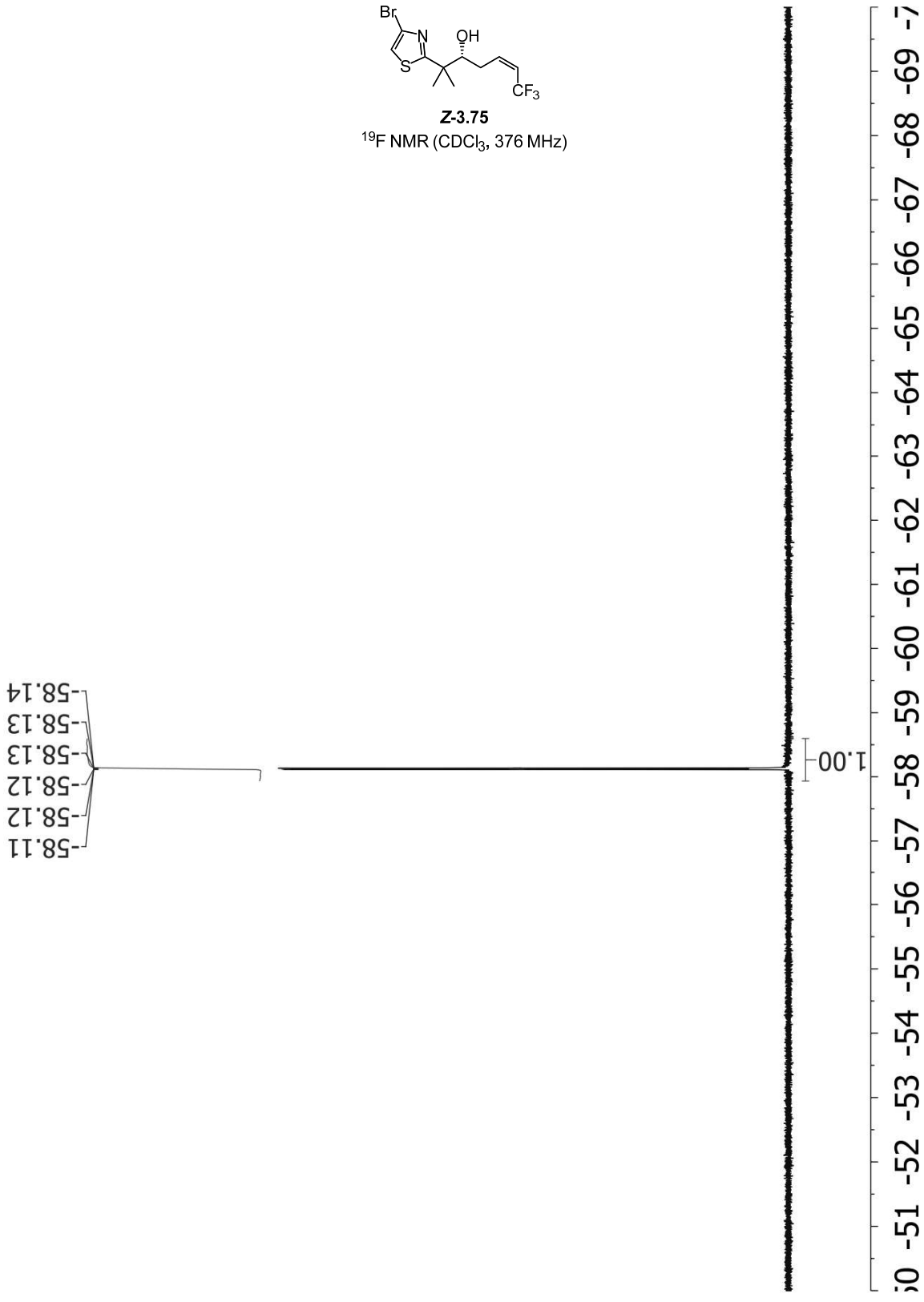

***Z*-3.75**

^{19}F NMR ($CDCl_3$, 376 MHz)

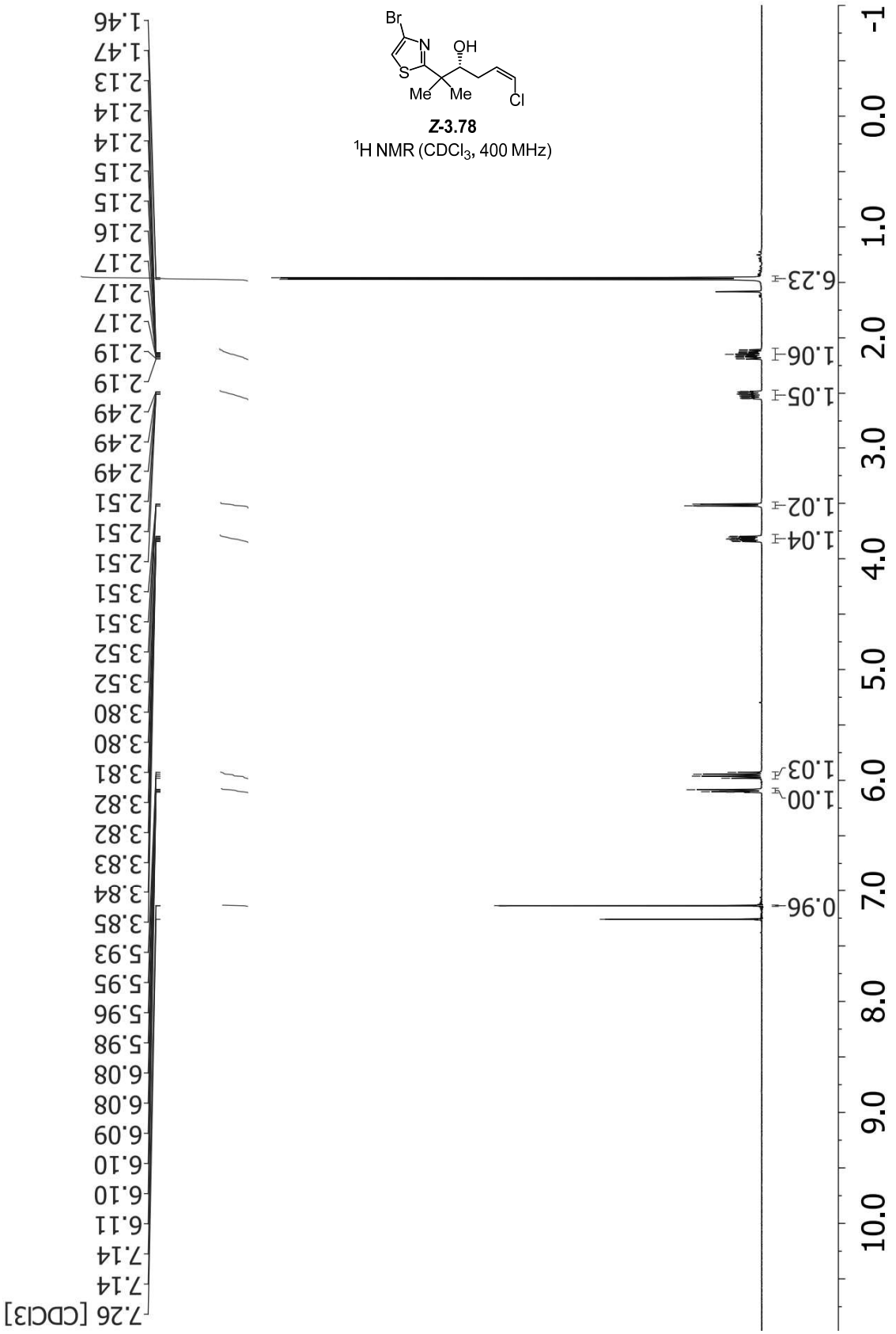
Br
N
OH
S
Me
Me
Cl
Z-3.78
1H NMR (CDCl3, 400 MHz)
7.26 [CDCl3]
6.23
1.06
1.05
1.02
1.04
1.03
1.00
0.96

Br
N
OH
S
Me
Me
Cl
Z-3.78
13C NMR (CDCl3, 150 MHz)
24.00
26.76
30.11
45.39
77.16
77.57
116.01
119.57
124.30
128.96
179.97

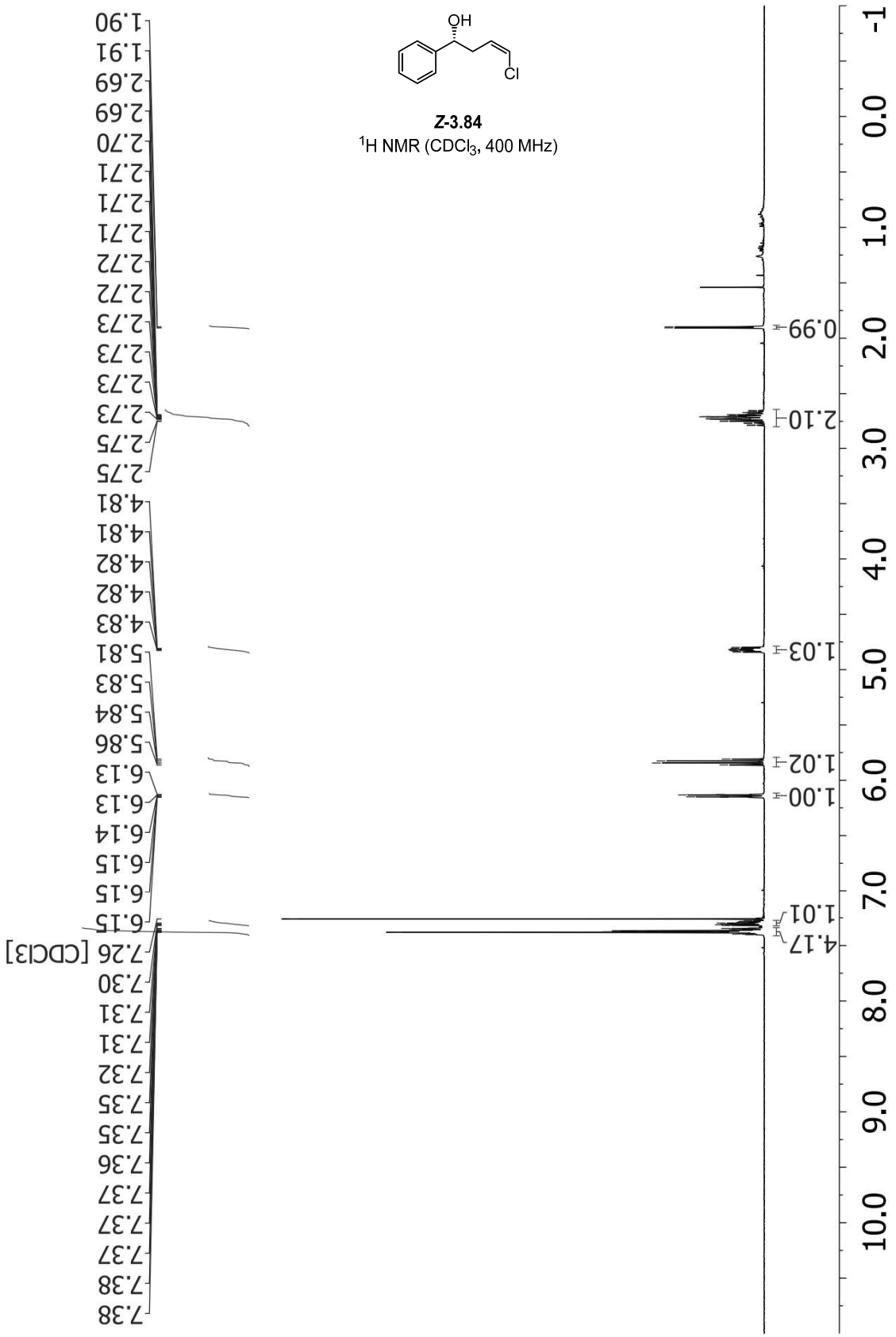
OH
Cl
Z-3.84
1H NMR (CDCl3, 400 MHz)
[CDCl3]
4.17
1.01
1.00
1.02
1.03
2.10
0.99

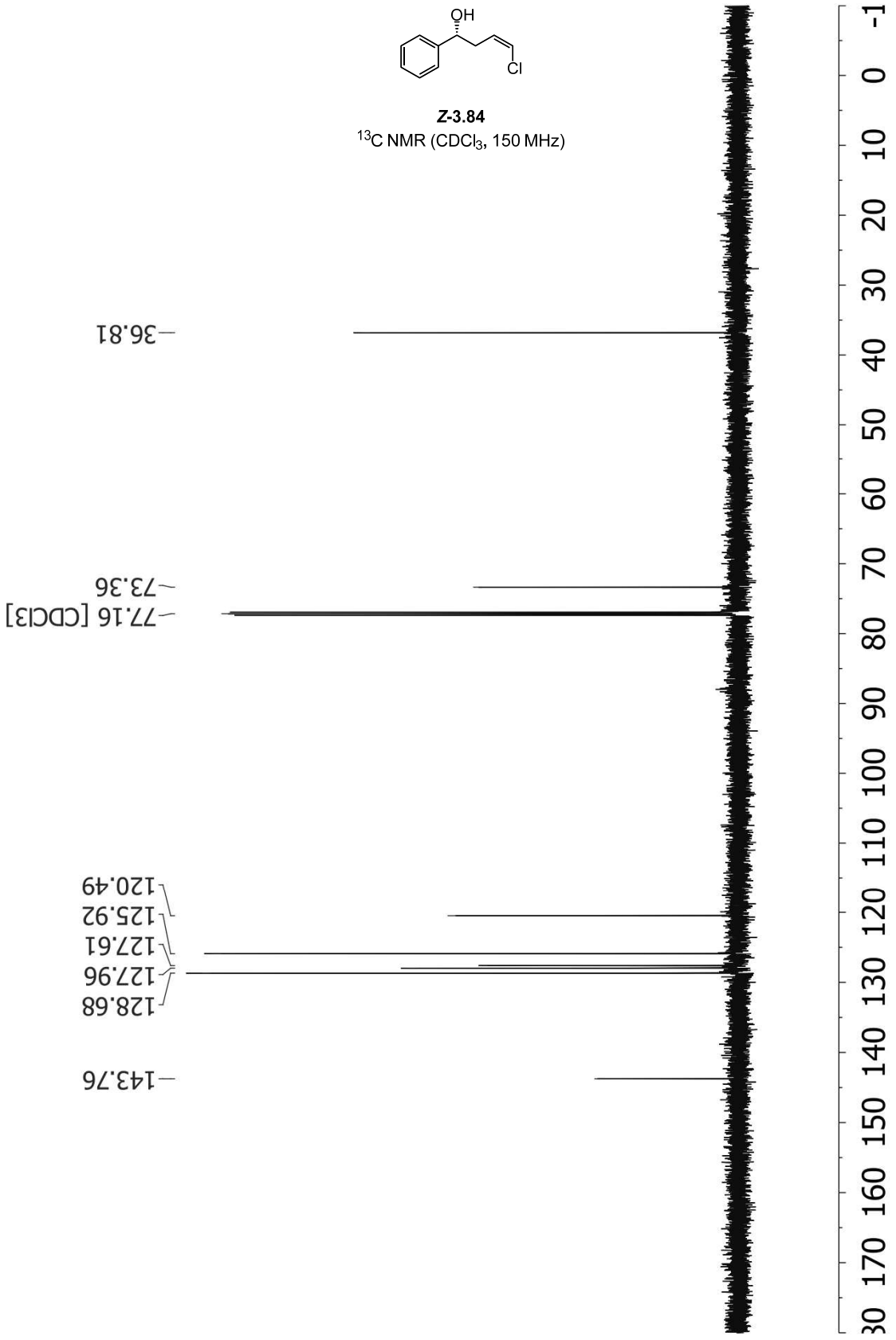
OH
Cl
Z-3.84
13C NMR (CDCl3, 150 MHz)
36.81
73.36
77.16 [CDCl3]
120.49
125.92
127.61
127.96
128.68
143.76
-1
0
10
20
30
40
50
60
70
80
90
100
110
120
130
140
150
160
170

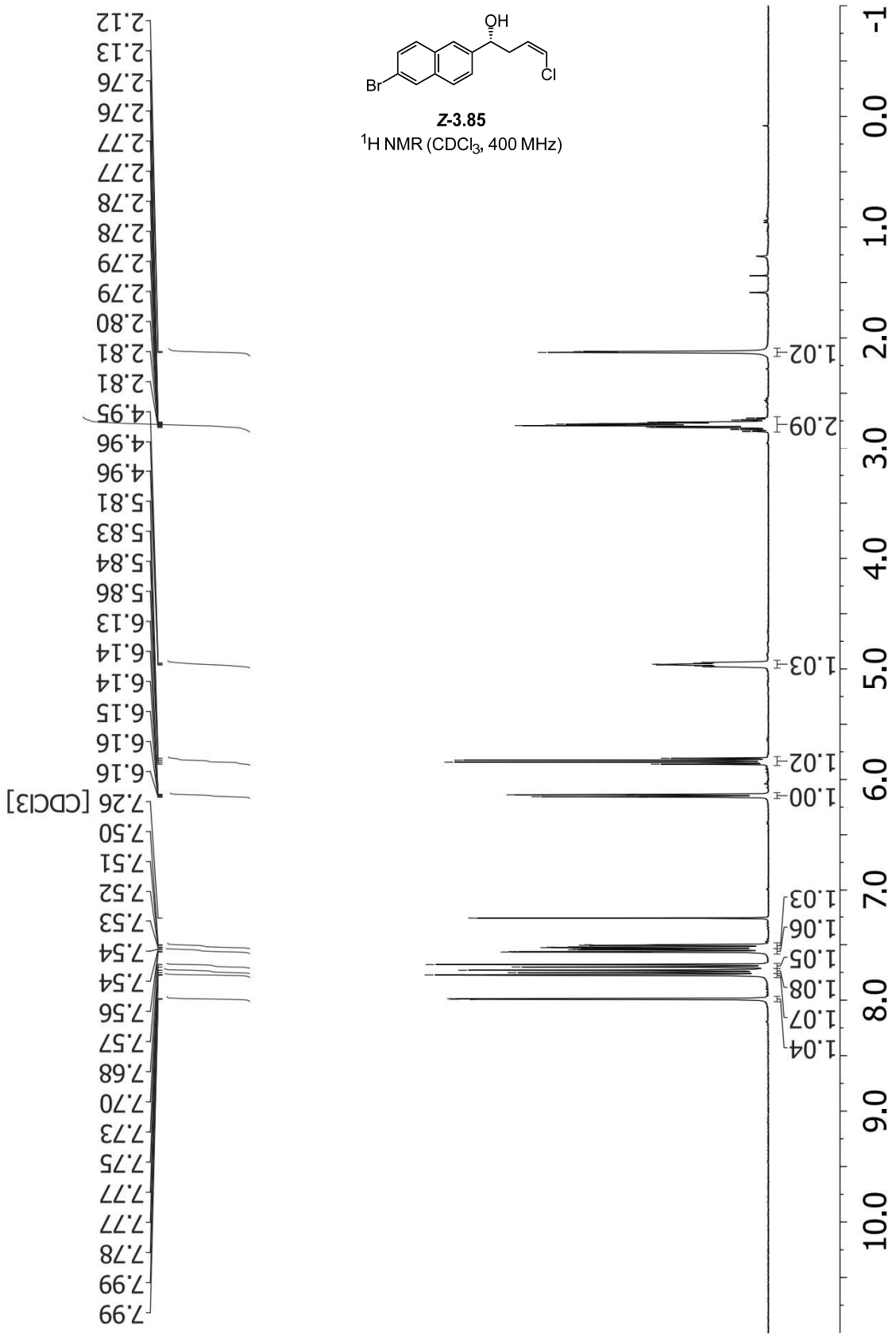
OH
Br
Cl
Z-3.85
1H NMR (CDCl3, 400 MHz)
[CDCl3]

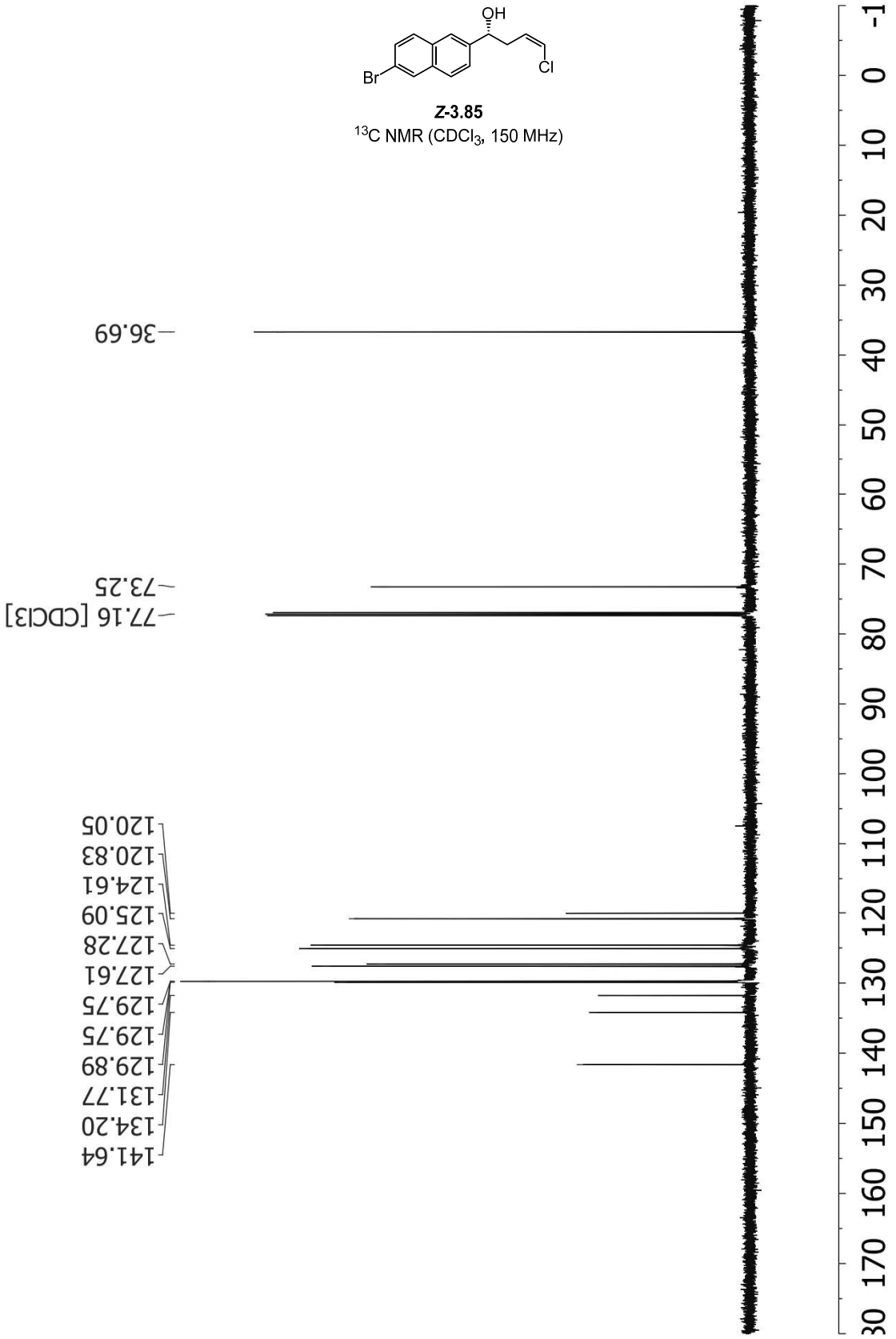
OH
Br
Cl
Z-3.85
13C NMR (CDCl3, 150 MHz)
36.69
73.25
77.16 [CDCl3]
120.05
120.83
124.61
125.09
127.28
127.61
129.75
129.75
129.89
131.77
134.20
141.64

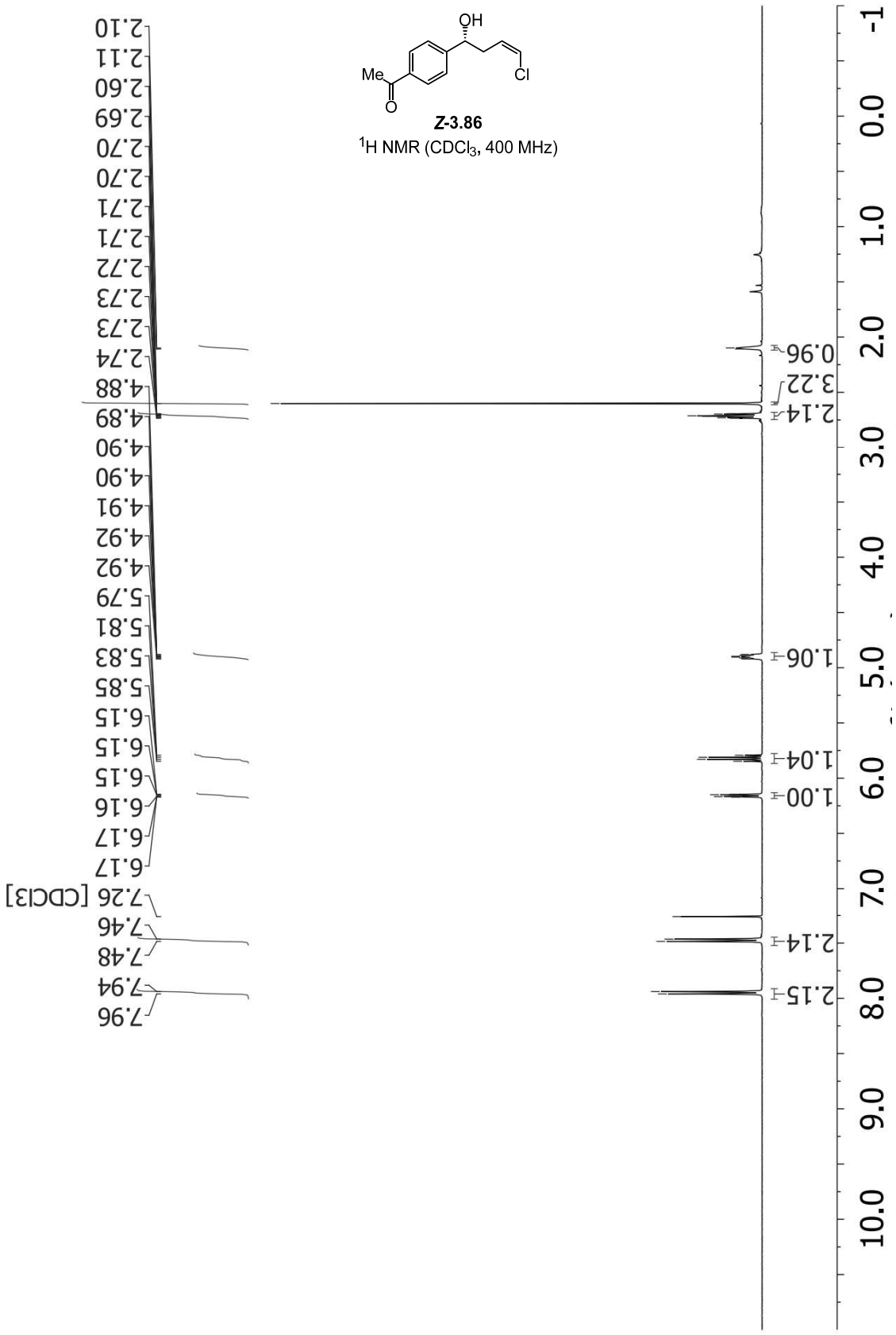
OH
Me
Cl
O
Z-3.86
1H NMR (CDCl3, 400 MHz)
2.10
2.11
2.60
2.69
2.70
2.70
2.71
2.71
2.72
2.73
2.73
2.74
4.88
4.89
4.90
4.90
4.91
4.92
4.92
5.79
5.81
5.83
5.85
6.15
6.15
6.15
6.16
6.17
6.17
7.26 [CDCl3]
7.46
7.48
7.94
7.96
0.96
3.22
2.14
1.06
1.04
1.00
2.14
2.15
-1
0.0
1.0
2.0
3.0
4.0
5.0
6.0
7.0
8.0
9.0
10.0

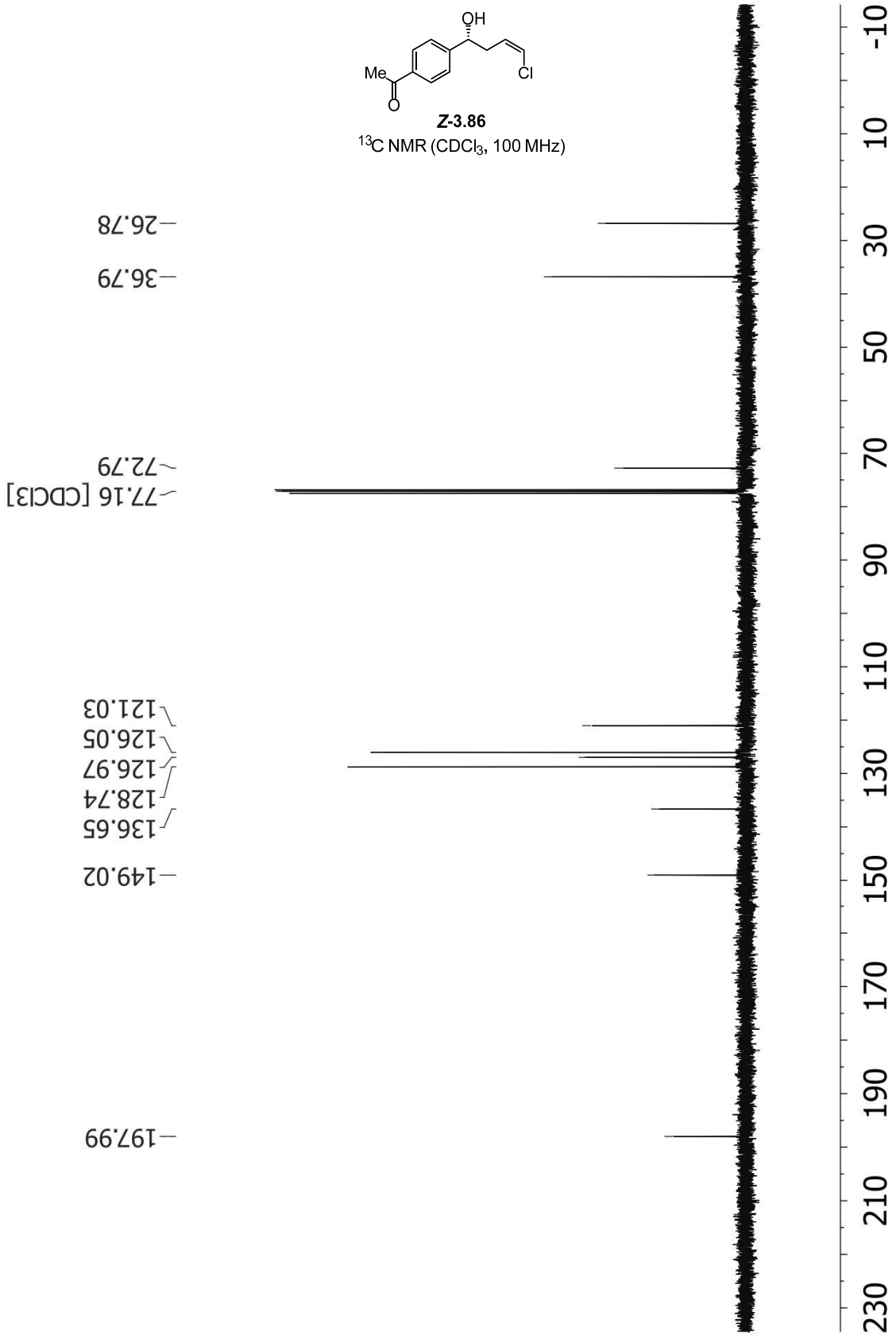
OH
Me
Cl
O
Z-3.86
13C NMR (CDCl3, 100 MHz)
26.78
36.79
72.79
77.16 [CDCl3]
121.03
126.05
126.97
128.74
136.65
149.02
197.99
-10
10
30
50
70
90
110
130
150
170
190
210
230

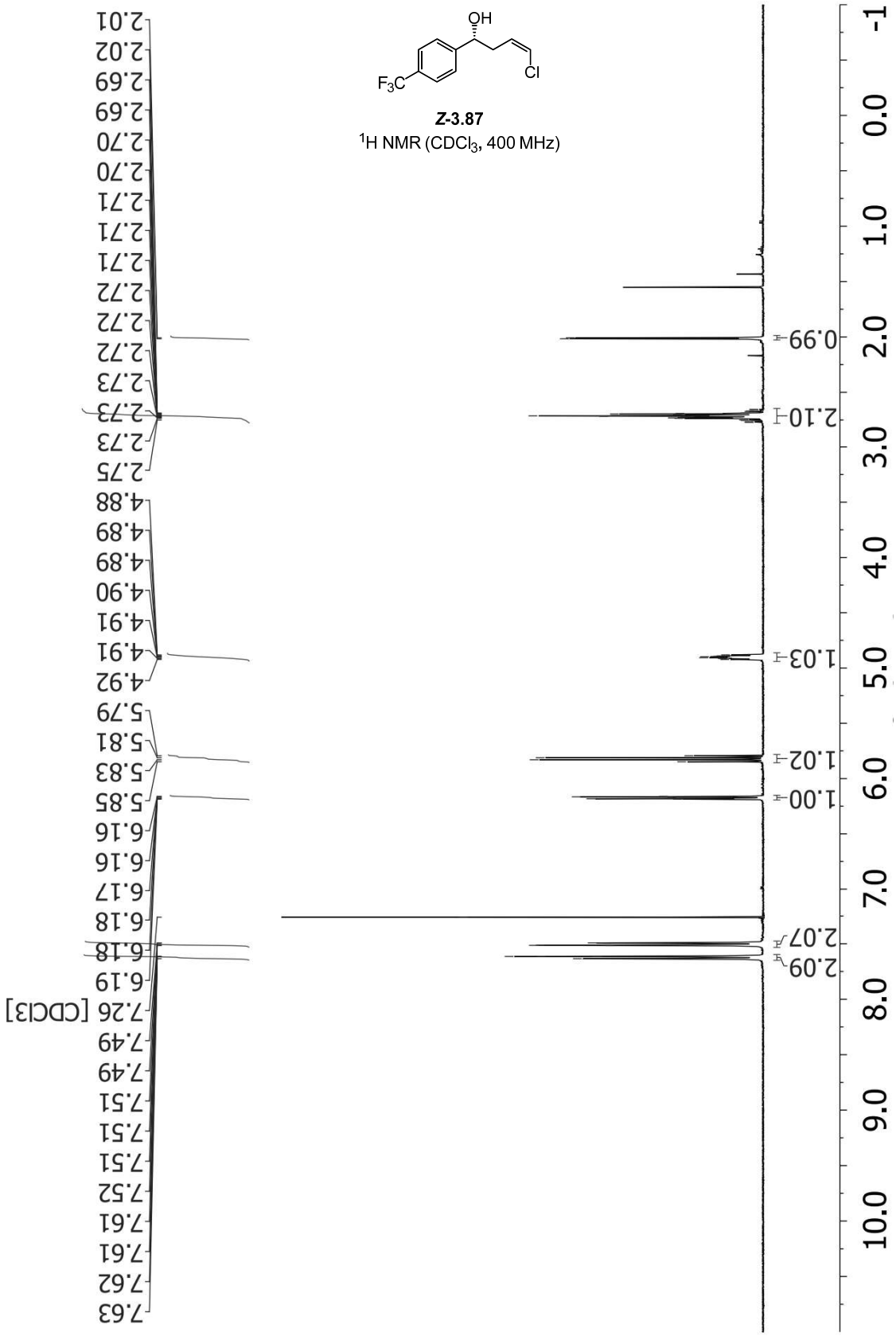
OH
F3C
Cl
Z-3.87
1H NMR (CDCl3, 400 MHz)
[CDCl3]

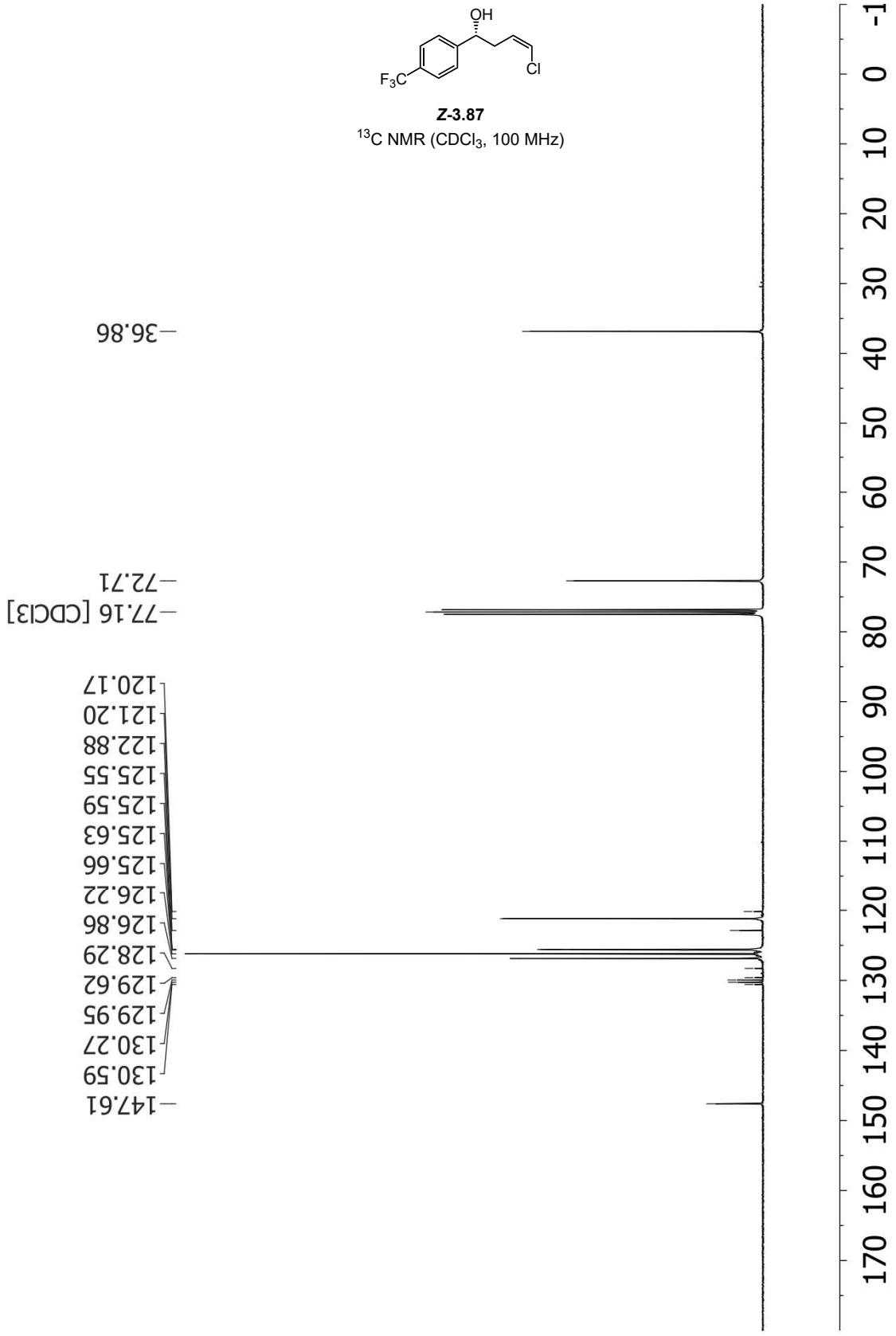
OH
F3C
Cl
Z-3.87
13C NMR (CDCl3, 100 MHz)
36.86
72.71
77.16 [CDCl3]
120.17
121.20
122.88
125.55
125.59
125.63
125.66
126.22
126.86
128.29
129.62
129.95
130.27
130.59
147.61
-1
0
10
20
30
40
50
60
70
80
90
100
110
120
130
140
150
160
170

***Z*-3.87**

^{19}F NMR ($CDCl_3$, 376 MHz)

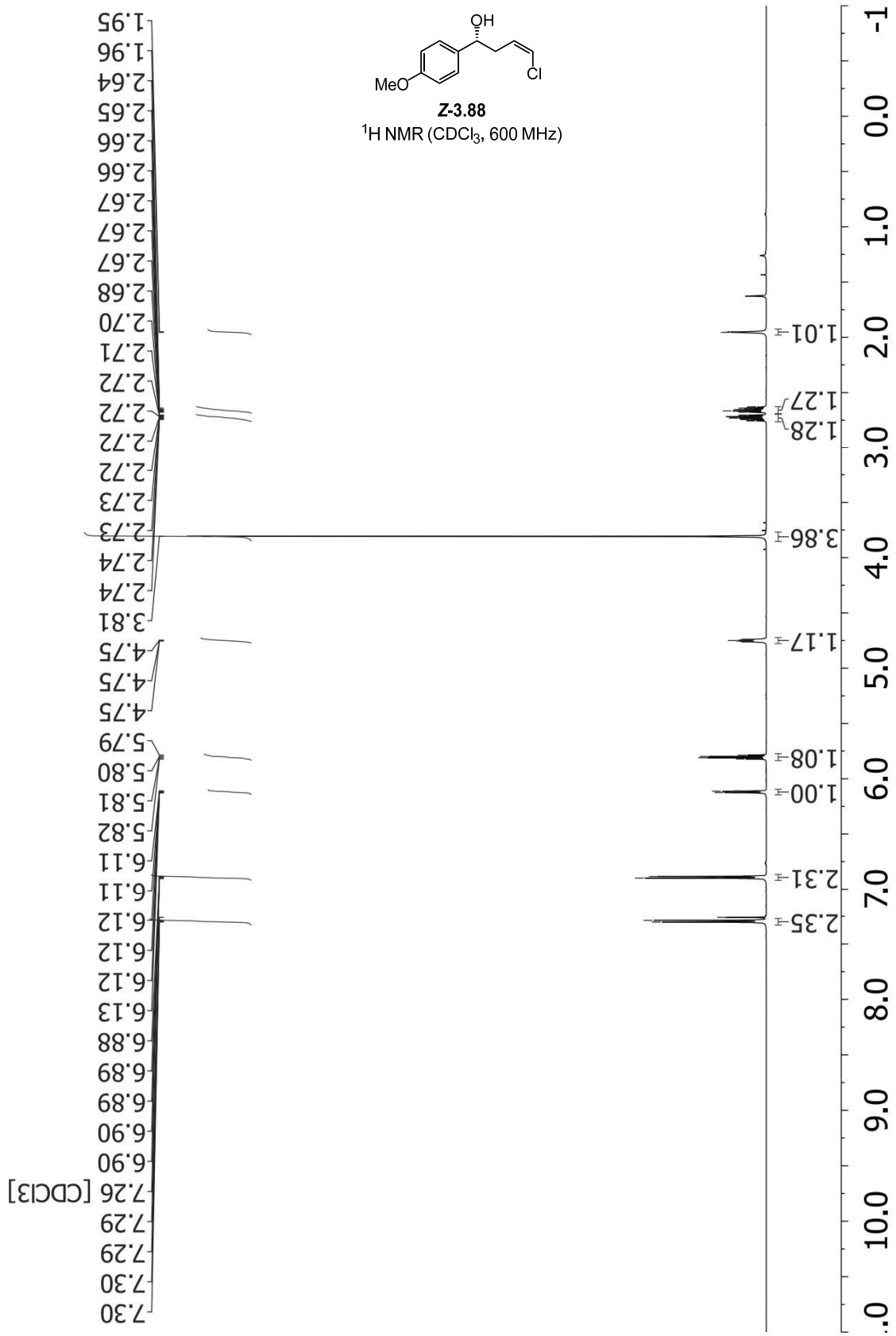
OH
MeO
Cl
Z-3.88
1H NMR (CDCl3, 600 MHz)
1.95
1.96
2.64
2.65
2.66
2.66
2.67
2.67
2.67
2.68
2.70
2.71
2.72
2.72
2.72
2.72
2.73
2.73
2.74
2.74
3.81
4.75
4.75
4.75
5.79
5.80
5.81
5.82
6.11
6.11
6.12
6.12
6.12
6.13
6.88
6.89
6.89
6.90
6.90
7.26 [CDCl3]
7.29
7.29
7.30
7.30
1.01
1.27
1.28
3.86
1.17
1.08
1.00
2.31
2.35
0.0
10.0
9.0
8.0
7.0
6.0
5.0
4.0
3.0
2.0
1.0
0.0
-1

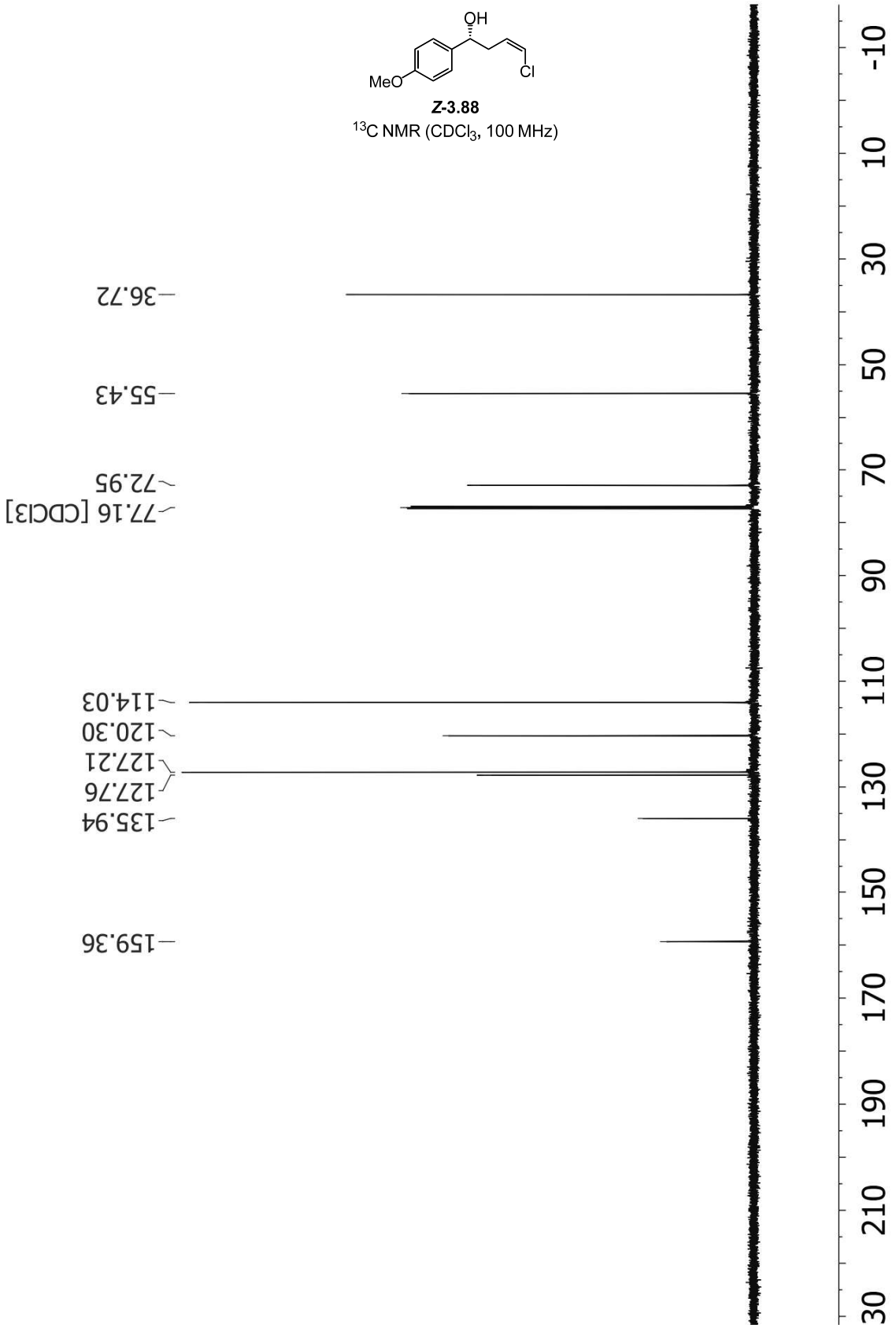
OH
MeO
Cl
Z-3.88
13C NMR (CDCl3, 100 MHz)
36.72
55.43
72.95
77.16 [CDCl3]
114.03
120.30
127.21
127.76
135.94
159.36
-10
10
30
50
70
90
110
130
150
170
190
210
30

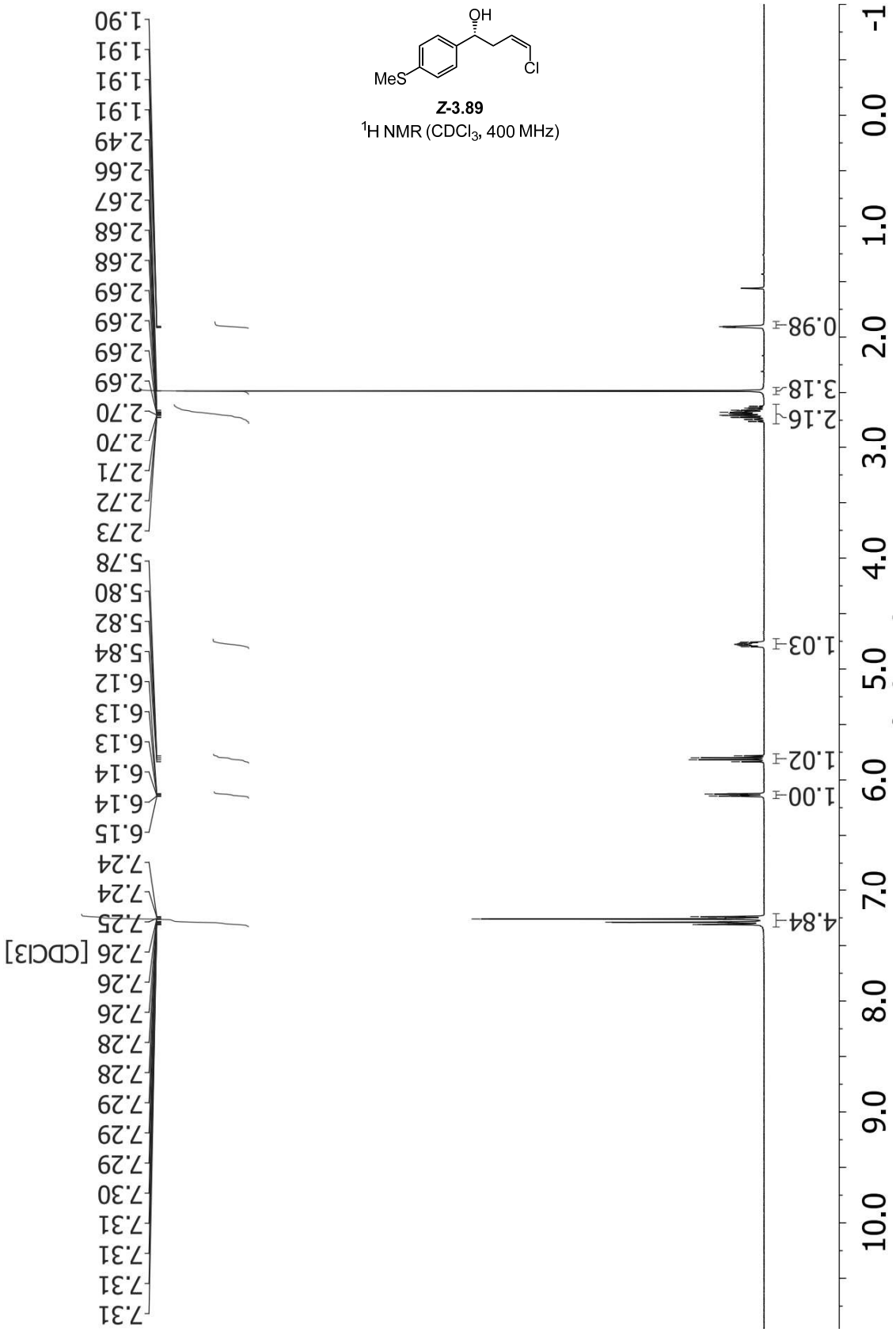
OH
MeS
Cl
Z-3.89
1H NMR (CDCl3, 400 MHz)
[CDCl3]

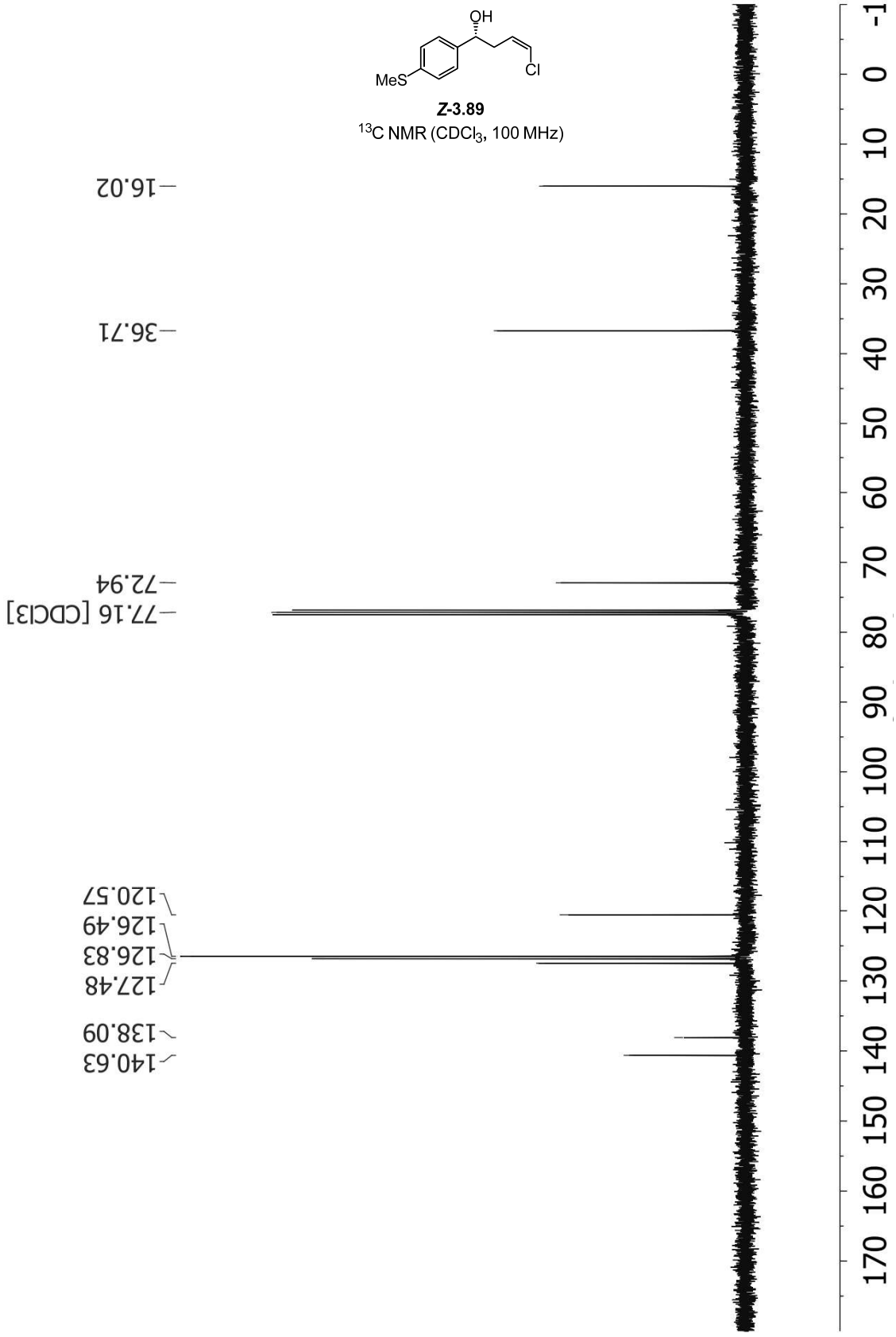
OH
MeS
Cl
Z-3.89
13C NMR (CDCl3, 100 MHz)
16.02
36.71
72.94
77.16 [CDCl3]
120.57
126.49
126.83
127.48
138.09
140.63
170 160 150 140 130 120 110 100 90 80 70 60 50 40 30 20 10 0 -1

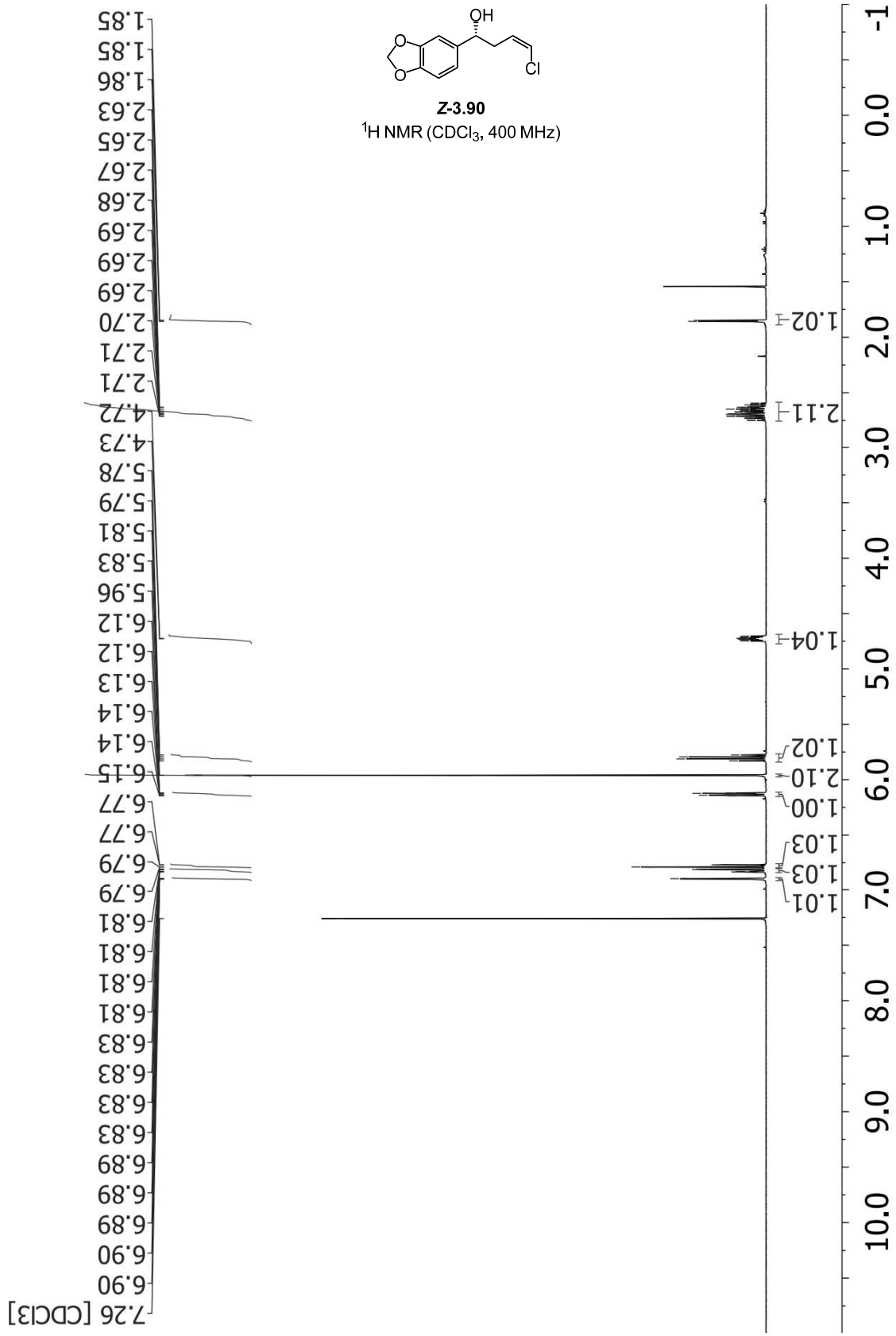
OH
O
O
Cl
Z-3.90
1H NMR (CDCl3, 400 MHz)
7.26 [CDCl3]
1.01
1.03
1.03
1.00
2.10
1.02
1.04
2.11
1.02

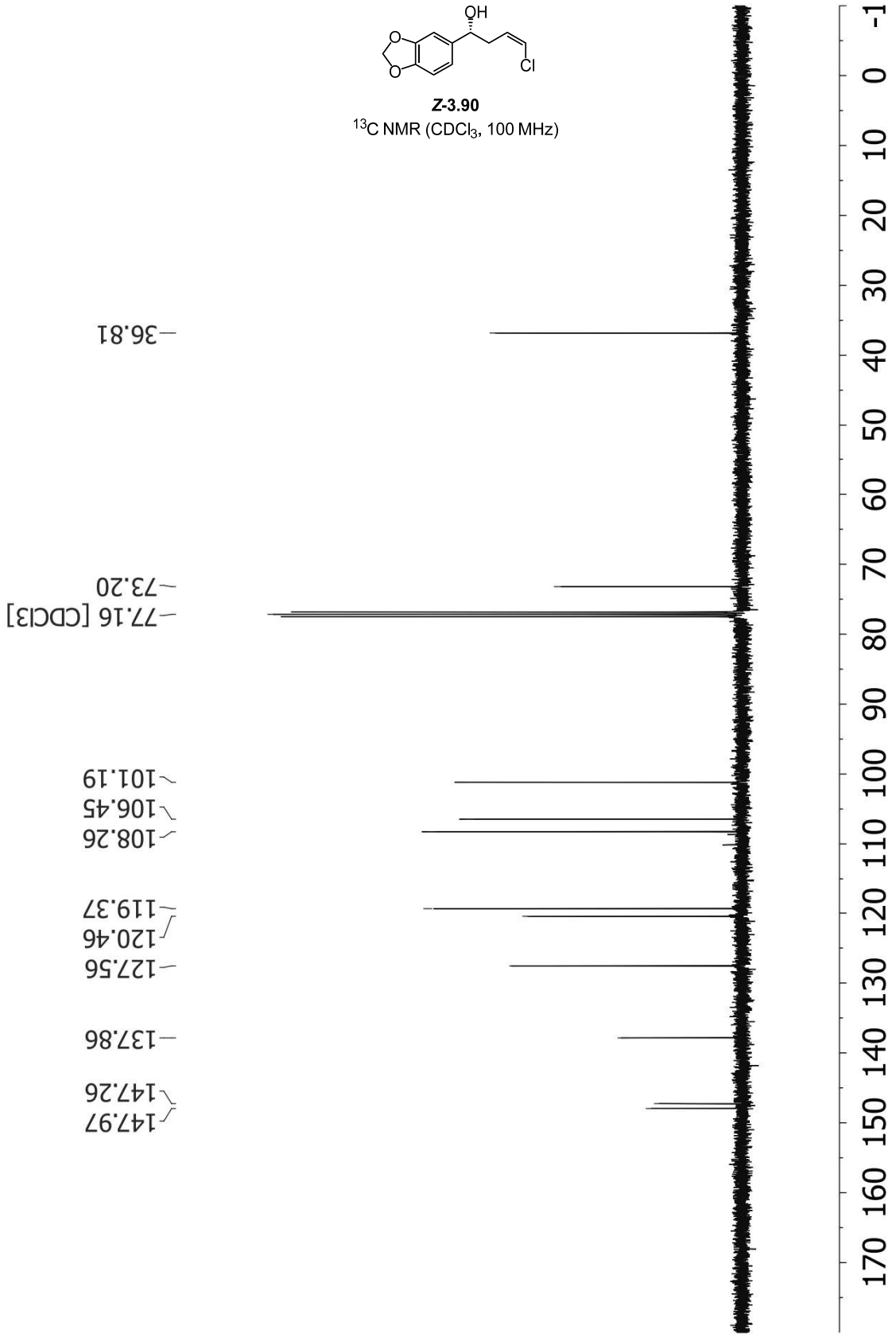
OH
O
O
Cl
Z-3.90
13C NMR (CDCl3, 100 MHz)
36.81
73.20
77.16 [CDCl3]
101.19
106.45
108.26
119.37
120.46
127.56
137.86
147.26
147.97
-1
0
10
20
30
40
50
60
70
80
90
100
110
120
130
140
150
160
170

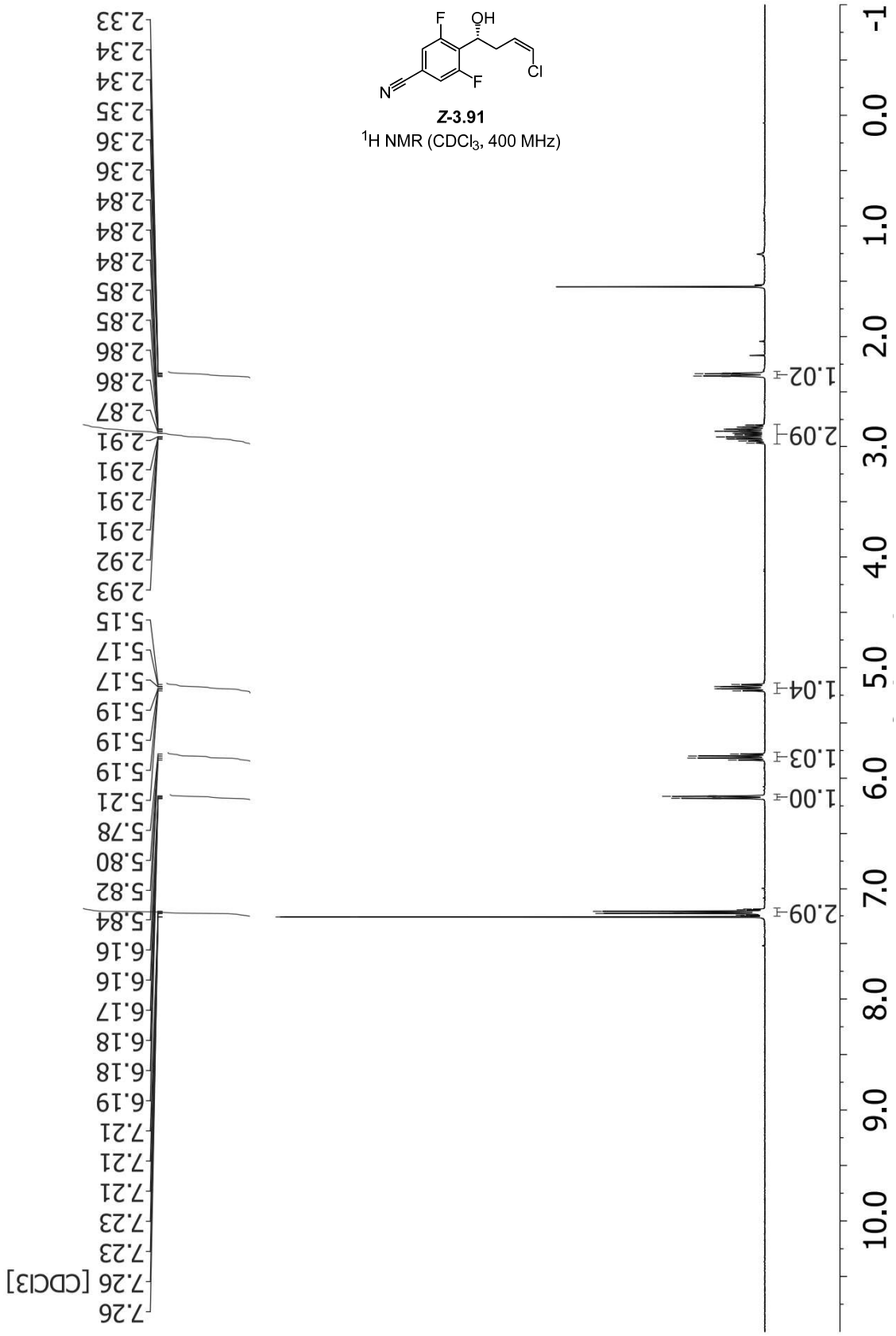
F
OH
Cl
F
N
Z-3.91
1H NMR (CDCl3, 400 MHz)
2.33
2.34
2.34
2.35
2.36
2.36
2.84
2.84
2.84
2.85
2.85
2.86
2.86
2.87
2.91
2.91
2.91
2.91
2.92
2.93
5.15
5.17
5.17
5.19
5.19
5.19
5.21
5.78
5.80
5.82
5.84
6.16
6.16
6.17
6.18
6.18
6.19
7.21
7.21
7.21
7.23
7.23
7.26 [CDCl3]
7.26
1.02
2.09
1.04
1.03
1.00
2.09
-1
0.0
1.0
2.0
3.0
4.0
5.0
6.0
7.0
8.0
9.0
10.0

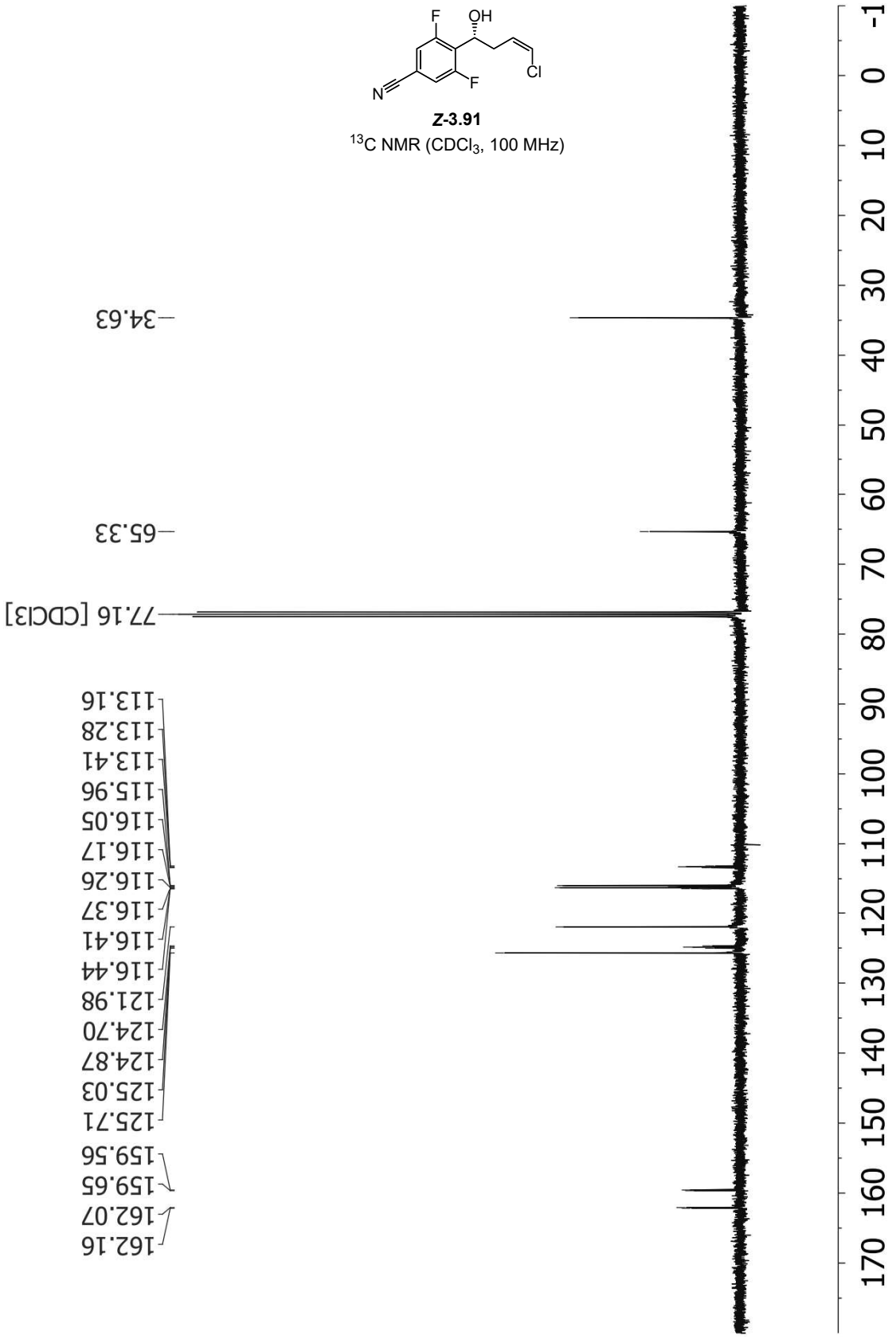
F
OH
Cl
F
N
Z-3.91
13C NMR (CDCl3, 100 MHz)
34.63
65.33
77.16 [CDCl3]
113.16
113.28
113.41
115.96
116.05
116.17
116.26
116.37
116.41
116.44
121.98
124.70
124.87
125.03
125.71
159.56
159.65
162.07
162.16

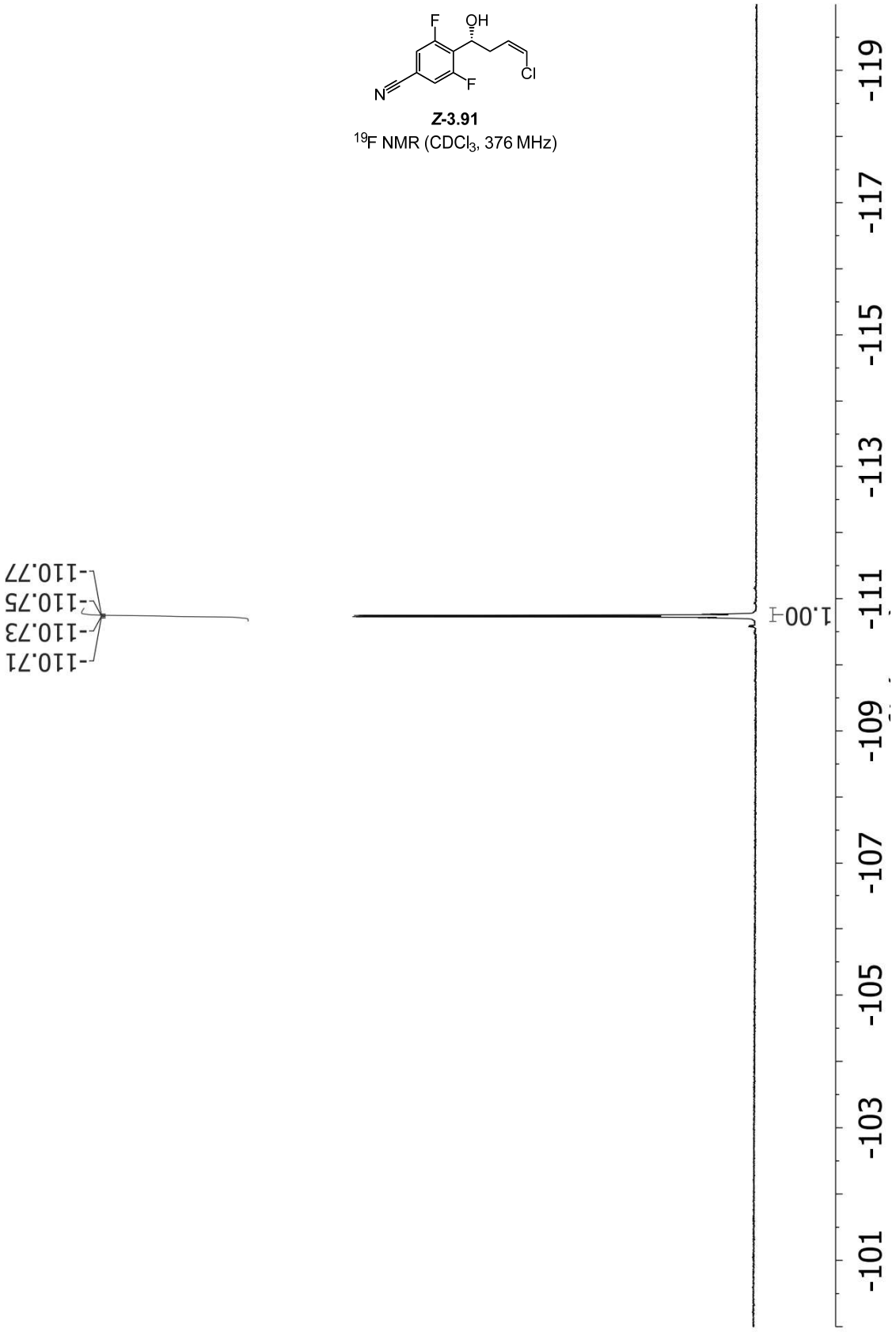

***Z*-3.91**

^{19}F NMR ($CDCl_3$, 376 MHz)

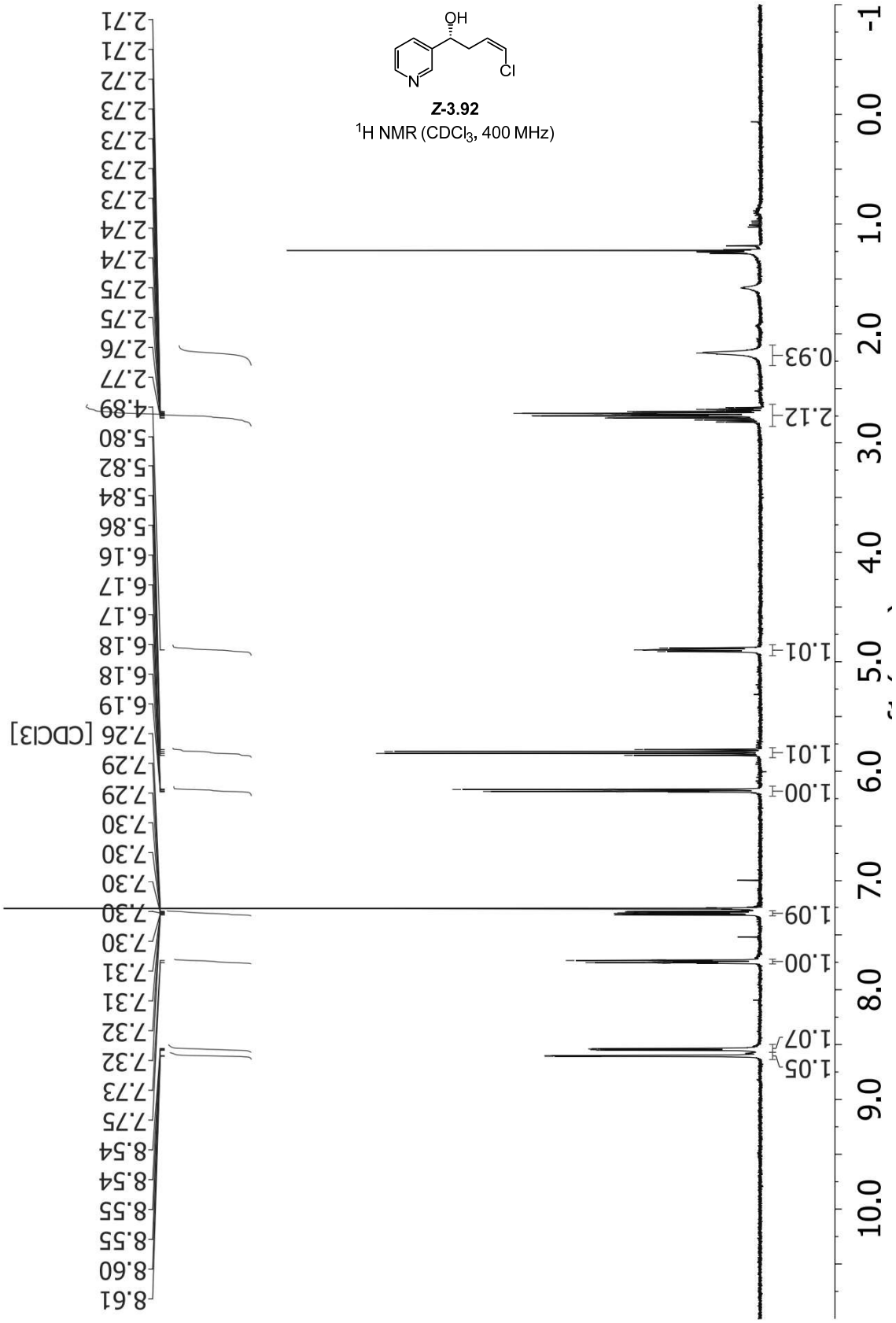
OH
N
Cl
Z-3.92
1H NMR (CDCl3, 400 MHz)
[CDCl3]

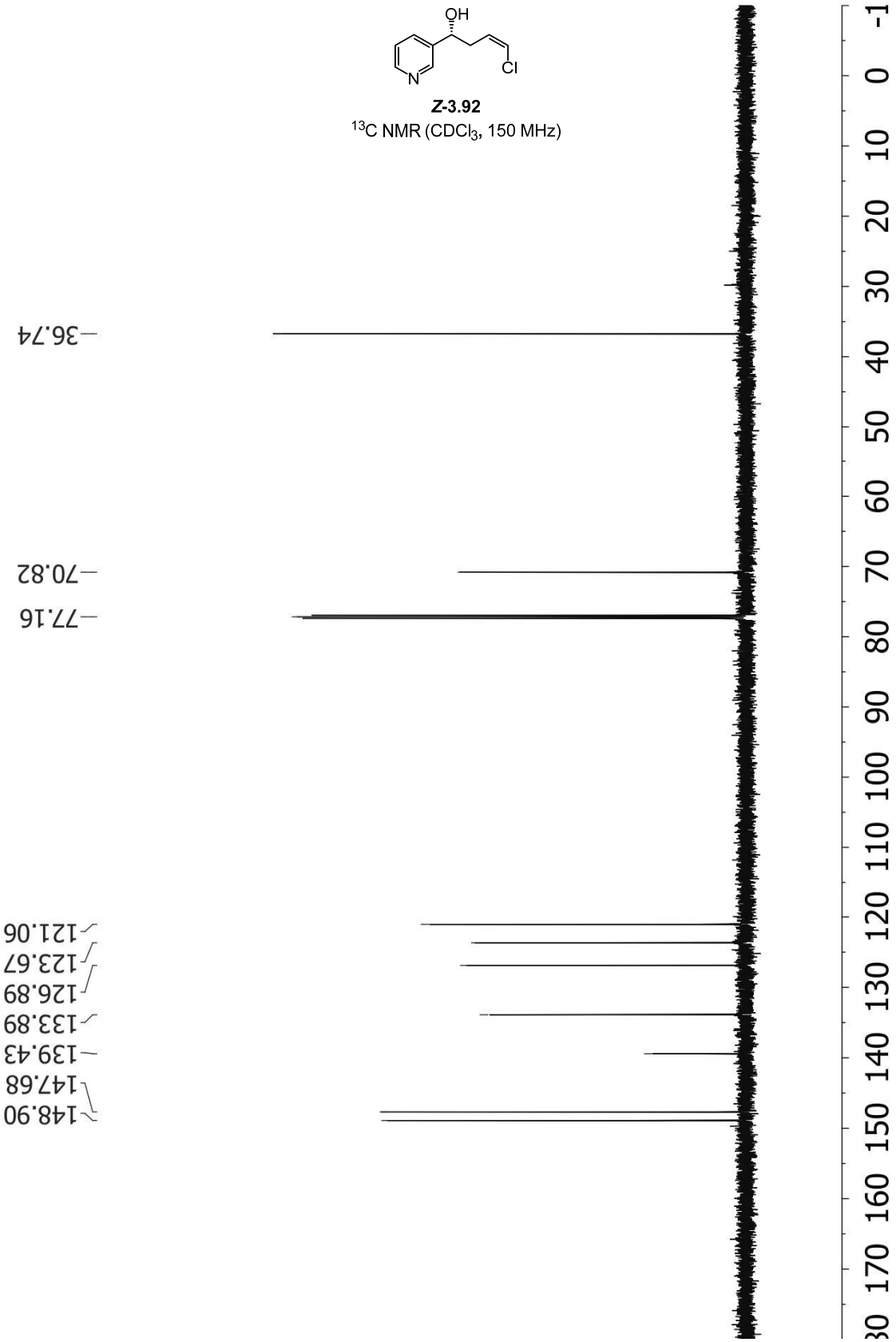
OH
N
Cl
Z-3.92
13C NMR (CDCl3, 150 MHz)
36.74
70.82
77.16
121.06
123.67
126.89
133.89
139.43
147.68
148.90

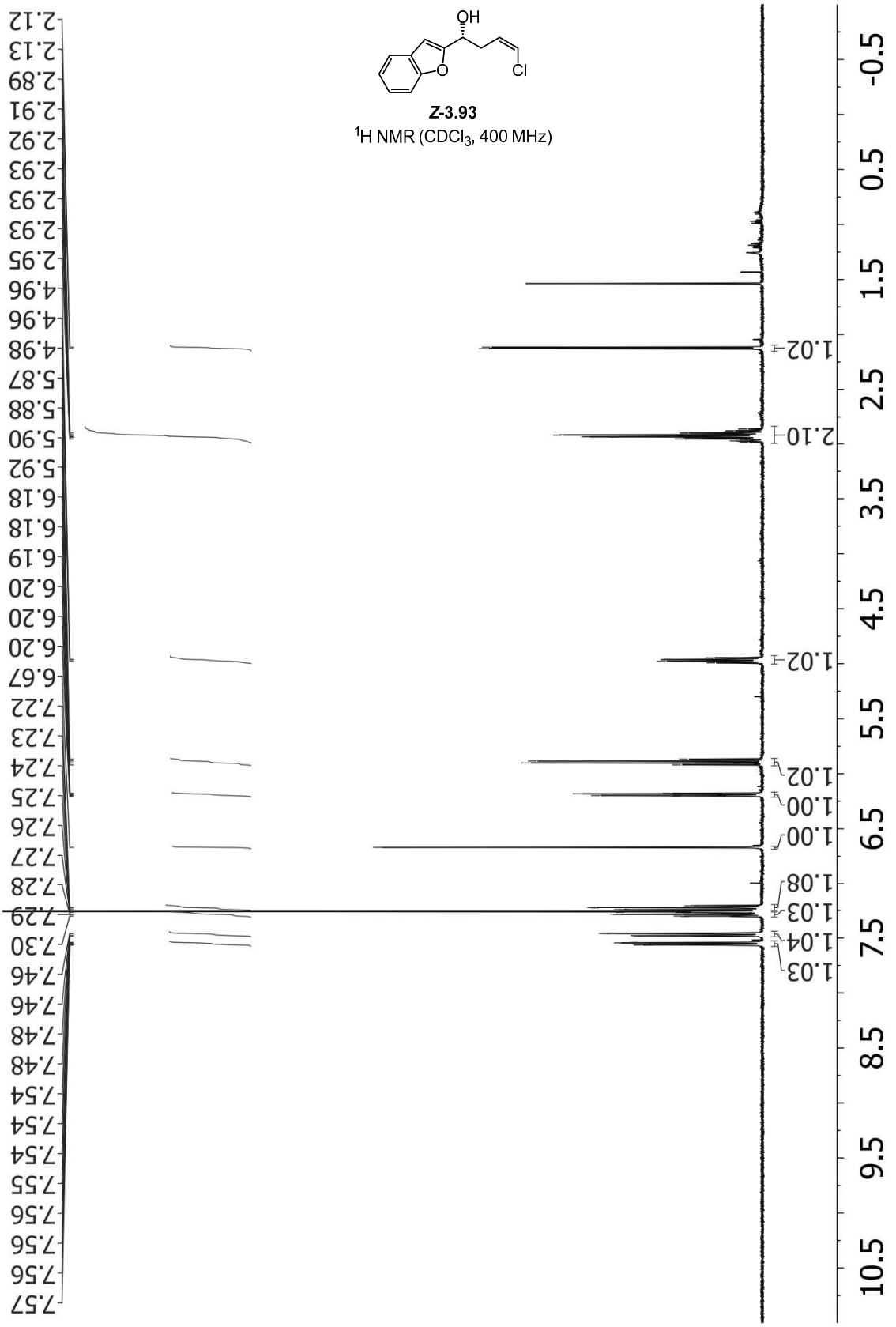
OH
O
Cl
Z-3.93
1H NMR (CDCl3, 400 MHz)
2.12
2.13
2.89
2.91
2.92
2.93
2.93
2.93
2.95
4.96
4.96
4.98
5.87
5.88
5.90
5.92
6.18
6.18
6.19
6.20
6.20
6.20
6.67
7.22
7.23
7.24
7.25
7.26
7.27
7.28
7.29
7.30
7.46
7.46
7.48
7.48
7.54
7.54
7.54
7.55
7.56
7.56
7.56
7.57
1.02
2.10
1.02
1.02
1.00
1.00
1.08
1.03
1.04
1.03
-0.5
0.5
1.5
2.5
3.5
4.5
5.5
6.5
7.5
8.5
9.5
10.5

OH
O
Cl
Z-3.93
13C NMR (CDCl3, 150 MHz)
33.47
67.19
77.16 [CDCl3]
103.09
111.40
121.08
121.28
123.02
124.49
126.64
128.12
154.94
158.33
170 160 150 140 130 120 110 100 90 80 70 60 50 40 30 20 10 0 -1

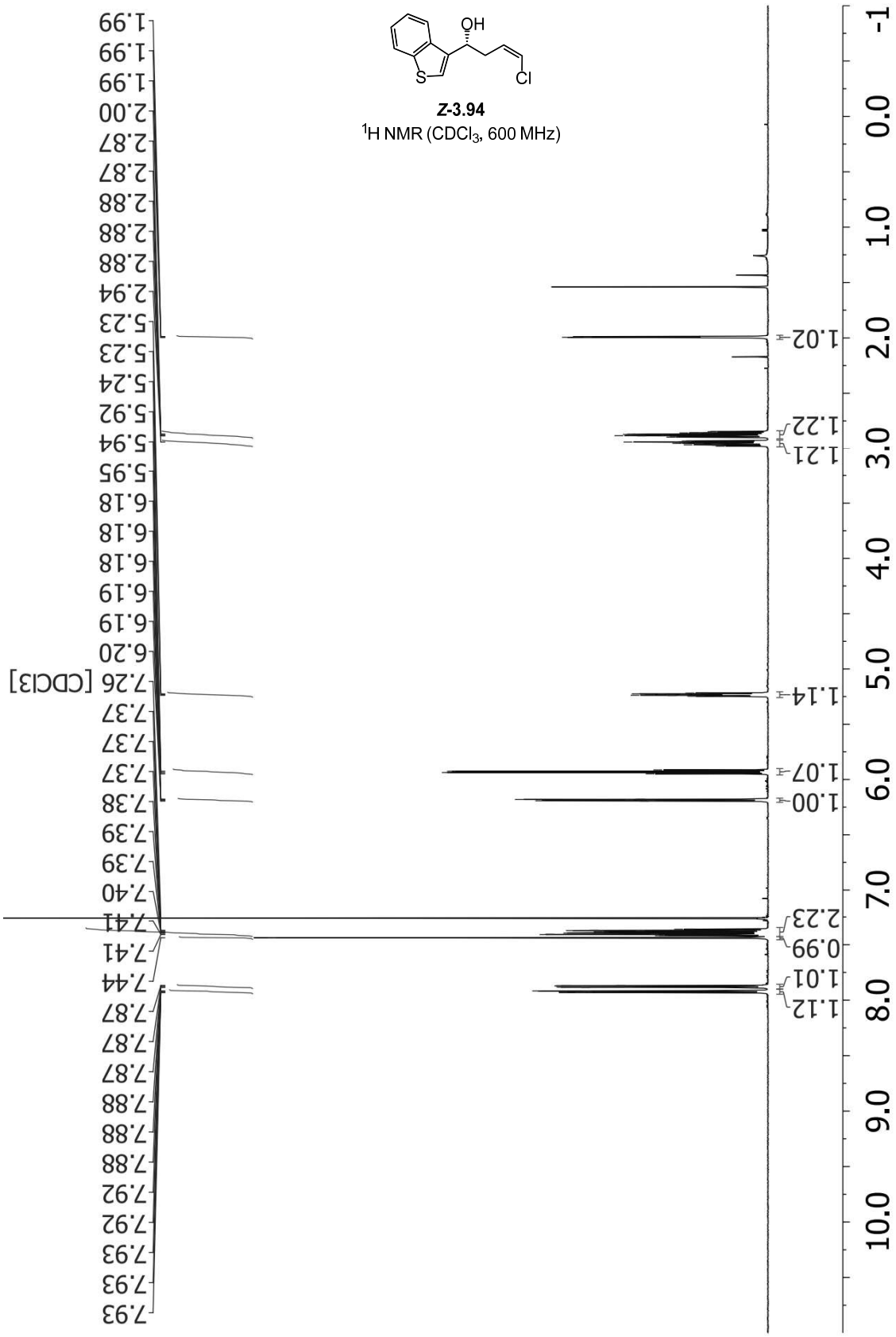
OH
S
Cl
Z-3.94
1H NMR (CDCl3, 600 MHz)
7.26 [CDCl3]
1.14
1.07
1.00
2.23
0.99
1.01
1.12
1.02
1.22
1.21

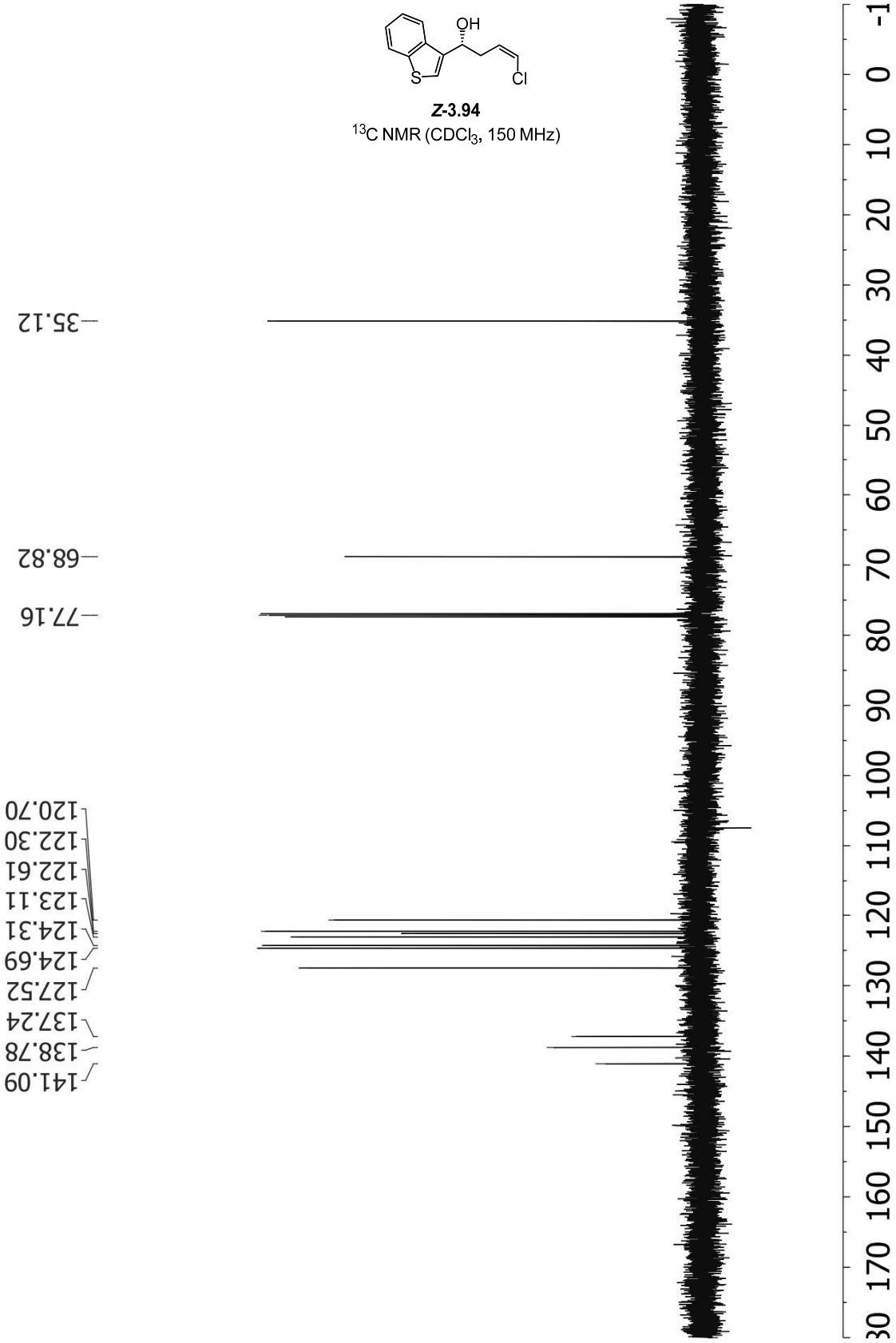
OH
S
Cl
Z-3.94
13C NMR (CDCl3, 150 MHz)
35.12
68.82
77.16
120.70
122.30
122.61
123.11
124.31
124.69
127.52
137.24
138.78
141.09
-1
0
10
20
30
40
50
60
70
80
90
100
110
120
130
140
150
160
170
180

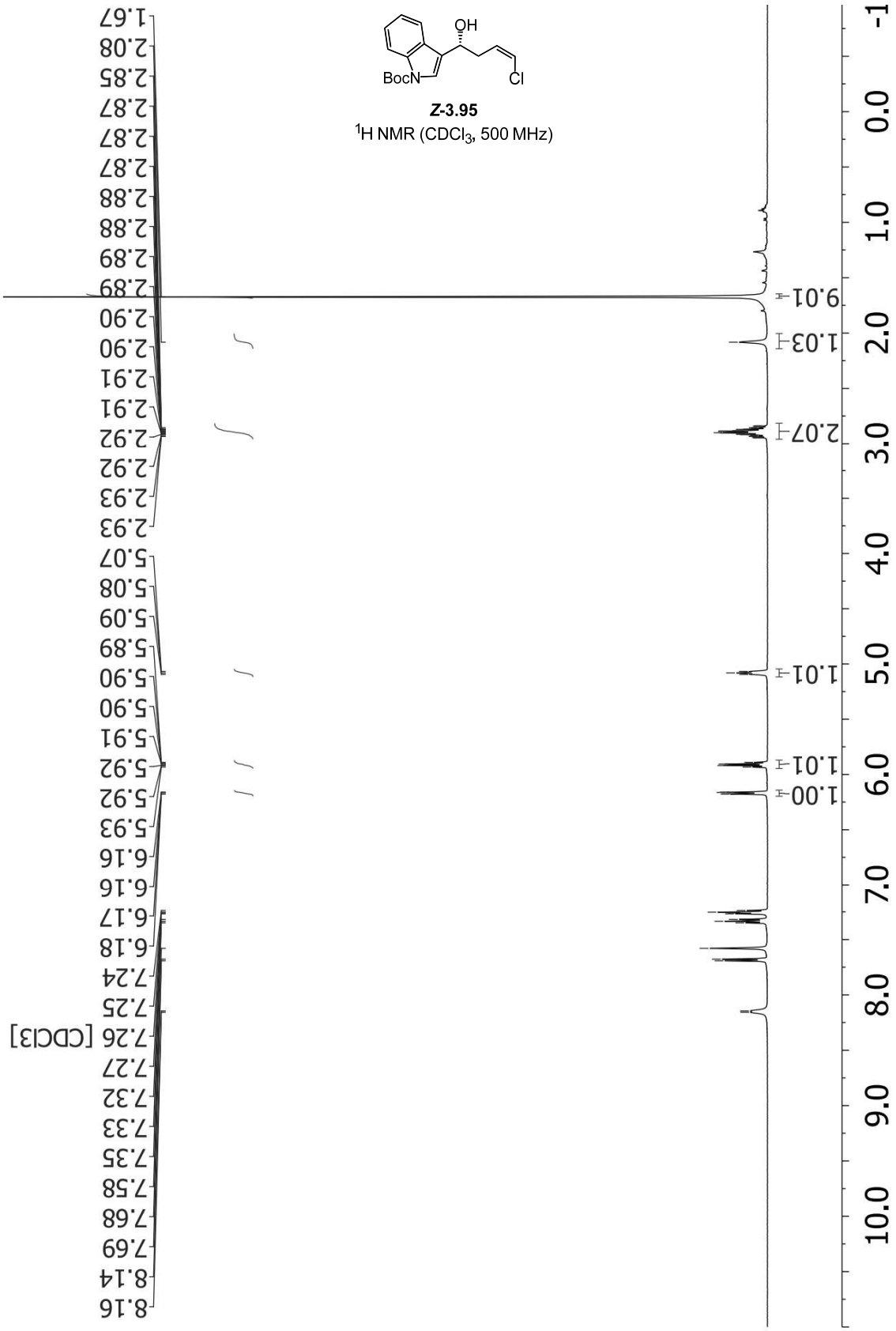
OH
BocN
Cl
Z-3.95
1H NMR (CDCl3, 500 MHz)
9.01
1.03
2.07
1.01
1.01
1.00
[CDCl3]

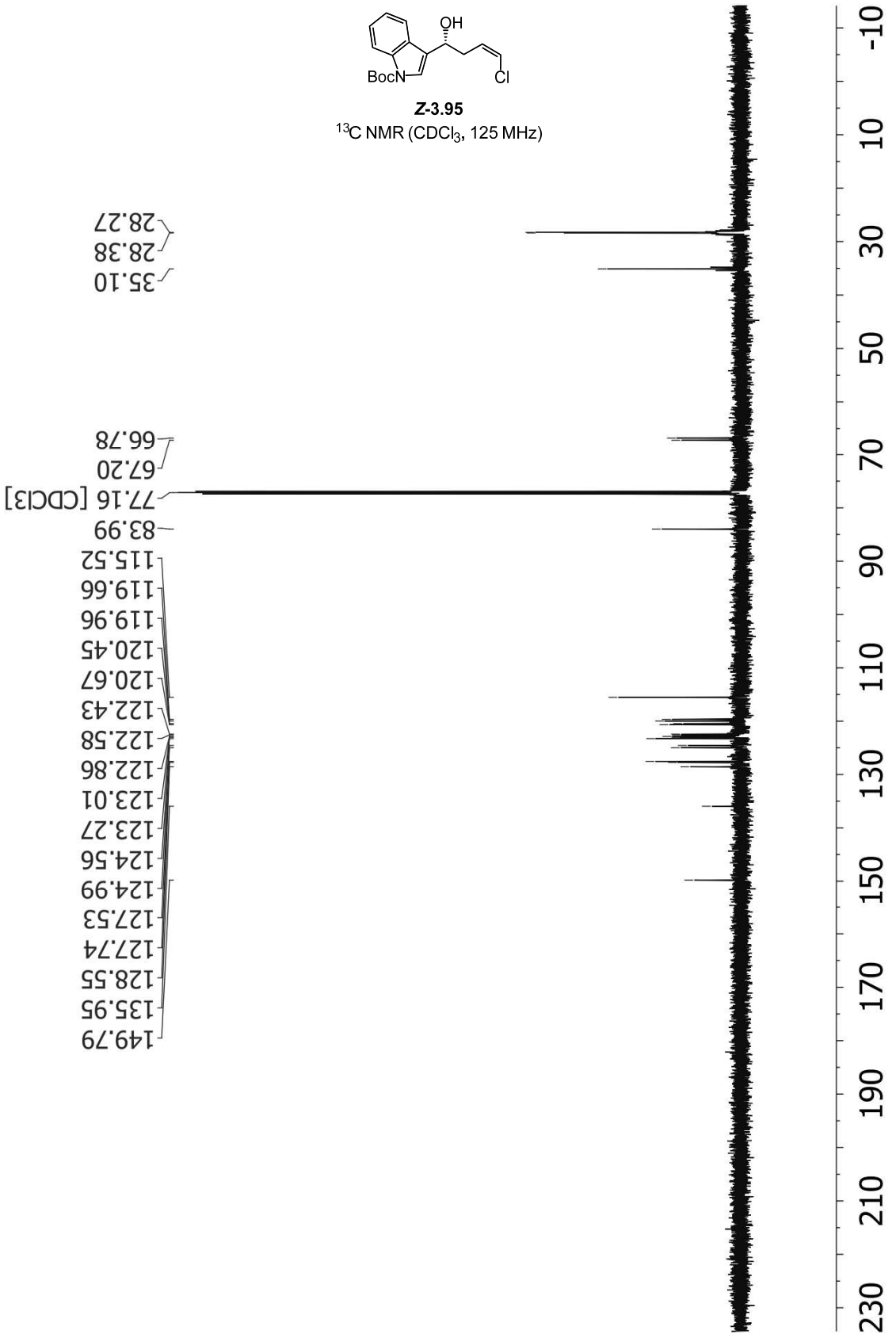
OH
BocN
Cl
Z-3.95
13C NMR (CDCl3, 125 MHz)
28.27
28.38
35.10
66.78
67.20
77.16 [CDCl3]
83.99
115.52
119.66
119.96
120.45
120.67
122.43
122.58
122.86
123.01
123.27
124.56
124.99
127.53
127.74
128.55
135.95
149.79
-10
10
30
50
70
90
110
130
150
170
190
210
230

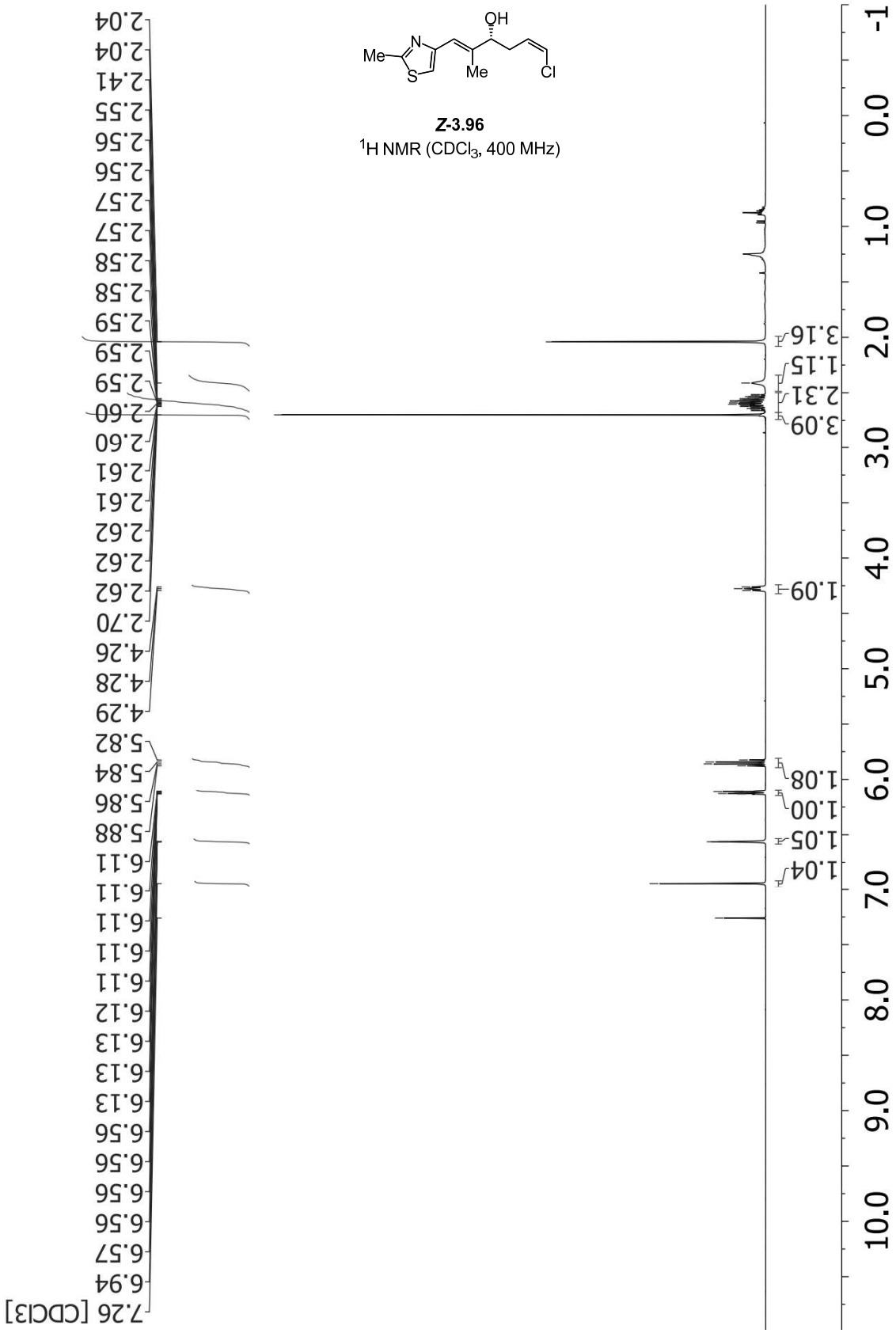
OH
N
Me
S
Me
Cl
Z-3.96
1H NMR (CDCl3, 400 MHz)
7.26 [CDCl3]
3.16
1.15
2.31
3.09
1.09
1.08
1.00
1.05
1.04

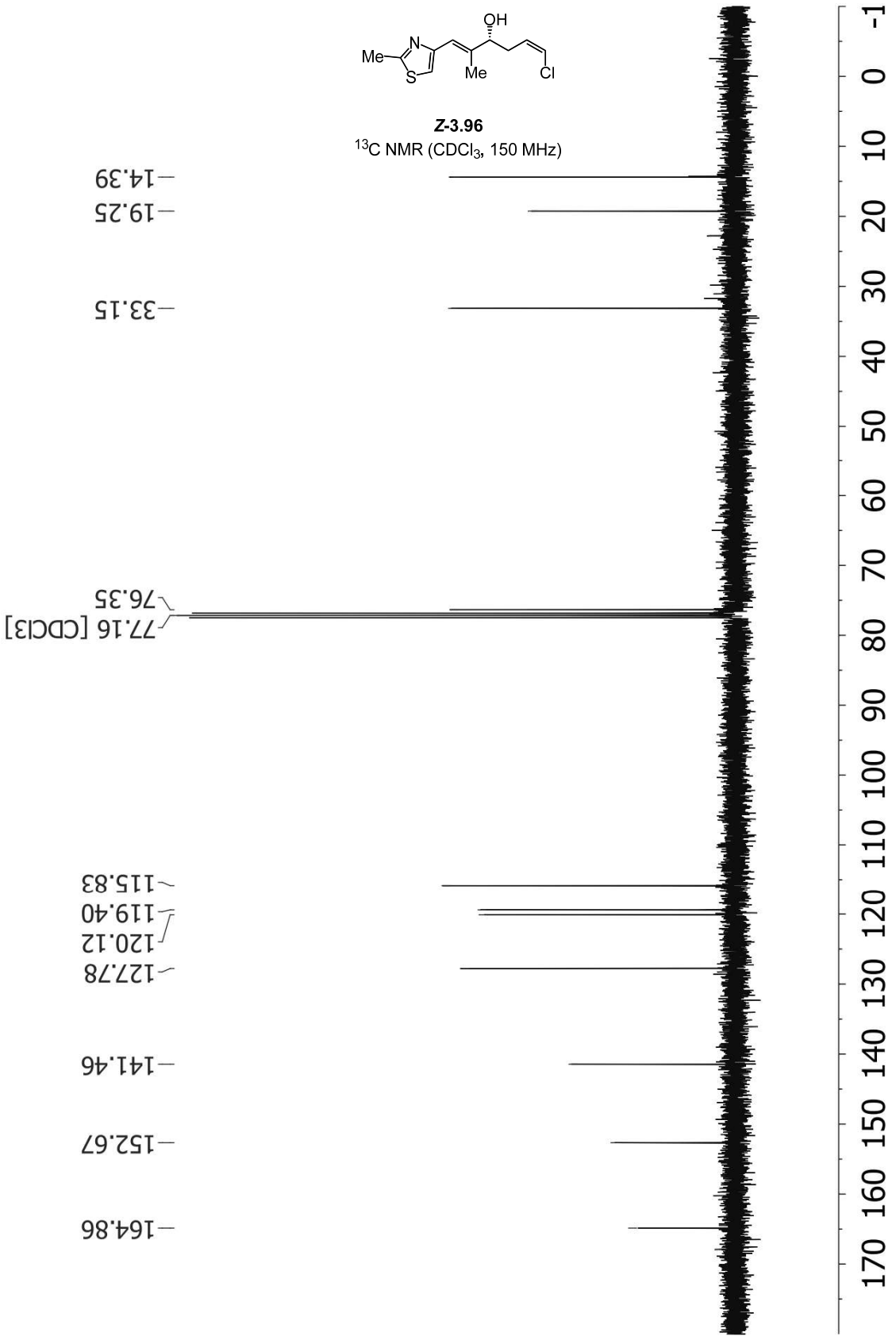
OH
N
Me
S
Me
Cl
Z-3.96
13C NMR (CDCl3, 150 MHz)
14.39
19.25
33.15
76.35
77.16 [CDCl3]
115.83
119.40
120.12
127.78
141.46
152.67
164.86
-1
0
10
20
30
40
50
60
70
80
90
100
110
120
130
140
150
160
170

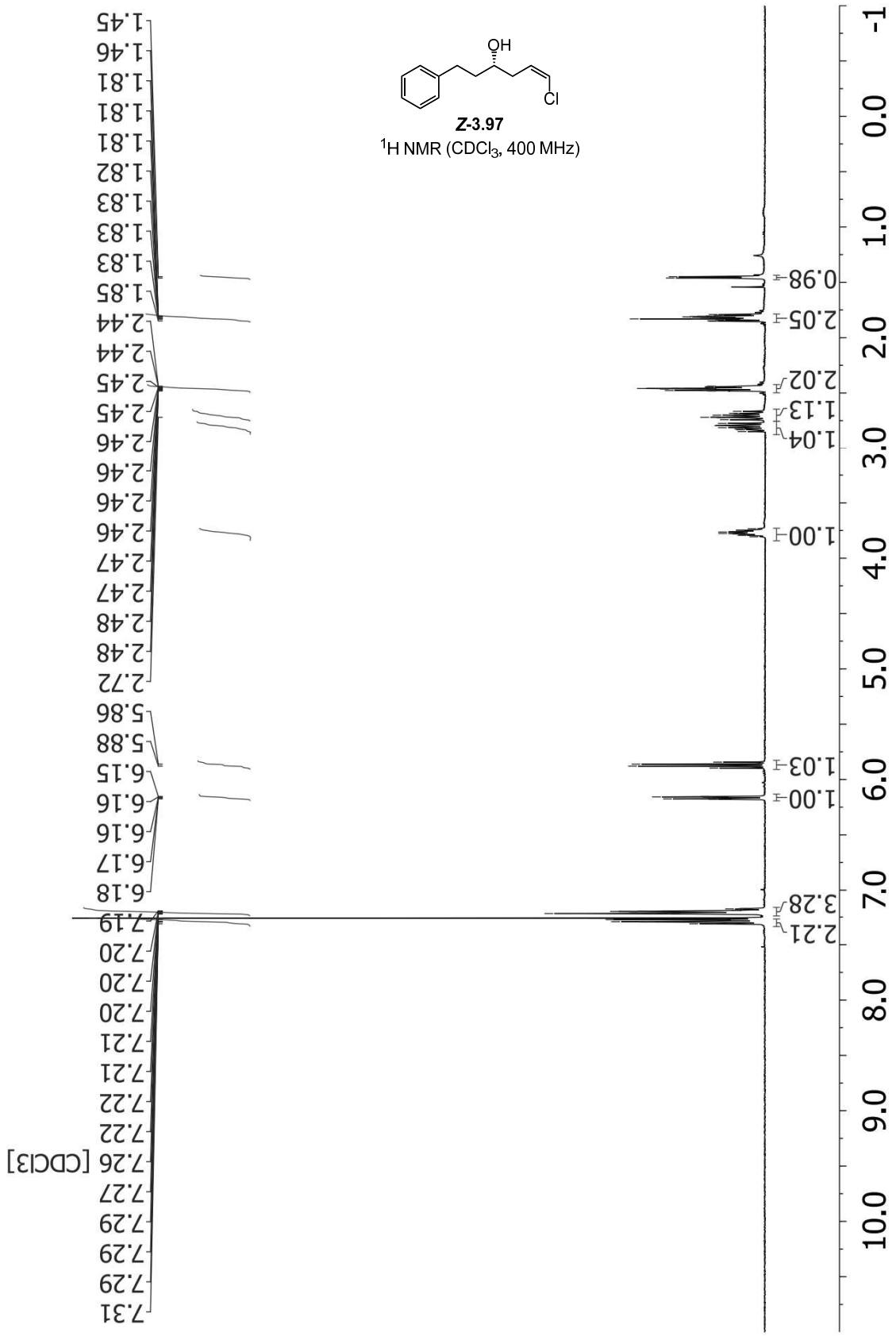
OH
Cl
Z-3.97
1H NMR (CDCl3, 400 MHz)
[CDCl3]

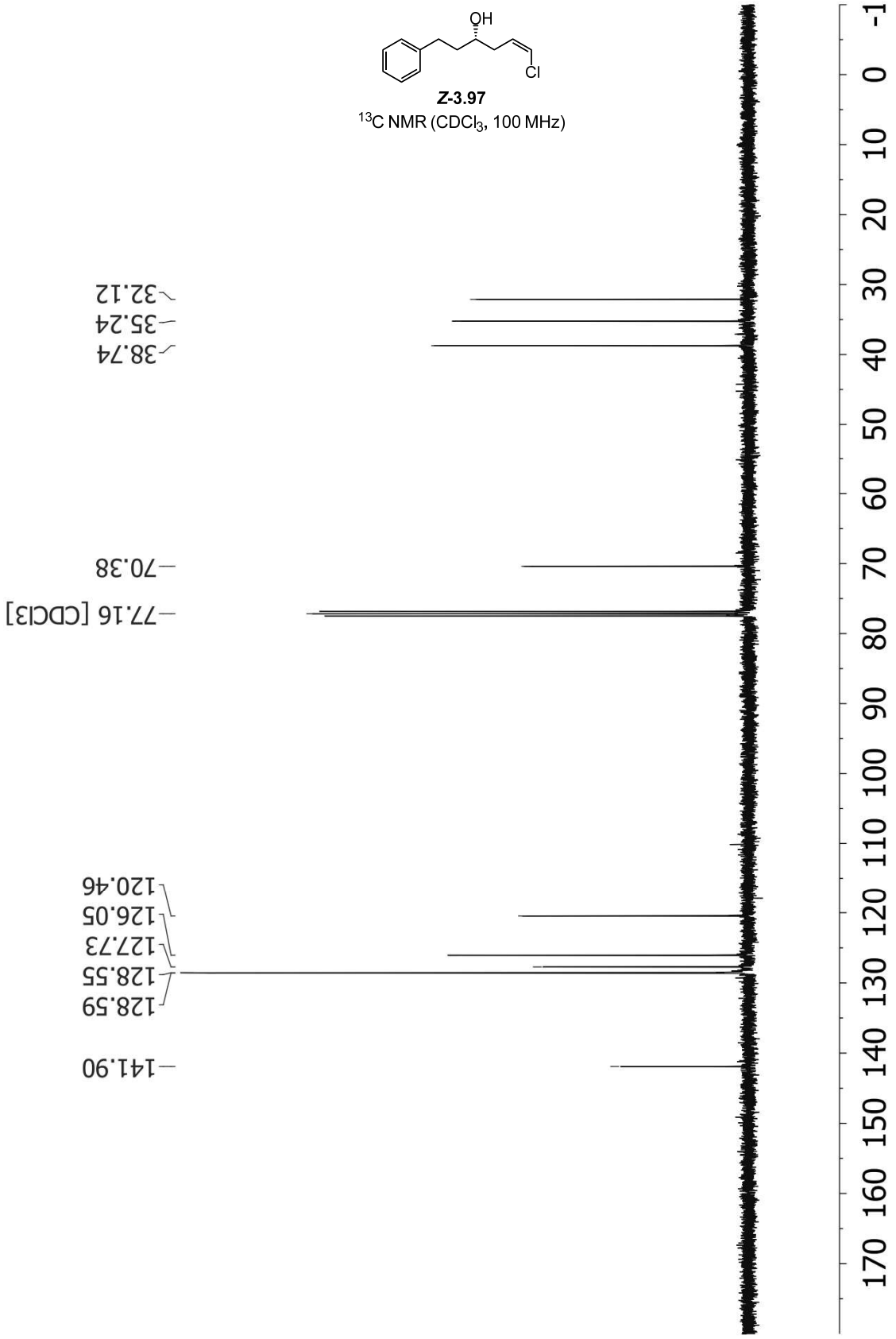
OH
Cl
Z-3.97
13C NMR (CDCl3, 100 MHz)
32.12
35.24
38.74
70.38
77.16 [CDCl3]
120.46
126.05
127.73
128.55
128.59
141.90
-1 0 10 20 30 40 50 60 70 80 90 100 110 120 130 140 150 160 170

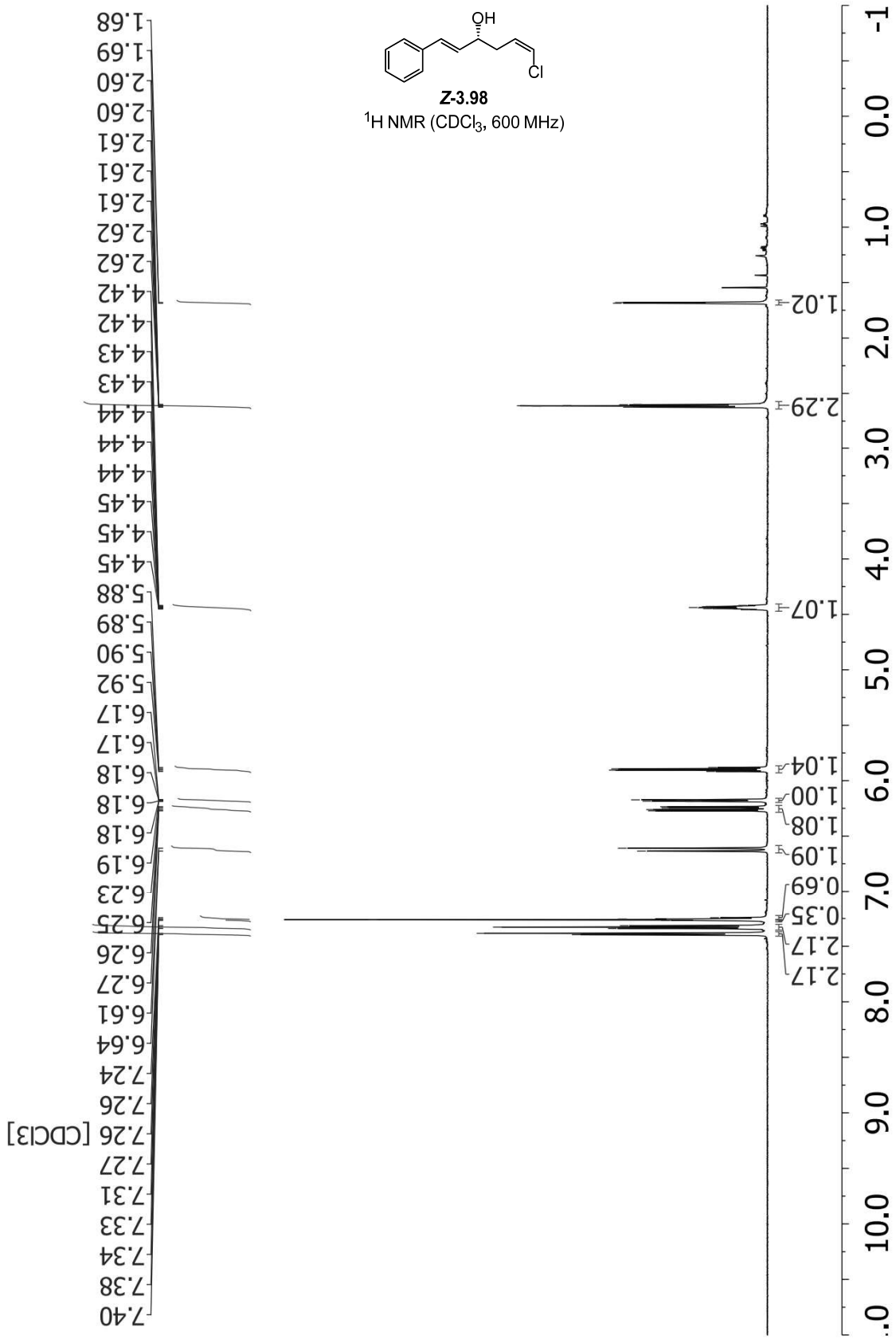
OH
Cl
Z-3.98
1H NMR (CDCl3, 600 MHz)
7.40
7.38
7.34
7.33
7.31
7.27
7.26 [CDCl3]
7.26
7.24
6.64
6.61
6.27
6.26
6.25
6.23
6.19
6.18
6.18
6.18
6.17
6.17
5.92
5.90
5.89
5.88
4.45
4.45
4.44
4.44
4.44
4.43
4.43
4.42
4.42
2.62
2.62
2.61
2.61
2.61
2.60
2.60
1.69
1.68
1.02
2.29
1.07
1.04
1.00
1.08
1.09
0.69
0.35
2.17
2.17
0.0
10.0
9.0
8.0
7.0
6.0
5.0
4.0
3.0
2.0
1.0
0.0
-1

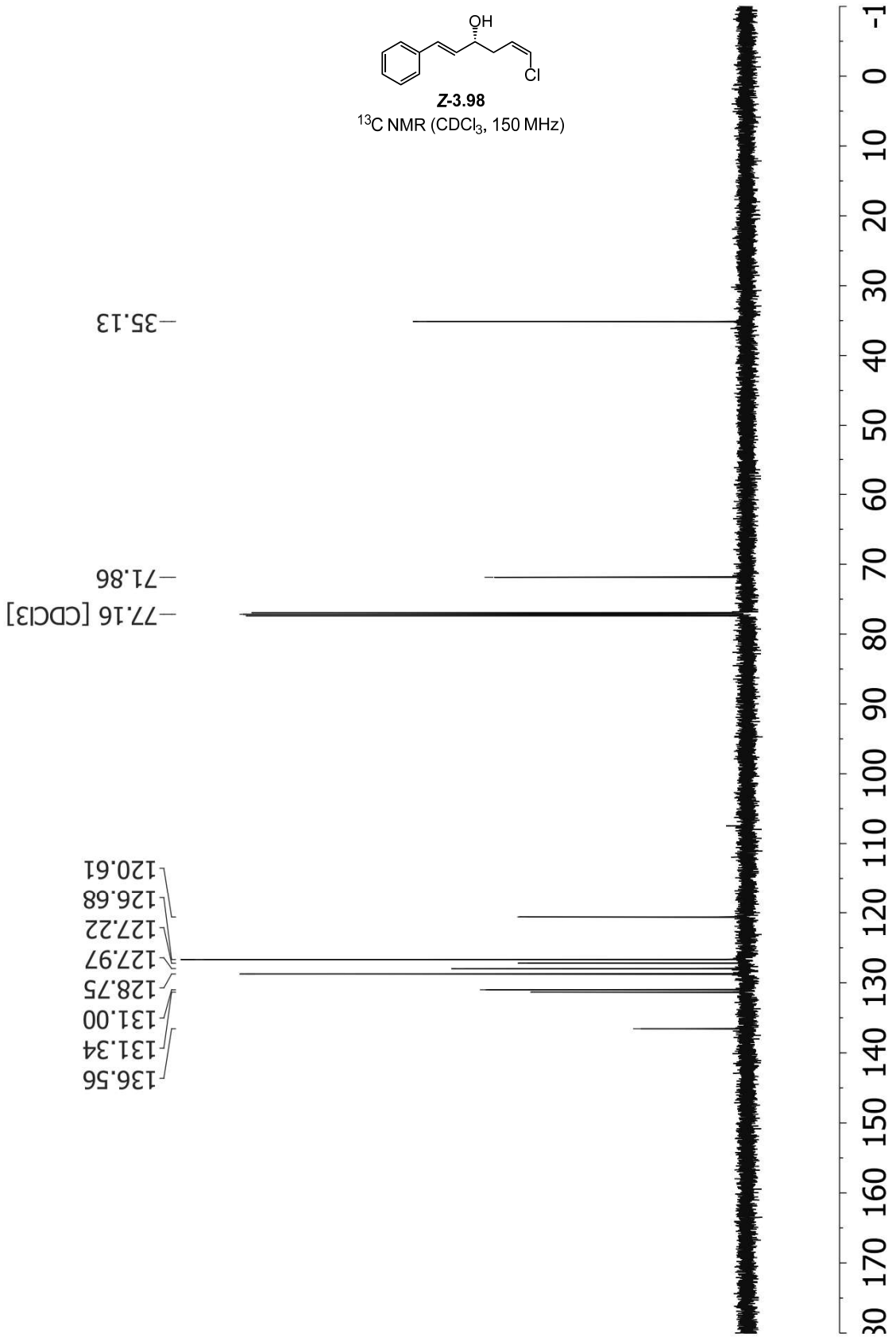
OH
Cl
Z-3.98
13C NMR (CDCl3, 150 MHz)
35.13
71.86
77.16 [CDCl3]
120.61
126.68
127.22
127.97
128.75
131.00
131.34
136.56

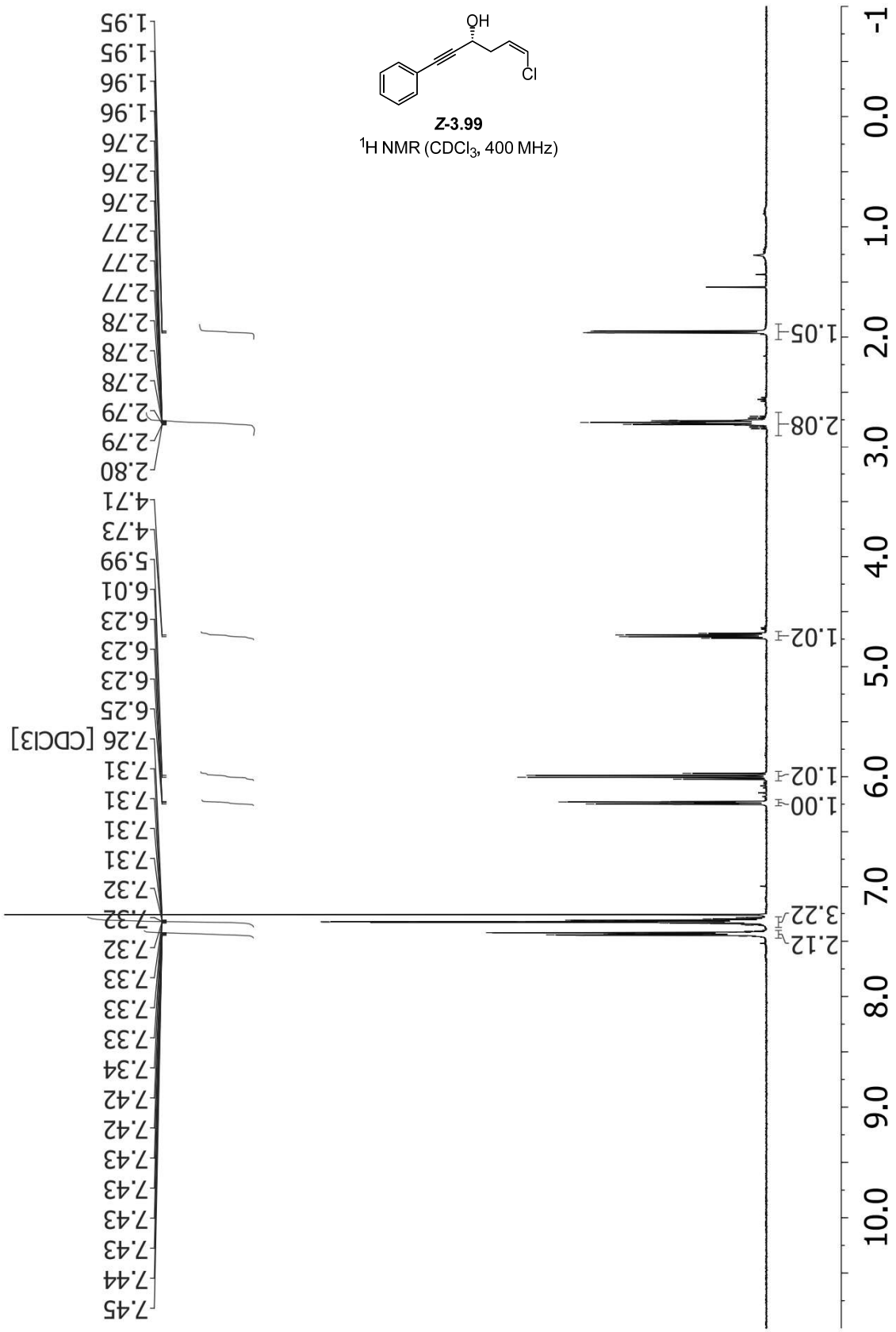
OH
Cl
Z-3.99
1H NMR (CDCl3, 400 MHz)
[CDCl3]
1.95
1.95
1.96
1.96
2.76
2.76
2.76
2.77
2.77
2.77
2.78
2.78
2.78
2.79
2.79
2.80
4.71
4.73
5.99
6.01
6.23
6.23
6.23
6.25
7.26
7.31
7.31
7.31
7.31
7.32
7.32
7.32
7.33
7.33
7.33
7.34
7.42
7.42
7.43
7.43
7.43
7.43
7.44
7.45
1.05
2.08
1.02
1.02
1.00
3.22
2.12
10.0
9.0
8.0
7.0
6.0
5.0
4.0
3.0
2.0
1.0
0.0
-1

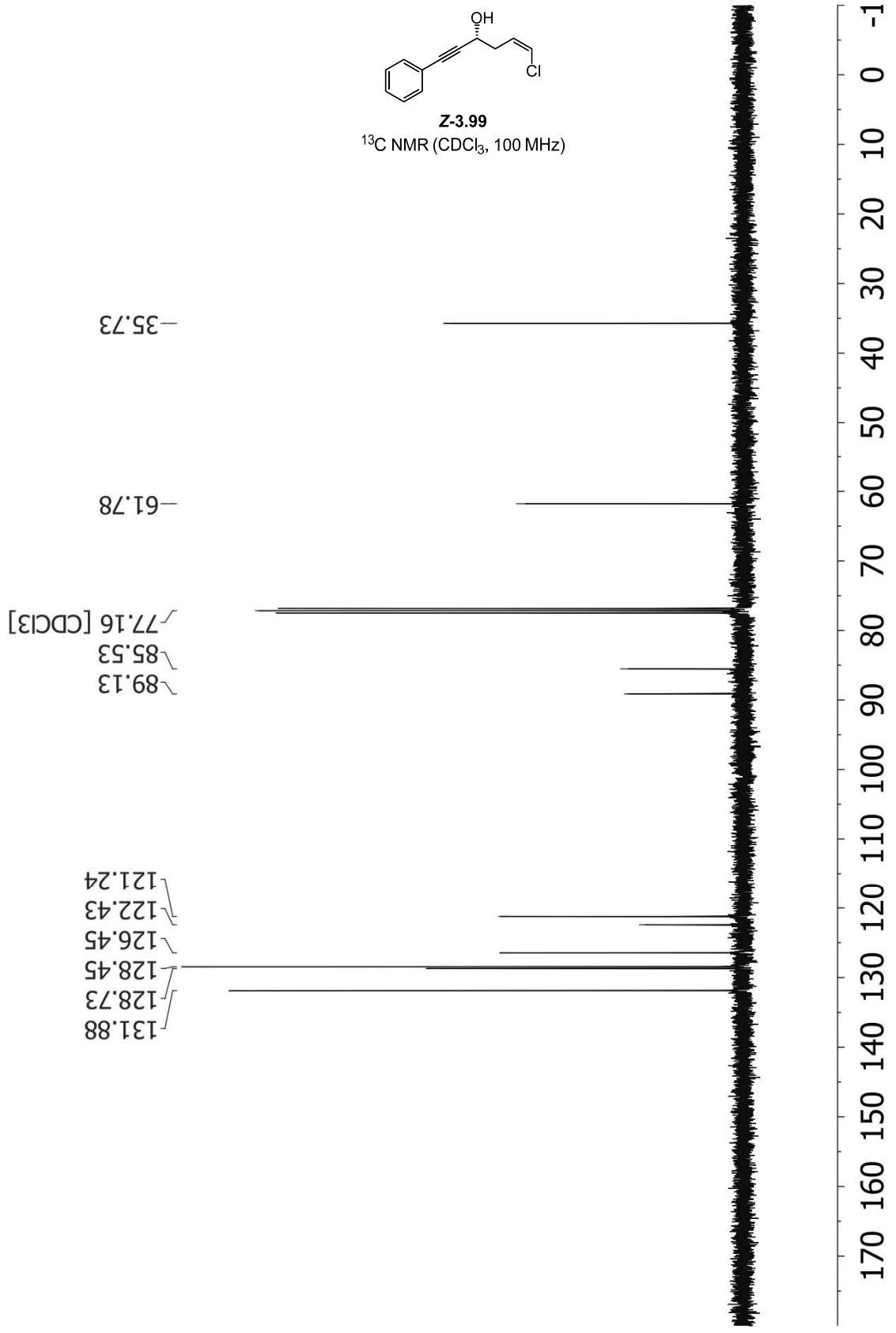
OH
Cl
Z-3.99
13C NMR (CDCl3, 100 MHz)
35.73
61.78
77.16 [CDCl3]
85.53
89.13
131.88
128.73
128.45
126.45
122.43
121.24
-1 0 10 20 30 40 50 60 70 80 90 100 110 120 130 140 150 160 170

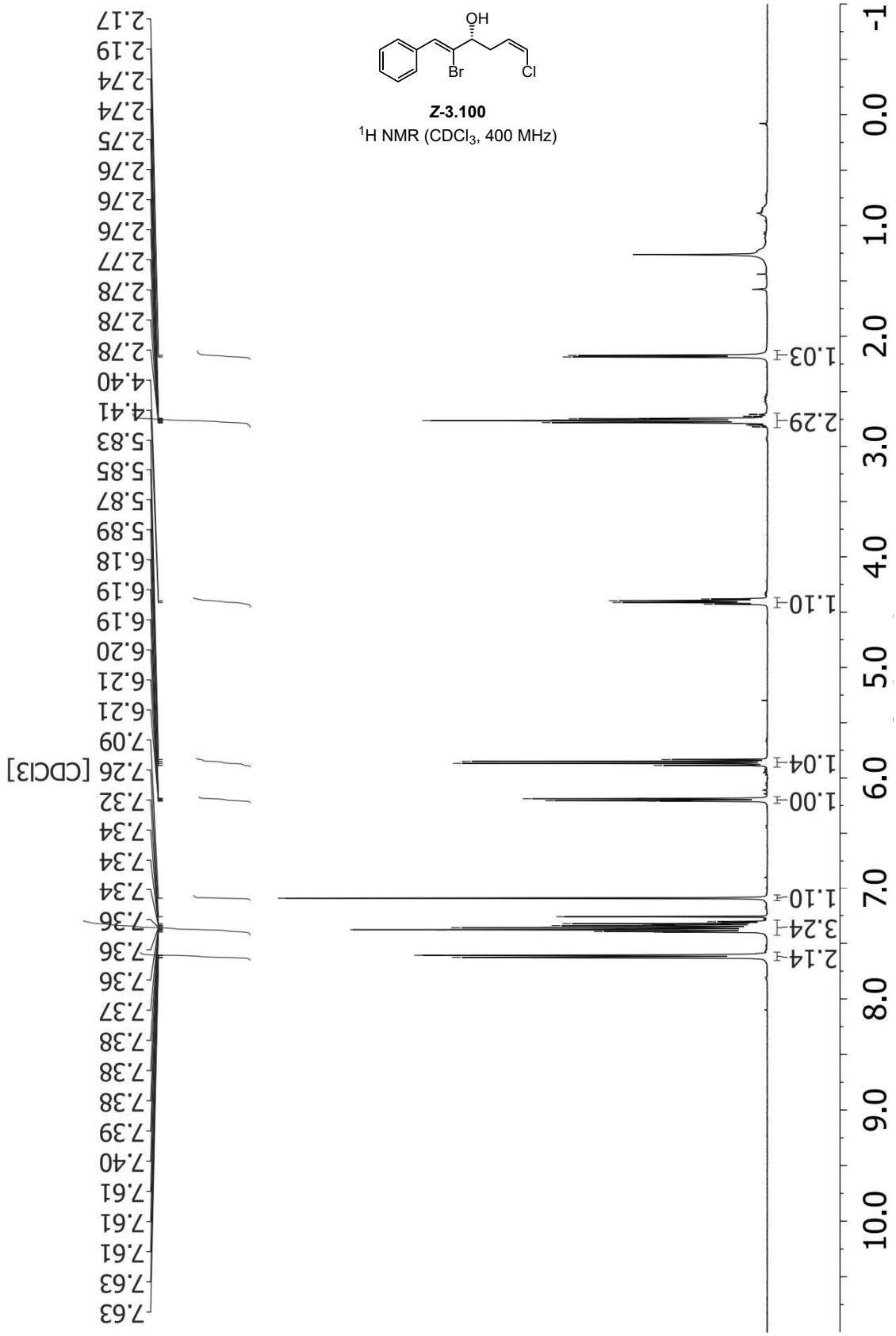
OH
Br
Cl
Z-3.100
1H NMR (CDCl3, 400 MHz)
[CDCl3]
1.03
2.29
1.10
1.04
1.00
1.10
3.24
2.14

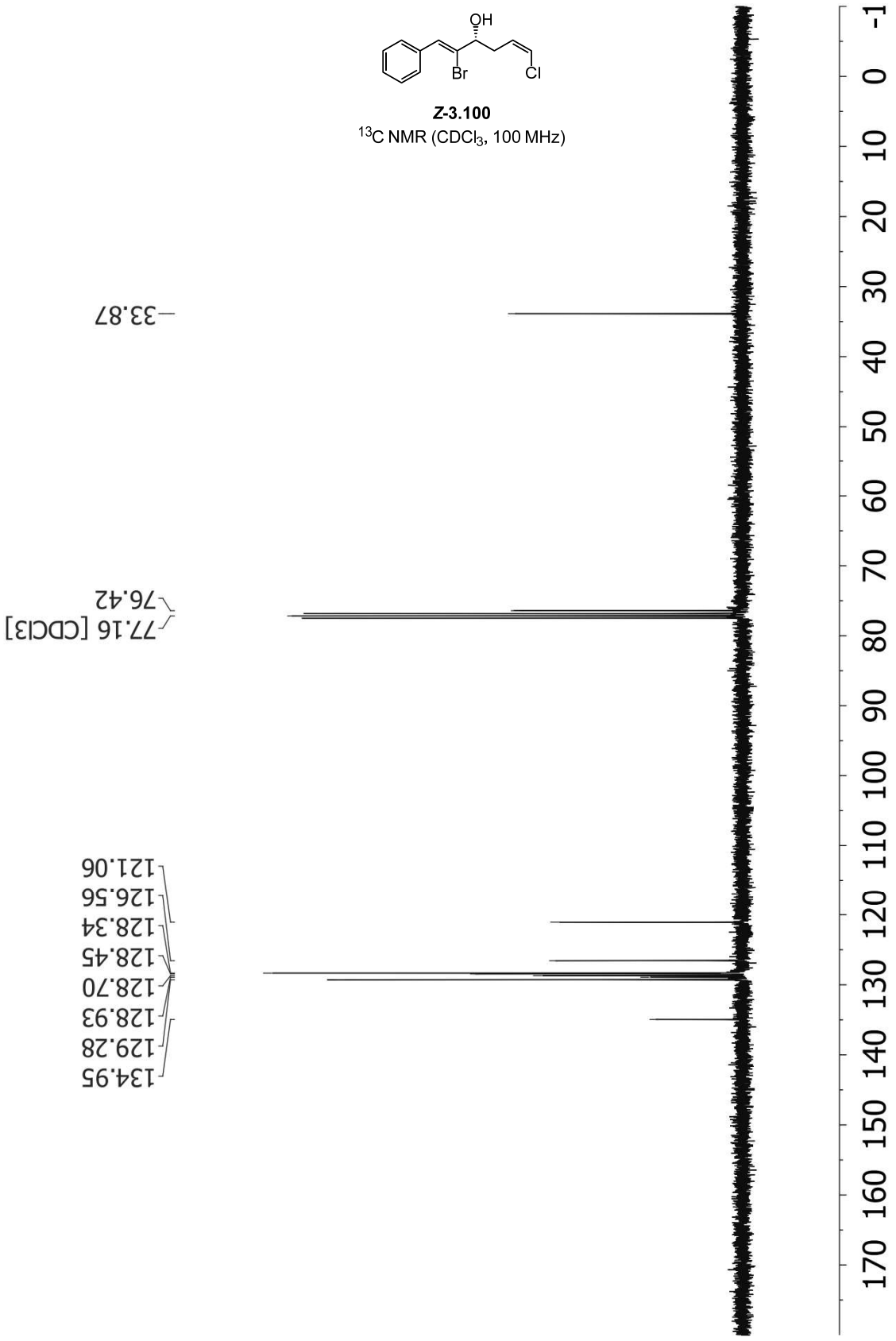
OH
Br
Cl
Z-3.100
13C NMR (CDCl3, 100 MHz)
33.87
77.16 [CDCl3]
76.42
134.95
129.28
128.93
128.70
128.45
128.34
126.56
121.06

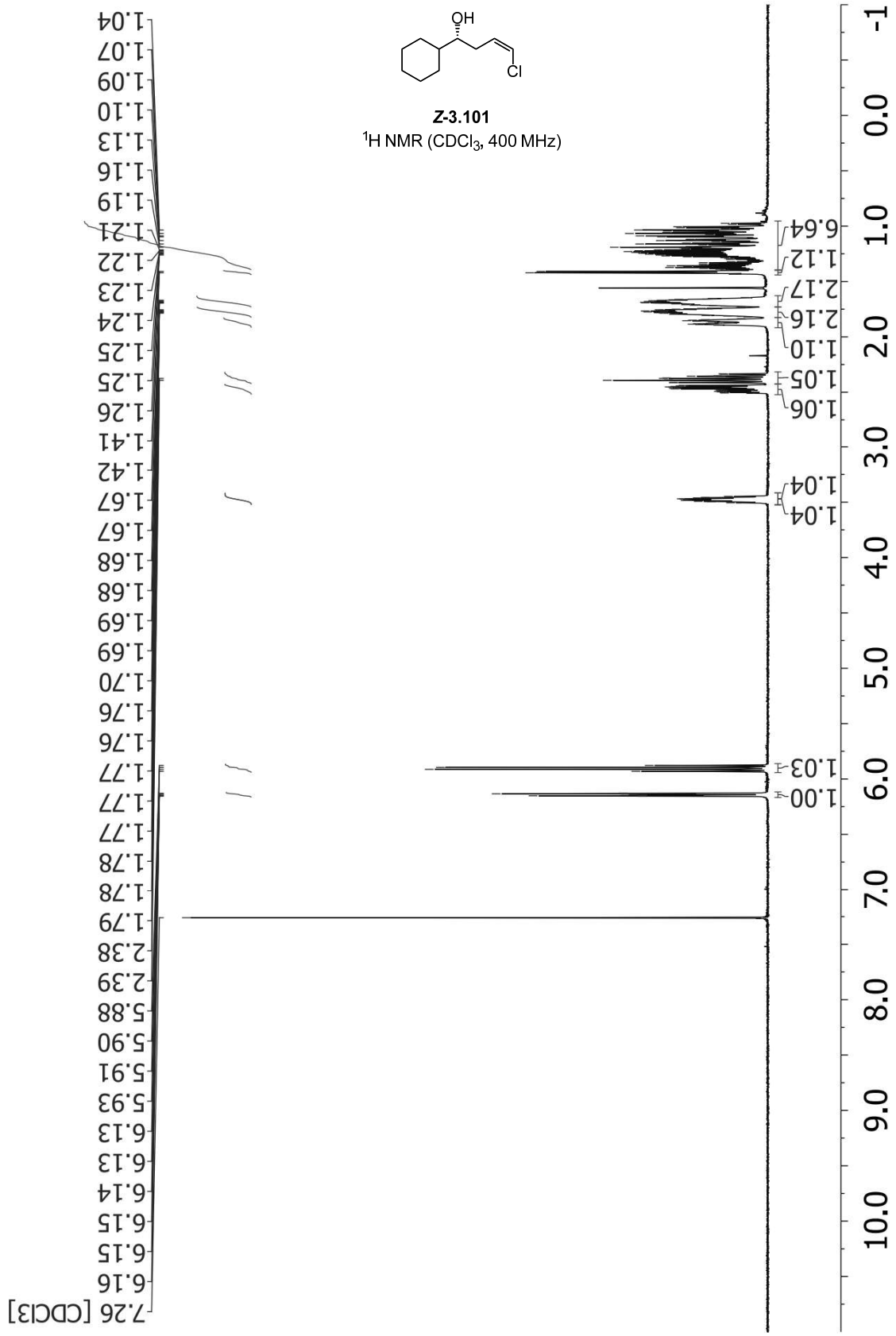
OH
Cl
Z-3.101
1H NMR (CDCl3, 400 MHz)
7.26 [CDCl3]
6.64
1.12
2.17
2.16
1.10
1.05
1.06
1.04
1.04
1.03
1.00

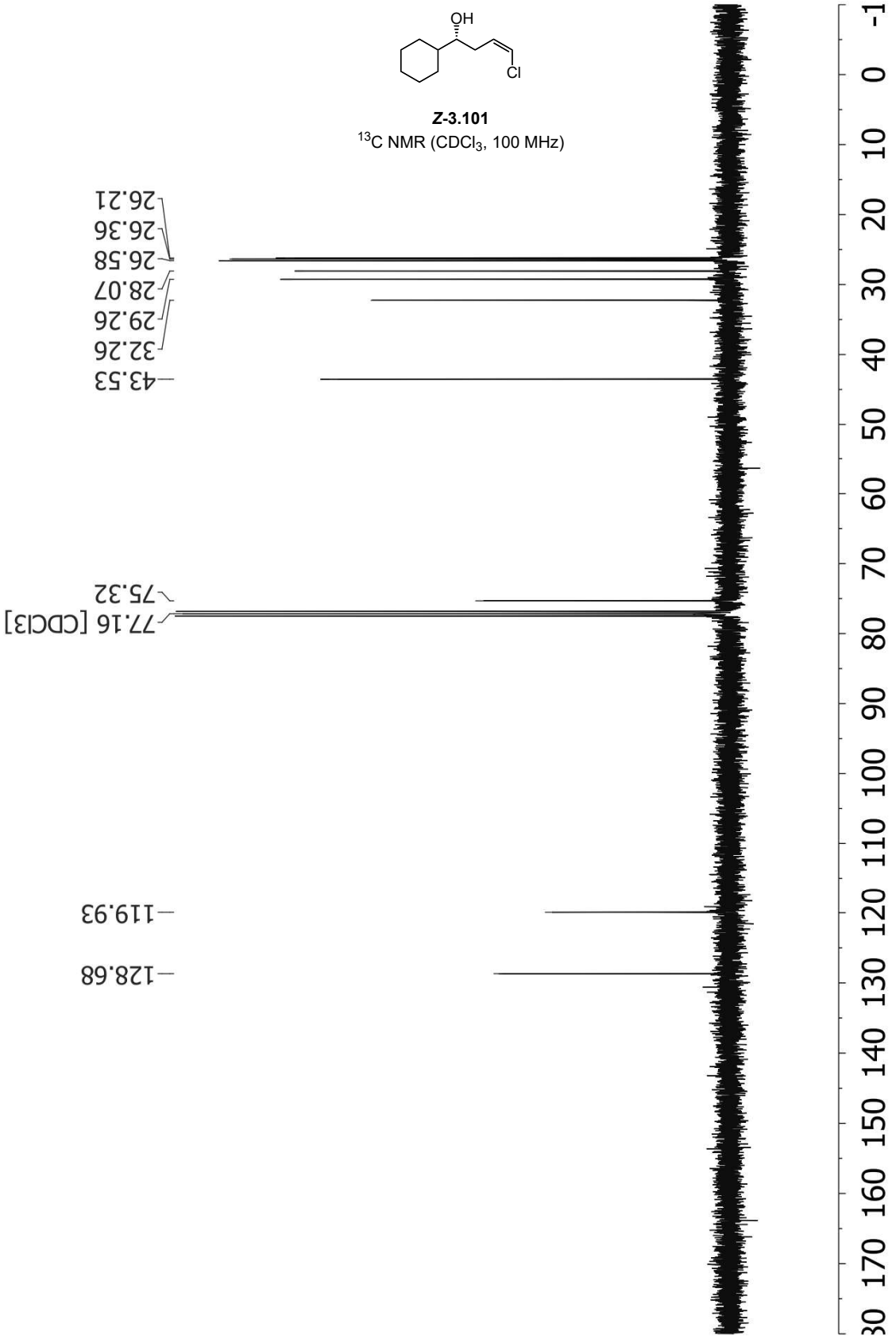
OH
Cl
Z-3.101
13C NMR (CDCl3, 100 MHz)
26.21
26.36
26.58
28.07
29.26
32.26
43.53
75.32
77.16 [CDCl3]
119.93
128.68

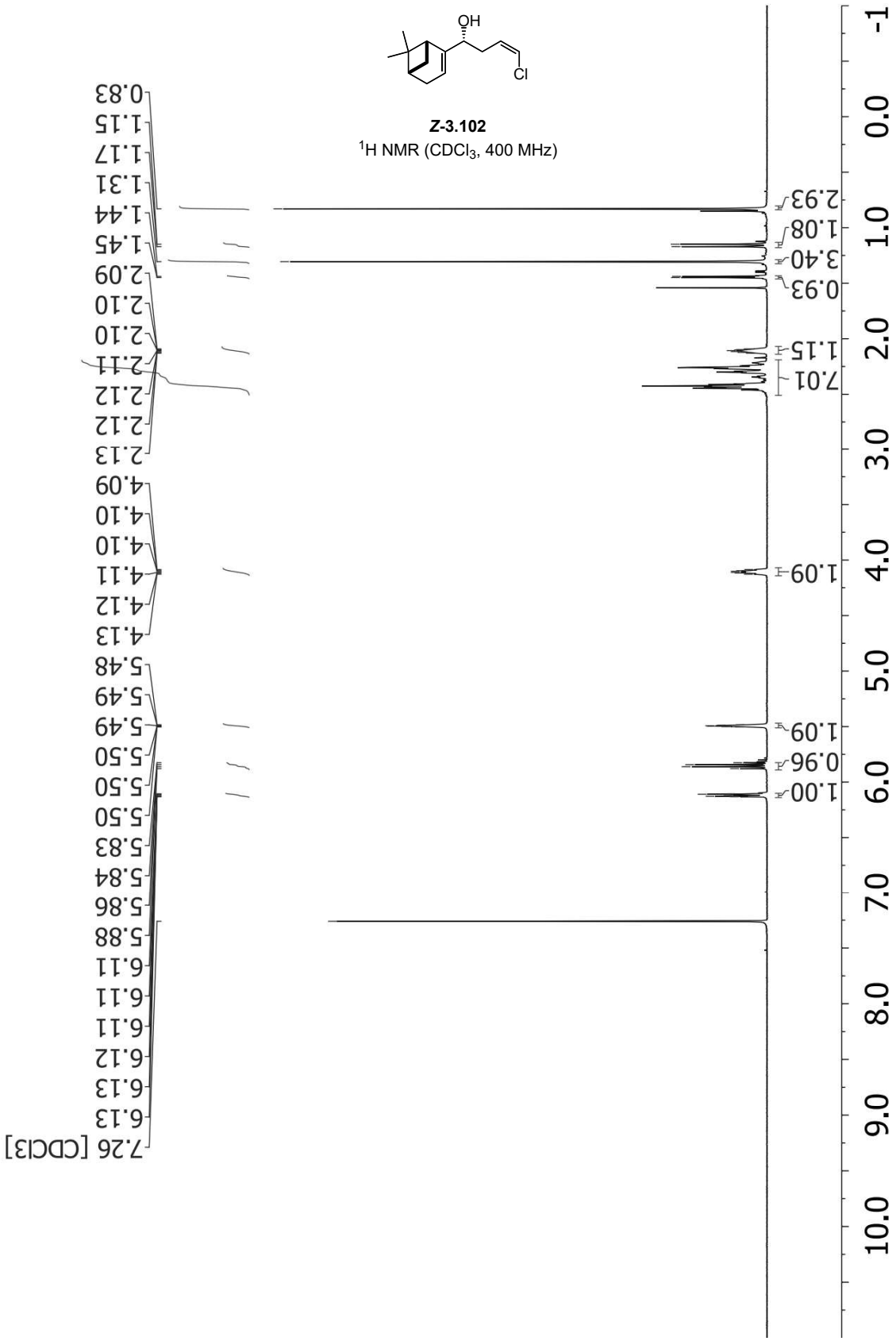
OH
Cl
Z-3.102
1H NMR (CDCl3, 400 MHz)
7.26 [CDCl3]
2.93
1.08
3.40
0.93
1.15
7.01
1.09
1.09
0.96
1.00

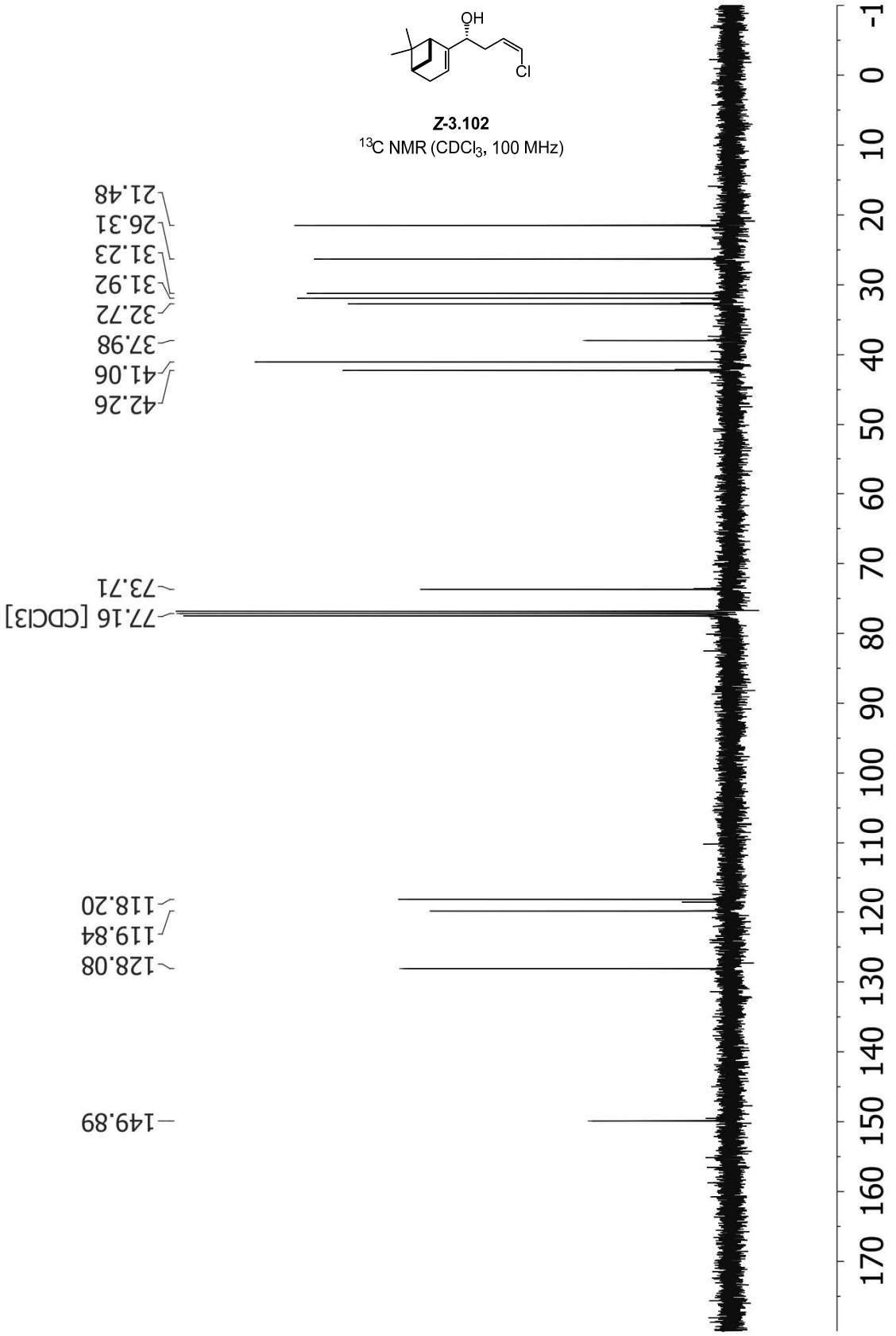
OH
Cl
Z-3.102
13C NMR (CDCl3, 100 MHz)
21.48
26.31
31.23
31.92
32.72
37.98
41.06
42.26
73.71
77.16 [CDCl3]
118.20
119.84
128.08
149.89
-1 0 10 20 30 40 50 60 70 80 90 100 110 120 130 140 150 160 170

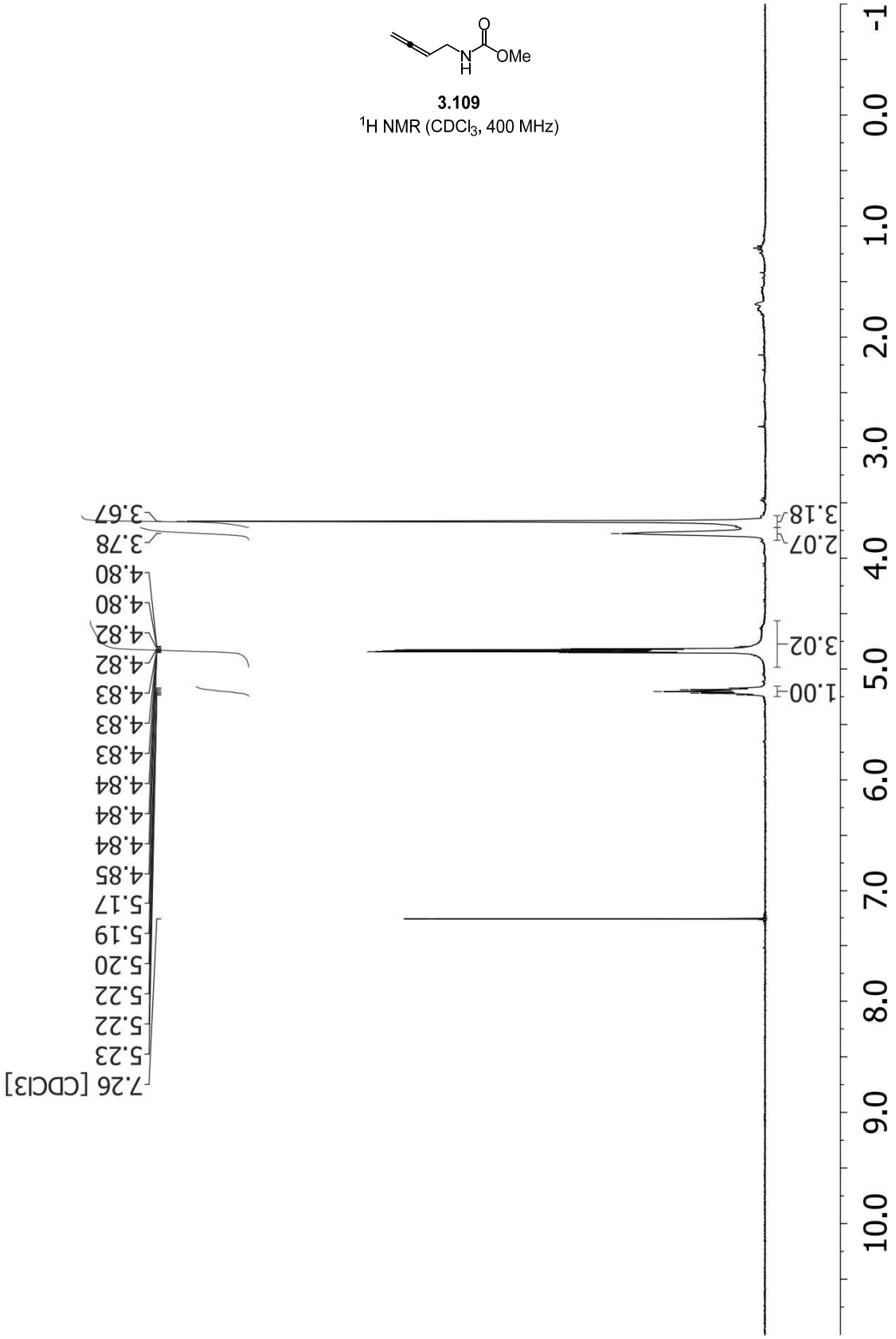
O
N
H
OMe
3.109
1H NMR (CDCl3, 400 MHz)
-1
0.0
1.0
2.0
3.0
4.0
5.0
6.0
7.0
8.0
9.0
10.0
3.18
2.07
3.02
1.00
3.67
3.78
4.80
4.80
4.82
4.82
4.83
4.83
4.83
4.84
4.84
4.84
4.85
5.17
5.19
5.20
5.22
5.22
5.23
7.26 [CDCl3]

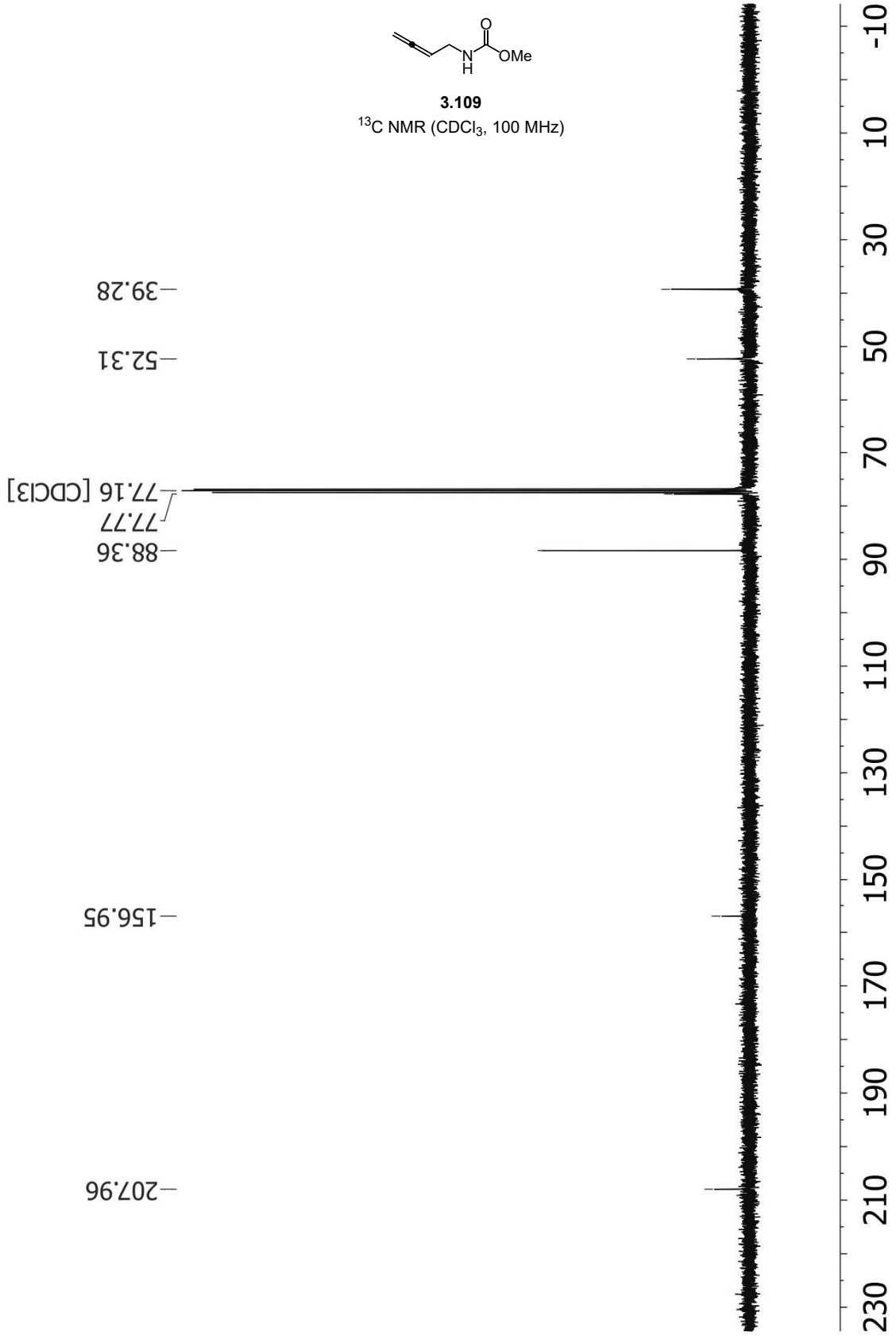
O
N
H
OMe
3.109
^{13}C NMR ($CDCl_3$, 100 MHz)
207.96
156.95
88.36
77.77
77.16 [CDCl3]
52.31
39.28
230
210
190
170
150
130
110
90
70
50
30
10
-10

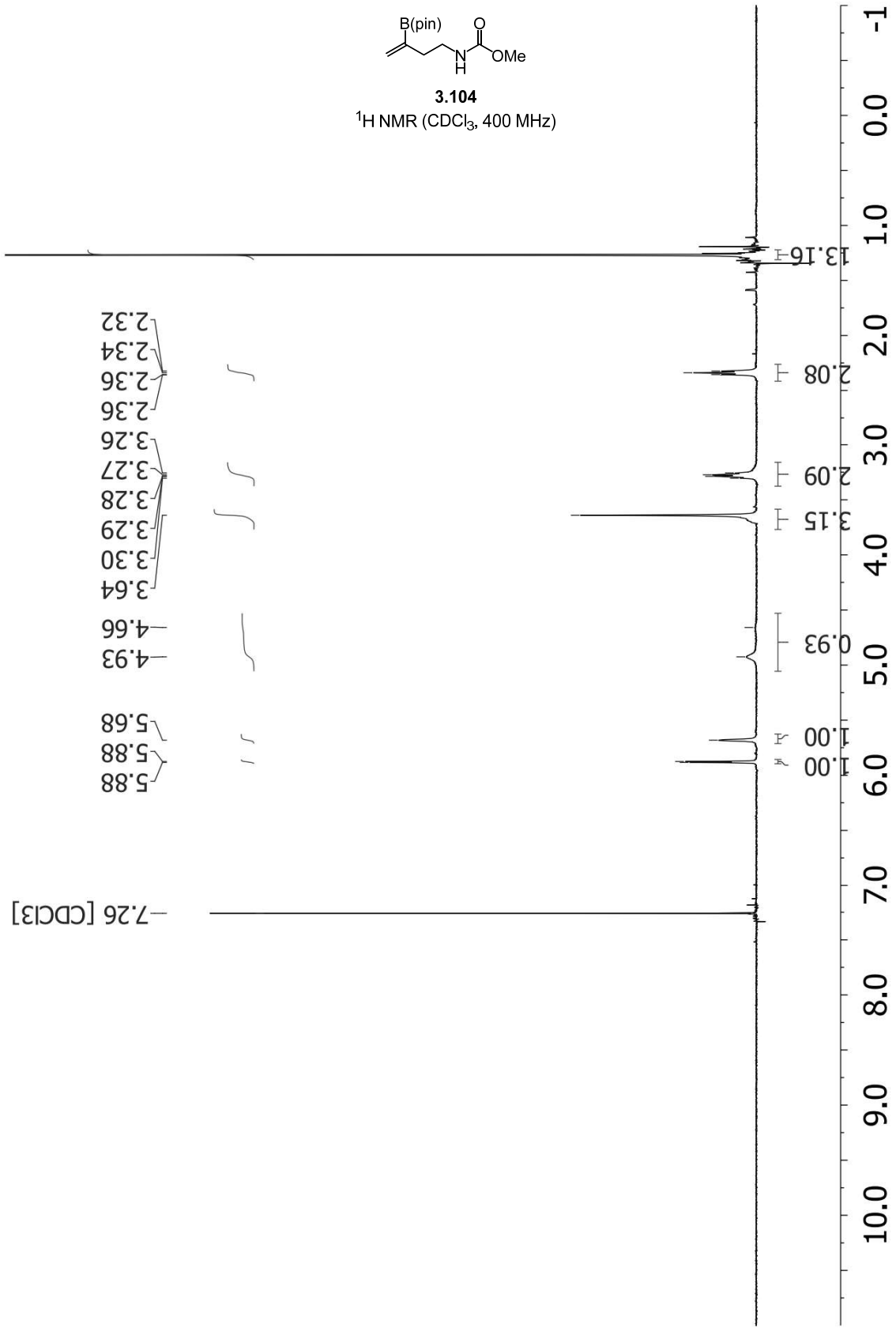
B(pin)
O
N
H
OMe
3.104
^{1}H NMR ($CDCl_3$, 400 MHz)
13.16
2.08
2.09
3.15
0.93
1.00
1.00
7.26 [CDCl3]
5.68
5.88
5.88
4.93
4.66
3.64
3.30
3.29
3.28
3.27
3.26
2.36
2.36
2.34
2.32

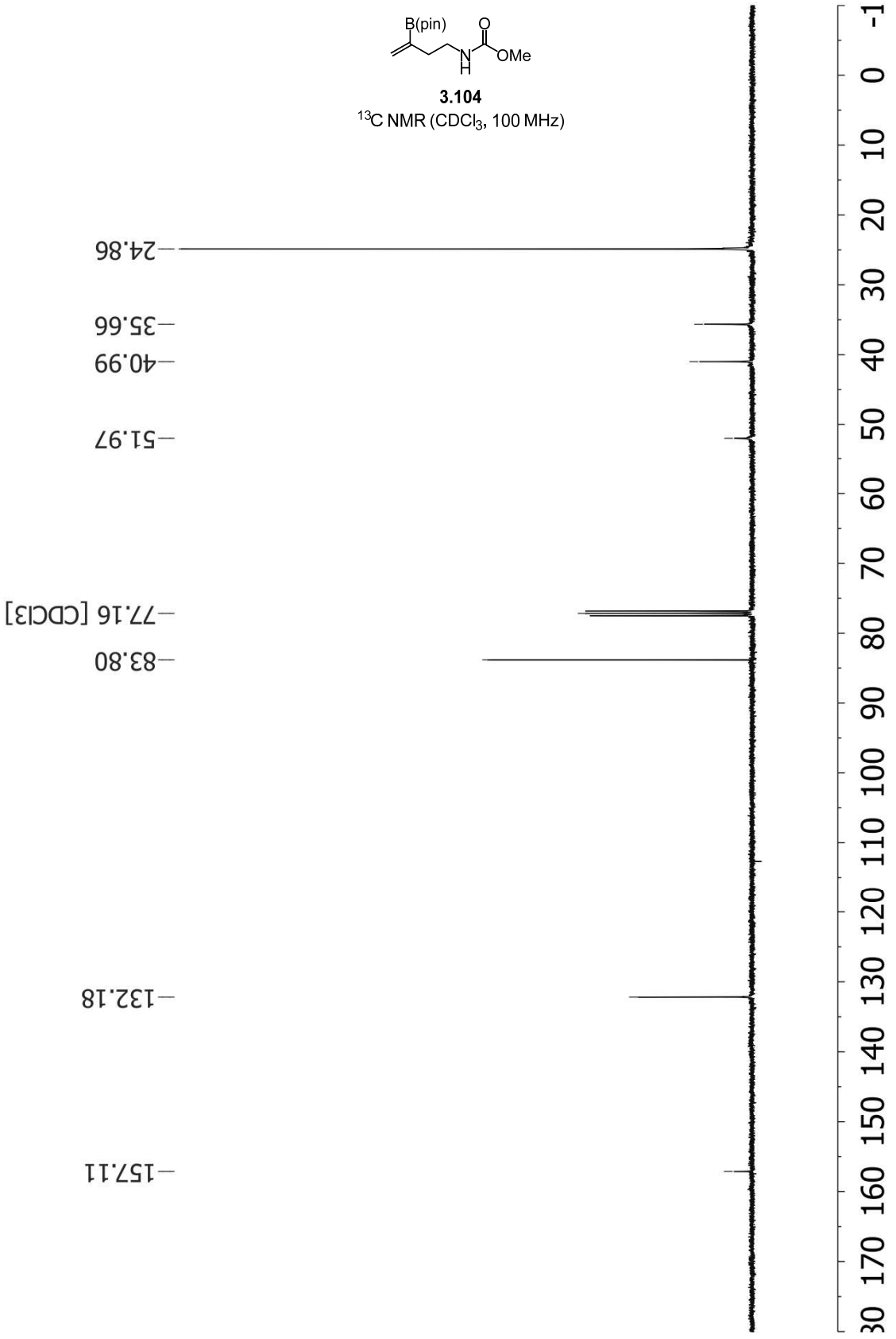
B(pin)
O
N
H
OMe
3.104
13C NMR (CDCl3, 100 MHz)
24.86
35.66
40.99
51.97
77.16 [CDCl3]
83.80
132.18
157.11
-1
0
10
20
30
40
50
60
70
80
90
100
110
120
130
140
150
160
170

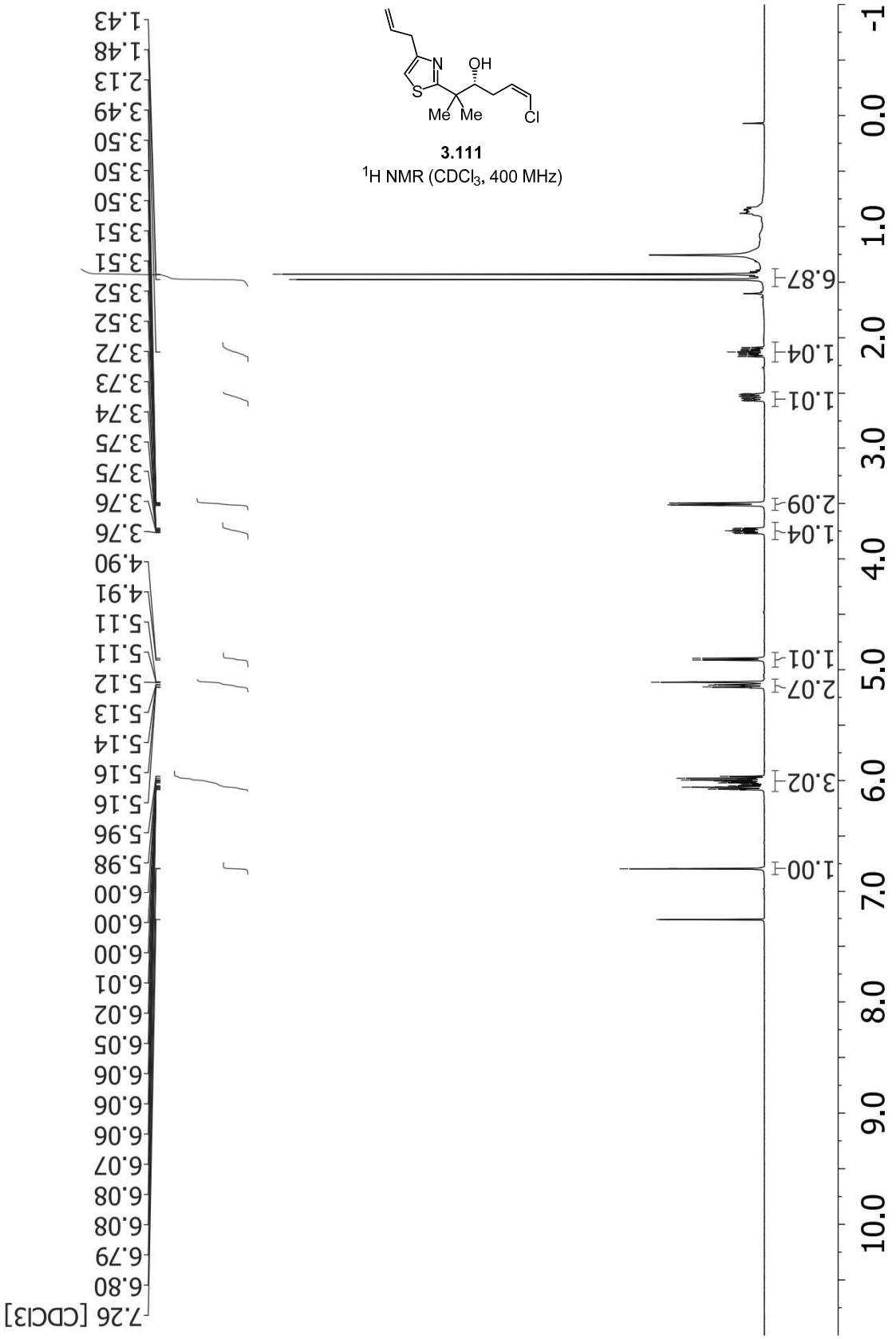
3.111
1H NMR (CDCl3, 400 MHz)
N
OH
S
Me
Me
Cl
7.26 [CDCl3]
6.87
1.04
1.01
2.09
1.04
1.01
2.07
3.02
1.00

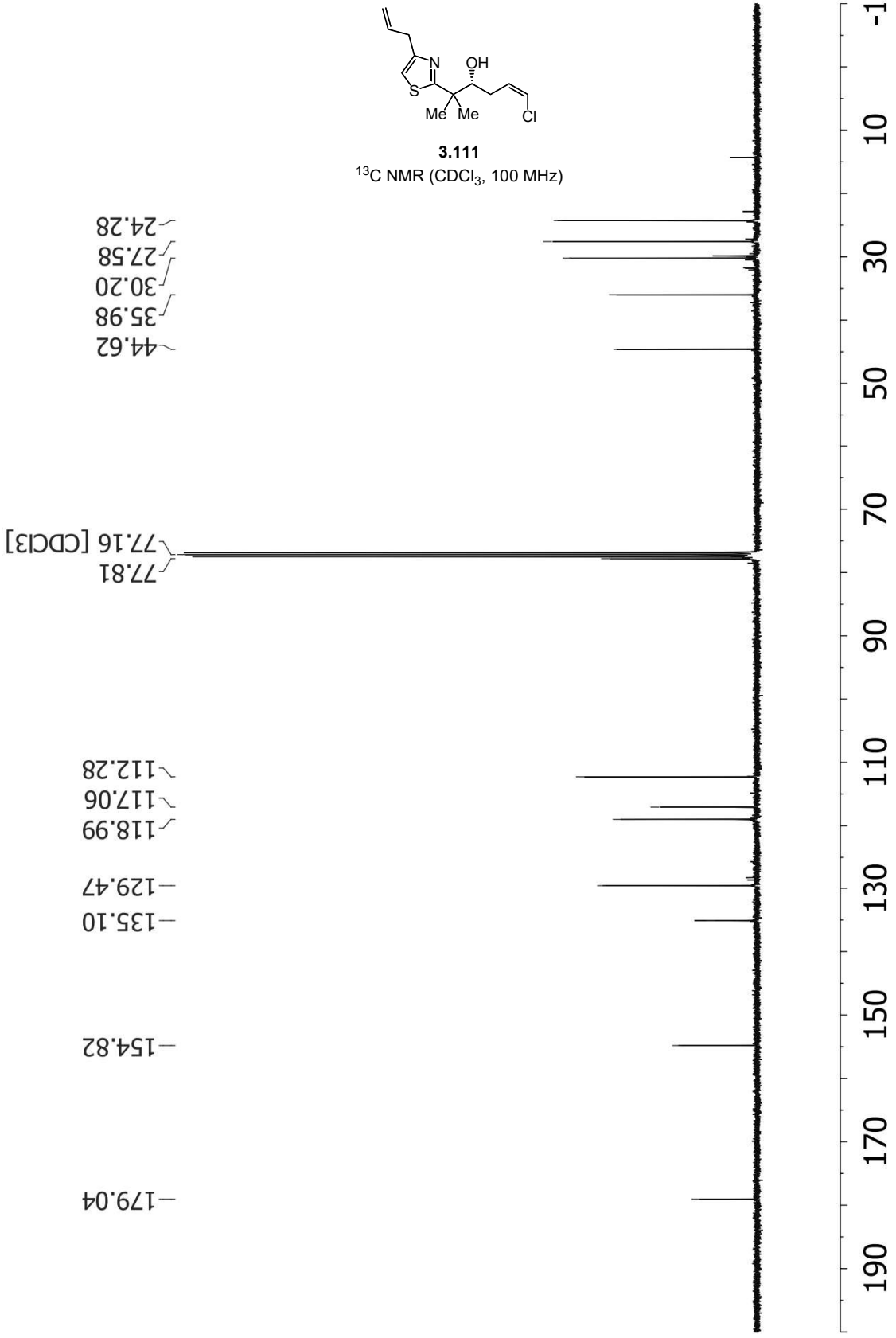
N
OH
S
Me
Me
Cl
3.111
13C NMR (CDCl3, 100 MHz)
24.28
27.58
30.20
35.98
44.62
77.16 [CDCl3]
77.81
112.28
117.06
118.99
129.47
135.10
154.82
179.04
-1
10
30
50
70
90
110
130
150
170
190

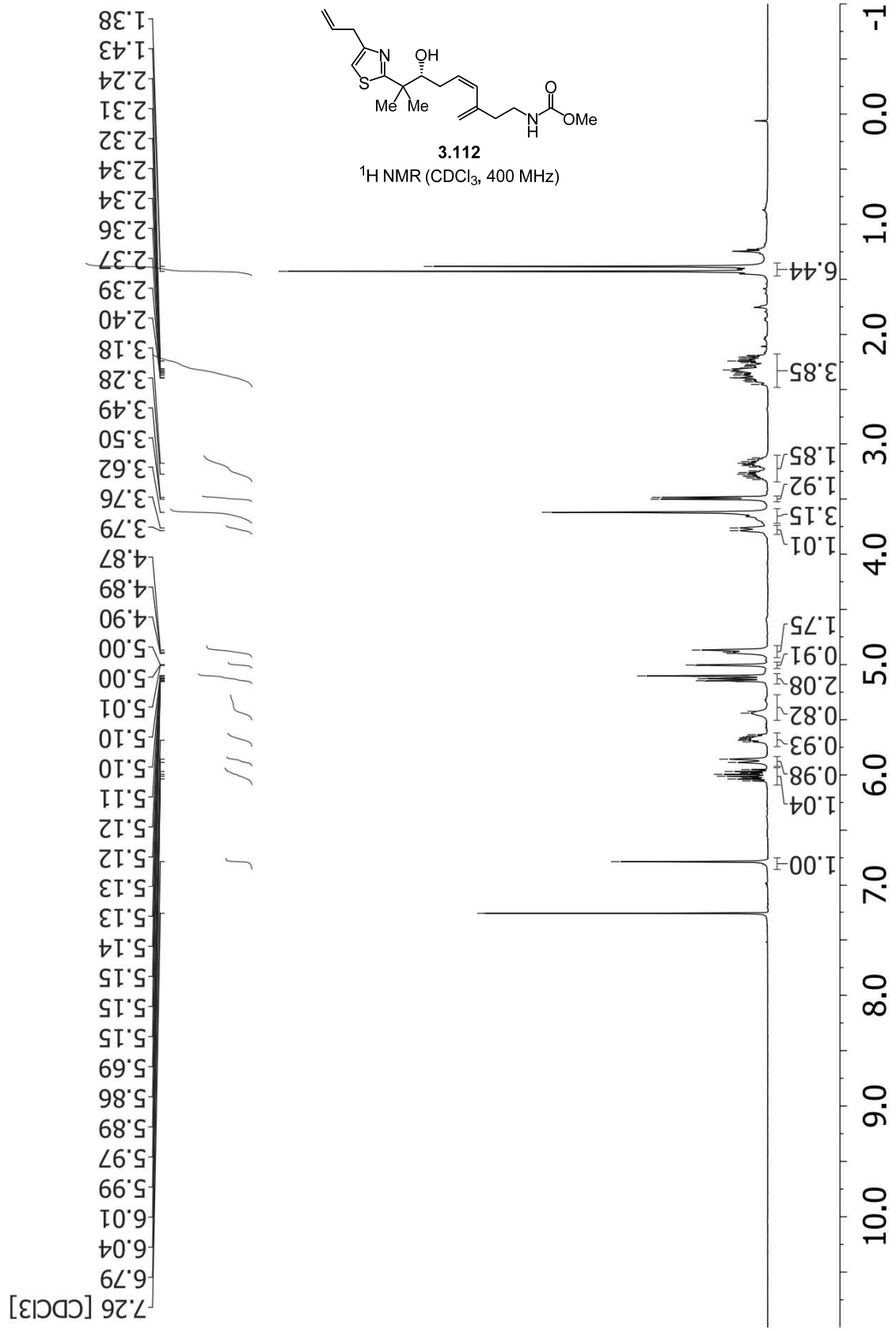
3.112
1H NMR (CDCl3, 400 MHz)
7.26 [CDCl3]
1.00
6.44
3.85
1.85
1.92
3.15
1.01
1.75
0.91
2.08
0.82
0.93
0.98
1.04

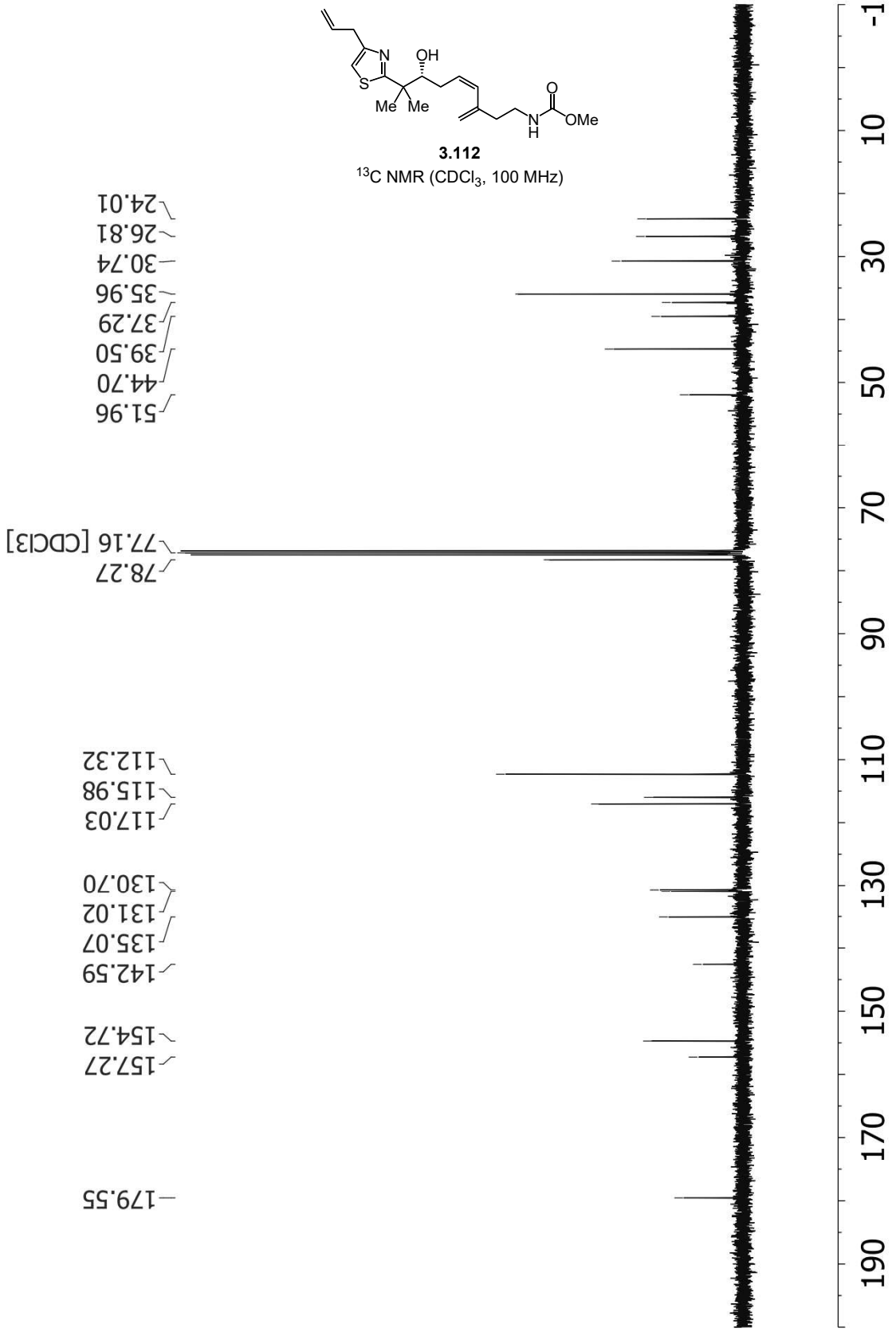
N
OH
S
Me Me
N
H
O
OMe
3.112
^{13}C NMR ($CDCl_3$, 100 MHz)
24.01
26.81
30.74
35.96
37.29
39.50
44.70
51.96
77.16 [CDCl3]
78.27
112.32
115.98
117.03
130.70
131.02
135.07
142.59
154.72
157.27
179.55
-1
10
30
50
70
90
110
130
150
170
190

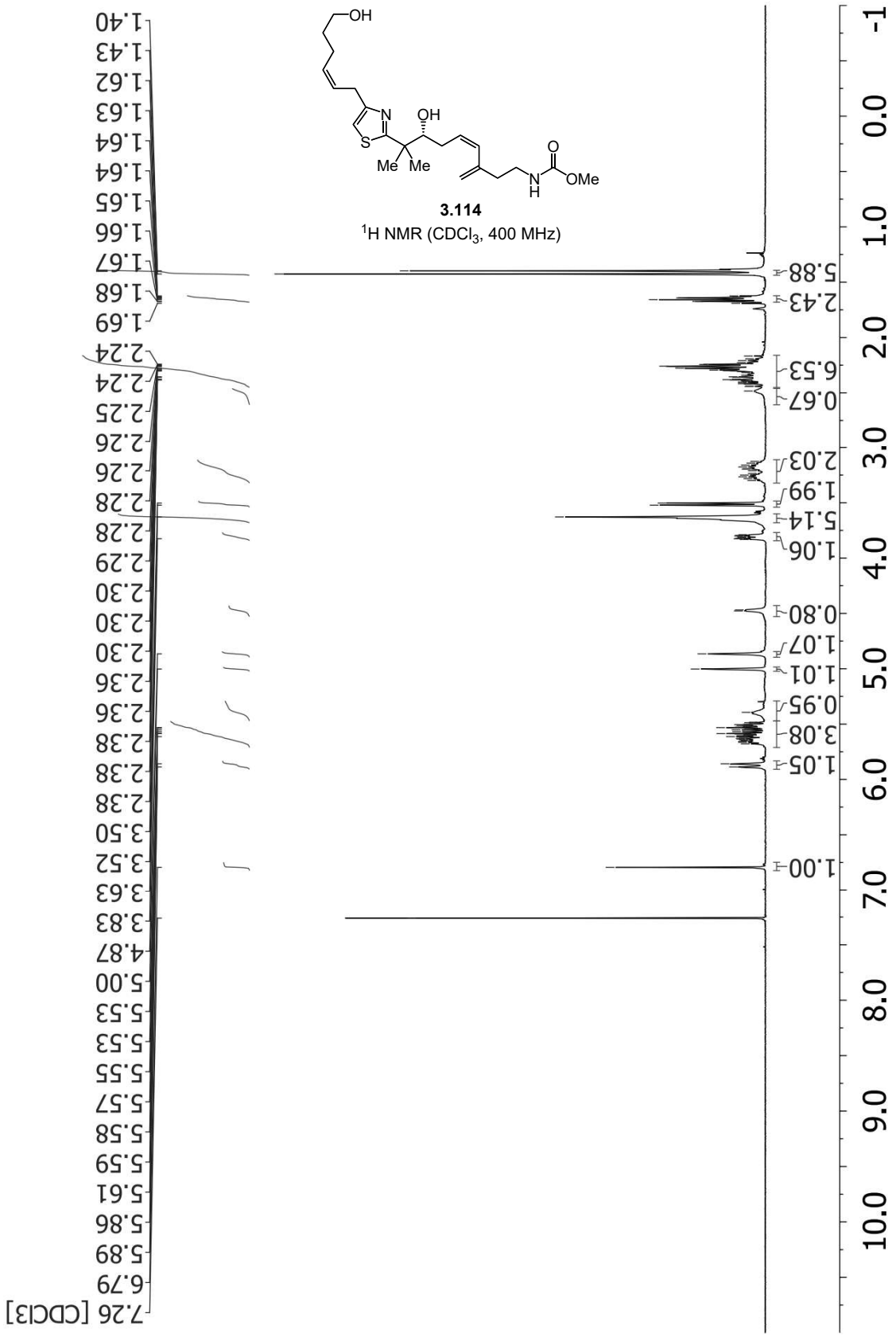
OH
N
OH
S
Me Me
O
N
H
OMe
3.114
1H NMR (CDCl3, 400 MHz)
7.26 [CDCl3]
1.00
1.05
3.08
0.95
1.01
1.07
0.80
1.06
5.14
1.99
2.03
0.67
6.53
2.43
5.88

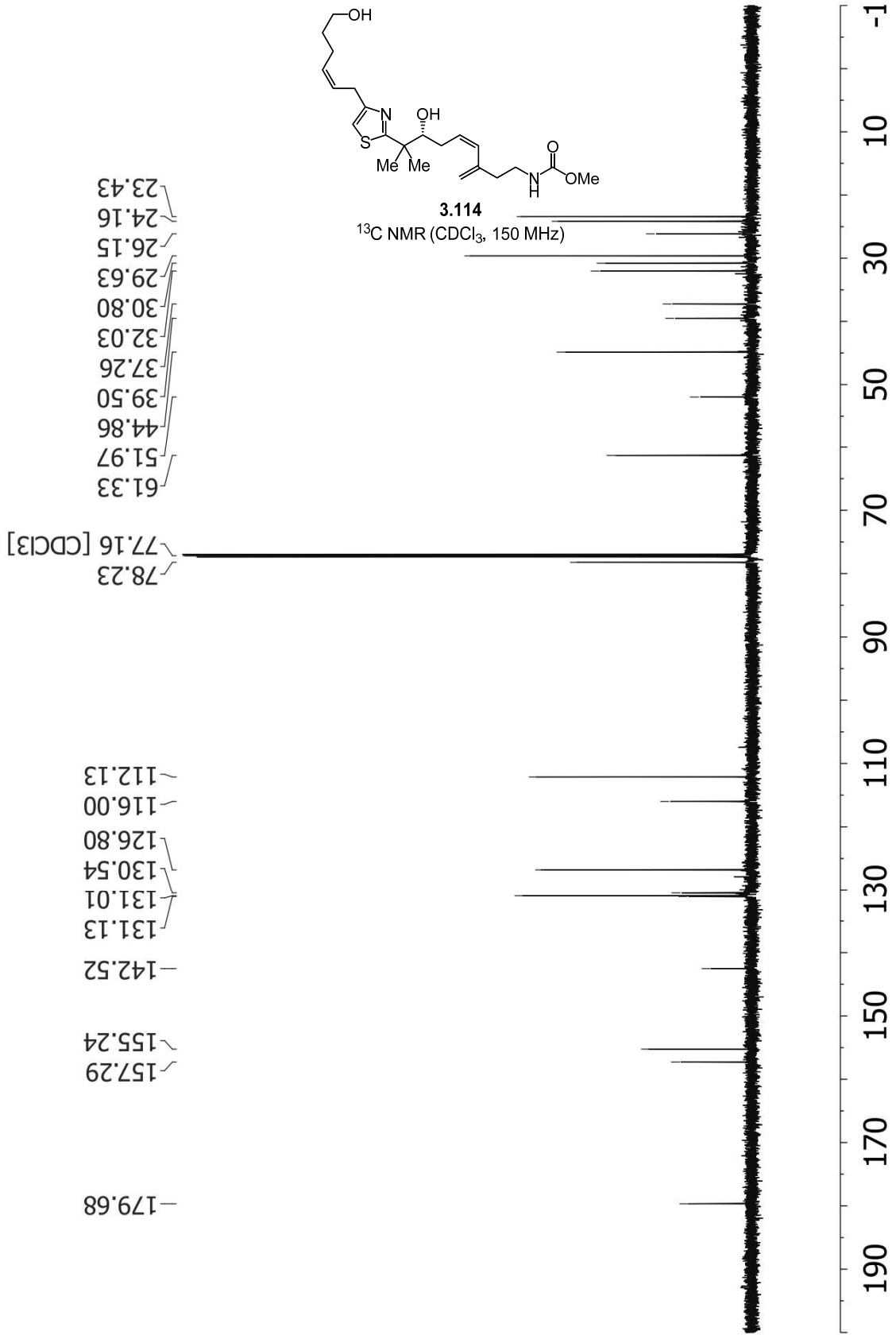
OH
N
OH
S
Me Me
O
N
H
OMe
3.114
^{13}C NMR ($CDCl_3$, 150 MHz)
23.43
24.16
26.15
29.63
30.80
32.03
37.26
39.50
44.86
51.97
61.33
77.16 [CDCl3]
78.23
112.13
116.00
126.80
130.54
131.01
131.13
142.52
155.24
157.29
179.68
-1
10
30
50
70
90
110
130
150
170
190

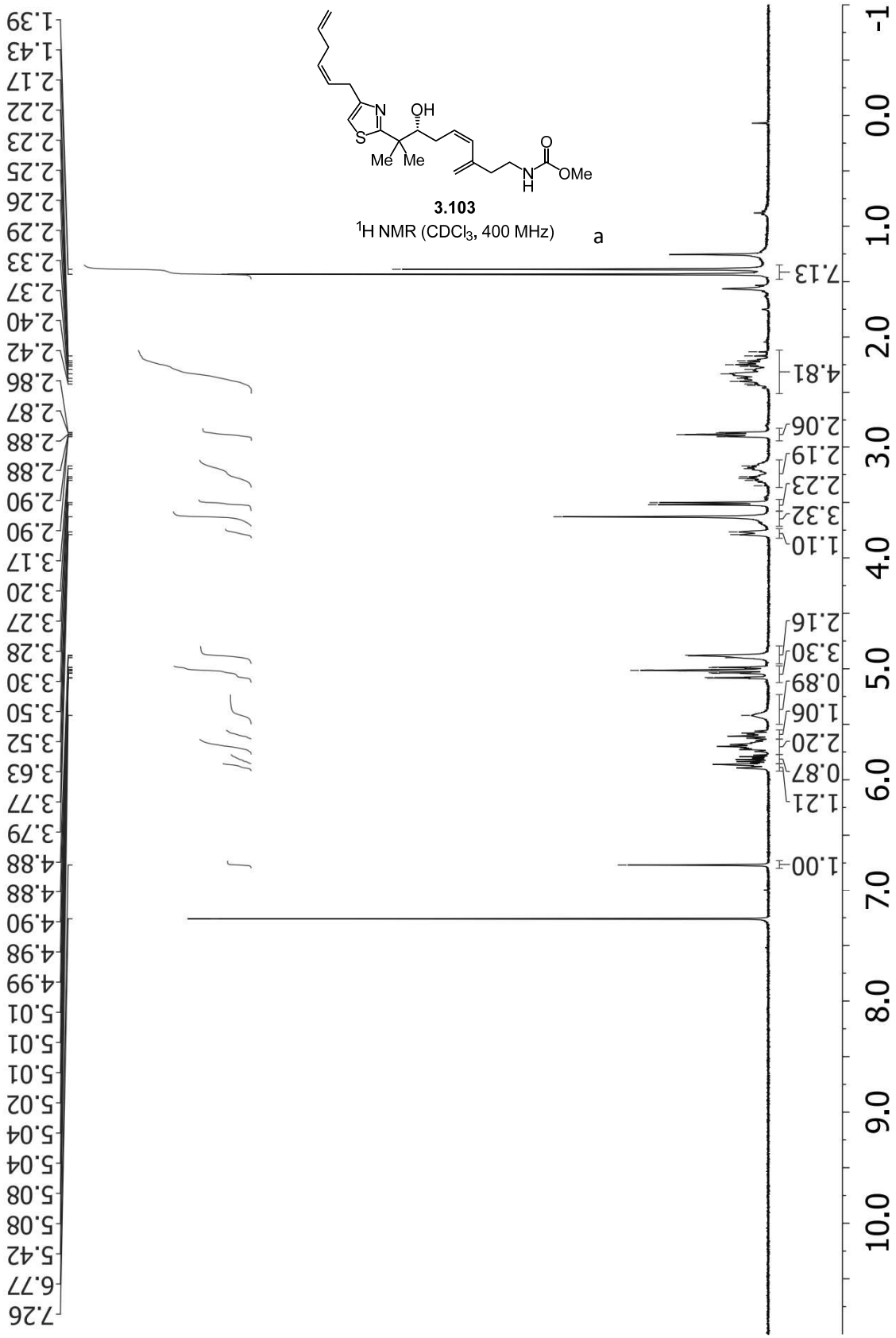
3.103
1H NMR (CDCl3, 400 MHz)
a
N
OH
S
Me Me
O
N
H
OMe

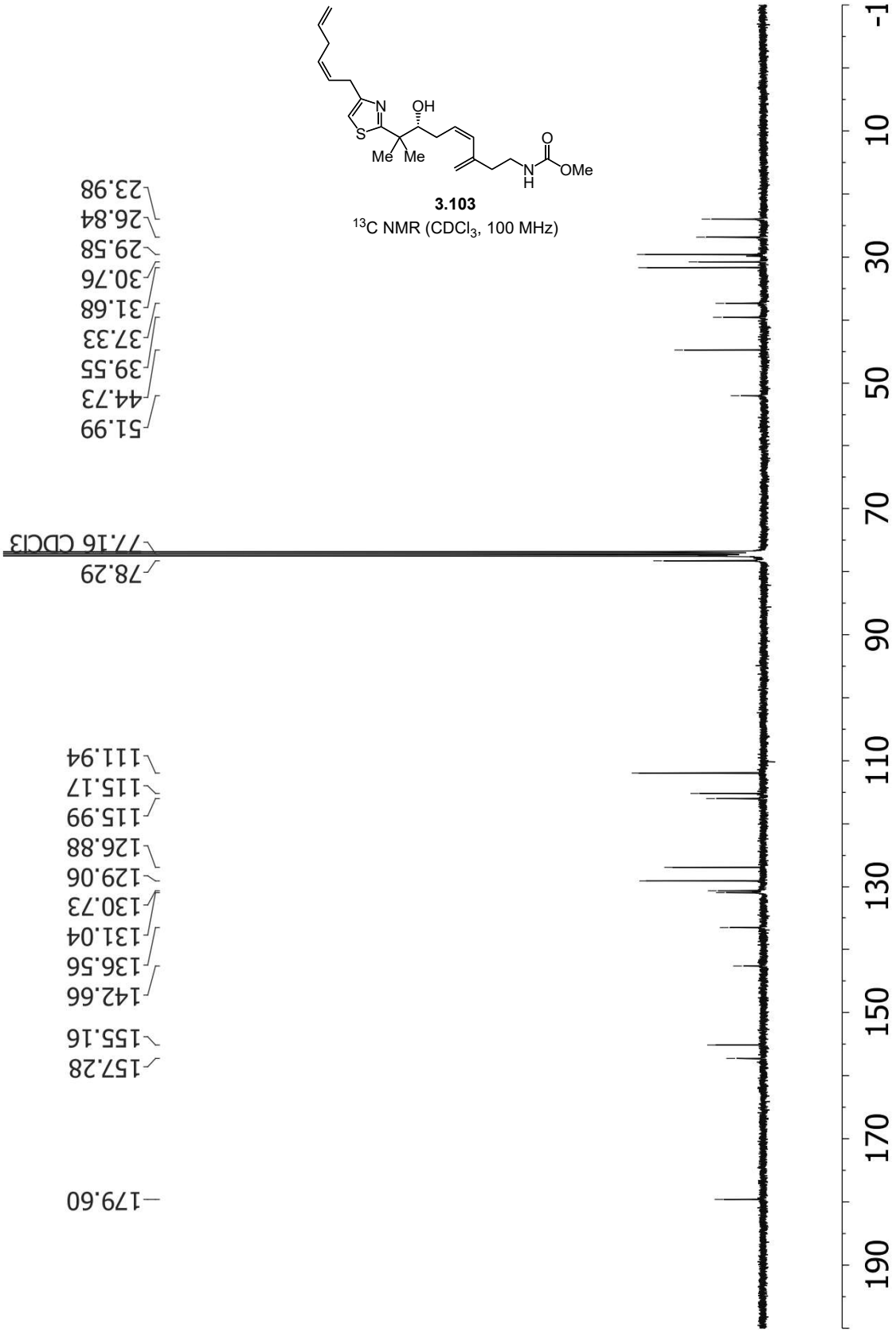
3.103
^{13}C NMR ($CDCl_3$, 100 MHz)
23.98
26.84
29.58
30.76
31.68
37.33
39.55
44.73
51.99
77.16 CDCl3
78.29
111.94
115.17
115.99
126.88
129.06
130.73
131.04
136.56
142.66
155.16
157.28
179.60
-1
10
30
50
70
90
110
130
150
170
190